PROCEEDINGS
OF THE
WEDNESDAY SLIDE
CONFERENCE 2019-2020

JOINT PATHOLOGY CENTER
SILVER SPRING, MD 20910
2019-2020

JOINT PATHOLOGY CENTER
VETERINARY PATHOLOGY SERVICE

Thanks to the Joint Pathology Center's amazing military and civilian staff members this 65th year of the Wednesday Slide Conference - it is truly a huge undertaking. Every single member of the JPC faculty, residents, and admin staff contributes to its success.

Special thanks to Ms. Keneyna Gathers, Ms. Andrea Cherilus, and Ms. Jessica Lewis for their help in organizing and keeping everything straight, and MAJ Erica Barkei for extra editing help, as my typing skills continue to fade with age.

Thanks also to our wonderful moderators, who travel from around the US to lend their expertise and make it such a valuable training experience for our staff and guests who join us each week. Unfortunately, we missed our last six moderators due to COVID-19 this year, we missed our weekly guests, and we especially missed the Wednesday gathering of our JPC Faculty and residents, but we toiled on and got the results out on time.

Most of all, a huge thank you to all of our contributors out there - your cases and your workups keep getting better every year - we couldn't do it without you.

We look forward to the kickoff of WSC 2020-2021 in the fall!

Bruce Williams, DVM
2019-2020 WSC Coordinator

WEDNESDAY SLIDE CONFERENCE 2019-2020

Case No.	JPC No.	Contr. No.	Species	Tissue	Diagnosis
Conference 1 – August 21, 2019					
1	4119798	NT-556/HA	Horse	Lung	Equine respiratory distress syndrome
2	4117511	17-0282	Dog	Lung	E-coli-associated pneumonia
3	4118594	P17-747	Ox	Lung	Contagious bovine pleuropneumonia
4	4129174	N198/18	Sheep	Ox	Ovine progressive pneumonia
Conference 2 – August 28, 2019					
1	4117378	Case #2	Lion	Cerebrum	Canine morbillivirus (CDV)
2	4118174	16GR108	Dog	Epididymis	Beagle pain syndrome, sperm granuloma
3	4084695	Case #2	Dog	Retro-orbital tissue	Granular cell tumor
4	4117447	14-1790	Dog	Vagina	Clitoral gland carcinom
Conference 3 – September 4, 2019					
1	4020435	W343-1	Pigeon	Pancreas, intestine	Pigeon paramyxovirus-1
2	4048789	14-102	Sheep	Lymph node	*Corynebacterium pseudotuberculosis*
3	4134828	2019B	Pig	Spleen	Classical Swine Fever
4	4135861	P17-969	Ox	Tongue	Foot and mouth disease
Conference 4 – September 18, 2019					
1	4087577	16-02795	Little red flying fox	Cerebrum	Australian bat lyssavirus
2	4111545	17-0894	Sheep	Liver	*Panicum* toxicosis
3	4116936	UMN VDL	Sheep	Nasal mucosa	*Salmonella arizonae*
4	4118633	M18-02265	Ox	Rumen	Kikuyu toxicosis
Conference 5 - September 25, 2019					
1	4121052	V17-00724	Sheep	Intestine	*Mycobacterium paratuberculosis*
2	4085120	160360	European brown hare	Liver	*Yersinia pseudotuberculosis*
3	4101226	Case 1	Rabbit	Kidney, liver	Rabbit hemorrhagic disease; *Eimeria steidae*
4	4119789	15-0463	Dog	Spinal cord	Spinal nephroblastoma
Conference 6 – October 2, 2019					
1	4118173	A15-62176	Cardinal tetra	Skin	*Flavobacterium columnare*
2	4120175	AP 17-4634	Zebrafish	Hindbrain	*Pseudoloma neurophilum*
3	4113195	AFRIMS Case 1	Zebrafish	Instestine	Intestinal adenocarcinoma
4	4117006	WSC 18-19 #2	Puerto Rican crested toad	Skin	Brown skin disease
Conference 7 – October 9 2019					
1	4135938	AP19-00238-9	Cat	Liver	Congenital hepatic fibrosis
2	4120038	16RD2093	Ox	Liver	*Crotalaria* toxicity
3	4101080	15-0318	Dog	Liver	Portosystemic shunt
4	4134512	19-117	Horse	Liver	Equine serum hepatitis

WEDNESDAY SLIDE CONFERENCE 2019-2020

Conference 8 – October 23 2019					
1	4135866	D19-007212	Dog	Uterus	Subinvolution of placental sites
2	4066220	15-1137	Goat fetus	Placenta	*Coxiella burnetti*
3	4102155	VS17005	Rhesus macaque	Uterus	Choriocarcinoma
4	4102428	TAMU 2017 WSC 2	Horse	Ovary	Hemorrhagic anovulatory follicle
Conference 9 – October 23, 2019					
1	4117005	WSC18-19 #1	Peahen	Liver	Marek's disease
2	4134827	2018A	Chicken	Tibial marrow	Chicken anemia agent
3	4135750	2018A	Chicken	Cecum	*Histomonas meleagridis*, intussusception
4	4085966	S699/14	Pigeon	Liver	Pigeon circovirus, pigeon herpesvirus
Conference 10 - November 20, 2019					
1	4135946	R17104D	Spiny lobster	Hepatopancreas	*Panulirus argus* virus-1 (PAV-1)
2	4132732	N18-0170	Oscar cichlid	Kidney	Renal cystadencarcinoma, mycobacteriosis
3	4136173	19H4111	Bearded dragon	Liver	Adenovirus
4	4138045	19-33870	Silvery salamander	Skin	*Amphibiocystidium sp.*
Conference 11 – December 4, 2019					
1	4116937	S17-1101	Dog	Skin	Erythema multiforme
2	4114031	WSC-SC-2	Cat	Skin	Pseudomycetoma
3	4122525	H18-0008-92	Cat	Pancreas, skin	Paraneoplastic alopecia
4	4137402	847/19	Cat	Skin	Cutaneous lymphocytosis
Conference 12 – December 11, 2019					
1	4032968	MSKCC/WMCRU HB	Hamster	Liver	Lymphoma, *Leishmania* sp.
2	4031109	A12-357	Rhesus macaque	Lung	SIV, *Pneumocystis carinii*
3	4118136	WSC Case 2 HE	Rat	Kidney	Chronic progressive nephropathy
4	4135947	L19-3350	Rabbit	Metatarsus	Botryomycosis
Conference 13 – January 8, 2019					
1	4130570	2019A208	Dog	Liver	Canine adenovirus-1
2	4038890	HSRL-425	Cat	Nose	*Cryptococcus*
3	4117383	18-2108 WSC3	Golden pheasant	Trachea, cecum	Avian herpesvirus-1, *Heterakis isolonche*
4	4118093	Rab51	Rabbit	Lung	*Emmonsia crescens*
Conference 14 – January 15, 2020					
1	4116557	18-4856	Turtle	Head	Vitamin A deficiency
2	4118632	2926	Asian small-clawed otter	Kidney	Oxalate urolithiasis
3	4136426	71618	Big brown bat	Kidney	*Nephroisospora eptesici*
4	4101490	016-045846	Red kangaroo	Liver, lung	Metastatic mammary carcinoma

WEDNESDAY SLIDE CONFERENCE 2019-2020

Conference 15 –January 22, 2019					
1	4128009	16N131-1	NOD mouse	Brain	*Klebsiella oxytoca*
2	4136806	MS18-3968	CYBB[ko] mouse	Spleen	Chronic granulomatous disease
3	4101223	17-1438 1-2	Mouse	Lung	*Mycoplasma pulmonis*
4	4103914	17N076	NOD scid mouse	Skin	Graft-vs.host response
Conference 16 – January 29, 2019					
1	4135077	S1809996	Pig	Lung	Porcine respiratory and reproductive syndrome
2	4167277	2015A	Pig	Jejunum	Porcine epidemic diarrhea virus
3	4136500	P590-19	Pig	Spinal cord	Porcine sapelovirus
4	4119040	N633-16	Pig	Skeletal muscle	Porcine circovirus-2
Conference 17 – February 5, 2019					
1	4117518	1235813-006	Cynomolgus macaque	Lung	*Mycobacterium tuberculosis*
2	4032584	WSC 2013 Case 1	Ox	Brainstem	Rabies
3	4134352	19N153	Sheep	Skeletal muscle	Nutritional myopathy
4	4119040	AFIP 2018 053/18	Cat	Pancreas	Chronic interstitial pancreatitis, islet amyloid, exocrine hyperplasia
Conference 18 – February 12, 2019					
1	4105224	17-325	Dog	Liver	Arteriovenous fistula
2	4032584	17/1060 Z	Dog	Aorta, spleen	*Aspergillus terreus*
3	4049886	WSC Cas 1	Squirrel monkey	Cerebrum	Amyloidosis
4	4135536	21465	Dog	Artery	Mucopolysaccharidosis
Conference 19 – February 19, 2019					
1	4117490	17041318	Ox	Spinal cord, heart	*Neospora caninum*
2	4136399	18-0311	Dog	Cerebellum	Ceroid lipofuscinosis
3	4032559	KSU VDL	Ox	Cerebellum	Medulloblastoma
4	4033564	WSC1920	Cat	Spinal cord	Ischemic myelopathy
Conference 20 – March 25, 2019					
1	4117493	T-1708131	Cat	Lung	Feline infectious peritonitis
2	4135747	19-2535	Sheep	Kidney	Malignant catarrhal fever/Ovine herpesvirus-2
3	4117883	Blank label	Ox	Lung	High altitude disease
4	4049442	LE-2	Pig	Haired skin	Porcine circovirus-2
Conference 21 – 3 April, 2019					
1	4066399	B-14-0576	Dog	Gingiva	Amyloid-producing ameloblastoma
2	4122528	H17-0922-03	Rabbit	Gingiva and alveolar bone	Carcinoma with odontodysplasia
3	4117676	S2018-0004	Red-tailed boa	Maxilla	Compound odontoma
4	4117660	AR17-0027-7 DVD	Prairie vole	Maxilla, cheek teeth	Odontodysplasia
Conference 22 – April 15, 2019					
1	4099471	NO-16-1279	Squirrel monkey	Heart	Encephalomyocarditis virus (EMCV)
2	4136179	Case 2 DVD	Rhesus macaque	Lung	Rhesus cytomegalovirus
3	4117676	61726-1	Colobus monkey	Cerebrum	*Balamuthia mandrillaris*
4	4100234	WSC 1920 Conf 22 Case 4 DVD	Spider monkey	Cecum, colon	*Clostridium difficile*

WEDNESDAY SLIDE CONFERENCE 2019-2020

Conference 23 – April 22, 2019					
1	4117530	69887	Cat	Lung	*Paragonimus kellicotti*
2	4119103	PV300	Dog	Peritoeneum	*Mesocestoides sp.*
3	4117380	61290	Turtle	Lung	Pentastomes
4	4101199	S1601842	Horse	Adrenal gland	*Halicephalobis gingivalis*
Conference 24 – April 29, 2019					
1	4084944	S62/16	Horse	Mesenteric artery	*Strongylus vulgaris*
2	4048931	Case 2	Horse	Small intestine	*Lawsonia intracellularis*
3	4117527	S1706449	Horse	Right dorsal colon	NSAID toxicosis
4	4083951	WSC Case 2 DVD	Horse	Pituitary gland	Adenoma of the pars intermedia
Conference 25 – May 6, 2019					
1	4137583	15/692	Horse	Subcutis	Undifferentiated pleomorphic sarcoma with giant cells
2	4115990	MU11478	Goat	Joint	*Mycoplasma mycoides mycoides subsp. capri*
3	4117671	17-137-W4	Pig	Foot, lung	*Trueperella pyogenes*
4	4115969	25681	Horse	Skeletal muscle	Systemic calcinosis

Joint Pathology Center
Veterinary Pathology Services

WEDNESDAY SLIDE CONFERENCE 2019-2020

C o n f e r e n c e 1

22 August 2019

CASE I: NT-556 (JPC 4119798).

Signalment: 4-day-old male Arabian foal (*Equus caballus).*

History: Foal was weak but ambulatory with expiratory dyspnea and tachypnea since birth and showed an elevated respiratory and cardiac rate and fever. Mucous membranes were hyperemic with multifocal petechiation of the oral mucous membranes and in the skin's ear inner side. The capillary refill time was less than 2 seconds. Pulmonary auscultation revealed snoring, wheezing, and crepitation with a diffuse and moderate alveolar pattern on thoracic radiographs. Supportive care and treatment, including positive pressure ventilation, were pursued without success and the foal was eventually euthanized.

Gross Pathology: Records indicate the horse to be in good body condition with multifocal petechiae of the oral mucous membranes and in the inner side of the pinna. Bilaterally, the lungs appeared markedly collapsed, were diffusely firm and heavy with an edematous consistency, and a reddish to gray discoloration.

Laboratory results: No clinically significant alterations detected in the blood, including an adequate level of immunoglobulins.

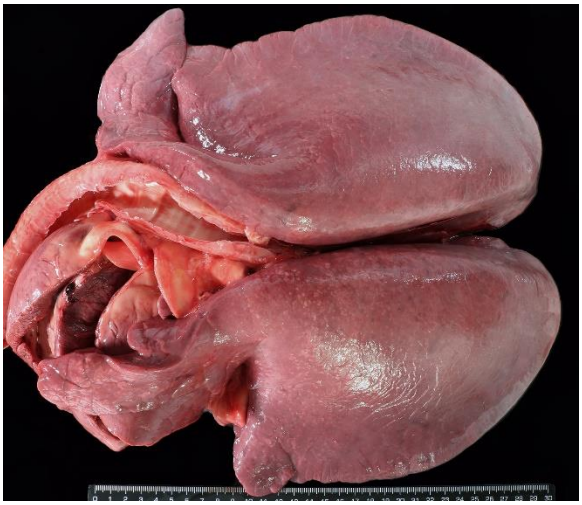

Lung, foal. There is diffuse pulmonary atelectasis with a firm, heavy and edematous consistency and reddish to gray coloration. (Photo courtesy of: Servie de Diagnostic de Patologia Veterinaria, Facultat de Veterinaria UAB, Bellaterra (Barcelona).

Microscopic Description:
Lung: Affecting all evaluated section there is a severe and diffuse thickening of alveolar septa as a result of moderate to intense hyperplasia of type II pneumocytes and mild septal inflammatory cells mostly lymphocytes, macrophages and neutrophils. In addition, the totality of alveolar, bronchial and bronchiolar lumens are markedly reduced (pulmonary atelectasis) with

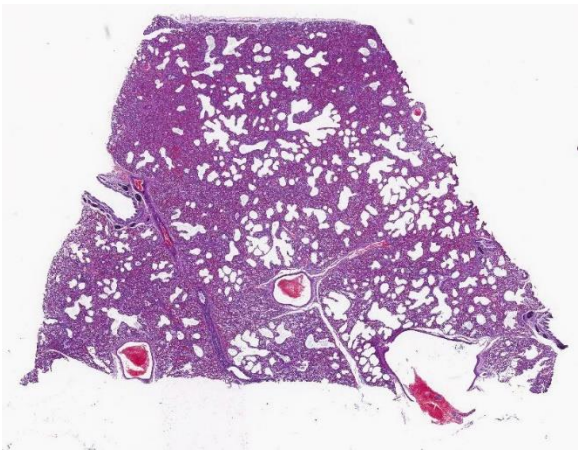

Lung, foal. A single section of lung is submitted. The lack of open alveoli suggests atelectasis. (HE, 4X)

multifocal aggregates of hypereosinophilic, homogeneous and amorphous material (fibrin) covering the alveolar walls or partially filling the alveolar lumens, and occasionally, bronchial lumens (hyaline membranes). Abundant foamy macrophages with occasional multinucleated cells, neutrophils, cellular and nuclear debris and mild edematous fluid are seen within alveolar lumens admixed with aforementioned hyaline membranes.

Contributor's Morphologic Diagnoses: Lung: Diffuse severe, subacute interstitial pneumonia with intra-alveolar and intra-bronchiolar hyaline membranes and diffuse severe pulmonary atelectasis.

Contributor's Comment: The histologic findings observed in this case such as the presence of hyaline membranes in alveolar and occasionally in bronchioles, as well as the severe and diffuse pulmonary atelectasis and the widespread presence of hyperplastic type II pneumocytes are compatible with the disease known as **Neonatal hyaline membrane disease** also known as Respiratory Distress Syndrome (RDS).

This syndrome is well recognized in premature or full-term foals but has not been further investigated in this species. Affected foals have respiratory distress from the time of birth, an expiratory grunt or "bark," hypoxemia, heart failure and/or convulsions and opisthotonos.[1] The lungs are diffusely atelectatic, plum-red, rubbery, and sink or become partially submerged in formalin.[1] Histologically, in addition to the thickened hypercellular alveolar septa expected in immature lung, hyaline membranes line collapsed alveoli and sometimes the small bronchioles. Alveoli are edematous, and cellular debris is occasionally noted.[1] Also the pathogenesis is not well established, is assumed that is occurs because of failure of the immature type II pneumocytes to secrete functional surfactant or surfactant dysfunction resulting in increased alveolar surface tension and alveolar and small bronchioles collapse at the end of expiration.[1] The tension and shear stress imparted on the lung during reinflation of these collapsed airspaces injures type I pneumocytes and club cells. [1]

This condition has been investigated primarily in humans, piglets and calves, but it also has been documented in premature puppies, lambs and primates. A familial form of neonatal respiratory distress is described in piglets with congenital fetal hypothyroidism and possibly hypoadrenocorticism, as thyroid hormone is necessary for maturation of type II pneumocytes. Affected piglets have diffuse alveolar damage with hyaline membranes and bronchiolar necrosis, as well as features suggesting hypothyroidism, including mildly prolonged gestation, fine hair coat, generalized edema, and thyroid follicular hyperplasia with lack of colloid. Other contributing factors in all species are fetal asphyxia, aspiration of meconium in amniotic fluid, reduction in pulmonary arteriolar blood flow, and inhibition of surfactant by fibrinogen, other serum constituents in edema fluid, or by

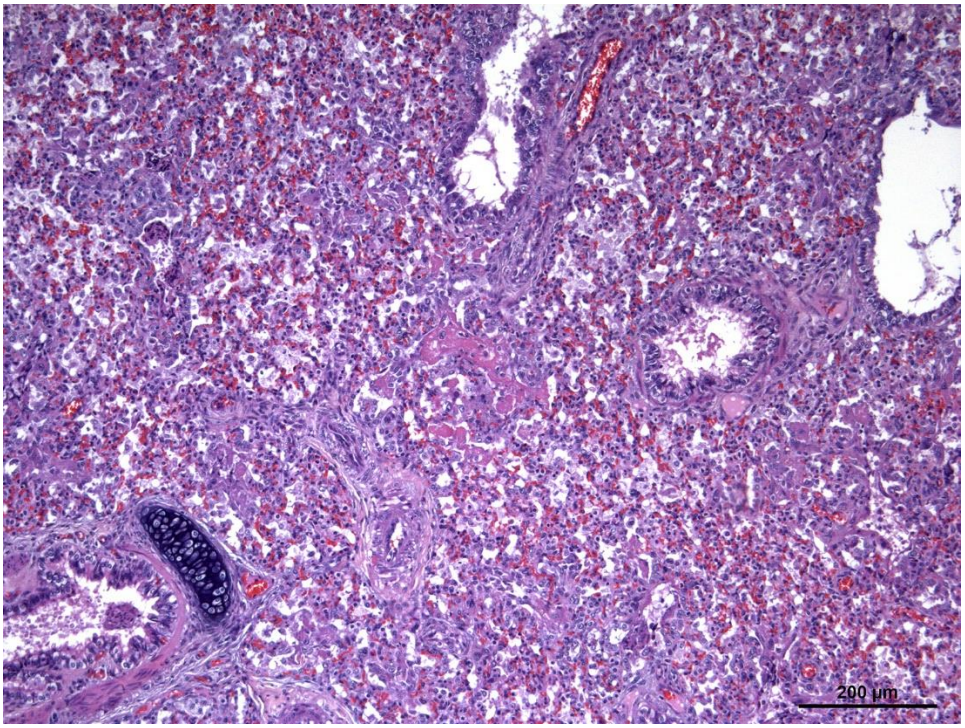

Lung, foal: There is diffuse and severe collapse of alveolar and bronchial lumina with multifocal aggregates of hypereosinophilic, fibrillar acellular material (fibrin) admixed with erythrocytes and inflammatory cells partially filling the alveoli extending along alveolar septa. (Photo courtesy of: Servie de Diagnostic de Patologia Veterinaria, Facultat de Veterinaria UAB, Bellaterra (Barcelona). (HE, 100X)

components in aspirated amniotic fluid. A similar condition is prevalent in cloned calves. In this case, the condition has also been associated with abnormalities of surfactant, but have not been adequately investigated in other species of domestic animals.

In humans, RDS is one of the main cause of respiratory distress in the newborn[9] and occurs soon after birth, and worsens during the first few hours of life.[9,11] Pulmonary edema plays a central role in the pathogenesis of RDS because of the excess lung fluid is attributed to epithelial injury in the airways, decreased concentration of sodium-absorbing channels in the lung epithelium, and a relative oliguria in the first 2 days after birth in premature infants. [9] Symptoms are similar than in domestic animals and include tachypnea, grunting, retractions and cyanosis.[7,10] The disease progresses rapidly,[5] with increased respiratory effort, intrapulmonary shunting, ventilation perfusion mismatch, and hypoxia with eventual respiratory failure.[9,11] The risk of RDS is inversely proportional to gestational age; RDS occurs in approximately 5% of near-term infants, 30% of infants less than 30 weeks gestational age, and 60% of premature infants less than 28 weeks gestational age.[9,11] Additional factors associated with development of RDS are male sex in Caucasians, infants born to mothers with diabetes, perinatal asphyxia, hypothermia, multiple gestations, cesarean delivery without labor, prematurity and presence of RDS in a previous sibling.[6,9,10,11]

The differential diagnosis of interstitial pneumonia in 1- to 4-month-old foals are bacterial or viral infections or treatment with erythromycin or other xenobiotics including 3-methylindole pyrrolizidine alkaloids and pentachlorophenol. *Rhodococcus equi*, or an aberrant response to that infection, is the main bacterial cause. Respiratory syncytial virus and equid herpesvirus 2 (EHV-2) are documented as the principal viruses for interstitial pneumonias. Other but less frequent causes are endotoxemia and *Pneumocystis carinii* infection. Because of the presence of severe and diffuse

hyperplasia of type II pneumocytes and the multinucleated cells in the lumen of alveolus, we performed immunohistochemistry to eliminate equine herpesvirus infection. No immunopositive cells were seen in any of the sections evaluated.

Contributing Institution:
Servei de diagnòstic de patologia veterinària, UAB (universitat Autònoma de Barcelona) Travessera dels Turons, Bellaterra, Barcelona, Spain

JPC Diagnosis: Lung: Pneumonia, interstitial, lymphohistiocytic, diffuse, marked, with type II pneumocyte hyperplasia, hyaline membrane formation and marked atelectasis.

JPC Comment: The contributor provides an excellent review of a disease in foals that replicates a very important and tragic disease in per-term human neonates.

Pulmonary surfactant is not only important for initial inflation of the lung, but for reinflation of the lung after end expiration as well. It is 80-90% by weight composed of lipid with approximately 70% of this in the form of dipalmitoylphosphtidylcholine.[5] Surfactant lipids are produced by Type II alveolar cells. This product, combined with surfactant proteins (SP) A-D, (produced by club cells) provide the reduction in surface tension required, but surfactant actually performs more functions in the lung.[5] Surfactant proteins are also known as collectins, and are part of the innate immune system.[5] Bacteria, viruses and some fungi have surface receptors for the lectin domains on the hydrophobic SPs A and D, allowing these proteins to participate in clearance activities for the pathogens. In addition, SP A and D also acts as immunomudulators, inhibiting allergen-induced lymphoproliferation, dendridic cell matureation, and eosinophil release of IL-8.[5]

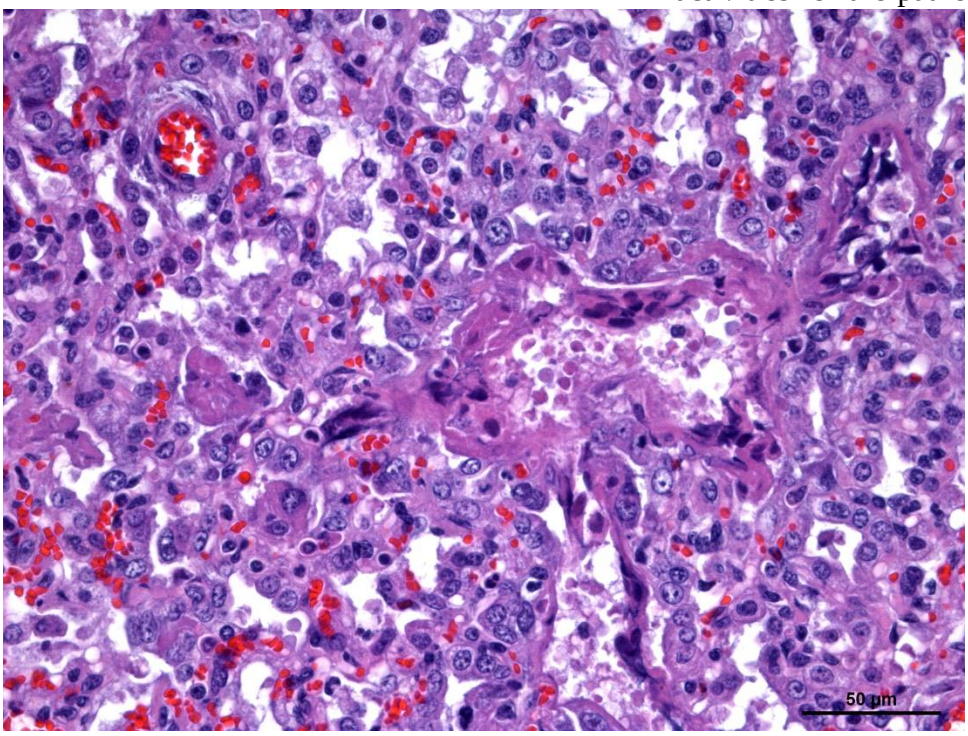

Lung, foal. There is diffuse type II pneumocytes hyperplasia as well as multifocal aggregates of fibrin covering the alveolar walls or partially filling the alveoli (hyaline membranes) admixed with foamy macrophages and occasional multinucleated cells. (Photo courtesy of: Servie de Diagnostic de Patologia Veterinaria, Facultat de Veterinaria UAB, Bellaterra (Barcelona). (HE, 400X).

In 1929, German scientist Kurt von Neergaard performed the first investigations on surface tension in atelectatic porcine lungs, noting the intense pressures required to inflate the lungs for the first time, similar to a baby's first breath.[3] Fifteen years later,

Dr. Peter Gruenwald, a New York pathologist, unaware of von Neergaard's experiments, repeated them on the lungs of stillborn infants, noting that the resistance to inflation appeared to be the result in increased surface tension. In the early 1950s, three independent researchers in different countries (one of whom, John Clements, worked at the US Army Chemical Center in Edgewood, Maryland) independently identified surfactant while studying the effects of nerve gas on the lungs.[3]

A research fellow, at the Harvard School of Medicine, Dr. Mary Avery, hearing of Clement's research, visited him to learn about this new "surface film" in the lung and devised a way to measure it in lung extracts from babies dying soon after birth. Her publication, "*Surface properties in relation to atelectasis and hyaline membrane disease*" in 1959, noted that it took 30 dynes of pressure to inflate the lungs of babies with hyaline membrane disease versus only 8 dynes in babies dying of other causes. One of the most high-profile infant deaths attributable to respiratory distress syndrome was Patrick Bouvier Kennedy, last child of John F. Kennedy and Jacqueline Kennedy, who died 39 hours after birth. [3]

1972 proved to be a banner year for treatment of neonatal hyaline membrane disease the discovery by Howie et al. that the administration of corticosteroids to mothers at risk for preterm birth reduced preterm rates of RDS by stimulating surfactant synthesis.[4] Finally, in the early 1980's , independent testing with modified bovine and porcine surfactants showed great promise, with five different formulations being put into clinical trials: 1) old synthetic or protein free, 2) natural minced lung extracts, 3) natural lung lavage extracts, 4) natural amniotic fluid extracts, and 5) synthetic protein analogues.[4] Today, prophylactic treatment with natural

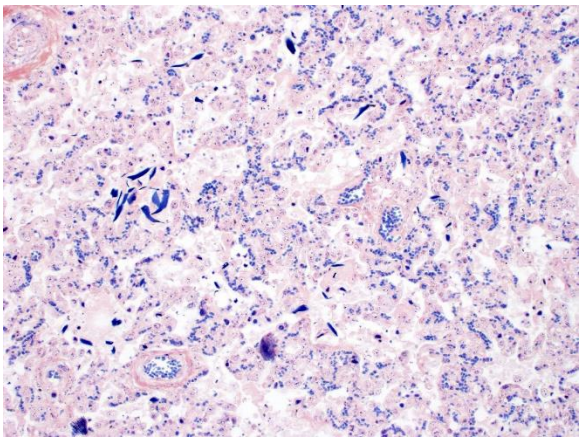

Lung, foal. A PTAH stain highlights the presence of squames within alveoli, which are often difficult to ascertain against a background of polymerized fibrin. (PTAH, 400X)

surfactants has been considered to decrease RDS by up to 50% and overall, neonatal mortality in the US by 6%.[4]

The moderator started off the conference with an admonition to residents to review pulmonary slides (of which today's conference has four) on a consistent basis, as well as reviewing the important segments of the lung that bear review on each slide. He then reviewed five basic categories of pneumonia – bronchopneumonia, interstitial, bronchointerstitial, embolic, and granulomatous, and defined his rare usage of the simple term "pneumonia" as a morphologic diagnosis (when the precise location of the inflammation cannot be localized to a particular segment).

This case generated spirited debate, and at the end of the discussion, we could not definitely identify equine respiratory disease as the cause of the histologic changes in this slide. While there was polymerized fibrin within alveoli, participants did not appreciate hyaline membrane formation. In addition, the distributed sections contained significant necrosis within terminal bronchioles, which was not described by the contributor. While these are non-specific findings, they are also

reminiscent of the well-known entity of interstitial and bronchointerstitial pneumonia seen in foals from 1 week to 9 months, for which a single definitive cause has not been established.[1] As mentioned by the contributor, possible causes for this syndrome includes viruses (RSV and EHV-2, aberrant responses to *Rhodococcus equi* or other common bacterial pathogens, surfactant dysfunction secondary to production of phospholipase A2 by alveolar macrophages, hyperthermia, or a variety of xenobiotics or toxins.

This slide was also reviewed by Dr. Kurt Williams, a subject matter expert in veterinary pulmonary pathology from Michigan State University. He agreed with our premise that the level of fibrin within the alveoli is not of the severity that one would expect with hyaline membrane disease and neonatal distress syndrome, but observed other changes in this particular slide that suggest a vascular reason for the notable changes. In this particular slide, there is significant increase in fibrous connective tissue of the pulmonary arterioles and "onion skinning" which suggests pulmonary hypertension. In addition, there is significant venous remodeling suggesting venous hypertension as well. Venous hypertension leads to an increase in pressure in pulmonary capillary pressure, which leads to the diffuse alveolar damage and fibrin exudation seen in this slide. In a young foal, this condition may result from significant cardiac disease, which was not described by the contributor. Intravascular pulmonary shunting might also result in concurrent arterial and venous hypertension. This was a very interesting case which answer lay beyond microscopic evaluation of the histologic specimen.

References:

1. Caswell JL, Williams KJ. Respiratory System. In: Maxie MG, ed. *Jubb, Kennedy, and Palmer’s Pathology of Domestic Animals*. Vol 2. 6th ed. St. Louis, MO: Elsevier; 2016: 515-516.
2. Dani C, Reali MF, Bertini G, Wiechmann L, Spagnolo A, Tangucci M, et al. Risk factors for the development of respiratory distress syndrome and transient tachypnoea in newborn infants. Eur Respir J 1999;14:155–9.
3. Halliday, HL. The fascinating story of surfactant. *J. Paediatrics Child Health* 2017; 53:327-332.
4. Halliday HL Surfactants: past present, and future. *J Perinatol* 2008: 28:s47-s56.
5. Han S, Mallampalli RK. The role of surfactant in lung disease and host defense against pulmonary infections. *Ann Am Thorac Soc* 2015; 12 (5): 765-774.
6. Hermansen CL, Mahajan A. Newborn respiratory distress. Am Fam Physician 2015;92(11):994–1002.
7. Leigh R. Sweet et al. Respiratory distress in the neonate: Case definition & guidelines for data collection, analysis, and presentation of maternal immunization safety data. Vaccine 35(48):6506-6517 · December 2017
8. McKenzie III HC. Disorder of foals. In: Reed SM, Bayly WM, Sellon DC ed. *Equine Internal Medicine*. 4th ed. St. Louis, MO: Elsevier; 2018: 1387-1391.
9. Pramanik AK, Rangaswamy N, Gates T. Neonatal respiratory distress: a practical approach to its diagnosis and management. Pediat Clin N Am 2015;62:453–69.

10. Reuter S, Moser C and Baack M. Respiratory distress in the newborn. Pediatr Rev. 2014 Oct; 35(10): 417–429.
11. Warren JB, Anderson JM. Newborn respiratory disorders. Pediatr Rev 2010;31 (12):487–95.

CASE II: 17-0282 (JPC 4117511).

Signalment: 11-year-old, female spayed, dachshund canine (*Canis familiaris)*

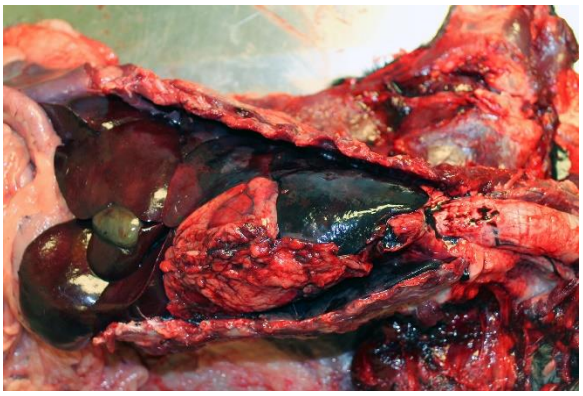

Lung, dog. The lungs are dark red and firm. (Photo courtesy of: Department of Pathobiology, University of Pennsylvania, School of Veterinary Medicine, Philadelphia, PA 19104 (http://www.vet.upenn.edu/diagnosticlabs)

History: After two weeks of boarding at the referring veterinarian, the dog became acutely lethargic, tachypneic, and had two episodes of vomiting. Evaluation at the veterinary clinic that day revealed pyrexia (temperature: 106.9 ^{o}F), mild coughing, and mucoid nasal discharge. Thoracic radiographs were unremarkable. The dog was administered a fluid bolus and then later received Lasix and supplemental oxygen. Although the temperature decreased to 101.8 ^{o}F, clinical signs of dyspnea and tachypnea progressed, and the dog developed epistaxis, hemorrhagic discharge from the mouth, as well as bloody diarrhea/melena. The

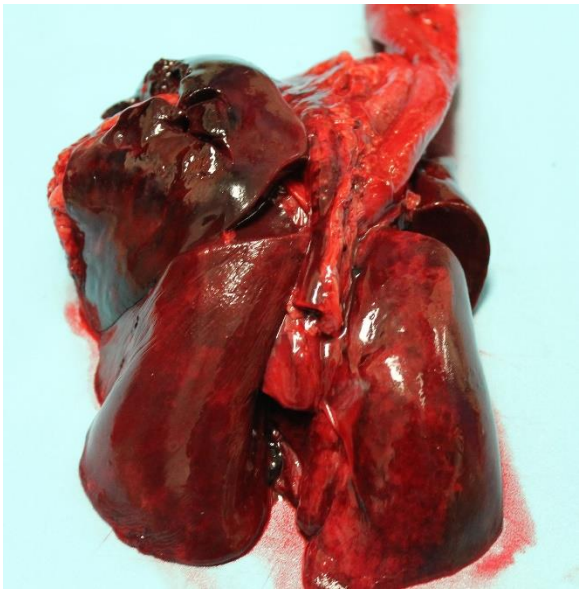

Lung, dog. The lungs fail to collapse and exuded copious amounts of a hemorrhagic fluid. (Photo courtesy of: Department of Pathobiology, University of Pennsylvania, School of Veterinary Medicine, Philadelphia, PA 19104 (www.vet.upenn.edu/diagnosticlabs)

temperature dropped to 95.4 ^{o}F the next morning and the dog died.

Gross Pathology: The pleural cavity contained approximately 125 mL of dark red slightly turbid fluid. The lungs were diffusely dark red, heavy, and firm with failure to collapse and generalized consolidation/"hepatization". Scattered throughout all lobes were pinpoint to 0.1 cm diameter hard white bony spicules. The pulmonary parenchyma exuded copious serosanguinous to hemorrhagic fluid on cut surface and sections from all lobes sank 10% formalin.

There was generalized venous congestion of the splanchnic vasculature. Few "paintbrush" hemorrhages were multifocally dispersed along the serosa of the descending colon. The mucosa of the stomach, duodenum, and orad jejunum were mottled tan-red and the luminal contents consisted of abundant partially digested blood and mucus.

Laboratory results: Aerobic culture of the lung postmortem yielded heavy growth of *Escherichia coli (E. coli*) and a second isolate of *Streptococcus* minor. Antimicrobial susceptibility testing results indicated that the E. coli isolate was sensitive to amikacin, cephalexin, enrofloxacin, imipenum, marbofloxacin, tetracycline, tobramycin, and trimethoprim/sulfamethoxazole.

Microscopic Description:
Lung: Multiple sections of lung are examined and similarly affected. Approximately 25-60% of the pulmonary parenchyma is disrupted by coagulative to lytic necrosis characterized by loss of tissue architecture with replacement by coalescing lakes of hemorrhage admixed with a dense inflammatory exudate. Airways are often occupied by high numbers of erythrocytes, toxic neutrophils, and foamy macrophages enmeshed in eosinophilic proteinaceous edema fluid and fibrillar fibrin. Scattered extracellular and intrahistiocytic short basophilic bacilli are occasionally observed within alveolar spaces, bronchioles, and bronchial lumina. The respiratory epithelium is often attenuated with cellular swelling, rounding, and loss of cilia (degeneration) or hypereosinophilia and pyknosis with luminal sloughing and exposure of a denuded basement membrane (necrosis). There is a paucity of bronchial associated lymphoid tissue. Pulmonary capillaries are occasionally distorted by luminal fibrin thrombi, and larger vasculature is multifocally variably obscured by deposition of hyalinized fibrin within the vessel wall (fibrinoid vascular necrosis). Other vessels are congested, lined by plump reactive endothelium, and surrounded by perivascular edema.

Alveolar septa multifocally contain low numbers of hematopoietic precursor cells (extramedullary hematopoiesis). Few small trabeculae of bone are randomly dispersed

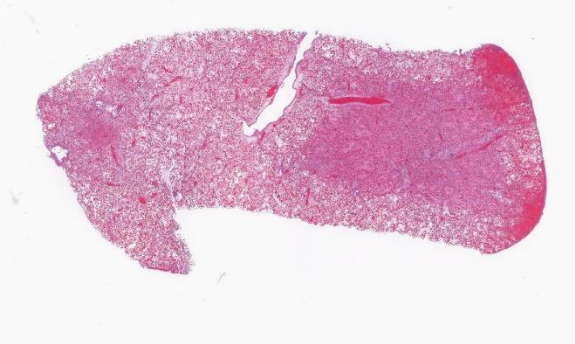

Lung, dog. A single section of lung is submitted for examination. At subgross magnification, diffuse severe congestion, edema, and subpleural hemorrhage is evident. (HE, 4X)

throughout the parenchyma. Rarely adjacent to larger airways are small clusters of histiocytes that contain finely granular black intracytoplasmic pigment. Histiocytes are intermingled with lymphocytes and fewer plasma cells.

Sections of the stomach, small intestine, and colon (slides not submitted) are diffusely hyperemic with marked transmural vascular congestion. Increased numbers of lymphocytes and plasma cells expand the gastrointestinal mucosa and there is occasional leukocyte exocytosis. Low numbers of neutrophils are intermingled within the superficial gastric mucosa.

Special staining of the lung reveals gram-negative bacilli within airways.

Clinical Signs– acute onset of dyspnea, tachypnea, pyrexia, and vomiting with rapid progression to epistaxis, hemoptysis, and melena

Contributor's Morphologic Diagnoses:
Lung:

1. Severe diffuse acute necrohemorrhagic and fibrinosuppurative pneumonia with numerous gram-negative bacilli

2. Multifocal heterotopic bone
3. Minimal multifocal pneumoconiosis

Stomach (not submitted):

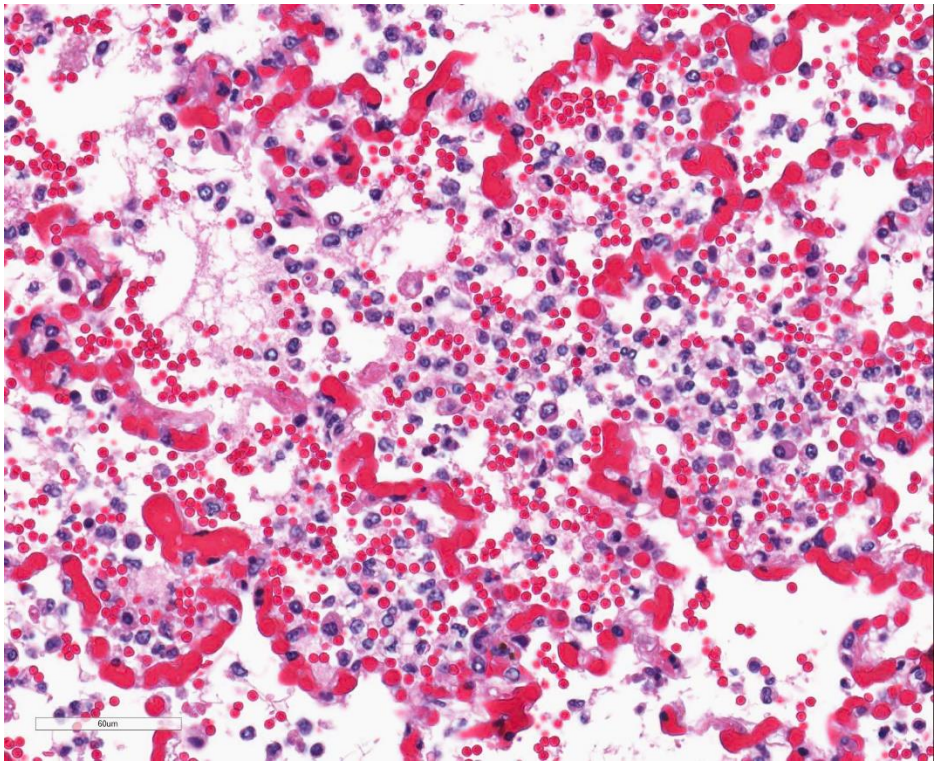

Lung, dog. There is extensive congestion and necrosis (discontinuity) of alveolar septa, with hemorrhage, fibrin polymerization, and numerous viable and degenerative neutrophils admixed with cellular debris. (HE, 389X)

1. Mild multifocal chronic neutrophilic and lymphoplasmacytic gastritis
2. Marked mural congestion

Small intestine, colon (not submitted):

1. Mild to moderate diffuse chronic lymphoplasmacytic enterocolitis
2. Marked mural congestion

Contributor's Comment: In dogs, bacterial pneumonia is most often attributed to opportunistic pathogens that occur as commensals of the normal microflora. Diagnosis therefore warrants an investigation for a predisposing cause that resulted in impairment of the pulmonary defense mechanism. Possible primary causes include viral infection (distemper, adenovirus-2, parainfluenza) or immunosuppression.[5,6,8,12] Aside from *Bordetella bronchiseptica*, which can be a primary pathogen, common opportunistic bacterial isolates include *Streptococcus* spp, *E coli*, *Pasteurella multocida*, and *Klebsiella pneumonia*e. Mixed bacterial infections are not infrequent. [5,6,8,12]

E. coli is often isolated in cases of aspiration pneumonia, and lesions are typically unilateral, necrotizing, and sometimes reveal the presence of foreign material within airways.[5] A predisposing factor to either aspiration pneumonia (i.e. dysphagia, regurgitation, megaesophagus) or bacterial pneumonia was not identified in this dog. Affected animals with either bacterial and/or aspiration pneumonia are susceptible to subsequent bacteremia, disseminated intravascular coagulation, and diffuse alveolar damage, which manifests clinically as acute respiratory distress syndrome (ARDS).[5]

Alternatively, mucosal barrier dysfunction in the gut can lead to bacterial translocation and hematogenous spread of the organism to the lungs.[5,7] Evaluation of the gastrointestinal tract in the present case revealed changes compatible with chronic inflammatory bowel

disease. No definitive foci of ulcers/erosions were identified, however the presence of neutrophils identified within the gastric mucosa could suggest mucosal barrier disruption.

Characterization and virulence typing of the *E. coli* isolate was unfortunately not pursued in this case. Previous reports of *E. coli*-associated hemorrhagic pneumonia in dogs have yielded isolates with an O serotype (specifically O4 and O6).[2,7,11] In a case series describing the disease in four dogs, Handt *et al*. identified the presence of the following virulence factors in all *E. coli* isolates: cytotoxic necrotizing factor 1 (CNF1), alpha hemolysin, and the adhesin factor papG allele III.[6] Both CNF1 and alpha hemolysin cause hemorrhage, necrosis, and edema [11,12] and are commonly produced by extraintestinal strains of pathogenic *E. coli*. [4,7,12] In another case report, the bacterial isolate was found to lack alpha hemolysin and instead possess fimbrial antigen K88.[2]

Extraintestinal pathogenic *E. coli* (ExPEC) harbor virulence factors not present in strains of commensal *E. coli*.[11] ExPEC are implicated in several human and animal disease conditions, including urinary tract infections, meningitis, septicemia, and pneumonia.[4,7,10] Review of the literature sometimes refers to these strains as necrotoxic or necrotoxogenic *E. coli*.[2,7] The pathogenesis of ExPEC involves bacterial adherence to the mucosal surface of the host epithelial cell, which is mediated by their adhesin encoded by papG. Colonization ensues, and there is initiation of the immune response via molecular triggers (i.e. TLR4) and subsequent production of proinflammatory cytokines.[11,12] While mechanisms of infection are uncertain, it has been hypothesized that animal affected by ExPEC may be immunocompromised secondary to stress, possibly induced by shipping or shelter overcrowding. These animals could be then be infected through inhalation following exposure to their own microflora or fecal contamination from a subclinical animal or human.[7,11]

It is worth noting that in both of these studies,[2,7] all dogs had a recent history of travel and were reportedly healthy prior to the development of peracute, fulminant, respiratory disease. Sudden death occurred in two dogs, while the remaining animals (including the current case) died within 24 hours following the onset of clinical signs. Clinical findings frequently included tachypnea, dyspnea, lethargy, and inappetance; when available, clinicopathologic abnormalities typically showed neutropenia with left shift. [2,7] A retrospective study specifically investigating hemoptysis determined that bacterial pneumonia was the most common underlying cause.[1] Consumption of expectorated blood from the respiratory tract was considered the most likely cause for melena in the present cause, however unidentified gastrointestinal ulcers cannot be ruled out.

Contributing Institution:
Department of Pathobiology
University of Pennsylvania, School of Veterinary Medicine
Philadelphia, PA 19104
www.vet.upenn.edu/diagnosticlabs

JPC Diagnosis: Lung: Pneumonia, interstitial, fibrinosuppurative, necrotizing, and hemorrhagic, diffuse, severe with multifocal necrotizing vasculitis

JPC Comment: The contributor has given an outstanding review of extraintestinal *E. coli* infection in the dog. A second pathogen was isolated from the lung in this animal, a minor population of non-speciated streptococci was also identified.

Within the last decade, several outbreaks of necrohemorrhagic pneumonia have been reported in confined dogs as a result of infection with *Streptococcus equi* var. *zooepidemicus*, a common commensal bacterium and opportunistic pathogen of horses.[3,9,10] One of these outbreaks affected over 1000 shelter dogs in less than one year.[9] Other smaller outbreaks affected animals within shelters and in one case, a university research colony.[10] Prior to this, it had been identified as a sporadic pathogen in dogs.[10]

In these outbreaks, infected dogs presented with respiratory signs of coughing, mucoid or hemorrhagic nasal discharge, and dyspnea, with some dying within 24-48 hours of clinical signs. At autopsy, pleural cavities often contained hemorrhage, and the predominant clinical signs were a necrotizing and fibrinous bronchopneumonia affecting all lobes and extending to the pleura. Numerous cocci are present within the cytoplasm of neutrophils, macrophages, or free within alveoli.[10]

While the pathogenesis of this disease is yet unknown, the potential for exotoxins of *S. equi* var. *zooepidemicus* has been postulated to cause an exuberant inflammatory response, such as may be seen in *S. equi* var. *equi* infection in horses and *S. pyogenes*, incriminated in toxic shock in humans. During the rapid clinical course of this condition, there is a marked elevation in a number of proinflammatory cytokines including IL-6, tumor necrosis factor, and interleukin-8 in the blood of infected animals. In these cases, *S. zooepidemicus* is routinely cultured from nasopharyngeal swabs or as a pure culture from affected lung tissue, and other common respiratory pathogens are seldom present. However, efforts to infect healthy dogs with cultures of *S. zooepidemicus* alone have not borne fruit, suggested as yet unexplained factors or co-pathogens in full-blown infection.

The moderator discussed the concept of diffuse alveolar phase, as well as the three phases of septal injury – exudative, proliferative (2-3 days later with type II pneumocyte hyperplasia) and repair (in which fibrosis may be seen in severe cases). Participants discussed the difficulty in this slide in differentiating hyaline membranes from necrotic alveolar walls or smooth muscle, as well as the remarkable amount of necrosis in the lung that apparently occurred within 24 hours in this animal.

References:

1. Bailiff NL, Norris CR. Clinical signs, clinicopathological findings, etiology, and outcome associated with hemoptysis in dogs: 36 cases (1990-1999). J Am Anim Hosp Assoc. 2002;38:125-133.
2. Breitschwerdt EB, DebRoy C, Mexas AM, et al. Isolation of necrotoxigenic *Escherichia coli* from a dog with hemorrhagic pneumonia. *J Am Vet Med Assoc*. 2005;226:2016-2019.
3. Byun JW, Yoon SS, Woo GH, Jung BY, Joo YS. An outbreak of fatal hemorrhagic pneumonia caused by *Streptococcus equi* subsp. *zooepidemicus* in shelter dogs. J Vet. Sci. 2009:10(3):269-271.
4. Caprioli A, Falbo, Ruggeri RM, et al. Cytotoxic necrotizing factor production by hemolytic strains of *Escherischia coli* causing extraintestinal infections. *J Clin Micro.* 1987:25:146-149.
5. Caswell JL, Williams KJ. Respiratory System. In: Maxie MG, ed. Jubb, Kennedy, and Palmer's Pathology of Domestic Animals. Vol. 2. 6th ed. St. Louis, MI: Elsevier; 2016: 564-569, 635-640.
6. Cohn, LA, Diseases of the Pulmonary Parenchyma. In: Ettinger SJ, Feldman

EC, Cote E. Textbook of Veterinary Internal Medicine. Vol. 2. 8th ed. Philadelphia, PA: WB Saunders Company; 2017:1113-1117.
7. Handt LK, Stoffregen DA, Prescott JS, et al. Clinical and microbiologic characterization of hemorrhagic pneumonia due to extraintestinal pathogenic *Escherichia coli* in four young dogs. *Comp Med*. 2003;53:663-670.
8. Lopez A, Martinson SA, Respiratory System, Mediastinum, and Pleurae. In: Zachary JM, ed. Pathologic Basis of Veterinary Disease. Vol. 6th ed. St. Louis, MI: Elsevier; 2017:546-547.
9. Pesavento PA, Hurley KF, Bannasch MJ, Artiushin S, Timoney JF. A Clonal Outbreak of Acute Fatal Hemorrhagic Pneumonia in Intensively Housed (Shelter) Dogs Caused by Streptococcus equi subsp. zooepidemicus. *Vet Pathol*. 2008:45:51-53.
10. Priestnall SL, Mitchell JA, Walker CA, Eries K, Brownlie J. New and emerging pathogens in canine infectous respiratory disease. *Vet Pathol2014:51(2)492-504.*
11. Sura R, Van Kruiningen HJ, DebRoy C, et al. Extraintestinal pathogenic *Escherichia coli*-induced acute necrotizing pneumonia in cats. *Zoonoses Public Health.* 2007;54:307-313.
12. Zachary JF, Mechanisms of Microbial Infections. In: Zachary JM, ed. Pathologic Basis of Veterinary Disease. Vol. 2. 6th ed. St. Louis, MI: Elsevier; 2017:151-153.

CASE III: P17-747 (JPC 4118594).

Signalment: 14 month old, female, Holstein-Friesian (*Bos Taurus*).

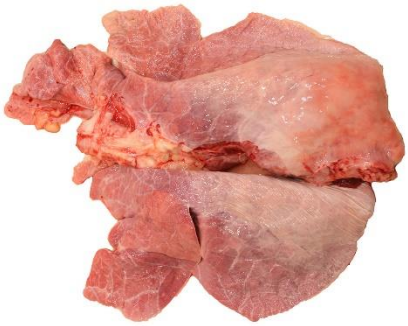

Lung, ox: There is marked fibrosis of the pleura overlying the caudal lobes, and a 25cm area of consolidation in the right pulmonary lobe. (Photo courtesy of: Friedrich-Loeffler-Institut, Department of Experimental Animal Facilities and Biorisk Management, Südufer 10, 17493 Greifswald-Insel Riems, https://www.fli.de/en/institutes/department-of-experimental-animal-facilities-and-biorisk-management-atb/)

History: This heifer was part of an experimental setting and inoculated by the intranasal and intratracheal route with 10^9 CFU of *Mycoplasma mycoides* subsp. *mycoides* (Mmm). The animal was humanely destroyed 4 weeks later and submitted for necropsy.

Gross Pathology: Lung: Multifocally, the pulmonary pleura was thickened and fibrotic with multiple adhesions to the thoracic wall. Only the right pulmonary caudal lobe was markedly enlarged and consolidated (25 cm in diameter). On cut section, there were variably sized bulging yellowish-grey to pale red and dry areas (necrosis) with marked interlobular fibrosis and distension of thrombosed lymph vessels. The left cranial lobe was diffusely atelectatic.

Laboratory results: PCR specific for Mmm in lung tissue - positive

Microscopic Description:
Lung: There are multifocal to coalescing areas of coagulative necrosis effacing 60% to 90% of the parenchyma (depending on location). Multifocally, there is mineralization in the central core of necrosis. Preexisting alveolar and bronchiolar lumina are replaced and expanded by an exudate composed of eosinophilic beaded fibrillar material (fibrin) admixed with large numbers of degenerate and few viable neutrophils, karyorrhectic debris and fewer alveolar macrophages, lymphocytes, and plasma cells. Adjacent and surrounding the necrotic foci the interlobular septa are markedly expanded up to 20 times by fibrovascular tissue (fibrosis) with numerous aggregated lymphocytes (lymphoid hyperplasia), scattered plasma cells and histiocytes (sequestration). Necrotic debris and homogenous eosinophilic material is present in various lymphatic vessels (thrombosis). Medium sized bronchi are surrounded by thick layers of connective tissue. In less consolidated areas alveoli coalesce and are expanded by clear space (emphysema) or partially contain eosinophilic fluid (edema).

Lung, ox: On cut section, areas of necrosis bulge from the surface, and the interlobular septa are markedly expanded. (Photo courtesy of: Friedrich-Loeffler-Institut, Department of Experimental Animal Facilities and Biorisk Management, Südufer 10, 17493 Greifswald-Insel Riems, https://www.fli.de/en/institutes/department-of-experimental-animal-facilities-and-biorisk-management-atb/)

Contributor's Morphologic Diagnoses:
Lung: Pleuropneumonia, fibrinonecrotizing, chronic, multifocal to coalescing, severe, with sequestrum formation, lymphoid hyperplasia, and interlobular fibrosis

Contributor's Comment: Contagious bovine pleuropneumonia (CBPP) is a notifiable highly contagious disease caused by *Mycoplasma mycoides* subsp. *mycoides* (Mmm). Mycoplasma are pleomorphic, non-motile and the smallest (0.3-0.8 µm) self-replicating bacteria which lack a true cell wall. There are over 200 Mycoplasma species, which are usually host-specific.[8]
Since small ruminants are not susceptible to the infection, Mmm is highly contagious for domestic cattle (*Bos taurus* and *Bos indicus*) of all ages. CBPP is also reported in bison, yak, and domestic buffalo.[1] Usually, CBPP has an incubation period of 3-6 weeks, but it can be longer up to 6 months. CBPP is mainly spread by inhalation of droplets from infected animals, but transmission can also occur via urine. Transplacental infection may occur as well. Currently the disease is endemic in Africa, especially in the Sahel Zone with neighboring countries where sporadic outbreaks are very common. Western Europe and Australia are considered free of CBPP.[1,8]

Cattle exhibit a pronounced age-dependent course of the disease, with calves up to 6 months showing arthritis mainly affecting the carpal and tarsal joints. In contrast, older animals primarily present with respiratory disease/distress caused by Mmm induced

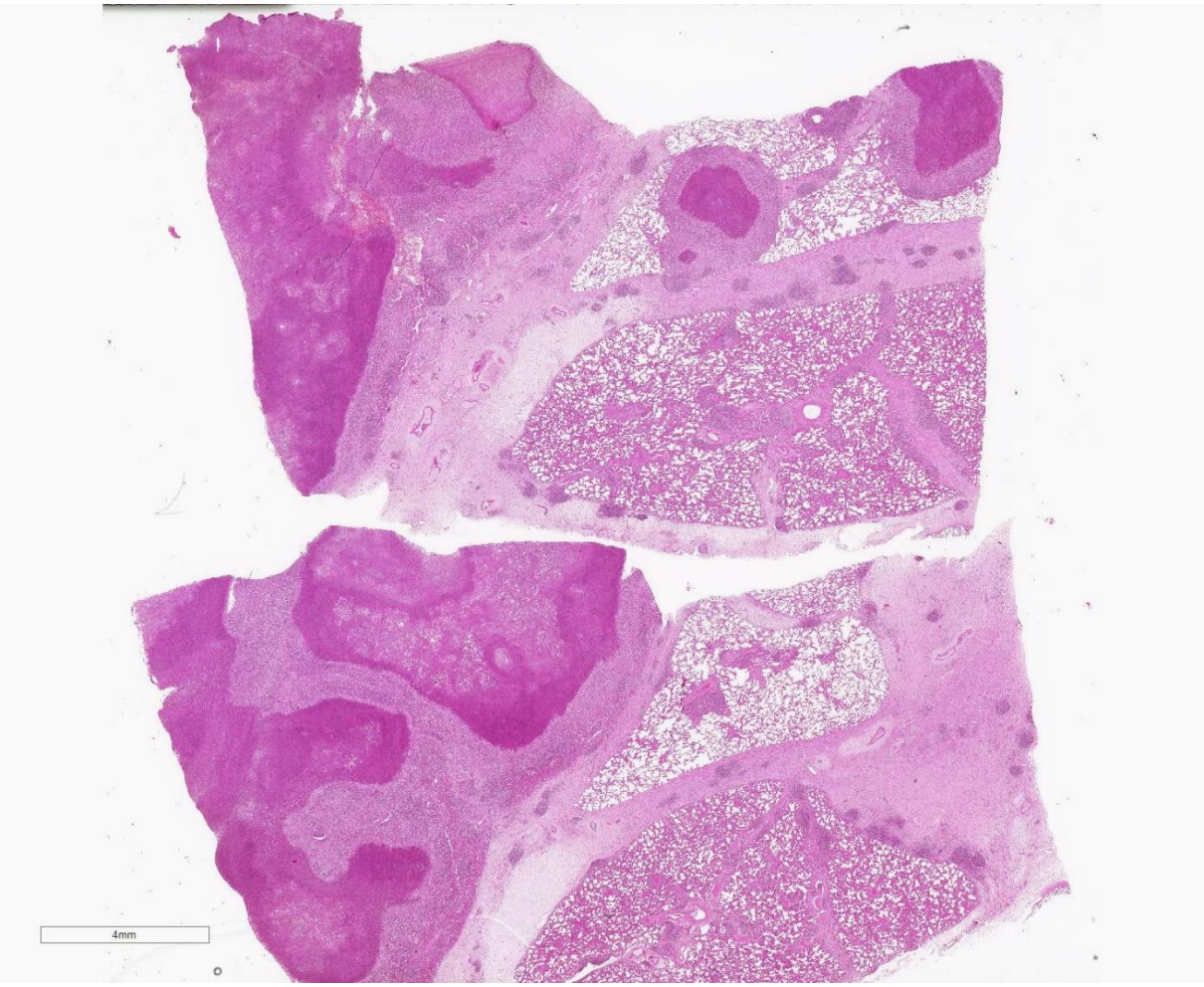

Lung, ox. At subgross magnification, lobules are separated by markedly edematous septa. Lobules exhibit large areas of necrosis, as well as variable degrees of atelectasis. (HE, 5X)

fibrinous pleuropneumonia. After infection of the respiratory tract, bacteremia develops secondarily. Whereas sudden death may occur in peracute cases, acutely ill animals commonly show fever, anorexia, and depression, followed by typical respiratory signs as dyspnea, mucoid nasal discharge, and coughing.[1,3] Commonly, affected animals show reduced milk production. Clinical signs may be absent in the chronic phase of the disease or affected animals show intermittent cough and fever, respectively, while shedding the organism intermittently.[1]

Specific gross lesions in CBPP depend on the course of disease. Severe congestion and hemorrhage are characteristic in the acute phase of fibrinous pleuropneumonia leading to red discoloration of lung tissue. The term 'pleuropneumonia' derives from early deposition of fibrinous exudate on the pleural surface resulting in accumulation of abundant yellow material in the pleural cavity. There is marked thickening and inflammation of the pleura leading to fibrinous pleurisy. On cut surface, dilatation and thrombosis of lymph vessels accompanied with interstitial edema lead to distension of interlobular septa giving the lung a marbled appearance. In chronic cases, areas of coagulative necrosis eventually develop into 'sequestra' by which

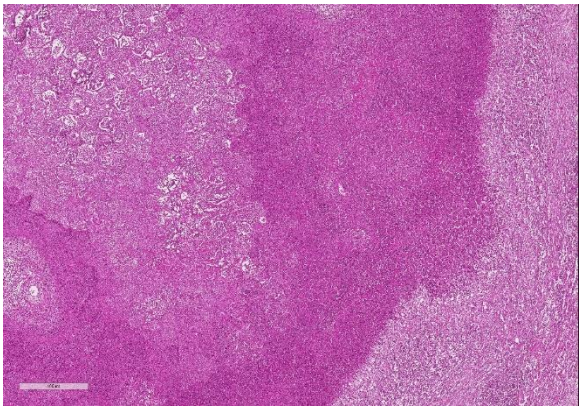

Lung ox. Large areas of central coagulative and more peripheral lytic necrosis are surrounded by a band of granulation tissue (right), forming a sequestrum. (HE, 100X)

necrotic lung parenchyma is encapsulated by connective tissue.[2]

Due to the fact that the animal in this case was part of a challenge model targeting the immune response, necropsy was performed only in the chronic phase of disease. Thus, histological lesions of the early stages of CBPP-=like hyperemia, interstitial edema and marked lymphangiectasia with lymphatic thrombosis and obstruction as well as diffuse fibrinous exudation were not present in the slides. Later on, neutrophils invade diffusely within the parenchyma and the fibrin deposits.[2,3,4] Since the branches of the bronchioles within the necrotic foci remain unchanged, the demarcation starts in an angiocentric way. From here and in broad layers with peripheral leukocyte accumulation and demarcation, a fresh granulation tissue extends towards the surrounding necrosis and yields the sequestrum.[4]

The pathogenicity of CBPP is not completely understood. Virulence factors of *Mycoplasma* species seem to be determined by intrinsic metabolic or catabolic pathway functions or by proper constituents of the mycoplasmal outer surface. It is unclear by which mechanisms Mmm can evade the killing by phagosome-lysosome fusion, which toxic molecules are produced that are responsible for cellular damage, and how vasculitis and thrombosis are induced. It is assumed that the bacterial membrane lipoprotein LppQ, is involved in the pathogenesis. The virulence of some Mmm strains seems to be related to the release of H_2O_2 which is cytotoxic.[5] Toxic galactan production, ciliary dysfunction, TNF-alpha dysregulation and immune-mediated vasculitis are also discussed to be involved in the pathogenic process of CBPP. Vasculitis and thrombosis of arteries,

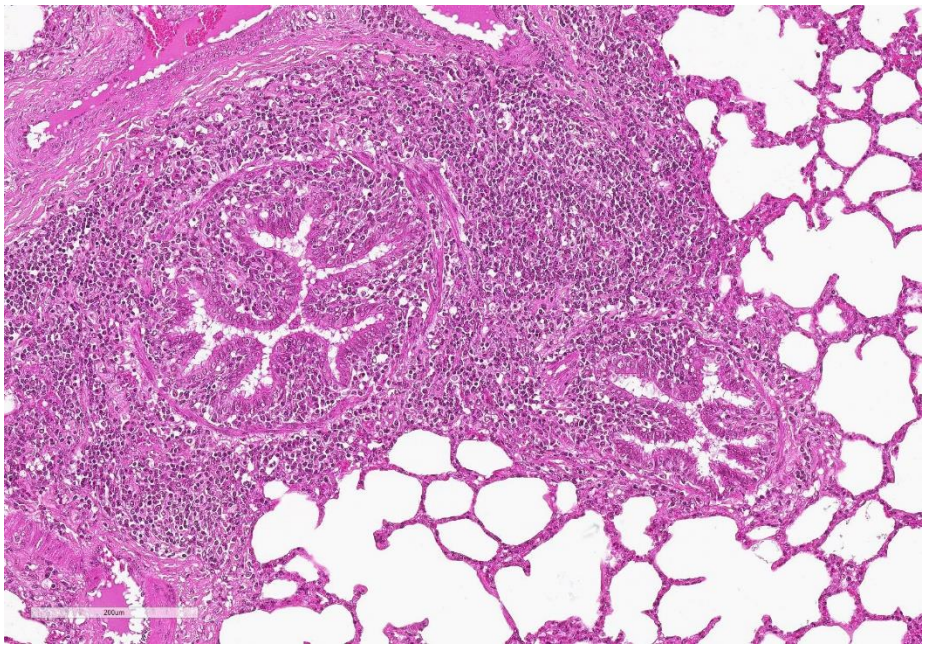

Lung, ox. In less affected lobules, bronchioles are surrounded by marked BALT hyperplasia and the submucosa and mucosa is infiltrated by numerous neutrophils and lymphocytes). (HE, 159X)

small caliber blood and lymphatic vessels are known to be crucial for the development of coagulative necrosis of lung tissue.[3] Little is known why CBPP is mainly restricted to the caudal pulmonary lobes and often occurs unilaterally.

Contributing Institution:
Friedrich-Loeffler-Institut
Department of Experimental Animal Facilities and Biorisk Management
Südufer 10
17493 Greifswald-Insel Riems
https://www.fli.de/en/institutes/department-of-experimental-animal-facilities-and-biorisk-management-atb/

JPC Diagnosis: Lung: Bronchopneumonia, fibrinosuppurative and necrotizing, multifocal, severe, with marked interlobular edema.

JPC Comment: The contributor has done an outstanding job in reviewing this pathogen, which, with the eradication of rinderpest, is considered to be the most important pathogen in affected countries.[7] It is the only bacterial disease currently on the OIE's "A" list of severe infectious animal disease,[7] Eradicated from much of the world, it has never been reported in South America and several Saharan and Middle Easter countries. It is considered eradicated in North America, much of Asia, Australia, and countries comprising the southern part of Africa. In the remaining part of sub-Saharan Africa, the disease is present and yet causes marked livestock losses. Current information on outbreaks of this disease may be found at the World Animal Health Information Service athttp://www.oie.int/wahis_2/public/wahid.php/Wahidhome/Home .

In the United States, the federal veterinary service, the US Bureau of Animal Industry, was founded in 1884, largely to eradicate the disease of contagious bovine pleuro-pneumonia. Its first director, Dr. Daniel

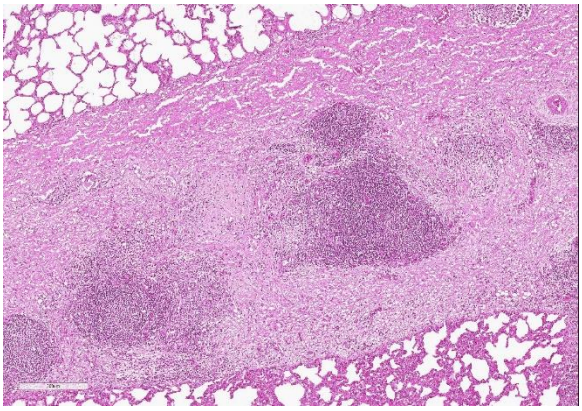

Lung, ox. Interlobular septa are markedly expanded by fibrous connective tissue, edema, and numerous lymphoid nodules (tertiary lymphoid centers) (HE, 69X)

Salmon had begun his years-long crusade to stamp out the disease in 1879, and was given the task of organizing the BAI in 1884, and established the Pathological Division in 1891. In addition to work on contagious bovine pleuropneumonia (which was eradicated from the United States in 1892, the BAI Pathological division did yeomans work in eradicating and developing vaccines for many other diseases, including foot-and – mouth disease, blackleg, tuberculosis, glanders, dourine, and Texas cattle fever (bovine babesiosis). Their groundbreaking research as a division of the USDA came to a halt in 1953 when their duties were transferred to the Agricultural Research Service, a newly created organization under the Eisenhower administration.[6]

MMM belongs to the so-called "*M. mycoides* cluster", containing MMM, *M. mycoides* susbsp *capri* (MMc), *M. capricolum* subsp *capricolum* (Mcc), *M. capricolum* susbsp. *capripneumoniae* (Mccp) and *M. leachii*, containing a number of closely related previous unclassified mycoplasmas. MMM's most closely related member of this cluster is *Mycoplasma mycoides* susbsp. *capri*, a bacterium which causes a syndrome called "MAKePS" in small ruminants, primarily goats, composed of mastitis,

arthritis, keratitis, pneumonia, and septicemia. It can also be identified in the ears of normal goats.[7]

The moderator reviewed several other severe fibrinosuppurative pleuropneumonias in cattle, and the subtle gross and histologic lesions that might help differentiate them, to include *Mannhemia hemolytic*a, *Histophilus somni*, *Pasturella multocida*, and *Mycoplasma bovis*, in addition to MMM.

References:

1. Caswell JL, Williams KJ. Respiratory system. In: Maxie MG ed. *Jubb, Kennedy and Palmer's Pathology of Domestic Animals*. Vol 2. 6th ed. Philadelphia, PA: Elsevier; 2016:551-554.
2. López A, Martinson SA. Respiratory System, Mediastinum, and Pleurae. In*:* Zachary JF, ed. *Pathologic Basis of Veterinary Disease*. 6th ed. St. Louis, MO: Mosby; 2017:519-520.
3. López A, Martinson SA. Respiratory System, Mediastinum, and Pleurae. In*:* Zachary JF, ed. *Pathologic Basis of Veterinary Disease*. 6th ed. St. Louis, MO: Mosby; 2017:532-533.
4. Nieberle K, Cohrs P, Lehrbuch der speziellen pathologischen Anatomie der Haustiere, Teil I, 5th ed. Jena: VEB Gustav Fischer Verlag; 1970: 270-274.
5. Pilo P, Frey J, Vilei EM. Molecular mechanisms of pathogenicity of *Mycoplasma mycoides subsp. mycoides SC*. *Vet J*. 2007;174(3):513-21.
6. Saunders, LZ. A history of the Pathological Division of the Bureau of Animal Industry, United States Departmen of Agriculture between 1891-1921. *Vet Pathol* 1989; 26:531-550.
7. Thiacourt F, Manso-Silvan L, Salah W, Barbe V, Vacherie B, Jacob D, Breton M, Dupuy V, Lomenech AM, Blanchard A, Sirand-Pugnet P. Mycoplasma mycoides, from "mycoides Small Colony" to "capri". A microevoluationary perspective. *BMC Genomics* 2011, 12:114-133.
8. Zachary JF. Mechanisms of microbial infections. In*:* Zachary JF, ed. *Pathologic Basis of Veterinary Disease*. 6th ed. St. Louis, MO: Mosby; 2017:170-171.
9. World Organization for Animal Health (2009). Contagious Bovine Pleuropneumonia. OIE, Paris. http://www.oie.int/fileadmin/Home/eng/Animal_Health_in_the_World/docs/pdf/Disease_cards/CONTAGIOUS_BOVINE_PLEUROPNEUMONIA.pdf

CASE IV: N198/18 (JPC 4120174).

Signalment: 3 year-old, female, Rasa Aragonesa sheep (*Ovis aries*)

History: The animal presented with signs of emaciation to the clinical service for ruminants (*Servicio Clínico de Ruminantes* – SCRUM) at the University of Zaragoza. Clinical examination of the animal showed respiratory dyspnea and increased respiratory sounds.

Gross Pathology: Prior to post-mortem examination, educational computed tomography (CT) scans were performed of the thorax and evinced a diffuse bronchointerstitial pattern and increased thickness of the bronchiolar walls. At necropsy, the sheep showed cachexia (1/5). The lungs were diffusely enlarged, grey, and had a rubbery-like firmness. Lung weight was also increased. Over the pulmonary

surface there were multifocal 1-2 mm grey dots. Mediastinal and tracheobronchial lymph nodes were enlarged.

Laboratory results: The blood count showed moderate normochromic, normocytic anemia.

Lung, sheep: At autopsy, the lungs were expanded, grey and firm with a rubbery texture. (Photo courtesy of: Universidad de Zaragoza. Departamento de Patología Animal, Web: (https://patologiaanimal.unizar.es/)

Quantitative PCR, considered positive when quantitation cycle (Cq value) was lower than 38, was performed in a lung sample. It was positive for *Visna-Maedi/Caprine Arthritis Encephalitis* virus (Cq value: 27,7) and for *Mycoplasma ovipneumoniae* (Cq value: 35,5) and negative for *Pasteurella multocida* and *Mannheimia haemolytica*.

Microscopic Description:
Lung: There is a diffuse inflammatory process that expands the alveolar septa of around the 100% of the section and there is multifocal prominent hyperplasia of bronchial/bronchiolar associated lymphoid tissue (BALT). Diffusely, alveolar septa are thickened up to 5 times by lymphocytes, histiocytes, plasma cells and rare neutrophils. BALT follicles show an enlarged diameter by increased numbers of centrocytes/centroblast (BALT hyperplasia). These follicles tend to coalesce and multifocally bulge towards the pleura. Multifocally, interstitial and bronchial/bronchiolar smooth muscle is enlarged and there is an increased number of myocytes/myofibroblasts (smooth muscle hypertrophy-hyperplasia).

Contributor's Morphologic Diagnoses: Lung: Pneumonia, interstitial, diffuse, severe, chronic with prominent BALT hyperplasia and smooth muscle hypertrophy-hyperplasia.

Condition: Maedi. Ovine Progressive pneumonia
Cause: Small ruminant lentivirus (Visna/maedi virus)

Contributor's Comment: This is the respiratory form of small ruminant lentiviruses. This respiratory disease is caused by a group of non-oncogenic exogenous retroviruses of the genus lentivirus that target immune cells, mainly macrophages.

The Small Ruminant Lentiviruses are a group of highly related single stranded RNA viruses with high mutational potential that affect mainly sheep but also goats.[1] These viruses induce chronic inflammation that usually remains subclinical. When it becomes clinical, the disease can express mainly in

Lung, sheep: Numerous grey dots over the surface of the lung correspond to lymphoid nodules within the pulmonary parenchyma. (Photo courtesy of: Universidad de Zaragoza. Departamento de Patología Animal, Web: (https://patologiaanimal.unizar.es/)

four different locations: lung, joints (mainly carpus), central nervous system and mammary gland.[3] The expression of each form as well as the gravity of the lesion depends on host immune response and the viral factors.[2,5]

The respiratory form, termed maedi or ovine progressive pneumonia, is the most common presentation of the disease in sheep.[1] The process consists of an afebrile chronic progressive pneumonia that leads to weight loss and marked dyspnea. Grossly, the lungs show a rubbery firm appearance and do not collapse when the thoracic cavity is opened. Microscopically, is characterized by an inflammatory interstitial pattern and formation of lymphoid nodules with germinal centers around bronchioles and vessels. Mild interstitial fibrosis and smooth muscle hypertrophy are usually present. Unlike goats, type II pneumocytes hyperplasia is rarely seen in sheep.
Neurologic form is characterized by leuokencephalomyelitis and demyelination that leads to ataxia and profound weight loss.[6] This form progresses faster than the respiratory one and usually occurs in adult sheep and goat kids (2-4 months). Articular form curse with arthritis affecting mainly the carpal joints.[4] The mammary form implies interstitial mastitis and is associated with agalactia.

The main route of transmission is aerosol, particularly under intensive housing. Colostrum transmission plays also an important role.[3] The virus infects a variety of cell types (mammary epithelium, fibroblast, endothelial cells, monocytes, choroid plexus) but its replication just occur in mature macrophages.[1] Lentiviral-infected macrophages produce cytokines that recruit and activate other leukocytes but also hence lentiviral replication. Indeed, clinical signs and histopathological lesions are the result of

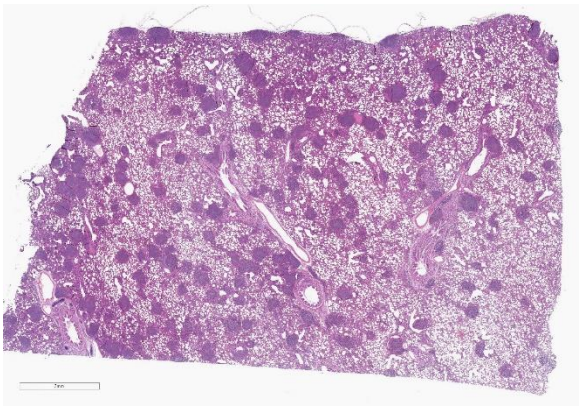

Lung, sheep: At subgross magnification, numerous lymphoid nodules are dispersed throughout the section. (HE, 8X)

the inflammatory process instead of the direct viral damage to the organ. There is neither treatment nor commercial vaccines for the disease, which is what makes immunization of the ovine population against the virus challenging.[8]

The main differential diagnosis of maedi is the classical form of ovine pulmonary adenocarcinoma (OPA). This disease is also presented as chronic progressive respiratory problems. However, there is abundant fluid production that leads to nasal exudate and the gross appearance of the lung shows consolidation of the apical lobes and ventral areas of the organ. The contribution of *Mycoplasma ovipneumoniae* should be taken into consideration in our case either as possible enhancer of the lentiviral infection or as secondary opportunistic pathogen.
Contributing Institution: Universidad de Zaragoza. Departamento de PatologíaAnimal
Web: https://patologiaanimal.unizar.es/

JPC Diagnosis: Lung: Pneumonia, interstitial, lymphohistiocytic, diffuse, moderate with peribronchiolar and perivascular lymphoid hyperplasia, and smooth muscle hyperplasia.

JPC Comment: The contributor provides a concise review of one of the most important respiratory diseases of small ruminants. The disease was first reported in South Africa in the eastern town of Graff-Rinet (hence the name "Graff-Rinet disease"). In 1923, it was identified in the United States by Dr. H.W. W Marsh (with various appellations such as "ovine progressive pneumonia" (OPP), "Montana progressive pneumonia", and "Marsh's progressive pneumonia"), and an errant combined paper by Dr. Marsh and Dr. E.V. Cowdry, determined that morphologically, the diseases of jaagsiekte (or ovine pulmonary carcinoma, OPA) and "Montana progressive pneumonia" were one and the same.[2]

The introduction of 20 infected Karakul sheep into Iceland in the early 1930's from Uzbehkistan introduced both OPA and ovine progressive pneumonia (OPP) to Iceland. [10] In 1935, cases of both were identified in Iceland, and cases of OPP (named "maedi" for "shortness of breath" in Icelandic) were identified in farms across the country and were traced back to the imported sheep. Maedi was not fully recognized as a disease different from OPA (jaagsiekte) until 1939 by Dr. G. Gislason, who further epidemiologically delineated the disease as a chronic progressive disease with a 2-3 year incubation period. He discovered that close housing of sheep spread the agent, and faced with a 20-30% mortality annually of older sheep, the Icelandic government slaughtered and replaced all sheep in affected areas and within 10 years, became the first country to eradicate OPP.[10] The disease still remains in all major sheep producing countries of the world, except for Australia and New Zealand, where it has never been seen.

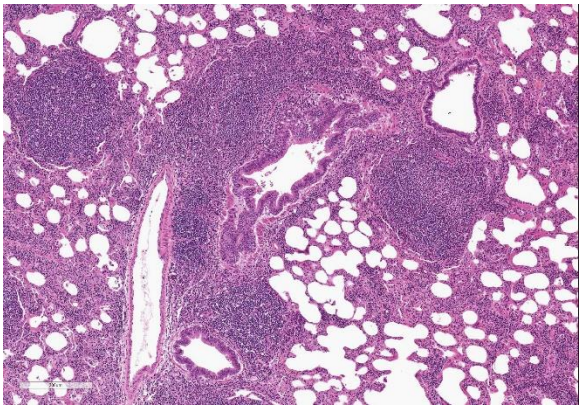

Lung, sheep: Lymphoid nodules are primarily adjacent to airways, but also extend along pulmonary vessels. Alveolar septa are markedly expanded and often atelectatic. (HE, 73X)

Research in Iceland continued on maedi and a related virus, visna with numerous transmission tests, and the viruses were finally isolated in 1957 (visna) and 1958 (maedi). Following the discovery of reverse transcriptase in these viruses, they became the prototype for the non-oncogenic retroviruses the lentiviruses (lenti="slow"), of which additional viruses, were have isolated, including the disease agents of equine infectious anemia (EIAV – 1976) and caprine arthritis-encephalitis (CAEV-1980.) After experimental cross infection of sheep by CAEV and goats by MVV, the three viruses were grouped together under the name small ruminant lentiviruses (SRLV).[10] The grouping is further reinforced by the ability of SRLVs to cause disease syndromes in sheep that have been previously identified in only in goats, such as viral arthritis.[5]

One of the other peculiarities of the SRLVs, like other lentiviruses, is its predilection for mutation, which may not only help it cross between small ruminant species, but also generate new quasi species, further confounding vaccinologists. Reproduction via reverse transcriptase is not a precise science, as insertional and deletion mutations occur with some frequency. While core genes of *gag* and *pol* are largely conserved, mutations are occasionally found in certain parts of *env* which result in variability,

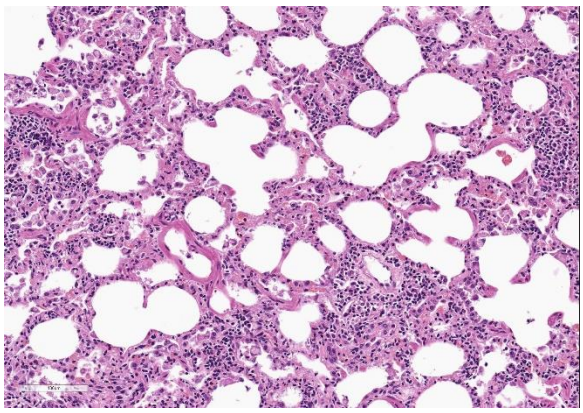

Lung, sheep: Alveolar septa are expanded by a combination of lymphocytes (often in aggregates), and macrophages, as well as patchy type II pneumocyte hyperplasia. There is moderate scattered interstitial smooth muscle hyperplasia. (HE, 202X)

particularly in antibody-binding regions. [1]

As mentioned above, small ruminant lentiviruses may infected a range of cells, but like other lentivirus, they show a particular tropism for cells of macrophage/monocyte lineages to include dendritic cells, mammary gland epithelium (helpful for transmission in colostrum to neonates) and the endothelia and microglia of the CNS (which may help in causation of visna in young lambs and kids.) The maedi-visna virus (MVV) is also unique among lentiviruses as it is the only one in which respiratory transmission is significant (although whether free viruses or exhaled infected cells is the culprit remains to be seen.)[1]

This entity has made a number of appearances in the WSC over the years (see WSC 1995-96, Conference 21, Case 3; WSC 2005-2006, Conference 23, Case 1; WSC 2009, Conference 10, Case 1).

In the conference, the participants reviewed and compared the different manifestation of small ruminant lentiviruses. One of the points of discussion was the difference in pneumonia seen in the goat versus the lamb; the pneumonia in goats is characterized by less prominent lymphoid follicles formation and marked type II pneumocyte hyperplasia and filling of alveoli with surfactant.

References:

1. Blacklaws BA. Small ruminant lentiviruses: Immunopathogenesis of visna-maedi and caprine arthritis and encephalitis virus. *Comp Immunol Microbiol Infect Dis*. 2012;35(3):259–269.
2. Cowdry EV and Marsh HW. Comparative pathology of South African Jagziekte and Montana progressive pneumonia of sheep. *J Exper Med*,1927:571-585.
3. Gayo E, Polledo L, Balseiro A, et al. Inflammatory Lesion Patterns in Target Organs of Visna/Maedi in Sheep and their Significance in the Pathogenesis and Diagnosis of the Infection. *J Comp Pathol*. 2018;159:49–56.
4. Minguijón E, Reina R, Pérez M, et al. Small ruminant lentivirus infections and diseases. *Vet Microbiol*. 2015;181(1–2):75–89.
5. Pérez M, Biescas E, Reina R, et al. Small Ruminant Lentivirus–Induced Arthritis. *Vet Pathol*. 2015;52(1):132–139.
6. Pinczowski P, Sanjosé L, Gimeno M, et al. Small Ruminant Lentiviruses in Sheep. *Vet Pathol*. 2017;54:413–424.
7. Polledo L, González J, Benavides J, et al. Patterns of Lesion and Local Host Cellular Immune Response in Natural Cases of Ovine Maedi-Visna. *J Comp Pathol*. 2012;147(1):1–10.
8. Pritchard GC, McConnel I. Maedi-Visna. In: Aitken ID, editor. Diseases of sheep. Fourth Edition. Oxford (UK): *Blackwell Publishing*; 2007. 217–223.

9. Reina R, de Andrés D, Amorena B. Immunization against small ruminant lentiviruses. Viruses. 2013;5:1948–1963.
10. Thormar H. The origin of lentivirus research: maedi-visna virus. *Curr HIV Res* 2013; 11:2-9.

Self-Assessment - WSC 2019-2020 Conference 1

1. Which of the following cell types is defective in equine respiratory distress syndrome?
    a. Type 1 pneumocytes
    b. Type II pneumocytes
    c. Alveolar macrophages
    d. Club cells

2. Which of the following is NOT a virulence factor in necrotoxic *E. coli*?
    a. VapA
    b. PapG
    c. Alpha hemolysin
    d. Cytotoxic necrotizing factor 1

3. Which of the following is not susceptible to infection by *Mycoplasma mycoides* subsp. *mycoides?*
    a. Yak
    b. Sheep
    c. Bison
    d. Buffalo

4. Calves infected with *Mycoplasma mycoides* subsp. *mycoides* are most likely to display which of these ?
    a. Encephalitis
    b. Otitis media
    c. Arthritis
    d. Hepatic granulomas

5. Which is not a common site of disease in sheep infected by lentivirus ?
    a. Brain
    b. Liver
    c. Joints
    d. Mammary gland

Please email your completed assessment for grading to Dr. Bruce Williams at bruce.h.williams12.civ@mail.mil. Passing score is 80%. This program (RACE program 33611) is approved by the AAVSB RACE to offer a total of 0.5 CE Credits, with a maximum of 12.5 CE Credits being available to any individual Veterinary Medical Professionals for the 2019-2020 Wednesday Slide Conference. This RACE approval is for the subject matter categories of: SCIENTIFIC using the delivery method of NON-INTERACTIVE DISTANCE. This approval is valid in jurisdictions which recognize AAVSB RACE.

Joint Pathology Center
Veterinary Pathology Services

WEDNESDAY SLIDE CONFERENCE 2019-2020

C o n f e r e n c e 2

CASE I: Case #2 (JPC 4117378).

Signalment: 9-year-old, male, African lion (*Panthera leo*).

History: Caesar was born in June 2007. He and his sister, Cleopatra, were purchased from a breeder in Louisiana by a man who lives in Austin and had a large ranch in the northern Hill Country. The owner contacted the Austin Zoo and Animal Sanctuary in spring 2009 wanting to surrender the pair as he could not get a permit from the county to keep them. Caesar and Cleopatra arrived at the Austin Zoo and Animal Sanctuary in May 2009. Cleopatra got sick in spring 2011 and was humanely euthanized in July 2011 after she was diagnosed with canine distemper virus (CDV) and developed seizure activity. Caesar had never shown any symptoms at this time. All of the large felids were vaccinated for CDV shortly after Cleopatra died. Caesar had a diminished appetite in December 2013 and started exhibiting unusual behavior (e.g. jumping around the walls of his den). His appetite returned in January 2014, but he became ataxic in March 2014. The ataxia became progressively worse until he was no longer able to get his feet under him to walk up the steps into his den. He was admitted to the Texas A&M CVM for examination. He had a high positive titer for toxoplasmosis and a low positive titer for CDV which was thought to be a result of his vaccination. He was alert with an excellent appetite while being treated for toxoplasmosis. After some instances of apparent improvement, he ultimately started star gazing, stopped eating and became nonresponsive, at which time he was humanely euthanized.

Cerebrum, lion. A slightly compressed section of cerebrum was submitted. No obvious lesions are present at subgross magnification. (HE, 5X)

Gross Pathology: Patient is emaciated (BCS 2/9). There are multiple, red, inflamed areas on skin from trauma and pressure sores.

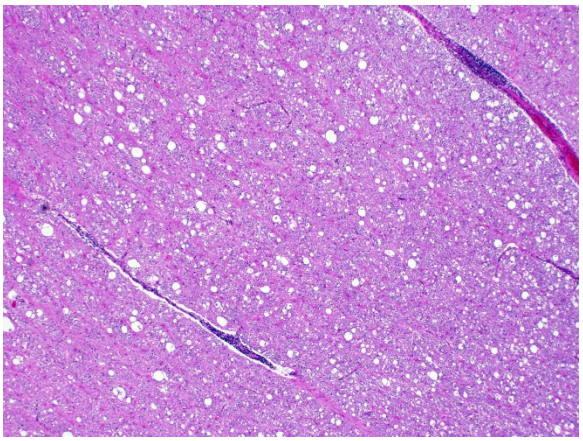

Cerebrum, lion. There is extensive vacuolation of the cortical white matter. In addition, Virchow-Robins space is multifocal expanded by low to moderate numbers of lymphocytes. (HE, 100X)

There is an abscess in the ventral neck associated with the right mandibular lymph node. The brain appears slightly shrunken. No other significant gross lesions are observed.

Laboratory results: Brain, positive for CDV by IHC.

Microscopic Description:
Cerebrum: Approximately 40% of myelin sheaths are lost with replacement by gitter cells (demyelination), or are markedly dilated (spongiosis) and occasionally contain swollen axons with bright eosinophilic axoplasm (spheroids) or gitter cells and cellular debris (Wallerian degeneration). Neurons and astrocytes often contain intranuclear viral inclusion bodies that marginate the chromatin and, rarely, 3-5 um eosinophilic intracytoplasmic viral inclusion bodies. Multifocally, there is vacuolation of the gray matter. Multifocally, there are small foci of glial nodules and numerous astrocytes with abundant eosinophilic cytoplasm and eccentric nuclei (gemistocytes). Occasionally, neuronal cell bodies are swollen and round with central chromatolysis (degeneration) or rarely, shrunken with bright eosinophilic cytoplasm with pyknotic nuclei (necrosis). Numerous neurons contain yellow to light green, granular material (lipofuscin). Multifocally, there is expansion of the Virchow Robin space around the blood vessels in the affected gray and white matter and leptomeninges by lymphocytes and plasma cells and lined by reactive endothelium.

Contributor's Morphologic Diagnoses: Cerebrum: Demyelination, multifocal, marked with spongiosis, spheroids, lymphoplasmacytic perivascular meningoencephalitis and eosinophilic intranuclear and intracytoplasmic viral inclusion bodies, African lion (*Panthera leo*), felid.

Contributor's Comment: Canine distemper virus (CDV) is an important, ubiquitous infectious disease of domesticated dogs[2], wild canids in the family Canidae[2] (e.g., dingo, fox, coyote, jackal, wolf), wild cats in Felidae (e.g., African lion[11], Bengal tiger[3], Amur tiger[18], leopard), Mustelidae[13] (e.g., weasel, ferret, mink, skunk, badger, marten, otter), Procyonidae[10] (e.g., raccoon, coati), Phocidae (e.g., Lake Baikal seal[5]), Rodentia (e.g., Asian marmot[18]) and nonhuman primate (e.g., rhesus macaque[16]) within the

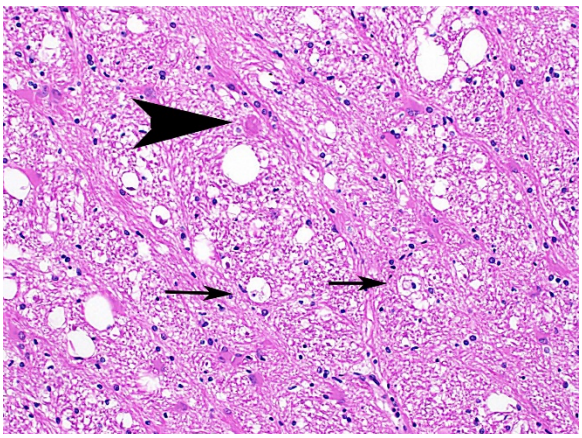

Cerebrum, lion. The vacuolation of the white matter is the result of numerous dilated myelin sheaths, some of which contain myelin debris and Gitter cells (arrows). Occasional spheroids are present (arrowhead). (HE, 400X)

genus *Morbillivirus* in the family *Paramyxoviridae*. Other morbilliviruses include rinderpest, peste des petits ruminants virus, cetacean morbillivirus, phocine distemper virus and the measles virus.

CDV causes systemic disease often with respiratory, gastrointestinal and central nervous system (CNS) involvement. There are four distinct forms of CNS disease: 1) classic CDV encephalitis; 2) multifocal distemper encephalomyelitis in mature dogs; 3) "old dog" encephalitis (ODE)[14]; and 4) post-vaccinal canine distemper encephalitis. In large felids, fatal neurologic disease is due to a distinct CDV variant. Specifically, in African lions, it is thought they contract the virus from feral dogs or hyenas[2]. CNS disease is most common, followed by gastrointestinal and respiratory disease; lesions of the hard pads are rare[10]. Generalized seizure activity, the most common neurologic abnormality, usually culminates in acute death[10].

CDV is a pantropic, negative-sense, single-stranded, enveloped RNA virus 150-300 nm in diameter. There is one recognized serotype with variable strain pathogenicity and tissue tropism. Virulence factors include hemagglutinin glycoproteins on the viral envelope, which mediate attachment to host cells and fusion glycoproteins which allow penetration of host cells and fusion of infected cells with uninfected cells[22]. Receptors include signaling lymphocyte activation molecule or SLAM (CD150)[21], which is leukocyte-restricted and mediates entry into cells and CD46 which is widespread.

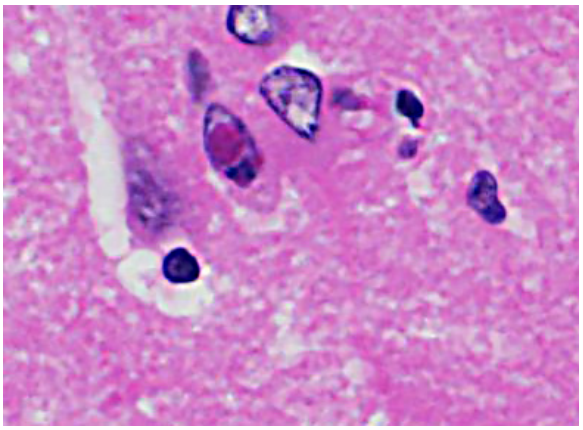

Cerebrum, lion. An astrocyte contains a large intranuclear viral inclusion. (HE, 400X)

Infection is via inhalation and the virus infects macrophages in the upper respiratory tract or lungs and replicates in the tonsils and lymph nodes in the first 24 hours. There is cell-associated viremia by two days postinfection with spread to all lymphoid tissues and blood lymphocytes by two to five days postinfection, followed by lymphocytolysis, leukopenia and immunosuppression. Animals with adequate humeral/cellular immunity neutralize the virus by 14 days postinfection and may not shed virus. Animals with delayed intermediate humeral/cellular immunity, have a viral infection/persistence in the mucosal epithelium and brain and may develop neurologic disease and disease associated with epithelial infection. Animals that fail to develop neutralizing antibody by eight or nine days postinfection have virus that disseminates to the respiratory, gastrointestinal, urogenital and central nervous systems. The integumentary, exocrine and endocrine systems may also be affected. CDV is shed in all excretions during the systemic phase of infection which makes secondary infections with Adenovirus, *Bordetella* sp., *Clostridium piliforme*, *Cryptosporidium* sp., *Escherichia coli*, *Encephalitozoon* sp., *Pneumocystis* sp., *Sarcocystis* sp., and *Toxoplasma* sp. common.

CNS lesions develop one to three weeks after systemic signs or may occur after a subclinical infection. The virus is spread

hematogenously to the brain and choroid plexus via macrophages shed into the cerebrospinal fluid and disseminates virus within the ventricles. The virus spreads to ependymal cells and spreads locally to infect astrocytes and microglia which leads to the characteristic white matter vacuolation (intramyelinic edema) thought to result from a direct effect of the virus on oligodendrocytes. ODE may be caused by infection with replication of a defective virus[12]. Post-vaccinal CDV occurs due to vaccination with a modified live vaccine and is often fatal in exotic carnivores (e.g., ferret, mink, lesser panda, grey fox). CDV rarely causes fatal encephalitis in young dogs, possibly due to immune stimulation by other canine viruses (e.g., canine parvovirus) at the time of vaccination. Vaccination of pregnant dogs can cause abortion or disease in puppies.

Disease with classic canine distemper is most common in 12-16 week old puppies. Early clinical signs include fever, conjunctivitis, coughing, vomiting, diarrhea, depression, anorexia and serous to mucopurulent oculonasal discharge. Clinical pathology reveals lymphopenia, thrombocytopenia, regenerative anemia, hypoalbuminemia, hypergamma- and alpha-globulinemia. After one to four weeks, clinical signs include neurologic disease (e.g., seizures, cerebellar or vestibular ataxia, paraparesis, myoclonus) with minimal or no signs of epithelial infection. Hyperkeratosis of the footpads and nose and enamel hypoplasia are late manifestations. Of note, 50-70% of infections are subclinical.

Multifocal distemper encephalomyelitis in mature dogs occurs when CDV infects dogs at four to eight years of age and is a rare, chronic, progressive disease, but is not preceded by signs of classic distemper[6].

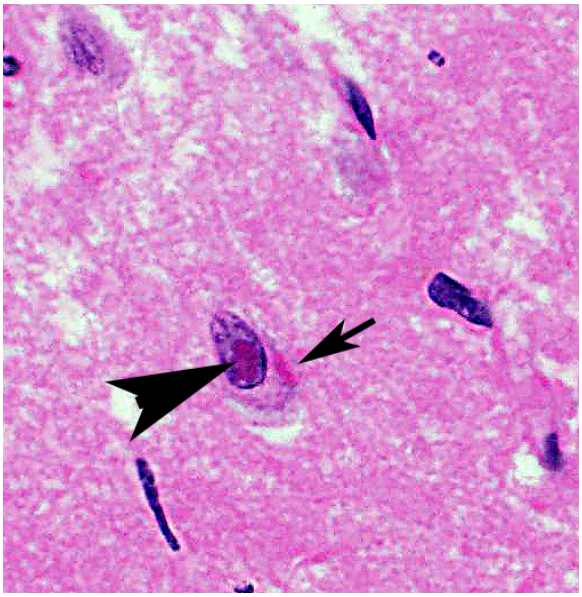

Cerebrum, lion. A small neuron contains both an intracytoplasmic viral inclusions (arrow) and an intranuclear viral inclusion (arrowhead). (HE, 400X)

There is a slow, progressive course of weakness and incoordination, but no seizures. "Old dog" encephalitis (ODE) is extremely rare; most cases occur in dogs past middle age. There is an insidious onset of circling, incoordination, compulsive walking and pushing against fixed objects, but no paralysis or convulsions. The disease progresses over three to four months to coma and death. Post-vaccinal canine distemper encephalitis affects young dogs one to three weeks post-vaccination with a modified live CDV vaccine. There is an acute/subacute clinical course which lasts one to five days. Clinical signs are similar to the furious form of rabies, to include aggressiveness and attack behavior.

Grossly, CNS lesions are uncommon, but white matter softening with brown discoloration, with or without hemorrhage and reduction in brain size with dilated ventricles, can be seen in ODE. Non-CNS lesions include bronchointerstitial pneumonia[7], catarrhal enteritis[17], conjunctivitis[15], hyperkeratosis of the foot

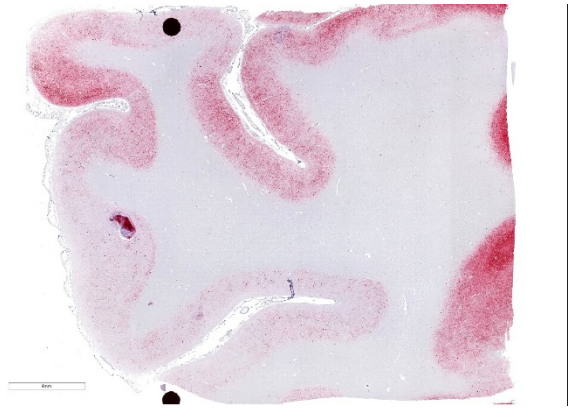

Cerebrum, lion. The cortical gray matter shows extensive immunostaining for canine distemper virus.

pads and nose[17], tonsillar enlargement[4], thymic atrophy[4], enamel hypoplasia[9] and metaphyseal osterosclerosis[9] in young growing dogs.

Histologically, eosinophilic intranuclear and/or intracytoplasmic viral inclusion bodies are most numerous 10-14 days postinfection. Intranuclear viral inclusion bodies are typically most obvious in the brain and intracytoplasmic viral inclusion bodies in the epithelium (especially the urinary bladder), but less obvious in the lymphoid tissues. In classic canine distemper, lesions usually involve both gray and white matter, but predominate in one. In the white matter there is demyelination, with early axon sparing, and status spongiosis with axonal degeneration and necrosis, which is most severe in the cerebellar peduncles, rostral medullary velum, optic tracts, hippocampal fornix, spinal cord and surrounding the fourth ventricle. There is also nonsuppurative encephalitis, gitter cells, astrocytosis and viral syncytia. In the gray matter, there are intranuclear viral inclusion bodies with or without intracytoplasmic viral inclusion bodies in the neurons, neuronal necrosis, mononuclear infiltrate surrounding necrotic neurons and nonsuppurative perivascular encephalitis with or without a mild meningitis.

In multifocal distemper encephalomyelitis in mature dogs, lesions are restricted to the CNS and are most prevalent in the cerebellum and white matter of the spinal cord. In contrast to ODE, the cerebral cortex is often spared. There is multifocal necrotizing non-suppurative encephalitis with rare intranuclear viral inclusion bodies in astrocytes and demyelination in the internal capsule and corona radiate. In ODE, the cerebral cortex and brainstem are consistently affected. The characteristic features are widespread nonsuppurative perivascular encephalitis, intranuclear viral inclusion bodies in neurons and astrocytes and neuronal necrosis. Viral antigen is detectable by immunohistochemistry, however the virus cannot be isolated from the brain. In post-vaccinal canine distemper encephalitis, the lesions are always restricted to the CNS and resemble classic canine distemper, but with relative sparing of white matter.

Ultrastructurally, tubular CDV nucleocapsids are seen in non-membrane bound intracytoplasmic aggregates[8]. Similar tubular structures may be seen in the nucleus despite lack of viral replication in the nucleus[8].There is also destruction of ensheathing myelin envelope[8]. Diagnostic tests used to identify CDV include virus isolation, immunohistochemistry and the fluorescent antibody test. Differential diagnosis for CNS lesions include *Toxoplasma gondii* or *Neospora caninum* (random, multifocal, necrotizing foci in the grey and white matter with protozoa at the margins of the lesions), rabies virus (intracytoplasmic viral inclusion bodies in the hippocampal neurons and Purkinje cells with occasional lymphocytic perivascular cuffing), pseudorabies virus (polioencephalomyelitis with or without ganglionitis and intranuclear viral inclusion bodies in the neurons of the spinal ganglia,

spinal cord, medulla and pons), granulomatous meningoencephalitis (progressive neurological disease of adult dogs with granulomatous inflammation), canine adenovirus type 1 (brainstem hemorrhages with mild vasculitis and intranuclear viral inclusion bodies in endothelial cells) and canine herpesvirus (usually puppies less than 21 days old with multifocal necrotizing lesions in many organs including lung, liver, kidneys and CNS).

Contributing Institution: United States Army Institute of Surgical Research Website: http://www.usaisr.amedd.army.mil/

JPC Diagnosis: Cerebrum: Meningoencephalitis, necrotizing and lymphoplasmacytic, diffuse, moderate, with marked demyelination, gliosis, and moderate numbers of neuronal and astrocytic intra-nuclear and intracytoplasmic viral inclusions.

JPC Comment: The contributor has done an excellent job in the description of the multisystemic pathogenesis of morbillivirus infection in the canine host, and much of this information is applicable to the disease in wild felids. Interestingly, transmission of virulent CDV to domestic cats has not been possible.[1] A report of autopsy findings in large felids in an outbreak in several zoos in North America notes that the histologic findings between the disease in large felids and in dogs are quite similar with the exception of marked Type II pneumocyte hyperplasia in large felids and a more mild and patchy meningoencephalitis than that seen in canine cases.[1]

The disease is not new in large felids; retrospective studies of archived tissues have identified CDV antigens in cases prior to its initial description in this species.[20] Most studies agree that outbreaks in large felids

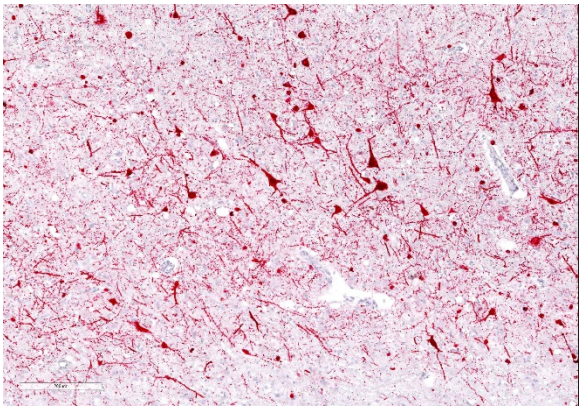

Cerebrum, lion. There is extensive immunostaining for canine distemper virus in cortical neurons.

represent spillover from infected dogs[1,14,20,21] and that this mode of transmission represents a very significant threat to a wide species of animals, many highly endangered, in both wild and captive settings. However, following widespread canine vaccination programs in proximity to the Serengeti ecosystem, the cyclic peaks in lion infections became desynchronized to those of the surrounding canine population, suggesting the possibility of other wildlife species may be maintaining and driving CDV infections in the lion population.[20,21] Widespread vaccination programs (generally aimed at vaccinating 95% of local dog populations) have shown some efficacy in decreasing spillover into wildlife; problems associated with direct vaccination of susceptible wildlife species include mode of vaccine delivery and administration of boosters (often requiring tranquilization and handling of animals), safety and efficacy of distemper vaccines in target species, and the logistics and costs of administering this type of program.[14]

Clinical signs in wildlife species are similar to that of domestic dogs, but may vary as a result of host age, immune status, and viral strain variability. One of the major determinants of strain virulence is genetic variation in the H protein, one of six structural proteins of the CDV virus.[14] The

H protein binds to two cellular receptors in susceptible cells, the signaling lymphocyte adhesion molecular (SLAM, CD150), which is present on the surface of T and B lymphocytes, macrophages, and dendritic cells. A second epithelial receptor, nectin-4, participates in cell entry as well as cell-to-cell spread.

The moderator reviewed various aspects of the pathogenesis and corresponding macroscopic and microscopic lesions of canine distemper virus in big cats as well as other susceptible carnivores. Peculiarities of CDV infection in large cats include prominent alveolar type 2 pneumocyte proliferation and a lack of inclusion bodies within the urinary bladder.[1] She also stated than in addition to being a very illustrative case of a classic lesion, she chose this case to add this entity to the WSC database, where it is the first instance of CDV in a large felid.

References:

1. Appel MJ, Yates RA, Foley GL, et al. Canine distemper epizootic in lions, tigers, and leopards in North America. *J Vet Diagn Invest*. 1994;6(3):277-288.
2. Beineke A, Baumgartner W, Wohlsein P. Cross-species transmission of canine distemper virus-an update. *One Health*. 13;(1):49-59.
3. Blythe LL, Schmitz JA, Roelke M, Skinner S. Chronic encephalomyelitis caused by canine distemper virus in a Bengal tiger. *J Am Vet Med Assoc*. 1983; 183(11):1159-1162.
4. Boes KM, Durham AC. Bone marrow, blood cells, and the lymphoid/lymphatic system. In: Zachary JF, eds. Pathologic Basis of Veterinary Disease. 6th ed. St. Louis, MO: Elsevier Mosby; 2017:759-760.
5. Butina TV, Denikina NN, Belikov SI. Canine distemper virus diversity in Lake Baikal seal (Phoca sibirica) population. *Vet Microbial*. 29;144(1-2):192-197.
6. Cantile C, Youssef S. Nervous system. In: Maxie MG, ed. Jubb, Kennedy, and Palmer's Pathology of Domestic Animals. Vol 1. 6th ed. St. Louis, MO: Elsevier; 2016:384-385.
7. Caswell JL, Williams KJ. Respiratory system. In: Maxie MG, ed. Jubb, Kennedy, and Palmer's Pathology of Domestic Animals. Vol 2. 6th ed. St. Louis, MO: Elsevier; 2016:574-576.
8. Cheville NF. Ultrastructural Pathology: The Comparative Cellular Basis of Disease. Ames, IA: Wiley-Blackwell; 2009:360-363.
9. Craig LE, Dittmer KE, Thompson KG. Bones and joints. In: Maxie MG, ed. Jubb, Kennedy, and Palmer's Pathology of Domestic Animals. Vol 1. 6th ed. St. Louis, MO: Elsevier; 2016:104-105.
10. Deem SL, Spelman LH, Yates, RA, Montali RJ. Canine distemper in terrestrial carnivores: a review. *J Zoo Wild/ Med*. 2000;31(4):441-451.
11. Harder TC, Kenter M, Appel MJ, Roelke-Parker, et al. Phylogenetic evidence of canine distemper virus in Serengeti's lions. *Vaccine*. 1995;13(6):521-523.
12. Headley SA, Amude AM, Alfieri AF, Bracarense AP, Alfieri AA, Summers BA. Molecular detection of canine distemper virus and the immunohistochemical characterization of the neurologic lesions in naturally occurring old dog encephalitis. *J Vet Diagn Invest*. 2009;21 (5):588-597.
13. Kiupel M, Perpifian. Viral diseases of ferrets. In: Fox JG, Marini RP, ed. Biology and Diseases of the Ferret.

3rd ed. Ames, IA: John Wiley & Sons, Inc.; 2014:439-450.
14. Loots AK, Mitchell E, Dalton DL, Kotze A, Venter EH. Advanceds in canine distemper fvirus pathogenesis research: a wildlife perspective. *J Gen Virol* 2017; 98:311-321.
15. Miller AD, Zachary JF. Nervous system. In: Zachary JF, eds. Pathologic Basis of Veterinary Disease. 6th ed. St. Louis, MO: Elsevier Mosby; 2017:890-891.
16. Origgi FC, Sattler U, Pilo P, Waldvogel AS. Fatal combined infection with canine distemper virus and orthopoxvirus in a group of Asian marmots (Marmota caudata). *Vet Pathol*. 2013;50(5):914-920.
17. Pesavento PA, Murphy BG. Common and emerging infectious diseases in the animal shelter. *Vet Pathol*. 2014;51 (2):478-491.
18. Qiu W, Zheng Y, Zhang S, et al. Canine distemper outbreak in rhesus monkeys, China. *Emerg Infect Dis*. 2011;17(8):1541-1543.
19. Seimon TA, Miquelle DG, Chang TY, et al. Canine distemper virus: an emerging virus in wild endangered Amur tigers (Panthera tigris altaica). *MBio*. 2013;4(4):e00410- 13.
20. Terio KA, McAloose D, Mitchell E. Felidae. *In:* Terio KA eds., Pathology of Wildlife and Zoo Animals, London, UK: Academic Press; 2018:pp 278-279.
21. Viana M, Cleaveland S, Matthiopoulos J, et al. Dynamics of a morbillivirus at the domestic-wildlife interface: Canine distemper virus in domestic dogs and lions. *Proc Natl Acad Sci U S A*. 2015 Feb 3;112(5):1464-9.
22. Wenzlow N, Plattet P, Witter R, Zurbriggen A, Grone A. lmmunohistochemical demonstration of the putative canine distemper virus receptor CD150 in dogs with and without distemper. *Vet Pathol*. 2007;44(6):943-948.
23. Zachary JF. Mechanisms of microbial infections. In: Zachary JF, eds. Pathologic Basis of Veterinary Disease. 6th ed. St. Louis, MO: Elsevier Mosby; 2017:225-226.

CASE II: 16GR108 (JPC 4118174).

Signalment: 1-year-old, male, Beagle (*Canis familiaris*).

History: Two-week exploratory toxicity study.

Gross Pathology: Unilateral (left) small epididymis was noted macroscopically.

Laboratory results: None

Microscopic Description: Epididymis: Within the epididymis, there is moderate focal arterial inflammation characterized by expansion of tunica intima with prominent endothelial cells, disruption of the internal elastic lamina, and presence of fibrin, cellular

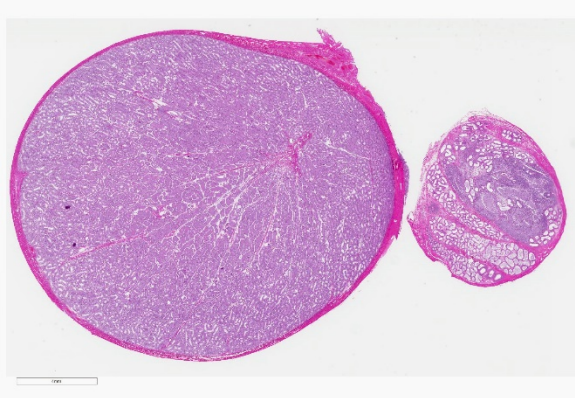

Testis and epididymis, dog. A section of testis (left) and epididymis (right). Approximately 33% of the epididymis is expanded by an inflammatory focus that replaces tubules. (HE, 6X)

debris, and inflammatory cells (lymphocytes, plasma cells and macrophages) in the tunica media and adventitia.
Disrupting ductular and stromal architecture is a focally extensive inflammatory reaction composed of a ring of macrophages, lymphocytes, and plasma cells (granuloma) surrounding a large focus of extravasated spermatozoa.

Contributor's Morphologic Diagnoses:
Epididymis: 1) Arteritis, lymphoplasmacytic, focal, moderate, subacute
2) Sperm granuloma, focal, moderate, subacute

Contributor's Comment:
This finding was unrelated to the test article because it occurred in just one animal without dose relationship and was consistent with idiopathic juvenile polyarteritis of young Beagles, a background finding in dogs.[1,2] Small to medium caliber arteries are most commonly affected by this form of vascular injury. Histologically, vascular changes are characterized by medial necrosis, mononuclear cell inflammatory infiltrates, intimal proliferation, and fibrinoid necrosis.[4,7,8] There is a higher incidence in males with a trend towards the epididymis as the organ most commonly affected. Differentiation from drug-induced vascular injury (DIVI) is important in toxicity studies.

DIVI includes vasoactive arteriopathy, toxic vasculitis, and hypersensitivity vasculitis. Histologic changes induced by vasoactive drugs include necrosis and inflammation in all three vessel layers, most commonly in small vessels of the skin, and an absence of fibrinoid necrosis. Toxic vasculitis affects small to medium-caliber vessels and is characterized morphologically by segmental fibrinoid necrosis and neutrophilic inflammation of the vessel wall, periadventitial tissue, and thrombosis.

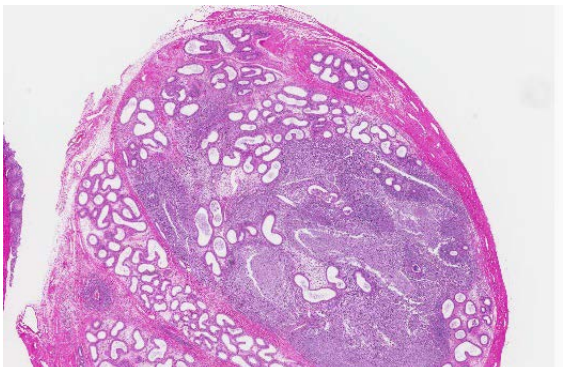

Testis and epididymis, dog. The epididymis is expanded by poorly formed granulomas which replace tubules. (HE, 18X)

Vasoactive arteriopathy represents the most common type of DIVI and primarily affects coronary arteries (vasodilators) and small arteries systemically (vasoconstrictors). Histologically, changes are characterized by medial hemorrhagic necrosis with minimal inflammation (vasodilators) and focal medial fibrinoid necrosis (vasoconstrictors).[1]

Epididymal sperm granulomas are typically an incidental finding and similarly not test article-related in the present case. There are multiple causes of sperm granulomas including, most commonly, trauma and inflammation, congenital ductular abnormalities, adenomyosis of epididymal ducts, parasitic lesions, and toxins.[2]

Contributing Institution:
Pfizer Drug Safety Research and Development
455 Eastern Point Rd.,
Groton, CT 06340
https://www.pfizer.com/partners/research-and-development

JPC Diagnosis:
1. Epididymis: Sperm granulomas, multiple.
2. Arteriole, head of the epididymis: Arteritis, necrotizing and granulomatous, chronic, diffuse, moderate.
3. Testis, seminiferous tubules: Atrophy and aspermatogenesis, diffuse, moderate.

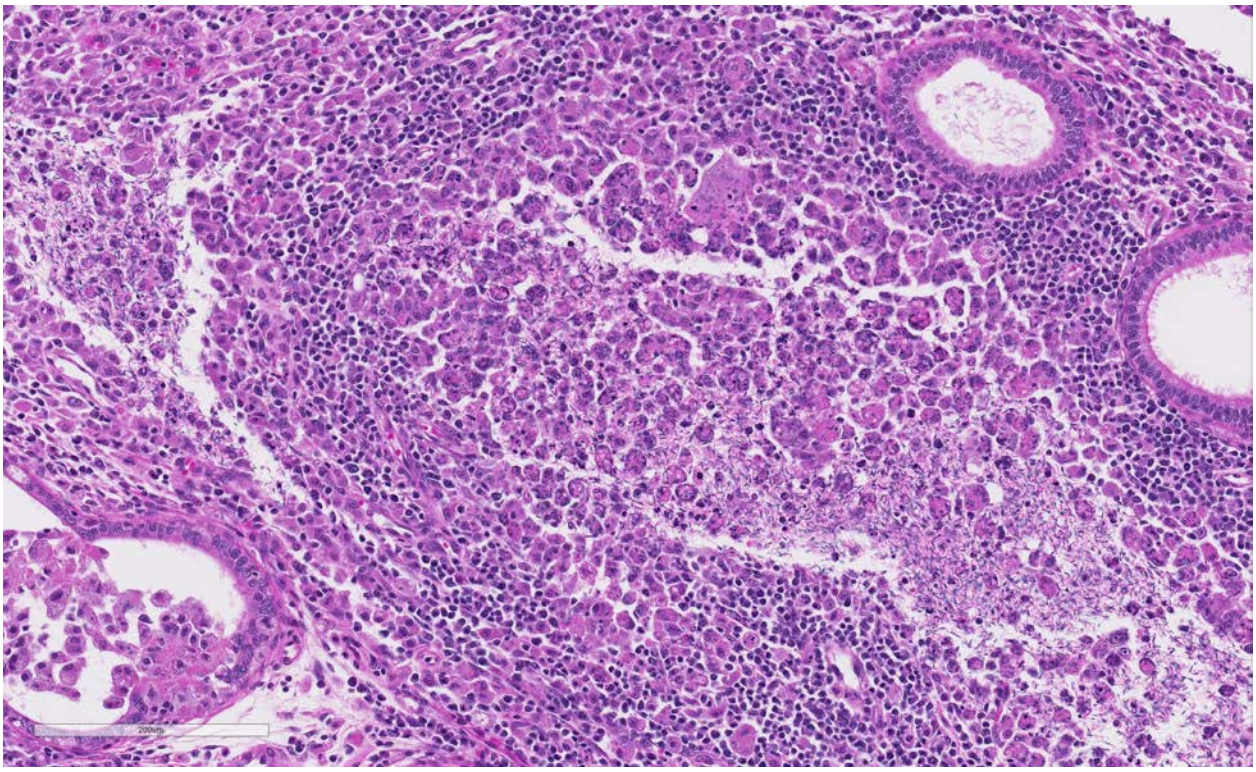

Testis and epididymis, dog. The granulomas are centered on free sperm in the interstitium, which are often engulfed by macrophages. Peripherally, the granuloma contains moderate numbers of lymphocytes and plasma cells and small amounts of collagen with plump fibroblasts. At lower left, macrophages infiltrate an epididymal tubule. (HE, 186X)

JPC Comment: Idiopathic juvenile polyarteritis of beagle dogs, first described in 1992 by Scott-Moncrieff et al. in 1992,[6] is one of the most well-known primary vasculitides in the dog. The term "primary" vasculitis comes from human medicine and refers to a vasculitis whose cause is unknown, versus "secondary" vasculitides, which have defined infectious causes, such as endotheliotropic viruses, or drugs (as described by the contributors). A retrospective study of canine vasculitis by Swann et al. in 2015[9] failed to disclose significant differences between the two groups; primary vasculitides were more common in female dogs (this case notwithstanding), and dogs with elevated serum globulin concentrations were seen with more frequency in dogs with primary vasculitides.

Idiopathic juvenile polyarteritis (IJP), also known as "beagle pain syndrome", is an acute febrile multisystemic vasculitis most often seen in dogs less than 36 months of age.[7] It is characterized by acute onset of fever and pain (often cervical) with animals assuming a characteristic hunched stance.[4] Vascular lesions range from a mild lymphohistiocytic perivasculitis to transmural arterial inflammation with fibrinoid necrosis with loss of elastic laminae, intimal and medial fibrosis, and marked perivascular inflammation.[4,7] Lesions are most commonly seen in the small-and medium-sized arterioles (i.e., arterioles other than the great vessels) of the cervical meninges, heart, and cranial mediastinum.[7] Animals with repeated episodes may develop gross signs of progressive bilateral atrophy of cervical and temporal muscles,[4] and histologic evidence of hepatic, splenic and renal amyloidosis.[4,7]

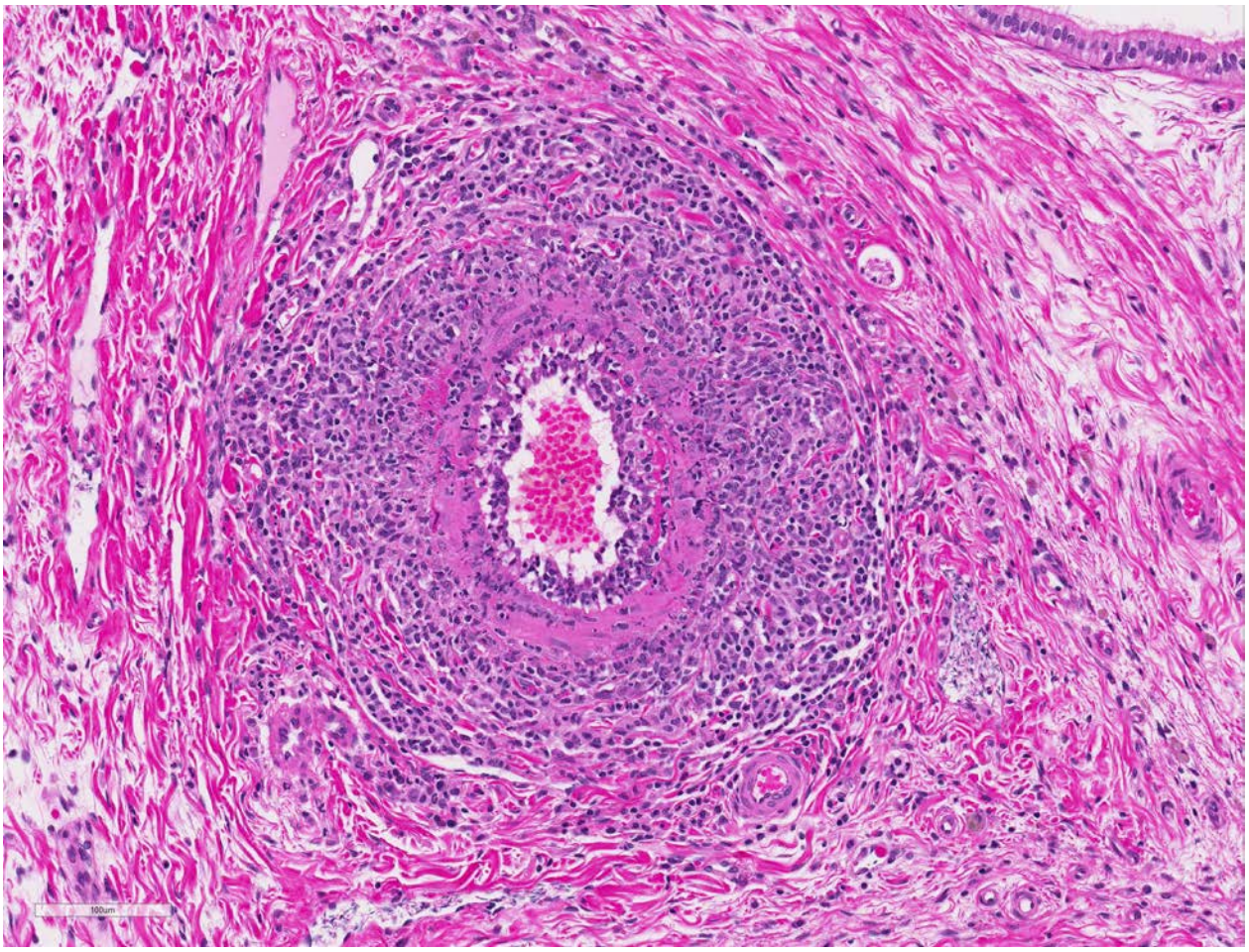

Testis and epididymis, dog. There is fibrinoid necrosis of an epididymal arteriole with marked infiltration of the adventitia and outer media by numerous neutrophils and macrophages. At its periphery, dilated lymphatics contain sperm. (HE, 218X)

Interestingly, a primary vasculitis affecting the testicular artery of raccoons has been reported.[5] Histologic lesions of segmental arteritis of the extratesticular (epididymis and spermatic cord) arterioles similar to that of IJP and other forms of polyarteritis nodosa were described. The lesions were seen in both wild and breeder animals of all ages.[5]

The blood-epididymis barrier (BEB) is an important factor in protecting maturing sperm from the immune system. This barrier protects developing spermatozoa in the testis and mature spermatozoa within the epididymal tubules not only from infiltrating inflammatory cells following injury, but also from cytokines released in local and systemic inflammatory conditions.[3] The breakdown of the BEB may result from traumatic injuries, developmental abnormalities, or the administration of testosterone and various chemicals and drugs. In addition, BEB barrier function diminishes with age. Sperm granulomas (which may be seen not only in the epididymis but also within the testis proper and vas deferens) are cardinal signs of breakdown of the BEB, and arise as a result of the antigenicity of spermatozoa.[3] An excellent review of factors contributing to the breakdown of the BEB and the resulting inflammatory process is provided in the 2014 article by Gregory and Cyr cited below.[3]

The moderator discussed the formation of sperm granuloma and the fact that the inception of spermatozoa formation does not occur until well after the immune system is formed, which is why sperm is so antigenic. She pointed out that the tail of the epididymis is more likely to be affected in infectious disease, while the head (caput) of the epididymis has a higher incidence of granuloma formation as a result of the presence of an increased number of abnormal ductules and reviewed the general pathology behind granuloma formation. She gave an excellent review of "beagle pain" syndrome, pointing out that the disease is not restricted to Beagles, nor is it always a painful condition. She chose this case as an example of a classic lesion as well as a descriptive case which has two concurrent processes.

References:

1. Clemo FAS, Evering WE, Snyder PW, et al. Differentiating spontaneous from drug-induced vascular injury in the dog. *Toxicol Pathol.* 2003;31(Suppl.):25-31.
2. Foley GL, Bassily N and Hess RA. Intratubular spermatic granulomas of the canine efferent ductules. *Toxicol Pathol.* 1995;23(6): 731-734.
3. Gregory M, Cyr DG. The blood-epididymis barrier and inflammation. *Spermatogenesis* 2014; 4(2)e97619-1 – e97619-13.
4. Hayes TJ, Roberts GK, Halliwell WH. An idiopathic febrile necrotizing arteritis syndrome in the dog: beagle pain syndrome. *Toxicol Pathol.* 1989;17(2):129-137.
5. Hamir AN, Palmer M, Li H, Stanko J, Rogers DB. Spontaneous idiopathic arteritis of the testicular artery in raccoons (*Procyon lotor*). *Vet Pathol* 2009; 46:1129-1132.
6. Scott-Moncrieff JC, Snyder PW, Glickman LT, Davis EL, Felsburg PJ. Systemic necrotizing vasculitis in nine young beagles. *J Am Vet Med Assoc* 1992; 201(10):1553-1558.
7. Snyder PW, Kazacos EA, Scott-Moncrieff JC, et al. Pathologic features of naturally occurring juvenile polyarteritis in beagle dogs. *Vet Pathol* 1995;32(4):337-345.
8. Son W. Idiopathic canine polyarteritis in control beagle dogs from toxicity studies. *J Vet Sci.* 2004;5(2):147-150.
9. Swann JW, Priestnall SL, Dawson C, Chang YM, Garden OA. Histologic and clinical features of primary and secondary vasculitis: a retrospective study of 42 dogs. *J Vet Diagn Investig* 2015; 27(4): 489-496.

CASE III: Case #2 (JPC 4084695).

Signalment: 12-year-old, spayed female, Mix breed (*Canis familiaris*).

History: Patient was referred to a local veterinary hospital because of left exophthalmos. A very large orbital contrast-enhancing mass compressing the left eye was revealed by computerized tomography (CT). The mass along with the left eye was surgically resected.

Gross Pathology: Grossly there was a whitish-gray, firm mass, approximately 5×4.3×3cm in diameter, located in the retrobulbar area. On cut surface, the mass was solid and whitish-marble, and completely involved the optic nerve.

Laboratory results: None

Microscopic Description: The tumor composed of sheets of closely packed large neoplastic cells supported by scant stroma harboring numerous small vessels.

Eye, dog. There is a 5x4x3 cm retrobulbar mass which involves the optic nerve. (Photo courtesy of: Setsunan University)

Neoplastic cells were large, mainly round to polygonal cells, with abundant eosinophilic granular cytoplasm. The nuclei showed minimal pleomorphism and hyperchromasia and tended to be situated towards the periphery of the cell. Mitoses were not observed. There were also few whorl-like structures. Abundant cytoplasmic eosinophilic granules were PAS-positive. Immunohistochemically, the neoplastic cells were diffusely positive for vimentin, but did not express cytokeratin AE1/AE3, neurofilament, GFAP and IBA-1.

Contributor's Morphologic Diagnoses: Eye: Orbital meningioma, granular cell type.

Contributor's Comment: Orbital meningioma can derive from the optic nerve arachnoid cap cells that extend through the dura mater into the connective tissues of the orbit. In the dog, which has the higher incidence among the domestic species, 82% of the meningiomas are intracranial, 15% are intraspinal, and the remaining 3% are retrobulbar or orbital.[5] Primary orbital meningiomas are generally thought to be slow growing and benign, but intraocular invasion and malignant variants with extracranial metastasis have been reported. Poodles, poodle crosses, Samoyeds, Samoyed crosses, German shepherds, and German shepherd crosses were the only breeds affected.[7] In the same study, the mean age at the time of diagnosis was 9 years (range: 3 to 7 years of age), and a male sex predisposition with a male:female ratio of 2:1 was also evident.[7] Clinically, they are frequently associated with unilateral protrusion of the ocular globe and blindness. Apparently there is no predilection for either side. Although not highly invasive, canine orbital meningiomas are difficult to remove, and local regrowth or extension through the optic foramen leading to blindness is a common complication.[7]

Orbital neoplasms are seen rarely in the dog, almost always present as slowly progressing, painless exophthalmos in older dogs, and are often malignant. A wide variety of tumor types can occur in the orbit, with fibroma, meningioma, osteosarcoma, malignant lymphoma, lipoma, rhabdomyomas, and lachrimal gland tumor.

In this case, histomorphological differentials are thought to be included rhabdomyomas, oncocytomas, and histiocytic sarcoma. Rhabdomyomas are benign skeletal muscle neoplasms that are characterized by glycogen-rich, eosinophilic, striated muscle

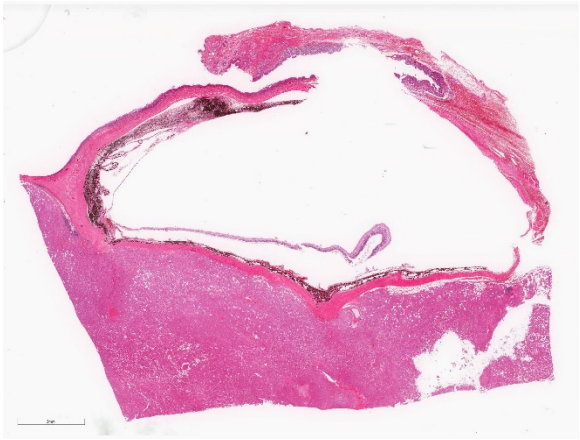

Eye, dog. Subgross magnification of a tangential section of the eye and the associated mass. The optic nerve is not visible in the submitted section. (HE, 8X)

cells with numerous mitochondria, and myofilaments. In oncocytomas, the abundant eosinophilic cytoplasmic granules correspond to large numbers of mitochondria. In histiocytic sarcoma, tumor cells sometimes contain many small vacuoles. Multinucleated giant cells with variably sized nuclei are common, and the mitotic rate is high in many areas.

The current classification of meningiomas in domestic animals describes nine histological types: meningothelial, fibrous, transitional, psammomatous, angiomatous, papillary, granular cell, myxoid and anaplastic.[4] Among these types, granular cell meningioma is specific to domestic animals, and does not exist in the WHO classification of human meningioma.[6] Otherwise, there are some reports of canine granular cell tumors in the meninges.[2,8,10] At present, the histopathological differences between granular cell meningiomas and granular cell tumors in the central nervous systems are obscure. Furthermore, the description of the histological characteristics of granular cell meningioma in the WHO classification for domestic animals is very similar to that of granular cell tumors. In the rat, there is convincing gross, histologic, and ultrastructural evidence suggesting that intracranial granular cell tumors originate from meningeal arachnoid cells and that some of these tumors may also contain

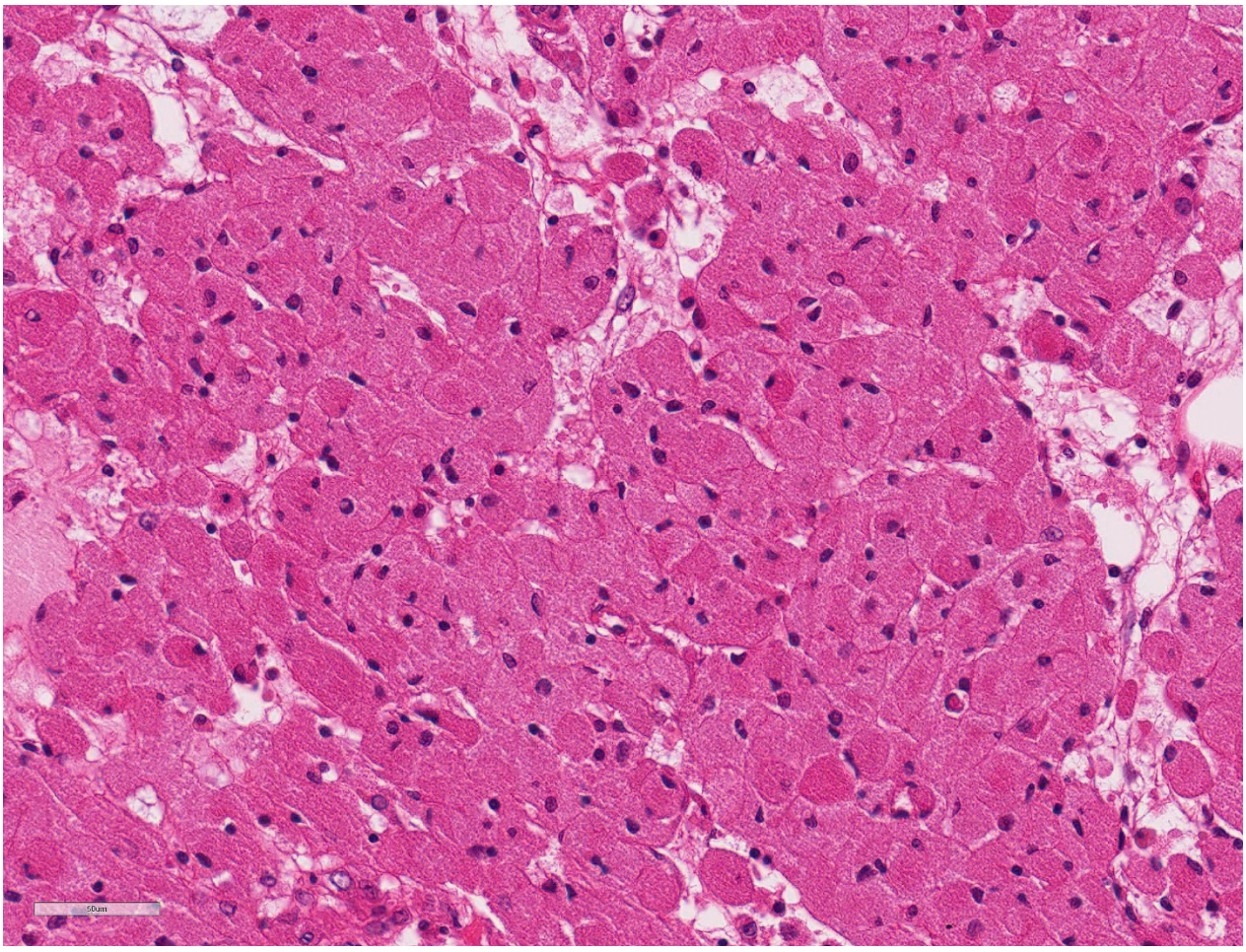

Eye, dog. Neoplastic cells range up to 3-0um in diameter, with abundant eosinophilic granular cytoplasm. (HE, 400X)

mixtures of both cell types.[2,12] The major meningeal involvement in both these canine tumors suggests that, as in the rat, they may be derived from a cell type forming the leptomeninges. Other support for this hypothesis is provided by a canine meningotheliomatous meningioma in which a substantial granular cell component has been described.[2,9]

JPC Diagnosis: 1. Retro-orbital fat: Granular cell tumor.
2. Eye: Retinal detachment and atrophy with diffuse severe ganglion cell loss. .
3. Eyelid: Conjunctivitis, lympho-plasmacytic, chronic, diffuse, mild.

JPC Comment: While careful consideration was given to the contributor's diagnosis of "orbital meningioma, granular cell type", we prefer the diagnosis of granular cell tumor in this case.

Much of the diagnostic confusion in this particular case arises from changes in the current classification of meningiomas. While present in the 1999 WHO Classification of Tumor of Domestic Animals[4] (referenced by the contributor), "granular cell meningioma" has been dropped in more recent classifications.[3] In addition, the images of the "granular cell meningioma" in the WHO Classification[4] are quite similar to those ascribed to "granular cell tumors" in other publications, including the paper by Higgins et al.[2,3]

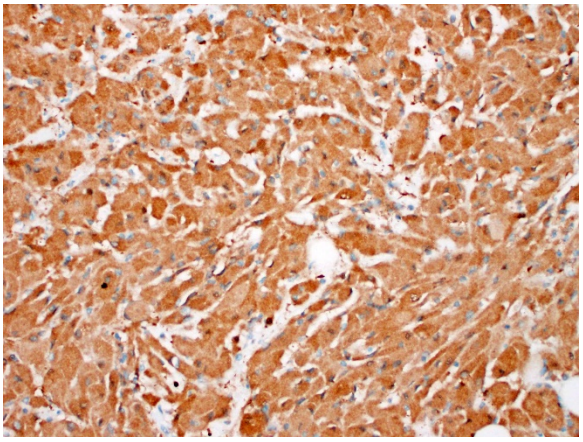

Eye, dog. Neoplastic cells demonstrate strong S-100 immunopositivity. (anti-S-100 400X)

A number of WSC cases have dealt with the unique classification of orbital meningioma in previous years, including WSC 2015-2016, Conference 20, Case 4 and WSC 2018-2019, Conference 7, case 4. A common feature of orbital meningiomas is the presence of chondroid or osseous metaplasia,[1,7] which is absent in this case, as are other features of meningioma. While a few granular cell meningiomas are present within the collection of the Comparative Ocular Pathology Lab of Wisconsin (COPLOW) (and one had been published)[11], these tumors all had areas of osseous and cartilaginous metaplasia, as well as areas of neoplastic cells that resemble those seen in more classic meningiomas of the meningotheliomatous type (Personal communication, Leandro Teixeira.) Careful examination of the available literature on canine orbital meningiomas[1,7] failed to disclose mention of a "granular cell type"; in one reference of an orbital meningioma with a "granular cell component",[9] the morphology is significantly different that that seen in this case, with central nucleolus and homogenous eosinophilic cytoplasm as compared to that seen here, in which the cytoplasm is granular and the nuclei are peripheralized and hyperchromatic.

Granular cell tumors have been described in the central nervous system of the rat, ferret, dog, and humans.[2] The etiology of these neoplasm remains in question, although prevailing theory in the rat, dog, and ferret is that they indeed are of meningothelial origin. Granular cell tumors in humans may be of astrocytic origin[2] (A JPC-run GFAP stain was negative). Additionally, they may have a similar appearance to oncocytic meningeal

variants in which the granules are numerous mitochondria rather than lysosomes, as seen in animal species (Personal communication, Jey Koehler, Auburn University).

The second morphologic diagnosis was suggested by Dr. Leandro Teixeira of COPLOW upon slide review: If you look at the retina in the slide it is completely devoid of ganglion cells. "This is due to compression of the optic nerve by the orbital neoplasm causing axonal (wallerian) degeneration and complete ganglion cell loss. This is a very important lesion since it is the reason these dogs go blind and thus I think it deserves a separate morphologic diagnosis." (Personal communication, Leandro Teixeira).

The moderator reviewed differential diagnosis of retro-orbital meningioma, oncocytoma, rhabdomyosarcoma, and granular cell tumor. In addition, in this particular case, a section was floated off the section for ultrastructural analysis and the granules in the cells were demonstrated to be lysosomes further cementing the diagnosis of granular cell tumor. The moderator also presented data supporting her contention that

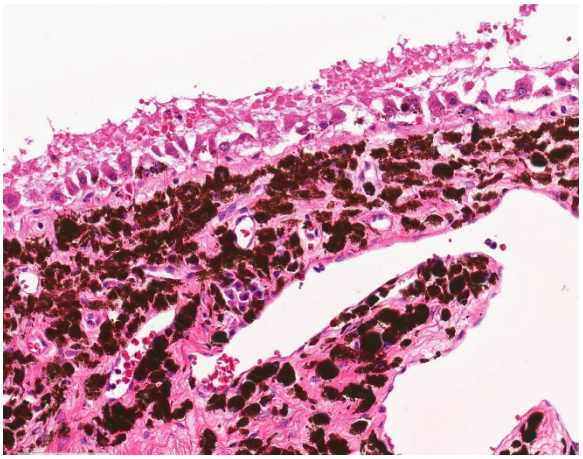

Eye, dog. The retina is detached. The pigmented retinal epithelium is markedly hypertrophic and covered with hemorrhage and fibrin. (HE 256X)

the morphology of granular cell tumors may be the result of widespread cellular degeneration and lysosomal overload, which might explain how various cell types in various organs in various species may attain a similar morphologic appearance.

References:

1. Dubielzieg, RR, Ketring KL, McLellan GJ, Albert DM. The optic nerve. *In:* Veterinary Ocular Pathology: A comparative review. Edinburgh UK: Saunders/Elsevier; 2010; pp. 410-411.
2. Higgins RJ, LeCouteur RA, Vernau KM, Sturges BK, et al. Granular cell tumor of the canine central nervous system: Two cases. 2001. *Vet Pathol.* 38: 620-627.
3. Higgins RJ, Bollen AW, Dickinson PJ, Siso-Llonch S. Tumors of the Nervous System. *In:* Tumors in Domestic Animals, Fifth Ed, Meuten DJ, ed.; Ames IA: Wiley Blackwell 2016; pp. 864-872.
4. Koestner A, Bilzer T, Fatzer R, Schulman FY, Summers BA, Van Winkle TJ. Meningioma In: *Histological Classification of Tumors of the Nervous System of Domestic Animals*. 2nd series. Vol. V. Washington, DC: Armed Forces Institute of Pathology; 1999: 27-29.

5. Koestner A, Higgins RJ: Tumors of the nervous system. In: *Tumors in Domestic Animals*, 4ed. Meuten DJ, Iowa State Press, Ames, 2002: 697–738.
6. Louis DN, Perry A, Reifenberger G, von Deimling A, et al. The 2016 World Health Organization classification of tumors of the central nervous system: A summary. 2016. *Acta Neuropathol.* 131(6):803-820.

7. Mauldin EA, Deehr AJ, Hertzke D, Dubielzig RR. Canine orbital meningiomas: a review of 22 cases. *Vet Ophthalmol*. 2000; 3:11-16.
8. Mishra S, Kent M, Haley A, Platt S, et al. Atypical meningeal granular cell tumor in a

dog. 2012. *J Vet Diagn Invest.* 24(1):192-197.
9. Perez V, Vidal E, Gonzalez N, Benavides J, et al. Orbital meningioma with a granular cell
component in a dog, with extracranial metastasis. *J Comp Pathol*. 2005; 133: 212- 217.
10. Sharkey LC, McDonnell JJ, Alroy J. Cytology of a mass on the meningeal surface of the left brain in a dog. 2004. *Vet Clin Pathol.* **33**: 111-114.

11. Shaw GC, Miller SN, Dubielzig RR, Teixeira LBC (2015). Granular cell variant of a canine orbital meningioma: a case report. American College of Veterinary Pathologists, American Society for Veterinary Clinical Pathology, and Society of Toxicologic Pathology Combined Annual Meeting, Minneapolis, Minnesota.
12. Yoshida T, Mitsumori M, Harada T, Maita K. Mmorphological and ultrastructural study of the histogenesis of meningeal granular cell tumors in rats. 1997. *Toxicol Pathol.* 25(2):211-216.

CASE IV: 14/1790 (JPC 4117447).

Signalment: 13-year-old spayed female Labrador retriever dog, *Canis familiaris*, canine

History: This dog presented for a mass on the vaginal floor. Complete blood count and chemistry were unremarkable.

Gross Pathology: 3cm diameter, asymmetrical, lobulated and highly vascular mass protruding from the vaginal floor.

Laboratory results: None

Microscopic Description: Vaginal floor mass: This is an expansile, fairly well-demarcated, unencapsulated, multilobulated

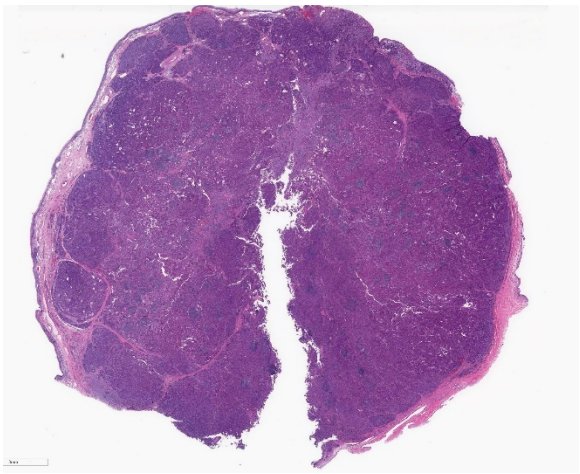

Vagina, dog. A large multilobulated neoplasm expands the submucosa, elevating the overlying ulcerated surface. Aggregates of lymphocytes may be seen at low magnification. (HE, 7X)

and peripherally invasive neoplasm composed of cuboidal to polygonal cells arranged in cords, acini, occasional rosettes (Figure 1) and solid areas with fine fibrovascular stroma. Neoplastic cells have indistinct cell borders, a moderate amount of eosinophilic cytoplasm, and round to oval finely stippled nuclei with prominent nucleoli. There is mild anisocytosis and anisokaryosis and one mitotic figure in 10 high power (400x) fields. Rafts of neoplastic cells are within multiple endothelial lined vessels (vascular invasion) (Figure 2) [varies by slide]. Scattered throughout the mass are perivascular clusters of lymphocytes and foci of hemorrhage with hemosiderin-laden macrophages.

Contributor Morphologic Diagnoses: Clitoral gland adenocarcinoma

Contributor Comment: Vaginal and vulvar tumors are uncommon neoplasms which typically occur in older, sexually intact females.[7] The majority of these neoplasms are benign and of smooth muscle or fibrocyte origin.[7] Few, individual case reports of epithelial neoplasms resembling apocrine gland anal sac adenocarcinomas

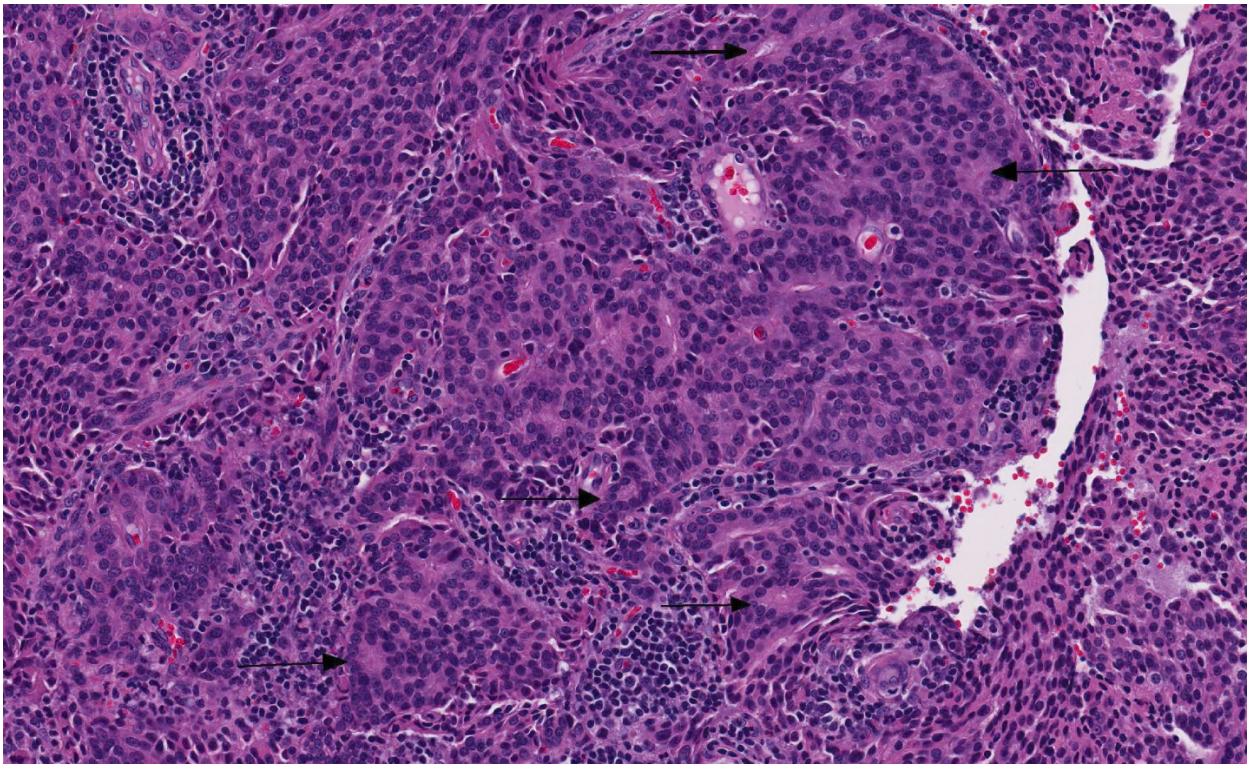

Vagina, dog. Neoplastic cells are arranged in nests and trabeculae, and rosettes are common (arrows). Numerous lymphocytes and fewer plasma cells are present within the stroma. (HE, 246X)

(AGASACA), but arising within the clitoral fossa, have been documented in the literature since 2010.[3,4,5,8] A case series published in 2018 has added 6 more cases to the literature.[8]

Clitoral gland carcinomas are thought to arise from individual apocrine glands within the fibro-fatty tissues of the canine clitoris. They typically present as ulcerated, multilobular masses protruding from the vulva. Histologically, these tumors closely resemble their anal sac counterpart, and it is possible that tumors at this location have been previously reported as AGASACAs. Tubular, rosette, and solid forms are described in the paper by Verin et al.,[8] although most tumors are mixed-type. Only carcinomas have been reported; a majority of cases have vascular invasion at the time of diagnosis.[8] Tumors that have been stained with neuroendocrine markers are typically uniformly positive for neuron-specific enolase, with mixed positivity for chromogranin A and synaptophysin and negative for S-100.[8]

Interestingly, in two earlier reports of clitoral gland adenocarcinoma in the dog, hypercalcemia of malignancy (HM) was a feature.[3,4] However, in the six cases reported recently, only 2 of 6 cases exhibited HM; one case confirmed an elevated parathormone-related hormone (PTHrp) as the likely cause.[8]

In this case, the animal received two doses of chemotherapy before treatment was stopped due to undesirable side effects. Although the neoplasm has recurred at the original site, there was no evidence of metastatic disease or hypercalcemia of malignancy more than 2 years after initial diagnosis and treatment.

Contributing Institution:
University of Tennessee, College of Veterinary Medicine, Department of Biomedical and Diagnostic Sciences http://www.vet.utk.edu/departments/path/index.php

JPC Diagnosis: Mass from vaginal floor: Clitoral gland adenocarcinoma.

JPC Comment: The contributor has done an outstanding job summarizing the histologic and clinicopathologic features of this uncommon neoplasm of the vulva of the dog. A 2016 paper by Rout et al.[5] describes the salient features of this tumor on cytologic evaluation: loosely cohesive and acini of epithelial cells with numerous "naked" nuclei in the surrounding milieu, suggestive of neuroendocrine carcinoma. Cell clusters may include capillaries or pink amorphous material.[5] In addition, clitoral gland adenocarcinomas, like the closely related tumors of the apocrine glands of the anal sac often metastasize to regional nodes; close examination of regional nodes (including the inguinal as well as medial and internal iliac nodes) for gross evidence of metastasis is recommended.[8]

Neoplasms of the clitoral gland are well known in the rat and these glands, as well as the preputial glands of males, are usually sampled in carcinogenicity and xenobiotic studies in the mouse and rat.[6] These modified sebaceous glands are located adjacent to the vagina, and their ducts empty into the clitoral fossa. Their growth and activity are regulated by a number of hormones, including sex hormones, as well as ACTH, prolactin, and growth hormones. In general, a range of lesions is seen in this gland similar to those seen in the mammary gland. [6]

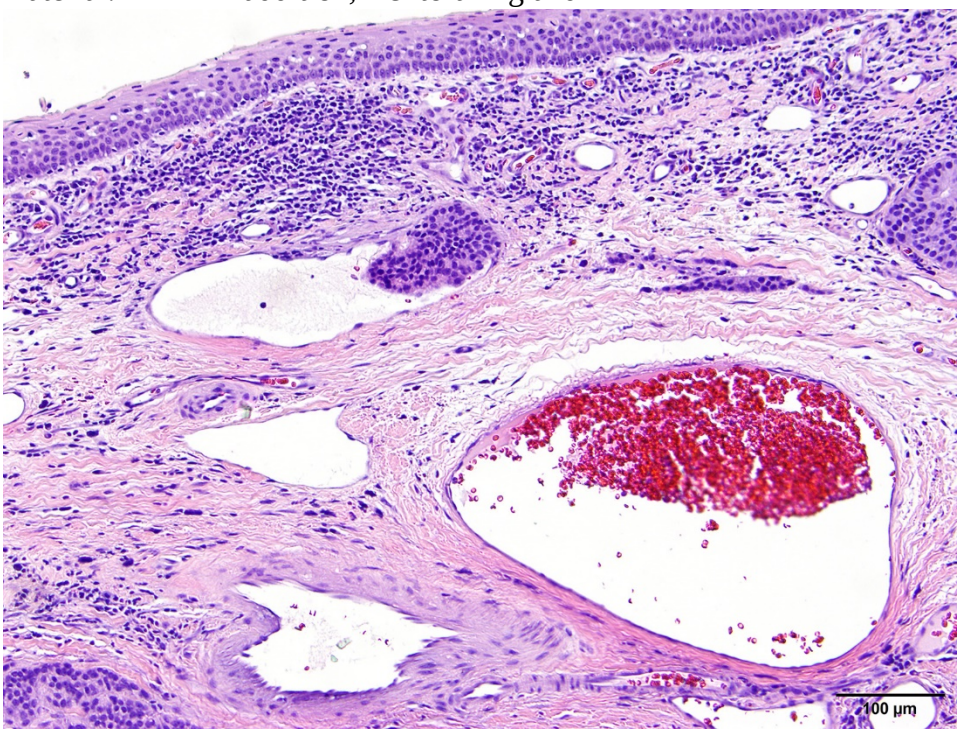

Vagina, dog. Neoplastic cells are occasionally present within submucosal lymphatics (HE, 246X) (Photo courtesy of: University of Tennessee, College of Veterinary Medicine, Department of Biomedical and Diagnostic Sciences http://www.vet.utk.edu/departments/path/index.php

In rodents, inflammatory changes of the clitoral gland may range from simple lymphocytic infiltrates to actual inflammation resulting from bacterial or fungal agents, or the presence of foreign bodies in adjacent tissue. Obstructed clitoral gland ducts may result in granulomatous inflammation. Hyperplasia, or less commonly atrophy, is seen in older animals. Clitoral gland neoplasms are often not large

enough to be observed grossly and necropsy, so this tissue (as well as preputial gland, mammary gland, and the rat Zymbal's gland) should be routinely harvested at necropsy.[6]

A range of neoplasms and subtypes have been observed in rodents. Adenomas of the clitoral glands, and are characterized as expansile growths with minimal atypia and few mitoses. [6] Clitoral gland carcinomas are generally larger with invasive growth, ulceration of the overlying skin, nuclear atypia and a high mitotic rate. Several subtypes (solid, cystic, papillary, papillary cystic, and mixed cell types) are described, but the current INHAND document does not recommend subtyping for regulatory activities. Squamous papillomas and malignant basal cell variants of clitoral gland adenocarcinomas are also described.[6]

In humans, the clitoris is covered by squamous mucosal epithelium without a glandular component.[2] The overwhelming majority of neoplasms arising in and around this organ in human are squamous cell carcinomas.[1] As the clitoris and surrounding tissues possess lymphatic drainage, malignancies from other areas of the body will rarely metastasize to this area.[1]

The moderator stated she chose this particular case as it not only is a new addition to the WSC database, but also has been recently published in the veterinary literature and would be very helpful for residents preparing for certifying examinations. She reviewed the various type of rosettes seen in various tumors including Homer-Wright (central region contains neuropil), Flexner-Wintersteiner (central region largely empty except cytoplasmic extensions from tumor cells), ependymal rosettes (central regions are empty), and pseudorosettes (surround a blood vessel). She also reviewed the various type of neoplasms whose cytologic appearance includes large numbers of "naked nuclei" to include a variety of neuroendocrine neoplasms, apocrine carcinomas of the anal sac, and clitoral adenocarcinoma.

References:

1. DuPont NC, Mabuchi S, Ries S, Berman ML. Sclerosing ductal carcinoma of the clitoris with microcystic adnexal carcinoma-like features. *J Cutan Pathol* 2009: 359-361.
2. Kurman RJ, Ronnett BM, Sherman ME, Wilkinson EJ. Anatomy of the lower female reproductive tract. *In*: AFIP Atlas of Tumor Pathology, Series 4: Tumors of the Cervix, Vagina, and Vulva. ARP Press, Silver Spring, MD, p. 20.
3. Mitchell KE, Burgess DM, Carrigan, MJ. Clitoral adenocarcinoma and hypercalcemia in a dog. *Aust Vet Pract* 2012; 42:279-282.
4. Neihaus SA, Winter JE, Goring RL, Kennedy FA, Kiupel M. Primary clitoral adenocarcinoma with secondary hyperpcalcemia of malignancy in a dog. *J. Am Anim Hosp Assoc* 2010; 46(3):193-196.
5. Rout ED, Hoon-Hanks LL, Gustafson TL, Ehrhart EJ, MacNeill AL. What is your diagnosis: Clitoral mass in a dog. *Vet Clin Pathol* 2016; 197-198.
6. Rudmann D, Cardiff R, Chouinard L, Goodman D, Kuttler K, Marxfeld, Molinolo A, Treumann S, Yoshizawa K. Proliferative and nonproliferative lesions of the rat and mouse mammary, Zymbals's, preputial, and clitoral glands. *Toxicol Pathol* 2012; 49: 7S-39S.
7. Thatcher C, Bradley RK. Vulvar and vaginal tumors in the dog: a

retrospective study. *J Am Vet Med Assoc.* 1983;183(6):690–692.

8. Verin R, Cian F, Stewart J, et al. Canine clitoral carcinoma: A clinical, cytologic, Histopathologic, Immunohistochemical, and Ultrastructural Study. *Vet Pathol.* 2018; epub ahead of print. DOI: 10.1177/0300985818759772

Self-Assessment - WSC 2019-2020 Conference 2

1. Which of the following is true concerning multifocal distemper encephalomyelitis?
    a. It is an acute fulminant disease of young animals 3-4 weeks following MLV administration.
    b. Classic distemper signs are not seen in affected animals.
    c. The most common sign is seizure activity.
    d. Of the variants of distemper, it is the only one that does not have a progressive course.

2. Which receptor mediates the entrance of canine distemper virus into cells?
    a. Fusion protein receptor
    b. Signaling lymphocyte activation molecule
    c. Hemagglutinin protein receptor
    d. CD45

3. Which of the following is NOT a form of drug-induced vascular injury?
    a. Toxic vasculitis
    b. Vasoactive arteriopathy
    c. Idiopathic juvenile polyarteritis of dogs
    d. Hypersensitvity vasculitis

4. Granular cell tumors of the central nervous system of the dog are thought to be derived from which cell of origin?
    a. Astrocytic
    b. Histiocytic
    c. Meningothelial
    d. Endothelial

5. Animals with clitoral gland adenocarcinomas may exhibit elevated blood levels of which of the following?
    a. Vegetative epithelial growth factor
    b. Inhibin
    c. Insulin-like growth factor
    d. Calcium

Please email your completed assessment for grading to Dr. Bruce Williams at bruce.h.williams12.civ@mail.mil. Passing score is 80%. This program (RACE program 33611) is approved by the AAVSB RACE to offer a total of 0.5 CE Credits, with a maximum of 12.5 CE Credits being available to any individual Veterinary Medical Professionals for the 2019-2020 Wednesday Slide Conference. This RACE approval is for the subject matter categories of: SCIENTIFIC using the delivery method of NON-INTERACTIVE DISTANCE. This approval is valid in jurisdictions which recognize AAVSB RACE.

Joint Pathology Center
Veterinary Pathology Services

WEDNESDAY SLIDE CONFERENCE 2019-2020

C o n f e r e n c e 3

Dr. Corrie Brown, DVM, PhD, Diplomate ACVP
Josiah Meigs Distinguished Teaching Professor
University Professor
Department of Pathology
University of Georgia College of Veterinary Medicine
2200 College Station Road Athens, GA, 30602

CASE I: W343-12 (JPC 4020435).

Signalment: Pigeon (*Columba livia*), age and sex unknown

History: An onset of high mortality affecting pigeons occurred in Victoria (Australia) in 2011. Clinical presentations in affected birds were lethargy, sudden death or neurological signs not further specified. Hundreds of birds were subsequently investigated, including racing pigeons, feral pigeons, domestic and commercial poultry and native birds of many species.

Gross Pathology: All the affected pigeons had diffuse pale and enlarged kidneys. The majority of birds also had enlarged spleens and grey mottled discoloration of the pancreas.

Laboratory results: Initial PCR testing for Newcastle Disease (APMV-1) was positive. Virus isolation and sequencing showed the virus to be the virulent strain of APMV-1. lmmunohistochemistry for paramyxovirus showed widespread immunoreactivity in the kidneys and in many cases pancreatic and splenic positivity were also observed.

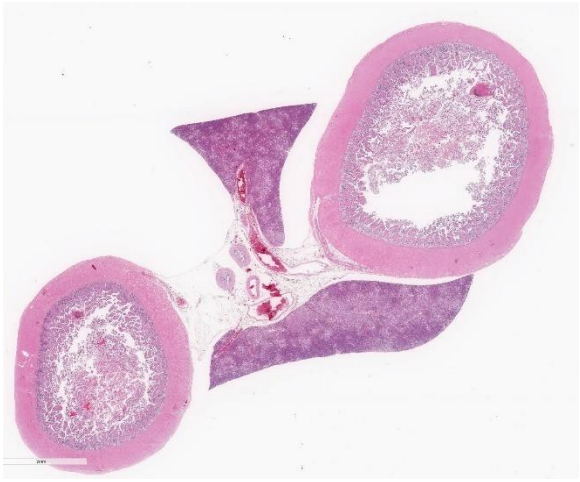

Pancreas and intestine, pigeon. Up to 50% of the pancreatic tissue is replaced by multifocal to coalescing areas of pallor (necrosis). (HE, 9X)

Microscopic Description: Pancreas: Multifocally and randomly distributed throughout the parenchyma there are numerous variably sized necrotic areas, characterized by disruption of normal architecture and stromal collapse, loss of cellular detail and accumulation of amorphous necrotic material, cellular debris and fibrin. There are scattered lymphocytes and plasma cells within the necrotic areas.

Small intestine: in the lamina propria of the mucosa there are small numbers of inflammatory cells, predominantly composed of lymphocytes and plasma cells. Not all slides: in the intestinal lumen there are few cross and longitudinal sections of nematode parasites, characterized by external cuticle, digestive tract, reproductive tract containing eggs with bipolar plugs, and hypodermal bacillary bands (consistent with *Capillaria* sp.).

Contributor's Morphologic Diagnoses:
1. Pancreatic necrosis, multifocal, acute, severe, pancreas, pigeon (*Columba livia*)
2. Mild, chronic, diffuse lymphoplasmacytic enteritis with intraluminal nematode parasites, consistent with *Capillaria* sp., small intestine, pigeon (*Columba livia*)

Contributor's Comment: The clinical, pathological and laboratory findings in this case are consistent with infection with avian paramyxovirus 1 (APMV-1). APVM-1 or Newcastle Disease Virus (NDV) belongs to the family of Paramyxoviridae, genus Avulavirus [1]
Different strains and isolates of NOV cause quite distinct clinical signs and severity of disease, even in the same host species. Based on the disease produced in chickens under laboratory conditions, NOV isolates have been placed in five pathotypes:

- viscerotropic velogenic, NOV strains that cause a highly virulent form of disease in which hemorrhagic lesions are characteristically present in the intestinal tract;
- neurotropic velogenic, NOV strains that cause high mortality following respiratory and nervous signs;
- mesogenic, NOV strains that cause respiratory and sometimes nervous signs with low mortality;

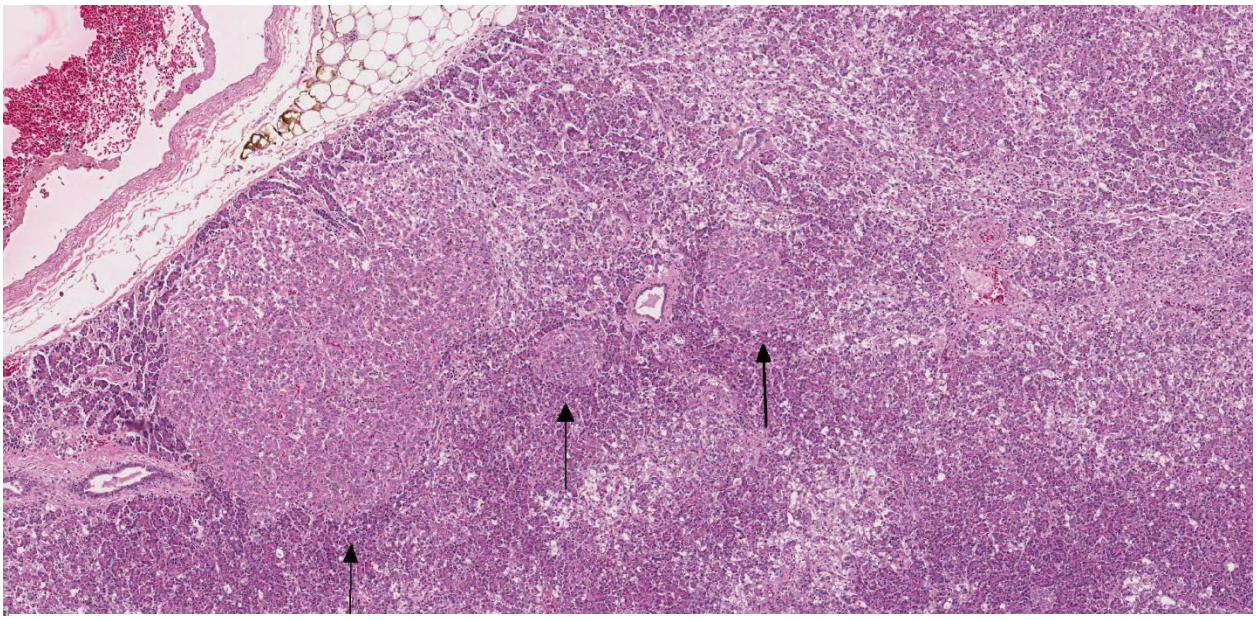

Pancreas, pigeon. Areas of necrosis are largely confined to acinar tissue, largely sparing islets (arrows). (HE, 95X)

- lentogenic, NOV strains that cause mild or unapparent respiratory infections;
- asymptomatic enteric, NOV strains that cause unapparent enteric infections.

However, such groups should be regarded only as a guide because there is always some degree of overlap and some viruses are not easily placed in a specific pathotype.[8]

Newcastle Disease (ND) is mainly a disease of poultry but NDV infections have been established in at least 241 species from 27 of the 50 orders of birds. All birds are probably susceptible to the infection, but the disease observed with any given virus may vary enormously from one species to another. Infection with NDV has been reported to infect animals other than birds, ranging from reptiles to humans.[1] APVM-1 has been responsible for outbreaks in pigeons in Africa, Middle East, Europe, Japan Canada and United States.[1] The variant nature of the virus enabled unequivocal demonstration of infection with this strain and for pragmatic purposes it became known as PPMV-1, although if this virus infects poultry, including pigeons reared for food, it fulfills the definitions of notifiable ND currently in use by the OIE.[2] Infection of feral and domestic pigeons with APMV-1 has been reported for the first time in Australia in August 2011.

In pigeons, neurological signs, such as torticollis, disturbed equilibrium, pecking aside seeds, paresis of wings or feet, and digestive symptoms (watery to hemorrhagic diarrhea) are frequently observed but respiratory signs are usually absent. Atypical digestive forms are being seen increasingly frequently and consist of persistent diarrhea without neurological signs.[1] The major clinical presentation in pigeons from the Australian outbreak were sudden death or neurological signs not further specified. Some of the birds submitted alive for euthanasia and autopsy had head tilt and/or ataxia.

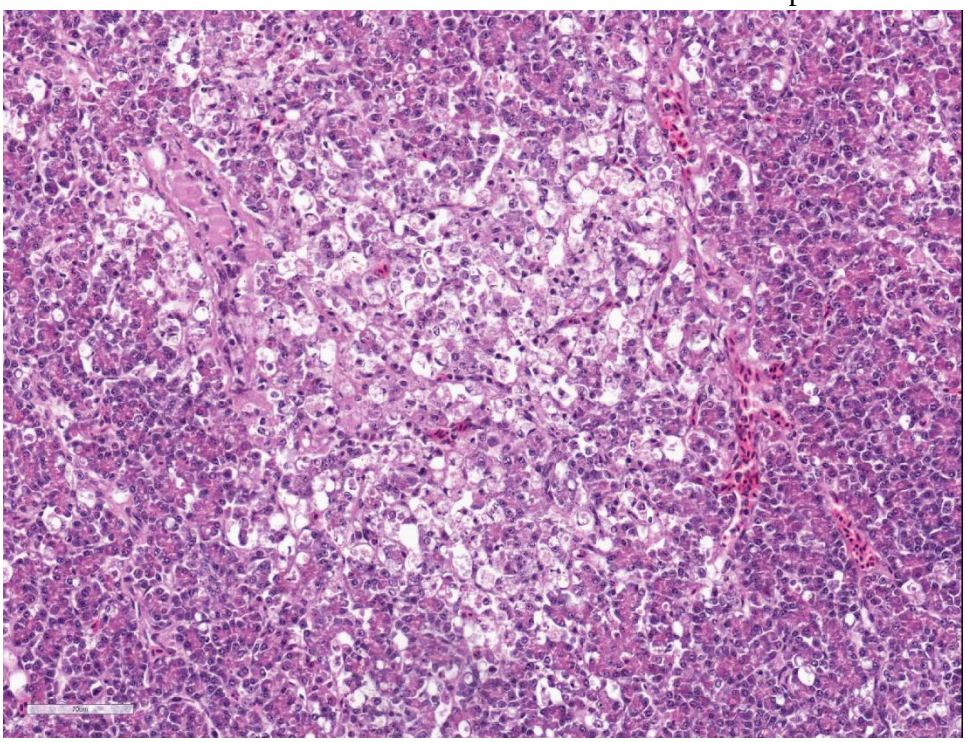

Pancreas, pigeon. In areas of necrosis, there is loss of acinar architecture with areas vacuolation and fragmentation of acinar cells and pyknosis. (HE, 313X)

Histologically, the main lesions were in the pancreas and kidney. Pancreatic necrosis was invariably present in all the pigeons examined, occasionally associated with a lymphoplasmacytic infiltrate. Renal lesions were

characterized by acute tubular necrosis, sometimes associated with a lymphoplasmacytic inflammation. Although behavioral and neurological disease was usually the presenting sign where sudden death had not intervened, histological lesions in the brain were rare and, where present, mild, limited to a mild lymphocytic infiltrate in the meninges. Similar lesions were described in the outbreaks previously reported in pigeons in Canada, United States and Europe; the lesions most commonly encountered were focal non-suppurative meningoencephalitis, lymphoplasmacytic infiltration in liver, pancreas and lung, multifocal hepatic necrosis, pulmonary congestion, piecemeal pancreatic necrosis, interstitial lymphoplasmacytic nephritis and tubular necrosis.[3,6]

In pigeons, experimental inoculation with the pigeon variant of PPMV-1 produced histological changes consistent with those we found in naturally infected pigeons, including pancreatic necrosis as well as necrotizing enterocolitis, necrotizing hepatitis with periportal hepatitis, pulmonary hemorrhage, tracheitis, and perivascular cuffing in the brain.[8]

The cases of PMV-1 infection in pigeons documented in the present report were not linked to any known Newcastle disease outbreaks in commercial poultry. The source of infection is not known, but in the previous European and Californian outbreaks the racing activities were the main means of transmission.[2,3]

Contributing Institution:
Faculty of Veterinary Science, University of Melbourne, Australia
www.vet.unimelb.edu.au

JPC Diagnosis: 1. Pancreas: Pancreatitis, necrotizing, random, multifocal to coalescing, moderate.
2. Small intestine: Enteritis, ulcerative, multifocal, mild.
2. Small intestine, lumen: Few adult adenopharsid (aphasmid) nematodes.

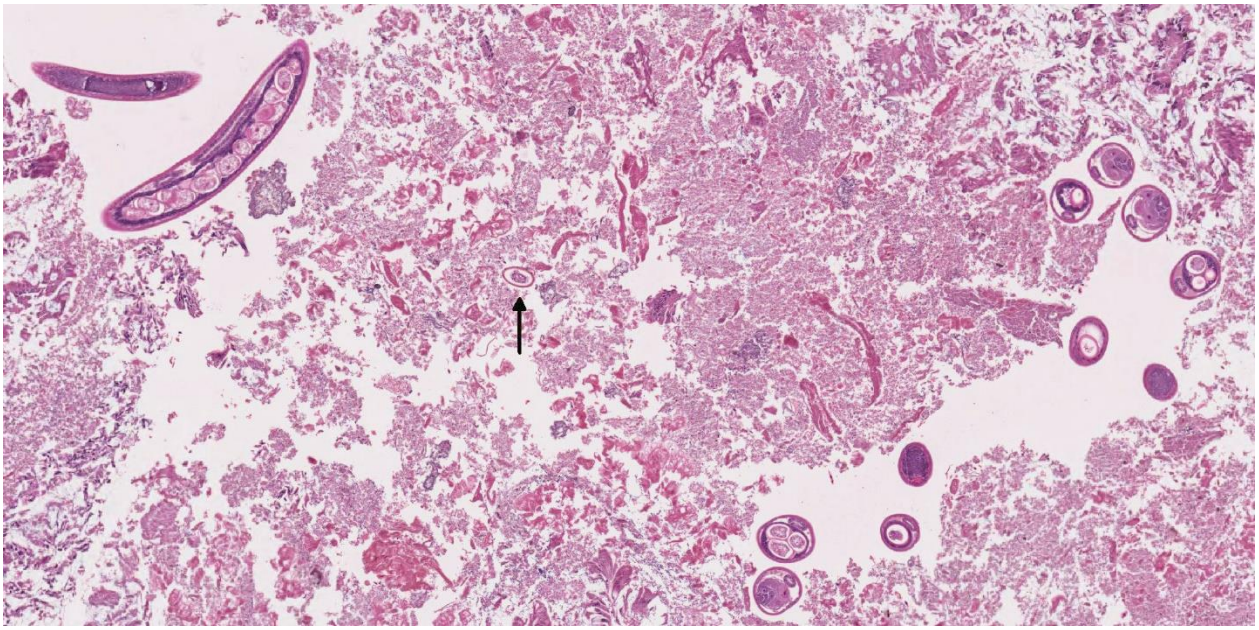

Intestine, pigeon. The lumen of the intestine contains cross sections of adult nematodes and rare eggs with bipolar plugs.

JPC Comment: Newcastle disease is a constant threat to the poultry industry worldwide, and the importance of not only recognizing its clinical signs, but also the pathogenesis and infection kinetics of this virus cannot be overestimated. This Tier 1 USDA Select agent has been reclassified from its previous genus Rubulavirus to a new genus of Avulavirus (which includes the previous rubulaviruses which infect birds). OIE reporting is required for velogenic and mesogenic viruses, and these strains are endemic in Asia, Africa, the Middle East and parts of Central and South America. An ongoing outbreak continues in California arising from backyard flocks (a similar outbreak spilled over into commercial poultry in California in 2003, resulting in losses of over three million birds and a cost of over $120 million).[4]

In addition to the infectious threat posed by illegal importation of backyard fowl in the US, several wild bird species pose a reservoir threat for virulent strain, including pigeons and doves, and waterfowl such as double-crested cormorants and swans, and upland game birds (pheasants and partridges)[5]. Most cases of Newcastle disease in pigeons are the result of pigeon-specific strains, denoted as pigeon paramyxovirus-1 (in order to differentiate them from the rest of the avulaviruses that infect birds.[5] Pet psittacines, including parrots, conures, budgerigars, and conures also develop neurologic disease after NDV infection, and a psittacine isolate was responsible for an outbreak of NDV in California in 1971.[5]

Strains of NDV virus have also been identified in wild anseriformes, shorebirds, and gulls, but not virulent fusion protein sequences have been identified.[4] Interestingly, bird surveys in many countries have found vaccine strain virus (lentogenic forms of the virus are often used in vaccination programs), which leads to concern that passaging through wild bird species may result in reversion to a more virulent strain. This particular event has occurred in poultry resulting in a 1998 outbreak in Australia, but not yet in wild birds.[4]

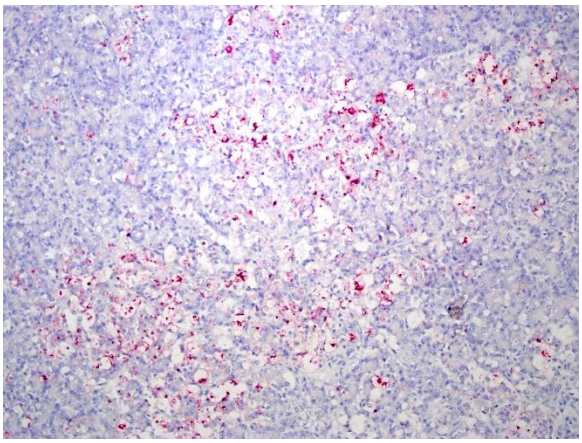

Small intestine, pigeon. Villi show extensive immunopositivity for avian paramyxovirus antigen within remnant epithelium as well as mesenchymal and inflammatory cells within affected villi. (anti-NDV, 400X) (Photo courtesy of: Dr. Corrie Brown, UGA Department of Veterinary Pathology).

Backyard fowl are a special problem to the biosecurity of our nation's poultry as a result of poor vaccination practices as well as their mobility. While all most all birds produced by the commercial industry receive one or more NDV vaccines during their lifetime (more long-lived birds like broiler-breeders may receive 3 or more vaccinations), estimates are that less than 10% of backyard birds are vaccinated,[4] and their exposure to other unvaccinated birds and potential wild reservoir birds makes the potential for an outbreak of mesogenic or velogenic NDV highly likely in this country.

Another area of concern is the minimal mutation required for transformation of an avirulent NDV into one of high virulence. The NDV genome encodes for 6 structural proteins – nucleocapsid protein,

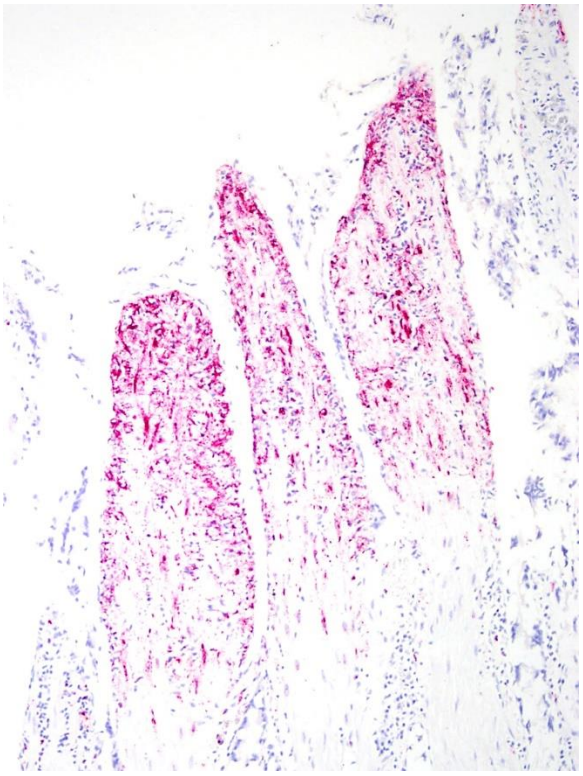

Pancreas, pigeon. Necrotic pancreatic cells and infiltrating inflammatory cells demonstrate strong immunopositivity for avian paramyxovirus. (anti-NDV, 400X) (Photo courtesy of: Dr. Corrie Brown, UGA Department of Veterinary Pathology).

phosphoprotein, a matrix protein, a fusion protein, a hemagglutinin-neuroaminidase protein, and an RNA polymerase. Virulence has been attributed to amino acids at the cleavage site on the fusion protein, with three or more lysine or arginine residues starting at position 133 and a phenylalanine residue at 117 are common to all virulent strains of the virus. Hence, mutations resulting in this particular lineup of amino acid residues in the fusion protein may potentially give rise to new and virulent strains of the virus.[4]

On a somewhat lighter note, Newcastle disease received its name from the second documented outbreak of Newcastle disease which occurred in Newcastle-on-Tyne, England in 1927. A previous outbreak in Java (the Dutch East Indies at the time) did not result in the disease being called "Dutch East Indies chicken fever" or some other appellation, presumably as public relations experts were not in great numbers in Indonesia at the time. It has been theorized that an even earlier outbreak of Newcastle Disease may have occurred in South Uist on the Outer Hebrides islands (where cormorants are occasionally shot and consumed by the inhabitants – with the offal presumably tossed out on the ground). An outbreak of this type was memorialized in the Gaelic poem "Call nan Cearc" (The Loss of the Hens) written by John Campbell in 1898.[7]

The moderator reviewed the disease causes by pigeon paramyxovirus, an avuloviral disease first identified in the 1980s which has spread around the world, largely as a result of racing pigeon enthusiasts and the mobility of their charges. The virus, belonging to the same family as NDV is not particularly pathogenic for poultry, although if it has a high intracerebral pathogeneicity index (a measurement of pathogenicity for NDV), it can halt trade.

The moderator also perfomed an immunohistochemical study on the stlide, using an anti-NDV antibody. The amount of staining within small intestinal villi was surprising, as attendees obviously misinterpreted much of the necrosis in this tissue as autolysis.

As a final note, the class Aphasmidia (to which *Capillaria* belongs), has recently been renamed Adenophorasda.

References:

1. Alexander DJ. Newcastle Disease and other avian Paramyxoviruses, Rev Sci Tech Off Int Epiz 19(2): 443-462, 2000
2. Alexander DJ: Newcastle disease in the European Union 2000 to 2009. Avian Pathol 40:547-58, 2011

3. Barton JT, Bickford AA, Cooper GL, Charlton BR, Cardona CJ: Avian Paramyxovirus Type 1 Infections in Racing Pigeons in California. I. Clinical Signs, Pathology, and Serology. Avian Dis Apr-36(2):463-8, 1992.
4. Brown VR, Bevins SN. A review of virulent Newcastle disease viruses in the United States and the ole of wild birds in viral persistence and spread. *Vet Research* 2017; 48:68-83.
5. Cattoli G, Susta L, Terregino C, Brown C. Newcastle disease: a review of field recognition and current methods of laboratory detection. *J Vet Diagn Invest* 2011, 23(4): 637-656.
6. Johnston KM and Key WO. Paramyxovirus infection in feral pigeons (*Columba livia*) in Ontario. Can Vet J 33: 796-800, 1992
7. MacPherson L.W. Some observation on the epizootiology of Newcastle Disease*Can J Comp Med* 1956; 20(5):155-168.
8. Pearson JE, Senne DA, Alexander DJ, Taylor WO, Peterson LA, Russell PH: Characterization of Newcastle disease virus (avian para-myxovirus-1) isolated from pigeons. Avian Dis. 31: 105-111, 1987.

CASE II: 14-102 (JPC 4048789).

Signalment: 8-month-old purpose-bred Dorset cross ewe (*Ovis aries)*

History: Received from supplier 17 days before euthanasia. Vaccinated for CD&T, pasteurellosis and orf 6 months previously. Negative Q fever serology. Dewormed with an avermectin at time of shipping. Eleven days after arrival she developed a 5 cm diameter subcutaneous abscess of the cranioventral neck near the angle of the mandible. FNA was performed and a sample was submitted for culture. The next day the abscess had ruptured and incompletely drained. When culture results were received, the decision was made to euthanatize.

Lymph node, sheep: There is a fibrous subcutaneous swelling at the angle of the jaw. (Photo courtesy of: Department of Comparative Medicine, Penn State Hershey Medical Center, http://www.hmc.psu.edu/comparativemedicine/)

Gross Pathology: At necropsy there was a firm fibrous subcutaneous swelling at the angle of the right mandible with a cutaneous scab. The left submandibular lymph node was firm (fibrosis) and exuded thick green material on cut section. There were several small (2-5 mm) tan nodules in the lungs and liver.

Laboratory results: Gram Stain of FNA: Large numbers of gram-positive rods.
Aerobic culture of abscess (PADLS PVL): Heavy growth of *Corynebacterium pseudotuberculosis*.

Microscopic Description: The lymph node is partially effaced by one large or several coalescing discrete, incompletely encapsulated pyogranulomas with a large central core of abundant necrotic cellular debris and degenerate neutrophils with numerous coarse basophilic refractile

Lymph node, sheep: When incised, the swelling exuded a green tenacious exudate. (Photo courtesy of: Department of Comparative Medicine, Penn State Hershey Medical Center, http://www.hmc.psu.edu/comparativemedicine/)

mineralized concretions. This is surrounded by a layer of moderate numbers of epithelioid and foamy macrophages with occasional multinucleate giant cells, mostly of the Langhans type. Peripheral to this are moderate to large numbers of plasma cells with fewer lymphocytes and macrophages, and rare Mott cells. There is abundant nascent (immature) and mature fibrosis circumscribing the lesion. The lymph node is mildly reactive with pale germinal centers, paracortical lymphoid hyperplasia, and medullary sinus plasmacytosis.

Similar pyogranulomas were present in the liver and lungs (tissue not submitted), often with prominent eosinophil infiltration.

Contributor's Morphologic Diagnosis:
Lymph node, left submandibular, pyogranuloma, focally extensive, chronic, moderate with mineralization

Contributor's Comment: Caseous lymphadenitis is a disease of small ruminants caused by infection with *Corynebacterium pseudotuberculosis* (*C. ovis*).[1,5] The agent is so named for the gross and histologic similarity of the pyogranulomas to those of tuberculosis, including mineralization and caseation. The organism generally gains entry through cutaneous wounds (often related to shearing or castration), although none were present in this case. Given the lesion location, infection via a wound in the oral cavity is likely. Organisms localize in the local draining lymph node. Infections can also spread internally, commonly to the lungs (as in this case), making this animal unsuitable for research purposes. The organism can survive intracellularly within macrophages due to a leukotoxic surface lipid, and infections tend to be persistent but subclinical. The characteristic green color of the gross exudate is imparted by the accumulation of eosinophils in the lesions. Inspissation of the exudate over time produces the classic lamellated cheesy material.

Corynebacterium pseudotuberculosis is a pleomorphic, gram-positive, non-motile, facultatively anaerobic member of the *Actinomycetaceae*.[1,3] Members of this group are notable for the mycolic acid content of the cell walls and prolonged environmental persistence. *Corynebacterium pseudotuberculosis* is closely related to *C. diptheriae and C. ulcerans.* There are two biochemically and genetically distinct biovars of *C. pseudotuberculosis,* biovar *ovis* (biotype 1) and biovar *equi* (biotype 2). The former is typically a pathogen of small ruminants and does not reduce nitrate; the latter is more commonly a pathogen of cattle and horses and does reduce nitrate. Infections in horses include pigeon fever (skeletal muscle abscesses) and ulcerative lymphangitis.[4] Virulence factors for this

organism include phospholipase D, a sphingomyelin-specific phospholipase, as well as mycolic acids within the cell wall.

Differential diagnosis for this case would include *Trueperella (Arcanobacterium) pyogenes*, *Staphylococcus aureus* (botryomycosis), *Actinobacillus lignieresii*, and *Mycobacterium bovis*. Gram positive organisms of veterinary importance can be remembered by the acronym SCRAMBLED SCENT, encompassing the genera:

- *Staphylococcus*
- *Clostridium*
- *Rhodococcus*
- *Actinomyces*
- *Mycobacterium*
- *Bacillus*
- *Listeria*
- *Erysipelothrix*
- *Dermatophilus*
- *Streptococcus*
- *Corynebacterium*
- *Enterococcus*
- *Nocardia*
- *Trueperella*

Subcutaneous reactions tocClostridial vaccines, particularly around the neck or scapula, can also be mistaken for CLA.

Contributing Institution:
Department of Comparative Medicine
Penn State Hershey Medical Center
http://www.hmc.psu.edu/comparativemedicine/

JPC Diagnosis: Lymph node: Pyogranuloma, focal.

JPC Comment: The contributor gives a concise review of *Corynebacterium pseudotuberculosis* infection in small ruminants. This gram-positive facultative intracellular pathogen, which may exhibit pleomorphism in tissue, such as coccoids and filamentous rods,[2] is best known for abscess formation in small ruminants, also affects a wide range of other species, including horses (as previously mentioned), cattle, camelids, deer, and humans. The bacterium was first identified by the French bacteriologist Edward Nocard from a cow, and three years later, by the Bulgarian Hugo von Priesz from a ewe.

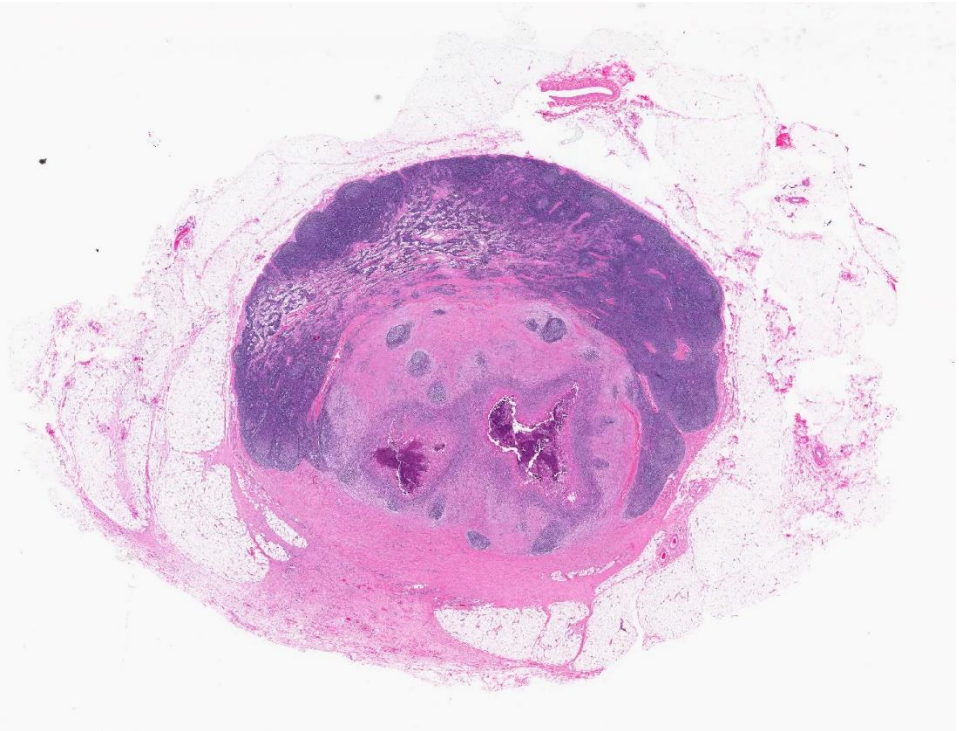

Lymph node, sheep: Approximately 50% of the node is effaced by a large abscess with a core of lytic material and a thick capsule. (HE, 5X)

For the next thirteen, it was referred to as the "Priesz-Nocard" bacterium, whereupon it was renamed *Bacillus pseudotuberculosis* in the atlas by prominent German bacteriologists Lehman and Neuman. In the 1923 first edition of Bergey's *Manual of Determinative Bacteriology* it was placed in the genus of *Corynebacterium,* where it remains today. It was at that time called *Corynebacterium ovis*, but after discovered to cause infection in a number of species, reverted back to *C. pseudotuberculosis* in 1948, by the sixth edition of that manual.[1]

In sheep, infection usually follows wound infection, and at shearing time, infected abscesses may be punctured, bacterial liberated in a common dip tank, and the bacterium may invade shearing wounds on other sheep or even penetrate intact skin. In addition to direct contact, the disease may also be spread by sheep with established respiratory infections coughing on the open wounds of penmates.[2] If the bacteria are not confined to and eliminated from the skin, the infection may progress to draining nodes.[6] Mature abscesses in the lymph nodes of sheep may achieve a greenish lamellated "onion-skin appearance" due to recurrent and alternating episodes of suppuration and encapsulation; in goats, the abscesses tend to demonstrate a more liquefied appearance. When the infection reaches the lymph nodes, the condition is considered persistent and lifelong.[1]

In sheep, especially older sheep, the infection may progress from peripheral lymph nodes to internal nodes or organs, especially the lungs, resulting in chronic systemic disease referred to as the "thin ewe syndrome" (apparently more common in the US than in other countries)[1]. The presence of abscesses within

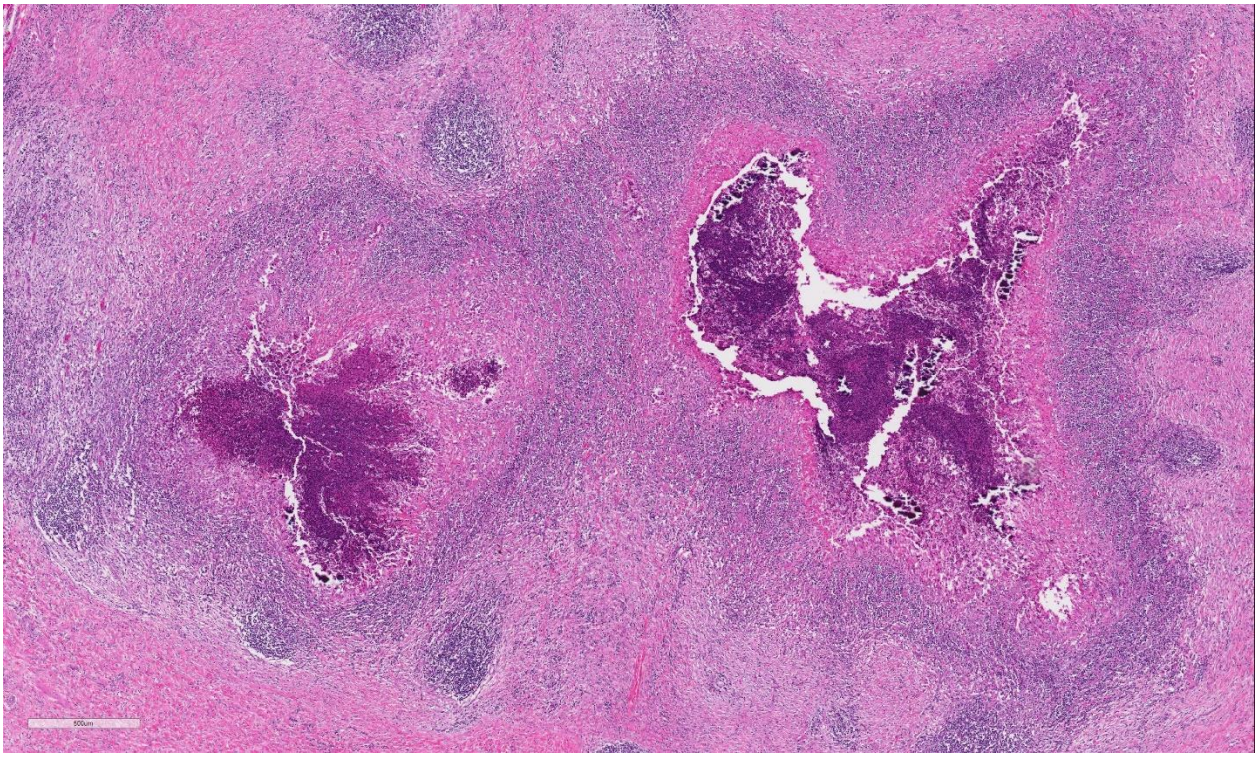

Lymph node, sheep: Higher magnification of the necrotic core of the abscess. Lymphoid aggregates are scattered throughout the abscess wall. (HE, 45X)

nodes and carcass meat generally results in condemnation, which, in countries which utilize lamb for religious celebration, may result in a loss of $200 per animal to the purveyor. Many countries have strict importation guidelines regarding contamination of small ruminants with this bacterium. The importance of CLA vaccination is exemplified by the decrease in CLA in Australia alone - in 1973, CLA among sheep in Western Australia was estimated at 58%; following introduction of a CLA vaccine in 1983, similar studies recorded a prevalence of 45%, which in turn dropped to 20% in 2002.[1]

In goats, lesions are more often severe, and abscesses tend to cluster in the nodes of the face and neck. The liquid nature of abscessed nodes is reminiscent of melioidosis (*Burkholderia pseudomallei* infection) in this species.[6] Other lesions associated with *C. pseudotuberculosis* in sheep and goats include mastitis (presumably resulting from local spread from abscessed supramammary nodes)[1] and polyarthritis in young lambs, but overall, the disease is rarely fatal, even in prolonged infection.[6]

Another disease caused by *C. pseudotuberculosis* in the horse is equine folliculitis and furunculosis (also referred to as equine contagious acne, , equine contagious pustular dermatitis and Canadian horsepox. It is most often seen at points of contact with tack in animals with pre-existent seborrheic dermatitis, and likely represents secondary invasion by bacteria spread on contaminated tack.[1]

The moderator, who did her PhD studying this agent, reviewed the various pathogenic factors which allow it to cause disease in a range of ruminants and horses. Like other higher bacteria, the presence of mycolic acid in the wall of the bacterium, which allows it

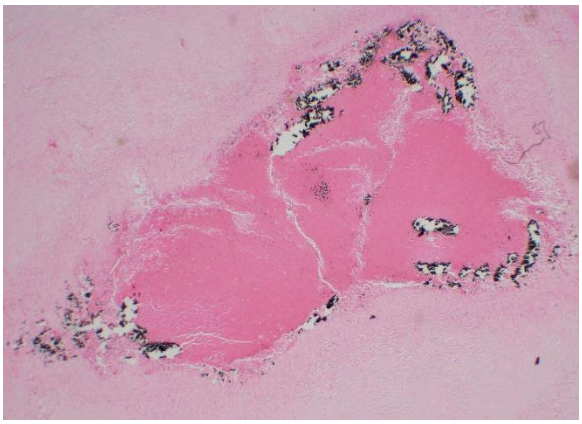

Lymph node, sheep: A Von Kossa stain highlights the mineral within the lesion. (von Kossa, 20X)

to resist digestion in phagocytes also lends a unique property to colonies in culture – the ability to slide easily across the plate, known as "shuffleboard colonies". Another virulence factor, phospholipase D, is important for tissue invasion. In sheep and goats, phospholipase D allows the bacteria to invade through sphingomyelin-containing endothelium, allowing for extensive intravascular spread of the bacterium. In the biovar infecting horses, the bacterium do not possess sufficient phospholipase D for intravascular spread, and must be introduced in a wound, resulting in a slow progressive lymphangitis.

The moderator also described the synergistic hemolysis-inhibition titers (with a rather rude acronym) which were used in the 1980s for diagnosis of occult infection of *C. pseudotuberculosis* in small ruminants in Brazil. The synergistic hemolysis-inhibition test detects antibodies to an exotoxin of *C. pseudotuberculosis* by the inhibition of a synergistic hemolysis between the toxins of *C. pseudotuberculosis* and *R. equi.*

References:

1 Baird GJ, Fontaine MC: Corynebacterium pseudotuberculosis and its role in

ovine caseous lymphadenitis. *J Comp Pathol* 2007:137(4)**:**179-210.
2. Dorella FA, Pacheco LGC, Oliveira SC, Miyoshi A, Azevedo. *Corynebacterium pseudotuberculosis:* microbiology, biochemical proterties, pathogenesis and molecular studies of virulence. *Vet Res* 2016; 17:201-218.
3 Soares SC, Silva A, Trost E, Blom J, Ramos R, Carneiro A, et al.: The pan-genome of the animal pathogen Corynebacterium pseudotuberculosis reveals differences in genome plasticity between the biovar ovis and equi strains. *PLoS One* 2013:8(1)**:**e53818.
4 Valentine BA, McGavin MD: Skeletal Muscle. In: McGavin MD, Zachary JF, eds. *Pathologic Basis of Veterinary Disease, Fourth Ed.* St. Louis, MO: Elsevier; 2007: 973-1039.
5 Valli VEO: Hematopoietic System. In: Maxie MG, ed. *Jubb, Kennedy, and Palmer's Pathology of Domestic Animals*. Fifth ed. Edinburgh: Saunders Elsevier; 2007: 107-324.
6. Valli VEO, Kiupel M. Bienzle D. In. Maxie MG, ed. *Jubb, Kennedy, and Palmer's Pathology of Domestic Animals.* Sixth ed. Edinburg: Saunders, Elesevier, 2016, pp 204-208.

CASE III: 2019B (JPC 4134828).

Signalment: Pig, *Sus scrofa domesticus*, LWD, 8-weeks-old, female

History: This is one of two experimental cases of pigs infected with classical swine fever virus (CSFV). This case was intraorally inoculated with 1mL of $10^{6.5}TCID_{50}$/mL of a strain of CSFV. Clinical signs of the animal were observed and total leukocytes in the whole blood of the pig were counted daily for 2 weeks. Clinical samples of the heparinized hole blood, sera, saliva, nasal swab and feces were collected for the detection of the virus gene by RT-PCR analysis.

The pigs inoculated with CSFV showed fever and abolition of appetite from 4 days post infection (dpi) and developed reddened skin lesion in hindlegs and conjunctivitis at 14 dpi. The pig was euthanized at 14 dpi.

Gross Pathology: In the pig infected with CSFV, multifocal infarction of the margin of the spleen was observed. Mild hyperemia on the brain was seen in the pig. Hemorrhagic lymph nodes in the pig were appeared. Button ulcers in the colon was find in the pig. There were no pathological findings in the respiratory organs in the pig.

Laboratory results: The body temperature of this CSFV inoculated pig was over 40^{o}C from 4 to 14 dpi. The decrease of leukocyte counts in blood (under 10,000 cells/µl) were also confirmed from 3 to 14 dpi. The viral RNA was detected from the blood samples from 4 dpi and from saliva, nasal swab and feces from 5 dpi in the pig.

Spleen, pig. Two sections of spleen are presented for examination. A large area of congestion and hemorrhage (peripheral infarct) is present in the bottom section. (HE, 7X)

Microscopic Description: Spleen: There were multifocal necrosis with hemorrhage, karyopyknosis and karyorrhexis in the red pulp. The lumen of some blood vessels was dilated and was occluded by a fibrin thrombus. Necrosis of arterial walls were occasionally observed; however, vasculitis was not prominent. The stromal and parenchymal cells in the wedge-shaped margin of the spleen was replaced by extravascular erythrocyte accumulation. The remaining stromal cells in that area showed necrosis with karyopyknosis and karyorrhexis (hemorrhagic infarction).

The white pulp in the adjacent parenchyma is of markedly reduced cellularity (lymphoid depletion) and almost of lymph follicles were atrophic.

Contributor's Morphologic Diagnosis:

1. Spleen, red pulp: Multiple fibrin thrombosis with hemorrhagic infarction, multifocal necrosis, moderate.
2. Spleen, white pulp: Lymphocyte depression, diffuse, severe.

Contributor's Comment: We confirmed that the characteristic lesion of multifocal infarction of the margin of the spleen arises following inoculation with CSFV by intraoral inoculation. The histological lesion of hemorrhagic infarction was reproduced experimentally; however, vasculitis was not prominent in this case, suggesting this case was in an early stage of an infection of CSFV.

Classical swine fever (CSF) is a highly contagious viral disease induced by CSFV of the genus *Pestivirus* in the family *Flaviviridae*.[3] This disease is widely distributed in the world including Asian countries. CSFV is classified into three genotypes (1, 2 and 3) and several subgenotypes (1.1–1.4, 2.1–2.3, and 3.1–3.4).[4,7] In East and Southeast Asia, several genotypes or subgenotypes of CSFV isolates including 1.1, 2.1-2.3 and 3.4 have been identified.[1,5] The virulence of the CSFV ranges from highly virulent with almost 100% mortality, to avirulent. The severity also depends on the condition of host animals including age, breeds and health status.[2]

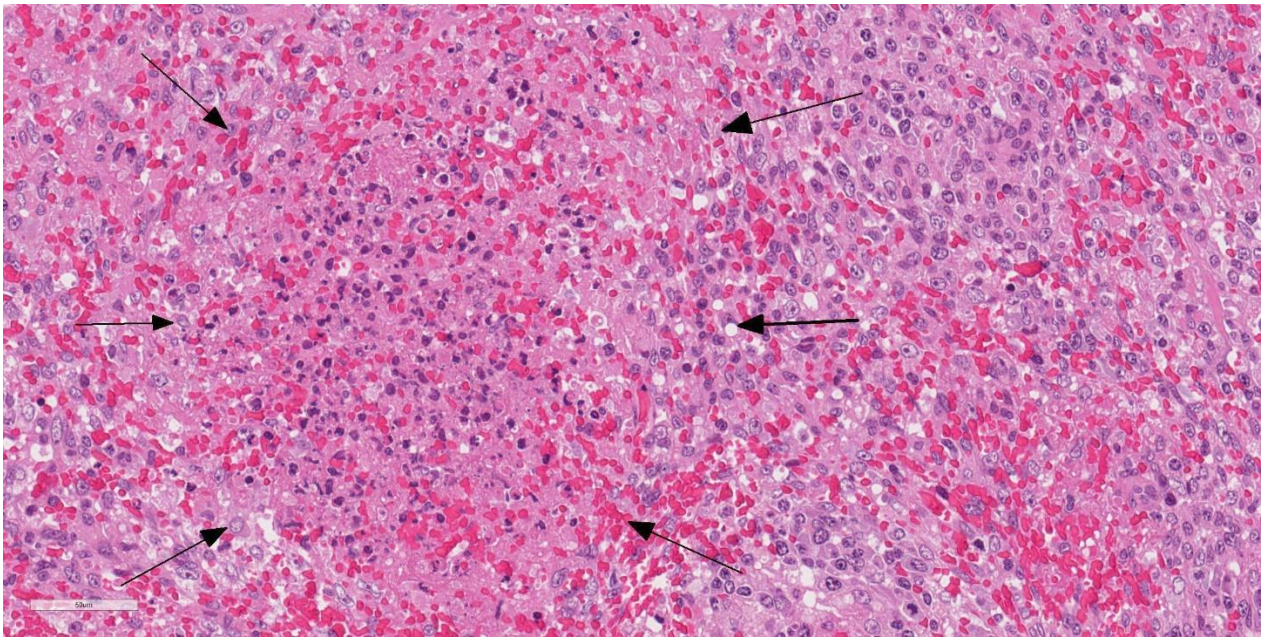

Spleen, pig. Within the red pulp, there are multifocal areas of lytic necrosis and fibrin deposition. (HE, 400X)

In the present experiment, the infected pigs developed clinical signs of lethargy, anorexia, reddish dermal macula and conjunctivitis. These clinical symptoms were quite mild, and the pig did not die within 2 weeks of the experimental period. These results suggest that the virulence of the CSFV used in this study is considerably lower than a high virulent strain of CSFV.[2]

Splenic infarction is considered pathognomonic for CSF.[2] Macrophage-driven cytokine storms following infection of CSFV play an important role of the pathogenesis of splenic infarctions in CSF. [2] A marked increase in macrophage/monocyte-derived pro-inflammatory cytokines such as TNFα, IL-1, and IL-6 is suggested to be the main mediator of systemic endotheliotoxicity. These cytokines induce endothelial swelling, followed by degeneration and necrosis of endothelial cells and fibrinonecrotizing vasculitis.[13] The formation of arterial infarcts at the multifocal sites of vasculitis within the spleen leads to vascular occlusion followed by ischemic necrotic cell death of the dependent parenchyma. A single splenic arterial supply with minimal anastomoses is an important predisposing factor for infarction in the spleen.[6] This infarction area is rapidly followed by hemorrhage from damaged blood vessels and inflow of erythrocytes from the surrounding parenchyma with intact perfusion leading to the commonly illustrated hemorrhagic infarcts.[6]

Severe lymphocyte depression is also common in the splenic white pulp of the CFSV-infected pigs. In acute stages of infection, CSF is accompanied by severe lymphopenia and resulting immunosuppression as well as granulocytopenia.[2,8,11] The infection of dendritic cells induces secretion of large amount of IFN-α which is a key element in the pathogenesis of CSF. The high serum level of IFN-α is suggested to be the central inducer of dysregulation of the immune system, which manifests as lymphocyte apoptosis, depletion and immunosuppression.[10]

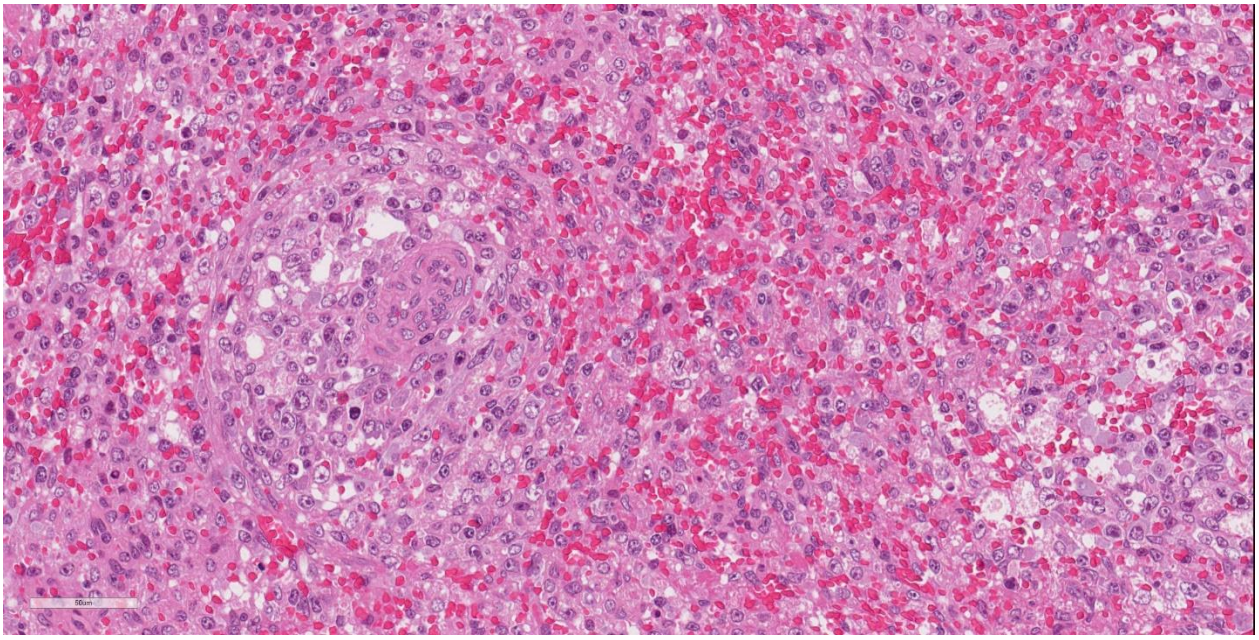

Spleen, pig. Splenic follicles (one at left) are devoid of lymphocytes but replete with macrophages. (HE, 400X)

The acute form of the disease is characterized by atypical clinical signs such as high fever, anorexia, gastrointestinal symptoms, general weakness and conjunctivitis during the first two weeks upon infection of CSFV and then skin lesions including hemorrhages, cyanosis or reddish macula appeared in different areas of the body such as the ear, limbs and ventral abdomen around two to four weeks after infection.[2,9] In this study, this typical skin lesion could find from 14 dpi in the inoculated pig and the clinical appearance was quite difficult to diagnose as CSF in this experimental study. The results in this study showed that the pigs infected with this strain of CSFV excrete viruses into the clinical samples and viral RNAs were detected from the blood samples, especially whole blood samples, from 4 or 5 dpi until at least 2 weeks after infection. Because it is difficult to detect clinical sigms in pigs infected with this strain, the results in this study are significantly valuable to establish countermeasures and diagnostic strategy for CSFVs that has similar characteristics with mild pathogenesis.

Contributing Institution:
3-1-5 Kannondai, Tsukuba, Ibaraki 3050856, Japan
National Institute of Animal Health
http://www.naro.affrc.go.jp/english/laboratory/niah/

JPC Diagnosis: 1. Spleen, margins: Necrosis, multifocal,l moderate, with thrombosis, hemorrhage and fibrin deposition (infarcts).
2. Spleen, white pulp: Lymphoid depletion, diffuse, severe.

JPC Comment: The contributor has done a nice job describing an investigation of the effects of intraoral inoculation of a mildly virulent strain of classical swine fever virus (CSFV). CSFV, a pestivirus in the same family as bovine viral diarrhea virus and border disease virus, is one of the most economically important viruses in the world. While a number of countries have eliminated the virus (United States, Canada, Mexico and many Western European countries), the virus remains endemic in many others, including China, India and many countries in Central and South America. A number of countries that had eliminated CSF have recently seen recurrences in light of a large current outbreak in China.[15]

The disease of classical swine fever is divided into acute and chronic forms. The acute form is also known as the "lethal" form (although both forms end with death of infected pigs) or the "transient" form (another odd choice of name.) In the acute form, clinical signs appear after 4-7 days, and non-specific (referred to as "atypical" signs) clinical signs of fever, pyrexia and gastrointestinal distress are the rule.[2] From 2-4 weeks, more diagnostic signs of including neurologic deficits, paralysis and convulsions appear, and are often accompanied by cutaneous hemorrhage and cyanosis of the extremities and abdomen (the so-called "typical" of classic signs of CSF. Due to the immunosuppression which accompanies CSF (such as seen in the section of spleen submitted in this case), respiratory and gastrointestinal disease may also be present. Infection of pregnant sows may result in abortions, stillbirths, and mummification.[2]

Chronic infections are usually associated with immunotolerant pigs who were infected during gestation. These infections, while prolonged and mostly associated with "atypical" signs, ultimately also result in death of infected animals; albeit with a longer course of several months in which they continually shed high levels of virus in the saliva, urine, feces and other secretions.
Death is often the result of immunosuppression, and affected animals

exhibit marked depletion of lymphoid organs and ulceration of the gastrointestinal tract.[2]

CSF control is based largely on two strategies – comprehensive culling (which is effective in countries which have eliminated the virus), and vaccination, which is practiced in countries in which the CSFV is endemic.[15] While many of these countries now mandate vaccination against CSV, small and medium pig farms (in which help irregular vaccination schedules or the maintenance of immune-tolerant animals) may help to maintain the virus in an endemic state. Vaccination failure may be further impacted by the presence of multiple genotypes in a given area or immunosuppressive coinfections by other viruses include PRRS virus and PCV-2. In some countries, the virus is maintained in the population of wild boars from which it may spill over into the domestic pig population, especially on small farms.[15]

Another potential weapon in the fight to eradicate CSV in endemic areas is the development of virus-resistant animals. Recently, Chinese scientists reported the development of genetically modified pigs using CRISPR-Caspase 9 mediated knock-in technology. Antiviral small haripin RNAS were inserted into porcine DNA at the *Rosa26* locus and transgenic pigs were produced by somatic nuclear transfer. F1-generation pigs were challenged with virulent virus and and developed only minor clinical symptoms and markedly decreased blood levels of virus as compared to non-transgenic controls.[12]

One of the more interesting aspects of this particular slide is the relatively mild changes noted in the splenic arterioles, which rather than a significant vasculitis (which would be expected given the endotheliotropism often exhibited by this virus) exhibited at best a mild vasculopathy with no mural inflammation and rare pyknosis of mural smooth muscle cells and a hint of protein within the wall. A spirited discussion of the usage of the terms vasculitis and vasculopathy for this change in the absence of any significant inflammation failed to yield a clear victor.

To further illustrate the marked lymphoid depletion in this specimen, a JPC-run CD20 highlighted the almost absolute lack of B-cells (a favorite target of CSFV), and a CD3 showed marked depletion of T-cells. An IBA-1 stain showed numerous macrophages, many of which appeared activated.

References:

1. Beer M, Goller KV, Staubach C, Blome S. Genetic variability and distribution of Classical swine fever virus. *Anim Health Res Rev* 2015:16(1):33–39.
2. Blome S, Staubach C, Henke J, Carlson J, Beer M. Classical swine fever-an updated review. *Viruses* 2017; 9(4) E86 doi:10.3390/v9040086.
3. Kirkland PD, Le Potier MF, Vannier P, Finlaison D. Pestiviruses. In: Zimmerman, J. J., Karriker, L. A., Ramirez, A., Schwartz, K. J. and Stevenson, G. W. eds. *Diseases of swine.* 10th ed. West Sussex: John Wiley & Sons; 2012; 538–553.
4. Lowings P, Ibata G, Needham J, Paton D. Classical swine fever virus diversity and evolution. *J Gen Virol* 1996; 77(Pt6):1311–1321.
5. Luo Y, Li S, Sun Y, Qiu HJ. Classical swine fever in China: a minireview. *Vet Microbiol* 2014; 172(1-2):1–6.
6. Mosier DA. Vascular Disorders and Thrombosis. In: Zachary JF, ed. *Pathologic Basis of Veterinary Disease*. 6th ed. St. Louis, Missouri: Elsevier; 2017; 44-72.

7. Paton DJ, McGoldrick A, Greiser-Wilke I, Parchariyanon S, Song JY, Liou PP, Stadejek T, Lowings JP, Björklund H, Belák S. Genetic typing of classical swine fever virus. *Vet Microbiol* 2000; 73(2-3):137–157.
8. Pauly T, König M, Thiel HJ, Saalmüller A. Infection with classical swine fever virus: Effects on phenotype and immune responsiveness of porcine T lymphocytes. *J Gen Virol* 1998; 79(Pt1):31–40.
9. Petrov A, Blohm U, Beer M, Pietschmann J, Blome S. Comparative analyses of host responses upon infection with moderately virulent classical swine fever virus in domestic pigs and wild boar. *Virol J* 2014; 11:134 doi: 10.1186/1743-422X-11-134.
10. Summerfield A, Ruggli N. Immune responses against classical swine fever virus: between ignorance and lunacy. *Front Vet Sci* 2015; 2-10.
11. Susa M, König M, Saalmüller A, Reddehase MJ, Thiel HJ. Pathogenesis of classical swine fever: B-lymphocyte deficiency caused by hog cholera virus. J Virol 1992; 66(2):1171–1175.
12. Xie Z, Pang D, Yuan H et al. Genetically modified pigs are protected from classical swine fever virus. *PLoS 1 Pathog* 2018; 14(2), e1007193.
13. Zachary JF. Mechanisms of microbial infections. In: Zachary JF, ed. *Pathologic Basis of Veterinary Disease*. 6th ed. St. Louis, Missouri: Elsevier; 2017; 132-241.
14. Zhou B. Classical swine fever in China – an update minireview. *Front Vet Sci* 2019; 6:187, 10.3389/fvets.2019.00187.

CASE IV: P17-969 (JPC 4135861).

Signalment: 7 months old, female, Holstein, *Bos taurus*, bovine.

History: The animal was experimentally infected with 10,000 ID_{50} foot-and-mouth disease virus (FMDV A IRN/22/2015) into the tongue. After 24 hours, the animal was euthanized and submitted for necropsy.

Gross Pathology:
Tongue: Multiple oval to round vesicles (aphthae), up to 3 cm diameter were multifocally present at the dorsum of the tongue.
Hoof: Multiple vesicles and pustules were also found on the left hoof within the interdigital space and bulb of the heel.

Laboratory results: None.

Microscopic Description:
Tongue. Expanding within the lingual mucosa, there is a 6.5 mm large, well-demarcated vesicle (vesiculopustule) which contains variable numbers of viable and degenerate neutrophils, erythrocytes, fibrillar beaded eosinophilic material (fibrin) and a low amount of proteinaceous fluid. The

Tongue, ox. The surface of the tongue contains severe discrete vesicles within the mucosa. (Photo courtesy of: Friedrich-Loeffler-Institut, Federal Research Institute for Animal Health, Department of Experimental Animal Facilities and Biorisk Management, Südufer 10, 17493 Greifswald – Insel Riems, Germany. https://www.fli.de)

adjacent epithelial cells are polygonal to round, swollen with hypereosinophilic cytoplasm, basophilic karrhyorectic and pyknotic nuclei (lytic necrosis), and are separated by intercellular edema (spongiosis). Diffusely, the epithelium is infiltrated by a large number of neutrophils, focally obscuring the basal epithelial layer. Predominantly, perivascular, moderate numbers of neutrophils and few macrophages are present within the submucosa and adjacent connective tissue. Endothelial cells are hypertrophic (endothelial activation).

Contributor's Morphologic Diagnosis:
Tongue. Glossitis, vesiculopustular, focal, suppurative, moderate, acute with intramucosal edema, Holstein (*Bos taurus*), bovine.

Contributor's Comment: Foot-and-mouth disease (FMD) is a highly contagious, viral disease of cloven-hoofed animals. The etiologic agent is the FMD virus (FMDV), a picornavirus, of which there are seven known FMDV serotypes: O, A, C, Asia 1, SAT1, SAT2, and SAT3[4,9]. Although FMD outbreaks are often of low mortality rates, morbidity is often high due to the characteristic vesicles within the mouth and on the feet, resulting in profound agricultural production and economic losses[2,9]. Furthermore, the high level of contagiousness of FMD and high tenacity of the FMDV pose a considerable challenge in controlling a disease outbreak.

In the United Kingdom in 2001, an outbreak of FMD resulted in the mass culling of over 6 million cattle and sheep, costing nearly $12 billion.[9] From 2010-2011, three outbreaks occurred in Japan and South Korea, with 3 million pigs, and 100,000 cattle being culled.[9,10] Throughout the FMD endemic regions, outbreaks are frequently reported and ongoing, including (as of June 17, 2019) 6,370 cases in Algeria, 968 in China, 386 in Malawi, 239 in Morocco, 6,391 in Mozambique, 1,200 in Sierra Leone, 1,220 in Zambia, and 2,108 in Zimbabwe[5]. Globally,

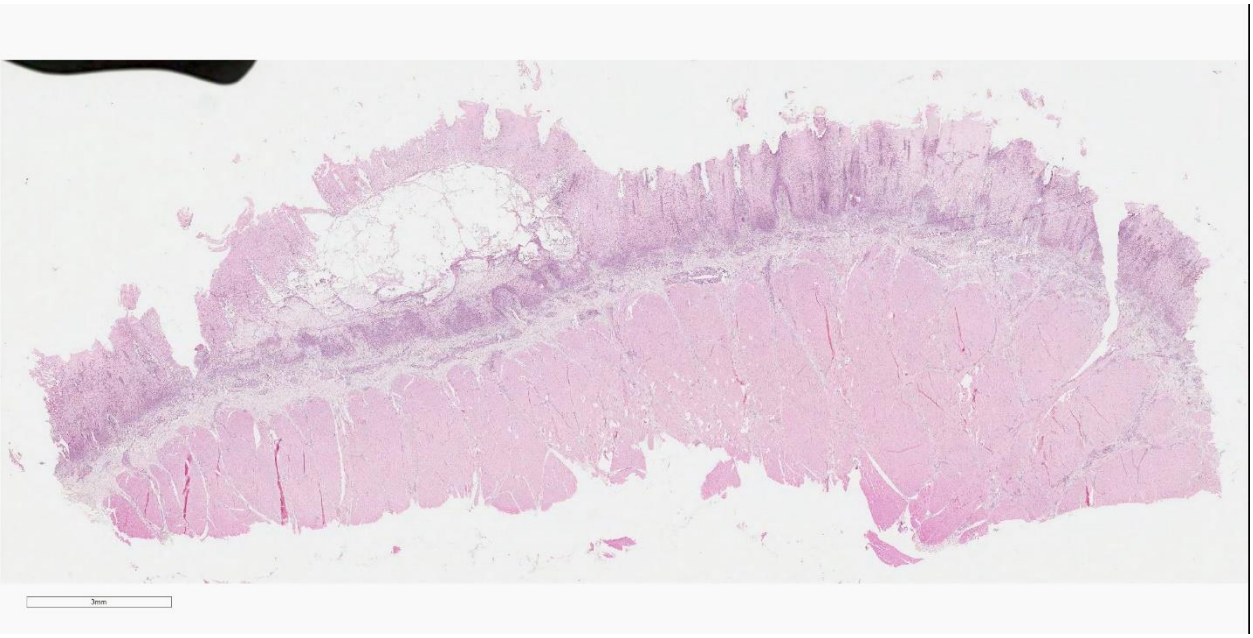

Tongue, ox. A large vesicle undermines approximately one-third of the mucosa. There is diffuse marked infiltration of the mucosa by innumerable neutrophils, largely concentrated at the edges of the vesicle as well as in the basal layers of the mucosa. (HE, 7X)

in the past 5 years (as of June 17, 2019), FMD outbreaks resulted in 376,367 cases, 12,201 deaths, 314,063 culls, with an estimated 3,650,220 animals identified as susceptible[5].

Although FMD constitutes a major global health threat, research into understanding the fundamental mechanisms of disease pathogenesis remains limited due to, in part, the necessary biosecurity and infrastructure to work with FMDV, as well as the diversity of viral serotypes and strains[2]. In general, FMD is designated into three stages: pre-viremia, viremia, and post-viremia[2]. The definitive location of viral entry remains to be elucidated, although the pharynx and larynx appear to be an important anatomical site.[2,9] Furthermore, although infected animals develop a profound viremia 1-2 days before the onset of clinical signs, the source of the viremia also remains poorly understood.[2,9] Vesicles often hold higher viral titers than the blood, however, viremia may occur prior to vesicle formation.[2] Other tissues with viral titers include the skin (whether or not lesions are present), lungs, lymph nodes, and heart.[2] After the clearance of viremia, approximately 50% of cattle may become persistent carriers, although to what degree the carriers pose a threat to naïve animals, also remains poorly understood.[1,2,4]

Clinically, FMD manifests as a fever 2-7 days post-infection, followed by the vesicle formation in the mouth and on the feet, which may rupture under mechanical stressors, thus forming large erosions[7]. Damage to the epithelium results in hypersalivation and lameness, ultimately leading to weight loss and a drop in milk production.[9,10] Characteristic histologic lesions include vacuolar degeneration of epithelial cells, leading to hydrophobic cell swelling, cellular degeneration, lysis, and intraepithelial edema.[9] Healing occurs first through fibrin exudation with neutrophilic granulocytes, to granulation tissue and re-epithelialization.[9]. In addition to classical lesions, FMDV also induces a fatal lymphocytic-histocytic myocarditis especially in young animals,

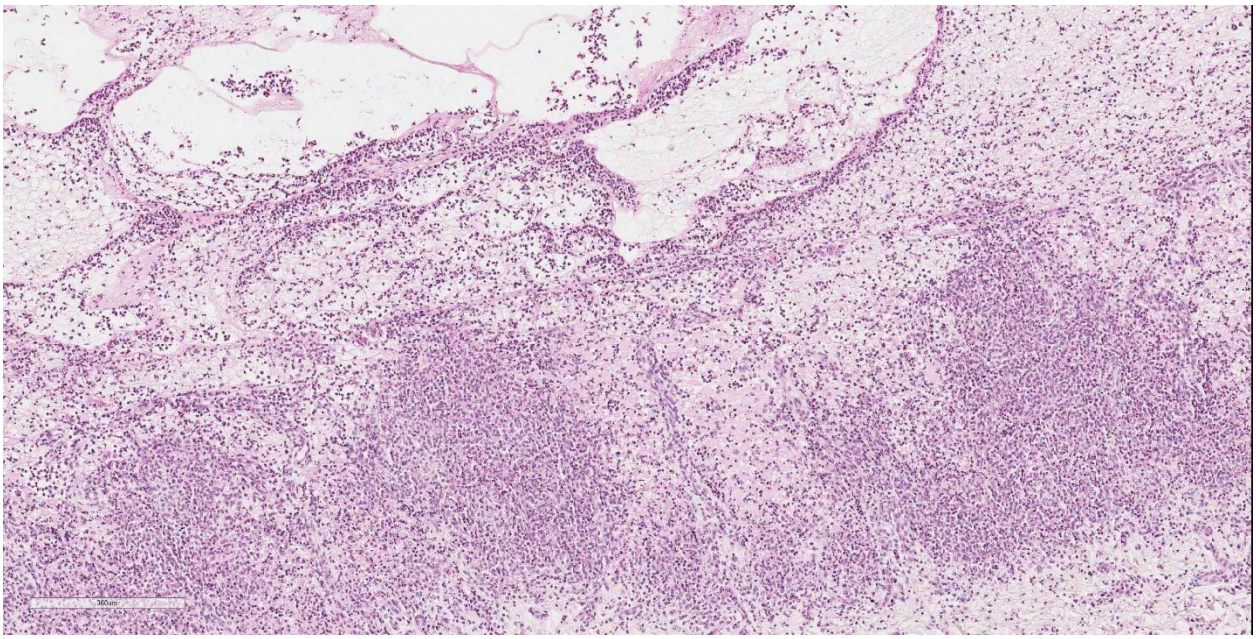

Tongue, ox. The floor of the vesicle and basal layers of the mucosa are outlined by a heavy infiltrate of neutrophils and cellular debris. (HE 97X)

characterized by small, grey-white foci within the myocardium of the left ventricle and septum.[4,9]

Important infectious differential diagnoses for ulcerative and erosive lesions include vesicular stomatitis (VS), vesicular exanthema in swine (VES), swine vesicular disease (SVD), bovine virus diarrhea (BVD), bluetongue virus (BTV), and malignant catarrhal fever (MCF).[9] Non-infectious causes include burns, trauma, and toxicants (selenium toxicity, cantharidin (blister beetle), toxic plants (buttercup, St. John's Wort, lantana, elderberry)), and photodermatitis.[3,9] Differentiation of these diseases may be made through laboratory diagnostics, including detection of the pathogen (antigen ELISA, PCR, viral isolation), histopathology, or antibodies produced by the infected animal[1,4,9] In many countries, prior to laboratory confirmation of disease, cases of vesicular lesions must be reported to official veterinarians in order to ensure prompt response and preparedness in the event of an FMD positive animal.

A primary objective in controlling FMD globally is immediate detection of disease, as well as controlling the movement of animals and animal products, and contacts with animals between countries.[9,10] It is imperative that animal health practitioners are trained to not only identify early cases of

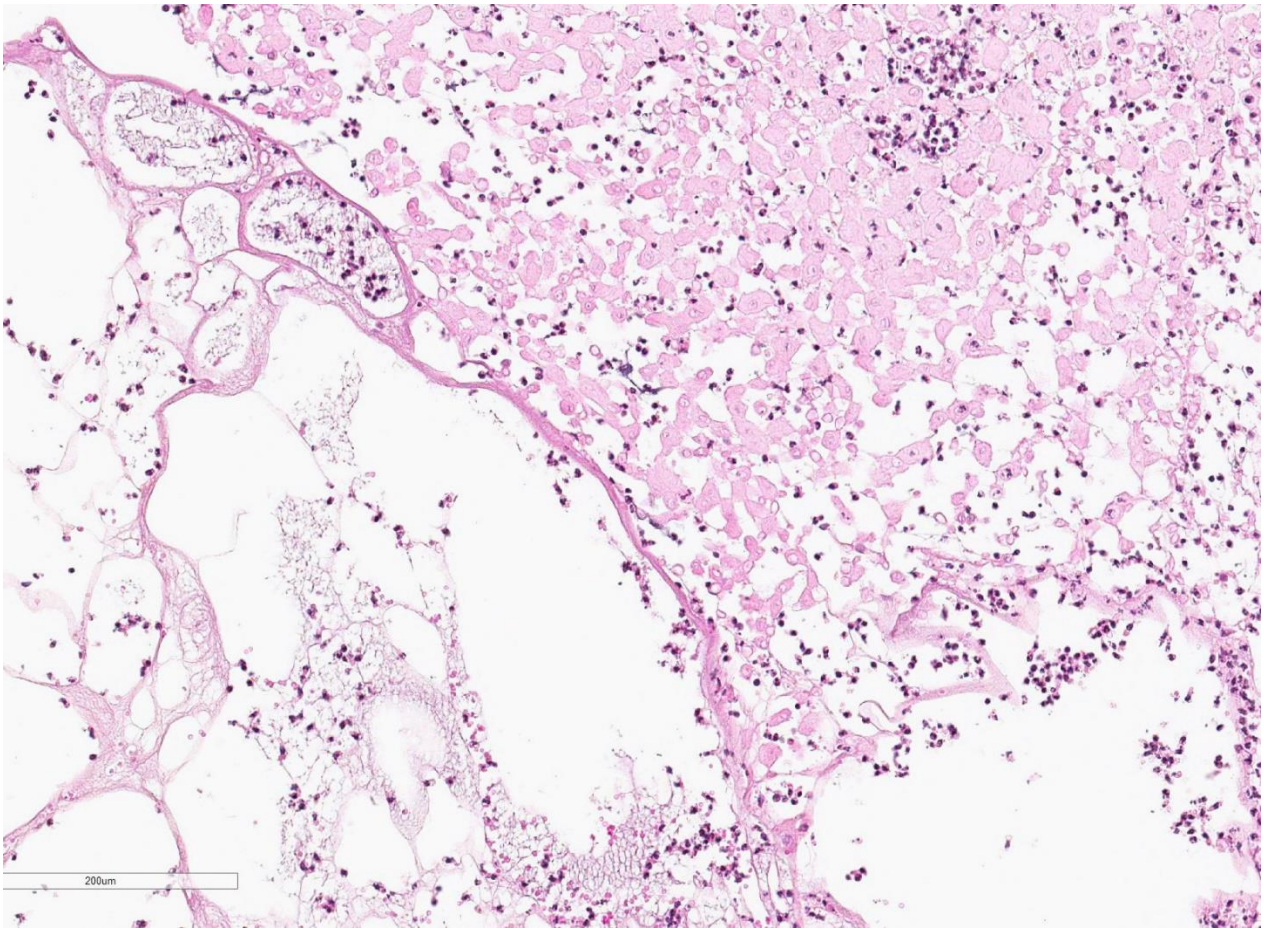

Tongue, ox. Adjacent to the vesicle, degenerating mucosal epithelial cells are rounded up and disassociated, furthering additional vesicle formation or enlargement. (HE, 173X)

FMD, but also practice high standards of biosecurity and workplace hygiene.[9] Although FMDV is sensitive to changes in pH (below 6.0, above 9.0) and standard disinfectants (2% sodium hydroxide, 0.2% hydrochloric acid, 2% formalin, 0.5% citric acid), a challenge lies in controlling potentially contaminated materials, as all secretions and excretions of an infected animal are considered infectious.[6] Furthermore, FMDV may survive in the soil for up to 28 days, in urine for 39 days, and fecal slurries for up to 6 months.[6] In addition, cattle that become carriers may continue to harbor virus for up to 3.5 years[1]. Vaccinations are available, however, a vaccine is not protective across serotypes, and vaccination does not prevent animals from becoming carriers.[2,9]

Contributing Institution:
Friedrich-Loeffler-Institut, Federal Research Institute for Animal Health, Department of Experimental Animal Facilities and Biorisk Management, Südufer 10, 17493 Greifswald – Insel Riems, Germany. https://www.fli.de

JPC Diagnosis: Tongue: Glossitis, vesicular and neutrophilic, multifocal to coalescing, severe.

JPC Comment: The contributor has done an outstanding job describing this disease of global veterinary importance with particular regard to cattle. The apthovirus that causes foot and mouth disease affects a range of other species, some of which may contribute significantly to the potentiation and duration of an outbreak. Small ruminants may facilitate the spread of outbreaks as lesions are often inapparent, and these animals are easily transported. In countries in the virus is endemic, African buffalos and impala have been documented as reservoir hosts and well as being able to pass the virus on to domestic cattle.[7]

Much of the available research has been performed on cattle; however, swine are a major component of the world's meat production as well, and the pathogenesis of the disease is significantly different in this species. Swine are considered amplifier hosts and have the ability to produced large amounts of virus, which may be transmitted

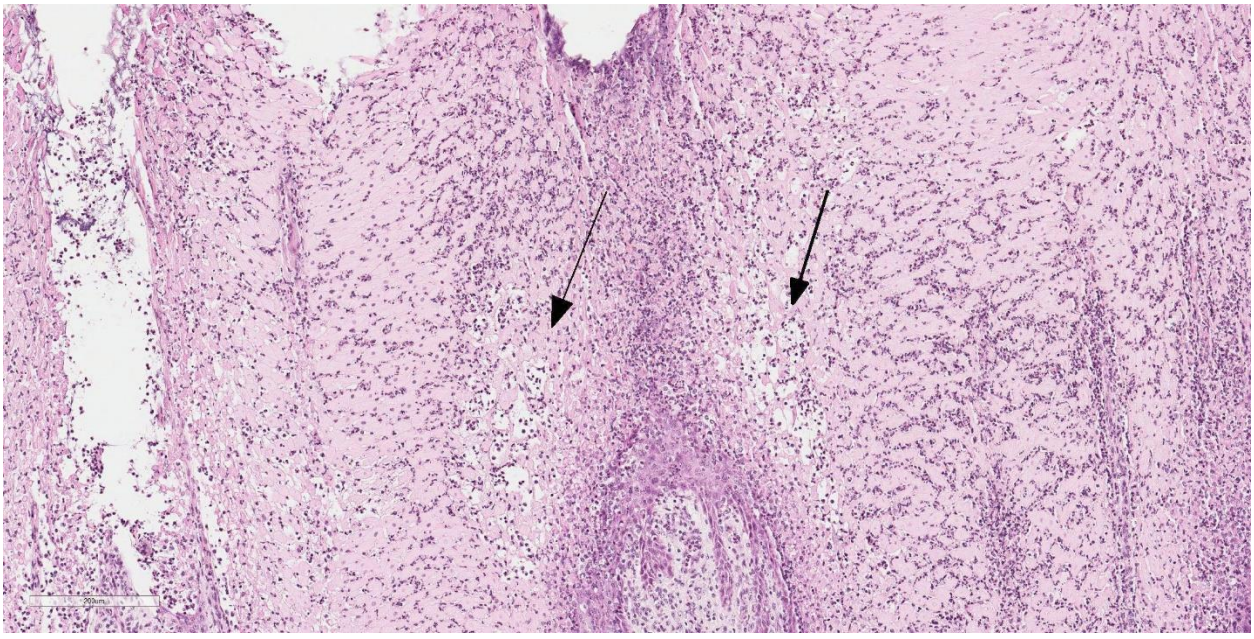

Tongue, ox. In mucosa adjacent to the vesicle, there is extensive transmigration of neutrophils and incipient vesicle development (arrows). (HE, 121X)

by aerosols to other farms. While the clinical signs of FMD in swine are similar to those in cattle, the pathogenesis of the disease in swine demonstrates considerable different.[8] Pigs are more susceptible to oral inoculation (through oropharyngeal tonsillar tissue) than via aerosol exposure which suggests that physical separation of pigs may be successful to decrease infection rates in swine, but not in cattle. During clinical disease, the highest quantities of virus is produced within vesicles in the oral cavity and feet; however, pigs exhale massive quantities of infectious FMDV, likely with tonsillar tissue as the source.[8] Convalescence occurs within 1-2 weeks, although serious injuries to the feet may resulting in secondary infection and persistent lameness. Pigs that clear the disease also apparently completely clear the virus with 17 days; carrier states apparently do not occur in this species.[8]

References:

1. Alexandersen S, Zhang Z, Donaldson AI. Aspects of the persistence of foot-and-mouth disease virus in animals – the carrier problem. *Microbes and Infection*. 2002; 4: 1099-1110.
2. Arzt J, Juleff N, Zhang Z, Rodriguez LL. The pathogenesis of foot-and-mouth disease I: Viral pathways in cattle. Transboundary and Emerging Diseases. 2010; 58: 291-304.
3. Holliman A. Differential diagnosis of diseases causing oral lesions in cattle. *In Practice*. 2005; 27: 2-13.
4. Longjam N, Deb R, Sarmah AK, Tayo T, Awachat VB, Saxena VK. A brief review on diagnosis of foot-and-mouth disease of livestock: conventional to molecular tools. *Veterinary Medicine International.* 2011.
5. OIE. World Animal Health Information Database. Accessed 17 June 2019. <http://www.oie.int/wahis_2/public/wahid.php/Diseaseinformation/Immsummary>
6. Owen JM. Disinfection of farrowing pens. *Rev. sci. tech. Off. Int. Epiz.* 1995; 14(2): 381-391.
7. Paton DJ, Gubbins S, King DP. Understanding the transmission of foot-and-mouth disease virus at different scales. *Curr Opin Virol* 2018; 28:85-91.
8. Stenfeldt C, Diaz-San Segundo F, de los Santos T, Rodriguez LL, Arzt J. The pathogenesis of foot-and-mouth disease in pigs. *Front Vet Sci* 2018; 3:41:10.3389/fvets.2016.00041.
9. Teifke JP, Breithaupt A, Haas B. Foot-and-mouth disease and its main differential diagnoses. *Veterinary Practice of Large Animals*. 2012; 40(G): 225-237.
10. Yoon H, Yoon SS, Wee SH, Kim YJ, Kim B. Clinical manifestations of foot-and-mouth disease during the 2010/2011 epidemic in the Republic of Korea. *Transboundary and Emerging Diseases.* 2012; 59: 517-525.

Self-Assessment - WSC 2019-2020 Conference 3

1. Which of the following strains of Newcastle disease virus causes mild or inapparent respiratory infection ?
    a. Mesogenic
    b. Lentogenic
    c. Bronchogenic
    d. Velogenic

2. Which of the following is usually NOT seen in paramyxovirus-infected pigeons?
    a. Neurologic signs
    b. Respiratory signs
    c. Gastrointestinal signs
    d. Paresis of the wings or feet

3. In addition to small ruminants, which other species is commonly infected by *Corynebacterium pseudotuberculosis*?
    a. Dogs
    b. Horses
    c. Poultry
    d. Amphibians

4. Which of the following is not true of the splenic infarcts seen in classical swine fever?
    a. They are venous in origin.
    b. They are the result of macrophage liberation of proinflammatory cytokines.
    c. Single blood supply in the spleen and lack of anastomoses play a role in their development.
    d. Cytokine storms play an important role in their development.

5. In additional to the classical vesicular lesions of foot and mouth disease, which of the following may be seen in young animals:
    a. Encephalitis
    b. Nephritis
    c. Myocarditis
    d. Bone marrow necrosis

Please email your completed assessment for grading to Dr. Bruce Williams at bruce.h.williams12.civ@mail.mil. Passing score is 80%. This program (RACE program 33611) is approved by the AAVSB RACE to offer a total of 0.5 CE Credits, with a maximum of 12.5 CE Credits being available to any individual Veterinary Medical Professionals for the 2019-2020 Wednesday Slide Conference. This RACE approval is for the subject matter categories of: SCIENTIFIC using the delivery method of NON-INTERACTIVE DISTANCE. This approval is valid in jurisdictions which recognize AAVSB RACE.

Joint Pathology Center
Veterinary Pathology Services

WEDNESDAY SLIDE CONFERENCE 2019-2020

C o n f e r e n c e 4

CASE I: 16-02795 (JPC 4087577)

Signalment: Adult (age and gender not specified) little red flying fox (*Pteropus scapulatus*).

History: This bat was in the care of a local wildlife rescue group, when its vocalisations became abnormal, then developed paresis which progressed to grand mal seizures. The bat was euthanased, and tissues submitted to the laboratory for exclusion of Australian Bat Lyssavirus (ABLV).

Gross Pathology: No gross lesions observed

Laboratory results: Immuno-histochemistry: Immunohistochemistry using monoclonal (HAM Mab 100) and polyclonal (Poly 663) antibodies raised against rabies nucleoprotein showed diffuse positive staining in neurons throughout the cerebral cortex and brainstem, and in cerebellar Purkinje fibres. ABLV antigen was most concentrated within neurons in the hippocampus, thalamus, and pons.

Microscopic Description:
Brain: Blood vessels throughout the brainstem and cerebrum are surrounded by lymphocytes and fewer plasma cells. Multifocally within the brainstem, thalamus and rarely in cerebellar Purkinje cells, neurons have one to numerous oval, well demarcated, eosinophilic intracytoplasmic inclusions (Negri bodies). The cranial nerve is diffusely infiltrated with many lymphocytes and fewer plasma cells. Meninges in the brainstem are focally expanded with neutrophils and lymphocytes, with fewer plasma cells.

Contributor's Morphologic Diagnosis:

1. Brain; brainstem, cerebrum, and cerebellum: Encephalitis, lymphoplasmacytic, subacute, diffuse, mild, with multifocal intraneuronal intracytoplasmic

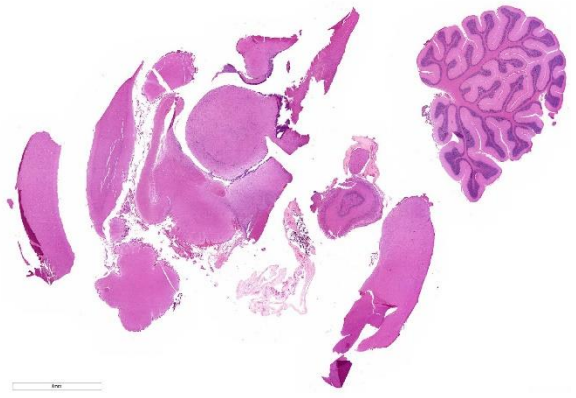

Brain, little red flying fox. The entire brain is submitted for examination. (HE, 8X)

eosinophilic inclusions (Negri bodies)
2. Ganglion: Ganglioneuritis, lymphoplasmacytic, subacute, diffuse, moderate
3. Meninges: Meningitis, neutrophilic and lymphocytic, subacute, focal, mild, with multifocal calcification

Contributor's Comment: Australian bat lyssavirus (ABLV) belongs to the genus *Lyssavirus*, family *Rhabdoviridae*, order *Mononegavirales*.[10] The genus *Lyssavirus* includes seven genotypes: rabies virus (RABV, genotype 1), Lagos bat virus (genotype 2), Mokola virus (genotype 3), Duvenhage virus (genotype 4), European bat lyssavirus 1 (EBLV-1, genotype 5), European bat lyssavirus 2 (EBLV-2, genotype 6), and Australian bat lyssavirus (ABLV, genotype 7). ABLV is most closely related to classical rabies (genotype 1), and vaccination against rabies provides protection against exposure to ABLV. Two variants of ABLV have been described, in pteropid and insectivorous bats.[5,6] Natural infections with ABLV have been described in horses,[11] with affected animals displaying clinical signs similar to those of classical rabies. There have been three reported cases of ABLV infection in Australia, all of which were fatal.[1,4,7,8]

Microscopic lesions typically associated with *Lyssavirus* infections include a nonsuppurative encephalomyelitis, with multifocal gliosis, neuronal degeneration, and rare oval, eosinophilic intracytoplasmic viral inclusions (Negri bodies).[2] The distribution of Negri bodies in domestic animals has been described as occurring most commonly in the hippocampus in carnivores, and in the Purkinje cells of herbivores.[2] Hooper et al. (1999) published a survey of

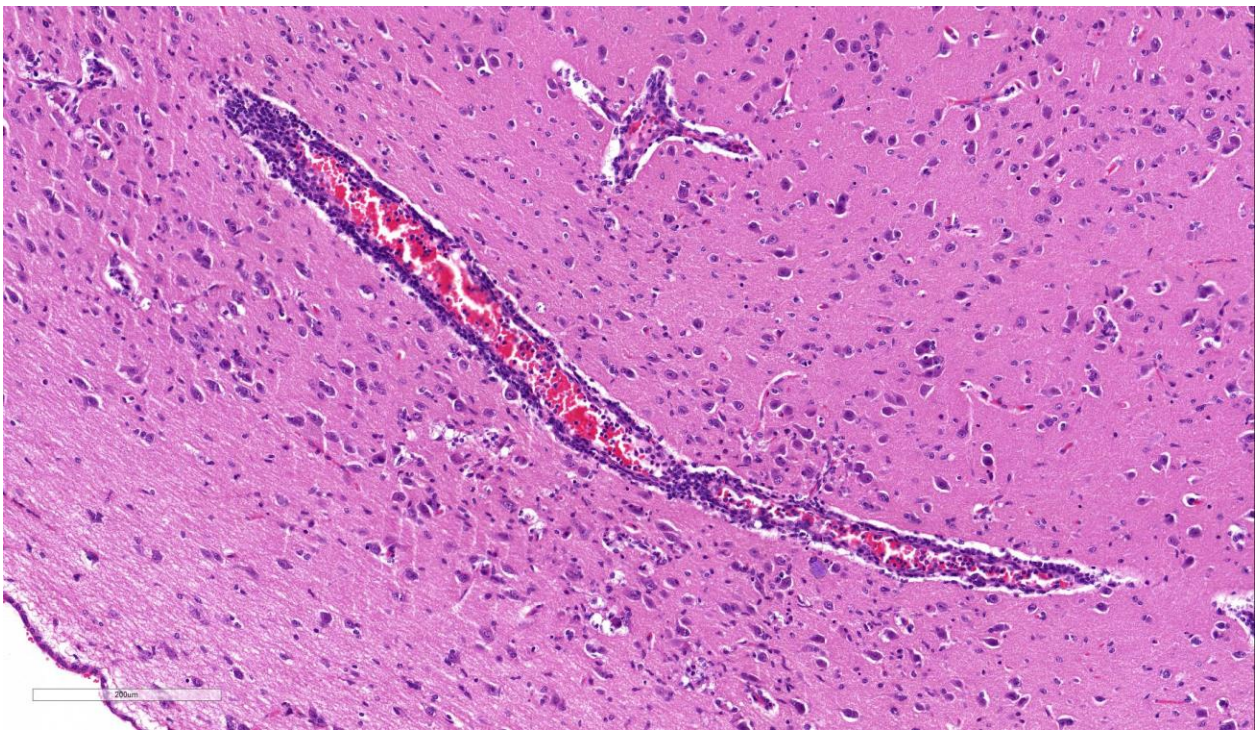

Thalamus, little red flying fox. Multifocally, scattered throughout the brain parenchyma, vessels are cuffed by low to moderate numbers of lymphocytes and rare plasma cells. There is a moderate gliosis and multifocal neuronal necrosis. (HE, 100X)

lesions in the brains of bats that had tested positive for ABLV, and reported lesions in the hippocampus, thalamus and midbrain, and medulla oblongata and pons.[9] The authors observed Negri bodies in only 9 of 21 bats. Immunoperoxidase staining using antibodies raised against rabies viral nucleoprotein revealed a reaction pattern with a distribution similar to that of microscopic lesions. Positive immunohistochemical staining was noted to occur in the absence of lesions. Positive immunohistochemical staining was also reported in the dorsal root ganglia and in ganglia of the alimentary system. There was only loose relationship between staining of Negri bodies on H&E section and the presence of virus in neurons.

In the present case, the relationship between immunohistochemical staining and the presence of Negri bodies was similarly loose, with many more inclusions apparent after immunohistochemical staining. In addition, immunohistochemical staining of intraneuronal inclusions demonstrated a widespread distribution of viral antigen. Neuronal necrosis and gliosis were not features in the current case. This case was unusual in our laboratory with submission of only the fixed brain rather than the whole fresh bat and ABLV exclusion through tissue sampling of swabs from the oral cavity, salivary gland, and brain for PCR.[11] Fresh salivary gland and brain tissues are subsequently sent to the national reference laboratory for direct fluorescent antibody testing, which is the international gold standard diagnostic test. While the results of immunohistochemical testing highlight the relative insensitivity of routine histology as a diagnostic method for *Lyssaviruses* it does demonstrate its ability to secure a positive diagnosis.

Bats are unique in that they are able to coexist with *Lyssaviruses*, as well as a number of

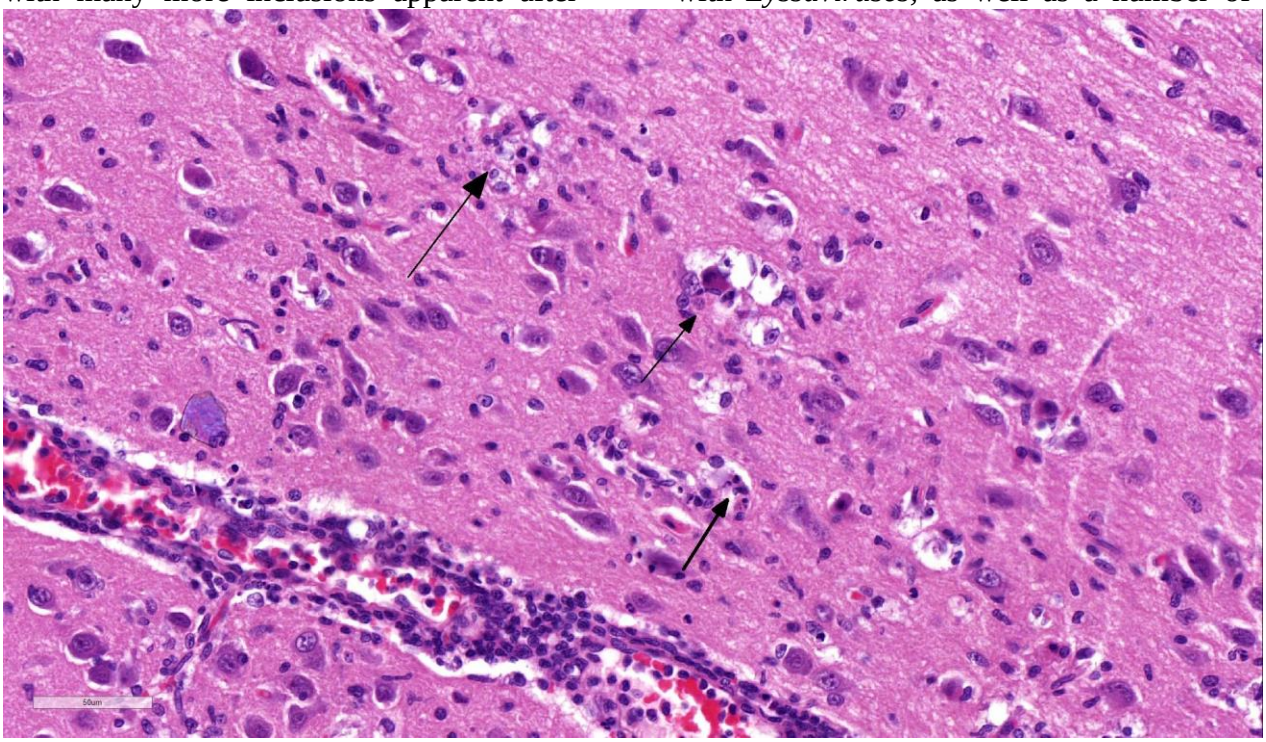

Thalamus, little red flying fox. Higher magnification of the field in fig 1-2. Neurons are shrunken and fragmented and surrounded by microglia (arrows). (HE, 400X)

other viruses that are lethal to most mammals (e.g. Hendra, Nipah, Severe acute respiratory system coronavirus [SARS-CoV], Ebola, Mekala, and Marburg viruses). Research indicates that the Australian black flying fox, *Pteropus alecto*, constitutively expresses interferon alpha genes,[14] and type III interferons that are differentially expressed compared to type I interferons.[13] However, the immunologic mechanisms by which bats are able to tolerate infection with these otherwise lethal viruses are only beginning to be unraveled.

Contributing Institution:
State Veterinary Diagnostic Laboratory
Elizabeth Macarthur Agricultural Institute
Woodbridge Rd
Menangle
NSW 2568
Australia

JPC Diagnosis: Brain: Meningo-encephalitis, diffuse, lymphoplasmacytic, mild with numerous neuronal intra-cytoplasmic viral inclusions.

JPC Comment: The contributor has done an outstanding job describing Australian bat lyssavirus (ABLV) and the peculiarities noted upon comparison of histologic and immunohistochemical evaluation on tissue from infected animals. This case compares favorably with a series of ABLV-infected bats by Hooper et al.[9] discussing the great variability of immunopositivity in neurons in tissues infected with lyssaviruses (similar to that in seen in rabies cases.) To maximize the diagnostic potential of immuno-histochemistry in suspect cases of any lyssavirus, submission (and evaluation) of tissues in addition to cerebrum is highly recommended, to include spinal cord and dorsal root ganglia, adrenal gland, and gastrointestinal tract (inclusions may be found in GI nerve plexes.)[9]

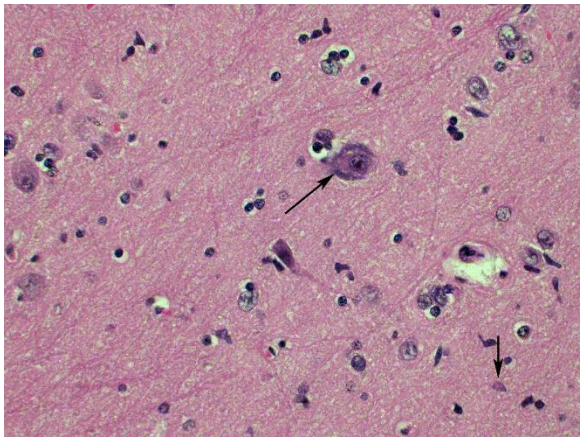

Thalamus, little red flying fox. Neurons often contain multiple intracytoplasmic 1-2um round viral inclusions (Negri bodies). (HE, 400X)

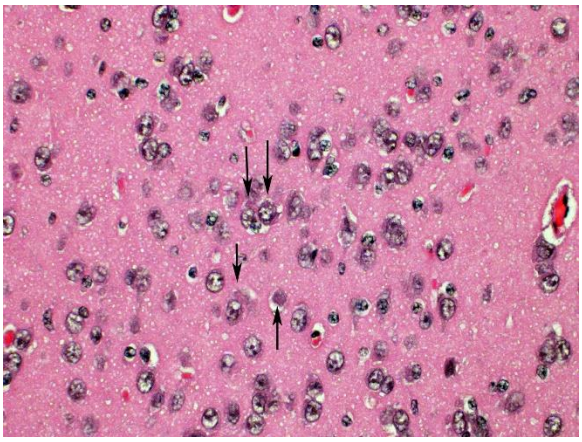

Olfactory cortex, little red flying fox. Neurons contain multiple intracytoplasmic 1-2um round viral inclusions (Negri bodies). (HE, 400X)

As previously noted, ABLV infection in humans is a rare finding, with only three reported cases, but with a mortality of 100%. Infection rates in wild bat population have been estimated at less than 1%, but purported to be markedly increased (5-10%) in sick or injured bats, the ones most likely to come into contact with humans. Like rabies, direct contact is required for zoonotic transmission, and in the documented cases of lyssavirus in humans, the latent period ranged from one month to 27 months.[4]

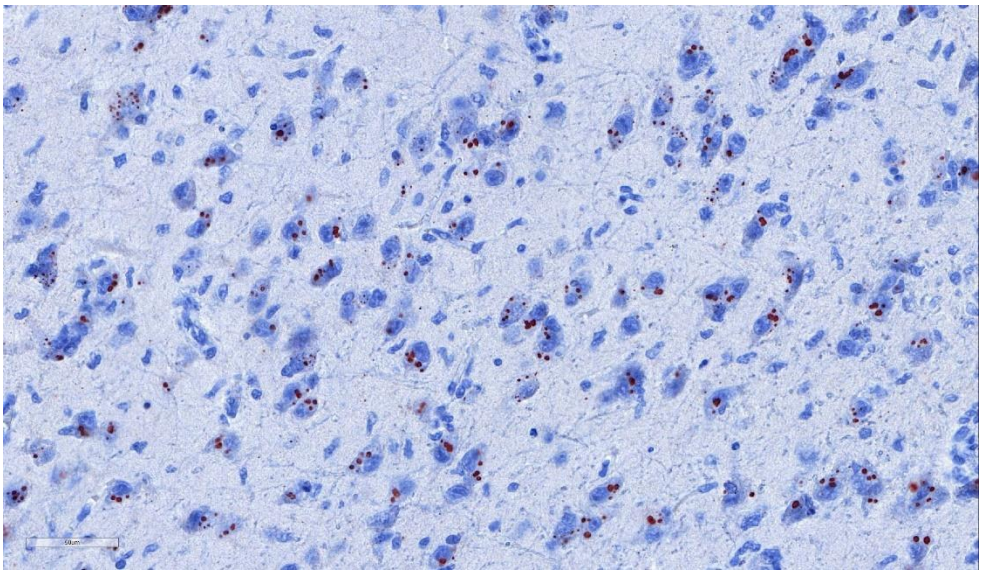

Cerebrum, little red flying fox. While difficult to see on HE, immunostaining for flying fox lyssavirus antigen shows its widespread location in neurons of the cerebrum. (Photo courtesy of: State Veterinary Diagnostic Laboratory, Elizabeth Macarthur Agricultural Institute, Woodbridge Rd. Menangle, NSW 2568 Australia)

Antemortem diagnosis of Australian bat lyssavirus in humans, as in rabies, is difficult. Neuroimaging is usually of little benefit. CSF pleocytosis is mild at best and present in only approximately 60% of cases.[4] Lyssaviral antibodies may appear late in the course of disease or not. The utility of nuchal skin biopsy (considered to be 98% specific) is yet to be verified in human cases of lyssavirus infection, but bat lyssavirus has been shown to cross-react with rabies RT-PCR, so this test, as well as salivary PCR should be considered.[4] Clinically, the three cases of zoonotic bat lyssavirus resembled the encephalitic or "furious" form of rabies, characterized by hyperactivity, agitation, and spasms, especially of the face. As treatment for lyssavirus has not been established, but post-exposure prophylaxis is considered to be protective if offered.[4]

In addition to ABLV and rabies, two types of lyssavirus have been identified in European bats – European bat lyssavirus types 1 and 2 (EBLV-1 and EBLV-2); EBLV-1 is further subdivided into subtypes 1a and 1b. Both types have been reported as causing neurologic rabies-like syndromes in man, as well as cats and sheep.[3]

The distributed slides psed a challenge for participants as few identified lesions in the submitted tissue other than the numerous Negri bodies. The slide posted online at https://www.askjpc.org had an identifiable ara of meningeal inflammation, and the parenchyma in its proximity exhibited gliosis with rare neuronal necrosis and satellitosis (Fig 1-3). The architecture of one of the submitted sections was unfamiliar to the participants; many identified it as hippocampus until Dr. Andrew Cartoceti of

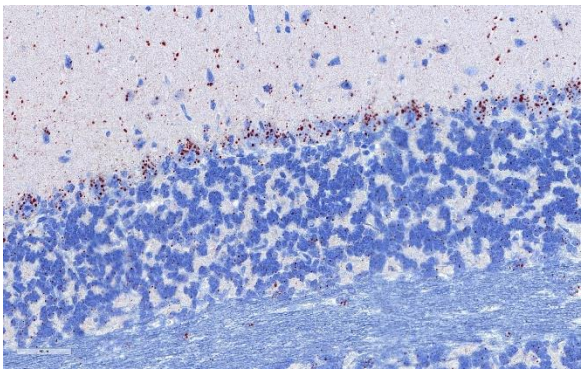

Cerebellum, little red flying fox. Intracytoplasmic inclusions of flying fox lyssavirus are present within neuronal cytoplasm of Purkinje cells as well as neurons of the granular cell layer.(Photo courtesy of: State Veterinary Diagnostic Laboratory, Elizabeth Macarthur Agricultural Institute, Woodbridge Rd. Menangle, NSW 2568 Australia)

the National Zoo identified it as olfactory cortex.

References:

1. Allworth A, Murray K, Morgan J: A human case of encephalitis due to a lyssavirus recently identified in fruit bats. *Communicable diseases intelligence* 1996:20**:**504-504.
2. Cantile C, Youssef S: Viral infections of the nervous system. In: Maxie G, ed. *Jubb, Kennedy & Palmer's Pathology of Domestic Animals:*. 6th ed.: Elsevier Health Sciences; 2016: 367-369.
3. Dacheau L, Larrous F, Mailles A et al. European bat lyssavirus transmission among cats, Europe. *Emerg Inf Dis* 2009; 15(2): 280-84.
4. Francis JR, Nourse C, Vaska VL, Calvert S, Northill JA, McCall B, et al.: Australian Bat Lyssavirus in a child: the first reported case. *Pediatrics* 2014:133(4)**:**e1063-1067.
5. Gould AR, Hyatt AD, Lunt R, Kattenbelt JA, Hengstberger S, Blacksell SD: Characterisation of a novel lyssavirus isolated from Pteropid bats in Australia. *Virus Res* 1998:54(2)**:**165-187.
6. Gould AR, Kattenbelt JA, Gumley SG, Lunt RA: Characterisation of an Australian bat lyssavirus variant isolated from an insectivorous bat. *Virus Res* 2002:89(1)**:**1-28
7. Grattan-Smith P, O'regan W, Ellis P, O'fFaherty S, McIntyre P, Barnes C: Rabies. A second Australian case, with a long incubation period. *Med J Austral* 1992:156(9)**:**651-654.
8. Hanna JN, Carney IK, Smith GA, Tannenberg AE, Deverill JE, Botha JA, et al.: Australian bat lyssavirus infection: a second human case, with a long incubation period. *Med J Aust* 2000:172(12)**:**597-599.
9. Hooper PT, Fraser GC, Foster RA, Storie GJ: Histopathology and immunohistochemistry of bats infected by Australian bat lyssavirus. *Australian Veterinary Journal* 1999:77(9)**:**595-599.
10. ICTV: Virus Taxonomy: 2015 Release.
11. Shinwari MW, Annand EJ, Driver L, Warrilow D, Harrower B, Allcock RJ, et al.: Australian bat lyssavirus infection in two horses. *Vet Microbiol* 2014:173(3-4)**:**224-231.
12. Smith IL, Northill JA, Harrower BJ, Smith GA: Detection of Australian bat lyssavirus using a fluorogenic probe. *Journal of Clinical Virology* 2002:25(3)**:**285-291.
13. Zhou P, Cowled C, Todd S, Crameri G, Virtue ER, Marsh GA, et al.: Type III IFNs in pteropid bats: differential expression patterns provide evidence for distinct roles in antiviral immunity. *J Immunol* 2011:186(5)**:**3138-3147.
14. Zhou P, Tachedjian M, Wynne JW, Boyd V, Cui J, Smith I, et al.: Contraction of the type I IFN locus and unusual constitutive expression of IFN-alpha in bats. *Proc Natl Acad Sci U S A* 2016:113(10)**:**2696-2701.

CASE II: 17-0894 (JPC 4111545).

Signalment: Merino, Female, 12 months old

History: 14 of 130 twelve month old lambs died during a two week period in late Autumn. Sheep were grazing pastures containing witchgrass (*Panicum capillare*)

Forage. Animals had been grazing pastures containing witchgrass (Panicum capillary capillare). (Photo courtesy of: Veterinary Diagnostic Laboratory, School of Animal and Veterinary Sciences, the University of Adelaide, Roseworthy, South Australia, 5371, Australia.

Gross Pathology: Cutaneous photo-sensitization of eyelids, muzzle and coronet bands. Severe generalized jaundice, very swollen yellow and firm liver with enhanced lobular pattern. Dark yellow-brown staining of kidneys.

Laboratory results: None performed.

Microscopic Description:
Liver: Lobar borders of liver are rounded. There is mild to moderate infiltration of periportal interstitium by lymphocytes, macrophages, and variable neutrophils, mild to moderate expansion of periportal fibrocollagenous connective tissue, and mild to moderate bile duct hyperplasia. Within periportal interstitium there are clear acicular clefts (crystal ghosts) surrounded by fibroblasts and collagen. Rare crystal ghosts are present in the bile ducts associated with tubular epithelial degeneration and attenuation, and less often present in the sinusoids. Diffusely, there is moderate hepatocellular swelling characterized by feathery to vacuolar cytoplasm and scattered individual cell necrosis, most notably in periportal regions. Kupffer cells are often enlarged with vacuolar to lightly pigmented cytoplasm, or clear cytoplasm. Bile canaliculi are sometimes distended by light brown-orange pigment (bile plugs).

Microscopic findings in other tissues included myocardial sarcocystosis, moderate to severe neutrophilic bronchointerstitial pneumonia, and renal tubular epithelial degeneration and cytoplasmic pigmentation (bilirubin, other) with pigmented tubular casts.

Sheep, presentation. Affected sheep had facial alopecia and swelling. (Photo courtesy of: Veterinary Diagnostic Laboratory, School of Animal and Veterinary Sciences, the University of Adelaide, Roseworthy, South Australia, 5371, Australia)

Contributor's Morphologic Diagnosis:
Liver: chronic-active mixed cholangio-hepatitis with cholestasis, periportal fibrosis and crystal ghosts (crystal cholangio-hepatopathy).

Contributor's Comment: Crystal-associated hepatopathy and secondary photosensitization in these lambs developed following exposure to witchgrass (*Panicum capillare*) in pasture. No crystals were observed under direct nor polarized light, however acicular clefts (crystal ghosts) were identified in the periportal interstitium, bile ducts and rarely in the sinusoids. The duration that lambs had been grazing this pasture prior to the onset of clinical signs was not recorded in the submission. Onset of hepatotoxicity in sheep experimentally exposed to another *Panicum* species, kleingrass (*Panicumn coloraturum*), was variable, occurring as early as three days to several weeks post initial exposure [1]. Following natural exposure of sheep to *P. schinzii*, the clinical appearance of hepatotoxicity was reported to have occurred within five days of the flock being moved onto affected pastures [2].

Sheep, presentation. Affected sheep had generalized icterus. (Photo courtesy of: Veterinary Diagnostic Laboratory, School of Animal and Veterinary Sciences, the University of Adelaide, Roseworthy, South Australia, 5371, Australia)

Crystal hepatopathy has been reported in ruminants and horses following exposure to *Panicum* grasses 1, as well as *Brachiaria* [3,4], and *Narthecium*[14] grass species. These plants contain steroidal saponins and affected ruminants often develop bile crystals composed of the calcium salts of steroidal saponin glucuronides.[6,8-10]

Hepatic lesions described in natural and experimental *Panicum* grass toxicity in sheep and horses include patchy or scattered

Sheep, liver: Livers were firm, swollen and yellow with an enhanced lobular pattern on cut surface. . Affected sheep had generalized icterus. (Photo courtesy of: Veterinary Diagnostic Laboratory, School of Animal and Veterinary Sciences, the University of Adelaide, Roseworthy, South Australia, 5371, Australia)

hepatocellular necrosis, vacuolation and swelling, nuclear chromatin clumping, presence of birefringent crystals in small bile ducts, bile canaliculi or within sinusoidal phagocytes, fibrosis, bile duct proliferation, and lymphocytic hepatitis.[1,7] Crystals may not always be observed; no crystals were identified in affected livers of horses and sheep following exposure to *Panicum dichotomiflorum*, [7] and this was thought to be to the short exposure time to the grasses (feeding trials only lasted 12 days). In experimental work done elsewhere, sheep grazing kleingrass for less than 10 days did not have observable crystals in the liver [1]. In kleingrass toxicity, crystals are reportedly

Sheep, kidney: Kidneys are icteric with a dark brown cortex (Photo courtesy of: Veterinary Diagnostic Laboratory, School of Animal and Veterinary Sciences, the University of Adelaide, Roseworthy, South Australia, 5371, Australia)

soluble in acidified ethyl alcohol, acetic acid, pyridine, chloral hydrate, and methanol, but not in xylene, petroleum ether, diethyl ether, acetone, water, or cold ethyl alcohol. [1]

Contributing Institution:
Veterinary Diagnostic Laboratory
School of Animal and Veterinary Sciences
The University of Adelaide,
Roseworthy, South Australia, 5371, Australia

JPC Diagnosis: Liver: Cholangiohepatitis, necrotizing and histiocytic, multifocal, mild, with mild bridging portal fibrosis, biliary hyperplasia, subcapsular hepatocellular loss intrahistiocytic and intraductal crystal formation.

JPC Comment: The genus *Panicum* is a large group of grasses containing up to 600 different species of grasses in tropical and temperate regions around the world.[13] The majority may be used as forage for livestock; however a limited number of species such as those mentioned above, may result in crystal associated hepatopathy, with the formation of crystals within bile ducts and resultant hepatic damage as the most important lesion. The biotransformed saponins within these plants are conjugated with gluruconic acid and excreted in the bile, where they may complex with calcium to form an insoluble salt. Photosensitization in affected animals is usually the result of biliary damage and inability to conjugate phytoporphyrins (phylloerythrin), a chlorophyll derivative produced by bacteria in the gastrointestinal tract. Phylloerythrin is a photoactive compound which is excited by ultraviolet light in lightly pigmented and poorly haired areas of the body.

A recent article by Sillman et al[12] details toxicity in 3-month Boer goats clearing a weedy livestock lot. After a month of the lot, affected animals developed icterus and inappetence with marked hyperbilirubinemia, elevated aspartate aminotransferase and variable levels of alanine aminotransferase. Examination of the lot showed a tremendous growth of *Panicum dichotomiflorum*. At autopsy, portal areas were mildly fibrotic and contained clusters of macrophages centered on large, acicular crystals. Mild hepatocellular vacuolation and biliary hyperplasia were also noted. Previous reports of *P. dichotomiflorum* described intoxication in a variety of species, including nursing and juvenile lambs and horses, although many reports note that other animals of various species, breeds, or ages grazing the same forage were unaffected. The report by Sillman et al. also notes the

Sheep liver. A section of liver is submitted with enhanced visibility of portal triads and a focal subcapsular scar. (HE,7X)

presence of tubular nephrosis in the goat, which had not been previously described. Evidence of photosensitization was not noted in these cases. [12]

Another recent report describes the first instance of hepatogenous photosensitization due to steroidal saponin toxicity in macropods. Steventon et al.[13] describes an outbreak of blindness or photophobia in 95 grey kangaroos in New South Wales, Australia. Affected animals developed icterus, photophobia (abnormal shade seeking behavior), and blindness resulting with severe corneal edema and inflammation and necrotizing dermatitis of the eyelids, pinnae, and forearms. Examination of the liver of affected animals revealed crystal formation in small bile ducts with mild granulomatous inflammation and portal fibrosis. The presence of crystal-associated damage and inflammation with bile ducts prompted examination of the site of the outbreak, which was dominated by a heavy growth of *Panicum gilvum* ("sweetgrass" or "sweet panic".)[13]

Sporidesmin, a plant saponin from spores of *Pithomyces chartarum* which causes a well-known syndrome of photosensitization ("facial eczema") and severe hepatic damage in New Zealand. The excretion of unconjugated sporidesmin in the bile results in oxidative injury to the biliary epithelium, leakage of biliary components into the surrounding tissue, and occasionally necrosis of vessels in adjacent parenchyma.[4] When complemented with concurrent ingestion of saponins of *Tribulus terrestris* a condition known as "geeldikkop" is created, in which crystal formation within bile ducts and within the whitish contents of the gallbladder is noted.[4]

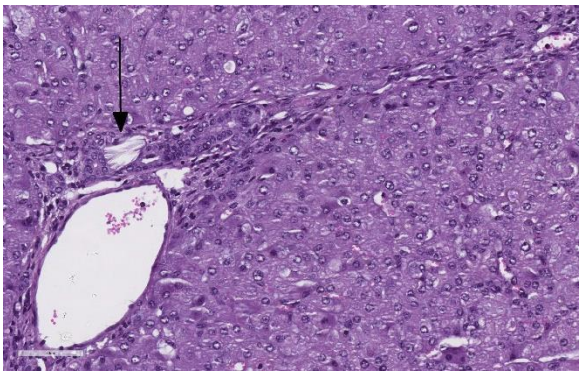

Sheep, liver: Portal areas contain increased profiles of bile ductules and small amounts of collagen. Sheaf-like crystals are present in close proximity to, or within bile ductules. (HE, 315X)

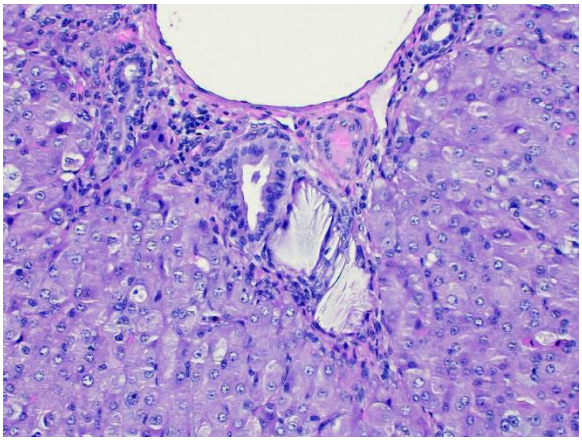

Sheep liver: Higher magnification of crystals within and adjacent to bile ducts. (HE, 400X)

Conference participants were impressed by the significant icterus demonstrated in the gross lesions in this case as compared with the relative lack of significant fibrosis and hepatocellular damage. While information about possible exposure to copper was not mentioned, a JPC-run rhodamine stain was considered unremarkable in this case.

References:

1 Bridges CH, Camp BJ, Livingston CW, Bailey EM: Kleingrass (Panicum coloratum L.) poisoning in sheep. *Vet Pathol* 1987:24(6)**:**525-531.

2 Button C, Paynter DI, Shiel MJ, Colson AR, Paterson PJ, Lyford RL: Crystal-Associated Cholangiohepatopathy and Photosensitization in Lambs.

Australian Veterinary Journal 1987:64(6)**:**176-180.
3 Cruz C, Driemeier D, Pires VS, Schenkel EP: Experimentally induced cholangiohepatopathy by dosing sheep with fractionated extracts from Brachiaria decumbens. *J Vet Diagn Invest* 2001:13(2)**:**170-172.
4. Cullen JM, Stalker MA. Liver and Biliary System. *In:* Maxie MG, ed. Jubb Kennedy and Palmers' Pathology of Domestic Animals, 6th Edition. St. Louis MO, Elsevier. Vol 2, , 338-340.
4 Graydon RJ, Hamid H, Zahari P, Gardiner C: Photosensitization and Crystal-Associated Cholangiohepatopathy in Sheep Grazing Brachiaria-Decumbens. *Australian Veterinary Journal* 1991:68(7)**:**234-236.
5 Holland PT, Miles CO, Mortimer PH, Wilkins AL, Hawkes AD, Smith BL: Isolation of the Steroidal Sapogenin Epismilagenin from the Bile of Sheep Affected by Panicum-Dichotomiflorum Toxicosis. *Journal of Agricultural and Food Chemistry* 1991:39(11)**:**1963-1965.
6 Johnson AL, Divers TJ, Freckleton ML, McKenzie HC, Mitchell E, Cullen JM, et al.: Fall panicum (Panicum dichotomiflorum) hepatotoxicosis in horses and sheep. *J Vet Intern Med* 2006:20(6)**:**1414-1421.
7 Lancaster MJ, Vit I, Lyford RL: Analysis of Bile Crystals from Sheep Grazing Panicum-Schinzii (Sweet Grass). *Australian Veterinary Journal* 1991:68(8)**:**281-281.
8 Miles CO, Munday SC, Holland PT, Lancaster MJ, Wilkins AL: Further Analysis of Bile Crystals from Sheep Grazing Panicum-Schinzii (Sweet Grass). *Australian Veterinary Journal* 1992:69(2)**:**34-34.
9 Munday SC, Wilkins AL, Miles CO, Holland PT: Isolation and Structure Elucidation of Dichotomin, a Furostanol Saponin Implicated in Hepatogenous Photosensitization of Sheep Grazing Panicum-Dichotomiflorum. *Journal of Agricultural and Food Chemistry* 1993:41(2)**:**267-271.
10 Regnault TR: Secondary photosensitisation of sheep grazing bambatsi grass (Panicum coloratum var makarikariense). *Aust Vet J* 1990:67(11)**:**419.
11. Sillman SJ, Lee ST, Clabrn J, Borush H, Harris SP. Fall panicum (Panicum dichotomiflorum) toxicosis in three juvenile goats. *J Vet Diagn Investig* 31(1):90-93.
12. Steventon CA, RAidal SR, Quinn JC, Peters A. Steroidal saponin toxicity in Eastern grey kangaroos;: A novel clinicotahologic presentation of hepatogenous photosensitization*J Wild Dis* 2019; 54(3):491-502.
13 Uhlig S, Wisloff H, Petersen D: Identification of cytotoxic constituents of Narthecium ossifragum using bioassay-guided fractionation. *J Agric Food Chem* 2007:55(15)**:**6018-6026.

CASE III: UMN VDL (JPC 4116936)

Signalment: 3-year-old ewe (*Ovis aries*) breed unknown.

History: Pesistent nasal discharge and labored breathing. This animal was euthanized.

Gross Pathology: There was a moderate amount of mucoid discharge in the nares. On coronal section, the nasal turbinates

Nasal mucosa, sheep. The mucosa lining the turbinates is diffusely hyperemic and markedly thickened, occasionally occluding the meatus. (Photo courtesy of: The University of Minnesota, College of Veterinary Medicine, Veterinary Diagnostic Laboratory.

(conchae) were diffusely and markedly thickened, with a roughened appearance and the meatuses were narrowed.

Laboratory results: Aerobic culture of a nasal swab yielded a 4+ predominant *Salmonella* sp. serotyping of this isolate performed by NVSL identified it as a serotype III 61:k:1,5,7 (*S. enterica* subspecies *arizonae).* Immuno-histochemistry for *Salmonella* sp. showed strong positive immunoreactivity distributed throughout the nasal mucosa and submucosa, with epithelial cells, goblet cells, macrophages, and extracellularly.

Microscopic Description: The mucosa of the nasal turbinate is markedly thickened by polypoid to finger-like projections of hyperplastic epithelial cells and dense infiltrates of plasma cells and lymphocytes admixed with few neutrophils, macrophages, and siderophages within the lamina propria and submucosa. The infiltrates within the lamina propria and submucosa separate and surround hyperplastic seromucous glands, which are often ectatic and contain intraluminal mucin and cellular debris. Glandular and surface epithelial cells often contain intracytoplasmic aggregates of indistinct, 1-2um diameter eosinophilic coccobacilli. There are moderate numbers of intraepithelial neutrophils, lymphocytes, and macrophages. There is multifocal follicular lymphocid hyperplasia within the submucosal lymphoid tissue and there are few coalescing pyogranulomas within the lamina propria and submucosa, which replace and compress adjacent glandular

Nasal mucosa, sheep. Gross section of fixed turbinate. The mucosa at the top is approximately normal size, demonstrating the marked proliferation of the mucosa lining the scrolls (Photo courtesy of: The University of Minnesota, College of Veterinary Medicine, Veterinary Diagnostic Laboratory. https://www.vdl.umn.edu/)

tissues. There is dense fibrous tissue expanding the submucosa (fibrosis).

Contributor's Morphologic Diagnosis: Nasal cavity – Rhinitis, proliferative, lymphoplasmacytic and pyogranulomatous, diffuse, marked, chronic with bacteria.

Contributor's Comment: Chronic proliferative rhinitis has been reported in sheep from the United States, Spain, and most recently Switzerland.[1,2,5] Affected breeds in published reports include Columbian, Dorset, Aragonasa, and Texel sheep. Clinical signs and associated lesions manifest n animals older than 1 year of age, and most published cases are between 4 and 7 years of age. The earliest published report was associated with *S. enterica* spp. *Arizonae* (serotype III).[1] Other reports have identified *Salmonella diarizonae* (serotype IIIb: 61:k:1, 5,(7)) as the associated organism.[2,5] This latter serotype is commonly isolated from sheep in several countries and is considered host-adapted.[3]

In a recent survey of US sheep flocks by the USDA, 66.4% of flocks were culture-positive for *Salmonella* spp. and 94.6% of the isolates were identified as serotype IIIb61:k:1, 5,(7)[4] The intestine and tonsils are commonly colonized without any clinical signs or pathologic findings. There are few sporadic reports of associated diarrhea in lambs, abortions, and a report of epididymo-orchitis in a ram.[3] The bacterium can be detected in fecal swabs of healthy animals and is likely maintained in sheep largely due to fecal-oral transmission and colonization.[3] The bacterium can also be detected in nasal swabs from animals with chronic proliferative rhinitis making this another possible source of infection for other animals in a given flock.[5]

Nasal mucosa, sheep. Histologic section of the sample in Fig 2. (Photo courtesy of: The University of Minnesota, College of Veterinary Medicine, Veterinary Diagnostic Laboratory. https://www.vdl.umn.edu/) (HE, 7X)

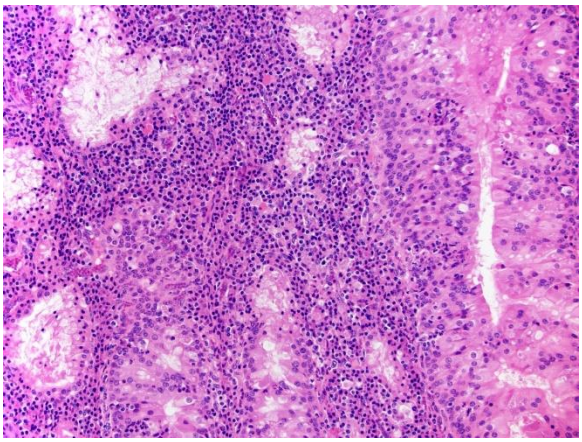

Nasal mucosa, sheep. The lamina propria is expanded by a dense, primarily plasmacytic infiltrated. Overlying mucosa is markedly hyperplastic and glands are mildly degenerate and filled with sloughed cells and mucin. (Photo courtesy of: The University of Minnesota, College of Veterinary Medicine, Veterinary Diagnostic Laboratory. https://www.vdl.umn.edu/) (HE, 200X)

In all case reports which included clinical findings, nasal discharge, respiratory distress, and dyspnea of increasing severity over weeks to years were reported.[1,2,5] Depending on severity and chronicity, "striking mouth-breathing" and loss of body condition may also occur.[3] This may be fatal unto itself or lead to euthanasia.

The gross and microscopic appearance of this case is consistent with all published cases. The most prominent light microscopic features are the polypoid projections formed

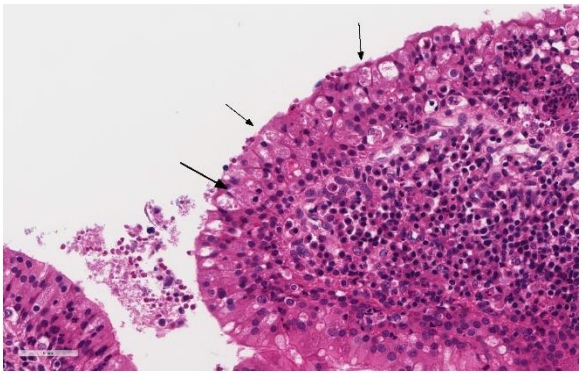

Nasal mucosa, sheep. Mucosal epithelial cells are multifocally expanded by intracytoplasmic aggregates of bacilli (arrows). (HE, 315X)

by hyperplastic epithelium and the infiltrate within the lamina propria and submucosa composed of large numbers of plasma cells, lymphocytes, neutrophils, and macrophages. Particularly prominent in this case were abundant, poorly visualized intracytoplasmic bacilli/coccobacilli within epithelial cells. Additional extracellular bacteria are evident with the aid of IHC. The factors which lead to this striking lesion in association with this common bacterium remain unknown. One recent study attempted to preproduce the disease in a controlled study with limited success.[3] Intranasal inoculation of bacteria led to elevated IFN-gamma over several months and bacteria were maintained in the respiratory tract for at least one year; however, the proliferative lesion was not reproduced. Upper respiratory tract diseases in sheep are most often seen related to infection by larvae of the bot fly *Oestrus ovis* (nasal myiasis; osteosis), leading to mild eosinophilic, catarrhal rhinitis. Enzootic nasal tumor, caused by enzootic nasal tumor virus -1 and -2 (oncogenic betaretrovirus) is another clinical differential, but is likely to cause a focal mass lesion and have a strikingly different histology appearance. Other sporadically occurring nasal tumors or space occupying lesion (e.g. lymphoma, non-viral adenocarcinoma and fungal granuloma) may also have similar clinical signs or gross lesions. Lastly viral pneumonias (e.g. respiratory syncytial virus, ovine adenovirus, parainfluenza 3) may present clinically as primarily upper respiratory signs.)

Contributing Institution:
The University of Minnesota, College of Veterinary Medicine, Veterinary Diagnostic Laboratory. https://www.vdl.umn.edu

JPC Diagnosis: Nasal mucosa: Rhinitis, proliferative**,** and lymphoplasmacytic, chronic, severe, with multifocal mucosal erosion and numerous intracytoplasmic bacilli.

JPC Comment: The contributor does an excellent and thorough writeup on the current knowledge of this uncommon but very characteristic lesion associated with *Salmonella* in sheep. This entity has made one previous appearance in the Wednesday Slide Conference (and must have made quite the impression during the AFIP residency of the moderator, who chose this counter-intuitive and unique lesion for a conference 29 years later.)

According to one report, there is concern over zoonotic potential for this bacterium within

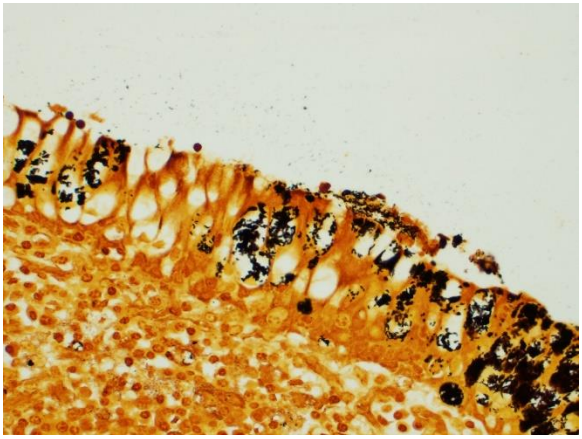

Nasal mucosa, sheep. A Warthin-Starry stain demonstrates the large numbers of intracytoplasmic bacilli. (WS 4.0, 200X)

this particular presentation, although there is no evidence demonstrating actual occurrence. This particular serovar is most commonly seen following transmission from infected snakes with vertebral osteomyelitis and oophoritis.[3]

Nasal mucosa, sheep. Immunostaining for Salmonella sp. antigen demonstrates widespread immunopositivity within the mucosal epithelium of the submitted section (Photo courtesy of: The University of Minnesota, College of Veterinary Medicine, Veterinary Diagnostic Laboratory. https://www.vdl.umn.edu/) (anti-Samonella spp., 200X)

References:

1. Meehan IT, Brogden KA, Courtney C et al. Chronic proliferative rhinitis associated with *Salmonella arizonae* in sheep. *Vet Pathol* 1992; 29:556-559.
2. Lacasta D, Ferrer LM, Ramos JJ et al. Chronic proliferative rhinitis associated with *Salmonella enterica* subspecies *diarizonae* serovar 61:k:1, 5,(7) in sheep in Spain. *J Comp Path* 2012; 147: 406-409.
3. Lacasta D, Figueras L, Bueso JP et al. Experimental infection with *Salmonella enterica* subsp. *diarizonae* serotype 61:k:1, 5,(7)in sheep: Study of cell-mediated immune response. *Small Rum Res* 2017; 149:28-33.
4. Salmonella on US Sheep Operations, 2011. USDA-APHIS, Veterinary Services Info Sheet. June 2013.
5. Stokar-Regenschiet N, Overesch G, Giezendanner R et al. *Salmonella enterica* subsp. *diarizonae* serotype 61:k:1, 5,(7) associated with chronic proliferative rhinitis and high nasal colonization rates in a Texel sheep in Switzerland. *Prev Vet Med* 2017; 145:78-82.

CASE IV: M18-02265 (JPC 4118633).

Signalment: 3 year 8 month-old, female Friesian, bovine (*Bos taurus*)

History: On a farm in the Hunter region of NSW Australia, 2/40 adult cows died suddenly. Three days prior to death, the herd had been moved onto a Kikuyu (*Pennisetum clandestinum*) paddock. It was also possible that the herd had not had access to water for 24h.

Gross Pathology: Necropsy was performed on 2 animals. Gross findings in the necropsied animals included severe dehydration and abundant liquid content of the rumen. Ruminal papillae tips had multifocal pale discoloration. Mucosa from reticulum and omasum presented with multifocal red areas. The cows were pregnant with fetuses aged at approximately 7-8 months gestation

Laboratory results: Results of serum biochemistry analysis on an animal from the same herd were consistent with the gross finding of severe dehydration (decreased renal perfusion resulting in mild elevations in Urea/Creatinine/Phosphate and Protein/Albumin/Globulin) and muscle damage possibly related to being recumbent prior to death (mild elevations in creatinine and AST). Serum D-lactate levels were at the top of the normal range

			Reference Range
GGT	27		0-35 U/L
GLDH	20		0-30 U/L
AST	181	H	0-120 U/L
BIL	3.0		0.0-24.0 umol/L
CK	6752	H	0-300 U/L
UREA	17.5	H	2.1-10.7 mmol/L
CREAT	492	H	0-186 umol/L
PHOS	3.28	H	0.80-2.80 mmol/L
URE/CREA	0.04		0.00-0.07
PROTEIN	128.5	H	60.0-85.0 g/L
ALBUMIN	49.6	H	25.0-38.0 g/L
GLOB	78.9	H	30-45.0 g/L
ALB/GLOB	0.6	L	0.7-1.1
BHB	0.80		0.00-0.80 mmol/L
CA	2.62		2.00-2.75 mmol/L
MG	2.02	H	0.74-1.44 mmol/L
D-LACT	0.5		0.0-0.5 mmol/L

A Total Alfatoxins qualitative strip test on a sample of the kikuyu was negative (<4ppb cut off)

Microscopic Description: Omasum: There is widespread disruption of epithelial tissue architecture with multifocal to coalescing aggregates of degenerate neutrophils, epithelial cells with eosinophilic cytoplasm and shrunken, pyknotic or karrhorhectic nuclei admixed with cellular debris (micropustules). There is diffuse separation of omasal mucosa from underlying tissue (interpreted to be partially due to artifact). The omasal lumen is filled with fragments of refractile plant material mixed with myriad of small basophilic cocci. The submucosa is diffusely, mild to moderate expanded with clear areas (edema), with multifocal mild to moderate coalescing infiltrates of neutrophils, lymphocytes and plasma cells with occasional macrophages.
Reticulum: There is multifocal to coalescing disruption of epithelial tissue architecture with multifocal to coalescing aggregates of degenerate neutrophils, epithelial cells with eosinophilic cytoplasm and shrunken, pyknotic or karrhorhectic nuclei (interpreted as necrotic epithelial cells) (micropustules) admixed with clear spaces (edema) and cellular debris. Subepidermal vessels are diffusely congested and interstitial fibroblasts and myofibers are multifocal separated out by increased amounts of clear space.

Contributor's Morphologic Diagnosis: Omasum: Omasitis, necrosuppurative, diffuse, moderate to severe with intracorneal pustules, Friesian, bovine (*Bos taurus*)

Reticulum: Reticulitis, necrosuppurative, multifocal to coalescing, moderate with intracorneal pustules, Friesian, bovine (*Bos taurus*)

Contributor's Comment: Kikuyu grass (*Pennisetum clandestinum)* is a perennial tropical pasture species commonly found on coastal regions of Australia growing between spring and autumn.[2] Poisoning occurs after ingestion of kikuyu after a period of rapid

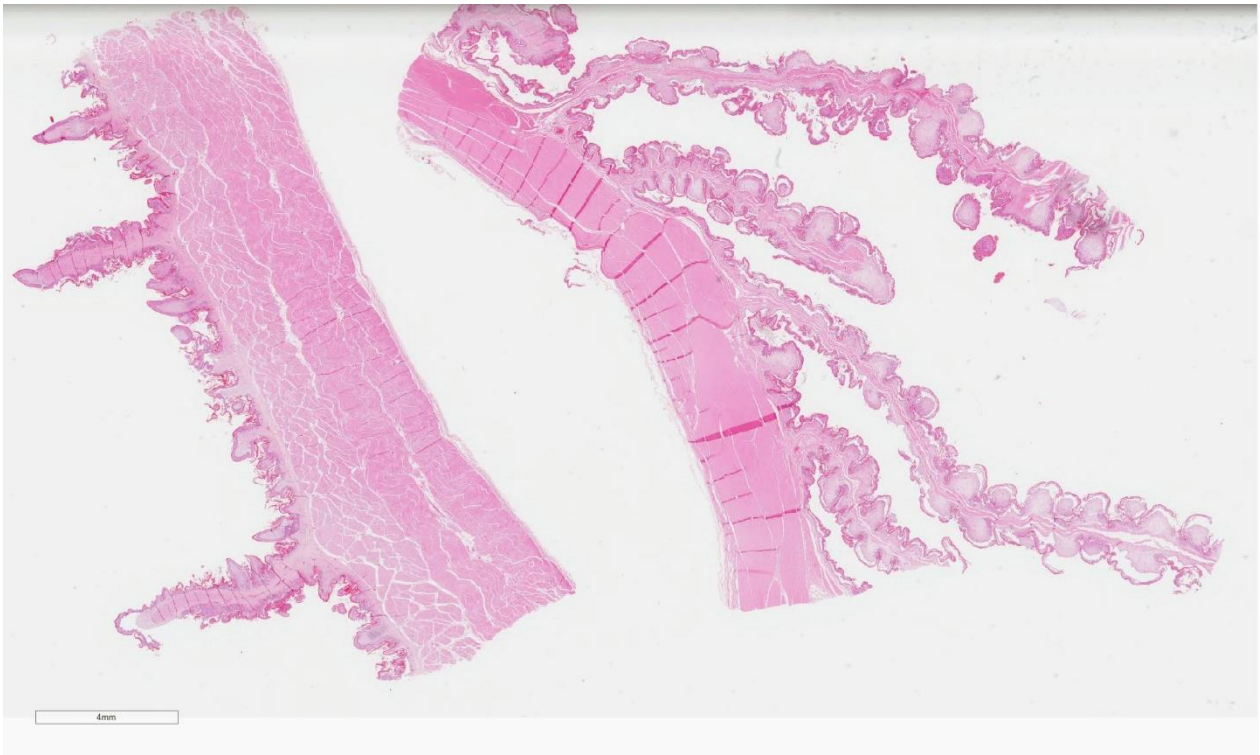

Ox, reticulum and omasum: At low magnification, the mucosa is multifocally lifted off of the underying mildly edematous submucosa. (HE, 5X)

growth in autumn following a period of summer drought. From a collation of outbreaks across 40 farms, between 13.6% and 64.2% cattle were affected of which between 16.7% and 95.6% died.[2] In an outbreak, signs of toxicity typically present on average 3 days (1-8 day range) post first grazing of kikuyu, with some cases progressing quickly to death over a subsequent week long period.[2] Clinical signs consist of drooling, dehydration, abdominal pain, sham drinking, depressed mentation, incoordination and recumbency. Other signs may include distended abdomen, rumen stasis, elevated temperature and both cardiac and respiratory distress.[2,3] A history of grazing kikuyu and a post mortem finding of a distended rumen containing a sloppy mix of pasture and fluid are highly suggestive of kikuyu poisoning. Additional supportive evidence from a post mortem includes hyperaemic mucosa of the forestomaches and abomasum, empty small intestine, dry contents in the large intestine and cardiac haemorrhages.[2] The most consistently reported histopathological lesion is segmental necrotising inflammation within the epithelium of the forestomach mucosa,[2-4] most frequently the omasum.[2] Cases of longer duration of exposure show mucosal inflammation regresses and epithelial repair occurring.[2]

There are multiple theories towards the toxin production that causes kikuyu poisoning. While produced seasonally, it is unknown if it is produced spontaneously by the plant, in response to a stimulus such as a pathogen or by a pathogen itself. Despite no reported cases of nitrate poisoning from kikuyu, one suggestion is the accumulation of nitrogenous compounds may be associated with toxin production.[2] Another is the association of armyworms and kikuyu in

some but not all cases[1]. Oral ingestion of fungi cultures and mycotoxins has produced similar kikuyu-like poisoning conditions in cattle, however isolation of these fungi and/or mycotoxins from kikuyu plants and soil associated with poisonings is not consistent.[1,2,6]

Other diseases with a similar presentation to kikuyu poisoning include metabolic disease such as hypocalcaemia and hypo-magnesemia, infectious diseases such as listeriosis and *Histophilus somni* meningoencephalitis, or other poisonings such as lead, salt or nitrate poisoning. Ruminal acidosis causes similar histological lesions, but is usually restricted to the rumen.

Contributing Institution: Elizabeth Macarthur Agricultural Institute, NSW, DPI https://www.dpi.nsw.gov.au

JPC Diagnosis: 1. Omasum: Omasitis, necrotizing, multifocal to coalescing, with numerous intracorneal pustules.

2. Reticulum: Reticulitis, necrotizing, multifocal to coalescing, with numerous intracorneal pustules.

JPC Comment: Kikuyu grass (*Pennisetum clandestinum*) is a drought-tolerant grass native to the region of Kenya that is home to the Kikuyu people. It has been adapted to be a lawn grass in dry regions of New Zealand, South Africa, and the Southwestern US (California). It has become popular on golf courses due to its dense nature and propensity to create challenging rough. It has been termed an invasive species in several countries due to its ability to overgrow other plant life, preventing other plants from sprouting and producing herbicidal toxins that compete with other plants.[5]

Toxicity is sporadic, with many animals grazing it with no ill effects. Outbreaks are

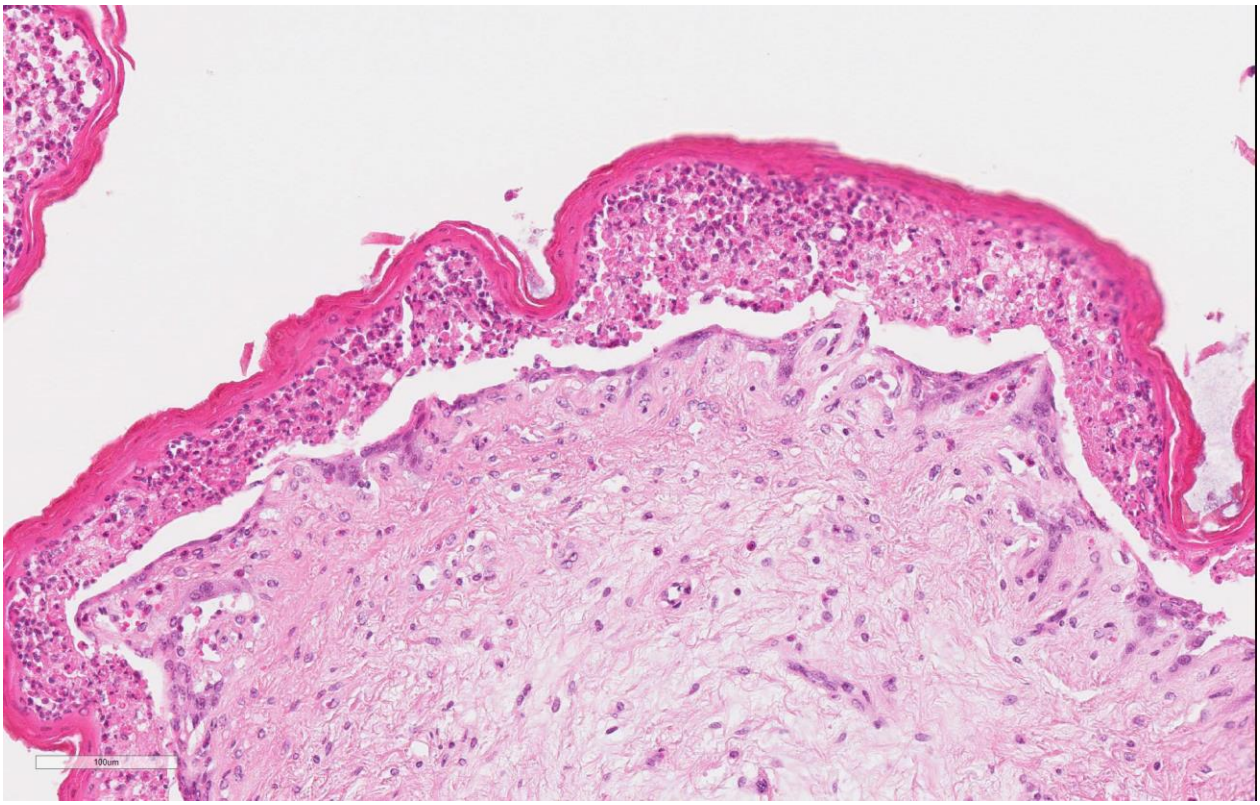

Ox, omasum. Coalescing intracorneal pustules often form clefts within the mucosa. (HE, 246X)

brief, geographically restricted, and lethal. A number of strains (with such names as "Whittet", "Crofts", and "Noonan") of kikuyu grass have been developed but do not appear to differ significantly in potential toxicity.[2]

The contributor mentions the "sloppy mix" of pasture and fluid in the rumen. This appears to be the result of a number of contributing factors, to include excess salivary production, ruminal stasis and a net outflow of fluid from the ruminal mucosa into the ruminal lumen. Animals will excessive amounts of ruminal fluid may "sham drink" (placing the head in or near water or playing in a water source without actual drinking) and die of dehydration due to third spacing of water into the rumen.[2]

The microscopic lesion demonstrated in this case is consistent with that described in cases of kikuyu poisoning – necrosis of the superficial layers of the ruminal, reticular, and omasal mucosa (stratum lucidum, granulosum, and spinosum) with profound infiltatin by neutrophils which lifts it off of the underlying stratum basale. Degenerative changes in the myocardium and kidney have been infrequently reported in association with this condition.[2]

The identity of the toxin in kikuyu grass is yet to be elucidated and is the subject of many theories regarding its identity and seasonality. The forestomach lesion is reminiscent of that seen with ingestion of *Baccharis* sp. plants by ruminants (WSC Conference 2012-2013, Conference 4, Case 2), which is the result of accumulation of fungus-produced trichothecene toxins. A kikuyu-lke condition has been reproduced in ruminants via feeding of fungal cultures from two pasture fungi, *Myrothecium* sp. and *Phoma* sp. which produce roridin and verrucarin toxins, respectively. Nitrates have often been incriminated in outbreaks of kikuyu grass, which accumulated nitrates during their reproductive period within their stems. Leaf damage by various insects have been theorized to increase the consumption of kikuyu stems in some outbreaks, or overgrazing may increase stem consumption. In most reported cases of kikuyu poisoning, nitrate levels were within normal limits in affected animals.[2]

References:

1. Botha C, Truter M, Jacobs A. Fusarium species isolated from Pennisetum clandestinum collected during outbreaks of kikuyu poisoning in cattle in South Africa. *Onderstepoort J Vet Res*. 1983;81(1):1-9. doi:10.4102/ojvr.v81i1.803.
2. Bourke C. A review of kikuyu grass (Pennisetum clandestinum) poisoning in cattle. *Aust Vet J*. 2007;85(7):261-267. doi:10.1111/j.1751-0813.2007.00168.x.
3. Gwynn R, Gabbedy B, Hophinkson W, Kay B, Wood Pm. Kikuyu Poisoning of Cattle in Western Australia. *Aust Vet J*. 1974;50(8):369-370. doi:10.1111/j.1751-0813.1974.tb14116.x.
4. Martinovich D, Smith B. Kikuyu Poisoning of Cattle 1. Clinical and Patholgical Findings. *N Z Vet J*. 1973;21(4):55-63. doi:10.1080/00480169.1973.34078.
5. "Pennisetum clandestinum (General impact)" Global Invasive Species Database, Invasive Species Specialist Group. (http: //www.issg.org/database/species/impact_info.asp?si=183&fr=1&sts=&lang-EN.
6. Ryley M, Bourke C, Liew E,

Summerell B. Is Fusarium torulosum the causal agent of kikuyu poisoning in Australia? In: *Australasian Plant Disease Notes*.Vol 2. Australasian Plant Pathology Society; 2007:133-135. doi:10.1021/jf991022b.

Self-Assessment - WSC 2019-2020 Conference 4

1. Which of the following is true regarding Australian bat lyssavirus?
    a. It usually results in fatal infections in bats.
    b. It is more closely related to several types of European bat lyssavirus than to classical rabies virus
    c. Meningoencephalitis is not seen in infected animals.
    d. Vaccination against rabies is protective against exposure to Australia bat lyssavirus.

2. Which of the following is most commonly seen in sheep grazing grasses of the species *Panicum*?
    a. Crystals in the bile ducts
    b. Uroliths
    c. Polioencephalomalacia
    d. Cardiac necrosis

3. Which of the following subspecies of *Salmonella enterica* has been identified as a cause of proliferative rhinitis in sheep?
    a. typhimurium
    b. dublin
    c. arizonae
    d. houtenae

4. Which of the following is the usual histologic lesion associated with kikuyu intoxication?
    a. Laminar cortical necrosis
    b. Granulomatous inflammation in the lung
    c. Epithelial necrosis of the forestomachs
    d. Renal tubular necrosis

5. The lesions associated with ingestion of kikuyu grass are similar to toxicity associated with grazing?
    a. Baccharis cordifolia
    b. Cestrum diurnum
    c. Solanum glaucophyllum
    d. Veratrum californicum

Please email your completed assessment for grading to Dr. Bruce Williams at bruce.h.williams12.civ@mail.mil. Passing score is 80%. This program (RACE program 33611) is approved by the AAVSB RACE to offer a total of 0.5 CE Credits, with a maximum of 12.5 CE Credits being available to any individual Veterinary Medical Professionals for the 2019-2020 Wednesday Slide Conference. This RACE approval is for the subject matter categories of: SCIENTIFIC using the delivery method of NON-INTERACTIVE DISTANCE. This approval is valid in jurisdictions which recognize AAVSB RACE.

Joint Pathology Center
Veterinary Pathology Services

WEDNESDAY SLIDE CONFERENCE 2019-2020

C o n f e r e n c e 5

25 September 2019

CASE I: V17-00724 (JPC 4121052).

Signalment: Three years old, female, breed not specified, *Ovis aries*, sheep

History: The ewe had poor weight gain especially in the winter with periodic loose, nonpelleted feces. The ewe had subcutaneous edema in the skin of the ventral mandibular area (bottle jaw).

Gross Pathology: There were segments of the small intestine that were thick and corrugated. The mesenteric lymph nodes were enlarged with numerous variably sized tan foci that effaced the lymph node parenchyma.

Laboratory results: The mesenteric lymph node was PCR positive for *Mycobacterium avium* subspecies *paratuberculosis* (MAP). MAP was not isolated on culture of the mesenteric lymph node.

Microscopic Description:
The lamina propria of multiple segments of the small intestine is markedly thickened by diffuse infiltrates of numerous macrophages, which are mixed with lesser numbers of lymphocytes. The infiltrates of macrophages result in blunting and widening of the

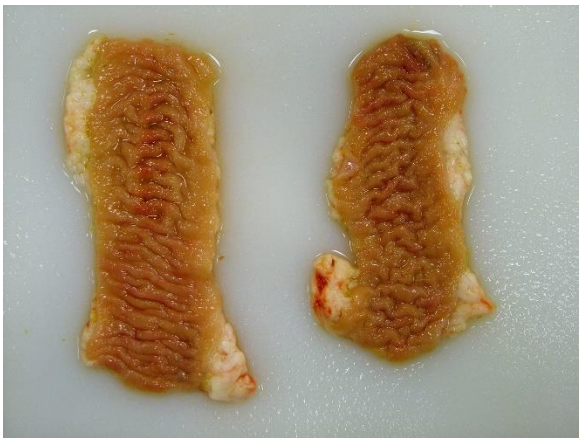

Intestine, sheep. Multifocally, the intestinal mucosa was thickened and rugose. (Photo courtesy of: New Mexico Department of Agriculture Veterinary Diagnostic Services, www.nmda.nmsu.edu/vds)

intestinal villi. The macrophages in the lamina propria contain numerous intracellular acid fast bacilli. There are occasional lymphatic vessels in the mesentery that are surrounded by and infiltrated by numerous macrophages with lesser numbers of lymphocytes and neutrophils (not present in all sections).

Contributor's Morphologic Diagnoses: Small intestine. Enteritis, granulomatous, diffuse, severe with numerous intracellular acid fast bacilli; etiology consistent with

Mycobacterium avium subspecies *paratuberculosis* (Johne's disease)

Contributor's Comment: Mycobacteria are thin rods that can vary in length from 0.2 to 10.0 µm.[7] Mycobacteria are acid-fast and are gram-positive, but the lipid in the cell wall typically prevents staining with a Gram stain. They are aerobic, oxidative, non-motile and do not form spores. Mycobacteria are typically slow-growing with a range of generation times of 2-20 hours.

Johne's disease is caused by *Mycobacterium avium* subspecies *paratuberculosis* (MAP).[6,7,8] Johne's disease occurs most commonly in domestic ruminants, but nondomestic ruminant species as well as non-ruminant species can be infected with MAP. MAP is shed in the feces of infected animals and is spread by fecal-oral transmission. Transmission of MAP to naïve animals typically occurs in young animals while they are still nursing while older animals are more resistant to infection. There are two strains of MAP: type I or S strain and type II or C strain. The type I strain of MAP was first isolated from sheep and is fairly species specific for sheep with only rare reports of cattle being infected with this strain. The type II strain of MAP was first isolated from cattle and can infect a multitude of species including cattle, sheep and goats. The type II strain of MAP is the most common.

Unlike in cattle where Johne's disease causes severe diarrhea, Johne's disease in sheep manifests as a wasting disease in the majority of sheep.[3,6,7,8] The intestinal thickening caused by granulomatous enteritis can involve the jejunum, ileum, cecum and colon, but are most common in the ileum.[2,3,6,7,8] The intestinal lesions of Johne's disease in sheep are typically mild, can be multifocal and easily missed at necropsy. Sheep with Johne's disease can also develop

Mesenteric lymph node, sheep. Mesenteric nodes were enlarged with variably-sized tan foci of inflammation. (Photo courtesy of: New Mexico Department of Agriculture Veterinary Diagnostic Services, www.nmda.nmsu.edu/vds)

granulomatous lymphangitis of lymphatic vessels in the mesentery as well as lymphadenopathy and granulomatous lymphadenitis of the mesenteric lymph nodes. Tubercle-like caseating mineralized granulomas are more common in the intestine, lymph vessels and mesenteric lymph nodes of sheep than they are in cattle. Lymph nodes other than mesenteric lymph nodes, the liver, the lungs and the spleen can also have small granulomas with MAP in sheep. The microscopic lesions of Johne's disease in sheep occur in two forms. One form consists of dense infiltrates of numerous macrophages in the mucosal epithelium of the intestine with numerous bacteria (the multibacillary form associated with a strong humoral immune response). The other form consists of focal to multifocal lymphocyte-rich infiltrates of macrophages in the mucosal epithelium of the intestine with few bacteria (the paucibacillary form associated with a cell-mediated immune response).

After ingestion of MAP, the mycobacteria gain access to the small intestine through M cells or epithelial cells over the submucosal Peyer's patches.[2,6,9] The mycobacteria then infect and survive in macrophages in the

Intestine, sheep. Subgross magnification demonstrates circumferential loss of villi with expansion of the lamina propria by a prominent cellular exudate. (HE, 7X)

intestinal mucosal epithelium and the mesenteric lymph nodes. In sheep experimentally infected with MAP, infection could be identified in most sheep by 18 months postinfection.[4] Infection was typically identified first in the mesenteric lymph nodes. Microscopic lesions could be identified 6-12 months after the identification of infection with MAP with the lesions usually being identified in the mesenteric lymph nodes first. The microscopic lesions and the disease in the sheep experimentally infected with MAP developed at variable rates with clinical signs first apparent at 24 months usually corresponding to the development of severe intestinal lesions. Although the intestinal lesions may be less severe in subclinical sheep, there is evidence of continuous fecal shedding of MAP in some subclinically infected sheep potentially resulting in a continuously infected environment.[10]

Diagnosis of Johne's disease in sheep, particularly of an individual sheep, can be more difficult than it is in cattle.[6,8,9] Isolation of mycobacterium from the feces or tissue from sheep is much more difficult than it is from cattle as the type I strain is difficult to isolate.[3,6,8,9] PCR can be used to detect MAP in feces and tissue of sheep, but molecular techniques are most likely useful on an individual animal basis and not a herd basis due to the cost of testing.[8,9] Serologic testing (ELISA and AGID) can be used for antemortem diagnosis of Johne's disease, but there are studies that indicate the usefulness of serologic testing depends on whether the sheep has the multibacillary form (a strong humoral immune response and more likely to be serologically positive) or the paucibacillary form (a cell-mediated immune response and more likely to be serologically negative).[8] In addition, the serologic tests can also cross react with *Corynebacterium pseudotuberculosis* (caseous lymphadenitis)

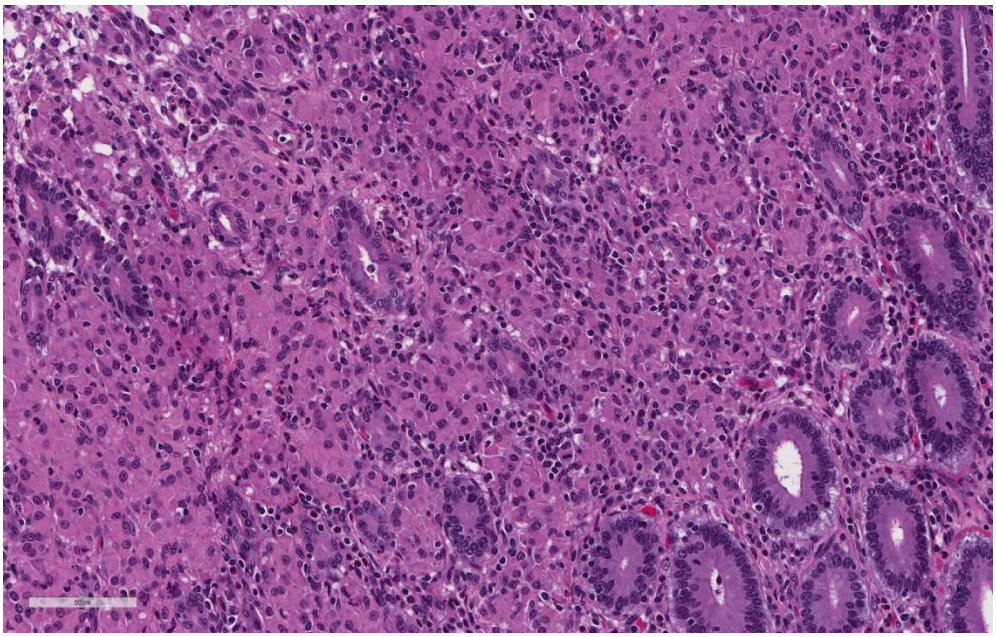

Intestine, sheep. Crypts are separated and replaced by sheets of histiocytes with abundant eosinophilic cytoplasm.

another wasting disease of sheep. The diagnosis of Johne's disease using histopathology collected postmortem or from rectal biopsy can also be difficult with the paucibacillary form of Johne's disease because it can have a multifocal distribution.[4,9]

Contributing Institution:
New Mexico Department of Agriculture
Veterinary Diagnostic Services
www.nmda.nmsu.edu/vds

JPC Diagnosis: Small intestine: Enteritis, histiocytic, diffuse, severe with marked villar and crypt loss, villar blunting and fusion, crypt abscesses and hyperplasia, and edema (with multifocal lymphohistiocytic lymphangitis).

JPC Comment: The contributor has provided a concise review of *Mycobacterium avium* susbsp. *paratuberculosis* (MAP) in ruminants with a focus on its peculiarities in sheep.

The economic importance of Johne's disease in sheep cannot be ignored. While reports in small ruminants, as compared to affected cattle are sketchy, annual mortality in affected flocks in Australia have averaged 6-7% annually, with some reaching up to 20%. Economic losses to the British sheep industry range up to 20 million pounds annually if replacement strategies are factored in. In Italy, MAP infection decreases profit efficiency by 20% in affected farms. [10] These are direct losses only; potential indirect losses arising from trade restrictions at the international and national levels are difficult to estimate. Unlike many other highly contagious diseases of serious economic import, the OIE as of yet considers this a non-

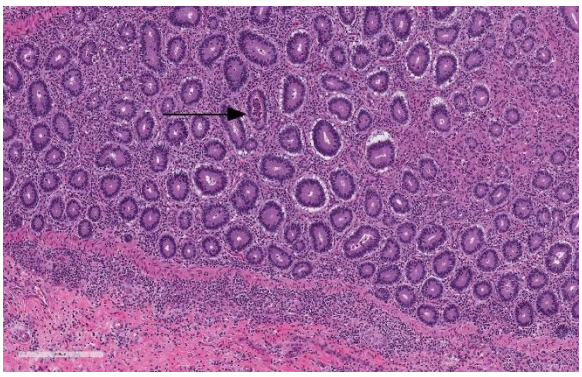

Intestine, sheep. The inflammatory infiltrate is less prominent in lamina propria surrounding the deep crypts and extends into the underlying submucosa. Rare crypt abscesses are present (arrow)

reportable disease and offers no guidance on paratuberculosis. Norway has had no known cases of MAP since 2015, and Sweden has been free of Johne's disease in cattle since 2008, but due to the insidious nature of this disease, all countries remain at risk.[10] Another risk factor is Johne's disease infection of non-domestic ruminant species including wild species of goats and sheep, deer, camelids, bison, rhinoceroses, and some species of marsupials may serve as additional reservoirs.

Another determining factor in the potential spread of Johnes's disease appears to be the differential susceptibility of various breeds to infection by MAP. In a recent article by Begg at al.,[1] Merino sheep (prized for their fine wool with an average value of 2-3 times more than mutton sheep) have the highest rate of clinical disease 14 months after oral inoculation at 42%, followed by Merino-Suffolk cross (36%), Border Leicester (12%) and Poll Dorset (11%). The authors were careful to point out that this may simply imply a longer disease duration Border Leicester and Poll Dorset breeds; however, this information is useful when considering control programs that emphasize a rapid decrease in environmental contamination by infected animals.[1]

Over the years, the MAP has been considered as a potential pathogen in humans in a number of conditions, yet never definitively incriminated. Numerous studies have identified potential risks for both waterborne (farm effluent) and foodborne (contaminated milk and meat) pathways for zoonotic transmission to humans, however at present, MAP is still not considered a zoonotic pathogen. One of the most common theories is that MAP may be a cause of IBD in humans, and is supported by circumstantial evidence including similar morphologies between Johne's disease and various forms of IBD including Crohn's disease, increases in IBD in areas in which animals demonstrate a 30% incidence of Johnes's disease and isolation in breast milk from mothers with IBD. However, Koch's postulated have never been fulfilled, and MAP has not yet been isolated with by ELISA-based or PCR in individuals with IBD. MAP has also been theorized to play a role in the generation of Type I diabetes in certain populations due to potential epitope mimicry between islet cell proteins GAD65 and ZNT8 with MAP proteins and HSP65 and MAP3865c,, respectively as well as and

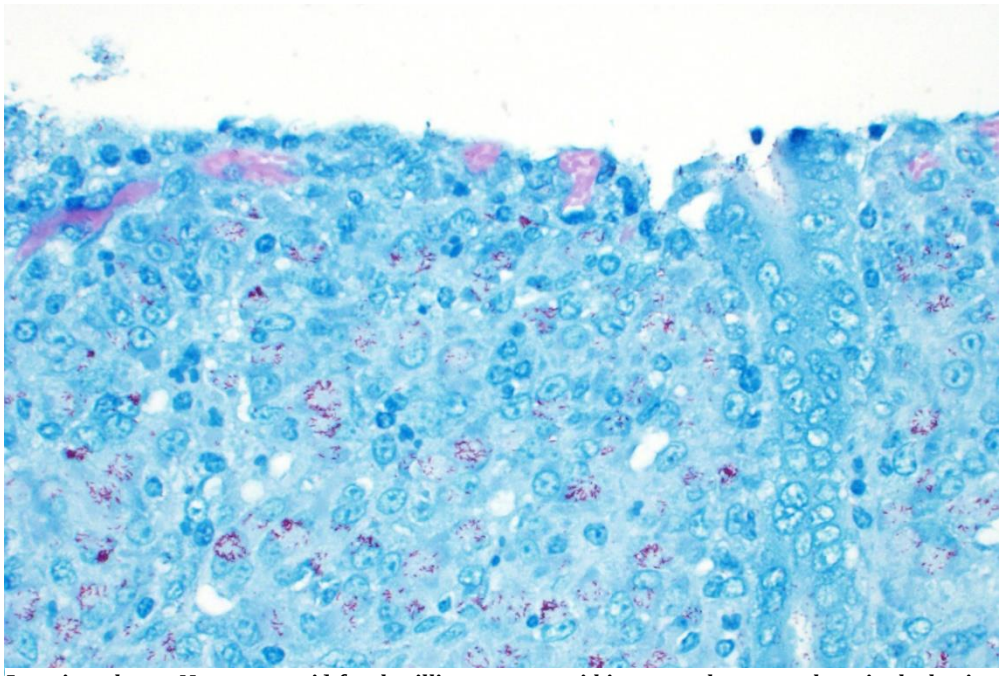

Intestine, sheep. Numerous acid-fast bacilli are present within macrophage cytoplasm in the lamina propria. (Ziehl-Nielsen, 400X)

immune responses to HSP65 have been seen in patients with rheumatoid arthritis and Hashimoto's thyroiditis. [4]

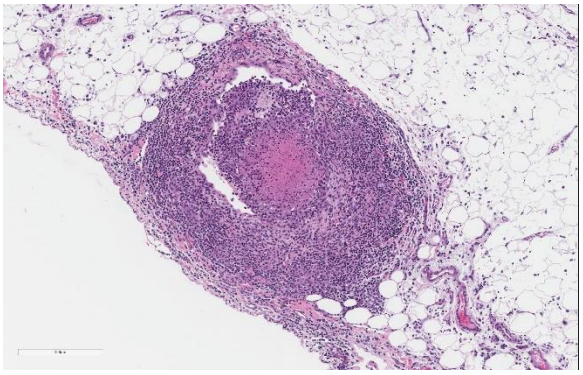

Intestine, sheep. Lymphohistiocytic inflammation is centered on lymphatics in the adjacent mesentery. (HE 95X)

The moderator discussed the difference between Ziehl-Nielsen and Fite-Furaco stains. "Acid- fastness" refers to microorganisms whose cell wall has a high lipid content of mycolic and long chain fatty acids, which cause them to bind the basic dye carbol-fuchsin, a stain which remains after strong decolorization with acid-alcohol (thus "acid-fast") The Fite-Furaco uses peanut oil and xylene to protect the wall of bacteria from decolorization and allows for the visualization of bacteria with less lipid content, such as *M. leprae* and *Rhodococcus equi*. The moderator also mentioned a newly discovered strain of the bacterium, called the type III B strain (as opposed to type I S and type II C strains) which is pathogenic for buffalo, and currently a problem in India.

References:

1. Boes KM and Durham AC. Bone marrow, blood cells and the lymphoid lymphatic system. In: Zachary JF, ed. *Pathologic Basis of Veterinary Disease*. 6th ed. St. Louis, MO. Elsevier; 2017: 724-804.
2. Carrigan MJ and Seaman JT. The pathology of Johne's disease in sheep. *Aust Vet J*. 1990; 67(2): 47-50.
3. Dennis MM, Reddacliff LA and Whittington RJ. Longitudinal study of clinicopathological features of Johne's disease in sheep naturally exposed to *Mycobacterium avium* subspecies *paratuberculosis*. *Vet Pathol*. 2011; 48(3): 565-575.
4. Garvey M. Mycobacterium avium subspecies paratuberculosis: A possible causative agent in human morbidity and risk to public health safety. *Open Vet J* 2018; 8(2):172-181
5. Gelberg HB. Alimentary system and the peritoneum, omentum, mesentery, and peritoneal cavity. In: Zachary JF, ed. *Pathologic Basis of Veterinary Disease*. 6th ed. St. Louis, MO. Elsevier; 2017: 324-411.
6. Markey B, Leonard F, Archambault HM, Cullinare A and Maguire D. Mycobacterial species. In: *Clinical Veterinary Microbiology*. 2nd ed. St. Louis, MO. Mosby Elsevier; 2013: 161-176.
7. Radostits OM, Gay CC, Hinchcliff KW and Constable PD. Diseases associated with bacteria – IV. In: *Veterinary Medicine A Textbook of the Diseases of Cattle, Horses, Sheep, Pigs and Goats*. 10th ed. Philadelphia, PA; 2007: 1007-1060.
8. Uzal FA, Plattner BL and Hostetter Jm. Alimentary system. In: Maxie G, ed. *Jubb, Kennedy, and Palmer's Pathology of Domestic Animals*. 6th ed (Vol 2). St. Louis, MO. Elsevier; 2016: 1-257.
9. Whittington RJ, Reddacliff LA, March I, McAllister S and Saunders V. Temporal patterns and quantification of excretion of *Mycobacterium avium* subspecies

paratuberculosis in sheep with Johne's disease. *Aust Vet J.* 2000; 78(1): 34-37.
10. Whittington R, Dopnat K, Weber MF et al. Tontrol of paratuberculosis: who, why, and how. A review of 48 countries. *BMC Vet Res* 2019; 15:198-227.

CASE II: 160360 (JPC 4085120).

Signalment: Adult, female, European brown hare (*Lepus europaeus*).

History: Found dead in the woods

Gross Pathology: At necropsy the animal presented a severe jaundice. Mesenteric lymph nodes were enlarged and on cut section they presented multiple coalescing foci of caseous necrosis. The spleen was severely enlarged and was characterized by 1 mm white foci also present in the liver and the kidneys.

Laboratory results: Bacteriology**:** *Yersinia pseudotuberculosis* in liver and spleen.

Microscopic Description:
Liver: 60% of hepatic parenchyma is characterized by the presence of multifocal to coalescing, 1mm in size, randomly distributed inflammatory lesions (Fig. 4). These lesions are composed, from the periphery to the center, by a moderate amount of macrophages, epithelioid cells and less multinucleated giant cells (Langhans and foreign body types) admixed with scant heterophils. The inflammatory cells surround some cells (macrophages and hepatocytes) with condensed (pyknosis) or fragmented nuclei (karyorrhexis), nuclear and cellular debris (necrosis). The center of the lesion is occupied by small, 1µm in length, coccobacillar basophilic organisms (bacterial

Liver, hare. Numerous 1mm white foci were present in the liver. (Photo courtesy of Laboratoire d'Histopathologie animale, Vetagro Sup, campus veterinaire, http://www.vetagro-sup.fr/)

colonies) enmeshed within an eosinophilic material (fibrin). Liver parenchyma presents severe and diffuse hydropic degeneration, characterized by enlarged cells with clear granular eosinophilic cytoplasm (glycogenosis). A multifocal single cell necrosis is also present. Within the sinusoids a moderate amount of heterophils and monocytes are present, as well as Kupffer cells (Kupffer cell hyperplasia). An extramedullary hematopoiesis is evident within Disse'space.

Contributor's Morphologic Diagnoses:
Liver: Hepatitis, granulomatous and necrotizing, multifocal to coalescing, severe chronic with bacteria consistent with *Yersinia pseudotuberculosis*.

Kidney (not submitted): Nephritis, granulomatous and necrotic, multifocal, chronic moderate with bacteria consistent with *Yersinia pseudotuberculosis*.

Spleen (not submitted): Splenitis, granulomatous and necrotic, multifocal to coalescing, chronic severe with ibacteria consistent with *Yersinia pseudotuberculosis*.

Spleen, hare. There was marked splenomegaly with coalescing white foci as well. (Photo courtesy of Laboratoire d'Histopathologie animale, Vetagro Sup, campus veterinaire, http://www.vetagro-sup.fr/)

Contributor's Comment: *Yersinia pseudotuberculosis* is a gram-negative, facultative intracellular coccobacillus, which occurs worldwide in wild rodents, lagomorphs and birds. Sporadic infections can occur in domestic animals and humans. It is shed in the feces by infected animals and it can survive and grow in the environment at low temperatures. Infection occurs by ingestion; the organism penetrates the intestinal mucosa through the M cells.[3] Then it migrates to the Payer's patches and by the lymphatic route to the mesenteric lymph nodes. If the organism becomes septicemic/bacteremic, it spreads to other organs, typically liver and spleen.

Pathogenic factors include:

- *Invasin*. This protein is expressed at low temperature conditions and it facilitates bacteria translocation through the intestinal epithelium into the lamina propria and Peyer's patches. Invasin binds to β1 integrins on cells, favoring bacterial-cell adhesion.
- *Type III secretion system* (T3SS): it is a virulence mechanism found in several gram-negative bacteria. It is composed of a needle-like syringe that injects into the host cell the effector proteins. After being attached to host cells, *Y. pseudotuberculosis* uses this system to inject the Yersinia outer proteins (Yops) [3]
- *Yersinia outer proteins* (Yops): there are 6 known Yops. These effector proteins alter the actin cytoskeletal structures to inhibit phagocytosis, induce apoptosis and downregulate proinflammatory responses. They are produced at 37°C environmental temperature, which means within the host.[3]

Gross typical lesions are white 1-10 mm foci in affected organs, mainly intestine, liver, spleen and mesenteric lymph nodes. In the large lesions a caseous necrosis is visible. Histologically, the lesions consist in micro abscesses composed of necrotic neutrophils with or without granulomatous reaction. Large bacterial colonies are easily visible.

In hares and rabbits differential diagnosis are *Yersinia enterocolitica* and *Francisella tularensis*. The three bacteria produce similar gross and histologic lesions and bacterial culture is necessary to identify them.

Contributing Institution:
Laboratoire d'Histopathologie animale, Vetagro Sup, campus vétérinaire, http://www.vetagro-sup.fr/

Liver, hare. At subgross magnification, there are numerous occasionally coalescing areas of necrosis. (HE, 7X)

JPC Diagnosis: Liver: Hepatitis, necrotizing, multifocal to coalescing, marked, with numerous colonies of bacilli.

JPC Comment: The genus *Yersinia* is a member of the family Enterobacteriaceae and consists of 18 species of gram-negative bacilli, three of which, *Y. enterocolitica*, *Y. pseudotuberculosis*, and the causative agent of plague, *Yersinia pestis* are pathogenic for animals, Nonhuman primates and man are considered extremely susceptible to infection by these pathogens, although *Y. enterocolitica (Yec)* was not considered as a human or veterinary pathogen until the late 1960s.[1] In contrast, a number of domestic and wildlife species including pigs, rodents, and wild birds, are and important reservoirs of this pathogens and considered significantly less susceptible to their pathogenic effects. (Interestingly, pork chitterlings (intestine) have been often identified as a source of food-borne illness to young children, during the cleaning and preparation phase.)[4] *Y. enterocolitica* has over 60 serotypes, but less than ten are pathogenic in primate hosts. It has six biotypes, of which one is highly pathogenic (1B), one is non-pathogenic (1A) and the remained, biotypes 2-5) are considered mildly pathogenic.[2]

The plasmid of *Yersinia* virulence (pYV) which encodes for many of the virulence factors mentioned by the contributor is the most important factor in pathogenicity. All biotypes are capable of mucosal invasion; however only those strains with the pYV can migrate from Peyer's patches to mesenteric nodes, and onward to establish the necrotic lesions in multiple organs demonstrated in this case. While this would logically mean that identifying plasmids are an easy way to identify pathogenic serotypes, it has been demonstrated that pathogenic bacteria may spontaneously lose this plasmid when

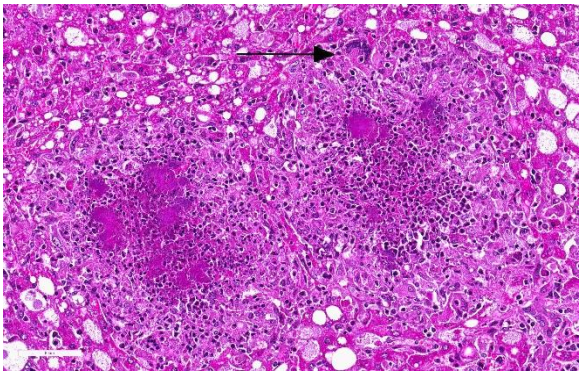

Liver, hare. Areas of lytic necrosis are centered on large bacterial colonies. Multinucleated giant cell macrophages are scattered at the periphery (arrow). (HE, 185X)

exposed to temperatures over 37C, prolonged storage, or frequent passaging.[2]

The primary site of translocation in the intestine is via the M cells. Some strains of *Yec* may cluster on M cells at a density of over 1000X that of the surrounding absorptive villar epithelium.[2] By five days after infection, M cells and Peyer's patches are usually destroyed[2], and the bacteria have migrated to mesenteric lymph nodes.

The contributor mentions several important virulence factors including the Type III secretion system, a unique needle-like system which actively injects yersinial outer proteins (Yops) into cells to aid in evasion of the immune response. A few other virulence factors also bear mentioning: mucoid *Yersiniae* factor, which closely resembles fimbriae of enterotoxigenic *E. coli* and assists in mucosal attachment in early stages of infection, and several heat-stable enterotoxins (which induce diarrhea in infected individuals).[2]

Yersinia enterocolitica has been a popular submission with seven cases in the last decade of the WSC alone (and over 25 since 1975). A list of more recent cases include: WSC 2018-2019 liver and spleen, African green monkey; WSC 2016-2017, Conf 8,

case 4, lung, African Green monkey; WSC 2015-2016, Conf 12, Case 3 liver and cecum, hare; WSC 2013-2014, Conference 1, Case 3, small intestine and lymph node blackbuck; 2011-2012, WSC Conference 3, Case 1, Liver and spleen, guinea pig; and WSC 2010-2011, Conf 15, Case, 1, intestine, Indian macaque.

References:

11. Bakker J, Kondova I, de Groot CW Remarqe EJ, Heidt, PJ. A report on Yersinia-related mortality in a colony of new world monkeys. *Lab Prim Newsletter*. 2007; 46(3):11-15.
12. Bancerz-Lisiel A, Pieczywek, M, Lada P, Szweda W. The most important virulence markers of Yersinia enterocolitica and their role during infection. *Genes* (Basel) 2018; 9(5):pii: E234, doi: 10:3390/genes9050235
13. Pha K, Navarro L: Yersinia type III effectors perturb host innate immune responses. World journal of biological chemistry **7:** 1-13, 2016
14. Sabina Y, Rahman A, Ray RC, Montet, D. *Yersinia enterocolitica*: Mode of transmission, molecular insights of virulence and pathogenesis of infection. *J Path* 2011; 1:1-10.

CASE III: Case 1 (JPC 4101226).

Signalment: 8-week-old female Rex cross rabbit, *Oryctolagus cuniculus.*

History: Found dead in the woods

Gross Pathology: The rabbit was one of several young rabbits housed and hand-reared at a rescue organization. Both this rabbit and its litter mate displayed symptoms

Liver, rabbit. The liver appeared grossly pale and enlarged; three separate white hepatic nodules measuring 3 to 5mm in diameter were present in the parenchyma. (Photo courtesy of: Institute of Veterinary Animal and Biomedical Sciences, Massey University, Private Bag 11222, Palmerston North, New Zealand 4442)

of lethargy, anorexia and hypothermia. Within 48 hours of the onset of clinical signs, the rabbit died. The litter mate and several other young rabbits in the organization also died in the days following this death.

Laboratory results: Bacteriology**:** *Yersinia pseudotuberculosis* in liver and spleen.

Microscopic Description:
Despite moderate autolysis of the tissues, the liver has multifocal areas of hepatocytes with reasonable preservation. Scattered amongst these areas, and throughout the hepatic lobule, are swollen eosinophilic hepatocytes with varying degrees of pyknosis, karyolysis and karyorrhexis (necrosis) and marked loss of chord architecture. In addition to these findings, there is marked multifocal distention of bile ducts with periductal fibrosis expanding and compressing the surrounding hepatic parenchyma. The biliary epithelium is hyperplastic and forms papillary projections into the lumen. Numerous epithelial cells contain asexual and sexual developmental stages of coccidia and the biliary duct lumina contain large numbers of oocysts. Moderate numbers of lymphocytes and plasma cells and smaller numbers of heterophils are admixed within the periductal fibrous tissue and the

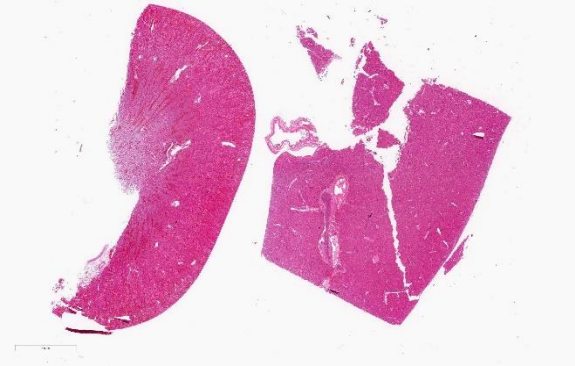

Kidney, liver, rabbit. Sections of both kidney and liver were submitted for examination. (HE, 5X)

connective tissue stroma of the papillary projections.

The kidney diffusely shows recent vascular congestion and tubular and glomerular hemorrhage. Intracapillary fibrin thrombi are present multifocally in glomeruli. Scattered renal tubular cells exhibit hypereosinophilic cytoplasm, pyknotic nuclei, karyorrhexis and karyolysis (necrosis).

Contributor Morphologic Diagnoses:
Liver: Hepatitis, acute, moderate to severe, random with hepatocellular necrosis
Liver: Cholangitis, proliferative, chronic severe with intraepithelial coccidia
Kidney: Nephritis, haemorrhagic, severe, acute, with multifocal glomerular thrombosis

Contributor Comment: In this case, the rabbit had two concurrent disease processes: hepatic coccidiosis (*Eimeria stiedae*) and rabbit hemorrhagic disease (RHD) caused by rabbit calicivirus. RHD was the cause of death, with hepatic coccidiosis as an incidental finding.

Rabbit hemorrhagic disease or viral hemorrhagic disease is caused by a calicivirus of the genus Lagovirus, which rapidly infects wild and domestic rabbits (*Oryctolagus cuniculi*). The virus was first identified in 1984 in China where it killed 140 million rabbits within months.[21] It was released in Australia and New Zealand as a method of pest control of wild rabbits and is endemic in the populations in those countries.[6,27]

The RHD virus is highly infectious, with a greater than 80% mortality rate, and it usually produces death in affected individuals within 48 to 72 hours of infection.[1,21] Death is due to acute liver damage and disseminated intravascular coagulation (DIC).[24] No clinical signs may be observed if the infection is peracute. Alternatively, they may manifest as anorexia, lethargy, pyrexia, conjunctival congestion and neurological signs such as ataxia, opisthotonos or paralysis in acute infections.[13,29] Other signs such as dyspnea, cyanosis, or hemorrhagic epistaxis may also be seen. Subacute infections result in milder clinical signs, with some rabbits surviving. Many rabbits with chronic infections will die within 1 to 3 weeks after a period of jaundice, weight loss and lethargy.[11]

The primary findings at necropsy include hepatomegaly with an enhanced lobular pattern, splenomegaly, renomegaly, pulmonary hemorrhage and oedema, blood-tinged nasal discharge or bloody foam in the tracheal lumen.[1,14] Additionally, hyperemia or sub-serosal hemorrhages may be found on

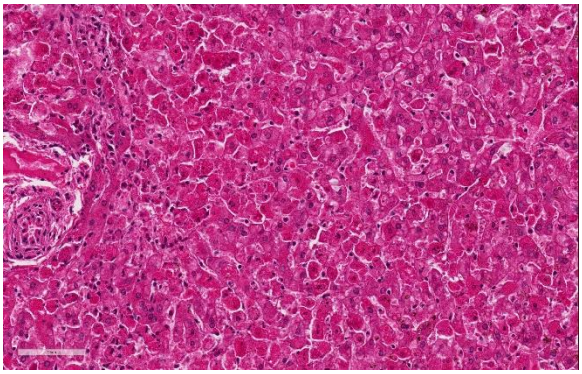

Liver, rabbit. Throughout the entire lobule, the majority (up to 80%) of hepatocytes are individualized, hypereosinophilic, with nuclear changes including peripheralized and crescentic chromatin or karyorrhexis. (HE, 321X)

multiple organs such as the intestine, pericardium, kidney and lungs.[1]

The primary histopathological lesion is an acute necrotizing hepatitis.[2] In adult rabbits, the virus has tropism for hepatocytes and can be detected in the liver a few hours post-infection.[2] Viral replication occurs primarily in hepatocytes in the centrilobular areas but also in Kupffer cells.[2,8-10,22] Additionally, viral antigen has been detected in macrophages of the spleen, alveoli, kidneys and small intestine.[22,23] The virus induces apoptosis in these cells, releasing viral progeny to infect other cells.[7] In younger rabbits, viral antigen has been detected only in rabbits greater than 4 weeks of age.[18,22] Younger rabbits appear to be resistant to the RHD virus. Rabbits less than 3 weeks of age are fully resistant, and this resistance decreases as rabbits increase in age to 8 weeks old, where mortality rates are the same as adult rabbits.[1]

The mechanism of resistance is unclear. It is thought to relate to viral attachment to the carbohydrate group of host-cell histo-blood group antigens (HBGA).[24,25] RHD attaches to HBGA H type 2, A type 2 and B type 2 oligosaccharides which are found on the surface of epithelial cells of the upper respiratory and digestive tracts. The expression of HBGA H type 2 seems to be mostly lacking in the upper respiratory and gastrointestinal tracts of resistant rabbits.[17] However, other factors must be involved in viral attachment to cells as hepatocytes, which are the main cell involved in viral replication, do not contain these HBGA receptors.[25] Additionally, in young rabbits, viral replication occurs only in a small fraction of hepatocytes, indicating other factors are involved in the resistance to this virus.[1]

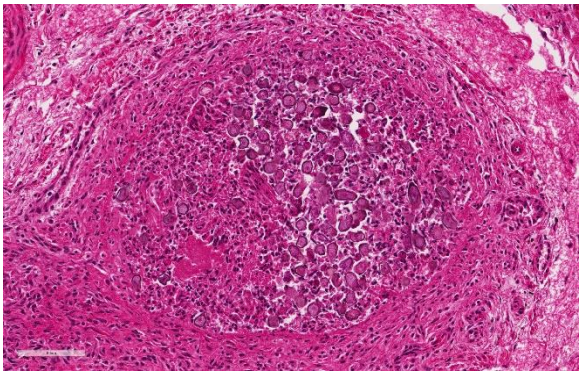

Liver, rabbit. Bile ductules contain numerous luminal oocysts. The lining epithelium is hyperplastic, but disorganized as a result of autolysis. (HE, 282X)

In this rabbit, hepatic coccidiosis, was an incidental finding that likely contributed to its poor condition. *Eimeria stiedae* is a common cause of morbidity and mortality in rabbits. Ten other species of *Eimeria* spp. infect the domestic rabbits but specifically infect the gastrointestinal tract.[15,17] Clinical signs for hepatic coccidiosis include a thin body condition, diarrhoea, a pot-bellied appearance and, in severe cases, icterus.[21]

Young, weanling rabbits are most often infected when ingestion of the sporulated oocyst from the environment occurs. The oocysts are shed after a prepatent period of 15 to 18 days, and once in the environment, are extremely resistant to disinfectants.[21]

Sporulated oocysts are ingested, where sporozoites are released to invade the duodenal mucosa and lamina propria.[18] It is possible that sporozoites are then transported to the liver via either lymphatic or hematogenous spread. Organisms have been found in macrophages in the lymphatics and in regional lymph nodes within 12 hours of exposure, in bone marrow within 24 hours and in the liver within 48 hours.[18,21] Once in the liver, sporozoites invade the epithelial cells of bile ducts to become trophozoites. Trophozoites undergo the asexual division of schizogony and merogony over several

generations to eventually form the macro- and microgametocytes involved in sexual division. Fertilization of a macrogametocyte by a microgametocyte to form an oocyst which is then shed in the feces.[18,21]

Contributing Institution:
Institute of Veterinary Animal and Biomedical Sciences, Massey University
Private Bag 11222, Palmerston North
New Zealand 4442

JPC Diagnosis: Liver: Hepatitis, necrotizing (it's really apoptosis), massive, diffuse, severe.
2. Liver, bile ducts: Epithelial hyperplasia, diffuse, mild to moderate, with intraluminal apicomplexan oocysts.

JPC Comment: The contributor has done an excellent review of a virus of global import in this species, as well as well-known common parasite of young rabbits.

The Czech v351 strain of rabbit lagovirus has been used in Australia and New Zealand (following illegal release on the South island) to control pest rabbits for a number of years.[14] However, even before this virus was released into a naïve population, wild rabbits demonstrated cross-reacting antibodies suggesting other similar viruses had previously circulated within this population. The first non-pathogenic rabbit calicivirus was identified in Italy, following seroconversion of animals in a rabbitry with no history of clinical disease. Shortly thereafter, a non-pathogenic strain of rabbit calicivirus with 88% was identified in Australia, and New Zealand. One common factor was that these viruses appeared to prevail in cool high-rainfall areas.[14] Additional "benign" viruses have also been identified in European hares in Australia, with evidence of previous recombination, confirming previous hypotheses of the origin of genetic diversity within this genus of virus.[12] In 2014, a recombinant strain of RHDV was identified in Australia which contained capsid and non-structural genes of non-pathogenic RHDV variants.[12]

Other interesting changes have been noted in RHDV since its release thirty years ago in Australia. In contrast to myxoma virus, which was also released into the wild to control pest rabbits and rapidly attenuated in virulence over time as local rabbits developed genetic resistance, pathogenic genotypes of Australian RHDV appear to have increased in virulence.[7] A comparison study of deaths in a closed population experiencing outbreaks back to the original release of RHDV noted that in outbreaks from 2007-2009 (as compared to the 1990's), more recent outbreaks demonstrated elevation in case fatality rates, disease duration (time to death), as well as the amount of virus produced in infected animals.[7]

The first lagovirus other than RHVD infecting rabbits in the United States was identified by Bergin et al in 2009. This virus, referred to as Michigan rabbit calicivirus

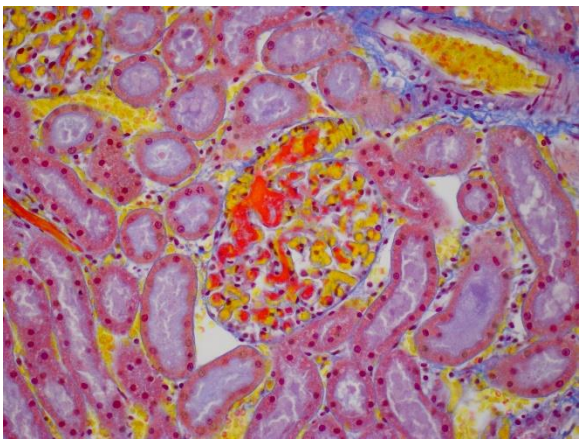

Kidney, rabbit. Fibrin thrombi within glomerular capillaries stains dark red. (Martius scarlet blue trichrome, 400X) (Photo courtesy of: Institute of Veterinary Animal and Biomedical Sciences, Massey University, Private Bag 11222, Palmerston North, New Zealand 4442)

occurred in a closed rabbitry with an approximately 32% case mortality and clinical and necropsy findings of epistaxis, vulvar hemorrhage, diarrhea, and ocular discharge. This virus averaged 79% homology with the RNA genome of RHDV virus. The rabbitry was ultimately depopulated.[5]

References:

1. Abrantes J, van der Loo W, Le-Pendu J, Esteves PJ. Rabbit haemorrhagic disease (RHD) and rabbit haemorrhagic disease virus (RHDV): a review. *Veterinary research* 2012; 43: 12.
2. Alonso C, Oviedo JM, Martin-Alonso JM, Diaz E, Boga JA, Parra F: Programmed cell death in the pathogenesis of rabbit hemorrhagic disease. *Arch Virol* 1998;143: 321-332.
3. Barriga OO, Arnoni JV. *Eimeria stiedae*: weight, oocyst output and hepatic function of rabbits with graded infections. *Experimental Parasitology* 1979; 48:407-414.
4. Barriga OO, Arnoni JV. Pathophysiology of hepatic coccidiosis in rabbits. *Veterinary Parasitology* 1981; 8:201-210.
5. Bergin IL, Wise AG, Bolin SR, Mullaney TP, Kiupel M, Maes. RK. Novel calicivirus identified in rabbits, Michigan, USA. *Emerg Infec Dis* 2009; 15(12)1955-1962.
6. Cooke BD. Rabbit haemorrhagic disease: field epidemiology and the management of wild rabbit populations. *Rev Sci Tech* 2002; 21:347-358.
7. Elsworth P, Cooke BD, Kovaliski J, Sinclair R, Holmes EC, Strive T. Increased virulence of rabbit hemorrhagic disease virus associated with genetic resitance in wild Australia rabbits. *Virology* 2014; 10:415-423.
8. Gelmetti D, Grieco V, Rossi C, Capucci L, Lavazza A. Detection of rabbit haemorrhagic disease virus (RHDV) by in situ hybridisation with a digoxigenin labelled RNA probe. *J Virol Methods* 1998; 72:219-226.
9. Jung JY, Lee BJ, Tai JH, Park JH, Lee YS: Apoptosis in rabbit haemorrhagic disease. *J Comp Pathol* 2000; 123:135-140
10. Kimura T, Mitsui I, Okada Y, et al. Distribution of rabbit haemorrhagic disease virus RNA in experimentally infected rabbits. *J Comp Pathol* 2001; 124:134-141.
11. Lavazza A, Capucci L. How Many Caliciviruses are there in Rabbits? A Review on RHDV and Correlated Viruses In: Alves PC, Ferrand N, Hackländer K, eds. *Lagomorph Biology*. 1st ed. Berlin, Germany: Springer 2008:263-278.
12. Mahar JE, Hall RN Shi M, Mourant R, Hung N, Strive T, Holmes EC. The discovery of three new hare lagoviruses reveals unexplored viral diversity in this genus. *Virus Evol* 2019; 5(1): vewz005.
13. Marcato PS, Benazzi C, Vecchi G, et al. Clinical and pathological features of viral haemorrhagic disease of rabbits and the European brown hare syndrome. *Rev Sci Tech* 1991; 10: 371-392.
14. Mitro S, Krauss H. Rabbit hemorrhagic disease: a review with special reference to its epizootiology. *Eur J Epidemiol* 1993; 9:70-78.
15. Moussa A, Chasey D, Lavazza A et al. Haemorrhagic disease of lagomorphs: evidence for a calicivirus. *Vet Microbiol* 1992; 33: 375-381.

16. Nicholson LJ, Mahar JE, Strive T, Zheng T, Holmes EC, Ward VK, Duckworth JA. Benign rabbit calicivirus in New Zealand. *Applied Env Microbiol* 2017; e00090-17
17. Nyström K, Le Gall-Reculé G, Grassi P et al. Histo-blood group antigens act as attachment factors of rabbit hemorrhagic disease virus infection in a virus strain-dependent manner. *PLoS Pathog* 2011; 7:1-22.
18. Owen D. Life cycle of *Eimeria stiedae*. *Nature* 1970; 227:304.
19. Pakandl M. Coccidia of rabbit: a review. *Folia Parasitologica* 2009; 56(3):153-166.
20. Park JH, Lee YS, Itakura C. Pathogenesis of acute necrotic hepatitis in rabbit hemorrhagic disease. *Lab Anim Sci* 1995; 45:445-449.
21. Percy DH, Barthold SW, Griffey SM. Rabbit In: *Pathology of Laboratory Rodents and Rabbits*. 4th ed. Ames, Iowa, USA: Blackwell Publishing; 2016: 253-323.
22. Prieto JM, Fernandez F, Alvarez V et al. Immunohistochemical localisation of rabbit haemorrhagic disease virus VP-60 antigen in early infection of young and adult rabbits. *Res Vet Sci* 2000; 68:181-187.
23. Ramiro-Ibáñez F, Martín-Alonso JM, García Palencia P, Parra F, Alonso C. Macrophage tropism of rabbit hemorrhagic disease virus is associated with vascular pathology. *Virus Res* 1999; 60:21-28.
24. Ruvoen-Clouet N, Blanchard D, Andre-Fontaine G, Ganiere JP. Partial characterization of the human erythrocyte receptor for rabbit haemorrhagic disease virus. *Res Virol* 1995, 146:33-41.
25. Ruvoen-Clouet N, Ganiere JP, Andre-Fontaine G, Blanchard D, Le Pendu J. Binding of rabbit hemorrhagic disease virus to antigens of the ABH histo-blood group family. *J Virol* 2000; 74:11950-11954.
26. Shien JH, Shieh HK, Lee LH. Experimental infections of rabbits with rabbit haemorrhagic disease virus monitored by polymerase chain reaction. *Res Vet Sci* 2000; 68:255-259.
27. Thompson J, Clark G. Rabbit calicivirus disease now established in New Zealand. *Surveillance* 1997; 24:5-6.
28. Ueda K, Park JH, Ochiai K, Itakura C. Disseminated intravascular coagulation (DIC) in rabbit haemorrhagic disease. *Jpn J Vet Res* 1992; 40:133-141.
29. Xu ZJ, Chen WX: Viral haemorrhagic disease in rabbits: a review. *Vet Res Commun* 1989; 13: 205-212.

CASE IV: 15-0463 (JPC 4119789)

Signalment: 9-month-old, male-entire, Rottweiler cross canine (*Canis familiaris*).

History: A deceased, male-entire, 9-month-old Rottweiler cross canine was submitted to the Murdoch University Anatomic Pathology diagnostic service for necropsy examination following barbiturate euthanasia. The dog had a progressive 5-week history of non-ambulatory bilateral hindlimb paresis progressing to paralysis and loss of deep pain; there was no history of prior trauma, clinical signs were non-responsive to carprofen. Otherwise the patient appeared healthy and well, and had been eating and drinking normally. At the time of euthanasia it had developed fecal and urinary incontinence and no pain was elicited on

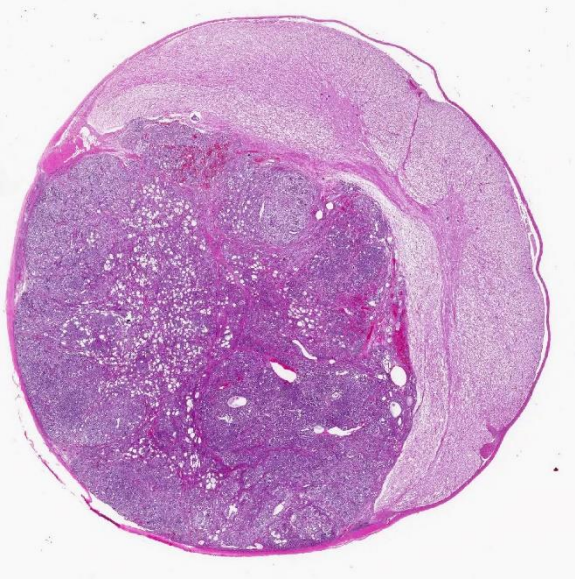

Spinal cord, dog. The spinal cord is compressed by a well-demarcated intradural neoplasm. (HE, 5X)

spinal palpation. A neurological examination carried out prior to euthanasia found the following:

- The panniculus reflex was absent caudal to L4 bilaterally, with a very sharp demarcation.
- Hind limbs: tonic-clonic patellar reflex bilaterally, cranial tibial clonic-tonic on left and intermittently tonic clonic on right. Withdrawal reflex bilaterally intact, sciatic unconvincingly present, absence of deep pain bilaterally on all digits. Negative Babinsky. Negative crossed extensor. Negative superficial sensation. No motor function exhibited.
- Anal tone: decreased to virtually absent.

The cadaver was unfortunately frozen and thawed prior to necropsy examination.

Gross Pathology: A focal, 10mm diameter, well-demarcated, mottled grey to pink-red nodule was identified within the spinal cord at the level of the T13/L1 intervertebral disc; its cut surface bulged slightly. Depending upon the level at which it was sectioned, the nodule was intradural and extramedullary, or intramedullary in location. The dorsal surfaces of the metatarsal regions bilaterally exhibited moderate, multifocal, chronic dermal erosions and ulcerations. The hindlimb musculature was mildly symmetrically atrophied.

Laboratory results: None performed.

Microscopic Description:
Thoracolumbar spinal cord: Effacing the grey matter, extending into the adjacent white matter and compressing the remaining adjacent spinal cord is a non-encapsulated, moderately well-demarcated, mildly infiltrative, moderately cellular neoplasm measuring 10mm in diameter. The neoplasm is composed of three distinct neoplastic cell populations. The first, epithelial, population forms tubules and acini lined by cuboidal, low columnar, to pseudostratified epithelium; frequently, the tubules form papillary projections (glomeruloid structures). 8 mitotic figures are seen in 10 HPF (400x) within this epithelial population. The second population consists of polygonal cells forming dense clumps or occasionally palisading along basement membranes; they possess indistinct cell borders, and a small amount of pink granular cytoplasm (primitive blastemal population). 12 mitotic figures are seen in 10 HPF (400x) within the blastemal population. The third and least abundant, mesenchymal, population is composed of

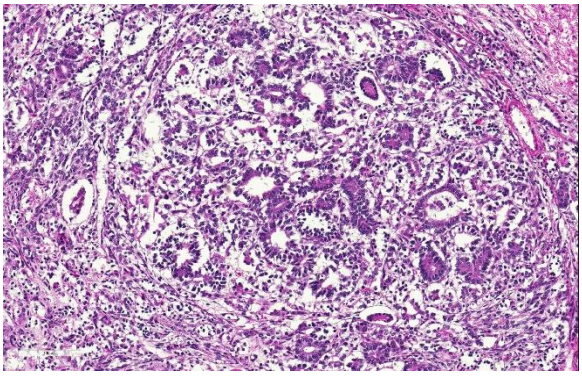

Spinal cord, dog. Neoplastic cells often form well-differentiated tubules, lined by columnar epithelium. (HE, 210X)

spindloid cells, forming loose streams which ramify throughout the other two populations, and occasional whorls. Spindloid cell nuclei are round to ovoid with a single indistinct nucleolus and finely stippled to lacy chromatin; their cytoplasm is eosinophilic with indistinct cell borders. 5 mitotic figures are seen in 10 HPF (400x) within the mesenchymal population. Blood vessels within the neoplasm are distended with erythrocytes (hyperaemia). The remaining spinal cord parenchyma contains large numbers of variably sized clear spaces (rarefaction, freeze-thaw post-mortem artefact).

Contributor's Morphologic Diagnoses: Spinal cord T13/L1: ectopic nephroblastoma.

Contributor's Comment: Microscopic evaluation of the mass found within the spinal cord at the level of T13/L1 reveals a neoplastic infiltrate, which, given the lack of a renal lesion, is consistent with a primary spinal ectopic nephroblastoma.

Unlike primary renal nephroblastomas (Wilms' tumor), which are reported in a wide range of domestic companion and production animal species, including dogs, primary spinal ectopic nephroblastomas are rarely reported neoplasms that occur in young dogs between 5 months to 4 years, the median age being 14 months.[1,4] Whilst they are rare, comprising merely approximately 1% of all canine primary CNS tumors, they are an important differential in the aforementioned age group.[4] Of course, secondary spinal nephroblastomas can arise as a result of metastasis from a primary renal nephroblastoma; however the lungs and liver are more common secondary sites, with over 50% of canine cases of primary renal nephroblastoma exhibiting widespread pulmonary and hepatic metastases.[6] Primary spinal ectopic nephroblastomas typically arise as a single mass, or sometimes multiple masses, at the level of the thoracolumbar junction between T10-L3[3,4] and exhibit both intramedullary and extramedullary intradural growth; extradural growth is also reported.[1,11]

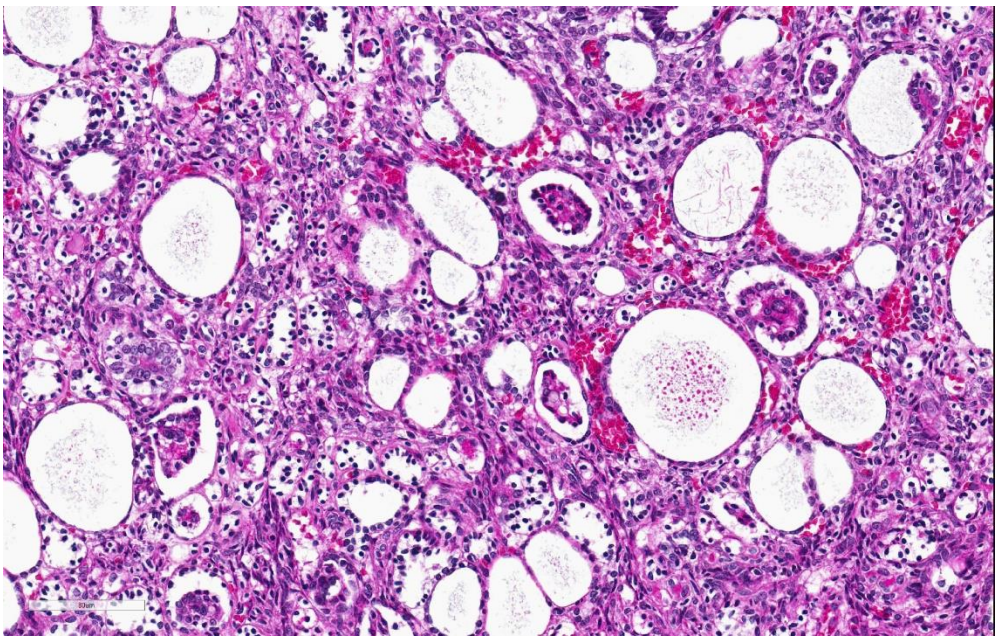

Spinal cord, dog. Ectatic tubules occasionally contain a papillary projection with peripheralized nuclei, resembling a fetal glomerulus. (HE, 300X)

Whilst historically German Shepherds and female dogs were thought to be predisposed[1], a breed and sex predisposition is not supported in more recent reports, with dogs of variable sizes and breeds reported.[3,4,11] Affected dogs exhibit clinical signs of a compressive myelopathy, i.e. progressive

unilateral or bilateral paraparesis, paraplegia, and/or ataxia; the duration of clinical signs is reported to range from 2 to 60 days, with the median being 14 days.[1,4] The prognosis appears variable, with one study involving 11 dogs having found the post-surgical resection median survival time to be 70.5 days;[1] whilst another reported a median survival time of 374 days post-surgery (6 dogs) or radiation (1 dog), and 55 days in 3 dogs only receiving palliative prednisone and gabapentin.[5,11] The latter study also found that tumor location was important for prognostication – dogs with intramedullary nephroblastoma (n = 4) had a much shorter median survival time (140 days) compared to 380 days in the 6 dogs with intradural but extramedullary nephroblastoma;[5] however, the 10 dogs in the study received varied treatment regimens. Previously it was not thought to metastasize,[10] however multifocal spinal nephroblastoma is reported in 2 dogs, consistent with intraspinal metastasis through the cerebrospinal fluid.[3,10] Metastasis to the caudal vena cava, adrenal glands, hepatic and mediastinal lymph nodes, pulmonary interstitium, bone marrow, and periosteum as well as extradural space of two vertebral bodies is reported in a single canine case with a dorsal retroperitoneal mass contiguous with a right renal tumor.[2] However, it is difficult to ascertain whether the primary neoplasm was of renal or spinal origin in the reported case.

Their histogenic origin remains unconfirmed and controversial, given the complexity of nephrogenesis; it is believed they originate from (a) ectopic metanephric blastema or, (b) mesonephric rest tissue, either of which become entrapped between the dura mater and the spinal cord during embryogenesis.[2,9] Nephrogenesis involves two embryologically distinct tissues - nephrogenic and ductogenic; the former developing from the intermediate mesoderm and progressing through the

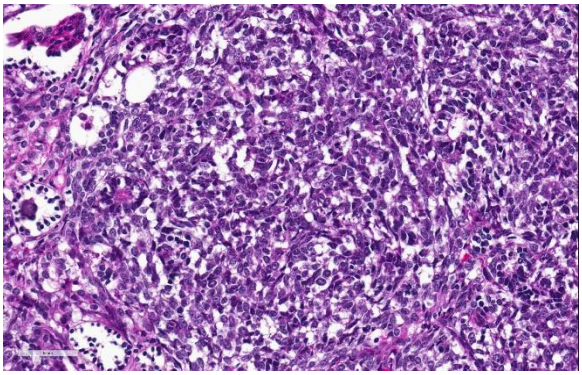

Spinal cord, dog. Less differentiated areas of the neoplasm are composed of nests of polygonal to spindle cells. (HE, 400X)

pronephros, mesonephros and metanephros phases.[12] In humans, this progression normally ceases after 36 weeks gestation, whereupon the renal metanephric blastema disappear.[12] Occasionally, the nephrogenic blastema fail to develop into normal mature renal parenchyma (however, it is not known whether arrest occurs at the mesonephros or metanephros phase in any given case[8]); persistent blastemal tissue is then referred to as nephrogenic rest tissue, which may undergo oncogenesis resulting in nephroblastoma[12] (either primary renal in the case of renal nephrogenic rests, or primary extrarenal in the case of ectopic rests). In humans, extrarenal nephroblastomatosis, i.e. ectopic immature renal tissue, has been reported in such ectopic sites as the inguinal canal, testis, lumbosacral area, adrenal gland, thorax, colon, and heart;[8,12] however, primary extrarenal nephroblastoma is rare, with few cases reported in the retroperitoneum and inguinal canal.[8]

Previously in the canine literature, this tumor was mistakenly thought to be of neuroectodermal origin, leading to its frequent misdiagnosis as one of the other main differentials for intradural spinal cord tumors in young dogs (i.e. ependymoma, medulloepithelioma, neuroepithelioma); it has also been erroneously classified as spinal

cord blastoma, poorly differentiated astrocytoma, and hamartoma.[4,5,10] Teratoma can be excluded due to the lack of other non-nephrogenic tissues within the neoplasm.[12] As seen in this case, ectopic nephroblastomas are characterized by a triphasic neoplastic population, comprised of epithelial, blastemal, and stromal cells, redolent of Wilms' tumor.[3,4,6] Distinctive histological features aiding diagnosis are the presence of tubules and acini, as well as glomerulus-like structures that resemble fetal glomeruli.[3,4] Metaplastic differentiation towards muscle, bone or cartilage is frequently reported in renal nephroblastomas,[6] however is not a feature of spinal ectopic nephroblastomas, with only 1 case reporting metaplastic cartilage formation.[3] Wallerian degeneration (multifocal myelin sheath distension, swollen axons, and myelomacrophages) attributable to a compressive myelopathy is commonly seen; however it was felt in this case post-mortem change due to freeze-thaw artefact obscured ability to observe such changes.

Immunohistochemistry can aid diagnosis, and also supports their ectopic renal origin.[10] The blastemal and mesenchymal (stromal) populations are immunoreactive for vimentin, whilst the epithelial population forming tubules/acini shows immunoreactivity for cytokeratin.[10] Immunoreactivity of polysialic acid to the blastemal nuclei is seen;[4,10] however the definitive antigenic marker is Wilms' tumor gene product (WT-1) – the blastemal nuclei in the glomerulus-like structures are typically strongly immunopositive.[4] There are, however, reports of canine cases that are negative for this marker; presumably due to abnormal antigen expression by tumour cells.[1,6] In human nephroblastoma, a poorer prognosis is seen in cases in which stronger blastemal WT-1 expression is observed,[1] however this correlation has not been found in canines. Primary spinal ectopic

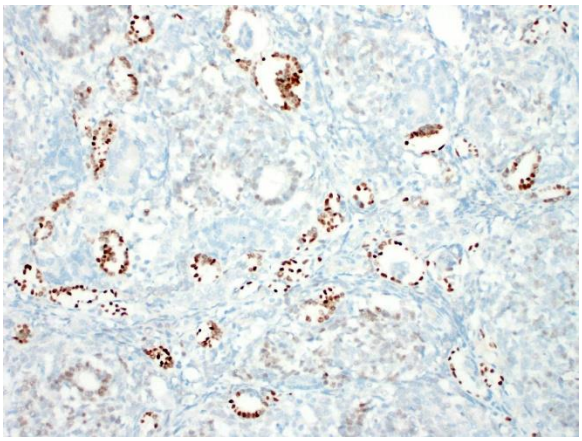

Spinal cord, dog. There is strong intranuclear staining of cells lining differentiated tubules as well as glomeruloid structures (arrow). (anti WT1, 200X)

nephroblastomas lack immunoreactivity with routine neuronal (SYN, NeuN, and TNF) and glial (Olig2, GFAP) markers.[4] Nephroblastomas lack immunoreactivity for GFAP and neurofilaments, yet their epithelial population is immunopositive for cytokeratin, which rules out the main differential diagnoses, the primitive neuroectodermal tumors;[4] in particular, ependymomas, given the perivascular pseudorosettes and true rosettes typical of ependymomas are similar to the tubules found in nephroblastomas.[10]

Contributing Institution:
Veterinary Pathology Department
School of Veterinary and Life Sciences
Murdoch University
90 South Street
Murdoch, Western Australia
6150, Australia
http://www.murdoch.edu.au/School-of-Veterinary-and-Life-Sciences/

JPC Diagnosis: Spinal cord: Ectopic nephroblastoma (spinal nephroblastoma)

JPC Comment: The contributor has done an excellent job summarizing this uncommon and very unique tumor of young dogs.

The Wilms tumor antigen is a tumor suppressor gene that it humans is found at 11p13. It functions as a regulator of transcription in the inner layer of intermediate mesoderm and inhibits transcription of several growth-promoting genes, and plays a critical role in the development of the genitourinary tract, spleen and mesothelium. First identified as a tumor suppressor gene in association with Wilm's tumors in humans, the name WT-1 would lead one to believe that the immunohistochemical stain targeting this gene product would be specific for Wilm's tumor. However, it is also present in a number of normal tissues, including CD-34 positive stem cells, glomerular podocytes and mesangial cells, Sertoli and granulosa cells, ovarian stroma and surface epithelium, uterine endometrial stroma and myometrium, and mesothelium.[7] It is expressed in a wide range of neoplasms in humans, including nephroblastoma, mesothelioma, metanephric adenoma, ovarian carcinoma, transitional cell carcinomas, among others.[7]

While nephroblastomas have been rarely identified as intra- and extradural masses in humans, it has almost always been a consequence of metastasis (10% of Wilm's tumor present with metastatic foci), and less commonly invasive growth through nerve root foramina. Development from rests of ectopic nephrogenic tissue has not yet been documented. Contrarily, there appears to be only one report of spinal nephroblastoma in the dog attributable to metastasis of a renal primary, as opposed to growth of ectopic metanephric blastema.[9]

References:

1. Brewer DM., Cerda-Gonzalez, S., Dewey, CW., Diep, AN., Van Horne, K., McDonough, SP. Spinal cord nephroblastoma in dogs: 11 cases (1985-2007). JAVMA. 2011; 238(5): 618-624.
2. Gasser, AM., Bush, WW., Smith, S., Walton, R. Extradural spinal, bone marrow, and renal nephroblastoma. J Am Anim Hosp Assoc. 2003; 39: 80–85.
3. Henker, LC., Bianchi, RM., Vargas, TP., de Oliveira, EC., Driemeier, D., Pavarini, SP. Multifocal spinal cord nephroblastoma in a dog. J Comp Path. 2018; 158: 12-16.
4. Higgins, RJ., Bollen, AW., Dickinson, PJ., Sisó-Llonch. S. Tumors of the Nervous System. In: Meuten DJ, ed. Tumors in Domestic Animals: 5th ed. Ames, IA: John Wiley & Sons Inc.; 2017: 863-864.
5. Liebel, F-X., Rossmeisel, JH., Lanz, O., Robertson, JL. Vet Surg. 2011; 40: 244-252.
6. Meuten, DJ., Meuten, TLK. Tumours of the urinary system. In: Meuten DJ, ed. Tumors in Domestic Animals: 5th ed. Ames, IA: John Wiley & Sons Inc.; 2017: 646-650.
7. Nakatsuka S, Oju Y Horiuchi T et al. Immunohistochemical detection of WT1 protein in a variety of cancer cells. *Mod Pathol* 2006; 19:804-814.
8. Oottamasathien, S., Wills, ML., Brock III, JW., Pope IV, JC. Primary extrarenal nephroblastomatosis. Urology. 2007; 184.e3-184.e4.
9. Petit A, Rubo A Durand C, Piolat C, Perret, Cecile P, Pagnier A, Plantaz, D, Sartelet H. A Wilms' tumor with spinal cord compression: An extrarenal origin?
10. Terrell, SP., Platt, SR., Chrisman, CL., Homer, BL., de Lahunta, A., Summers, BA. Possible intraspinal metastasis of a canine spinal cord nephroblastoma. Vet Pathol. 2000; 37: 94-97.
11. Traslavina, RP., Aleman, M., Affolter, VK., LeCouteur, RA., Ramsamooj, R., Higgins, RJ. Pathology in practice. Spinal cord (ectopic) nephroblastoma in a dog. J Am Vet Med Assoc. 2013; 242(12): 1661-1663.

12. Wu, Y., Zhu, X., Wang, X., Wang, H., Cao, X., Wang, J. Extrarenal nephroblastomatosis in children: a report of two cases. BMC Pediatrics. 2014; 14: 255-259.

Self-Assessment - WSC 2019-2020 Conference 5

1. Which of the following is true regarding Johne's disease in sheep?
    a. It results in severe diarrhea.
    b. Caseating tubercles in the lymph nodes are mover common than they are in cattle.
    c. Paucibacillary forms are associated with a strong humoral response
    d. Multibacillary forms are associated with a strong cell-mediated response.

2. Which of the following is NOT true concerning testing for Johne's disease in sheep.
    a. PCR is not recommended for herd testing
    b. ELISA tests may cross-react with *Corynebacterium pseudotuberculosis.*
    c. Some studies indicate that paucibacillary forms may result in false negatives on serologic tests.
    d. Rectal biopsies are the best source of positive testing for paucibacillary forms.

3. Which of the following virulence factors of Yersina alters the actin cytoskeleton to inhibit phagocytosis?
    a. Yersinial outer proteins
    b. endotoxin
    c. Invasin
    d. Type III secretion system

4. Which of the following is true concerning rabbit hemorrhagic disease?
    a. This disease primarily results in mortality in animals less than 3 weeks of age.
    b. Apoptosis is the main route of hepatocellular necrosis and viral spread to adjacent cells.
    c. The first identification of the virus was in the United States in the mid-1980s.
    d. The virus shows primary tropism for macrophages.

5. Which of the following is true concerning spinal nephroblastoma in the dog?
    a. It is most commonly the result of metastasis from a renal primary tumor.
    b. It is primarily a tumor of dogs 5 years of age or older.
    c. Metaplastic differentiation town muscle, bone, and cartilage is commonly seen in this tumor.
    d. Wilms tumor-1 (WT-1) is a good marker for this variant of nephroblastoma.

Please email your completed assessment for grading to Dr. Bruce Williams at bruce.h.williams12.civ@mail.mil. Passing score is 80%. This program (RACE program 33611) is approved by the AAVSB RACE to offer a total of 0.5 CE Credits, with a maximum of 12.5 CE Credits being available to any individual Veterinary Medical Professionals for the 2019-2020 Wednesday Slide Conference. This RACE approval is for the subject matter categories of: SCIENTIFIC using the delivery method of NON-INTERACTIVE DISTANCE. This approval is valid in jurisdictions which recognize AAVSB RACE.

Joint Pathology Center
Veterinary Pathology Services

WEDNESDAY SLIDE CONFERENCE 2019-2020

C o n f e r e n c e 6

2 October 2019

Conference Moderator:
Dr. Jeff Wolf, DVM
Senior Pathologist
Chief Scientific Officer/Pathology Manager
EPL, Inc.
Sterling, VA

CASE I: A15-62176 (JPC 4118173).

Signalment: Adult (age unknown), female, cardinal tetra (*Paracheirodon axelrodi*) fish

History: Following transport by air, high mortalities began in the group of fish approximately 24-hours after arrival in quarantine facilities at a public aquarium. There were no reported gross lesions. Skins scrapes, gill, and fin clips were reported as negative for external parasites.

Gross Pathology: Four fish were received whole fixed in formalin. Skin surfaces contained multiple, ill-defined areas of pallor and scale loss suggestive of erosion or ulceration.

Laboratory results: N/A

Microscopic Description: There is severe ulceration of the dorsal cranial region, snout, and lips, extending onto the ventral mandibular region and into the oropharynx. Lesions are characterized by extensive epithelial loss, with variable loss or necrosis of dermal connective tissues. Remaining dermal tissues are pale staining, have lost morphologic detail and are infiltrated by masses of a monomorphic population of slender, approximately 4-6 um long, bacterial rods. Necrosis and edema extend into underling muscle and adjacent soft tissues, including the olfactory rosette. Affected myofibers are similarly pale staining, with coagulated, vacuolated and fragmented

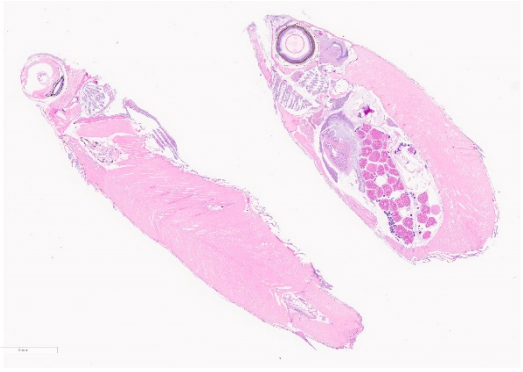

Body, cardinal tetra: Two sagittal sections of the tetra are submitted for examination. (HE, 5X)

cytoplasm, devoid of cross striations. Associated hypodermal adipose and areolar connective tissues are edematous, contain abundant cellular debris, and have lost tinctorial properties and morphologic detail. Bacteria are scattered throughout. Inflammatory responses vary from none to infiltration by small to moderate mixed populations of lymphocytes and macrophages. A focal area of hemorrhage extends from the forebrain into the cranial cavity.

Contributor's Morphologic Diagnosis: Facial skin: Ulcerative dermatitis, necrotizing, acute, focally extensive, severe, with slender bacterial rods, and subadjacent necrotizing myositis, cellulitis, and olfactory mucosal necrosis

Contributor's Comment: Microscopic examination reveals ulcerative skin lesions containing large numbers of long, slender bacterial rods consistent with *Flavobacterium columnare*, the causative agent of columnaris disease. Similar ulcerative lesions were present in all fish examined, varying only in lesion distribution and severity. Additional findings included the presence of several encapsulated larval nematodes in the coelomic cavity.

Columnaris disease occurs worldwide in many wild and cultured freshwater fish, including tropical aquarium species.[3] In the southeastern United States it is a major pathogen affecting channel catfish aquaculture.[4] The term "saddle back" is commonly used to describe symmetrical lesions over the dorsum of the back, but this is only one manifestation of the disease, which frequently involves various combinations of the gills, perioral area, fins, and caudal peduncle. The clinical course of disease, acute to chronic, and extent of lesions is dependent on the virulence of the bacterial strain involved.[3] Lesions generally begin as foci of depigmentation and erosion, but can rapidly progress to large ulcers with exposure of underlying skeletal muscle. Lesions often have a yellowish discoloration and narrow hemorrhagic border. Microscopically, lesions are primarily necrotizing, often in the presence of massive numbers of the long slender bacteria, particularly within dermal connective tissues. Bacteria are readily visualized in H&E- and Giemsa-stained sections. Despite the large numbers of bacteria and their destructive nature in tissue, inflammatory cell infiltration is often minimal. Secondary infection

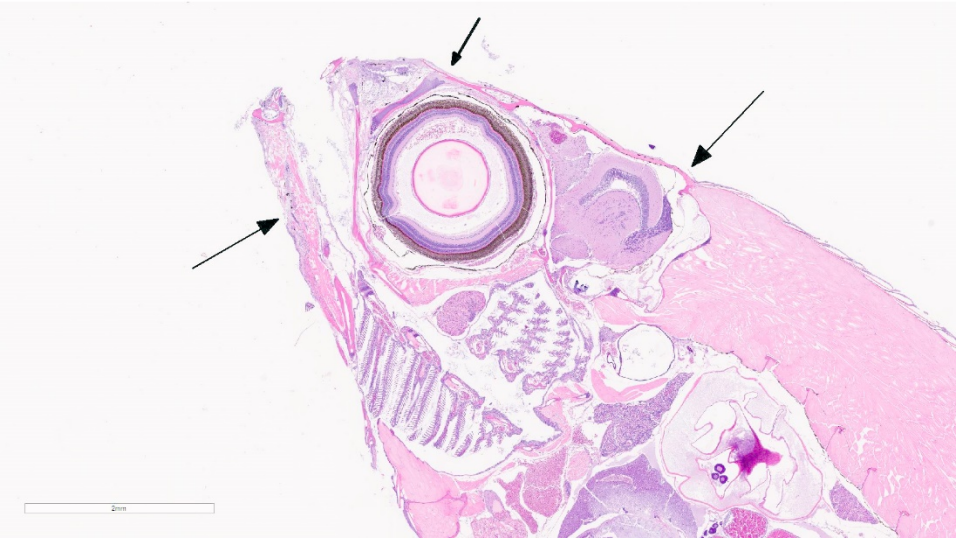

Body, cardinal tetra: There is diffuse loss of the epithelium over the face and within the oral cavity between the two arrows. (HE, 19X)

by the oomycete *Saprolegnia* sp. is common.[3,4]

Flavobacterium columnare is widespread in freshwater environments and survival is promoted in hard alkaline water with high organic loads. While highly virulent strains of *F. columnare* exist, the bacteria often presents as a typical opportunist following episodes of environmental stress, such as transport, as seen in this case. Other environmental factors conducive to infection include higher temperatures, high stocking densities, elevated nitrite levels, and slow water flow. Disease pathogenesis is poorly understood, but may initially involve factors related to the ability of the bacteria to respond to chemotaxic factors, adhere to host surfaces, and aggregate in thick mats. Three genomovars of *F. columnare* with variable pathogenicity are known to exist. Pathogenicity is enhanced by the presence of a thick capsule and the production of chondroitin AC lyase, which degrades chondroitin sulfates and hyaluronic acid in connective tissues. Extracellular proteases also contribute to tissue damage and promote invasion. Some studies indicate impairment of the host alternative complement pathway through sialic acid production and it is hypothesized that lack of inflammation may be related to the production of pro-apoptotic factors that inhibit phagocytes. Reported disturbances in blood parameters, presumably the result of water imbibition, include decreases in PCV, electrolytes and serum proteins.[3]

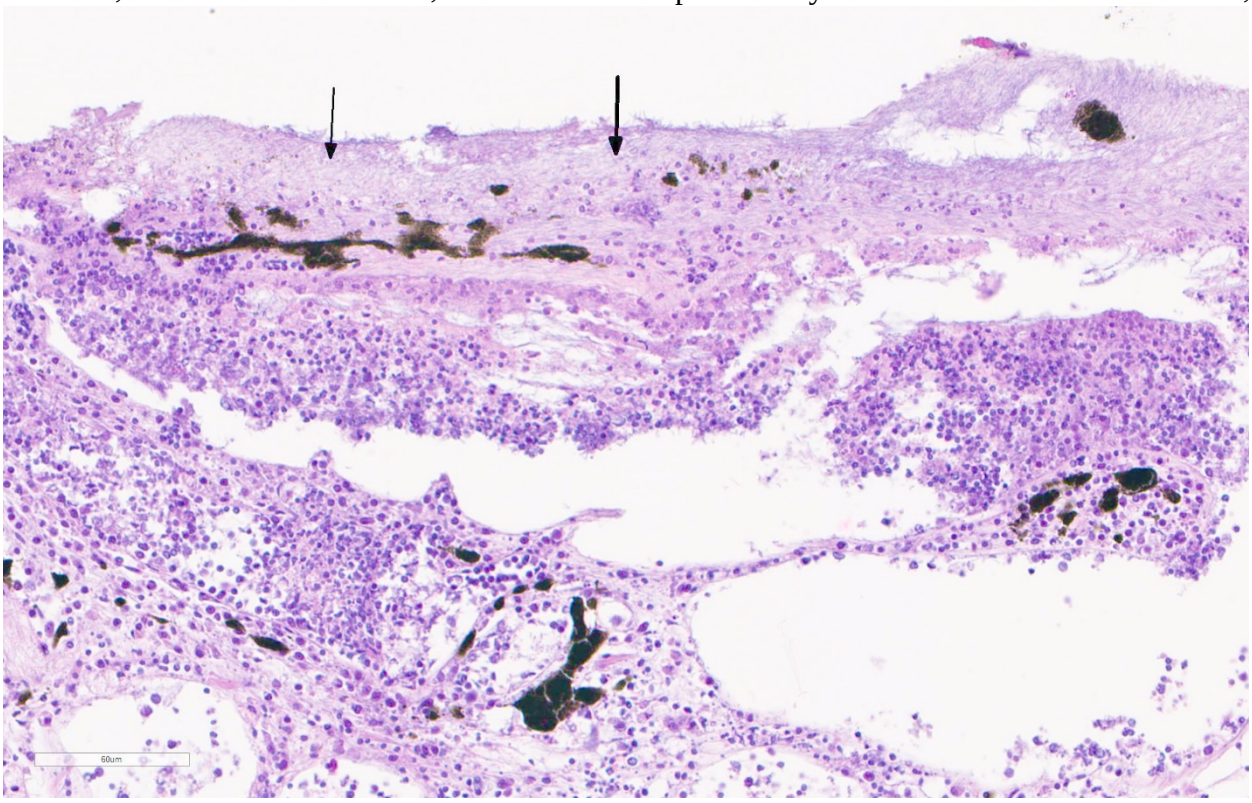

Snout, cardinal tetra. The denuded dermis of the snout is edematous, infiltrated by innumerous degenerate lymphocyte and histiocytes, and is covered by a mat of 1x5 um filamentous bacilli which are present at all levels of the inflamed dermis.(HE, 200X)

The name “columnaris disease” has been used consistently since the condition was first described in 1922. However, the taxonomic status of the agent has been revised numerous

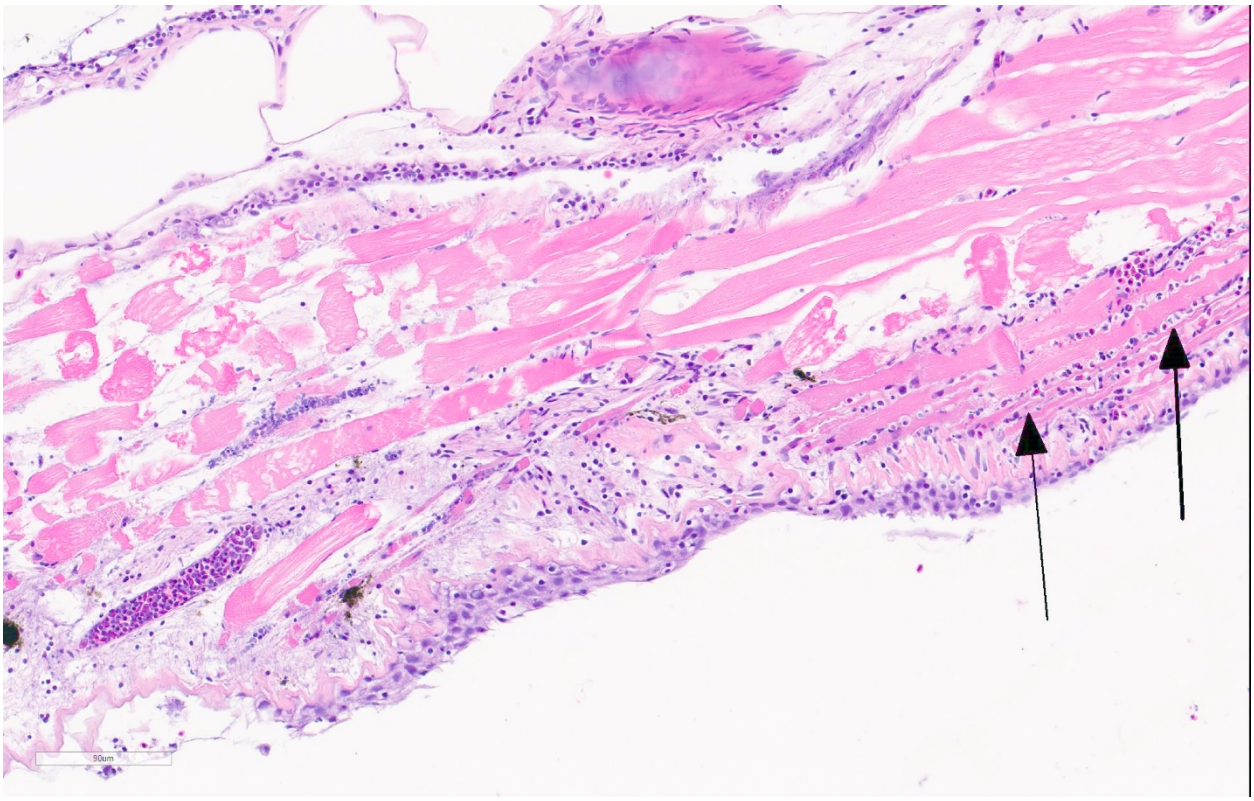

Jaw, cardinal tetra. The skeletal muscle of the jaw is multifocally necrotic, as evidenced by vacuolation, fragmentation, and loss of satellite nuclei, and infiltrated by degenerate inflammatory cells. The interstitium contains numerous filamentous bacilli. (HE, 234X)

times and includes the earlier combinations *Bacillus columnaris*, *Chondrococcus columnaris*, *Cytophaga columnaris*, and *Flexibacter columnaris*.[3] The current name, *Flavobacterium columnare*, was recognized in 1996.[2] The genus *Flavobacterium* contains additional important fish pathogens that can produce lesions similar to *F. columnare*, including *Flavobacterium psychrophilum*, the cause of coldwater or peduncle disease in salmonid and other cold freshwater species,[6] and *Tenacibaculum maritimum*, in marine fish.[1] Collectively, bacteria in this gram-negative genus average 2-5 µm in length, although forms up to 40 µm can occur. Longer rods are flexible and move by gliding motility. Colonies are typically yellow, a product of non-diffusible carotenoid or flexirubin-type pigment production.[2]. Isolation of the bacteria in culture requires the use of low nutrient agar media, such as Shieh or tryptone yeast extract salts (TYES). The organism will now grow on standard bacterial media such as trypticase soy agar (TSA). Confirmatory diagnostic tests include ELISA, FA, and LAMP methods, as well as conventional and qPCR procedures.[3]

Contributing Institution:
Department of Pathology, College of Veterinary Medicine, University of Georgia, Athens, GA 30602, www.vet.uga.edu/VPP

JPC Diagnosis: Head: Dermatitis, necrotizing**,** and lymphocytic, focally extensive severe, with skeletal muscle degeneration and necrosis and innumerable filamentous bacilli.

JPC Comment: The contributor has given us an outstanding review of this common bacterial pathogen of a wide range of

freshwater fish. *Flavobacterium columnare* has been seen as a causative factor in a number of large-scale fish dieoffs, to include multiple species in separate reported dieoffs in the Buffalo Pound and Blackstrap Lakes, which affected yellow perch and lake whitefish respectively, and several thousand carp in the St. Lawrence river.[8] In these mortality events, *F. columnare* was considered one of a number of factors, to include environmental stress due to ambient heat and lessened oxygen availability, and other bacterial pathogens, including *Aeromonas hydrophila* which was co-cultured from the dead fish.[8]

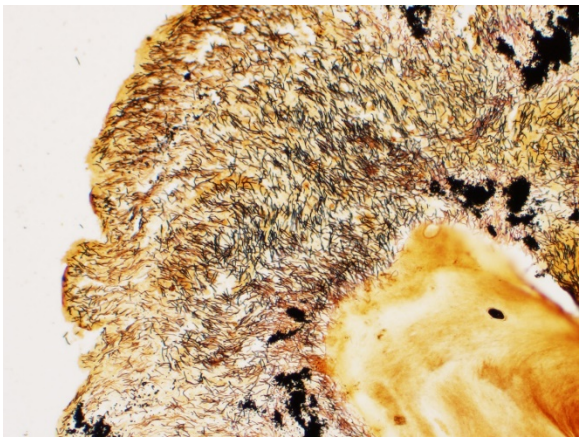

Snout, cardinal tetra. A silver stain demonstrates the large number of Flavobacterium infiltrating the denuded dermis and underlying tissue. (Warthin-Starry 4.0, 400X)

Increased water temperature has been noted as a major contributoring factor to the increase in *F. columnare* infections on a global basis. It was identified in a study by Pulkkinen et al. as a major factor in the increase in virulence of *F. columnare* over a period of 23 years in salmon farms in Finland. In addition to higher temperatures causing stress to fish,[6] global warming also extends the periods in which *F. columnare* can grow and cause outbreaks, as well as facilitate faster tissue invasion by virulent strains as increase in chondrolysin lyase activity (facilitating dermal invasion) is seen at higher temperatures.[3] In farmed fish, increased stocking levels contribute to outbreaks of *F. columnare* by increasing the organic load in the water, as well as nitrate concentration and the possibility for co-infections with other bacterial pathogens or ectoparasites.[3]

The moderator commented on the acute nature of the lesion which was illustrated by the lack of granulomatous inflammation, and believes that many of the inflammatory cells present within the lesion are lymphocytes and few are actually tissue macrophages (as would fit with the history of fish death within 24 hours after the stress of transport, as well as the normal progress of the disease – "the fish go down quickly".) as bacteria may be lost before autopsy, the moderator recommends wet-mounted skin scrapings in animals that are still living. After approximately 15 minutes, F. columnare will assume a typical "haystack" formation for which it is famous.

A differential diagnosis for facial necrosis in ornamental fish is spaC-type *Erysipelothrix.*[5] This report describes a disease of ornamental fish resulting in facial cellulitis, necrotizing dematitis and myositis and disseminated coelomitis with numerous colonies of gram-positive organisms. *Erysipelothrix* was recovered by from numerous animals but were genetically divergent from existing species of *E. rhusiopathae* and *E. tonsillarum* known to be pathogenic in fish and marine mammals.[5]

References:

1. Avendaño-Herrera R, Toranzo AE, Magariños B. Tenacibaculosis infection in marine fish caused by Tenacibaculum maritimum: a review. *Dis Aquat Org.* 2006; **71**: 255-266.

2. Bernardet J –F, Segers P, M. Vancanneyt M, Berthe F, Kersters K, Vandamme P. Cutting a Gordian Knot: Emended classification and description of the genus *Flavobacterium*, emended description of the family *Flavobacteriaceae*, and proposal of *Flavobacterium hydatis* nom. nov. (Basonym, *Cytophaga aquatilis* Strohl and Tait 1978) Int J Syst Bacteriol. 1996; **46**: 128-148.

3. Declerq AM, Haesebrouck F, Van den Broeck W, Bossier P, Decostere A. Columnaris disease in fish: a review with emphasis on bacterium-host interactions. *Vet Res*. 2013; **44**: 27.

4. Durburow RM, Thune RL, Hawke JP, Camus AC. Columnaris disease, a bacterial infection caused by Flavobacterium columnare. Southern Regional Aquaculture Center Publication No. 479. 1998.

5. Pomaranski EK, Reichley SR, Yanong, R, Shelley J, Pouder DB, Wolf JC, Kenelty KV, Ven Bonn B, Oliaro F, Byrne B, Clothier KA, Griffen MJ, Camus AC, Soto E. Characterizatioj of spaC-type Erysipelothrix sp. isolates causing systemic disase in ornamental fish. *J Fish Dis* 2017; 41(1): 49-60.

6. Pulkkinen K, Suomalainen LR, Read AF, Ebert D, Rintamakk P, Valtonen ET. Intensive fish farming and the evoluation of pathogen virulence: the case of columnaris disease in Finland. *Proc R Soc B* 2010; 277:593-600

7. Starliper CE. Bacterial coldwater disease of fishes caused by Flavobacterium psychrophilum. J Adv Res. 2011; **2**: 97-108.

8. Scott SJ, Bollinger TK. Flavobacterium columnare: an important contributing factor to fish die-offs in southern lakes of Saskatchewan, Canada. *J Vet Diagn Investig* 2014; 26(6)832-835.

CASE II: AP 17-4634 (JPC 4120175).

Signalment: 10-month-old male wildtype line (unspecified), zebrafish, *Danio rerio*

History: A wild-type control zebrafish for a leukemia study was swimming in circles and removed from the study for pathology evaluation.

Gross Pathology: No notable gross findings were observed.

Laboratory results: N/A

Microscopic Description:
There are randomly distributed and variably sized cross-sections of parasitic complexes containing numerous spores within the white mater of the posterior brain and brain stem. The majority of parasitic spores appear as uninucleate structures by H&E staining and are approximately 3.0 µM wide x 5.0 µM long with posterior vacuoles. Low numbers of glial cells are found at the periphery of some complexes while the neuropil appears devoid of cells at other locations were

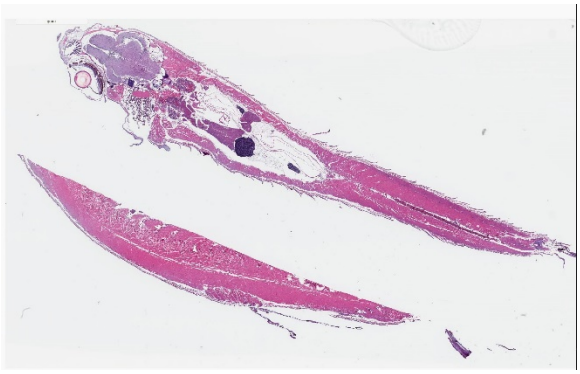

Zebrafish, sagittal sections. Two sections are presented for examination. No lesions are present on subgross examination. (HE 5X)

complexes are observed. Spores were not detected in other sampled tissues.

Contributor Morphologic Diagnosis:
Brain, neuropil: Parasitic complexes, multifocal, with morphology that is most consistent with *Pseudoloma neurophilia* infection.

Contributor Comment: *Pseudoloma neurophilia* is a commonly encountered and well described microsporidian parasite of zebrafish. Unlike other microsporidia, *P. neurophilia* does not appear to form xenomas. Histologic and ultrastructural studies of oral exposure to the proliferative parasitic stages show that early developmental phases interface with zebrafish host cells through a glycocalyx-like coating. Sporophorous vacuoles are then formed where the sporogonic stages remain to undergo karyokinesis, producing tetranucleate stages that then divide into uninucleate sporoblasts and spores. Spores remaining within these parasite complexes may or may not elicit an immune response.[1]

Recent studies are better clarifying the genomic basis of P. neurophila infections as well as the effects of silent infections on research.[1,4,8-10] P. neurophilia may be transmitted either through a vertical or horizontal route. It often presents in zebrafish colonies as a chronic, subclinical infection that primarily affects the brain and skeletal muscle.[5] Infected fish demonstrate a range of presentations included altered behavior, reduced growth or spinal deformities (e.g., lordosis and kyphosis). Alternatively, there may be no visible indications of infections and only baseline mortality rates for a facility. The variable clinical presentations and the potential for false negatives using either histology or molecular testing when conducting sentinel surveillance makes eradication of microsporidial infections challenging. Additionally data gathered from fish from infected colonies has the potential for inconsistent results for behavioral, immunology and hematopoiesis studies. The negative effects of microsporidial infections in colonies used for research studies is especially profound when immuno-suppressive therapies, like gamma irradiation, are used as parasitic infections often worsen. Interestingly aspects of the subclinical disease as well as understanding how these infections become clinically significant following immunosuppression in zebrafish are being advanced as one way to study aspects of microsporidial infections in humans.[4,6,8,9]

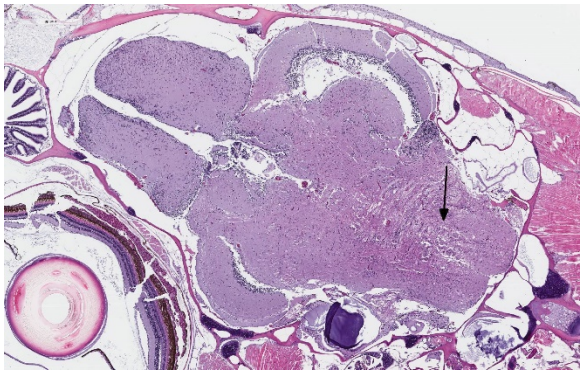

Brain, zebrafish. A cluster of microsporidial sporophorous vesicles are present within the hindbrain. (HE, 36X)

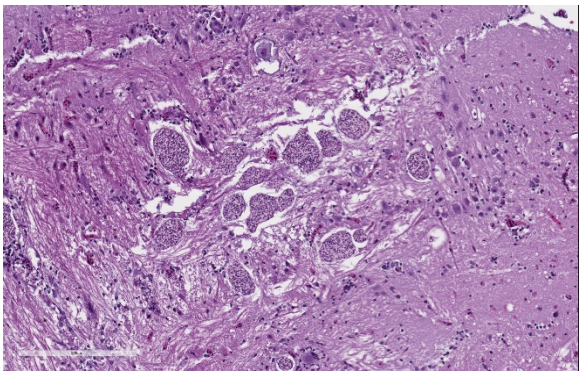

Brain, zebrafish. Sporophorous vesicles measures up to 60um in diameter and contain numerous spores. (HE 200X)

Contributing Institution:
Department of Pathology, College of Veterinary Medicine, University of Georgia, Athens, GA 30602, www.vet.uga.edu/VPP

JPC Diagnosis: Hindbrain: Microsporidial xenomas, multiple.
2. Skeletal muscle: Degeneration and necrosis, multifocal.

JPC Comment: *Pseudoloma neurophilium* is a common microsporidial parasite of zebrafish. Transmission occurs vertically and horizontal routes of transmission are the result of consumption of environmentally resistant spores in water contaminated by carcasses and eggs. Standard sterilization techniques, such as bleaching, do not impact spores, and spores contained within embryonated eggs are shielded from disinfectants.[9]

A recent study also demonstrated reduced survivability of *P. neurophila* spores following cryopreservation.[3] This is an important finding as cryopreservation of sperm is widely used in the maintenance and distribution of many strain type zebrafish used in research. Other zebrafish pathogens examined in this fashion were *Mycobacterium marinum* and *chelonae* (minimal impact upon freezing and thawing), and eggs of *Pseudocapillary tomentosa* (no survival).[3]

Due to their social nature, zebrafish are used in a wide variety of behavioral research studies on human diseases, such as autism, schizophrenia, depression, and PTSD, as well as to study the behavioral effects of a wide variety of pharmaceuticals.[8,11] Startle behavior, shoaling, and interfish distance of laboratory zebrafish are all interpretable responses in judging behavioral abnormalities. Fish infected with *P. neurophilia* have been shown to have

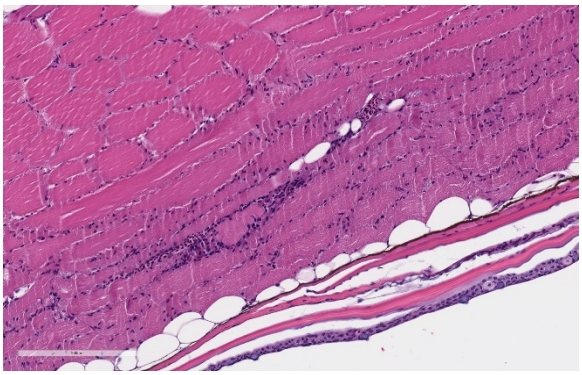

Skeletal muscle, zebrafish. Multifocally, occasional myofibers of the skeletal muscle are shrunken, granular, and low numbers of lymphocytes and histiocytes invade the perimysium. (HE, 200X)

abnorming shoaling behavior and interfish distance, which may potentially complicate behavioral studies using this animal model.[11]

A recent publication from the research group at Oregon State University at Corvallis, one of the leading groups in the area of zebrafish research, recently identified a number of species of aquarium fish that may also be infected with *P. neurophilia* in a mixed-species aquarium setting.[7] While long considered to be an infection restricted to *Danio rerio*, there are now five families and eight species which have been identified to be infectable with this parasite. The species include giant danio, medaka, fathead minnows, goldfish, platys, Siamese fighting fish, and neon tetras.[7]

Contributing Institution:
St. Jude Children's Research Hospital, Department of Pathology
https://www.stjude.org/research/departments-divisions/pathology.html

References:

1. Cali, A., et al., Development, ultrastructural pathology, and taxonomic revision of the microsporidial genus, *Pseudoloma* and its type species *Pseudoloma*

neurophilia, in skeletal muscle and nervous tissue of experimentally infected zebrafish (*Danio rerio*). *J Eukaryo Micro* 2012; 59(1): 40-48.
2. Matthiew, JL, et al. *Pseudoloma neurophilia* n. g., n. sp., a new microsporidium from the central nervous system of the zebrafish (*Danio rerio*). *J Eukaryo Micro* 2001; 48(2):227-233.
3. Norris, LJ, Watral V, Kent ML. Survival of bacterial and parasitic pathogens from zebrafish (*Danio rerio*) after cryopreservation and thawing. *Zebrafish* 2018; 15(2):188-201.
4. Ramsay JM, et al., *Pseudoloma neurophilia* (Microsporidia) infections in zebrafish (*Danio rerio*): effects of stress on survival, growth and reproduction. *Dis Aquatic Org* 2009. 88(1):69-84.
5. Sanders JL et al., Verification of intraovum transmission of a microsporidium of vertebrates: *Pseudoloma neurophilia* infecting the zebrafish, *Danio rerio*. PLoS ONE, 2013; 8(9):e76064.
6. Sanders, J.L., V. Watral, and M.L. Kent. Microsporidiosis in zebrafish research facilities. *ILAR Journal / National Research Council*, Institute of Laboratory Animal Resources, 2012; 53(2): p. 106-113.
7. Sanders JL, Watral V, Stidworthy MF, Kent ML. Expansion of the known host range of the microsporidium, *Pseudoloma neurophilia*. Zebrafish 2016; Supp 1:S102-S107.
8. Spagnoli, S., L. Xue, and M.L. Kent, The common neural parasite *Pseudoloma neurophilia* is associated with altered startle response habituation in adult zebrafish (*Danio rerio*): Implications for the zebrafish as a model organism. Behavioural brain research, 2015. 291: p. 351-360.
9. Spagnoli, S.T., et al., *Pseudoloma neurophilia* infection combined with gamma irradiation causes increased mortality in adult zebrafish (*Danio rerio*) compared to infection or irradiation alone: new implications for studies involving immunosuppression. *Zebrafish*, 2016. 13(Suppl 1): p. S-107-S-114.
10. Spagnoli, S.T., et al., *Pseudoloma neurophilia*: A retrospective and descriptive study of nervous system and muscle Infections, with new implications for pathogenesis and behavioral phenotypes. *Zebrafish* 2015; 12(2):189-201.
11. Spagnoli S, Sanders J, Kent M. The common neural parasite *Pseudoloma neurophilia* causes altered shoaling behavior in adult laboratry zebrafish and its impoicatiobs for neurobehavioral research. *J Fish Dis* 2017; 40(3):443-446.

CASE III: AFRIMS Case 1 (JPC 4113195).

Signalment: Adult, male zebrafish (*Danio rerio)*

History: This animal was one of four maintained in a private aquarium and was >1 year old. The animal progressively (1 month)

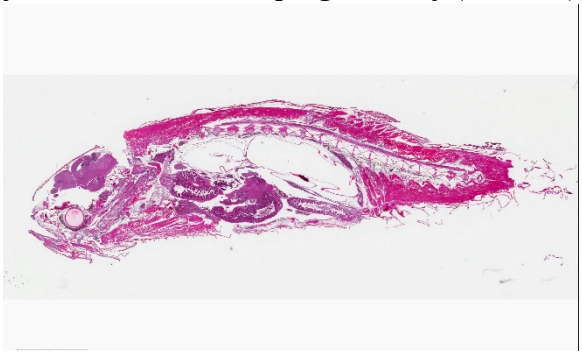

Presentation, zebrafish. A sagittal section of a zebrafish is submitted for examination. (HE 7X)

was observed to have developed a swollen abdomen and then became anorexic for 1 week. The last two days prior to euthanasia, the animal lost buoyancy control and swam irregularly within the water column. Necropsy did not reveal any abnormalities. All other animals in the tank were within normal limits.

Gross Pathology: Necropsy did not reveal any abnormalities.

Laboratory results: N/A

Microscopic Description:
Intestine: Multifocal to coalescing, markedly expanding and effacing the intestinal mucosa and submucosa and extending multifocally into the muscularis is a densely cellular, unencapsulated, poorly circumscribed neoplasm composed of polygonal cells arranged in abortive tubules in which the cells pile up and frequently have lost polarity, as well as disorganized islands and trabeculae on a fine fibrovascular stroma. Neoplastic cells have variably distinct cell borders, small to moderate amount of basophilic granular cytoplasm, oval to elongate nuclei with dense, finely stippled chromatin and occasionally 1 distinct nucleolus. Mitoses are infrequent at approximately 1 per 3 high powered fields observed. There is moderate anisocytosis and anisokaryosis, and often neoplastic cells within tubules appear to undergo maturation to mucoid cells which are characterized by large polygonal cells with abundant microvacuolated eosinophilic cytoplasm and small peripheralized nuclei with dense chromatin and no observable nucleoli. No mitoses were observed in this population. Neoplastic tubules are occasionally either occluded by the proliferating cells or are rarely ectatic and contain eosinophilic cellular and karyorrhectic debris, mucous, sloughed cells, scattered granulocytes and lymphocytes.

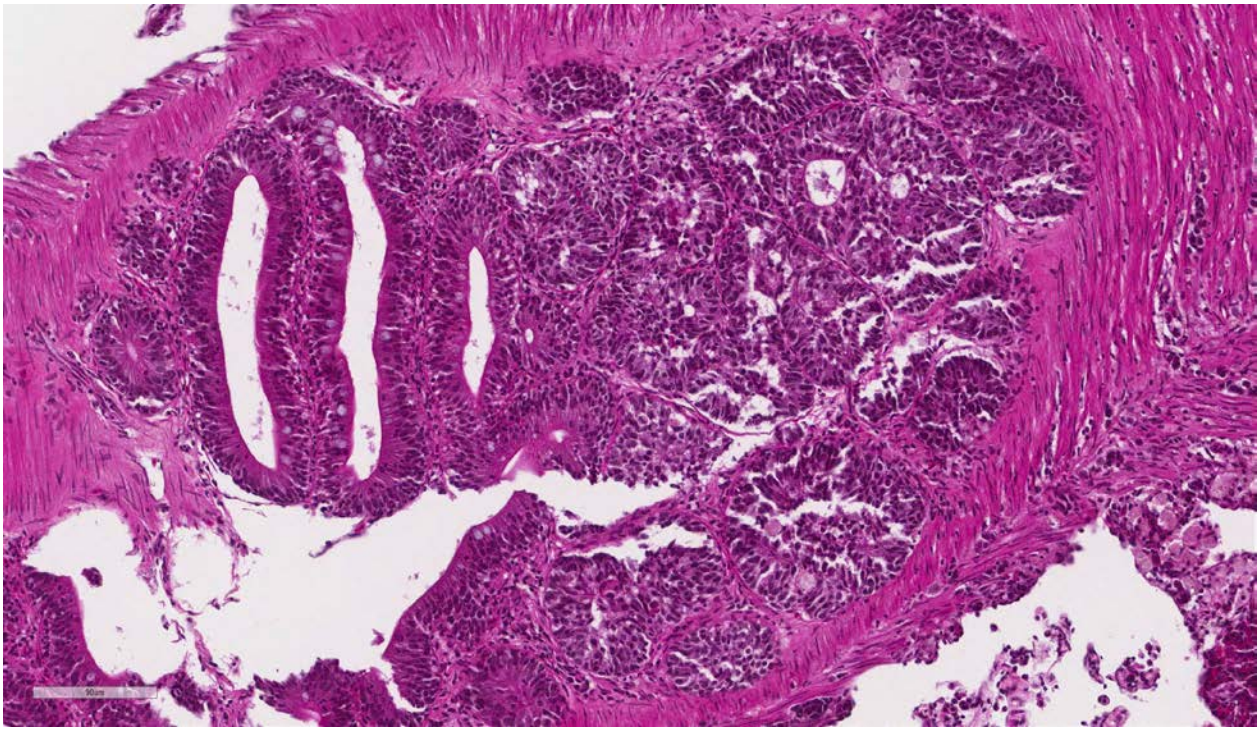

Intestine, zebrafish. The architecture of the large segment of the intestine at right is markedly altered, with a loss of typcal villar arthcitecture, and formation of prominent acini which resemble crypts. (HE, 100X)

Multifocally, extending transmurally and occasionally disrupting the serosal surface, the myocytes within the affected muscularis are separated, surrounded and replaced by small islands of neoplastic cells, eosinophilic amorphous material (edema), streams of lymphocytes and granulocytes. In these areas, myocytes are vacuolated and swollen (degenerate). Adjacent mucosa, unaffected by the neoplastic process, is frequently hyperplastic with epithelial piling and formation of papillary fronds which occasionally occlude the crypts. Focally, within a pancreatic vessel there is an organizing fibrin thrombus; however neoplastic cells are not observed within vessels or lymphatics. Occasionally rhabdomyocytes within the body wall are degenerate, necrotic or atrophic and separated by the previously described edema and inflammatory cells.

Liver; kidney; rectum; branchial arch; gill; thyroid gland; esophagus; oral cavity; brain; eye; spinal cord; vertebral column; air sac: No significant findings.

Contributor's Morphologic Diagnosis:
Intestine: Adenocarcinoma

Contributor's Comment: Fish have been and continue to be used extensively as comparative animal models for human neoplastic disease, and the zebrafish is by leaps and bounds the primary species employed. There are many reasons why zebrafish have made such headway into the fields of cancer research, and while the adult animal may appear to share little with primates, there are a wide range of evolutionarily preserved signaling pathways, translational regulation of cellular division and molecular markers of neoplasia which make fish extremely relevant to comparative pathology studies.[5,9,10,11] Furthermore, the

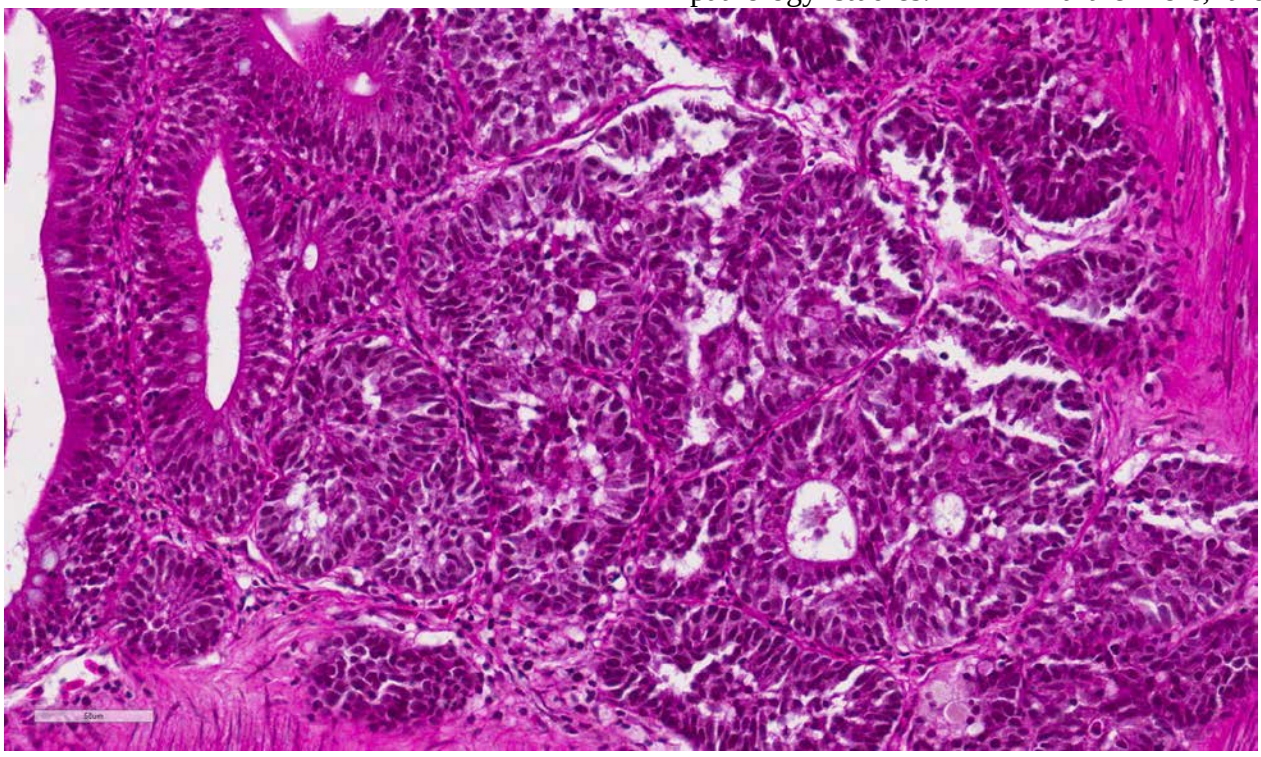

Intestine, zebrafish. Areas of dysplasia and acinar formations of neoplastic cells replace normal architecture. (HE, 234X)

embryology of fish and humans share significant commonality and as such present a valuable resource for study of the development of human disease, especially with embryonal tumors.[5,10] A recent and extremely exciting development of a transparent adult zebrafish allows for in vivo assessment of neoplastic metastatic behavior using labeled neoplastic cells.[13]

In addition to spontaneous tumors, neoplastic disease has been induced in fish and in particular in zebrafish using a variety of methods. genetic manipulation, xeno-transplantation, chemical carcinogenesis, forward and reverse genetic screens and radiation induction of neoplasia have all been described.[5,9,10,11,12] Mutant zebrafish lines have been created which are highly susceptible to the development of tumors, especially, but not limited to, those which are rare in other vertebrate species such as chordomas, pineocytomas, hepatoblastomas, ocular medulloepitheliomas and olfactory esthesioneuroepitheliomas.[12]

Zebrafish lack a stomach, and as such, the esophagus connects directly to the intestine. At a cellular level, with the exception of Paneth cells, the zebrafish intestine is composed of all of the same cell types which make up the intestinal tract in mammalian species. The intestine is a contiguous simple tube which has morphological differences at the cellular level, primarily associated with the cellular populations and changes in the epithelium along its length, but that does not have macroscopic features which allow differentiation of large and small sections. [6,10]

Intestinal adenocarcinoma in zebrafish has been reported to occur with some frequency

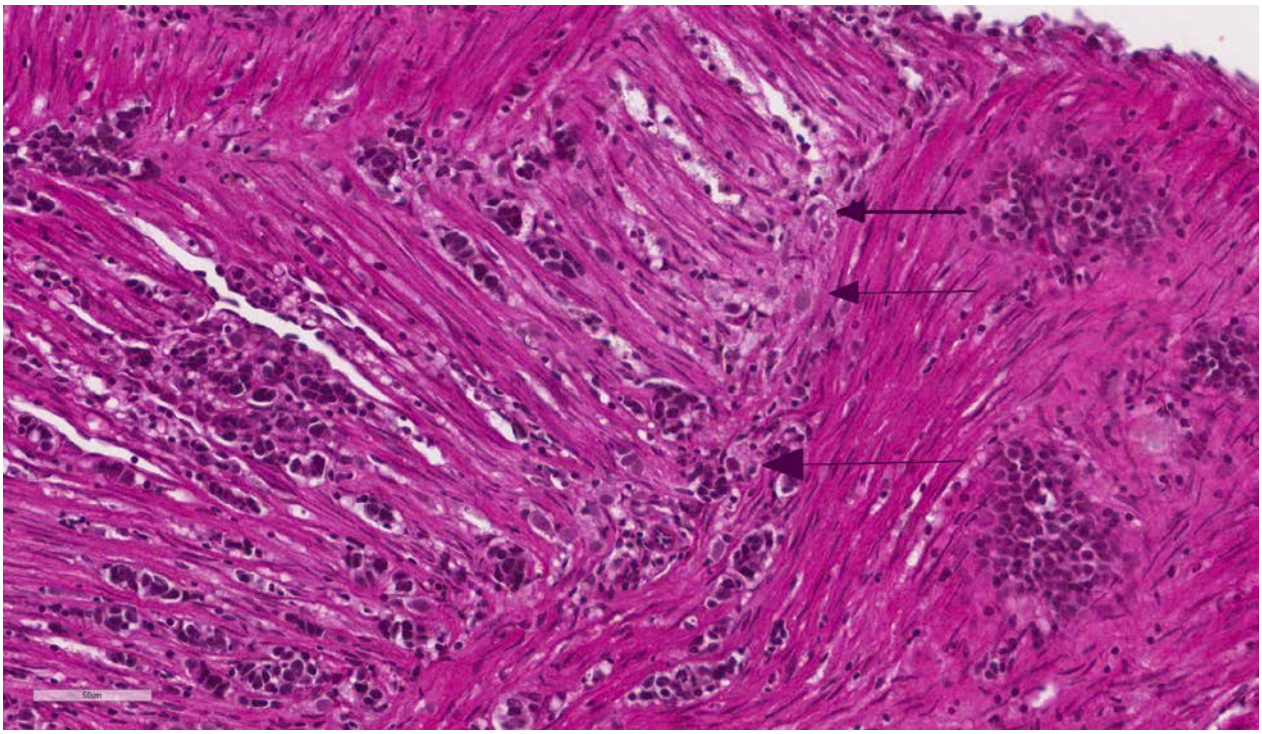

Intestine, zebrafish. Neoplastic cells, seen here infiltrating the intestinal wall, have two morphologies – a more mature mucous-like cells, and more numerous small cells with a small rim of eosinophilic cytoplasm surrounding a hyperchromatic nucleus. (HE,400X)

as a spontaneous neoplasm,[2,3,7,10,11] as well as occurring in the genetically modified adenomatous polyposis coli-deficient zebrafish (APC) model.[2,3,10] Additional reports of experimentally induced intestinal tumors have been associated with other genetically modified zebrafish lines, animals exposed to carcinogens and transgenic as well as in association with the nematode parasite, *Pseudocapillaria tomentosa*.[4,10]

A large study was conducted at Oregon State University examining submissions to the Zebrafish International Resource Center (ZINC) over a 10-year period. Approximately 2% of the cases submitted during that period were diagnosed with intestinal lesions, and of those, 113 tumors were diagnosed, with greater than 50% receiving diagnoses of adenocarcinomas.[7] The histopathological criteria for diagnosis of the various intestinal lesions, which were described in the evaluation, are abstracted below as Table 1 adapted from Paquette et al.'s retrospective study on intestinal neoplasia in zebrafish.[7]

Table 1. Defining Histological Signs of Intestine Presentations as Observed within Zebrafish Submitted to the Zebrafish International Resource Center Diagnostic Service 2000-2012[7]

Intestinal Presentation	**Defining Signs**
Normal Intestine	One cell thick layer of columnar epithelial cells lining mucosal folds with basally-oriented oval nuclei; mucosal folds become progressively shorter caudally, causing "villi" (the normal undulating structure of the intestinal wall appears villous, but lacks the true anatomic characteristics of villi) to appear shorter as the intestine approaches the excretory vent (anus); lamina propria, but no submucosa; inner circular and outer longitudinal smooth muscle layers invest the intestine throughout its length. Mucosal mucus (goblet) cells can be observed and increase in number distally.
Hyperplastic Intestine	Multilayered and increased numbers of epithelial cells, especially within basilar mucosal folds; "piling-up" of mucosal epithelial cells; nuclear pseudostratification; enhanced nuclear basophilia; pseudocrypt formation resulting from increased mucosal folding; anisokaryosis frequently observed and increased mitotic figures.
Dysplastic Intestine	Features of hyperplastic intestine in addition to increased nuclear and cellular pleomorphism, and occasionally aberrant mitotic figures, the

	loss of nuclear polarity and disorganization or absence of pre-existing histoanatomic architecture
Intestinal adenocarcinoma	Features of dysplastic intestine plus formation of disorganized pseudocrypts with invasion deep into the lamina propria and frequently through the basement membrane into the underlying muscularis layers; bizarre mitotic figures; neoplastic epithelial cells are pleomorphic and may be columnar, cuboidal or attenuated; hyperchromatic nuclei; annular strictures and fibroplasia frequently accompany tumorigenesis; pseudocrypts formed by the folding of neoplastic mucosal epithelium often resembled pseudoacinar structures that contained intraluminal sloughed rafts of necrotic neoplastic cells
Intestinal small cell carcinoma	Sheets and nests of round, polygonal or fusiform cells with minimal cytoplasm; hyperchromatic nuclei with granular chromatin and inconspicuous nucleoli; extensive fibroplasia; tumor cells occasionally formed an insular or organoid pattern characteristic of neuroendocrine tumors.
Intestinal tubular/tubulovillous adenoma	Focal adenomatous polypoid structures with clusters resembling mammalian glandular colonic crypts. The pseudocrypts often are lined by hyperplastic mucosal epithelium where the cells are crowded and have hyperchromatic nuclei. Increased mitotic figures are observed. Tubulovillous adenoma is essentially similar to tubular adenoma with a combination of both villous and pseudocrypt structures

The neoplasm in this case was diagnosed as part of the histopathological evaluation of the sampled tissues, rather than as a post-mortem necropsy finding. The clinical symptomology prior to euthanasia is consistent with the final diagnosis, however is relatively non-specific for any abdominal neoplasm as well as a wide range of other pathological processes. The histo-pathological features of this tumor are consistent with a diagnosis of intestinal adenocarcinoma.

Contributing Institution:
Armed Forces Research Institute of Medical Sciences (AFRIMS). http://afrims.amedd.army.mil/usamd-afrims.html

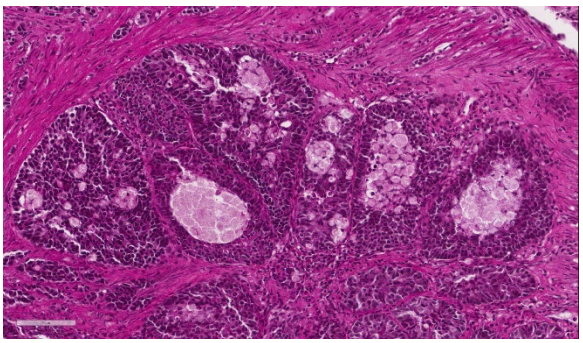

Intestine, zebrafish: Dilated acinar lumina contain sheets of necrotic mucus-producing cells. (HE, t34X)

JPC Diagnosis: 1. Intestine: Adenocarcinoma.
2. Pancreas: Intestinal adenocarcinoma, metastatic.

JPC Comment: The contributor has provided an excellent and comprehensive review of this neoplasm and its importance in a common laboratory species. Realizing the complexity of diagnosis of these tumors based solely on their morphologic appearance,[7] Paquette et al. in 2015[8] published a study detailing the immunohistochemical profile of these tumors, identifying them as neoplasms of epithelial origin (rather than their primary differential of tumors of neuroendocrine origin.) These neoplasms stained positive for AE1/AE3 (cytokeratin), while no tumors exhibited any immunopositivity for neuroendocrine markers (chromagranin A or S-100.)[8]

An interesting study by the Oregon State group in 2018 strongly suggests that this particular entity is transmissible.[1] The condition has been identified across zebrafish of multiple genetic backgrounds, suggesting genetics did not play a strong role. Feeding diets of fish with a high prevalence to fish with a low prevalence did not increase the frequency of the finding, suggesting diet was not a factor. Connecting tanks of fish with high prevalence to those of low prevalence in the same recirculating system did not result in a spike in tumors. Following a cohabitation protocol with fish with a known high incidence of the tumor, sampling of the biome of these fish with high-throughput 16S rRNA sequencing was performed, which indicated a high rate of infection in animals with tumors with a yet unidentified species of *Mycoplasma*, presumably spread to naive fish via a fecal-oral route. The authors do admit that a) other agents, potentially oncogenic viruses, may still be causative or play a role in causation, and b) the *Mycoplasma* infection may be a result of the pathological change rather than its cause. They recommend managing fish with the condition as having a potentially transmissible condition.[1]

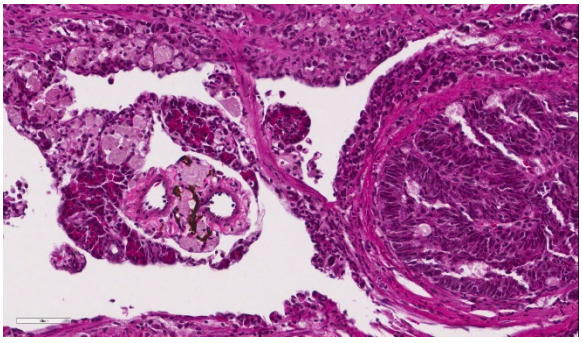

Intestine, zebrafish: Neoplastic cells infiltrate the pancreas (left) and line the intestinal serosa (right). (HE, 400X)

References:

1. Burns AR, Watral V, Sichel S, Spagnoli S, Banse AV, Mittge E, Sharpton TJ, Gullemin K, Kent ML. Transmission of a common intestinal neoplasm in zebrafish by co-habitation. *J Fish Dis* 2018 41(4):569-579.

2. Feitsma H, Cuppen E. Zebrafish as a cancer model. *Mol Cancer Res*. 2008; **6**:685-694. Shive HR. Zebrafish models for human cancer. *Vet Pathol*. 2013; 50:468-482.

3. Haramis AP, Hurlstone A, van der Velden Y, et al. Adenomatous polyposis coli-deficient zebrafish are susceptible to digestive tract neoplasia. *EMBO Rep.* 2006;**7**:444–449.

4. Kent ML, Bishop-Stewart JK, Matthews JL, et al. Pseudocapillaria tomentosa, a nematode pathogen, and associated neoplasms of zebrafish (Danio rerio) kept in research colonies. *Comp Med*. 2002;**52**:354–358.

5. Langheinrich U, Hennen E, Stott G, Vacun G. Zebrafish as a model organism for the identification and characterization of drugs and genes affecting p53 signaling. *Current Biol*. 2002; 12:2023-2028.

6. Menke AL, Spitsbergen JM, Wolterbeek APM, et al. Normal anatomy and histology of the adult zebrafish. *Tox Pathol*. 2011;**39**:759-775.

7. Paquette CE, Kent ML, Buchner C, et al. A retrospective study of the prevalence and classification of intestinal neoplasia in zebrafish (Danio rerio). *Zebrafish*. 2013; **10**:1-9.

8. Paquette, CE, Kent ML, Peterson TS, Wang R, Roderick HD, Lohr CV. Immunohistochemical characterization of intestinal neoplasia in zebrafish indicated epithelial origin. *Dis Aquat Org* 2015; 116(3): 191-197.

9. Setlow RB, Woodhead AD, Grist E. Animal model for ultraviolet radiation induced melanoma: Platyfish-swordtail hybrid. *Proc Natl Acad Sci USA*. 1989;**86**:8922-8926.

10. Shive HR. Zebrafish models for human cancer. *Vet Pathol*. 2013; **50**:468-482.

11. Shive HR, West RR, Embree LJ et al. brca2 and tp53 collaborate in tumorigenesis in zebrafish. *PLoS ONE*. 9(1): e87177.doi:10.1371/journal.pone.0087177.

11. Spitsbergen JM, Kent ML. The state of the art of the zebrafish model for toxicology and toxicologic pathology research - Advantages and current limitations. *Tox Pathol*. 2003;3(Suppl.):62-87.

13. White RM, Sessa A, Burke C, et al. Transparent adult zebrafish as a tool for in vivo transplantation analysis. *Cell Stem Cell*. 2008; 2:183–189.

CASE IV: WSC 18-19 #2 (JPC 4117006).

Signalment: 1-year-old, male, Puerto Rican crested toad *(Peltophryne lemur)*

History: The toad was found dead in its enclosure after an approximately several weeks long treatment for skin issues.

Gross Pathology: At necropsy, the toad was moderately desiccated and the skin of the ventrum and legs was diffusely brown and was easily peeled away from the body.

Laboratory results: N/A

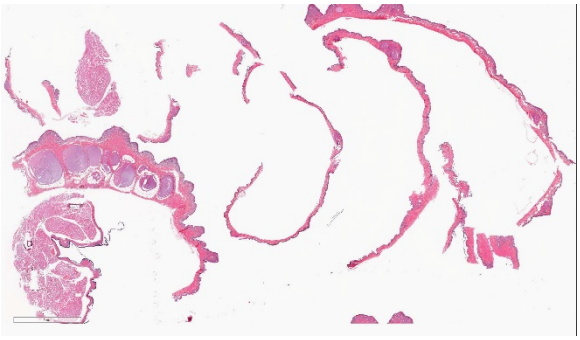

Skin, Puerto Rican crested toad. Multiple sections of skin are submitted for examination. (HE, 5X)

Microscopic Description:
There is multifocal to diffuse hyperplasia of the epidermis which is often covered by orthokeratotic hyperkeratosis. This keratin layer is often deep brown. Within the hyperplastic epidermis there are rare apoptotic keratinocytes and intracellular edema (spongiosis).There is a nearly diffuse layer of prominent melanocytes within the superficial dermis immediately adjacent to the basal layer of the epidermis. There is frequent thickening of the dermal Eberth-Katschenko (calcium) layer.

Contributor Morphologic Diagnosis:
Skin, Epidermal hyperplasia, orthokeratotic hyperkeratosis, spongiosis, rare keratinocyte apoptosis, and dermal melanocytosis, moderate, diffuse with thickened Eberth-Katschenko layer

Contributor Comment: The changes seen in the sections of skin from the submitted toad are consistent with the entity described as Brown Skin Disease of Puerto Rican Crested Toads (PRCT). Brown skin disease (BSD) is an idiopathic disease that has only been described in this species of toad.

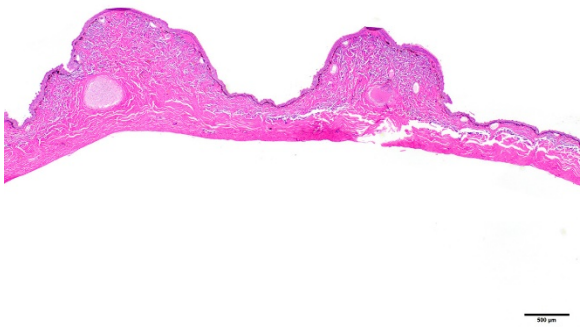

Skin, Puerto Rican crested toad. Epidermal hyperplasia with markedly thickened Eberth-Katschenko layer. (HE, 20X) (Photo courtesy of: Kansas State Veterinary Diagnostic Laboratory, Department of Diagnostic Medicine/Pathobiology)

Grossly the disease is characterized by leathery, brown discoloration of the skin that can occur anywhere on the body with abnormal shedding of the skin (dysecdysis) particularly on the ventrum.[1] Microscopically BSD is typically characterized by epithelial hyperplasia, spongiosis, orthokeratotic or parakeratotic hyperkeratosis with “nuclear ghosts” in keratinized epithelial cells, and occasional basal layer disorganization.[1] Other features include single cell necrosis throughout the epithelium, erosion or ulceration, and thickening of the Eberth-Katschenko layer (a normal layer of mineralization present in the skin).[1] See Crawshaw et al for excellent comparisons of normal and affected PRCT skin histology images.

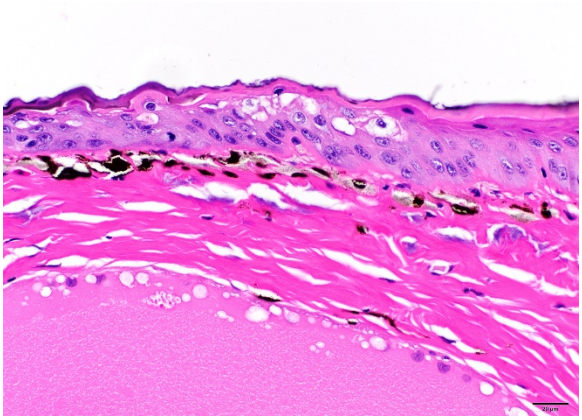

Skin, Puerto Rican crested toad. Epidermal hyperplasia with spongiosis and increased dermal melanocytes (HE, 400X) (Photo courtesy of: Kansas State Veterinary Diagnostic Laboratory, Department of Diagnostic Medicine/Pathobiology)

Examination of many cases has failed to reveal a cause for the disease. Attempts at bacterial cultures have revealed growth of a number of different bacterial genuses including *Aeromonas, Acinetobacter*, and many others but these have been considered normal flora or contaminants and attempts to identify common fungi of toads including chytrid fungi have all been negative.[1] In one study, supplementation of Vitamin A in 48 captive born PRCT failed to reduce the

severity of disease when it developed.[2] Further testing for bacterial or fungal organisms was not pursued in this case. Another PRCT was submitted from the same zoological collection and was similarly diagnosed with BSD. In that case bacterial culture of the skin revealed abundant growth of *Providencia rettgeri, Acinetobacter sp., Pseudomonas putida, Citrobacter freundii, Enterococcus faecalis, Microbacterium sp., and Staphylococcus sp. (non-hemolytic).* Fungal cultures of this second toad revealed unidentified yeast and further testing was not pursued.

Puerto Rican Crested Toads are a threatened species and have been listed as endangered by the International Union for Conservation of Nature (IUCN) since 1987.[1] Since then a number of the species have been housed in a number of zoos in an attempt to save the species. Given the lack of a convincing infectious cause for this disease is it possible that a genetic component contributes to this disease. Evidence for this includes the initial case of BSD occurring in one male of a group of four toads that represented the last four of the "Northern" race of PRCT, six offspring from a pairing of this same group, and multiple animals from succeeding generations from this initial pairing.[1] Despite this, cases of BSD have occurred in unrelated individuals from the "Southern" race housed at different zoos in close proximity to affected animals and on similar diets thus the true etiology remains elusive.[1]

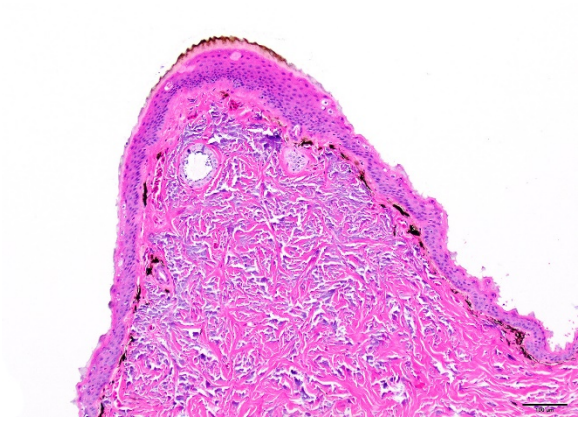

Skin, Puerto Rican crested toad. Epidermal hyperplasia with brown orthokeratotic hyperkeratosis, increased dermal melanocytes, and thickened Eberth-Katshenko layer (HE, 100X) (Photo courtesy of: Kansas State Veterinary Diagnostic Laboratory, Department of Diagnostic Medicine/Pathobiology)

Contributing Institution:
Kansas State Veterinary Diagnostic Laboratory, Department of Diagnostic Medicine/Pathobiology, www.ksvdl.org

JPC Diagnosis: Skin: Epidermal hyperplasia and hyperkeratosis, diffuse, marked, with dermal melanosis and mineralization.

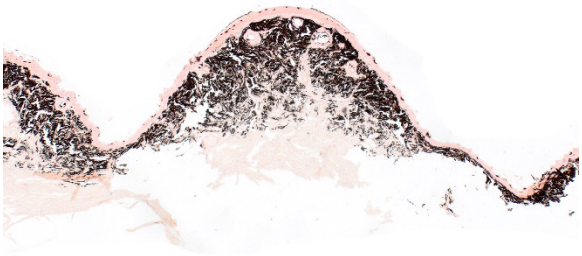

Skin, Puerto Rican crested toad. Thickened Eberth-Katshenko layer highlighted with Von Kossa staining (Von Kossa, 40X) (Photo courtesy of: Kansas State Veterinary Diagnostic Laboratory, Department of Diagnostic Medicine/Pathobiology)

JPC Comment: The contributor has provided a concise review of this species-specific disease which unfortunately is a problem in a threatened species. The contributor describes the common finding of brown leathery skin in affected toads, which does not apparently contain an increase in dermal melanocytes to explain the coloration. Attempts to soak and remove affected skin from individuals have been successful, but the disease recurs again soon after.[1]

A wide range of environmental factors (to include husbandry issues) and infectious

agents have been incriminated as causing skin lesions in anurans. Once considering the problem of dysecdysis (abnormal skin shedding), low humidity, low temperature, and poor nutrition have all been implicated in this dysecdysis.[2]

Hypovitaminosis A has been particularly incriminated in amphibians with dysecdysis. Like all other species, retinoids must be obtained via the det in the form of provitamin A carotenoids or preformed Vitamin A. When absorbed, enterocytes hydrolyze dietary retinol esters or carotenoids to retinol where they are combined with dietary fat and cholesterol to form retinyl ested-laden chylomicons and resecreted. Dissolution of chylomicra in circulation allows the delivery of retinoids to peripheral tissues; remaining retinoids are taken up by the liver. In the skin, retinoids perform an important function in the regulation of gene transcription and affect processes of cellular proliferation, differentiation, and apoptosis.[2]

References:

1. Crawshaw G, Pienkowski M, Lentini, A, et al. Brown Skin Disease: A Syndrome of Dysecdysis in Puerto Rican Crested Toads (*Peltophryne lemur).* Zoo Bio. 2014. 33:558-564.
2. Dutton C, Lentini A, Berkvens, et al. The Effect of Supplementation with Vitamin A on Serum and Liver Concentrations in Puerto Rican Crested Toads (*Peltophryne lemur)* and its lack of Impact on Brown Skin Disease. Zoo Bio. 2014. 33: 553-557.

Self-Assessment - WSC 2019-2020 Conference 6

1. Which of the following is NOT true regarding columnaris disease in fish?
    a. The inflammation seen in areas of bacterial invasion is generally overwhelming.
    b. The disease is characterized by acute mortality following massive sepsis.
    c. The causative agent is considered an opportunistic invader.
    d. Secretion of digestive enzymes degrade ground substance in connective tissue.

2. Flavobacterium columnaris is which of the following?
    a. Gram-positive
    b. Gram-negative

3. Which of the following is not seen with infection in zebrafish by *Pseudoloma neurofiliis*?
    a. Spinal deformities
    b. Altered behavior
    c. Exopthalmos
    d. Reduced growth

4. Which of the following is not a characteristic of intestinal adenocarcinoma in the zebrafish?
    a. Organoid patterns characteristic of neuroendocrine tumors
    b. Features of dysplasia within the intestine
    c. Bizarre mitotic figures
    d. Psedoacinar structures containing sheets of necrotic neoplastic cells

5. The Eberth-Katschenko layer is which of the following?
    a. A rudimentary system of alarm cells in the skin of amphibians
    b. A layer of cutaneous mineralization
    c. A suture line in the skin where shedding begins
    d. A line of openings of toxin producing glands in toads.

Please email your completed assessment for grading to Dr. Bruce Williams at bruce.h.williams12.civ@mail.mil. Passing score is 80%. This program (RACE program 33611) is approved by the AAVSB RACE to offer a total of 0.5 CE Credits, with a maximum of 12.5 CE Credits being available to any individual Veterinary Medical Professionals for the 2019-2020 Wednesday Slide Conference. This RACE approval is for the subject matter categories of: SCIENTIFIC using the delivery method of NON-INTERACTIVE DISTANCE. This approval is valid in jurisdictions which recognize AAVSB RACE.

Joint Pathology Center
Veterinary Pathology Services

WEDNESDAY SLIDE CONFERENCE 2019-2020

C o n f e r e n c e 7

9 October 2019

Conference Moderator:
Dr. John Cullen, VMD, PhD, DACVP, FIAT
Professor, Anatomic Pathology
College of Veterinary Medicine
North Carolina State University
Raleigh, North Carolina

CASE I: AP19-00238-9 (JPC 4135938).

Signalment: 12-year-old female spayed domestic longhaired cat (*Felis catus*)

History: The patient presented to the NCSU Small Animal Emergency Service on 1/19/19 with a history of steady decline over the past several months with weight loss, anorexia, and vomiting. Over the last few days, the patient had also developed neurologic signs. The primary veterinarian's bloodwork found elevated liver enzymes (ALT of 166, AST of 124, ALP of 311, total bilirubin of 2.8, and conjugated bilirubin of 1.5), a mildly elevated SDMA (16, reference 0-14 ug/dl), mildly reduced BUN (15, reference 16-37), and a mildly reduced creatinine (0.8, reference 0.9-2.5). Abdominal ultrasound identified bilateral chronic nephropathy with small nephroliths or dystrophic mineralization and a splenosystemic collateral vessel. The primary veterinarian treated with a renal diet, ursodiol, and lactulose. The owners felt clinical signs did not improve. On physical exam at NCSU, she had a reduced BCS and moderate muscle wasting and was quiet and depressed with intermittent responsiveness. Due to concern for the quality of life, euthanasia was elected.

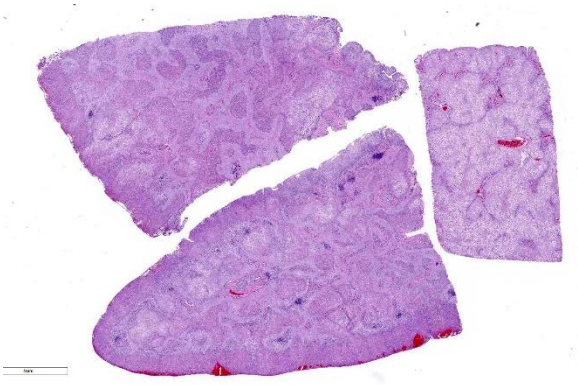

Liver, cat. Three sections of liver are submitted for examination. Approximately 50% of the hepatic parenchyma is replaced by anastomosing bands of dense fibrous connective tissue, which contain randomly scattered cellular aggregates (HE, 5X)

Gross Pathology: Arising from the splenic vein and connecting to the caudal vena cava

in the region of the left kidney is a large shunt vessel up to 4 mm in diameter. Additionally, connecting the portal vein and caudal vena cava in the cranial abdomen are two small (1 mm in diameter), tortuous vessels. The liver is mildly reduced in size, weighing 67 g (2.9% of total body weight; normal is 3-4). The liver is diffusely markedly pale red to tan and moderately firm. Over the diaphragmatic surface of the right lateral liver lobe is a 2.0 x 0.8 cm region of hemorrhage and mild depression. The parenchyma subjacent to this focus is markedly firm. The right kidney is mildly reduced in size compared to the left kidney and has multifocal
chronic infarcts up to 2 cm in diameter. No abnormalities are identified externally in the brain.

Laboratory results: No additional findings

Microscopic Description:

Liver: Replacing 20-50% of the hepatic parenchyma is robust, portal-to-portal bridging mature collagenous stroma, and within this stroma are markedly increased numbers of small caliber bile duct profiles. Bile ducts often have irregular to absent lumina, are tortuous with occasional branching, and frequently occur at the limiting plate directly adjacent to periportal hepatocytes. Mildly increased numbers of arteriole profiles accompany hyperplastic bile ducts. Portal veins are frequently reduced in diameter or absent. Within this bridging fibrosis are mild, multifocal infiltrates of lymphocytes and plasma cells. In the subcapsular region, sinusoids are multifocally markedly congested. The mesothelium is regionally hypertrophied. Variably 15-75% of hepatocytes, in a patchy predominantly centrilobular to midzonal distribution, contain one to multiple, small to

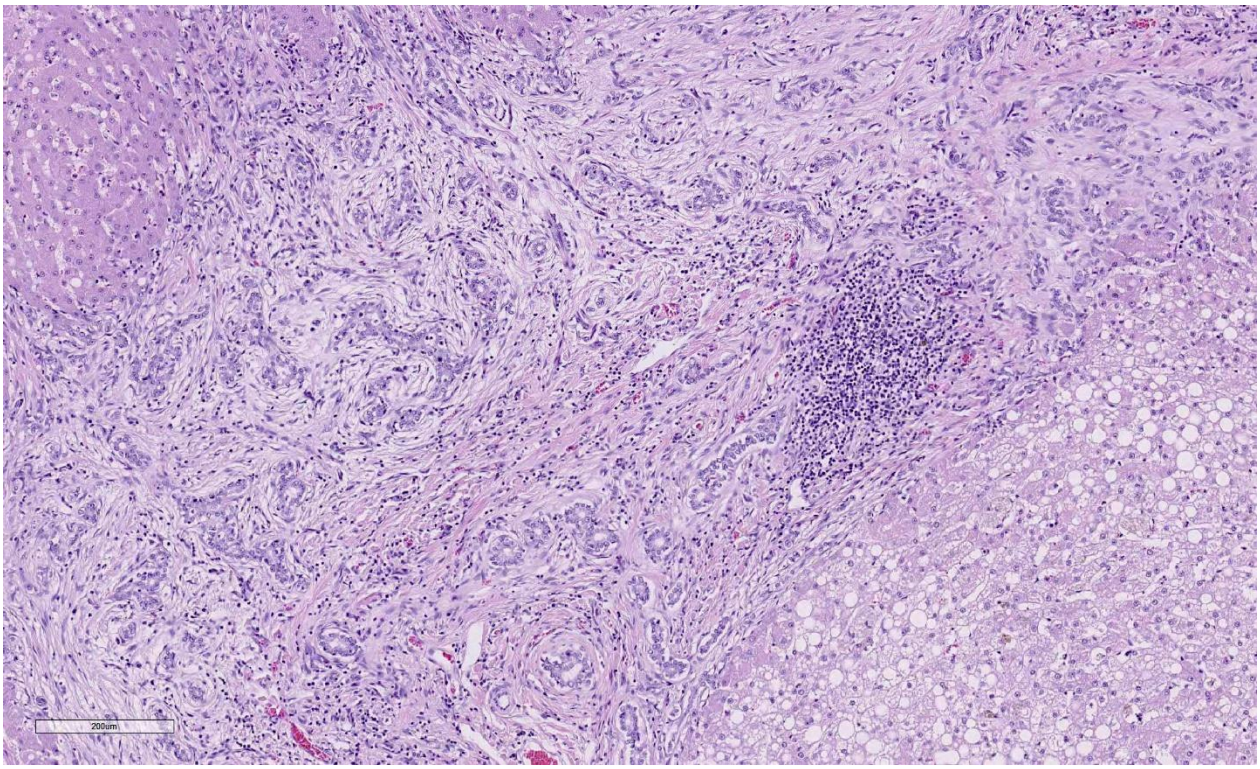

Liver, cat. Higher magnification of the dense bands of fibrous connective tissue which expands and bridges portal areas and largely effaces the periphery of the hepatocellular lobule. There is marked biliary hyperplasia in areas of fibrosis, and scattered areas of lymphoplasmacytic inflammation. (HE, 107X)

large, discrete, clear, lipid type vacuoles. Scattered within the parenchyma are occasional pigment granulomas composed of foamy macrophages that are occasionally laden with golden-brown pigment (suspected hemosiderin).

Contributor's Morphologic Diagnosis: Liver:
a. Marked, portal-to-portal bridging fibrosis with marked ductular reaction, portal vein hypoperfusion, mild arteriolar hyperplasia, and mild lymphoplasmacytic chronic hepatitis (consistent with congenital hepatic fibrosis)
b. Moderate, multifocal to coalescing, hepatic lipidosis

Contributor's Comment: The clinical history, gross findings, and histologic findings in this case, are all consistent with congenital hepatic fibrosis (CHF). CHF is a condition resulting from abnormal development at the ductal plate affecting small interlobular bile ducts.[3,10] CHF is histologically characterized by periportal to bridging fibrosis with numerous small often irregular bile ducts and a reduction in the number of portal vein branches.[3] In humans, the fibrosis has been shown to be progressive.[10] Inflammation and cholestasis are generally absent, and regenerative hyperplasia is not typically a feature.[3] Sequelae include portal hypertension, ascites, and acquired extrahepatic portosystemic shunts. These signs may be the result of progressive fibrosis or altered and insufficient portal vein architecture.[3]

CHF is a morphologic diagnosis but not a single clinical entity and instead is the result of a spectrum of conditions that affect the ductal plate.[4] In humans, isolated CHF is rare but reported, and CHF is more often associated with fibrocystic diseases (FCDs),

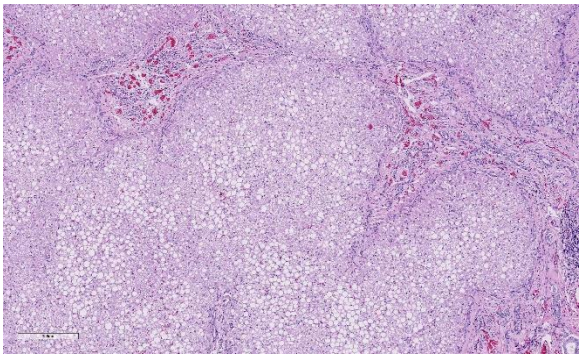

Liver, cat. Remaining hepatic parenchyma is vaguely nodular, with marked hepatocellular lipidosis and swelling. (HE, 400X)

including polycystic kidney disease (PKD).[10] While inheritance is most commonly autosomal recessive, X-linked and autosomal dominant inheritance are also described. Notably, although FCDs are currently categorized by phenotype, in the future, gene-based classification may significantly alter distinction among the FCDs.[10]

In the veterinary literature, there are relatively few reports of CHF. Species in which CHF has been reported include dogs[3,14,17], cats[1,19], aborted and neonatal calves[2,18], foals including Swiss Freiberger horses and multiple other breeds[5,11,12], an African green monkey[17], and a colony of Sprague-Dawley rats now used as a model for human autosomal recessive CHF[15]. In a case series of five dogs, all dogs presented at one year of age or younger with signs of liver disease.[3] Several other series of hepatic/hepatoportal fibrosis in young dogs have been published but do not expressly diagnose CHF versus other causes of hepatic fibrosis.[14,16]

There are two reports describing CHF in cats. One report describes CHF in cats with polycystic kidney disease (PKD), an autosomal dominant disorder for which Persian cats are predisposed.[1] Among cases of PKD, 28% had CHF, and 17% had both CHF and liver

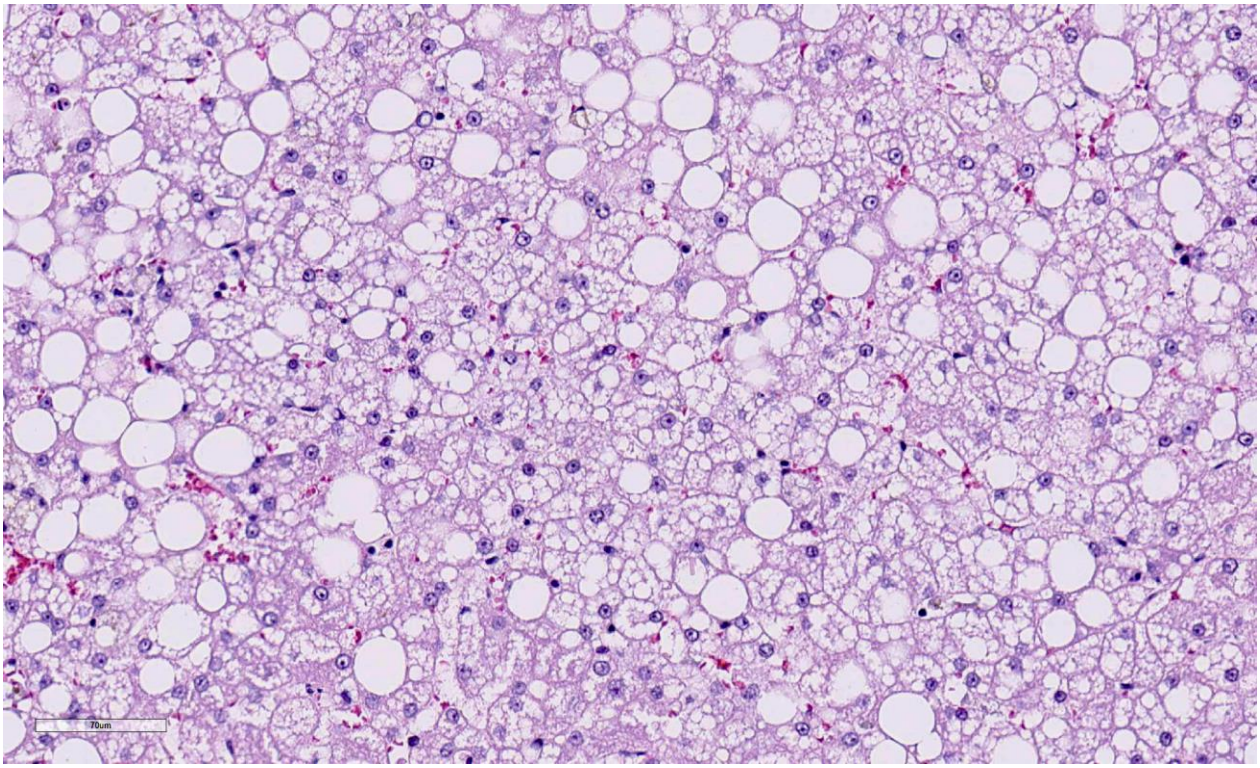

Liver, cat. Higher magnification of hepatocytes with marked swelling, lipidosis, and loss of sinusoidal architecture. (HE, 200X)

cysts. The age range for CHF-affected cats in this report was 1 to 13 years, and one of those cats had clinical signs of liver disease. [3] Additionally, there is a report of two cats with CHF and secondary acquired portosystemic shunts, and in this report, both cats also had evidence for concurrent PKO, as well as in one cat a concurrent congenital portosystemic shunt.[19] Interestingly in the case presented here, the cat lacked gross and histologic evidence of PKD, suggesting that in contrast to what is reported in the literature, CHF is not exclusively a manifestation of PKD in cats. Additionally, this case demonstrates that in contrast to dogs, CHF may progress more slowly in cats than in dogs and not become clinically relevant until later in life.

Contributing Institution:
North Carolina State University College of Veterinary Medicine
https://cvm.ncsu.edu/research/departments/dphp/programs/pathology/

JPC Diagnosis: Liver: Fibrosis, portal and bridging, diffuse, severe, with marked biliary hyperplasia, hepatocellular loss, nodular hepatocellular regeneration, and hepatocellular lipidosis.

JPC Comment: In humans, congenital hepatic fibrosis (CHF) is an autosomal recessive disease resulting from a mutation on PKDH1, whose gene product encodes fibrocystin/polyductin, a ciliary protein expressed in cholangiocytes as well as renal tubular epithelium.[6] In humans, CHF is part of the fibropolycystic diseases (FCDs), which also include autosomal dominant and autosomal recessive polycystic kidney disease, Caroli's disease, and von Meyenburg complexes (biliary hamartomas).[6,9] While a rare condition in humans (estimated in 1 in

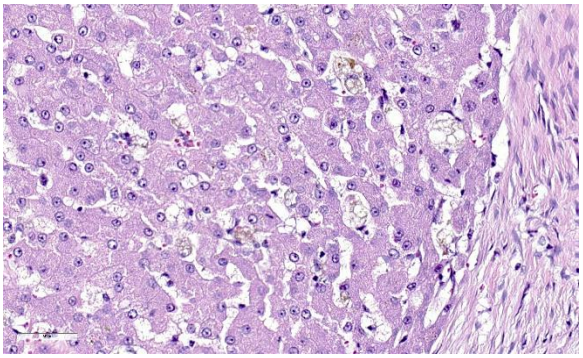

Liver, cat. Individualized or small aggregates of macrophages contain brown lipofuscin pigment (lipogranulomas), indicative of hepatocellular loss. (HE, 400X)

20,000 live births) it often occurs with diseases of other organs as well as other congenital diseases, including Joubert Syndrome and Bardet-Biedl Syndrome.[6]

In most other conditions resulting in progressive hepatic fibrosis. Fibrosis is a reparative response to a previous necrotizing or inflammatory insult.[6,9] In CHF, fibrosis is genetic, resulting from lack of remodeling of the ductal plate, the embryologic precursor to the intrahepatic bile ducts. The lack of remodeling ultimately results in the persistence of immature biliary structures, cystic malformation, and prominent peribiliary fibrotic responses. The actual function of polycystin is not known is thought to be involved as a regulator of transcription of various proteins involved in proliferation, differentiation, tubulogenesis and cell-matrix interactions.[6,9]

The clinical spectrum of CHF in humans is extremely broad and depends largely on whether polycystic disease is present in other organs. Cases of "pure" CHF may remain undetected into middle age. One of the most important consequences of fibropolycystic disease in humans is the development of portal hypertension, which often results in clinical symptoms of hematemesis and melena in 30-70% of cases; clinical signs related to cholangitis are less common, which may ultimately require hepatic resection or transplantation. Portal hypertension in such cases ultimately may require hepatic resection or transplant.[6,9]

The contributor discusses a previous report of cats with CHF and PKD. Hepatic fibrosis has been reported in between 22-48% of cats with feline polycystic kidney disease, although clinical signs associated with liver failure are rare.[8] Genetic testing for PKD became available following that report, and was found to be associated with a C>A mutation in exon 29 of *PKD1* (polycystic kidney disease 1). In a feline case of combined CHF and PKD1 reported in 2015, genetic testing revealed a wild-type sequence at this position, suggesting an alternate pathogenesis, or perhaps a mutation not yet described in the cat, and is similar to the case described herein which PKD was not a concurrent condition.[8]

Upon close inspection of the submitted sections, the moderator commented on the zone of exclusion of relatively unaffected tissue. This is supplied by a subset of bile ducts of the smallest caliber at the periphery

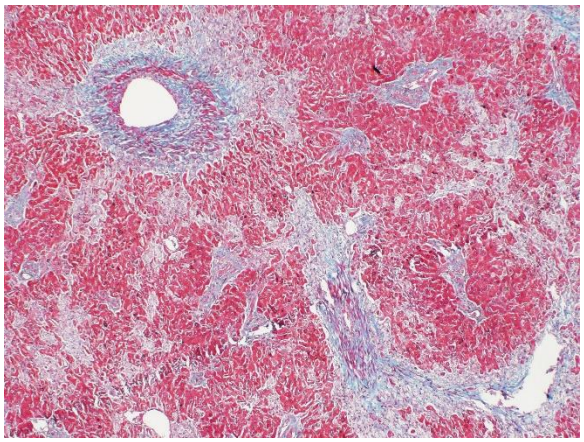

Liver, cat. A Masson's trichrome stain demonstrates the severity of the fibrosis. There is extensive fibrosis around sublobular veins, effacing the draining lymphatics, and fibrosis bridges smaller portal triads. (Masson's, 100X)

of the liver lobe, suggesting that the process is affecting ducts of a particular size, such as the lobular and interlobular ducts rather than the smallest ductules which supply the sublobular case. The lack of pigmented macrophages suggests a limited amount of continuing damage to bile ducts at this pint in the development of this lesion. The moderator interpreted the nodularity of the parenchyma as simple entrapment of hepatocytes without the formation of regenerative nodules (which are not commonly seen in cats.)

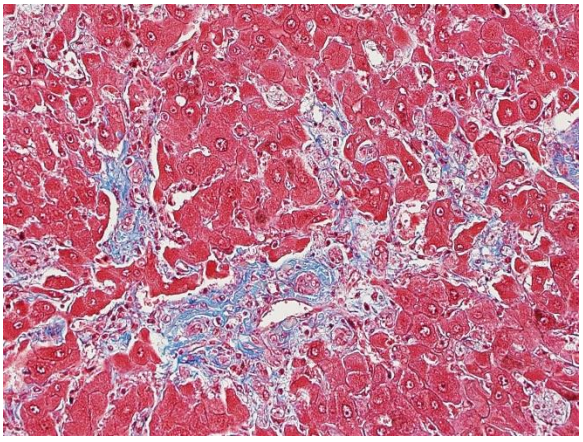

Liver, cat. Higher magnification of the portal triads show their expansion by abundant collagen. (Masson's, 200X)

The moderator commented that hepatic fibrosis is an uncommon finding in cats except for this particular condition. In dogs, the diseases generally results in death within 6-10 months, but cats may go on for years. Dogs develop considerable portal hypertension which does not appear to be of great clinical importance in affected cats (which also much less commonly result in the development of acquired portosystemic shunts than in dogs).

References:

1. Bosje JT, Van den lngh TS GAM, van der Linde-Sipman JS. Polycystic kidney and liver disease in cats. Veterinary Quarterly. 1998;20(4), 136-139.

2. Bourque AC, Fuentealba IC, Bildfell R, Daoust PY, Hanna P. Congenital hepatic fibrosis in calves. Can Vet J. 2001 ;42:145-146.

3. Brown DL, Van Winkle T, Cecere T, Rushton S, Brachelente C, & Cullen JM. Congenital hepatic fibrosis in 5 dogs. Vet Pathol. 2010;47(1):102-107.

4. Desmet VJ. What is congenital hepatic fibrosis?. Histopathology. 1992;20(6),465- 478.

5. Drogemuller M, Jagannathan V, Welle M, et al. Congenital hepatic fibrosis in the Franches-Montagnes horse is associated with the polycystic kidney and hepatic disease 1 (PKHD1) gene. PLoS One. 2014;9:e110125.

6. Fabris L, Fiorotto R, Spirli C, Cadamuro M, Mariotti V, Perugorria MJ, Bnales JM, Srazzabosco M. Pathobiology of inherited biliary diseases: a roadmap to understand acquired liver diseases. *Nat Rev Gastroenterol Hepatol* 2019; 16(8):497-511.

7. Giouleme 0, Nikolaidis N, Tziomalos K, et al. Ductal plate malformation and congenital hepatic fibrosis: clinical and histological findings in four patients. Hepatology Research. 2006;35(2):147-150.

8. Guerra JM, Daniel AGT, Cardoso NC, Grandi F, Quieroga F, Cogliati B. Congenital hepatic fibrosis and polycystic kidney disease not linked to C>A mutation in exon 29 of PKD1 in a Persian cat. *J Fel Med Surg Open Rep* 2015; doi: 10,1177, 2055116915619191

9. Guerra JA, Kampa KC, Zapparoli M, Alves VAF, Ivantes CAP. Congenital hepatic fibrosis and obliterative portal venopathy without portal hypertension – a review of literature based on an asymptomatic case. *Arch Gastroenterol* 2018; doi: 10.1590/S0004-2803.201800000-91.

10. Gunay-Aygun M, Gahl WA, Heller T. Congenital hepatic fibrosis overview. In: GeneReviews®[lnternet]. University of Washington, Seattle, 2014. Accessed 14 Apr 2019 at< https://www.ncbi.nlm.nih.gov/books/NBK2701/>.
11. Haechler S, Van den lngh TS, Rogivue C, Ehrensperger F, Welle M. Congenital hepatic fibrosis and cystic bile duct formation in Swiss Freiberger horses. Vet Pathol. 2000;37:669-671.
12. Molin J, Asfn J, Vitoria A, et al. Congenital hepatic fibrosis in a purebred Spanish horse foal: pathology and genetic studies on PKHD1 gene mutations. Vet Pathol. 2018;55:457-461.
13. Rothuizen J, Van Den lngh TS, Voorhoutm G, Van Der Luer RJT, Wouda W. Congenital porto-systemic shunts in sixteen dogs and three cats. Journal of Small Animal Practice. 1982;23(2):67-81.
14. Rutgers HC, Haywood S, Kelly DF. Idiopathic hepatic fibrosis in 15 dogs. The Veterinary record. 1993;133(5),115-118.
15. Sanzen T, Harada K, Yasoshima M, Kawamura Y, Ishibashi M, Nakanuma Y. Polycystic kidney rat is a novel animal model of Caroli's disease associated with congenital hepatic fibrosis. The American journal of pathology. 2001; 158(5): 1605-1612.
16. Van TOI, Rothuizen J. Hepatoportal fibrosis in three young dogs. The Veterinary record. 1982; 110(25),575-577.
17. Wallace S, Blanchard T, Rabin L, Dick E, Allan J, Hubbard G. Ductal plate malformation in a nonhuman primate. Vet Pathol. 2009;46:84-87.
18. Yoshikawa H, Fukuda T, Oyamada T, Yoshikawa T. Congenital hepatic fibrosis in a newborn calf. Vet Pathol. 2002;39:143-145.
17. Zandvliet MM, Szatmari V, van den lngh T, Rothuizen J. Acquired portosystemic shunting in 2 cats secondary to congenital hepatic fibrosis. Journal of veterinary internal medicine. 2005;19(5),765-767.

CASE II: N 544/17 (JPC 4120038).

Signalment: 24-month-old, male, Nelore (*Bos taurus indicus*), bovine

History: A lot containing 200 steers was allocated on a 125-hectare pasture (Property A) consisting of *Brachiaria brizantha*. The pasture was heavily invaded by *Crotalaria spectabilis*. The steers remained in this paddock for two months, when two of them died after showing weight loss, jaundice and increased abdominal volume. After the death of these two steers, another 150 steers of the same lot were shipped to a feedlot (Property B). After remaining for 50 days in property B, another eight steers became ill and died. Three of them were necropsied. Another 15 bovines died on property B in the subsequent two months.

Liver, ox. The liver was firm and with multifocal to coalescingt yellowish areas. (Photo courtesy of: Universidade Federal de Mato Grosso, Hospital Veterinário-HOVET, Laboratório de Patologia Veterinária, Av. Fernando Correa da Costa 2367, Bairro Boa Esperança, Cuiabá, MT, CEP 78060-900. http://www1.ufmt.br/ufmt/unidade/?l=ppgvet)

Gross Pathology: The cadaver was in poor body condition, there was about 20 liters of yellowish translucent fluid in the abdominal cavity. The liver was firm and with multifocal to coalescent yellowish areas.

Laboratory results: Analyses for aflatoxin done in the ration fed to the affected steers in the feedlot resulted negative for aflatoxin.

Microscopic Description: The liver architecture is disorganized by marked fibrosis, multifocal biliary duct hyperplasia and mild to moderate scattered hepatomegalocytosis.

Contributor's Morphologic Diagnosis: Liver, hepatocyte loss, fibrosis, bile duct hyperplasia and hepatomegalocytosis. Lesions compatible with pyrrolizidine alkaloid poisoning.

Contributor's Comment: *Crotalaria* spp. (Papilionaceae) are herbaceous plants and woody shrubs known colloquially as rattlepod or rattlebox because, as the seeds become loose within the pod, they rattle when the pods are shaken.[10] There are more than of 600 species in the genus *Crotalaria* distributed worldwide; most of these species are poisonous for livestock.[4] Forty of them were identified in Brazil and *C. mucronata*, *C. juncea*, *C. spectabilis*, and *C. retusa* were proven toxic for livestock under natural conditions. *C. mucronata* and *C. juncea* are associated with interstitial pneumonia[3], while *C. retusa* and *C. specatabilis* are associated with chronic hepatotoxicosis.[2,10] The toxic principle in *Crotalaria* spp. are dehydropyrrolizzidine alkaloids (DHPAs). DHPAs and their N-oxides are present in plant families such as Boraginaceae, Asteraceae, Orchidaceae, and Fabaceae.[8]

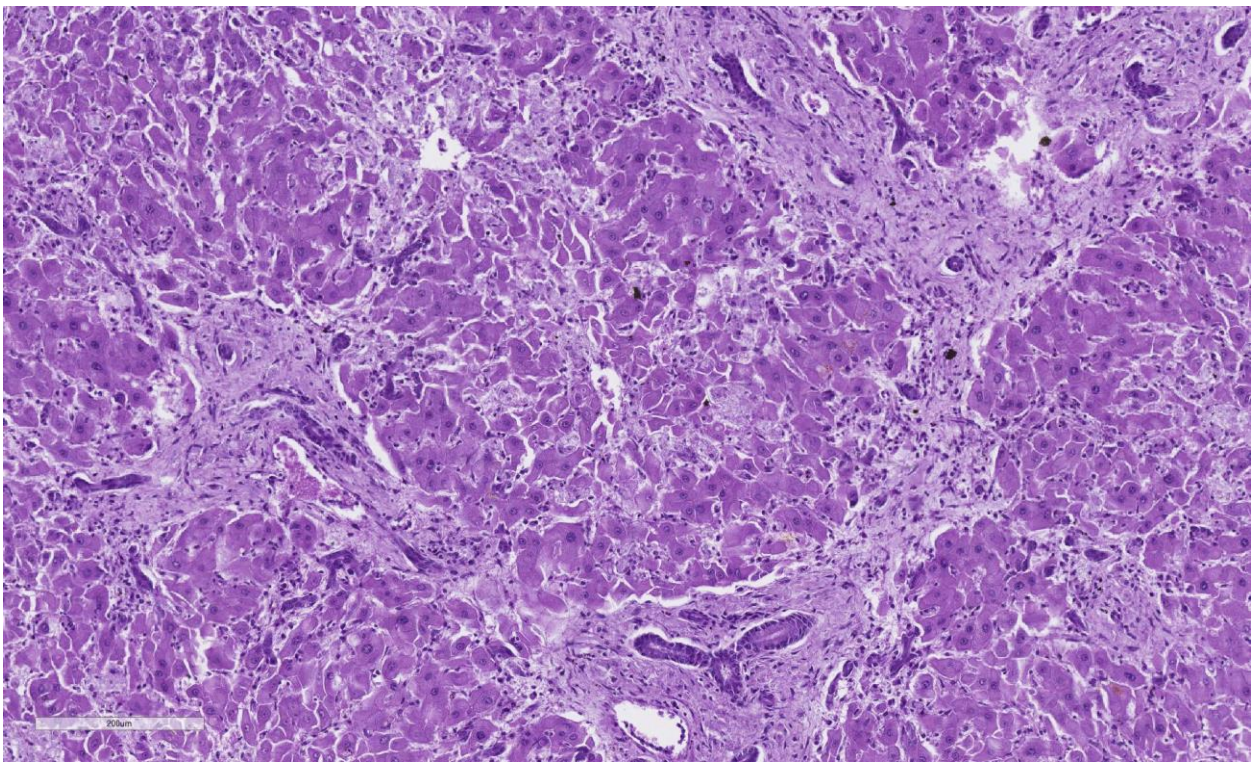

Liver ox. The submitted section of liver demonstrates a complex pattern of bridging fibrosis and hepatocellular loss. (HE, 130X)

DHPAs are stable chemical compounds which are biotransformed in the liver by cytochrome P-450 enzymes into toxic metabolites and pyrrole alcohols. These metabolites are alkylating agents that inhibit mitosis, resulting, in the case of the liver, in very large hepatocytes (megalocytes) – a condition referred to as hepatomegalocytosis. As the hepatocytes are lost and dropped out due to necrosis, bile duct proliferation and fibrosis occur.[6] At pasture, the Crotalaria poisoning is usually a chronic condition characterized by hepatomegalocytosis, fibrosis and bile duct proliferation.[6] However the ingestion of high doses of the plant can cause acute centrilobular necrosis.[1]

The diagnosis of intoxication by *C. spectabilis* in the steers of this report was based on clinical signs, an abundance of the plant in Property 1, and pathological changes which are similar to the ones describe in livestock poisoned by species of *Crotalaria.*[6,7] Poor body condition and ascites found in the necropsied steers ruselted from chronic hepatic disease and hepatic failure. Differential diagnosis should include other DHPAs-containing plants such as species of *Senecio*, *Cynoglossum*, *Amsinckia*, *Heliothropium*, and *Echium*. Table 1 includes some *Crotalaria* species and respective DHPAs.[4,5]

Table 1- Some *Crotalaria* species and their isolated pyrrolizidine alkaloids[4,5]

Species	Alkaloids
C. spectabilis	Monocrotaline, spectabiline, retusine
C. retusa	Monocrotaline, retusamine
C. pallida	Integerrimine, nilgirine, acetyl nilgirine, usaramine
C. incana	Anacrotine, integerrimine, usaramine
C. sagittalis	Monocrotaline

Contributing Institution:
Universidade Federal de Mato Grosso, Hospital Veterinário-HOVET, Laboratório de Patologia Veterinária, Av. Fernando Correa da Costa 2367, Bairro Boa Esperança, Cuiabá, MT, CEP 78060-900. http://www1.ufmt.br/ufmt/unidade/?l=ppgvet

JPC Diagnosis: Liver: Fibrosis**,** portal and centrilobular, bridging, diffuse, severe, with marked hepatocellular degeneration, necrosis, and loss, lipogranuloma formation, and megalocytosis.

JPC Comment: Dehydropyrrolizine alkaloid (DHPA) toxicosis is a common toxicosis of ruminants and herbivores, with up to 350 DHPA containing plant species in the southern US alone (Paul Stromberg, personal communication).

DHPAs can produce disease in animals by a variety of acute and chronic toxicity and are documented carcinogens. The base chemical is composed of fused five-members carbons rings; toxic DHPAs have a 1.2 unsaturation. Progressive esterification of the based chemical, such as diesters and macrocyclic diesters appears to increase toxicity.[9]

DHPAs required oxidation by cytochrome P450s within the liver to develop their toxic pyrroles, which react with many essential cellular proteins (including glutathione) as well as nucleic acids. Hepatocytes, the site of activation, and endothelial cells are most often affected, resulting in hepatocellular degeneration and necrosis, with sequelae of fibrosis, biliary proliferation, and ultimately cirrhosis.[9]

Most livestock toxicity results when animals

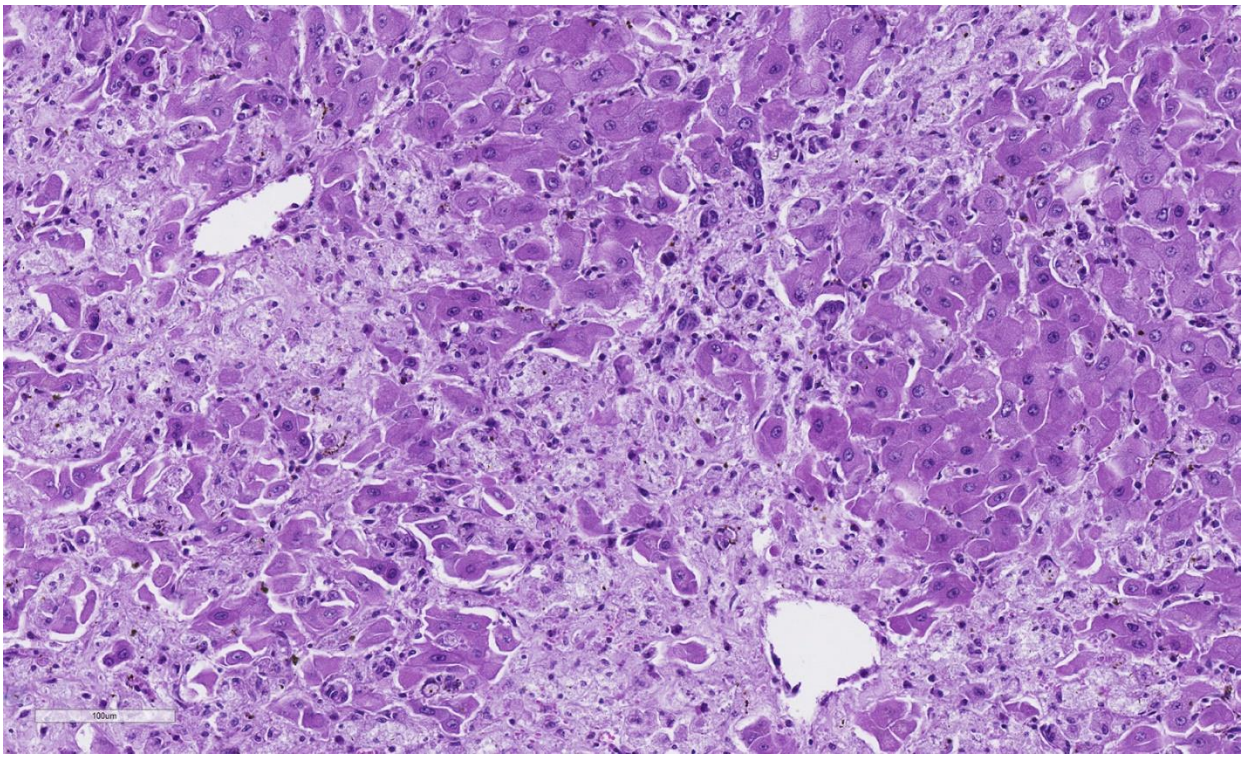

Liver, ox: Fibrous bands extend to central veins and there is significant loss of centrilobular and midzonal necrosis. (HE, 200X)

consume toxic plants in the absence of alternative forage, but poisoning also occurs when DHPA-containing plants are harvested and fed in hay. (This type of toxicity also occurs in humans; thousands of people in Afghanistan and Tajikistan were poisoned when DHPA containing plants were harvested and processed into flour.) There is significant species variation with regard to susceptibility of DHPA toxicity, with pigs and chickens being considered highly susceptible, cattle horses, and rats moderately susceptible, and mice, sheep and goats being relatively resistant, leading to the somewhat risky "practice" of using small ruminants to clear forage areas containing plants high in PAs.

The disease in poisoned humans is somewhat different than in livestock, with endothelial damage in the liver predominating. Endothelial damage in humans leads to fibrosis of hepatic sinusoid and central veins, resulting in portal hypertension and veno-occlusive disease. Tragically, due to the susceptibility of human fetuses and neonates, they may develop fatal hepatic disease by transplacental or transmammary passage of toxic metabolites, while their pregnant or nursing mothers are unharmed.

A number of tests have been developed in recent years that help to quantitate the toxic and carcinogenic properties of various pyrollizzidine alkaloids, including an *in vitro* chicken, mouse and rat hepatocyte protocol, an *in vivo* chick system in which orally dosed chicks are given measured disease of various DHPAs and the damage to their livers measured at 7 days post inoculation, and a carcinogenic model using heterozygous p53 knockout mice which are fed DHPAs in pelleted feed for 12 months, after which they are autopsied and carcinogenic effects in various organs are compared.

The moderator marveled at the amount of macrophages present in this section, which is not especially characteristic of most cases of DHPA toxicity, but surmised that it may be another toxic principle in the pastures grazed by the affected beeves. He suggested the possibility of concurrent toxicity with a sapinogen intoxicant.

References:

1. Anjos BL, Nobre VMT, Dantas AFM et al. Poisoning of sheep by seeds of *Crotalaria retusa*: Acquired resistance by continuous administration of low doses. *Toxicon*. 2010;**55**:28-32.
2. Boabaid FM, Alberton RL, Ubiali DG et al. Acute poisoning by *Crotalaria spectabilis* seeds in pigs of Mato Grosso State, Brazil. In: Riet-Correa F, Pfister J, Scild AL, et al. ed. *Poisoning by Plants, Mycotoxins, and Related Toxins*. Cambridge:CAB International; 2011:148-153.
3. Boghossian, M.R., Peixoto, P.V., Brito, M.F., Tokarnia, C.H., Aspectos clínico-patológicos da intoxicação experimental pelas sementes de *Crotalaria mucronata* (Fabaceae) em bovinos. *Pesq. Vet. Bras.* 2007;**27**(4):149-156.
4. Burrow GE, Tyrl RJ. *Toxic Plants of North America*. 2th ed. Ames: Wiley-Backwell; 2013:535-541.
5. Fletcher MT, McKenzie MA, Blaney BJ. Pyrrolizidine Alkaloids in *Crotalaria* Taxa from Northern Australia: Risk to Grazing Livestock. *J. Agric. Food Chem*. 2009;**57**:311-319.
6. Lucena RB, Rissi DR, Maia LA et al. Intoxicação por alcaloides pirrazolidinicos em ruminantes e equinos no Brasil. *Pesq. Vet. Bras.* **30**(5):447-452.
7. Nobre VMT, Riet-Correa F, Dantas AFM et al. Intoxication by *Crotalaria retusa* in ruminants and equidaein the State of Paraíba, Northeastern, Brazil. In: Acamovic T, Stewart CS, Pennycott TW. ed. *Poisoning by Plants, Mycotoxins, and Related Toxins*. Cambridge:CAB International; 2004:275-279.
8. Stegelmeier, B.L. Pyrrolizidine alkaloid-containing toxic plants (*Senecio*, *Crotalaria*, *Cynoglossum*, Amsinckia, *Heliotropium*, and *Echium* spp.). *Vet. Clin. North. Am. Food Anim Pract.* 2011;**27**,419-428.
9. Stegelmeir BL, Colegate SM, Brown AW. Dehydropyrrolizidine Alkaloid Toxicity, Cytotoxicity, and Carcinogencity. *Toxins* 2016; 8(12). pii: E356.
10. Tokarnia, C.H., Döbereiner, J., Peixoto, P.V., Poisonous plants affecting livestock in Brazil. *Toxicon*. 2002;**40**:1635-1660.

CASE III: 15-0318 (JPC 4101080).

Signalment: 6-month-old intact male Mi-Ki dog (*Canis familiars*).

History: The puppy presented with a history of lethargy, hyporexia, occasional vomiting, and abnormal behavior including opisthotonus and head pressing. A single seizure was observed, which resolved with diazepam. Following diazepam administration, the puppy became stuporous with a lack of menace response and bilaterally decreased pupillary light reflexes. The puppy's mentation gradually improved with treatment (lactulose, metronidazole, omeprazole, ondansetron and intravenous fluids with dextrose). The patient was sedated with butorphanol and alfaxalone for an abdominal ultrasound, and became obtunded

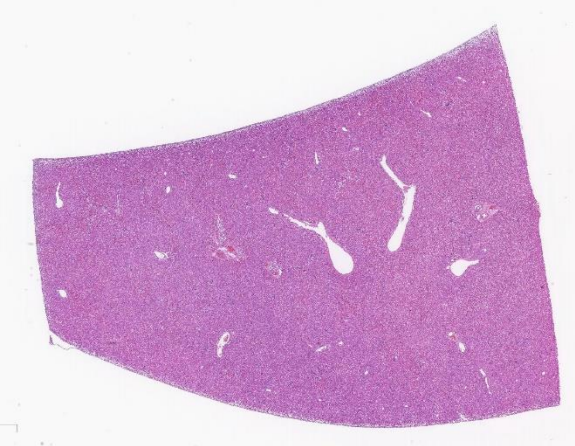

Liver, dog. One section of liver is submitted for examination. There are no apparent lesions at subgross examination. (HE, 5X)

with abnormal vocalization that persisted despite supportive care. Due to a poor prognosis, the puppy was euthanized.

Gross Pathology: The puppy weighed 1.9 kg with adequate visceral adipose. The liver was diffusely small with normal lobation, color, and consistency. A single dilated and tortuous anomalous vessel, approximately 3 mm wide, connected the gastroduodenal vein with the caudal vena cava. There was mild, bilaterally symmetric dilation of the lateral ventricles. The brain was otherwise grossly unremarkable. The lungs were mildly, diffusely wet and oozed a small amount of serosanguineous fluid and foam on cut section. Sections of lung from all lobes floated in formalin. No other gross lesions were observed.

Laboratory results: Chemistry abnormalities: Albumin 2.8 g/dL, Globulins 2.2 g/dL, Creatinine 0.3 mg/dL, ALP 177 U/L, Phosphorous 6.6 mg/dL, Glucose 66 mg/dL, Cholesterol 67 mg/dL
Ammonia: 213 µmol/L (reference range: 11-35 µmol/L)
Bile acids: 112 µmol/L (pre-prandial) and 104 µmol/L (post-prandial)
Urine specific gravity: 1.026
Urine sediment: 11-20 ammonium biurate crystals /hpf

Imaging: Abdominal ultrasonography identified a small liver with a suspected single extrahepatic portosystemic shunt from the right gastric or gastroduodenal vein to the caudal vena cava.

Microscopic Description: The liver is composed of small hepatic lobules with irregularly and closely spaced portal triads. Portal triads contain increased numbers of arteriolar profiles and portal venules are often small or absent. Larger portal tracts contain dilated lymphatic vessels. Cords of hepatocytes surrounding portal tracts are thin, and individual hepatocytes are small, with a small amount of eosinophilic, occasionally finely vacuolated cytoplasm. The periportal sinusoids are infrequently dilated. Some sections contain randomly distributed small foci of inflammation composed of low numbers of lymphocytes, macrophages, and neutrophils, with individually necrotic hepatocytes. Scattered rarely throughout the parenchyma of some sections are small clusters of lipid and golden-brown pigment laden macrophages with fewer lymphocytes (pigment lipogranulomas).

In sections of brain (not submitted), the white matter, and to a lesser extent, the grey matter throughout the cerebrum and midbrain contain numerous variably sized, discrete to coalescing clear vacuoles. The lateral ventricles are mildly bilaterally and symmetrically enlarged.

Contributor's Morphologic Diagnosis: Dog, liver: hepatopathy characterized by lobular hypoplasia with hepatocellular atrophy, increased arteriolar profiles, and portal vein hypoplasia

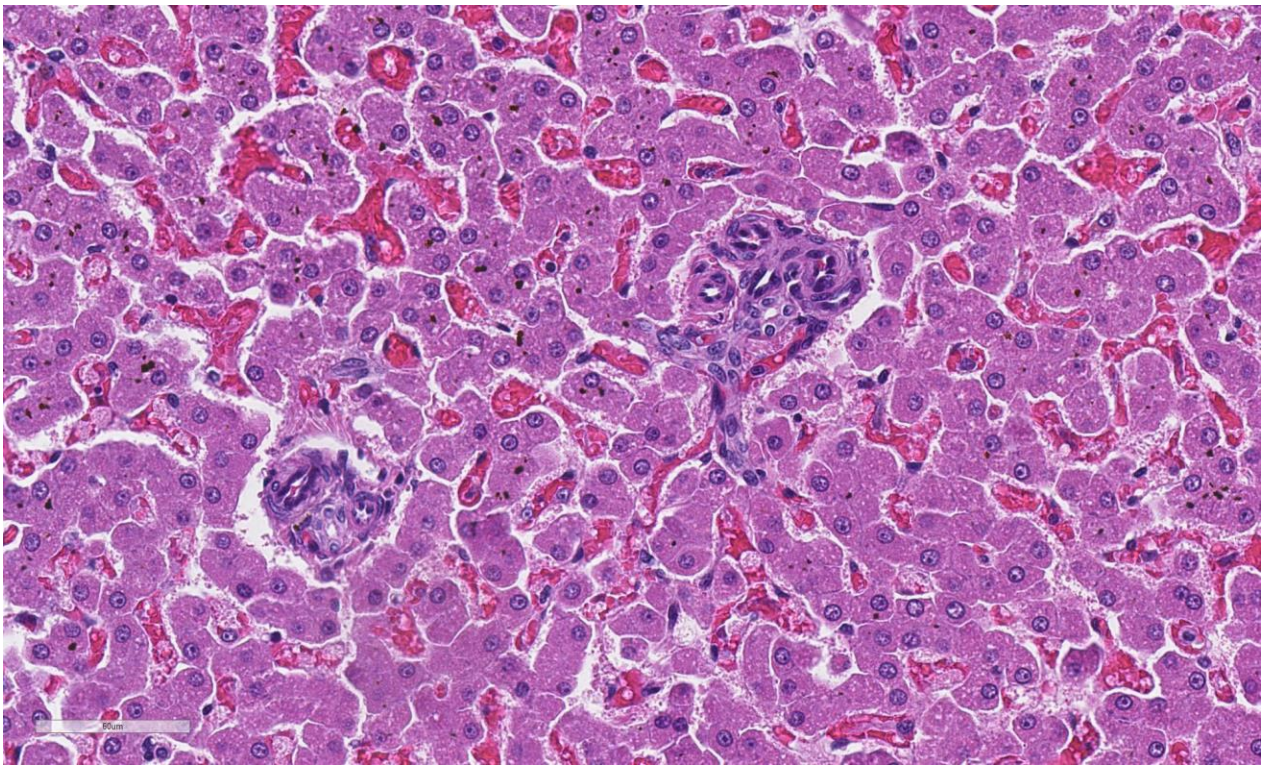

Liver, dog. Portal areas contain numerous profiles of arterioles, bile ductules, but lack profiles of portal veins. Due to hepatocellular atrophy (best adjudged by comparing the size or Kupffer cell nuclei to hepatocyte size), portal triads are often closely apposed. (HE, 400X)

Dog, liver: mild multifocal random lymphohistiocytic and neutrophilic hepatitis with single cell necrosis

Contributor's Comment: Portosystemic shunts are any anomalous connections of the portal circulation to the systemic circulation that bypass the liver. Acquired hepatic shunts are distinguished from congenital shunts on ultrasonography, exploratory laparotomy, or gross examination, as acquired shunts are typically composed of multiple anastomosing vessels rather than a single large vessel. Acquired shunts most often arise secondary to portal hypertension, such as in cirrhosis or portal vein obstruction, but can also develop in the presence of microvascular malformations[1,2].

Congenital hepatic shunts are categorized into intra- and extrahepatic shunts, and are thought to be an inherited condition in some breeds (Cairn terriers, Yorkshire terriers, Irish wolfhounds, Maltese, Australian cattle dogs)[3,4,5,6]. Large breed dogs tend to develop intrahepatic shunts, most commonly due to a patent ductus venosus[6]. Extrahepatic shunts are more common in small breed dogs and cats, most frequently connecting the portal vein, gastric vein, or splenic vein with the caudal vena cava or azygous vein[1]. Patients often present at less than 1 year of age, but can progress into adulthood before clinical signs become apparent. Clinical signs may include an overall small size compared to littermates, depressed mentation, circling, seizures, and other manifestations of hepatic encephalopathy. Clinical pathology findings can include microcytosis, hypoalbuminemia, hypocholesterolemia, hypoglycemia, low BUN, increased bile acid concentration, hyperammonemia, and ammonium biurate crystalluria[1,7].

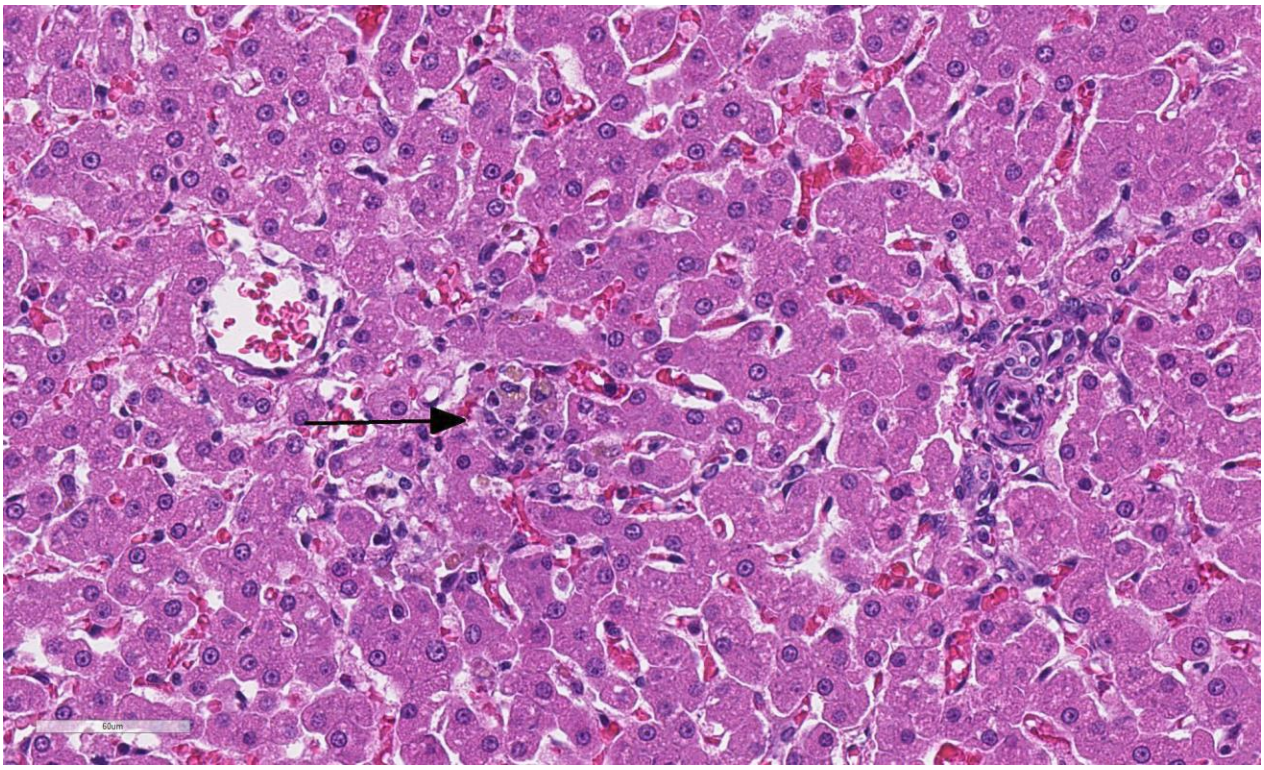

Liver, dog. Scattered throughout the section are small aggregates of hemosiderin and lipid-laden macrophages (microgranulomas) (arrows). (HE, 400X)

Blood in the portal circulation contains hepatotrophic growth factors such as insulin, glucagon, and hepatocyte growth factor, which are essential for normal hepatocellular development[8]. Lack of blood flow and delivery of growth factors to the developing liver results in small hepatic lobules and hepatocytes, increased arteriolar profiles, small to absent portal veins, and pigment lipogranulomas[2,9]. These histologic features are characteristic of portal vein hypoperfusion; however, are not specific for a portosystemic shunt. Similar histologic lesions are also seen in cases of primary portal vein hypoplasia[1,2].

Primary portal vein hypoplasia is the current preferred term for conditions previously described as microvascular dysplasia, hepatoportal fibrosis, and idiopathic noncirrhotic portal hypertension[2]. In contrast to a portosystemic shunt, portal vein hypoplasia can result in portal hypertension, ascites, and acquired shunts[1,2]. Microscopically, portal fibrosis and bile duct hyperplasia are sometimes noted in addition to the characteristic histologic features of portal vein hypoperfusion[2,7]. Without an adequate history, clinical findings or imaging results, it is often impossible to differentiate between primary portal vein hypoplasia and congenital portosystemic shunts with histology alone. Concurrent primary portal vein hypoplasia and congenital portosystemic shunts have been reported in dogs[7].

In this case, the microscopic hepatic and brain lesions correlated well with the gross identification of a distinct anomalous vessel, clinical signs, and clinical pathologic abnormalities. This constellation of findings is consistent with an extrahepatic congenital portosystemic shunt and hepatic

encephalopathy. The cause of the mild, multifocal random hepatitis is unclear, though the distribution suggests possible early sepsis rather than an ischemic or toxic etiology.

Contributing Institution: University of Pennsylvania, School of Veterinary Medicine, Department of Pathobiology
http://www.vet.upenn.edu/research/academic-departments/

JPC Diagnosis: Liver, portal veins: Hypoplasia, diffuse, severe, with lobular and hepatocellular atrophy

JPC Comment: The contributor has provided a concise but illustrating explanation of congenital hepatic shunts and portal vein hypoplasia in the dog.

In a recent study of 125 dogs with developmental hepatic vascular disease[8], the initial diagnosis was confirmed in 89.3% of cases in which suspicion of portosystemic shunt was raised following liver biopsy, demonstrating the sensitivity of liver biopsy in such cases. In this study, animals were divided into those with intrahepatic shunts, those with extrahepatic shunts, and those with hepatic microvascular dysplasia – portal vein hypoplasia. Cases of microvascular dysplasia without apparent shunting were most commonly seen in Yorkshire terriers. In addition to more classic histologic findings of compressed lobules, multiple sections of tortuous arterioles in portal triads, and absence of portal veins within triads, this study also noted consistent but less common histologic lesions. Approximately 20% of cases of either intra- or extrahepatic shunting had hypertrophy of smooth muscle around sublobular veins, which increased to 80% in cases of microvascular dysplasia. Fibrosis of the central veins was noted in 22% of extrahepatic shunts and microvascular dysplasia but 60% of intrahepatic shunts. Calcification was visible in approximately 2% of animals with developmental hepatic vascular disease, but did not appear to be the result of dystrophic calcification of the vessel wall itself. Finally, lipogranuloma formation appeared to be most common in extrahepatic shunts (50%) but twenty percent or less in the other two categories, and tended to be more prominent in older dogs in the study.[8]

Regarding evalution of this particular specimen, the moderator made several observations. The moderator mentioned that in liver biopsies (not autopsies) you should not see sinusoids, else you are likely viewing hepatocellular atrophy. You may see it in autopsy specimens following postmortem consumption of glycogen, resulting shrinkage up to 33% of overall size. Addtionally, in humans, 20% of subcapsular portal triads lack portal veins, which could be problematic in small biopsies with few portal triads to evaluate. The moderator reiterated a generalization from his previous visits that the visualization of any lymphatics in the liver is evidence of disease but not specific to any particular one – evaluation of serum proteins, vascular or biliary disease, inflammation, etc. should all be considered, but it should never be considered a normal finding. In cases of microvascular dysplasia, dilated lymphatics is likely the result of decreased venous but normal arterial perfusion, as well as concomitant hypoproteinemia.

References:

1. Cullen JM, Stalker MJ. Liver and biliary system. In: Maxie MG, ed. *Jubb, Kennedy, and Palmer's Pathology of Domestic Animals*. Vol 2. 6th ed. St. Louis, MO: Elsevier; 2016:266-268.
2. Cullen JM, van den Ingh TSGAM, Bunch SE, Rothuizen J, Washabau RJ, Desmet VJ.

Morphological classification of the circulatory disorders of the canine and feline liver. In: WSAVA Standards for Clinical and Histological Diagnosis of Canine and Feline Liver Diseases. St. Louis, MO: Elsevier Limited;2006:51-52; 47-52.
3. van Straten G, Leegwater PAJ, de Vries M, van den Brom WE, Rothuizen J. Inherited congenital extrahepatic portosystemic shunts in Cairn terriers. J Vet Intern Med. 2005;19:321-324.
4. Tobias KM. Determination of inheritance of single congenital portosystemic shunts in Yorkshire terriers. J Am Anim Hosp Assoc. 2003;39:385-389.
5. van Steenbeek FG, Leegwater PAJ, van Sluijis FJ, Heuven HCM, Rothuizen J. Evidence of inheritance of intrahepatic portosystemic shunts in Irish wolfhounds. J Vet Intern Med. 2009;23:950-952.
6. Tisdall PLC, Hunt GB, Bellenger CR, Malik R. Congenital portosystemic shunts in Maltese and Australian cattle dogs. 1994;71(6):174-178.
7. Schermerhorn T, Center SA, Dykes NL, Rowland PH, Yeager AE, Erb HN, Oberhansley K, Bonda M. Characterizaton of hepatoportal microvascular dysplasia in a kindred of Cairn terriers. J Vet Intern Med. 1996;10(4):219-230.
8. Sobczak-Filipiak M, Szarek J, Badurek I, Pdmanabhan J. Trebacz P, Januchta-Kurmin M, Galanty M. Retrostpective liver histomorphological analysis in dogs in instances of clinical suspicion of congenital portosystemic shunt. *J Vet Res* 2019; 63:243-249.
9. van Steenbeek FG, van den Bossche, Leegwater PAJ, Rothuizen J. Inherited liver shunts in dogs elucidate pathways regulating embryonic development and clinical disorders of the portal vein. Mamm Genome. 2012;23:76-84.

CASE IV: 19-117 (JPC 4134512).

Signalment: 15-year-old, castrated male, Quarter Horse (*Equus caballus*)

History: This horse presented to ambulatory service with an acute onset of illness. Clinical examination revealed a normal respiratory rate, normal heart rate and a temperature of 100.7 ^{o}F. There was severe icterus and dark brown urine dripped from the penis. Gut sounds were decreased in all 4 quadrants. When moved, the horse collapsed and euthanasia was elected. The horse was not vaccinated. There was no history of feed change, medications, travel or exposure to toxins.

Gross Pathology: Gross examination revealed a carcass in good nutritional condition with no evidence of dehydration and moderate autolysis. Dark red urine dripped from the prepuce. There was diffuse and severe icterus. A scant amount of serosanguinous fluid was noted in the peritoneum. The liver was small and flaccid weighing 3.8 kg or 0.7% body weight (normal range 1.2-1.5%). On section, an enhanced reticular pattern was noted. The

Liver, horse. The liver was small, flaccid, and weighed 3.8 kg or 0.7% body weight (normal range 1.2-1.5%). (Photo courtesy of: Diagnostic Services Unit, University of Calgary, Faculty of Veterinary Medicine, https://vet.ucalgary.ca/dsu).

small intestinal content was hemorrhagic. The urinary bladder was filled with dark red urine and the discoloration did not clear following centrifugation (pigmenturia). There was diffuse splenic congestion consistent with barbiturate euthanasia.

Laboratory results: PCR was positive for equine parvovirus (EqPV-H). PCR was negative for equine pegivirus (EPgV), non-primate hepacivirus (NPHV) or equine hepacivirus and Theiler's disease-associated virus (TDAV). PCR was negative for *Leptospira* species.
Urine sediment: 11-20 ammonium biurate crystals /hpf

Microscopic Description: Liver: Four sections are available for examination with varying degrees of autolysis and postmortem bacterial overgrowth. Diffusely, the hepatic lobules are distorted and reduced in size owing to marked loss of centrilobular and midzonal hepatocytes. This is accompanied by stromal collapse and sinusoidal congestion. Individualized periportal hepatocytes remain along the periphery of the lobules. Periportal hepatocytes have abundant cytoplasm containing multiple, large, well-defined vacuoles consistent with macrovesicular fatty change. Large, multinucleated hepatocytes are frequently observed (hepatocellular giant cell or syncytial cell formation). Kupffer cells contain a moderate amount of light brown, granular pigment. The portal units are expanded by minimal fibrosis, infrequent duplication of the bile ducts and a scant infiltrate of mononuclear inflammatory cells including lymphocytes, histiocytes and plasma cells. Copper was not observed on rhodanine stain and a scant amount of iron restricted to the Kupffer cells was noted on Perls' Prussian blue stain.

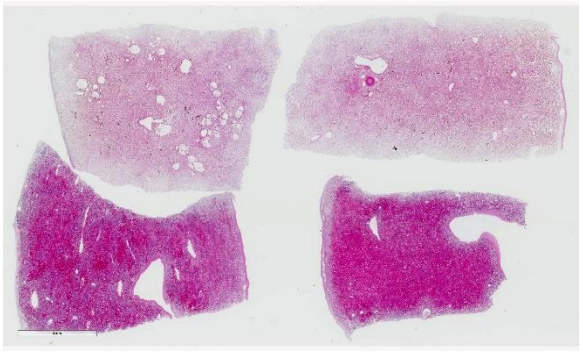

Liver, horse. Four sections of liver are submitted for evaluation; the two sections at top are poorly preserved. (HE, 5X)

Kidney (not shown on slide): Multifocally renal tubules are ectatic, are lined by attenuated epithelium and contain granular to hyaline, bright orange to red material interpreted to be heme pigment.

Contributor Morphologic Diagnosis: Liver: Hepatocellular loss and degeneration, submassive, severe, subacute with stromal collapse, mild portal hepatitis and syncytial cell (giant cell) formation

Contributor Comment: Based on the clinical course of disease, gross pathology, histopathology, PCR results and lack of exposure to known hepatotoxins, this is interpreted to be a case of equine serum hepatitis or Theiler's disease. Serum hepatitis is a long recognized cause of acute liver failure in horses. Theiler's disease was first described in 1919 in horses following vaccination using equine antiserum against African horse sickness.[4,13] The disease is reported globally and is typically observed following administration of equine biological products including tetanus antitoxin, botulinum antitoxin, antiserum against *Streptococcus equi*, pregnant mare's serum and equine plasma.[5,14] Of these products, serum hepatitis is most commonly associated with tetanus antitoxin possibly because it is the most frequently used.[14] Similar to the current case, a number of cases of equine

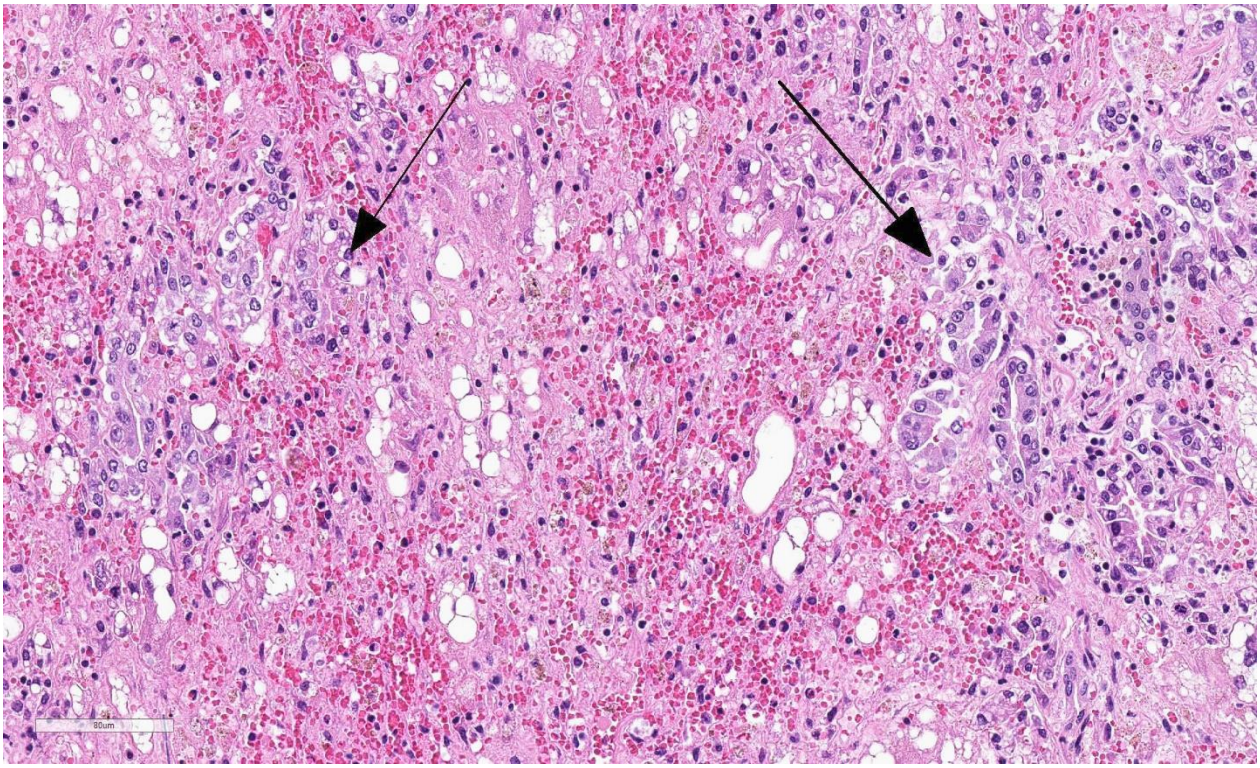

Liver, horse. There is almost total loss of hepatocytes between portal triads (arrows). The intervening space contains abundant hemorrhage, numerous siderophages, and few degenerating remnant hepatocytes with contain one or more large clear vacuoles within their cytoplasm. (HE, 267X)

serum hepatitis are not associated with administration of equine biologicals raising the specter of horizontal transmission from contaminated medical equipment and insect vectors such as tabanid flies. [2,3,15]

The typical incubation period is 4-10 weeks, but can be as long as 14 weeks.[4,5,14] The onset of clinical disease is sudden with rapid progression to death. Lethargy, icterus, photosensitivity, fever and neurological signs including hyperexcitability, blindness and ataxia are reported.[4,13] Morbidity rates vary from 1-18% in outbreaks and mortality rates are between 50-90%.[14]

Typical biochemical findings include marked elevation in liver enzyme values (primarily SHD and AST and to a lesser degree GGT), direct and indirect bilirubin and bile acids.[5,14] Reported gross lesions include icterus, ascites, serosal and renal petechiae, and intestinal hemorrhage. The liver is small and limp due to the hepatocellular loss and is often described as having a "dishrag" appearance. Cut surface reveals a highlighted zonal pattern.[2, 4] Acute hepatic necrosis and hemorrhage are not features of serum hepatitis. Microscopic features are instead more chronic than the clinical course suggests and are dominated by hepatocellular loss with collapse and distortion of the reticulin framework as seen in the current case. There may be few surviving periportal hepatocytes which demonstrate hepatocellular vacuolation consistent with macrovesicular lipidosis. Additional microscopic features include variable numbers of apoptotic hepatocytes, deposition of bile pigments in Kupffer cells and hepatocytes, mild fibroplasia in the portal units and variable ductular proliferation. Inflammation is not robust, but a diffuse infiltrate of lymphocytes, plasma cells,

histiocytes and neutrophils may be present.[2, 4]

While the association between serum hepatitis and administration of equine biologics has been known for 100 years and a blood-borne virus has long been suspected, the etiologic agent of Theiler's disease has eluded the veterinary profession. Since 2012, four emerging viruses have been identified and studied for their possible association with equine hepatitis. Three are in the family *Flaviviridae* including equine pegivirus (EPgV), non-primate hepacivirus (NPHV) or equine hepacivirus, and Theiler's disease-associated virus (TDAV). The fourth is equine parvovirus-hepatitis (EqPV-H). NPHV, closely related to hepatitis C virus, is hepatotropic and hepatic disease following experimental transmission is documented.[9] TDAV was first identified in an outbreak of acute clinical hepatitis in horses following administration of botulinum antitoxin of equine origin.[3] However, retrospective analysis of samples indicated the presence of EqPV-H in all TDAV positive samples indicating coinfection initially missed do to methodology.[5] EPgV is a common infection of horses in the United States and Western Europe, but the virus is not hepatotropic and has not been associated with hepatic disease.[6] Recently, EPgV infection was associated with a reduced risk of having increased liver enzyme activity indicating that EPgV is an unlikely cause of equine hepatitis.[10] In 2018, a novel equine parvovirus (equine parvovirus-hepatitis, EqPV-H) was discovered in the liver and serum of a horse succumbing to Theiler's disease and experimental administration of EqPV-H positive tetanus antitoxin samples resulted in viremia and subclinical or clinical hepatic disease in 2 horses. This study also revealed EqPV-H viremia in 13% of normal horses tested suggesting that many infected horses don't develop clinical disease.[5] More recently, 2 companion studies demonstrated EqPV-H infection in 18 consecutive cases of serum hepatitis and EqPV-H infection in 9/10 horses with Theiler's disease in the absence of equine biologic product administration. In both studies, the 3 additional flaviviruses implicated in equine hepatitis were absent or rarely present.[14,15] These recent studies support the role of EqPV-H in Theiler's disease, but further studies are required to unequivocally demonstrate that EqPV-H is the cause of serum hepatitis.

In the standard veterinary pathology textbooks, giant cell formation is not described as a feature in equine serum hepatitis and was an unexpected feature in this case. There is a single report of Theiler's disease in a Canadian horse in which multinucleated hepatocytes are described.[13] Giant-cell hepatitis (GCH) is well-described in humans and is characterized by parenchymal inflammation with formation of large multinucleated hepatocytes.[11] It is most commonly seen in neonates, and occurs rarely in adults where it is known as post-infantile GCH.[11,16] It is considered to be a nonspecific tissue reaction to various stimuli and therefore is not specific to an etiology. The pathogenesis is unknown and may be due to hepatocyte nuclear proliferation without subsequent cell division or membrane fusion of neighboring hepatocytes.[11] In infants, a recent study indicated that most cases of GCH were idiopathic. In this case series, panhypopituitarism was the most common recognizable clinical association with fewer cases attributed to biliary atresia, Alagille syndrome, bile salt defects, neonatal hemochromatosis, SCID, and viral infections.[16] In adults, giant cell transformation occurs with a variety of insults including viral hepatitis (hepatitis A, hepatitis B, non A, non B hepatitis, hepatitis C, and Epstein-Barr virus), autoimmune hepatitis, and with a variety of drugs and herbal remedies.[11] Giant cell hepatitis is an

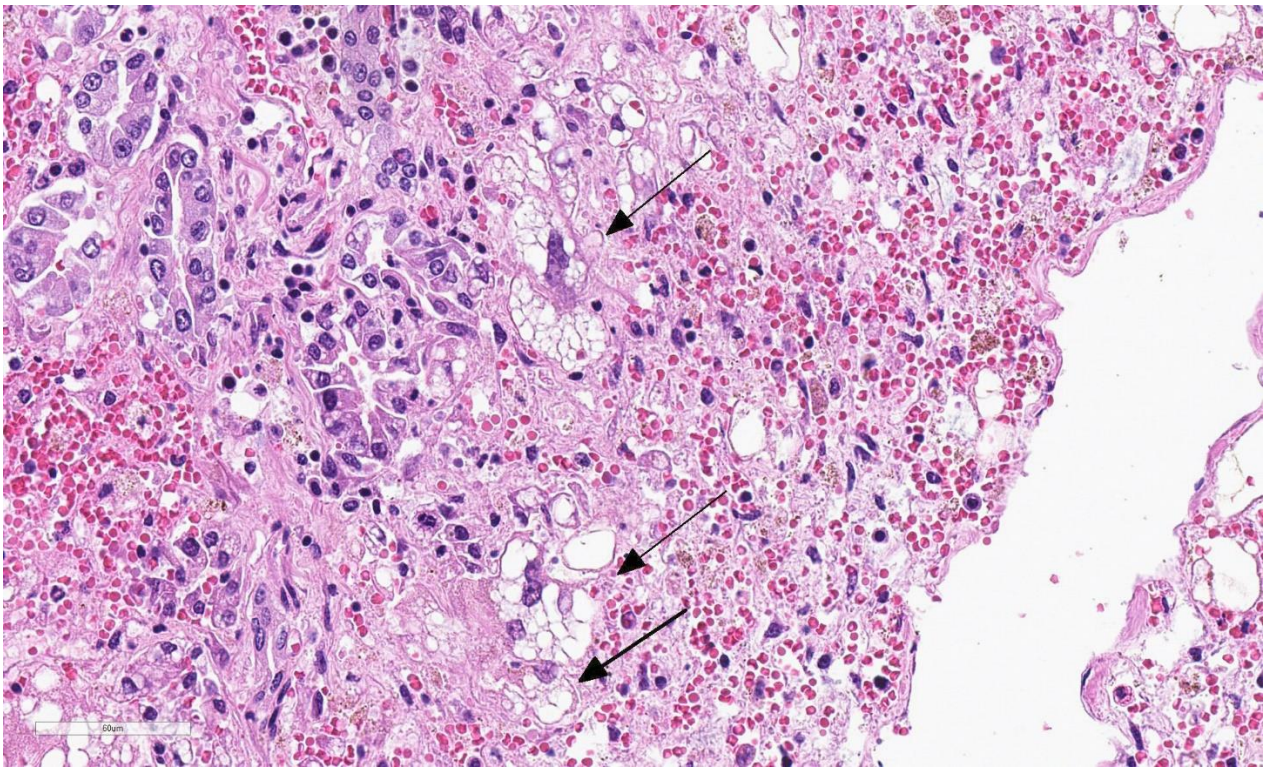

Liver, horse. Remaining periportal hepatocytes (located adjacent to portal triads) (arrows)are expanded by numerous clear lipid vacuoles. (HE, 400X)

uncommon lesion in animals but has been recorded in cats, calves and foals.[4] In foals, giant cell transformation has been reported in cases of neonatal isoerythrolysis[1] and in aborted foals with suspected leptospirosis.[17]

In the absence of muscle injury in this horse, the dark red appearance to the urine and pigmentary nephrosis were interpreted as hemoglobinuria and hemoglobinuric nephrosis indicative of intravascular hemolysis. Common causes of intravascular hemolysis and hemoglobinuria in horses include immune-mediated hemolytic anemia; a number of infections including piroplasmosis, equine infectious anemia, leptospirosis, and clostridial hepatitis; drug toxicity; toxic plants including red maple, *Brassica* species and membranes of the onion family; and hepatic failure. Hemolysis secondary to hepatic failure is presumed in this case and intravascular hemolysis is described in the terminal stages of Theiler's disease.[2] The mechanism for intravascular hemolysis in cases of liver failure in horses is unknown; however, bile acids or their salts are considered possible hemolytic factors.[8]

Contributing Institution:
Diagnostic Services Unit
University of Calgary, Faculty of Veterinary Medicine
https://vet.ucalgary.ca/dsu

JPC Diagnosis: Liver: Degeneration, necrosis and loss, massive, diffuse, severe, with stromal collapse and hepatocellular lipidosis**.**

JPC Comment: The contributor has done an outstanding job summarizing the history, pathogenesis, and current thought regarding this very dramatic and well-known disease of the horse.

Sir Arnold Theiler 1867-1936), for which this disease still bears his name, was a Swiss veterinarian and researcher of great importance in the area of veterinary research and education in South Africa. As the state veterinarian for the South African Republic, he developed he first vaccine against rinderpest. In 1919, he was the first to describe acute serum hepatitis in animals vaccinated against African horse sickness. As the first director of the Onderstepoort veterinary Research Institute, he was instrumental in leading the research team in their investigations of many diseases of the region including East Coast fever (caused by *Theileria parva),* sleeping sickness, heartwater, malaria, and African Horse sickness. He shortly became the dean of the newly built University of Pretoria Faculty of Veterinary Science, and worked there until his passing.

Since the identification of an equine parvovirus as the putative agent of equine serum hepatitis, a number of groups have begun the process of determining the extent of its presence in a variety of equine biologics, including horse serum from a variety of providers. In one study,[7] 11 out of 18 samples of serum from providers in the US, Europe, Canada, New Zealand and South America demonstrated the presence for equine parvovirus-hepatitis (EqPV-H) using gel electrophoresis of the qPCR products and anti-EQPv-H antibodies were also detected in the same samples, although both fetal-based serum products tested negatively. While the presence of the putative agent has only been definitively identified in conjunction with disease in the US and China at this time, this study shows that the putative agent is truly of global origin.[7]

One of the classic syndromes associated with equine serum hepatitis and the reason it has longed been considered an infectious disease rather than just a reaction to biologics is the propensity for horses in contact to develop the disease. A 2018 study[15] reports the results of identification of EPv-H from 10 cases of apparent serum hepatitis on 6 different properties and the results of screening of in-contact horses which had not previously received any equine biologicals. In this study, animals with clinical infection were 80% positive, while in-contact animals were 48% positive, suggesting that these animal may be subclinical infected. Samples from infected animals were also tested for other viruses that had previously been associated with equine serum hepatitis (non-primate hepacivirus A), EPgV (pegivirus E) and EDAV (pegivirus D) were not identified in this study. [15]

Due to the massive degeneration, necrosis and hemorrhage affecting much of the four sections on the slide, this proved to be a deceptively difficult slide to describe. A common artifact was present in many of the slides which appears as blue spicular crystals within vacuoles of fat which was interpreted as calcium stearate crystals.

References:

1. Boyle AG, Magdesian KG, Ruby RE. Neonatal isoerythrolysis in horse foals and a mule foal: 18 cases (1988-2003). *J Am Vet Med Assoc*. 2005; 227(8): 1276-1283.

2. Brown DL, Van Wettere AJ, Cullen JM. Hepatobiliary system and exocrine pancreas. In: Zachary JF, ed. *Pathologic Basis of Veterinary Disease*. 6th ed. St. Louis, USA: Elsevier; 2017: 412-470.

3. Chandriani S, Skewes-Cox P, Zhong W, et al. Identification of a previously undescribed divergent virus from *Flaviviridae* family in an outbreak of serum hepatitis. *Proc Natl Acad Sci* USA. 2013; 110(15): E1407-E1415.

4. Cullen JM, Stalker MJ. Liver and biliary system. In: Maxie MG, ed. *Jubb, Kennedy, and Palmer's Pathology of Domestic Animals*. 6th ed. St. Louis USA: Elsevier; 2016: 259-351.

5. Divers TJ, Tennant BC, Kumar A, et al. New parvovirus associated with serum hepatitis in horses after inoculation of common biological product. *Emerg Infect Dis*. 2018; 24(2): 303-310.

6. Kapoor A, Simmonds P, Cullen JM, et al. Identification of a pegivirus (GB virus-like virus) that infects horses. *J Virol*. 2013; 87(12): 7185-7190.

7. Meister TL, Tegtmeyer B, Postel A, Cavalleri JMV, Todt D, Stang A, Steinmann E. Equine parvovirus-hepatitis frequently detectable in commercial equine serum pools. *Viruses* 2019; 11(5):E461.

8. Ramaiah SK, Harvey JW, Giguere S, Franklin RP, Crawford PC. Intravascular hemolysis associated with liver disease in a horse with marked neutrophil hypersegmentation. *J Vet Intern Med*. 2003; 17:360-363.

9. Ramsay JD, Evanoff R, Wilkinson TE, et al. Experimental transmission of equine hepacivirus in horses as a model for hepatitis C virus. *Hepatology*. 2015; 61(5): 1533-1546.

10. Ramsay JD, Evanoff R, Mealey RH, Simpson EL. The prevalence of elevated gamma-glutamyltransferase and sorbitol dehydrogenase activity in racing Thoroughbreds and their association with viral infection. *Equine Vet J*. 2019 Mar 8. doi:10.1111/evj.13092.

11. Shetty S, Janarthanan K, Leelakrishnan V, Nirmala V. Giant-cell hepatitis-rare entity in adults. *J Clin Exp Hepatol*. 2016; 6(3): 244-245.

12. Smith HL, Chalmers GA, Wedel R. Acute hepatic failure (Theiler's disease) in a horse. *Can Vet J*. 1991; 32: 362-364.

13. Sturgeon B. Theiler's disease. *Vet Rec*. 2017; 180(1):14-15.

14. Tomlinson JE, Kapoor A, Kumar A, et al. Viral testing of 18 consecutive cases of equine serum hepatitis: a prospective study (2014-2018). *J Vet Int Med*. 2019; 33: 251-257.

15. Tomlinson JE, Tennant BC, Struzyna A, et al. Viral testing of 10 cases of Theiler's disease and 37 in-contact horses in the absence of equine biologic product administration: a prospective study (2014-2018). *J Vet Int Med*. 2019; 33: 258-265.

16. Torbenson M, Hart J, Westerhoff M, et al. Neonatal giant cell hepatitis: histological and etiological findings. *Am J Surg Pathol*. 2010; 34(10): 1498-1503.

17. Wilkie IW, Precott JF, Hazlett MJ, Maxie MG, van Dreumel AA. Giant cell hepatitis in four aborted foals: a possible leptospiral infection. *Can Vet J*. 1988; 29:1003-1004.

Self-Assessment - WSC 2019-2020 Conference 7

1. Which of the following is the cause of congenital hepatic fibrosis?
    a. Intrahepatic arteriovenous shunting
    b. Genetic abnormalities resulting in overproduction of type 1 collagen by hepatic stellate cells
    c. Drug-associated toxicity targeting biliary epithelium
    d. Ductal plate abnormality

2. Which of the following is the cause of megalocytosis associated with pyrollizzidine intoxication?
    a. Hepatocyte fusion
    b. Cytoplasmic invagination resulting in karyomegaly
    c. Inhibition of mitosis through DNA alkylation
    d. Activation of endogenous retrovirus with replication of random segments of DNA

3. Which of the following is NOT a characteristic histologic finding in the livers of dogs with congenital hepatic shunts in the dog?
    a. Absence of portal veins
    b. Multiple profiles of tortuous arterioles
    c. Lipogranulomaas
    d. Micronodular hemosiderosis

4. Which of the following most often precedes onset of Theiler's disease in the horse?
    a. Insect bites
    b. Administration of equine biologicals
    c. Use of contaminated instruments
    d. Exposure to swampy ground

5. Viruses from which of the following families have been incriminated as potential causes of Theiler's disease?
    a. Herpesviruses and filoviruses
    b. Herpesviruses and flaviviruses
    c. Flaviviruses and parvoviruses
    d. Flaviviruses and pestiviruses

Please email your completed assessment for grading to Dr. Bruce Williams at bruce.h.williams12.civ@mail.mil. Passing score is 80%. This program (RACE program 33611) is approved by the AAVSB RACE to offer a total of 0.5 CE Credits, with a maximum of 12.5 CE Credits being available to any individual Veterinary Medical Professionals for the 2019-2020 Wednesday Slide Conference. This RACE approval is for the subject matter categories of: SCIENTIFIC using the delivery method of NON-INTERACTIVE DISTANCE. This approval is valid in jurisdictions which recognize AAVSB RACE.

Joint Pathology Center
Veterinary Pathology Services

WEDNESDAY SLIDE CONFERENCE 2019-2020

C o n f e r e n c e 8

23 October 2019

Conference Moderator:
Dr. Dalen Agnew, DVM, PhD, DACVP
Associate Professor
Pathobiology and Diagnostic Investigation
Michigan State University
College of Veterinary Medicine
East Lansing, Michigan

CASE I: D19-007212 (JPC 4135866).

Signalment: 21-month-old female Welsh Corgi mixed breed dog

History: Following spay procedure; a section of uterus was submitted for biopsy evaluation.

Gross Pathology: Arising from the splenic vein and connecting to the caudal vena cava in the region of the left kidney is a large shunt vessel up to 4 mm in diameter. Additionally, connecting the portal vein and caudal vena cava in the cranial abdomen are two small (1 mm in diameter), tortuous vessels. The liver is mildly reduced in size, weighing 67 g (2.9% of total body weight; normal is 3-4). The liver is diffusely markedly pale red to tan and moderately firm. Over the diaphragmatic surface of the right lateral liver lobe is a 2.0 x 0.8 cm region of hemorrhage and mild depression. The parenchyma subjacent to this focus is markedly firm. The right kidney is

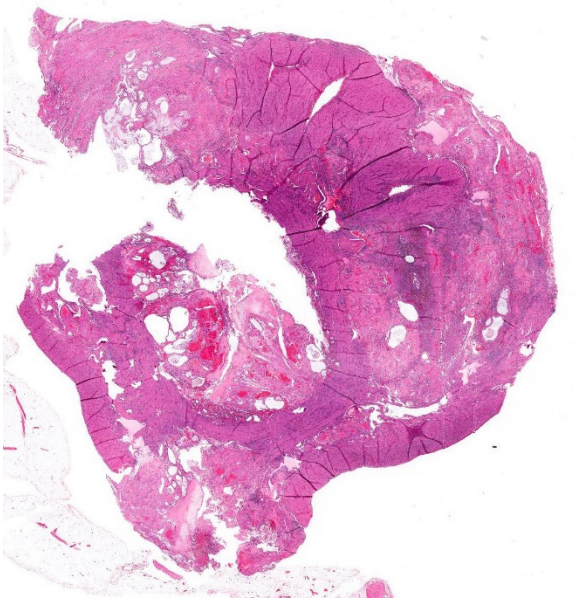

Uterus, dog. A cross section of uterus is submitted for examination. At low magnification, the endometrium is expanded by numerous dilated glands and areas of hemorrhage. The myometrium is focally expanded at left by plaques of collagen and bands of a dense cellular infiltrate. (HE, 5X)

mildly reduced in size compared to the left kidney and has multifocal
chronic infarcts up to 2 cm in diameter. No abnormalities are identified externally in the brain.

Laboratory results: NA

Microscopic Description: Uterus: Diffusely and markedly expanding the endometrium, extending into the luminal space, and infiltrating into the myometrium are markedly ectatic endometrial glands which are admixed and/or surrounded by a coagulum of degenerate neutrophils, eosinophilic karyorrhectic and cellular debris, congested blood vessels, multifocal hemorrhage, hemosiderin, fibrin, and sloughed epithelial cells. These sloughed cells are similar to those lining remaining intact endometrium and are tall columnar epithelial cells with contain highly vacuolated cytoplasm. The myometrium is multifocally infiltrated by large numbers of lymphocytes, plasma cells and hemosiderin-laden macrophages. Multifocally, within the endometrial coagulum and the underlying myometrium are scattered aggregates of irregularly shaped syncytial trophoblast cells which contain up to 6-10 nuclei with abundant eosinophilic cytoplasm and multifocal mild mineralization. There is focal rupture of the serosa with transmural proliferation/invasion of endometrial glands, hemorrhage, fibrin, and yellow pigment (hematoidin).

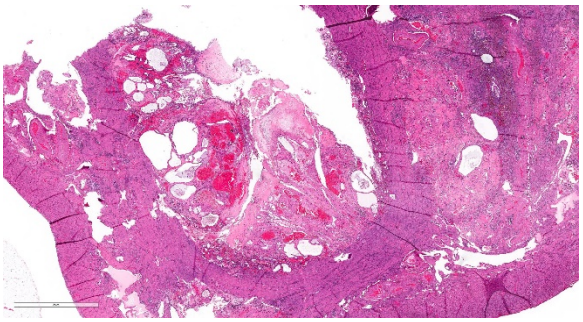

Uterus, dog. Higher magnification of the endometrium. Nodules of endometrium at left contain large ectatic glands; at right, the endometrium is largely replaced by a dense collagenous band. (HE, 20X)

Contributor's Morphologic Diagnosis: Uterus: Necrosis, hemorrhage, and mineralization with syncytial trophoblast retention, endometrial hyperplasia, and serosal rupture

Condition: Subinvolution of placental sites (SIPS)

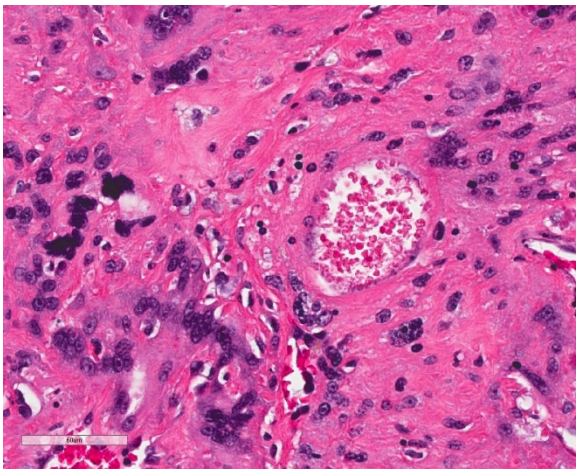

Uterus, dog. Bands of endometrial collagen are infiltrated by anastomosing cords of trophoblasts which demonstrate erythrophagocytosis and the presence of brightly eosinophilic hematin within their cytoplasm. (HE, 400X)

Contributor's Comment: Clinical presentation of subinvolution of placental sites (SIPS) typically consists of blood-tinged vaginal discharge that extends past the normally expected 7-10 days post-whelping[1], sometimes lasting for months. The condition occurs most commonly in young dogs and the cause is unknown. Prolonged bleeding and extensive loss of blood can lead to anemia and occasionally death. Affected dogs are also prone to ascending infections.

Normal uterine involution in dogs takes 12-15 weeks[3]. In dogs with SIPS gross lesions consist of some or all of the placental attachment areas (ellipsoidal enlargements)

being thickened, rough, grey to brown and hemorrhagic with the inter-placental sites appearing normal.

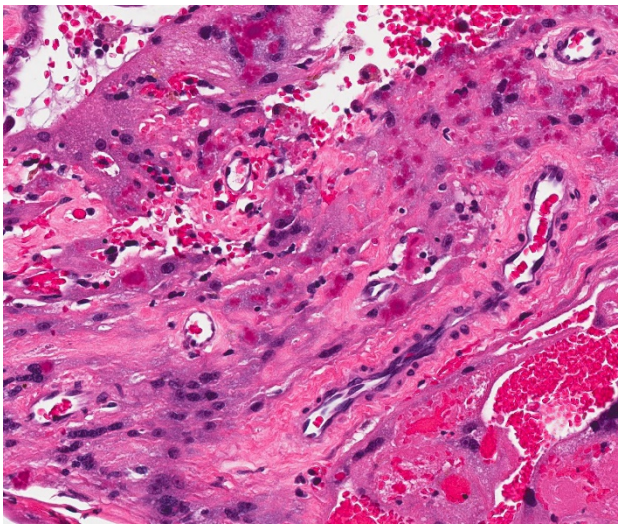

Uterus, dog. Numerous syncytiotrophoblasts remain within the collagenous bands as well. (HE, 400X)

Microscopically, SIPS are characterized by a luminal coagulum of abundant necrotic cellular debris, hemorrhage, and within the deeper layers of endometrium, syncytial trophoblasts or decidual cells that have a vesiculate nucleus and highly vacuolated cytoplasm due to progesterone stimulation. The retained trophoblastic cells fail to degenerate and subsequently invade into the deeper glandular layer and myometrium. [2] These trophoblastic cells also inhibit normal thrombus formation leading to prolonged bleeding. [4] Mineralization and infiltration of lymphocytes, plasma cells, and macrophages often occur in these areas of necrosis. The syncytial trophoblasts or decidual cells may invade deeper layers including the myometrium and also may cause serosal rupture (as seen in this submitted case) leading to escape of the contents into the peritoneal cavity causing fatal peritonitis [1]. Spontaneous recovery generally occurs in healthy dogs and in prolonged cases ovariohysterectomy must be performed for resolution of the condition[4,5].

Other differentials for hemorrhagic vaginal discharge include endometritis, neoplasia, coagulopathies, brucellosis and other bacterial infections.

Contributing Institution:
North Carolina State University College of Veterinary Medicine
https://cvm.ncsu.edu/research/departments/dphp/programs/pathology/

JPC Diagnosis: Uterus, Endometritis, chronic-active and necrohemorrhagic , diffuse, severe, with numerous myometrial trophoblasts and syncytiotrophoblasts, adenomyosis, endometrial progesterone effects, vascular thrombosis and mural rupture.

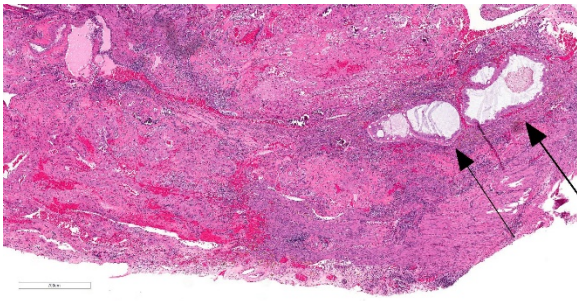

Uterus, dog. The endometrium (serosa at bottom) is markedly expanded by collagen, trophoblasts, inflammatory cells, and several endometrial glands (arrows). (HE, 33X)

JPC Comment: In domestic species, subinvolution of placental sites is a condition unique to the bitch. In humans, subinvolution of the placental site (also known as non-involution of the placental site or subinvolution of the uteroplacental arteries), is an uncommon cause of postpartum bleeding in older multiparous women. Unlike the dog, in humans it is most often diagnosed within several weeks postpartum, although cases have been diagnosed as long

as 6 years after the most recent parturition.[6] In humans, this condition is different from the bitch, in that hemorrhage is usually the result of failure occlusion of the placental vessels.

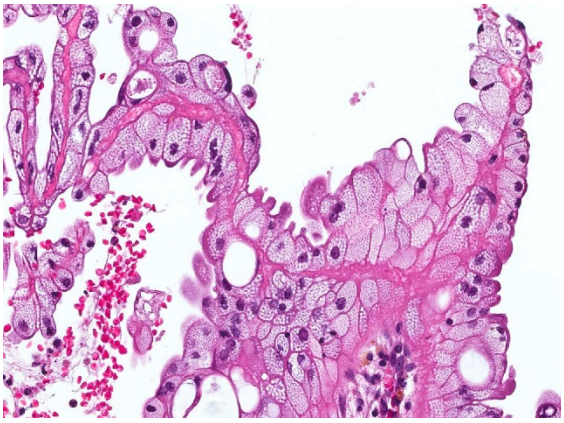

Uterus, dog. The epithelium lining the endometrial surface and endometrial glands is hypertrophic with numerous cytoplasmic vacuoles (progesterone effect). (HE, 324X)

During mid- to late gestation in humans, endovascular trophoblasts actually replace the endothelial lining of the uteroplacental arteries, expressing endothelial –type markers and angiogenic factors resulting in significant remodeling of the arterial bed to create low-resistance high-flow arteries to supply the needs of the developing fetus.[6] Within days after birth, these trophoblasts disappear, resulting in endarteritis, thrombosis, and occlusive mural fibrosis of these vessels, which coincides with loss of the decidua and endomyometrium in the remainder of the uterus, and limits blood loss during this process. While the pathogenesis of this process has not yet been fully elucidated, it is likely that the lack of involution of placental vessels results from abnormal immunologic recognition, as the normal deposition of immunoglobulin (IgG, IgM, and IgG) and complement proteins (C1q, C3d, C4) seen in normally involuted arteries is not seen in those associated with subinvolution. Additionally, remnant endovascular trophoblasts in non-involuting placental vessels express high levels of the anti-apototic protein Bcl-2.[6]

The moderator pointed out the focal area of rupture of the wall of this uterus, obviously complicating the prognosis in this case. The cause of the mural rupture is likely the result of ischemia due to multifocal thrombosis in this case. The moderator also commented on the presence of abundant hyaline collagen lacking fibroblasts within the section, which is a characteristic feature of involution in the dog. These collagen plaques form over the surface within 3 days of parturition to form a sort of hemostatic bandage over the profound vascularity of the deeper degenerating layers of the endometrium. The moderator also discussed the importance of discussing the complete disorganization of the endometrium in SIPS as compared to normal involution, which may be helpful in distinguishing between normal involution and SIPS in cases with incomplete history. The depth of the trophoblasts is also helpful in making this distinction.

The moderator also pointed out the presence of abundant reddish crystalline material in trophoblasts and syncytiotrophoblasts which

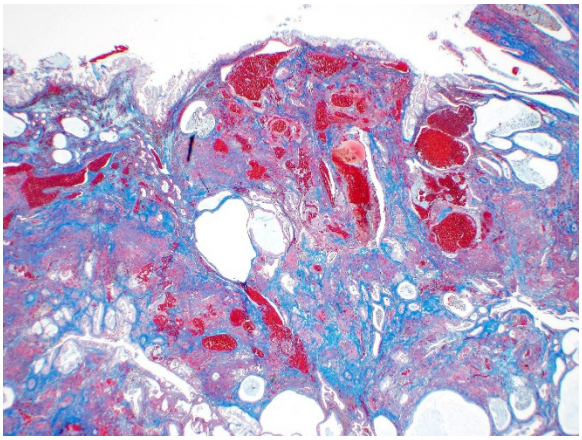

Uterus, dog. A trichrome stain demonstrates the amount of collagen within the remaining endometrium. (Masson's trichrome, 20X)

was interpreted as hematin, a blood breakdown pigment. Within these cells, as opposed to macrophages, the breakdown of hemoglobin is incomplete, more closely resembling hemoglobin crystals than hemosiderin granules.

References:

1 In: Maxie MG, ed. *Jubb, Kennedy and Palmer's Pathology of Domestic Animals*. 6 ed.; 2016: 358-464.

2 Al-Bassam MA, Thomson RG, O'Donnell L: Involution Abnormalities in the Postpartum Uterus of the Bitch. *Veterinary Pathology* 1981:18(2)**:**208-218.

3 Al-Bassam MA, Thomson RG, O'Donnell L: Normal postpartum involution of the uterus in the dog. *Canadian journal of comparative medicine : Revue canadienne de medecine comparee* 1981:45(3)**:**217-232.

4 Johnston SD, Root Kustritz MV, Olson PS: *Canine and feline theriogenology*. Philadelphia, PA: Saunders, 2001.

5 Sontas HB, Stelletta C, Milani C, Mollo A, Romagnoli S: Full recovery of subinvolution of placental sites in an American Staffordshire terrier bitch. *Journal of Small Animal Practice* 2011:52(1)**:**42-45.

6. Wachter DL, Thiel F, Agaimy A. Subinvolution of the placental site six years after last delivery. *Int J Gynecol Pathol* 2011; 581-582.

7. Weydert JA, Benda JA: Subinvolution of the Placental Site as an Anatomic Cause of Postpartum Uterine Bleeding: A Review. *Archives of Pathology & Laboratory Medicine* 2006:130(10)**:**1538-1542.

CASE II: 15-1137 (JPC 4066220).

Signalment: Three late term dairy goat fetuses (breed not specified)

History: Multiple late term abortions occurred in a large dairy goat herd. Submitted samples included fixed tissues, tissue pools, abomasal fluid and serum from one of the aborting dams.

Gross Pathology: The submitting veterinarian reported that the placentas had hemorrhages and pinpoint white foci on the cotyledons. Fetal spleens and livers were enlarged.

Laboratory results: Placentas were positive for *Chlamydophila* by antigen ELISA. PCR for *Toxoplasma gondii* was negative on placenta and brain. No *Campylobacter* was isolated and PCR for BVD was negative. FA for *Leptospira* was negative. A single dam serum was positive for antibodies to *Coxiella* but negative for *Brucella abortus*, BVDV and *Toxoplasma*. Immunohistochemistry for *Coxiella burnetii* on the placenta was positive.

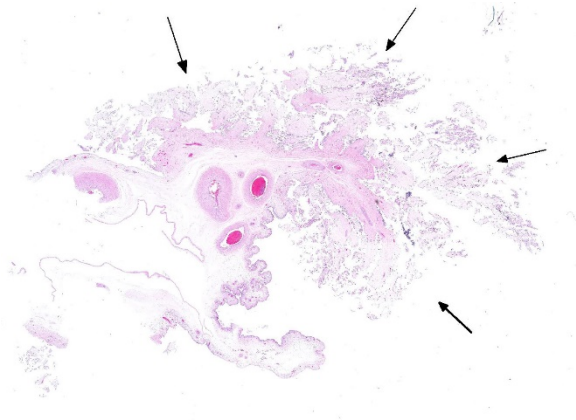

Placenta, goat fetus. A cross section of chorioallantois with cotyledon (arrows) is submitted for examination. (HE, 5X)

Microscopic Description: In sections of placenta from 2 fetuses, there were multifocal areas of necrosis and inflammation. Cotyledons and intercotyledonary placenta were infiltrated by neutrophils and macrophages. Fibrin admixed with degenerate inflammatory cells covered the cotyledonary surface. The intercotyledonary interstitium was infiltrated by inflammatory cells, and a few scattered blood vessels were necrotic and inflamed). Multiple chorionic epithelial cells were expanded by the presence of discreet vacuoles containing numerous bacterial organisms. Gimenez-tained sections highlighted the intracellular organisms. Gimenez-positive organisms were identified as *Coxiella burnetii* by immunohistochemistry.

Other lesions (not submitted) included multifocal gliosis within sections of cerebrum in two of the fetuses. No organisms were identified histologically. Sections of livers, lungs, spleens and kidneys had no histologic lesions.

Contributor's Morphologic Diagnosis: Multifocal necrotizing placentitis with vasculitis and intracellular bacterial organisms (*Coxiella burnetii*)

Contributor's Comment: *Coxiella burnetii* is a well-recognized cause of abortion in sheep goats and, to a lesser extent, cattle.[9] In one large study of goat abortions, *C burnetii* was second only to *Chlamydia psittaci (Chlamydophila abortus)* in numbers of cases of bacterial abortion in goats.[6] Infected animals remain as a reservoir, shedding large numbers of organisms during subsequent abortions or at normal parturitions. Organisms are also shed in feces and milk,[3] Ruminant reservoirs are the major source of infection in people, in whom the organism causes the zoonotic disease Q fever.[1] Although cattle are major shedder of *C burnetii*, especially in milk[6], the organism is not a major abortifacient in that species.[5]

Transmission is by inhalation or fecal-oral routes. Infected animals may abort in late

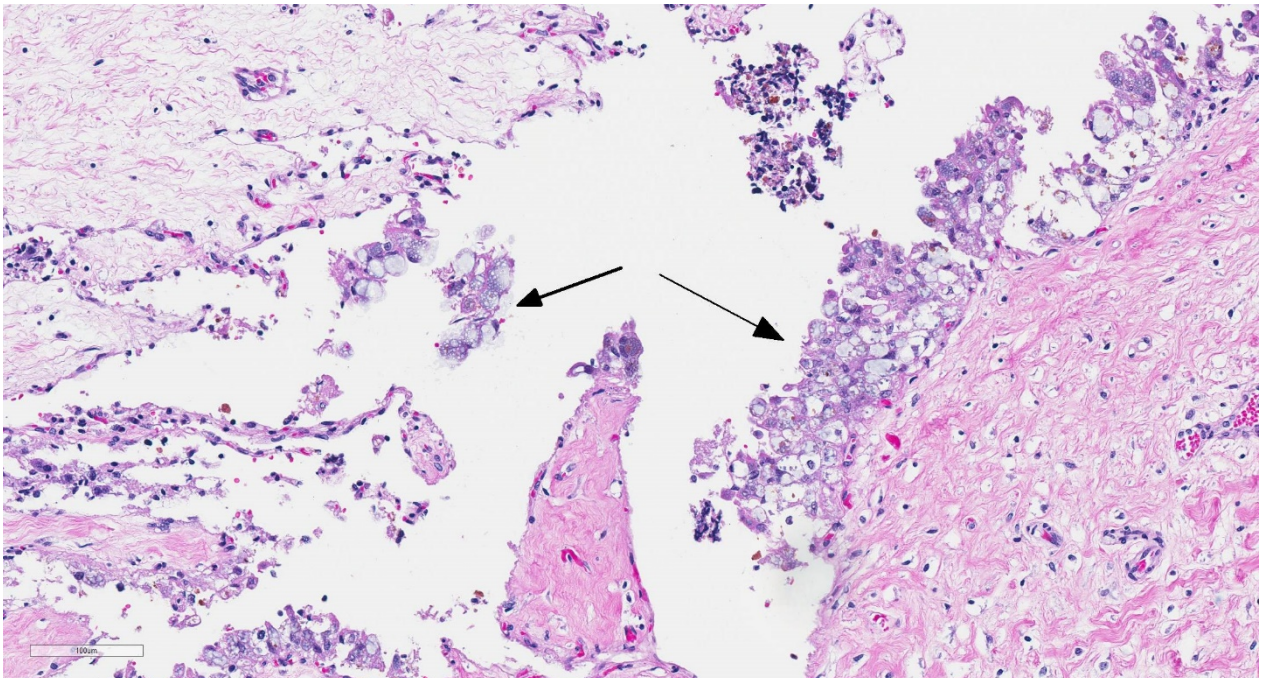

Placenta, goat fetus. There is marked loss of cotyledonary epithelium. Remaining trophoblasts ((right arrow) and sloughed trophoblasts are swollen by the presence of numerous intracytoplasmic bacilli. (HE, 142X)

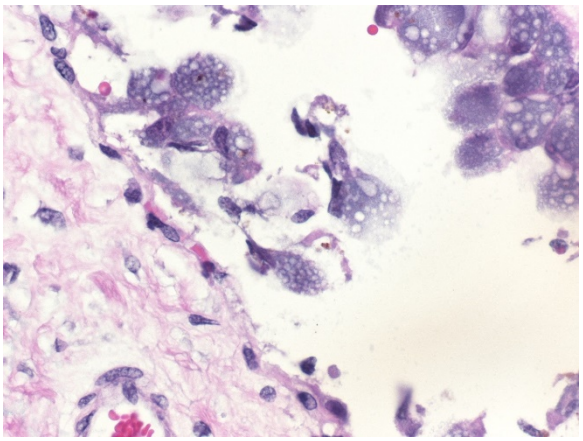

Placenta, goat fetus. Higher magnification of trophoblasts with numerous C. burnetti within their cytoplasm. This pathogen gives infected cells a unique "bubbly" appearance. (HE, 400X) (Photo courtesy of: Department of Veterinary Microbiology and Pathology, and the Washington Animal Disease Diagnostic Laboratory, Washington State University, Pullman, WA www.vetmed.wsu.edu)

gestation or give birth to weak kids. Fetal lesions are minimal but gross evidence of placentitis is present.[9] Characteristic histologic lesions are necrotizing intercotyledonary placentitis with intracellular organisms; vascultitis is less prominent than in chlamydial placentitis. Both *C burnetii* and *C abortus* are Gimenez-positive. In this case, since antigen ELISA for *Chlamydophila* was positive, immunohistochemistry was needed to identify the organisms as *C burnetii*. *C abortus* should also cause multifocal necrosis in fetal liver and spleen, which was not seen in this case. This case was also interesting in that cerebral glial nodules suggested *Toxoplasma* infection, but PCR for *T gondii* on placenta and brain was negative.

The human disease Q fever, caused by infection with *C burnetii*, was first reported in Australia in 1935 but has a worldwide distribution.[1]. Only 40% of infected people show any clinical signs. The more common acute disease manifests as flu-like symptoms, pneumonia or hepatitis; chronic infections manifest primarily as endocarditis.[2] Most reported cases are of the acute disease. Cases in the US are most often reported from western and plains states where ranching and rearing of cattle are common. Cases are most commonly reported in spring in summer, coinciding with birthing season for ruminants. Incidence of disease increases with age and persons with immune compromise, or those in contact with livestock are at higher risk.

C burnetii is an obligate intracellular organism in the order Rickettsiales. It infects monocytes and macrophages and survives within the acidic environment of the phagosome. Intracellular survival depends upon inhibition of phagosome-lysosome fusion. Control of the infection requires intact cell mediated immunity; lymphocytes of people with chronic infections fail to proliferate in response to *C burnetii* antigen, whereas lymphocytes of people with acute infections do respond.[2]

Contributing Institution:

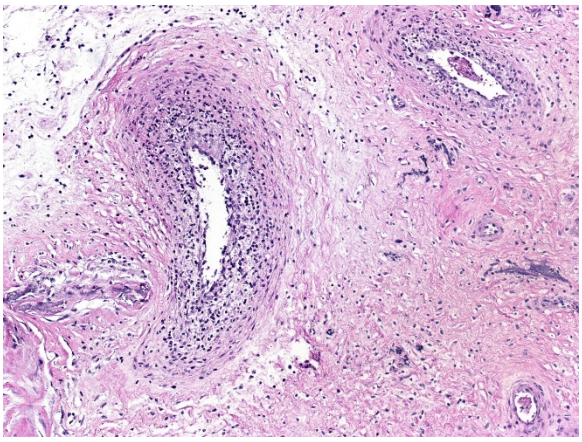

Placenta, goat fetus. There is loss of endothelium and there are numerous viable and degenerate neutrophils and cellular debris within the walls of chorionic vessels (vasculitis) (HE, 400X) (Photo courtesy of: Department of Veterinary Microbiology and Pathology, and the Washington Animal Disease Diagnostic Laboratory, Washington State University, Pullman, WA www.vetmed.wsu.edu)

Department of Veterinary Microbiology and Pathology, and the Washington Animal Disease Diagnostic Laboratory, Washington State University, Pullman, WA 99164-7034 www.vetmed.wsu.edu

JPC Diagnosis: Chorioallantois: Placentitis, necrotizing, diffuse, severe, with multifocal moderate vasculitis, and numerous intratrophoblastic coccobacilli.

JPC Comment: *Coxiella burnetii*, the causative agent of Q fever, is a bacterium whose wall is similar to that of a gram-negative bacillus; however, its wall does not stain with Gram stains, requiring a Gimenez stain to disclose its location.[4] As an obligate intracellular parasite, it produces a reproductive vacuole that resembles a phagolysosome with an acidic pH, acid hydrolysates, and cationic peptides. To survive in this harsh environment, it has developed important buffering strategies, including the production of basic proteins, sodium-proton exchanges to combat oxidative stress ,and osmoprotectants to prevent osmotic damage.[4] In vitro experiments have determined that there are actually two variants of the coccobacillus, a reproductively active "large-cell variant" which is the replicative form, and an environmentally stable small cell variant, which has numerous cross-links in its peptidoglycan wall to give it additional resistance to environmental stresses such as dessication, chemical, and heat stress.[4]

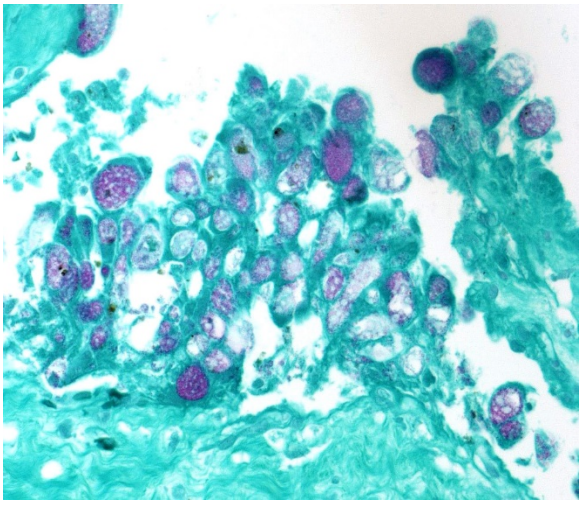

Placenta, goat fetus. Bacilli within trophoblasts stain positively with a Gimenez stain. (Gimenez, 400X) (Photo courtesy of: Department of Veterinary Microbiology and Pathology, and the Washington Animal Disease Diagnostic Laboratory, Washington State University, Pullman, WA www.vetmed.wsu.edu)

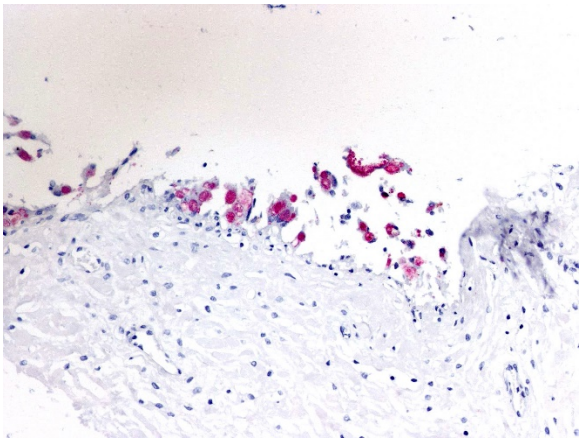

Placenta, goat fetus. Coccobacilli within trophoblasts stain immunopositively for C. burnetti. (anti-C. burnetti, 400X) (Photo courtesy of: Department of Veterinary Microbiology and Pathology, and the Washington Animal Disease Diagnostic Laboratory, Washington State University, Pullman, WA www.vetmed.wsu.edu)

Q fever, short for *query* fever, was first identified by Dr. John Derrick in meat-packing workers in Queensland Australia in 1935 who developed an acute febrile illness but were negative on blood and serologic tests for known pathogens at the time.[7] Transmission to guinea pigs and other laboratory animals ultimately resulted in the identification of rickettsia within the spleen. The clinical signs of Q fever – high fever, headaches and a slow pulse resembled other rickettsial diseases of the time including typhus and psittacosis, but lacked the rash common to the other two diseases. [7]

In humans, Q fever has been seen in all

countries except New Zealand. While ruminants have been the traditional reservoirs, in recent years, a number of additional species have been reported as shedding the bacillus, to include cats, marine mammals, psittacines, reptiles, and ticks.[4] In the absence of a suitable host, *C. burnetii* also possesses the ability to utilize free-living amebae as a reservoir for the small-cell, vegetative form.[4] Q fever is most common seen in persons who come in contact with infected animals, including farmers, abattoir works, lab workers, and veterinarians.[7] Transmission has also been seen following ingestion of raw milk or fresh goat cheese.[7] Q fever has many various acute and chronic manifestations, or may be asymptomatic. When it became a reportable disease in the US in 1999, case numbers increased by 250% in the next 5 years.[4] While it most often presents as an influenza-like illness, more serious manifestations, such as pneumonia, hepatitis, or endocarditis are seen. [10] Endocarditis is the most common chronic disease associated with *C. burnetii* infection in humans and has been seen following valve transplants. [10] In cases of endocarditis, as vegetation may be absent of small, resulting in a long latent period. [10]

Between 2007 and 2010, a country-wide outbreak of Q fever occurred in the Netherlands with over 40,000 cases estimated, especially in the provinces of Noord-Brabant, Gelderland, and Limburg, centers of goat farming. The outbreak coincided with a marked increase in high-intensity dairy goat farming in proximity to urban areas. On some of these farms, abortion levels due to *Coxiella* exceeded 60%, leading to requirements for reporting of abortions and widespread immunization of goats. With cases still on the rise, in 2008, the Dutch government was forced to slaughter over 50,000 goats in order to minimize the public health risk.

The moderator discussed the presence of a brown granular pigment within the trophoblasts. While initially interpreted as hemosiderin by most participants, he offered the possibility of meconium and uptake by the trophoblasts. He noted the unusual lack of necrotic debris between the cotyledonary villi in this particular case. He also registered, during the description in this case, a personal enmity toward the words “admixed” and “coccobacilli”.

References:

1. CDC Info, Q fever, Epidemiology and Statistics update June 2019. http://www.cdc.gov/qfever/stats/index.html
2. Angelakis E and Raoult D. Q fever. Vet Microbiol 2010; 140:297-309.
3. Berri M, Rousset E, Champion JL, et al. Goats may experience reproductive failures and shed Coxiella burnetti at two successive parturitions after a Q fever infection. Res in Vet Sci 2007; 83:47-52.
4. Eldin C, Melenotte C, Mediannikov O, Ghigo E, Millon M, Edouard S, Mege JL, Maurin M, Raoult D. From ! Fever to Coxella burnetii infection: a paradigm Change. *Clin Micorbiol Rev* 2017; 30(1) 115-190.
5. Garcia-Ispierto I, Tutusaus J, Lopez-Gatius F. Does Coxiella burnetii affect reproduction in cattle? A clinical update. Reprod Dom Anim 2014; 49:529-535.
6. Moeller RB. Cases of caprine abortion: diagnostic assessment of 211 cases (1991-1998). J Vet Diagn Invest 2001; 13:265-270.
7. Reimer LG. Q fever. *Clin Micro Rev* 1993; 6(3):193-198.
8. Rodolakis A, Berri M, Hechard C, et al. Comparison of Coxiella burnetii shedding in milk of dairy bovine,

caprine and ovine herds. J Dairy Sci. 2007; 90:5352-5360.
9. Schlafer DM and Miller RB. Female genital system IN *Jubb, Kennedy and Palmer's Pathology of Domestic Animals*, Vol. 1, 5th Edition, GM Maxie, ed. Elsevier Saunders, Edinburgh, 2007.
10. Weiner Well Y, Fink D, Schlesinger Y, Raveh D, Rudensky B, Yinnon AM. Q fever endocarditis; not always expected. *Clin Micorbiol Infect* 2010; 6:359-362.

CASE III: VS17005 3 (JPC 4102155).

Signalment: 9-year-old, female rhesus macaque (*Macaca mulatta)*

History: This animal received 4Gy whole body irradiation three years prior to presentation. It had a history of menorrhagia and anemia (Hct 14.8%). A hysterectomy was performed to prevent further blood loss. During the procedure the uterus was found to be adhered to the right side of the abdominal wall.

Gross Pathology: The uterus weighed 4.5g and the endometrium at the apex of the uterus was irregularly thickened up to 1.5mm.

Laboratory results: None.

Microscopic Description: The superficial endometrium is expanded and effaced in areas by an unencapsulated, poorly demarcated neoplasm composed of sheets of pleomorphic neoplastic cells supported by fine stroma, which projects into the lumen in some areas. Aggregates of macrophages, lymphocytes and few eosinophils and granular leukocytes are scattered throughout. The neoplastic cells have variably distinct cell borders, are round to polygonal, have abundant eosinophilic vesicular cytoplasm, 1-12 oval nuclei with stippled chromatin, and 1-2 nucleoli. Mitoses are rare. A few cells, especially towards the lumen, have undergone degeneration and necrosis. The remaining endometrium has few scattered dilated glands lined by epithelial cells with basally arranged nuclei, without mitoses.

Contributor's Morphologic Diagnosis: Uterine trophoblastic tumor

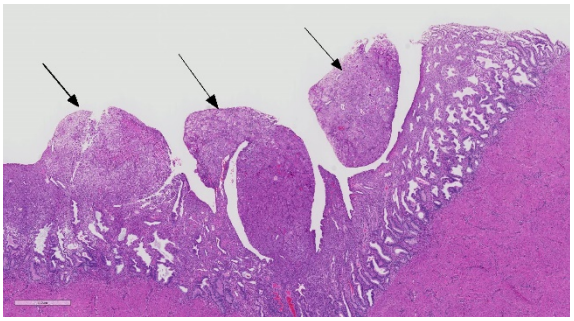

Uterus, rhesus macaque. Multiple nodules of a neoplasm abut or occupy the superficial endometrium. Subjacent glands are mildly dilated. (HE, 28X)

Contributor's Comment: Gestational trophoblast disease (GTD) is a rare disease of pregnancy, a result of abnormal differentiation of trophoblasts, but may also rarely develop from germ cells in the absence of pregnancy.[13] Since trophoblasts lack the common regulatory pathways that prevent the development of neoplasms, either molar gestations/hydatiform moles or trophoblastic tumors can develop.[16] Hydatiform moles are abnormal pregnancies characterized by aberrant chromosomal changes. Women greater than forty years of age and younger than 20 are more likely to develop molar gestations/hydatiform moles. Uterine epithelioid trophoblastic tumors have been reported in a red-tailed guenon (*Cercopithecus ascanius*)[4] and an African green monkey (*Chlorocebus aethiops sabaeus*).[2] Ovarian nongestational

trophoblastic tumors (2 choriocarcinomas and 1 epithelioid trophoblastic tumor) have been reported in captive macaques.[6,7,10,15]

Trophoblast tumors can be classified into one of three subcategories: choriocarcinomas, placental site trophoblastic tumors, and epithelioid trophoblastic tumors. Choriocarcinomas are malignant tumors composed of bilaminar cytotrophoblasts and syncytiotrophoblasts without chorionic villi. In some cases, these represent a component of mixed germ cell tumors of the ovary. Pure nongestational choriocarcinomas are extremely rare in humans. Typically the neoplastic cells are strongly positive for human chorionic gonadotrophin (β-hCG) and weakly positive for human placental lactogen (hPL).[14] Placental site trophoblastic tumors are composed of sheets of variably sized trophoblasts with single to multiple nuclei with atypia. These cells may permeate the myometrium and blood vessels.[3] The cells are usually positive for hPL and variably positive for β-hCG and placental-like alkaline phosphatase (PLAP).[9,14] Epithelioid trophoblastic tumors are composed of sheets of monomorphic intermediate trophoblasts which resemble the chorionic membrane.[3] The cells are variably immunoreactive for placental-like alkaline phosphatase (PLAP) and hPL but strongly immunoreactive for E-cadherin and epidermal growth factor receptor.[9,14]

The clinical signs associated with GTD vary widely. Symptoms usually present within the first trimester and include bleeding and anemia, a larger than normal uterus for the gestational age, hyperemesis, pre-eclampsia, hyperthyroidism and respiratory distress. Abnormal fetal organs observed by ultrasonography and markedly elevated serum hCG can aid in the clinical diagnosis. Histopathology and immunohistochemistry provides a confirmatory diagnosis. The treatment options of trophoblast tumors depend on the stage of the tumor. [13,16]

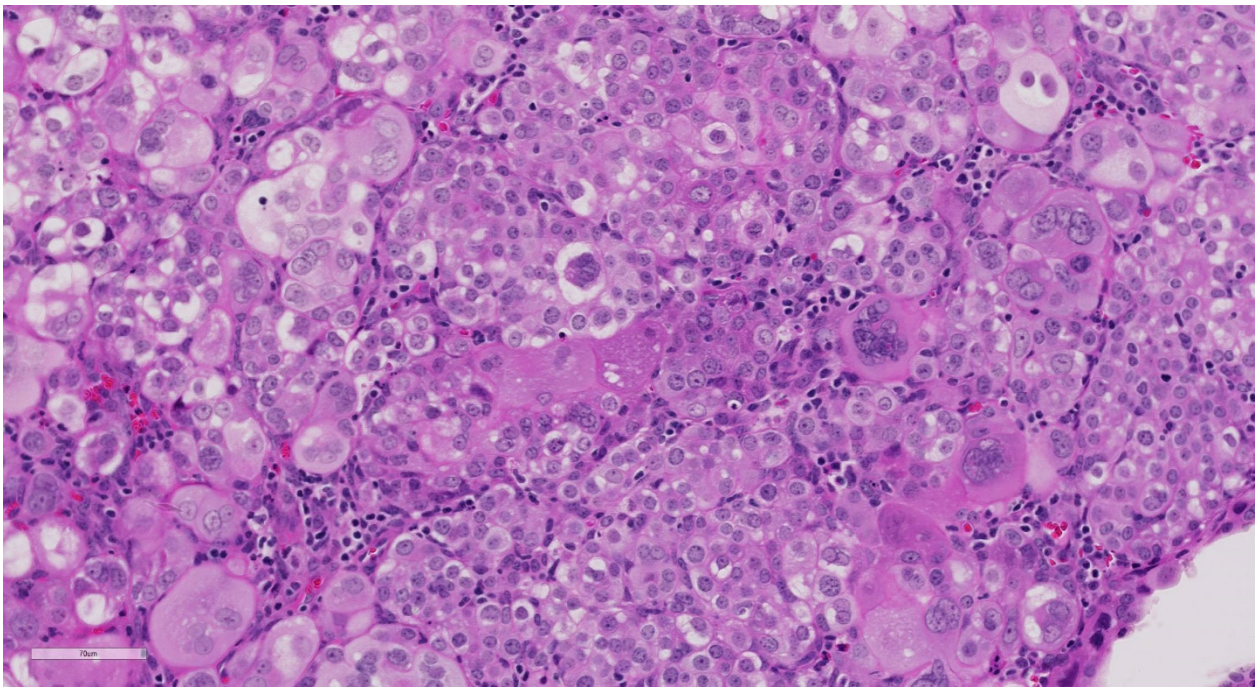

Uterus, macaque. The neoplasm is composed of two distinct populations of cells – uninucleated polygonal cells resembling cytotrophoblasts, and larger multinucleated cells resembling syncytiotrophoblasts. (HE, 205X)

Contributing Institution:
Wake Forest School of Medicine
Department of Pathology, Section on Comparative Medicine
Medical Center Boulevard / Winston-Salem, NC 27157
www.wakehealth.edu

JPC Diagnosis: Uterus: Choriocarcinoma

JPC Comment: The contributor has presented a concise yet informational description of a confusing set of neoplasms that are extremely rare in all species. These tumors are a subset of gestational trophoblastic disease, which as stated above, includes hydatiform moles.[1]

Hydatiform moles (hydatiform meaning cystic, mole simply referring to a clump of growing tissue) arise during pregnancy from non-viable eggs that implant in the uterus, and are the most common of the gestational trophoblastic diseases. These eggs have lost the nucleus, and hence the maternal DNA. The mole, a parthenogenetic zygote, results from fertilization by a spermatozoa undergoing mitosis following combining with the egg (resulting in a 46 XX phenotype) or alternatively two haploid spermatozoa (resulting in a 46 X,Y karyotype.)[1] Even more rarely a normal egg may be fertilized by two sperm which reduplicate themselves (resulting in a 69, XXY karyotype) – known as a partial mole. Partial moles, due to the presence of maternal DNA may have discernable, but disorganized fetal elements within their structure.[1]

Moles may often be grossly differentiated from true trophoblastic tumors grossly and histologically by their grapelike appearance (owing to their development of chorionic villi, not seen in the true trophoblastic tumors. and histologically, but the presence of chorionic villi, which are not present in the true trophoblastic tumors. They may be invasive, growing into the wall of the uterus, or actually turn into choriocarcinomas (this happens into 4% of tumors.)[1]

The true trophoblastic tumors, as mentioned by the contributors, include choriocarcinoma, the placental site trophoblastic tumor (PSTT), and epithelioid trophoblastic tumor (ETT), and their differentiation histologically is based on morphology and immunohistochemistry (reviewed above in the contributor's comments.)[12] Choriocarcinomas are by far the most malignant and common of the three, often demonstrating significant invasion of the uterus and distant metastasis in approximately 40% of human cases. The other two tumors are far less common and both are derived from the intermediate trophoblast. PSTT is the rarest subtype with 1 per 100.000 pregnancies.[9] These are slow growing malignancies that most affect women of reproductive age and are seen following a normal or ectopic pregnancy or miscarriage, with rare cases affecting post-menopausal women. Because of its similarities to a normal implantation site, it was initially called a "placental pseudotumor".[9] The cellular population of the placental site trophoblastic tumor is monomorphic as composed to the dimorphic population of choriocarcinomas, and its immunohistochemical profile is the reverse, with strong staining for hPL and weak staining for hCG (as the choriocarcinoma stains strongly for hCG and weakly for hPL.[11] Interestingly, the differential levels of these hormones are often used as a clinical test for these particular neoplasms as well. The third neoplasm, epithelioid trophoblastic tumor (ETT) was first diagnosed in humans by Shih and Silverberg in 1998[2], and is also a neoplasm of intermediate trophoblasts (as is the PSTT) but resemble those of the chorionic villi, rather than the placental site

(as seen with the PSTT). The neoplastic cells stain weakly for hCG and HPL, but strongly for cytokeratin and inhibin –A, epithelial growth factor, and e-cadherin.[2] A review of the immunohistochemical staining patterns for the various types of gestational trophoblastic diseases is presented in Table 1.

Since the submission of this case, this case has also been presented at the 2018 Satellite Sympoisum of the National Toxicology Program at the annual meeting of the Society of Toxicologic Pathologists, the minutes of which were subsequently published in *Toxicologic Pathology*. The presenter described the immunohistochemical findings for this neoplasm including a general immunpositivity for hCG and strong positivity in the multinucleated cells. The cells stained diffusely positive for pancytokeratin, but failed to stain for human placental lactogen, placental alkaline phosphatase, and p63. There were rare foci of CD10 immunopositivity, and these cells failed to stain with hCG and pancytokeratin. Based on these findings, the contributor and the participants at the conference prefer a diagnosis of choriocarcinoma. This is in agreement with the immunohistochemical stains run at the Joint Pathology Center,

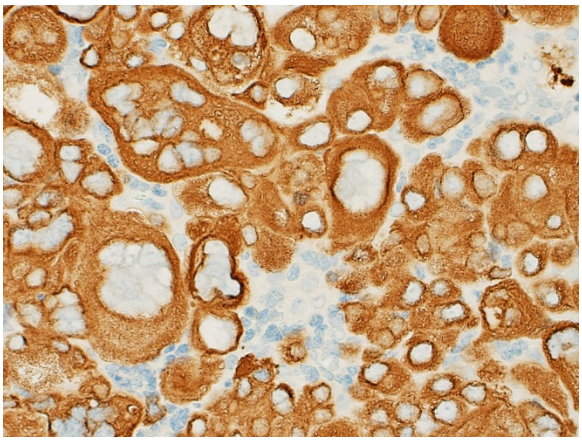

Uterus macaque. Both cell populations are strongly positive for cytokeratin (AE1-AE3, 400X)

which demonstrated patchy but strong immunopositivity of the syncytio-trophoblastic population for hCG, and a weaker staining pattern for HPL and weak to absent staining of cytotrophoblasts for both. As expected, both populations stained strongly positive for cytokeratin, but this is not useful in differentiating any of the three trophoblastic tumors. Based on this findings and the histologic appearance of the tumor, we are in agreement with the contributor that this tumor is best classified as a choriocarcinoma.

Table 1. A Summary of the Immunohistochemical Staining Properties of Different Types of Gestational Trophoblastic Disease Compared to the Presented Lesion.

Immunohistochemistry Stain	ETT	PSTT	CC	Mole	PSN	Lesion
Human chorionic gonadotrophin	±	±	+	+	−	+
Human placental lactogen	±	+	±	+	−	−
Pancytokeratin	+	+	+	+	+	+
p63	+	−	±		+	−
CD10	−	±	±	+		Focal
Placental alkaline phosphatase	−	−	−	+	+	−
α-inhibin	+	+	+	+	+	
Mel-CAM (CD146)	±	+	+		−	
Ki67 index	Moderate	Moderate	High	Low	Low	

Note: Select references were used to compile these data (Bentley 2003; Hui et al. 2014; Kalhour et al. 2009; Kommoss et al. 2001; Shih, Seidman, and Kurman 1999; Shih and Kurman 2004; Yokouchi et al. 2011). ETT = epithelioid trophoblastic tumor; PSTT = placental site trophoblastic tumor; CC = choriocarcinoma; PSN = placental site nodule.

Table 1. Immunohistochemical staining properties of trophoblastic diseases.[5]

The moderator mentioned that based on the thickness of the uterus, the endometrium is likely hyperplastic (a change of little significance in this particular slide).

References:

1. Braga A, Mora P de Melko AC, Noguieria-Rodrigues A, Amim Junior J, Resenda-Filhon J, Seckl MJ. Challenges in the diagnosis and treatment of gestational trophoblastic neoplasia worldwide. *World J Clin Oncol* 2019; 10(2):28-37.
2 Chu D, Shih IM, Knezevich M, Sheth S: Uterine epithelioid trophoblastic tumor in an African green monkey (Chlorocebus aethiops sabaeus). *J Am Assoc Lab Anim Sci* 2007:46(2)**:**92-96.
3 Cline JM, Wood CE, Vidal JD, Tarara RP, Buse E, Weinbauer GF, et al.: Selected Background Findings and Interpretation of Common Lesions in the Female Reproductive System in Macaques. *Toxicologic Pathology* 2008:36(7)**:**142S-163S.
4 Cooper TK, Shih IM, Gabrielson KL: Uterine epithelioid trophoblastic tumour in a red-tailed guenon (Cercopithecus ascanius). *J Comp Pathol* 2005:133(2-3)**:**218-222.
5. Elmore SA, Carreira V, Labriola CS et a. Proceedings of the 2018 National Toxicology Program Satellite Symposium. *Toxicol Pathol* 2018; 46(8)865-897.
6. Farman CA, Benirschke K, Horner M, Lappin P: Ovarian choriocarcinoma in a rhesus monkey associated with elevated serum chorionic gonadotropin levels. *Vet Pathol* 2005:42(2)**:**226-229.
7. Giusti AM, Terron A, Belluco S, Scanziani E, Carcangiu ML: Ovarian epithelioid trophoblastic tumor in a cynomolgus monkey. *Vet Pathol* 2005:42(2)**:**223-226.
8.. Lucas R, Cunha TM, Santos FB. Placental site trophoblastic tumor: a case report and review of the literature. *Obstet Gyn Radiol* 2015; 9(4):14-22
9.. Luiza JW, Taylor SE, Gao FF, Edwards RP: Placental site trophoblastic tumor: Immunohistochemistry algorithm key to diagnosis and review of literature. *Gynecol Oncol Case Rep* 2014:7**:**13-15.
10. Marbaix E, Defrere S, Duc KH, Lousse JC, Dehoux JP: Non-gestational malignant placental site trophoblastic tumor of the ovary in a 4-year-old rhesus monkey. *Vet Pathol* 2008:45(3)**:**375-378.
11. Shih IM, Kurman RJ. Epithelioid trophoblastic tumor: a neoplasm distinct from choriocarcinoma and placental site trophoblastic tumor simulating carcinoma. *Am J Surg Pathol* 1998; 22(11):1393-1403.
12. Silverberg SG, Kurman RJ. Gestational trophoblastic disease. *In:* Atlas of Tumor Pathology, Vol 3. Tumors of the Uterine Corpus and Gestational Trophoblastic Disease. ARP Press, Washington D.C. 1991,
13. Stevens FT, Katzorke N, Tempfer C, Kreimer U, Bizjak GI, Fleisch MC, et al.: Gestational Trophoblastic Disorders: An Update in 2015. *Geburtshilfe Frauenheilkd* 2015:75(10)**:**1043-1050.

14. Sunish Mohanan JC, Nancy Kock, Hermina Borgerink, Justin Vidal, Ross Tarara, J. Mark Cline. : Uterine Trophoblastic Tumors in Cynomolgus Macaques (Macaca fascicularis). Poster: Wake Forest School of Medicine.
15. Toyosawa K, Okimoto K, Koujitani T, Kikawa E: Choriocarcinoma and teratoma in the ovary of a cynomolgus monkey. *Vet Pathol* 2000:37(2)**:**186-188.
16. *Williams Gynecology, Third Edition*: McGraw-Hill Education, 2016. https://accessmedicine.mhmedical.com/book.aspx?bookID=1758

CASE IV: TAMU 2017 WSC 2 (JPC 4102428).

Signalment: 7-year-old, American Quarter Horse mare, *Equus ferus caballus*

History: Four weeks prior to presentation at the end of April, this working Quarter Horse mare had had a tooth extraction under anesthesia. Approximately 2 weeks prior to presentation, the horse became dyspneic with a nasal discharge and coughing. She was treated with Uniprim (trimethoprim and sulfadiazine) without resolution, and at 5 days before presentation, her treatment was switched to doxycycline, banamine and Previcox (NSAID's Cox-2 inhibitor). Because the dyspnea worsened, she was taken to a veterinarian, and she was found to be febrile (103.6F) and severely dyspneic. She was referred to TAMU, and at presentation, the mare continued febrile, and dyspneic with a bilateral nasal discharge. Ultra sound showed bilateral consolidation with a flocculent, pleural effusion especially on the right where a hypoechoic fluid pocket at the level between ribs 9-15 in which gas was trapped was noted.

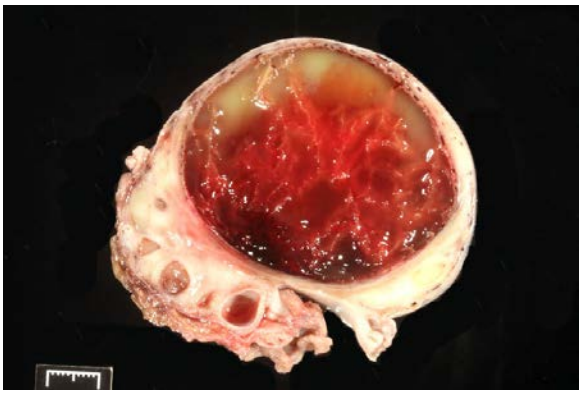

Ovary, horse. The left ovary weighed 268g and had a 4.6x4.6x5.2 cyst with a 1.5mm wall and hemorrhagic gelatinous content. (Photo courtesy of: Texas A&M University, College of Veterinary Medicine and Biomedical Sciences http://vetmed.tamu.edu/vtpb.)

The chest drains were lavaged daily, and the mare receive LRS fluids, antibiotics (gentamicin then chloramphenicol) and antiinflammatories; however, the lesion and signs progressed, and she was euthanized after 3 days of hospitalization

Gross Pathology: A 422 kg (929 lb) seven-year-old, red roan, Quarter Horse mare with a white sock on the right hind and in adequate body condition is necropsied on April 27, 2017.

INTEGUMENTARY/SPECIAL SENSES: Shaved areas include: 10x10cm on the right mid thorax and 10x10 cm on the right side of the mid-cervical neck. A 3 cm, linear, superficial abrasion is caudal to the right eye.

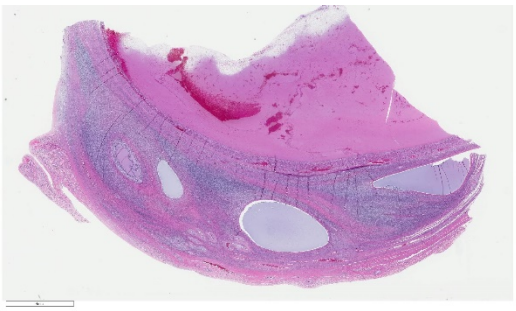

Ovary, horse. A section of ovary with a hemorrhagic cyst at top and normal ovary with visible primary and secondary follicles in the adjacent normal ovary. (HE 7X) (Photo courtesy of: Texas A&M University, College of Veterinary Medicine and Biomedical Sciences http://vetmed.tamu.edu/vtpb.)

RESPIRATORY: Approximately 5 L of yellow to grey, turbid fluid are in the pleural cavity, and a large amount of yellow, friable material is admixed with the fluid and firmly adhered to the lung (fibrinopurulent pleuritis). Diffusely, the costal and diaphragmatic pleura are dark red and markedly thickened (reactive mesothelium). The ventral lungs are diffusely firm and dark red (bronchopneumonia). In the middle of the right lung is a focal, 10x10x15 cm cavitation that connects to bronchi and contains a large amount of tan, casts of grey red, moist, friable material (Aspiration Pneumonia with sequestrum formation).

CARDIOVASCULAR (Heart weight: 4.19 kg; Right ventricular wall: 1 cm; Left ventricular wall: 3 cm): The pericardium is markedly and irregularly thickened and dark red (reactive mesothelium). The right side of the heart is mildly thickened (hypertrophy, pulmonary hypertension).

ENDOCRINE: A 1.5x0.5 cm, raised, pink to grey, mass is in the pituitary gland (pituitary adenoma, presumed).

GENITAL: The left ovary (268 g) is oval with a 4.6X4.6X5.2 cm cyst having a 1-2 mm-thick, yellow wall and containing a yellow and red, fibrillary and gelatinous content (submitted).

INTEGUMENTARY/SPECIAL SENSES, **MUSCULOSKELETAL**, **HEMIC & LYMPHATIC URINARY** (Right kidney weight: 1.47 kg; Left kidney weight: 1.56 kg),

DIGESTIVE, **LIVER/PANCREAS** (Liver weight: 9.1 kg), **NERVOUS** (Brain weight: 550 g): No significant findings.

Laboratory results: Hyper-gammaglobulinemia: globulins 5.4g/dL (92.2-3.8g/dL)
Mature neutrophila PMN 10,153/uL (2260-8580/uL)
Monocytosis 1287/uL (0-1000/uL)
Hyperfibrinogenemia 700mg/dL (100-400 mg/dL)
Thoracocentesis/trans-tracheal wash culture: Streptococcus zooepidemicus 4+, Bacteroides pyogenes 2+ and Fusobacterium spp. 4+

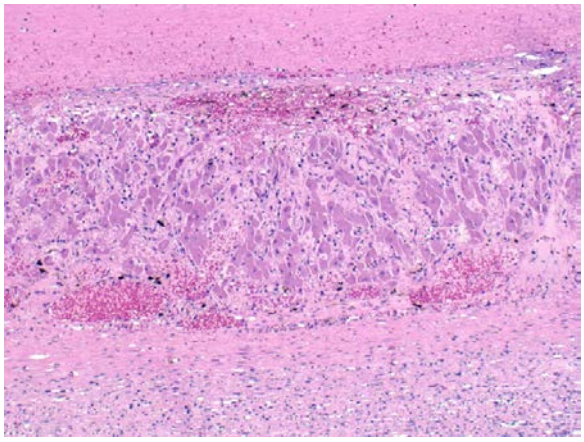

Ovary, horse. The wall of the cyst contains an inner layer of fibrovascular tissue and a thicker outer layer of well-vascularized luteinized thecal cells. (HE 100X) (Photo courtesy of: Texas A&M University, College of Veterinary Medicine and Biomedical Sciences http://vetmed.tamu.edu/vtpb.)

Microscopic Description: Ovary: The section consists of a border of ovarian capsule with a zone of ovarian cortex/stroma containing an occasional egg, various developing and atretic follicles and many hilar vessels. Below this cortical tissue is a band of normal fibromuscular ovarian stroma that ends as a discrete cyst. Moving centripetally into the cyst Is a 5-15 luteal cell-thick lining in a fine, well vascularized stroma and with an inner thin layer of fibrous connective tissue. The central portion of the cyst has pools of free erythrocytes with fine, poorly organized fibrin and fibrillary material. The vessels in the luteal tissue are engorged and several have paucicellular, homogeneous walls (necrosis) with occasionally partial thrombosis. Luteal tissue has some siderophages, but most dark pigment seen is acid hematin. Occasional sections have a hilar artery with segmental, mild, mononuclear cell cuffing.

Contributor's Morphologic Diagnosis: Ovarian luteal cyst (Hemorrhagic anovulatory follicle-derived)

Contributor's Comment: This is an example of a hemorrhagic anovulatory follicle in the progression of becoming a luteal cyst. Hemorrhagic anovulatory follicles (HAFs) are a common but rarely described lesion seen in equine necropsies and equine biopsy submissions. It is odd that their description is not in veterinary pathology texts.

HAF's are an "event" described in the current veterinary literature by theriogenologists as a major cause of equine infertility [1,2,3,4,5,6] and most recently in human medicine as a model for women's luteinized, unruptured-follicle syndrome.[1] This "event" must be discussed in view of the horse's reproductive physiology, because the HAF is similar if not identical to the transitional follicle, an ovarian structure considered normal during the physiologic anovulatory period of the mare during winter's short photoperiod. Our case occurred at the end of April. The structure should be discussed with an understanding of the equine corpus hemorrhagicum (CH) and corpus luteum (CL). The CH and CL are triangular structures with the apex angled toward the ovulation fossa, and the CH fills in rapidly and usually completely to form a CL [5,7] after ovulation and without significant fibrosis. Theriogenologists know HAFs are a common, if not the most common, lesion associated with anovulation and occur in 5-25% of mares during the breeding season.[2.3.4.5.6] In ultrasound of HAFs, the follicular fluid has echogenic foci and swirling fibrin-like strands. Macroscopically on section, the hemorrhagic center is characteristically mottled yellow red,

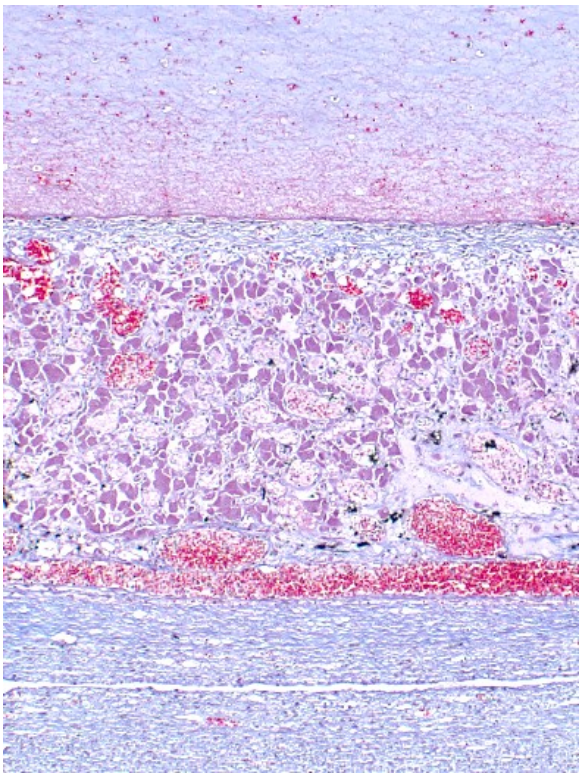

Ovary, horse. A Masson's trichrome demonstrates the amount of collagen within the inner layer and exterior to the cyst wall. (HE 100X) (Photo courtesy of: Texas A&M University, College of Veterinary Medicine and Biomedical Sciences http://vetmed.tamu.edu/vtpb.)

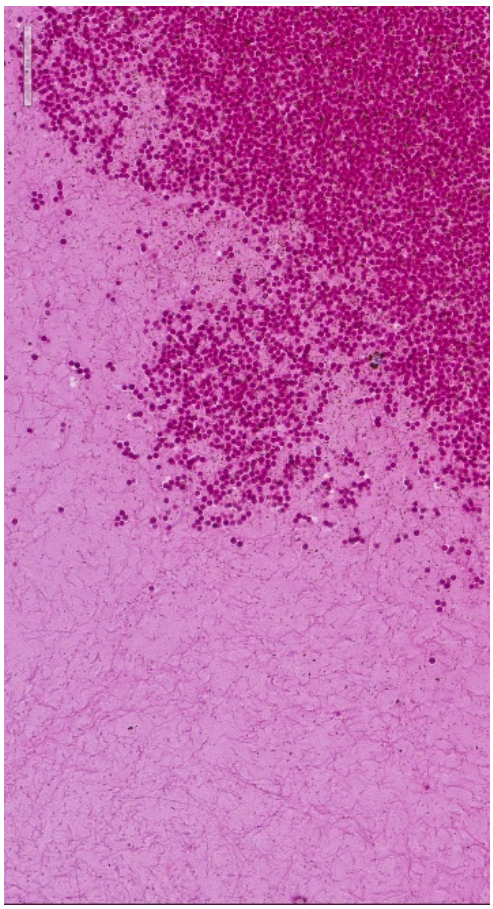

Ovary, horse. The cyst contents are composed primarily of eosinophilic protein, some polymerized fibrin, and hemorrhage. (HE 100X) (Photo courtesy of: Texas A&M University, College of Veterinary Medicine and Biomedical Sciences http://vetmed.tamu.edu/vtpb.)

somewhat gelatinous and obviously different from a clot or thrombus. The blood does not flow out of an HAF when it is sectioned. Nor do you see characteristic layering of a large thrombus. Some mares will have several HAFs in a breeding season, and some mares are more predisposed to having them. They are more frequent in old mares. Although, like transitional follicles, HAFs are not treated routinely, some work has been done to discover how to induce them in order to understand the natural pathophysiology of the HAF in the breeding season. Variable success at inducing HAFs has been achieved with administration of prostaglandin, LH and NSAIDs using various regimen. Most recently, dosing mares with the COX-2 inhibitor, flunixin meglumine, resulted in 100% HAF induction.[1]

When do veterinary pathologists see them? They are common in necropsies of mares with chronic bacterial diseases (like this case) and in cases of endotoxemias and colics. Interestingly, they appear in biopsy services as specimen from ovariectomies where they clinically are diagnosed granulosa cell tumors by rDVM's. In such biopsy cases, history of an episode of colic in the previous 10 days is common/predictable. One can certainly think that products of sepsis and endotoxemias could both disrupt adenohypophyseal hormone release and generate interleukins and prostaglandins with the result of an anovulation. Most recently, our lab also sees them in ovaries coincident with abscesses induced by follicular aspirations, an increasingly common manipulation.

Are HAFs related to luteal cysts? The luteal tissue is well-vascularized and with DIC, hemorrhage accumulates in follicles that do not ovulate. Had the mare of this case survived, the hemorrhage would have increased due to the vascular lesions you see in the luteal wall. Follicle-sized cysts later form larger, spherical, blood-filled luteinized cysts. It is a rare ovarian hematoma that does not have a luteinized wall.[a]

The old mantra was that "cystic ovarian disease as described in the cow does not occur in the mare",[7] but there may be more similarities than previously believed. This is a case of an HAF progressing into a luteinized cyst and/or ovarian hematoma, but looked at from a pathologist's perspective and taken from a necropsy case.

Contributing Institution:

Texas A&M University, College of Veterinary Medicine and Biomedical Sciences (Departmental Web site address)**:** http://vetmed.yamu.edu/vtpb

JPC Diagnosis: Ovary: Hemorrhagic luteal cyst (hemorrhagic anovulatory follicle OK)

JPC Comment: The contributor brings up excellent points on a fairly common cause of ovulation failure in older mares that rarely merits more than a line in most pathology texts. This lesion is a rarity in most surgical biopsy practices as especially as it is often successfully treated with prostaglandin therapy. It is most often seen as an incidental finding at autopsy, especially in animals dying suddenly of other causes.

Anovulatory hemorrhagic follicles (AHF), also known as persistent anovulatory follicles, will grow (especially during transition phases of spring and autumn) but fail to rupture, and has been estimated to occur between 4.4-13% of all ovulations in mares, with the higher percentages seen in older mares.[4]

While the true cause of this lesion is not known, quite a few theories abound as to its development. These include: a) insufficient gonadotrophic stimulation to induce ovulation; b) reduced follicular secretion of estrogen; c) physical blockage of passage of the developing follicle to the ovarian fossa; d) aberrant production of matrix metalloproteinases, required for tissue remodeling during ovulation and corpus luteal production, or e) overuse of ovulation-stimulating drugs, or f) abnormalities in angiogenesis during corpora lutea formation, or vascular regression during luteolysis.[4]

This slide is an excellent example of an AHF, with the characteristic wall consisting of a thin inner fibrovascular layer and a thicker outer layer of luteinized cells which is heavily vascularized and may be the source of significant ovarian hemorrhage which may be life-threatening. Immunohistochemistry

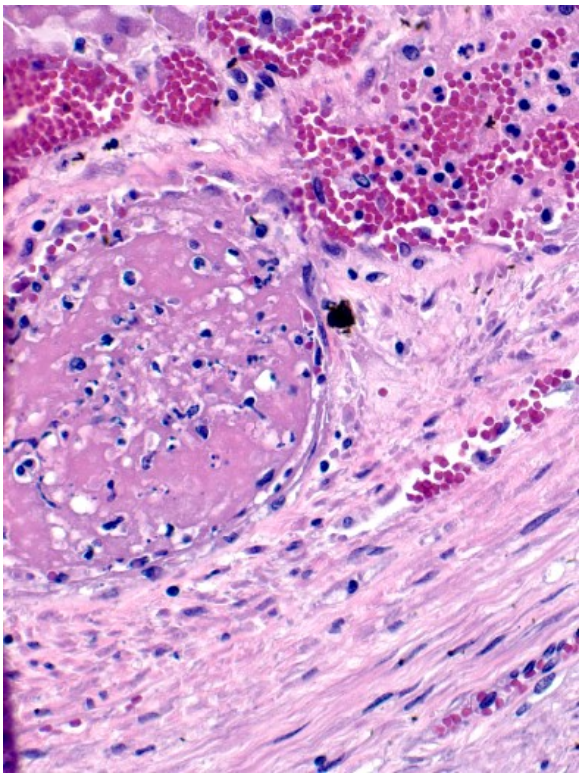

Ovary, horse. Multiple vessels within the luteinized thecal layer are thrombosed. (HE 400X). (Photo courtesy of: Texas A&M University, College of Veterinary Medicine and Biomedical Sciences http://vetmed.tamu.edu/vtpb.)

is not generally necessary for diagnosis, but these follicles often express an immunohistochemical profile similar to normal luteinized cells of corpora hemorrhagica and corpora lutea, with the exception of a decreased expression of Flk-1, a receptor for vascular endothelial growth factor (VEGF).[4]

The moderator commented briefly on the presence of thrombosed capillaries within this layer of luteinized cells surrounding the HAF, ascribing the thrombosis to the sepsis seen in this horse rather than the degeneration of the HAF itself.

References:

1. Bashir ST, Gastal, MO,Tazawa SP, Tarso SGS, Hales DB, Cuervo-Arango J, Baerwald

AR, Gastal EL. The mare as a model for luteinized unruptured follicle syndrome: intrafollicular endocrine milieu. Reproduction 2016 151: 271-83.
2. Cuervo-Arango J, Newcombe JR. Risk Factors for the Development of Haemorrhagic Anovulatory Follicles in the Mare. Reprod Dom Anim 2010 45:473–480.
3. Cuervo-Arango J, Newcombe JR. Ultrasound Confirmation of Ovulation in Mares: A Normal Corpus Luteum or a Haemorrhagic Anovulatory Follicle? Reprod Dom Anim 2013 48:105-11.
4. Ellenberger C, Muller K, Schoon H-A, WilsherSR, Allen WR. Histological and Immunohistochemical Characterization of Equine Anovulatory Haemorrhagic Follicles (AHFs). 2008.44:395-405.
5. Ginther OJ, Gastal EM, Gastal MO, Beg MA. Incidence, Endocrinology, Vascularity, and Morphology of Hemorrhagic Anovulatory Follicles in Mares. J EQ Vet Sci 2007 27:130-139.
6. McCue PM, Squires EL. Persistent anovulatory follicles in the mare. Theriogenol 2002. 58:561-43.
7. Roberts SJ. Veterinary Obstetrics and Genital Diseases (Theriogenology). 1986 David and Charles Inc. North Pomfret, VT, pp 585- 587.
a. JF Edwards Platform Presentation: "Transitional ("Autumn") Follicles in the Mare." 39th Annual Meeting Am. College of Veterinary Pathologists, Kansas City, MO, 11-3-1988.

Self-Assessment - WSC 2019-2020 Conference 8

1. What is the normal duration of uterine involution of the canine uterus?
    a. 2-4 weeks
    b. 8-10 weeks
    c. 12-15 weeks
    d. 20-24 weeks

2. Which of the following is the best histochemical stain for *Coxiella burnetii*?
    a. Gram
    b. Twort's
    c. Machiavello
    d. Gimenez

3. Which of the following has not been identified as a potential source of *C. burnetii* for humans?
    a. Pet birds
    b. Ticks
    c. Fish
    d. Reptiles

4. Which of the following is the predominant cell type in choriocarcinoma?
    a. Neoplastic epithelial cell
    b. Uterine stroma
    c. Trophoblast
    d. Chorionic epithelium

5. Admininstration of which of the following will result in the formation of a hemorrhagic anovulatory follicle?
    a. Prostaglandin
    b. COX-2 inhibitor
    c. Estrogen
    d. Progesterone

Please email your completed assessment for grading to Dr. Bruce Williams at bruce.h.williams12.civ@mail.mil. Passing score is 80%. This program (RACE program 33611) is approved by the AAVSB RACE to offer a total of 0.5 CE Credits, with a maximum of 12.5 CE Credits being available to any individual Veterinary Medical Professionals for the 2019-2020 Wednesday Slide Conference. This RACE approval is for the subject matter categories of: SCIENTIFIC using the delivery method of NON-INTERACTIVE DISTANCE. This approval is valid in jurisdictions which recognize AAVSB RACE.

Joint Pathology Center
Veterinary Pathology Services

WEDNESDAY SLIDE CONFERENCE 2019-2020

C o n f e r e n c e 9

30 October 2019

Conference Moderator:
Frederic Hoerr, DVM, MS, PhD
Veterinary Diagnostic Pathology, LLC
638 South Fort Valley Road
Fort Valley, Virginia, 22652 USA

CASE I: WSC18-19 #1 (JPC 4117005).

Signalment: Three-year-old Peahen (*Pavo cristatus*)

History: A reportedly three-year-old peahen was presented deceased for necropsy examination following a weeklong history of being lethargic with no mobility in her legs. She was eating and drinking well. The peahen had whitish diarrhea few days before death. The other 11 birds in the group were acting normally.

Gross Pathology: The bird was in good body condition with adequate pectoral muscling. Diffusely, the pericardial sac was mildly thickened by a large amount of white chalk-like material which was adhered to its surface. The kidneys appeared pale and on cut section, there was white granular material throughout the renal parenchyma.

The inner wall of the coelomic cavity and the surfaces of the visceral organs including the liver and abdominal air sacs were covered in small quantities of fine white powder-like material. The duodenal contents were mixed with white granular material throughout.

Liver, heart, peahen. Diffuse thickening of pericardium and pinpoint lesions on liver consistent with urate deposition. (Photo courtesy of: Kansas State University Veterinary Diagnostic Laboratory/Dept. of Diagnostic Medicine/Pathobiology, http://www.ksvdl.org)

The right stifle joint had significant sub-capsular hemorrhage that extended into the adjacent muscle. Subcutaneously and intramuscularly along the medial aspect of the left tibiotarsus were extensive dark red areas (hemorrhage).

No significant gross lesions were seen in the oral cavity, trachea, lungs, esophagus, crop, proventriculus, gizzard, jejunum, caecum, colon, uterus, ovaries, liver, lymph nodes, spleen or brain.

Laboratory results: The pooled liver and kidney sample was positive for Marek's disease virus by real-time PCR.

Microscopic Description: Liver: Diffusely, the normal hepatocellular architecture is disrupted by an accumulation of large numbers of medium to large sized lymphocytes and lymphoblasts that moderately expand the sinusoidal spaces. The pleomorphic lymphoid cells are more concentrated around the central veins (centrilobular area). These lymphoid cells contain small to moderate amounts of basophilic to amphophilic, homogenous cytoplasm with round to oval nuclei with coarsely stippled chromatin and indistinct nucleoli. Approximately 20-25% of the neoplastic lymphocytes appear degenerate with fragmented nuclei that appear as basophilic pyknotic bodies of variable sizes. Similar lymphoid infiltrates were present in the kidneys, proventriculus, ventriculus, small intestine, ceca, spleen, ovary, and globes.

Immunohistochemistry:
Immunohistochemical staining showed strong positive reactivity of the lymphocytes for CD3 and negative for CD20 and CD79a.

Contributor's Morphologic Diagnosis:
Liver: Lymphoid infiltration, diffuse, severe, with scattered hepatocyte necrosis.

Liver, peahen. A section of liver is submitted for examination. Even at low magnification, a retiform pattern of cellular infiltration, especially prominent in proximity to blood vessels is evident. (HE, 7X)

There are approximately 3-5 mitotic figures per HPF (400X). Multifocally, the hepatocytes are mildly compressed by the infiltrating lymphoid cells and occasionally few hepatocytes show single cell necrosis with hypereosinophilic cytoplasm, pyknotic nuclei, and a clear space around them.
Contributor's Comment: Liver: Diffusely, the normal hepatocellular architecture is disrupted by an accumulation of large numbers of medium to large sized lymphocytes and lymphoblasts that moderately expand the sinusoidal spaces. The gross lesions of visceral gout with deposition of urates on the heart, liver, and kidneys were most likely the result of impaired renal function caused by infiltration of neoplastic lymphocytes. Many neoplastic diseases in poultry are caused by viral etiologies. A list of the viral induced neoplastic diseases seen in poultry are provided in Table 1.

Table 1: Transmissible neoplasms [2].			
Virus type	Nucleic acid type	Virus classification of etiological agent	Neoplastic diseases
Retrovirus	RNA	Leukosis/sarcoma Group	**Leukoses** Lymphoid leucosis Erythroblastosis Myeloloblastosis **Sarcomas and other connective tissue tumors** Fibrosarcoma, fibroma Myxosarcoma, myxoma Osteogenic sarcoma, osteoma Histiocytic sarcoma Related neoplasms Hemangioma Nephroblastoma Hepatocarcinoma Osteopetrosis
		Reticuloendotheliosis Group (REV)	Reticuloendotheliosis Lymphoid leucosis
Herpesvirus	DNA	Marek's disease virus	Marek's disease

(Table adapted from Swayne DE, ed., *Diseases of Poultry* 2017.)

Confirmatory diagnosis of the visceral form of Marek's disease requires histopathological examination, identification of MDV, by PCR and/or demonstration of MATSA antigen on tumor cells by immunohistochemistry.

Marek's disease is a cell-associated lymphoproliferative disease that is commonly seen in domestic chickens and less commonly in other birds. This is believed to be the first report of Marek's disease in this species of peafowl. A novel herpesvirus that was most closely related to gallid herpesvirus-3 was previously reported in three peafowls that had hepatocellular necrosis with intranuclear eosinophilic inclusions.[9]

The causative agent of Marek's disease, gallid herpesvirus 2, belongs to the genus *Mardivirus*, subfamily: Alphaherpesvirinae and family: Herpesviridae. The genus *Mardivirus* consists of different serotypes: Serotype 1 MDV (gallid herpesvirus type 2), Serotype 2 MDV (gallid herpesvirus type 3) and Serotype 3 herpesvirus of turkeys (meleagrid herpesvirus type 1). Serotypes 2 and 3 are non-oncogenic.[7] The serotype-1 MDV consists of Marek's disease virus of varying pathogenicity based on which they are classified as mild (mMDV), virulent (vMDV), very virulent (vvMDV) and very virulent + (vv+MDV).[8] Clinical signs can occur in chickens as early as 4 weeks of age and are commonly seen in birds between 12 and 24 weeks of age. The disease occurs in four distinct syndromic forms:[7]

1) Classical form: Mainly characterized by neurological signs with partial or complete

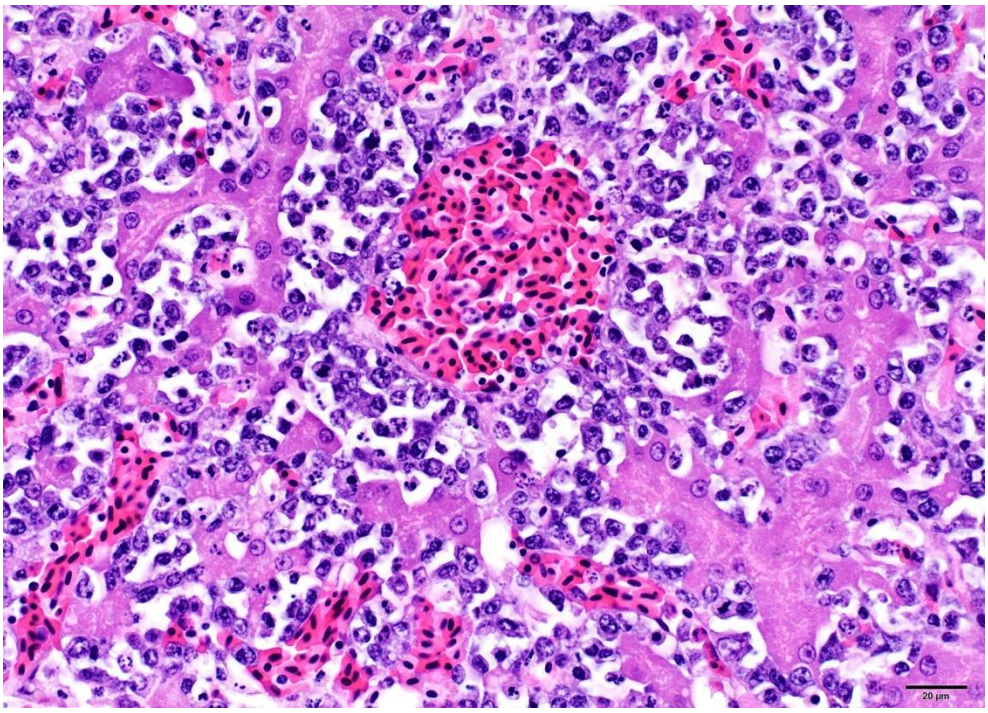

Liver, peahen. Neoplastic lymphocytes fill hepatic sinusoids around a central vein with mitotic figures and evidence of cellular necrosis. Several mitotic figures and numerous apoptotic cells are present within the neoplastic population. Neoplastic cells are also present within the lumen of the central vein. (H&E, 400X) (Photo courtesy of: Kansas State University Veterinary Diagnostic Laboratory/Dept. of Diagnostic Medicine/Pathobiology, http://www.ksvdl.org)

paralysis of legs and wings. Other common clinical signs include torticollis, dilation of crop, gasping, and respiratory distress depending on the nerves affected.

2) Acute form: Involves the formation of lymphomas in the visceral organs causing anorexia, depression, weight loss, and diarrhea.

3) Acute cytolytic form: Commonly seen in infections caused by vvMDV strains. It is characterized by high mortality with severe atrophy of lymphoid organs.

4) Transient paralysis: This is an uncommon form that lasts for about 24-48h and is usually associated with edema of the brain causing varying degrees of ataxia, paresis or paralysis of the legs, wings and neck.

Following infection by direct or indirect aerosol route through inhalation of cell-free virus particles within feather dander, the pathogenesis of MDV is very complex and is influenced by the age, immune status, and genetic susceptibility. MD pathogenesis is characterized by four phases:[3,10]

1) Early cytolytic phase: seen within 2-7 days post infection (dpi). Initial infection of lung epithelial cells and production of viral Interleukin-8 (vIL-8) recruits the innate immune cells resulting in infection of macrophages and B-cells. By as early as 24 hr pi, the macrophages and dendritic cells can disseminate the virus from lungs to B cells and CD4+ T cells in the bursa of Fabricius, spleen, and thymus. During the cytolytic phase, large numbers of B-cells within the spleen along with CD4+ T cells in cecal tonsils undergo apoptosis and contribute to immunosuppression. A semi productive lytic viral replication in B cells and production of vIL-8 leads to recruitment and infection of T-cells which then leads to viremia and systemic spread of infection.

2) Immune evasion and latency phase: occurs between 7-10 dpi. MDV integrates into the genome of the infected CD4+ T cells leading to immune evasion and establishment of latency.

3) Cutaneous infection, replication and shedding: latently infected CD4+ T cells migrate to cutaneous feather follicles, where

they infect the feather follicle epithelium. The resulting fully productive viral replication causes syncytia formation, and secretion of mature virions in skin dander. Aggregates of small lymphocytes with intranuclear inclusions can be seen in perifollicular areas by 7 dpi. These lymphoid aggregates develop into either cutaneous tumors or degenerate to form necrotic foci.

4) Proliferative phase: occurs around 28 dpi and is characterized by formation of CD4+ T cell visceral lymphoma. Meq (Marek's EcoQ) gene has been shown to be important for transformation and Meq protein is consistently expressed in lymphoma cells and tumor cells[5]. The infection in transformed cells is nonproductive.

The two important and most common lymphomatotic diseases are Marek's disease and lymphoid leukosis (ALV) differential diagnosis of the two is confusing. Table 2 describes the important features for their differential diagnosis.

Table 2: Gross and microscopic features for differential diagnosis of Marek's disease and lymphoid leukosis[1]

Feature	**Marek's disease**	**Lymphoid leukosis**
Age	Few days to many weeks	Not less than 16 weeks
Clinical signs	Frequent paralysis	Nonspecific
Incidence	Usually more than 5% in unvaccinated flocks	Rarely more than 5% of infected flocks
Gross lesions		
Neural enlargement	Frequent	Absent
Bursa of Fabricius	Diffuse enlargement or atrophy	Nodular tumors
Proventriculus, skin and muscle tumors	May be present	Usually absent
Microscopic lesions		
Neural involvement	Frequent	Absent
Cytology of tumors	Usually pleomorphic lymphoid cells consisting of lymphoblasts, small, medium and large lymphocytes and reticulum cells	Lymphoblasts of uniform morphology, usually of clonal origin
Category of neoplastic lymphoid cell involved	T lymphocyte	B lymphocyte

(Table adapted from Pattinson M et al., *Poultry Diseases* 2008.)

Marek's disease virus is transmitted horizontally only, and appropriate hygiene precautions and vaccination can prevent its spread in hatching eggs and day-old chicks. ALV and REV can be transmitted both horizontally and vertically and avian leukosis and REV can be controlled by virus eradication at the primary breeding level.

Gross Pathology: The presence of enlarged peripheral nerves and/or visceral lymphomas are commonly seen in Marek's disease, but these lesions are not pathognomonic[9]. Some of the commonly seen lesions include: 1) Enlargement of peripheral nerves (brachial, sciatic and coeliac plexus, abdominal vagus,

and intercostal nerves) with loss of cross-striations and glistening appearance. The affected nerves are edematous and greyish or yellowish in appearance. 2) Development of lymphoid tumors in visceral organs of birds less than 16 weeks of age. 3) Discoloration of the iris and irregularity of the pupil. 4) Lymphomas in the skin around feather follicles.

Microscopic lesions: Affected nerves and visceral tumors contain mixed populations of small to large lymphocytes, lymphoblasts, plasma cells, and macrophages. The peripheral nerves affected in classical and acute forms show three types of lesions: A-type lesions (proliferative type) is characterized by infiltration of proliferating lymphoblasts, small to large lymphocytes, and macrophages; B-type lesion (inflammatory type) is characterized by edema and infiltration of small lymphocytes, plasma cells with proliferation of Schwann cells; C-type lesion (minor infiltrative type) is characterized by mild scattering of small lymphocytes and plasma cells, generally seen in birds with no clinical signs or gross lesions. The proportion of different cell types varies with stage of disease and virulence of the virus with aggressive lymphomas containing of a higher proportion of lymphoblasts.

Immunohistochemistry characteristics: MD tumor cells commonly express MHC-II and T cell markers such as CD4. 5-40% of the tumor cells express MATSA, less than 5% of the cells express IgM. Viral antigens pp38[4] and meq can be detected in tumor cells[5] by immunohistochemistry, fluorescent antibody tests or *in situ* hybridization.[10]

Contributing Institution:
North Carolina State University College of Veterinary Medicine

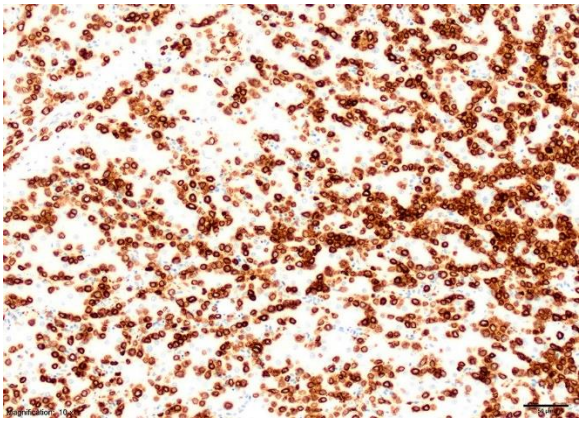

Liver, peahen. Neoplastic lymphocytes stain strongly positive for CD3. (anti-CD3, 200X) (Photo courtesy of: Kansas State University Veterinary Diagnostic Laboratory/Dept. of Diagnostic Medicine/Pathobiology, http://www.ksvdl.org)

JPC Diagnosis: Liver: Lymphoma, large cell.

JPC Comment: The contributor has done an excellent job in reviewing Marek's disease, one of the most common neoplastic diseases of poultry (and unusual in the fact that it is caused by an alphaherpesvirus (avian alphaherpesvirus-2) rather than a gammaherpesvirus (lymphocryptovirus, rhadinovirus) which is more typical of herpesvirus-driven oncogenesis.)

Joszef Marek (1868-1952) was a noted Hungarian veterinarian, professor of pathology, and ultimately director of the veterinary school in Budapest. In 1907, he first described a peculiar neurological disease which he noticed in his backyard chickens, causing drooping of the wings, and paresis (and ultimately paralysis) of the legs. His multivolume textbook on animal pathology and therapeutics, written at the turn of the century with colleague F. Hutyra, was translated into numerous languages and enjoyed great popularity for decades. He discovered the use of ditrol to control liver flukes, and was awarded the Hungarian Kossuth prize for science in 1949.

Two reports (2016 and 2018) have also described Marek's disease in peafowl – one in the Indian peafowl (*Pavo cristatus*)[2] more commonly known as the "peacock" and one in a green or Javan peafowl (*Pavo muticus)*[8]. Both reports, which describe the pathologic features as well as immunophenotyping of the neoplastic lymphocytes and identification of Marek's disease virus Serotype 1 by PCR, share a number of similarities with this case, including the presence of disease in adult birds.[2,8]

The contributor lists a number of causes of lymphoproliferative disease in poultry, including the common Marek's disease and avian leukosis, the less common avian reticulendotheliosis (a virus that may transform both B and T cells in affected birds), and the relatively unknown retrovirus which causes lymphoproliferative disease in turkeys (with a catchy syndromic name of lymphoproliferative disease in turkeys.)[1,6]

LPDV virus is an exogenous retrovirus which causes lymphoid tumors in some galliforms, especially wild turkeys. The virus was identified first in Europe in the 1970's, and not in North America until 2009.[6] In a study of 800 wild turkeys over a 37 year period,[6] lymphoid neoplasia was seen in approximately 7% of cases, and LPDV virus was identified in over half of those by PCR. In infected birds with neoplastic disease, skin tumors are most common (44%) with liver lesions in 30%. In a few birds in which the lymphocytes were immunophenotyped, the neoplasms appeared to be of T-cell origin, but additional information needs to be performed in this area.[6]

The moderator cautioned on the over interpretation of histologic changes in a single HE slide to differentiated between Marek's disease and lymphoid leukosis. While a positive immunohistochemical test for CD-3 is very helpful in further narrowing the potential diagnosis, definitive diagnosis is still best determined by real-time PCR (performed by the contributor in this case and positive.)

References:

1 Allison AB, Keel MK, Philips JE, Cartoceti AN, Munk BA, Nemeth NM, Welsh TI Thomas JM Crum JM et al. Avian oncogenesis induced by lymphoproliferative dissease virus: a neglected or emerging retrovirual pathogen *Virology* 2014; 450-451:2-12 doi: 10.1016/jvirol 2013.11.037. .

2 Blume GB, Cardoso SP, Oliveira MLB, Maziolli MP, Gomez SYM, Reis Junior JL, Sant Ana FIF, Martins NRS. Visceral Marek's disease in white peafowl (Pavo cristatus). *Arch Bras Med Vet Zootec* 2016:68(6)1602-1608

3 Boodhoo N, Gurung A, Sharif S, Behboudi S: Marek's disease in chickens: a review with focus on immunology. *Veterinary Research* 2016:47(1)**:**119.

4 Gimeno IM, Witter RL, Hunt HD, Reddy SM, Lee LF, Silva RF: The pp38 Gene of Marek's Disease Virus (MDV) Is Necessary for Cytolytic Infection of B Cells and Maintenance of the Transformed State but Not for Cytolytic Infection of the Feather Follicle Epithelium and Horizontal Spread of MDV. *Journal of Virology* 2005:79(7)**:**4545-4549.

5 Nair V: Latency and tumorigenesis in Marek's disease. *Avian Dis* 2013:57(2 Suppl)**:**360-365.

6. Neidringhaus,KD, Nemeth NM, Sellers HS, Brown JD, Fenton HMA. Multicentric round cell neoplasms and their virsal associataions in wild turkeys (Melagris gallopavo) in the southeastern United States. *Vet*

Pathol 2019; doi 10.1177/0300985819864306
7. Pattison PM, Bradbury J, Alexander D. eds., In: *Poultry Diseases*. 6th ed.: Saunders Ltd.; 2008: 258-275.
8. Ranjbar VR, Khordadmehr R. Marke's disease in a peafowl (Pavo muticus); pathological, immunohistochemical and molecular studies. Conference proceedings. *Appr Poultr Dairy Vet Sci:* 2018.
9 Seimon TA, McAloose D, Raphael B, Honkavuori KS, Chang T, Hirschberg D, et al.: A novel herpesvirus in three species of pheasants: Mountain peacock pheasant (Polyplectron inopinatum), Malayan peacock pheasant (Polyplectron malacense), and Congo peafowl (Afropavo congensis). *Veterinary pathology* 2012:49(3)**:**482-491.
10. Swayne DE, ed. Neoplastic Diseases. *Diseases of Poultry*. 13 ed.; 2017.
11. Witter RL: Increased virulence of Marek's disease virus field isolates. *Avian Dis* 1997:41(1)**:**149-163.

CASE II: 2018A (JPC 4134827).

Signalment: 14-day-old, female, SPF chicken (*Gallus gallus*)

History: A 1-day-old chick was inoculated intramuscularly with chicken anemia virus (CAV) that was isolated in Japan in 2017. The bird exhibited petechial hemorrhage of wings on 11 days post inoculation (DPI), depression and dropping wings on 12 DPI, and was found dead on 13 DPI.

Gross Pathology: The bone marrow, spleen and kidney were pale. The thymus was atrophied. The liver was enlarged.

Presentation, chicken. On Day 12 post IM inoculation with chicken anemia agent, the chicken exhibiting petechial hemorrhages and drooping wings. (Photo courtesy of: National Institute of Animal Health, National Agriculture and Food Research Organization (NARO), 3-1-5Kannondai, Tsukuba, Ibaraki 3050856, Japan, (WSC ID95), http://www.naro.affrc.go.jp/english/niah/index.html).

Laboratory results: CAV was reisolated from the liver of the inoculated bird.

Microscopic Description: Bone marrow of tibiotarsus: Hematopoietic cells and erythrocytes were significantly decreased and were replaced by loose connective tissues. Low number of the large atypical cells were scattered in the extravascular spaces. Some of the atypical cells contained one to a few small eosinophilic nuclear inclusion bodies.

Contributor's Morphologic Diagnosis:
Bone marrow: Hypoplasia, severe, with occasional large atypical cells with small eosinophilic intranuclear inclusion bodies.

Contributor's Comment: The chicken anemia virus (CAV) was first detected in Japan in 1979.[18] CAV currently belongs to the *Gyrovirus* genus, Anelloviridae family.[9] CAV is a non-enveloped, icosahedral virus measuring about 19 nm in diameters, with a circular, single-stranded DNA genome.[4,13,18]

Femur, chicken. The bone marrow is extremely pale. (Photo courtesy of: National Institute of Animal Health, National Agriculture and Food Research Organization (NARO), 3-1-5Kannondai, Tsukuba, Ibaraki 3050856, Japan, (WSC ID95), http://www.naro.affrc.go.jp/english/niah/index.html).

Chickens are considered only natural hosts of CAV. CAV is ubiquitous in flocks around the world, and most flocks carry antibodies regardless of vaccination.[10-12,20]

CAV is mainly transmitted vertically through eggs and causes anemia, anorexia and lethargy to chicks.[19,21] Hematocrit values decline less than 10% of normal in severe cases.[3,16] Infection with CAV alone in chickens of 2-week-old or older is subclinical.[16] If clinical signs develops in these chicks, immune depression is suspected.[6]

CAV targets hemocytoblasts in the bone marrow and T lymphoblasts in the thymus cortex, leading to hypoplasia of the bone marrow and atrophy of the thymus lobules.[1,2] Damage to the bone marrow and the lymphatic tissues causes anemia, circulatory failure and low platelets, and which develop the pale colored viscera and hemorrhagic lesions. The liver swelling and atrophy of the bursa of Fabricius can also be seen.[17,18]

Histologic findings include depletion of hematopoietic tissues in the bone marrow and depletion of lymphocytes in the lymphoid tissues.[17] Eosinophilic intranuclear inclusion bodies can be observed in the bone marrow and the thymus of the infected birds.[5] The inclusion bodies are occasionally detected in the spleen, proventriculus, lung, kidney, bursa of Fabricius and skin.[15] CAV infection needs to be differentiated from infectious bursal disease (IBD). Infection of highly pathogenic IBD virus make lesions similar to CAV infection in lymphoid tissues, bone marrow and skeletal muscle.[7,8,14] However, in IBD infection, inclusion bodies are not observed.

Tibia and fibula, chicken. The bone marrow is diffusely and severely hypoplastic. (HE 9X)

Contributing Institution:
National Institute of Animal Health,
National Agriculture and Food Research Organization (NARO)
3-1-5Kannondai, Tsukuba, Ibaraki 3050856, Japan
(WSC ID95)
http://www.naro.affrc.go.jp/english/niah/index.html

JPC Diagnosis: 1. Tibial bone marrow: Necrosis and atrophy, diffuse, severe, with edema and rare hemocytoblastic and osteoclastic intranuclear inclusions.

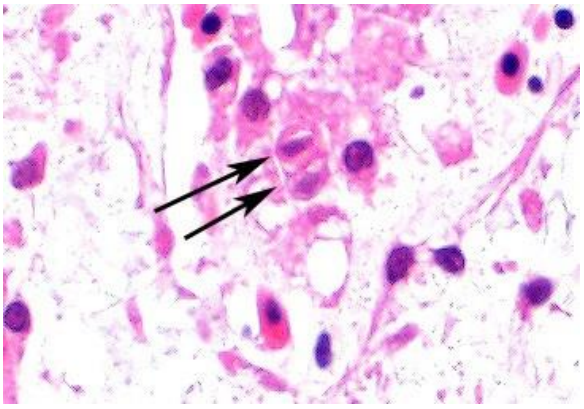

Tibial bone marrow, chicken. Few remaining hematoblasts contain large rhomboid intranuclear inclusions (arrows).

JPC Comment: Chicken anemia agent is a major cause of immunosuppression in young chickens on a global basis, and is often associated with other diseases, such as necrotic dermatitis, hemorrhagic syndrome, aplastic anemia syndrome, and blue wing disease.

This slide is an excellent representation of the changes noted in experimental infections with this agent. Following injection with a virulent strain of CAV, bone marrow cellularity begins to decrease approximately between 4-8dpi.[5,15] Large hematopoietic cells, larger than normal pre-erythroblasts are present within the intra- and extravascular spaces. These cells frequently contain intranuclear inclusions, as do degenerating hematopoietic cells. From days 12-20, (the time period from which this particular slide was collected), there is severe depletion of both erythropoietic and granulocytic cells. Inclusions may be more common seen in osteoclasts during this period, as few hemocytic precursors remain.[5] Similar changes proceed apace along this timeline within the thymus, bursa, and splenic white pulp as well. Intranuclear inclusions may be seen within lymphocytes in all of these tissues.[15]

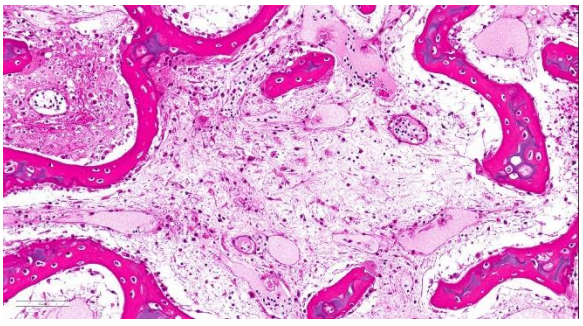

Tibial bone marrow, chicken. Higher magnification of the tibial bone marrow demonstrating the absolute lack of progenitor cells and equally few erythrocytes within blood vessels. (HE 350X).

In surviving birds, the bone marrow and lymphoid begin to repopulate by day 16dpi and day 24 dpi, with tissue recovery by day 32dpi.[15] In one study, 35 of 50 (70%) of inoculated birds succumbed to the disease, mostly between days 14 and 18.[17]

The importance of infection with chick anemia agent is far more than early and permanent immunosuppression in chicks infected within the first few days of life. Earlier in the day, the moderator had presented a lecture on immunosuppressive disease suggesting that a second wave of immunosuppression may be seen in animals infected with chick anemia agents at approximately 18 days of age due to profound thymic atrophy. If injected later, it may also potentiate the effects of other

immunosuppressive agent, such as IBD, resulting in significant immunosuppression and related diseases (reovirus, respiratory disease, clostridiosis, E. coli, coccidosis) in affected birds from 18-35 days.

The assembled participants discussed the difficulty of discerning the intranuclear inclusions in this disease. There was general agreement that they were in hemocytoblasts and osteoclasts, but agreement on what were inclusions and what were degenerating nuclei was more difficult to come by.

References:

1. Adair BM, McNeilly F, McConnell CD, McNulty MS. Characterization of surface markers present on cells infected by chicken anemia virus in experimentally infected chickens. *Avian Dis.* 1993; **37**:943-950.

2. Adair BM. Immunopathogenesis of chicken anemia virus infection. *Dev Comp Immunol.* 2000; **24**:247-255.

3. Campbell TW, Ellis C. Appendices. In: *Avian & exotic animal hematology & cytology.* 3rd ed. Oxford, UK: Blackwell Publishing; 2007:246.

4. Goryo M, Suwa T, Matsumoto S, Umemura T, Itakura C. Serial propagation and purification of chicken anaemia agent in MDCC-MSBI cell line. Avian Pathol. 1987; **16**:149-163.

5. Goryo M, Suwa T, Umemura T, Itakura C, Yamashiro S. Histopathology of chicks inoculated with chicken anaemia agent (MSB1-TK5803 strain). *Avian Pathol.* 1989; **18**:73-89.

6. Imai K, Mase M, Tsukamoto K, Hihara H, Yuasa N. Persistent infection with chicken anaemia virus and some effects of highly virulent infectious bursal disease virus infection on its persistency. *Res Vet Sci.* 1999; **67**:233-238.

7. Inoue M, Fukuda M, Miyano K. Thymic lesions in chicken infected with infectious bursal disease virus. *Avian Dis.* 1994; **38**:839-846.

8. Inoue M, Fujita A, Maeda K. Lysis of myelocytes in chickens infected with infectious bursal disease virus. *Vet Pathol.* 1999; **36**:146-151.

9. International committee on taxonomy of viruses https://talk.ictvonline.org/ictv-reports/ictv_9th_report/ssdna-viruses-2011/w/ssdna_viruses/139/anelloviridae

10. McNulty MS, Connor TJ, McNeilly F, Kirkpatrick KS, McFerran JB. A serological survey of domestic poultry in the United Kingdom for antibody to chicken anaemia agent. *Avian Pathol.* 1988; **17**:315-324.

11. McNulty MS, Connor TJ, McNeilly F. A survey of specific pathogen-free chicken flocks for antibodies to chicken anaemia agent, avian nephritis virus and group a rotavirus. *Avian Pathol.* 1989; **18**:215-220.

12. McNulty MS, Connor TJ, McNeilly F, Spackman D. Chicken anemia agent in the United States: isolation of the virus and detection of antibody in broiler breeder flocks. *Avian Dis.* 1989; **33**:691-694.

13. McNulty MS, Curran WL, Todd D, Mackie DP. Chicken anemia agent: an electron microscopic study. Avian Dis. 1990; **34**:736-743.

14. Nunoya T, Otaki Y, Tajima M, Hiraga M, Saito T. Occurrence of acute infectious bursal disease with high mortality in Japan and pathogenicity of field isolates in specific-pathogen-free chickens. *Avian Dis.* 1992; **36**:597-609.

15. Smyth JA, Moffett DA, McNulty MS, Todd D, Mackie DP. A sequential histopathologic and immune-cytochemical study of chicken anemia virus infection at one day of age. *Avian Dis.* 1993; **37**:324-338.

16. Takagi S, Goryo M, Okada K. Pathogenicity for chicks of six isolation of chicken anemia virus (CAV) isolated in the past two years ('93 '94). *J Jpn Soc Poulf Dis.* 1996; **32**:90-97.

17. Taniguchi T, Yuasa N, Maeda M, Horiuchi T. Hematopathological changes in dead and moribund chicks induced by chicken anemia agent. *Natl Inst Anim Health Q (Tokyo).* 1982; **22**:61-69.

18. Yuasa N, Taniguchi T, Yoshida I. Isolation and some characteristics of an agent inducing anemia in chicks. *Avian Dis.* 1979; **23**: 366-385.

19. Yuasa N, Yoshida I. Experimental egg transmission of chicken anemia agent. *Natl Inst Anim Health Q (Tokyo).* 1983; **23**:99-100.

20. Yuasa N, Imai K, Tezuka H. Survey of antibody against chicken anaemia agent (CAA) by an indirect immunofluorescent antibody technique in breeder flocks in Japan. *Avian Pathol.* 1985; **14**:521-530.

21. Yuasa N, Imai K. Pathogenicity and antigenicity of eleven isolates of chicken anaemia agent (CAA). *Avian Pathol.* 1986; **15**:639-645.

CASE III: 2018A (JPC 4135750).

Signalment: 9-month-old, Ancona hen, *Gallus gallus domesticus*

History: One hen in a flock of 12 was euthanized following a 7-days history of ataxia progressing to unilateral paresis.

Gross Pathology: The bone marrow, spleen and kidney were pale. The thymus was atrophied. The liver was enlarged.

Laboratory results: None performed.

Microscopic Description: At the level of the grossly identified cecal intussusception, the mucosa and submucosa of the intussusceptum are segmentally disrupted by lytic necrosis and granulomatous inflammation. In the areas of necrosis, the mucosa is replaced by a large aggregate of cellular and nuclear debris, fibrin, myriad mixed bacteria, hemorrhage

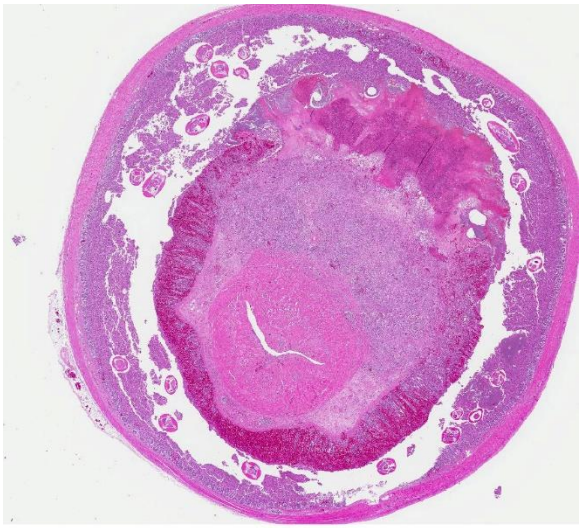

Cecum, chicken. A segment of cecum has telescoped into another, resulting in severe congestion and mucosal hemorrhage within the intussuscipiens. Within the lumen of the intussusceptum, there are numerous cross sections of adult ascarids. (HE, 12X)

and several weakly eosinophilic protozoal trophozoites (histomonads). Trophozoites are round, 7-17 µm diameter, with a single, central, 3 µm diameter nucleus. The underlying lamina propria and submucosa are expanded by abundant macrophages, multinucleated giant cells (foreign body and Langhans-type), lymphocytes, plasma cells, few heterophils, plump fibroblasts (fibrosis), tortuous capillaries (neovascularization), and extracellular and intrahistiocytic trophozoites. The remaining mucosa of the intussusceptum is diffusely expanded by hemorrhage and superficial enterocytes are sloughed. The cecal lumen contains numerous cross and tangential sections of adult, female nematodes and few nematode eggs. The adult nematodes have a thin smooth cuticle, lateral alae, lateral cords, coelomyarian musculature, and a psuedocoelom containing a digestive tract lined by columnar cells with a brush border, a simple esophagus, an ovary, a muscular vagina and a uterus containing ova in various stages of development and few sperm. Intraluminal nematode eggs are oval and ~40 x 60 µm, with a thick smooth shell surrounding a uninucleate zygote. The mucosa of the examined sections of the intussuscipiens is multifocally attenuated, disrupted by autolysis, and the lamina propria is infiltrated by moderate to abundant lymphocytes and plasma cells.

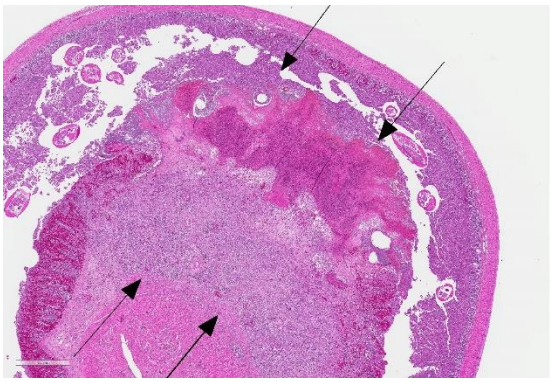

Cecum, chicken. Segmentally, within the intussuscipiens, there is an extensive area of lytic necrosis within the mucosa which expands the submucosa (arrows). (HE, 23X)

Other findings: Lymphocytic meningitis and peripheral neuritis, consistent with Marek's disease.

Contributor's Morphologic Diagnosis:
Cecal intussusception and typhlitis, granulomatous and necrotizing, segmental, subacute to chronic, severe, with adult nematodes (consistent with *Heterakis gallinarum*) and protozoal trophozoites (consistent with *Histomonas meleagridis*)

Contributor's Comment: Blackhead disease (histomoniasis) is caused by the protozoan flagellate *Histomonas meleagridis*. Classically this parasite is transmitted when susceptible species (i.e. gallinaceous birds, ducks, geese, game birds, and zoo birds) ingest *H. meleagridis*-infected ova or adults of the intermediate host, *Heterakis gallinarum* (cecal worm of poultry). In addition to this mode of transmission, turkeys can acquire infection through cloacal contact with contaminated feces and retrograde transport of histomonads to the ceca; a process known as cloacal drinking.[2] Once in the ceca, *H. meleagridis* can invade the cecal mucosa and cause local inflammation and necrosis, as seen in this case. However, lesions only develop if the ceca are co-colonized by certain types of bacteria (e.g. *E. coli*, *Clostridium perfringens*, *Bacillus subtilis*, *Salmonella* sp.). The importance of bacteria in the pathogenesis of histomoniasis has been demonstrated in studies showing that *H. meleagridis* is avirulent in germ-free ceca[6] and gnotobiotic turkeys.[1] In some birds, histomonads subsequently invade the portal circulation and spreads to the liver to cause

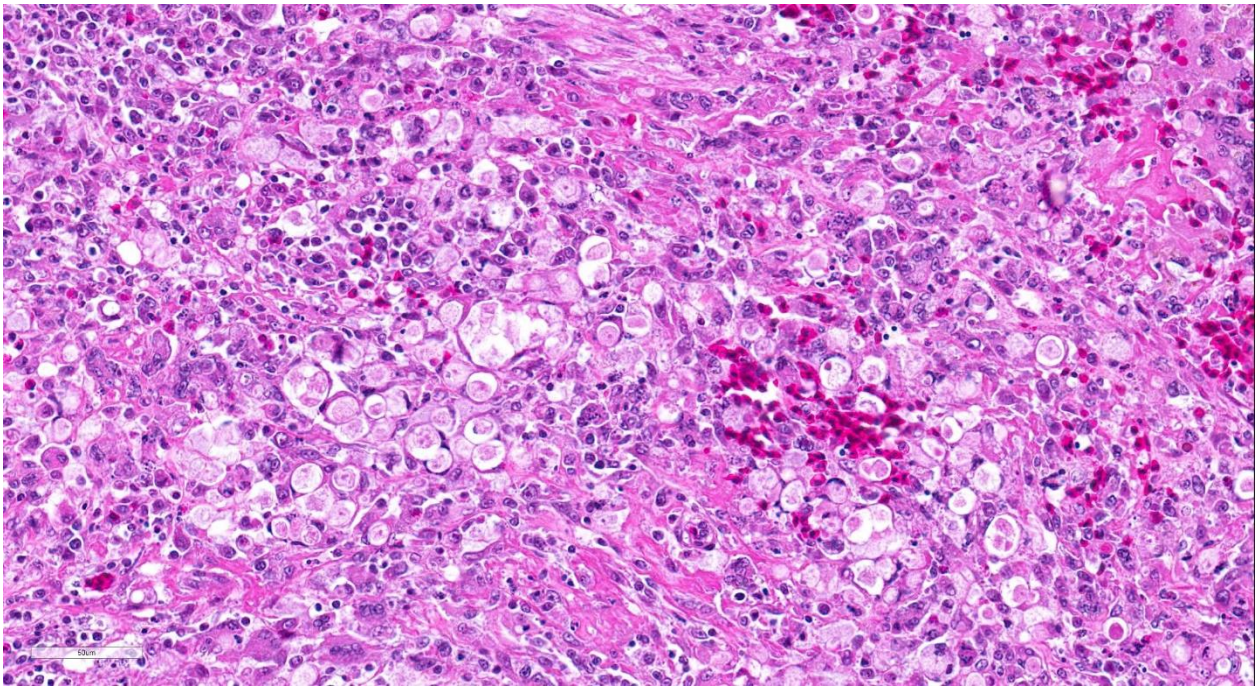

Cecum, chicken. Within the submucosa numerous histomonads are present within macrophages and occasionally free within the inflammatory infiltrate. (HE, 400X)

necrotizing and fatal hepatitis. This was not observed in the present case and the clinical signs that led to euthanasia were attributed to concurrent Marek's disease.

Turkeys are highly susceptible to developing systemic histomoniasis, with mortality rates reaching 100% in some flocks.[8] Conversely, in chickens, *H. meleagridis* causes relatively low mortality (10-20%) and high to low morbidity characterized by decreased egg production, and decreased weight gain.[1,8] This difference in susceptibility is not fully understood, but current data indicate that innate and adaptive immune responses play an important role.[9] In chickens, histomonads elicit an innate immune response (i.e. increased expression of IL-1β, CXCLi2, and IL-6) in the cecal tonsils within the first 24 hours of infection.[10] Turkeys, however, do not upregulate these pro-inflammatory cytokines until the organism is detectable in the liver.[10] In addition, one study of the adaptive immune response demonstrated that chickens have a higher percentage of IFN-ɣ mRNA expressing cells in the cecum prior to infection, suggesting these cells may play a protective role in histomoniasis.[7] In contrast, the number of IFN-ɣ positive cells in the ceca of unvaccinated turkeys initially decrease following infection and then increase coincident with cecal inflammation and necrosis. It is thought that the intensity of these delayed immune responses is an important contributor to the severity of disease in turkeys.[7,10]

Management of histomoniasis in commercial and backyard flocks has become more difficult in recent years because the last drug approved for the prevention of blackhead disease was disallowed in the U.S. in 2016.[1] Several alternative therapies are currently being investigated, but none have been proven to be sufficiently efficacious for broad application and a protective vaccine is not available.[1] Therefore, traditional environmental management practices (e.g.

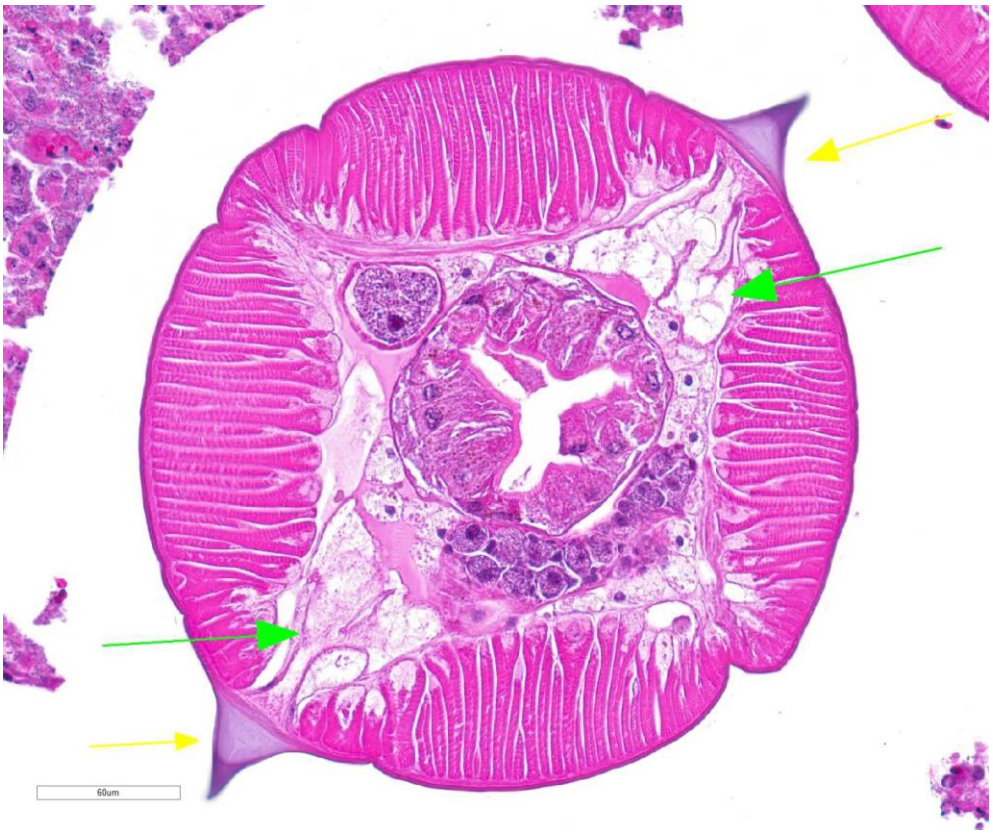

Cecum, chicken. Cross-sections of adult nematodes are present within the luminal debris. This adult female has a thin cuticle with lateral alae (yellow arrows), prominent lateral chords (green arrows), tall coelomyarian/polymyarian musculature, an intestine with tall columnar epithelium and a brush border, and numerous cross sections of the uterus with developing eggs. (HE, 253X)

biosecurity, management of soil and litter, avoid comingling highly susceptible species with chickens, etc.) are of increasing importance in the prevention of this disease.

Contributing Institution:
Washington Animal Disease Diagnostic Laboratory (WADDL); Department of Veterinary Microbiology and Pathology, Washington State University.
https://waddl.vetmed.wsu.edu/
https://vmp.vetmed.wsu.edu/

JPC Diagnosis: 1. Cecum: Intussuception.
2. Cecum: Typhlitis, necrohemorrhagic and granulomatous, transmural, multifocal to coalescing, marked with numerous amebic trophozoites.
3. Cecum, lumen: Adult ascarids, multiple.

JPC Comment: With the recent removal of nitarsone, the last remaining feed additive targeting flagellates, the economic importance of *Histomonas meleagridis* is greater than ever before. A recent retrospective of the disease in commercial turkeys was published in 2018[4], in concert with similar retrospective studies in France and Germany. In the California study, most cases occurred in warmer months from April to October, likely due to the longer survival of trophozoites outside the host during these months. Affected birds ranged from 2 weeks to 15 months; and the disease is less frequent, but no less severe in older birds. In most autopsied birds, histomoniasis was considered the primary cause of death. Histomonads were observed outside of the cecum and liver in 12/66 cases; other affected organs included spleen kidney, bursa, proventriculus, pancreas, lung, and crop. In five out of the 66 cases, the infection spread to all houses in the facility but cecal worms were only seen in 2 out of 66 cases, suggesting other forms of spread and the possibility of more resistant forms.[4]
H. meleagridis has recently been characterized in peafowl.[2] They may be

experimentally infected with *H. meleagridis*, but natural infections are rare. In a recent retrospective of infected peafowl, characteristic gross and histologic lesions associated with *H. meleagridis* (necrotizing typhlitis and hepatitis) were noted in each case, however, no birds had concurrent *H. gallinarum* infection. One bird had a concurrent infection with *Tetratrichomonas gallinarum*; the significance of this infection in facilitating the histomonad infection (seen with a number of other bacteria as mentioned by the contributor) is yet unclear.[2]

Interestingly, in a retrospective of common mortality in commercial egg-laying chickens, intussusception (classified along with volvulus under "twisted intestine") ranked seventh in the top fifteen causes of normal mortality at 3.5% of 3337 necropsies. Intussusception ffis reported to occur frequently secondarily to coccidiosis, necrotic enteritis, or intestinal parasitism, although in that particular study, intestinal parasites were not found. Affected birds demonstrate emaciation and atrophy of the reproductive tract, suggesting that the lesions are generally chronic in nature.[3] The moderator discussed the possibility of a number of cases of intussusception seen in non-parasitized birds perhaps being the result of skipping a feeding day in pullets, similar to the so-called "re-feeding syndrome" seen in humans.

References:

1. Clark S, Kimminau E. Critical Review: Future Control of Blackhead Disease (Histomoniasis) in Poultry. *Avian Dis*. 2017;61**:** 281-288.
2. Clarke LL, Beckstead BM, Hayes JR, Rissi D. Patholoic and molicular charcterization of histomoniasis in peafowl (Pavo cristatus). *J Vet Diagn Investig* 2017; 29(2):237-241.
3. Fulton RM. Causes of normal mortality in commercial egg-laying chickens. *Avian Dis* 2017; 61(3): 289-295.
4. Hauck R, Stoute S, Chin RP, Senties-Cue CG, Shivaprasad HL. Retrospective sutdy of histomoniasis (blackhead) in California turkey flocks 2000-2014.
5. Hu J, Fuller L, McDougald LR. Infection of turkeys with Histomonas meleagridis by the cloacal drop method. *Avian Dis*. 2004;48**:** 746-750.
6. Kemp RL. The failure of Histomonas meleagridis to establish in germ-free ceca in normal poults. *Avian Dis*. 1974;18**:** 452-455.
7. Kidane FA, Mitra T, Wernsdorf P, Hess M, Liebhart D. Allocation of Interferon Gamma mRNA Positive Cells in Caecum Hallmarks a Protective Trait Against Histomonosis. *Front Immunol*. 2018;9**:** 1164.
8. McDougald LR. Blackhead disease (histomoniasis) in poultry: a critical review. *Avian Dis*. 2005;49**:** 462-476.
9. Mitra T, Kidane FA, Hess M, Liebhart D. Unravelling the Immunity of Poultry Against the Extracellular Protozoan Parasite Histomonas meleagridis Is a Cornerstone for Vaccine Development: A Review. *Front Immunol*. 2018;9**:** 2518.
10. Powell FL, Rothwell L, Clarkson MJ, Kaiser P. The turkey, compared to the chicken, fails to mount an effective early immune response to Histomonas meleagridis in the gut. *Parasite Immunol*. 2009;31**:** 312-327.

CASE IV: S699/14 (JPC 4085966).

Signalment: Hessian crop pigeon, juvenile (< 1 year), weight: 440 g, female

History: The examined animal came from a private breeding livestock. Several pigeons

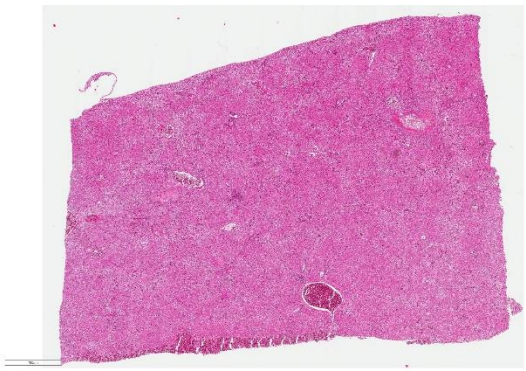

Liver, pigeon: A section of liver is submitted for examination. At low magnification, a retiform pattern of hepatic glycogenosis is evident upon close inspection as are scattered foci of hemorrhage. (HE, 30X)

died without any clinical symptoms. Treatment was not applied.

Gross Pathology: Both liver and kidneys showed multifocal beige to dark-brown colored foci, in diameter 0.2-0.3 mm, extending to subjacent parenchyma. In the lungs multifocal moderate acute hemorrhages were diagnosed. The pigeon was in good body condition.

Laboratory results: Molecular biological examination:
PCR for Pigeon Herpesvirus (PiHV): positive
PCR for Pigeon Circovirus (PiCV): positive

Parasitological examination:
Detection of a small number of coccidial oocysts

Microscopic Description: Liver: There are multifocal areas of acute necrosis, in some areas associated to the portal fields. These areas are demarcated by a moderate infiltration with predominantly histio-cytes/macrophages, some lymphocytes and a few neutrophils and plasma cells and a very mild beginning fibrosis. In numerous intralesional hepatocytes large (5-10 µm) amphophilic to basophilic intranuclear inclusion bodies type Cowdry A can be detected. Partly these large inclusions possibly seem to be located in the cytoplasm of the hepatocytes as well. Furthermore numerous hepatocytes show intranuclear eosinophilic inclusion bodies (ca. 3 µm) type Cowdry B. There is a diffuse moderate irregularity and dissociation of the cords of hepatocytes with a diffuse moderate anisocytosis and anisokaryosis of the hepatocytes. Multifocal a mid-zonal to peripheral lobular localized degeneration of hepatocytes is detected. In the periphery of areas of necrosis a few round and lightly basophilic structures (councilman-bodies) can be noticed.
With reference to the portal fields a mild to moderate hyperplasia of bile ducts and a very mild interstitial fibrosis with fibroplasia is obvious. Additionally, in the cytoplasm of several hepatocytes and Kupffer cells a small amount of light brown to green and of golden-yellow to light green fine and coarse granules is detected, most likely consistent with a mild hemosiderosis and a mild storage of bile pigment. Diffuse moderate hyperemia and multifocal mild acute hemorrhages are obvious.

Contributor Morphologic Diagnosis:
Liver: hepatitis, necrotizing and histiocytic/granulomatous, multifocal, polyphasic, moderate with numerous intranuclear inclusion bodies.

Contributor's Comment: Circoviruses are very small (15-20 nm in diameter) non-enveloped icosahedral viruses with circular single-stranded DNA. Because of their small size circoviruses are dependent on cellular enzymes of the host for their replication. Therefore, tissues with rapid cell proliferation, such as lymphoid tissue, are affected by circovirus.[2,7] Beside the pigeon circovirus (PiCV) three other circoviruses are known to be infectious pathogens of

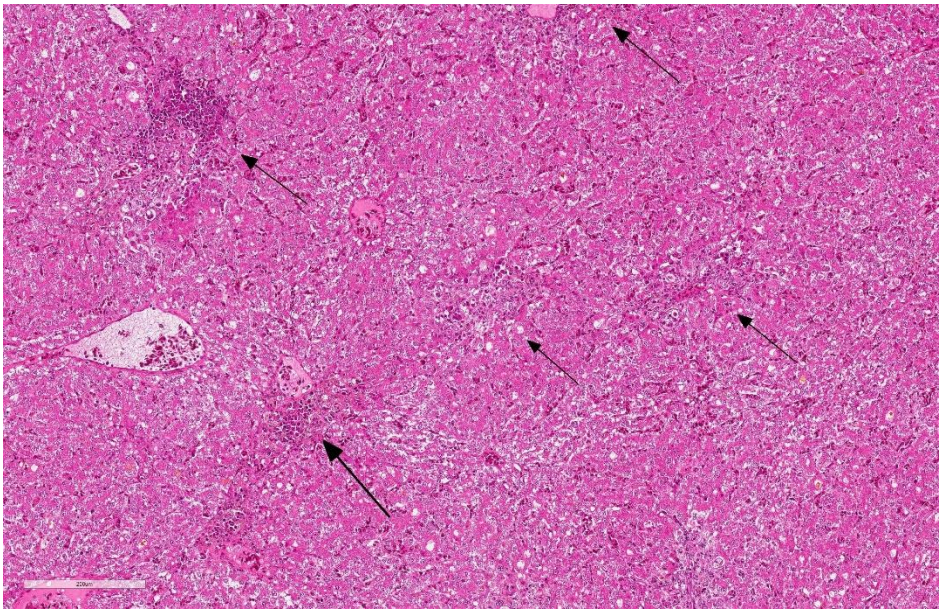

Liver, pigeon: Randomly scattered throughout the section are numerous foci of necrosis in which hepatocytes are individualized, shrunken, and hypereosinophilic. Nuclei of hepatocytes at the periphery often contain a single intranuclear viral inclusions surrounded by a clear halo. (HE, 146X)

spontaneous diseases. Chicken anemia virus (CAV) in fowl, which has been reclassified in the genus Gyrovirus, psittacine beak and feather disease (PBFD) in psittacine birds and porcine circovirus (PCV) in pigs.[4]

The PiCV was first identified in the USA but since it has been reported in many European countries, in North America, Australia and South Africa, probably a worldwide distribution is assumed. The practice of the pigeon sports probably supported the worldwide spread of the virus.[2]

Typically PiCV infects, as in the present case, young pigeons under one year of age. The way of transmission is not fully understood yet, but most infections seem to occur an oral way. Additionally, an egg-transmitted infection is also to be taken in consideration.[5]

Clinical signs can be lethargy, growth retardation, poor race performance and various symptoms caused by secondary bacterial or parasitic infections induced by immunosuppression. In contrast to PBFD a dystrophy and loss of feathery or beak deformations can only be seen rarely in PiCV infections. PiCV is normally associated with high morbidity and varying mortality, depending on secondary infections. In necropsy gross findings are usually very rare, atrophy of the bursa of Fabricius can occur. Other lesions often result from the secondary infections. A common histopathological finding is necrotizing bursitis and large (up to 15µm) basophilic intracytoplasmic inclusion bodies in the cells of the lymphoid follicles. Rarely these inclusion bodies are seen in other organs, such as spleen, thymus and GALT/BALT.[1,2,4,5] Definitive diagnosis can be made by PCR or in situ hybridisation. The Pi(CV) is found in the bursa of Fabricius, spleen, thymus, kidney, respiratory system and liver. As PiCV can be detected in clinically and histopathologically normal pigeons, many PiCV infections seem to be subclinical.[5]

The young pigeon disease syndrome (YPDS, swollen gut syndrome) is a multifactorial disease in young pigeons, aged from 4 to 12 weeks. Its etiological agent(s) is (are) still unknown. The PiCV plays an important role in YPDS by inducing immunosuppression. Other possibly involved infectious agents are pigeon herpesvirus, pigeon adenovirus, avian polyomavirus and bacterial pathogens such as *Spironucleus columbae* and *Escherichia coli*.[5]

Herpesviruses are large (180-250 µm in diameter) enveloped viruses with double-stranded DNA and an icosahedral capsid. Their replication occurs within the nucleus of the host cell.

Pigeon herpesvirus-1 (PiHV-1) has a worldwide distribution. Pigeons are the natural hosts of PiHV-1, in which it remains latent. Adult pigeons are asymptomatic carriers. Squabs are infected very early in life by latently infected pigeons feeding the squabs with cropmilk. The squabs are protected if they received maternal antibodies conferred with egg yolk. These pigeons also become asymptomatic carriers. In case the egg yolk does not contain any maternal antibodies, the emerging squabs are fully susceptible for PiHV-1 infection and develop clinical symptoms.

Adult pigeons (latent carriers) often appear completely healthy, although PiHV-1 can be isolated from the pharynx of these birds. Susceptible young birds develop clinical symptoms. In necropsy retarded development and pharyngitis, partly associated with small foci of necrosis and small ulcers are observed. In generalized infections the histopathological examination reveals necrosis in the liver and the spleen. Intranuclear inclusion bodies in hepatocytes are common findings.

Infection with *Trichomonas gallinae*, *Chlamydia* spp. or avian paramyxovirus should be considered as differential diagnoses.

Serological examinations (in positive cases) can only provide information about the infection state of the animal. Diagnosis of PiHV-1 infection should be confirmed by virus isolation.[3,9]

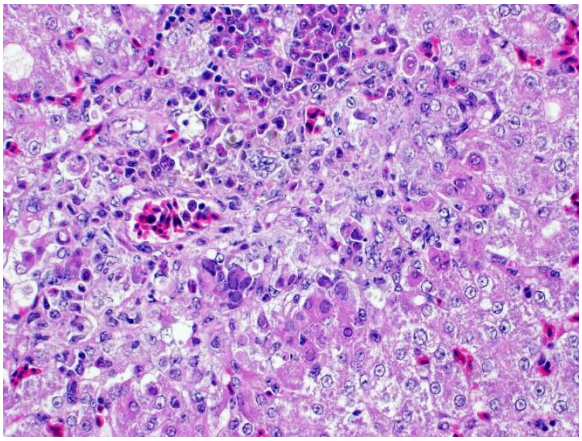

Liver, pigeon: Areas of necrosis are infiltrated by moderate numbers of heterophils (top) and macrophages. Nuclei of hepatocytes at the periphery often contain intranuclear viral inclusions. (HE, 400X)

Contributing Institution:
Institut für Veterinär-Pathologie, Veterinärmedizinische Fakultät Leipzig, Universität Leipzig, Germany (http://www.vetmed.uni-leipzig.de/ik/wpathologie)

JPC Diagnosis Liver: Hepatitis, necrotizing, random, multifocal, subacute, with small eosinophilic and large basophilic intranuclear viral inclusions.

JPC Comment: The contributor does an excellent job at describing two common viral infections in pigeons, only one of which can be diagnosed by examining this particular slide.

Like most alphaherpesviruses, the course of herpesviral disease is most often subclinical in the natural host, but may cause significant damage is other species. In the pigeon, most infections are latent, but may recrudesce in times of stress or concurrent disease. In Belgium, 50% of pigeons have antibodies to the virus; when affected with other respiratory pathogens, PHV-1 can be isolated in the pharynx of up to 80% of birds.[4] In adult birds, clinical disease is limited to the respiratory tract with necrotizing lesions in

the mouth, pharynx and larynx; superficial bacterial lesion results in more severe lesions.[9] Necrotizing hepatitis is most often seen in young birds which did not receive maternal immunity through the egg yolk, making this an intriguing potential cause of "young pigeon disease syndrome".

The disease in pigeons, is eclipsed by the disease in owls and falcons who have preyed upon infected pigeons. PCR studies have demonstrated that the herpesvirus that causes "hepatosplenitis infectiosa strigum" or "hepatosplenitis" in raptors is identical to columbid-herpesvirus 1, once again illustrating the severe disease which often results when alphaherpesviruses jump into aberrant hosts. For more information on the disease in raptors, see the following WSC cases – WSC 2017-2018 Conf 15 Case 1, WSC 2014-2015 Conferenc 13, case 4, WSC 2010-2011, Conference 8, Case 1.

Pigeon circovirus (PiCV) was first diagnosed in Canada in 1986, and shortly after, was diagnosed in many countries around the world. In recent studies, infection rates in flocks range averaged around between 75 and 80% in China and Europe, with similar rates in healthy and unhealthy birds. [6] The potential transmission of this disease in racing birds as well as cosmopolitan pigeons is extremely high. While mortality in affected flocks in two-month- to 1-year-old pigeons may be up to 100%[9], the potential of circoviruses to cause lymphoid necrosis and immunosuppression in affected birds may be even more profound.[9]

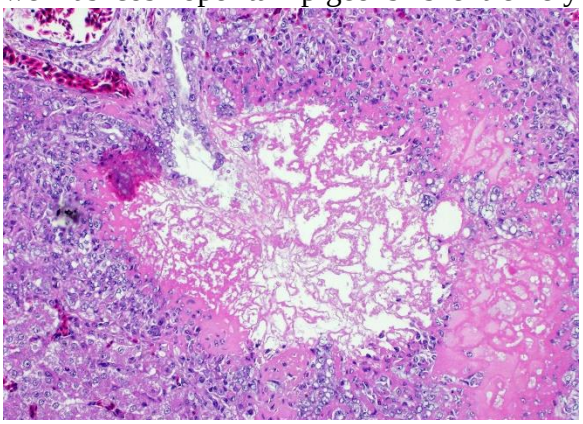

Liver, pigeon. Areas of necrosis extending into portal areas breach the biliary epithelium, resulting in release of bile into the surrounding parenchyma and liquefactive necrosis. (HE, 400X)

"Young pigeon disease syndrome", (YPDS) as mentioned by the contributor, is a syndrome of disease which appears closely interrelated with the immunosuppressive effects of pigeon circovirus, much like the many syndromes associated with porcine circovirus-2. It was first described in the 1980s, and affects birds from 4-12 weeks of age, resulting in anorexia, ruffled feathers, regurgitation and diarrhea, excessive crop liquid, and polyuria. In affected flocks, morbidity approaches 20% and mortality 50%. As the contributor has stated, a variety of infectious agents, in addition to PiCV have been incriminated, to include pigeon adenoviruses and herpesviruses. A recent study of birds with YPDS in Poland demonstrated a 44.5-100% infection rate with PiCV, and the second most common viruses in affected birds was pigeon herpesvirus-1, at approximately 30%.[7] Pigeon adenovirus was not identified in any flocks in this study.

The characteristic botryoid basophilic intracytoplasmic inclusions of pigeon circovirus are largely restricted to lymphoid tissues, and would not likely be seen within hepatocytes in this case, although there was great variation in size and shape of the inclusions in this case. While the age of this bird may or may not be consistent with the syndrome of YPDS, and the evidence is circumstantial at best, it is interesting to ponder the effects of PiCV in generating clinical systemic herpesviral disease in a mature bird.

References:

1. Abadie J, Nguyen F, Groizeleau C, Amenna N, Fernandez B, Guereaud C, Guigand L, Robart P, Lefebvre B, Wyers M: Pigeon circovirus infection: Pathological observations and suggested pathogenesis. Avian Pathology. 2001; 30(2): 149-158

2. Duchatel JP, Szeleszcuk P: Young pigeon disease. Medycyna Wet. 2011; 67(5): 291-294

3. Kaleta EF Herpesvirus der Tauben. In: Kaleta EF and Krautwald-Junghanns M-E ed. Kompendium der Ziervogelkrankheiten. Hannover: Schlütersche GmbH & Co. KG Verlag und Druckerei; 1999; 292-294

4. Marlier D, Vindevogel H: Viral infections in pigeons. The veterinary journal. 2006; 172: 40-51

5. Raue R, Schmidt V, Freick m, Reinhardt B, Johne R, Kamphausen L, Kaleta EF, Müller H, Krautwald-Junghanns M-E: A disease complex associated with pigeon circovirus infection, young pigeon disease syndrome. Avian Pathology. 2005; 34(5): 418-425

6. Stenzel TA, Pestka D, Tyklowski B, Smialek M, Knocicki A. Epidemiological investigation of selected pigeon viral infections in Poland. *Vet Rec*

7. Todd T: Circoviruses: immunosuppressive threats to avian species. Avian Pathology. 2000; 29: 373-394

8. Todd T: Avian circovirus diseases: lessons for the study of PMWS. Veterinary Microbiology. 2004; 98: 169-174

9. Vindevogel H, Duchatel JP. Pigeon Herpesvirus Infection. In: Calnek BW, Barnes HJ, Beard CW, Reid WM, Yoder Jr. HW ed. Diseases of Poultry. Ninth Edition. Ames: Wolfe Publishing Ltd; 1991; 665-667

Self-Assessment - WSC 2019-2020 Conference 9

1. Which of the following diseases is not caused by a retrovirus?
    a. Marek's disease
    b. Avian leukosis
    c. Avian reticuloendotheliosis
    d. Lymphoproliferative disease of turkeys

2. How is Marek's disease transmitted between birds?
    a. Feces
    b. Dander
    c. Respiratory secretions
    d. Coitus

3. Which of the following organs is most affected by infection with chick anemia agent?
    a. Brain
    b. Cecum
    c. Liver
    d. Bursa

4. Which of the following is true concerning infection in poultry with *Histomonas meleagridis*?
    a. Concurrent bacterial factor in important to establish infection.
    b. Histomonad infection is limited to the liver and ceca in the turkey.
    c. Chickens, as abnormal hosts, have a higher mortality rate than turkeys.
    d. The frequency of infection increases with age in turkeys.

5. Viruses from which of the following virus families have NOT been incriminated as potential causes of "young pigeon disease syndrome"?
    a. Herpesviruses
    b. Adenoviruses
    c. Flaviviruses
    d. Circoviruses

Please email your completed assessment for grading to Dr. Bruce Williams at bruce.h.williams12.civ@mail.mil. Passing score is 80%. This program (RACE program 33611) is approved by the AAVSB RACE to offer a total of 0.5 CE Credits, with a maximum of 12.5 CE Credits being available to any individual Veterinary Medical Professionals for the 2019-2020 Wednesday Slide Conference. This RACE approval is for the subject matter categories of: SCIENTIFIC using the delivery method of NON-INTERACTIVE DISTANCE. This approval is valid in jurisdictions which recognizeAAVSB RACE.

Joint Pathology Center
Veterinary Pathology Services

WEDNESDAY SLIDE CONFERENCE 2019-2020

C o n f e r e n c e 10

20 November 2019

CASE I: R17104D (JPC 4135946).

Signalment: Caribbean spiny lobster (*Panulirus argus)* of unknown sex and age

History: In 2016, 14 Caribbean spiny lobsters (*Panulirus argus)* were collected off of Summerland Key, Florida to supplement the resident population at a large public aquarium. The lobsters were transported and placed in quarantine at a separate facility. After 5 months, lobsters began showing clinical signs of lethargy and dying in the molt. Samples of hemolymph were submitted to the Louisiana Aquatic Diagnostic Laboratory (LADL) at Louisiana Animal Disease Diagnostic Laboratory (LADDL) and the University of Florida for PCR for White Spot Syndrome Virus (WSSV) and *Panulirus argus* Virus 1 (PaV1), respectively. Upon obtaining the PCR results, the remaining lobsters were euthanized and gross necropsies were performed on site at the quarantine facility. Formalin-fixed tissues were submitted to LADL for histopathological evaluation.

Gross Pathology: There were no significant gross lesions in the lobsters examined.

Laboratory results:
PCR for White Spot Syndrome Virus (WSSV): Negative
PCR for *Panulirus argus* Virus 1 (PaV1): Positive

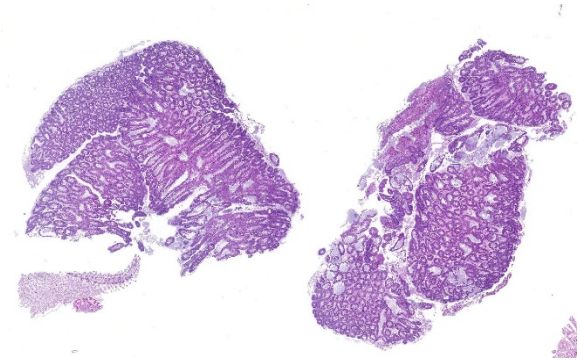

Hepatopancreas, lobster. Multiple sections of hepatopancreas are submitted. At low magnification, there is dilation of hepatopancreatic tubules which are filled with a bluish-grey material. (Photo courtesy of: Louisiana Animal Disease Diagnostic Laboratory (LADDL), School of Veterinary Medicine, Louisiana State University (http://www1.vetmed.lsu.edu/laddl/index.html)

Microscopic Description: Hepatopancreas: Throughout the hepatopancreas, the hemal sinuses are variably dilated and increased in size in comparison to the adjacent tubules. The dilated sinuses are filled with a moderate to abundant amount of circulating hemocytes and proliferative spongy connective tissues. Fixed phagocytes surrounding the hepatopancreatic tubules are variably enlarged, with multifocal disruption of the typical rosette-like arrangement. Circulating hemocytes, fixed phagocytes, and spongy connective tissue cells often have enlarged, hypertrophic nuclei that contain large eosinophilic to amphophilic inclusion bodies, occasionally surrounded by a clear halo, with margination of the nuclear chromatin along the nuclear membrane (Cowdry-type A inclusion bodies). The cytoplasm of the affected cells often contain smaller, variably-sized, round eosinophilic globules. There are subjectively decreased numbers of reserve inclusion cells throughout the hepatopancreas. In few areas, the epithelial cells lining the hepatopancreatic tubules are variably decreased in size or completely absent, and the lumen contains a moderate amount of basophilic granular material and few individual sloughed epithelial cells.

In addition to the hepatopancreas, similar eosinophilic intranuclear inclusion bodies were observed within spongy connective tissue cells of the exoskeletal membrane (not included in submission).

Contributor's Morphologic Diagnosis: Hepatopancreas: Hepatopancreatitis, moderate, diffuse, chronic, with mild to moderate hepatopancreatic atrophy and numerous eosinophilic intranuclear inclusion bodies

Contributor's Comment: As a brief overview, the normal hepatopancreas of

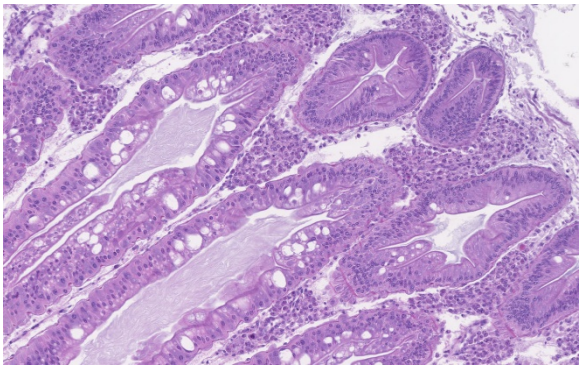

Hepatopancreas, lobster. H&E. 100X. The hemal sinuses are variably dilated and filled with variable numbers of circulating hemocytes and proliferative spongy connective tissue. (HE 100X)

most decapod crustaceans is a large compact paired glandular organ that surrounds the midgut and occupies a large portion of the cephalothorax.[2] The hepatopancreas is surrounded by a connective tissue membrane and each half consists of two or three lobes comprised of a complex network of blind-ending tubules, which are connected to the midgut gland through common absorptive ducts.[2,8] With exception of the distal closed end, each tubule is lined by a single cell layer of epithelial cells, which are divided into subtypes including the embryonic E-cells, fibrillar F-cells, resorptive or absorptive R-cells, and secretory B-cells.[2] The embryonic cells reside within the apical portion of the tubule, while the remaining cell types (B-, R-, and F-cells) reside within the digestion zone.[8] An outer basement membrane separates the tubules from the hemal sinuses, which contain an arteriole surrounded by a rosette-like structure of fixed phagocytes, which remove foreign material from the hemolymph, and reserve inclusion cells, which contain polysaccharides such as glycogen and proteins such as hemocyanin.[3,6,8]

Panulirus argus Virus 1 (PaV1) was discovered approximately 20 years ago as the first naturally occurring pathogenic virus of

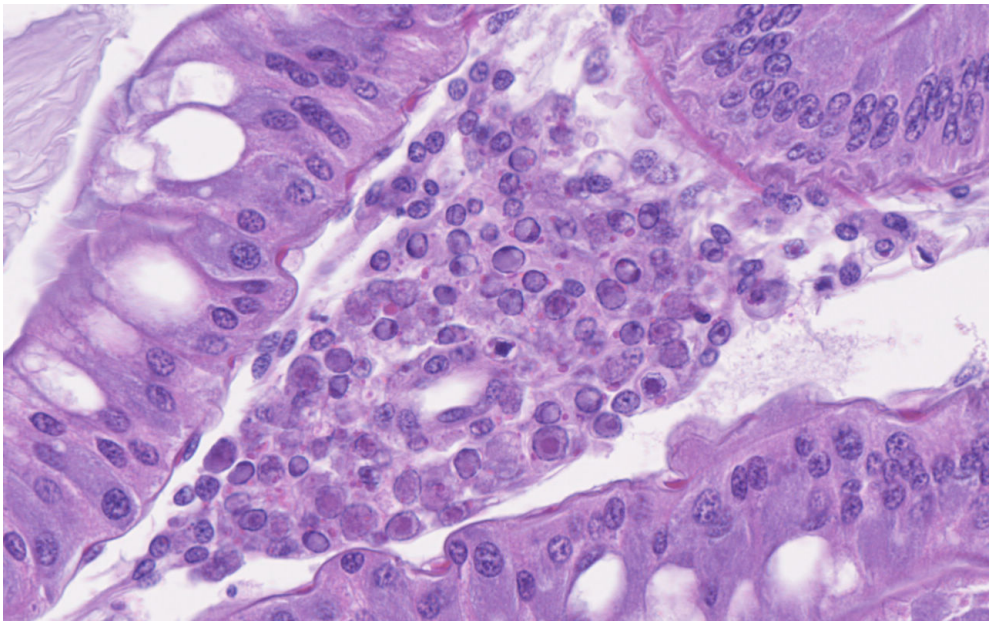

Hepatopancreas, lobster. Fixed hemocytes within the hepatopancreas frequently have hypertrophic nuclei containing large eosinophilic Cowdry-type A inclusion bodies. (HE, 600X) (Photo courtesy of: Louisiana Animal Disease Diagnostic Laboratory (LADDL), School of Veterinary Medicine, Louisiana State University (http://www1.vetmed.lsu.edu/laddl/index.html)

lobsters.[1,3-7] PaV1 was first detected in juvenile Caribbean spiny lobsters (*Panulirus argus*) from the Florida Keys, Florida, USA, but has since been detected throughout the Caribbean Sea, including reports from St. Croix, St. Kitts, Yucatan (Mexico), Belize, and Cuba.[1,3,6] At the time of submission, Caribbean spiny lobsters are the only reported affected host of the virus.[6] PaV1 is one of the most significant pathogens affecting spiny lobsters and is believed to be associated with a decline in the spiny lobster fishery in the Florida Keys.[6,7] Additionally, these lobsters are shipped internationally, which could play a role in the potential spread of the virus. The virus is not yet classified, but shares morphological characteristics with Herpesviridae and Iridoviridae; it is an unenveloped, icosahedral DNA virus with an approximately 182 nm nucleocapsid that develops within the infected host cells' nuclei.[6]

The virus is most prevalent within and nearly always lethal to the smallest juvenile lobsters, with a decrease in prevalence correlating with increase in the size of lobster; adults may harbor the virus, but do not typically exhibit signs of disease.[1,6] Healthy lobsters tend to avoid diseased lobsters, which may explain reduced disease transmission, but may also lead to increased shelter competition and increased predation on the infected lobsters.[1,6] Heavily infected lobsters become lethargic and sedentary, cease feeding, and eventually die of metabolic exhaustion.[1,6]

During early stages of infection, the virus has an apparent predilection for the fixed phagocytes of the hepatopancreas, which later lyse and infect proliferating spongy connective tissue cells and circulating hemocytes, including hyalinocytes and semi-granulocytes.[1,3,5] As mentioned above, the fixed phagocytes and circulating hemocytes play an important role in phagocytosing foreign materials from the hemolymph.[6,8] The circulating hemocytes affected include hyalinocytes and semigranulocytes; granulocytes, as well as fibrous connective tissue cells are not affected.[1,3] All affected cell types are derived from the mesoderm, suggesting that the virus may have a tropism for this developmental germ layer.[6] In heavier infections, virtually all spongy connective tissue cells are infected and hepatopancreatic tubules become atrophied,

with depletion of reserve inclusion cells, leading to metabolic wasting and death.[6]

The hemolymph of affected lobsters has a characteristic white, milky appearance and fails to clot.[6,7] Histopathologic lesions can be observed within 10-15 days of infection and include alterations to the fixed phagocytes and spongy connective tissue with enlarged nuclei containing Cowdry-like inclusion bodies.[8] Molecular diagnostics including polymerase chain reaction (PCR) and fluorescent *in situ* hybridization (FISH) have been utilized for disease confirmation.[4-6]

In this case, the abundance of intranuclear eosinophilic inclusion bodies coupled with the positive PCR result were diagnostic for *Panulirus argus* Virus 1 (PaV1). In addition to the intranuclear inclusions, eosinophilic globular material was observed within the cytoplasm of the infected cells. The origin of this material has yet-to-be determined, but based on electron microscopy, we believe this material could be virus-induced particles within the cytoplasm. As another alternative, the histologic appearance is somewhat similar to the eosinophilic globular aggregates associated with reserve inclusion cells and therefore, these globules may represent polysaccharide aggregates such as glycogen. The areas with loss of hepatopancreatic epithelium and intraluminal basophilic granular material are believed to be euthanasia-induced artifacts, though virally-induced change cannot be ruled out. However, PaV1 has not been reported to affect hepatopancreatic epithelium, so this is considered less likely.

Contributing Institution:
Louisiana Animal Disease Diagnostic Laboratory (LADDL), School of Veterinary Medicine, Louisiana State University (http://www1.vetmed.lsu.edu/laddl/index.html)

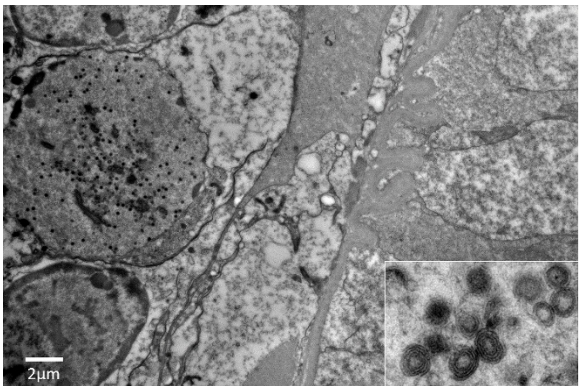

Hepatopancreas, lobster. An electron micrograph of the intracytoplasmic globular material within reserve inclusions cells contains potential virus-induced particles. (Photo courtesy of: Louisiana Animal Disease Diagnostic Laboratory (LADDL), School of Veterinary Medicine, Louisiana State University (http://www1.vetmed.lsu.edu/laddl/index.html)

JPC Diagnosis: 1. Hepatopancreas: Hepatopancreatitis, interstitial, hemolytic, diffuse, moderate, with numerous eosinophilic intranuclear inclusion bodies.
2. Hepatopancreas, gill, midgut; circulating hemocytes: Eosinophilic intranuclear inclusion bodies.
3. Hepatopancreas: Atrophy, tubular, diffuse, severe.

JPC Comment: The contributor has done an outstanding job of describing the pertinent anatomy of the decapod hepatopancreas as well as illustrating this important disease of spiny lobsters. Many pathologists are likely unfamiliar with the anatomy of the lobster, and are directed to reference 8 below, an excellent review of the gross and histologic anatomy of the lobster at: https://scholarworks.wm.edu/cgi/viewcontent.cgi?article=1005&context=reports (reference 8)

Many pathologists (as well as the majority of conference participants) are largely unaware of the diseases of spiny lobsters. In addition to Panulirus argulus virus-1, spiny lobsters are host to a number of infectious, parasitic,

and syndromal conditions of interest.

At this time, PaV1, appears to be the only natural viral infection of spiny lobsters, although it appears they may be natural hosts for the virus that causeswhite spot syndrome virus, a viral disease clinically seen in shrimp.[6]

Spiny lobsters are host however, to a number of bacterial pathogens. *Aerococcus viridans* is a gram-positive bacillus that is most common in holding facilities but has been identified in Cuban spiny lobsters. This agent results in a reddish disocloration of the shell, pink hemolymph and coagulopathies when introduced through a broken exoskeleton. "Shell disease" is a condition caused by a numer of chitinoclistic gram-negative bacterial, including bacteria from the genera *Vibrio, Aeromonas, Pseudomonas, and Shewanella*. This multifoal erosion of the shell may occur randomly on the exoskeleton, or in spiny lobsters, affect the tail fan. In addition, *Vibrio* sp. may cause disseminated disease in spiny lobsters, especially larvae, but also may be cultured from hemolymph in apparently normal individuals of this species. Fouling bacteria, such as *Leucothrix mucor* damage eggs and larvae of lobsters in culture. Several species of microsporidia are also seen in the spiny labsters, and may affect the meat quality of infected animals.[6]

A number of fungi infect spiny lobsters,. Oomycetes and phycomycetes usually infect the eggs and larvae, and are more common when water quality is poor. *Fusarium solani* results in black shell disease, melanization which is often seen in a variety of diseases affecting the exoskeleton in this species. Cilites are often found as commensals on the exterior of lobsters particular in cultures.[6]
A number of helminth parasites are described in spiny lobsers, to include digenetic trematodes, which utilitze them as intermediate hosts and encyst as metacercariae in the msuculature. Connective tissues of metacestodes may encyst in connective tissues. Rotifers, copepods, and amphipods are often symbionts or commensals in spiny lobsters or their egg clutches.[6]

Disease syndromes in lobsters generally are associated with interesting names, even if their etiology is unknown. "Turgid lobster syndrome" occurs in spiny lobsters in New Zealand and Australia, is characterized by swelling of the arthrodial membranes, and a causative agent is unknown. Australia is also host to "pink lobster syndrome" in which the meat turns pink to yellow and is unpalatable. Mass mortality evens have been documented by habitat alteration such as hypoxia events, algal blooms, and mass strandings.[6]
The moderator reviewed the anatomy and histology of the lobster. In discussing the most appropriate morphologic diagnosis for this case, the moderator discussed a preference for the term "hemocytic" rather than granulocytic due to the difficulties in distinguishing the two on routine light microscopy. Atrophy of the hepatopancreas in this case is especially profound as normal hepatopancreas is filled with lipid vacuoles, and few remained in this particular specimen, but it was added as a separate morphologic diagnosis as it was difficult to establish whther it resulted from the viral infection, or simply diminished nutritional status as a consequence of captivity.

References:

1. Behringer DC, Butler MJt, Shields JD, Moss J. Review of *Panulirus argus* virus 1--a decade after its discovery. *Dis Aquat Organ*. 2011;94**:** 153-160.
2. Gibson R, Barker PL. The Decapod Hepatopancreas. *Oceanogr Mar Biol Ann Rev*. 1979;17**:** 285-346.

3. Li C, Shields JD, Ratzlaff RE, Butler MJ. Pathology and hematology of the Caribbean spiny lobster experimentally infected with Panulirus argus virus 1 (PaV1). *Virus Res*. 2008;132**:** 104-113.
4. Li C, Shields JD, Small HJ, et al. Detection of Panulirus argus Virus 1 (PaVI) in the Caribbean spiny lobster using fluorescence in situ hybridization (FISH). *Dis Aquat Organ*. 2006;72**:** 185-192.
5. Montgomery-Fullerton MM, Cooper RA, Kauffman KM, Shields JD, Ratzlaff RE. Detection of Panulirus argus Virus 1 in Caribbean spiny lobsters. *Dis Aquat Organ*. 2007;76**:** 1-6.
6. Shields JD. Diseases of spiny lobsters: a review. *J Invertebr Pathol*. 2011;106**:** 79-91.
7. Shields JD, Behringer DC, Jr. A new pathogenic virus in the Caribbean spiny lobster Panulirus argus from the Florida Keys. *Dis Aquat Organ*. 2004;59**:** 109-118.
8. Shields JD, Boyd RA: Atlas of Lobster Anatomy and Histology. *In*: Special Papers in Marine Science. Virginia Institute of Marine Science, College of William and Mary, 2014

CASE II: N18-0170 (JPC 4132732).

Signalment: Adult (≥4 years) female Oscar, cichlid (*Astronotus ocellatus)*

History: On August 9, 2018 the patient presented for rapid gilling. Upon physical examination the gill filaments were thickened, erythematous and mottled red to light pink. A black spot on the gill filaments of the first right gill arch was seen, and a trematode was observed on a gill clip. The patient was treated with 10 ppt NaCl baths, ceftazidime and praziquantel injections but no improvement was seen. Due to quality of life concerns, euthanasia with MS-222 was elected on August 19, 2018.

Gross Pathology: On gross examination there is abundant mucus coating the entire

fish. The caudal pole of the kidney is expanded by a dark, mottled, red-brown to tan, 3.5 x 2.5 x 2.5 cm multinodular mass. ***Viscera, oscar. Gross necropsy photo with coelomic wall retracted cranially. Orientation: Dorsal aspect is to the top of the photo, cranial aspect is to the left. a) liver b) ovary c) spleen d.) mass e) GI f) swim bladder. (Photo courtesy of: Smithsonian's National Zoo and Conservation Biology Institute, https://nationalzoo.si.edu/animals/veterinary-care)***

The mass is partially encapsulated, soft, wet, friable, and located ventral to the swim bladder. The kidney is similarly mottled and attached by apparent renal tissue to the mass**.** No other abnormalities are seen.

Laboratory results:
Renal mass cytology - Rafts of epithelial cells. Cells occasionally surround acellular material (possible mineral) in a tubule-like formation.

Microscopic Description: Preexisting renal tissue is identified by renal tubules and glomeruli. Greater than 90% of the normal renal tissue is expanded and obliterated within the original renal capsule by a neoplastic mass with lobules separated by a fibrovascular stroma. Neovascularization is noted throughout the mass within the interstitium. The mass is primarily cystic forming distinguishable lumina up to 1.8 mm in diameter containing viable and degenerate erythrocytes, indistinct cellular debris, and eosinophilic fluid. The cells lining these

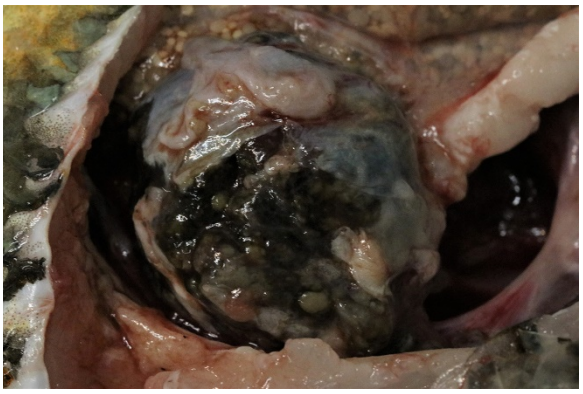

Kidney, oscar. Renal mass in situ, connection with trunk kidney. (Photo courtesy of: Smithsonian's National Zoo and Conservation Biology Institute, https://nationalzoo.si.edu/animals/veterinary-care)

spaces are well-differentiated, cuboidal to occasionally columnar epithelium exhibiting mild anisocytosis and anisokaryosis. Each cell contains a moderate amount of eosinophilic occasionally vacuolated cytoplasm, and a single round, centrally to apically located nucleus. Nuclei have finely stippled to vesicular chromatin and 1-2 basophilic nucleoli. No mitotic figures are seen. The interstitium of the mass is moderately expanded by macrophages containing golden brown pigment (hemosiderin), lower numbers of lymphocytes and plasma cells and regions of neovascularization. Numerous coalescing organized granulomas are present within cystic lumina and the interstitium. They range from 0.1 mm solitary granulomas to 3 mm coalescing granulomas. The granulomas consist of a necrotic core of brightly colored eosinophilic cellular and karyorrhectic debris contained by an inner layer of concentric compressed epithelioid macrophages surrounded by a thicker layer of foamy macrophages. Hemosiderophages are prominent throughout the interstitium and occasionally within outer foamy layers of granulomas. Scattered mineralization is present within granulomas. There are areas within the mass where disorganized and coiled membranes of cuboidal epithelium are seen (likely handling artifact).

Slide N18-0170-2 Acid Fast –There are abundant intracellular and extracellular robust acid-fast rods (1 x 3 um) within granulomas.

Contributor Morphologic Diagnosis:

Kidney, posterior: Cystadenoma with concomitant multifocal, subacute to chronic, granulomatous nephritis with acid-fast bacilli

Contributor Comment: Renal tumors in teleosts (bony fish) are generally quite rare with the most common reports being nephroblastic tumors both in rainbow trout (associated with toxin exposure) and in Japanese eels (*Anguilla japonica*).[4,5] Most reports are of single cases, including a cystic adenocarcinoma in a European eel (*Anguilla Anguilla*), an adenoma in a brown bullhead catfish (*Ameiurus nebulosus*), and a papilliferous cystadenoma of the mesonephric duct in a Chinook salmon.[4,5] However, the tumor featured in this case is a well described tumor of this species and has been seen in multiple *A. ocellatus* specimens including three from the National Cancer Institute's Registry of Tumors in Lower Animals, one from North Carolina State

Kidney, oscar. The renal mass measures 5.7 x 2.5 x 2.7 cm. Numerous tan granulomas are visible on the service. (Photo courtesy of: Smithsonian's National Zoo and Conservation Biology Institute, https://nationalzoo.si.edu/animals/veterinary-care)

University College of Veterinary Medicine[10] and one from the University of Veterinary Medicine Veterinarplatz, Vienna Austria.[2] The clinical presentation was similar in all cases where recorded (abdominal distention and deteriorating condition despite medical therapy). While there were minor differences between reported tumor specimens (+/- granulomas, mineral crystals), all appeared cystic and originated from the posterior kidney and, with the exception of one case where there was invasion of surrounding tissue, all cases appeared benign.[7] In addition to the cases listed above, another oscar in the same aquarium this one died on August 1, 2018. That fish was also an adult (>4 years) female that presented with a smooth, firm, white tissue was protruding from the vent which was not able to be reduced. On necropsy a mass that was similar grossly to the mass in this case fish was found. Histologic examination identified it to be a renal cystadenoma but there were no granulomas in that case. Based on the number of specimens of the same species with similar tumors and lack of literature to indicate otherwise, it can be inferred that oscar cichlids are predisposed to renal cystadenomas. It is unknown whether this tumor occurs in wild individuals or if its development is due in part to low genetic diversity of the captive-bred population. Other potential etiologies of this tumor cannot be ruled out; it could be a unique species response to an unidentified environmental factor or an as-yet-unidentified microbe such as in proliferative kidney disease in goldfish caused by the myxozoan *Hoferellus carassii*.[7]

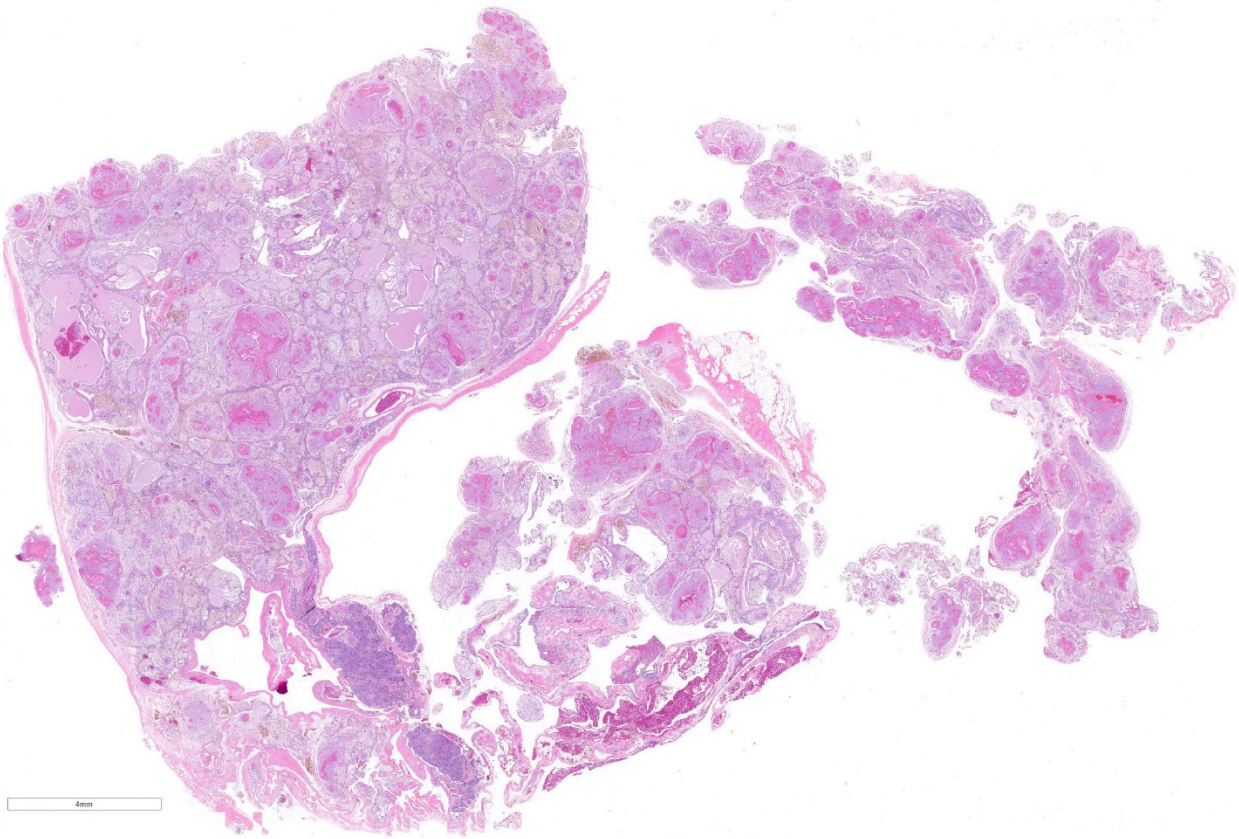

Kidney, oscar. A section of kidney is submitted. 95% of the kidney is effaced by a large cystic neoplasm studded with granulomas. Normal kidney is present in the section (arrows) (HE, 7X)

Clinical signs attributable to the tumor are nonspecific, though it can be presumed that the neoplasm (and in this case infection with mycobacteria) may have affected renal function and that large tumor size may have had an impact on buoyancy. This tumor's abnormal tissue likely provided a permissive environment predisposed to secondary infection. Smaller granulomas were noted in heart, liver, spleen, and ovary, and other animals in this tank had also been previously diagnosed with mycobacteriosis. In the case presented, opportunistic mycobacteriosis is an unsurprising, though florid, complication of both systemic and tissue-specific disease associated with the neoplasm.

Mycobacteria are slow growing, acid-fast staining bacilli that are natural occupants of water systems and opportunistic pathogens. They form biofilms within pipes and on surfaces of aquariums which makes them resistant to many forms of filtration and disinfectants. This makes eradication of mycobacteria from a system difficult. Opportunistic infections of fish within a contaminated system can occur when those fish are inflicted with external injuries or stress. Pathogenicity varies depending on the species of mycobacteria ranging from mild, chronic infections of a few fish to acute system wide infections with mortalities of 30-100%. Infection often results in granuloma formation, most notably within the liver and kidneys but diffuse disease can be seen, especially with the more pathogenic strains.[11] This case provides an example of environmental, host, tissue, and pathogen interactions resulting in dramatic pathology.

Contributing Institution:
https://nationalzoo.si.edu/animals/veterinary-care

JPC Diagnosis: 1. **Kidney**: Renal cystadenoma.

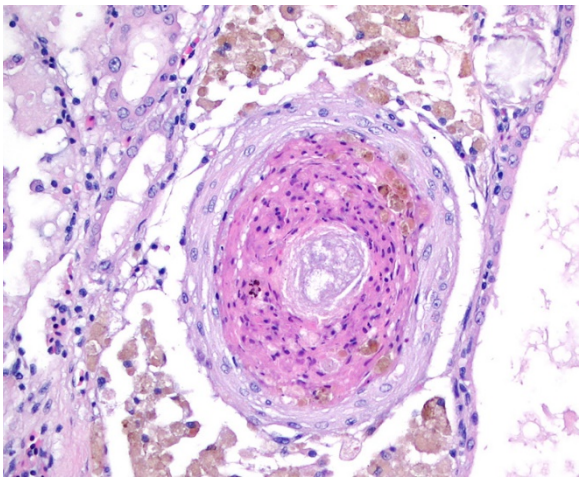

Viscera, oscar. Granuloma, composed of lamellated epithelioid macrophages and centered on a bacterial colony and associated cellular debris. (HE, 400X) (Photo courtesy of: Smithsonian's National Zoo and Conservation Biology Institute, https://nationalzoo.si.edu/animals/veterinary-care)

2. Kidney: Granulomas, numerous

JPC Comment: The contributor has done an excellent job of describing renal adenoma/cystadenoma in fishes. Benign renal neoplasms are rare tumors in animals, as they rarely cause clinical signs and are primarily diagnosed at autopsy. Many reports, as in fish, are single case reports, with large studies of renal neoplasms in dogs, where they amounted to 3% of cases overall, and in slaughtered cattle with an incidence of one in 13,500. Another survey of 6706 cattle at slaughter yielded no benign tumors. Due to the rarity of benign tumors in domestic species, definitive criteria of benignancy have not been well established.[8] As well-differentiated malignancies and benign tumors may overlap in histologic appearance, arbitrary criteria of 2cm diameter is often used, but tumors of this size may be problematic. Mitoses over 10 per 2.37mm suggest malignancy in the absence of more definitive criteria, including invasion and metastasis.[8]

A similar problem has been encountered in

human medicine, in which metastasis has been documented repeatedly in tumors less than 3cm in diameter. Current human protocols define adenomas as tumors less than 0.5cm with densely packed tubules or papillary projections and bland nuclei with the low mitotic rate. Benign renal neoplasms are also encountered in higher incidence in cases of pyelonephritis and renal vascular disease and are reported in high frequency along with renal cysts in von-Hippel-Landau syndrome in children.[9]

Mycobacteriosis is a common, serious, and often lethal disease affecting fish and other poikilotherms in aquatic environment. As mentioned by the contributor, the ability for this species (and related species such as *Nocardia)* to survive in biofilms in recirculating systems, results in recurrent infections which are the bane of aquarists.[1]

This condition, which has appeared numerous times in poikilotherms in the WSC over the years, has played primary and secondary roles (as in this case.) The kidney appears to be one of the most common (if not the most common) organ affected along with the spleen, and granulomas are often seen as well in the liver, gills, mesentery, gonads, and choroid.[1] In the kidney, both discrete granulomas and diffuse granulomatous inflammation (as demonstrated in this slide) are seen.[1] The process of development of inflammatory lesions in affected fish has been studied in detail, characterized, and divided largely into temporal phases.[6] Subacute infections are characterized by diffuse infiltration of macrophages in infected organs with caseonecrotic centers. The chronic proliferative form is characterized by the formation of "hard" and "soft" granulomas, differentiated largely by the presence of fibrous connective tissue in the "hard" granulomas.[6] Calcification (as seen in this slide) occurs in more chronic lesions.[6]

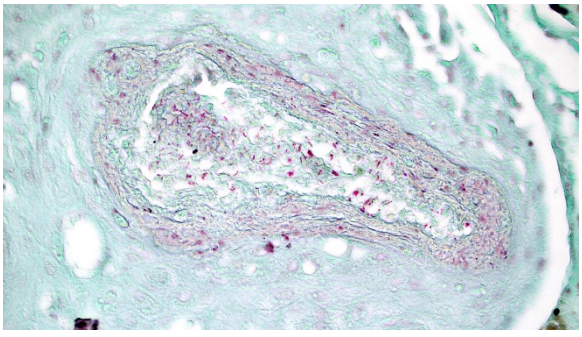

Viscera, oscar. Acid fast stain revealing numerous acid fast positive rods 1x2 um consistent with Mycobacterium spp. (Acid-fast, 400X) (Photo courtesy of: Smithsonian's National Zoo and Conservation Biology Institute, https://nationalzoo.si.edu/animals/veterinary-care)

A range of studies have demonstrated several paths of transmission in fish, including cutaneous wounds (common in bettas raised for export), transovarial transmission, and ingestion (demonstrated by feeding infected fish carcasses).[3] Commonly isolated species include *M. marinum, M. fortuitum, M. chelonae, M. peregrinum and M. abscessus.*[1] The moderator discussed additional differentials for the neoplasm in this case, to include polycystic kidney disease and obstructive cystic disease. The lack of epithelial attenuation within the large cysts tends to rule out obstruction as a cause, but polycystic kidney disease, remained a concern based solely on the histology. The moderator reviewed pertinent renal anatomy and histology in the fish, as well as general pathology of mycobacteriois, and a quick review of gross lesions in fish disease.

References:

1. Frasca S, Wolf JC, Kinsel MJ, Camus AC, Lombardini ED. Osteichthyes. *In* Terio KA, McAloose D, St. Leger J. Pathology of Wildlife and Zoo Animals. London, UK. Associated Press, pp. 964-966.

2. Hochwartner O, Loupal G, Wildgoose WH, Schmidt-Posthaus H. *Occurrence of spontaneous tumours of the renal proximal tubules in oscars Astronotus ocellatus*. Dis Aquat Organ. 2010. 89:185–189.
3. Jacobs JM, Stine CB, Baya Am, Kent ML. A review of mycobacteriosis in marine fish. *J Fish Dis 2009; 32(2): 119-130.*
4. Lee BC, Hendricks JD, Bailey GS. *Rare renal neoplasms in Salmo gairdneri exposed to MNNG (N-methyl-N'-nitro-N-nitrosoguanidine).* Diseases of Aquatic Organisms. 1989. 6:105-111.
5. Lombardini ED, Hard GC, Harshbarger JC. *Neoplasms of the Urinary Tract in Fish*. Veterinary Pathology. 2014. 51:1000–1012.
6. Lewis, S, Chinabut S. Mycobacteriosis and nocardiosis. *In:* Woo PTK, Bruno DW, eds. Fish Diseases and Disorders vol 3, ed. 2. Cambridge MA; CAB International 2011; pp. 397-423.
7. Noga EJ. *Fish Disease: Diagnosis and Treatment (2nd edition).* 2013. Wiley-Blackwell. 239-240.
8. Meuten DJ, Meuten TLK. *In* Meuten DJ, ed. Tumors in Domestic Animals, 5th ed., Ames Iowa, John Wiley and Sons, Inc., 2017; pp 634-638.
9. Murphy WM, Grignon DJ, Perlman EJ. *In*: AFIP Atlas of Tumor Pathology: Tumors of the kidney bladder and related urinary structures. Washington DC, ARP Press, Inc., 2004, pp.160-162.
10. Petervary N, Gillette DM, Lewbart GA, Harshbarger JC. *A spontaneous neoplasm of the renal collecting ducts in an Oscar, Astronotus ocellatus (Cuvier), with comments on similar cases in this species.* Journal of Fish Diseases. 1996. 19:279-281.
11. Racz A, Dwyer T, Killen SS. *Overview of a disease outbreak and introduction of a step by step protocol for the eradication of Mycobacterium haemophilum in a Zebrafish system.* Zebrafish. 2018. DOI: 10.1089/zeb.2018.1628.

CASE III: 19H4111 (JPC 4136173).

Signalment: Juvenile (approximately 2 months), unknown sex, bearded dragon (*Pogona vitticeps*)

History: A recently-adopted juvenile bearded dragon presented for 2-3 day history of lethargy and neurologic abnormalities (star-gazing behavior, intermittent head-tilt, inability to ambulate). Coelomic distention and a significant amount of intestinal contents were observed upon trans-illumination. Severe lethargy and depression persisted following administration of antibiotics, therefore euthanasia and post-mortem examination was elected.

Gross Pathology: The body was considered to be thin and exhibited mild autolysis. The liver was markedly enlarged, diffusely pale yellow to tan, and nodular.

Viscera, bearded dragon. The liver is enlarged, yellow, and has a nodular appearance. (Photo courtesy of: Iowa State University, College of Veterinary Medicine, Department of Veterinary Pathology, Ames, IA 50010-1250, https://vetmed.iastate.edu/vpath)

Laboratory results:
Electron microscopy results revealed intranuclear icosahedral virions consistent with adenovirus, and smaller icosahedral virions suspected to be dependovirus. Whole-genome sequencing confirmed bearded dragon adenovirus in liver samples.

Microscopic Description: Liver: There is hepatocellular disintegration and loss with mild fibrosis and few discernable portal tracts. Diffusely hepatocytes display varying degrees of cytoplasmic microvesicular lipid type vacuolar change. Occasionally, individual or groups of hepatocytes are hypereosinophilic with pyknotic nuclei. In some areas, hepatic bile ducts are proliferative. Frequently, the hepatocyte nuclei are markedly enlarged (karyomegaly) with deeply basophilic round to irregularly-shaped intranuclear inclusions that occasionally displace the chromatin to the periphery. There are multifocal areas of hemorrhage and infiltrates of inflammatory cells consisting of heterophils, lymphocytes, plasma cells, and macrophages.

Other findings: (Not included in slide submission)

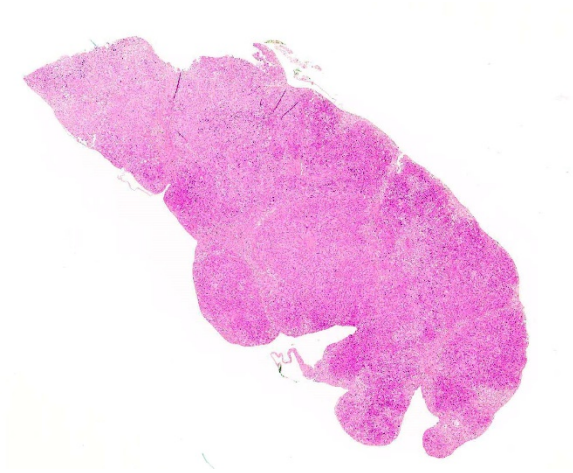

Liver, bearded dragon. The liver has a nodular appearance as a result of bands of fibrosis bridging portal areas. In addition, there are multiple areas of subcapsular hepatocellular loss and fibrosis which give the capsule and undulant appearance. (HE, 19X)

Intestine: There are moderate numbers of apicomplexan organisms in various stages of development within the intestinal mucosa. Mucosal enterocytes show intraepithelial microgametes and macrogametes. Some enterocytes appear degenerate and vacuolated with karyomegalic intranuclear basophilic inclusions. The lamina propria is infiltrated by a small number of lymphocytes, plasma cells, and heterophils.

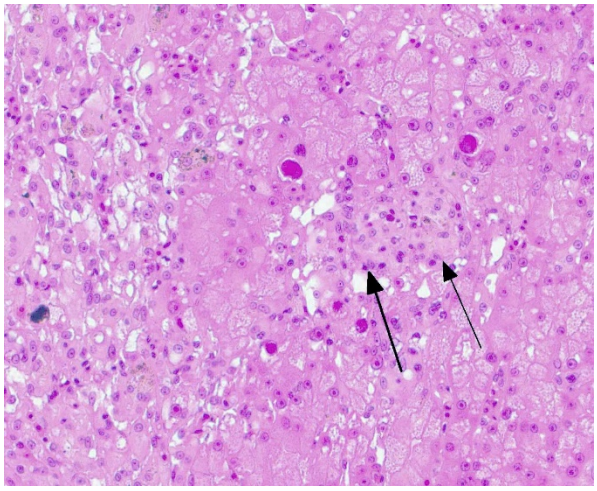

Liver, bearded dragon. At the periphery of attenuated nodules, hepatocytes contain a large intranuclear adenoviral inclusion, may be eosinophilic and rounded up, and there are nodular aggregates of macrophages (arrows). At left, hepatocytes contain small amounts of lipofuscin and melanin. (HE, 400X)

Lungs: Occasional, pneumocytes have karyomegalic nuclei with intranuclear, basophilic viral inclusions.

Pancreas: Pancreatic acinar cells occasionally have karyomegalic nuclei with intranuclear, basophilic viral inclusions.
Kidney: Renal tubular epithelium occasionally have karyomegalic nuclei with intranuclear, basophilic viral inclusions.

Contributor Morphologic Diagnosis:
Liver: Hepatitis, necrotizing, lymphocytic, random, multifocal with biliary hyperplasia, hepatocellular fatty degeneration, karyomegaly and basophilic intranuclear

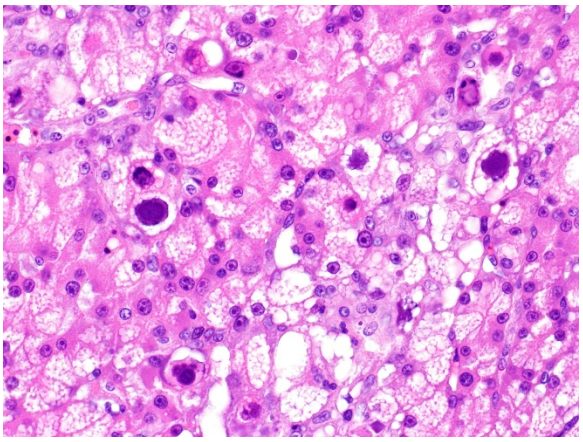

Liver, bearded dragon. Higher magnification of hepatocytes displaying adenoviral intranuclear inclusions and profound microvesicular lipidosis of hepatocytes. (HE, 400X) (Photo courtesy of: Iowa State University, College of Veterinary Medicine, Department of Veterinary Pathology, Ames, IA 50010-1250, https://vetmed.iastate.edu/vpath).

inclusion bodies, (consistent with adenovirus)

Intestine: Enteritis, lymphoplasmacytic, multifocal, moderate, with intraepithelial apicomplexans (coccidiosis) and intranuclear, basophilic inclusion bodies (consistent with adenovirus)

Contributor Comment: Adenoviruses are non-enveloped, linear, dsDNA viruses with an icosahedral nucleocapsid ranging in size from 80-110 nm. Agamid adenovirus-1 belongs to the *Atadenovirus* genera, one of five accepted *Adenoviridae* genera. It is the most widespread of atadenoviruses and has been described in other reptiles such as chelonians, snakes, crocodiles, and chameleons.[7,9] Genomic sequencing techniques have facilitated the characterization of numerous other squamate viruses within this genera, including chameleonid adenovirus 1 in chameleons, eublepharid adenovirus 1 in leopard geckos and fat-tailed geckos, helodermatid adenovirus 1 in Gila monsters and Bearded lizards, scincid adenovirus 1 in blue-tongued skinks, and snake adenovirus 1 and 2 in various snake species.[14]

Agamid adenovirus-1 is a common infection of bearded dragons (*Pogona vitticeps*), as well as other squamates. Clinical signs vary from asymptomatic or mild ill-thrift (e.g., weight loss, lethargy), to severe enterohepatic (e.g., diarrhea, weakness, anorexia) and neurological signs (e.g., head tilt, circling, opisthotonus) as well as death.[1-3,7-11] Disease is thought to manifest from stress-associated viremia, afflicting juveniles more so than adults. Agamid adenovirus-1 is most prevalent among captive breeding colonies though has been isolated from free-

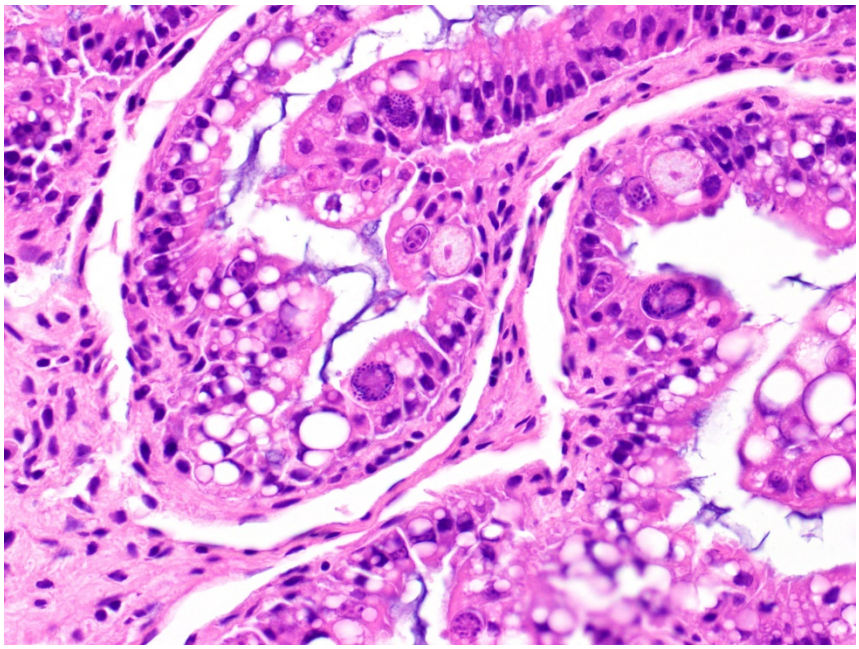

Intestine, bearded dragon. Coccidial schizonts and gametocytes are present within intestinal epithelium. (HE, 400X) (Photo courtesy of: Iowa State University, College of Veterinary Medicine Department of Veterinary Pathology, Ames, IA 50010-1250, https://vetmed.iastate.edu/vpath).

range bearded dragons, which are native to Australia.[3,6,9]

Disease caused by adenoviruses in various species is typically enterohepatic or respiratory in nature.[7,9] There are, however, exceptions to this generalization (see Table 1). Many species do not show outward clinical signs of adenovirus except in the presence of immunosuppression or another primary infection. Numerous cases of agamid adenovirus-1 are reported with concurrent coccidiosis (*Isospora* or *Eimeria* spp.) which also tend to be incidental, except in severe infestations or otherwise compromised bearded dragons.[5,8,11] Other reported comorbidities include *Cryptosporidium* spp., fungal infections, and other viruses (e.g., dependovirus).[7,12] Transmission is primarily fecal-oral, therefore, prevention is aimed at maintaining a hygienic environment and quarantining new colony additions.[9,11]

Antemortem diagnosis of agamid adenovirus-1 can be made via PCR on choanal-cloacal swabs at select diagnostic laboratories, which is preferred to serology due to lower sensitivity.[3,4,6] Postmortem diagnosis is based on presumptive karyomegalic, basophilic, intranuclear adenoviral inclusions and necrosis, particularly within the liver. Viral inclusions may be visualized within hepatocytes,

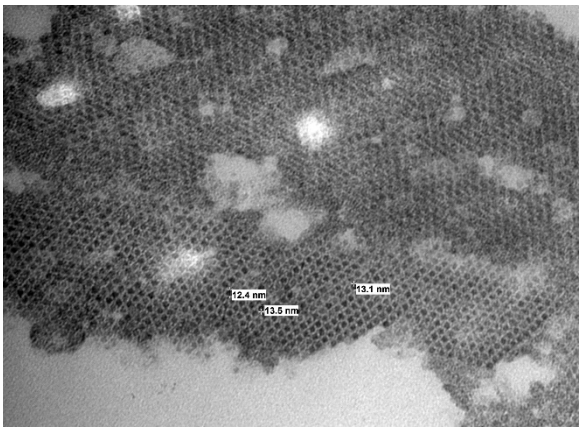

Liver, bearded dragon. Icosahedral virions measuring 12.4 nm to 16.3 nm are seen intracellularly, compatible with dependovirus. (Photo courtesy of: Iowa State University, College of Veterinary Medicine, Department of Veterinary Pathology, Ames, IA 50010-1250, https://vetmed.iastate.edu/vpath).

enterocytes, esophageal epithelium, myocardium, endocardium, lung, renal tubular epithelium, brain glial and epithelial cells, and/or within the pancreas.[3,7,11] Other molecular techniques such as electron microscopy, in situ hybridization, and next gen sequencing are useful in obtaining a definitive diagnosis or further characterizing adenoviruses.[1,3,4,8,14] Despite this virus being typically host-specific, phylogenetic evidence supports some cross-over and viral adaptation through co-evolution in novel host species.[1,2,14]

Genus	Virus(es)	Reported Disease/Syndrome
Atadenovirus	Agamid adenovirus 1	Hepatitis, enteritis, encephalitis
	Duck adenovirus 1	Egg drop syndrome
	Cervine adenovirus 1	Vasculitis, hemorrhagic disease, pulmonary edema
	Caprine adenovirus 1	None to mild respiratory disease
	Ovine adenovirus 7	None to mild respiratory disease
Aviadenovirus	Fowl adenovirus 2, 8, 11	Inclusion body hepatitis
	Fowl adenovirus 4	Hepatitis-hydropericardium syndrome virus
	Fowl adenovirus 1	Gizzard erosion
	Avian adenovirus 1	Quail bronchitis virus
	Turkey adenovirus 1 & 2	Decreased egg production

	Duck adenovirus 2	Hepatitis (rarely)
Ichtadenovirus	Sturgeon ichtadenovirus A	
Mastadenovirus	Canine adenovirus 1 Canine adenovirus 2 Bovine adenovirus Equine adenovirus 1 & 2 Porcine adenoviruses 1-5 Guinea pig Rabbit adenovirus 1 Goat adenovirus 2 Ovine adenovirus 1-5 Caprine adenovirus	Infectious canine hepatitis Infectious canine tracheobronchitis Pneumonia and enteritis (secondary pathogen) Bronchopneumonia in immunocompromised (SCID) Mild respiratory disease, enteritis, encephalitis Asymptomatic, or pneumonia (high mortality) Diarrhea Severe respiratory and enteric disease in lambs None to mild respiratory disease
Siadenovirus	Frog siadenovirus A Raptor siadenovirus A Psittacine adenovirus 2 Budgerigar adenovirus 1 Gouldian finch adenovirus 1 Silawesi tortoise adenovirus 1 Turkey adenovirus 3	Hemorrhagic enteritis (turkeys), marble spleen (pheasants), avian adenovirus splenomegaly (broiler chickens)

Table 1. Adenoviruses of importance in animal species

Contributing Institution:

Iowa State University
College of Veterinary Medicine
Department of Veterinary Pathology
Ames, IA 50010-1250
https://vetmed.iastate.edu/vpath

JPC Diagnosis: Liver: Hepatitis, necrotizing, multifocal to coalescing, chronic, moderate with fibrosis and numerous hepatocellular intranuclear viral inclusions

JPC Comment: The contributors have done an excellent job discussing adenoviral infection in a wide range of species. Adenoviral hepatitis has made a number of appearances in the WSC over the years below. (Table 2).

In addition to the listing of infected lizards mentioned by the contributor, adenoviruses have also been documented in eastern bearded dragons, savannah and emerald monitors, Rankin's dragon lizard, central netted dragons, western striped tree dragons, green anoles, Jackson's and mountain chameleons, , common agamas, and Tokay geckos.[10] Most if not all adenoviral infections in lacertids focus primarily on the liver. Clinical signs may range from none to acute CNS signs to chronic wasting and gross findings are usually minimal. Histology in affected livers usually is that of a necrotizing

hepatitis, and the biliary epithelium is also affected in some species. In addition to hepatocytes, intranuclear inclusions may be seen in a range of other cells, including enterocytes, endothelial cells, renal tubular epithelium, glomeruli, exocrine pancreas, and oral mucous membrane.[10] Proliferative changes have been reported (primarily affecting the tracheal and esophageal mucosa) in Jackson chameleons.[10] Coinfections are common, including dependoparvovirus (reported as a hepatic coinfection in bearded dragons with adenovirus)[7,10], ranavirus, iridovirus, and gastrointestinal parasites such as coccidia and helminths.[10] Nile crocodiles) also have an adenovirus which results in hepatitis as well.[7] While adenoviruses are well-known for their disease-causing effects in multiple species, including humans, adenoviruses are also on the forefront of human medicine, especially in the areas of gene therapy and vaccine delivery. As adenovirus DNA does not incorporate into the viral genome during transcription such as say retroviral DNA, they are an ideal vector for the delivery of genes or antigenic materials on a therapeutic basis.[13] An issue that faces adenovirus vectors, however, is the prevalence of antibodies to many common human adenoviruses in potential patients (arising from the mild infections of the respiratory, GI, and urinary tracts that adenovirus cause in immunocompetent individuals. The use of adenoviruses linked to animal, but not human, disease (such as chimpanzee adenoviruses) has been proposed to solve this issue, but concern about potential generation of severe cross-species disease has tempered its current usage.[13]

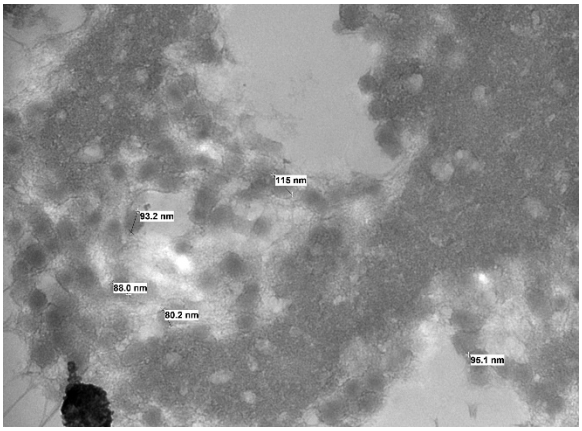

Liver, bearded dragon. Larger icosahedral virions measuring 80.2 nm to 115 nm are seen intranuclearly, compatible with adenovirus. (Photo courtesy of: Iowa State University, College of Veterinary Medicine, Department of Veterinary Pathology, Ames, IA 50010-1250, https://vetmed.iastate.edu/vpath).

WSC 2018-2019, Conf 21, Case 2 WSC 2013-2014, Conf 16, Case 4 WSC 1987 Conf 29, Case 2	Chicken
WSC 2018-2019, Conf 16, Case 1 WSC 2012-2014, Conf 1 Case 3 WSC 1996-1997, Conf 20, Case 4	Dog
WSC 2009-2010, Conf 9, Case 3 WSC 1995-1996, Conf 29, Case 2	Bearded Dragon
WSC 2007-2008, Conf 23, Case 3 WSC 1997-1998, Conf 29, Case 4	Falcon
WSC 1991, Conference 6, Case 2	Chimpanzee

Table 2. Adenoviral hepatitis in the WSC

The moderator reviewed the pertinent gross anatomy of the bearded dragon. The moderator gave a brief discussion of dependoviruses, which often are seen as coinfections with adenovirus, as they

"depend" on the viral machinery of adenoviruses for replication.

References:

1. Bak E-J, Jho Y, Woo G-H. Detection and phylogenetic analysis of a new adenoviral polymerase gene in reptiles in Korea. *Arch Virol*. 2018: 1-7.
2. Benge SL, Hyndman TH, Funk RS, et al. Identification of helodermatid adenovirus 2 in a captive central bearded dragon (pogona vitticeps), wild gila monsters (heloderma suspectum), and a death adder (acanthophis antarcticus). *J Zoo Wildl Med*. 2019;50: 238-242.
3. Doneley R, Buckle K, Hulse L. Adenoviral infection in a collection of juvenile inland bearded dragons (Pogona vitticeps). *Aust Vet J*. 2014;92: 41-45.
4. Fredholm DV, Coleman JK, Childress AL, Wellehan Jr JF. Development and validation of a novel hydrolysis probe real-time polymerase chain reaction for agamid adenovirus 1 in the central bearded dragon (Pogona vitticeps). *J Vet Diang Invest.* 2015;27: 249-253.
5. Hallinger MJ, Taubert A, Hermosilla C, Mutschmann F. Captive Agamid lizards in Germany: Prevalence, pathogenicity and therapy of gastrointestinal protozoan and helminth infections. *Comp Immunol Microbiol Infect Dis*. 2019;63: 74-80.
6. Hyndman TH, Howard JG, Doneley RJ. Adenoviruses in free-ranging Australian bearded dragons (Pogona spp.). *Vet Microbio*. 2019;234: 72-76.
7. Jacobson ER. Viruses and viral diseases of reptiles. In: Infectious diseases and pathology of reptiles: color atlas and text. Boca Raton, FL: CRC Press; 2007:395-460.
8. Kim DY, Mitchell MA, Bauer RW, Poston R, Cho D-Y. An outbreak of adenoviral infection in inland bearded dragons (Pogona vitticeps) coinfected with dependovirus and coccidial protozoa (Isospora sp.). *J Vet Diang Invest*. 2002;14: 332-334.
9. Marschang RE. Viruses infecting reptiles. *Viruses*. 2011;3: 2087-2126.
10. Orrigi, F. Lacertilia. *In In* Terio KA, McAloose D, St. Leger J. Pathology of Wildlife and Zoo Animals. London, UK. Associated Press, pp. 875.
11. Schilliger L, Mentré V, Marschang RE, Nicolier A, Richter B. Triple infection with agamid adenovirus 1, Encephaliton cuniculi-like microsporidium and enteric coccidia in a bearded dragon (Pogona vitticeps). *Tierarztl Prax Ausg K*. 2016;5.
12. Schmidt-Ukaj S, Hochleithner M, Richter B, Hochleithner C, Brandstetter D, Knotek Z. A survey of diseases in captive bearded dragons: a retrospective study of 529 patients. *Vet Med (Praha)*. 2017;62: 508-515.
13. Tatsia N, Ertl HCJ. Adenoviruses as vaccine vectors. *Mol Therap* 2004. (10)4: 616-630
14. Wellehan JF, Johnson AJ, Harrach B, et al. Detection and analysis of six lizard adenoviruses by consensus primer PCR provides further evidence of a reptilian origin for the atadenoviruses. *J Virol.* 2004;78: 13366-13369.

CASE IV: 19-33870 (JPC 4138045).

Signalment: Adult, female Silvery Salamander *(Ambystoma platineum)*

History: This wild salamander was found dead in the water in late March at a local state park in central Illinois.

Gross Pathology: Examined is a 12.0 g adult female Silvery Salamander *(Ambystoma platineum)* in fair postmortem condition. There are numerous, discrete, 1-3 mm in diameter white, flat to slightly raised cutaneous

Skin, salamander. Multiple randomly arranged white nodules are present across the body surface. (Photo courtesy of: University of Illinois at Urbana-Champaign, Veterinary Diagnostic Laboratory http://vetmed.illinois.edu/vet-resources/veterinary-diagnostic-laboratory/)

foci scattered throughout the entire surface of the body (Figure 1). There are few discrete 1-2 mm in diameter white to tan flat foci within the subcapsular surface of the liver. The remaining viscera are unremarkable.

Laboratory results:
FV3 Ranavirus qPCR was negative.

Microscopic Description: Skin: Mostly confined within the epidermis and rarely expanding the dermis are large numbers of variably sized intraepidermal cysts (sporangia) packed with round, 5-10 µmin diameter, eosinophilic globular spores with scant crescent- shaped pale eosinophilic variably granulated cytoplasm. The sporangia mostly distend the mid to basal portions of the epidermis. There are moderate numbers of coccobacilli enmeshed in between the spores. There is minimal leukocytic reaction towards the cysts. The remaining epidermis is moderately hyperplastic with multiple segments of prominent superficial cornification.

Special staining of sporangia within the liver with Grocott's Methenamine Silver (GMS) and Periodic acid-Schiff (PAS) is performed. The GMS stain highlights in black the majority of the spore's capsule and parts of the internal contents. Diffusely, the entire spore structure has strong reaction for PAS.

Other findings: (Not included in slide submission)
Intestine: There are moderate numbers of apicomplexan organisms in various stages of development within the intestinal mucosa. Mucosal enterocytes show intraepithelial microgametes and macrogametes. Some enterocytes appear degenerate and vacuolated with karyomegalic intranuclear basophilic inclusions. The lamina propria is infiltrated by a small number of lymphocytes, plasma cells, and heterophils.

Lungs: Occasional, pneumocytes have karyomegalic nuclei with intranuclear, basophilic viral inclusions.

Pancreas: Pancreatic acinar cells occasionally have karyomegalic nuclei with intranuclear, basophilic viral inclusions.

Kidney: Renal tubular epithelium occasionally have karyomegalic nuclei with intranuclear, basophilic viral inclusions.

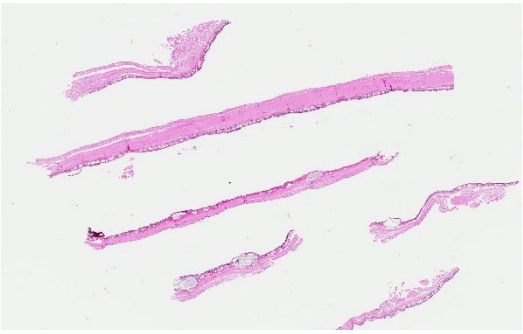

Skin, salamander. Multiple sections of skin are submitted for examination. There are multiple irregularly round nodules which elevate the epidermis. (HE, 9X)

Contributor Morphologic Diagnosis:
Skin (bodywide): Numerous intraepidermal Mesomycetozoan sporangia

Contributor Etiologic diagnosis:
Cutaneous amphiocystidiosis

Contributor Comment: The cause of death in this salamander is likely multifactorial. The presence of cutaneous amphiodiocystidiosis may be considered an incidental finding, however the concurrent visceral involvement (liver) in this case might suggest significant infection secondary to immune suppression or damaged defense mechanisms. A primary infectious etiology was not identified, so clinical deterioration due to environmental factors cannot be ruled out.

Amphibiocystidium is a genus of fungal-like parasites that cause characteristic skin nodules in amphibians of Europe and North and South America. A member of the class Mesomycetozoea, these protists arose at the animal-fungal divergence and were historically considered either protozoan or fungal.[7]

Mesomycetozoans are found in marine and freshwater environments as commensals or parasites to invertebrates, fish, amphibians, birds, and mammals.[8] *Amphibiocystidium* is closely related to the genuses *Dermocystidium,* which is a primary pathogen of salmonid fish, and *Rhinosporidium,* which causes clinical disease in birds and mammals, including humans.[7]

Grossly, *Amphibiocystidium* spp. cause multifocal, regular, 3-5 mm in diameter

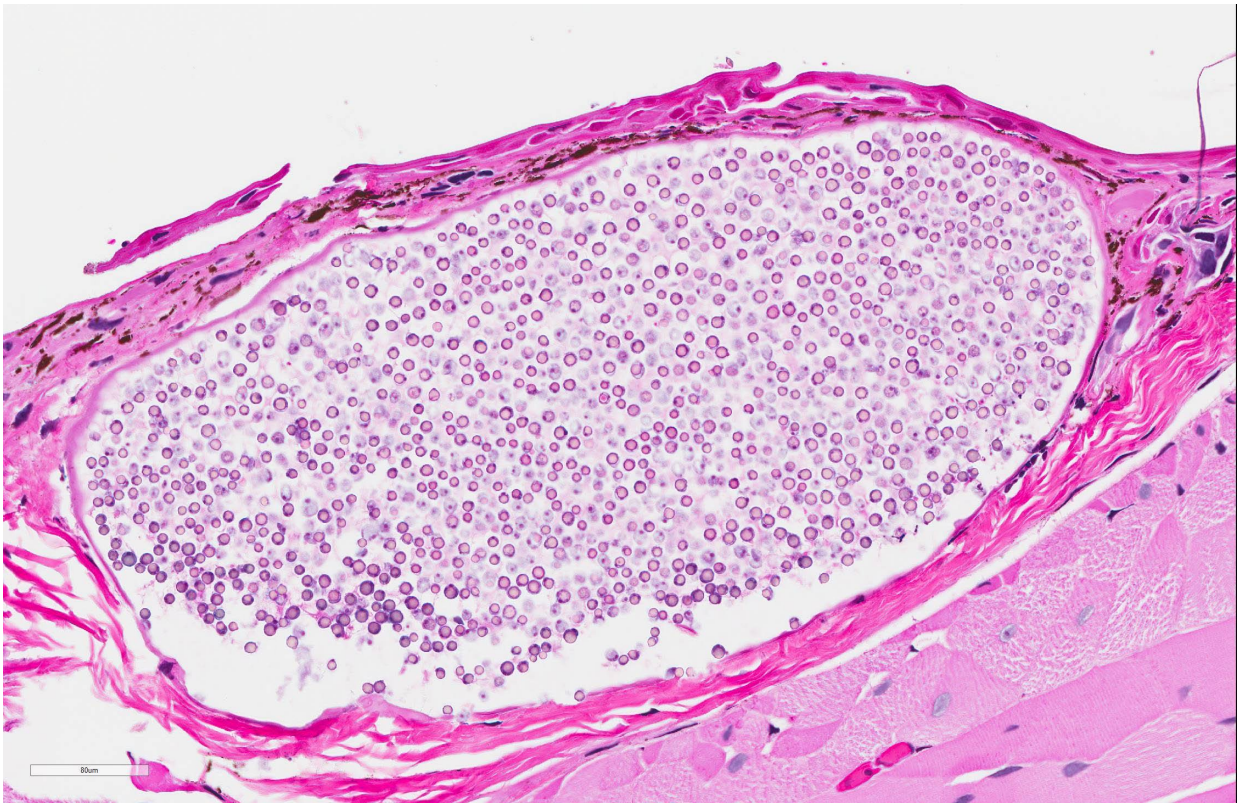

Skin, salamander. Cutaneous sporangia measure 0.3 to 0.6 mm, are bound by a thin hyaline wall, and contain numerous 10um endospores (HE, 270X)

often spherical, "C" or "U"-shaped skin nodules that are sometimes ulcerated. These lesions must be grossly differentiated from encysted parasites (particularly *Clinostomum* sp. trematodes) or granulomas caused by higher order bacteria or fungi.

Microscopically, studies report several 100-600 µm cysts (sporangia) containing myriad 2-6 µm endospores.[7] An inflammatory cell infiltrate composed primarily of lymphocytes and macrophages may be found in the vicinity of these cysts. The associated epidermis may be hyperplastic. Histologic lesions must be differentiated from unidentified alveolate protozoa observed in ranid frogs, which have been associated with mortality events in free-ranging ranid tadpoles in the United States.[8] Tissues affected by alveolate protozoa will be infiltrated by large numbers of 6-9 µm spherical basophilic spores in absence of a host inflammatory response, and spores are positive for periodic acid-Schiff (PAS), Grocott's methenamine silver (GMS), and Congo Red stains.[8]

The phylogeny of *Amphibiocystidium* is still unsettled; the genus was recently created to encompass members of the

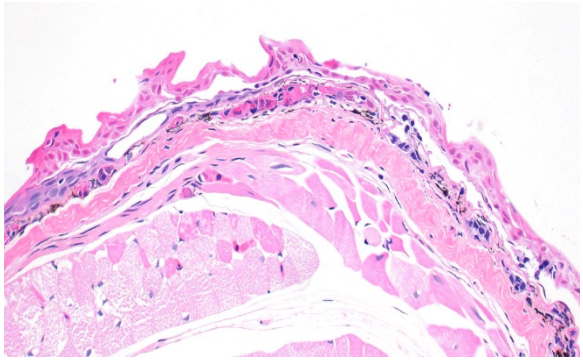

Skin, salamander. Multifocally, there are areas of epidermal necrosis in which the full thickness of the epidermis has lost differential staining and is separated from the underlying dermis. (HE, 100X)

Dermocystidium, Dermomycoides, and *Dermosporidium* spp. affecting amphibians, interpreted as monophyletic,[6] and may also include the related genus *Amphibiothecum,* a parasite of American toads *(Anaxyrus americanus).* Predominant species of *Amphibiocystidium* include A. *ranae, A. viridescens.* and A. *pusula.*[7]

Amphibiocystidium spp. have been reported to affect both anuran and caudate species in Europe, where it has been detected for over a century, and was more recently discovered in North America.[9] Although lethal infections have been documented, the large majority of reported cases are associated with low morbidity and mortality.[2] The life cycle and pathogenesis of *Amphibiocystidium* is largely unknown.[3] Although clinical challenge studies have yet to be performed, a 7-year survey of a natural population of Italian stream frogs *(Rana italica)* found no appreciable negative effects of *Amphibiocystidium* infection; however, ecological and host-specific factors influencing susceptibility were not assessed in this study.[2]

Primarily attributed to climate change and emerging pathogens such as chytrid fungus *(Batrachochytrium dendrobatidis)* and ranaviruses, the current massive decline in global amphibian populations

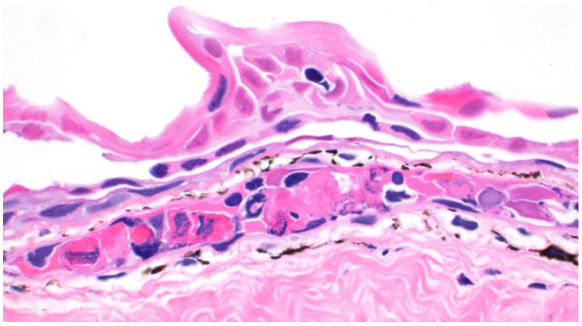

Skin, salamander. Higher magnification of an area of epithelial necrosis. The vessel in the dermis beneath is thrombosed and contains numerous granulocytes. (HE, 400X)

has emphasized the need to understand the myriad of other infectious agents affecting amphibian species, most of which have yet to be well-described and understood.[9,10] Some of these agents, such as *Amphibiocystidium,* have been found in amphibians co-infected with *Batrachochytrium dendrobatidis,* with several other reports implying but not confirming co-infection.[1] Many of these agents, such as *Amphibiocystidium* have unknown pathogeneses and have yet to undergo clinical studies.

Contributing Institution:
University of Illinois at Urbana-Champaign, Veterinary Diagnostic Laboratory
http://vetmed.illinois.edu/vet-resources/veterinary-diagnostic-laboratory/

JPC Diagnosis: 1. Skin, epidermis: Numerous sporangia.
2. Skin, epidermis: Necrosis, multifocal, with vasculitis, dermatitis, and epidermal hyperplasia.

JPC Comment: The contributor has done an outstanding job in this review of *Amphibiocystidium*, an emerging mesomycetozoan pathogen. The Mesomycetozoae are a class of organisms that contain ten different genera of saprophytic and parasitic organisms (grouped by 18s ribosomal DNA analysis) which have changed in classification over the years, previously being referred to as both fungi and protists. Their grouping was initially called the "DRIP clade", an acronym composed of its initial members *Dermocystidium,* rosette agent, *Ichthyophonus* and *Psorospermium*. With the exception of *Rhinosporidium*, parasitic species primarily infect aquatic animals. Most of these agents have poorly documented life cycles.[5]
Rhinosporidium seeberi is the most well-known of the group, due to its propensity to infect higher vertebrates, including dogs, horses, and humans. It is thought that most infections arise via traumatized epithelium. Nasal polyps are the most common and identifiable lesions associated with infection and in humans (account for 70% of lesions; however, humans have demonstrated a range of other staging areas, including the palpebral and bulbar conjunctiva (15%), sclera, lacrimal sac, and genital mucous membranes. No immunity is developed against rhinosporidiosis, although rarely spontaneous regression has been noted.[4]

The term "rosette agent" refers to a unique species of mesomycetozoan (*Sphaerothecum*

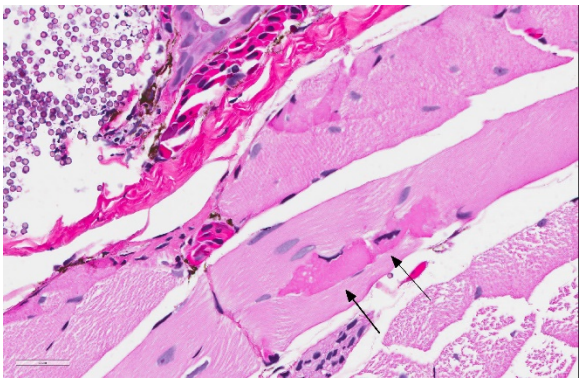

Skin, salamander. There are rare necrotic myocytes scattered randomly through skeletal muscle. (HE, 340X)

destruens) which was first identified in China and appears to have been spread through the aquaculture trade to Europe and the US in association with another invasive species, its natural host the stone moroko (*Pseudorasbora parva).* It has been identified in over 4 species, including salmon, carp, and sea bass. This mesomycetozoan results in systemic and often fatal infection in aberrant hosts, but invading gills, liver, kidney, intestine, and gonads. The spores pass from infected fish in both urine and seminal fluid. The parasite has the ability to infect both salmonids and cyprinids, with great potential to impact global piscine biodiversity as well as have a profound impact on aquaculture and food security.[12]

Mesomycetozae have made a number of appearances in the Wednesday Slide Conference:
Rhinosporidium seeberi: (WSC 2017-2018 Conf 3, Case 3-horse, WSC 2016-2017 Conf 8, Case 1-horse, WSC 2010-2011 Conf 14, Case 3-horse, WSC 2002-2003 Conf 11, Case 3-dog, among others); *Ichthyophonus* (WSC 2001-2002 Conf 24, Case 4 – rainbow trout, WSC 2015-2016 Conf 13, Case 1 – red-spotted newt); *Dermocystidium* (WSC 2015-2016 Conf 13, Case 1-tetra, WSC 2010-2011 Conf 22, Case 3-koi); and *Perkinsus* (classified at the time on the shifting sands of the mesomycetozoans-but now classified as in the phylum Perkinsozoa) (WSC 2013-2014, Conf 12, Case 3 – abalone).
A pathologist from the National Zoo in attendance commented on the presence of myonecrosis in this slide and the frequency with which it is seen in fresh autopsies on amphibians, to the point that he considered these changes to be almost artifactual in this case. Several participants, including the moderator saw areas in which the epidermis was diffusely pink and without differential staining, and mildly separated with serum pooling. One area was associated with a focal area of granulocyte aggregation. Spirited discussion greeted this finding (which may not have been present on all slides), but its cause is unclear. The moderator also discussed the peculiar life cycle of this gynogenic species, in which all specimens are female, and mating with males of another species. The sperm of the male (usually blue-spotted or Jefferson salamanders) stimulates egg development, but does not contribute to the DNA of the offspring. The moderator also discussed the difficulty (per Dr. Alan Pessier of Washington State University) of definitively differentiating *Amphibiocystidium* from *Perkinsus* based on HE slides.

References:

1. Borteiro C, Cruz JC, Kolenc F, et al. Dermocystid-chytrid coinfection in the Neotropical frog Hypsiboas pulchellus (Anura: Hylidae). *J Wildl Dis*. 2014;50(1):150-153.
2. Fagotti A, Rossi R, Canestrelli D, et al. Longitudinal study of Amphibiocystidium sp. infection in a natural population of the Italian stream frog (Rana italica). *Parasitology.* 2019:1-8.
3. Gonzalez-Hernandez M, Denoel M, Duffus AJ, Garner TW, Cunningham AA, Acevedo-Whitehouse K. Dermocystid infection and associated skin lesions in free- living palmate newts (Lissotriton helveticus) from Southern France. *Parasitology International.* 2010;59(3):344-50.
4. John D, Selvin SST, Irodi A, Jacob P. Disseminated rhinosporidiosis with conjunctival involvement in an immunocompromised patient. *Mid East Afr J Ophthal* 2017; 24(1):51-53.
5. Mendoza L, Taylor JW, Ajello L. The class *Mesomycetozoea*: a heterogenous group of micro-organisms at the animal-fungal

boundary. *Ann Rev Microbiol* 2002; 56:315-244.

Pascolini R, Daszak P, Cunningham AA, et al. Parasitism by Dermocystidium ranae in a population of *Rana esculenta* complex in Central Italy and description of Amphibiocystidium n. gen. *Dis Aquat Org*. 2003;56(1):65-74.

6. Pereira CN, Di Rosa I, Fagotti A, Simoncelli F, Pascolini R, Mendoza L. The pathogen of frogs Amphibiocystidium ranae is a member of the order Dermocystida in the class Mesomycetozoea. *J Clin Microbial.* 2005;43(1):192-198
7. Pessier A. Amphibia. In: Terio, K. A., McAloose, D., & Leger, J. S, eds. *Pathology of Wildlife and Zoo Animals.* Academic Press; 2018:915-944.
8. Pessier AP. Hopping over red leg: The metamorphosis of amphibian pathology. *Vet Path*. 2017;54(3):355-357
9. Pessier AP. Management of disease as a threat to amphibian conservation. *International Zoo Yearbook*. 2008;42(1):30-39.
10. Raffel TR, Bommarito T, Barry DS, Witiak SM, Shackelton LA. Widespread infection of the Eastern red-spotted newt (Notophthalmus viridescens) by a new species of Amphibiocystidium, a genus of fungus-like mesomycetozoan parasites not previously reported in North America. *Parasitology.* 2008;135(2):203-215.
11. Sana S, Harodouin EA, Gozlan RE, Ercan D, Tarkan AS, Zhang T, Andreou D. Origin and invasion f the emerging infectious pathogen *Sphaerothecum destruens.*

Self-Assessment - WSC 2019-2020 Conference 10

1. Which of the following organs is most commonly affected by Panulirus argulus-1 infection ?
    a. Exoskeleton
    b. Gills
    c. Intestinal tract
    d. Hepatopancreas

2. Which of the following is true about renal cystadenomas?
    a. They are more common than renal malignancies.
    b. They often have a high mitotic rate.
    c. Size has been used a criteria for morphologic diagnosis.
    d. Theyare easily differentiated from carcinomas.

3. Which of the species of non-tuberculous mycobacteria has not been commonly isolated in fish?
    a. M. cheloniae
    b. M. marinum
    c. M. fortuitum
    d. M. genovense

4. Adenoviral infections in lacertids primarily affect which organ?
    a. Intestine
    b. Lung
    c. Liver
    d. Brain

5. *Amphibiocystidium* is most closely related to which of the following genera of pathogenic organisms?
    a. Chlorella
    b. Rhinosporidium
    c. Histoplasma
    d. Balantidium

Please email your completed assessment for grading to Dr. Bruce Williams at bruce.h.williams12.civ@mail.mil. Passing score is 80%. This program (RACE program 33611) is approved by the AAVSB RACE to offer a total of 0.5 CE Credits, with a maximum of 12.5 CE Credits being available to any individual Veterinary Medical Professionals for the 2019-2020 Wednesday Slide Conference. This RACE approval is for the subject matter categories of: SCIENTIFIC using the delivery method of NON-INTERACTIVE DISTANCE. This approval is valid in jurisdictions which recognize AAVSB RACE.

Joint Pathology Center
Veterinary Pathology Services

WEDNESDAY SLIDE CONFERENCE 2019-2020

Conference 11

4 December 2019

Conference Moderator:

Charles W. Bradley, VMD, DACVP
Assistant Professor, Pathobiology
University of Pennsylvania School of Veterinary Medicine
4005 MJR-VHUP
3900 Delancey Street
Philapdelphia, PA, 19104

CASE I: S17-1101 (JPC 4116937).

Signalment: 4-year-old spayed female Bernese mountain dog (*Canis familiaris*).

History: The animal had a one year history of skin changes including multifocal alopecia, crust formation and discolorations, whose underlying cause could not be identified. The animal had been treated with high doses of dexadreson and cyclosporine, resulting in a mild and slow improvement of the skin lesions. Two weeks before death the animal started limping and a rupture of the cruciate ligament was suspected. The animal was euthanized because of the questionable prognosis of the skin lesions in combination with the cruciate rupture and recurrent episodes of fever of unknown origin (temperature >39.8°C).

Haired skin, dog. Around the bridge of the nose, the mouth and eyes, there are multiple sharply circumscribed partially hairless areas with severe crust formation. (Photo courtesy of: Institute of Veterinary Pathology, Vetsuisse Faculty (University of Z Zurich), Winterthurerstrasse 258, CH-8057 Zurich, Fax number +41 44 635 89 34, http://www.vetpathology.uzh.ch)

Gross Pathology: On both sides of the trunk extending to the axillas and groin, on the nasal bridge, on the ears, and around the

Haired skin, dog. Around the bridge of the nose, the mouth and eyes, there are multiple sharply circumscribed partially hairless areas with severe crust formation. (Photo courtesy of: Institute of Veterinary Pathology, Vetsuisse Faculty (University of Z Zurich), Winterthurerstrasse 258, CH-8057 Zurich, Fax number +41 44 635 89 34, http://www.vetpathology.uzh.ch)

eyes and mouth, there were multiple, sharply demarcated, hairless or partially hairless areas of skin with brown to grey discoloration and crust formation. Around these hairless areas, the fur was clotted with crusty, brown material. Bilaterally adjacent to the caudal aspect of the tongue, there were red, papillary masses of soft tissue and approximately 1 x 2 x 0.5 cm observed (histologically identified as chronic-active necrotizing and suppurative inflammation with granulation tissue formation). On the left cheek, there was a pale yellow, soft mass in the subcutis (lipoma). On the right knee joint the drawer test was positive with increased mobility of the joint. The joint was filled with turbid, slightly flocculent synovial fluid and both anterior and posterior cruciate ligaments were ruptured (right sided complete cruciate ligament rupture with secondary chronic multifocal gonitis on the right side with follicle formation). The liver was markedly enlarged and displayed round edges (diagnosed histologically as steroid induced hepatopathy).

In the right cranial lobe of the lung, there was a firm, poorly demarcated structure palpable in the parenchyma. On the serosal surface of the left middle lobe, there were multiple plaque-like, sharply circumscribed, brown depositions of material observed (histologically identified as multifocal calcifications of pulmonary basal membranes with reactive histiocytic inflammation).

Laboratory results:

Ultrasound and radiography: no abnormalities detected.Hematology/blood chemistry: no abnormalities detected

Microscopic Description:

All layers of the epidermis and also the follicular infundibular epithelium contain rounded, hypereosinophilic keratinocytes with pyknotic nuclei (apoptosis). Multifocally, apoptotic keratinocytes are surrounded by lymphocytic infiltrations (satellitosis). Within the epidermis there are multifocal accumulations of neutrophils, separating the superficial from the deeper

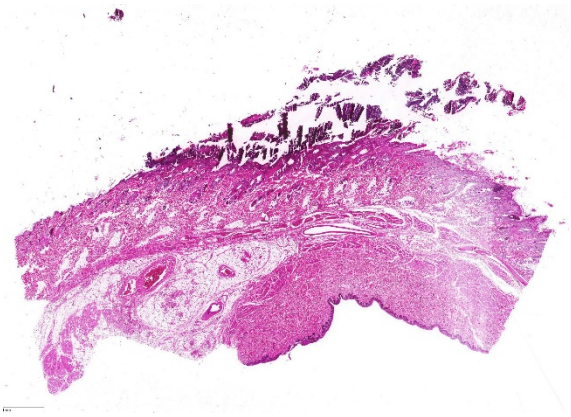

Haired skin, dog. The submitted section of haired skin contains a focally thickened area of epidermis with a hypercellular area of suppurative dermatitis. (HE, 7X).

epidermal layers (interpreted as pustule formation). The superficial dermis and the dermo-epidermal junction show ribbon-like, severe infiltrations of lymphocytes, plasma cells and fewer macrophages, separating the dermo-epidermal junction into areas which are variably clearly visible or severely obscured. Lymphoid infiltrates are observed in the basal layer and macrophages containing brown pigment (melanin) are visible in the dermis (melanin incontinence). Multifocally the stratified layer is thickened and multifocally nuclei can be observed also in the superficial keratinocytes (parakeratotic and orthokeratotic hyperkeratosis). Furthermore, the epidermal surface is covered by serocellular crusts and accumulations of (partially degenerate) neutrophils. In the superficial areas, low numbers of thick-walled, round structures with a clear center and approximately 5- 10 µm in diameter (interpreted as *Candida* spores) are observed. The neutrophilic infiltrates extend multifocally deep into the dermis or into the hair follicles (secondary suppurative pyoderma and folliculitis).

Contributor's Morphologic Diagnosis: Skin, chronic multifocal to coalescing interface dermatitis, with apoptotic keratinocytes, lymphocytic satellitosis and with secondary crust formation, parakeratotic hyperkeratosis, suppurative pyoderma and folliculitis (consistent with erythema multiforme)

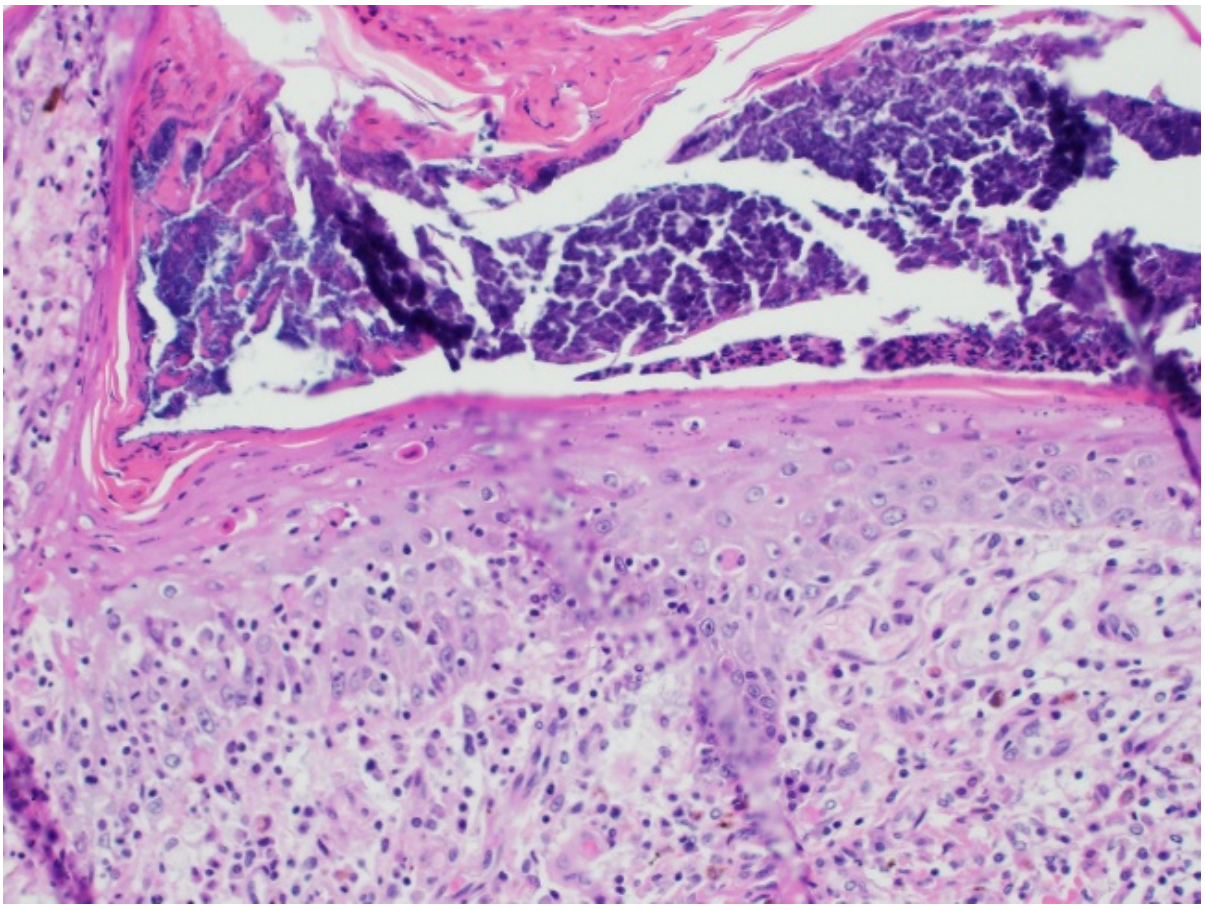

Haired skin, dog. The submitted section of haired skin contains a focally thickened area of epidermis with a hypercellular area of suppurative dermatitis. (HE, 7X)

Contributor's Comment: Erythema multiforme is a rare skin disease in dogs and cats and has also been described in horses, cattle, swine, ferrets and anecdotally in goats.[3,6,7] The nomenclature and definitions of erythema multiforme (EM), Stevens-Johnson syndrome (SJS) and toxic epidermal necrosis (TEN) in veterinary literature are conflicting and therefore confusing.[7,8] In human medicine, EM, SJS and TEN were considered to be different severities of the same disease. Nowadays it is accepted that EM and SJS/TEN represent separate conditions.[8]

The pathogenesis of erythema multiforme in animals is still poorly understood.[3,6,7,8] Possible etiologies include adverse drug reactions (CADR), e.g. against sulphonamides, other antibiotics, and levamisole. Neoplasia, food (including commercial dog food and beef/soy diet), nutraceutical products and infections are reported triggers for erythema multiforme in canine patients.[3,4,6,7,8] However, proven causalities by re-challenge are rare and a multicentric study revealed that only 19% of the canine EM cases were drug related.[5] The histological characteristics and pattern indicate a misdirected immune response against keratinocytes, which is lymphocyte-

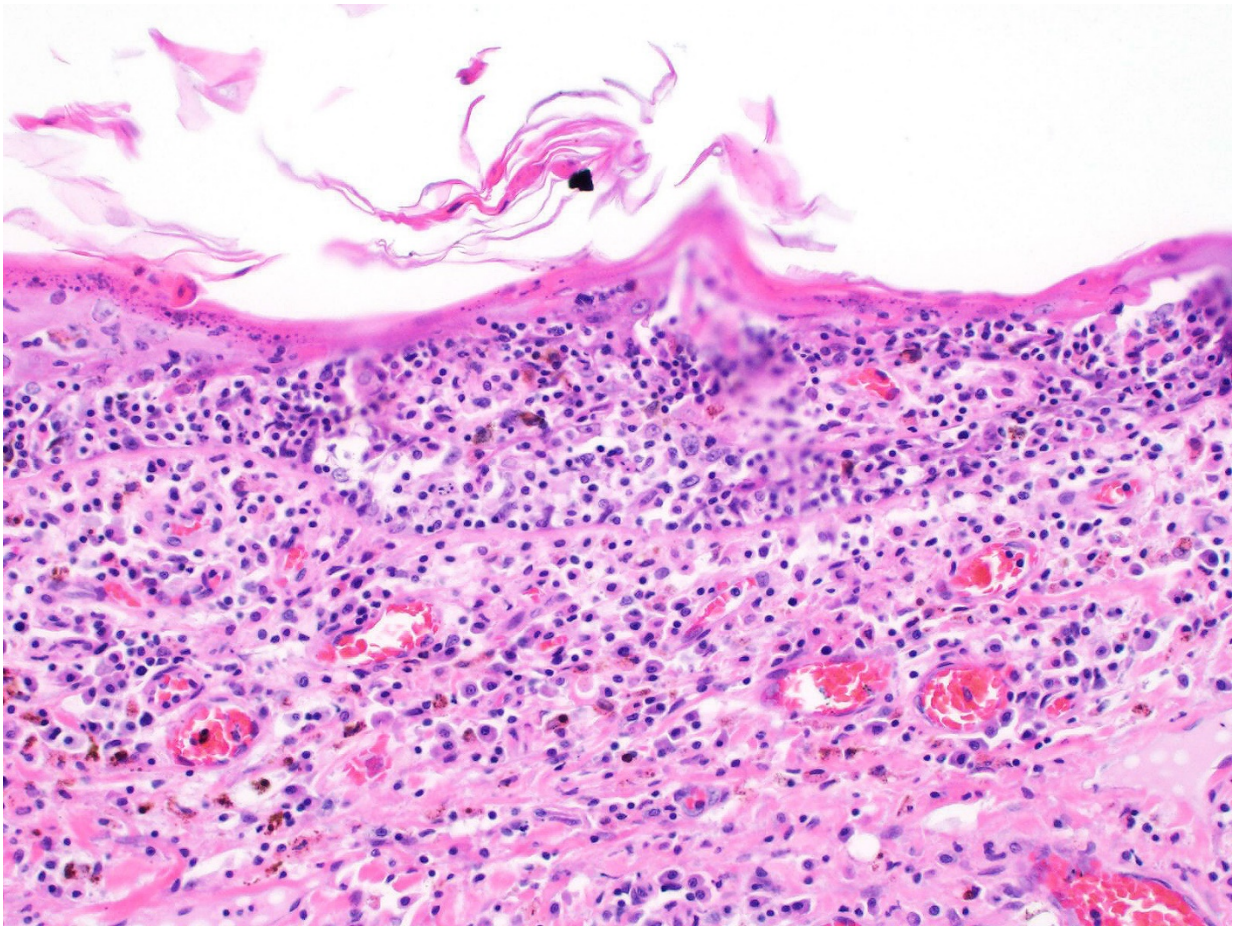

Haired skin, dog. The epidermis is infiltrated by large numbers of lymphocytes and macrophages. (HE, 400X).

mediated with direct cytotoxicity of target cells.[6,8]

Clinical lesions

In dogs, lesions are normally bilateral and involve the trunk, groin and axilla and also the inner pinna, footpads and mucocutaneous junctions.[3,8] Canine and feline lesions consist of erythematous macules, papules and plaques. Lesion borders are indurated and lesion centers are clear with discolorations to cyanotic or purpuric. Central crusting of lesions is common, but in canine patients this may extend to heavily crusted and/or scaly plaques.[7,8]

Histology – typical lesions

Microscopic lesions in canine erythema multiforme are similar to those in human patients.[3,8] Classic lesions include interface dermatitis, with cell death occurring in all epidermal (suprabasilar and basal) layers, accompanied by satellitosis (lymphoid infiltrates around apoptotic keratinocytes).[3,6,7,8] Intraepidermal mononuclear cells are mainly lymphoid, but Langerhans cells have also been identified.[3,8.] In canine patients the follicular infundibular epithelium is regularly affected and hyperkeratosis and parakeratosis are common, which is not the case in human patients.[3,7,8] Yager et al. further suggest that hydropic degeneration of the basal layer may not be such a prominent feature in canine patients compared to humans.[8]

Diagnosis and differential diagnoses

Erythema multiforme in the dog includes a wide range of clinical lesions, leading to a long list of differential diagnoses such as urticaria, demodicosis, dermatophytosis, bacterial folliculitis, superficial spreading pyoderma and bullous autoimmune skin diseases.[3,7,8] The presence of scaling-crusting lesions additionally includes superficial necrolytic dermatitis, zinc-responsive dermatoses or other cornification disorders as possible differential diagnoses.[3,8] Diagnosis of canine erythema multiforme therefore is often based on a combination of anamnesis, gross, and histological findings.[3,6] Yager et al. emphasize the importance of taking the anamnesis and gross lesions into consideration when giving a diagnosis of erythema multiforme.[8]

Contributing Institution:

Institute of Veterinary Pathology
Vetsuisse Faculty (University of Zurich)
Winterthurerstrasse 258, CH-8057 Zurich
Fax number +41 44 635 89 34
http://www.vetpathology.uzh.ch

JPC Diagnosis: 1. Haired skin: Dermatitis, interface, lymphohistiocytic, diffuse, modearate, with transepidermal and follicular keratinocyte apoptosis.

2. Haired skin: Dermatitis, suppurative, multifocal to coalescing, severe, with diffuse moderate ortho-and parakeratotic hyperkeratosis and bacterial cocci.

JPC Comment: The contributor has compiled an excellent overview of the three entities of erythema multiforme, Stevens-Johnson syndrome (SJS) and toxic epidermal necrosis (TEN), syndromes about which there remains to this day a lot of disagreement in the veterinary literature. Comparison with the human disease has advanced knowledge in these chronic and occasionally fatal syndromes and provided an excellent starting point, but the differences in the human disease and its veterinary counterpart are profound as well. Moreover, the literature lacks a critical number of well-documented cases of these diseases, and many of the cases in the older literature may, upon further review in light of more recent advances in veterinary dermatology, may have been incorrectly diagnosed.

In spite of significant disagreement in the veterinary literature from the last decade on these uncommon diseases, there are considerable points of agreement (many already mentioned by the contributor, but worthy of mentioning again):

1. Erythema multiforme (EM) and STS/TEN represent independent and different diseases, rather than opposite poles of a spectrum of immune-mediated disease.
2. Both EM and STS/TEN are mediated at least in part (STS/TEN) or in toto by cytotoxic lymphocytes directed against altered keratocyte antigens.

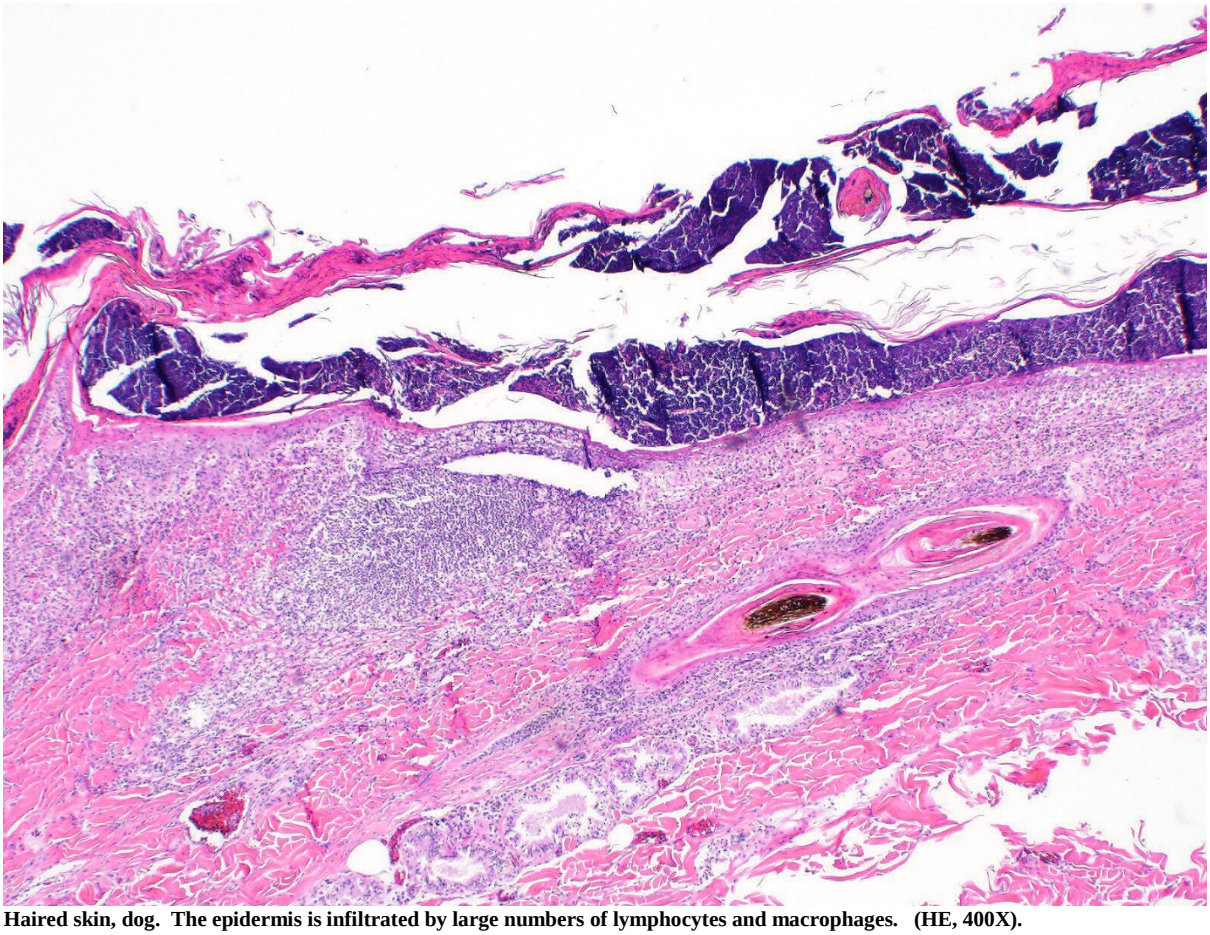

Haired skin, dog. The epidermis is infiltrated by large numbers of lymphocytes and macrophages. (HE, 400X).

3. There is considerable overlap in the histologic diagnosis of these diseases, and these findings must be closely correlated with clinical findings and history for a definitive diagnosis.
4. The histologic diagnosis of erythema multiforme is not a straightforward diagnosis and bears a number of differential diagnoses that should be considered before this diagnosis is rendered.

The reliable diagnosis of EM via STS/TEN has been confusing in both human and veterinary medicine for years. Early attempts at classification of these diseases[5] were based on human schema and proposed classification on five categories: type of skin lesions, distribution, mucosal involvement, systemic signs, and precipitating factors. Areas of significant variation include types of lesions (in which epidermal detachment is useful for identifying STS/TEN) and mucosal involvement (in which an absence of mucosal involvement is seen only with EM. It may, however be seen with EM, so its presence is not of diagnostic utility). On a purely academic note, one of the few differentiating factors between Stevens-Johnson syndrome (STS) and toxic epidermal necrolysis (TEN) (and likely the reason that they are so often lumped together) is that STS should have <10% epidermal detachment) and TEN >30%. Regarding mucosal involvement, several classifications have tried to characterize mucosal involvement, either due to severity or the number of mucosal sites affected, but this criteria is still under evaluation.[1,8] Significant overlap occurs in the remaining categories.

There is also significant disagreement and uncertainty yet remaining in the exact pathogenesis of the lesions in EM and STS/TEN. EM is characterized by lymphocytic targeting of individual keratinocytes, which SJS/TEN lesions are lymphocyte poor, with extensive areas of epidermal necrosis and lifting. Early SJS/TEN lesions resemble the pattern seen in EM, while later lesions with large confluent areas of necrosis suggest a progression to either waves of apoptosis,[8] soluble mediators of inflammation such as reactive oxygen species, granulysin, and soluble Fas ligand, or programmed cell death (necroptosis) A recent publication established the death of keratinocytes in TEN to be an apoptotic event, as seen in its human counterpart[2], but this does not explain the complete pathogenesis of this disease.

As complex as the diagnosis of STS/TEN may be, the correct diagnosis of erythema multiforme may be even more complex due to the variable histologic presentation and potential differential diagnosis. Lymphocytic-driven keratinocyte apoptosis at all levels of the epidermis and indeed, full-thickness epidermal necrosis may also be seen in EM lesions. The potential for hyperkeratosis in EM cases (also known as “hyperkeratotic” or “old dog” EM also brings cornification or clinical scaling disorders into the differential diagnosis. [8] Moreover, cases complicated by other secondary bacterial diseases or opportunistic infectious agents (as illustrated by this particular case) pose an additional diagnostic challenge.

The moderator stressed the importance of a good history as well as an optimal sample (often from the center of the lesion in which devitalization and lesion development in the differentiation of EM/SJS/TEM on surgical biopsy. As these three lesions may also resemble each other on a single biopsy sample, in the absence of a good history and clinical distribution of lesions, the prudent surgical pathology may withdraw to a conclusion that the biopsy likely is within the EM/SJS/TEM spectrum, but refrain from the desire to place it in one of the three categories. In the cat, exfoliative dermatitis associated with thymoma (and even a few without) may also present as a cytotoxic dermatitis which resembles EM.

References:

1) Banovic F, Olivry T, Bazzle L., Tobias JR, Atlee, B, Zabel S, Hensel N, Linder KE. Clinical and microscopic characteristics of canine toxic epidermal necrolysis. *Vet Pathol* 2015; 53(2):321-330.
2) Banovic F, Dunston S, Linder KE, Rakich P, Olivry, T. Apoptosis as a mechanism for keratinocyte death in canine toxic epidermal necrolysis. *Vet Pathol* 2017; 54(2): 249-253.
3) Boehm TMSA, Klinger, CJ, Udraite L, Mueller RS. Targeting the skin – erythema multiforme in dogs and cats. *Tierärztl Prax Kleintiere.* 2017; 45:352-356.
4) Favrot C, Olivry T, Dunston SM, Degorce-Rubiales F, Guy JS. Parvovirus Infection of Keratinocytes as a Cause of Canine Erythema multiforme. *Vet Pathol.* 2000; 37:647-649
5) Hinn AC, Olivry T, Luther PB et al. Erythema multiforme, Stevens-Johnson syndrome and toxic epidermal necrolysis in the dog: clinical classification, drug exposure, and histopathologic correlations. *J Vet Allergy Clin Immunol* 1998:6:13-20
6) Itoh T, Nibe K, Kojimoto A, et al. Erythema Multiforme Possibly Triggered by Food Substances in a Dog. *J. Vet. Med. Sci.* 2006; 68(8):869-871
7) Jubb, Kennedy, Palmer. *Pathology of Domestic Animals*. 6th ed. St. Louis, Elsevier Saunders; 2016.
8) Yager J.A, Erythema multiforme, Stevens-Johnson syndrome and toxic epidermal necrolysis: a comparative review. Vet dermatol 2014; 25: 406-e64.

CASE II: WSC-SC-2 (JPC 4114031).

Signalment: 7 year old, male neutered Munchkin, *Felis catus*

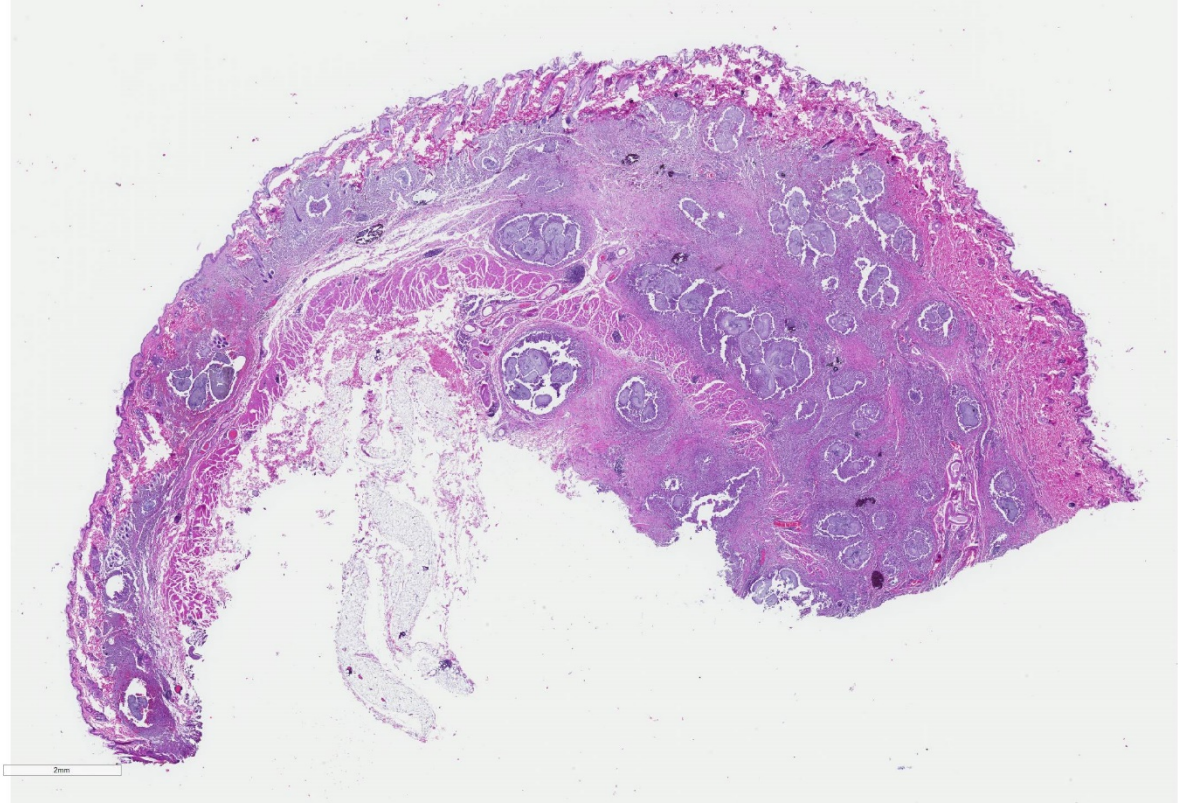

Haired skin and subcutis, cat. The superficial and deep dermis is expanded with large grains surrounded by a rim of inflammatory cells and fibrous connective tissue (HE, 7X)

History: Since birth, the patient has suffered from chronic dermatophytosis, which was diagnosed on histopathology when the cat was approximately 1 year old. The cat was treated with ketoconazole and lime sulfur dips. Since then, the cat intermittently developed raised, alopecic skin lesions that would t wax and wane without treatment. Four months prior to the current submission, the cat had lost 40% of his body weight and had intermittent vomiting. Physical examination revealed multiple mammary nodules. A complete left chain mastectomy was performed and submitted for histopathologic examination.

Gross Pathology: Two sections of formalin fixed pigmented haired skin with subcutis and mammae. The dermis and subcutis was markedly thickened and nodular around the teats. When sectioned, the tissue was firm and mottled light tan and brown.

Laboratory results:

Bloodwork and cytology was performed by the referring veterinarian. Bloodwork

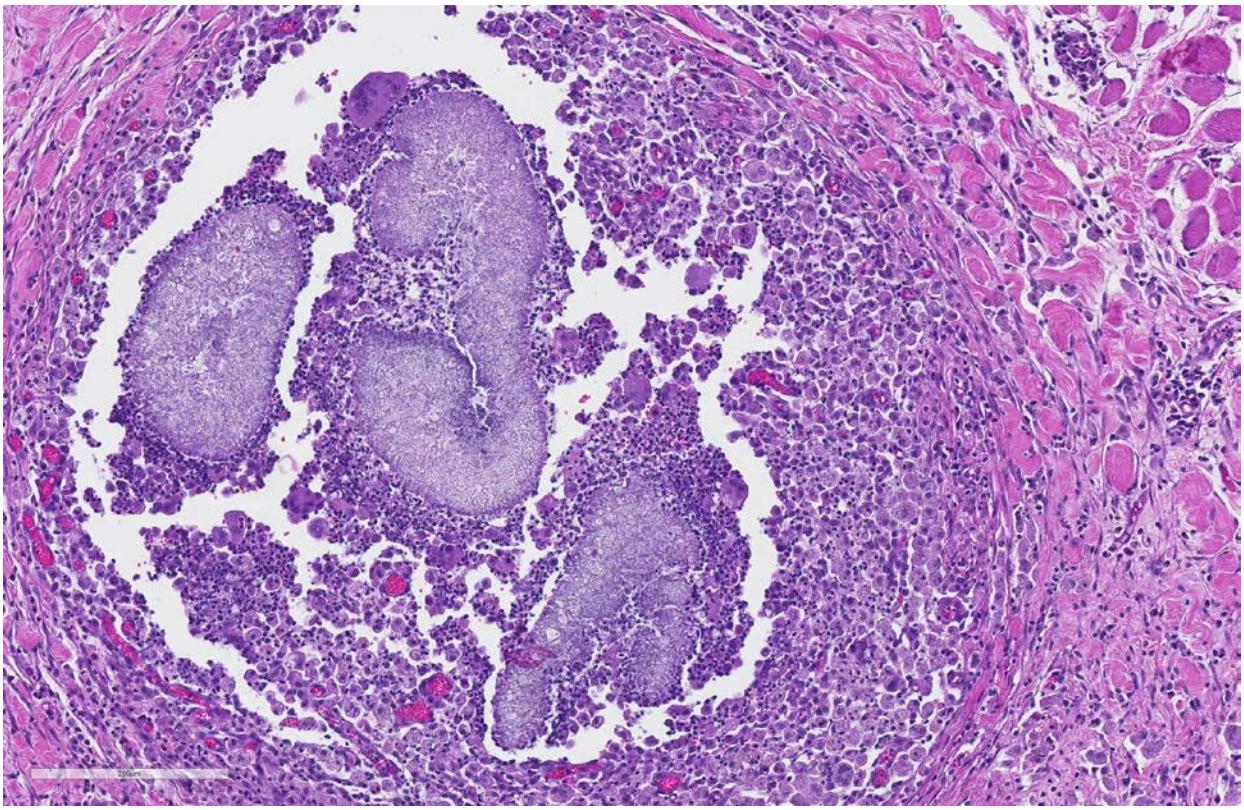

Haired skin and subcutis, cat. Higher magnification of "grains" (fungal hyphae enmeshed in antigen-antibody complexes), and surrounded by macrophages, neutrophils, and rare giant cells. (HE, 180X)

revealed elevated liver values. Cytology of a mammary nodule was suggestive of adenocarcinoma.

Microscopic Description:

The sections of lightly pigmented, haired skin have intense nodular and diffuse infiltrates extending from the deep dermis into the subcutis that often efface the dermis and subcutis. The nodules are composed of large mats of hyphae embedded in granular eosinophilic material that is slightly radiating and forms irregularly-shaped tissue grains (Splendore-Hoeppli material). The hyphae are often tangled and irregularly arranged, are approximately 5-7 micrometers in diameter, have parallel walls with frequent bulbous dilations, are septate and have rare acute-angle branching. The mats of hyphae and Splendore-Hoeppli material are surrounded by many foamy and epithelioid macrophages, Langhans and foreign body-type multinucleated giant cells and neutrophils. Some large nodules have a thin peripheral rim of fibrous tissue containing moderate numbers of fibroblasts. Many macrophages and multinucleated giant cells are moderately to markedly distended with abundant amorphous to globular material that stains intensely eosinophilic with a PAS histochemical stain and black with GMS histochemical staining (presumptive dermatophyte remnants). On H&E sections this phagocytized material is

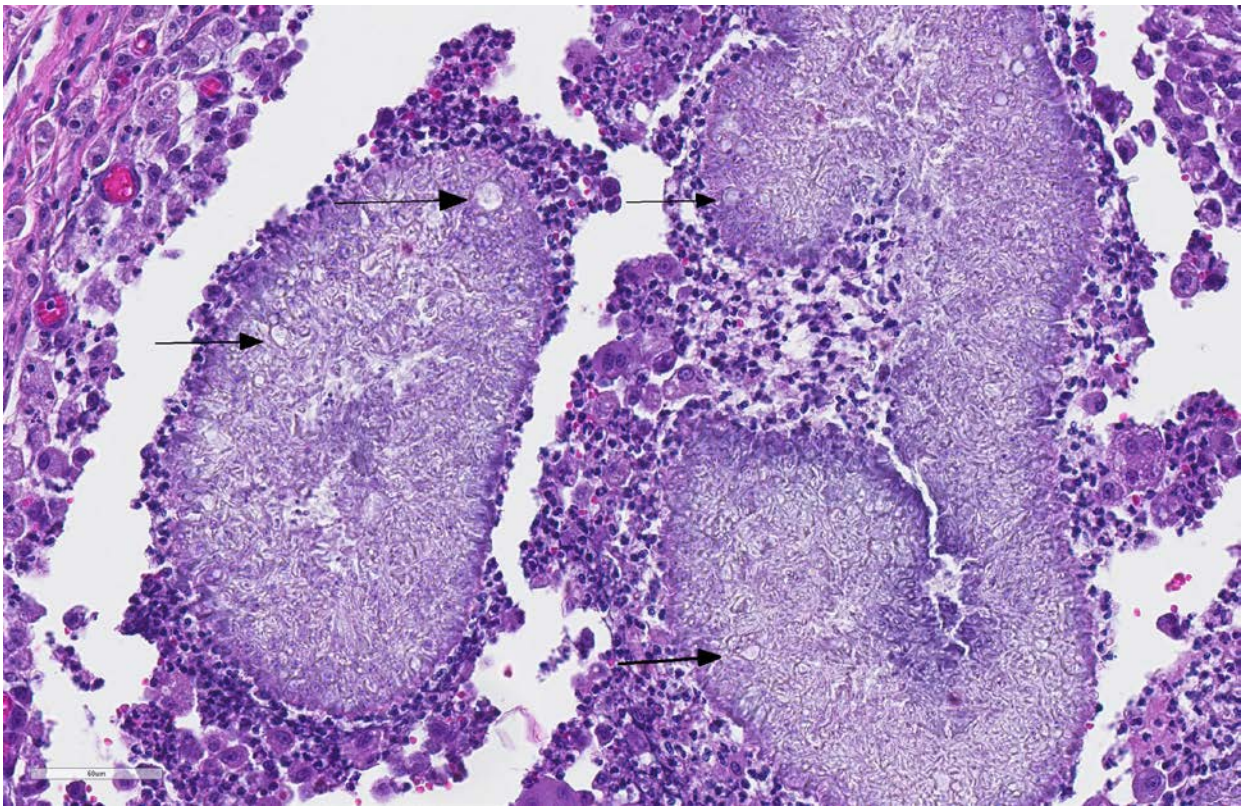

Haired skin and subcutis, cat. Higher magnification previous field, demonstrating a better view of aggregated fungal hyphae and dilated terminal swellings (arrows). (HE, 400X)

clear with pale eosinophilic hyphal margins. Within lower numbers of macrophages and multinucleated giant cells there are fragments of hyphae with parallel walls, bulbous dilations, and septae. Also within the nodular to diffuse infiltrate there are often small moderate-sized aggregates of mineralized material that contain abundant, similar hyphae. Areas of mineralization are most common within the superficial margins of the infiltrate. Within tissue that is not effaced, there are nodules composed of many lymphocytes and few plasma cells and macrophages surrounding blood vessels in the deep dermis and subcutis. There is a clear line of demarcation between the nodular to diffuse infiltrate within the deep dermis and superficial dermis. Within the superficial dermis there are perivascular and interstitial infiltrates composed of lower numbers of lymphocytes, plasma cells, mast cells and few neutrophils. The overlying epidermis has an irregular, papillated appearance and there is mild to marked basket-weave and compact orthokeratotic hyperkeratosis. PAS and GMS histochemical stains do not reveal hyphae along the epidermal surface or within follicles.

Contributor's Morphologic Diagnosis:

Dermatitis, pyogranulomatous, multifocal and focally extensive, chronic, severe, with myriad fungal hyphae embedded within Splendore-Hoeppli material, deep dermis and subcutis of the ventral abdomen.

Contributor's Comment: The histologic findings were most consistent with dermatophytic pseudomycetoma. Dermatophytic pseudomycetomas are deep dermal to subcutaneous atypical dermatophyte infections with nodules that frequently ulcerate and form draining tracts. Pseudomycetomas have been reported to range from 1-8 cm in diameter and can mimic neoplasia, as in this case.[4,5,7] Initially, the nodules are small and non-painful, so disease is often chronic before detections, particularly in long-haired cats. Dermatophytic pseudomcyetoma is most commonly caused by *Microsporum canis* and has almost exclusively been reported in Persian cats and to lesser extent Himalayan cats.[5,7,9] The lesions have been reported to occur with or without a history of skin trauma and occur more commonly on the head, neck, dorsum, tail, flanks or limbs,[5,7] and lesions on the ventral abdomen are uncommonly reported.[5] The granules present within the tissue and fistulous tracts have been described as white, yellow, or light brown.[5]

The histomorphology of hyphae in tissue alone is an inaccurate method to identify fungi/dermatophytes and culture and/or PCR are needed for definitive diagnosis. Unfortunately in this case, fresh tissue was not obtained at the time of surgery, as neoplasia was suspected, and an infectious etiology was not on the referring veterinarian's differential list because of the clinical presentation and fine needle aspirate results. We did submit formalin fixed paraffin embedded (FFPE) tissue for pan-fungal PCR, and despite the large numbers of hyphae within the lesions, PCR failed to identify the organisms. In a case report of four cats with dermatophytic pseudomycetomas, PCR performed using FFPE tissue failed to identify the dermatophytes one of the two cases in which *Microsporum canis* was confirmed with culture, and in two of the cases that had characteristic lesions, but in which tissue was not submitted for culture.[5]

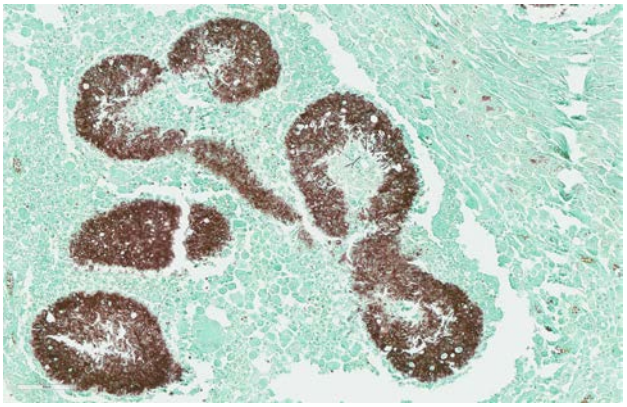

Haired skin and subcutis, cat. Dermatophyte hyphae stain strongly with a Grocott's methenamine silver (GMS, 271X)

Dermatophytic pseudomycetomas are very similar to true eumycotic mycetomas as the organisms are present in tissue as grains or granules, however there is a difference in the formation of the granules in that there is less amorphous eosinophilic material (cement-like substance) within the grains in mycetomas, and more Splendore-Hoeppli material is present in pseudomycetomas.[7,9] Pseudomycetomas are formed by dermatophytes and bacteria that are not members of the Actinomycetales order.[9]

The pathogenesis of dermatophytic pseudomcyetoma is unclear, and most reported cases lack the history of trauma preceding the development of the lesions. It is believed that furunculosis resulting from

typical dermatophyte infections may lead to the migration of dermatophyte hyphae into the deep dermis and subcutis, followed by development of pseudomycetomas.[5,6] An underlying immunosuppression or a selective immunodeficiency is thought to underlie the susceptibility of Persian cats to conventional dermatophytosis and dermatophytic pseudomycetoma.[5,7] Others have hypothesized that long-haired cat breeds, such as Himalayan and Persian cats may be more susceptible due to incomplete grooming of the hair coat and long hair, which may predispose to more chronic dermatophytosis and furunculosis.[5,6] In this case, although there was a chronic history of dermatophytosis in this cat, there was no histologic evidence of dermatophytosis in the dermis, epidermis and hair follicles. There has been one case report, of intra-abdominal dermatophytic granulomatous peritonitis in a Persian cat.[4] The authors in this case report hypothesized that generalized dermatophytosis at the time the cat was spayed may have led the inoculation of dermatophyte hyphae in to the abdomen, despite the surgery occurring several years prior to diagnosis. The significant weight loss, vomiting, and increasing liver values inhis cat, raises the possibility of systemic involvement. One thought we had was that the body confirmation of this cat breed with very short legs could have been a predisposing factor for the development of these pseudomycetomas, possibly due to traumatic furunculosis that could be more common in a Munchkin cat with chronic dermatophytosis, due to an increased likelihood of contact to the ventral abdomen against contact surfaces during play, etc due to the short stature of the breed.

Treatment of dermatophyte pseudomycetomas in cats is difficult with variable responses to anti-fungal medications alone.[4,5,6,10] It has been suggested that wide surgical excision and concurrent treatment with oral itraconazole prior to and after wide surgical excision are beneficial in the treatment of dermatophytic pseudomycetoma with results ranging from long-term disease free interval prior to recurrence to presumptive clinical cure of up to 2 years and 8 months at the time of publication.[5] In another paper the use of oral terbinafine resulted in resolutions of dermatophytic mycetomas in two cats. One cat's (Persian) clinical signs require continual pulse therapy of the drug as the lesions recurred after compete discontinuation. The other cat had no recurrence for 28 months after discontinuation of the medication at the time of publication.[2] Dermatophytic pseudomycetoma has been rarely been reported in dogs, with reported cases occurring in a Manchester Terrier, two Yorkshire Terriers, and a Chow Chow.[1,7]

Contributing Institution:

University of Florida
College of Veterinary Medicine
Department of Comparative, Diagnostic, and Population Medicine
http://cdpm.vetmed.ufl.edu/

JPC Diagnosis: Haired skin and subcutis: Pyogranulomas, multiple, with dermal fibrosis, Splendore-Hoeppli material,

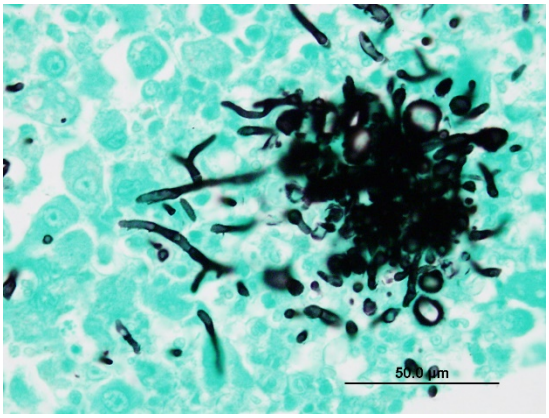

Haired skin and subcutis, cat. Higher magnification of the argentaffinic fungal hyphae, demonstrating parallel walls, dichotomous branching, septation, and terminal bulbous swellings. (GMS, 1000X) (*Photo courtesy of:* University of Florida, College of Veterinary Medicine, Department of Comparative, Diagnostic, and Population Medicine, http://cdpm.vetmed.ufl.edu/)

and numerous intradermal fungal hyphae (pseudomycetoma).

JPC Comment: The contributor has done an outstanding job on describing this uncommon finding in cats, and even more rare in other veterinary species. The terminology of this condition continues to be confusing, with mycetoma, eumycotic mycetoma, actinomycotic mycetoma, bacterial mycetoma, and pseudomycetoma all floating around in the liteature.

A mycetoma cotains three distinguishing features: 1) the formation of a nodular fibrotic inflammatory lesion, 2) formation of draining tracts, and 3) the grossly visible presence of fungal or bacterial grains.[3,4] When bacteria are at the center of the grains, the term bacterial mycetoma may be applied.[11] More specific bacterial terms may be utilized, such as "actinomycotic mycetoma" in cases of subcutaneous infection with *Actinomyces, Nocardia,* and *Actinomadura* spp.[2] Eumycotic mycetomas are caused by species of true fungi (non-dermatophyte), which are enmeshed in "grain cement" which contains melanin, proteins, and lipids.[2]

The usage of the term pseudomycetoma is somewhat less well-defined. In humans, pseudomycetomas are smaller, do not form draining tracts, and are often on parts of the the body other than the feet.[3] Bacterial cultures are usually negative. The material that binds the hyphae into grains is Splendore-Hoeppli material, which may be composed of antigen-antibody complexes, major basic protein, or both.[3] In the veterinary literature, the term pseudomycetoma is used to describe mycetomas resulting from dermatophyte infection of subcutaneous tissue, while in other publications the term is used to describe fungal species that have been traumatically implanted (most of which are dermatophytes as well). Many authors now prefer the term "dermatophytic pseudomycetoma" which provides both agent and method of traumatic implantation to deep tissues.[6,7,8] It should be pointed out that dermatophytic pseudomycetoma is a separate (and disparate) disease from superficial dermatophytic infection.[3]

In humans, mycetomas are considered endemic in certain parts of the world within the so-called "mycetoma belt"which included India, Sudan, and Mexico.[2] These forms of deep fungal infection are true mycetomas, without representation from dermatophytes. The nycetomas in question are most often seen in the feet, with disfiguring lesions, multiple draining sinuses, and variably colored and shaped

grains. Deep surgical excision of of grains under aseptic conditions is important in diagnosis, as direct visualization and culture of fungal hyphae within the grains is paramount.[2] Grains that wash out through draining tracts are not considered appropriate for diagnosis. Serodiagnostic test have proved valuable in certain instances, and PCR testing of grains shows great promise in parts of the "mycetoma belt" where they have been employed.[2]

The moderator also noted the bulbous swellings on the end of the hyphae within the deep dermis. While usually seen in dermatophytic mycelia, these "chlamydiospore-like" structures are also seen in pseudomycetomas for unknown reasons. In vary rare cases, in Persian cats, the sexual stage of *Microsporum canis*, *Arthrosporum canis*, has been isolated.

References:

1. Abramo F, Vercelli A, Mancianti F. Case report: two cases of dermatophytic pseudomycetoma in the dog: an immunohistochemical study. *Vet Dermatol*. 2001;12:203-207.
2. Ahmed, AA, van de Sande W, Fahal AH. Mycetoma laboratory diagnosis: review article. *PLoS Neg Trop Dis* 2017: 11(8): e0005638.
3. Berg JC, Hamacher KL, Roberts GD. Pseudomycetoma caused by Microscopum canis ina n immunosuppressed patient: a case report and review of the literature. *J Cutan Pathol* 2007: 34:431-434.
4. Black SS, Abernathy TE, Tyler JW, et al. Intra-abdominal dermatophytic pseudomycetoma in a Persian cat. *J Vet Intern Med*. 2001;15:245-248
5. Bonifaz A, Tirado-Sanchez A, Calderon L, Saul M, Araiza J, Hernandezz M, Gonzalez GM, Pnce RM. Mycetoma: Experience of 482 cases in a single center in Mexico. *PLos Negl Trop Dis*
6. Chang, Shih-Chieh, et al. Dermatophytic pseudomycetomas in four cats. *Vet Dermatol.* 2010;22:181-187.
7. Duangkaew, L, et al. Cutaneous blastomycosis and dermatophytic pseudomycetoma in a Persian cat from Bangkok, Thailand. Medical Mycology Case Reports 15 (2017) 12-15.
8. Giner J, Bailey J, Juan-Salles C, Joiner K, Martinez-Romero EG, Oster S. Dermatophytic pseudomycetomas in two ferrets. *Vet Derm* 2018: 29:452-e154.
9. Gross TL, et al. Skin Diseases of the Dog and Cat: Clinical and Histopathologic Diagnosis. 2nd Ed. 288-291. 2005.
10. Mauldin, EA and Peters-Kennedy, J. Integumentary System. In Jubb, Kennedy, and Palmer's Pathology of Domestic Animals. Edited by: M. Grant Maxie Vol. 1, 6th Ed. 2016, Elsevier. pp. 653-659.
11. Martoreall, Jaime, Gallifa N, Fondevila D, Rabanal RM. Bacterial pseudomycetoma in a dwarf hamster. *Eur Soc Vet Derm* 2006: 17:449-452.

12. Nuttall TJ, German AJ, Holden SL, Hopkinson C, and McEwan NA Successful resolution of dermatophyte mycetoma following terbinafine treatment in two cats. The Authors Journal Compilation ESVD and ACVD. 2008;19:405-410.

CASE III: H18-0008-92 (JPC 4122525).

Signalment: Unknown age (adult), european, male neutered, cat (*Felis catus*).

History: This cat was found dead in the street by a passerby and brought to the *Centre Hospitalier Universitaire Vétérinaire d'Alfort* (ChuvA) of the *Ecole Nationale Vétérinaire d'Alfort* (EnvA). We were unable to find and contact the owner despite the presence of a microchip. As a consequence, no information regarding the medical history was available. A necropsy was performed for pedagogic purpose.

Gross Pathology: The animal was severely cachectic and dehydrated. The skin of the ventral abdomen, ventral thorax, ventral neck, flanks and all legs was alopecic, thin, smooth and focally erythematous. Remaining hairs could be easily removed. The pawpads were smooth, erythematous and sometimes shiny. A 2-cm-diameter, unencapsulated but rather well-demarcated, lobulated, firm, white mass was found at the extremity of the left pancreatic lobe. On cut section, the mass was cystic. The pancreatic lymph node was slightly enlarged, firm and white. Numerous firm, ill-demarcated, 1-3-cm in diameter, often umbilicated, white masses were found in the liver and on the abdominal side of the diaphragm.

Presentation, cat. The cat is cachectic, and the skin of the abdomen, ventral thorax, flanks and legs, is thin, smooth, and reddened. (Photo courtesy of: Unité d'Histologie et d'Anatomie pathologique, BioPôle Alfort, Département des Sciences Biologiques et Pharmaceutiques, Ecole Nationale Vétérinaire d'Alfort).

Laboratory results: None.

Microscopic Description: SKIN: The main dermatopathologic pattern was non-inflammatory adnexal atrophy.

The epidermis was slightly and diffusely acanthotic. The *stratum corneum* was diffusely thin, compact and orthokeratotic, with focally areas of parakeratosis. There was diffuse and severe follicular atrophy of hairless telogen type. Hair follicles were reduced to thin and tortuous epithelial cords surrounded by a thick, homogenous and glassy sheath of collagen. Sebaceous and apocrine glands were present and only minimally atrophic.

There was a slight increase in the number of dermal mast cells. The hypodermis was diffusely and severely atrophic with only few and small remaining adipocytes.

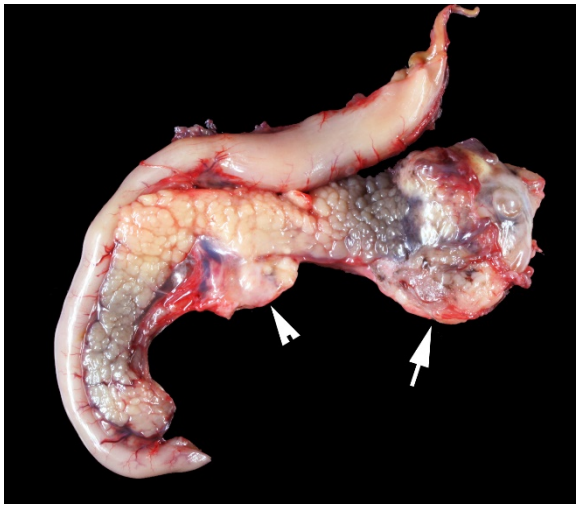

Pancreas, cat. A 2-cm-diameter, unencapsulated but rather well-demarcated, lobulated, firm, white mass was found at the extremity of the left pancreatic lobe (arrow) . The pancreatic lymph node was enlarged (arrowhead) (Photo courtesy of: Unité d'Histologie et d'Anatomie pathologique, BioPôle Alfort, Département des Sciences Biologiques et Pharmaceutiques, Ecole Nationale Vétérinaire d'Alfort).

PANCREAS: A rather well-circumscribed but infiltrating and only partially encapsulated, highly cellular neoplasm developed in the pancreas. Neoplastic epithelial cells formed cords and nests supported by a moderately abundant fibrovascular stroma. Cells were polygonal to cuboidal, had a high nucleocytoplasmic ratio, a scant brightly eosinophilic cytoplasm and a central to paracentral round nucleus with a prominent eosinophilic nucleolus and coarse chromatin. Cytonuclear atypias were marked with anisocytosis and anisokaryosis, occasional binucleation, hyperchromatic nuclei. The mitotic count was moderate (7 mitoses per 10 high-power 0,237-mm^2-fields). A large central area of necrosis was present. No lymphovascular emboli were found but several images of perineural invasion were present at the periphery.

In the remaining pancreatic parenchyma, the lobulation was prominent due to a moderate to marked thickening of interlobular septa by fibrosis and multifocal lymphoplasmacytic infiltrates. Affected lobules often had rounded borders. Some pancreatic ducts were dilated and/or filled with degenerated neutrophils. There were also multiple foci of exocrine lobular hyperplasia.

Contributor's Morphologic Diagnosis:

SKIN: Follicular atrophy, severe, diffuse, with telogen hairless follicles and diffuse slight epidermal acanthosis and compact *stratum corneum*, findings consistent with feline paraneoplastic alopecia.

PANCREAS:

1. Pancreatic adenocarcinoma.
2. Pancreatitis, neutrophilic and lymphoplasmacytic, chronic-active, multifocal, moderate with interstitial fibrosis (chronic interstitial pancreatitis).
3. Exocrine nodular hyperplasia.

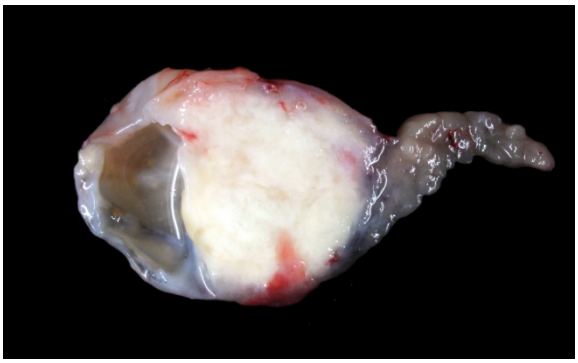

Upon dissection, the pancreatic nodule was cystic as a result of central necrosis. (Photo courtesy of: Unité d'Histologie et d'Anatomie pathologique, BioPôle Alfort, Département des Sciences Biologiques et Pharmaceutiques, Ecole Nationale Vétérinaire d Alfort)

Name of the disease: Feline paraneoplastic alopecia.

Contributor's Comment: Paraneoplastic syndromes (PNS) are non-neoplastic but neoplasm-associated disorders that cannot be readily explained neither by the location of the primary tumor or its metastases, nor by the elaboration of hormones indigenous to the tissue from which the tumor arose.[7,11,14] PNS can be associated to both benign or malignant tumors and some PNS are highly specific of particular tumors.[7,11] PNS are important to recognise because they can be the first sign of a tumor, can be used as a marker of the disease (as such, they may indicate recurrence) or because they can cause significant clinical problems.[6] If the tumor is removed, resolution of the PNS usually occurs. Recurrence or persistence of a PNS may indicate tumor recurrence, incomplete excision and/or metastases.

In people, it is expected that 10-50% of patients with a malignancy will experience at some point a PNS.[7,14] In veterinary medicine, the exact frequency of PNS is unknown but several cutaneous PNS of internal tumors (mainly cancers) have been described and are summarized in table 1. More cutaneous PNS are described in humans.[14]

In many veterinary textbooks and papers, we found that nodular dermatofibrosis associated with renal cystadenocarcinoma in dogs is often described as a cutaneous PNS.[9,11,14] We believe that this disease should be regarded as a genetic tumor syndrome in which dermatofibromas represent markers of the disease rather than PNS. Indeed, dermatofibromas usually precede, rather than follow, renal cystadenocarcinomas and thus appear to develop independently from them.[3,14] Furthermore, there are evidence that dermatofibromas develop first because they reflect haploinsufficiency in dermal

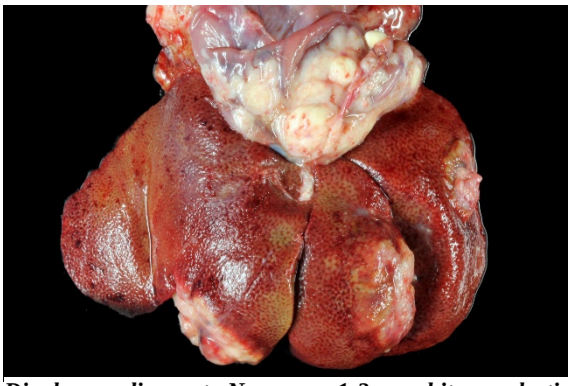

Diaphragm, liver cat. Numerous 1-3 cm white neoplastic nodules are present on the abdominal side of the diaphragm (above) and within the liver (below). (Photo courtesy of: Unité d'Histologie et d'Anatomie pathologique, BioPôle Alfort, Département des Sciences Biologiques et Pharmaceutiques, Ecole Nationale Vétérinaire d'Alfort)

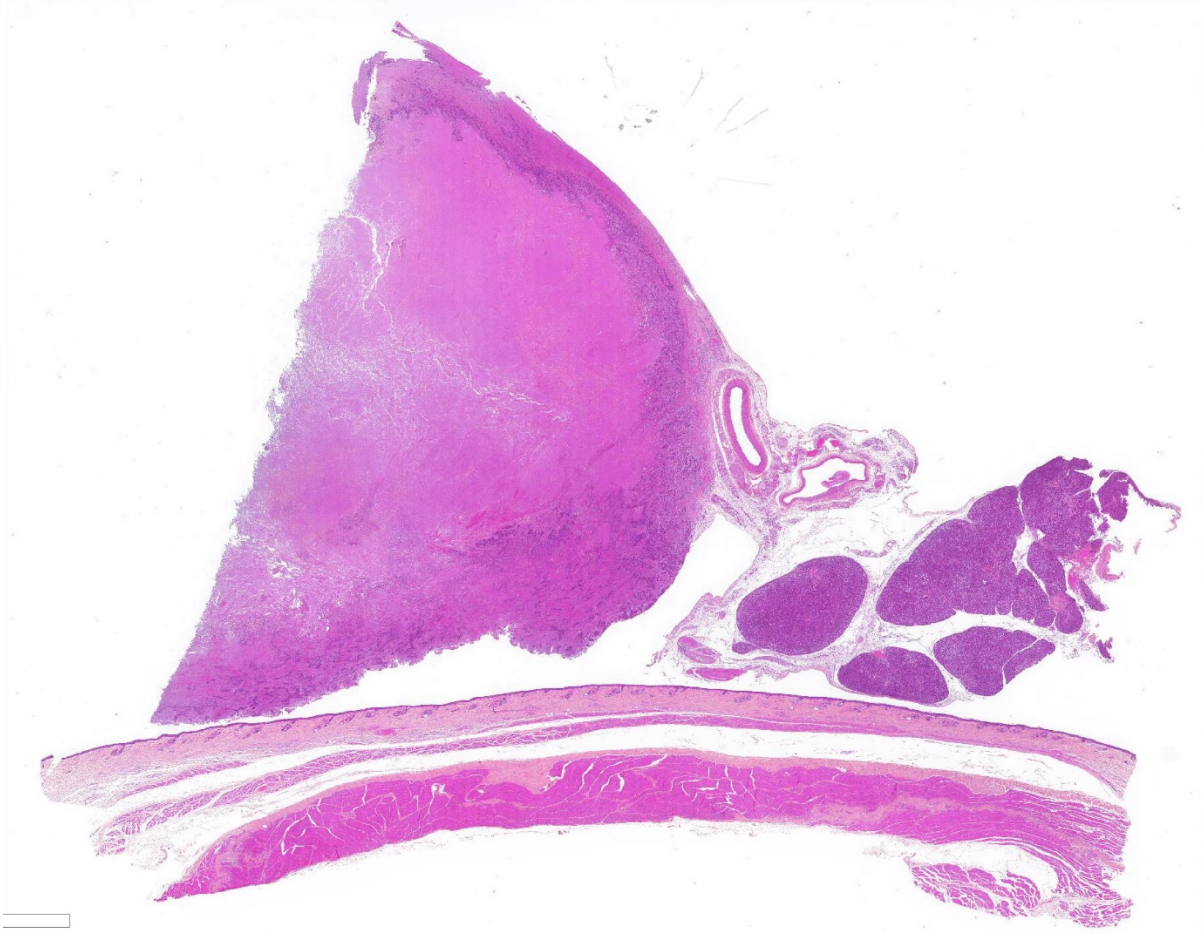

Pancreas, haired skin, cat. A largely necrotic section of the pancreatic nodule (above, left), and a section of haired skin (below) is submitted for examination. (HE, 7X).

fibroblasts whereas renal cystadeno-carcinomas develop later because they require a second-hit mutation (loss of heterozygoty) in the Birt–Hogg–Dubé gene. This resembles fibrofolliculomas associated with renal cancers in Birt–Hogg–Dubé syndrome in humans.[3]

Feline paraneoplastic alopecia has been associated with pancreatic adenocarcinoma, bile duct carcinoma, hepatocellular carcinoma, neuroendocrine pancreatic carcinoma, intestinal adenocarcinoma and hepatosplenic plasma cell tumor, the first one being the most frequent cause.[1,4,9,14] In most cases, paraneoplastic alopecia is recognized in advanced stages of the disease and affected cats are usually euthanized due to an extremely poor prognosis. The mechanism underlying feline paraneoplastic alopecia has not been elucidated. In the rare cases in which excision of the primary tumor was performed, hair regrowth was observed but alopecia then returned when metastases developed.[4] Interestingly, alopecia has been described in a woman with a bile duct

PNS	Most common associated tumor	Main dermatologic features	Main cutaneous histopathological features	Comments
Feline paraneoplasic alopecia	Pancreatic or biliary carcinoma	Progressive alopecia, easily epilated hair, glistening skin, sometimes footpad involvement	Nonscarring alopecia with follicular telogenization, miniaturization and atrophy	Also weight loss. Late in the course of malignancy. Possible secondary infections (*Malassezia* spp.)
Feline thymoma-associated exfoliative dermatitis	Thymoma	Progressive erythema and scaling, alopecia, waxy debris between digits and in nail beds	Cell-poor hydropic interface dermatitis with hyperkeratosis. Sebaceous gland often absent.	Assumed to be immune-mediated (resembles graft-versus-host reaction)
Feminization syndrome	Testicular tumors, in particular Sertoli cell tumors	Bilateral symmetrical alopecia, linear preputial dermatosis, gynecomastia, pendulous prepuce	Epidermal thinning, follicular keratosis and atrophy, sebaceous gland atrophy	Also myelosuppression and behavioral changes. Believed to be related to sex hormone aberration (hyperestrogenism and/or testosterone:oestrogen imbalance)
Superficial necrolytic dermatitis	Glucagonoma	Foot pad hyperkeratosis, alopecia and erosions with crusts on pressure points, mucocutaneous junctions, the muzzle, perineal area and feet	Parakeratosis, keratinocytic edema/necrosis and basal cell hyperplasia (French flag or red, white and blue epidermal appearance)	Also found in cases of hepatocutaneous syndrome which is more frequent.
Para-neoplastic pemphigus	Lymphoma, splenic sarcoma (other?)	Erythematous vesiculo-bullous lesions of head, trunk and limbs	Suprabasal cleft-forming acantholysis, dyskeratotic or necrotic keratinocytes at all epidermal levels, basal vacuolization, intense epidermal exocytosis of inflammatory cells	Also severe, erosive stomatitis with involvement of upper digestive and respiratory tracts. One reported case in a dog associated with mediastinal lymphoma

Table 1: Main features of cutaneous PNS in dogs and cats.[7,11]

carcinoma who presented a round alopecic area just on the top of the skull. A complete removal of the liver tumor allowed hair to grow back until metastases developed.[2]

In cats, differential diagnoses for acquired alopecia should include dermatophytosis, demodicosis due to *Demodex cati*, immune-mediated lymphocytic mural folliculitis, pseudopelade and vasculitis for primary alopecia. *Cheyletiella blakei, Notoedres cati,*

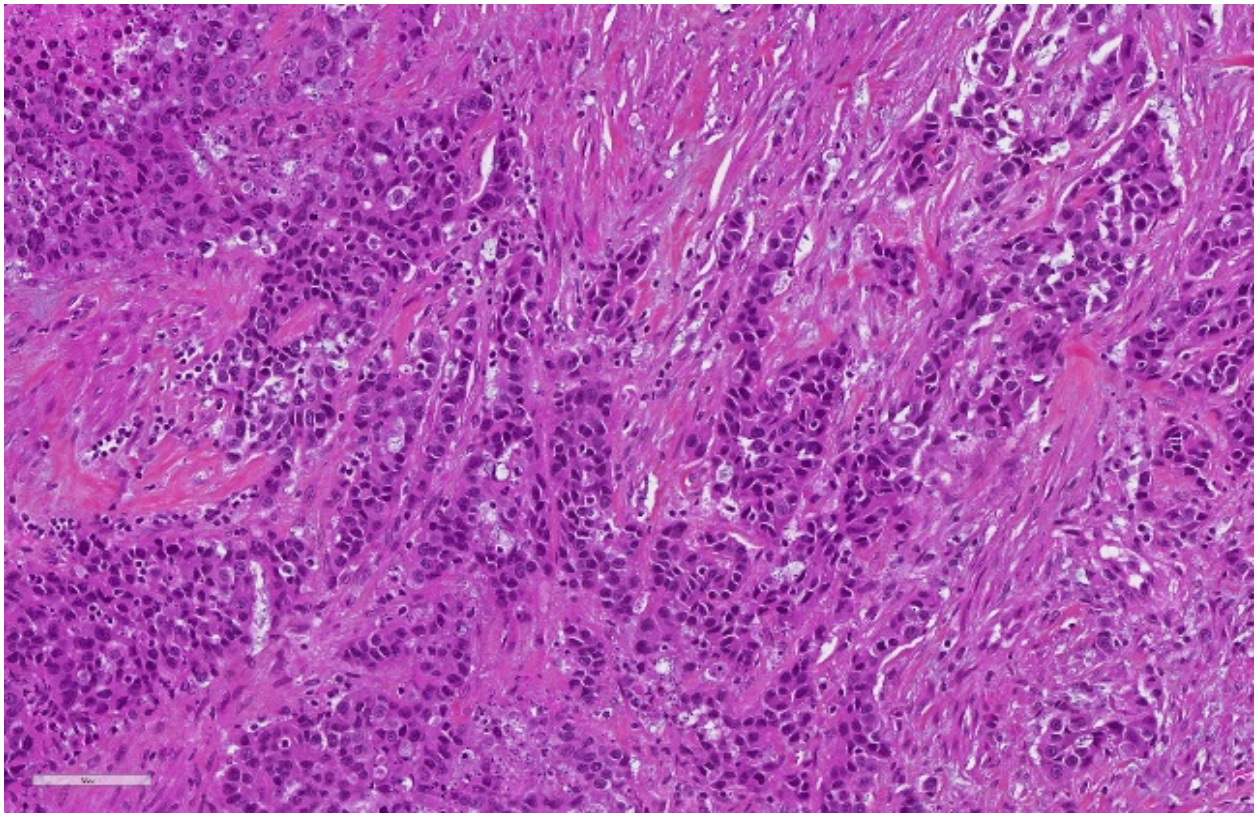

Pancreas, cat. Nests and cords of epithelial cells with small amount of granular eosinophilic cytoplasm infiltrate the capsule of the nodule at the edge of the large necrotic central focus. Many of these cells are undergoing necrosis as well. (HE, 267X)

Demodex gatoi, allergic disease, cutaneous infections with bacteria and/or fungi or fleas should be considered as a cause for secondary alopecia. Other causes such as *telogen effluvium*, hyperadrenocorticism and hypothyroidism occur very rarely in cats.[1,4]

Interestingly, in this case, the remaining pancreatic parenchyma had lesions of chronic pancreatitis. Chronic inflammation is well known as a predisposing factor for cancer and there are numerous examples: *Helicobacter pylori*-associated gastritis causing gastric lymphoma in humans, *Spirocerca lupi*-infestation causing esophageal sarcomas in dogs, etc.[7,11] Many studies have found a link between chronic pancreatitis and pancreatic malignancy in humans.[5,12,13,15,16] It is thus tempting to speculate that the chronic pancreatitis may have favored the development of a pancreatic adenocarcinoma in this case.

Contributing Institution:

Unité d'Histologie et d'Anatomie pathologique, BioPôle Alfort, Département des Sciences Biologiques et Pharmaceutiques, Ecole Nationale Vétérinaire d'Alfort

JPC Diagnosis:

1. Pancreas: Pancreatic exocrine carcinoma.
2. Pancreas: Pancreatitis, interstitial, subacute, diffuse, mild, with acinar atrophy.
3. Pancreas, islets: Amyloidosis, diffuse, mild.
4. Haired skin: Follicular atrophy, diffuse, severe, with loss of hair shafts, and mild acanthosis.

JPC Comment: The contributor has provided an excellent review of feline paraneoplastic alopecias, and their speculation on the exclusion of nodular dermatofibrosis from the classification of paraneoplastic syndromes as well as on the potential inflammatory origin of the pancreatic neoplasm in this cat are logical and appear sound.

Pancreatic exocrine neoplasia is an uncommon entity in dogs and cats, although hyperplastic lesions of the exocrine pancreas is very common in older individuals. Subtypes of pancreatic exocrine carcinoma include ductal, acinar, and less common hyalinizing, clear cell, and undifferentiated.[10] These neoplasms are subtyped by the primary discernable pattern of the neoplastic cells. In this particular case, as the majority of the neoplasm is necrotic, and only cells infiltrating the capsule are viable, a definitive pattern is not available, making

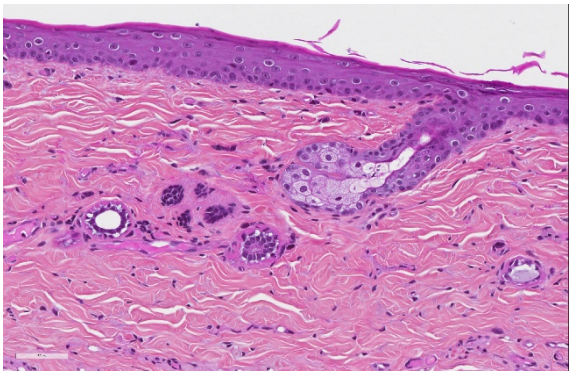

Pancreas, cat. There is diffuse severe atrophy of hair follicles which lack hair shafts. The apocrine glands are also atrophic with vacuolated epithelium. Sebaceous glands are normal. The Overlying epidermis is mildly acanthotic with a small amount of parakeratosis. (HE, 346X)

subtype of this neoplasm untenable in this particular case. A 2011 report suggested that loss of expression of tight junction protein claudin-4 might result in cellular detachment and invasion in poorly-differentiated neoplasm and was suggested as a marker of poorly differentiated tumors.[6]

In cats, this is a neoplasm of older animals (median 11.6 years).[8,10] They progress rapidly with animals presenting with weight loss, and anorexia, occasionaly vomiting, and a palpable abdominal mass. [8,10] Involvement of the liver or bile duct by metastatic foci or explants may result in icterus or elevated liver enzymes. In the cat, these are usually solitary masses, but may also infiltrate and efface the pancreas as well. [8,10] Untreated, the medial survaval time is 97 days, while animals receiving surgical treatment or chemotherapy survive an average of 165 days. [8] One retrospective study identified diabetes mellitus in 15% of cats with pancreatic malignancies.[10]

In dogs, pancreatic adenocarcinomas present with similar signs, and may also

present either as solitary masses or infiltrate the pancreas. Unlike the cat, elevated levels of amylase and lipase may be seen as a result of pancreatitis.[8] Metastasis, often to the liver and local lymph nodes is seen in the majority of cases. Hyalinizing pancreatic adenocarcinoma, a rare variant (WSC 2013-2014, Conference 2, Case 4), occasionally arises as a solitary mass in the right lobe of the pancreas. The nature of the hyalinized stroma in these tumors is not known, but it is not amyloid, as it does not stain with antibodies for serum amyloid A, light chains, amylin, or alph-1-antitrypsin.

References:

1. Affolter V, Gross TL, Ihrke P, Walder E. Atrophic diseases of the adnexa. In: *Skin diseases of the dog and cat: clinical and histopathologic diagnosis*. Blackwell Publishing; 2005:480–517.
2. Antoniou E, Paraskeva P, Smyrnis A, Konstantopoulos K. Alopecia: a common paraneoplastic manifestation of cholangiocarcinoma in humans and animals. *Case Rep*. 2012;2012:bcr2012006217–bcr2012006217.
3. Gardiner DW, Spraker TR. Generalized Nodular Dermatofibrosis in the Absence of Renal Neoplasia in an Australian Cattle Dog. *Vet Pathol*. 2008;45:901–904.
4. Grandt L-M, Roethig A, Schroeder S, et al. Feline paraneoplastic alopecia associated with metastasising intestinal carcinoma. *J Feline Med Surg Open Rep*. 2015;1:205511691562158.
5. Hamada S, Masamune A, Shimosegawa T. Inflammation and pancreatic cancer: disease promoter and new therapeutic target. *J Gastroenterol*. 2014;49:605–617.
6. Jakab CS, Rusvai M, Demeter Z, , Szab³ Z, Kulka J. Expression of claudin-4 molecule in canine exocrine pancreatic acinar cell carcinomas. *Histol Histopathol.* 2011;26:1121-1126.
7. Kumar V, Abbas AK, Aster JC. Neoplasia. In: *Robbins & Cotran Pathologic Basis of Disease*. Elsevier; 2014:189–242.
8. Linderman, MJ, Brodsky EM, Lorimier LP, Clifford CA, Post GS. Feline exocrine pancreatic carcinoma: a retrospective study of 34 cases. *Vet Comp Oncol* 2018; 11:208-212.
9. Mauldin EA, Peters-Kennedy J. Integumentary system. In: Vol. 1, *Jubb, Kennedy, and Palmer's pathology of domestic animals*. Grant, M M; 2007:509–736.
10. Munday JS, Lohr CV, Kiupel M. Tumors of the alimentary tract. In: *Tumors of Domestic Animals*. John Wiley & Sons 2017: 597-600.
11. Newkirk KM, Brannick EM, Kusewitt DF. Neoplasia and Tumor Biology. In: *Pathologic Basis of Veterinary Disease*. Elsevier; 2017:289–321.
12. Pinho AV, Chantrill L, Rooman I. Chronic pancreatitis: A path to pancreatic cancer. *Cancer Lett*. 2014;345:203–209.
13. Raimondi S, Lowenfels AB, Morselli-Labate AM, Maisonneuve P, Pezzilli R. Pancreatic cancer in chronic pancreatitis; aetiology, incidence, and early detection. *Best Pract Res Clin Gastroenterol*. 2010;24:349–358.
14. Turek MM. Cutaneous paraneoplastic syndromes in dogs and cats: a review of the literature. *Vet Dermatol*. 2003;14:279–296.
12. Witt H, Apte MV, Keim V, Wilson JS. Chronic Pancreatitis: Challenges and

Advances in Pathogenesis, Genetics, Diagnosis, and Therapy. *Gastroenterology*. 2007;132:1557–1573.

13. Xu Z, Vonlaufen A, Phillips PA, et al. Role of Pancreatic Stellate Cells in Pancreatic Cancer Metastasis. *Am J Pathol*. 2010;177:2585–2596.

CASE IV: 847/19 (JPC 4137402).

Signalment: 17-year-old, neutered female, Domestic Shorthair (*Felis catus*), feline

History: This cat was found dead in the street by a passerby and brought to the *Centre Hospitalier Universitaire Vétérinaire d'Alfort* (ChuvA) of the *Ecole Nationale Vétérinaire d'Alfort* (EnvA). We were unable to find and contact the owner despite the presence of a microchip. As a consequence, no information regarding the medical history was available. A necropsy was performed for pedagogic purpose.

Gross Pathology: Two skin biopsies from areas with alopecia and crusting measuring 0.8 x 0.7 x 0.4 cm and 0.8 x 0.6 x 0.4 cm respectively, were fixed in formalin and submitted.

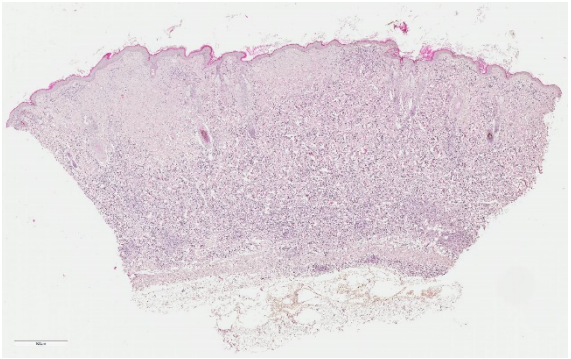

Haired skin, cat The superficial and deep dermis are diffusely infiltrated with lymphocytes which appear more densely packed in the deep dermis and form multiple nodular aggregates. (HE, 30X)

Laboratory results:

Cytological examination of a superficial skin lesion identified few neutrophils but no evidence of bacterial or fungal structures. Microbiological and a fungal culture were negative, too.

Microscopic Description:

Haired skin: Multifocally to coalescent the dermis is loosely infiltrated by mostly uniform, small round cells (Fig. 1) with scant or only minimal pale amphophilic cytoplasm and dark round to oval nuclei with condensed chromatin consistent with mature lymphocytes. The infiltrate abuts the epidermal and follicular epithelia but infiltrates them only occasionally (Fig. 2).

The deep dermis contains perivascular to nodular aggregates of tightly packed mature lymphocytes with almost no cytoplasm and dense basophilic nuclei (Fig. 3). Mitotic figures were not seen.

Small numbers of mast cells, plasma cells and neutrophils are loosely intermingled. The epidermis shows mild to moderate epidermal hyperplasia and mild orthokeratotic hyperkeratosis.

Immunohistochemistry (Fig 4) identified almost all cells in the superficial and deep dermis as CD3-positive T cells. The small, tightly packed aggregates in the deep dermis consisted of PAX5-positive B cells.

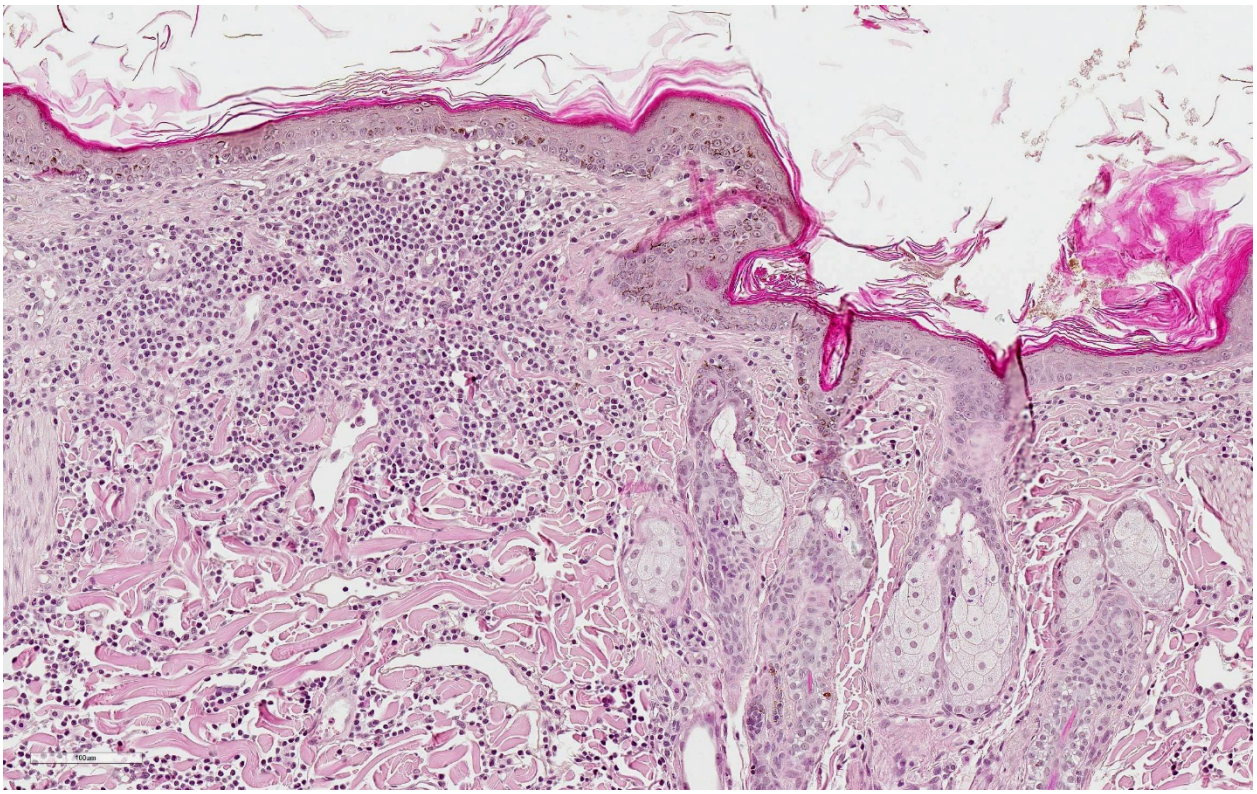

Haired skin, cat. Lymphocytes within the superficial dermis with sparing of the mildly spongiotic epidermis, mild orthokeratotic hyperkeratosis, and mild superficial dermal edema. (HE, 200X)

Contributor's Morphologic Diagnosis:

Haired skin: cutaneous lymphocytosis, moderate to severe, diffuse

Contributor's Comment: Cutaneous lymphocytosis is an uncommon disease and has been described in cats, dogs and humans [1,2,11]. The condition is most often seen in older cats, without a breed predisposition, but a slight predominance in females. The etiology is unknown.[2]

The typical clinical presentation is characterized by acute onset with slow progression.[2] Cutaneous lymphocytosis is mostly a solitary lesion showing alopecia, erythema and scaling, with or without crusting or ulceration. Pruritus can be seen in more than half of the cases, most commonly affecting the lateral thorax but also various other body sites (legs, pinnae, flank, neck, abdomen, hip, digit and planum nasale for instance).[2] It is a relatively benign disease with rare occasions of systemic illness in some cats and dogs associated with anorexia, weight loss and well-differentiated T-cell infiltrates in internal organs.[1,2] In most of the cases, treatment with glucocorticoids resulted in marked improvement of the clinical outcome.[2]

Cutaneous lymphocytosis in cats and dogs resembles cutaneous pseudolymphoma (lymphocytoma cutis, cutaneous lymphoid hyperplasia) in humans, a reactive proliferation of well-differentiated T- or B-cells in the skin of humans. In most cases, hypersensivity reaction to various antigenic stimuli has been described (such as arthropod bites, vaccination, tattoo dyes, drugs and contactants).[6,7,10]

In human cases, malignant transformation has been observed in some cases with systemic lymphoid involvement including enlarged mesenteric lymph nodes, infiltration of the liver, pancreas, stomach,

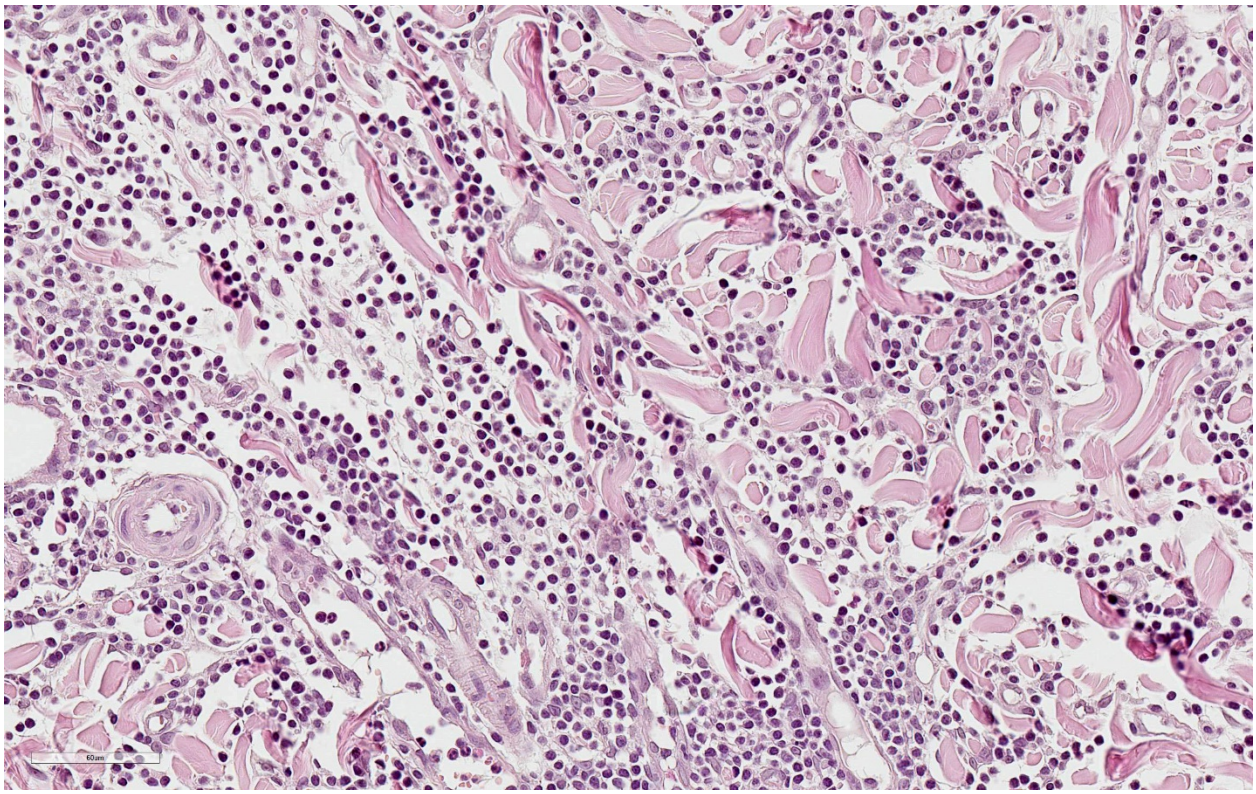

Haired skin, cat. Lymphocytes are small, bland, and diffusely expand the dermis. (HE, 400X)

kidney and heart by T lymphocytes and B cell infiltration of the small intestine.[4,8,11]

Histologically, cutaneous lymphocytosis in dogs and cats is characterized by proliferation of well differentiated CD3-positive T cells in the superficial and deep dermis and in most cases also nodular aggregates of CD79-positve B-cells in the dermis.[2,4,11] In some cases, a T-cell receptor gamma gene rearrangement (TCRγ) can be verified suggesting that this condition is a low-grade or indolent T cell lymphoma.[3]

As a differential for cutaneous lymphocytosis, cutaneous T cell lymphoma must be considered. Cutaenous histiocytosis may be difficult to clinically or histologically differentiate from well-differentiated cutaneous malignant lymphoma with predominance of mature. However, histopathology of cutaneous T cell lymphomas often identifies epitheliotropic lymphoma characterized by a diffuse superficial or follicular epitheliotropic infiltrates of medium sized to large lymphocytes / lymphoblasts and in some cases additional Pautrier's intraepidermal aggregates. In non-epitheliotropic lymphomas a deep dermal and subcutaneous infiltration of small to blastic lymphoid cells (bottom heavy configuration) with a variable mitotic activity can be seen.[9]

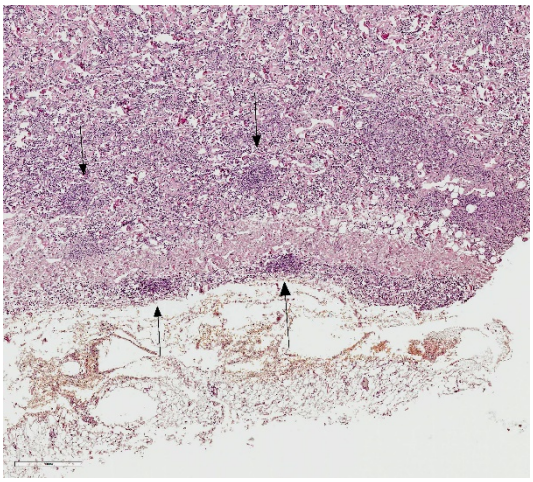

Haired skin, cat. Nodular aggregates of lymphocytes are present in the deep dermis (arrows). (HE, 400X)

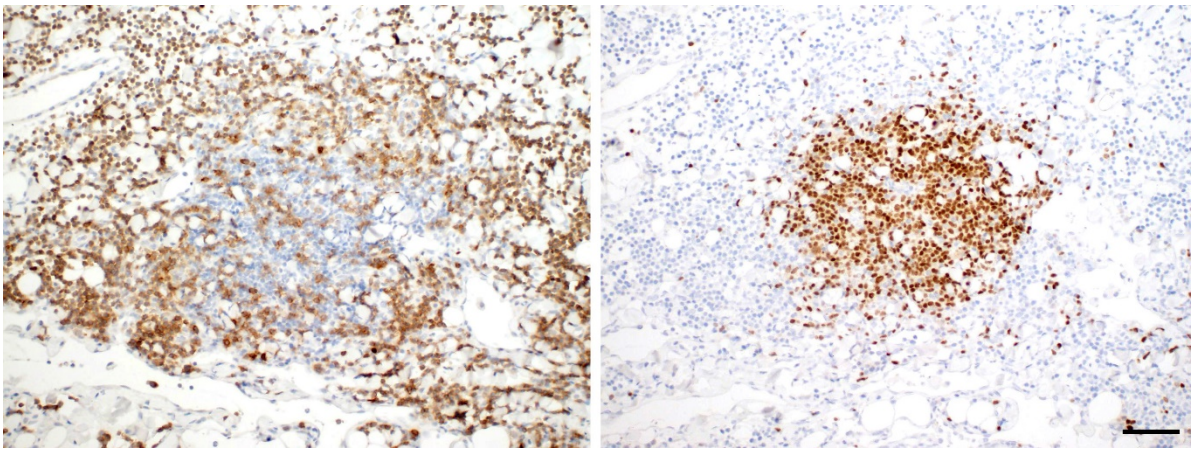

Haired skin, cat. Immunohistochemistry of nodules in the deep dermis demonstrates the preponderance of diffusely arrayed CD 3-positive T-cells (similar to that in all levels of the dermis) at left, and a nodular aggregate of PAX-5 positive B cells at right. (Ianti-CD#, and anti PAX-5, 400X) . (Photo courtesy of: Department of Veterinary Pathology, Freie Universität Berlin http://www.vetmed.fu-

Contributing Institution:

Department of Veterinary Pathology, Freie Universität Berlin http://www.vetmed.fu-berlin.de/en/einrichtungen/institute/we12/index.html

JPC Diagnosis: Haired skin: Lymphocytosis, diffuse, marked, with mild acanthosis and orthokeratotic hyperkeratosis.

JPC Comment: The contributor has provided an excellent review of this uncommon entity in the dog and cat. This particular specimen appears to very closely match descriptions in the veterinary literature. Immunohistochemical stains run at the JPC revealed the infiltrate to be overwhelmingly populated by CD-3 positive T-cells, with scattered aggregates of CD-20 and Pax-5 positive B cells in the deeper regions of the dermis.

In Gross et al, while the condition share most features in dogs and cats, cases in the dog often demonstrate a Grenz or lymphocyte-free zone in the superficial dermis at the dermo-epidermal junction.[5]

The attendees found it of note that a PubMed search for Dr. Nicolas Kluger[7] (cited below) yielded 77 publications on dermatologic conditions involving tattoos.

References:

1. Affolter VK, Gross TL, Moore PF. Indolent cutaneous T-cell lymphoma presenting cutaneous lymphocytosis in dogs. *Vet Dermatol*. 2009 Oct 20;5- 6:577-585.
2. Gilbert S, Affolter VK, Gross TL, et al. Clinical, morphological and immunohistochemical characterization of cutaneous lymphocytosis in 23 cats. *Vet Dermatol*. 2004 Feb 15;1:3-12.
3. Gilbert S, Affolter VK, Schmidt P, et al. Clonality studies of feline cutaneous lymphocytosis. *Vet Dermatol*. 2004 Aug 15;S1:24.
4. Gilliam AC, Wood GS. Cutaneous lymphoid hyperplasia. *Semin Cutan Med Surg*. 2000 Jun 19;2:133-141.
5. Gross TL. Ihrke PJ, Walder EJ, Affolter VK. Lympocytic tumors. In: *Skin Disesaes of the dog and cat: clinical and histopathologic diagnosis, 2nd Ed.* Oxford UK Backwell Science 2003; .. 872-875.
6. Hartsock RJ. Postvaccinal lymphadenitis. Hyperplasia of

lymphoid tissue that stimulates malignant lymphomas. *Cancer*. 1968 Apr 21;4:632- 649.

7. Kluger N, Vermeulen C, Moguelet P, et al. Cutaneous lymphoid hyperplasia (pseudolymphoma) in tattoos: a case series of seven patients. *J Eur Acad Dermatol Venereol*. 2010 Feb 24;2:208-213.
8. Lackey JN, Xia Y, Cho S, et al. Cutaneous lymphoid hyperplasia: a case report and brief review of the literature. *Cutis*. 2007 Jun 79;6:445-448.
9. Pariser MS, Gram DW. Feline cutaneous lymphocytosis: case report and summary of the literature. *J Feline Med Surg*. 2014 Sep 16;9:758-763.
10. Rijlaarsdam JU, Willemze R. Cutaneous pseudolymphoma: classification and differential diagnosis. *Seminars in Dermatology*. 1994 Sep 13;3:187-196.\
11. Rook KA. Canaine and Feline Cuatneous epitheliotropic lymphoa and cutaneous lymphocytosis. *Vet Clin Small Anim* 2019: 49:67-81.
12. Wood GS. Inflammatory diseases that stimulate lymphomas: cutaneous pseudolymphomas. In: Goldsmith AL, Katz SI, Gilchrest BA, et al. eds. *Fitzpatrick's dermatology in general medicine*. New York, NY: McGraw Hill Medical; 2008:1402-1408.

Self-Assessment - WSC 2019-2020 Conference 11

1. Which of the following diseases is characterized by detachment of 30% or more of the epidermis ?
    a. Erythema multiforme
    b. Stevens-Johnson syndrome
    c. Toxic epidermal necrolysis
    d. “Old dog” erythema multiforme

2. Which of the following is NOT true.
    a. EM, STS, and TEN are variations in severity of the same disease.
    b. The histomorphology of EM and STS/TEN are unique and definitive when compared.
    c. Both EM and STA/TEN are mediated by lymphocytoxicity against altered lymphocyte antigens.
    d. The diagnosis of EM is not straightforward and there are often many differentials.

3. Which of the following is characteristic of pseudomycetoma when compared to mycetoma?
    a. Grains
    b. Fungal hyphae
    c. Subcutaneous nodules
    d. Splendore-Hoeppli material

4. Which of the following has not been cited as a cause of feline paraneoplastic alopecia?
    a. Hepatocellular carcinoma
    b. Renal cystadenocarcinoma
    c. Pancreatic carcinoma
    d. Intestinal adenocarcinoma

5. Which of the following is the predominant lymphocyte subset in cutaneous lymphocytosis?
    a. CD3+T cell
    b. B-cell
    c. NK cell
    d. CD8+ T cell

Please email your completed assessment for grading to Dr. Bruce Williams at bruce.h.williams12.civ@mail.mil. Passing score is 80%. This program (RACE program 33611) is approved by the AAVSB RACE to offer a total of 0.5 CE Credits, with a maximum of 12.5 CE Credits being available to any individual Veterinary Medical Professionals for the 2019-2020 Wednesday Slide Conference. This RACE approval is for the subject matter categories of: SCIENTIFIC using the delivery method of NON-INTERACTIVE DISTANCE. This approval is valid in jurisdictions which recognize AAVSB RACE

Joint Pathology Center
Veterinary Pathology Services

WEDNESDAY SLIDE CONFERENCE 2019-2020

Conference 12

11 December 2019

CASE I: MSKCC/WMC/RU HB (JPC 4032968).

Signalment: Young adult, intact female Syrian hamster (*Mesocricetus auratus*)

History: Both animals are from the same group of eight hamsters that were shipped together three weeks prior to being experimentally inoculated with *Leishmania donovani*. All animals were administered intraperitoneal preparations of *Leishmania* derived from tissue homogenates of previously infected hamsters. Shortly after treatment, seven of the eight animals became acutely lethargic and dehydrated with perineal staining. Multiple animals were found dead and the remainder with euthanized as clinical signs progressed.

Gross Pathology: The abdomen is moderately distended and there is mild perineal fecal staining.

Approximately 1-2ml of slightly turbid, serosanguinous fluid is present within the abdominal cavity. The mesentery is markedly thickened and diffusely white. Intestinal loops are firmly adhered to one another by mesenteric adipose tissue which

Viscera, hamster: A single mass incorporates much of the abdominal viscera, including the liver, spleen, multiple loops of gut, and mesentery. (Photo courtesy of: Memorial Sloan-Kettering Cancer Center, 1275 York Ave, New York, New York, 10065, http://www.mskcc.org/research/comparative-medicine-pathology).

envelopes the spleen and uterus, and is adhered to the visceral surface of the liver. Mesenteric lymph nodes are enlarged and poorly demarcated, blending into the surrounding mesentery. The cecum is moderately distended by feed material and the distal colon is empty.

The liver is enlarged (10.6% of bodyweight) with rounded margins, and is diffusely pale tan and friable with an enhanced reticular

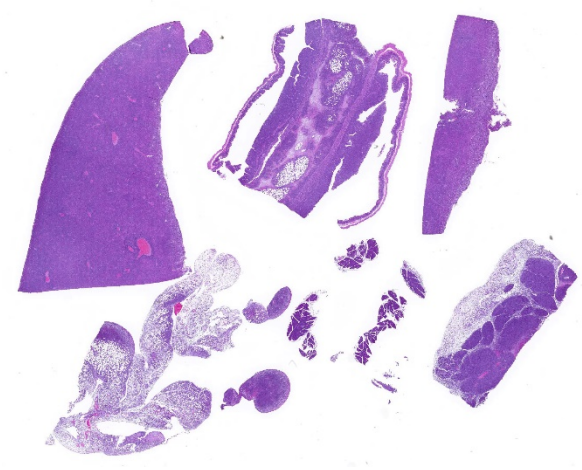

Viscera, hamster: Sections of liver, omentum, and pancreas are all infiltrated by a densely cellular neoplasm. (HE, 9X)

pattern. The kidneys are mildly enlarged, pale tan and swollen. The pancreas and peripancreatic adipose tissue are mottled tan to red and firm.

In the right cranial lobe of the lung, there was a firm, poorly demarcated structure palpable in the parenchyma. On the serosal surface of the left middle lobe, there were multiple plaque-like, sharply circumscribed, brown depositions of material observed (histologically identified as multifocal calcifications of pulmonary basal membranes with reactive histiocytic inflammation).

Laboratory results:

Cytology of the abdominal fluid revealed moderate numbers of small to medium sized lymphocytes, fewer large round cells, and small numbers of mesothelial cells and macrophages. Impression smears of the liver were highly cellular and composed predominantly of large round cells, approximately 10-20um in diameter, with a high nuclear to cytoplasmic ratio, large round nucleus, finely clumped chromatin, multiple nucleoli, and a small amount of basophilic cytoplasm.

Microscopic Description:

Mesentery including mesenteric lymph nodes, spleen and pancreas (variably includes small intestine): A poorly demarcated neoplastic infiltrate dissects throughout the mesentery which is extensively adhered to the splenic capsule, pancreas, mesenteric lymph nodes and intestinal serosa. Neoplastic round cells are arranged into densely cellular, unencapsulated sheets that variably efface the splenic and lymph node parenchyma and extensively disrupt the small intestinal muscularis and mucosa. Neoplastic cells have indistinct margins, a moderate amount of amphophilic cytoplasm and 10-15um diameter, round nuclei with coarsely stippled chromatin and variably conspicuous nucleoli. Frequent cells are necrotic and tingible body macrophages are scattered throughout the infiltrate. Anisocytosis and anisokaryosis are moderate and up to 7 mitotic figures are present per high power field (x400). Large areas of acute coagulative necrosis are scattered throughout mesenteric lymph nodes, variably accompanied by aggregates of fragmented mineral material (dystrophic mineralization). Scattered macrophages in remnant subcapsular sinuses and at the margins of necrotic foci contain dozens of oval-shaped, 2-3um diameter, intracytoplasmic protozoa with a 1-2um, basophilic nucleus and a variably distinct, perpendicular kinetoplast (*Leishmania* amastigotes).

Liver: An intense neoplastic infiltrate diffusely percolates throughout hepatic sinusoids, disrupting hepatic cords, obscuring portal tracts and lining the tunica intima of frequent central veins. Frequent hepatocytes are dissociated with hypereosinophilic cytoplasm and pyknotic nuclei (necrosis).

Contributor's Morphologic Diagnosis:

Mesentery including mesenteric lymph nodes, spleen, pancreas and small intestine: Lymphoma

Mesenteric lymph nodes: Severe, acute, multifocal to coalescing, necrotizing splenitis with intrahistiocytic protozoa, etiology consistent with *Leishmania* sp.

Contributor's Comment All eight hamsters received intraperitoneal preparations of *Leishmania donovani* derived from tissue homogenates of previously infected animals. Within three weeks, all animals became acutely lethargic and dehydrated or died acutely. Gross and histologic findings were similar in all animals, which were characterized by intense mesenteric infiltrates of neoplastic round cells. The histologic appearance of neoplastic cells is most consistent with lymphoma. Consistent with the experimental history, scattered macrophages located at the margins of necrotic foci within the mesenteric lymph nodes contained cytoplasmic amastigotes. All animals were inoculated with *L. donovani* as part of a study investigating host immunoregulation of visceral leishmaniasis.

Protozoa of the family Trypanasomatidae, genus *Leishmania* cause a spectrum of disease in people ranging from subclinical infection to severe, disseminated cutaneous, mucocutaneous and visceral disease. Visceral leishmaniasis (VL) is the most severe form of disease and may be fatal. *Leishmania donovani* is the predominant cause of VL in East Africa and India, whereas *L. infantum* and *L. chagasi* predominate in the Mediterranean and Latin America, respectively.[1] The domestic dog is an important reservoir host for the latter two species. Humans are the only known reservoir of *L. donovani.*

Leishmania sp. proliferate in the midgut of phlebotomine sandflies where the flagellated leptomonad form appears as a leaf-shaped promastigote.[5] Upon transmission to mammalian hosts, the organism assumes the aflagellated, obligate intracellular leishmanial form, or amastigote, which proliferates within macrophages and dendritic cells of susceptible hosts. These are approximately 2um diameter with a basophilic nucleus and perpendicularly oriented kinetoplast.

Host susceptibility to clinical disease relates to the *Leishmania* species involved and individual host factors such as immunocompetence. In susceptible hosts, VL may cause persistent fever, leukopenia, hypergammaglobulinemia and hepatosplenomegaly. Chronic immune-complex deposition may result in glomerulonephritis in people. Clinical and pathologic findings are similar in dogs, consisting predominantly of hepatic granulomas, splenomegaly and lymphadenopathy.[5]

The Syrian hamster is a widely used experimental model of VL, developing clinical signs and lesions that recapitulate human and canine disease including splenic lymphoid depletion, hepatic granulomas and amyloid deposition within the spleen and liver.[1] Glomerulonephritis and inflammatory myopathies have also been reported. Despite developing clinical disease and lesions that closely approximate human VL, a lack of reagents and a poor immune response to infection are limiting factors in the Syrian hamster model, particularly for evaluation of vaccination strategies. Murine models have also been utilized to identify genes that play an important role in the pathogenesis of VL. In some mouse strains (eg. CBA) genetic resistance is conferred by the gene *Slc11a1*, which encodes a phagosomal membrane protein that limits intracellular *Leishmania* multiplication by Fe^{2+} deprivation.[1] Susceptible mouse strains (eg. BALB/c, C57BL/6) with impaired *Slc11a1* expression are susceptible to *Leishmania*; however, even susceptible mice typically overcome visceral infection.

Given the severity of the neoplastic infiltrate in all animals, the cause of death in these animals was determined to be lymphoma, rather than visceral leishmaniasis. Outbreaks of transmissible lymphoma due to *hamster polyomavirus* (HaPV) infection have been reported in hamster colonies causing lymphoma epizootics that affect up to 80% of young, naïve animals.[2] HaPV was initially described in association with epitheliomas in older hamsters.[3] Tumors arise from the epithelium of the hair follicle forming keratin-filled, cystic masses. Large

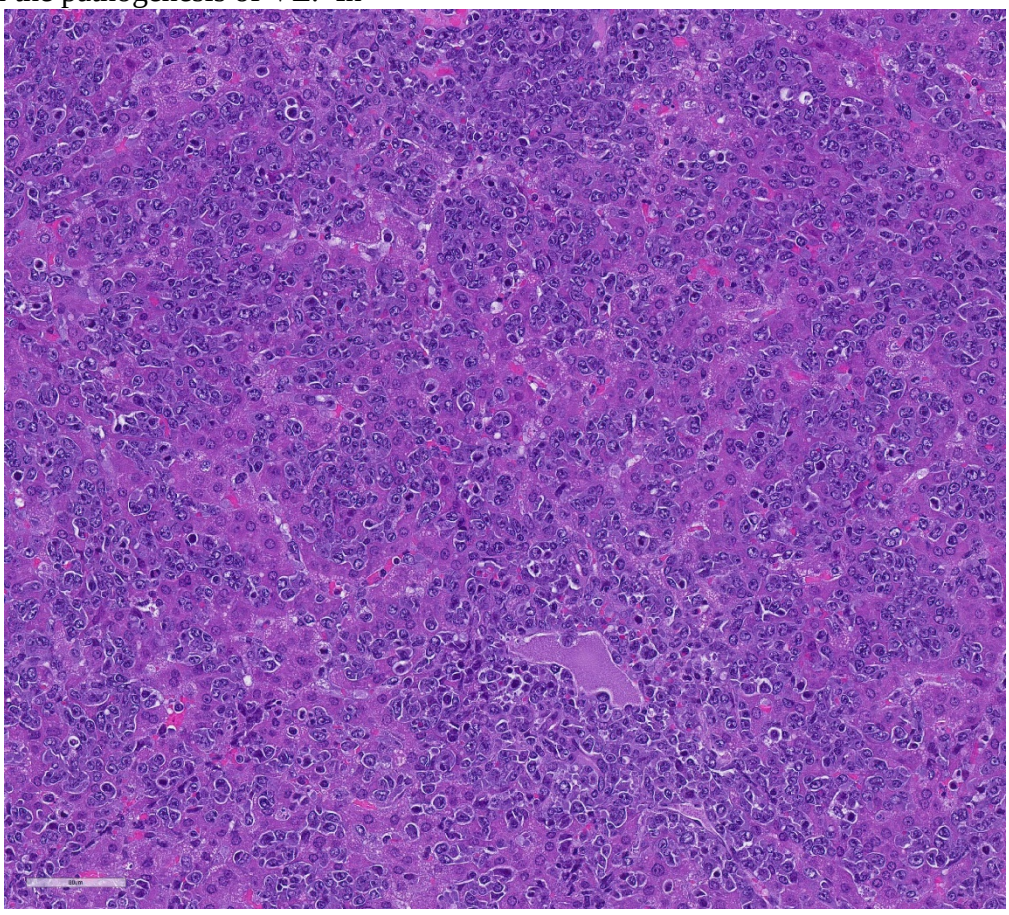

Liver, hamster: The liver is diffusely infiltrated by neoplastic lymphocytes which efface its normal sinusoidal pattern. (HE, 279X)

numbers of virus particles are detectable in keratinizing cells of epitheliomas. This contrasts with HaPV-associated lymphomas, which do not contain infectious virus, although thousands of copies of extrachromosomal viral DNA are present within neoplastic cells. Ha-PV associated lymphoma typically arises in the mesentery with infiltration of the liver, kidney, thymus, and other viscera. Tumors are usually lymphoid, although erythroblastic, myeloid and reticulosarcomatous forms may occur[3]. In enzootically infected, older hamsters the virus persists subclinically in the kidneys with intermittent shedding in urine.

In this case HaPV infection was suspected based on the clinical presentation but could not be confirmed by PCR (IDEXX RADIL). Lymphoma is rare in young hamsters and the rapid neoplastic progression in this group is highly suggestive of epizootic HaPV.[2] Ultrastructural imaging was not pursued as virus particles are not typically present in neoplastic lymphocytes.

It is unclear whether affected animals developed lymphoma prior to arrival at our facility or whether intraperitoneal *Leishmania* inoculation was the source of the tumor. It is possible that the tissue homogenate from which the inoculum was derived was infected with HaPV. It is also possible although somewhat less likely, that the donor animal had spontaneous lymphoma that was then transmitted to subsequent animals in the tissue homogenate. Transmissible tumors in the dog (canine transmissible venereal tumor) and Tasmanian devil (devil facial tumor disease) are associated with downregulation of tumor cell MHC expression, allowing successful allograft and proliferation in

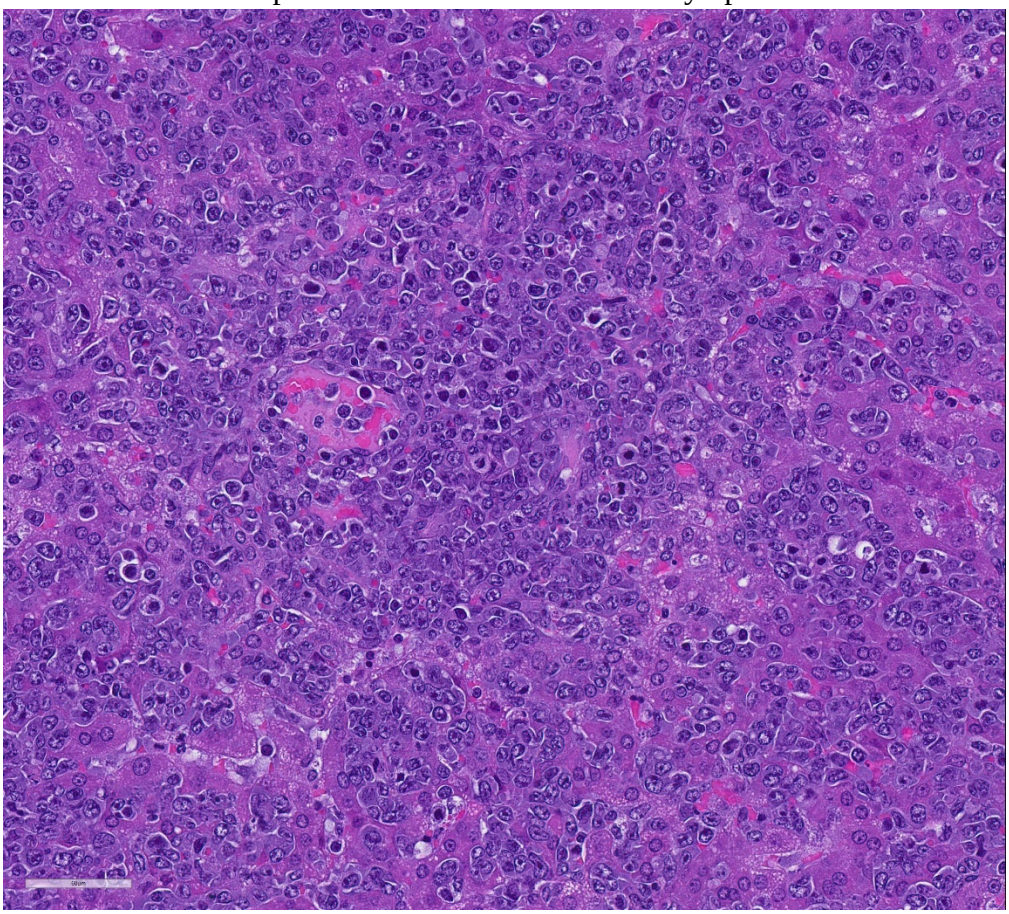

Liver, hamster: High magnification of the field in 1-3, demonstrating the large size of the neoplastic cells, abundant granular basophilic cytoplasm and high mitotic rate. (HE, 315X)

the absence of a host immune response.[4]

Contributing Institution:

Memorial Sloan-Kettering Cancer Center
1275 York Ave
New York, New York, 10065
http://www.mskcc.org/research/comparative-medicine-pathology

JPC Diagnosis: 1. Liver, spleen, omentum, pancreas: Lymphoma.
2. Liver, spleen, omentum, pancreas, macrophages: Intracytoplasmic amastigotes, rare.

JPC Comment: The contributor has provided an excellent review of leishmaniasis as well as the use of the Syrian hamster as the animal model for its visceral

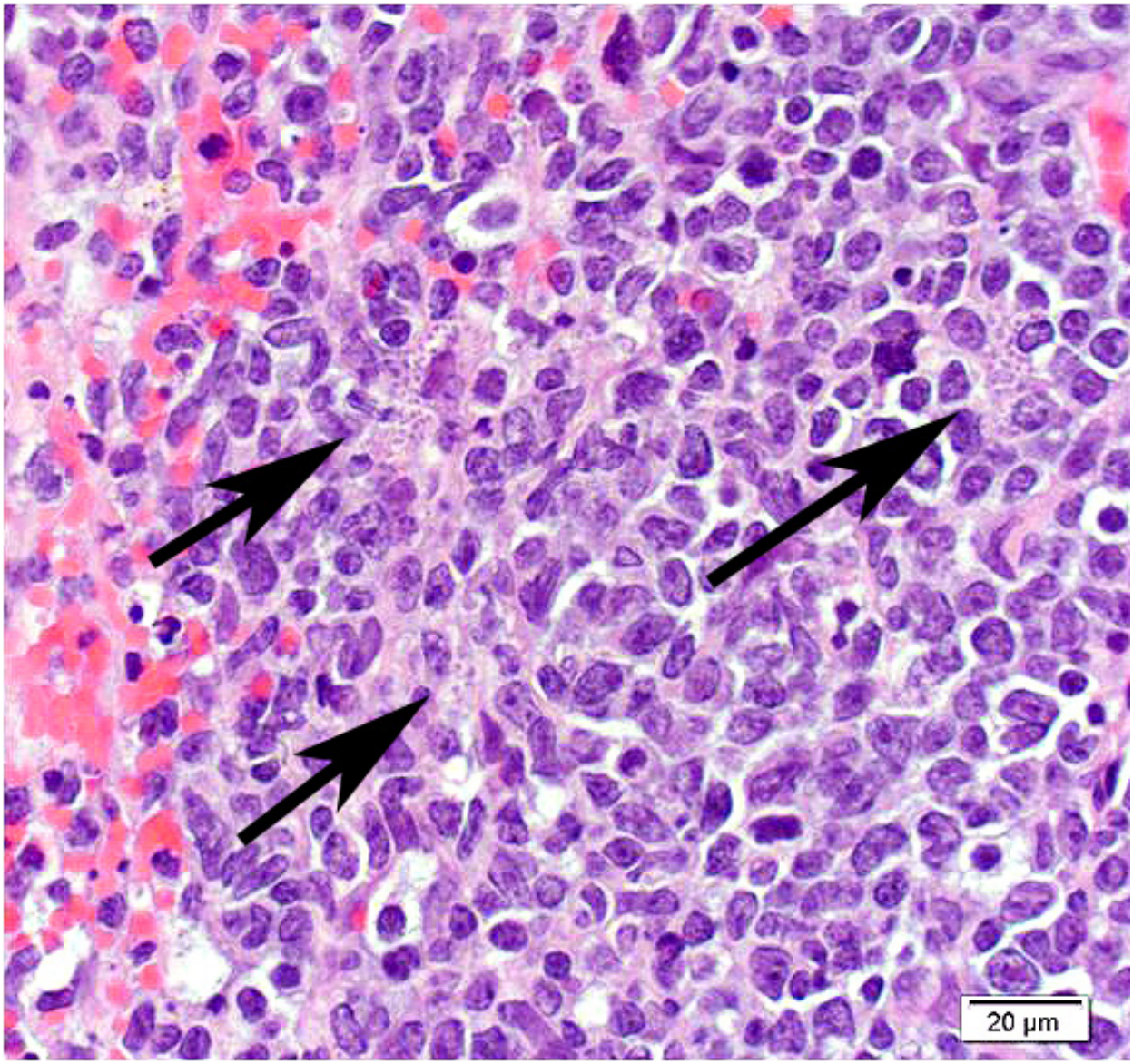

Spleen, hamster. Macrophages contain multiple intracytoplasmic amastigotes. (HE, 400X).

form. *Leishmania* has appeared multiple times in the Wednesday Slide Conference in the dog (WSC 2015-2016, Conf 17, Case 3, WSC 2013-2014 Conf 3, Case 3, WSC 2009-2010, Conf 13, Case 4, @WC 2007-2008, Conference 5, case 2). It has appeared twice in the hamster (WSC 1998-1999, Conf 10, Case 2 and WSC 1971-1972, Conference 22, case 2). The reader is directed to the comments on these cases for additional information.

The history of leishmaniasis is an ancient one, with identification of *Paleoleishmania* in fossilized form within the proboscis and gut of 100-million-year-old fly preserved in amber. Written records of cutaneous leishmaniasis begin in Assyrian tables describing "oriental sore", and *Leishmania* DNA has been recovered from Egyptian and Peruvian mummies. Evidence for immunization agains Leishmania dates back to ancient Arabia, whose physicians vaccinated children with exudate from the sores of active lesions or exposed them to sand flies to prevent the occurrence of disfiguring facial scars. Numerous reports in more modern times of "Allepo", "Jericho" and "Baghdad boil" are present in Middle Eastern literature, and numerous reports from explorers of the New World, including Francisco Pisarro described a similar scarring condition. Visceral leishmaniasis, or kala-azar, was first described by military surgeon Willian Twining in 1827 in India. Scottish pathologist William Boog Leishman was the first to observe and describe the amastigotes of *Leishmania* in autopsy of soldiers in India as well as infected rats. Weeks later, an Irish pathologist working at Madras veterinary college identified similar structures in Inidan subjects with splenomegaly and recurring fever. In 1903, Dr. William Ross identified the structures first described by Leishman and Donovan as a new species and not a degenerate trypanosome or piroplasm (as was currently thought at the time) and named the agent *Leishmania donovani*.

Currently visceral leishmaniasis remains a significant problem in 14 high-risk tropical countries, but numbers of cases, especially in India, appear to be on the decline. International travel and international transport of blood products (blood is not routinely checked for anti-leishmanial antibodies) has resulted in cases of VL in non-endemic countries. Ongoing instability in the Middle East and refugee crises also helps to import cutaneous forms of leishmaniasis into areas where it formerly was at a very low level.

Unfortunately, in the submitted sections, the changes associated with visceral leishmaniasis are greatly overshadowed by the large cell lymphoma presuably resulting from activation of hamster polyomavirus. Few of the participants noticed the presence of amastigotes within macrophages, as amastigote-laden macrophages were often overshadowed by the profound neoplastic infiltrate and the scattered apoptotic cells contained within.

References:

1. Nieto A *et al*. Mechanisms of resistance and susceptibility to experimental visceral leishmaniosis: BALB/c mouse versus syrian

hamster model. *Vet Res*. 2011;42(1):39

2. Percy DH and Barthold SW; Hamster. In: Pathology of Laboratory Rodents and Rabbits, Eds. Percy DH and Barthold SW, 3rd ed. pp181-183. , Wiley-Blackwell, Ames, IA, 2007
3. Scherneck S, Ulrich R and Feunteun J. The hamster polyomavirus--a brief review of recent knowledge. *Virus Genes*. 2001;22(1):93-101
4. Siddle HV et al. Reversible epigenetic down-regulation of MHC molecules by devil facial tumour disease illustrates immune escape by a contagious cancer. *Proc Natl Acad Sci U S A*. 2013;110(13):5103-8
5. Steverding D. The history of leishmaniasis. *Parasit Vect* 2017; (10):82-89.
6. Valli V; Hematopoietic System. In: Jubb, Kennedy & Palmer's Pathology of Domestic Animals, Ed. Maxie GM, 5th ed., pp.302-304, Saunders Elsevier, Philadelphia, PA, 2007

CASE II: A12-357 (JPC 4031109).

Signalment: 4 year old male rhesus macaque (*Macaca mulatta*).

History: This rhesus macaque was inoculated with SIVsmE6601:1 as part of a research study. Six months post inoculation, the animal was noted to have poor appetite and acute weight loss (18% body weight over 2 weeks). Clinical examination two days prior to euthanasia revealed severe respiratory distress with nasal discharge and wheezing, along with liquid diarrhea and a severe neutrophilic leukocytosis. Due to poor prognosis and progression towards simian acquired immunodeficiency syndrome, the animal was humanely euthanized.

Gross Pathology: The animal was in poor body condition with no appreciable body fat. The mucosa of the stomach was thickened and edematous. The duodenum was diffusely hyperemic. The liver and kidneys had pale foci scattered throughout the parenchyma extending through cut sections. All lung lobes were diffusely reddened and severely mottled dark red or pale brown and markedly thickened and firm.

Laboratory results: N/A

Microscopic Description:

Lung: Primarily focused around bronchi and bronchioles and involving approximately 40% of the tissue examined, alveolar spaces are filled with inflammatory cells consisting of neutrophils, epithelioid macrophages, and multinucleated giant cells admixed with edema, fibrin, cellular and karyorrhectic

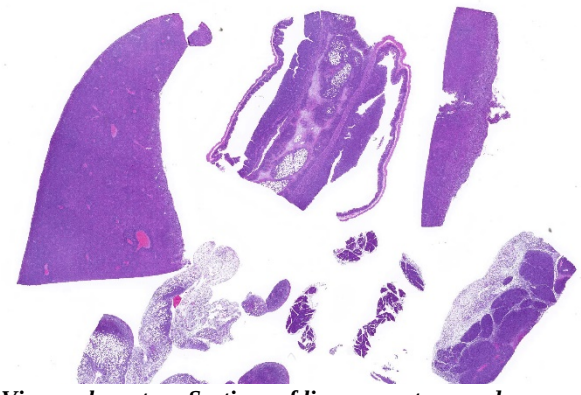

Viscera, hamster: Sections of liver, omentum, and pancreas are all infiltrated by a densely cellular neoplasm. (HE, 9X)

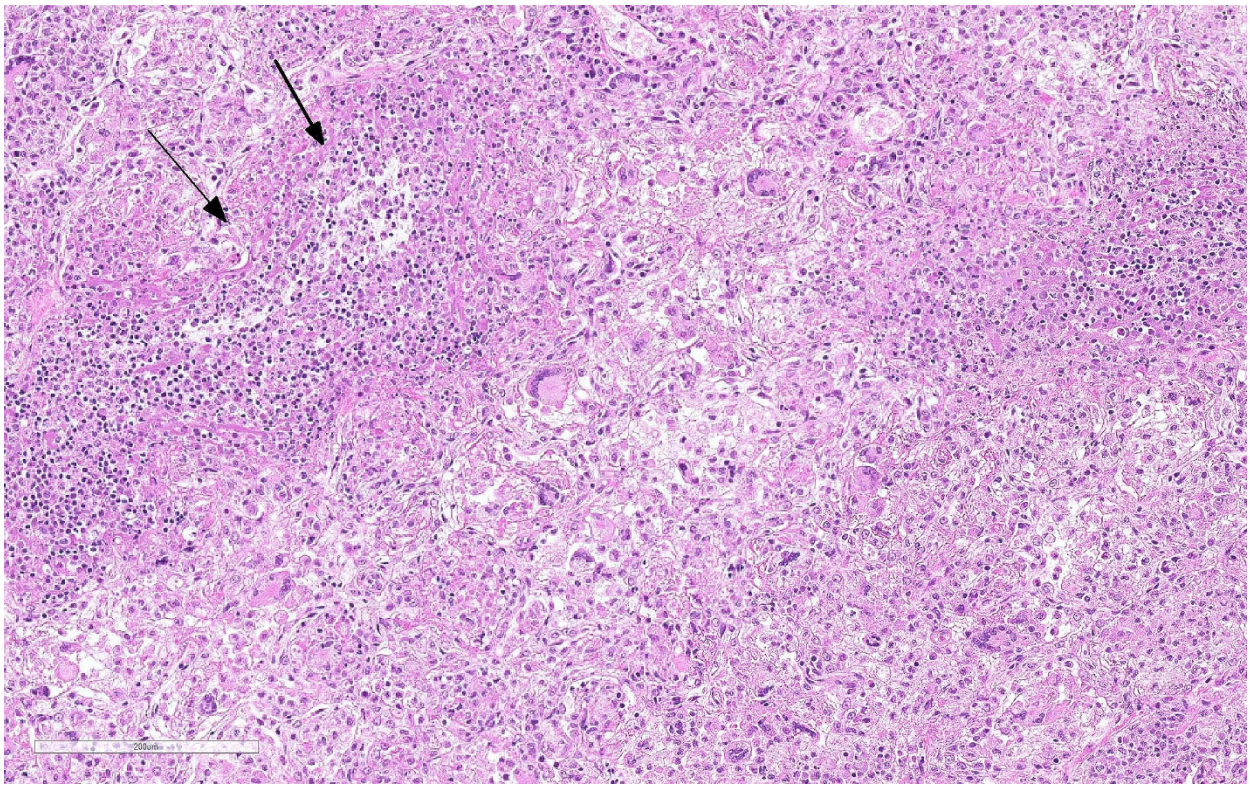

Lung, rhesus. Alveolar architecture is obscured by a mixed cellular infiltrate containing numerous macrophages, neutrophils and multinucleated viral syncytia. Airways are effaced as well (arrows). (HE, 276X)

debris, and extravasated red blood cells. Within several areas of inflammation are bacterial colonies (not present on each slide). The lumina of several bronchioles are partially occluded by neutrophils, histiocytes, cellular and karyorrhectic debris, and fibrin. Multifocally within alveolar spaces, are aggregations of foamy, eosinophilic fungal organisms (*Pneumocystis carinii*).

Contributor's Morphologic Diagnosis:

Lung: Multifocal, severe, chronic bronchointerstitial pneumonia with SIV giant cells and *Pneumocystis carinii*

Contributor's Comment Lentiviruses are a subfamily of retroviruses and include human immunodeficiency virus (HIV), simian immunodeficiency virus (SIV), equine infectious anemia virus (EIAV), ovine lentivirus (OvLV), bovine immunodeficiency virus, and feline immunodeficiency virus (FIV). Lentiviruses cause chronic disease syndromes including immunodeficiency, encephalitis, pneumonia, arthritis, anemia, thrombocytopenia, and lymphoid hyperplasia. SIV has proven a useful model to study HIV pathogenesis, as the virus is morphologically identical to HIV by electron microscopy, serologically related to HIV, and cytopathic for $CD4^+$ T cells.[7] SIV infected macaques develop peripheral lymphadenopathy, splenomegaly, diarrhea, weight loss, skin rash, pneumonia, septicemia, and hemogram abnormalities including leukopenia, lymphopenia, neutropenia, anemia, and thrombocytopenia. The appearance of multinucleate giant cells

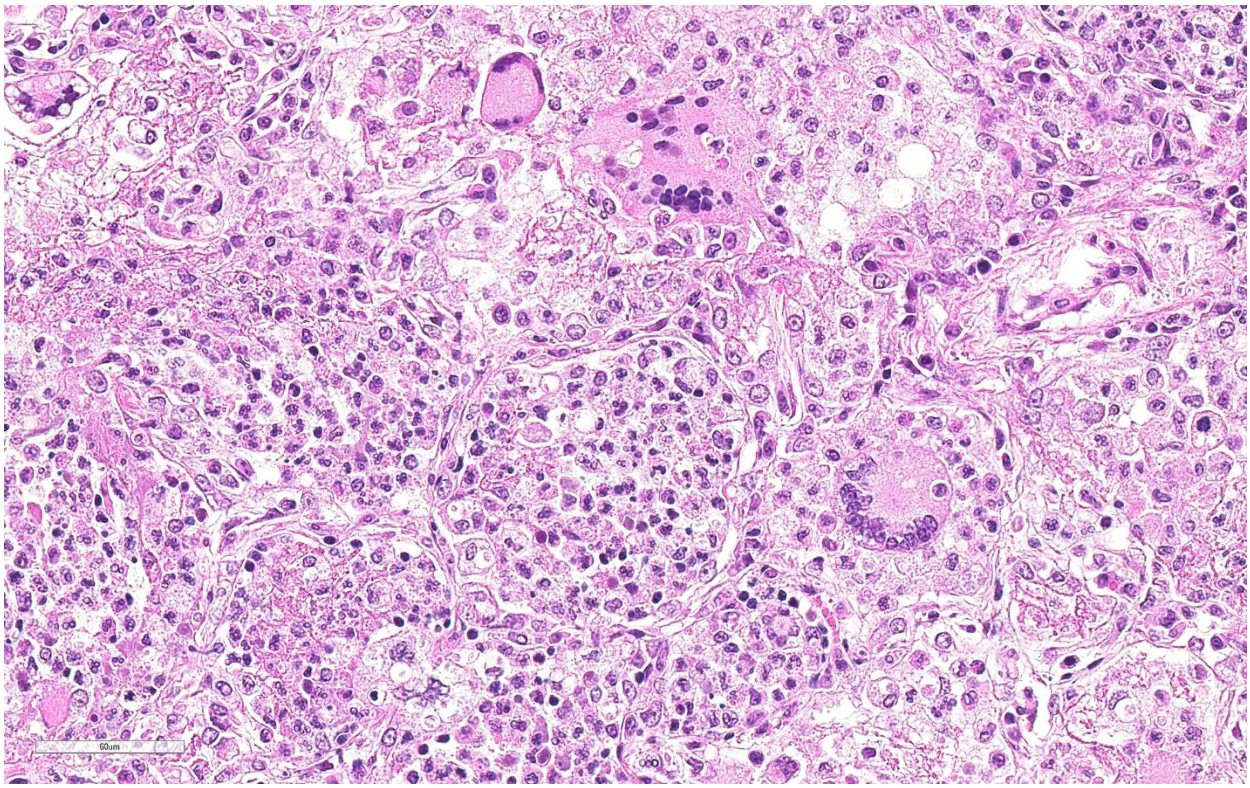

Lung, rhesus. Macrophages and neutrophils fill alveoli along with scattered viral syncytial giant cells. (HE, 400X)

is often an indication of terminal phase of disease progression.[7]

The most common pulmonary lesion in HIV is a lymphocytic and histiocytic pneumonia, centered around vessels and bronchioles.[6] Interestingly, when this syndrome occurs, HIV- infected individuals have lower incidence of opportunistic infections and longer survival times. SIV is similar, and macrophage-tropic strains cause pneumonia.[1,2,6]. If these infected macrophages go on to form giant cells, this is generally the terminal phase of SAIDS. If it infects macrophages and there is a T cell response in the lung, humans with the disease get pneumonia, but not OIs and death.

Pulmonary opportunistic infections in both AIDS patients and SAIDS-infected monkeys include *Pneumocystis carinii*, *Mycobacterium avium-intracellulare*, cytomegalovirus, *Cryptosporidium parvum* as well as other bacteria, fungal, and viral organisms. Pulmonary conditions reported to occur secondary to AIDS or SAIDS include Kaposi's sarcoma, nonspecific pneumonitis, pulmonary lymphoma, pulmonary lymphoid hyperplasia, and lymphocytic interstitial pneumonia. *Pneumocystis carinii* infection in macaques is characterized by foamy pink exudate within alveoli, extensive lymphocytic infiltration, and type II pneumocyte hyperplasia.[3]

Pulmonary multinucleate giant cells and histiocytic infiltrates have been observed in

SIV infected rhesus macaques.[7] Viral antigen (p26 and p14) has been observed on theses syncytial cells and smaller macrophages in alveolar spaces, circulating in pulmonary blood vessels, and in the sinusoids of tracheobronchial lymph nodes of moribund animals.[2] These cells have also been labeled with a-1-antichymotrypsin, indicating macrophage origin. This spectrum of lesions is seen in monkeys that are free from CMV.[2] The more common pulmonary change in SIV infection is perivascular mononuclear inflammation between 2-8 weeks after inoculation. SIV arrives at the lung hematogenously likely within lymphocytes or macrophages. This characteristic infiltrate of multinucleate giant cells reflects the final stage of disease where the immune system is unable to restrict viral replication in macrophages. Disseminated giant cell disease is a characteristic of terminal AIDS/SAIDS.[3,8]

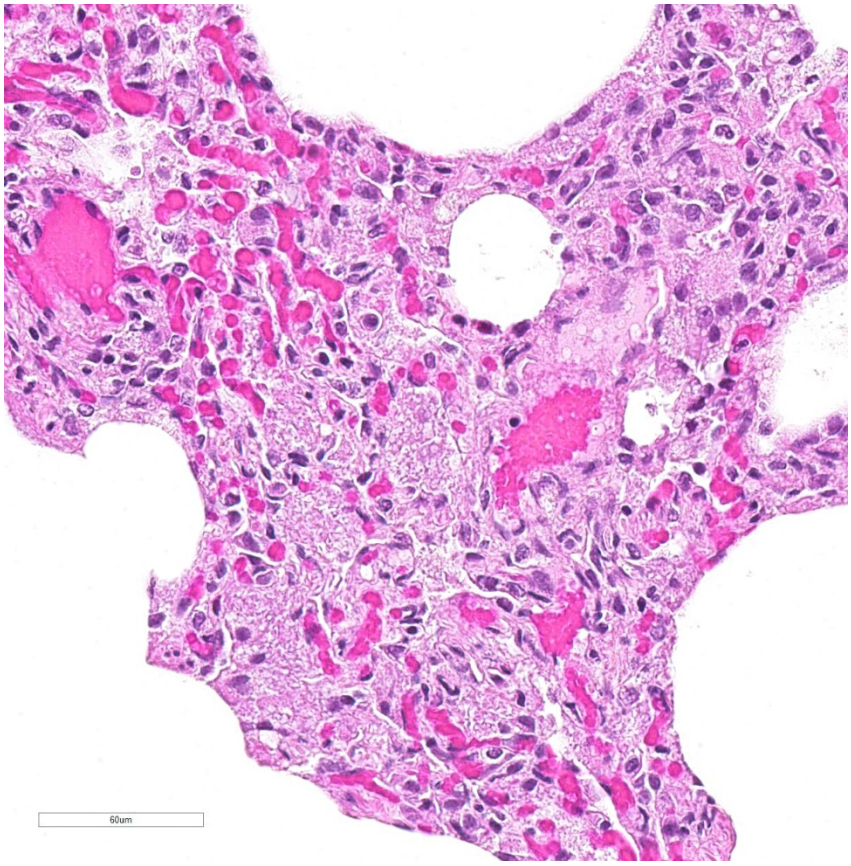

Lung, rhesus. In less damaged areas of the section, alveoli are filled with macrophages and eosinophilic flocculent protein. (HE, 400X).

Contributing Institution:

Harvard Medical School
Division of Comparative Pathology
New England Primate Research Center
One Pine Hill Drive
Southborough, MA 01772|
www.hms.harvard.edu/NEPRC

JPC Diagnosis: Lung: Pneumonia, interstitial, histiocytic, with abundant fungal cysts, neutrophils and numerous viral syncytia.

JPC Comment: The contributor provides a concise overview of pulmonary SIV infection in the macaque, which very closely approximates common events as seen in HIV infected humans.

The fungus *Pneumocystis carinii* was first identified in post-World-War II Europe in malnourished children, and prior to the onset of the HIV epidemic in the 1980s, was most

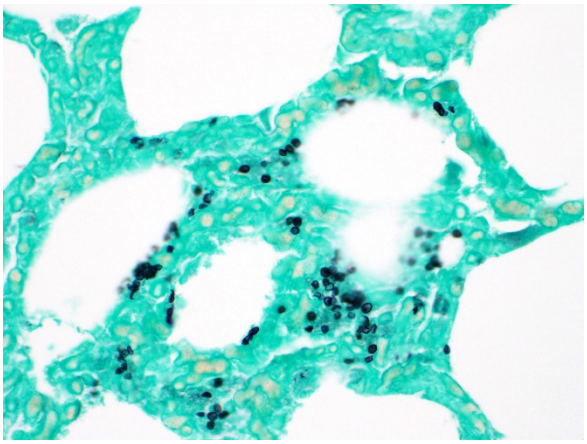

Lung, rhesus. Asca of Pneumocystis carinii are embedded in the flocculent proteinaceous exudate. (GMS, 400X).

often seen in patients undergoing chemotherapy. Infection elicits humoral and cell mediated responses in affected individuals with the $CD4^+$T-cell-driven response considered the most important in combating infection. Asci, or cystic forms, have beta-glucan within their cell wall, which is recognized by alveolar macrophages and epithelial which ultimately prime the T-cell response. Various inflammatory responses, including Th1, Th2, and Th17 responses all been identified in various cases of PCP, however, none have been shown to be intrinsic to disease clearance. Trophozoites, whch lack a cell wall, do not stimulate the response, and may actively inhibit it. Macrophages also appear to be the primary cell responsible for killing the fungus.

Coinfection by *Pneumocystis carinii* in SIV-infected macaques with AIDS is a common finding, especially in terminal stages of the disease. Experimental models of *Pneumocystis carinii* pneumonia (PCP) infection in rhesus macaques have been established via pulmonary airway inoculation of SIV-infected animals, which allows the ability to study the pathogenesis of PCP in immunosuppressed patients. Characteristic findings in this model parallels those seen in natural infection, with an initial increase in $CD8^+$ T cells in the lung and bronchiolo-alveolar lavage fluid of affected animals until they constitute over 90% of $CD3^+$ T-cells. Infiltration of neutrophils into the lung generally heralds the onset of clinical disease and are considered a major cause of pulmonary damage in PCP.

It was generally accepted for many years among SIV researchers that the African nonhuman primates, which infected with lentiviruses do not progress to AIDS, as characterized by $CD4^+$ depletion, opportunistic infections, and neoplasia. A 2009 paper by Pandrea et al[8] chronicled progressive SIV infection in African green monkeys, mandrills, sooty and black mangabeys, and HIV infection in baboons and chimpanzees. While the viral loads required to infect these species is considerably higher than required to infect Asian macaques, and potentially higher than natural infection, it may be wise to consider same- and cross-species infection with lentivirus a “persistently non-progressive” rather than “non-pathogenic” infection in these species.[8]

References:

1 Babas T, Vieler E, Hauer DA, Adams RJ, Tarwater PM, Fox K, Clements JE, Zink MC: Pathogenesis of SIV pneumonia: selective replication of

viral genotypes in the lung. Virology **287:** 371-381, 2001

2 Baskin GB, Murphey-Corb M, Martin LN, Soike KF, Hu FS, Kuebler D: Lentivirus-induced Pulmonary Lesions in Rhesus Monkeys (*Macaca mulatta*) Infected with Simian Immunodeficiency Virus. Vet Pathol **28:** 506-513, 1991

3 Baskin GB, Murphey-Corb M, Watson EA, Martin LN: Necropsy Findings in Rhesus Monkeys Experimentally Infected with Cultured Simian Immunodeficiency Virus (SIV)/Delta. Vet Pathol **25:** 456-467, 1988

4. Board KF, Patil S, Lebedeva I, CapuanoIII S, Trichel AM, Murphey-Corb M, Rajakumar PA, Flynn JL, Haidaris CG, Noris KA. Experimental Penumocystic carinii pneumonia in simian immunodeficiency virus-infected rhesus macaques. *J Inf Dis 2*003; 187:576-588.

5. Hoving JC, Kolls JK. New advances in understanding the host immune response to Pneumocystis. *Curr Opin Microbiol* 2017; 40:65-71

6. Mankowski JL, Carter DL, Spelman JP, Nealen ML, Maughan KR, Kirstein LM, Didier PJ, Adams RJ, Murphey-Corb M, Zink MC: Pathogenesis of Simian Immunodeficiency Virus Pneumonia. Am J of Pathol **153:** 1123-1130, 1998

7. McClure HM, Anderson DC, Fultz PN, Ansari AA, Lockwood E, Brodie A: Spectrum of disease in macaque monkeys chronically infected with SIV/SMM. Vet Immunol Immunop **21:** 13-24, 1989

8. Pandrea I, Silvestri G, Apetrei C: AIDs in African NHP hosts of SIVs: A New Paradigm of SIV Infection. Cur HIV Res **7:** 57-72, 2009

CASE III: WSC Case 2 HE (JPC 4118136).

Signalment2-year-old, intact male, Harlan Sprague-Dawley rat (*Rattus norvegicus)*

History: This rat was a terminal sacrifice (Test Day 730) animal from the control (untreated) group of a chronic, 2-year carcinogenicity study. No clinical signs or gross lesions were noted.

Gross Pathology: N/A

Laboratory results: N/A

Microscopic Description:

There is marked, irregular undulation along the capsular cortical surface. Diffusely throughout the cortex, there is moderate loss of renal tubules with replacement and wide separation of remaining tubules by abundant interstitial fibrous connective tissue, edema, and mixed inflammatory cells, including predominantly small lymphocytes and plasma cells. Low numbers of brown, granular pigment-laden (hemosiderin-laden) macrophages are also scattered throughout the cortical interstitium. Multifocal small

interstitial hemorrhages are also present. The majority of remaining renal tubules are moderately to marked dilated and vary from empty to often filled with eosinophilic proteinaceous fluid or protein (hyaline) casts. Occasionally, a few scattered tubules have sloughed, necrotic epithelial cells and/or small intraluminal clusters of degenerative neutrophils admixed with necrotic cellular and nuclear debris and rare erythrocytes. Renal tubular epithelial changes range from cytoplasmic swelling and vacuolization (degeneration) to attenuation and atrophy. The tubular basement membrane is often thickened and hyalinized. Frequent scattered regenerative tubules are also present. Regenerative tubules are lined by one or multiple layers of crowded, plump epithelium characterized by slight cytoplasmic basophilia and large, vesicular nuclei with a single prominent nucleolus and increased mitoses. Rarely, a small papillary projection of jumbled renal tubular epithelium projects into the lumen. The majority of glomeruli are enlarged with glomerular tufts segmentally to globally

Kidney, rat. Subgross changes include an irregular contour of the capsule, diffuse ectasia of tubules, protein casts and interstitial hypercellularity predominantly within the outer stripe of the medulla, and mild dilation of the renal pelvis. (HE, 7X)

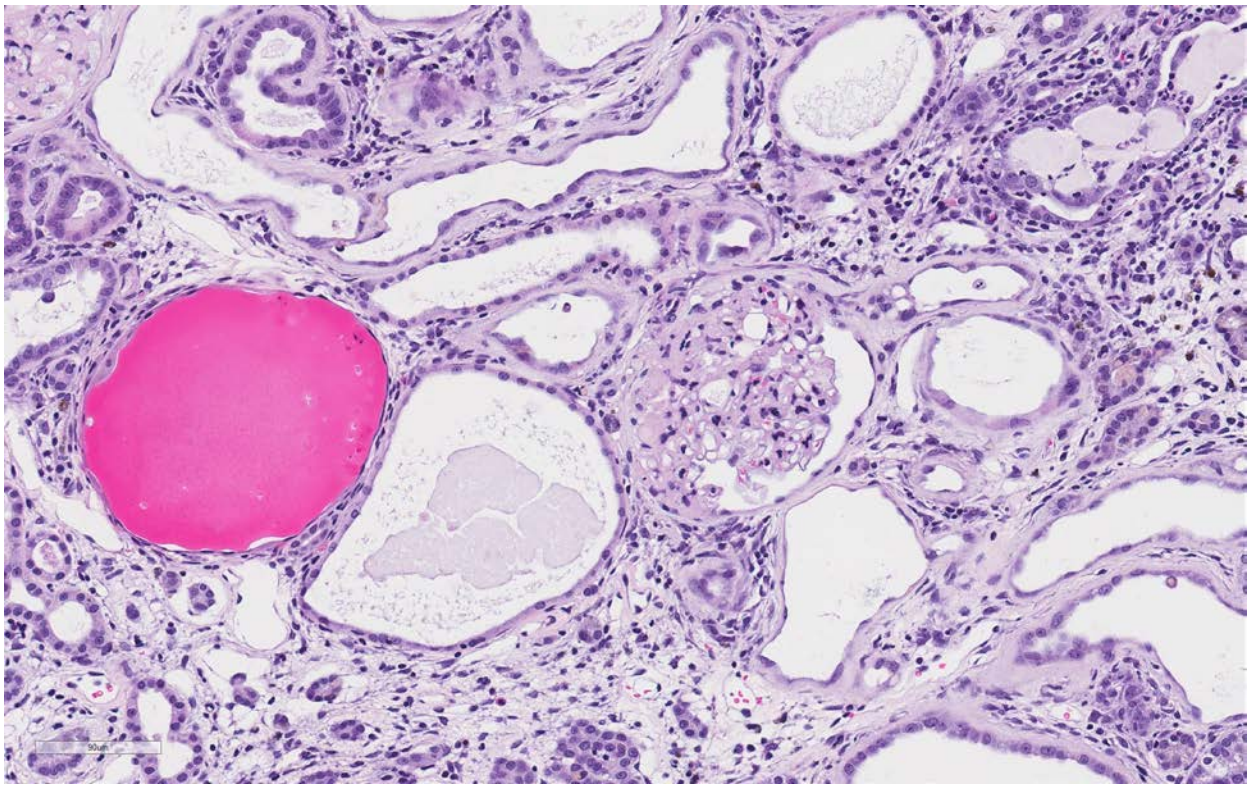

Kidney, rat. There is marked expansion of the interstitium with edema, collagen, and lymphocytes, plasma cells, and rare neutrophils. Tubules are markedly ectatic, often lined by attenuated epithelium, have a thickened basement membranes, and contain luminal protein. Other tubules within areas of fibrosis are shrunken and atrophic. The glomerulus at center has markedly thickened capillary basement membrane and early Synechiae formation approximately 50% around Bowman's membrane. (HE, 150X)

expanded by increased mesangial fibrous connective tissue, Bowman's capsule thickened and hyalinized, and periglomerular fibrosis (glomerulosclerosis). The parietal epithelium lining Bowman's capsule is often hypertrophied and glomerular tufts are multifocally adhered to Bowman's capsule (synechiae). The urinary space is often moderately dilated. A few shrunken, obsolescent glomeruli are also seen.

Contributor's Morphologic Diagnosis:

Kidney: Tubular degeneration, atrophy, necrosis, and regeneration, diffuse, severe with thickened basement membranes, tubular ectasia and hyaline casts, chronic interstitial nephritis and fibrosis, and glomerulosclerosis, segmental to global (chronic progressive nephropathy)

Contributor's Comment: Chronic progressive nephropathy (CPN) is very common in all conventional strains of laboratory rat, with the highest incidence and severity in the Fischer 344 and Sprague-Dawley strains.[2-4] The disease also occurs at a higher incidence and with progressively greater severity in male rats than in female rats.[2-4,6] CPN is also a very common spontaneous renal disease of aging laboratory mice.[3-4,6] A similar disease has been described in the gerbil, common marmoset, and naked mole rat. [5,6,8] In guinea pigs, segmented nephrosclerosis shares some features with CPN.[5]

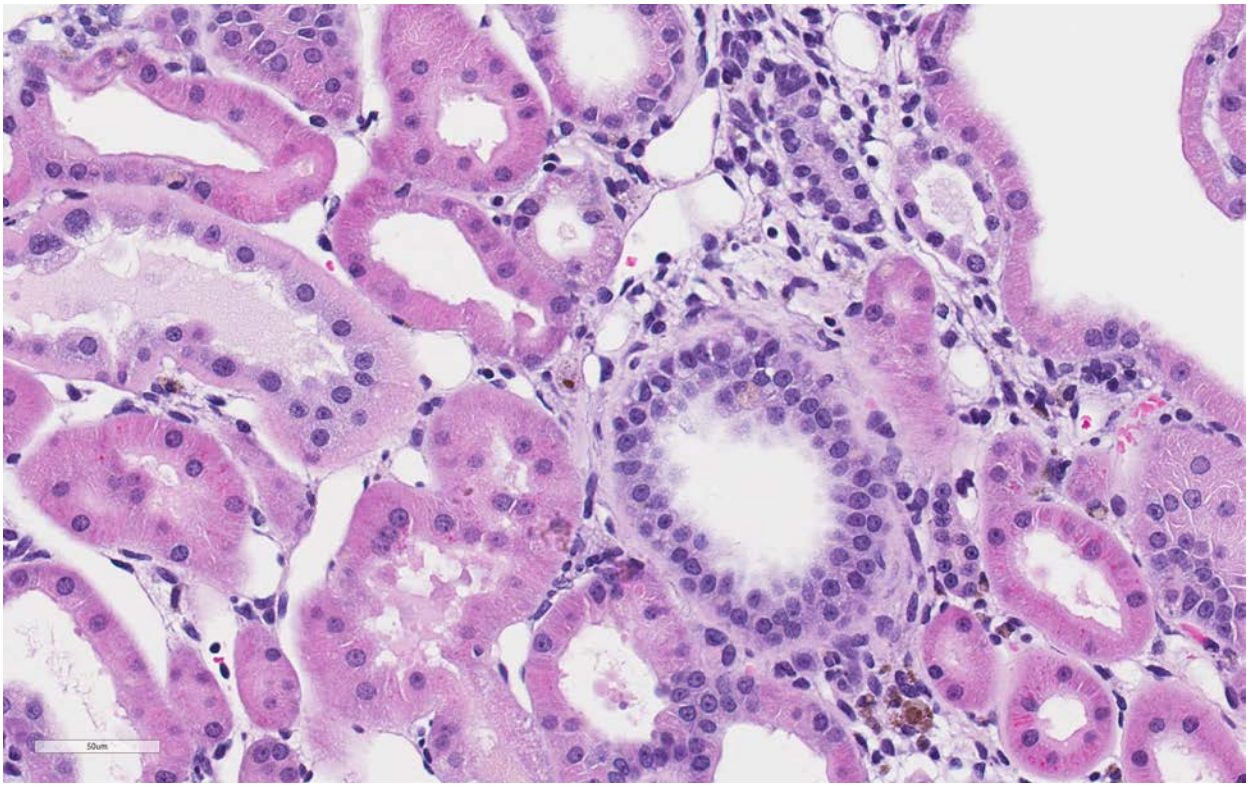

Liver, rat. Regenerating tubules are characterized by cytoplasmic basophilia and nuclear crowding. (HE, 276X)

CPN is a major cause of morbidity and mortality in laboratory rats.[3,4] Although commonly thought of as an aging disease, many rats start developing the earliest lesions of CPN as juveniles (2-3 months old).[3] The disease progresses throughout the life of the animal, eventually leading to end-stage renal disease in the rat.[2-4] Renal failure from CPN can sometimes account for up to 50% or more of unscheduled male rat deaths in chronic carcinogenicity bioassays.[3]

The cause of CPN is unknown[2-4], although Manskikh recently proposed a hypothesis for an expanding somatic mutant clone of precursor cells of tubular epithelium as the inciting cause.[6] A number of dietary and hormonal factors are known to influence the incidence and severity of disease. The primary diet-related factors of importance are total caloric intake as well as source and amount of protein in the diet. Restricting caloric intake and reducing protein in the diet can reduce the incidence and severity of CPN. With regard to hormonal factors, the sex predisposition of the disease is linked to the presence of androgens, rather than an absence of estrogen.[2-4]

Classically, the glomerulus has been thought to be the primary target, with hyperfiltration being the underlying basis for the pathogenesis.[3-5] This theory has been perpetuated due to the influence of high protein diets on disease progression and the associated clinical pathology finding of albuminuria in affected animals. However, this proposed glomerular hyperfiltration pathogenesis has not been proven; in fact, in aging rats, there is no evidence for a causal

relationship between glomerular capillary blood pressure and the structural damage to glomeruli, arguing against this theory of a primary hemodynamic mechanism.[4] Additionally, the earliest lesion of CPN that is detectable by light microscopy is actually a renal tubular lesion – a focal simple tubular hyperplasia of the P1 segment of a proximal tubule. This focal tubular lesion progresses to a small focus of affected tubules within a nephron and eventually to involve adjacent nephrons. Tubular basement membrane thickening is often a very prominent feature. Glomerular lesions generally develop later in the course of the disease.[2-4] However, it cannot be ruled-out that a functional alteration in the glomerulus which cannot be detected microscopically may occur prior to this tubular lesion. During later and more severe stages of the disease, CPN is predominantly characterized by both degenerative and regenerative tubular changes, including numerous protein casts, as well as prominent segmental to global glomerulosclerosis.[1-3] In severe grade cases, vesicular alteration of the renal papilla can be seen.[7] Deposition of interstitial extracellular matrix (fibronectin, thrombospondin, collagens I and III) and infiltration by mononuclear inflammatory cells is often seen as well but these components are generally mild and not prominent features of the disease.[1-3] Notably, vascular lesions are not a part of the disease.[3,4]

With regard to experimental studies and chronic carcinogenicity bioassays, some chemicals can induce exacerbation of CPN and, given the proliferative nature of the disease, advanced CPN is itself a risk factor for a marginal increase in the incidence of renal tubule tumors.[2-4] In humans, the most common renal diseases are diabetic nephropathy and hypertensive nephropathy. The biology and lesions of rat CPN do not mirror those of either of these nephropathies nor of any of the additional known, less common nephropathies of humans; there is no known counterpart of rat CPN in humans.[3] As such, there is debate over the conclusions that can be drawn from chronic carcinogenicity bioassays using rats regarding small increases in the incidence of renal tubule tumors and the relevance to human health. When designing experiments and interpreting the data from studies using the laboratory rat, relevance for species extrapolation to humans needs to be considered, particularly with regard to determining nephrotoxic effects and risk for renal tumor development.

Contributing Institution:

National Toxicology Program
National Institute of Environmental Health Sciences
111 TW Alexander Drive, PO Box 12233
Research Triangle Park, NC 27709

https://www.niehs.nih.gov/research/atniehs/labs/lep/ntp-path/index.cfm

JPC Diagnosis: Kidney: Nephritis, interstitial, chronic, diffuse, severe, with membranous glomerulonephritis, synechiae, tubular loss, degeneration, necrosis, and regeneration, and marked interstitial fibrosis.

JPC Comment: The contributor has provided an excellent review of chronic progressive nephropathy of rats (CPN), a

very common age-related finding in laboratory rodents, which may have an important and deleterious effect on analysis in chronic studies.

From a strain perspective, Sprague-Dawley and Fischer 344 appear to be the most affected by this condition, followed by Wistar, Long-Evans, and Brown Norway strains, with Buffalo and Osborne-Mendel the most resistant.[1] The changes are grossly apparent only in the later stages of disease, presenting as kidneys which are decreased in size with an irregular contour, and a golden, rather than brick-red coloration.

Microscopically, lesions may be seen as early as 2-3 months of age in male rats of predisposed strains as individual regenerative tubules within the cortex with basophilic cytoplasm, epithelial crowding, and an irregularly thickened basement membrane. Affected tubules will accumulate hyaline material in their lumen over time, predominantly in inner stripe of the outer medulla (descending loop of Henle). Over time, individual diseased and regenerative tubules become enlarging foci, hyaline casts extend into the cortex, and eosiniophlic droplets may be seen in tubular epithelium (most prominently in males). Visible glomerular changes develop at this time. Shortly, interstitial inflammation (beginning at the cortical medullary junction) and fibrosis develops.[1]

End stage CPN is characterized by involvement of the entire kidney and various effects in other organs: hyperplasia of the chief cells of the parathyroid gland as well as metastatic calcification in a number of organs, including the kdney, lung, media of large arteries, and the gastrointestinal tract. An additional lesion of end-stage CPN, which may be overlooked with the myriad and severe changes of the glomeruli, tubules, and interstitium, is papillary hyperplasia of the epithelium of the renal pelvis. This lesion consistst of projections of hyperplastic transitional epithelium containing large dilated vessels which project into the pelvic lumen.[1]

Clinicopathologic findings in affected animals include marked proteinuria and aluminuria and resulting hypoproteinemia, hypoalbuminemia, and hypercholesterolemia, demonstrating the severity of the glomerular damage. Decreased functional renal mass results in hyperphosphatemia, and serum calcium is decreased as a result of Starling's law as well as hypoalbuminemia. Serum nitrogen and creatinine values increase only in late stages of the disease.[1]

References:

1. Seely JC, Hard GC, Blankenship B. Urinary Tract. *In: Boorman's Pathology of the rat: reference and atlas, 2nd edition,* Suttie A, Leininger JR, Bradley AE, eds. London, Academic Press 2018; pp 135-137.
2. Hard GC, Banton MI, Bretzlaff RS, et al. Consideration of Rat Chronic Progressive Nephropathy in Regulatory Evaluations for Carcinogenicity. *Toxicol Sci*. 2013;132(2): 268-275.
3. Hard GC, Johnson KJ, Cohen SM. A comparison of rat chronic progressive nephropathy with human renal disease –

implications for human risk assessment. *Crit Rev Toxicol*. 2009;39(4):332-346.
4. Hard GC, Khan KN. A Contemporary Overview of Chronic Progressive Nephropathy in the Laboratory Rat, and Its Significance for Human Risk Assessment. *Toxicol Path*. 2004;32:171-180.
5. Manskikh VN. Hypothesis: Chronic Progressive Nephropathy in Rodents as a Disease Caused by an Expanding Somatic Mutant Clone. *Biochemistry Moscow*. 2015;80(5):689-693.
6. Manskikh VN, Averina OA, Nikiforova AI. Spontangenous and Experimentally Induced Pathologies in the Naked Mole Rat (*Heterocephalus glaber*). *Biochemistry Moscow*. 2017;82(12):1504-1512.
7. Souza NP, Hard GC, Arnold LL, Foster KW, Pennington KL, Cohen SM. Epithelium Lining Rat Renal Papilla: Nomenclature and Association with Chronic Progressive Nephropathy (CPN). *Toxicol Path.* 2018;46(3):266-272.
8. Yamada N, Sato J, Kanno T, Wako Y, Tsuchitani M. Morphological Study of Progressive Glomerulonephropathy in Common Marmosets (*Callithrix jacchus*). *Toxicol Path*. 2013;41:1106-1115.

CASE IV: L19-3350 (JPC 4135947).

Signalment: 7-year-old, intact female, Flemish giant domestic rabbit (*Oryctolagus cuniculus*)

History: The rabbit presented with a 1-month history of severe subcutaneous swelling, erythema, ulceration and abscess formation of the left hindlimb extending from the hock to the digits. A focal area of mild subcutaneous swelling was also noted on the plantar surface of the right hindlimb metatarsal area with a similar exudate on cut surface. The animal was housed on a wire cage outdoors with no bedding. Decreased borborygmi were noted on auscultation and the haircoat in the perineal region was stained with feces. Due to the severity of the lesions, which would require limb amputation, euthanasia was elected.

Gross Pathology: The left metatarsal region is markedly swollen, with multifocal ulceration and fistulous tracts that extend to

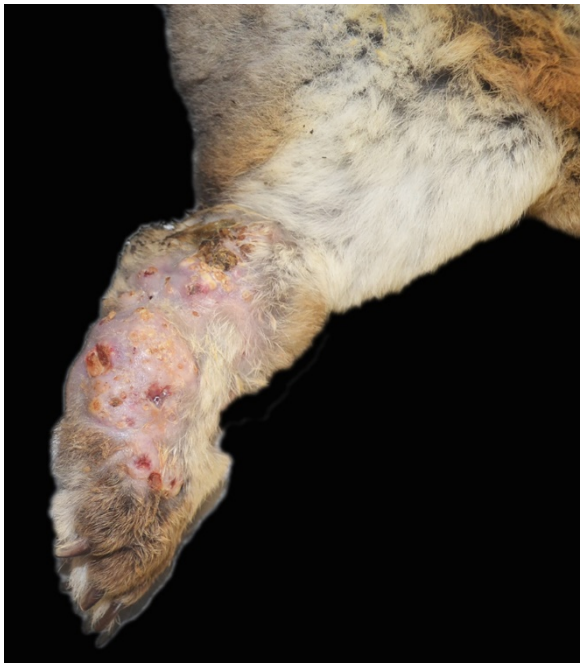

Metatarsus, rabbit The left metatarsal region is swollen, with multifocal ulceration and fistulous tracts. (Photo courtesy of: Louisiana Animal Disease Diagnostic Laboratory (LADDL), School of Veterinary Medicine, Louisiana State University (http://www1.vetmed.lsu.edu/laddl/index.html)

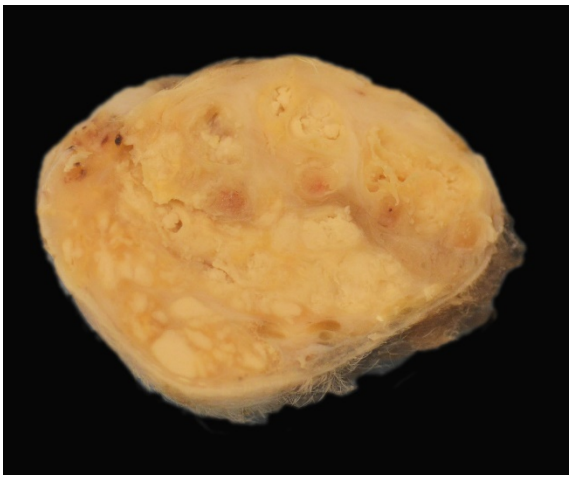

Metatarsus, rabbit. Multifocal abscesses containing abundant, inspissated, white to pale yellow, granular exudate are seen on cut surface. (Photo courtesy of: Louisiana Animal Disease Diagnostic Laboratory (LADDL), School of Veterinary Medicine, Louisiana State University (http://www1.vetmed.lsu.edu/laddl/index.html)

the plantar surface of the paw On cut surface, the subcutis is effaced by multifocal abscesses containing abundant, inspissated, white to pale yellow, granular exudate extending to the periosteum of the underlying metatarsal and phalangeal bones.The distal right metatarsal region has a 0.5 cm diameter focal abscess within the subcutis.

Laboratory results: Bacteriology: Skin – Moderate growth of *Pseudomonas aeruginosa*

Microscopic Description:

Haired skin (left distal hindlimb): The dermis and panniculus are effaced by multifocal to coalescing areas of liquefactive necrosis characterized by abundant hypereosinophilic cellular debris, hemorrhage, numerous heterophils and colonies of coccobacillary bacteria surrounded by abundant intensely eosinophilic (hyalinized) material frequently forming radiating, club-like projections (Splendore-Hoeppli reaction). The areas of necrosis are peripherally delimited by abundant foamy histiocytes and proliferation of dense fibrous connective tissue. There are occasional dilated lymphatic vessels. The cortical bone of the metatarsal and phalangeal bones represented in the sections have variable areas of periosteal bone proliferation and occasional Howship's lacunae containing osteoclasts. Other histologic changes variably represented in the sections include proliferation of the synovial membrane within tendon sheaths along with moderate infiltration of lymphocytes and plasma cells; skeletal muscle atrophy, regeneration and replacement by fibrous connective tissue characterized by shrunken myofibers, multinucleated myocytes and moderate endomysial infiltration of lymphocytes and plasma cells; and peripheral nerve fiber degeneration and loss characterized by marked vacuolization and deposition of mucinous matrix and/or fibrous connective tissue within the endoneurium. Histologic changes within the epidermis and adnexa are also variably represented in the

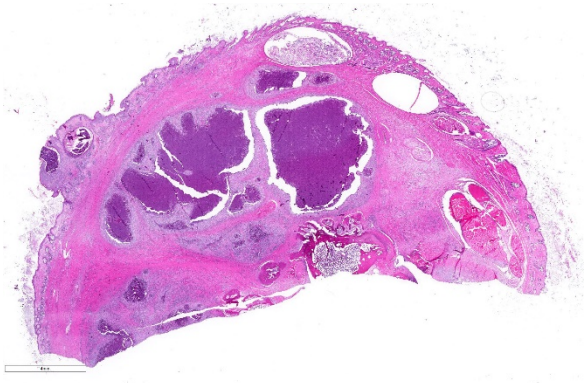

Partial cross section, metatarsus. Within the deep dermis, focally extending to the epidermis and abutting the bone, there are numerous multifocal to coalescing pyogranulomas. There is a proliferative reaction arising from the cortex of the underlying bone. (HE, 7X)

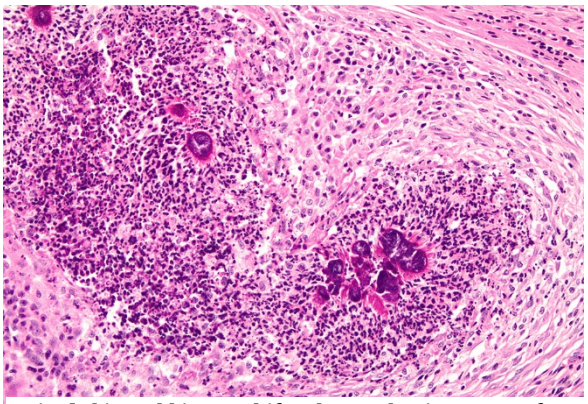

Haired skin, rabbit. Multifocal to coalescing areas of necrosis with numerous colonies of bacteria delimited by abundant Splendore-Hoeppli reaction. (HE, 200X) (Photo courtesy of: Louisiana Animal Disease Diagnostic Laboratory (LADDL), School of Veterinary Medicine, Louisiana State University (http://www1.vetmed.lsu.edu/laddl/index.html)

sections. The epidermis is markedly hyperplastic with occasional pustules and crusts, and multifocal transepidermal elimination of necrotic debris and bacterial colonies into the epidermal surface or into the lumen of hair follicles is also noted (Figure 4). Multiple hair follicles are markedly dilated and filled with abundant keratin (comedone), and the adnexa are frequently delimited by moderate numbers of lymphocytes and plasma cells. Special stains performed (Gram, Gridley, Giemsa, Steiner, and Fite's) characterized bacterial colonies as being composed by short rod-shaped gram-negative bacteria that also stain strongly basophilic with Giemsa (Figures 5 and 6). No fungal organisms, spirochetes or acid-fast bacteria were identified.

Additional histologic findings (not represented in the sections) include marked myeloid hyperplasia with a left shift, mild to marked extramedullary hematopoiesis in the liver and spleen, and abundant intravascular heterophils within pulmonary capillaries and larger vessels.

Contributor's Morphologic Diagnosis:

Skin (left distal hindlimb): Dermatitis and panniculitis, pyogranulomatous, multifocal to coalescing, severe, with abundant large intralesional gram-negative bacterial colonies and Splendore-Hoeppli reaction.

Contributor's Comment: Botryomycosis, also known as bacterial pseudomycetoma, is a term that commonly refers to a chronic bacterial infection of the skin and subcutis caused by non-filamentous bacteria that tend to form grossly visible colonies as tissue grains within the lesions (noted in this case as a granular exudate).[11] This condition affects multiple animal species including equids, cattle, dogs, hamsters, mice, rats, rabbits and guinea pigs.[1-6,9,12,14-16] It has to be differentiated from actinomycotic and eumycotic mycetomas, which usually present with similar gross and histologic lesions. Actinomycotic mycetomas are frequently associated with subcutaneous *Actinomyces* spp. or *Nocardia* spp. infections, which can be differentiated histologically using special stains including Gram and modified acid-fast: *Actinomyces* spp. are gram-positive, non-acid-fast, filamentous bacteria, and *Nocardia* spp. are gram-positive and variably acid-fast filamentous bacteria. Eumycotic mycetomas are caused by a variety of fungi that can be readily identified using stains such as methenamine silver.

Botryomycotic lesions usually develop in the skin and subcutis, but frequently extend deeply, affecting the underlying muscle and bone. Visceral lesions are uncommon but have been reported in multiple species as well.[2,4,15] Grossly, lesions are characterized

by firm, focal to multifocal nodules containing a white to yellow exudate with a gritty texture (tissue grains) that tend to ulcerate and/or develop fistulous tracts as observed in this case. Additional histologic findings in this rabbit included marked myeloid hyperplasia with a left shift, mild to marked extramedullary hematopoiesis in the liver and spleen, and abundant intravascular heterophils within pulmonary capillaries and larger vessels; all of these most likely related to the inflammatory response secondary to the infection.

The Splendore-Hoeppli phenomenon has been reported as a classic histologic feature of botryomycosis. Although its composition is not fully characterized, it is reportedly

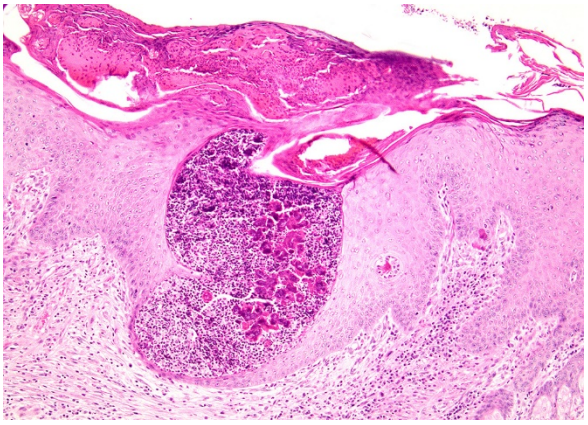

Haired skin, rabbit. The epidermis has multifocal areas of transepidermal elimination of necrotic debris and bacterial colonies and superficial serocellular crusts. (HE, 100X) (Photo courtesy of: Louisiana Animal Disease Diagnostic Laboratory (LADDL), School of Veterinary Medicine, Louisiana State University (http://www1.vetmed.lsu.edu/laddl/index.html)

composed of necrotic debris and deposition of immune complexes.[8] While in some cases deposition of immunoglobulins was observed via immunohistochemistry and immunoelectron microscopy, in other instances this material may be composed of eosinophilic major basic protein.[8,13] Differences in composition may be associated with the specific causative agent and probably other factors such as disease stage and previous treatments.[8]

Even though the pathogenesis of botryomycosis is not well understood, it is believed that the pyogranulomatous inflammation develops as a consequence of the complex interactions between the host response and the agent's virulence factors. It is speculated that the inability to clear the infection may be associated with a polysaccharide coating synthesized by the bacteria. Coagulase-positive staphylococci (mainly *S. aureus*) are the most common causative agents of botryomycosis, but other bacteria including *Pseudomonas* spp., *Streptococcus* spp., *Actinobacillus* spp., *Pasteurella* spp., *Proteus* spp., *Escherichia coli*, *Trueperella* spp. and *Bibersteinia* spp. have also been identified. This condition is generally secondary to wound contamination or traumatic lesions; in this case it was likely associated with poor housing conditions with no bedding. Usually, the bacteria are not well recognizable on H&E sections, in which special stains can aid in ruling out actinomycotic bacteria (actinomycotic mycetoma) and fungi (eumycotic mycetoma). Bacterial and/or fungal culture is required in order to confirm the etiologic agent. In this case, bacterial colonies were gram negative and basophilic with a Giemsa stain, consistent with the culture of *Pseudomonas aeruginosa*. The Gram and

Giemsa stains highlighted the radiating, club-like projections within the Splendore-Hoeppli material.

Contributing Institution:

Louisiana Animal Disease Diagnostic Laboratory (LADDL), School of Veterinary Medicine, Louisiana State University (http://www1.vetmed.lsu.edu/laddl/index.html)

JPC Diagnosis: Partial cross section of leg: Dermatitis and cellulitis, pyogranulomatous (heterophilic and granulomatous), multifocal to coalescing, severe, with Splendore-Hoeppli material and numerous bacilli.

JPC Comment: The contributor has provided an excellent review of the condition of botryomycosis, a unique histologic lesion that may be seen in a variety of species and tissues, and results from several common bacterial genera as mentioned by the contributor. It should be stressed that while Splendore-Hoeppli material, which may be composed of immunoglobulins, major basic protein, or both is a component of botryomycotic lesions, it may be seen in a number of other lesions other than botryomycosis, including many fungal and helminth infections, as well as surrounding a variety of inert materials within the skin and subcutis.[8]

Pseudomonas aeruginosa is a ubiquitous gram-negative organism of soil and aquatic environments, which, as a result of its intrinsic and expanding antibiotic resistance,

Haired skin, rabbit. Bacterial colonies are gram-negative. The Gram stain intensely highlights the club-like projections typical of the Splendore-Hoeppli reaction. (Gram, 400X) (Photo courtesy of: Louisiana Animal Disease Diagnostic Laboratory (LADDL), School of Veterinary Medicine, Louisiana State University (http://www1.vetmed.lsu.edu/laddl/index.html)

is a particulary worrisome opportunistic wound invader. It is a common opportunist in hospital settings, and the second most common isolate in ventilator-related infection.[5]

P. aeruginosa is a potent infectious agent in acute infections (with a host of virulence factors) and chronic infections (which are facilitated by its formation of biofilms). The bacterium possess flagella and type 4 pili, which provide a means of motility and cellular adhesion respectively, but also can stimulate an inflammatory response.[5] Like many other pathogenic gram-negative bacilli, it possesses a Type 3 secretion system, a needle-like evolutionary flagellar derivative, which allows it to inject exotoxins directly through a pore in the cell membrane. It possesses four exotoxins –

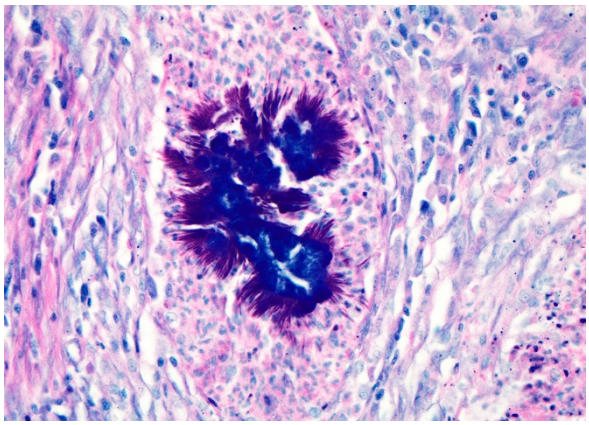

Haired skin, rabbit. Bacterial colonies are intensely basophilic on a Giemsa stain. Club-like projections typical of the Splendore-Hoeppli reaction are also highlighted. (Giemsa, 400X) (Photo courtesy of: Louisiana Animal Disease Diagnostic Laboratory (LADDL), School of Veterinary Medicine, Louisiana State University (http://www1.vetmed.lsu.edu/laddl/index.html)

exoU, exoS, exoS, and exoY – although often not all. ExoS has a deleterious effect on the actin cytoskeleton and exoU is a potent phospholipase. [5]

Chronic infections in wounds, burns, and ventilator-assisted patients (particularly patients with cystic fibrosis who are often immunosuppressed) are largely mediated by *P. aeruginosa*'s ability to create biofilms.[10] Biofilms are highly structured communities attached to each other and a surface, and act as a single unit directed by the secretion of diffusible molecules called autoinducers by dominant bacilli in their midst. Pathogenic strains of *Pseudomonas aeruginosa* produce three autoinducers which help organize biofilms in a variety of situations. [10]

One of the most deleterious effects of biofilms is the diffusional resistance they provide against antimicrobials and some autoinducers upregulate the production of beta-lactamases by *P. aeruginosa*, deactivating beta lactam antibiotics on the surface of the biofilm before they can diffuse into its depths. Moreover, biofilms protect their community from humoral aspects of immunity such as antibodies as well as impairing phagocytosis by their sheer size.[10]

References:

1. Akiyama H, Kanzaki H, Tada J, Arata J. Staphylococcus aureus infection on cut wounds in the mouse skin: experimental staphylococcal botryomycosis. *J Dermatol Sci.* 1996;11(3)**:**234-238.

2. Bostrom RE, Huckins JG, Kroe DJ, Lawson NS, Martin JE, Ferrell JF, et al. Atypical fatal pulmonary botryomycosis in two guinea pigs due to Pseudomonas aeruginosa. *J Am Vet Med Assoc.* 1969;155(7)**:**1195-1199.

3. Bridgeford EC, Fox JG, Nambiar PR, Rogers AB. Agammaglobulinemia and Staphylococcus aureus botryomycosis in a cohort of related sentinel Swiss Webster mice. *J Clin Microbiol.* 2008;46(5)**:**1881-1884.

4. Casamian-Sorrosal D, Fournier D, Shippam J, Woodward B, Tennant K. Septic pericardial effusion associated with pulmonary and pericardial botryomycosis in a dog. *J Small Anim Pract.* 2008;49(12)**:**655-659.

5. Gellatly SL, Hancock REW. Pseudomonas aeruginosa: new insights into pathogenesis and host

defenses. *Pathog Dis* 2013: 67:159-173.

6. Grosset C, Bellier S, Lagrange I, Moreau S, Hedley J, Hawkins M, et al. Cutaneous Botryomycosis in a Campbell's Russian Dwarf Hamster (Phodopus campbelli). *J Exotic Pet Med.* 2014;23(4)**:**389-396.

7. Hedley J, Stapleton N, Priestnall S, Smith K. Cutaneous Botryomycosis in Two Pet Rabbits. *J Exotic Pet Med.* 2019;28(1)**:**143-147.

8 Hussein MR. Mucocutaneous Splendore-Hoeppli phenomenon. *J Cutan Pathol.* 2008;35(11)**:**979-988.

9. Loader H, Lawrence KE, Brangenburg N, Munday JS. Cutaneous botryomycosis in a crossbred domestic pig. *N Z Vet J.* 2018;66(4)**:**216-218.

10. Mulcahy LR, Isabella VM, Lewis K. Pseudomonas aeruginosa biofilms in disease. *Microb Ecol* 2017

11. Padilla-Desgarennes C, Vazquez-Gonzalez D, Bonifaz A. Botryomycosis. *Clin Dermatol.* 2012;30(4)**:**397-402.

12. Percy DH, Barthold SW. *Pathology of Laboratory Rodents and Rabbits*. Ames, IA: Blackwell Publishing, 2007.

13. Read RW, Zhang J, Albini T, Evans M, Rao NA. Splendore-Hoeppli phenomenon in the conjunctiva: immunohistochemical analysis. *Am J Ophthalmol.* 2005;140(2)**:**262-266.

14. Shapiro RL, Duquette JG, Nunes I, Roses DF, Harris MN, Wilson EL, et al. Urokinase-type plasminogen activator-deficient mice are predisposed to staphylococcal botryomycosis, pleuritis, and effacement of lymphoid follicles. *Am J Pathol.* 1997;150(1)**:**359-369.

15. Share B, Utroska B. Intra-abdominal botryomycosis in a dog. *J Am Vet Med Assoc.* 2002;220(7)**:**1025-1027, 1006-1027.

16. Shults FS, Estes PC, Franklin JA, Richter CB. Staphylococcal botryomycosis in a specific-pathogen-free mouse colony. *Lab Anim Sci.* 1973;23(1)**:**36-42.

Self-Assessment - WSC 2019-2020 Conference 12

1. Which of the following viruses may result in lymphoma in infected hamsters?
    a. Gammaherpesvirus
    b. Retrovirus
    c. Papillomavirus
    d. Polyomavirus

2. Which of the following is the vector for leishmaniasis?
    a. Mosquitoes
    b. Sandflies
    c. Ticks
    d. Reduviid beetles

3. Which of the following cell types is responsible for killing *Pneumocystis carinii* infection ?
    a. $CD4^+$ T cells
    b. $CD8^+$ T cells
    c. Neutrophils
    d. Macrophages

4. Which of the following microscopic changes appears first in chronic progressive nephropathy of rats??
    a. Tubular regeneration
    b. Interstitial inflammation
    c. Papillary hyperplasia of pelvic epithelium
    d. Glomerular synechiation

5. Which of the following is not a virulence factor of *Pseudomonas aeruginosa*?
    a. Vap protein
    b. Flagella
    c. Pili
    d. Type 3 secretion system

Please email your completed assessment for grading to Dr. Bruce Williams at bruce.h.williams12.civ@mail.mil. Passing score is 80%. This program (RACE program 33611) is approved by the AAVSB RACE to offer a total of 0.5 CE Credits, with a maximum of 12.5 CE Credits being available to any individual Veterinary Medical Professionals for the 2019-2020 Wednesday Slide Conference. This RACE approval is for the subject matter categories of: SCIENTIFIC using the delivery method of NON-INTERACTIVE DISTANCE. This approval is valid in jurisdictions which recognize AAVSB RACE.

Joint Pathology Center
Veterinary Pathology Services

WEDNESDAY SLIDE CONFERENCE 2019-2020

Conference 13

8 January 2020

CASE I: 2019A208 Case 2 (JPC 4130570).

Signalment: 4 months, female, Rhodesian Ridgeback, *Canis familiaris*, dog

History: The dog was presented on emergency for acute lethargy, anorexia and melena. Blood examination revealed increased CK and liver enzymes. On echography and clinical examination generalized lymphadenopathy was noticed. Soon the dog developed neurological signs with decreased consciousness, compulsive behavior and head pressing (forebrain disorder.) Also coagulopathy due to severe thrombocytopenia with increased coagulation times (PT and aPTT) was present. In 24 hours there was a progression of symptoms with neurological deterioration. Finally cardiac arrest developed with unsuccessful reanimation; the clinicians postulated hemorrhagic disorder, infectious or immune mediated encephalitis and metabolic encephalopathy as main differential diagnosis. Vaccination and deworming was up to date.

***The liver is somewhat flaccid. Serosal hemorrhages are present on the colon. (Photo courtesy of: The University of Ghent,* https://www.ugent.be/di/di05/nl)**

Gross Pathology: The liver was moderately pale, enlarged with a scant amount of fibrin strands on the capsule. There were several ruptures secondary to reanimation causing hemoabdomen. Spleen and lymph nodes were severely enlarged. The mesenteric lymph nodes were clearly edematous on cut surface. Many hemorrhages were seen at the serosal surfaces. Also severe edema of the gallbladder and melena was present. Dispersed small hemorrhages were present in the basal nuclei of the cerebrum and in the thalamus of the brain on cut surface.

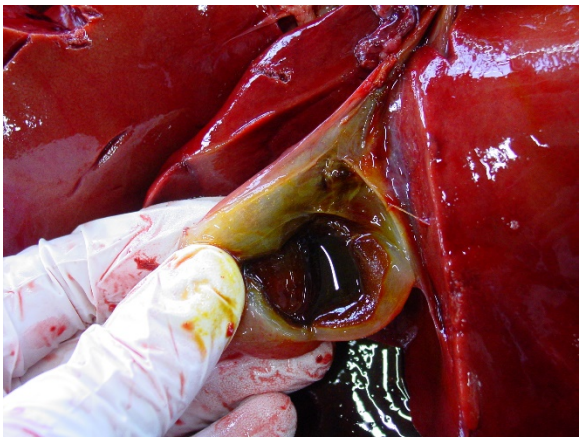

***Gallbladder, dog. There is marked edema of the gallbladder wall. (Photo courtesy of: The University of Ghent,* https://www.ugent.be/di/di05/nl)**

Laboratory results:

- Blood examination: increased CK 1199U/L (99-436), increased GOT/GPT and bile acids (no value available), thrombocytopenia 23 K/µL (148-484) and increased PT 18s (11-17) and aPTT 144s (72-102).

-Toxoplasmosis and neosporosis were excluded (IgG/M-determination.)

- Parvovirosis and angiostrongylosis were tested with a negative result.

Microscopic Description:

Multifocal in the midzonal to centrilobular region, areas of coagulation necrosis are present. This is characterized by swollen, eosinophilic, well circumscribed hepatocytes with a dark small, fragmented nucleus. In these areas loss of tissue architecture is present with pooling of red blood cells. Multifocal distributed, several hepatocytes and Kupffer's cells contain large, intranuclear basophilic inclusions surrounded by a clear halo with margination of chromatin. In the sinusoidal spaces, there is a moderate increased amount of lymphocytes. There is a large subcapsular bleeding (secondary to liver rupture due to cardiac reanimation). On immunohistochemical staining for Canine adenovirus, there are numerous hepatocytes and Kupffer's cells with positive staining nuclei.

Contributor's Morphologic Diagnosis:

Severe multifocal midzonal to centrilobular hepatic necrosis with large basophilic intranuclear viral inclusion bodies, consistent with canine adenovirus type 1.

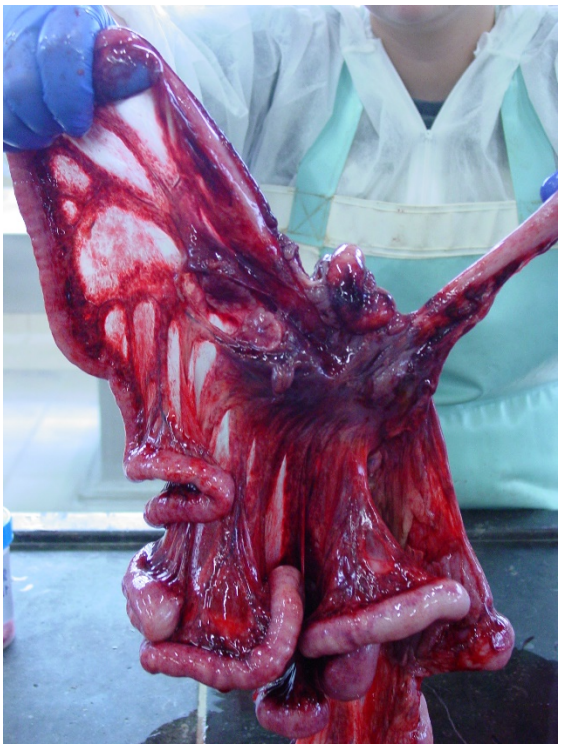

***There is marked ecchymotic to suffusive hemorrhage of the mesentery and the mesenteric root. (Photo courtesy of: The University of Ghent,* https://www.ugent.be/di/di05/nl)**

Contributor's Comment: Non-enveloped dsDNA virus → family: Adenoviridae → genus: Mastadenovirus ; there are 2 types.[10]

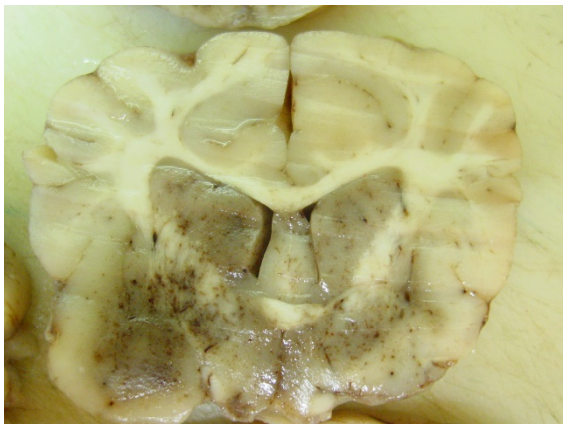

***There are hemorrhages within both gray and white matter within the diencephalon. (Photo courtesy of: The University of Ghent,* https://www.ugent.be/di/di05/nl)**

- Canine adenovirus - 1 (CAV-1) causes infection in numerous mammalian carnivores belonging to the *Canidae, Mustelidae* and *Urisdae*. In dogs, it causes infectious canine hepatitis (ICH) also called fox encephalitis or Rubarth's disease.[9] This virus causes a systemic infection mainly targeting the hepatocytes, endothelial and mesothelial cells. CAV-1 can cause a severe often fatal disease in juveniles. Death is very rare in animals older than 2 years of age. Clinical symptoms are variable, often vomiting, melena, fever and abdominal pain is present. In some cases nonspecific nervous signs occur. In a minority of cases there is acute death without preceding symptoms. During the recovery phase uni- or bilateral corneal edema can develop ("blue eye").[5] Years of widespread vaccination reduced the incidence of this disease in domestic animals in many countries to almost zero. In wildlife species CAV-1 is widespread, primarily as a subclinical infection but epizootic disease occurs1. In foxes neurological symptoms are more frequently present than in dogs being the reason for its less popular name: fox encephalitis virus.[2]
- CAV-2 causes a mild self-limiting infection of the upper respiratory tract and plays a role in the pathogenesis of infectious tracheobronchitis (ITB) known as kennel cough. Because of antibody cross-reaction it is used for CAV-1 vaccine production.[2]

Pathogenesis:

Infection occurs through oronasal transmission. After reaching the oropharyngeal tonsils, tonsillitis develops accompanied by fever. The virus spreads to local lymph nodes and reaches the bloodstream through the lymph flow causing viremia which lasts 4-8 days. In a following phase the primary targets: hepatic parenchymal cells and endothelial cells (in al organs) get infected[4.] Viral replication causes cell lysis and necrosis.[13] Hepatic necrosis ensues at about day 7 (of experimental infection).[2] Lesions in other organs are mainly secondary to vascular injury causing hemorrhage and edema. In a further stage, disseminated intravascular coagulation (DIC) can occur.[10] This is caused by lysis of endothelial cells with activation of coagulation cascade and aggregation of thrombocytes. This causes increased consumption of clotting factors and thrombocytes resulting in consumptive coagulopathy.[11] Several organ systems can be affected including the liver, kidney, lymph nodes, thymus, gastric serosa, pancreas and subcutaneous tissues.[12] Edema of the gallbladder can be very prominent and is most likely due to increased vascular permeability secondary tot vascular injury.

Gallbladder edema is a pathognomonic sign at necropsy.[7] The central nervous system can be also be targeted causing an encephalitis with often inconspicuous lesions.

During the convalescent phase (day 7-21 days post infection) deposition of immune complexes (antigen-antibody) in the cornea can occur causing complement fixation and neutrophilic activation (type III hypersensitivity). The neutrophilic proteases cause diffuse hydropic degeneration of corneal endothelium and secondary stromal edema. The interstitial fluid accumulation causes deformation of corneal collagen fibers creating a blue-white aspect of the cornea ("*blue eye*"). The same mechanism happens in a small percentage of dogs 6-7 days after vaccination with modified live virus. In some cases inflammation proceeds and causes interstitial keratitis and permanent fibrosis. Alongside the corneal edema, anterior uveitis and glomerulonephritis can develop because of type III hypersensitivity.[4,8]

Gross findings:

- Hepatomegaly; turgid and friable with sometimes a mottled yellowish aspect, fibrin strands at the capsular surface[6]
- Edema and intramural bleeding of the gallbladder (pathognomonic)[7]
- Enlarged, hemorrhagic, edematous lymph nodes
- Serosal bleeding (paintbrush lesions)

Gross lesions in other organs are inconstant:[5]

- Hemorrhagic kidney infarctions (in young puppies)
- Enlarged, edematous tonsils (tonsillitis)
- Hemorrhages in the lungs, brain (midbrain and brainstem) and metaphyses of the long bones (ribs).
- Multifocal mucosal petechiae and subserosal hemorrhage[11]
- Corneal edema ("blue eye")

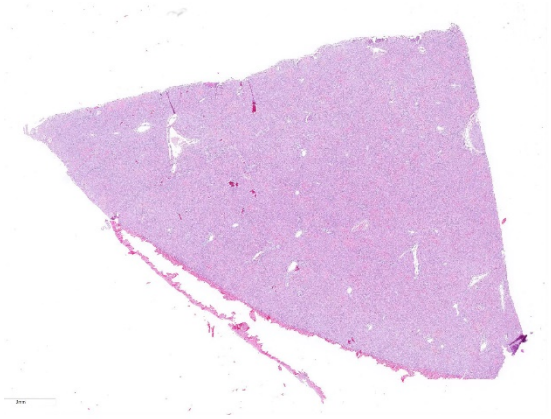

Liver, dog: A section of liver is submitted for examination. Upon close subgross inspection, there are areas of pallor and hemorrhage scattered throughout the section, as well as acute hemorrhage overlying the capsule. (HE, 7X)

Histological findings:

Liver:

- Centrilobular (periacinar) zonal necrosis (resembling acute hepatotoxicity.) In convalescence, hepatic regeneration occurs rapidly. After 2 weeks small foci of hepatocellular necrosis may be present. Foci of regenerating Kupffer's cells may be present for another 2 weeks[6]
- Intranuclear, large, basophilic inclusion bodies in endothelial cells, hepatocytes or Kupffer's cells. Viral inclusions can be present after 4 days of experimental infection. At day 5-6-7 inclusions are most numerous, from day 8 numbers decline rapidly (in experimental infection)[2]

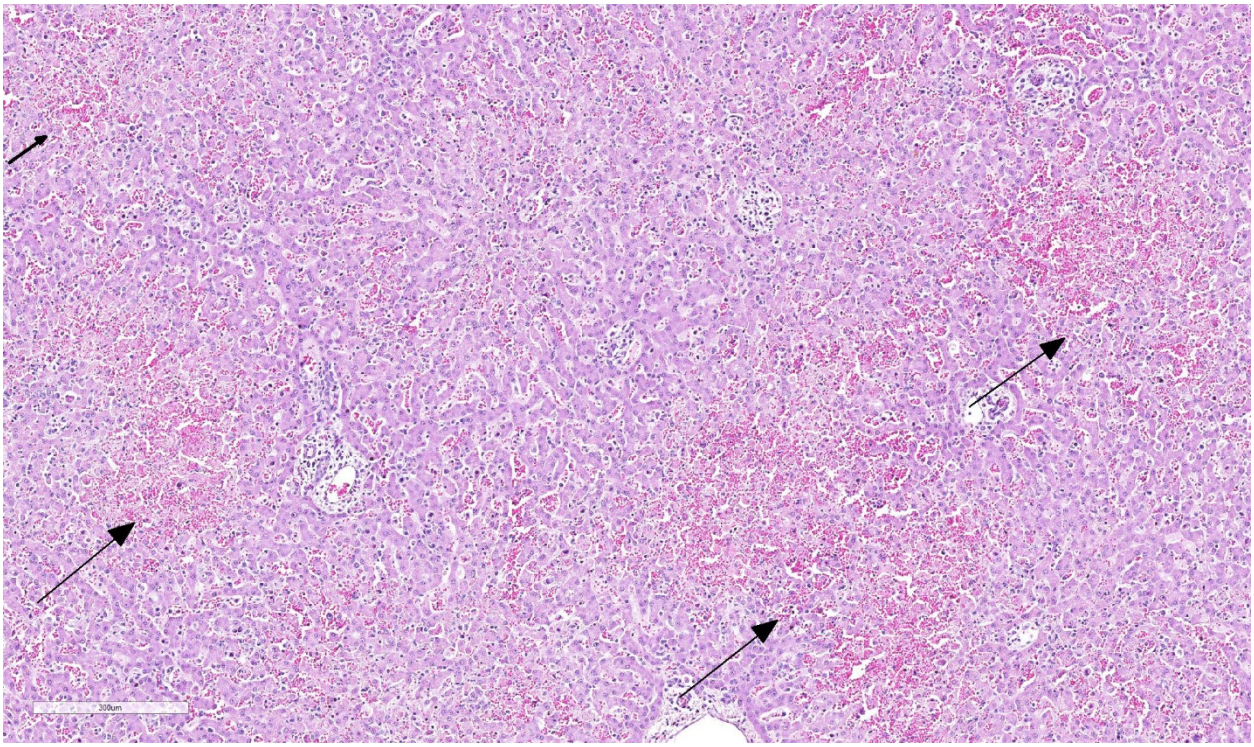

Liver, dog: Areas of pallor correspond to foci of hemorrhage and necrosis. (HE, 88X)

- Fatty change
- Blood filled dilated sinusoids (because of loss of hepatocytes)
- Intact reticulin framework
- Mild leukocytic infiltration, mostly degenerating neutrophils

Other organs: Microscopic lesions in other organs are mainly secondary to endothelial damage.

- Brain: Hemorrhages of small vessels with rare intranuclear inclusions in endothelial cells which can be in relation with small foci of demyelination. Encephalitis can develop with very subtle lesions characterized by a mononuclear vasculitis with rarely more than a single perivascular monolayer of cells and hemorrhage[9]
- Lymphoreticular organs: Congestion, lymphocytolysis in lymphoid follicles and in the white pulp of the spleen,[9] inclusions can be present in reticulum cells
- Kidney: Occasional intranuclear inclusion body in the glomerular mesangium cells or in the epithelial cells of the proximal convoluted tubule.[9]. Glomerulonephritis and secondary chronic interstitial nephritis can develop because of deposition of immune complexes in later stages.[1,4]
- Lung: areas of hemorrhagic consolidation with hemorrhage, edema and fibrin formation in the alveoli with often inclusions in alveolar capillaries.
- Eye: corneal edema due to hydropic degeneration of corneal endothelium which can develop into interstitial keratitis and permanent fibrosis. Intranuclear inclusions can be present in a few degenerating endothelial

cells. There can be accompanying anterior uveitis characterized by accumulation of lymphocytes and plasma cells perivascular in the iris and ciliary body.[8]

- In every organ macrophages with intranuclear inclusions can be present.5

Contributing Institution:

University of Ghent
https://www.ugent.be/di/di05/nl

JPC Diagnosis: Liver: Hepatitis, necrotizing, multifocal, mild to moderate, with edema and numerous eosinophilic hepatocellular and endothelial intranuclear viral inclusion bodies.

JPC Comment: The contributor has given us an excellent and very comprehensive review of canine adenovirus-1 in the dog.

Liver infection with adenovirus have been a popular, although not especially diagnostically challenging, submission over the years in a number of species. This case marks the seventh time that CAV-1 has appeared in the WSC in the last forty years. Adenovirus in the liver of chickens (inclusion body hepatitis) has appeared a total of six times, with falcon adenovirus and bearded dragon (agamid) adenovirus appearing twice. (The complete list of adenoviral submittions over the years is well over a hundred, with pulmonary infections being the most common overall.)

In 1998, a case of CAV-1 in a skunk which manifested as fatal necrotizing hepatitis was reveiwed in conference number 4, suggesting that this virus may cause disease in other wildlife species outside of canids.

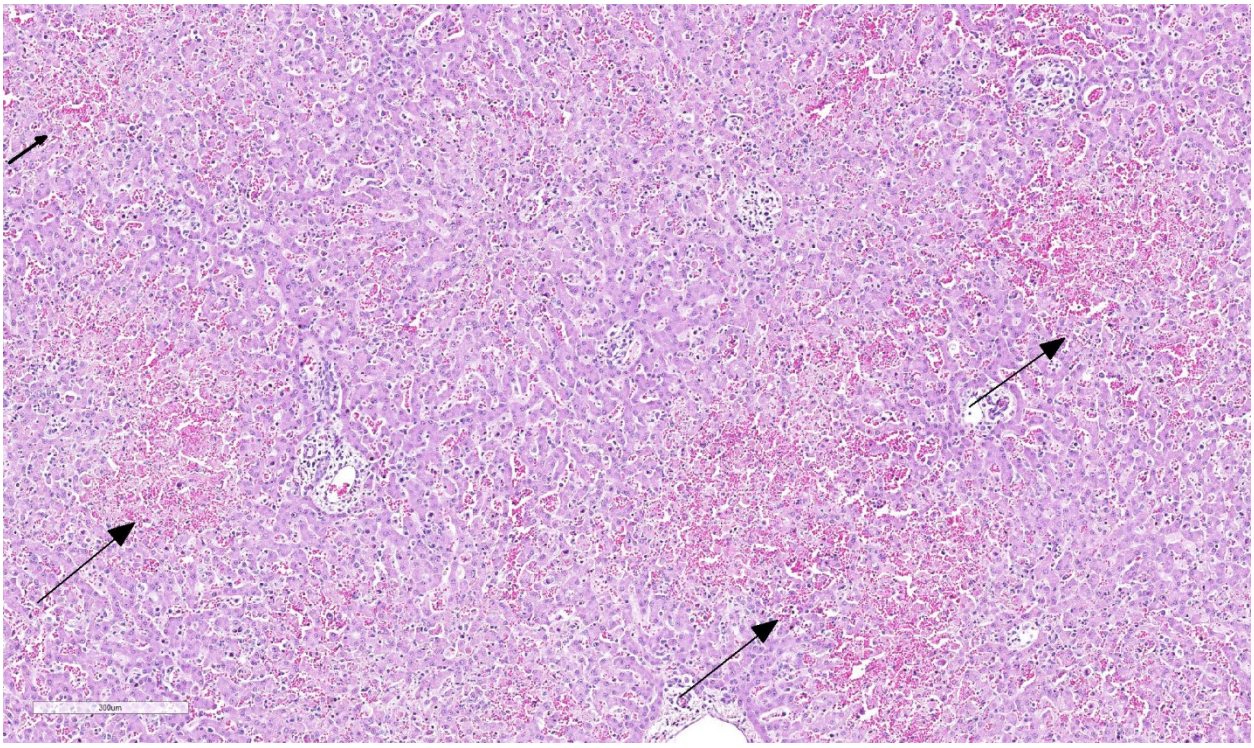

Liver, dog: Within and at the periphery of foci of necrosis, hepatocellular and endothelial cell nuclei are expanded by an eosinophilic viral inclusion which is often surrounded by a clear halo. (HE, 400X)

Although the conference results incorrectly identify skunks as canids (they are mustelids!), foxes, wolves and coyotes have certainly developed fatal disease associated with CAV-1. Skunks indeed have their own adenovirus (skunk adenovirus-1, first identified in 2015[5]) which also causes fatal hepatitis (casting a bit of doubt over our 1998 case of CAV in a mustelid.) While adenoviruses are generally considered species-specific, skunk adenovirus-1 has been identified as causing pneumonia and trachieitis in pygmy hedehogs as well.[6] Several species of adenoviruses have also been identified by nested PCR in mustelids in the United Kingdom, but associated disease has not been ascribed to these viruses.[11]

The most spirited discussion on this very classic case regarded the location of necrosis. While textbooks often discuss a characteristic pattern of centrilobular necrosis in affected animals, the typical pattern for viral hepatic infection would be expected to be random. Additionally, within many areas of necrosis, effete hepatocytes contain a basophilic stippling which some participants questioned might be an apicomplexan cyst. However, the material stained stongly positive with a Prussian Blue stain indicated that the material was iron-based. The cause of the ferrugination of occasional degenerate/necrotic cells was not clear.

References:

1. Balboni A, Verin R, Morandi F, et al. Molecular epidemiology of canine adenovirus 1 and type 2 in free-ranging red foxes (*Vulpes vulpes*) in Italy. Veterinary Microbiology. 2013; (162): 551-557.
2. Cabasso VJ. Infectious canine hepatitis virus. Annals of the New York Academy of Sciences. 1962; (101): 498-514.
3. Cabasso VJ. Infectious canine hepatitis. In: *Infectious Diseases of Wild Animals*, Davis, Karstad, Trainer eds., Ames: Iowas State University Press, Ames, Iowa, 1981.
4. Cianciolo RE, Mohr FC. Urinary System. In: Maxie MG, ed. *Jubb, Kennedy, and Palmer's Pathology of Domestic Animals*. Vol. 2. 6th ed. St. Louis MO: Elsevier Ltd; 2016:410.
5. Lozak RA, Ackford JG, Slaine P, LiA, Carman S, Campbell D, Welch MK, Kropinskin AM, Nagy, E. Characterization of a novel adenovirus isolated from a skunk. *Virology* 2015; 485:16-24.
6. Needle DB, Selig M, Jackson KA, Delwart E, Tighe E, Leib SL, Seuberlich T, Pesavento PA. Fatal bronchopneumonia caused by skunk adenovirus 1 in an African pygmy hedgehog.
7. Stalker MJ, Hayes MA. Liver and biliary system. In: Maxie MG, ed. *Jubb, Kennedy and Palmer's Pathology of Domestic Animals.* 5th ed. Vol 2. New York, NY: Elsevier Saunders; 2007:348-351.
8. Vandevelde M, Higgins RJ, Oevermann A. Inflammatory diseases. In: *Veterinary Neuropathology: Essentials of Theory and Practice.* 1th ed. West Sussex, UK: John Wiley & Sons Ltd; 60-61.
9. Wilcock BP, Njaa BL. Special Senses. In: Maxie MG, ed. *Jubb, Kennedy, and Palmer's Pathology of Domestic Animals*. Vol. 1. 6th ed. St. Louis MO: Elsevier Ltd; 2016:452-453.

10. Walker D, Abbondati E, Cox AL, et al. Infectious canine hepatitis in red foxes (Vulpes vulpes) in wildlife rescue centres in the UK. Veterinary Record. 2016; (178) : 421.
11. Walker D, Gregory WF, Turnbull D, Rocchi M, Meredith AL, Philbey AW, Sharp CP. Novel adenoviruses detected in British mustelids, including a unique aviadenovirus in the tissues of pine martens. *J Med Microbio*l *2017; 66:1177-1182.*
12. Wong M, Woolford L, Hasan NH, Hemmatzadeh F. A Novel Recombinant Canine Adenovirus Type 1 Detected from 2 Acute Lethal Cases of Infectious Canine Hepatitis. Viral Immunology. 2017; (30): 258-263.
13. Wigton DH, Kociba GJ, Hoover EA. Infectious Canine Hepatitis: Animal Model for Viral-Induced Disseminated Intravascular Coagulation. Blood. 1976; (47): 287-296.
14. Zachary JF. Mechanisms of microbial infections. In: Zachary JF, ed. *Pathologic Basis of Veterinary Disease*. 6th ed. St. Louis, MO: Elsevier; 2017:207.

CASE II: HSRL-425 CVM-WU-2 (JPC 4038890).

Signalment: 3-year-old intact male feral domestic short hair cat (*Felis catus*)

History: An approximately 3-year-old 4.5 kg intact male feral, DSH (*Felis catus*) was presented to a veterinary hospital in Pomona, California. A good Samaritan used a live trap to capture the animal after she noticed excessive swelling in the nasal region. She was bitten during the capture process. The swelling was localized over the bridge of the nose and had a 3 cm ulcerated area that was bleeding excessively. Due to financial constraints and prognosis, the cat was euthanized and submitted for necropsy and rabies testing.

Upon initial examination, there was gross swelling at the bridge of the nose, and the eyes were nearly shut due to the severe conjunctivitis with abundant secretion. Dorsal to the nasal planum, there was an ulcerated area about ~3cm in diameter that had missing skin, covered by partially clotted blood mixed with necrotic debris.

Gross Pathology: The cat was in thin body condition with a large (3cm in diameter) ulcerated area on a severely swollen space-occupying lesion on the bridge of the nose. No gross abnormalities were found upon examination of internal organs. The cat was underweight and was ~10% dehydrated. A nasal swab was performed and stained with Diff Quik. Fungal organisms were visualized; however, narrow or broad based budding could not be identified. A tentative diagnosis of cryptococcosis was given.

Nasal planum has a large bulging mass (5cm in diameter) that expands and deforms the dorsal planum. The bulging mass has a superficial 3cm in diameter ulceration that connects with the nasal cavity. The ulcer is covered by partially clotted blood mixed with necrotic debris. The philtrum is intact. On cut section the mass is solid and occupies the nasal cavity replacing the turbinates and sinuses.

Laboratory results:

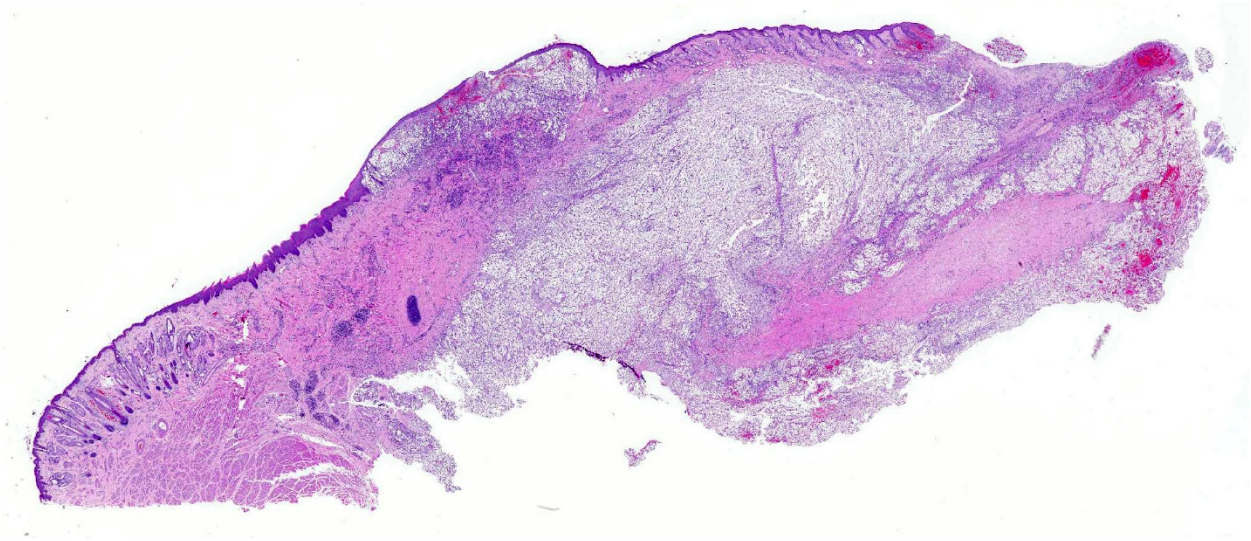

Mucocutaneous junction and haired skin, bridge of nose: The section contains a central area of mucus membrane. A large inflammatory nodule effaces 50% of the dermis and abuts the mucosal epithelium (center) (HE, 7X)

The brain was submitted *in toto* for rabies testing. Rabies testing was negative.

Microscopic Description:

Tissues submitted for histopathology included lung, liver, kidney, eye and portions of the nasal mass.

Skin from nasal area (from mucosa to haired skin): There is a locally extensive inflammatory area that extends to the deep limits of the examined sample. The submucosa is severely distorted and replaced by numerous round yeasts admixed with histiocytes, occasional multinucleated giant cells, and plasma cells. The yeasts vary from round with a thick wall to oval slightly pink transparent cells. These cells vary from 5-25 µm in diameter. The blastoconidia (asexual reproduction) is characterized by narrow based budding. The yeasts have a clear, thick capsule that gives the characteristic empty space around the yeast. The overlying epithelium is variably ulcerated with occasional acanthosis.

Nasal sections stained with PAS stain in addition to routine H&E staining show characteristic fungal organisms.

The eye was examined. There is severe suppurative inflammatory conjunctivitis with no fungal organism observed.

The other tissues show no significant changes.

Contributor's Morphologic Diagnosis:

Morphologic Diagnosis: Nasal planum: Chronic, locally extensive, severe granulomatous rhinitis with superficial focal dermal ulceration and hemorrhage

Contributor's Comment: Cryptococcus is an important dimorphic, basidiomycetous encapsulated fungal organism causing disease in humans and animals.[3,5] Cats seem to be the most susceptible species.[3,5]

It is an encapsulated fungus that replicates by narrow based budding (blastoconidia - asexual reproduction also called vegetative

stage). The organism has also a sexual stage of reproduction called basidiospores rarely found in the natural cases. The infection occurs by environmental exposure and is not thought to be transmissible from one infected animal to another. The main environmental source is bird excreta, mainly pigeons.[3,5,12]

Cryptococcus are aerobic, non-fermentative organisms that form mucoid colonies on a variety of media. Virulence factors utilized by the yeast include its polysaccharide capsule, melanin, mannitol, and enzymes such as phospholipase, laccase and superoxide dismutase. Phopholipase and laccase are unique to *C. neoformans* and *C. gatti* and are thought to increase pathogenicity by interfering with the host immune response. The severity of the disease is the result of the combination of the virulence factors coupled with the immune status of the patient.[1,3,12]

The thick polysaccharide capsule interferes with the protective immune reaction against the yeast preventing successful phagocytic. There is some evidence to correlate the immune status of the patient to the inflammatory response against the organism. The most susceptible patients have T-cell deficiencies. In cats there is no breed or gender predisposition. Cats younger than 6 years appeared to be at higher risk. Retroviral infection in cats is not considered a risk factor. The most common presentations in cats include upper respiratory (like in this case), cutaneous, or central nervous system.[1,3,5,10,11]

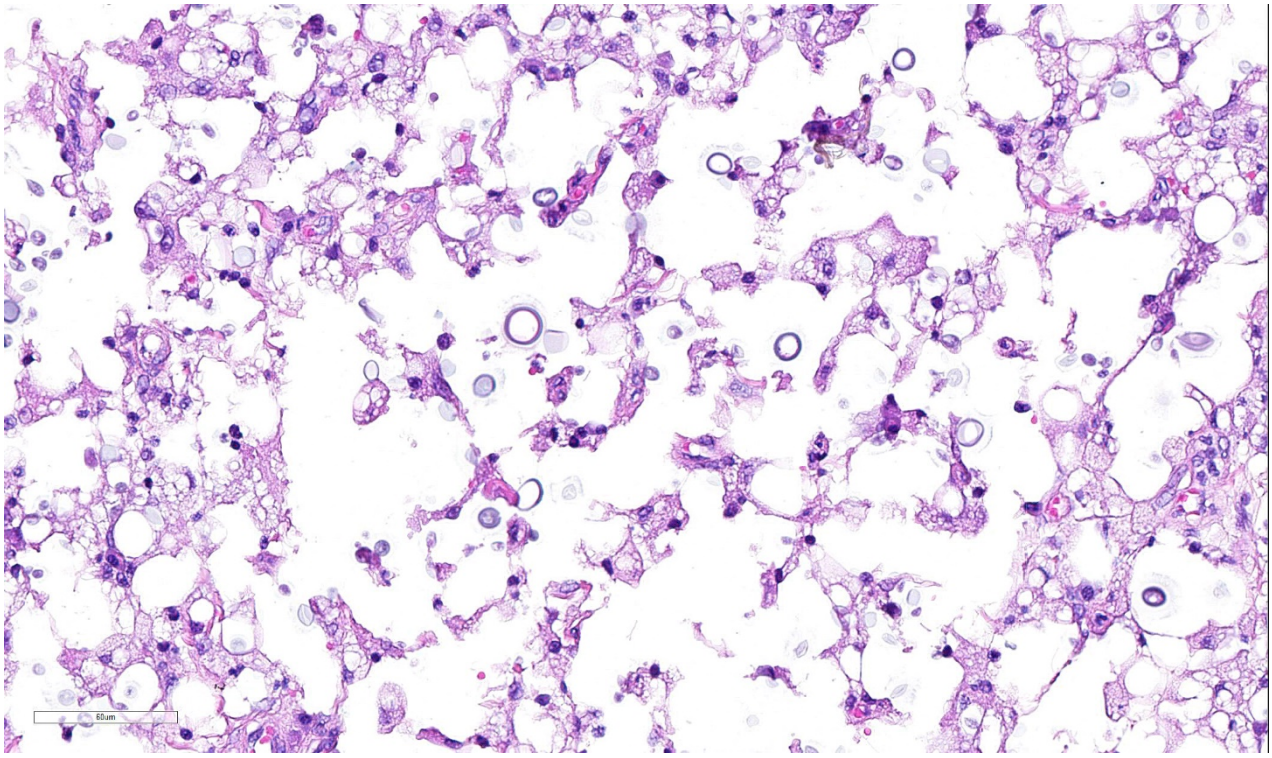

Nose, cat. High magnification of one of the inflammatory nodules demonstrates numerous spherical to concave 6-15um yeasts with a 1-2um cell wall, amphophilic cytoplasm, and a 2-10 clear capsule, engulfed by numerous foamy macrophages. (HE, 400X)

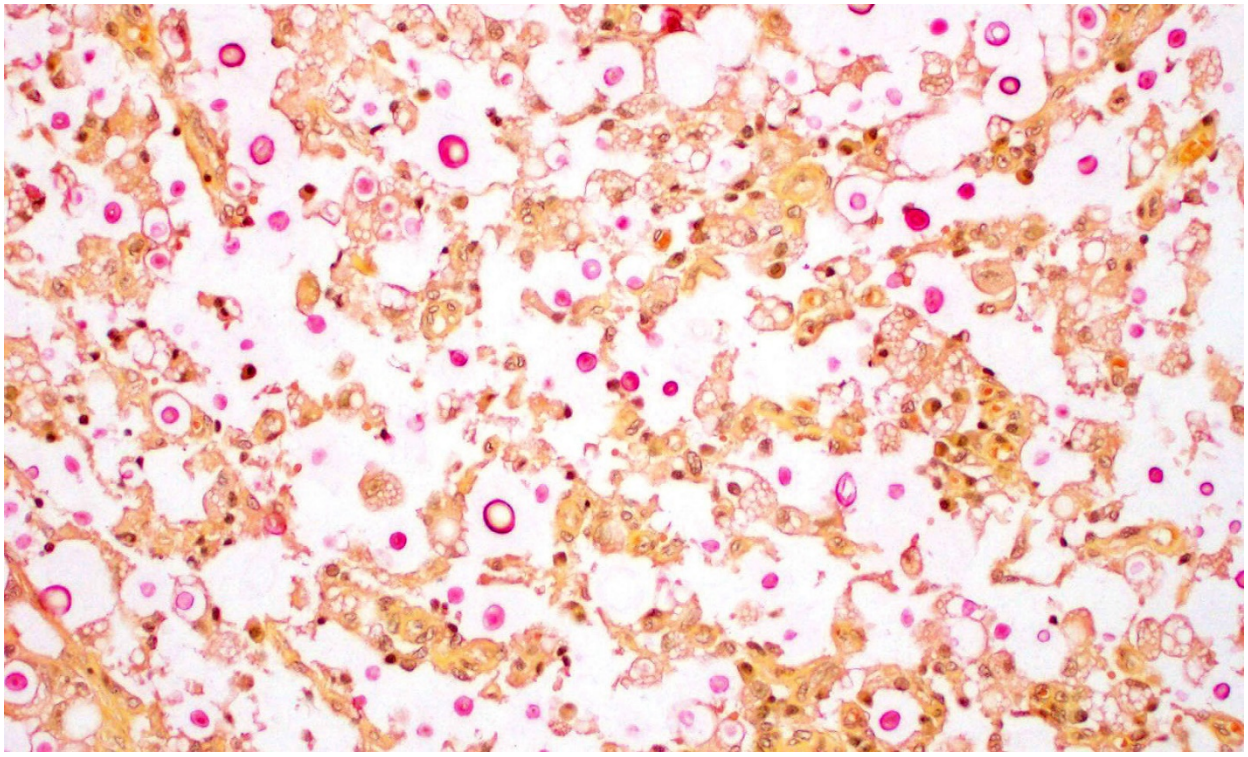

Nose, cat. A mucicarmine stain demonstrates the capsule around the yeast. The clear space delineates the capsules previous area, but it retracts upon fixation. (Mucicarmine, 400X)

There are about 40 different species within the genus of *Cryptococcus*. *C. neoformans* is the only pathogenic species. There are 4 species of *Cryptococcus neoformans* recognized which are separated in 4 different serotypes (A-D). The different types have different geographic distribution as well as virulence. *C. gatti* is considered being the most pathogenic.[5,9] *C. gatti* (Cg) has been identified as an emerging infectious disease that not only affects immunosuppressed patients but also those with a intact immune response.[1,2,3,5,6].

The lesions caused by *Cryptococcus spp* are composed of exclusively fungal organisms and minimal inflammatory response. The inflammatory reaction and fungal morphology is very characteristic however the differential diagnosis regarding the organisms includes coccidiodomycosis, *Candida*, and *Histoplasma*.[1,3,5,7] Histopathology, supported by silver stains (Gomori methenamine silver – GMS) or polysaccharide stains (periodic acid- Schiff - PAS) is the fastest and cost effective means of achieving a diagnosis when fungi are suspected. The diagnosis is made by the identification of the typical encapsulated yeast in cytology or histopathology. Its polysaccharide capsule positive to mucicarmine and Alcian blue stain is characteristic. The cerebrospinal fluid of affected patients can be stained with India ink to identify the organism. However alternative molecular diagnostic tests have been developed to achieve a definite diagnosis, including serum cryptococcal antigen that is thought to be the best way to reach a definitive diagnosis. Molecular

diagnostic test are also available including PCR, amplified fragment length polymorphism (AFLP) analysis and Multilocus Sequence Typing (MLST).[9]

Contributing Institution:

College of Veterinary Medicine
Western University of Health Sciences
http://www.westernu.edu/xp/edu/veterinary/about.xml

JPC Diagnosis: Mucocutaneous junction, nose: Dermatitis, granulomatous, multifocal to coalescing, severe with numerous intra- and extracellular yeasts.

JPC Comment: In 1894, *Cryptococcus neoformans* was simultaneously identified as a human and juice pathogen by pathologist Otto Busse (from a granulomatous lesion in the tibia of a 31-year-old woman), and Italian scientist Francesco Sanfelipe (from peach juice). The true pathogenic nature of *C. neoformans*, however, was not realized until the 1980's when immunosuppressed AIDS patients provided appropriate venue for its pathogenic abilities and a tragic opportunity for widespread research.[7]

The basics of *Cryptococcus* infection are well known, and reviewed by the contributor above. In the last decade, a number of new insights have been gained into the pathogenic mechanisms of cryptococcal infection.

Size in important in many phases of cryptococcal infection. Infection is most likely the result of inhalation, but not of the yeasts of the size seen in this case (6-15um) which are too large for inhalation into the deeper airways of the lung (usually 5um or less). Infection more likely occurs from desiccated cells or spores, which set the stage for latent infection which is stimulated to growth by immunosuppression later in life.[8]

Another instance in which yeast size impacts pathogenesis is the formation of atypical yeast forms which helps cryptococcus in establishing latent infection or perpetuating its disease-causing growth phase. Unusually small forms, known as metabollically inactive "drop" or "micro" cells measure 2-4um and possess a thickened cell wall, making them attractive for phagocytosis by macrophages and likely important in latent infection.[8] Another atypical form resides at the opposite pole of the size spectrum – "titan" cells, polyploid cells which exceed 12um in diameter. These cells have a highly crosslinked resistant capsule and also a thickened cell wall with chitin to assist in phagocytosis evastioh. The production of host chitinases need to break down these forms appears to be detrimental to the overall inflammatory response.[8]

Two distinct pathogeneic species, Two distinct species, *Cryptococcus neoformans* and *Cryptcoccus gatti* exist within the genus since 2000. They differ in host requirements, with *C. neoformans (*and its subspecies *C. neoformans* var. *grubii*) causing disease in immunosuppressed hosts, and *C. gatti* infecting immunocompetent animals. One of the commonly infected animals in Australia, unfortunately, is the koala, which lives among species of eucalyptus trees which naturally host the sexual phase of the fungus.[4] In some parts of Australia, especially on the eastern coast, colonization rates of of 94-100% occur in koalas, and may act as a reservoir and amplifying host. Affected koalas present with pneumonia and miningoencephalitis, but many koalas possess subclinical infections which provide a resource for studying latent infection.[4]

One of the attendees from the National Zoo mentioned that animals that had been treated long term with antifungal agents may have grealy reduced to absent capsules, and that additionally, this fungus may be pigmented. *Cryptococcus* also has an organelle known as a microsome, which allows it to metabolize xanthine and urates, which facilitates its survival in bird feces.

References:

1 Buchanan, K. L., & Murphy, J. W. (1998). What makes Cryptococcus neoformans a pathogen?. *Emerging infectious diseases*, *4*(1), 71.

2. Castrodale L. *Cryptococcus gattii:* an emerging infectious disease of the Pacific Northwest. State of Alaska Epidemiology Bulletin. September 1, 2010, no. 27. http://www.epi.alaska.gov/bulletins/docs/b2010_27.pdf

3. Chandler FW and Watts JC. Pathologic Diagnosis of Fungal Infections. ASCP Press Chicago USA 1987 p161-175.

4. Chen SCA, Meyer W, Sorrell TC. Cryptococcus gatti infections. *Clin Microbiol Rev* 2014 27(4):980-1024.

5. Guarner, J., & Brandt, M. E. (2011). Histopathologic diagnosis of fungal infections in the 21st century. *Clinical microbiology reviews*, *24*(2), 247-280.

6. Krockenberger, M. B., & Lester, S. J. (2011). Cryptococcosis—Clinical Advice on an Emerging Global Concern. *Journal of feline medicine and surgery*, *13*(3), 158-160.

7.-Lamm, Catherine G., Sterrett C. Grune, Marko M. Estrada, Mary B. McIlwain, and Christian M. Leutenegger. "Granulomatous rhinitis due to Candida parapsilosis in a cat." Journal of Veterinary Diagnostic Investigation (2013).

8. May RC, Stone NRH, Wiesner DL, Bicanic T, Nielsen K. Cyrptococcus: from environmental saprophyte toblobal pathogen. *Nat Rev Microbiol* 2016; 14(2):106-117.

9. Sidrim, J. J. C., Costa, A. K. F., Cordeiro, R. A., Brilhante, R. S. N., Moura, F. E. A., Castelo-Branco, D. S. C. M. & Rocha, M. F. G. (2010). Molecular methods for the diagnosis and characterization of Cryptococcus: a review. *Canadian journal of microbiology*, *56*(6), 445-458.

10. Simmer M, Secko, D. A Peach of a Pathogen: Cryptococcus Neoformans

The Science Creative Quarterly. August 2003. Accessed July 2013. http://www.scq.ubc.ca/a-peach-of-a-pathogen-cryptococcus-neoformans/

11. Sykes, J. E., B. K. Sturges, M. S. Cannon, B. Gericota, R. J. Higgins, S. R. Trivedi, P. J. Dickinson, K. M. Vernau, W. Meyer, and E. R. Wisner. "Clinical signs, imaging features, neuropathology, and outcome in cats and dogs with central nervous system cryptococcosis from California." *Journal of Veterinary Internal Medicine* 24, no. 6 (2010): 1427-1438.

12. Trivedi, Sameer R., Richard Malik, Wieland Meyer, and Jane E. Sykes. "Feline cryptococcosis: impact of current research on clinical management." Journal of Feline Medicine & Surgery 13, no. 3 (2011): 163-172.

CASE III: 18-2108 WSC #3 HE (JPC 4117383).

Signalment: 3-1yr female red golden pheasant (*Chrysopholus pictus).*

Trachea, ceca, colon, golden pheasant. There are numerous <3mm nodules within the muscularis and serosa of the cecum and colon of this bird. (Photo courtesy of: Connecticut Veterinary Medical Diagnostic Laboratory at the University of Connecticut, http://cvmdl.uconn.edu/)

History: A pheasant flock of 50 birds was experiencing respiratory signs, including nasal congestion, puffy eyes, and ocular discharge. Twelve pheasants died over approximately one month. The owner purchased an additional 12-16 new pheasants from Michigan and Ohio. These new pheasants seemed thin, weak, and lethargic. They were introduced directly into the original flock without a quarantine period. There were no further deaths in the original flock, but eight of the new pheasants died within a three-week period. This golden pheasant was submitted for necropsy together with two Impeyan pheasants for necropsy, both of which had a severe mucopurulent infraorbital sinusitis and rhinitis.

Gross Pathology: The pheasant weighed 470g and was in good body condition. There were innumerable firm yellow to reddened nodules each up to 3mm in diameter covering the serosal surfaces of the distal segment of the gastrointestinal tract, affecting the ceca most severely but with additional nodules over the colorectum, ileum, and distal jejunum. These nodules were also present in the mucosa of the ceca. No gross lesions were identified in the nasal cavities, trachea, or lungs of this pheasant.

Laboratory results:

Aerobic and *Mycoplasma* cultures from the affected sinuses of the two Impeyan pheasants yielded no growth.

Microscopic Description:

Cecum, ileum, and colorectum: Many well-circumscribed nodules, each up to 3mm in diameter and becoming confluent, expand the submucosa, muscularis externa and

Trachea, ceca, colon, golden pheasant. Multiple sections of trachea, cecum, and colon are submitted for examination. At subgross magnification, numerous nodules may be seen within the sections of gut, and larval and adult ascarids may be viewe3d within them. (HE, 7X)

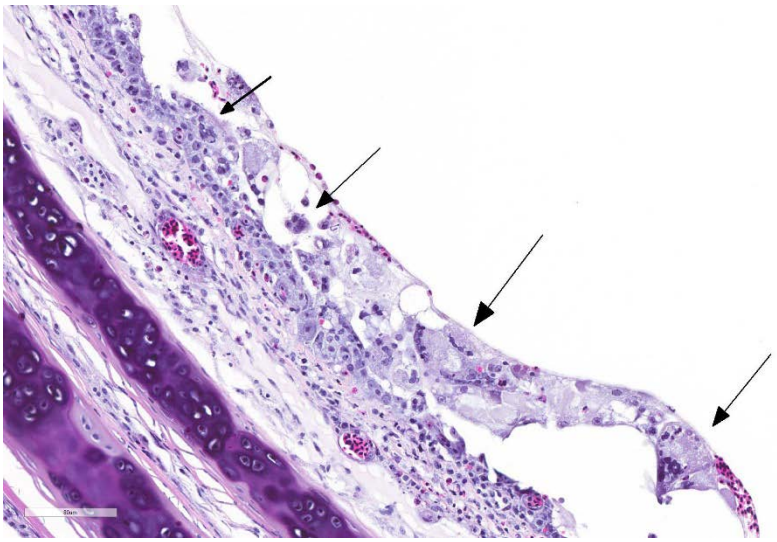

Trachea, golden pheasant. Within the exudate of overlying the disordered, ulcerated and hyperplastic mucosa, there are numerous multinucleated viral syncytia. (HE, 275X)

serosa, and are sometimes pedunculated from the serosal tissue. The cecum is most severely affected. Nodules consist primarily of spindle cells with a large volume of pale eosinophilic cytoplasm and indistinct cell borders, having large round to oval nuclei with vesicular chromatin and a prominent nucleolus. Cells are arranged in whorls, and sometimes interlacing streams and bundles. Nodules are infiltrated by mild to moderate numbers of macrophages and small lymphocytes with fewer plasma cells, and are surrounded by a thin collagenous capsule. Many of these nodules contain nematode parasites of 0.3mm in diameter in cross section or tangential section. Nematodes are characterized by a thin smooth cuticle with lateral alae and a thin hypodermis, large lateral chords, and thick polymyarian, coelomyarian musculature. A pseudocoelom contains a distinct digestive tract with columnar enterocytes, and non-embryonated eggs are present in a uterus in some sections. Some of these nematodes are degenerate and fragmented and are surrounded by increased numbers of leukocytes, including multinucleated giant cells and heterophils. There is moderate congestion of vessels within some nodules with occasional extravasation of erythrocytes, and there are occasional aggregates of hemosiderin-laden macrophages. Additional nematodes are rarely present in the cecal lumen. There is some variation among slides and sections.

TRACHEA: There is circumferential erosion of the tracheal epithelium, and the tracheal mucosa is covered by a thin pseudomembrane composed of fibrillar eosinophilic material (fibrin) admixed with heterophils, sloughed degenerate cells, and small numbers of erythrocytes. The epithelium contains large syncytial cells with up to 25 nuclei, which slough into the tracheal lumen. Nuclei in syncytial cells often contain large hyaline eosinophilic to basophilic viral intranuclear inclusions that peripheralize the chromatin. Individual epithelial cells sometimes contain amphophilic to basophilic inclusions. Cilia are absent from most of the remaining epithelium which is attenuated to a low cuboidal level in certain areas, while in other areas there is a reparative process where epithelium is 4-5 cells thick and disorganized, and nuclei are large with prominent nucleoli. The subjacent

submucosa is expanded by edema and low to medium numbers of heterophils, macrophages, and lymphocytes; mucus glands are not seen.

Contributor's Morphologic Diagnosis:

Cecum, ileum, and colorectum: Atypical nodular mesenchymal proliferation, submucosal, mural and serosal, severe, with granulomatous inflammation and intralesion adult nematodes, morphology consistent with *Heterakis* spp.

Trachea: Tracheitis, fibrinonecrotizing, diffuse, severe, with epithelial syncytia formation and intranuclear viral inclusion bodies, consistent with gallid herpesvirus-1.

Contributor's Comment: The microscopic findings in this pheseant are characteristic for gallid herpesvirus type 1 (GaHV-1), the cause of infectious laryngotracheitis, and for *Heterakis* infection.

GaHV-1 is a member of the genus *Iltovirus*, subfamily *alphaherpesviridae* of the *herpesviridae* family[3]. The disease was first described in poultry in the United States in 1925[3], and in pheasants in 1931. Pheasants, pea fowl, and very young turkeys are also susceptible, while quail, guinea fowl, and non-galliform birds are resistant.[2] Birds that survive become lifelong carriers that may continue to shed, and wind can carry the virus between backyard flocks and larger production facilities. The virus is susceptible to disinfectants and to light exposure, but can survive in moist litter for 4 days or in dry litter for 20 days. Naturally infected birds develop clinical illness 6-14 days post-exposure.[3] Viral replication is limited to the respiratory epithelium; latency is achieved by infection of the trigeminal ganglion.[3] Birds affected in an epizootic can develop bloody mucus throughout the upper respiratory tract and experience severe respiratory distress and high mortality, while enzootic forms can cause varying degrees of mucoid tracheitis, conjunctivitis, and sinusitis, with lower mortality.[3]

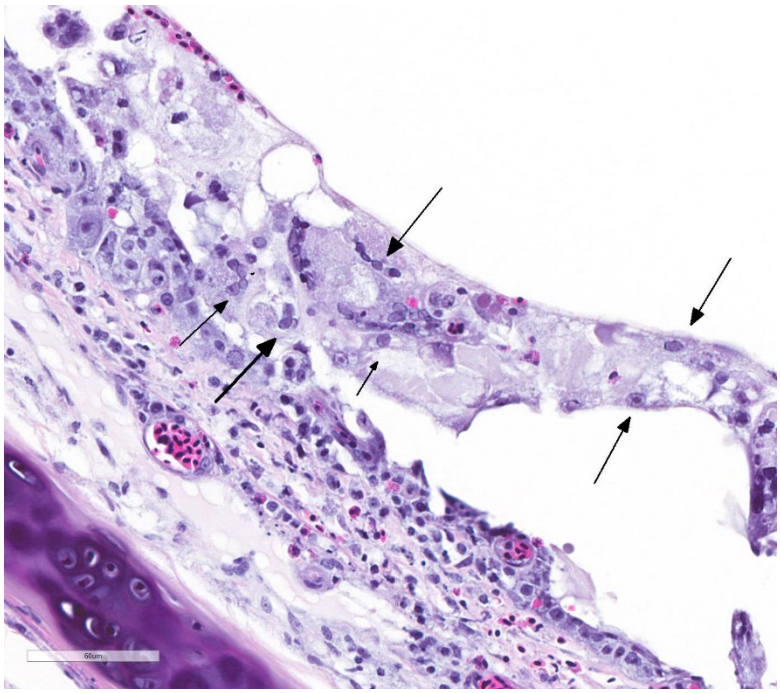

Trachea, golden pheasant. Amphophilic intranuclear inclusions are present within sloughed epithelium as well as within nuclei of viral syncytia (arrows). (HE, 400X)

Though this bird did not have significant rhinitis or sinusitis on gross anatomic examination, the two Impeyan pheasants submitted concurrently did have marked exudates in their upper respiratory tracts,

Cecum and colon, golden pheasant. Multiple nodules of proliferating spindle cells are present within the wall of the gut, and extend into the adjacent mesentery. A cross section of an adult female ascarid is present within one of the nodule.

and characteristic intranuclear inclusions in sloughed syncytial cells were identified on histopathology on all three birds. These inclusions are pathognomonic and can be identified with hematoxylin and eosin stain or with Giemsa.[3] Where GaHV-1 is suspected but inclusions are absent, viral isolation from chicken embryo liver cells, detection of GaHV-1 antigen by direct fluorescent antibody or immunohistochemical staining, or GaHV-1 DNA detection by PCR are appropriate.[3] Serology is not generally advised due to cross-reactivity with vaccine-induced antibodies.[3] Differential diagnoses for affected birds include infection by avian paramyxovirus (Newcastle disease), avian influenza, adenovirus infection, and avian coronaviruses.[3]

Heterakis spp infection is common in many galliform species. The life cycle is direct but earthworms may serve as paratenic hosts, making eradication of infection from birds on pasture or earthen lots exceedingly difficult.[1,8] *Heterakis dispar* has been reported in pheasants and is relatively non-pathogenic, while *H. gallinarum* and *H. isolonche* have both been reported to cause typhlitis in pheasants. *H. gallinarum* is infrequently a major primary pathogen in poultry, however it serves as a transport host for the protozoal parasite *Histomonas meleagridis*, which causes blackhead disease in turkeys and sometimes in chickens. However, in pheasants, there are no reports of histomoniasis, and disease is due to the nematode itself.

Heterakis isolonche is usually more pathogenic and has been reported to cause

high mortality in pen-reared pheasants.[8] It causes extensive nodule formation in the distal digestive tract due both to granuloma formation and marked proliferative host response, with the ceca most severely affected. These nodules sometimes rupture, causing peritonitis/coelomitis.[4] Second-stage larvae of *H. isolonche* are released from eggs in the gizzard, migrate to the ceca, then penetrate the mucosa[1]. In the submucosa, the larvae spark a proliferative response resulting in the yellow to pink to dark brown nodules seen grossly.[1] The worms frequently reside in the nodules.[1] Previous studies have variably characterized the nodules associated with these worms as granuloma, fibroma, fibrohistiocytic neoplasia, or leiomyoma, indicating the variability in response and limited studies attempting to characterize the proliferating cells. [4,5,6,9]

While lesions are sometimes reported as benign neoplasia, there is a case report of metastatic lesions of neurofibroblastic origin developing in the lung and liver of a 9-year-old ring-necked pheasant (*Phasianus colchicus*).[7]

Some consider *H. isolonche* to be an example of a nematode that induces neoplasia.[1] *Spirocerca lupi* is known to induce fibrosarcoma and osteosarcoma in the esophagus of dogs.[12] In our case, trichrome stain revealed no collagen among the proliferating fusiform cells, and immunohistochemical staining for smooth muscle actin and CD68 for cells of macrophage lineage were both negative, with appropriate staining of muscularis externa and individual inflammatory cells serving as appropriate internal positive controls, respectively. *H. gallinarum* and *H. isolonche* are very similar worms, and are

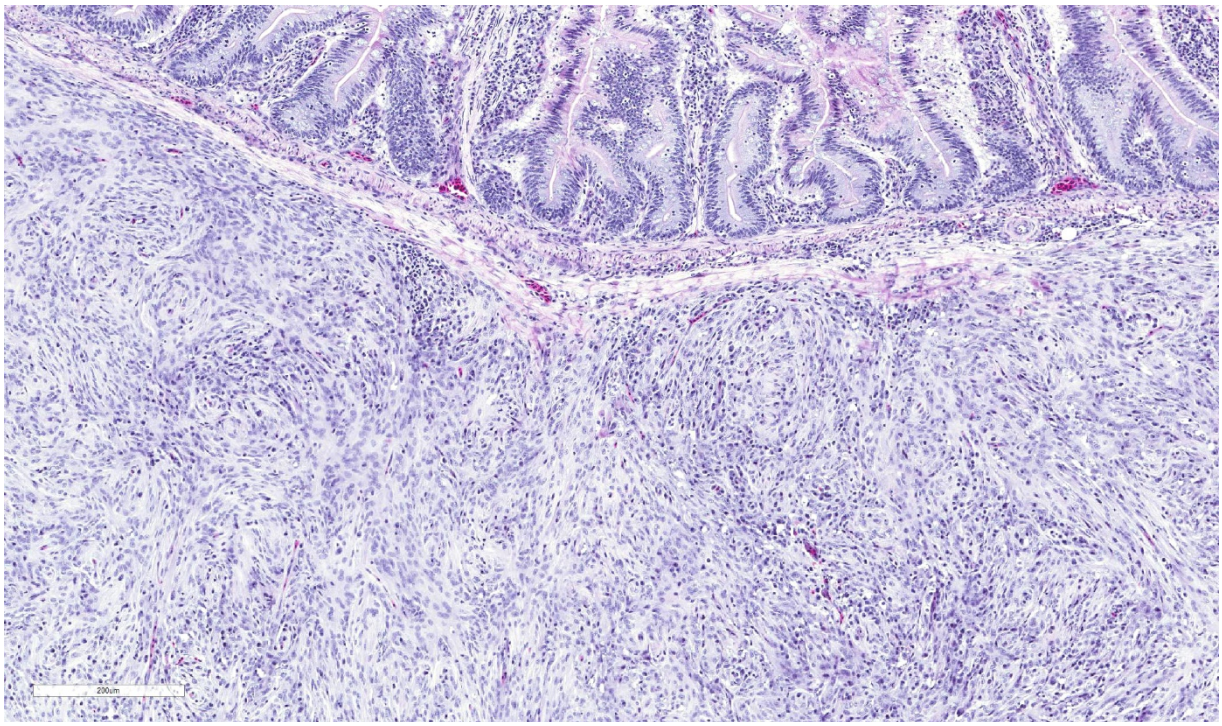

Nodules are composed of tight interlacing bundles of spindle cells with widely scattered lymphocytes and macrophages. (HE, 131X) (HE, 22X)

usually differentiated at the gross level. *H. isolonche* is slightly longer that *H. gallinarum*, and its spicules are more symmetrical than those of *H. gallinarum.*[8] In this case, intraluminal worms were not recognized grossly and are rarely seen on histologic section, features consistent with the life cycle of *H. isolonche* and not of *H. gallinarum*.

Of relevance to this case, there are multiple case reports describing increased pathogenicity in certain pheasant species including golden pheasants, though these cases do not describe the extensive involvement of the tunica muscularis externa or serosa of the ceca and surrounding digestive tract as seen in this bird.[4,5,6,9]. A cause for the increased disease severity in golden pheasants has not been elucidated, however parallels between the migrations of strongyles in equids, of hookworms in Southern fur seals, and of *H. gallinarum* in other galliform species may provide further insight. [4,11,12]

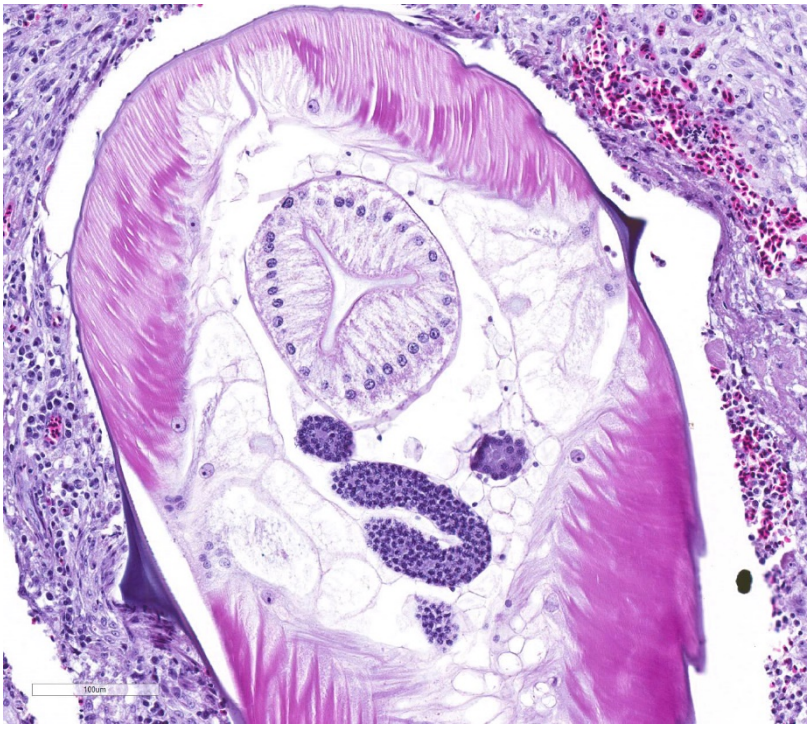

Cecum, golden pheasant. A tangential section of an intranodular ascarids exhibits lateral alae, a thin cuticle, lateral chords, polymyarian coelomyarian musculature, an intestine with numerous columnar uninucleate epithelium and multiple cross-sections of gonad. (HE, 219X)

Contributing Institution:

Connecticut Veterinary Medical Diagnostic Laboratory at the University of Connecticut,

http://cvmdl.uconn.edu/

JPC Diagnosis: 1. Trachea: Tracheitis, necrotizing and heterophilic, moderate with multifocal ulceration, epithelial intranuclear viral inclusion bodies and viral syncytia.

2. Cecum, large intestine, coelom: Typhlitis, colitis, and coelomitis, granulomatous, multifocal, moderate, with nodular spindle cell proliferations, and adult and larval ascarids.

JPC Comment: The participants agreed that this was a challenging descriptive exercise, with two distinct entities, as well as an adult nematode to describe. While most WSC submissions allow participants to focus on a single pathologic agent and process, there are two excellent unrelated conditions ongoing in this submission.

One of the characteristics of infectious laryngotracheitis and a number of other

alphaherpesviruses, (to include herpes simplex virus 1 and 2, anatid herpesvirus-1, and a number of others - but certainly not all) is the formation of characteristic syncytial cells, (prominent in this particular specimen.) In ILT, syncytial cells are commonly seen in the exudate overlying the remnants of the intact mucosa; these are virally infected, mutated, and degenerating cells which have lost contact with adjacent epithelium, a process that usually results in epithelial death. In alphaherpesvirus infection, membrane fusion is a key element of initial cell entry and lateral spread of virus in tissues It requires four envelope proteins, gB, gD, gH, and gL. When mutated, the gB and gK genes confer hyperfusogenicity on HSV and an accelerated and exaggerated process result in the formation of syncytial cells. Essenctially, the formation of syncytia is a normal process associated with viral transfection gone haywire as a result of mutation.

The contributor has also done an excellent job in discussing the unique proliferative change resulting from infection with *H. isolonche* in pheasants. This precise histogenesis of these nodules have not to date been elucidated. Immunostaining for smooth muscle, desmin, IBA-1, and histochemical staining for collagen failed to identify a smooth muscle or histiocytic origin for these nodules, and a literature review fails to elucidate their origin as well. It is good to have some things that modern science cannot explain.

There are a few other species of *Heterakis* species of note. *Heterakis* gallinarum in itself does not cause any significant disease, but is a host for *Histomonas melagridis*, a protozoan parasite which causes necrotizing typhlitis and hepatitis in turkeys and other poultry species. *Heterakis bonasae* infects the ceca of ruffed grouse and bobwhite quail and heavy infections may result in ill thrift and death . *Heterakis spumosa* is largely a historical pathogen in laboratory rodents which infects the cecum or colon and is not considered pathogenic.

The contributor mentioned parasites which may result in neoplasia in their host. Other examples include *Opisthorchis felineus* and *Clonorchis sinensis* which cause cholangiocarcinoma in cats and humans; *Cysticercus fasciolaris* which was documented to cause hepatic sarcoma in rats; *Trichosomoides crassicauda* which causes of the urothelium in rats; and *Schistosoma haematobium* a well-known cause of transitional cell carcinoma of urinary bladder in humans.

References:

1. Abdul-Aziz T, Barnes HJ. *Heterakis isolonche* Infection in Pheasants. In: Abdul-Aziz, T, Barnes, HJ. *Gross Pathology of Avian Diseases: Text and Atlas.* Madison, WI: Omnipress; 2018: 181.

2. Crawshaw GT, Boycott BR. Infectious Laryngotracheitis is Peafowl and Pheasants. *Avian Dis.* 1982; 2: 397-401.

3. García M, Spatz S, Guy JS. In: Swayne DE, ed. *Diseases of Poultry* 13th Ed. Ames, IA: John Wiley & Sons, Inc; 2013: 161-180.

4. Griner LA, Migaki G, Penner LR, McKee Jr. AE. Heterakidosis and Nodular Granulomas caused by *Heterakis isolonche* in the Ceca of Gallinaceous Birds. *Vet Pathol.* 1977: 582-590.

5. Halajian A, Kinsella JM, Mortazavi P, Abedi M. The first report of morbidity and mortality in Golden Pheasant, *Chrysolophus pictus*, due to a mixed infection of *Heterakis gallinarum* and *H. isolonche* in Iran. *Turk J Vet Anim Sci*. 2013; 37: 611-614.

6. Helmboldt CF, Wyand DS. Parasitic neoplasia in the golden pheasant. *J Wildl Dis* 1972; *8*: 3-6

7. Himmel L, Cianciolo R. Nodular typhlocolitis, heterakiasis, and mesenchymal neoplasia in a ring-necked pheasant (*Phasianus colchicus*) with immunohistochemical characterization of visceral metastases. *J Vet Diagn Invest.* 2017; 4: 561-565.

8. McDougald, LR. Internal Parasites. In: Swayne DE, ed. *Diseases of Poultry* 13th Ed. Ames, IA: John Wiley & Sons, Inc; 2013: 1123-1124.

9. Menezes RC, Tortelly R, Gomes DC, Pinto RM. Nodular Typhlitis Associated with the Nematodes *Heterakis gallinarum* and *Heterakis isolonche* in Pheasants: Frequency and Pathology with Evidence of Neoplasia. *Mem Inst Oswaldo Cruz.* 2003; 8: 1011-1016.

10. Okubo Y, Uchida H, Wakata K, Suzuki T, Shibata T, Ikeda H, Tamaguch M, Cohen JB, Glorioso, JC, Tagaya M, Hamada H. Tahara H. Syncytial mutations do not impair the specificyt of entry and spread of a glycopeotein d receptor-retargeted herpes simplex virus. *J of Virol* 2016; 90(24)11096-1

11. Seguel M, Muñoz F, Navarette MJ, Paredes E, Howerth E, Gottdenker N. Hookworm Infection in South American Fur Seal (*Arctocephalis australis*) Pups: Pathology and Factors Associate with Host Tissue Damage and Pathology. *Vet Pathol*. 2017; 2: 288-297.

12. Uzal FA, Plattner BL, Hostetter JM. In: Maxie MG, ed. *Jubb, Kennedy, and Palmer's Pathology Of Domestic Animals* 6th Ed. St. Louis, MO: Elsevier; 2016: 34-35.

CASE IV: Rab 51 (JPC 4118093).

Signalment: Adult (age unknown), female entire, wild European rabbit, *Oryctolagus cuniculus*.

History: This rabbit is from a group of wild rabbits shot for population control and subsequently submitted for post mortem examination for research and teaching purposes (institutional Ethics and Welfare Committee reference: CR240).

Gross Pathology: The lungs have a light brown to pink surface and a firm, gritty texture. A large number of coalescing granulomas that measure up to 1 mm in diameter expand the pulmonary parenchyma on cut surface (Fig. 1). Tracheobronchial lymph nodes have smooth, homogenous and cream capsular and cut surfaces and measure approximately 8x5x5 mm.

There are multifocal, randomly distributed, well demarcated, cream foci within the liver

Lung, rabbit. Numerous 1mm granulomas expand the pulmonary parenchyma. (Photo courtesy of: Department of Veterinary Medicine, The Queen's Veterinary School Hospital, University of Cambridge. Cambridge CB3 0ES, UK. https://www.vet.cam.ac.uk)

parenchyma and level with or slightly raised from the capsular surface. These foci measure up to 2 mm in diameter (gross and microscopic findings confirmed concurrent *Eimeria stiedae* infection).

Laboratory results:

None available.

Microscopic Description:

Greater than 90% of the pulmonary parenchyma is expanded by a large number of multifocal to coalescing granulomas surrounding thick walled adiaspores. Adiaspores measure 200-300µm in diameter and have a wall which consists of a bright eosinophilic, approximately 3µm thick outer layer, a 30-40µm thick pale eosinophilic middle layer and a variably prominent, 2-3µm thick, basophilic inner layer. The adiaspore wall surrounds a foamy, variably pale basophilic core. Large numbers of concentrically arranged heterophils, macrophages, and epithelioid macrophages, small to moderate numbers of lymphocytes and plasma cells, moderate numbers of multinucleated giant cells (foreign body type, 10-50 nuclei) and variable numbers of fibroblasts surround the adiaspores. At the center of some granulomas are degenerate adiaspore remnants admixed with heterophils or a core of necrotic debris. Granulomas multifocally extend up to or raise the visceral pleural surface. Adiaspore walls are intensely and stain intensely with periodic acid-Schiff stain.

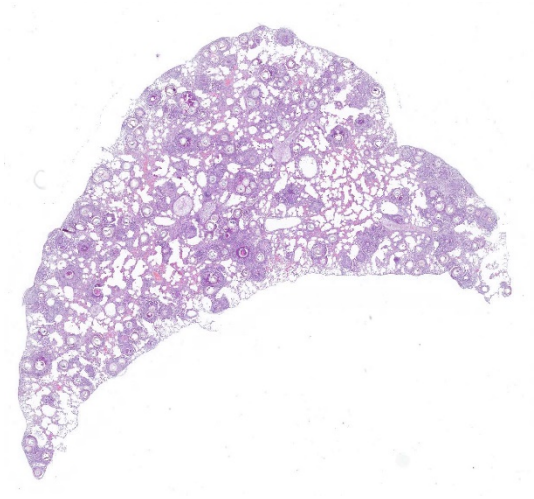

Lung, rabbit. A section of lung is submitted for examination. Even at low magnification, coalescing granulomas centered on adiaspores are visible. (HE, 6X)

Contributor's Morphologic Diagnosis:

Pneumonia, granulomatous and heterophilic, chronic, multifocal to coalescing, severe; lungs, with adiaspores consistent with *Emmonsia crescens*.

Contributor's Comment Adiaspiromycosis is associated with two causative agents: *Emmonsia crescens* and *Emmonsia parva*, which are saprophytic dimorphic fungi of the *Ajellomycetaceae* family. *E. parva* is distributed in small geographical areas in North America, Asia, Australia, and eastern Europe, has a small adiaspore diameter (10-20μm) and grows up to 40°C. *E. crescens* has a worldwide distribution, large adiaspores (up to 300μm), and grows up to 37°C.[14]

Following inhalation of conidia from soil, adiaspores develop and increase in size in host tissue which leads to granulomatous pneumonia in the host[3]. Small mammals such as rodents[5,7] and mustelids[9] are most commonly affected, but adiaspiromycosis has also been sporadically reported in larger mammals such as horses[12], deer[11], badgers[10], foxes[10] and dogs[8]. Adiaspiromycosis occurs rarely in humans and has a range of presentations from solitary pulmonary nodules to disseminated pulmonary disease and is occasionally fatal. A disseminated, extrapulmonary form has been described in immunosuppressed patients with acquired immunodeficiency syndrome and in one HIV-positive patient on immunosuppressive therapy following liver transplant.[1]. Adiaspiromycosis has been previously reported in cottontail rabbits (*Sylvilagus audubonii*) in New Mexico[15] and is recognized in *Oryctolagus cuniculus* as a historic, occasional, pathogen of laboratory rabbits.

In this case, a wild European rabbit (*Oryctolagus cuniculus*) exhibited granulomatous pneumonia which was particularly marked both grossly and microscopically.[6] All lung lobes were affected. Additionally, the cortex and medulla of the tracheobronchial lymph node were multifocally expanded by moderate numbers of adiaspores, with a similar histological appearance to those in the lungs,

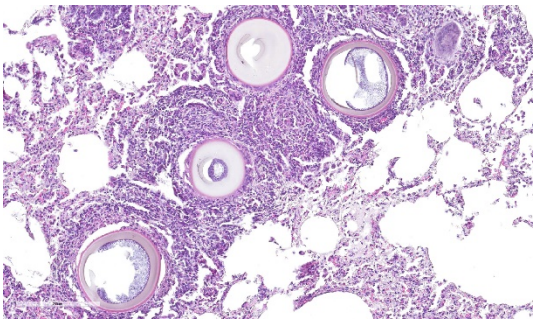

Lung, rabbit. A section of lung is submitted for examination. Even at low magnification, coalescing granulomas centered on adiaspores are visible. (HE, 6X)

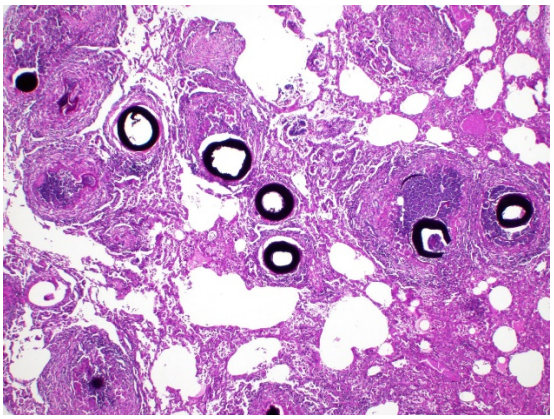

Lung, rabbit. Adiaspore cell walls stain strongly with periodic acid-Schiff. (PAS, 40X)

and surrounded by large numbers of epithelioid macrophages, moderate numbers of multinucleated giant cells (foreign body type, 10-50 nuclei) and fewer heterophils. Adiaspores do not replicate within host tissue and so the extent and severity of this case was most likely related to inhalation of large numbers of conidia. Adiaspore morphology was considered most consistent with *E. crescens* due to the diameter.

E. crescens infection can be confirmed by microdissection of adiaspores and PCR amplification using *Emmonsia* specific primers followed by DNA sequencing.[2,12] In this case microdissection and PCR of formalin-fixed tissue was attempted using *Emmonsia* specific primers however no *Emmonsia* specific DNA was identified. This may have been due to the limitations of using formalin-fixed tissue for PCR amplification rather than fresh tissue. Fungal culture was not attempted, but culture of *E. crescens* is reported to be challenging and frequently unsuccessful.[2]

Recent phylogenetic studies have led to taxonomic revisions of *E. parva* and *E. crescens*. In one study, *E. parva* was shown to cluster in the *Blastomyces* genus (*B. parvus)*[4], and other members of the *Emmonsia* genus with a yeast tissue form have been reclassified into the *Emergomyces* genus. It has, therefore, been proposed that *Emmonsia crescens* be assigned to the new genus *Adiaspiromyces.*[4,6]

Contributing Institution:

Department of Veterinary Medicine, The Queen's Veterinary School Hospital, University of Cambridge. Cambridge CB3 0ES, UK. https://www.vet.cam.ac.uk

JPC Diagnosis: Lung: Pneumonia, interstitial, granulomatous**,** diffuse, moderate, with numerous extracellular adiaspores**.**

JPC Comment: The contributor has submitted an excellent review of adiospiromycosis in animal species, from its pathogenesis to the nmost recent development in classification of this organism.

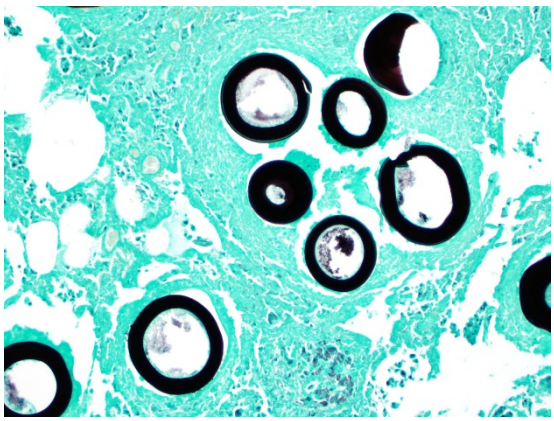

Lung, rabbit. Adiaspore cell walls also stain strongly with silver stains, although their necessity in this case, like PAS, is questionable. (Gomori methenamine silver, 40X)

Dr. Chester W. Emmons, 1900-1985.

Historically, the first description of adispiromycosis as a pulmonary infection was first in rabbits by Dr Chester Wilson Emmons (1900-1985) of the National Institutes of Health. During his tenure at the NIH, he was the first medical mycologist at the NIH as well as the head of the medical mycology section at the National Institute for Allergic and Infectious Disease. Dr. Emmons designated the fungus as *Haplosporium parvum*, but it was reexamined in 1959 by Cifrerri and Montemartini, who renamed the organism *Emmonsia parvum.* Interestingly (at least for this particular conference), Dr. C.W. Emmons, during his tenure at NIH, is also credited for identifying the ecological niche for *Cryptococcus neoformans*.

In 1960 Emmons himself added a second species, *E. crescens*, and proposed adiaspiromycosis as a more descriptive name for the disease. The name adiaspiromycosis is derived from Greek - "a" for not or without, "dia" – by or through, and sporo, for seed - ultimately in reference to the fact that the spores to do replicate or disseminate within tissue. The severity of disease is largely the result of inoculum size and the ability of the host to mount an immune response.[13]

The first human case of adispiromycosis was reported in 1964, and most cases of this relatively rare fungal infection have been reported to the result of *E. crescens* (which has been reported in over 120 mammalians species as well.) Most cases of *E parva* have been seen in immunosuppressed hosts. A syndrome of granulomatous conjunctivitis in children in the Amazon basin has been described with *Emmonsia,*[13] although *Rhinosporidium* could not be completely excluded.

Until recently, *Emmonsia* was limited to two speceis, *E. crescens and E. parvum.* However, a cluster of new *Emmonsia*-like fungi have been isolated in human patients with atypical disseminated mycotic infections behaving more like more traditional dimorphic fungi such as *Blastomyces*, highlighting the close relationship of these two genera. (In fact, *E parva* is theorized to be closer genetically to *Blastomyces dermatitidis* than to *E. crescens.* Seven new species of *Emmonsia* have been identified since the 1990's (usually in individual immunosuppressed patients), with only one becoming a named species (*E. pasteuriana.)* Newer species of *Emmonsia* also differ from the historical members of the genus in that rather than exhibiting simple increase in size, they possess the ability to convert to replicative yeasts and disseminate to other tissues.[13]

References:

1. Anstead GM, Sutton DA, Graybill JR. Adiaspiromycosis causing respiratory failure and a review of human infections due to Emmonsia and Chrysosporium spp. *J Clin Microbiol*. 2012;50:1346–1354.
2. Borman AM, Simpson VR, et al. Adiaspiromycosis due to Emmonsia crescens is Widespread in Native British Mammals. *Mycopathologia*. 2009 Oct 16;168:153–163.
3. Caswell JL, Williams KJ. Respiratory system. In: Maxie MG, ed. Jubb, Kennedy, and Palmer's Pathology of Domestic Animals. 6th ed. Vol. 2. St. Louis, MO: Elsevier, 2016:584– 585.
4. Dukik K, Muñoz JF, Jiang Y, et al. Novel taxa of thermally dimorphic systemic pathogens in the Ajellomycetaceae (Onygenales). *Mycoses*. 2017;60:296–309.
5. Fischer OA. Adiaspores of Emmonsia parva var. crescens in lungs of small rodents in a rural area. *Acta Vet. Brno*. 2001;70:345–352.
6. Hughes K, Borman AM. Adiaspiromycosis in a wild European rabbit, and a review of the literature. *J Vet Diagnostic Investig*. 2018; Published online May 2.
7. Kim, T; Han, J; Chang, S; et al. Adiaspiromycosis of an apodemus agrarius captured wild rodent in Korea. Lab Anim Res. 2012;28:67–69.
8. Koller LD, Patton NM, Whitsett DK. Adiaspiromycosis in the lungs of a dog. *JAVMA*. 1976 Dec 15;169:1316–1317.
9. Křivanec K, Otčenášek M. Importance of free living mustelid carnivores in circulation of adiaspiromycosis. *Mycopathologia*. 1977;60:139–144.
10. Křivanec K, Otčenášek M, Šlais J. Adiaspiromycosis in large free living carnivores. *Mycopathologia*. 1976;58:21–25.
11. Matsuda K, Niki H, Yukawa A, et al. First detection of adiaspiromycosis in the lungs of a deer. *J Vet Med Sci*. 2015;77:981–983.
12. Pusterla N, Pesavento PA., Leutenegger CM, et al. Disseminated pulmonary adiaspiromycosis caused by Emmonsia crescens in a horse. *Equine Vet J*. 2002;34:749–752.
13. Schwartz IS, Kenyon C, Feng P, Govender NP, Dukik, K, Sigler L, Jiang Y, Stielow JB, Munoz JF, Cuomo CA, Botha A, Stchigel AM, de Hoog GS. 50 years of Emmonsia dseease in humans: the dramatic emergence of a cluster of novel fungal pathogens. *PLOS Pathogens* 2015; 11(11): e1005198.
14. Sigler L. Ajellomyces crescens sp. nov., taxonomy of Emmonsia spp., and relatedness with Blastomyces dermatitidis (teleomorph Ajellomyces dermatitidis). *J Med Vet Mycol*. 1996;34:303–314.
15. Taylor RL, Miller BE, Rust JH. Adiaspiromycosis in small mammals of New Mexico. *Mycologia*. 2017;59:513–518.

Self-Assessment - WSC 2019-2020 Conference 13

1. Which of the following is true concerning canine adenovirus-1?
    a. It most commonly results in pneumonia in infected animals.
    b. Primary targets are macrophages and lymphocytes in affected animals.
    c. Gallbladder edema is a pathognomonic sign at autopsy.
    d. Anterior uveitis results from Type IV hypersensitivity 2-3 weeks following infection

2. Which of the following is not a canid species susceptible to CAV-1?
    a. Coyotes
    b. Skunks
    c. Foxes
    d. Wolves

3. Which of the following is not a virulence factor of *Cryptococcus*?
    a. Laccase
    b. Superoxide dismutase
    c. Phospholipase
    d. Type 3 secretion system

4. Which of the following is true about *Heterakis isolonche* infection in golden pheasants?
    a. Mortality is most often the result of co-infection with *Histomonas meleagridis*.
    b. Cockroaches are the intermediate hosts for *Heterakis sp.*
    c. *Heterakis dispar* is the most pathogenic species for pen-reared pheasants.
    d. *Heterakis isolonche* is associated with a fibroblastic nodular response in pheasants.

5. Which of the following genera of fungi is *Emmonsia* most closely related to?
    a. Blastomyces
    b. Cryptococcus
    c. Histoplasma
    d. *Coccidiomycosis*

Joint Pathology Center
Veterinary Pathology Services

WEDNESDAY SLIDE CONFERENCE 2019-2020

C o n f e r e n c e 14

15 January 2020

Dr. Neel Aziz
Supervising Veterinary Pathologist
Smithsonian Conservation Biology Institute
National Zoological Park
Washington DC, 20008

CASE I: 18-4856 2 (JPC 4116557).

Signalment: Western Pond Turtle, female adult.

History: The turtle was found on a road in Waterloo campground in Lebanon, Oregon. Eyes were swollen bilaterally. Fed ensure and cat foot but ate very little. Treated with eye ointment and baytril.

Gross Pathology: A 468g male Western Pond Turtle (*Actinemys marmorata*) is necropsied on 10/6/2017 in fair body condition and mild post mortem autolysis. Eyelids are markedly swollen bilaterally with thick, light yellow, caseous material present under the lids. Globes are not appreciated grossly. Approximately 30% of the total lung parenchyma is red and firm and thick, light yellow, caseous material oozes out on cut surfaces.

Laboratory results: N/A.

Microscopic Description:

Cross sections of the skull, brain, and eyes. There is hyperplasia and hyperkeratosis of the eyelids and external ear canal. There is marked squamous metaplasia and layered keratin accumulation within the nasal vestibule, more prominent on one side, with dilation of some sinus mucous glands containing moderate numbers of heterophils. In one of these heterophil-rich foci there is rimming layer of epithelioid macrophages and multinucleate giant cells with small numbers of bacteria visible in the exudate. Other glands in the region (ophthalmic or sinus mucous glands) multifocally show moderate to severe squamous metaplasia and occasional keratin accumulation. There are multifocal, asymmetric areas of marked osteoclast activity.

Head, pond turtle: A transverse section through the head at the level of the globe demonstrates marked expansion of the lacrimal glands. (HE, 7X)

Contributor's Morphologic Diagnosis:

Whole body: Emaciation

Multiple organs: Squamous metaplasia consistent with hypovitaminosis A;

Sinuses: Severe diffuse heterophilic rhinitis with squamous metaplasia and keratin accumulation

Other lesions:

Lungs: severe chronic active heterophilic and proliferative bronchointerstitial pneumonia with bacteria

Eyelids/eye: Hyperplastic keratoconjunctivitis

Ears: Bilateral severe hyperplastic otitis media

Contributor's Comment: Histopathology is consistent with hypovitaminosis A; squamous metaplasia with keratinization was observed in multiple tissues throughout the body. Other disease processes may be occurring simultaneously/secondarily, (opportunistic bacteria) but the most severe lesions were due to the vitamin deficiency.

The cause of the increased bone resorption/osteoclast activity is unknown. As the change is not generalized, a Vitamin D deficiency/hypocalcemia is unlikely. , In addition, clinical reports of hypovitaminosis D in turtles mention paradoxical minera-

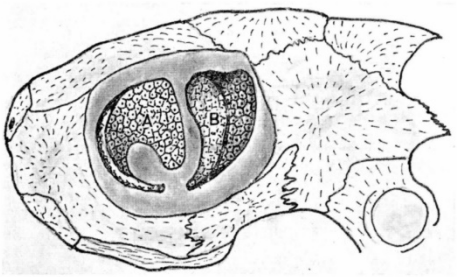

Fig. 1. Topography of the ophthalmic glands in the terrapin (diagrammatic). The Harderian gland (A) is anteromedial or rostral. The lachrymal gland (B) is posterolateral or temporal. The globe fits into the cup formed by the two glands.

Head, pond turtle: Illustration of the position of Harderian and lacrimal glands within the orbit of the turtle. (Photo courtesy of: Elkan E, Zwart P. The ocular disease of young terrapins caused by Vitamin A deficiency. Pathol Vet 1967; 4:201-222.)

lization of soft tissues (including muscle, renal tubules, etc) and such changes are lacking here. In this case, osteoclasis often occurred near areas of squamous metaplasia, so perhaps local tissue swelling/pressure was the force for osseous remodeling.

Contributing Institution:

Oregon Veterinary Diagnostic Laboratory, Carlson College of Veterinary Medicine, Oregon State University, Corvallis, Oregon 97331.
https://vetmed.oregonstate.edu/diagnostic

JPC Diagnosis: 1. Lacrimal glands and ducts: Squamous metaplasia, diffuse, severe, with marked hyperkeratosis, and diffuse glandular degeneration, heterophilic adenitis, and dochitis.

2. Skull, vomer and frontal bone: Bone resorption, diffuse, marked.

JPC Comment: This slide is an excellent example of squamous metaplasia seen in the lacrimal glands in chelonians as a result of Viamin A deficiency.

The 1967 paper in *Pathologia Veterinaria (* the forerunner of *Veterinary Pathology)* by Elkan and Zwart is an outstanding reference on the systemic effects of Vitamin A deficiency in the "young terrapin", as well as a tremendous example of scientific prose, the like of which we do not see today in modern publications.[3] While a quotation of the entire first page is poor form (and the reader can download it online), a short snippet is illustrative of how far current medical writing has fallen - "In vain do the textbooks on herpetology mention the exacting dietary requirements of juvenile terrapns, in vain their advice on how to meet these requirements…Neither the sellers nor the buyers read these books, presuming that a plastic bowl and some 'ant's eggs' suffice to keep a juvenile terrapin alive. The annual holocaust among the imported terrapins proves the error of this assumption."[3]

As mentioned by the contributor, Vitamin A deficiency in chelonians is a systemic process, rather than just one confined to the structures of the orbit.[3] Squamous metaplasia also occurs in the external ear, where it has been associated with aural "abscessation" in a number of chelonian species in association with a mixed flora of gram-negative bacilli, presumably ascending

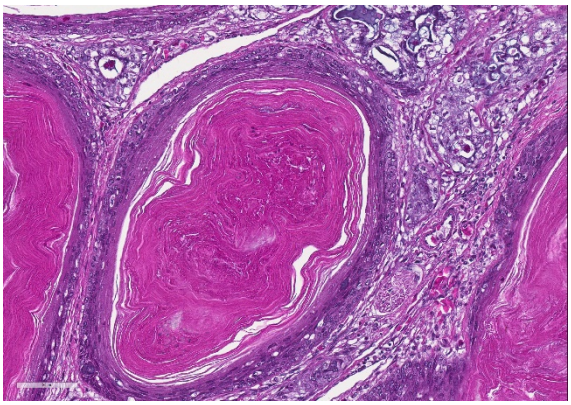

Lacrimal gland, pond turtle. Lacrimal glands or ducts are markedly expanded by a wall of multiple layers of stratified squamous epithelium and their lumina are filled with lamellar keratin. (HE, 283X)

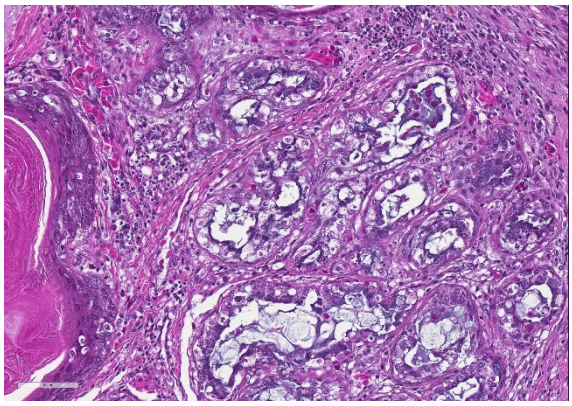

Lacrimal gland, pond turtle. Remaining lacrimal glands are shrunken and cuboidal and infiltrated by low to moderate numbers of heterophils. A low number of epithelial cells are pyknotic or fragmented. The interstitium is infiltrated by low numbers of heterophils and lymphocytes. (HE, 283X)

from the Eustachian tube.[1,7] In addition, squamous metaplasia accompanied by excessive keratinzation occurs in other organs as well. Pancreatic ducts are thickened, hyperkeratotic, and ensheathed in heterophils. In the kidney, collecting ducts are distended and occluded by keratin debris, often resultin in severe nephritis. Blockage by keratin debris may also be seen in the ureters and urinary bladder. Degenerative and inflammatory changes were noted by Elkham in the thyroid and liver, but squamous metaplasia was not documented in these animals.[3]

Some participants had difficulty in orienting themselves on the submitted section, and there was considerable variation between sections (necessitated by the submission requirement of 165 sections.) As illustrated by Elkham and Zwart, the chelonian globe fits into the cup formed by the two glands, the anteromedial Harderian gland, and the posterolateral lacrimal gland.[3] It is preseumed that the lacrimal gland is present in the submitted sections due to its position lateral to the globe. The ear canal is not present on these sections. Moreover, at this stage of lesion development, the participants had great difficulty determining which of the large keratin filled structures might be derived originally from glands or ducts. Isolated mucus cells were present within the walls of several dilated keratin-filled structures, which would not be consistent from ductal derivation, but at this level of change, it is difficult and likely unnecessary to be certain. Some participants had focal granulomas within the sinuses and adjacent skeletal muscle within their sections.

The effects of Vitamin A deficiency have been documented in a wide range of poikilothermic and homothermic species. In crocodiles, squamous metaplasia result in similar changes in the conjunctiva and kidenys, as well as nodular distentions of the ostia of the lingual glands.[2] In captive anurans, squamous metaplasia may be seen in mucus glans of the skin, tongue, oral mucosa, esophagus, cloaca, renal tubules, oviduct, and bladder.[5] Periocular gland squamous metaplasia has been seen in penguins.[8] Squamous metaplasia may be seen in other species of birds, including psittacines in a wide range of tissues including glands of the oral cavity, esophagus, salivary gland and respiratory tract. Protruding keratin masses from

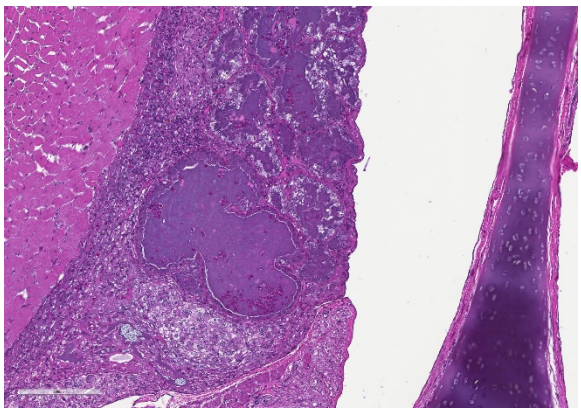

Nasal glands, pond turtle. Unilaterally nasal glands are ectatic and filled with abundant basophilic secretory product and often infiltrated with heterophils, which expand the interstitium as well.

esophageal glands are classsic lesions associated with Vitamin A deficiency in poultry. Squamous metaplasia of Harderian glands, although not to the level seen in chelonians, has also been seen in laboratory rodents as well.[3] In suckling calves, it has been incriminated in a sider range of ocular abnormalitis to include cataract formation, lens luxation, micropthalmia, and reduction in the size of the optic nerve.[9]

While it might be thought that in present days, Vitamin A deficiency and related opthalmic disease would be a rarity, the human species has found new ways to impair its ability to take in this important dietary ingredient. Starvation still rules in many parts of the world, but in developed nations, hypovitaminosis A is still seen, as a result of restrictive and monotonous diets (including vegan diets, "cafeteria" and "junk food" diets, and eating disorders.[4] Malabsorptive syndromes, to include bariatric surgery also accounts for a number of cases each year. While signs of deficiency are system wide, well-documented ocular diseases associated with Vitamin A in humans include night blindness, xeropthalmia ("dry eye") Bitot's spot (a buildup of keratin located superficially in the conjunctiva associated with corneal drying), keratitis and keratomalacia.[4]

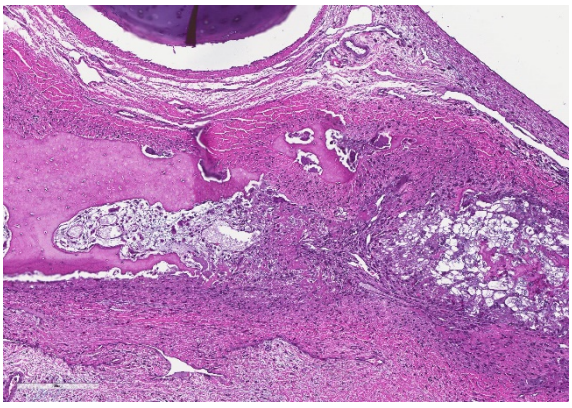

Skull, pond turtle. There is marked remodeling of the bones of the skull including the vomer bone (seen here, suggestive of starvation. (HE, 150X)

Several pathologists attending the conference suggested that bacterial infection or chronic irritation should also be considered in the potential differential diagnosis for this particular lesion in light of the lack of information on husbandry of this particular animal. Dr. Andrew Cartoceti of the National Zoo mentioned that samples for Vitamin A should be packaged in a brown container due to the susceptibility of the compound to sunlight. The active resorptionof the bones of the skull in this animal was attributed to protein and caloric malnutrition.

References:

1. Brown JD, Richards JM, Robertson J, Holladay S, Sleeman JM. Pathology of aural abscesses in free-living Eastern box turtles. *J Wildl Dis* 2004; 40(4): 704-712.
2. Conley JK, Shilton CM. Crocodilia. *In: Pathology of Wildlife and Zoo Animals* Terio KA, McAloose D, St Leger J eds., 2019; London: Associated Press, p. 849
3. Elkan E, Zwart P. The ocular disease of young terrapins caused by Vitamin A deficiency. *Pathol Vet* 1967; 4:201-222.
4. Faustino JF, Rieiro-Silva A, Dalto RF, de Souza MM, Furtado JMF, de Melo Rocha G, Alves M, Rocha EM. Vitamin A and the eye: an old tale for modern times. *Arch Brazil Opthamol* 2016; 79(1):56-61.
5. Pessier, A. Amphibia. *In: Pathology of Wildlife and Zoo Animals* Terio KA,

McAloose D, St Leger J eds., 2019; London: Associated Press, p. 921-922.
6. Reavill DR, Dorrestein G. Psittacines, Coliiformes, Musophagiformes, Cuculiformes. *In: Pathology of Wildlife and Zoo Animals* Terio KA, McAloose D, St Leger J eds., 2019; London: Associated Press, p. 770
7. Rodriguez CE, Duque AMH, Steinberg J, Woodburn DB. Chelonia. *In: Pathology of Wildlife and Zoo Animals* Terio KA, McAloose D, St Leger J eds., 2019; London: Associated Press, p. 831-832.
8. Stidworthy MF, Denk D. Sphisciformes, Gaviiformes, Podicipediformes, Procellariformes, and Pelecaniformes. *In: Pathology of Wildlife and Zoo Animals* Terio KA, McAloose D, St Leger J eds., 2019; London: Associated Press, p. 651.
9. No authors listed. Range of ocular deformities in calves due to hypovitaminosis A. *Vet Record* 2014; 174(10)244-247.

CASE II: 2926 (JPC 4118632).

Signalment: 7-year-old, male, Asian small-clawed otter (*Aonyx cinerea*).

History: This otter was presented to a veterinary hospital with a short history of anorexia. Marked increases of blood urea nitrogen, creatinine, inorganic phosphorus, and ammonia were noted in serum biochemistry. Radiographs indicated numerous (more than 20) calculi in both kidneys, ureters, and urinary bladder. Lithotomy was performed, and approximately 30, up to 10.2 mm in diameter, yellowish-green to white calculi were removed from the ureters and urinary bladder. The otter persistently showed anorexia and died at seventh day after the surgery.

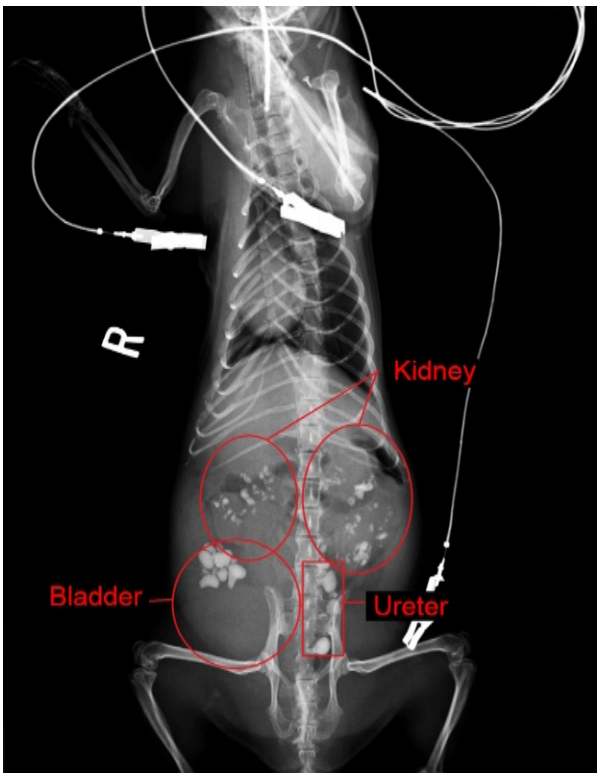

Radiograph, Asian small clawed otter. This radiograph demonstrates numerous radiopaque uroliths within the kidneys, ureter, and bladder. (Photo courtesy of: Laboratory of Comparative Pathology, Graduate School of Veterinary Medicine, Hokkaido University, https://www.vetmed.hokudai.ac.jp/)

Gross Pathology: The animal showed mild emaciation and dehydration at necropsy. Multiple yellowish-green calculi, maximum 6 mm in diameter, were noted in the renal pelves, ureters, and urinary bladder. Both ureters dilated moderately. Some renal lobes were mildly atrophic with fibrosis.

Laboratory results:

Blood urea nitrogen, 215.2 mg/dl (reference range: 9.2 – 29.2 mg/dl in dogs); creatinine, 6.6 mg/dl (0.4 – 1.4 mg/dl in dogs); inorganic

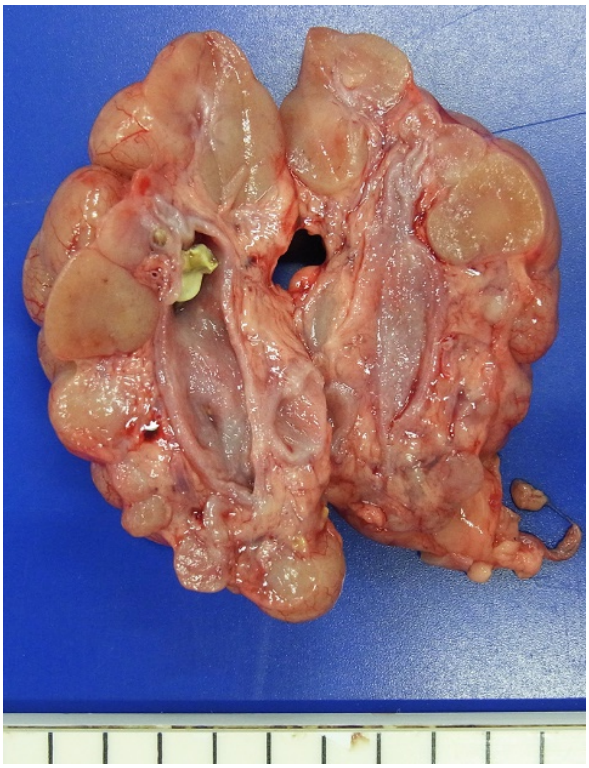

Kidney, Asian small-clawed otter. The major calyx is markedly dilated and contains a large urolith. Uroliths can also be identified in minor calyces and there is marked atrophy of several lobules. (Photo courtesy of: Laboratory of Comparative Pathology, Graduate School of Veterinary Medicine, Hokkaido University, https://www.vetmed.hokudai.ac.jp/)

phosphorus, 25.8 mg/dl (1.9 – 5.0 mg/dl in dogs); ammonia, 247 µg/dl (16 – 75 µg/dl in dogs).

Microscopic Description: Kidney: Diffuse moderate interstitial fibrosis is observed. A few lymphocytes infiltrate into the interstitium of the medulla. Prismatic pale yellowish crystals scatter in the lumina of renal tubules, collecting ducts, and dilated renal pelvis. These crystals show birefringence under polarized light. Degeneration and necrosis of the tubular epithelial cells and intraluminal protein cast formation are noted in the medulla.

Contributor's Morphologic Diagnosis: Kidney: Oxalate urolithiasis and nephropathy, chronic, multifocal, moderate.

Contributor's Comment: Urolithiasis is frequently observed in otters such as Asian small-clawed otters (*Aonyx cinerea*), North American river otters (*Lontra canadensis*), or Eurasian otters (*Lutra lutra*).[1-3,6,8] It has been reported that 16.7% of free-ranging North American river otters[5] and 23.4% of free-ranging Eurasian otters[1] had uroliths. The prevalence of uroliths appears to increase in captive populations, as urolithiasis has been found in 66.1% of captive Asian small-clawed otters[2] and 64.7% of captive Eurasian otters[1].

In Asian small-clawed otters, the majority of affected individuals had bilateral renal calculi.[2] In addition, about one-thirds of individuals with renal calculi also had cystic calculi.[2] Ureteral obstruction due to uroliths causes dilation of ureters, hydronephrosis,

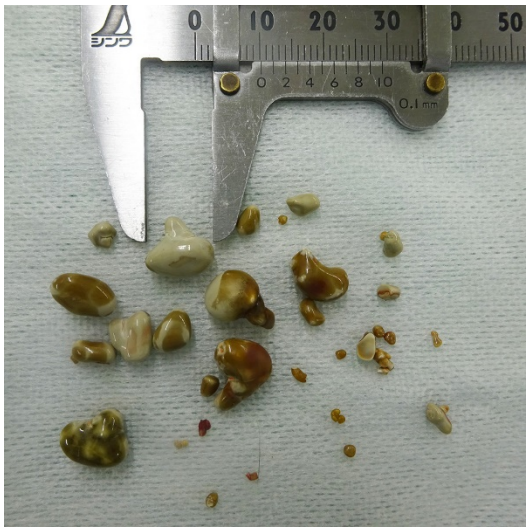

Uroliths, Asian small-clawed otter. Numerous oxalate crystals were retrieve from the urinary tract of this individual. (Photo courtesy of: Laboratory of Comparative Pathology, Graduate School of Veterinary Medicine, Hokkaido University, https://www.vetmed.hokudai.ac.jp/)

and pyelonephritis.[4] In the affected animals, renal disease can be the cause of, or a contributing factor in, the deaths.[2] Calculi are

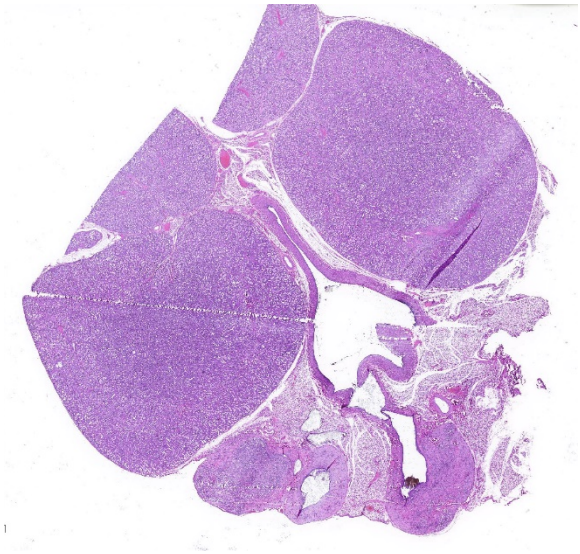

Kidney, Asian small-clawed otter. A section of kidney is presented for examination. Lobules at top have no gross lesions. Two lobules at bottom are markedly shrunken and the calyx contains a brownish occlusive urolith. (HE, 5X)

mainly composed of calcium oxalate or ammonium acid urate.[1,2,4]

In North American river otters, bilateral renal calculi are not common, and the majority of otters with calculi are generally healthy without gross renal abnormalities.[5] Only severely affected animals showed bilateral calculi or ureteral obstruction.[3] Although calculi have not been systematically analyzed so far, calcium phosphate and urate have been reported as a primary component of the calculi.[3,6]

In Eurasian otters, only one-thirds of total cases showed bilateral renal calculi and calculi were restricted to within the kidney in the majority of affected animals.[8] Only a few severely affected individuals showed ureteral or cystic calculi.[1,8] The main component of calculi is ammonium acid urate.[1,8]

Gender does not affect the susceptibility to urolithiasis in otters.[1,2,6] Meanwhile, age appears to relate to the prevalence of urolithiasis or disease severity. The positive rate or the number of uroliths increase with age in North American river otters and Eurasian otters.[1,6,8] In Asian small-clawed otters, renal disease was more frequently reported as the cause of death in older individuals.[2]

Although husbandry, diet, genetics, chronic infections, or metabolic disorders have been suggested as contributing factors, the exact mechanisms for the high prevalence of urolithiasis in otters have remained unknown. Since the prevalence of urolithiasis is higher in captive populations, it is possible that the captive diet may contribute to urolithiasis to some extent.[2] Meanwhile, as a significant portion of free-ranging individuals also have uroliths, there might be a predisposing factor to urolithiasis in otters. It is noteworthy that the main components of uroliths differ among species of otters as with the species-dependent difference in stone composition in

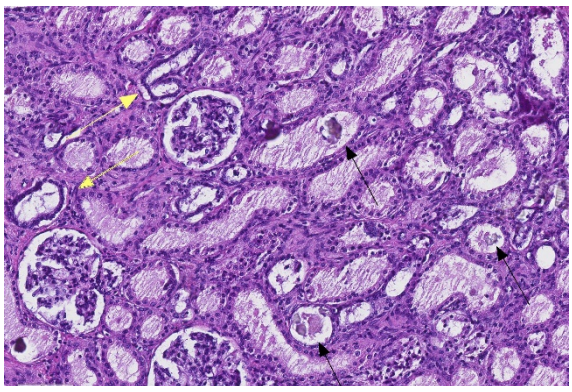

Kidney, Asian small-clawed otter. In other, more normal lobules, tubular lumina often contain oxalate crystals (black arrows) or epithelium is attenuated and mineralized (yellow arrows) (HE, 92X)

Mustelid sp.	Captive or Free Ranging	Stone Type	Reported Prevalence	Associated Lesions	Possible Risk Factors
Asian small clawed otter	Captive	Mix of urate and calcium oxalate	66%–89%	Not reported	Older age (>2 years)
Eurasian otter	Free ranging	Ammonium acid urate	10.2%	Nephrolithiasis	Dietary purine intake, protein quality, and digestibility
North American river otter	Free ranging	Calcium phosphate	16.2%	Not reported	Older age, capture location
North American river otter	Free ranging	Uric acid	0.33%	Bilateral nephrolithiasis, expanded renal calyces, marked hydroureter, mild renal medullary loss, and cortical tubular atrophy	Not reported
Wolverine	Free ranging	Ammonium acid urate with magnesium ammonium phosphate and calcium phosphate	8.9%	Nephroliths were unilateral in 87.5% of cases.	Older age (>2 years) males

Table 1. Urolithiasis in Otters and Wolverines. From Terio, McAloose. St Leger eds., *Pathology of Wildlife and Zoo Animals*., 2019.[10]

dogs.[6] In addition, disease severity is also different among species, *i.e.*, Asian small-clawed otters show severer lesions compared with North American river otters or Eurasian otters. Therefore, genetic factors predisposing to urolithiasis might also differ among species. As effective, preventive measures against urolithiasis in otters have not been established, periodic evaluations of uroliths would be important in captive populations such as routine abdominal radiographs, evaluation of serum creatinine and blood urea nitrogen, and urinalysis.[2]

Contributing Institution:

Laboratory of Comparative Pathology, Graduate School of Veterinary Medicine, Hokkaido University. https://www.vetmed.hokudai.ac.jp/

JPC Diagnosis: Kidney, pelvis: Oxalate urolithiasis, diffuse, severe, intratubular oxalate crystals, and diffuse moderate chronic interstitial fibrosis.

JPC Comment: The contributor provides an excellent review of urolithiasis in captive otters, which can be a significant management problem in zoological collections. Table 1 is an recapitulation of the various types of uroliths and prevalence in otter and wolverines.

Table 1. Urolithiasis in Otters and Wolverines. From Terio, McAloose. St Leger eds., *Pathology of Wildlife and Zoo Animals*., 2019.[10]

Other mustelids also develop uroliths on a fairly frequent basis, which may result in obstruction. Struvite urolithiasis is well-documented in ferrets and farmed mink. In pet ferrets, protein composition (with higher amounts of plant proteins than a wild mustelid would normally take in) are thought to be one of several causative factors. In farmed mink, urolithiasis is likely multifactorial, as the sexes have distinct seasonal predisposition to development of uroliths, with pregnant females developing stones in the spring, and male kits in the fall. Concurrent bacterial infection with *Staphylococcus intermedius* is common in mink, but bacterial infection is uncommon in the affected ferret.[10]

Oxalate nephrosis/nepholithiasis/urolithiasis is well known in a number of other species. Cheetahs, and less commonly cougars, jaguards and leopards may develop oxalate nephrosis with crystal development in tubules, acute renal failure, azotemia and death. Toxicosis, such as may be seen with ethylene glycol ingestion has been ruled out in most cases, but the pathogenesis of this disease remains unclear.[9]

Marsupials also commonly suffer from oxalate nephrosis, which is best known in the koala, but may also be seen in wallabies, possums, and potoroos. Mild oxalate neprhosis is a common finding in koalas in collections around the world, so dietary contributions are unlikely. Once again, the pathogenesis of oxalate nephrosis in these species is unknown.[5]

In domestic species, oxalate uroliths are the second most common type of calculus with small breeds such as miniature poodles, miniature schnauzers, Bichons, Lhasa Apsos and Shih-Tzus being predisposed. They may be encountered in a numbr of conditions other than ethylene glycol toxicosis, including hyperparathyroidism, hypercalcemia, and increased levels of endogenous and exogenous steroids. In ruminants (and in koalas), oxalate-degrading bacteria are a common flora of the rumen and lower tract, likely lessening the effect of a high-oxalate diet in certain locales.

Participants identified a focal area of extreme cortical and medullary atrophy of one of the lobules within the section of kidney adjacent to a large oxalate crystal. The area was interpreted as an area of obstruction if not actual pressure necrosis and focal hydronephrosis.

References:

1. Bochmann M, Steinlechner S, Hesse A, Dietz HH, Weber H. Urolithiasis in free-ranging and captive otters (*Lutra lutra* and *Aonyx cinerea*) in Europe. *J Zoo Wildl Med.* 2017;48:725-731.
2. Calle PP. Asian small-clawed otter (*Aonyx cinerea*) urolithiasis prevalence in North America. *Zoo Biol.* 1988;7:233-242.
3. Grove RA, Bildfell R, Henny CJ, Buhler DR. Bilateral uric acid nephrolithiasis and ureteral hypertrophy in a free-ranging river otter (*Lontra canadensis*). *J Wildl Dis.* 2003;39:914-917.
4. Higbie CT, Carpenter JW, Armbrust LJ, Klocke E, Almes K. Nephrectomy in an Asian small-clawed otter (*Amblonyx cinereus*) with pyelonephritis and hydronephrosis secondary to ureteral obstruction. *J Zoo Wildl Med.* 2014;45:690-695.
5. Higgins D, Rose K, Spratt D. Monotremes and marupials. . *In: Pathology of Wildlife and Zoo Animals* Terio KA, McAloose D, St Leger J eds., 2019; London: Associated Press, p. 458.
6. Niemuth JN, Sanders CW, Mooney CB, Olfenbuttel C, DePerno CS, Stoskopf MK. Nephrolithiasis in free-ranging North American river otter (*Lontra Canadensis*) in North Carolina, USA. *J Zoo Wildl Med.* 2014;45:110-117.
7. Roe K, Pratt A, Lulich J, Osborne C, Syme HM. Analysis of 14,008 uroliths from dogs in the UK over a 10-year period. *J Small Anim Pract.* 2012; 53: 634-640.
8. Simpson VR, Tomlinson AJ, Molenaar FM, Lawson B, Rogers KD. Renal calculi in wild Eurasian otters (*Lutra lutra*) in England. *Vet Rec.* 2011;169:49.
9. Terio KA, McAloose D, Mitchell E. Felidae. *In: Pathology of Wildlife and Zoo Animals* Terio KA, McAloose D, St Leger J eds., 2019; London: Associated Press, p. 268.
10. Williams BH, Burek Huntington KA, Miller M. Mustelids. *In: Pathology of Wildlife and Zoo Animals* Terio KA, McAloose D, St Leger J eds., 2019; London: Associated Press, p. 281.

CASE III: 71618 (JPC 4136426).

Signalment: Adult male big brown bat (*Eptesicus fuscus*); 24 g, wet fixed.

Wild caught, Maryland, USA. (Submitted partially fixed in 10% neutral buffered Formalin)

History: This adult male big brown bat (*Eptesicus fuscus*) was found dead two months after being captured in Maryland for use in a research colony. It had been

Kidney, big brown bat. Multiple sections of kidney are submitted for examination. One section contains multiple 2mm renal cysts, including one collapsed subcapsular cyst. (HE, 5X).

vaccinated for rabies and treated for mites, but no experimental manipulation had been performed.

Gross Pathology: The right kidney has 4 bulging, rounded, pale tan structures, 2-5 mm diameter. On cut section these are restricted to the cortex and contain pale tan, turbid fluid.

Laboratory results:

- Blood examination: increased CK 1199U/L (99-436), increased GOT/GPT and bile acids (no value available), thrombocytopenia 23 K/µL (148-484) and increased PT 18s (11-17) and aPTT 144s (72-102).

-Toxoplasmosis and Neosporosis were excluded (IgG/M-determination.)

- Parvovirosis and Angiostrongylosis were tested with a negative result.

Microscopic Description:

Expanding and compressing the renal cortex are multifocal cystic structures, which vary in size from 0.5 to 2 mm in diameter, and are surrounded by a 1-5 micron hyaline wall. The inner surface of the cyst is lined by 2-3 layers of hypertrophied and hyperplastic renal tubular epithelial cells. Epithelial cells contain numerous meronts and macrogametocytes, and rare microgametocytes. Within the cyst lumen

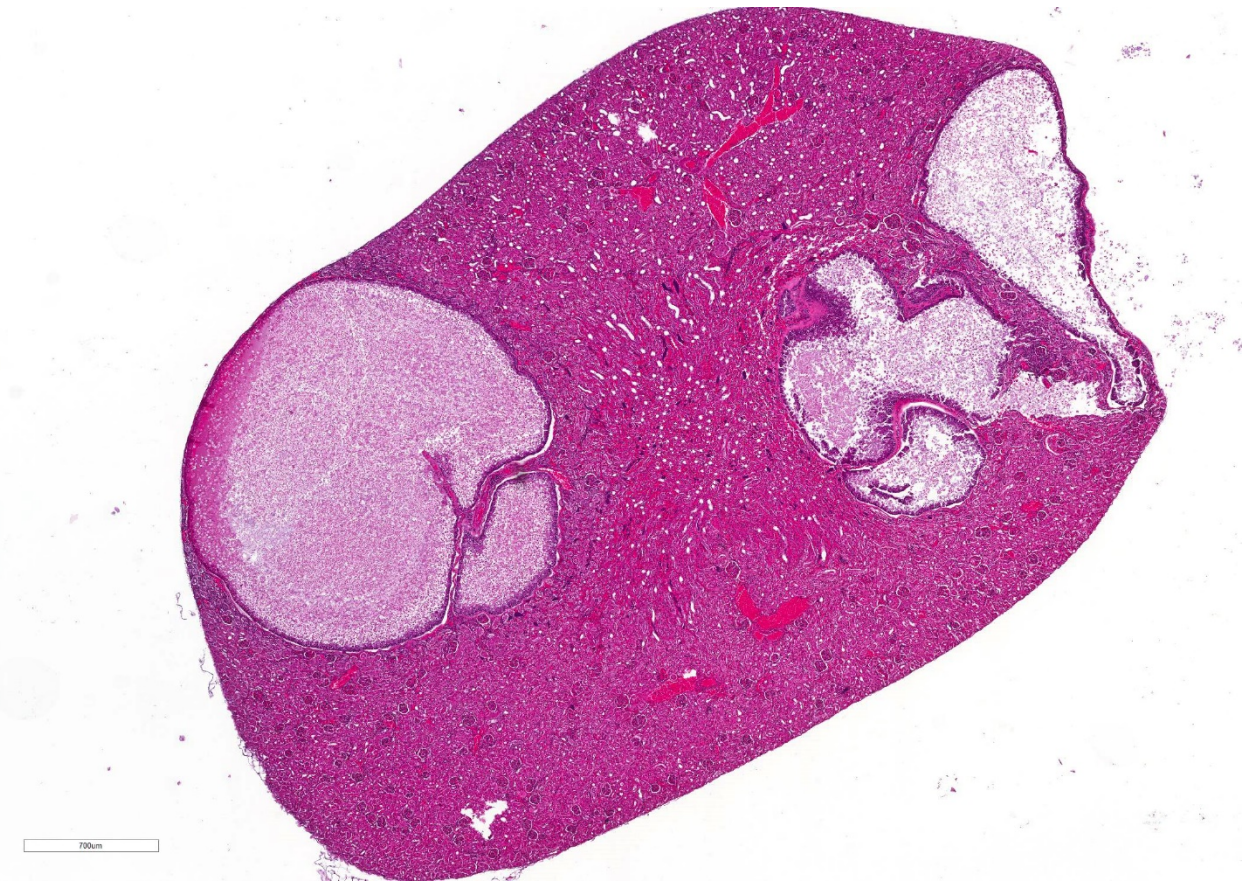

Kidney, big brown bat. Higher magnification of the renal cysts. Each cyst is lined with epithelium and surrounded by a thin eosinophilic capsule, and contain eosinophilic flocculent material. (HE, 26X).

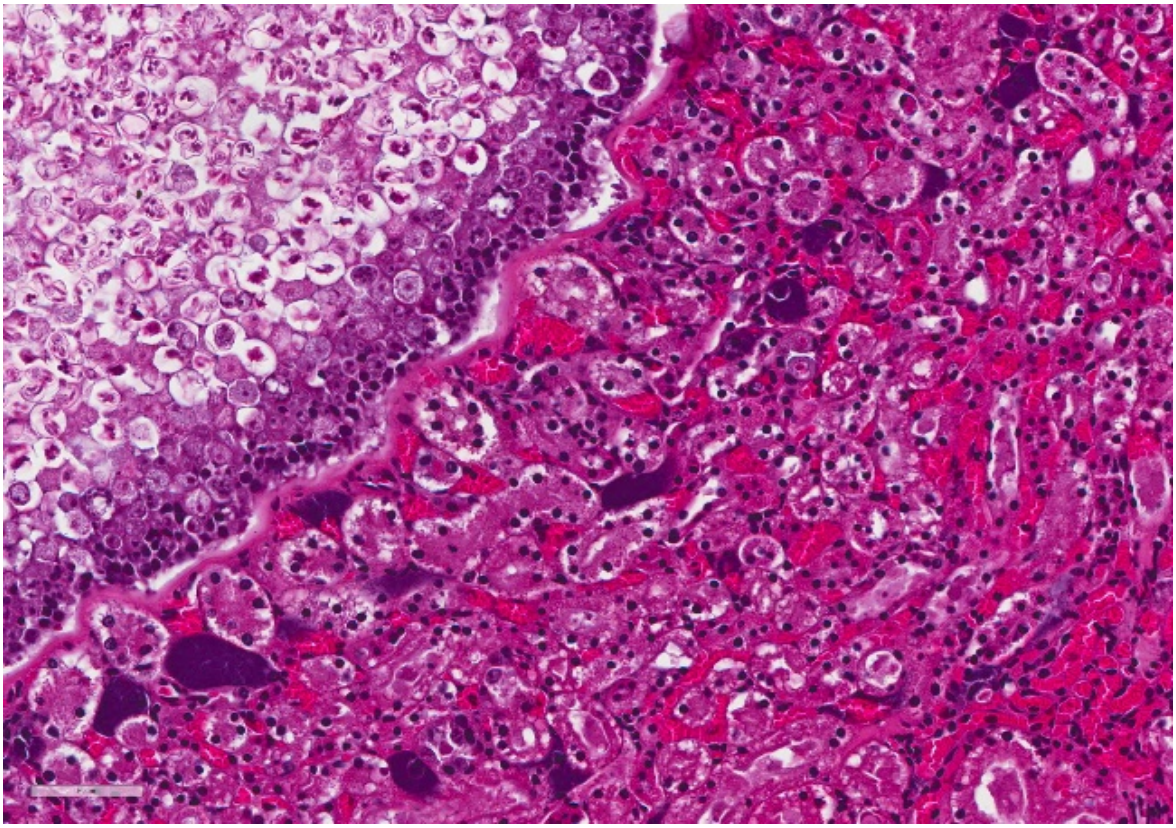

Kidney, big brown bat. Dilated tubule at upper left. The cyst is lined by hyperplasia epithelium which often contain coccidial gamonts. The lumen is filled with gametocytes and sporulating oocysts. At the periphery, there is marked congestion and capillaries often contain bacterial colonies (post-mortem overgrowth). (HE, 400X).

are numerous round-to-oval, ~15-micron diameter oocysts with a thin, delicate eosinophilic capsule, which contain 2 sporocysts each containing 4 sickle-shaped sporozoites. Within the cyst lumen are occasional erythrocytes and abundant eosinophilic debris. Scattered throughout the cortex and medulla of both kidneys are multiple rafts of deeply basophilic bacteria, with no tissue response.

Contributor's Morphologic Diagnosis:

Kidney: coccidiosis, chronic, multifocal, moderate, with cystic renal tubules

Contributor's Comment: Renal coccidiosis has recently been described as an incidental postmortem lesion in wild big brown bats, caused by the coccidian parasite *Nephroisospora eptesici*.[5] The organism was first described in 2010, after being identified in the kidneys of 29 wild big brown bats in Minnesota.[5] Although renal coccidiosis had been previously reported in other species of bats, the causative organisms had not been fully characterized.[1,2,3]

Nephroisospora eptesici is a member of the family Sarcocystidae, most closely related to *Besnoitia* spp. Unlike related apicomplexans, *Nephroisospora eptesici* has a single-host life cycle, with the complete life cycle occurring in the kidney.[5] Unlike other coccidians with a single-host life cycle, such as *Eimeria* spp., *Nephroisospora eptesici* is believed to have evolved from an

ancestor which required two hosts.[5] Thus, the single-host life cycle is a derived trait. The biology and host specificity of this organism remain to be elucidated. However, reports of morphologically similar coccidian parasites in other bats and the recent identification of *Nephroisospora* genetic material contaminating a published bat genome suggest that related organisms exist, although they have not been fully described.[1,2,3,4]

The associated gross lesions are white-to-beige spherical, well-demarcated cystic structures within the renal cortex.[5] Histologically, these structures represent cystically dilated renal tubules enclosed by a PAS-positive hyaline membrane, which contain numerous intracellular and extracellular coccidian organisms representing all life stages.[5] Oocysts within the lumen of the cystic tubules contain 2 sporocysts, which each contain 4 sporozoites.[5] Periodic acid-Schiff (PAS) and Feulgen special stains can be used to better demonstrate protozoal structures.

Renal coccidiosis due to *Nephroisospora eptesici* is rarely associated with inflammation, and is not believed to be responsible for clinical disease.[5] The primary significance of renal coccidiosis in bats is as an obfuscating factor in research. Genetic material of an undescribed *Nephroisospora* species has recently been identified as a contaminant in the published genome of David's myotis (*Myotis davidii*).[4]

Abundant intravascular bacteria, without associated inflammatory response, were noted in the kidneys and other tissues. These were considered to represent postmortem overgrowth, as no wounds or other nidus of bacterial infection were identified. Another bat autopsied from this colony had similar cystic structures in the kidneys. In that case, the structures had central mineralization, indiscernible organisms, and associated lymphoplasmacytic inflammation. These were considered to represent degenerating parasitic cysts.

Contributing Institution:

Johns Hopkins University, School of Medicine
Department of Molecular and Comparative Pathobiology
Broadway Research Building, #811

733 N. Broadway
Baltimore, MD 21205
http://mcp.bs.jhmi.edu/

JPC Diagnosis:

1. Kidney, tubules: Cysts, focally extensive, with numerous intraepithelial microgamonts and schizonts and sporulating intraluminal oocytes.

2. Kidney, tubules: Intraluminal bacterial colonies, numerous.

JPC Comment: The contributor has provided an excellent review of the species-specific renal coccidian *Nephroisospora eptesici.*

Coccidia that parasitize the kidney in their natural hosts are uncommon; the vast majority infect the gastrointestinal tract in

natural hosts. Renal apicomplexans typically infect the renal epithelium, with a number of species undergoing schizogony in more proximal segments of the tubular epithelium and gametogony in more distal aspects. Bradyzoite-laden cysts of a number of apicomplexan may be found within the kidneys, such as *Neospora* or *Besnotia*, but these cysts are usually found within inflammatory or mesenchymal cells and do not infect renal epithelium.

Klossella is an apicomplexan that infects renal tubules of horses (*K. equi*), and guinea pigs (*K cobayae*), as well as mice (*K. muris and mabokensis*), opossum (*K. tejara*), Australian water rats (*K. hydromyos*), snakes (*K. boyae*), and a number of unidentified species in other rodents and marsupials. *Klossiella sp.* characteristically undergo the first wave of schizogony in glomerular epithelial cells, with second waves of schizogony in proximal convoluted tubles and gametogony in the loop of Henle and beyond. Like most renal coccidians, clinical disease is rare; tubular nephrosis and interstitial nephritis is generally subclinical.[6]

Eimeria also has several species that infect the kidney, with *E. truncata* of geese the most well known, but also *E. boschai* and *somatarie* in ducks, and *E. christianseni* in swans and several unnamed species in owls. . These apicomplexans also rarely cause clinical disease except in young and stsress birds, which may manifest with emaciation. Severe outbreaks may result in mortality.[7]

Not all participants had seen the concentration of bacilli within the renal vessels as a postmortem findings, and their identity generated enthusiastic discussion. A Von Kossa Stain was negative, and the bacilli stained with a Brown-Brenn Gram stain.

References:

1. Boulard Y. Etude morphologique des coccidies (Adeleidae). *Klossiella killicki* n. sp. chez des microchiropterae Africans et *Klossiella tejerai* Scorza, 1957, chez un marsupial sud-americain. *Bulletin of the Museum of Natural History, 3rd series no. 284, Zoology.* 1975:194:83–89.
2. Gruber AD, Schulze CA, Brügmann M, Pohlenz J. Renal coccidiosis with cystic tubular dilatation in four bats. *Vet Pathol.* 1996;33:442–445.
3. Kusewitt DF, Wagner JE, Harris PD. Klossiella sp. in the kidney of two bats (Myotis sodalist). *Vet Parasitol.* 1977;3:365–369.
4. Orosz F. Two recently sequenced vertebrate genomes are contaminated with apicomplexan species of the Sarcocystidae family. *Int J Parasitol.* 2015;45(13):871-8.
5. Wünschmann A, Wellehan JF Jr, Armien A, Bemrick WJ, Barnes D, Averbeck GA, Roback R, Schwabenlander M, D'Almeida E, Joki R, Childress AL, Cortinas R, Gardiner CH, Greiner EC. Renal infection by a new coccidian genus in big brown bats (Eptesicus fuscus). *J. Parasitol*. 2010;96(1):178-183

6. http://www.askjpc.org/vspo/show_page.php?id=WDJ3V1B1eVJidHQyV3AwNGVZZHdmUT09
7. http://www.askjpc.org/vspo/show_page.php?id=V0Uzd2w5eFJvb3I5UllaWG9aUTNRZz09

CASE IV: 016-045846 26 (JPC 4101490).

Signalment: A 10 year-old, female intact, Red Kangaroo (*Macropus rufus)*

History: A ten year old, intact, female Red Kangaroo *(Macropus rufus)* was submitted for necropsy from a local zoo. The animal had presented acute dyspnea two days prior to death, and radiography was performed revealing extensive mixed pulmonary pattern. A large mass in the right inguinal area was noted, and the mammary gland was slightly enlarged. The animal was unresponsive to supportive care, including fluid therapy, antibiotics and analgesics, among others. Three years before, the animal had an arthrodesis and stem cell therapy in the right hock due to severe traumatic injury. Also, a wallaby peer from the same enclosure had died from gastrointestinal histoplasmosis recently.

Gross Pathology: The right axillary lymph node was moderately enlarged with a large amount of surrounding fat. On cut section, it was cavitated and contained serosanguinous fluid. The subcutis in the left inguinal area had a focally extensive area of hemorrhage, measuring 2 x 4 x 5 cm (biopsy-induced, as per the history in the submission form) with an underlying, thickly encapsulated, 2 cm in diameter, round mass with a solid, dark brown, necrotic center. The right inguinal lymph node was markedly enlarged, with a cavitated, straw-colored fluid-filled center. All other lymph nodes examined were dark-red, cavitated and fluid-filled. Bilaterally, the caudal nipples were diffusely enlarged and blue (cyanotic). The left caudal mammary gland was diffusely and markedly enlarged and firm, measuring 9 x 5 x 3 cm 2 x 0.7 x 3 cm, with two additional lobules measuring 4.5 x 3.5 x 2 cm and 2 x 1.5 x 1 cm. On cut section, they were cavitated, filled with serosanguinous fluid and a solid, tan area that contained a focal, necrotic center.

The thoracic cavity contained 130 mL of straw-colored, cloudy fluid. Affecting about 75 % of the pulmonary parenchyma, there were multifocal to coalescing, variably sized, dark red to tan, firm nodules, some of them with an umbilicated center. The pleura was diffusely thickened and cloudy. Adjacent to the right ovary and corresponding with the right lumbar lymph node, there was an approximately 6.5 x 3.5 x 3 cm, multilobulated, firm, tan mass firmly adhered to the caudal vena cava at the iliac bifurcation. The endothelium of the caudal vena cava at this site had multifocal 1 mm in diameter, firm nodules. On cut section, the mass was solid tan, with a brown, necrotic center. The pelvis of the right kidney was markedly distended with moderate atrophy of the renal medulla. Along the urinary bladder, following the ureteral insertion, there were multifocal, 4 mm in diameter, firm, tan nodules situated in a linear pattern.

Laboratory results: N/A.

Microscopic Description:

Lungs: Affecting approximately 70% of the sections examined, the parenchyma is effaced, replaced and compressed by a well-demarcated, unencapsulated, moderately cellular neoplasm arranged in acini, nests and tubules supported by a thick fibrovascular stroma, and intermixed with variably sized areas of hemorrhage and congestion. The neoplastic cells are polygonal, with variably distinct cell borders, a scant, finely vacuolated, eosinophilic cytoplasm, and a single, round to oval, vesicular nuclei with up to two

Lung, red kangaroo. Numerous 1mm noduless expand the pulmonary parenchyma. (Photo courtesy of: Kansas State University-Veterinary Diagnostic Laboratory and the Department of Diagnostic Medicine/Pathobiology, Manhattan, KS 66506. http://www.ksvdl.org/)

distinct basophilic nucleoli. There are marked features of anisocytosis and anisokaryosis with occasional binucleated cells, and there are seven mitotic figures per ten 600X fields examined. The mitotic figures are occasionally multipolar and bizarre. Frequently, the ductules formed by the neoplastic cells are filled with red blood cells, and foamy macrophages that often contain intracytoplasmic, brown, granular pigment (hemosiderin). The remaining alveolar spaces are either markedly compressed, congested or filled with an extracellular, eosinophilic fibrillar material (fibrin), hemorrhage and increased numbers of alveolar macrophages.

Liver: Affecting around 30% of the sections examined, the hepatic parenchyma is effaced, replaced and compressed by the same neoplastic population as described for the lungs. Occasionally in the portal triads, there are neoplastic cell emboli within the lumen of the vessels and there is a mild to moderate, biliary duct hyperplasia. The remaining hepatocytes, especially those in proximity of the neoplasm, contain a golden brown, granular pigment (suspected bilirubin) and several intracytoplasmic, clear vacuoles that occasionally push the nuclei eccentrically (vacuolar degeneration). The sinusoidal spaces are diffusely and mildly congested.

Contributor's Morphologic Diagnosis:

Lungs and Liver: Mammary carcinoma, metastatic.

Contributor's Comment: Other tissues affected that were histologically evaluated include right and left mammary glands, inguinal and lumbar lymph nodes, liver, lung and adrenals. Many sections had neoplastic cells as neoplastic emboli or closely associated with the vasculature. The lumbar lymph node was markedly enlarged, compressing the adjacent ureter causing unilateral hydroureter and hydronephrosis.

Immunohistochemistry for vimentin, cytokeratin (AE1/AE3) and chromogranin, as well as Grimelius staining for argyrophilic granules were performed to rule-out a neoplasm of non-mammary origin, such as neuroendocrine cells as suggested by occasional "pseudorosette-like" structures within the neoplasm. The neoplastic cells were strongly positive for cytokeratin, and the surrounding scirrhous reaction was vimentin positive. All other immuno- and histochemical-staining performed were negative (no internal control nor validation for a red kangaroo was performed for chromogranin immunohistochemical staining).

The mammary glands are classified as mammalian-specific modified subcutaneous apocrine sweat glands of ectodermal and mesodermal origin with a function of new-born nourishment and passive immunity. [2] Neoplasms are infrequently reported in *Macropodidae*, with little literature available regarding mammary adenocarcinomas in Red Kangaroos (*Macropus rufus)* which according to few studies, is the most common neoplasm along with oral squamous cell carcinomas in this species. [5] However, mammary neoplasms are exceedingly common in dogs, cats and humans. [2] In dogs, which has the highest incidence among domestic species, most mammary tumors are clinically benign regardless of their phenotype. [1, 4] Mammary carcinomas are very heterogeneous and complicated, creating increasingly intricate

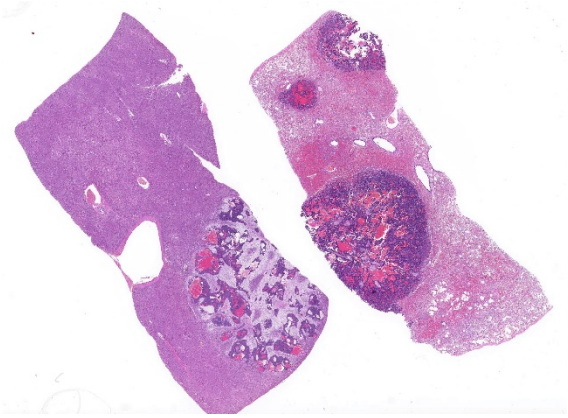

Liver and lung, red kangaroo. Both sections contain one or more well-demaracated neoplastic nodules. (HE, 6X)

classification schemes in order to characterize them. Nevertheless, simple, solid and complex carcinomas are the most prevalent type reported in the dog, with variable survival times but low metastasis. [4] It must be pointed that cytology and metastasis potential, most commonly via lymphatics, does not correlate well.[4] Dogs have a higher incidence of mammary neoplasm development in the caudal glands, while cats do not have a predilection site within the mammary chain. [4]

Generally, six main features are characterized as prognostically important in mammary tumors, which include metastasis to draining lymph node, intravascular tumor emboli, peripheral invasion, unique histological phenotype, histological grade (dysplasia and mitotic rate), and tumor size. In general, mammary carcinomas in cats with a size more than 3 cm in diameter have poorer prognosis, with shorter survival time.[1,2,4] In addition, less differentiated carcinomas have a greater metastasis chance and therefore, have shorter survival time. Many risk factors are associated in the development of mammary neoplasms in dogs and cats, such as age, reproductive status, exogenous hormone exposure, breed susceptibility, diet, and obesity.

Grading schemes for carcinomas, using an adaptation of the Elson and Ellis/Nottingham method for human breast carcinomas are available, although there are few cases with good follow-up. This scheme is based on the degree of tubular formation, nuclear pleomorphism, and mitotic index. [1,2]

According to the limited literature available, mammary tumors are one of the most common neoplasms in Red Kangaroos *(Macropus rufus)* and exceedingly common in dogs, cats and humans, with a heterogeneous, and complicated classification and characterization, but frequently malignant in the feline and benign in the canine population.

Contributing Institution:

Kansas State University-Veterinary Diagnostic Laboratory and the Department of Diagnostic Medicine/Pathobiology, Manhattan, KS 66506. http://www.ksvdl.org/

JPC Diagnosis: Liver, lung: Carcinoma, metastatic.

JPC Comment: The attendees agreed that without the history or a mammary mass, it would be difficult to identify the multiple metastatic foci as of mammary origin. We agree with the contributor's differential diagnosis of neuroendocrine carcinoma based on the morphology of the neoplastic cells as well as the tendency to form rosettes or rosette like structures within the submitted sections. In concurrence with the contributor's findings, a

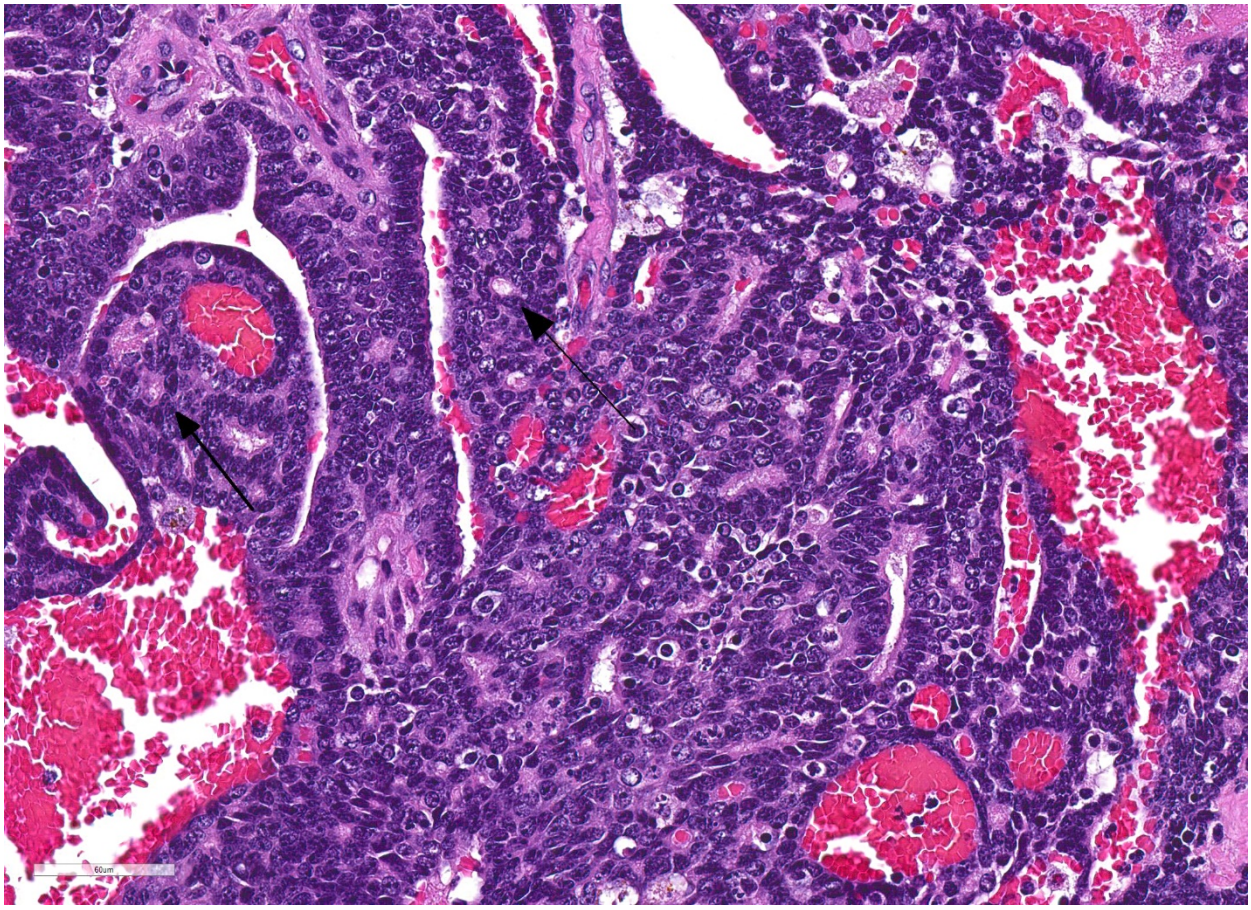

Lung, red kangaroo. The neoplasm is composed of closely packed, nest and cords of epithelial cells which occasionally form tubules (arrows). Areas of necrosis and dropout often contain hemorrhage and there are scattered individual apoptotic cells. (HE, 400X)

JPC-run chromagranin and synaptophysin were both negative in this case.

As mentioned by the contributor, neoplasia in kangaroos is likely underreported, but also appears to be relatively uncommon based on available literature. There are no previous submssions of neoplasia in kargaroos in the WSC, and no mentions of macropod neoplasia in the recently published *Pathology of Wildlife and Zoo Animals*, edited by Terio et al. In a 2007 report on 28 kangaroos autopsied in a major metropolitan zoo in the 1990's, six developed neoplastic disease, two of which were mammary neoplasia (additionally, two developed oral squamous cell carcinoma, with one lymphoma and one gastric lipoma). A review of the available literature at the time, revealed a similar incidence of reports of mammary gland adenocarcinoma (3/17) and oral cavity (3/17).

Using the tammar wallaby as a model, the mammary gland of the marsupial has recently been investigated by Khalil et al. and shows significant difference from other mammals, likely because of the type of young (extremely immature and almost fetal in nature) that it bears following an extremely short gestation (26.5) day gestation.. Pouch young remain attached to the teat for 100 days, where upon they detach and suckle periodically for up to an additional 110 days in the pouch. Marsupials have developed a lactation strategy consistnt with these distinct periods of nursing. In the phase of lactation during permanent attachment of the altricial yound, the milk is high in complex carbohydrates and low in fat and protein. Following detachment from the nipple during a period of rapid growth, eventual exit of the joey from the pouch, and a gradual involution of the mammary gland, the composition of the milk changes to a high protein, low carbohydrate composition, In addition, a number of novel milk proteins inclding SOD3 which protects agains mammary gland toxicity, as well as a number of other proteins which protect the mammary gland from potential infection during a period of milk stasis.

References:

1. Foster RA. *Female Reproductive System and Mammae.* In:Zachary JF Pathologic basis of Veterinary Disease, 6th ed. 2016:1191-1192
2. Goldschmidt MH, Peña L, Zapulli V. Tumors of the Mammary Gland. In; Meuten DJ, ed. *Tumors in Domestic Animals.* 5th ed. 2016: 723-765
3. Keller, AK , Nevarez JG, Rodriguez D, Gieger T, Gumber S Diagnosis and Treatment of Anaplastic Mammary Carcinoma in a Sugar Glider (*Petaurus breviceps*) Journal of Exotic Pet Medicine 2014; 23(3): 277-282
4. Schlafer DH, Foster RA. *Female Genital System.* In:Maxie M. G. Jubb, Kennedy and Palmer's Pathology of Domestic Animals, 6th ed; 3: 460-463.
5. Suedmeyer W, Johnson G. Survey of neoplasia in red kangaroos (*Macropus rufus),* 1992-2002, in a zoological collection Journal of Zoo and Wildlife Medicine 2007; 38(2):231-239.

Self-Assessment - WSC 2019-2020 Conference 14

1. Squamous metaplasia may be seen in which of the following organs in turtles affected with hypovitaminosis A?
    a. External ear
    b. Pancreas
    c. Kidney
    d. All of the above

2. Esophageal glandular squamous metaplasia is seen in which of the following in association with hypovitaminosis A?
    a. Ruminants
    b. Primates
    c. Birds
    d. Fish

3. Which of the following is NOT a virulence factor of *Cryptococcus*?
    a. Laccase
    b. Superoxide dismutase
    c. Phospholipase
    d. Type 3 secretion system

4. *Nephroisospora eptesici* in big brown pats is most closely related to which genus of coccidia?
    a. *Besnoitia*
    b. *Toxoplasma*
    c. *Eimeria*
    d. *Isospora*

5. Fill in the blank. Mammary glands are modified _____ glands.
    a. Sebaceous
    b. Paracrine
    c. Apocrine
    d. Holocrine

Please email your completed assessment for grading to Dr. Bruce Williams at bruce.h.williams12.civ@mail.mil. Passing score is 80%. This program (RACE program 33611) is approved by the AAVSB RACE to offer a total of 0.5 CE Credits, with a maximum of 12.5 CE Credits being available to any individual Veterinary Medical Professionals for the 2019-2020 Wednesday Slide Conference. This RACE approval is for the subject matter categories of: SCIENTIFIC using the delivery method of NON-INTERACTIVE DISTANCE. This approval is valid in jurisdictions which recognize AAVSB RACE.

Joint Pathology Center
Veterinary Pathology Services

WEDNESDAY SLIDE CONFERENCE 2019-2020

C o n f e r e n c e 15

22 January 2020

Dr. Cory Brayton, DVM, PhD, DACVP, DACLAM,
Director, Phenotypic Core
Associate Professor of Molecular and Comparative and Pathobiology
Johns Hopkins School of Medicine
Baltimore MD

CASE I: 16N131-1 (JPC 4128009).

Signalment: 3.5mo old, female, NOD.*Cg-Prkdc*^{scid}*Il2rg*^{tm1Wjl}/SzJ (NOD-SCID-gamma/NSG) mouse (*Mus musculus*)

History: This mouse was xenografted in the mammary fat pad at 6 weeks of age with tumor cells from a breast cancer patient. The mouse presented moribund, hunched and scruffy two months later, and was subsequently euthanized.

Gross Pathology: The xenograft tumor was not observed at gross necropsy. The mouse was in poor body condition, with marked depletion of external and internal adipose stores. The lungs were mottled dark red, and the spleen was dark red to black and smaller than normal. The small intestine contained small amounts of mucous, and few fecal pellets were present in the descending colon.

Laboratory results: N/A.

Microscopic Description: In sections of brain, there was a severe inflammatory infiltrate composed exclusively of mature and degenerate neutrophils within the third and lateral ventricles, extending into the subjacent neuropil of the hippocampus and cerebrum with associated fragmentation and rarefaction of the neuropil. Several colonies of short rod-shaped bacteria with peripheral clearing were observed within areas of necrosis. The meninges were expanded with a mild inflammatory infiltrate composed predominantly of neutrophils. In sections of lung, multiple arteries contained variably sized accumulations of fibrin, neutrophils, and fewer macrophages, some containing similar rod-shaped bacteria. The perivascular interstitium and alveolar walls were multifocally thickened with few neutrophils and macrophages, some of which contained intracytoplasmic bacteria. In sections of liver, there were few small inflammatory foci composed of degenerate neutrophils associated with hepatocellular

Brain, NOD SCID mouse: Multiple sections of the brain are submitted with cerebellum and brainstem (top left), diencephalon (middle) and telencephalon (inverted at bottom right). The lateral ventricles (black arrows), third ventricle (blue arrow) and fourth ventricle (green arrow) are distended and contain a cellular exudate. (HE, 5X).

necrosis and rod-shaped bacteria, and there were increased numbers of inflammatory cell infiltrates within portal areas, composed primarily of lymphocytes, macrophages, and fewer neutrophils. Occasionally rod-shaped bacteria were observed in Kupffer cells. In sections of bone marrow, there was diffuse and marked myeloid hyperplasia. Hucker-Twort gram stain on sections of brain revealed gram negative rod-shaped bacteria.

Contributor's Morphologic Diagnosis:
1. Brain: Meningoencephalitis, suppurative, locally extensive, severe, with rod-shaped bacterial colonies.

2. Lung: Pneumonia, suppurative and embolic, multifocal, moderate, with rod-shaped bacterial colonies.

3. Liver: Hepatitis, suppurative and embolic, multifocal, minimal, with rod-shaped bacterial colonies.

4. Bone marrow: Myeloid hyperplasia, diffuse, marked.

Contributor's Comment: *Klebsiella spp*. are gram-negative rod-shaped bacteria that are typically commensals in mice, and are not a significant cause of naturally occurring disease. *K. oxytoca* is ubiquitous in the environment, and can be isolated from the gastrointestinal tract, nasopharynx, lung, skin, and mucous membranes of healthy animals and humans.[2,7,14] However, these organisms may become opportunistic pathogens in certain situations, and in both humans and animals infections with *K. pneumoniae* and *oxytoca* are most commonly associated with clinical disease. *Klebsiella oxytoca* can cause suppurative lesions in various organ systems in mice, particularly the reproductive tract, where it has been associated with suppurative endometritis, salpingitis, and perioophortitis often progressing to peritonitis and abscess formation. Other reported opportunistic infections in rats and mice include perianal dermatitis, otitis media, cystitis, pyelonephritis, keratoconjunctivitis, Harderian gland adenitis, oral infection, subcutaneous, abdominal and hepatic abscesses, pneumonia, meningitis, endotoxemia and septicemia. [1,3,8,14] In humans, *Klebsiella oxytoca* and *pneumoniae* are considered important causes of nosocomial infections in hospitalized patients, and has been implicated in community acquired pneumonia, adult and

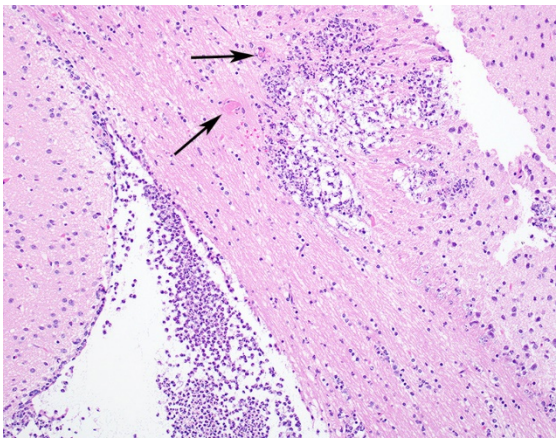

Brain, NOD SCID mouse: Neutrophils occupy the lateral ventricle and infiltrate the adjacent parenchyma, resulting in cavitation and thrombosis of parenchymal capillaries (arrows). (HE, 200X). (Photo courtesy of: In Vivo Animal Core, Unit for Laboratory Animal Medicine, University of Michigan Medical School, Ann Arbor, MI 48109 http://animalcare.umich.edu/business-services/vivo-animal-core)

neonatal sepsis and bacteremia, septic arthritis, soft tissue abscesses, and urinary tract infections, and chronic nasal infections.[1,2,10] *K. oxytoca* is also suspected to be the etiologic agent responsible for antibiotic-associated hemorrhagic colitis (AAHC) in humans, which occurs following antibiotic therapy and is characterized by bloody diarrhea, abdominal cramping and segmental hemorrhagic typhlocolitis [1,2,14]. Antibiotic therapy has been shown to promote abnormal colonization by *Klebsiella spp.* in humans[1] and rodents,[5] and an animal model of AAHC has been developed using oral administration of antibiotics in rats followed by oral infection with *K. oxytoca*.[6]

Immune status of the host plays an integral role in the pathogenesis of disease by *Klebsiella spp*. Certain strains and genetically modified mouse lines are more prone to developing lesions associated with *Klebsiella spp*. infection. Suppurative otitis media, urogenital tract infections, and pneumonia have been reported in substrains of C3H/HeJ mice and NMRI- *Foxn1*^{nu} mice, and LWE.1AR1 rats, and chronic renal inflammatory lesions and ascending urinary tract infections in NOD.Cg-*Prkdc*^{scid} *Il2rg*^{tm1Wjl}/SzJ (NSG) mice. [1,2,4,7,14] C3H/HeJ substrains are hyporesponsive to lipopolysaccharide (LPS) produced by gram-negative bacteria, due to a single amino acid substitution in the toll-like receptor 4 (TLR4) protein, NMRI- *Foxn1*^{nu} (nude) mice lack a thymus and are therefore T-cell deficient, and LEW.1AR-*iddm* rats are at risk for infection secondary to development of diabetes mellitus. Finally, NSG mice have multiple mutations including the *Prkdc* severe combined immune deficiency (scid) mutation, IL2 gamma deficiency, mutation of the C5 complement gene, and a novel MHC haplotype which leads to lack of normal T

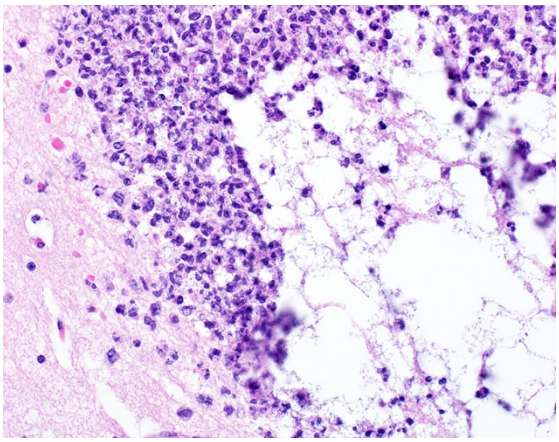

Brain, NOD SCID mouse: Neutrophils occupy the lateral ventricle and infiltrate the adjacent parenchyma, resulting in cavitation and thrombosis of parenchymal capillaries (arrows). (HE, 200X). (Photo courtesy of: In Vivo Animal Core, Unit for Laboratory Animal Medicine, University of Michigan Medical School, Ann Arbor, MI 48109 http://animalcare.umich.edu/business-services/vivo-animal-core)

and B lymphocytes and NK cells, and deficient cytokine and complement signaling and function.[4] Increasing age may also play a contributory role in pathogenesis of *Klebsiella* infection, as suppurative reproductive lesions due to *K. oxytoca* infection have been reported in National Toxicology Program (NTP) chronic chemical carcinogenesis bioassays.[3]

Klebsiella exerts its pathogenic effects by taking advantage of an immunosuppressed or immunocompromised host, and through the use of several virulence factors. The presence of a distinct polysaccharide capsule observed as a peripheral clearing on routine light microscopy is correlated with virulence of the organism, enabling it to resist phagocytosis and bactericidal components of serum.[1,7,10] In addition, several in vitro studies in humans and in mice have shown that *K. oxytoca* produces a cytotoxin, tilivalline, which induces cell death through inhibition of DNA synthesis.[2,14] Furthermore, genomic studies on tilivalline-producing *K. oxytoca* in both humans and mice revealed a number of genes associated with virulence potential.[2] Finally, a substrain of *K. oxytoca* (TNM3) has been shown to produce an immunosuppressive polysaccharide, AZ9, which is associated with decreased IL4 and IFNg responses leading to an overall depressed Th2-type immune response.[11,12]

In the present case, lesions were clearly representative of a septicemic process with multiple suppurative and embolic lesions in several organs including the lung, liver, and brain, and a myeloid response in the bone marrow. By light microscopy and gram staining, the observed peripheral clearing around the gram-negative, rod-shaped bacterial organisms is characteristic of *Klebsiella spp*. The affected animal in this case was a NSG mouse, which as previously discussed is a severely immunodeficient mouse model prone to opportunistic infection. These mice are commonly used to model development, progression, and metastasis of human tumor cells in vivo, through xenotransplantation experiments.

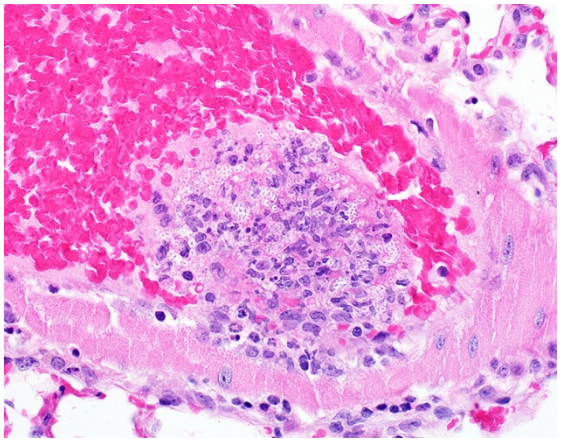

Lung, NOD SCID mouse: Septic fibrinocellular thrombi are present within the lumen of pulmonary arterioles. Incorporated macrophages and neutrophils often contain encapsulated bacilli within their cytoplasm. (HE, 400X). (Photo courtesy of: In Vivo Animal Core, Unit for Laboratory Animal Medicine, University of Michigan Medical School, Ann Arbor, MI 48109 http://animalcare.umich.edu/business-services/vivo-

The source of the infection is unknown, but it is possible that *K. oxytoca* was introduced through human contact as this organism can be spread from humans to rodents,[1] or through environmental contamination. One major concern with the presence of such opportunistic organisms in animals maintained with a well-defined hygienic status (specific pathogen-free) is that they are becoming more common and relevant as causes of disease in such colonies,[1] so

knowledge of these organisms is imperative to maintaining high standards of animal welfare and research quality. Furthermore, in experiments utilizing immunocompromised mice for serial tumor passage or xenograftment, transfer of tumor cells or other biologic material contaminated with infectious agents such as *Klebsiella* is a potential significant risk factor to the health recipient mice, as well as the quality of the experimental outcome due to morbidity and mortality secondary to opportunistic, and unexpected, infection.

Contributing Institution:

In Vivo Animal Core, Unit for Laboratory Animal Medicine

University of Michigan Medical School

Ann Arbor, MI 48109

http://animalcare.umich.edu/business-services/vivo-animal-core

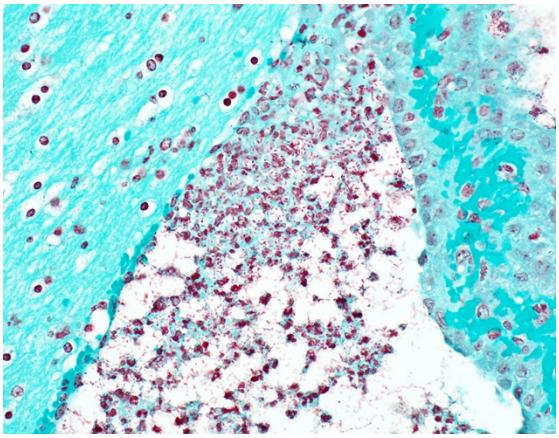

Cerebrum, NOD SCID mouse. Numerous discrete encapsulated gram-negative bacilli are present within the ventricular exudate. (Hucker-Twort, 400X) (Photo courtesy of: In Vivo Animal Core, Unit for Laboratory Animal Medicine, University of Michigan Medical School, Ann Arbor, MI 48109 http://animalcare.umich.edu/business-services/vivo-animal-core)

JPC Diagnosis: Brain: Ventriculitis, periventriculitis, and meningitis, necrotizing and suppurative, multifocal to coalescing, severe, with vasculitis, thrombosis gliosis, and numerous bacilli.

JPC Comment: The contributor has provided an outstanding and thorough review of this opportunistic infection in laboratory rodents, especially immunosuppressed models.

Tilvallin, as mentioned bythe contributor, is a gene product of *K. oxytoca* which induces apoptosis and loss of barrier integrity *in vitro* in human epithelial cells, which suggests a possible pathogenesis inhuman antibiotic-associated hemorrhagic colitis (AAHC).[12] Further investigation of the biosynthesis of this compound has demonstrated a number of other secondary metabolites, also pyrrolobenzodiazpines (PBD), including tilmysin and culdesacin. The combination of tilmysin with indole actually yields tilvallin. The PBD family of compounds are potent cytotoxic agents which demonstrate both antibacterial and anticancer activity due to DNA alkylation and formation of PBD-DNA adducts. In addition, tilvallin is also a microtubule stabilizing agent, a class of compunds that shift the balance of cellular tubulin from soluble to polymerized and are widely used as anticancer agents. This class also includes taxol, a widely used chemotherapeutic[12].

In 2011, the *Enterobacteriaceae* genus *Raoultella* (named after the French bacteriologist Didier Raoult) was separated from Klebsiella through the use of molecular techniques, as well as the identification of

growth at 10^{o} C and use of L-sorbose as a carbon source). This genus include four species: *Raoultella ornithinolytica, R. planticola, R. terrigena, and R. electrica.*[9] These bacilli are found in plants and soli in aquatic environments. R. ornithinolytica and R. planticola are considered emerging human pathogen, which results in biliary tract infections in elderly or immunosuppressed patients with malignancies or who have undergone invasive procedures. It is considered likely that a number of *Klebsiella* infections diagnosed historically may actually be of bacilli of this genus.[9]

The moderator discussed *Rodentibacter pneumotropica* as a common opportunist in immunosuppressed mice (which is usually difficult to see on HE and special stains), which highlights that the name of this common opportunist has changed within the last few years (for those who are trying to keep up with the microbiologists. The moderator also commented on the description of a "smaller than normal" spleen, as the normal weight of the spleen of an immunocompent mouse is 0.2g, and of a NOD-SCID mouse is 0.02g, highlighting not only the size difference of spleens, but the need to use absolute weights in this species. As this was a xenograft animal, the moderator wondered about the possibility of irradiation prior to engraftment in this individual further complicating this picture. Unfortunately lab data was not available in this case to distinguish between *K. oxtyoca* and *K. pneumoniae* in this case, so the moderator was loathe to pick one species over the other.

References

1 Bleich A, Kirsch P, Sahly H, Fahey J, Smoczek A, Hedrich HJ, et al.: Klebsiella oxytoca: opportunistic infections in laboratory rodents. *Lab Anim* 2008:42(3)**:**369-375.

2 Darby A, Lertpiriyapong K, Sarkar U, Seneviratne U, Park DS, Gamazon ER, et al.: Cytotoxic and pathogenic properties of Klebsiella oxytoca isolated from laboratory animals. *PLoS One* 2014:9(7)**:**e100542.

3 Davis JK, Gaertner DJ, Cox NR, Lindsey JR, Cassell GH, Davidson MK, et al.: The role of Klebsiella oxytoca in utero-ovarian infection of B6C3F1 mice. *Lab Anim Sci* 1987:37(2)**:**159-166.

4 Foreman O, Kavirayani AM, Griffey SM, Reader R, Shultz LD: Opportunistic bacterial infections in breeding colonies of the NSG mouse strain. *Vet Pathol* 2011:48(2)**:**495-499.

5 Hansen AK: Antibiotic treatment of nude rats and its impact on the aerobic bacterial flora. *Lab Anim* 1995:29(1)**:**37-44.

6 Hogenauer C, Langner C, Beubler E, Lippe IT, Schicho R, Gorkiewicz G, et al.: Klebsiella oxytoca as a causative organism of antibiotic-associated hemorrhagic colitis. *N Engl J Med* 2006:355(23)**:**2418-2426.

7 MacArthur CJ, Pillers DA, Pang J, Degagne JM, Kempton JB, Trune DR: Gram-negative pathogen Klebsiella oxytoca is associated with spontaneous chronic otitis media in Toll-like receptor 4-deficient

C3H/HeJ mice. *Acta Otolaryngol* 2008:128(2)**:**132-138.

8 Percy DH, Barthold S. W.: *Pathology of Laboratory Rodents and Rabbits*. 4th ed. Ames, IA: Blackwell Publishing; 2016: 50-72.

9. Ponce-Alonse M. Rodrigues-Rojas L, del Campo R, Canton, R, Morosini MI. Comparison of different methods for identificatio of species of the genus Raoultella: report of 11 cases of Rasoultella causing bacteraemia and literature review. *Clin Microbiol Infect* 2016; 22:252-257.

10 Sahly H, Podschun R: Clinical, bacteriological, and serological aspects of Klebsiella infections and their spondylarthropathic sequelae. *Clin Diagn Lab Immunol* 1997:4(4)**:**393-399.

11 Sugihara R, Matsumoto Y, Ohmori H: Suppression of IgE antibody response in mice by a polysaccharide, AZ9, produced by Klebsiella oxytoca strain TNM3. *Immunopharmacol Immunotoxicol* 2002:24(2)**:**245-254.

12 Sugihara R, Oiso Y, Matsumoto Y, Ohmori H: Production of an immunosuppressive polysaccharide, AZ9, in the culture of Klebsiella oxytoca strain TNM3. *J Biosci Bioeng* 2001:92(5)**:**485-487.

13. Unterhauser K, Potil L, Scheiditz GS, KKeienesberger S. *et al.* Klebsiella oxytoca enterotoxins tilimycin and tilivalline have distinct host DNA-damaging and microtubule-stabilizing activities. *Proc Natl Acad Sci USA* 2019; 116(9): 3774-3783.

14 Whary M, Baumgarth, N., Fox, J. G., Barthold, S. W.: Biology and Diseases of Mice. In: Fox JF, Anterson, L. C., Otto, G. M., Pritchett-Corning, K. R., Whary, M. T., ed. *Laboratory Animal Medicine*. 3rd ed. Amsterdam: Academic Press; 2015.

CASE II: MS18-3968 (JPC 4136806).

Signalment: Adult, male, albino, CYBB[ko] mouse, Mus musculus

History: NSG.Cybb[KO] mouse observed with scruffy hair coat, slightly hunched posture and pale ears. Mice of this strain have been spontaneously dying. These mice are on corn cob bedding and are provided with TMS antibiotic water. The feed is regular rodent chow and is autoclaved with the cage setup. The antibiotic water is made by sterilizing tap water in the autoclave and then adding TMS at the room in a Biological Safety Cabinet (BSC). The cages are sterile when they arrive at the room with aseptic technique used to transfer the mice from the dirty cage to the clean cage. All manipulation is performed in a BSC.

Spleen and pancreas, CYBB[ko] mouse. A section of spleen, pancreas, and mesentery is submitted. The spleen is 4-5 times normal thickness and normal follicular and sinusoidal architecture is not evident. (HE, 5X)

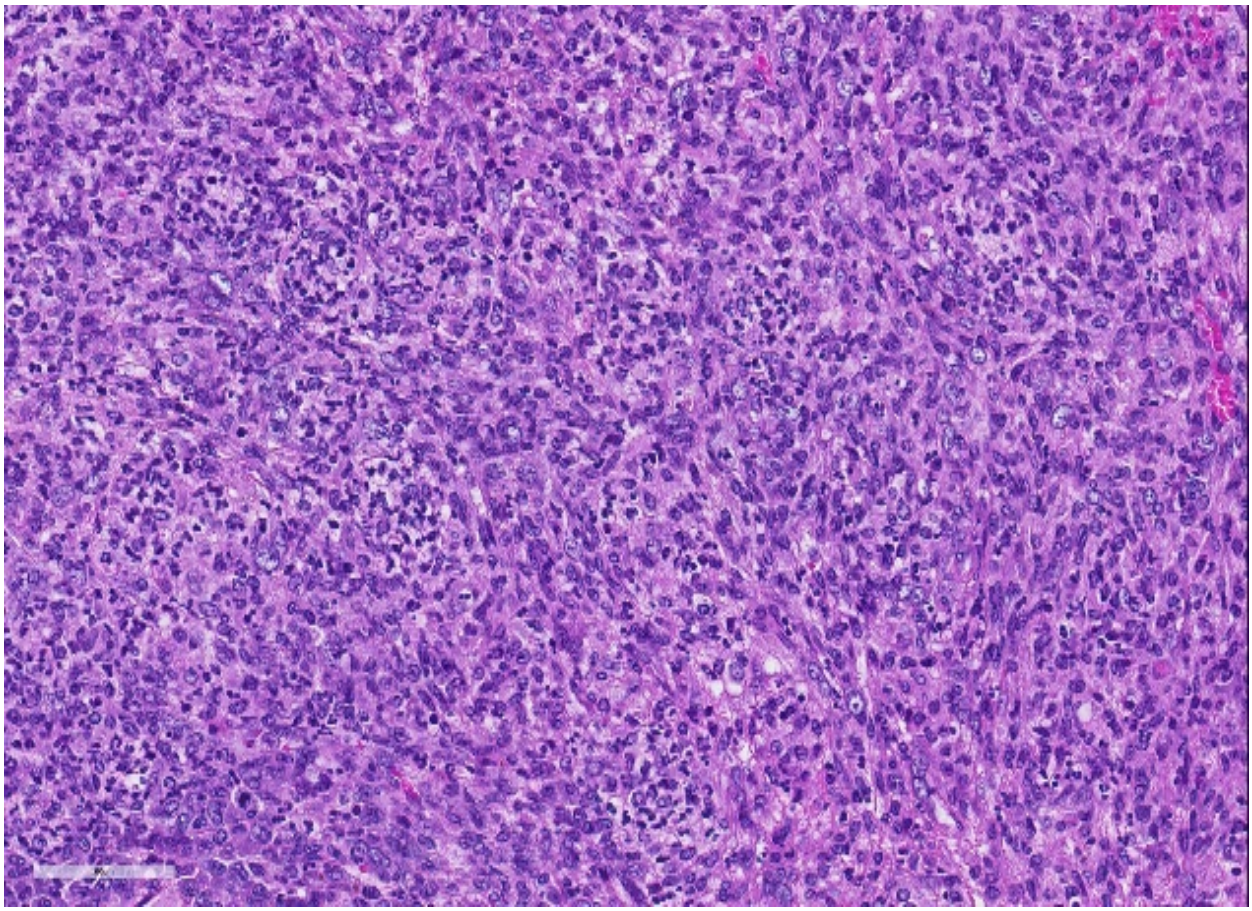

Spleen, CYBB[ko] mouse. Effacing approximately 50% of the splenic architecture in a nodular pattern are large numbers of macrophages (often spindling), admixed with large numbers of neutrophils. Mitotic figures are common. (HE, 400X)

Gross Pathology: Presented for necropsy was a live adult male white mouse. The animal appeared to be in good nutritional condition. The animal had a roughened hair coat, yet was alert and active in the transport box. The animal was euthanized with CO2.

Upon opening the carcass, adequate adipose stores were observed. The subcutis was slightly tacky indicating mild dehydration. Upon opening the peritoneal cavity, the spleen was enlarged approximately three times normal size and contained multifocal to coalescing pale tan masses that expanded above the capsular surface. The liver was also enlarged approximately three times normal size with multifocal to coalescing pale tan slightly raised masses scattered throughout.

Upon opening the pleural cavity, the lungs contained numerous light red pinpoint scattered foci. There was a 1 mm in diameter clear cyst in the right caudal lung lobe.

Lesions were not observed in the brain, heart, kidneys, pancreas, the entire male reproductive tract, and the entire gastrointestinal tract that has scant ingesta/digesta throughout and multiple formed feces in the descending colon.

Laboratory results: Microbiology yielded *Candida parapsilosis* from the liver.

Microscopic Description: Spleen – Multifocal to coalescing granulomas with epitheliod macrophages, many with neutrophils, and a coarse fibrous connective tissue network are observed. In a number of these are intracellular, one to a few, 1-5 um round to oval yeast organisms with a clear halo, and which a number are seen budding on PAS stain. The adjacent parenchyma has a moderate granulocytic hyperplasia. Similar lesions were observed in the liver, and yeast were observed in the liver, kidneys (tubulitis) and lungs (alveolitis).

Contributor's Morphologic Diagnosis:

Spleen, splenitis, pyogranulomatous and fibrosing, multifocal to coalescing, severe, chronic with intralesional yeast, *Candida parapsilosis*

Contributor's Comment:
NSG.Cybb{KO} mice are a genetically altered mouse strain that is severely immunocompromised. NSG (NOD.Cg-Prkd^{scid} Il2rg$^{tm1Wjl/}$SzJ) is a lymphocyte deficient strain, and Cybb KO (CYBB gene is located on X-chromosome, and encodes the gp91^{phox} protein) is the most common

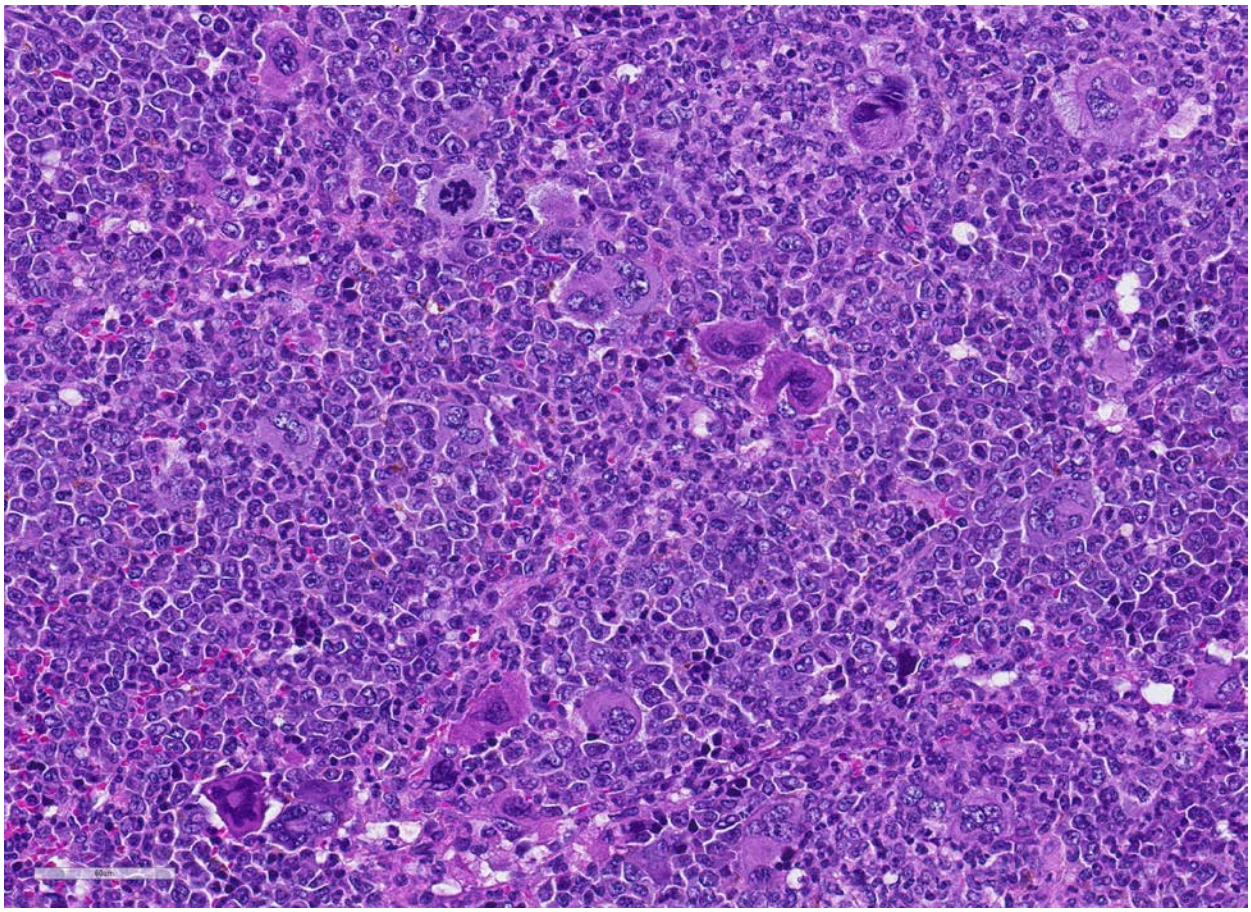

Spleen, CYBB[ko] mouse. The splenic red pulp is filled with immature granulocytes with a predominance of band cells (with doughnut-shaped nuclei), and fewer islands of hyperchromatic erythrocyte precursors as well as megakaryocytes. (HE, 400X)

form of Chronic Granulomatous Disease (CGD).[12] CGD is an immunodeficiency with a defect in phagocytes (macrophages, neutrophils) to produce reactive oxygen species (ROS) which are needed for microbicidal activity. Normally, ROS are generated by phagocyte NADPH oxidase. This enzyme is composed of 5 subunits; 2 plasma membranes and 3 cytosolic. Membrane bound are transmembrane glycoproteins (gp), one with 91kD mass called $gp91^{phox}$ (phox for phagocyte oxidase; also known as NOX2[neutrophil oxidase-2]) and a 22kD gp called $p22^{phox}$. These two form a heterodimer. The 3 cytosolic subunits ($p40^{phox}$, $p47^{phox}$, $p67^{phox}$) form a heterotrimer. The genes of the five components are CYBB [cytochrome b beta] located on the X-chromosome encoding $gp91^{phox}$, CYBA [cytochrome b alpha]encoding $p22^{phox}$, NCF1[neutrophil cytosol factor] encoding $p47^{phox}$, NCF2 encoding $p67^{phox}$, and NCF4 encoding $p40^{phox}$.[10]

The most common form of CGD involves the CYBB gene (deletion, frameshift, nonsense, missense, splice site mutation) that affects mostly males because of the predominant mode of genetic transmission (X- chromosome).[8] Interestingly, heterozygous mothers of affected males will carry a proportion of innate immune cells that are fully oxidase deficient. These individuals are prone to both infectious complications and autoimmune diseases. Of note, the risk of developing autoimmune disease was not at all related to degree of residual oxidase activity as it is in developing an infection. This suggests that even the presence of a minority of cells with absent oxidase activity predisposes to a dysregulated immune response in a dominant form.[12]

CGD appears to be a dysregulated granulomatous inflammation in various organs including the GI tract, respiratory tract, as well as the eye and urinary tract. In some patients a true autoimmune disease was exhibited; systemic lupus erythematosus, rheumatoid arthritis, inflammatory bowel disease, Sjogren's syndrome and atopic dermatitis. Interestingly, a large percentage of human patients did not show any evidence of infection.[13]

Some patients with CGD suffer from a variety of recurrent bacterial and fungal diseases. The most common bacterial infections include *Staphylococcus aureus, Klebsiella spp., Burkholderia cepacia, Serratia marcescens* and *Salmonella spp.*[9,14] Fungal infections include *Aspergillus fumigatus, A. nidulans, A. niger, A. flavus, Zygomycota* (primarily *Rhizopus spp.), Candida spp., Trichosporon spp., Paecilomyces spp., Scedosporium spp., Penicillium spp., Acremonium spp., Alternaria spp., Inonotus spp., Exophiala, Chrysosporium spp., Fusarium spp., Microascus spp., and Hansela spp.*[7,15] *A. nidulans* seems to have a unique interaction with CGD hosts.[7] *Geosmithia argillacea* has recently been shown to be mistakenly identified *as Paecilomyces spp.* in the past.[6] Dimorphic yeast form infections are exceedingly rare with only one reported case each of *Coccidioides immitis,*[14] *Histoplasma capsulatum,*[14] *and Sporothrix schenckii.*[14]

In this case *Candida parapsilosis* was the pathogenic yeast identified. *Candida* species are mainly found in the gastrointestinal tract of humans[9]. *C. parapsilosis* is found frequently on the skin and hands[11]. Although commensal, they can become pathogenic when host defense mechanisms or anatomical barriers are compromised.[10] *C. parapsilosis* is currently the second leading cause of candidemia which is associated with a high morbidity and mortality rate in humans.[12] In CGD humans, *Candida* species were isolated from meningitis, fungemia, lymphadenitis.[13]

C. parapsilosis is actually a complex of 3 distinct genetic species: *C. parapsilosis sensu stricto, C. orthopsilosis* and *C. metapsilosis.*[2,10] Polymorphisms in the genes COX3 (mitochondrial gene cytochrome oxidase subunit 3), SADH (secondary alcohol dehydrogenase) and SYA1 (putative alanyl-tRNA synthetase) distinguish the three species.[5] Virulence of *C. parapsilosis* is related to factors such as cell wall constituents, adhesion to biotic and abiotic structures leading to biofilm formation, and extracellular enzymes such as aspartic proteases, phospholipases and lipases. Aspartic proteases promote tissue colonization and invasion by rupturing host mucosal membranes. They may also aid in dispersion of biofilms. Phospholipases promote rupture of host cell membranes. Lipases help with acquiring nutrition, support fungal growth, mediate adhesion to cells and tissues, and coordinate yeast interactions with enzymes and immune cells during the infectious process.[11]

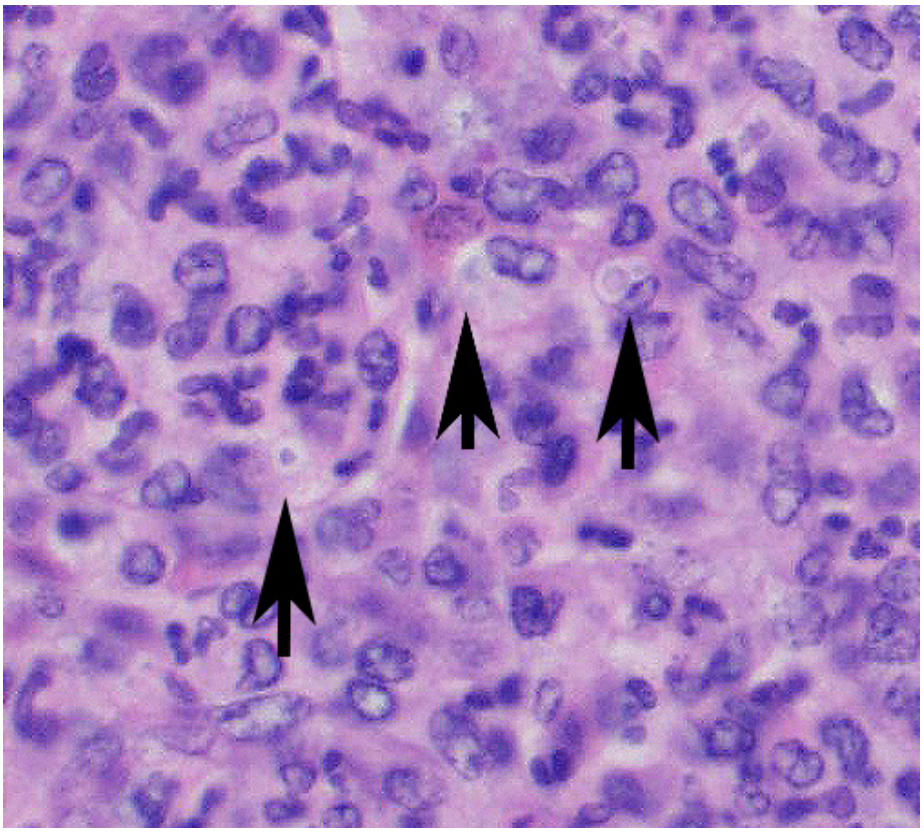

Spleen, CYBB[ko] mouse. Macrophages contain one or more 3-5um intracytoplasmic yeasts. (HE, 400X)

Initial attachment of *Candida* to host cells is followed by cell division, proliferation (forming yeast and pseudohyphae) and subsequent biofilm formation. Biofilm formation is an important virulence factor as it confers significant resistance to antifungal therapy by

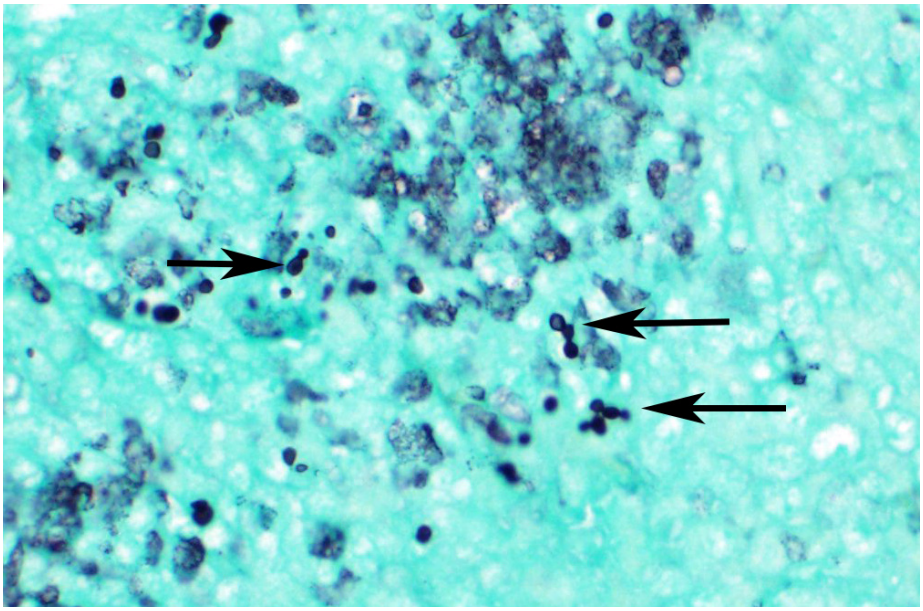

Spleen, CYBB[ko] mouse. A silver stain demonstrates budding yeasts. (GMS, 400X)

Division of Veterinary Resources
National Institute of Health
9000 Rockville Pike
Bldg. 28A, Room 107
Bethesda, MD20892

JPC Diagnosis: 1. Spleen: Splenitis, pyogranulomatous, diffuse, severe, with intrahistiocytic yeasts. 2. Spleen, red pulp: Extramedullary hematopoiesis, diffuse, severe.

limiting the penetration of substances through the matrix (water, ions, carbohydrates, proteins and nucleic acids) and protecting fungal cells from host immune responses[14]. Morphologically, *C. parapsilosis* is unable to form true hyphae, but forming pseudohyphae is associated with virulence.[11]

This case is somewhat baffling given that the animal was in a sterile environment with sterile bedding, caging and water yet still was exposed to *Candida*. However, in humans, *C. parapsilosis* is frequently isolated from hands and from sterile body sites. Thus, human transmission may have been possible. Overall, three mice developed similar lesions, with two having recognizable yeast organisms on histopathology. One should be vigilant and be alert for uncommon infections in a laboratory setting.

Contributing Institution:

JPC Comment: The contributor has provided an excellent review of this animal model of an uncommon inherited primary immunodeficiency, the mechanism of the immunodeficiency, as well as a review of Candida sp. in general as well as *C. parasilopsis*, the particular pathogen in this case.

As mentioned by the contributor, chronic granulomatous disease (CGD) is an uncommon X-linked immunodeficiency in humans resulting in frequent bacterial and fiungal infections. Patients with CGD may possess a defect in one of four different structural proteins in NADPH oxidase.[8,10] NADPH oxidase catalyzes the transfer of a single electron from NADPH to molecular oxygen, generating one of four reactive oxygen species, from the superoxide radical, including the peroxynitrite anion, hydroxyl anion, hypochlorous acid, and nitryl chloride. [8,10]

The contributor mentions the many types of fungal infection which are seen in immunsuppressed individuals. The reason for this is that mononuclear phagocyte activity is the major driver of resistance to systemic mycoses. Patients suffering from systemic mycosis have shown consistent benefit from concurrent administration of macrophage colony-stimulating factor. Patients with CGD are treated with continuous antibacterial and antifungal medications, and the only current long-term treatment is allogeneic hematopoitic stem cell transplants.

Interestingly, this WSC conference submission is not the JPC's first encounter with this mutant strain of mouse from the National Institutes of Health, Following a rotation at the Dept. of Veterinary Resources at the NIH, then resident Dr. Shannon Lacy (himself a former resident coodinator of the Wednesday Slide Conference published an article about infection seen in this same strain of knockout mice with another saprophytic fungus, *Trichosporoon beigelli*.[8] Like *Candida, Trichosporoon* is part of the normal flora of human skin and GI tract. This was the first report of disseminated trichosporoonosis in the laboratory mice of any immunosuppressed strain.[8]

The moderator noted that in this case, the yeasts in the submitted slide did not make either pseudohyphae or hyphae, which is consistent with the literature. *C. parapsilosis* apparently makes pseudohyphae in culture and within biofilms and not in tissue. It also does not produce true hyphae.

References:

1. Antachopoulos C. Invasive fungal infections in congenital immunodeficiencies. *Clin Microbiol Infect.* 2010; 16:1335-1342.
2. Bertini A, De Bernardis F, Hensgens LAM, Sandini S, Senesi S, Tavanti A. Comparison of *Candida parapsilosis, Candida orthopsilosis,* and *Candida metapsilosis* adhesive properties and pathogenicity. *Int J Med Microbiol.* 2013; 303:98-103.
3. Bonassoli LA, Bertoli M, Scidzinski TIE. High frequency of *Candida parapsilosis* on the hands of healthy hosts. *J Hosp Infect.* 2005; 59:159-162.
4. Cavalheiro M, Cacho Teixeira M. *Candida* biofilms: Threats, challenges, and promising strategies. *Frontiers Med* 2018; 5:1-15.
5. De Aguiar Cordeiro R, Alencar S, de Souza Collares Maia Castelo-Branco, et al. *Candida parapsilosis* complex in veterinary medicine: A historical overview, biology, virulence attributes and antifungal susceptibility traits. *Vet Microbiol.* 2017; 212:22-30.
6. DeRavin SS, Challipalli M, Anderson V, Shea YR, Marciano B, Hilligross D, Marquesen M, DeCastro R, et al. *Geosmithia argillacea:* An emerging cause of invasive mycosis in human chronic granulomatous disease. *Clin Infect Dis.* 2011; 52(6):e136-e143.
7. Henriet S, Verweij PE, Holland SM, Warris A. Invasive fungal infections in patients with chronic

granulomatous disease. In: Curtis N, et al. eds. *Advances in Experimental Medicine and Biology. Hot topics in infection and immunity in children IX*. New York, NY; Springer Science;2013: 27-55.
8. Lacy SH, Garnder DJ, Olson LC, Ding L, Holland SM, Bryant MA. Disseminated trichosporonosis in a murine model of chronic granulomatous disase. *Comp Med* 2003; 53(3): 303-308.
9. Rider NL, Jameson MB, Creech CB. Chronic granulomatous disease: Epidemiology, pathophysiology, and genetic basis of disease. *JPIDS.* 2018; 7(S1):S2-S5.
10. Roos D. Chronic granulomatous disease. *Br Med Bull*. 2016; 118:53-66.
11. Silva S, Negri M, Henriques M, Oliveira R, Williams DW, Azeredo J. *Candida glabrata, Candida parapsilosis,* and *Candida tropicalis:*biology, epidemiology, pathogenicity and antifungal resistance. *FEMS Microbiol Rev* 2012; 36:288-305.
12. Sweeney CL, Choi U, Liu C, Koontz S, Ha S_K, Malech HL. CRISPR-mediated knockout of Cybb in NSG mice establishes a model of chronic granulomatous disease for human stem-cell gene therapy transplants. *Hum Gene Therap.* 2017; 28(7):565-575.
13. Thomas DC. How the phagocyte NADPH oxidase regulates innate immunity. *Free Rad Bio Med*. 2018; 125:44-52.
14. Trotter JR, Sriaroon P, Berman D, Petrovic A, Leiding JW. *Sporothrix schenckii* lymphadenitis in a male with X-linked chronic granulomatous disease. *J Clin Immunol*. 2014; 34:49-52.
15. Winkelstein JA, Marino MC, Johnston RB, Boyle J, Curnette J, Gallin JI, Malech HL, et al. Chronic granulomatous disease. Report on a national registry of 268 patients. *Medicine (Baltimore)*. 2000; 79(3):155-169.

CASE III: 17-1438 1-2 (JPC 4101223)

Signalment: Two-month-old, intact female mouse, *Mus musculus*.

History: The mouse was purchased from a non-conventional vendor (pet shop) and it was enrolled in a study as model of autoimmune colitis. The animal was submitted for euthanasia and necropsy given the loss of body weight (10% in the previous 2 weeks) and hunched posture. No other mouse in the group, from the same source and in the same experimental conditions, exhibited any similar or different sign of disease.

Gross Pathology: The lung lobes are diffusely expanded, firm and mottled (Fig.1). Within the cranial regions there are

Lungs, mouse. There are extensive areas which is most prominent in the left lung. Airways are multifocally markedly ectatic, nodular in appearance and filled with exudate. (Photo courtesy of: Laboratory of Comparative Pathology; Hospital for Special Surgery, Memorial Sloan Kettering Cancer Center, The Rockefeller University, Weill Cornell Medicine. https://www.mskcc.org/research-areas/programs-centers/comparative-medicine-pathology)

multiple grey-white nodules measuring about 0.5 to 1 mm in diameter (consistent with bronchiectasis).

Laboratory results: PCR for Mycoplasma spp. on fresh frozen lung tissue was positive

Microscopic Description: About 80 % of the parenchyma is affected in a multifocal to coalescing fashion by the infiltration and accumulation of a large number of mostly viable and occasionally degenerated neutrophils, admixed with few foamy macrophages, obliterating the lumen of alveoli, bronchioles and bronchi (Fig.2). The adjacent parenchyma is atelectatic. Few bronchial and bronchiolar structures exhibit distorted outlines with dilation (bronchiectasis and bronchiolectasis), thickening of the lining epithelium with piling up of nuclei (hyperplasia), and luminal narrowing by polypoid-like structures, formed by a fibrous stalk and lined by one or more layer of cuboidal to columnar epithelium (bronchiolitis obliterans). Multifocally the respiratory epithelium is replaced by one or more layers of cells with features of squamous epithelium (squamous metaplasia, Fig. 3). Large cuffs composed of lymphocytes and plasmacells surround the intrapulmonary branches of the bronchial tree. Protein rich fluid is multifocally present within few alveoli (alveolar edema).

Contributor's Morphologic Diagnosis:

Lungs: suppurative bronchopneumonia, subacute, severe with bronchiectasis, bronchiolectasis, bronchiolitis obliterans and squamous metaplasia, consistent with *M. pulmonis* infection

Contributor's Comment: *Mycoplasma* is a genus of bacteria belonging to the order Mycoplasmatales, family Mycoplasmataceae, class Mollicutes. The class name indicates the lack of a wall around the cell membrane, which is a peculiar feature of these bacteria. As such

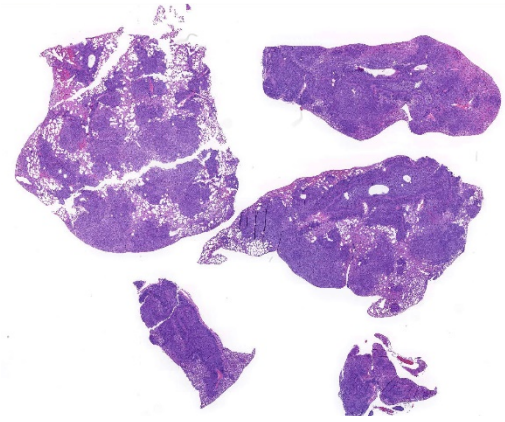

Lungs, mouse. Multiple sections of lung are submitted. Inflammatory changes are focused on airways and affect from 80-100% of each section. (HE, 6X)

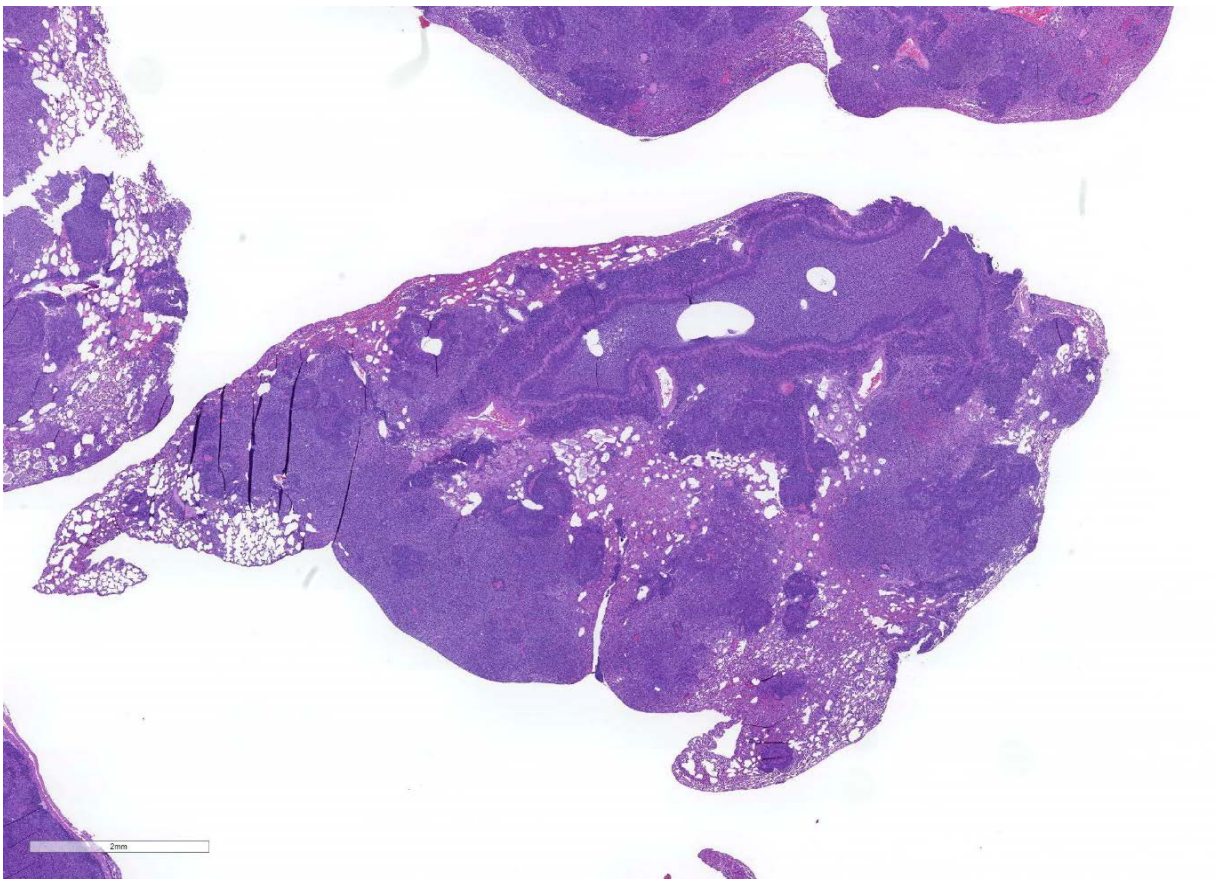

Lungs, mouse. Multiple sections of lung are submitted. Higher magnification of an affected lobe with a markedly dilated, exudate-filled airway (bronchiectasis). (HE, 15X)

they are classified as gram-indeterminate. Mycoplasmae are divided into 2 clusters: hemotropic and pneumoniae, based on 16S sequencing.

The "pneumoniae" Mycoplasma are often non-pathogenic and are found in the genital and respiratory tracts. Mycoplasma species that are hosted in laboratory mice are: *M. pulmonis*, *M. arthritidis*, *M. neurolyticum*, *M. collis*, *M. muris*, however *M. pulmonis* only is a significant pathogen.

Factors such as Sendai virus infection, high concentration of ammonia in the environment and co-infection with *Pasteurella pneumotropica* play an important role in the clinical onset of the disease in subclinically infected mice. The modern husbandry standards of mouse facilities and health monitoring plans in research institutions contributed to decrease the incidence of mycoplasmosis despite the rather high percentage of infected animals.

Overall, mice are less susceptible than laboratory rats to the disease, however susceptibility to the disease varies upon the mouse strain, with the B6 being resistant and the C3H quite sensitive. Moreover, females seem to develop more severe forms. The natural disease in immunocompetent mice is usually characterized by weight loss, respiratory symptoms and head tilt or vestibular signs in case of concomitant

otitis. Immunodeficient mice on the other hand develop arthritis.[8]

Colonization of the respiratory tract is mediated by adhesion through special organelles of *Mycoplasma* organism to cilia, with consequent ciliostasis and retention of mucus.[7]

Grossly, mucopurulent exudate can be seen in the tympanic bulla, nasal passages and airways. When the disease is subacute or even chronic consolidation of the lung parenchyma and mottling, especially in the cranioventral regions can be appreciated.

Variably sized pearl-white to tan nodules can be observed. On cut section, they reveal a wall and a lumen partially or completely obliterated by exudate that correspond to dilated bronchial structures (bronchiectasis).

Histologically, the main and most consistent features are the luminal collection of viable and degenerated neutrophils in the nasal cavities, tympanic bullae, lower airways and the infiltration of lymphocytes and plasma cells forming cuffs around bronchi and bronchioles. Abscess formation as well as squamous metaplasia of the respiratory epithelium can be observed in chronic cases.

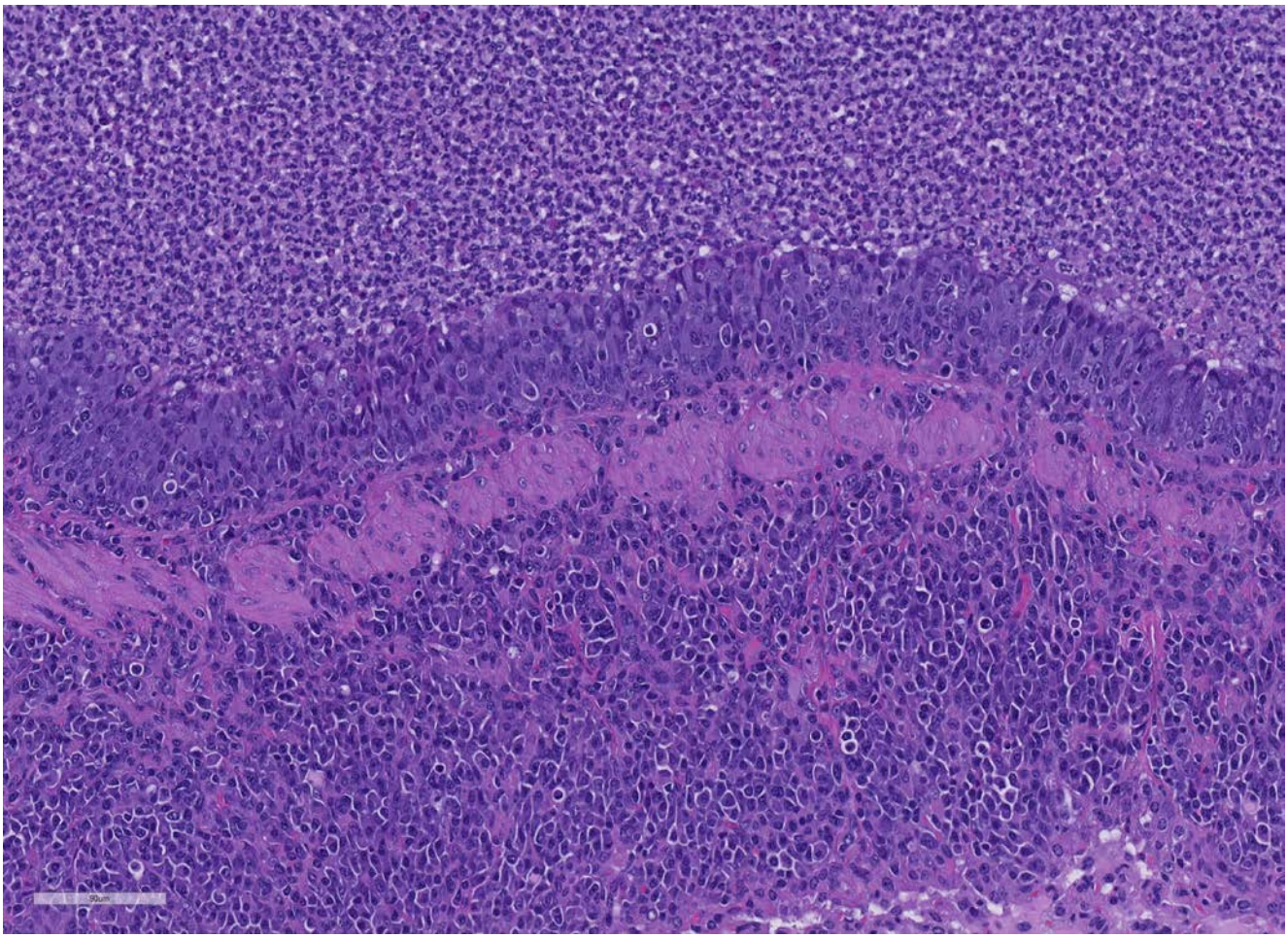

Lungs, mouse. The ectatic lumen (top) is filled with numerous viable and degenerate neutrophils. The hyperplastic epithelium (center) is infiltrated with neutrophils and lymphocytes, and below the wall of smooth muscle, there is accumulation of large numbers of lymphocytes and plasma cells. (HE, 242X)

The lymphoplasmacytic infiltrate is reported to be more prominent in rats than in mice.[8] The mycoplasmal membrane is decorated with high frequency variation antigens which act as superantigens, stimulating the humoral response in the infected host. Lymphoid hyperplasia around the airways is a consistent feature of the enzootic pneumonia of swine, caused by *M. hyopneumoniae.*[7]

Mycoplasma have the ability to establish infection thanks to several bacterial factors that prevent phagocytosis and killing by macrophages, which are the first line defense, and increased adherence to host's mucosal surfaces.[3,6,9] Capsular polysaccharide is an antiphagocytic factor.[4] *Mycoplasma pulmonis* produces a polysaccharide called EPS-I which has roles in cytoadherence, protection from complement, inhibition of biofilm formation.[1,2] It acts moreover as second shield defense against macrophage binding and phagocytosis. EPS-I appears to provide maximal defense against host response when present together with a long Vsa protein.[8] Vsa are a family of surface lipoproteins produced by mycoplasmas.[10,11-13] They vary in phase and size. Size variation in particular reduces binding of the bacteria by macrophages beside inhibiting biofilm formation and protecting from complement action similarly to EPS-I.

Contributing Institution:

Laboratory of Comparative Pathology; Hospital for Special Surgery, Memorial Sloan Kettering Cancer Center, The Rockefeller University, Weill Cornell Medicine.

https://www.mskcc.org/research-areas/programs-centers/comparative-medicine-pathology

JPC Diagnosis: Spleen: Splenitis, pyogranulomatous**,** diffuse, severe, with intrahistiocytic yeasts.

2. Spleen, red pulp: Granulocytic and myeloid hyperplasia, diffuse, severe.

3. Spleen, white pulp: Lymphoid hypoplasia, diffuse severe (consistent with genotype).

JPC Comment: Mycoplasma, in all their minimalized finery, embody much of what we know about what is actually necessary for the development of cellular life. In 1962, the National Aeronautic Space Administration (NASA) embarked on a continuing search for extraterrestial life, and suggesting that if found, it would be extremely simple, leading a generation of scholars to look on our own planet for what that form of life would resemble.[9] In doing so, the early investigations into mycoplasma, the simplest form of life with the ability of independent growth in artificial media, were purued.

Mycoplasa are indeed the essence of a "stripped down" life form, considered a "minimal" cell. They did not start as simple organisms at the base of the evolutionary tree which did not progress over billions of year, but evolved contrary to typical evolution, shedding large parts of its genome, as well as an independent lifestyle

for a very specialized parasitic one, becoming ever simpler and representing the absolute minimal requirements for cellular life.

Three species of mycoplasma have the smallest genome of all cellular life forms, with *M. genitalium*, a cause of urethritis in humans, having the smallest genome at 580,076 base pairs (contained in circular DNA).[5,9] In order to achieve this amazing housecleaning, mycoplasmas have sacrificed many of their genes, relegating themselves to a very particular parasitic (or in the case of some insect mycoplasmas) symbiont lifestyles.

One of the obvious results of the shedding of "excess genes" is their lack of a cell wall. Unlike most bacteria possess a cell wall, cell membrane, and cytoplasmic membrane, the evolutionary transition from their presumptive gram-positive roots, mycoplasma have jettisoned both the cell wall and cytoplasmic membrane, making themselves osmotically fragile and unable to live in the extra-organism (or extracellular environment for those species who live within other cells), but facilitating other interesting behavior such as direct fusion of their membranes with their host ro target cells to facilitate homeostatic or cytopathic endeavors).[9] (The lack of the a cell wall is also the reason why mycoplasma are resistant to many traditional antibiotics, which attack bacterial cell walls.)

Another reduction cementing their parasitic lifestyle is the deletion of all genes involved in amino acid, fatty acid and cofactor biosynthesis. Mycoplasma must receive all nutrients (and in the proper concentrations) from the host to survive, a feautre that prevented their growth in the laboratory for many years. Many continue to be fastidious in their requirements, often failing to grow as a result of mild "overdosing" of required amino acids or other nutrients in media.[9] (They are however, excellent parasites of cell cultures, with estimates of up to as many of 80% of cell cultures globally containing living mycoplasmas as "part of doing business".)[9]

Additional gene deletions have affected energy metabolism, leaving mycoplasmas to depend on glycolysis as their main, however ineffective means of energy production. They also are lacking in genes coding for elements of the Kreb's cycle or any cytochromes, damning these processes as "nice to have" but not essential for cellular life.[9]

One other way that mycoplasmas have adopted a stripped down life cycle is their lack of "redundant" genes. For most cellular functions in traditional bacteria, such as E.coli, each function as built-in redundancy, with anywhere from 2-6 separate genes for the same function. Mycoplasmas in generally possess a single gene for each function, which when knocked out as part of genomic investigation, most often results in death of the cell, or rarely, revision to non-pathogenicity.[9]

With all of this loss of genetic material, it is interesting that *M. genitalium*, the cellular organism with the smallest genome in the world, yet possesses twice the number of genes that investigations in the "minimal

cell set" described by molecular biologists as the requirements for life and reproduction.[5] It would appear that *Mycoplasma* as a genus still has some housecleaning to do.

One of the most interesting morphologic changes in this particular slide is the marked hyperplasia of bronchiolar epithelium which appears to extend into adjacent alveoli by lepidic growth. While the cause of this change is not evident, the moderator and other renowned mouse pathologists with whom she consulted on this case suggested the possibility of a concurrent virus which may may not have been tested for, such as Sendai or pneumonia virus of mice.

References:

1. Bolland JR, Dybvig K. *Mycoplasma pulmonis* Vsa proteins and polysaccharide modulate adherence to pulmonary epithelial cells. FEMS Microbiol. Lett. 2012;331:25–30
2. Bolland JR, Simmons WL, Daubenspeck JM, Dybvig K. Mycoplasma polysaccharide protects against complement. Microbiology. 2012;158:1867–1873
3. Davis JK, Davidson MK, Schoeb TR, Lindsey JR. Decreased intrapulmonary killing of *Mycoplasma pulmonis* after short-term exposure to NO_2 is associated with damaged alveolar macrophages. Amer. Rev. Resp. Dis. 1992;145:406–411
4. Finlay BB, Falkow S. Common themes in microbial pathogenicity. Microbiol. Rev. 1989;53:210–230
5. Glass JI, Merryman C, Wise KS, Hutchison III CA, Sith HO. Minimal cells, real and imagined. *Cold Spring Harbor Perspect Biol* 2017; 9:a023861.
6. Hickman-Davis J, Michalek SM, Gibbs-Erwin J, Lindsey JR. Depletion of alveolar macrophages exacerbates respiratory mycoplasmosis in mycoplasma-resistant C57BL mice but not mycoplasma-sensitive C3H mice. Infect. Immun. 1997;65:2278–2282
7. Maxie G. Jubb Kennedy Palmer's Pathology of Domestic Animals 6th ed. Elsevier; 2015 vol. 2: 533-35.
8. Percy DH, Barthold SW. Mouse. In: Percy DH, Barthold SW , eds. Pathology of Laboratory Rodents and Rabbits. 3rd ed. Ames, IA: Blackwell; 2007: 3–124.
9. Razin S, Yogev D, Naot Y. Molecular Biology and Pathogenicity of Mycoplasmas. *Micorbiol Mo Biol Rev* 1998; 1094-1156.
10. Shaw BM, Daubenspeck JM, Simmons WL, Dybvig K. EPS-I polysaccharide protects Mycoplasma pulmonis from phagocytosis. FEMS Microbiol Lett. 2013 Jan;338(2):155-60. doi: 10.1111/1574-6968.12048.
11. Shaw BM, Simmons WL, Dybvig K. The Vsa shield of *Mycoplasma pulmonis* is antiphagocytic. Infect. Immun. 2012;80:704–709

12. Simmons WL, Dybvig K. The Vsa proteins modulate susceptibility of *Mycoplasma pulmonis* to complement killing, hemadsorption, and adherence to polystyrene. Infect. Immun. 2003;71:5733–5738.
13. Simmons WL, Denison AM, Dybvig K. Resistance of *Mycoplasma pulmonis* to complement lysis is dependent on the number of Vsa tandem repeats: shield hypothesis. Infect. Immun. 2004;72:6846–6851.
14. Simmons WL, Dybvig K. Biofilms protect *Mycoplasma pulmonis* cells from lytic effects of complement and gramicidin. Infect. Immun. 2007;75:3696–3699.

CASE IV: 17N076 (JPC 4103914).

Signalment: ~6 months; Female; NOD.*Cg-Prkdc*^{scid} *IL2rg*^{tm1Wjl}/SzJ (aka NOD-*scid*-gamma, NOD-*scid* IL-2Rγ^{null}, NSG™ mouse); *Mus musculus*

History: A NOD-*scid*-gamma (NSG™) mouse was presented for progressive diffuse hair loss and scaling dermatitis. (NSG™

Presentation, NSG IL-2 Rg null mouse. The mouse has complete alopecia affecting the entire hair coat, with scaling dermatitis predominantly on the interscapular dorsum (Photo courtesy of: Unit for Laboratory Animal Medicine, In Vivo Animal Core, University of Michigan, 2800 Plymouth Road, B36-G178, Ann Arbor, MI 48109 http://animalcare.umich.edu/business-services/vivo-animal-core)

mice are typically fully haired). Four months prior to presentation, the mouse had undergone chemical depletion of the native hematopoietic compartment and adoptive transfer of human $CD3^+$-depleted bone marrow mononuclear cells, followed 2 weeks later by human $CD3^+$ T cell transfer. The experimental intent was to create a humanized hematopoietic system, which could then be used to assess effects of experimental agents on the hematopoietic system.

Gross Pathology: The mouse had complete to partial alopecia affecting the entire hair coat, with scaling dermatitis predominantly on the interscapular dorsum

Laboratory results:

- PCR was performed on skin using primers specific for *Corynebacterum bovis*: results were negative
- Aerobic culture of skin grew few - *Staphylococcus aureus* and rare *Enterococcus faecium*

Microscopic Description: Skin: In sections of haired skin, there is multifocal vacuolar change within the basilar epidermal and adnexal epithelium, evidenced by shrinking and separation of adjacent keratinocytes with occasional intracytoplasmic vacuolation and occasional dyskeratosis. Shrunken cells with pyknotic nuclei, consistent with apoptotic keratinocytes, are multifocally present in the same areas. Additionally, there is a mild to moderate interface and adnexal dermatitis comprised of lymphocytes and macrophages adjacent to and infiltrating the basal epithelium, outer root sheath of follicular epithelium, and sebaceous gland epithelium. Multifocal lymphocytic and macrophagic dermal infiltration and mild dermal fibrosis are also present. The overlying epidermis has moderate diffuse orthokeratotic hyperkeratosis and the stratum granulosum is prominent (hypergranulosis).

Other organs evaluated (not shown) included the lungs, liver, kidneys, uterus, spleen, mesenteric lymph nodes, pancreas, gastrointestinal tract, and bone marrow. The lungs contained diffuse peribronchial and peribronchiolar lymphocytic infiltration, with occasional intraepithelial infiltrates. The liver and kidneys showed infrequent, perivascular and peribiliary (in liver) mononuclear to lymphocytic infiltration. The bone marrow, spleen, and lymph nodes were highly cellular with appropriate distribution of erythroid and myeloid precursors in marrow and red pulp and with appropriate lymphoid cellularity and organization in the spleen and lymph nodes.

Contributor's Morphologic Diagnosis:

Skin: Dermatitis, interface and adnexal, lymphohistiocytic, with basilar vacuolar change, orthokeratotic hyperkeratosis, and dermal fibrosis, chronic, multifocal, moderate

Contributor's Comment: The gross and histologic findings in this case were consistent with graft-vs-host disease secondary to a protocol intended to generate immunologically "humanized" mice.

NSG™ mice[2,7] have three immune-related defects, consisting of:

1) The genetic background "NOD/ShiLtJ", which is a polygenic defect of the innate immune system resulting in impaired phagocytosis and defective antigen presentation by macrophages and dendritic cells
2) Severe combined immunodeficiency ("scid") mutation arising from loss of function of the gene *Prkdc*. *Prkdc* encodes the catalytic subunit of the protein complex that controls ligation of V(D)J DNA fragments during T cell receptor or immunoglobulin gene recombination in lymphocytes. Its absence results in failure to generate mature, functional B or T lymphocytes.
3) A targeted null mutation of the IL2 receptor γ chain, which blocks receptor recognition of cytokines IL-2, IL-4, IL-7, IL-9, IL-15, and IL-21. This further impacts murine hematopoietic development and results in a lack of mature, functional NK cells (development requires IL-15).

Because of these broad immunologic defects, NSG™ mice are often the recipient strain of choice for experimental engraftment, including the transfer of human

Haired skin, NSG IL-2 Rg null mouse. Three sections of skin are presented for examination. (HE, 6X)

hematopoietic cells to generate mice with a "humanized" immune system.[2,7] These humanized mouse protocols involve irradiation or chemical depletion of the native murine hematopoietic compartment and transfer of either human fetal bone marrow, liver, and thymus (BLT) or human bone marrow or peripheral blood-derived $CD34^+$ stem cells. Engrafted cells migrate to bone marrow and differentiate to all lineages of the mature immune system.

Humanized mouse protocols carry the potential for development of graft-vs-host disease (GVHD), in which human donor T cells are primed against murine antigens presented by graft-derived human cells, generating an immune response against murine host tissues. To avoid this, grafts are typically depleted of mature CD3+ cells to allow immature T cells, which will ostensibly regard host tissues as "self", to develop from the graft. Nevertheless, GVHD has been reported in humanized NSG™, most commonly in mice receiving BLT, but occasionally in mice receiving $CD34^+$-selected, $CD3^+$-depleted stem cells grafts.[2-5] Engraftment of non-$CD3^+$-depleted, peripheral blood mononuclear cells (PBMCs) has also been used to purposefully induce GVHD for study of pathogenesis or interventional strategies.[1,3]

In this mouse, the most severely affected organs were the skin and the lung. Organs affected by GVHD in NSG™ mice resemble those targeted in human GVHD, with skin, lung, liver, gingiva, and intestinal tract variably affected, depending on the type of graft, the individual mouse, or the stage of disease.[3,6] Organ specificity may relate to T cell homing receptor expression.[1] GVHD can occur acutely or have a more insidious, chronic course. Chronic GVHD may have a more complicated pathogenesis involving autoantibody production and impaired development of central or peripheral tolerance in graft-derived T cells. In both acute and chronic GVHD, MHC I-mediated presentation of murine antigen by graft-derived cells plays a key role, as GVHD preferentially occurs in mice receiving human grafts with specific HLA class I antigen haplotypes, particularly those associated with autoimmune disease in humans.[5] GVHD in this mouse clinically resembled chronic GVHD as it occurred 4 months after grafting- this is much longer than the typical presentation of acute GVHD in NSG mice (3-4 weeks post-engraftment).[9]

The key feature of cutaneous GVHD is interface dermatitis with basilar keratinocyte apoptosis.[5] This ranges from a mild interface dermatitis with vacuolar change to a lichenoid (band-like) infiltration. In chronic GVHD, orthokeratotic hyperkeratosis and dermal fibrosis (dermal sclerosis) become more prominent and inflammation may be more severe, although there is considerable variation and features of acute and chronic GVHD may be present in the same individual.[5]

The key feature of chronic pulmonary GVHD in humans is the appearance of bronchiolitis obliterans, believed to result from chronic inflammation and fibrotic remodeling of small airways. In this mouse case, bronchiolitis obliterans was not apparent and changes were confined to a

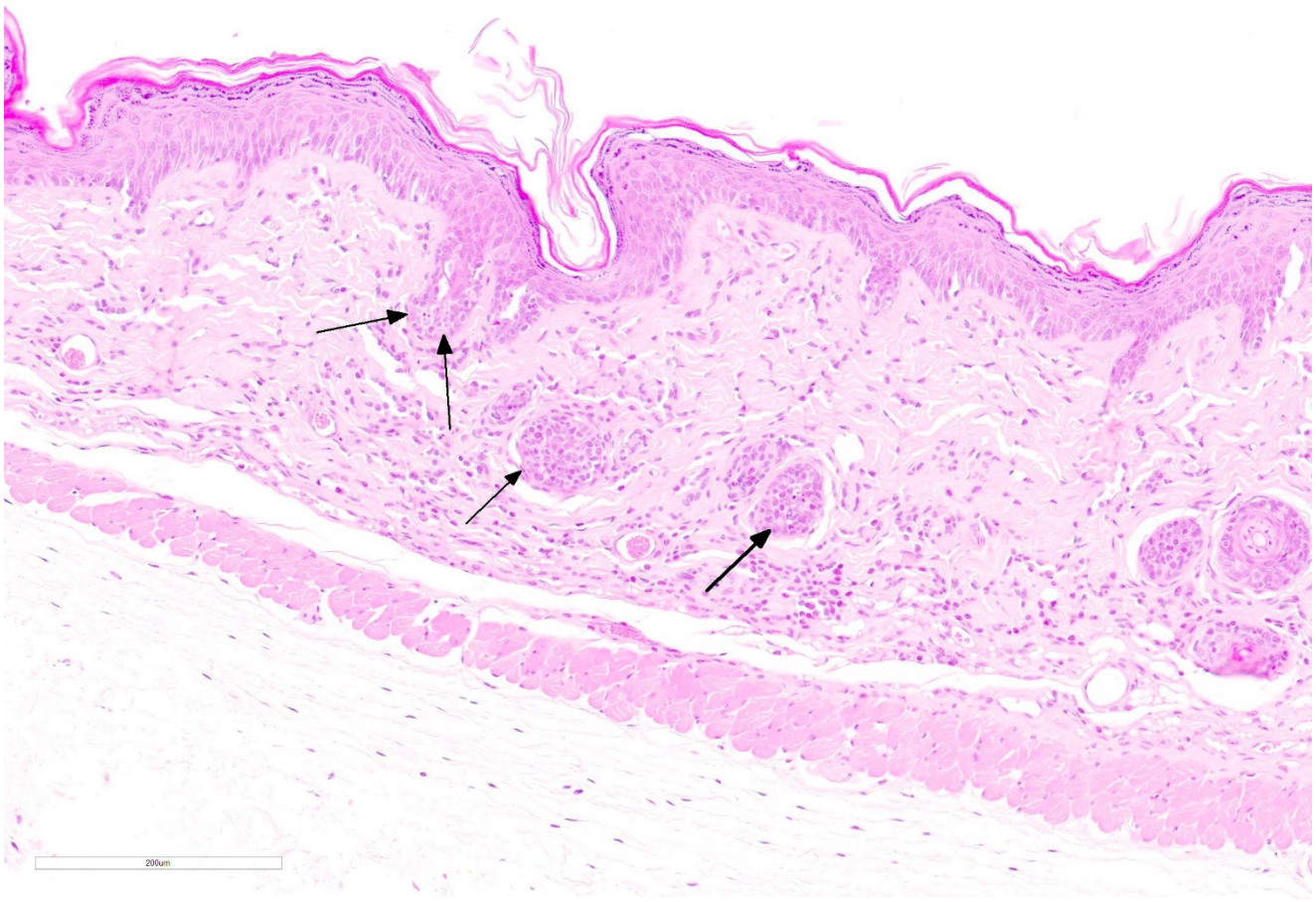

Haired skin, NSG IL-2 Rg null mouse. There is mild lymphohistiocytic interface dermatitis of the epidermis, follicles, and adnexa; and intercellular edema of the the basal epithelium. (HE 400X) ((Photo courtesy of: Unit for Laboratory Animal Medicine, In Vivo Animal Core, University of Michigan, 2800 Plymouth Road, B36-G178, Ann Arbor, MI 48109 http://animalcare.umich.edu/business-services/vivo-animal-core)

pronounced lymphohistiocytic bronchiolitis. It may be that fibrotic changes of the airway would develop with time. A recent survey of human patients with clinically suspected GVHD-associated bronchiolitis obliterans showed that 9 of 33 biopsies showed only lymphocytic bronchiolitis without fibrosis – this may represent an earlier stage of disease progression.[5]

Contributing Institution:

Unit for Laboratory Animal Medicine
In Vivo Animal Core
University of Michigan
2800 Plymouth Road, B36-G178
Ann Arbor, MI 48109

http://animalcare.umich.edu/business-services/vivo-animal-core

JPC Diagnosis: Haired skin: Dermatitis, lymphohistiocytic, diffuse, mild to moderate, with epidermal and follicular basal cell apoptosis, intra- and extracellular edema, epidermal hyperplasia, hypergranulosis, and orthokeratotic hyperkeratosis.

JPC Comment: For a wide range of hematologic malignancies, a cure is only availble through the use of allogeneic hematologic stem cell transplants (allo-HSCT).[4,7,8] Over a million of these procedures have been completed within the last decade[4], in which a combination of radation and chemotherapy is used to eliminate neoplastic or genetically abnormal cells of the hematopoetic compartment which are then replaced with hematopoetic stem cells from an allogeneic donor possessing differences in human leucocyte antigens (HLA) or major (MHA) and minor histocompatibility antigens (miH).[4] In the most simple terms, the syndrome of graft-versus host disease results from when cells from an immunocompetent donor recognize and attack the tissues of the immunocompromised recipient (who is incapable of mounting a response against the donor's cells). GHVD is a major cause of morbidity in allo-HSCT recipients, affecting up to 40-60%, and also accounting for 15% of mortality.[7]

In humans, cutaneous GVHD is considered the earliest and most common manifestation and may wraant a poor progosis.[4,7] A macular rash affecting a number of body parts, including the palms and soles, is its hallmark. This condition, in addition to vomiting and jaundice resulting from small bile duct damage and cholestasis, forms the basis for early diagnosis of acute GVHD.[8]

GVHD is divided into classic acute GVHD in which symptoms appear within 100 days (often 2-3 weeks following engraftment) and are consistent with the triad described above, and late onset acute GVHD which also shares these symptoms but appears after 100 days. Chronic GVHD represents 50% of all cases and 25% of mortalities occurs after the 100 day period.

In humans, the rash seen in aGVHD are usually centered on hair follicles, a useful early sign for diagnosis.[4,7] Histologically, the lesion in humans is very similar to that seen in the mouse model (and in this case), with vacuolar degeneration of the basal layer, dyskeratotic keratinocytes, and a mild lymphocytic infitrate at the dermo-epidermal junction that may infiltrate the epidermis beginning at the rete ridges and hair follicles.[7] The population of lymphocytes is predominantly $CD4^+$ and $CD8^{+,}$ and their presence in the epidermis suggests that they are donor lymphocytes attacking keratinocytes expressing different MHA antigens.[8]

Chronic forms of cutaneous GVHD (cGVDH) appear to be more common overall, and are reported in between 60 and 80% of patients. The most commonly recognized forms include lichenoid GVHD and sclerodermatous cGVHD. Lichenoid cGVHD exhibits most of the histologic signs descrbed about, with a macular hyperkeratotic rash. Sclerodermatous cGVHD may result in fibrosis at any level of the skin and ultimately may be disfiguring.[7]

One positive aspect of GVHD is associated with an effect known as graft-versus-leukemia (GVL). It well-documented that these patients have lower relapse rates of hematologic malignancies, and is a useful benefit in paitents with reduced intesity regimens to clear the body of neoplastic hematologic cells.[4]

Many participants had *Corynebacterium bovis* on ther list of differentials, but the moderator pointed out the lack of follicular hyperkeratosis, the mininal inflammation, and the proliferation of the stratum spongiosum, rather than the stratum granulosum, as in this case.

References:

1. Ali N, Flutter B, Sanchez Rodriguez R, *et al*. Xenogeneic graft-vs-host disease in NOD-*scid* IL-2Rγ^{null} mice display a T-effector memory phenotype. *PLoS One*. 2012; 7(8):e44219.
2. Ishikawa F, Yasukawa M, Lyons B, *et al.* Development of functional human blood and immune systems in NOD/SCID/IL2 receptor (gamma) chain (null) mice. *Blood.* 2005; 106(5):1565-73.PMC1895228.
3. King MA, Covassin L, Brehm MA, *et al*. Human peripheral blood leukocyte non-obese diabetic-severe combined immunodeficiency-interleukin-2 receptor gamma chain gene mouse model of xenogeneic graft-vs-host-like disease and the role of host major histocompatibility complex. *Clin Exp Immunol.* 2009;157(1):104-18.
4. Rodriguez KS, Oliverira-Ribeiro C, de Abreu Fiuza Gomes S, Knobler R. *Am J Clin Dermatol* 2018; 19:33-50.
5. Shulman HM, Cardona DM, Greenson JK, *et al*. Histopathologic diagnosis of chronic graft-vs-host disease. NIH consensus development project on criteria for clinical trials in chronic graft-vs-host disease. II. The 2014 Pathology Working group report. *Biol Blood Marrow Transplant*. 2014; 21(4):589-603.
6. Sonntag K, Eckert F, Welker C, *et al.* Chronic graft-vs-host-disease in CD34+ humanized NSG^{TM} mice is associated with human susceptibility HLA haplotypes for autoimmune disease. *J Autoimmun*. 2015; 62:55-66.
7. Villareal CDV, Perez JCJ, Alanis JCS, Candiani JC. Cutaneous graft-versus-host disease after hematopoietic stem cell transplant – a review. *An Bras Dermatol* 2016; 91(3):336-343.
8. Zeiser R, Blazar BR. Acite graft-versus-Host diseas biology, prevention, and therapy.
9. https://www.jax.org/strain/005557

Self-Assessment - WSC 2019-2020 Conference 15

1. Which of the following is not a predisposing factor for *Klebsiella oxytoca* infection?
    a. Age
    b. Immunosuppression
    c. Gender
    d. Antibiotic administration

2. Chronic granulomatous disease is an inherited immunodeficiency resulting from deficiency of what in phagocytes?
    a. Lysozyme
    b. Reactive oxygen species
    c. DNA ligase
    d. Mitochondrial ATPase

3. Which of the following gene families is still viable in mycoplasma?
    a. Adhesins
    b. Cell wall
    c. Amino acid biosynthesis
    d. Kreb's cycle

4. Coinfection with which other bacterium may result in clinical onset of symptoms in mice infected with *Mycoplasma pulmonis*?
    a. *CAR bacillus*
    b. *Pasteurella pneumotropica*
    c. *Proteus vulgaris*
    d. *Mycoplasma arthriditis*

5. Which is not part of the histologic lesion of cutaneous graft-versus-host disease?
    a. Interface dermatitis
    b. Basilar cell vacuolation
    c. Basilar keratinocyte apoptosis
    d. Mitoses at all levels of the epidermis

Please email your completed assessment for grading to Dr. Bruce Williams at bruce.h.williams12.civ@mail.mil. Passing score is 80%. This program (RACE program 33611) is approved by the AAVSB RACE to offer a total of 0.5 CE Credits, with a maximum of 12.5 CE Credits being available to any individual Veterinary Medical Professionals for the 2019-2020 Wednesday Slide Conference. This RACE approval is for the subject matter categories of: SCIENTIFIC using the delivery method of NON-INTERACTIVE DISTANCE. This approval is valid in jurisdictions which recognize AAVSB RACE.

Joint Pathology Center
Veterinary Pathology Services

WEDNESDAY SLIDE CONFERENCE 2019-2020

C o n f e r e n c e 16

29 January 2020

Dr. Ingeborg Langohr, DVM, PhD, DACVP
Professor
Department of Pathobiological Sciences
Louisiana State University School of Veterinary Medicine
Baton Rouge, LA

CASE I: S1809996 (JPC 4135077).

Signalment: A 3-month-old, male, mixed-breed pig (*Sus scrofa*)

History: This pig had no previous signs of illness, and was found dead.

Gross Pathology: Approximately 70% of the lungs, primarily in the cranial regions of the lobes, were patchy dark red, and firm compared to the more normal areas of lung.

Laboratory results: Porcine reproductive and respiratory syndrome (PRRS) PCR was positive from splenic tissue, and PRRS IHC was strongly immunoreactive within the cytoplasm of macrophages in the affected lung tissue. Porcine influenza virus PCR, porcine circovirus – 2 IHC, and *Mycoplasma hyopneumoniae* IHC were all negative. Small numbers of *E. coli* were isolated from the cranioventral lung with aerobic culture.

Microscopic Description: The interstitium within the section is diffusely infiltrated by moderate to large numbers of predominantly mononuclear cells along with edema. There is abundant type II pneumocyte hyperplasia lining alveolar septae and many of the alveolar spaces have central areas of necrotic macrophages admixed with other mononuclear cells and fewer neutrophils. Occasionally there is free nuclear basophilic

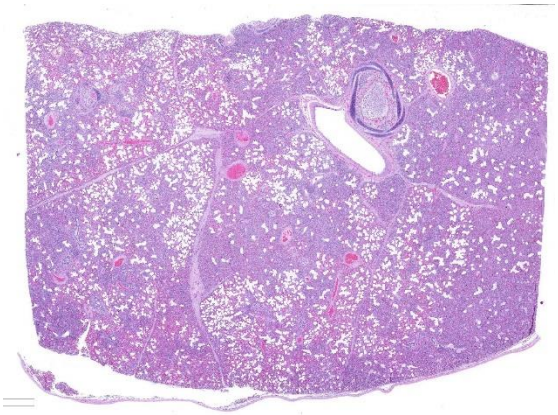

Lung, pig (HE, 6X). There is diffuse consolidation of the lung. At low magnification, airway are filled with exudate and the pleura and interlobular connective tissue are mildly expanded.

debris in these alveolar spaces as well as proteinaceous fluid. Bronchioles are occasionally variably filled with neutrophils, and many regions of BALT are mildly hyperplastic.

Contributor's Morphologic Diagnosis:

1. Lung: severe, acute, regionally extensive to patchy, interstitial pneumonia with marked type II pneumocyte hyperplasia and intra-alveolar macrophage necrosis
2. Lung: mild, acute, multifocal, cranioventral bronchopneumonia with mild BALT hyperplasia

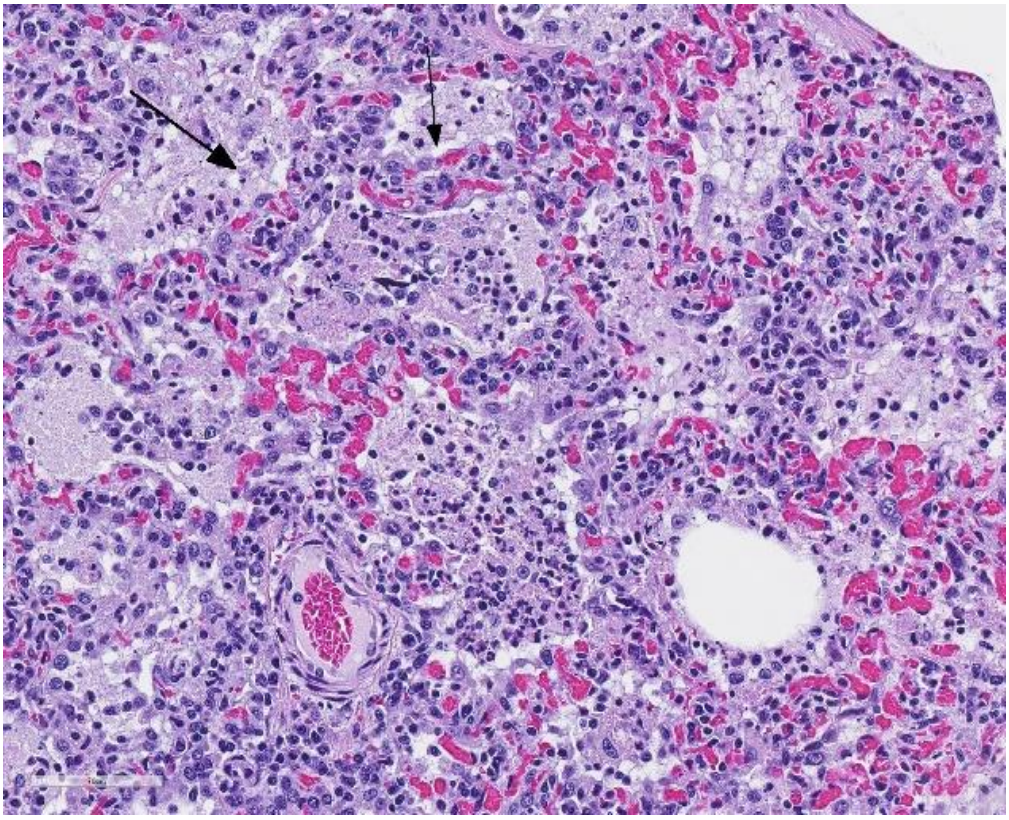

Lung, pig. Alveolar septa (arrows) are markedly expanded by a combination of macrophages (infiltrating and activated intravascular), congestion and edema. (arrows). Alveoli are filled with viable and degenerate neutrophils,

Contributor's Comment: Gross and histologic lesions were consistent with a patchy, severe interstitial pneumonia in this case. The most predominant features of the pneumonia were abundant type II pneumocyte hyperplasia as well as the large number of necrotic macrophages admixed with basophilic nuclear debris within the alveolar spaces. These histologic features are highly suggestive of porcine reproductive and respiratory syndrome (PRRS) virus induced interstitial pneumonia; however these features are not always present depending on the chronicity of the pneumonia, among other variables.[2] PRRS virus was detected in the affected lung with PCR and large numbers of macrophages had strong cytoplasmic immunoreactivity with PRRS IHC.

PRRS is caused by PRRS virus, an arterivirus, and is characterized by two overlapping disease presentations, reproductive impairment or failure, and respiratory disease in pigs of any age.[4] It causes estimated yearly economic losses of 660 million dollars in the USA and similar losses in most other countries.[1] The respiratory syndrome is seen more often in young growing pigs but also occurs in naïve finishing pigs and breeding stock.[4] In the respiratory syndrome, the virus is transmitted from an infected pig to the tonsil

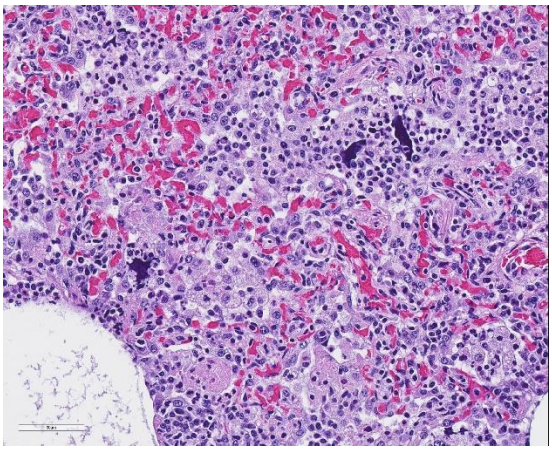

Lung, pig. Deeply basophilic aggregates of degenerated chromatin are often reported in in cases of PRRS. (HE, 354X)

or upper respiratory system of another pig where primary replication occurs in lymphoid tissues.[4] Viremia follows and may persist for several weeks.[4] The virus infects and compromises the function of pulmonary alveolar and intravascular macrophages resulting in interstitial pneumonia and appears to increase susceptibility of the lungs to other pathogens.[2] Secondary bronchopneumonia is common as was present in the current case.

Systemic infection commonly results in lymphocytic infiltrates in multiple organs, including lymphoplasmacytic rhinitis, myocarditis, endometritis and myometritis, and lymphohistiocytic meningoencephalitis and choroiditis, characterized by perivascular cuffs, vasculitis, gliosis and glial nodules.[2] Vasculitis, fibrin thrombi and rarely fibrinoid necrosis may occur in any organ.[2] A mild mononuclear vasculitis within the brain was also present in the current case, presumably due to PRRS.

Some pigs survive infection and become carriers, which is epidemiologically the most significant aspect of the infection. Commonly, once in a herd, this virus will persist indefinitely as the virus causes immune dysregulation during a critical time in immunological development, allowing the virus to persist.[1] One recently proposed method for this persistence is altered thymocyte development due to the viral infection leading to "holes" in the T cell repertoire resulting in poor recognition of PRRSV and other neonatal pathogens.[1] Currently, there are no effective treatment protocols for acute PRRS infections, and vaccination has not been as efficacious as hoped.[1] Prevention is the primary means of control.[3]

Contributing Institution:

California Animal Health & Food Safety Laboratory, San Bernardino Branch

https://cahfs.vetmed.ucdavis.edu/locations/san-bernardino-lab

JPC Diagnosis: JPC Diagnosis: 1. Lung: Pneumonia, interstitial, lymphohistiocytic, diffuse, severe, with type II pneumocyte hyperplasia, intra-alveolar macrophage necrosis and marked peribronchiolar and perivascular lymphoid hyperplasia.
2. Lung: Bronchopneumonia, necrotizing and suppurative, diffuse, mild

JPC Comment: The contributor provided a concise but informative review of porcine respiratory and reproductive syndrome.

This particular virus is a global problem within the swine industry around the globe and one of its most costly and continuing problem. Two genotypes exist, type 1 (Europe) and type 2 (North America). A number of difficulties are associated with PRRS infection, including a high virus mutation rate which may result in outbreaks in previously vaccinated herds, prolonged intection, and shedding via a number of routes, to include ingestion, inhalation, venereal and transplacental routes.[3] Fortunately, the virus is relatively fragile in

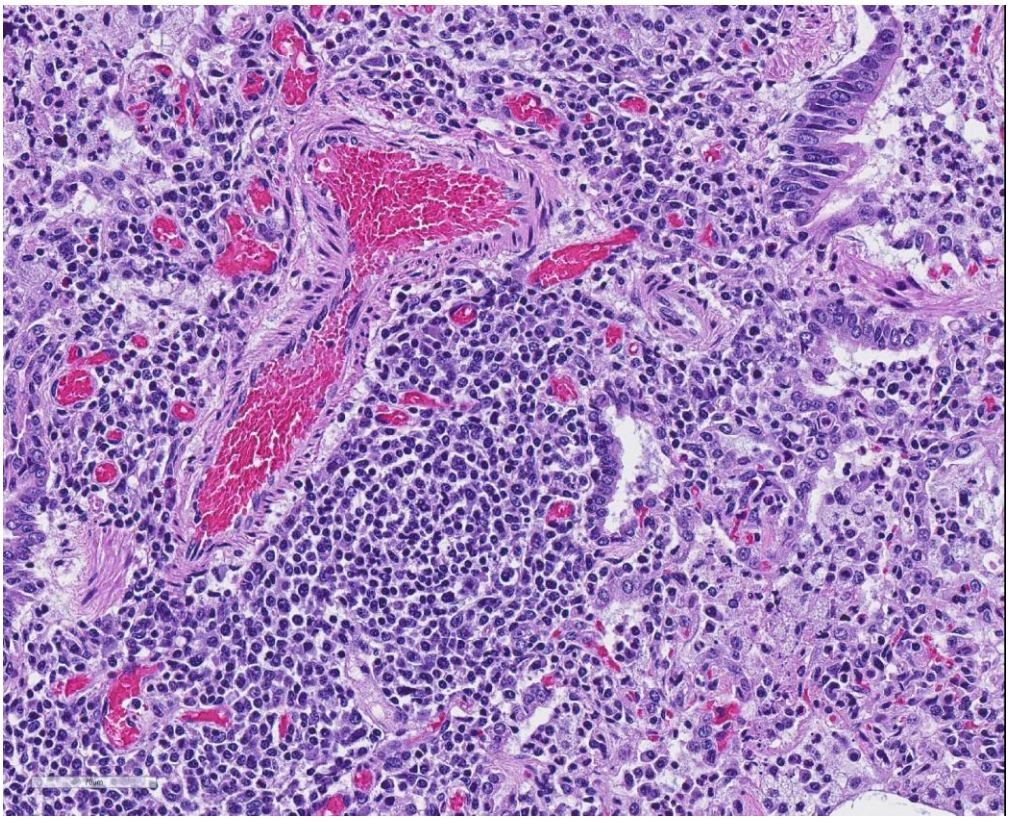

Lung, pig. Large cuffs of lymphocytes and plasma cells surround vessels of all sizes. (HE, 315X)

the environment.

PRRS infection generally revolves around macrophage infection, initially in tonsillar, nasal, or sites of pulmonary infection with infection of alveolar, interstitial, and intravascular macrophages, bronchiolar epithelium, and endothelium. Systemic viremia may occur in less than 12 hours with infection of macrophages, monocytes, and dendritic cells in many tissues. Within the lung, infection of macrophages results in markedly decreased macrophage phagocytosis, oxidative burst and cytokine release, predisposing the lungs to secondary bacterial infection. Additionally, the virus induces the release of the immunsuppressive cytokine IL-10 from infected macrophages, further diminishing both the innate and adaptive immune response.[3]Apoptosis of alveolar and intravascular macrophages are also common in infected animals but may not represent a consequence of viral infection.[2]

A number of reproductive abnormalities are seen in infected herds. In naïve herds, upt to 50% of sows may abort and 10% may die. It is a recognized cause of SMEDI (stillbirth, mummification, embryonal death and infertility). Hemorrhage of the umbilical cord due to fibrinoid necrosis and suppurative inflammation of the umbilical artery has been considered to be a characteristic gross lesion.[2] The persistence of one or more strains in endemic herds may result in continued losses from waves of abortions from successive generations of gilts.[2]

The presence of numerous necrotic macrophages and aggregates of bluish chromatin in the alveoli was considered diagnostic for PRRS by attendees. The moderator mentioned that while the presence of intra-alveolar necrotic macrophages are an excellent diagnostic feature for PRRS, they are not present in all cases. Some participants considered the presence of viable and degenerative neutrophils, especially within alveoli and smaller airways, evidence of a secondary

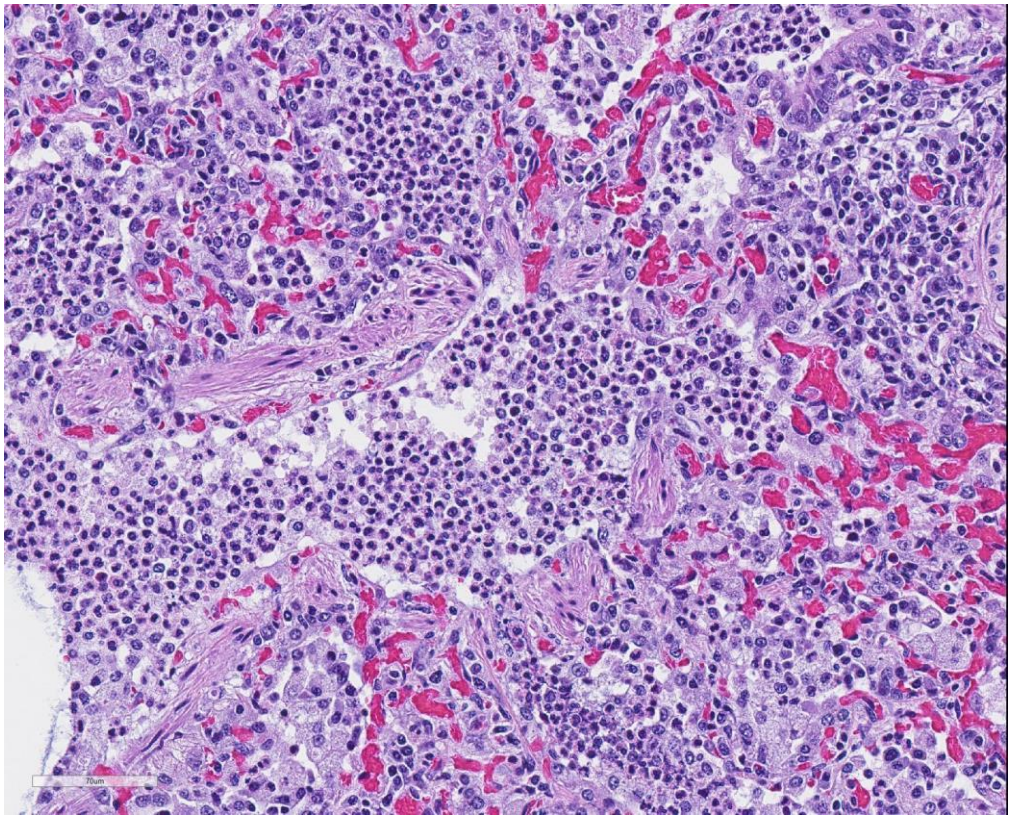

Lung, pig. Airways and surrounding alveoli denuded of epithelium and filled with viable and degenerate neutrophils suggest the strong possibility of a concomitant bacterial pneumonia. (HE, 315X)

bacterial infection further complicating the pneumonia in this pig. Attendees differed in their attribution of the BALT hyperplasia to either the interstitial pneumonia or a secondary bacterial infection.

While discussing this case, the moderator walked the participants through a number of differential diagnosis for lung diseases which should be tested for in cases such of this. Epitheliotrophic viruses such as swine influenza and swine coronavirus were discussed as potential viral agents, and bacteria such as *Streptococcus suis*, *Bordetella bronchiseptica*, and *Pasteurella multocida*. The moderator cautioned that some viruses, such as swine influenza, are present for only a short time in the epithelium, and that immunohistochemistry for viral antigen may be negative in more long-standing lesions. The moderator also raised the possibility of this case being a case of "proliferative and necrotizing pneumonia", an acute disease of weaner and grower pigs, in which severe acute disease results in dyspnea. In this condition the entire lobe, or only cranial and middle lobes may be affected, and lymphadenopathy is a consistent feature. The etiology of this condition is yet unknwon and may be the result of infection of certain strains of the PRRS virus, PCV, HeN2, alone or in combination.[2]

The presence of numerous necrotic macrophages and aggregates of bluish chromatin in the alveoli was considered diagnostic for PRRS, and the perivascular cuffs of lymphocytes and plasma cells were considered significant corroborative evidence for this diagnosisSome participants considered the presence of viable and degenerative neutrophils, especially within alveoli and smaller airways, evidence of a secondary bacterial infection further complicating the pneumonia in this pig.

References:

1. Butler JE, Sinkora M, Wang G, Stepanova K, Li Y, Cai X.

Perturbation of thymocyte development underlies the PRRS pandemic: A testable hypothesis. Front Immunol. 2019; 10:1077.
2. Caswell JL, Williams KJ. The respiratory system. In: Maxie MG, ed. Jubb, Kennedy, and Palmer's Pathology of Domestic Animals. 6th ed. Vol 2. St. Louis, MO: Elsevier Saunders; 2016:523-526.
3. Zachary JF. Mechanisms of Microbial infection. In: McGavin MD, Zachary JF, eds. *Pathologic Basis of Veterinary Disease.* 5th ed. St. Louis, MO: Mosby Elsevier; 2012:214-215.
4. Zimmerman JJ, Benfield DA, Dee SA, Murtaugh MP, Stadejek T, Stevenson GW, Torremorrell M. Porcine reproductive and respiratory syndrome (porcine arterivirus). In: Zimmerman JJ, Karriker LA, Ramirez A, Schwartz KJ, Stevenson GW, eds. *Diseases of Swine.* 10th ed. Ames, IA: Blackwell Publishing; 2012: 52,461-480.

CASE II: 2015A (JPC 4167277).

Signalment: Four-day-old crossbreed piglet (*Sus scrofa domesticus*)

History: This pig had no previous signs of illness, and was found dead.

Gross Pathology: At necropsy, the stomach was filled with undigested curdled milk. The small and large intestines were distended by watery yellow-to-greenish undigested milk, and intestinal walls were thin. No gross lesions were detected in other organs.

Laboratory results: RT-PCR for porcine epidemic diarrhea (PED) virus (PEDV) and transmissible gastroenteritis (TGE) virus (TGEV) was performed, the expected size of amplification products for PEDV gene, but not TGEV gene, were obtained. The RT-PCR products were directly sequenced and confirmed as PEDV gene.

Jejunum, 4-day-old piglet. Four cross-sections of jejunum are submitted for examination. (HE, 5X)

Microscopic Description: Severe atrophy of villi was detected in all segments of the small intestine. There were vacuolated epithelial cells throughout the small intestine. Immunohistochemical analysis revealed presence of PED viral antigen in the cytoplasm of epithelial cells lining the jejunum. No histopathologic lesions were detected in other organs.

Contributor Morphologic Diagnosis:

Jejunum: Enteritis, villous atrophy, acute, diffuse, severe.

Contributor Comment: PEDV is an enveloped, positive-sense, single-stranded RNA virus that belongs to the order *Nidovirales*, family *Coronaviridae*, genus *Alphacoronavirus*. PED was first observed among English feeding and fattening pigs in 1971, and then emerged in many European, Asian and North American countries.[9] PED is a highly contagious disease of swine of all ages, and has become a devastating issue in many pig-raising countries in Asia and North America.[1,4,5,7] In October 2013, a PED outbreak was recurred and confirmed in

Jejunum, 4-day-old piglet. Low magnification of a of cross section of jejunum shows marked villar blunting and fusion, as well as hemorrhage within the

on the jejunum and ileum. The diffuse villus atrophy of the small intestine is characteristic of the two disorders.[9] The presence of PED virus is confirmed by immunohistochemistry and RT-PCR.[9]

Contributing Institution:

National Institute of Animal Health, Japan.
http://www.naro.affrc.go.jp

/org/niah/

JPC Diagnosis: Intestine: Villar blunting, diffuse, severe, with villar enterocyte vacuolar degeneration, villar fusion, and mild crypt hyperplasia.

Japan after an absence of seven years in the country.[3] 38 out of 47 prefectures are affected until August 2014, and 817 have been affected among 5,570 farms.[3] PEDV isolates from this outbreak are genetically related to the PEDV isolates recovered from China and the USA in 2013.[3] Several new variants of PEDV emerged in the global pig population.[1,4,5,7] The spike protein of PEDV plays pivotal roles in viral entry and inducing the neutralizing antibodies in natural hosts.[6] Attenuated live vaccines using cell-culture-adapted PEDVs have long been used in Asia for the control of PEDV.[6,8] Recently, it was reported that an inactivated vaccine made from a U.S. field isolate is immunogenic in pigs.[2]

PED is characterized by vomiting and watery diarrhea, followed by dehydration, and a high mortality among suckling pigs.[5,9] Differential diagnoses for vomiting and diarrhea in pigs include PED and TGE, both of which have indistinct gross and histologic lesions centered mainly

JPC Comment: Porcine epidemic virus (PEDV) outbreaks were common in Europe in the 1970s and 1980s, and in Asia in the 1980s to 2000s. The first outbreak of PEDV in the United States occurred in April 2013 with explosive epidemics of diarrhea and vomiting affecting all ages, and resulting in 90-95% mortality in suckling pigs.[9]

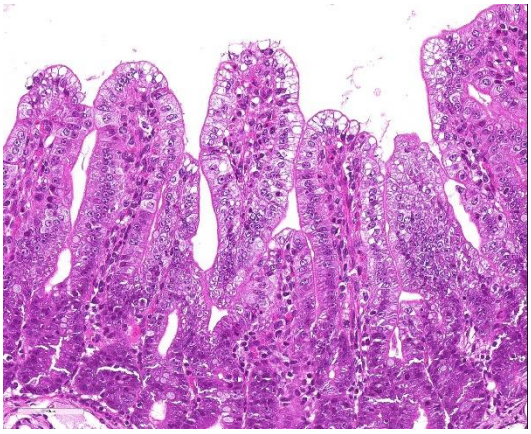

Jejunum, 4-day-old piglet. There is degeneration of villar tip enterocytes characterized by the presence of large vacuoles. (HE, 337X)

Jejunum, 4-day-old piglet. Multifocally, remaining villi demonstrate fusion. (HE, 347X)

In affected pigs, the main and often only sign of disease is watery diarrhea affecting up to 100% of pigs in all age groups, although piglets are more commonly affected. Experimental studies have demonstrated a 22- to 36-hour incubation period with viral replication in villous epithelium in all segments of the small intestine (viral replication can also been seen in colonic epithelium, but without obvious cellular degeneration).[9] Villus:crypt ratios in affected pigs are decreased from 7:1 to 3:1 or less. Characteristic vacuolar change of the villous epithelium resemble that seen with the coronavirus that causes transmissible gastroenteritis (TGE) in pigs, but are considered somewhat less pronounced.[9]

Clinical signs of disease on farms with naïve animals mimic those of epidemic transmissible gastroenteritis virus (TEGV) infection. Mortality is highest in piglets of 1 week of age or less, which often die of dehydration after 3-4 days of illness. Older pigs recover after about a week although recurrent diarrhea may occur in times of stress during intestinal repair, and sows may exhibit depression but no gastrointestinal signs.[10] The disease in the breeding facility is self-limiting, and tends to disappear once sows develop immunity and can produce colostral antibodies.[10]

Other coronaviruses of interest, but of less repute can also cause clinical disease in swine. A betacoronavirus known as hemagglutinating encephalomyelitis virus results in a disease known as vomiting and wasting disease. Infection is consided widespread among swine, although clinical disease is incommon. The virus, as the name suggests, possesses the ability to spontaneous agglutinate the erythrocytes of a number of species, including laboratory rodents.[10] The virus infects the respiratory epithelium of pigs less than 4 weeks of age, which lack protective antibodies. The virus ascends to the CNS via trigeminal, vagal, or spinal nerves. Vomiting in affected pigs is triggered by replication in the vagal sensory ganglion or in nerves that terminate in the vomiting center. Prolonged vomiting results in wasting; young piglets may die of dehydration, older pigs become emaciated.[10]

Another lesser known member of the Coronaviridae family is porcine torovirus, one of three species of totTorovirus, all of which rarely cause clinical disease. but they rarely cause clinical disease. In diarrheic pigs, seroprevalence for porcine torovirus

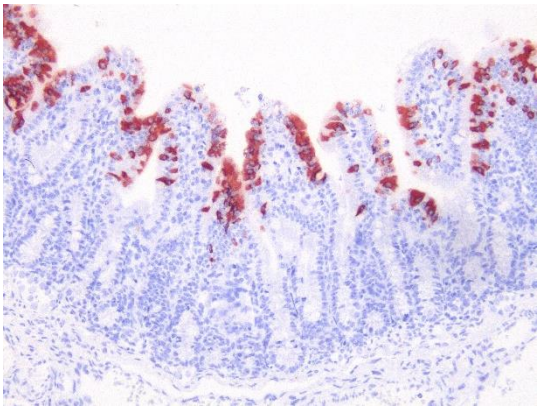

Jejunum, 4-day-old piglet. PED antigen is restricted to villar enterocytes. (anti-PED, 400X) (Photo courtesy of: National Institute of Animal Health, Japan. http://www.naro.affrc.go.jp/org/niah/)

may be high in many countries; however, concomitant enteric pathogens are simultaneously identifed in approximately 75% of cases so a direct link between porcine torovirus and true enteric disease is difficult to prove.[10]

The moderator mentioned the normal crypt ratio of 7:1 for a normal piglet, which demonstrates the marked villar blunting in this individual. A pathologist in the audience comment on the thin muscular tunics; the moderator noted that the muscular tunics of the intestine are thickest in proximity of the gastroduodenal junction and diminish caudally.

The moderator mentioned a number of other coronaviruses causing enteric disease in pigs including the porcine deltacoronavirus, and a bat-origin alphacoronavirus which resulting in almost 25,000 dead piglets on 4 farms in China in October 2017.

References:

1. Chen Q, Li G, Stasko J, Thomas JT, Stensland WR, Pillatzki AE, Gauger PC, Schwartz KJ, Madson D, Yoon KJ, Stevenson GW, Burrough ER, Harmon KM, Main RG, Zhang J. Isolation and characterization of porcine epidemic diarrhea viruses associated with the 2013 disease outbreak among swine in the United States. *J Clin Microbiol.* 2014;**52**(1)**:**234–243.
2. Collin EA, Anbalagan S, Okda F, Batman R, Nelson E, Hause BM. An inactivated vaccine made from a U.S. field isolate of porcine epidemic disease virus is immunogenic in pigs as demonstrated by a dose-titration. *BMC Vet Res.* 2015;**11**(1):62.
3. European Food Safety Authority (EFSA), Parma, Italy. Scientific Opinion on porcine epidemic diarrhoea and emerging porcine deltacoronavirus. EFSA Panel on Animal Health and Welfare (AHAW). *EFSA J.* 2014;**12**(10):3877.
4. Huang YW1, Dickerman AW, Piñeyro P, Li L, Fang L, Kiehne R, Opriessnig T, Meng XJ. Origin, evolution, and genotyping of emergent porcine epidemic diarrhea virus strains in the united states. *mBio.* 2013;**4**(5):e00737–13.
5. Lee S, Lee C. Outbreak-related porcine epidemic diarrhea virus strains similar to US strains, South Korea, 2013. *Emerg Infect Dis.* 2014;**20**(7):1223-1226.
6. Sato T, Takeyama N, Katsumata A, Tuchiya K, Kodama T, Kusanagi K. Mutations in the spike gene of porcine epidemic diarrhea virus associated with growth adaptation in vitro and attenuation of virulence in vivo. *Virus Genes.* 2011;**43**(1):72-78.
7. Song D, Huang D, Peng Q, Huang T, Chen Y, Zhang T, Nie X, He H, Wang P, Liu Q, Tang Y. Molecular characterization and phylogenetic analysis of porcine epidemic diarrhea viruses associated with outbreaks of severe diarrhea in piglets in jiangxi, china 2013. *PLoS One.* 2015;**10**(3):e0120310.
8. Song DS, Oh JS, Kang BK, Yang JS, Moon HJ, Yoo HS, Jang YS, Park BK. Oral efficacy of Vero cell attenuated porcine epidemic diarrhea virus DR13 strain. *Res Vet Sci.* 2007;**82**(1):134-140.
9. Stevenson GW, Hoang H, Schwartz KJ, Burrough ER, Sun D, Madson D, Cooper VL, Pillatzki A, Gauger P, Schmitt BJ, Koster LG, Killian ML, Yoon KJ. Emergence of Porcine epidemic diarrhea virus in the United States: clinical signs, lesions, and viral genomic sequences. *J Vet Diagn Invest.* 2013;**25**(5):649-654.
10. Zimmerman JJ, Benfield DA, Dee SA, Murtaugh MP, Stadejek T, Stevenson GW, Torremorrell M. Coronaviridae. In:

Zimmerman JJ, Karriker LA, Ramirez A, Schwartz KJ, Stevenson GW, eds. *Diseases of Swine*. 10th ed. Ames, IA: Blackwell Publishing; 2012: 514-521.

CASE III: P590-19 (JPC 4136500).

Signalment: 5½ week-old, neutered male, crossbred Landrace, Sus scrofa domesticus, domestic pig.

History: Two out of 950 weanling piglets showed clinical signs described as paresis progressing to paralysis affecting mostly the forelimbs; they were otherwise alert. The piglets were euthanized and rapidly brought to our diagnostic laboratory for a complete autopsy.

Gross Pathology: No gross lesions were seen.

Laboratory results: PCR for PRRSV at our institution was negative on samples of brainstem and spinal cord. Similar samples were sent to the Iowa State University's Veterinary Diagnostic Laboratory for PCR and were positive for porcine sapelovirus and negative for porcine teschovirus.

Spinal cord, piglet. At low magnification, focal areas of inflammation are visible within the ventral horns (arrows). (HE, 5X)

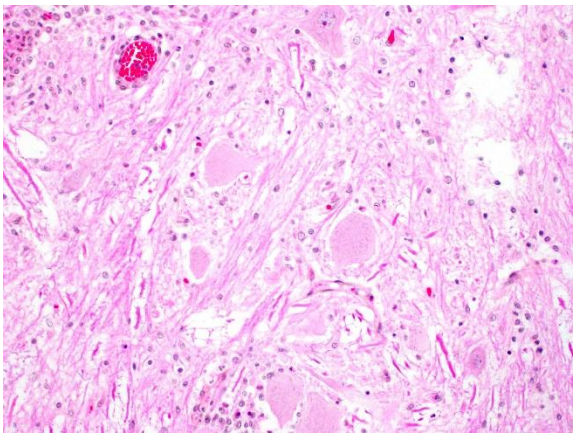

Spinal cord, piglet. Throughout the grey matter, neurons in early stages of degeneration are multifocally swollen, with a loss of Nissl substance (chromatoysis) (HE, 400X)

Microscopic Description: In this section of spinal cord, lesions involve the grey matter, predominantly the ventral horns. There is marked neuronal degeneration, necrosis and loss. Necrotic neurons are surrounded, infiltrated and eventually replaced by activated microgliocytes (neuronophagia and microglial nodules) with a few admixed neutrophils (Fig. 1). Necrotic neurons are shrunken with a hypereosinophilic, sometimes vacuolated cytoplasm, and the nucleus is often not visible. There is mild to moderate, multifocal perivascular cuffing by lymphocytes with fewer plasma cells also involving, but to a lesser degree, the leptomeninges.

Contributor Morphologic Diagnosis:

Mild to moderate lymphoplasmacytic poliomyelitis with marked neuronal degeneration/necrosis (nonsuppurative necrotizing poliomyelitis).

Contributor Comment: These lesions were diffuse in the spinal cord, but more severe in the cervical and cranial thoracic segments, consistent with the reported

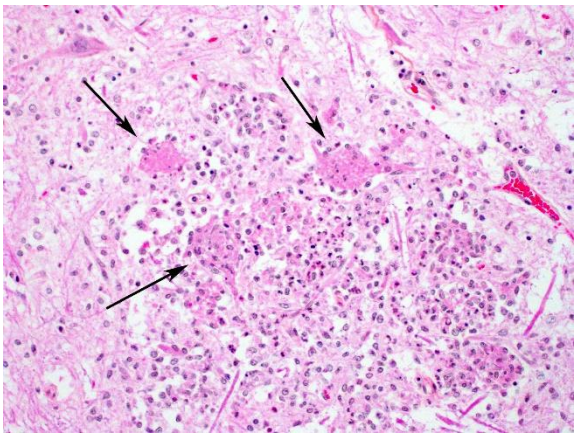

Spinal cord, piglet. There are numerous neuronophagic nodules within the gray matter, containing fragmentd and disintegrating neurons admixed with numerous glial cells, macrophages, and fewer neutrophils and eosinophils. (HE, 400X)

clinical signs. Lesions similar in nature and intensity were present in the brainstem, mainly in the medulla and pons, but also involved the white matter, albeit more mildly. Significant lesions were not present in the cerebellum or cerebrum (minimal lymphocytic meningitis) nor in other organs. The nature of the lesions, i.e. nonsuppurative inflammation involving preferentially the grey matter with neuronal necrosis and microglial nodules, was highly suggestive of a neuronotropic viral infection. Selenium toxicosis causes bilateral symmetrical poliomyelomalacia in the ventral horns, but it was not considered here as it is malacic (necrosis of all CNS components, not only neurons) in nature, and does not cause neuronophagia/microglial nodules or inflammation (although primarily malacic conditions will eventually incite inflammation with microglia, macrophages, and gitter cells). The viral etiologies considered in our geographical area (northeastern North America) were porcine teschovirus A (PTV), porcine sapelovirus A (PSV), porcine hemagglutinating encephalomyelitis virus (PHEV) and, to a lesser degree, porcine reproductive and respiratory syndrome virus (PRRSV) and porcine circovirus type 2 (PCV-2). These viruses are all specific to the porcine species (in natural disease). The final diagnosis, based on histopathology and PCR results, was encephalomyelitis due to PSV infection.

Porcine teschovirus A (PTV), formerly known as porcine enteroviruses (PEV) 1-7 and 11-13, is a member of the *Picornaviridae* family, which also includes porcine sapelovirus A (PSV) and porcine enteroviruses (PEV).[1] PTV causes a polioencephalomyelitis in pigs known as Teschen and/or Talfan disease; it has also been associated with reproductive failure. Teschen disease, the first one reported, is clinically severe (high morbidity and mortality) and limited mostly to Europe while Talfan disease, reported 20 years later, is a milder form (infection is usually asymptomatic) and is cosmopolitan.[1,2,7] Porcine sapelovirus A (PSV), formerly known as porcine enterovirus (PEV) 8, also causes a polioencephalomyelitis that is essentially similar to PTV, and has only been relatively recently reported in North America in 11 week-old pigs (20% morbidity; 30% mortality); it has also been associated with enteritis, pneumonia and reproductive failure. In contrast to PTV, the

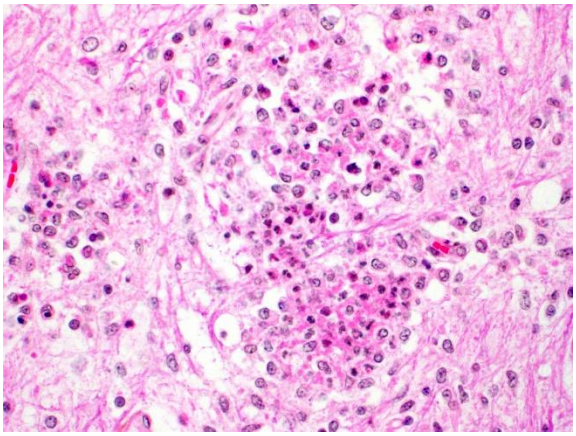

Spinal cord, piglet. Glial nodules mark areas of neuronal demise. (HE, 400X)

pathogenesis of PSV polioencephalomyelitis is still largely unknown and, to our knowledge, the disease has not been experimentally reproduced; PSV, but not PTV, is known to be cytopathic in porcine kidney cells.[1] Both PSV and PTV, like PEV, can be found in feces of normal pigs; thus, CNS sampling must be done as aseptically as possible.[1] Microscopic lesions in PTV and PSV are characterized by nonsuppurative polioencephalomyelitis with neuronal degeneration/necrosis and gliosis. Lesions are usually present throughout the neuraxis with some minor differences in the severity and distribution of lesions.[1,10]

PHEV, the only neurotropic porcine coronavirus, causes "vomiting and wasting disease" and/or encephalomyelitis in piglets less than 4 weeks of age, generally in 1-3 week-old piglets. It causes a nonsuppurative encephalomyelitis with neuronal degeneration involving predominantly the grey matter of the brainstem and proximal spinal cord.[2,6]

Although it is a systemic infection, PRRS has rarely been reported to cause predominantly central nervous system (CNS) lesions and clinical signs (neuroinvasive/ neurovirulent).[3,8] Lesions described in the CNS are lymphohistiocytic encephalitis (grey and white matter), with or without vasculitis, and/or meningitis;[3,9] in published reports we found, the spinal cord has apparently not been examined. Neuronal degeneration/ necrosis is not however a feature even in these cases and PRRSV is not considered a neuronotropic virus, although it was detected in neurons in one case.[3,7] PRRS is a common disease in Quebec and a generally mild lymphohistiocytic meningitis and/or encephalitis is often present along with the classical interstitial pneumonia and other lesions (e.g. lymphohistiocytic interstitial myocarditis).

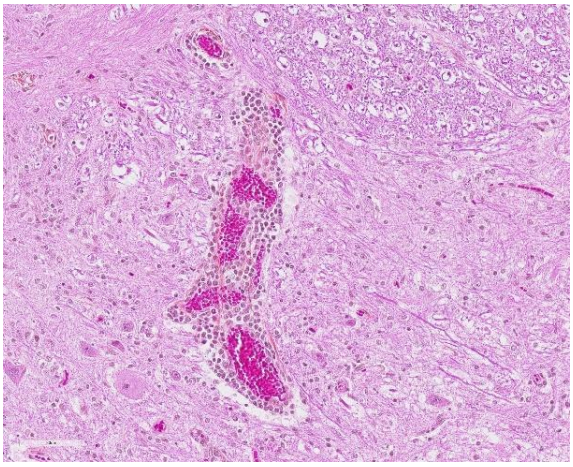

Spinal cord, piglet. Vessels within the grey matter are cuffed by several layers of lymphocytes and few macrophages, and the surrounding gray multifocal is multifocally gliotic and infiltrated by some of these cells. (HE, 400X)

PCV-2 also causes a systemic infection that results in a spectrum of diseases known as "porcine circovirus disease" (PCVD) or "porcine circovirus-associated disease" (PCVAD), the best known being postweaning multisystemic wasting syndrome (PMWS). CNS lesions are reported in PCVAD, but the role of PCV-2 is often not clear; they are generally mild and non-specific, e.g. nonsuppurative encephalitis and/or meningitis.[2,4,8] Neurological disease has rarely been reported with PCV-2 infection; in these cases, reported CNS lesions include cerebellar vasculitis and granulomatous meningoencephalomyelitis with multinucleated cells. These lesions were seen concurrently with systemic lesions typical of PMWS (e.g. widespread lymphoid depletion with granulomatous inflammation).[4,8]

Other possible causes of nonsuppurative polioencephalitis ± myelitis in pigs include

rabies (Lyssavirus), pseudorabies (suid herpes 1/varicellovirus; not present in Canada), West Nile virus (flavivirus) infection and "blue eye disease" (rubelavirus; Mexico). Although it is called encephalomyocarditis (cardiovirus), this disease is mainly a necrotizing myocarditis with generally minimal CNS lesions.[2,10]

Contributing Institution:

Faculty of veterinary medicine, Université de Montréal: https://fmv.umontreal.ca/faculte/departements/pathologie-et-microbiologie

JPC Diagnosis: Spinal cord, grey matter: Poliomyelitis, lymphocytic, diffuse, marked with neuronal necrosis, neuronophagia, glial nodule formation, and meningitis.

JPC Comment: The contributor provided an excellent review of neuronotropic viruses that target the spinal cord in swine.

Porcine sapelovirus is a member of the family Picornaviridae and was previously known as porcine enterovirus-8. There are historically two other species within the sapeloviruses, an avian species with one serotype and a simian species with three, hence the name "sapelovirus" for **s**imian, **a**vian, and **p**orcine **e**ntero-**l**ike viruses. More recently, the avian virus was moved to the genus *Anativirus*, and sapeloviruses have been discovered in the fecal flora of the sea lion and of a house mouse.[11]

Porcine sapelovirus has been identified in the feces of both healthy and diseased swine around the world.[5] It may result in SMEDI-like fetal mortality if inoculated into gilts on day 30 of gestation or earlier. In addition to neurologic disease, it may result in pneumonia and diarrhea as well. Histologic lesions in the intestine are those of villous atrophy.[5]

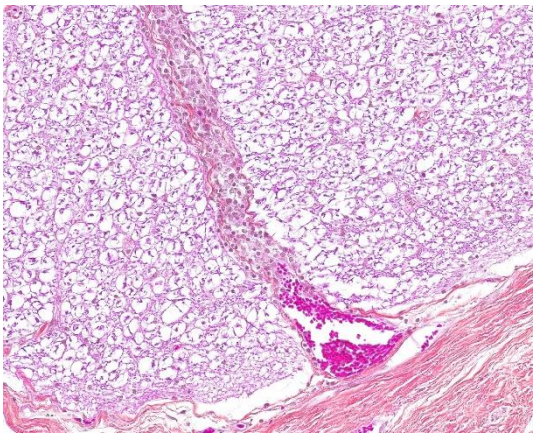

Spinal cord, piglet. Perivascular cuffs of lymphocytes extend along Virchow Robins spaces at the periphery of the spinal cord. (HE, 100X)

While most commonly transmitted by fecal-oral contact, this virus is environmentally resistant, and may also be transmitted through fomites. Diarrheic disease is seen intially in experimentally inoculated 50- to 60-day-old pigs, which is followed by ataxia and paraparesis and ultimately paralysis approximately five days later. Death occurs in an additional 2-3 days due to encephalitis. Humoral immunity is important in protection against sapelovirus infection, with maternal colostrum and early IgA production being considered protective against infection in weanlings.[5]

The moderator reviewed a number of viral and nutritional/toxic possibilities for lesions in the gray matter of the spinal cord.

References:

1. Arruda PH, Arruda BL, Schwartz KJ, et al. Detection of a novel sapelovirus in central nervous tissue of pigs with polioencephalomyelitis in the USA. *Transbound Emerg Dis*. 2017;64(2):311-315.
2. Cantile C, Youssef S. Nervous system. In: *Jubb, Kennedy and Palmer's Pathology of domestic animals*, vol.1.

Sixth Edition. Elsevier. St.Louis, MO, 2016:250-406.
3. Cao J, Li B, Fang L, et al. Pathogenesis of nonsuppurative encephalitis caused by highly pathogenic porcine reproductive and respiratory syndrome virus. *J Vet Diagn Invest*. 2012;24(4):767-71.
4. Drolet R, Cardinal F, Houde A, et al. Unusual central nervous system lesions in slaughter-weight pigs with porcine circovirus type 2 systemic infection. *Can Vet J*. 2011;52(4):394-7.
5. Horak S, Killoran K, Leedom Larson KR. Porcine sapelovirus. Swine Health Information Center and Center for Food Security and Public Health, 2016. http://www.cfsph.iastate.edu/pdf/shicfactsheet-porcine-sapelovirus.
6. Mora-Díaz JC, Piñeyro PE, Houston E, et al. Porcine Hemagglutinating Encephalomyelitis Virus: A Review. Front Vet Sci. 2019;6:53.
7. Salles MW, Scholes SF, Dauber M, et al. Porcine teschovirus polioencephalomyelitis in western Canada. *J Vet Diagn Invest*. 2011;23(2):367-73.
8. Seeliger FA, Brügmann ML, Krüger L, et al. Porcine circovirus type 2-associated cerebellar vasculitis in postweaning multisystemic wasting syndrome (PMWS)-affected pigs. *Vet Pathol*. 2007;**44**(5):621-34.
9. Thanawongnuwech R, Halbur PG, Andrews JJ. Immunohistochemical detection of porcine reproductive and respiratory syndrome virus antigen in neurovascular lesions. *J Vet Diagn Invest*. 1997;9(3):334-7.
10. Vandevelde M, Higgins RJ, Oevermann A. Inflammatory diseases. In: *Veterinary Neuropathology*. First Edition. Wiley-Blackwell. Chichester, West Sussex, 2012:48-80.
11. Murine sapelovirus. https://www.picornaviridae.com/sapelovirus/msv/msv.htm

CASE IV: N633-16 (JPC 4119040).

Signalment: 5½ week-old, neutered male, crossbred Landrace, *Sus scrofa domesticus*, domestic pig.

History: This animal was raised in a swine farm located in the state of Rio Grande do Sul, Brazil, and was part of an outbreak which occurred in three distinct swine growing-finishing sites. This outbreak affected pigs with age ranging from 80 to 120 days, and it lasted 60 days. The three sites had a total of 2152 pigs, of which 92 died during the outbreaks. All these pigs, including the one submitted, showed clinical signs of apathy, weight loss, diarrhea, cyanosis, and reddening of the ears, abdomen, and distal parts of the thoracic and hind limbs over a clinical course of 7 to 10 days. In addition, approximately 30 animals from the affected group, including the case referred, displayed stiff gait, muscle weakness, hind limb paresis, and recumbency. Euthanasia was elected due to the poor prognosis and progression of clinical signs.

Gross Pathology: Grossly, the muscular lesions consisted of multifocal to coalescing pale discoloration of the skeletal muscles,

Presentation, 5.5-week-old pig. Affected pigs demonstrated hind limb paresis. (Photo courtesy of: Faculdade de Veterinária, Universidade Federal do Rio Grande do Sul, Setor de Patologia Veterinária, http://www.ufrgs.br/patologia/)

Hind limb, 5.5-week-old pig. Muscles of the hindlimbs demonstrate severe pallor. (Photo courtesy of: Faculdade de Veterinária, Universidade Federal do Rio Grande do Sul, Setor de Patologia Veterinária, http://www.ufrgs.br/patologia/)

which was severe for the hind limbs, moderate for the thoracic limbs, and mild for the dorsal lumbar skeletal muscles. Other lesions included generalized lymphadenomegaly with whitish and reddish inter-mixed areas on the cut surface; enlarged kidneys with multifocal to coalescing pinpoint to round whitish areas; and splenomegaly with infarcts and multifocal white pulp hyperplasia. The liver was enlarged with diffuse orange-reddish discoloration; the skin had ulcers and irregular reddened lesions on the limbs and ear cyanosis.

Laboratory results:

Immunohistochemistry (IHC) was performed on lymphoid tissue and was characteristic of PCVD, with intense immunostaining in the cytoplasm of macrophages and multinucleated giant cells and moderate immunostaining of endothelial cells. In addition to that, IHC was performed on skeletal muscle tissue, and it showed intense multifocal immunostaining mainly in the cytoplasm and nuclei of inflammatory cells, while mild immunostaining was evidenced in the cytoplasm of endothelial cells, necrotic fibers, and skeletal muscle satellite cells.

DNA was obtained from the lymph nodes, spleen, and skeletal muscle of this pig, from which a polymerase chain reaction (PCR)

product of 481 bp was amplified. DNA extraction and PCR for PCV2 were performed as described previously.[4] The PCR products were sequenced, which indicated 99% identity with sequences in GenBank from the PCV2b genotype.

Microscopic Description: Some submitted slides have two to three sections of skeletal muscle, one of which is from the affected animal and presents prominent histological lesions, and the other ones is a section of normal skeletal muscle from an unaffected control pig. The affected tissue section is characterized by multifocal to coalescing, intense hyaline and floccular necrosis of myofibers, which have swollen and hypereosinophilic sarcoplasm with loss of striations, pyknotic nuclei, in addition to myofiber fragmentation with an intense inflammatory infiltrate of macrophages and multinucleated giant cells, sometimes occupying the whole myofiber sarcoplasm.

Mesenteric lymph nodes, 5.5-week-old pig. There is marked mesenteric lymphadenomegaly. (Photo courtesy of: Faculdade de Veterinária, Universidade Federal do Rio Grande do Sul, Setor de Patologia Veterinária, http://www.ufrgs.br/patologia/)

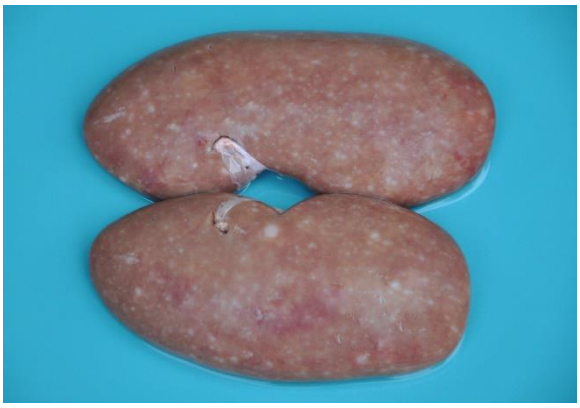

Kidney, 5.5-week-old pig. The kidneys are enlarged with white foci. (Photo courtesy of: Faculdade de Veterinária, Universidade Federal do Rio Grande do Sul, Setor de Patologia Veterinária, http://www.ufrgs.br/patologia/)

This pig had also in the interstitial and perivascular spaces a moderate inflammatory infiltrate of macrophages, multinucleated giant cells, lymphocytes, and plasma cells, as well as multifocal mild hemorrhage, endothelial cell hypertrophy, mild multifocal thrombosis, as well as occasional regenerating myofibers.

Contributor Morphologic Diagnosis:

Multifocal to coalescing, severe, subacute, granulomatous necrotizing myositis.

Contributor Comment: In the present case, final diagnosis of granulomatous necrotizing myositis due to porcine circovirus infection was reached through the association of clinical, gross, histopathological, immunohistochemical, and molecular findings. Porcine circovirus type 2 (PCV2) is a nonenveloped, circular, single-stranded DNA virus,[17] which presents four genotypes: PCV2a, PCV2b, PCV2c,[3,9,15] and PCV2d.[5,18] The virus is associated with multiple clinical syndromes in pigs, collectively known as porcine circovirus diseases (PCVD).[11] Clinically, PCVD may vary, and affected pigs usually display progressive weight loss, dyspnea, diarrhea, and lymphadenopathy. Histologically, lymphoid depletion and infiltration of histiocytes and multinucleated giant cells are observed in lymphoid organs.[6] In addition to these organs, PCV2 lesions have been described in the kidneys, small and large intestines, stomach, liver, lungs, central nervous system (CNS), and heart.[2,10,11,14]

Even though systemic disease is frequently observed associated with such viral infection, skeletal muscle lesions caused by PCV2 had not been described in the scientific literature prior to the present case, which has been recently published.[7] The etiology of such particular pathological feature is not completely elucidated. Occasionally, PCV2 infection may induce vascular lesions,,[8,11,13] which could induce necrotic changes; however, only mild vascular alterations within skeletal muscle of affected pigs were observed. Thus, we propose that the skeletal muscle lesions observed are most likely a direct effect of the viral infection, since positive immunostaining was noted in the sarcoplasm of myocytes and in macrophages within the muscle.

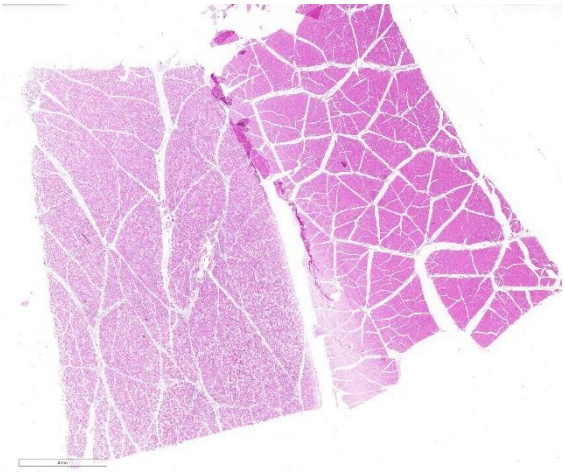

Skeletal muscle, 5.5 week old pig. Two sections of skeletal muscle are presented for examination. The section at left demonstrates marked pallor and diffuse cellular interstitial infiltrate visible at low magnification (HE, 7X)

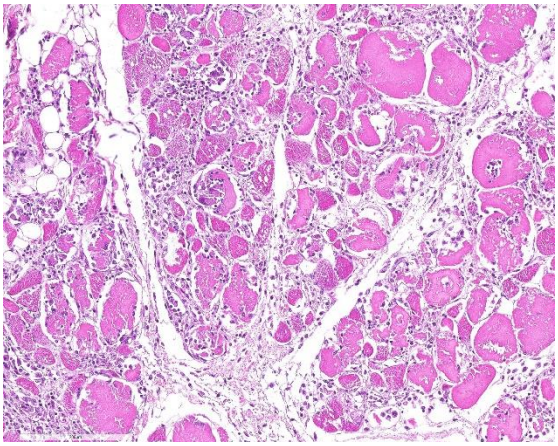

Skeletal muscle, 5.5 week old pig. Through the section of muscle, there is myofiber degeneration and necrosis with variation in fiber size, fragmentation, myofibrillolysis, and infiltration of necrotic myofiber by macrophages. The endomysium and perimysium is edematous and infiltrated by moderate numbers of macrophages and giant cells. (HE, 179X)

Based on the gross findings observed in the present case, ionophore toxicity and vitamin E/selenium deficiency should be included as the main differential diagnosis.[1,16] Vitamin E/selenium deficiency most commonly affects weaned pigs and, microscopically, causes mineralization of degenerate fibers, whereas ionophore poisoning causes a monophasic and multifocal degeneration of myofibers.[1] However, the affected pigs in this outbreak did not consume ionophore antibiotics, and the skeletal muscle microscopic lesions were primarily characterized by granulomatous necrotizing myositis, which causes distinct lesions from the above mentioned toxic and metabolic myopathies.[1,16]

Contributing Institution:

Faculdade de Veterinária
Universidade Federal do Rio Grande do Sul
Setor de Patologia Veterinária
http://www.ufrgs.br/patologia/

JPC Diagnosis: Skeletal muscle: Myositis**,** necrotizing and granulomatous, diffuse, severe, with multifocal vasculitis.

JPC Comment: The contributor summarizes work that he and a team of investigators published in the journal *Veterinary Pathology* in 2018, which was the first published report of skeletal muscle lesions associated with porcine circovirus-2. The potential infection of skeletal muscle (in addition to a long list of other tissues, many of which have appeared in the WSC, as listed below) by porcine circovirus has been considered for a number of years, as it was demonstrated that naïve pigs could be infected by feeding skeletal muscle from PCV-2 infected pigs.

In the report by Konradt et al.,[7] the granulomatous and necrotizing myositis seen in these animals was not an isolated manifestation of porcine circovirus disease, but one of a number of lesions of a group of pigs afflicted by PCD. In these animals , lymphoid tissue, including the spleen,

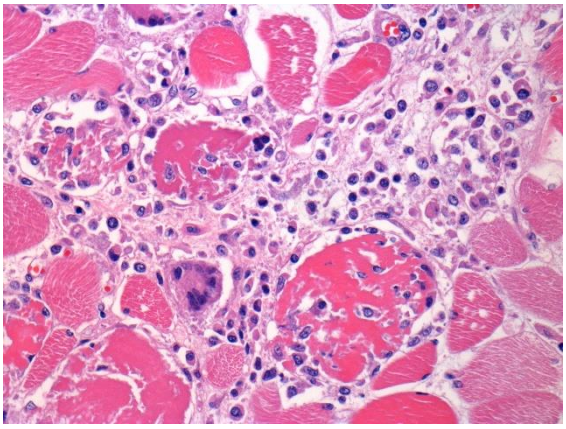

Skeletal muscle, 5.5 week old pig. Higher magnification of degenerating and necrotic myofibers. Some myotubes are devoid of a myofiber and contain numerous macrophages. A multinucleated giant cell macrophage is present at center. (HE, 400X) (Photo courtesy of: Faculdade de Veterinária, Universidade Federal do Rio Grande do Sul, Setor de Patologia Veterinária,

tonsils and lymph nodes, showed marked depletion of lymphocytes and granulomatous inflammation with giant cells. (Multinucleated giant cells macrophages appear to be a relatively constant feature in areas of inflammation in PCV-2 infected pigs, and also appeared in this slide, scattered through the interstitial infiltrate.) Affected pigs in this study also exhibited lymphohistiocytic vasculitis and fibrinoid necrosis in a number of organs including the skeletal muscle, lyphoidtissue, kidney liver, skin, and leptomeninges. Several pigs additionally exhibited granulomatous enteritis, predominantly in proximity to Peyer's patches.[7]

The moderator mentioned a very important point about granulomatous inflammation in this particular case. While widespread damage to muscle often incites a histiocytic response as part of cleanup, the number of epithelioid macrophages within the interstitium exceeds that which would be expected as a result of muscular necrosis and should be interpreted as granulomatous inflammation.

The moderator closed discussion of this case with a comprehensive review of PCV-2, PCV-2b, and PCV-3.

Since 2007, porcine circovirus and the many and varied manifestations of porcine circovirus-associated disease has been an oft-used viral disease and swine disease in the WSC. While space and time prohibit the recapitulation of myriad presentations of PCVD within this comment, the reader is encouraged to visit the various cases listed below (used as exemplars for common manifestations of PCVD) for a wealth of information on this important swine disease.

Conference 17, Case 2, 2018-2019 Conference 8, Case 2, 2016-2017	Granulomatous myocarditis
Conference 5, Case 1, 2017-2018	Granulomatous interstitial pneumonia with arteritis
Conference 21, Case 4, 2014-2015	Cerebellar hemorrhage
Conference 25, Case 1, 2013-2014 Conference 1, case 4, 2007-2008	Granulomatous hepatitis with marked hepatocellular degeneration and loss
Conference 7, Case 3, 2011-2012	Granulomatous interstitial nephritis
Conference 8, Case 4, 2009-2010	Porcine dermatopathy and nephropathy syndrome
Conference 17, Case 4, 1997-1998	Granulomatous lymphadenitis

Table 1 – Previous PCV submissions to the WSC.

References:

1. Cooper BJ, Valentine BA. Muscle and tendon. In: Maxie M, ed. Jubb, Kennedy, and Palmer's Pathology of Domestic Animals. Edinburgh, UK: Elsevier; 2016: 164–248.

2. Correa AM, Zlotowski P, de Barcellos DE, et al. Brain lesions in pigs affected with postweaningmultisystemic wasting

syndrome. J Vet Diagn Invest. 2007; 19(1):109–112.

3. Dupont K, Nielsen ED, Baeko P, et al. Genomic analysis of PCV2 isolates from Danish archives and a current PMWS case-control study supports a shift in genotypes with time. Vet Microbiol. 2008;128(1–2):56–64.

4. Ellis J, Krakowka S, Lairmore M, et al. Reproduction of lesions of postweaningmultisystemic wasting syndrome in gnotobiotic piglets. J Vet Diagn Invest. 1999;11(1):3–14.

5. Franzo G, Cortey A, Olvera D, et al. Revisiting the taxonomical classification of porcine circovirus type 2 (PCV2): still a real challenge. Virol J. 2015;12(131): 1–8.

6. Kim J, Chae C. Necrotising lymphadenitis associated with porcine circovirus type 2 in pigs. Vet Rec. 2005;156(6):177–178.

7.Konradt G, Cruz RAS, Bassuino DM, et al. Granulomatous Necrotizing Myositisin Swine Affected by Porcine Circovirus Disease. Vet Pathol. 2018; 55(2):268-272.

8. Langohr IM, Stevenson GW, Nelson EA, et al. Vascular lesions in pigs experimentally infected with porcine circovirus type 2 serogroup B. Vet Pathol. 2010; 47(1):140–147.

9. Olvera A, Cortey M, Segale´s J. Molecular evolution of porcine circovirus type 2 genomes: phylogeny and clonality. Virology. 2007;357(2):175–185.

10. Opriessnig T, Janke BH, Halbur PG. Cardiovascular lesions in pigs naturally or experimentally infected with porcine circovirus type 2. J Comp Path. 2006; 134(1):105–110.

11. Opriessnig T, Meng XJ, Halbur PG. Porcine circovirus type 2 associated disease: update on current terminology, clinical manifestations, pathogenesis, diagnosis, and intervention strategies. J Vet Diagn Invest. 2007;19(6):591–615.

12. Opriessnig T, Patterson AR, Meng XJ, Halbur PG. Porcine circovirus Type 2 in muscle and bone marrow is infectious and transmissible to naïve pigs by oral consulption. *Vet Microbiol* 2009; 133 (1-2), 54-64.

13. Resendes AR, Segale´s J. Characterization of vascular lesions in pigs affected by porcine circovirus type 2–systemic disease. Vet Pathol. 2015;52(3):497–504.

14. Segale´s J, Allan GM, Domingo M. Porcine circovirus diseases. In: Straw BE, Zimmerman JJ, D'Allaire S, Taylor DJ, eds. Diseases of Swine. 9th ed. Ames, IA: Blackwell; 2006:299–307.

15. Segale´s J, Olvera A, Grau-Roma L, et al. PCV-2 genotype definition and nomenclature. Vet Rec. 2008;162:867–868.

16. Shimshoni JA, Britzi M, Pozzi PS, et al. Acute maduramicintoxicosis in pregnant gilts. Food ChemToxicol. 2014;68:283–289.

17. Tischer I, Gelderblom H, Vettermann W, et al. A very small porcine virus with circular single-stranded DNA.Nature. 1982;295(5844):64–66.

18. Xiao CT, Halbur PG, Opriessnig T. Complete genome sequence of a novel porcine circovirus type 2b variant present in cases of vaccine failures in the United States. J Virol. 2012;86(22):12469–12473.

Self-Assessment - WSC 2019-2020 Conference 16

1. The primary cellular target for the arterivirus that causes PRRS is which of the following?
    a. Macrophage
    b. T-cell
    c. Endothelial cell
    d. B-cell

2. The lesions of porcine endemic diarrhea virus are most similar to what other virus in pigs?
    a. Transmissible gastroenteritis virus (TGEV)
    b. Porcine hemaggluinating and vomiting virus
    c. Porcine torovirus
    d. Porcine astrovirus

3. Which of the following is NOT seen in association with porcine sapelovirus?
    a. Ataxia
    b. Diarrhea
    c. Embryonal death
    d. Icterus

4. What is the characteristic finding in the lymphoid tissues of pigs infected with PCV-2?
    a. Lymphoid hyperplasia
    b. Lymphoid depletion with granulomatous inflammation
    c. Malignant transformation to lymphoma
    d. No change

5. True or false. Basophilic intracytoplasmic inclusions are seen within degenerating skeletal muscle fibers in animals demonstrating PCV-associated disease.
    a. True
    b. False

Please email your completed assessment for grading to Dr. Bruce Williams at bruce.h.williams12.civ@mail.mil. Passing score is 80%. This program (RACE program 33611) is approved by the AAVSB RACE to offer a total of 0.5 CE Credits, with a maximum of 12.5 CE Credits being available to any individual Veterinary Medical Professionals for the 2019-2020 Wednesday Slide Conference. This RACE approval is for the subject matter categories of: SCIENTIFIC using the delivery method of NON-INTERACTIVE DISTANCE. This approval is valid in jurisdictions which recognize AAVSB RACE.

Joint Pathology Center
Veterinary Pathology Services

WEDNESDAY SLIDE CONFERENCE 2019-2020

C o n f e r e n c e 17

5 Feb 2020

CASE I: 1235813-006 (JPC 4117518).

Signalment: Three year old, male cynomolgus macaque (*Macaca fascicularis*) from China.

History: This animal was found dead on day 109 of a 6 month routine general toxicity study. There were no reported clinical signs. Routine infectious agent screens and three consecutive tuberculosis skin tests were negative with the exception of measles which was positive after a live vaccine.

Gross Pathology There were moderate, focal to multifocal, tan foci on the liver and lung with moderate swelling of the mediastinum. Skin discolorations with abrasions / scabs were present on the ventral abdomen and right forelimb.

Laboratory results: The tan foci were PCR positive for *Mycobacterium tuberculosis* group and culture yielded slow growing acid fast bacilli identified as *Mycobacterium tuberculosis*.

Microscopic Description: Throughout approximately 90% of examined lung there was multifocal to coalescing granulomatous inflammation often forming discrete granulomas with central eosinophilic flocculent debris (caseating necrosis) with or without basophilic granular mineralization. This central area was surrounded by

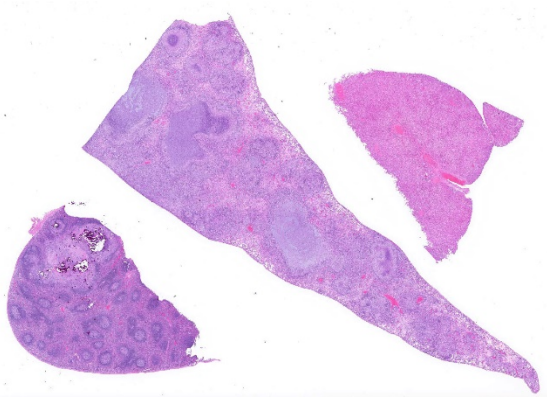

Liver, lung, spleen, cynomolgus monkey: Granulomas are easily visualized in the lung (middle) and spleen (bottom left) at subgross magnification. The granulomas in the spleen are heavily mineralized. (HE, 5X)

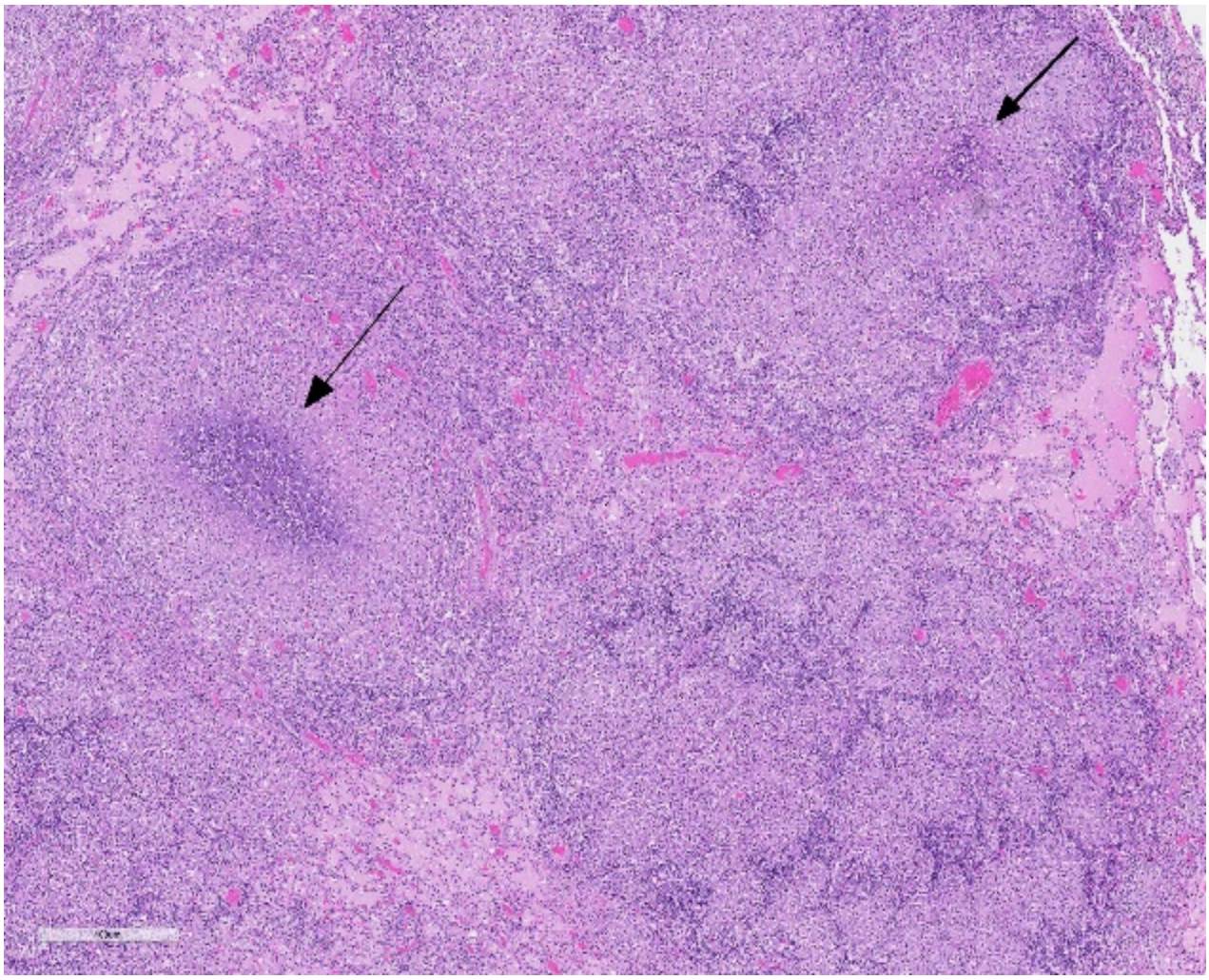

Lung, cynomolgus monkey. There are many areas of coalescing granulomatous inflammation in the lung. More mature granulomas are centered on an area of necrotic debris. (HE, 53X

epithelioid macrophages, multinucleated giant cells, a rim of lymphocytes and variable fibroblasts/fibrosis. Similar solitary discrete granulomas were seen in the spleen, liver, and mediastinum (mediastinum not submitted). There was an increase in number and prominence of germinal centers in the spleen (follicular hyperplasia) as well as frequent multifocal type 2 pneumocyte hyperplasia in the lung.

Ziehl-Nielsen acid fast staining of the lung revealed rare acid fast bacilli within the cytoplasm of macrophages or multinucleated giant cells, and/or free within the necrotic/mineralized areas.

Contributor's Morphologic Diagnosis:

Granulomatous pneumonia, severe, diffuse with focal hepatic and splenic granulomas and scant acid-fast bacilli.

Contributor's Comment: *Mycobacterium tuberculosis* (*M.tb*) is a cosmopolitan organism that infects approximately 1/3 of the world's human population and is a leading cause of death due to infectious disease. It is also an increasing public health

concern due to 1) emerging multidrug resistant and extensively drug resistant *M.tb* and 2) the increasing risk of death in HIV infected people.[20] Tuberculosis was considered the cause of 40% of all HIV-related deaths in 2016.[20] Roughly 10% of people infected with *M.tb* go on to develop active contagious disease with the remaining individuals either clearing the bacteria (approximately 10%) or harboring latent disease. These latent carriers create a reservoir of tuberculosis which can reactivate during times of stress or immune suppression and disseminate M.tb to naïve populations of humans[20] or spread the disease to susceptible animals (reverse zoonosis).[13]

In an NHP necropsy, *M.tb* often presents as tan or creamy white nodules (granulomas), predominantly within the lung, but also with systemic involvement. Other common causes of tan nodules or granulomas within the lung includes foreign body (kaolin), protozoan (*Toxoplasma gondii)*, bacterial (*Nocardia* sp), mycotic (*Coccidioides immitis*, *Coccidioides posadasii*, *Histoplasma capsulatum*, *Blastomyces*

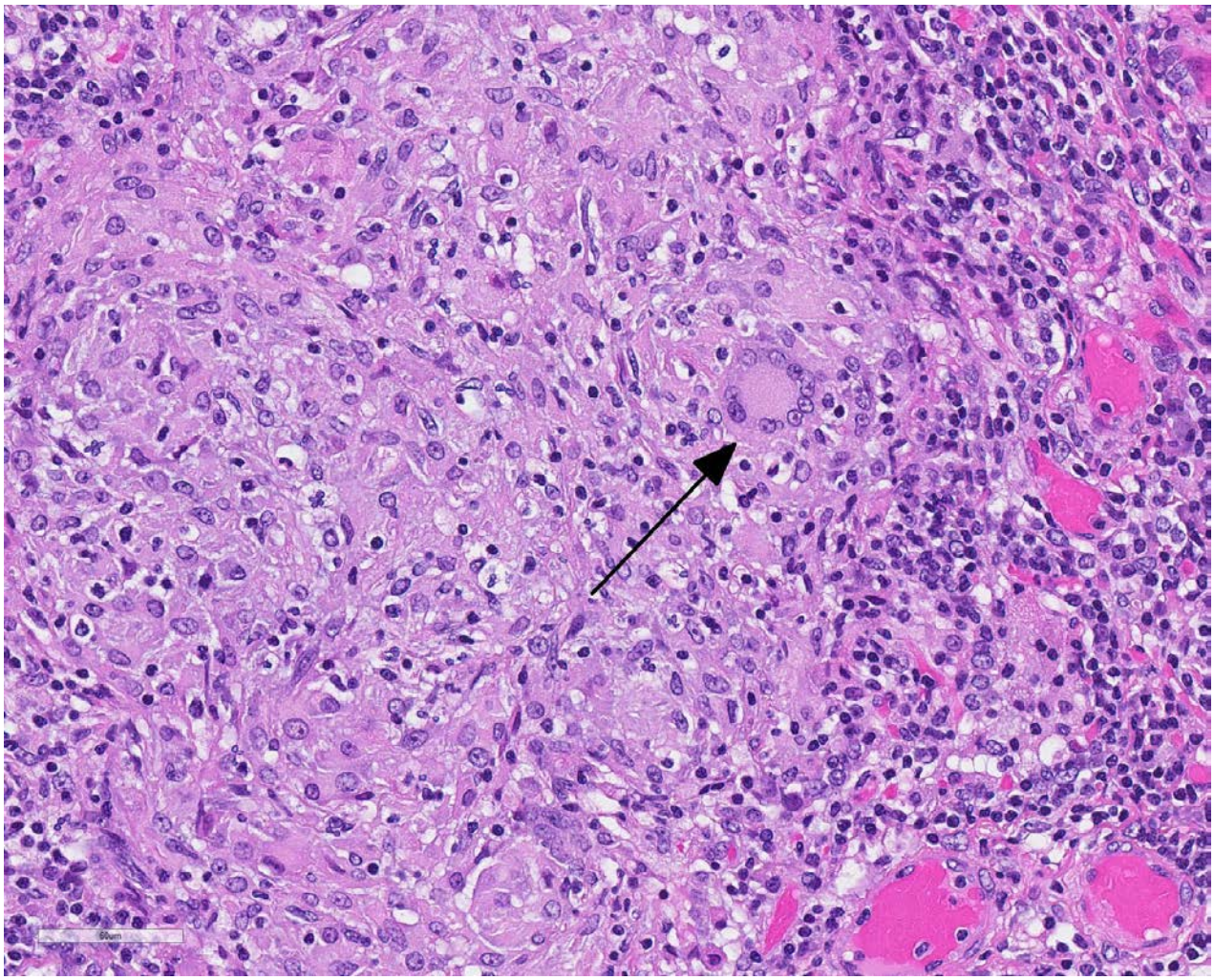

Lung, cynomolgus monkey. There are many areas of coalescing granulomatous inflammation in the lung. More mature granulomas are centered on an area of necrotic debris. (HE, 53X

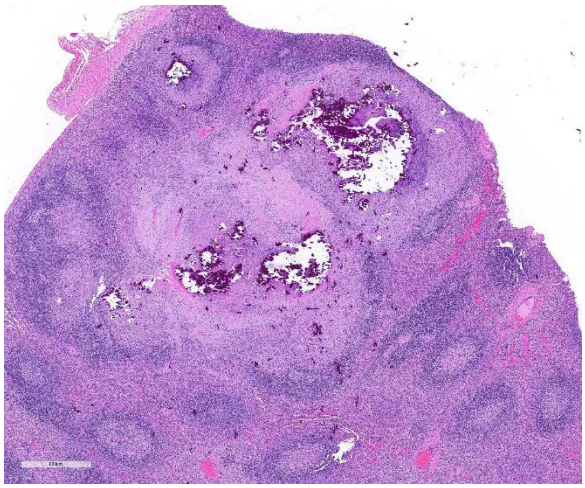

Spleen, cynomolgus monkey. Similar granulomas are present at one end of the section of spleen, but with a high content of crystalline mineral in the center. There is marked follicular hyperplasia of the white pulp through the remainder of the section, and the normal sinusoidal architecture is effaced by marked reticuloendothelial hyperplasia. . (HE, 331X)

dermatitidis, and *Cryptococcus neoformans*) and parasitic organisms (*Pneumonyssus simicola* (acariasis), *Taenia* cysts, *Echinococcus* cysts, *Mesocestoides* tetrathyridia, *Spirometra* spargana, and *Filaroides* and *Filariopsis* nematodiasis), Histology can distinguish between these diagnoses based on the appearance of the organisms.[11]

M.tb and mycobacteria in general are unusual among bacteria due to the high lipid content and relative thickness of their cell wall compared to gram-positive and gram-negative bacteria. The thick mycobacterial cell wall is relatively impermeable, does not take up crystal violet (Gram stain variable), and is responsible for the acid fast staining properties of mycobacteria. Immunologically, the lipid component of the mycobacterial cell wall is particularly effective at recruiting an immune response and has been commonly used as an adjuvant in vaccines to recruit a desired robust immune response to antigens of interest. The protein (antigen) and lipid components together during mycobacterial infection result in sensitization of the animal to tuberculosis proteins. Sensitized animals then react to purified mycobacterial protein derivative (PPD) in a skin test with a Type IV hypersensitivity reaction resulting in a cell mediated immune reaction after 2-3 days. Non-responders, or animals that fail to demonstrate a positive response to the PPD skin test in the face of mycobacterial infection (as seen in this monkey) are thought to be due to immunologic anergy.[3] Anergy is a failure of the animal to produce a Type IV delayed type hypersensitivity reaction upon PPD exposure. The exact cause of anergy in *M.tb* infection is unknown; although, in general, it is a lack of response of cell mediated immunity due to tyrosine kinase blockage and reduced IL-2 receptor signaling, among other mechanisms.[17] In *M.tb* infection a weak cell-mediated immune response (high IL-4) is thought to be associated with anergy.[7]

Another feature of the mycobacterial cell wall is its role in allowing the bacteria to evade the host immune system. In part, the success of *M.tb* is due to the highly infectious nature of the bacteria. It is thought that as few as 10 bacteria can cause disease.[18] Once within the host, mycobacteria are engulfed by macrophages into phagosomes. Under normal circumstances within a macrophage, phagosomes mature and fuse with lysosomes exposing the bacteria to destructive chemicals and lytic enzymes leading to bacterial death. Mycobacteria

have evolved mechanisms to avoid phagosome-lysosome fusion and survive within macrophages. For example, components of the mycobacterial cell wall interrupt the normal traffic of the phagosome to the lysosome by preventing recruitment of key molecules in phagosomal maturation such as the Rab5 to Rab7 conversion.[1] Phagosome maturation arrest in *M.tb* is thought to involve specific cell surface receptors (i.e. mannose receptor) and mycobacterial cell wall components (i.e. lipoarabinomannan and SapM enzyme)[5]. Ultimately, whether the mycobacteria are destroyed or remain active or latent within the host depends upon the infectious dose, the host immune response, and the environment of the infection.[3] A host response characterized by a Th2 cytokine response (IL-4) is associated with mycobacteria infection and Th1 cytokine response (IL-12, TNF-α, and IFN-γ) is associated with bacterial clearance.[1]

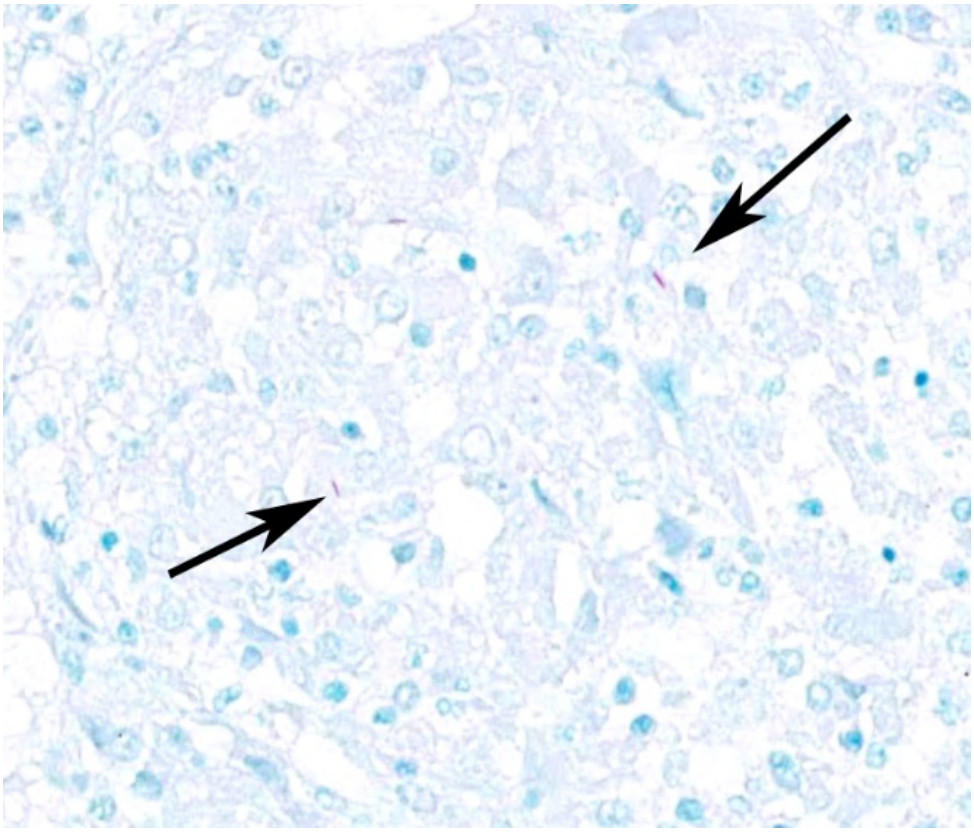

Lung, cynomolgus monkey. Acid-fast bacilli (arrow) are rarely seen within the granulomas. (Ziehl-Nielsen, 400X)(Image courtesy of: MPI Research, a Charles River Company, https://www.mpiresearch.com)

There are many mycobacteria that cause significant human and animal diseases. The histologic features of these diseases range from structured granulomas (often associated with few bacteria/paucibacillary infection) to more diffuse macrophage infiltration (often associated with numerous bacteria/multibacillary infection). Granulomas, or tubercles, have four histologic features: 1) central caseous necrosis with or without mineralization, 2) surrounded by epithelioid macrophages and Langhans multinucleated giant cells, 3) surrounded by lymphocytes with or without neutrophils and peripheral fibrosis, 4) tubercles contain rare acid fast bacilli which are found within macrophages, multinucleated giant cells, and/or the caseous core. In paucibacillary mycobacterial diseases, gross observations are crucial to identifying areas to look for

these rare bacilli as bacteria are not typically found outside of the structured granulomas.[3]. Multibacillary infection is more variable with few to sheets of infiltrating macrophages containing few to numerous acid fast bacilli. Leprosy (*Mycobacterium leprae)* is centered on nerves and can be paucibacillary and granulomatous or multibacillary and diffuse depending upon the strength of the cell mediated immune response with a stronger cell mediated response associated with the paucibacillary infection.[7] Common mycobacterial species involved in disease are listed in Table 1.

Contributing Institution:

MPI Research; a Charles River company
https:///www.crl.com
https://www.mpiresearch.com

JPC Diagnosis:
1. Lung: Bronchopneumonia, granulomatous, multifocal to coalescing, severe.
2. Spleen: Splenitis, granulomatous, multifocal to coalescing, severe, with mineralization.
3. Liver: Hepatitis, granulomatous, multifocal, moderate.

JPC Comment: The contributor has provided an excellent review of infection by *M tuberculosis*, (which has also been a popular submission in non-human primates as well as various models over the years).

The very early history of *Mtb* is still conjecture, but early strains may have infected hominids up to three million years ao with modern strains originating some 15,000-20,000 years ago. Eqyptian mummies have demonstrated skeletal deformitis reminiscent of "Pott's disease", and are even present in Egyptian art. The first written documents about TB appeared in India and Chinica dating back to 3000 to 2000 years ago.[2]

TB was well known and referred to as *phthisis* in ancient Greece. Isocrates first suggested the contagious nature of "the king's evil". The Romans recognized the fist symptomatology of TB and recommended fresh air, milk, and sea voyages as treatment[2].

Pulmonary TB was well known in Middle Ages Europe, with scrofula, a form of TB affecting the cervical nodes, described as a new clinical form. Before the first surgical interventions in the removal of "scrofula", the touch of English or French royalty was considered a cure (and continued in France until 1825).[2]

The true infectious nature of "phthisis" and "consumption" was expounded upon by English physician Benjamin Martin, and the disease was first called "tuberculosis" Johan Schonlein in the mid 19th century. The industrial revolution and poorly ventilated and overcrowded workplaces and housing with poor sanitation resulting in a fluorishing of TB, with up to 15% of workers dying of tuberculosis in 1838-1839 in England alone. The anemic pllor of the afflicted resulted in another name – "the white plague". The "white plague" reached a zenith in the mid-1800s, resulting in almost one in four deaths in Europe and North America[2].

The 1800s also brought a new and revised view of tuberculosis, with numerous renowned clinicians connecting the dots between miliary disseminated disease, tubercules, consolidation, pleurisy and pulmonary cavitation. In 1843, German

Mycobacteria	Species Affected	Systems involved and/or Gross appearance	Typical histologic appearance
M. tuberculosis	humans, NHPs, elephants, psittacine birds (zoonosis and reverse zoonosis) exotic ungulates, marine mammals, carnivores[14], dogs, cats, pigs, cattle Potential reservoir species: humans	Granulomas – lung and systemic (i.e. liver, spleen, etc.)	granulomas
M bovis	cattle, dogs/cats, humans, cervids, swine, horses deer, elk, bison, buffalo, goats, camels, llamas, swine, elephants, rhinoceroses, dogs, foxes, cats, mink, badgers, humans, NHPs, pigs, goats, warthogs, cats, mustelids, humans Potential reservoir species: badgers, brush tailed possums, swamp buffalo, buffalo, bison, various species of deer	**cattle:** granulomas – lung and systemic (lymph nodes, gastrointestinal tract, etc) **dogs and cats**: skin nodules or thickening/inflammation **humans**: pulmonary granulomas or gastrointestinal inflammation **cervids**: pulmonary granulomas, superficial lymphadenitis with draining tracts (DDx: *Fusobacterium necrophorum* **horses**: Gastrointestinal thickening/ granulomas **swine**: systemic granulomas	granulomas **dogs and cats:** unstructured pyogranulomatous inflammation of the skin dissecting along facial planes. (Note: central necrosis and paucibacillary help to distinguish from feline leprosy); often more granulation tissue with few scattered macrophages.
M avium subspecies *avium* and *hominissuis*[6]	birds > swine, cattle, horses, sheep, NHPs, humans	**birds**: thin body condition with intestinal and hepatic > systemic granulomas (lungs, air sacs, spleen, bone marrow and skin) **humans**: lymphadenitis, granulomas – lung and/or systemic	granulomas
M. avium paratuberculosis	cattle, goats, sheep	muscle atrophy/wasting; thickened mucosa of the ileum, large intestine, enlarged draining nodes; intimal plaques/mineral in thoracic aorta **small ruminants**: granulomas (enteric or vascular/lymphatic)	multibacillary – unstructured granulomatous enteritis with villus atrophy **sheep**: lepromatous neuritis reported
M.microti[18]	voles, humans	**voles**: gastrointestinal granulomas **humans**: pulmonary granulomas	granulomas
M.africanum[4]	humans	Pulmonary granulomas	granulomas

M.avium intracellularae complex (MAC)	dogs, cats	atypical mycobacterial skin infection - singe to multiple cutaneous and subcutaneous nodules, plaques, macules or diffuse swelling In cats: thickened, hardened tissue in the inguinal fat	multibacillary unstructured pyogranulomatous dermatitis and panniculitis. Can resemble feline leprosy. Occasionally fibroplasia may be marked and the lesion may appear as a spindle cell neoplasm
M. marinum[10]	fish humans	fish: systemic disease (potential route of infection skin trauma or gastrointestinal tract) humans: skin granulomas > pulmonary granulomas	granulomas
M. kansasii	humans	cervical lymphadenitis; pulmonary granulomas	granulomas
M.scrofulaceum[15]	humans	cervical lymphadenitis "scrofula"	granulomas
saprophytic Mycobacteria (*M. smegmatis, M. fortuitum, M. chelonae*[8], *M. phlei, M. thermoresistible, M. xenopi*)	dogs/cats	Focal thickened skin / inflammation	atypical mycobacterial skin infection - Similar to MAC although paucibacillary and clear vacuoles surrounded by neutrophils and peripheral epithelioid macrophages. Organisms can be found within the clear vacuoles
M. leprae[9]	armadillos, sooty mangabeys, chimpanzees, cynomolgus macaques, red squirrels	Multifocal to coalescing granulomatous dermatitis with loss of sensation/body parts on face, hands, and feet.	granulomas (tuberculoid) to unstructured (lepromatoid) granulomatous inflammation centered on nerves
M lepraemurium	rodents, cats	often head and limb cutaneous or subcutaneous nodules with or without alopecia or ulceration, often 1-3 year old cats	granulomatous dermatitis and/or panniculitis – large, pale, foamy macrophages; tuberculoid (organized granulomas) to lepromatous (sheets of cells); nerve involvement is only sporadic (distinct from human leprosy
Mycobacterium?	Cats	Feline tuberculosis syndrome in adult cats with firm skin nodules with draining tracts	pyogranulomatous dermatitis and panniculitis
Mycobacterium?	Dogs	canine leproid granuloma syndrome – firm painless nodules mainly on the head and dorsal pinnae of short coated breeds	acid fast bacteria identified, but not cultured; histo description unavailable

Table 1. Common mycobacterial infection in nonhuman primates.

physician Philipp Klencke was able to reproduce the human and bovine disease n rabbits. In 1850, the "sanatorium cure" was described for the first time by Hermann Berhmer, a botany student suffering from TB himself, and was used for the next 100 years as a mainstay of treatment for TB patients.[2]

In 1882, Robert Koch identified, isolated, and for the first time visualized the tubercle bacillus of *Mycobacterium tuberculosis* in a number of manifestations of tuberculosis, including pulmonary, scofulaceous, extra-pulmonary, and meningeal lesions

.

Following on his work, Paul Ehrlich developed alternate methods of staining, which in the hands of Franz Ziehl and Friedrich Neelson, became the first acid alcohol method for demnstrating the bacillus in tissue.[12]

In 1895, Wilhelm Konrad von Rontgen discovered the use of X-rays and became the first physician to visualize and detect TB lesions in the lungs; X-rays were an inexpensive method of diagnostic screening together with the tuberculin skin sensitivity test until the 1950s. In 1890 Koch himself developed a concentrated filtrate of cultured tubercle bacilli which he called "tuberculin" or "Koch's lymph" which he believed, could actually cure the disease. However, when injected, it cause violnt ractions, high fever, expansion of pre-existing lesions, and a severe reaction at the site, which he noted on self-incoulation. While it never did cure the disease, it was noted that infected individuals would develop "allergy" upon injection, resulting in an effected diagnostic method. The tuberculin and its method of use in the skin continued to be refined until the development of tuberculin purified protein defivative (PPD) by American biochemists Florence Seibert and Esmond Long in 1930, which was able to also detect latent subclinical infections.[12]
Vaccination for TB over the years has been problematic at worst, ineffective most of the time, and today is used only in aras with a high prevalence of childhood disease and in people in the military and healthcare with a high risk of exposure. The most successful advance in vaccination came in 1905 by two French bacteriologists, Albert Calmette and Camille Guerin at the Pasteur Institute, who developed a live attenuated vaccine from a non-virulent stratin. Over 100,000 children were vaccinated with this strain in the 1930s across Europe. Unfortunately 250 children were vaccinated with a BCG vaccine accidentally contaminated with a virulent strain in Lubeck Germany; 73 died and 135 developed clinical tuberculosis. Childhood vacination continued in post-WWII Europe and Asia to combat a resurgence of TB, but ultimately was discontined in the 1970s, when strict control programs were considered sufficient to control the spread.[12]

In 1993, the World Health organization declared TB a global emergency, and in 1995 defined the directly observed treatment, short-course strategy (DOTS) control policy, which has decreased the global incidence of TB by 1.5% each year, and overall mortality from TB has declined 22% from 200-2015. With new and effective anti-tuberculosis chemotherapeutic agens, the strategy of early diagnosis and targeted therapy is now considered to have the best cost/benefit ratio for treating this worldwide disease.[12]

The moderator and attendees reviewed a number of genpath concepts regarding mycobacterial infections, a number of of species and concepts regarding mycobacterial infections in a variety of species, and some diseases that might grossly cause nodules in the lungs of non-human primates. She mentioned the current theory of aortic mineralization in cattle with severe granulomatous disease as being the result of production of 1,25-cholecaliferol by the large numbers of macrophages in this disease and hypercalcemia.

References:

1. Ashenafi S, Aderaye G, Bekele A, Zewdie M, Aseffa G, Hoang ATN, Carow B, Habtamu M, Wijkander M, Rottenberg M, Aseffa A, Andersson J, Svensson M, Brighenti S. Progression of Clinical Tuberculosis is Associated with a Th2 Immune Response Signature in Combination with Elevated Levels of SOCS 3. 2014. Clin Immunol.151:84-99.
2. Barberis I, Bragazzi NL, Galluzo L, Martini M. The history of tuberculosis: from the first historical records to the isolation of Koch's bacillus. *J Prev Med Hyg* 2017; 58:E9-12.
3. Caswell JL, Williams KJ. Respiratory System. In: Jubb, Kennedy, and Palmer's Pathology of Domestic Animals. Vol 2. 5th ed. Editor: Maxie MG. Philadelphia, PA: Elsevier; 2007: 606-610
4. de Jong BC, Antonio M, Gagneux S. *Mycobacterium marinum* – Review of an Important Cause of Human Tuberculosis in West Africa. 2010. PLOS Negl Trop Dis. 4(9):1-9
5. Deretic V, Singh S, Master S, Harris J, Roberts E, Kyel G, Lee HH, Vergne I. *Mycobacterium tuberculosis* inhibition of phagolysosome biogenesis and autophagy as a host defence mechanism. 2006. Cell Microbio 8(5):719-727
6. Dhama K, Mahendran M, Tiwari R, Singh SD, Kumar D, Singh S, Sawant PM. Tuberculosis in Birds: Insights into the *Mycobacterium avium* Infections. 2011. Vet Med Intern. 1-14
7. Ginn PE, Mansell JEKL, Rakich PM. Skin and appendages. In: Jubb, Kennedy, and Palmer's Pathology of Domestic Animals. Vol 1. 5th ed. Editor: Maxie MG. Philadelphia, PA: Elsevier; 2007: 688-689
8. Greer LL, Strandberg JD, Whitaker BR. *Mycobacterium chelonae* Osteoarthritis in a Kemp's Ridley Sea Turtle (*Lepidochelys kempii)*. 2003. J Wild Dis 39(3): 736-741
9. Honap TP, Pfister LA, Housman G, Mills S, Tarara RP, Suzuki K, Cuozzo FP, Sauther ML, Rosenberg MS, Stone AC. *Mycobacterium leprae* Genomes from Naturally Infected Nonhuman Primates. 2018. PLOS Negl Trop Dis. 12(1):1-17
10. Lescenko P, Matlova L, Dvorska L, Bartos M, Vavra O, Navratil S, Novotny L, Pavlik I. Mycobacterial Infection in Aquarium Fish. 2003. Vet Med –Czech (3):71-78
11. Lowenstine LJ, Osborn KG. Respiratory System Diseases of Nonhuman Primates. In: Nonhuman Primates in Biomedical Research: Diseases. Vol 2. Editors: Abee CR, Mansfield K, Tardif S, Morris T. London, UK: Elsevier; 2012: 413-48.
12. Martini M, Besozzi G, Barberis I. The never-ending story of the fight against tuberculosis: from Koch's bacillus to global control programs. *J Prev Med Hyg* 2018:E241-247.
13. Messenger AM, Barnes AN, Gray GC. Reverse Zoonotic Disease Transmission (Zooanthroponosis): A Systematic Review of Seldom-Documented Human Biological Threats to Animals. 2014. PLOS One 9(2):1-9
14. Montali RJ, Mikota SK, Cheng LI. Mycobacterium tuberculosis in Zoo and Wildlife Species. 2001. Rev Sci Tech 20(1):291-303
15. Moulis G, Martin-Blondel G. Scrofula, the King's Evil. 2012. CMAJ 184(9).

16. Pieters J. *Mycobacterium tuberculosis* and the macrophage: Maintaining a Balance. 2008. Cell Host & Microbe 3:399-407
17. Schwartz RH. T cell Anergy. 2003. Annu Rev Immunol 21:305-334
18. Smith NH, Crawshaw T, Parry J, Birtles RJ. *Mycobacterium microti*: More Diverse Than Previously Thought. 2009. J Clin Microbiol. 47(8):2551-2559
19. Yan L, Cui H, Xiao H, Zhang Q. Anergic Pulmonary Tuberculosis is Associated with Contraction of the Vd2+T cell Population, Apoptosis, and Enhanced Inhibitory Cytokine Production. 2013. PLOS One 8(8):1-8
20. http://www.who.int/news-room/fact-sheets/detail/tuberculosis

CASE II: WSC 2013 Case 1 (JPC 4032584).

Signalment: 119.2 kg (262.8 lb), 5-month-old, female, Hereford calf (*Bos primmigenus*)

History: The day prior to euthanasia, the calf was found struggling to walk, and within 4 hours was recumbent. Four days previously, another 6-month-old heifer calf was found dead on this farm.

Gross Pathology: Body condition was good with visible subcutaneous and visceral fat. There was mild interlobular septal edema in the lungs and a large amount of blood exuded from the cut surface. Few pinpoint to 3mm diameter white foci were present both on the surface and within the parenchyma of the liver. There was mild enlargement of the spleen (interpreted as a result of euthanasia). The serosa of the terminal segment of the ileum was reddened and the contents were watery and red. The urinary bladder contained a moderate amount of clear urine. Normally formed feces were present in the rectum.

Laboratory results: Immunofluorescence Test for Rabies Virus Antigen: Positive

Microscopic Description: Medulla oblongata: Multifocally, blood vessels are surrounded by 1 to 6 cell thick cuffs of lymphocytes with lesser numbers of macrophages and plasma cells. There are occasional mild perivascular hemorrhages with edema. Increased numbers of glial cells, including astrocytes, microglia and oligodendrocytes, are present in the neuropil. Low numbers of neurons in areas of gliosis have one or multiple 2-4 um diameter, round to oval, eosinophilic, cytoplasmic inclusions (Negri bodies).

Contributor's Morphologic Diagnosis:

Medulla oblongata: Encephalitis, lymphocytic, plasmacytic and histiocytic, multifocal, moderate, with gliosis and neuronal intracytoplasmic inclusions (Negri bodies), etiology consistent with rabies virus (RABV)

Contributor's Comment: The microscopic and immunofluorescence findings in this calf indicate rabies encephalitis. Rabies virus (RABV) is a lyssavirus in the family Rhabdoviridae that causes acute, progressive encephalitis that is almost invariably fatal.[6] Two biotypes of RABV exist, i.e. "fixed" virus and "street" virus.[3] Fixed RABV is the

Brainstem, 5-month-old calf. One cross section of the brainstem is presented for examination. There are no apparent lesions at subgross magnification. (HE, 6X)

stabilized laboratory biotype, which is highly neurotropic but does not create Negri bodies and is not secreted in saliva, while street RABV is the wild biotype that circulates in nature.[3] All mammalian species can be infected by RABV, which is most commonly transmitted by bites of carnivores or bats. The virus can also enter via sensory nerve endings of the skin and mucous membranes, which has been observed in rare instances of aerosol exposure and ingestion (e.g. cannibalism and scavenging).[5] RABV infection has been documented after human organ transplantation, e.g. cornea, kidney, pancreas and liver.[5] The principal reservoir vector species within the USA and Canada vary by geographic region. Skunks, foxes and raccoons are important reservoir vectors in the continental United States and Canada, with raccoons of particular importance along the Atlantic coast, coyotes in southern Texas, and arctic foxes in Alaska.[3,4] In central and South America, dogs are the most important reservoir vector, with rabies also reported in terrestrial wildlife, e.g. monkeys, wolves, skunks and foxes. The Indian mongoose (*Herpestidae auropunctatus*) has become an important vector species in the Caribbean after its introduction to control rodents.[5] In Europe, the red fox is the principal reservoir vector, although dogs and the raccoon dog (*Nyctereutes procyonoides*) in Eastern Europe may serve as independent reservoir species or spill-over hosts dependent on the fox rabies cycle.[5] In Africa and Asia, dogs are important reservoirs with spillover to other species a major problem, for example, rabies accounts for 25,000-30,000 human deaths annually in India[8] and threatens the endangered Ethiopian wolf (*Canis simensis*) and the African wild dog (*Lycaon pictus*). Australia, New Zealand, Japan and the British Isles are free of RABV infection, but other lyssavirus species exist in bats in at least some of these countries.[5] Fructivorous, insectivorous and vampire bats are capable of transmitting RABV.[3,4]

The bite of a rabid animal delivers the virus into the striated muscle and connective

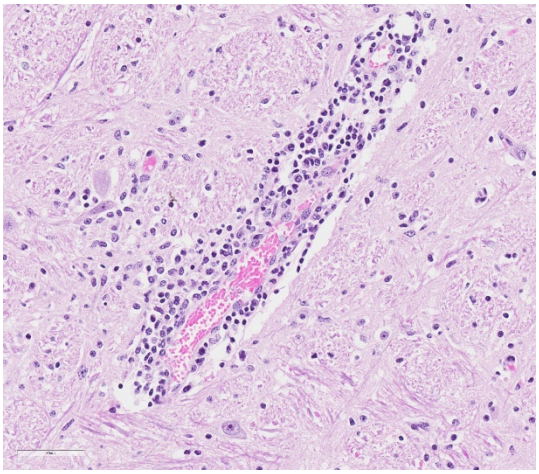

Brainstem, 5-month-old calf. Multifocally within the brainstem, Virchow-Robins spaces are expanded by 4-5 layers of lymphocytes and fewer histiocytes. (HE, 108X)

tissue at the site of inoculation. At the site of entry, the virus replicates for a short period in myocytes, then buds from the sarcolemma to invade the neuromuscular junction through conjugation with nicotinic acetylcholine receptors. Virus is then taken up at the axon terminus and delivered by retrograde axoplasmic flow within neurons to spinal cord and brain.[3,4] Subsequent replication occurs in the limbic system and neocortex.[3,4] The surface-exposed viral coat glycoprotein (RVG) is responsible for the neurotropism of RABV by binding to several neural tissue receptor molecules, specifically the neuronal cell adhesion molecule (NCAM) and the p75 neurotrophin receptor (p75NTR).[3] In animal species that serve as vectors, the viral genome moves centrifugally from the central nervous system through peripheral nerves to a variety of tissues including the adrenal medulla, nasal mucosa, cornea, epidermis and most importantly, the salivary glands.[1,3] In the salivary gland of these hosts, virions bud from plasma membranes at the apical (luminal) surface of mucous cells and into the intercellular canaliculi, and are released in high concentrations into the saliva resulting in highly infectious saliva.[2,3,4]

Following a 1-8 week incubation period, the clinical course of rabies is usually acute, lasting 1-2 days, but occasionally lasting up to 14 days. Following a prodromal phase, aberrant behavioral patterns occur in the infected animal. There are two recognized clinical forms of disease: furious and dumb or paralytic.[3] Clinical features of the furious form include restlessness, nervousness, aggression, inability to swallow water, hypersalivation, exaggerated response to light and sound, and hyperesthesia. Following the furious phase, paralysis and recumbency ensues. Terminally, there are often convulsive seizures, coma and then respiratory arrest.[2,3,4]

Gross anatomical lesions specific to RABV infection are typically not evident. Histological lesions of rabies are those typical of nonsuppurative encephalomyelitis with ganglioneuritis. Inflammatory and degenerative changes are usually most severe from the pons to the hypothalamus and in the cervical spinal cord, with relative sparing of the medulla oblongata.[3] The inflammatory reaction typically is one of perivascular cuffing and focal gliosis, although inflammatory changes may be minimal or absent in some cases.[3] Intracytoplasmic viral inclusions, known as Negri bodies, are present most commonly in the hippocampus of carnivores and in cerebellar Purkinje cells of herbivores. Negri bodies are found in neurons that are otherwise histologically normal and are reported to be scarce in regions where inflammation is the most severe.[3] The most severe lesions are commonly found in dogs, whereas other species (particularly ruminants, which are highly susceptible) may have minimal perivascular cuffing and few glial nodules in spite of having numerous Negri bodies.[3] In ruminants, gliosis is prominent in both the white and gray matter. Perivascular cuffs are composed mostly of lymphocytes, and a ring of hemorrhage largely confined to the perivascular space is commonly found surrounding cuffed vessels.

Contributing Institution:

Department of Pathobiology and Veterinary Science
Connecticut Veterinary Medical Diagnostic Laboratory
University of Connecticut
www.patho.uconn.edu

JPC Diagnosis:
Brainstem: Meningitis, lymphocytic, diffuse, mild, with gliosis and occasional neuronal intracytoplasmic viral inclusions.

JPC Comment: As in Case 1 of this conference, a thorough and wide-ranging review by the contributor allows us to discuss some of the interesting aspects of the medical history of this well-known and global disease. The etymology of the word rabies itself is controversial, with authorites splet on whether it derived from the word *rabias*, meaning "rabies" in Latin or the Sanskrit terms *rabhas* or *rabhasa.*[7]

Rabies has likely been known to humans ever since the domestication of dogs, estimated at up to 30,000 years ago. The first actual mention of rabies (and penalties for owners of rabid dogs) were found in Sumerian tablets dating back to 1930 BC – "If a dog becomes rabid […] and the dog bites a man and causes his death, the owner of the dog shall pay forty shekels of silver; if it bites a slave and cuses his death, he shall pay fifteen shekels of silver". At this time, herbs were often used as first attempts to cure the disease, and failing that, incantations at the local temple. Dogs were thought to be more likely to become rabid during a lunar eclipse, particularly if it occurred at the year's end.[7]

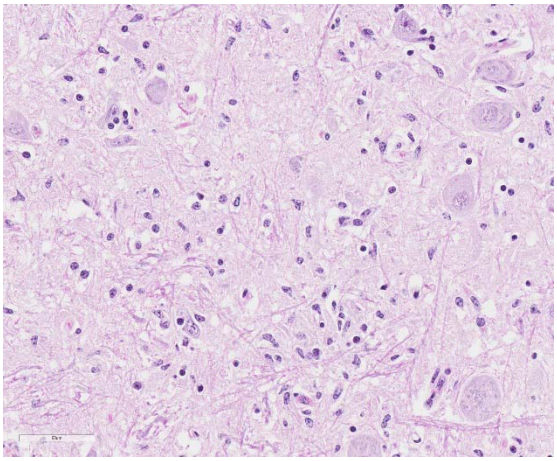

Brainstem, 5-month-old calf. There is a mild to moderate gliosis within brainstem nuclei, and occasionally poorly formed glial nodules (arrows). (HE, 400X)

Many cultures in antiquity made attempts to prevent the transmission of disease. In Persia, cutting off a dogs tail when they are 40 days old was done to protect them from the bite of another rabid animals. One prevention mistep in China during the Jin dynasty was to treat by applying the biting dog's brain tissue to the bite wound to prevent disease." Pedianus Doscorides, a Roman physician living in Turkey may have started down a more appropriate path, calling for the heat cauterization of bites by rabid dogs, but this was later denounced by other Roman doctors as unnecessary brutal.[7]

In ancient Greece, many medical texts showed an increasing awareness of rabies and its effects, with detailed recunts of its symptoms in man and animals, recognition of a latency period between the bite and onset of symptoms, and even palliative care.[7]

The Middle Ages showed an advance in the diagnosis of clinical rabies with hydrophobia described in affected humans (and noted to be absent in dogs), paralyic rabies, and the need for thorough cleansing of bite wounds as a potential treatment (although the agent was still considered to be a toxin). Religion impacted early vaccination, with dogs vaccinated with a white-hot "Key of Saint Hubert" to prevent

the contraction of rabies, and eventually was applied to the wounds of people bitten by dogs believed to be rabid. Alternatively, an incision would be made in the unfortunate bite victim, and threads from the Saint's cassock were implanted, accompanied by prayers and fasting. Patients not responding to these surefire cures were unfortunately suppressed between mattresses (an alternative form of treatment in Europe until the nineteenth century. [7]

The Renaissance saw rabies as a major entry in medical texts of the time, with an entire volume written on it by Dr. Julien Le Paulmier. The practices at Saint-Hubert were condemned, and cleansing the wound thoroughly was considered a beneficial practice among clinicians. As the saliva of infected dogs was now being looked at as the potential vector for transmission of the disease, an enterprising Prussian artillery general Kazimierz Siemienowicz tried filling hollow artillery shells with the saliva of rabid dogs and firing them at the enemy in the mid 1600's. [7]

The exploration of the new world brought dog-associated rabies to a continent which had largely recognized only bat-associated rabies, and spread to local wildlife such as mongooses in the Caribbean islands. [7]

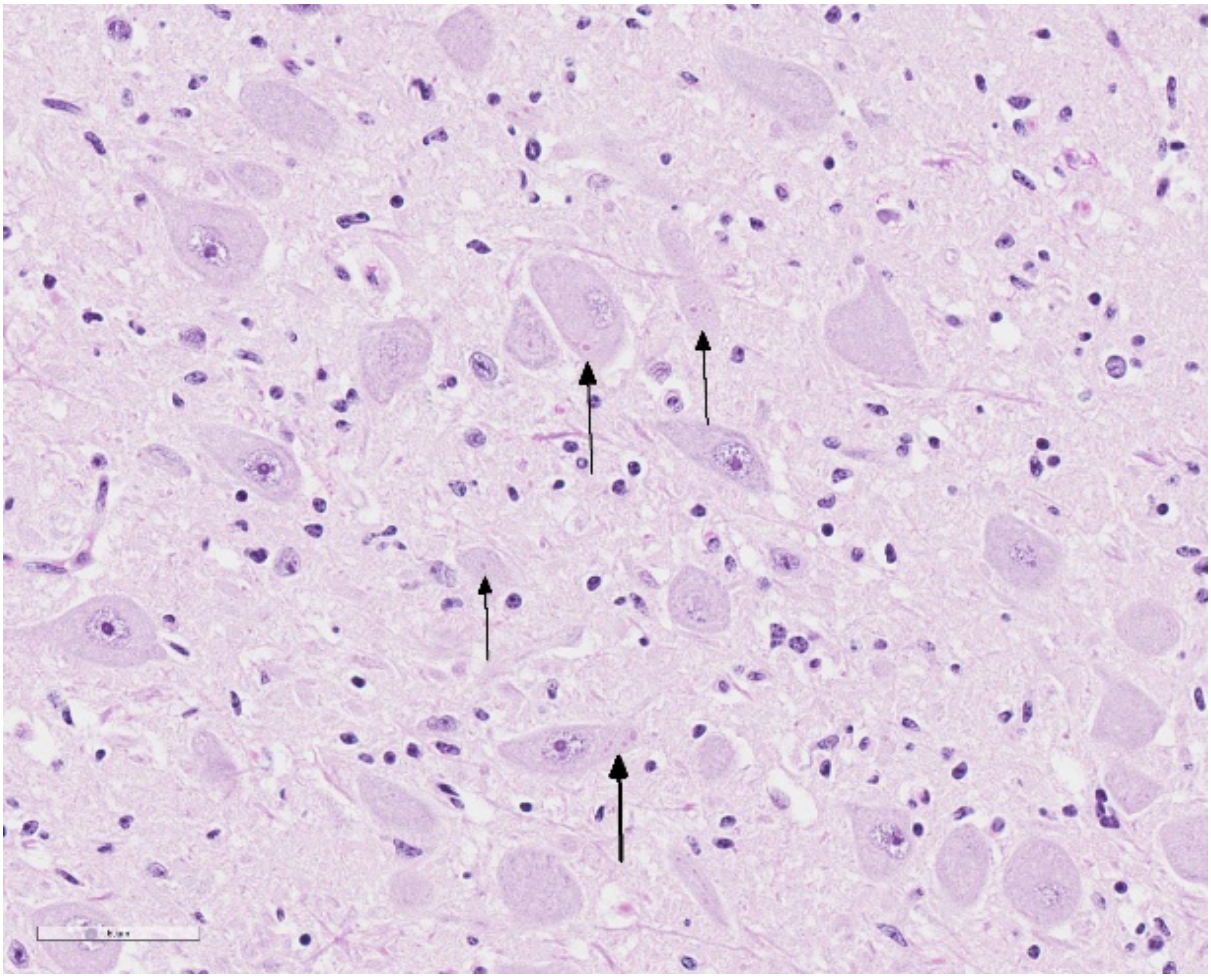

Brainstem, 5-month-old calf. Within the subependymal brainstem nuclei, neurons often contain one or more irregularly round 2-3um intracytoplasmic inclusions (Negri bodies) (HE, 400X).

In Renaissance Europe, the perception of the pathogenesis was evolving. The current thought was that rabies was transmitted by "seeds" (*semina*) in the saliva, and that transmission after a bite wound was an inconstant event. The first 15-day quaratine period was proposed by Joseph-Ignace Guillotin (yes, that Guillotin) in 1776. Conversely, he also suggested inoculation experiments on prisoners awating capital punishment (which was supported by Louis Pasteur years later), but thankfully this practice did not occur. Advances in treatment continued to lag behind, with application of the "hair of the dog" to the wound, and even eating omelets flavored with "dog-rose root" (previoulsy suggested over a fifteen hundred years before) as examples of treatments of the time. [7]

In the early 1800's, the newly minted "scientific approach" made great strides on elucidating the transmission of rabies and potential prevention. In 1813-1814, several researchers in Europe clearly transmitted the disease with the saliva of rabid dogs humans, and sciatic nerve tissue from a rabid cat. Francois Magendie, 30 years later, first suggested the agent was not a poison but a virus, and in 1879, Paul-Henri Duboue first proposed the theory of neuronal transmission. [7]

It was in this time of significant advance that Louis Pasteur was developing a live attenuated vaccine developed by a dessication technique and successfully used on dogs subsequently challenge with live rabies virus. The first human trial, tried on a child who was exhibiting sign of rabies, was met with failure, but a second trial, on 9-year-old Joseph Meister, only two days after the bite of a rabid dog and before the demonstration of any clinical signs was a success. Over 11 days, a total of 13 injections with initially attenuated and progressively more virulent virus allowed Master Meister to develop immunity against the virus and survive. A second successful attempt three months later in another child proved the efficacy of post-exposure prophylaxis, and since that time, PEP has saved countless lives around the world. In 1932, the League of Nations published records of over 115,000 patients that had received PEP, with a combined rabies mortality of oly 0.4%).[7]

Research on the virus itself proceeds apace during this time. In 1903, Adelphi Negri and Lina Luzzani-Negri desibed the fist RABV-neuronal interaction and the cytoplasmic inclusions that still bear their names. The virus itself was first visualized ultrastructually in the early 1960s, and its viral genome was mapped in 1988. These and many other advances allowed modification and shortening of PEP protocols, and laid the groundwork for marked advances in vacine research. [7]

However, these advances have only transformed rabies from a globally prevalent scourge, to a global neglected disease, following its eradication in North America and Europe. As of 2017, na estimated 59,000 people die each year of rabies, easily eclipsing similar deaths from Ebola outbreaks. Current attempts to curb these numbers include significant vaccination efforts in animal species, and human rabies vaccination in endemic areas. [7]

Thre was spirited discussion among participants on formulating a morphologic diagnosis for the relatively minimal inflammationin this case. The term meningitis was ultimately used (although no inflammation was seen in the meninges proper, as the lymphocytes and plasma cells appeared to be confined with Virchow-Robin's space around vessels, (an extension of the meninges). Other participants

preferred “perivascular encephalitis” but the inflammation did not appear to extend into the adjacent brainstem parenchyma, and still others preferred “perivascular cuffing.”

References:

1. Balachandr A, Charlton K. Experimental rabies infection of non-nervous tissues in skunks (*Mephitis mephitis*) and foxes (*Vulpes vulpes*). *Vet Pathol*. 1994;31:93-102.
2. King AA, Turner GS. Rabies: a review. *J Comp Path*. 1993;108:1-39.
3. Maxie MG, Youssef S. Nervous system. In: Maxie MG, ed. Jubb, Kennedy and Palmer’s, *Pathology of Domestic Animals,* vol. 1. 5th ed. Edinburgh, UK: Elsevier Limited; 2007:413-416.
4. Murphy FA, Gibbs EPJ, Horzinek MC, Studdert MJ. *Veterinary Virology*, 3rd ed. San Diego, CA: Academic Press; 1999:432-439.
5. Nel LH, Markotter W. Lyssaviruses. *Crit Rev Microbiol.* 2007;33:301-324.
6. Stein LT, Rech RR, Harrison L, Brown C. Immunohistochemical study of rabies virus within the central nervous system of domestic and wildlife species. *Vet Pathol.* 2010;47:630-633.
7. Tarantola A. Four thousand years of concepts relating to rabies in animals and humans, its prevention and its cure. *Trop Med Inf Disease* 2017; 2(2). Pil E5. Doi: 10.3390/tropicalmed202005.
8. Wunner WH, Briggs, DJ. Rabies in the 21st century. *PLoS Negl Trop Dis.* 2010;4(3):e591.

CASE III: 19N153 (JPC 4134352).

Signalment: 3-month-old, male, mixed breed, *Ovis aries*, sheep.

History: In a property with 108 ewes with their lambs with average age of 3 months, 13 lambs got sick. Signals were first noticed by the animals’ caretaker on April 4, 2019, and included paresis, decubitus, nasal discharge, and cough. On April 6, 2019, 10 affected lambs had died, two of which were submitted to necropsy. The remaining three were referred to the Veterinary Teaching Hospital (VTH). Clinical examination showed rales on pulmonary auscultation, hyperemic ocular mucous membranes, and mucous nasal discharge, and the lambs were treated with Se/Vit E, flunixin meglumine and Ceftiofur. Two of them completely recovered and one died on the second day from the start of treatment. The results of the bloodwork performed at the VTH are presented in Table

Hindlimb, lamb. The heavy muscle groups of the hind limb are partially white and opaque, with a chalk-like appearance. (Photo courtesy of: Laboratory of Anatomic Pathology, Universidade Federal de Mato Grosso do Sul. https://www.ufms.br/)

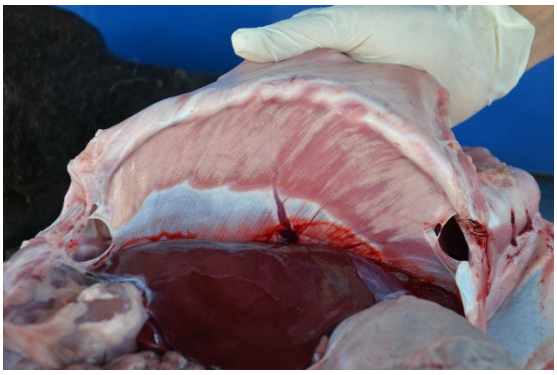

Diaphragm, lamb. The diaphragm has white and opaque stripes as if they were painted-brushed. (Photo courtesy of: Laboratory of Anatomic Pathology, Universidade Federal de Mato Grosso do Sul, https://www.ufms.br/)

1. Some of the lambs the remained at the property presented a subclinical increase in the muscle enzymes activity. In total, three lambs were necropsied, and presented similar gross and histological lesions.

Lambs were fed with 33 kg of ration manufactured on the property that included soybean hull, soybean meal, calcium carbonate and 63 kg of silage from Mombasa grass. Mombasa silage was being offered for the last 48 days. Previously sorghum silage has been provided to the lambs. The lambs were vaccinated and dewormed at 30, 60 and 90 days. The ewes were fed the ration at night ewes spent the day in Tifton pickets.

Gross Pathology: The cadaver is of an intact male lamb, undefined breed, with a brown wool coat with light areas, in a fair body nutritional status. The conjunctiva is of normal color, and the oral mucosa is pale. There is opacity of the left cornea (probably due to trauma while in decubitus). Multiple, focal, small to extensive, white-opaque chalk-like areas are observed in several muscle groups (Figure 1). The intensity of the lesions varied from mild (+) to severe (+++). These lesions distributed bilaterally and symmetrically in following muscles: supra-spinous (++), radial carpi (+), lateral digital extensors of the carpus, infra-spinosus (+), triceps (+++), brachiocephalic (++), gluteus medius (+++), semitendinosus (++), semimembranosus (+++), vastus medialis, (+++), gastrocnemius (+++), vastus lateralis (++), longissimus dorsi (+++), diaphragm (++) (Figure 2), and tongue (+) and musculi colli.

The craniodorsal region of the right (the side of decubitus) lung is diffusely dark-red, firm and without crepitation. This aspect extends to portions the right caudal lobe. Large quantities of *Haemonchus contortus* were in the abomasal lumen, admixed with pasty dark-red abomasal content.

Microscopic Description: Skeletal muscle (semimembranous): Transverse and longitudinal sections of the skeletal muscles were analyzed. Multiple myofibers are either reduced in size or markedly swollen. Segments of affected myofibers are homogeneously hypereosinophilic, with loss of sarcoplasmic striations and, lumpy cleavage of many myofibers (floccular degeneration); the nucleus of these myofibers is pyknotic and shrunken; these changes are more evident in cross-sections. The sarcoplasm of the affected myofibers is moderate to markedly cluttered by fine to dense, basophilic, and birefringent granular material (mineralization). Randomly, in the endomysium, small foci of lymphocytes, plasma cells, and macrophages are seen. Also, satellite there is marked proliferation and swollen of satellite cells, and occasional multinucleated cells and nuclei with mitotic

figures (attempts in regeneration) can be seen in the cytoplasm of degenerating/necrotizing myofibers. Some myofibers are slender, tapered and clear and contain multiple satellite cells arranged in rows in the sarcoplasm (myotubules). This latter finding is most often observed in longitudinal sections.

Within the lumen of pulmonary alveoli and bronchioles are small or moderate amounts of inflammatory cells, predominantly intact neutrophils. In the lumen of the alveoli, there is also amorphous eosinophilic material (edema), eosinophilic fibrillary material (fibrin) and moderate quantities of alveolar macrophages. Occasionally, in the bronchial lumen, small, long, slender fibers measuring about 100 μm in length and the slightly birefringent wall and light center are seen. Those structures are compatible with plant fibers. There are sparse hemorrhagic foci.

There is moderate hepatocellular vacuolar degeneration. There are no lesions in the spleen, kidney, adrenal, myocardium, intercostal, diaphragm, and encephalon.

Contributor's Morphologic Diagnosis:

1) Necrotizing acute or subacute myopathy, multifocal, polyphasic, with prominent calcification and myofiber regeneration
2) Lung, bronchopneumonia, suppurative, multifocal, moderate, associated with scattered intrabronchiolar vegetable fibers (consistent with aspiration pneumonia) (not submitted)

Contributor's Comment Nutritional myopathies are important diseases of calves,[1,18] lambs, swine,[19] and foals,[15] but has been described occasionally in more than 20 animals species including rabbits,[13] birds,[11,19] goats,[17] reptiles,[10] and man.[19] The condition was first described in the 1930s and has since been attributed to Se/Vit E deficiency.[13]

The disease is a dominant part of the veterinary literature on muscle diseases[8] and is also known as nutritional myodegeneration, white muscle disease, stiff-lamb disease, nutritional muscular myopathy (although use of this latter denomination is not recommended). Several syndromes are associated with deficiency of Se, Vit E, or both in domestic animals, such as nutritional myopathy, degenerative myelopathy in horses, degenerative encephalopathy in birds, retention of placenta in cattle, hepatosis dietetica in pigs, mulberry heart disease in pigs, exudative diathesis in pigs[7] and chickens, steatitis (yellow fat disease) in cats, and immune system compromise;[19] in people this nutritional deficiency is known in China for inducing a degenerative cardiomyopathy known as Keshan disease.[19]

The pathogenesis of nutritional myopathy due to Se/Vit E deficiency is not entirely understood. In these cases, as is customary, the usual suspects are lined up, and free radicals (FRs) are the main ones. Se/Vit E are responsible for the protection of cell membranes against the action of FRs, which mediate cell membrane damage.[16] FRs are chemical specimens that have an unpaired electron in the most external orbit of the atom. FRs include reactive oxygen species such as superoxide (O2) and reactive nitrogen species such as NO.[16] Because they

possess this unpaired electron, FRs readily reacts with organic substances causing the peroxidation of the phospholipids, proteins and nucleic acids of the cellular membrane, leading the cell to necrosis. The protection of membranes is partly the responsibility of selenium-containing enzymes, and more than 30 selenoproteins are known[7] and are part of the glutathione peroxidase/glutathione reductase system.[4,9]

Test	♀1	♀2	♂3	Reference value
RBC's 10^6/µL	10,89	13,59	7,3	9-15
Hemoglobin (g/dL)	8,2	9,7	5,6	9-15
PCV (%)	28,8	35,6	20,2	27-45
MCV (fL)	26,4	26,2	27,7	28-40
MCH (g/dL)	28,5	27,2	27,7	31-34
Leukocytes (mm^3)	25.500	14.600	7.600	4.000-12.000
Neutrophils (mm^3)	20.910	9.928	4.636	3.000-6.000
Lymphocytes (mm^3)	4.590	4676		1.000-9.000
Platelets (mm^3)	1.574.000	1.337.000	1.406.000	300.000-600.000
AST (UI/L)	1.839,10	8.268,40	14.174,50	98-278
Creatinine (mg/dL)	0,4	0,3	0,4	1,2-1,9
Creatine kinase (UI/L)	2.068,10	14.333,70	57.384,50	8,1-12,9
GGT (UI/L)	-	-	-	20 a 52
BUN (mg/dL)	-	-	-	17,12 a 42,8
Tortal protein (g/dL)	5,93	5,46	5	6,0 a 7,9
Globulin (g/dL)	3,03	2,96	2,8	3,5 a 5,7
Albumin (g/dL)	2,9	2,5	2,2	2,4 a 3,0

Table 1. Nutritional myopathy. Laboratory tests performed in the three affected lambs referred to the VTH. Lamb # 3 died. The other two recovered after treatment.

If any condition deprives the organism from these mechanisms, the cellular membranes become physiologically defective, allowing the influx of calcium into the cytosol,

resulting in the accumulation of calcium in the mitochondria. Damaged mitochondria fail to maintain the energetic needs of the cell, which results in cell necrosis, which manifests, in the myofiber, as floccular necrosis. The membrane injury allows the leakage of enzymes such as creatine kinase (CK), whose increased activity into the serum is a sign of muscle injury.[7] One way to confirm the disease is by determining low levels of selenium in the food and carcasses of the affected animal, increased serum CK activity and histological findings of muscle degeneration.[7]

Several factors influence the transfer of Se from the soil to the plants, among them soil alkalinity (which favors the absorption of Se), type of plant (plants differ in their capacity to store selenium) and the presence of sulfur that competes with selenium, which is lower in the spring and in the rainy season.[7,8]

Data on selenium levels in Brazilian soils are scarce. However, outbreaks of nutritional myopathy are described in the South,[2] the Northeast,[1] and North[3] of the country. In the South outbreaks occur mainly from July to August (winter, rainy season). Morbidity may be low but may reach 20%.

Feed with concentrates with a high content of fatty acids favors the occurrence of Se/Vit E deficiency. On the other hand, in animals fed concentrate, the availability of selenium may also be decreased as a consequence of the low pH of the rumen. Animals may die acutely without premonitory signs or after onset of apathy, dyspnea, and blood-filled foamy nasal discharge. There is marked tachycardia (150-200 bpm) and temperature is normal.[7] In the acute form the treatment is usually ineffective. The most common form is the subacute with clinical course from a few days to a week, and mainly affects calves and lambs. The affected animals can be found in decubitus.

Clinical signs include muscle stiffness, difficulty in locomotion, muscle tremors, abnormal postures, apathy, and death. Occasionally it is possible to observe bilateral and symmetrical swelling of the gluteus, dorsolumbar muscles and muscles of the shoulders. The involvement of the diaphragm and the pharyngeal and esophageal muscles is responsible for the dysphagia seen in clinic cases.[7] Dysphagia results in aspiration pneumonia, so typical in cases of nutritional myopathy[2] and that occurred in the lambs of this outbreak. The subacute form (as in this report) generally responds well to treatment with Se/Vit E and animals recover within 3-5 days. Myoglobinuria is not a common sign in young animals but may occur sporadically in adult animals.[8]

Gross lesions are seen in the skeletal muscles and myocardium. They are bilaterally symmetrical and affected the muscles with a heavy load. The type of affected muscle varies with the age of the affected animal. In lambs the muscles of the neck and tongue (involved in suckling) are the most affected. In slightly older animals, muscles of the shoulder, thigh and diaphragm are most affected.[8] Calcification of well-developed lesions leaves the chalky (opaque white) muscle, which gives rise to the name and "white muscle disease.[2]

Microscopic changes in the myofibers vary somewhat between species, but are mostly the same. Usually they are polyphasic and include hyaline degeneration with loss of myofiber striations, floccular necrosis, marked proliferation of satellite cells, and an influx of neutrophils and macrophages into the sarcoplasmic tube. Secondary

Name of Condition	Epidemiology and Pathology
Senna occidentalis and *S. obtusifolia* toxicosis	Degenerative lesions are marked in the skeletal muscles and very mild, if any, in the myocardium. Mineralization of muscle lesions are mild or absent. Mostly monophasic lesions. Myoglobinuria is a common clinical sign. Treatment with Se/vit E is ineffective.[5]
Ionophore toxicosis	Ionophores are food additives, therefore the disease occurs in animals being fed commercial rations. Lesions are in both, myocardium and skeletal muscle. In ruminants, lesions are prominent in the myocardium. Mineralization of the lesions is not a feature. Mostly monophasic lesions. Myoglobinuria is part of the clinical picture. Treatment with Se/vit E is ineffective.
Nutritional myopathy (Se/vit E responsive disease)	Usually affects fast-growing young animals (2-4 month-old). Degenerative lesions occur in both skeletal and myocardial muscles. Myocardial lesions are not present in all cases.[7] There is extensive mineralization of the lesions, which gives an opaque soft chalk-like gross appearance to the lesions (which does not occur in the other degenerative diseases mentioned in this table). Mostly polyphasic lesions. When instituted early in the course of disease treatment with Se/Vit E is effective. Myoglobinuria is usually not part of the clinical picture, except in sporadic cases in adult animals.
Gossypol toxicosis	Monogastric animals, such as pigs, are more susceptible to gossypol toxicity than ruminants. Necropsy lesions do not always include muscle degeneration (Mostly polyphasic lesions). Acute hydrothorax, hydropericardium, ascites and subcutaneous edema are part of necropsy findings. Hepatic lesions of centrilobular necrosis in pigs intoxicated with gossypol can be severe.
Downer syndrome	Usually affects well-nourished, well-fed, animals with large muscle masses. The lesion is well demarcated and focal or focally extensive and results from pressure (ischemia). Lesions tend to be polyphasic. It affects the parts in decubitus, usually those close to bony prominences. Muscle hemorrhages, ulcerative lesions on the skin that correspond to the decubitus site may be associated with these lesions and aid in the differential diagnosis.

calcification is marked. The regeneration of muscle fibers is remarkable.[13]

The diagnosis is based on the characteristic clinical signs, associated to the clinical pathology and anatomopathological findings. Segmental necrosis of myofibers with calcification is typical of this disease, but not diagnostic. Confirmation of the diagnosis requires the determination of levels of selenium and α-tocopherol in tissues (renal cortex and liver for Se and liver for α-tocopherol). As the serum activity of glutathione peroxidase is highly correlated with blood levels of Se, the activity of this enzyme in the blood is used to assess levels of Se in tissues. Se and α-tocopherol analysis are useful because they differentiate cases of segmental myonecrosis from causes other than Se/Vit E deficiency.

The differential diagnosis should include toxic myopathies such as those caused by *Senna occidentalis* (coffee senna)[5] and *S. obtusifolia*[6] that frequently produce intoxication in cattle in this part the world, or by ionophore antibiotics, another common livestock toxicosis in this region. In cases of toxic myopathy, the agent must be investigated in the feed and the presence of the plant should be determined in the pasture. Some aspects of differential diagnosis are shown in Table 2.

Contributing Institution:

Department of Pathobiology and Veterinary Science
Connecticut Veterinary Medical Diagnostic Laboratory
University of Connecticut
www.patho.uconn.edu

JPC Diagnosis: Skeletal muscle: Myocyte degeneration and necrosis, polyphasic, diffuse, moderate, with mineralization and rare myocyte regeneration.

JPC Comment: Another excellent and far-ranging discourse on the entity of nutritional myopathy by the contributor allows us to explore some less common avenues of Vitamin E deficiency, this time the human disease associated with hypovitaminosis E.

While there are eight different forms of Vitamn E, four each in the tocopherols and four in the tocotrienols (which all are absorbed in the small intestine), the liver can metabolize only one, alpha-tocopherol. The other seven forms are excreted. Low Vitamin E diets are seen in emerging countries; in developing countries, diseases impacting absorption are the most common cause. In the US, although studies have shown that 90% of men and 96% of women 19 years or older have diets deficient in Vitam E, only 0.1% of this demographic have deficient serum levels of alpha tocopherol.

The most common causes of Vitamin E deficiency in humans include premature low birth weight (premature infants have low vitamin E reserves due to limited placental transfer), mutations in hepatic tocopherol transfer proteins, various causes of fat malabsorption, cystic fibrosis (as patients are unable to secrete pancreatic enzymes which help absorp within E, short bowel or inflammatory syndromes, abetalipoproteinemia, and a genetic mutation of chromosome arm 8q.

The known beneficial effects of Vitam E in humans are in the areas of antioxidants,

immunomodulatory, and antiplatelet effects. Vitamin E supplementations may impact the development of coronary artery disease by preventing oxidative changes to LDLs. It enhances lymphocyte prolfieration while decreased the production of prostaglandin E2 and serum lipid peroxides. By the combination of decreasing LDL oxidation and reducing PGE2, this in turn reduces platelet aggregation as well as inhibiting protein kinase C.

True disease is uncommon in hypovitaminosis E in humans. One of the manifestations arises from a lack of its antioxidant properties in the nervous system. One particular genetic disease arising from this deficiency is known as ataxia with isolated vitamin E deficency (AVED). This autosomal recessive disorder results from a mutation in the gene which codes for the alpha-tocopherol transfer portein and maps to chromosome 8q13. It manifests from the age 2 onward with ataxia, hyporeflexia, and difficulty with upward gaze. The deficient alpha-tocopherol transfer protein delivers Vitamin E to Purkinje cells and other neurons, leading to free redical stress, oxidative damage and cellular dysfunction in these cells. A similar condition, Friedreich ataxia, may mimic AVED, but results from a genetic mutation of the FXN gene, which results in oxidative stress due to iron buildup in neuronal mitochondria.

References:

1. Amorim SL, Oliveira ACP, Riet-Correa F, Simões SVD, Medeiros RMT, Clementino IJ. Distrofia muscular nutricional em ovinos na Paraíba. [Nutritional muscular dystrophy in sheep in Paraíba] Nutritional muscular dystrophy in sheep in Paraíba. *Pesq Vet Bras*. 2005;25(2):120-124. In portuguese.

2. Barros CSL, Barros SS, Santos MN, Metzdorf LL. Miopatia nutricional em bovinos no Rio Grande do Sul. *Pesq Vet Bras*. 1988;8:51-55. In portuguese.

3. Bezerra SFB, Batista JS, Melo DEB, Lima Neto, Souza E, Farias YJMD. Miopatia nutricional em ovinos no Rio Grande do Norte [Nutricional myopathy in sheep in Rio Grande do Norte] *Acta Vet Bras*. 2007;1(2):60-63. In portuguese.

4. Brigelius-Flohe R, Traber MG. Vitamin E: function and metabolism. FASEB 1999; 13:1145-1155.

5. Carmo PMS, Irigoyen LF, Lucena RB, Fighera RA, Kommers GD, Barros CSL. Spontaneous coffee senna poisoning in cattle: report on 16 outbreaks. *Pesq Vet Bras*. 2011;31:139-146.

6. Carvalho AQ, Carvalho NM, Vieira GP, et al. Intoxicação espontânea por *Senna obtusifolia* em bovinos no Pantanal Sul-Mato-Grossense. [Spontaneous poisoning by Senna obtusifolia in cattle from the Pantanal of Mato Grosso do Sul] *Pesq Vet Bras*. 2014;34:147-152. In portuguese.

7. Constable PD, Hinchcliff KEW, Done SH, Grünberg W. Nutritional diseases and/or vitamin E deficiencies. In: Veterinary Medicine. A Textbook of the Diseases of Cattle, Horses, Sheep, Pigs and Goats. 11th ed. Vol. 2. St. Louis, MO: Elsevier; 2017:1458-1478.

8. Cooper BJ, Valentine BA. Muscle and tendon: nutritional myopathy. In: Maxie, MG, ed. Jubb, Kennedy, and Palmer's Pathology of Domestic Animals. 6th ed. Vol. 1. St. Louis, MO: Elsevier; 2016:214-218.

9. Da Costa LA, Badawi A, El-Sohemy A. Nutrigenetics and modulation of oxidative stress. *Ann Nutr Metab*. 2012;60(Suppl. 3):27-36.

10. Gabor LJ. Nutritional degenerative myopathy in a population of captive bred *Uroplatus phantasticus* (satanic leaf-tailed geckoes). J *Vet Diagn Invest*. 2005;17:71-73.

11. Giri DK, Miller DL, Thompson LJ, Mailler L, Styer E, Baldwin C. Superoxide dismutase expression and oxidative damage in a case of myopathy in brown pelicans (*Pelecanus occidentalis*). *J Vet Diagn Invest*. 2007;19:301-304.

12. Gordon N. Hereditary vitamin-E deficiency. *Developmental Medicine & Child Neurology* 2001; 43:133-135.

13. Hadlow WJ. Myodegeneration of nutritional origin. In: Innes JRM, Sauders LZ, eds. Comparative Neuropathology. New York, NY: Academic Press; 1962: 173-186.

14. Kennick TR, Coleman M. Vitamin E Deficiency. In: StatPearls, StatPearls Publishing LLC, Treasure Island, FL, 2019.

15. Löfstedt J. White muscle disease of foals. *Vet Clin North Am Eq Pract*. 1997;13:169-185.

16. Miller MA, Zachary JF. Mechanisms and morphology of cellular injury, adaptation and death: free radicals. In: Zachary JF, ed. Pathologic Basis of Veterinary Disease. 6th ed. Elsesvier, St Louis, MO: Elsevier; 2017:16.

17. Ross AD, Gee CG, Jackson ARB, Hall E, Greentree PL. Nutritional myopathy in goats. *Aust Vet J*. 1989;66(11):361-363.

18. Smith DL, Palmer SJ, Hulland TJ, McSherry BJ, Blackwell TE. A nutritional myopathy enzootic in a group of yearling beef cattle. *Can Vet J*. 1985;26:385-390.

19. Van Vleet JF, Ferrans VJ. Etiologic factors and pathologic alterations in selenium-vitamin E deficiency and excess in animals and humans. *Biol Trace Elem Res*. 1992;33:1-21.

CASE IV: AFIP 2018 053/18 (JPC 4119040).

Signalment: 5 year, 8-month-old spayed female DSH cat (*Felis silvestris*)

History: This cat presented with polyuria, polydipsia and cystitis. A diagnosis of diabetes mellitus was confirmed. The cat

Pancreas, cat. There is mild pancreatomegaly and several lightly colored nodular masses scattered though the parenchyma. (Photo courtesy of: Swedish University of Agricultural Sciences, Department of Biomedical Sciences and Veterinary Public Health, Section of Pathology, BOX 7028, SE 750 07, Uppsala, Sweden, https://www.slu.se/en/departments/biomedical-sciences-veterinary-public-health/)

was treated with insulin, but blood glucose concentrations remained high despite treatment. For this reason, a presumptive diagnosis of insulin resistant diabetes was made, and the concentration of insulin-like growth factor (IGF)-1 in serum was measured. Later, the cat developed severe and recurrent vomiting, whereby it was humanely euthanized and submitted for necropsy.

Gross Pathology: The cat was in good body condition with well-developed musculature. The pancreas was moderately enlarged and showed multiple lightly colored, homogenous, nodular structures measuring up to 5 mm in diameter. The pituitary gland was moderately enlarged.

Laboratory results: S-Glucose >20 mmol/l (reference range 3.5-6 mmol/l)

S-Fructosamine >500 µmol/l (reference range 190-350 µmol/l)

Serum Insulin-like Growth Factor (S-IGF-1) >3050 µg/l (reference range 100-1200 µg/l)

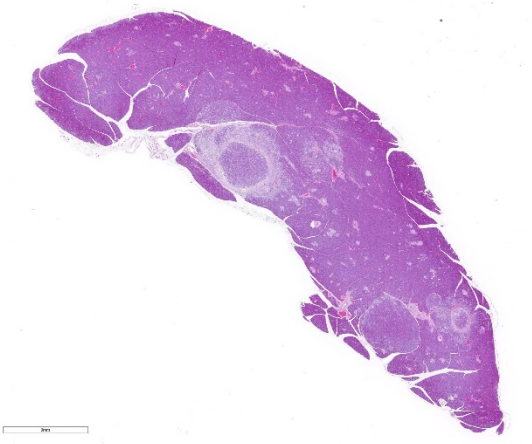

Pancreas, cat. A section of pancreas is submitted for examination. There are numerous nodules throughout the section, some with prominent fibrous capsules, and adjacent areas of pallor with loss of exocrine tissue. (HE, 7X)

Histologically, a well-circumscribed proliferation of well-differentiated acidophil cells was confirmed in the pituitary gland, consistent with an acidophil cell adenoma.

Microscopic Description: The exocrine parenchyma shows several well-circumscribed nodules, composed of variable amounts of well-differentiated acinar and ductal cells, often with reduced cytoplasmic staining properties. Surrounding nodules, and multifocally separating lobules as well as acinar and ductular structures, are variable amounts of fibrous tissue, multifocally expanded by numerous lymphocytes and small numbers of plasma cells. Multifocally, ductular structures are dilated and show epithelial attenuation and loss. Within lumina are moderate numbers of neutrophils and macrophages, as well as smaller amounts of eosinophilic, amorphous material (secretion), occasionally admixed with cellular debris. Diffusely, Langerhans's islets show moderate to marked cellular loss and are expanded by abundant amphophilic to lightly eosinophilic extracellular amorphous material (amyloid). Multifocally, small numbers of cells within the islets show an expanded vacuolated cytoplasm.

In Congo-red stained section (not provided), the extracellular material in the islets was confirmed to be amyloid by exhibiting apple-green birefringence in polarized light.

Contributor's Morphologic Diagnosis:

1. Pancreas, multifocal nodular hyperplasia/adenomas
2. Pancreas, pancreatitis, multifocal, interstitial, chronic, moderate, lymphocytic with multifocal acinar/ductular dilation and neutrophilic inflammation
3. Pancreas: islet amyloidosis, diffuse, severe, with cellular degeneration and loss

Contributor's Comment Diabetes mellitus is a disease characterized by loss of glycemic control with resulting fasting hyperglycemia. In cats, insulin resistant diabetes mellitus, resulting from inadequate tissue response to high insulin level is frequent, similar to diabetes mellitus type II in humans.[10]

Several pancreatic changes of the endocrine islets are associated with diabetes mellitus in cats, including loss of insulin-producing β-cells and amyloidosis of the islets. According to a recently published article, diabetic cats had approximately 65% lower median number of insulin-producing cells compared to control cats.[18] The mechanism of amyloidosis is related to co-secretion of insulin and islet amyloid polypeptide (IAPP).[11] The presence of amyloid can be verified histologically by staining with Congo Red, as was performed in this case, with amyloid protein exhibiting apple-green birefringence in polarized light.[4] Thioflavin-S or T can also be used to detect amyloid, and may be useful due to poor staining with Congo red in cats.[4,8] Historically, amyloidosis has been considered a consistent feature of diabetes mellitus in

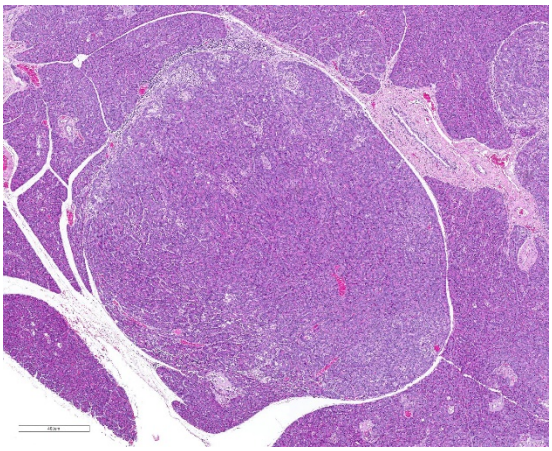

Pancreas, cat. There are several large areas of exocrine hyperplasia scattered throughout the section. (HE, 58X)

cats, and sometimes the cause of insulin dysregulation.[9,16] However, this association and causality has been questioned in recent years, and a newly published paper failed to find increased deposits of amyloid in the pancreas of diabetic cats compared to controls.[18]

The degree to which inflammation plays a role in feline diabetes remains controversial. According to one study, the number of neutrophils and macrophages in pancreatic islets was similar between cats with diabetes mellitus and control cats, however the presence of T- and B-cells combined seemed more frequent in islets of diabetic cats compared to non-diabetic cats.[18] In another study, expression of mediators regulating inflammation and oxidative stress was seen in cats with hyperglycemia and obesity, suggesting that these markers increase in the early development of diabetes mellitus.[8]

In addition to diabetes mellitus resulting from inadequate tissue response to high insulin level, a known cause of feline diabetes mellitus is acromegaly.[16]

Acromegaly is a clinical condition characterized by overgrowth of connective tissue and enlargement of viscera, resulting from chronic excessive secretion of growth hormone (GH), also known as hypersomatotropism.[16,19] According to one author, nodular pancreatic hyperplasia is commonly encountered in acromegalic cats on post mortem examinations.[14] Acromegaly may cause diabetes mellitus due to a GH-induced postreceptor defect in insulin action in target tissues.[14] GH measurements in blood has traditionally been used to diagnose acromegaly. However, S-IGF1 has replaced this parameter in recent years, due to limited GH assay availability.[3,13] Presence of an acidophil cell adenoma in the pituitary gland, together with severely elevated serum IGF values, suggest that the diabetes mellitus in this case was a result of hypersomatotropism due to neoplastic GH-secretion.

Pancreatitis is frequently diagnosed in cats,; the chronic form being more prevalent than the acute form.[2] In the acute form, neutrophilic infiltrates along with acinar cell and peripancreatic fat necrosis is observed, meanwhile chronic pancreatitis is dominated by non-suppurative infiltrates of

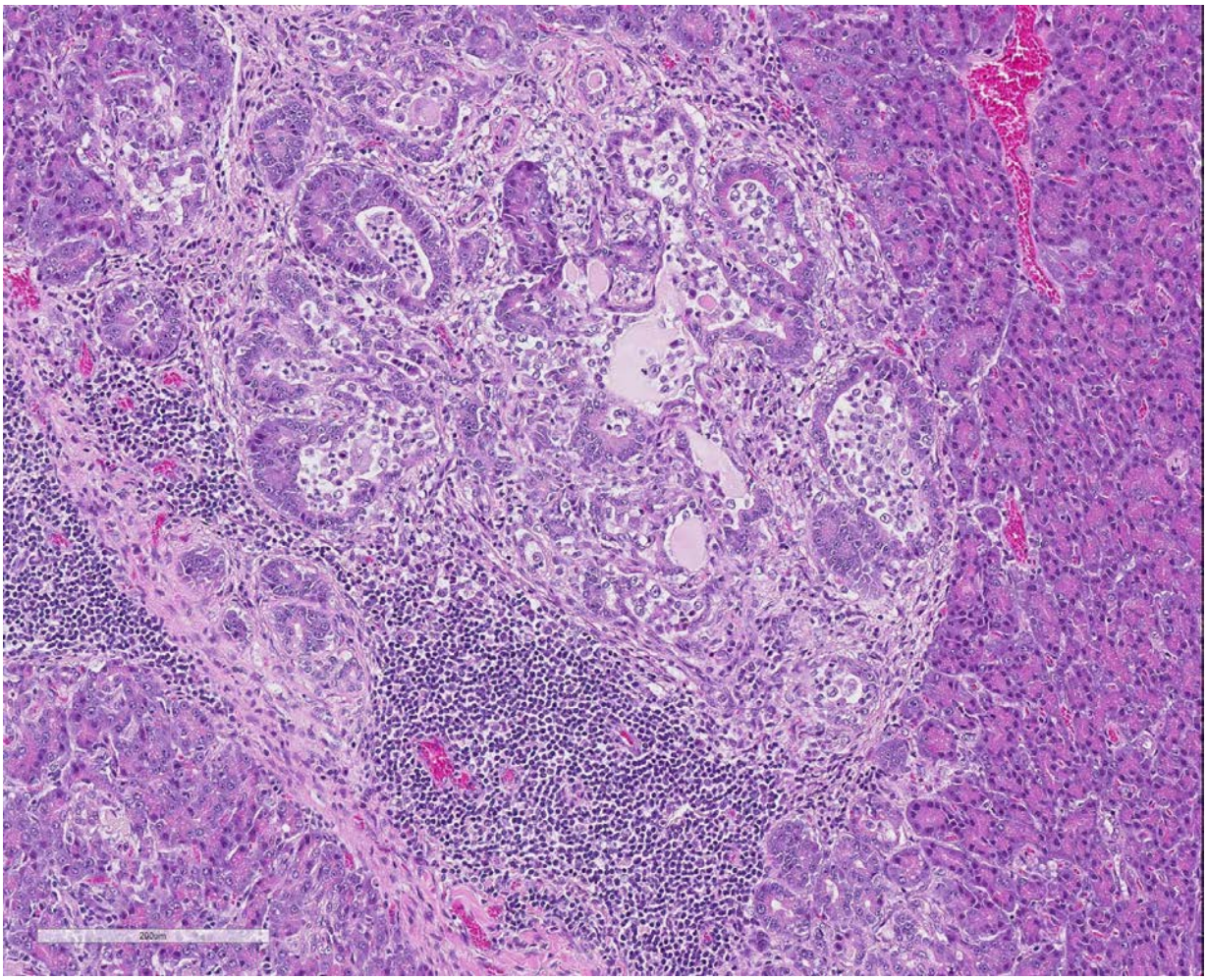

Pancreas, cat. There are several large areas of exocrine hyperplasia scattered throughout the section. (HE, 58X)

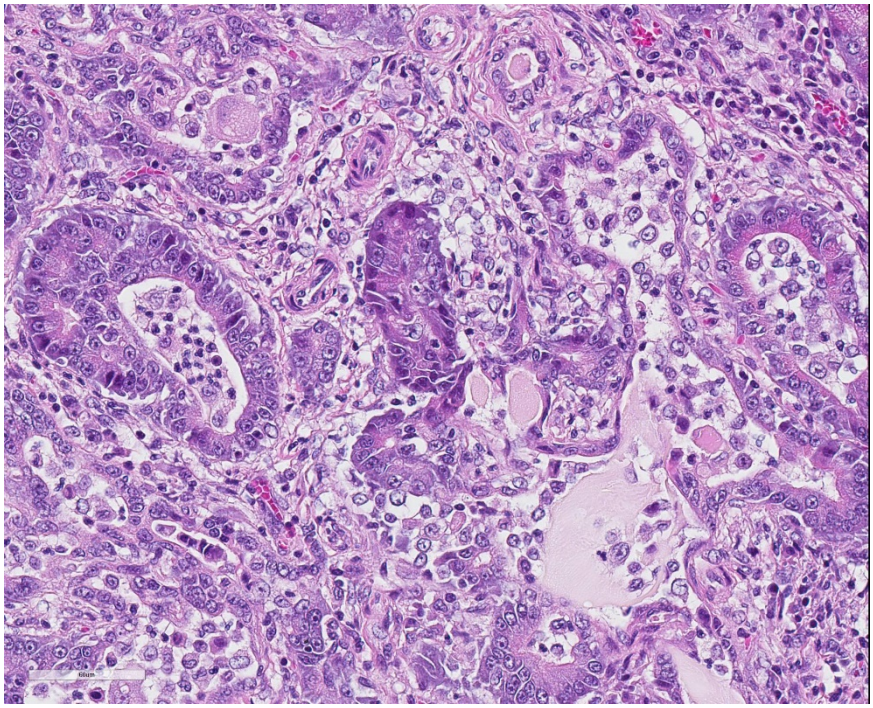

Pancreas, cat. Higher magnification of a focus of interstitial pancreatitis. In these areas, it is difficult to distinguish degenerating from regenerating acini or pancreatic ducts. (HE, 400X)

lymphocytes, accompanied by fibrosis and acinar atrophy.[6,10] Pancreatitis in cats may coexist with inflammatory bowel disease and cholangitis.[1] Moreover, pancreatitis is often observed in conjunction with a diagnosis of diabetes mellitus, and may be subclinical.[5,18] Anecdotally, the concurrent condition of diabetes mellitus and pancreatitis can make glycemic control more "brittle".[5] However, it is not clear whether the pancreatitis leads to diabetes mellitus, or if the diabetes mellitus causes pancreatitis.[5] It has been shown that the number of neutrophils is increased in pancreatic exocrine tissue in cats with hyperglycemia.[18] According to another study, the degree of inflammation of the exocrine pancreas is not significantly associated with diabetes nor ketoacidosis. However, the mitotic index of acinar cells, as measured by Ki67 and PCNA, is increased in cells in the near vicinity of pancreatic islets in cats with diabetes, possibly due to chronic pancreatitis.[17]

The gross nodular changes in the pancreas corresponded histologically to well-defined benign proliferations of exocrine pancreatic tissue. In summary, these were determined to be representative of nodular hyperplasias or adenomas. Nodular hyperplasia can be seen in several organ systems of aging individuals including the liver, adrenals, thyroid glands, spleen and pancreas.[10,13,17] In the pancreas these changes are usually considered clinically silent. In other organs, nodular hyperplasia has been discussed as a response to tissue injury or due to chronic pituitary hormone stimulation.[12] In this case, it is unclear if the nodular changes are purely hyperplasic or represent an adenomatous change. Possibly, the chronic inflammation could contribute to the increased amount of fibrous tissue surrounding nodules.

Contributing Institution:

Swedish University of Agricultural Sciences
Department of Biomedical Sciences and Veterinary Public Health, Section of Pathology
BOX 7028
SE 750 07, Uppsala, Sweden

https://www.slu.se/en/departments/biomedical-sciences-veterinary-public-health/

JPC Diagnosis: 1. Pancreas: Pancreatitis, interstitial, necrotizing and lympho-histiocytic, chronic, multifocal mild to moderate.

2. Pancreas, islets of Langerhans: Amyloidosis, diffuse, severe.

3. Pancreas, exocrine tissue: Hyperplasia, nodular multifocal, moderate.

JPC Comment: While the theoretical interplay of the three visualized lesions of chronic interstitial pancreatitis, islet amyloidosis, and exocrine hyperplasia, as well as the fourth lesion of an enlarged pituitary (which was neither submitted or further described in this case) and its discussion by the contributor is interesting to ponder; the participants had seen these three lesions independently and in various combination frequently in older cats, and were reticent to assign a relationship between any of the three, or the concomitant increased levels of serum growth hormone. (Also interesting is that this particular cat was less than 6 years of age.) Amylin, or islet associated peptide is toxic to islet cells in addition to resulting in effacement and atrophy as a result, but the presence of islet amyloid in the cat should not be interpreted as *prima facie* evidence of diabetes in the cat.[10]

The contributor mentions the possibility of elevated growth hormone levels and acromegaly in this particular individual as a potential cause of diabetes. Diabetes in acromegalic cats is a result of the catabolic

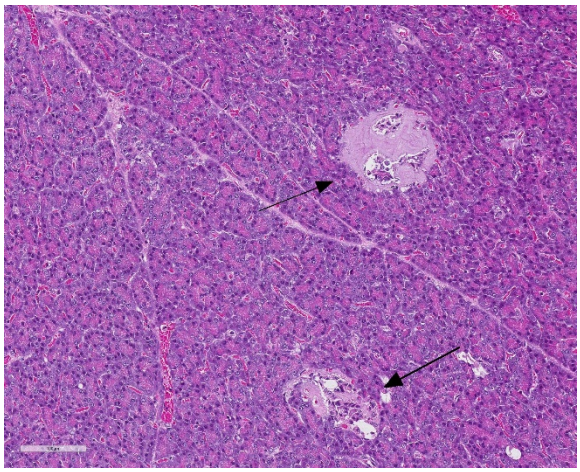

Pancreas, cat. Islets are largely replaced by amyloid. (HE, 203X)

effects of growth hormone, which causes insulin resistance through the generation of a postreceptor defect in the action of insulin or target cells with resulting diminished carbohydrate utilization as well as gluconeogenesis.[7] Various studies have demonstrated the concurrent presence of diabetes mellitus in between 20 and 50% of acromegalic human patients. One study of 1221 diabetic cats demonstrated 26.1% to have elevated serum insulin-like growth factor (secreted by the liver) and of this subset, 89% demonstrated pituitary neoplasms.[15]

Another effect of growth hormone release by a pituitary somatotroph tumor in an acromegalic patient is due to the anabolic effects of insulin-like growth factors, which results in increased protein synthesis and tissue growth. Affected cats demonstrate a characteristic clinical appearance (colloquially referred to as a "gangster cat" due to increased body weight, prognathia inferior, a broad face, enlarged paws, respiratory stridor, and often cardiac and abdominal organomegaly). While not seen

in all patients, these changes were not documented in the history of this case.[7]

Chronic interstitial pancreatitis is the typical pattern of inflammation of the pancreas in species other than the dog, and in cats, generally arises from an inflammatory process beginning in the ducts. Histologically, as seen in this case, ducts may contain exudate, may be dilated or stenotic, and are often surrounded by bands of fibrous connective tissue which may communicate with the interlobular stroma. Aggregates of lymphocytes and plasma cells are not uncommon in inflamed areas.[10]

References:

1. Armstrong PJ, Williams DA. Pancreatitis in cats. *Top Companion Anim Med*. 2012;27(3):140-7.
2. Bazelle J, Watson P. Pancreatitis in cats: is it acute, is it chronic, is it significant? *J Feline Med Surg*. 2014;16(5):395-406.
3. Berg RI, Nelson RW, Feldman EC et al. Serum insulin-like growth factor-I concentration in cats with diabetes mellitus and acromegaly. *J Vet Intern Med.* 2007;21(5):892-8.
4. Cianciolo, RE, Mohr, FC. Urinary System. In: Maxie MG, ed. Jubb, Kennedy, and Palmers Pathology of Domestic Animals. 6th ed. Philadelphia, PA:Saunders Elsevier; 2016:377-463.
5. Davison, J. Diabetes mellitus and pancreatitis--cause or effect? *Small Anim Pract.* 2015;56(1):50-9.
6. De Cock HEV, Forman MA, Farver TB et al. Prevalence and histopathologic characteristics of pancreatitis in cats. *Vet Pathol*. 2007;44(1):39-49.
7. Fracassi F, Salsi M, Sammartano F, Bo, Kooistra HS. Acromegaly in a non-diabetic cat. *J Fel Med Surg Open Rep* 2(1):2055116916646585. doi: 10.1177/2055116916646585.
8. Herndon AM, Breshears MA, McFarlane D. Oxidative modification, inflammation and amyloid in the normal and diabetic cat pancreas. *J Comp Pathol.* 2014;151(4):352-62.
9. Johnson KH, O'Brien TD, Jordan K et al. Impaired glucose tolerance is associated with increased islet amyloid polypeptide (IAPP) immunoreactivity in pancreatic beta cells. *Am J Pathol.* 1989;135(2):245–250.
10. Jubb, KVF, Stent, AW. Pancreas. In: Maxie MG, ed. Jubb, Kennedy, and Palmers Pathology of Domestic Animals. 6th ed. Philadelphia, PA:Saunders Elsevier; 2016:353-373.
11. Kahn SE, D'Alessio DA, Schwartz MW et al. Evidence of cosecretion of islet amyloid polypeptide and insulin by β-cells. *Diabetes.* 1990;39(5):634-8.
12. Newman SJ, Steiner JM, Woosley K et al. Correlation of age and incidence of pancreatic exocrine nodular hyperplasia in the dog. *Vet Pathol.* 2005;42(4):510-3.
13. Niessen SJ. Feline acromegaly: an essential differential diagnosis for the difficult diabetic. *J Feline Med Surg.* 2010;12(1):15-23.
14. Niessen SJ, Church DB, Forcada Y. Hypersomatotropism, acromegaly, and hyperadrenocorticism and feline diabetes mellitus. *Vet Clin North Am Small Anim Pract.* 2013;43(2):319-50.

15. Niessen SJ, Forcada Y, Mantis P, Lamb CR, Harrington N, Fowkes R, Korbonis M, Smith K, Church. Studying Cat (*Felis catus)* diabetes: Beware of the acromegalic imposter. *PLoS One* 2015; 29;10(5):e0127794. doi: 10.1371/journal.pone.0127794.
16. O'Brien TD. Pathogenesis of feline diabetes mellitus. *Mol Cell Endocrinol.* 2002;29:197(1-2):213-9.
17. Rosol, TJ., Gröne, A. Endocrine Glands. In: Maxie MG, ed. Jubb, Kennedy, and Palmers Pathology of Domestic Animals. 6th ed. Philadelphia, PA:Saunders Elsevier; 2016:270-356.
18. Zini E, Osto M, Moretti S et al. Hyperglycaemia but not hyperlipidaemia decreases serum amylase and increases neutrophils in the exocrine pancreas of cats. *Res Vet Sci.* 2010;89(1):20-6.

Self-Assessment - WSC 2019-2020 Conference 17

1. Which of the following is NOT a key event in the survival of *Mycobacterium tuberculosis* within macrophages?
    a. Th_2 response
    b. Phagosome maturation arrest
    c. IL-4 secretion by infected macrophages
    d. Impaired trafficking of lysosome to phagosome

2. Which of the following cells typically best demonstrates Negri bodies in ruminants?
    a. Cerebellar nuclei
    b. Hippocampus
    c. Purkinje cells
    d. Red nuclei and obex

3. Which of the following is the most common histologic finding in rabies?
    a. Perivascular cuffing of lymphocytes
    b. Laminar cortical necrosis
    c. Neuronophagia
    d. Glial nodule formation

4. Which of the following is true concerning nutritional myopathy?
    a. It is usually monophasic.
    b. Regeneration of muscle cells is prominent
    c. Mineralization is minimal.
    d. Lesions are restricted to skeletal muscle as cardiac muscles has high levels of endogenous antioxidants.

5. Which of the following is the most common cause of interstitial pancreatitis in the cat?
    a. Islet amyloid deposition
    b. High levels of dietary unsaturated fatty acids
    c. Vitamin E deficiency
    d. Inflammatory lesions in the pancreatic ducts

Please email your completed assessment for grading to Dr. Bruce Williams at bruce.h.williams12.civ@mail.mil. Passing score is 80%. This program (RACE program 33611) is approved by the AAVSB RACE to offer a total of 0.5 CE Credits, with a maximum of 12.5 CE Credits being available to any individual Veterinary Medical Professionals for the 2019-2020 Wednesday Slide Conference. This RACE approval is for the subject matter categories of: SCIENTIFIC using the delivery method of NON-INTERACTIVE DISTANCE. This approval is valid in jurisdictions which recognize AAVSB RACE.

Joint Pathology Center
Veterinary Pathology Services

WEDNESDAY SLIDE CONFERENCE 2019-2020

C o n f e r e n c e 18

12 Feb 2020

Timothy Cooper, DVM, PhD DACVP
Pathology Department
NIH/NIAID
Integrated Research Facility
Frederick, MD

CASE I: 17-325 (JPC 4105224).

Signalment: 8-month, male intact Old English Sheepdog, *Canis familiaris*, dog

History: The dog was presented to the Internal Medicine Service for evaluation of a 4 month period of daily vomiting, frequent diarrhea, depression following meals, and lack of weight gain.

Gross Pathology: A large mass of vessels was seen surrounding gallbladder and infiltrating into the liver at surgery. A biopsy including the gallbladder, vessels, and adjacent hepatic parenchyma was submitted for histopathology.

Laboratory results: Serum chemistry revealed elevations in activity of ALP (204 IU/L) and ALT (76 IU/L); serum ammonia concentration was elevated at 40 umol/L. Complete blood count revealed a moderate, normocytic, normochromic anemia with a hematocrit of 24.6%. A CT confirmed the presence of a large arterioportal malformation centered at the gallbladder and falciform fat as well as multiple acquired extrahepatic portosystemic shunts, moderate ascites, and left-sided liver atrophy.

Microscopic Description: Liver, gall bladder: Two sections of liver and gallbladder are examined. Surrounding the common bile duct and gall bladder is a mass-like proliferation of numerous

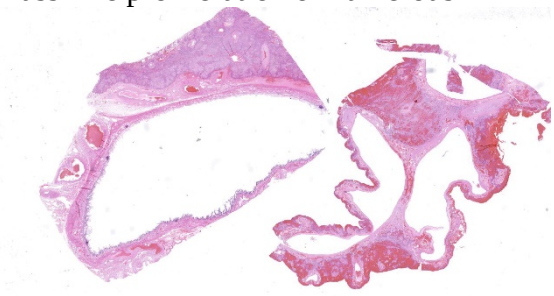

Liver, dog. Two sections of liver are presented. The section at left has a markedly dilated gallbladder within; the section at right contains multiple sections of a markedly dilated and tortuous muscular artery with a 10mm diameter. (HE, 5X)

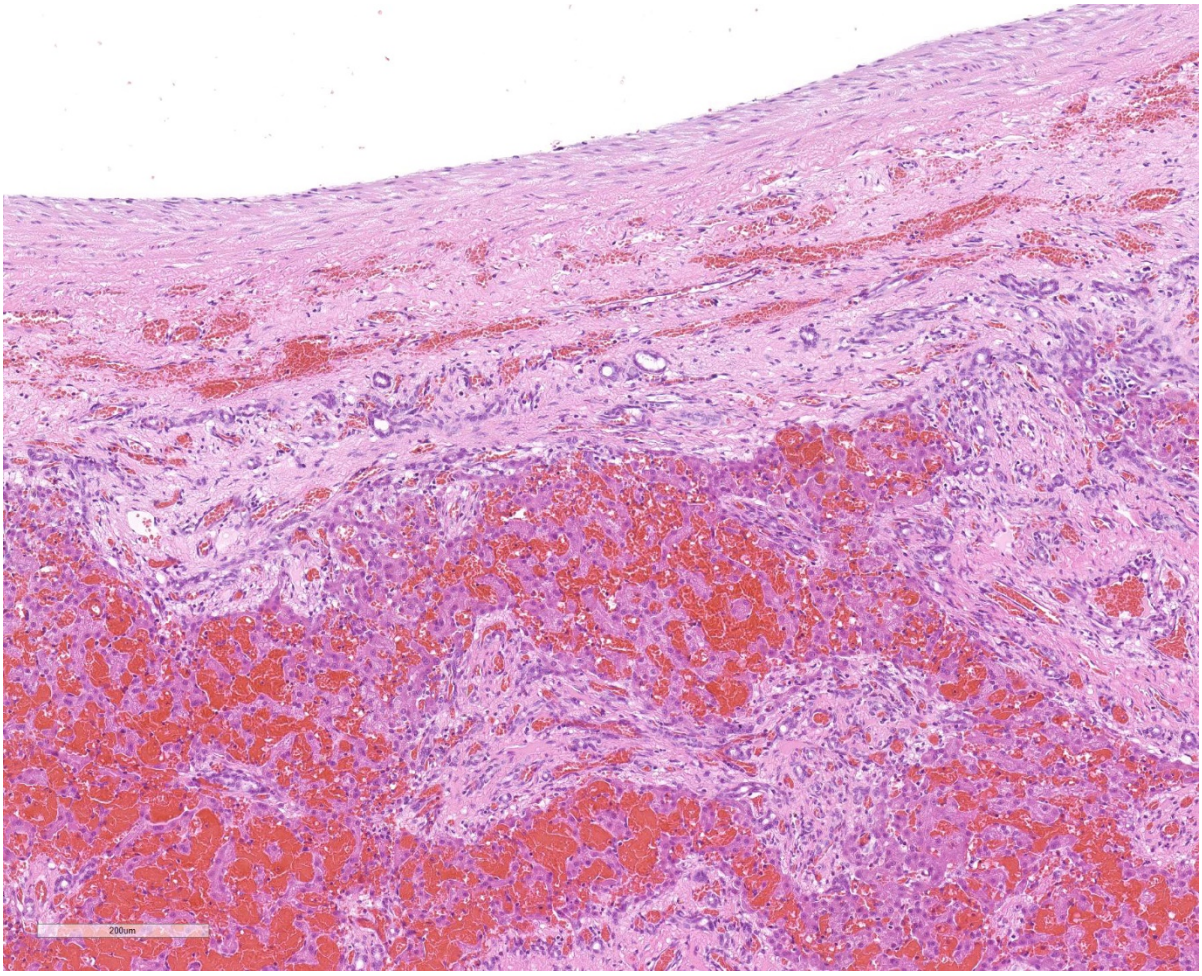

Liver, dog. Higher magnification of the wall of the arteriovenous connection. From top – smooth muscle cells of the wall are separated by abundant fibrillar collagen, with extends into the adjacent adventitia, effacing the tunica externa. This fibrosis extends into the adjacent parenchyma, replacing hepatocytes and entrapping bile ductules. Peripherally, there is marked fibrosis and arteriolar and ductular hyperplasia within portal areas which extends into the adjacent parenchyma, and severe dilation of hepatic sinusoids. (HE, 127X)

tortuous, small to large, well-differentiated arteries and veins, which rarely anastomose, and dissect or compress the hepatic parenchyma. The endothelium of veins and arteries is occasionally hypertrophied. Arterial and arteriolar walls are diffusely moderately thickened by subintimal edema, pale basophilic, mucinous matrix, and irregular fibers as well as by moderate to marked smooth muscle hypertrophy of the tunica media. The internal elastic lamina is frequently fragmented or absent (confirmed by Verhoeff-Van Gieson stain). The walls of veins and venules are markedly thickened and resemble arteries (arterialization). There is expansion of the tunica intima by irregular fibers and the tunica media by smooth muscle hypertrophy. The lymphatics surrounding the abnormal arteries and veins, those deep to the hepatic capsule, within portal tracts, and surrounding central veins are frequently moderately to markedly ectatic. The adjacent hepatic parenchyma is compressed by the vessels, with multifocal atrophy of the hepatic lobules. Additionally, there are

markedly increased numbers of bile duct profiles in portal tracts and isolated within the hepatic parenchyma; these bile ducts are frequently surrounded by concentric lamellar fibrosis (“onion-skinning”) . Portal tracts also have increased numbers of small arteriolar profiles and portal vein profiles are largely absent. Centrilobular hepatocytes are frequently atrophied and diffusely, hepatocytes are mildly to moderately swollen by diaphanous vacuolar change (glycogen type). Scattered throughout the parenchyma are individual necrotic hepatocytes. There is moderate stellate cell hypertrophy; hypertrophied stellate cells frequently contain large, clear, spherical vacuoles (lipid).

Contributor’s Morphologic Diagnosis:

Liver, gallbladder: Arteriovenous fistula with multifocal hepatic compression and atrophy, marked biliary and arteriolar hyperplasia, portal vein hypoperfusion, and moderate, diffuse glycogen-type hepatic vacuolation

Contributor’s Comment: The diagnostic imaging, gross and histologic findings of this biopsy sample are consistent with a diagnosis of a hepatic arteriovenous fistula. Arteriovenous (AV) fistulae can be

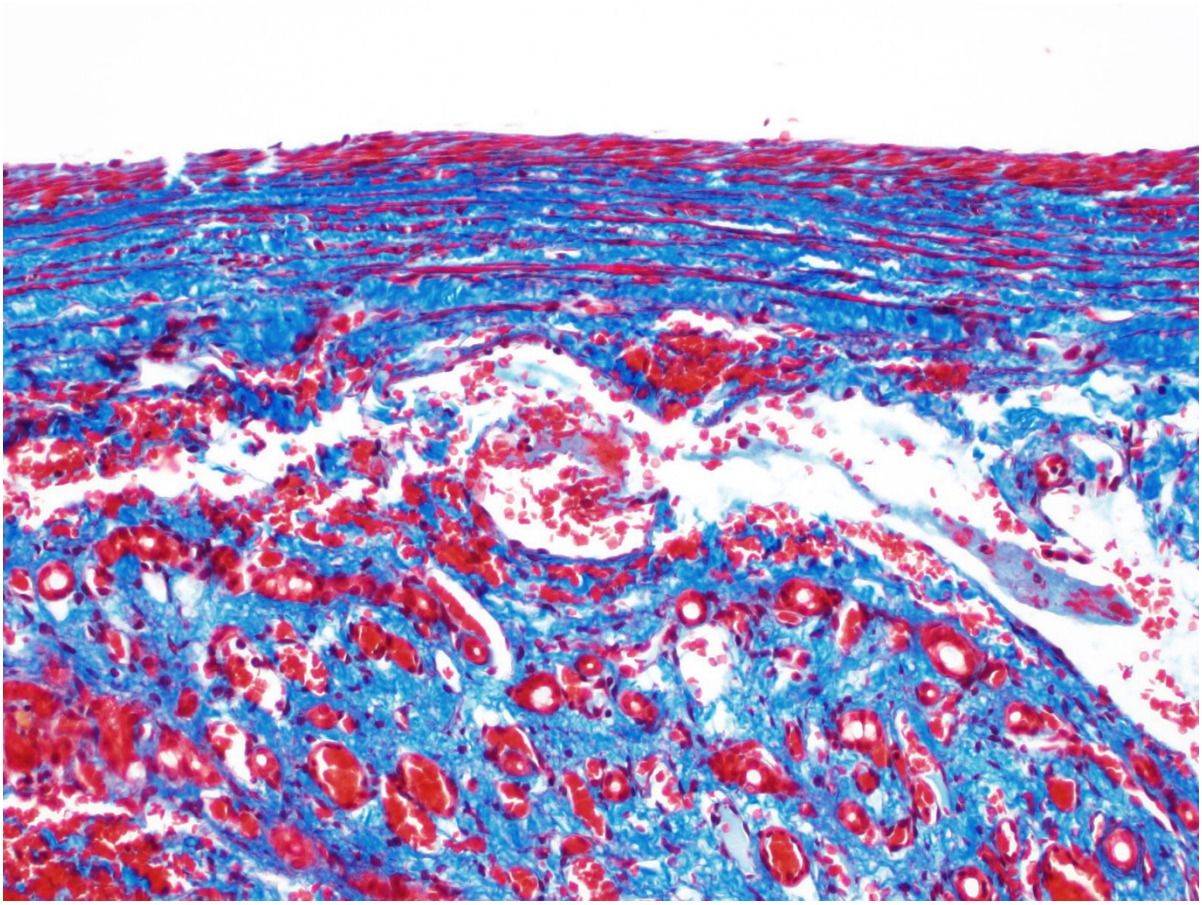

Liver, dog. A Masson’s trichrome stain demonstrates the large amount of collagen within the wall of the fistula. (HE, 400X)

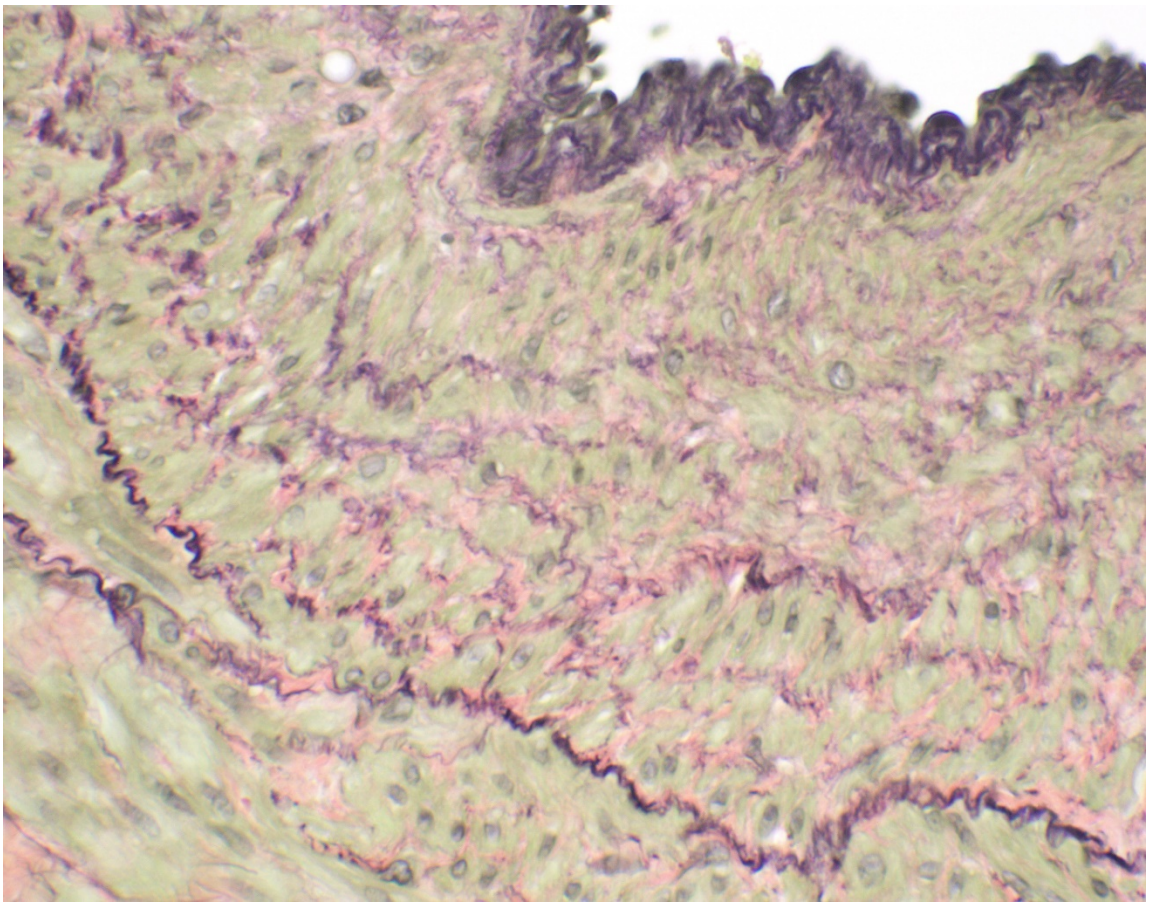

Liver, dog. A Verhoeff-van Gieson stain demonstrates the lack of an internal elastic lamina as well as deposition of elastin fibers between smooth muscle cells in the media (Verhoef- van Gieson, 400X)

congenital or acquired; acquired AV fistulae are documented to occur following trauma, rupture of arterial aneurysms into a vein, inflammation or necrosis of adjacent vessels, and iatrogenically (typically surgical intervention) [3,5,6]. AV fistulae have been reported in a variety of locations, including intrahepatic, pulmonary, and on the limbs.[3,6] They have been reported in dogs, cats, horses, cattle, and humans.[3,6]

Clinical signs of AV fistulae depend on the location; typically signs are associated with increased hydrostatic pressure within veins and subsequent increased intra-lymphatic pressure.[3,6] In fistulae involving abnormal blood flow to the liver, ascites, hepatic encephalopathy and synthetic liver failure can occur, resulting in depression, seizures, vomiting, and diarrhea. [2,3,6,9,12]

Gross findings of AV fistulae usually show one or more anastomoses of a large vein and large artery, surrounded by a tangle of medium and small arteries and venules that contribute to a mass effect. In hepatic arteriovenous fistulae, anastomosis typically involves the portal vein and hepatic artery.[2,3,6,9,12] However, there are reports of involvement of the cystic artery in humans.[10] Microhepatia is commonly observed due to abnormal portal blood flow.

Portal hypertension may result in the development of numerous portocaval acquired shunts.

Histology of AV fistulae reveals mass-like proliferations of abnormal arteries and veins, with arterialization of veins. The internal elastic lamina is frequently fragmented, split, or duplicated; in both veins and arteries, the tunica intima is expanded by smooth muscle invasion and hypertrophy, increased deposition of elastin fibers, edema, and mucinous matrix. The tunica media of veins and arteries also exhibits smooth muscle hypertrophy. Additionally, fibrinoid necrosis may be observed. Elastin (Verhoeff-Van Gieson) and trichrome (Gomori's trichrome) stains highlight the deposition of elastin fibers and fiber fragmentation as well as the fibrosis that often accompanies the fistulae.[3,5,6]. In fistulae that affect the liver, lesions resembling portocaval shunting occur, including absence or diminution of portal veins, marked biliary and arteriolar proliferation, hepatocyte atrophy, and lymphangiectasia. [2,3,6,9,12] Sinusoids near the fistulae are frequently dilated and congested. Liver lobes away from the fistulae may be normal with little parenchymal change.[3]

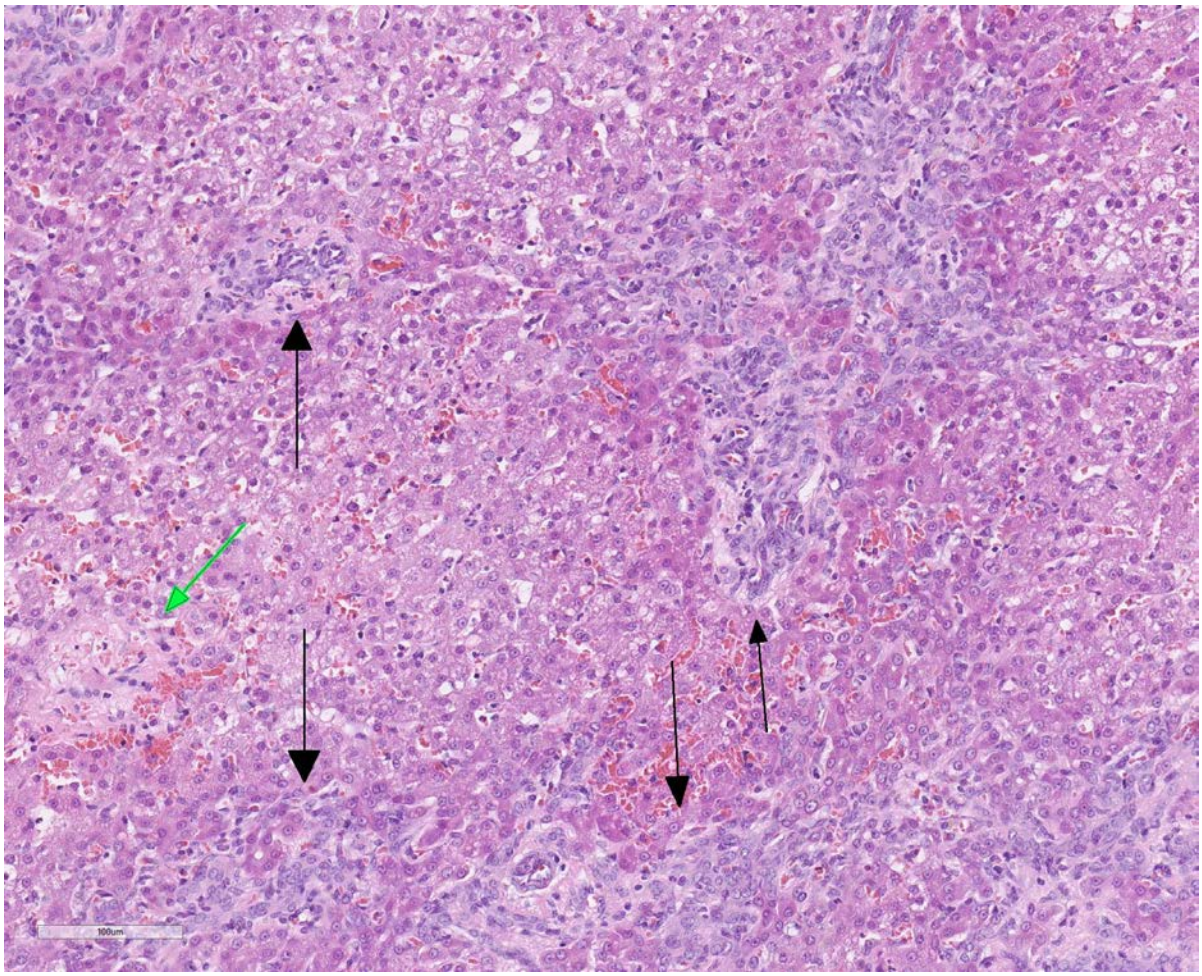

Liver, dog. At a distance from the arteriovenous fistula, portal triads are expanded by marked biliary hyperplasia and fibrosis (black arrows). There is hepatocellular necrosis and loss surrounding a central vein (green arrow).) (HE, 400X)

Treatment of AV fistulae is dependent upon location; advanced imaging such as ultrasonography, computed tomography, and magnetic resonance imaging can facilitate therapeutic intervention. Surgical excision, interventional techniques, and coil embolization have been described in a variety of cases.[5,8].

Contributing Institution:

North Carolina State University, College of Veterinary Medicine, Department of Population Health and Pathobiology
https://cvm.ncsu.edu/research/departments/dphp/

JPC Diagnosis: Liver: Aberrant arterial connection, focal, severe, with arterial and venous intimal and medial hyperplasia and fibroelastosis, hepatocellular atrophy, congestion, and hemorrhage.

JPC Comment: The contibutor has done an excellent and concise review of arteriovascular fistulae in the dog. Intrahepatic arteriovenous fistulae are most often acquired in humans as a result of surgical intervention, such as hepatic biopsy, transhepatic intervation such as percutaneous cholangiography, surgery or transplantation, and occasionally as a result of trauma. They may also arise within neoplasms (most commonly those which have an endothelial vasoproliferative component, such as infantile hemangiomas).[4]

In the dog, as in this case, they are likely congenital malformations that often result in portal hypertension as a result of the pressure differential between the hepatic artery and the low-pressure system of the portal circulation. In most affected dogs, large, pulsating vessels on the surface of one or more affected lobes are seen during surgery[6]; Doppler imaging is a commonly used imaging modality for diagnosis.[4,11] As mentioned by the contributor, microhepatia is a common finding in affected dogs, but the affected lobes are enlarged by the presence of the fistulae.[6] The WSAVA Liver Standardization group, in their 2006 tome, *Standards for Clinical and Histological Diagnosis of Canine and Feline Liver Diseases*, put forth their "strong impression" that arteriovenous fistulas are usually associated with portal vein hypoplasia, based on the observation that recovery from portal hypoperfusion has never been truly recorded following surgical resection of affected lobes.[11]

This particular case demonstrates the need for special stains for all microscropic evaluation of vascular lesions, and especially arteriovenous fistulae which have significant mural changes. On HE examination, the thickness of the arterial wall can be estimated, and gross disorder of smooth muscle cells can be identified, but much of the fine detail is obvious only after employment of various histochemical stains. A stain for elastin, such as Movat's pentachrome or Verhoeff-van Gieson, is imperative to identify fragmentation or loss of the internal elastic membrane. Loss of the internal elastic lamina allows migration of smooth muscle cells to the tunica interna, where they may dedifferentiate to a secretory phenotype and engage in arterial wall remodeling by synthesizing extracellular matrix components.[1] A stain for collagen, such as a Masson's trichrome, will demonstrate the amount of collagen within the remodeled intima; and a Movat's pentachrome will also demostrate excess intercellular elastin fragments as well.

The presence of two sections of liver, one containing sections of the fistula as well as one taken nearby, show significant

difference in degree of hepatocellular atrophy. While there is atrophy of hepatocytes in both sections (as is common in dogs with congenital and marked decreases in portal blood flow), there is significant hepatocellular loss in proximity to the fistulae, likely due to compression from the expanded vasculature as well. Examination of the portal triads in the section further away from the fistulae is informative as well, as portal areas contain numerous profiles of hepatic arterioles and bile ductules, but few visible profiles of portal veins. The marked siusoidal dilatation and hemorrhage is the result of the shunting of blood from the hepatic artery into the portal vein, and the generated pressure also results in dilation of lymphatics in both section, most prominently and strikingly around the sublobular veins (the so-called "rose window" effect, per personal communication, Dr. John Cullen.

The moderator adeptly summarized the changes in the slide by stating that "when you see arteries looking like veins and veins looking like arteries, you must add arteriovenous fistula or malformation to your differential diagnosis". The moderator noted another particular histologic finding in this section in the walls of hypertrophic arterioles – the apparent formation of two distinct layers of smooth muscle, oriented perpendicularly to each other – not a specific finding , but an indication of arterial wall disease.

The moderator opined that in the diagnosis of arteriovenous malformations, imagining is the gold standard, and hopefully the histology is supportive – diagnosis solely on histology may be problematic. The participants discussed the difference between arteriovenous "fistula" and "malformation". Arteriovenous fistulas are composed of a single connection between arteries and veins and the histologic findings may be more obvious on histology; artiovenous malformastions are multiple connections often formin a niduls of connections which may or many not be as easily discerned on histology.

Finally, the discusion of chronic congestion versus hemorrhage, which obscured much of the hepatic parenchyma on the slide was determined to be complicated by the fact that this sample was a biopsy.

References:

1. Aiello VD, Gutierrez PS, Chaves MJF, Lopes AAB, Higuchi ML, Ramires JAF. Morphology of the Internal Elastic lamina in arteries from pulmonary hypertensive patients: a conocal laser microscopy study. *Mod Pathol* 2003; 16(5):411-416.
2. Booler, H. Congenital Intrahepatic Vascular Anomaly in a Clinically Normal Laboratory Beagle. Tox Path. 2008, 36: 981-984
3. Cullen, JC and Stalker, MJ. Liver and Biliary system. In: Maxie MG, ed. *Jubb, Kennedy, and Palmer's Pathology of Domestic Animals*. Vol 2. 4th Edition. St. Louis, MO: Elsevier; 2016. 266.
4. Gallego C, Miralles M, Marin C, Muyor P, Gonzalez G, Garcia-Hidalgo E. Congenital hepatic shunts. *RadioGraphics* 2004; 24:755-772.
5. Leach, S.B., Fine, DM., Schutrumph, RJ., Britt, LG., Durham, HE., Christiansen, K. Coil embolization of an aorticopulmonary fistula in a dog. J Vet Cardiol. 2010; 12: 211-216.
6. Moore, P. F. and Whiting, P. G. Hepatic lesions associated with intrahepatic arterioportal fistulae in dogs. Vet Path. 1986; 23 (1): 57-62.

7. Robinson, WF and Robinson, NA. Cardiovascular system. In: Maxie MG, ed. *Jubb, Kennedy, and Palmer's Pathology of Domestic Animals*. Vol 2. 4th Edition. St. Louis, MO: Elsevier; 2016. 56.
8. Saunders, AB., Fabrick, C., Achen, SE., Miller, MW. Coil embolization of a congenital arteriovenous fistula of the saphenous artery in a dog. J Vet Intern Med. 2009; 23: 664-664.
9. Schaeffer, IGF., et al. Hepatic arteriovenous fistulae and portal vein hypoplasia in a Labrador retriever. JSAP. 2001; 42: 146-150.
10. Tajima, H., Hosaka, J., Tajma, N., Kumazaki, T. Arteriovenous malformation of the gallbladder. Eur. Radiol. 1997; 7: 333-334.
11. Rothuizen J, Bunch SE, Charles JA, Cullen JM, Desmet VJ, Szatmari V, Twedt DC, van den Ingh TSGAM, Ven Winkle T, Washabau RJ. Morphological classification of circulatory disorders of the canine and feline liver. . *In:* WSAVA Standards for Cinical and Histological Diagnosi of Canine and Feine Liver Disease. Edinburgh, Saunders-Elsevier, 2006, pp 53-55.
12. Yoshizawa, K., Oishi, Y., Matsumoto, M., Fukuhara, Y., Makino, N., Noto, T. Fujii, T. Congenital Intrahepatic arteriovenous fistulae in a young beagle dog. Tox Path. 1997; 25: 495-499.

CASE II: 17/1060 Z (JPC 4032584).

Signalment: 4 year old, female spayed, Bull Arab (canine)

History: Sudden death. The week before death, the animal was showing signs of hind limb/spinal pain. Radiographs at that time revealed a sublumbar mass and fluid in the caudal abdomen, fluid PCV/TP 15/70.

Gross Pathology: Abdominal cavity: The abdomen contains approximately 1300 ml of dark red, slightly turbid fluid (blood) admixed with tens of variably sized, friable, soft dark red material (blood clots). The dorsocaudal abdomen, ventral to lumbar vertebrae 6 and 7 and the iliopsoas muscles, contains a poorly demarcated, approximately 11 x 5 x 4 cm, firm mass which surrounds and replaces approximately 7 cm of the aorta. On cut section, the mass is mottled dark pink to dark red and cavitated. The caudal aspect of the mass is friable with roughened edges and contains approximately 10 ml of clotted blood (site of rupture).

Spleen: The tail of the spleen contains a focal, poorly demarcated, approximately 1cm in diameter, raised, irregular, soft mass, which is mottled dark red to tan on cut surface.

Kidney: The medulla of the right kidney contains a focal, 0.9 x 0.5 x 0.4 cm depressed area, which contains less than 1

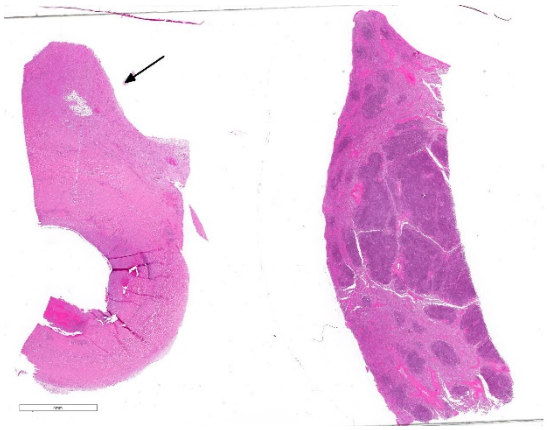

Aorta and spleen, dog. The wall of the aorta (left) is markedly thickened and fibrous connective tissue partially effaces the adventitial adipose tissue (arrow.) Areas of hypercellularity are evident in the aortic wall. Large areas of hypercellularity coalesce within the splenic parenchyma (right). (HE, 7X)

ml of turbid, mucoid, viscous, yellow fluid (granuloma).

Gross morphological diagnoses:

Abdominal cavity: Aortic arteritis, aneurysm with rupture and haemoabdomen

Spleen: Granulomatous Splenitis, focal, moderate, chronic

Kidney: Granulomatous nephritis, focal, moderate, chronic

Laboratory results:

Fungal culture:

Spleen: Very small fungal colonies isolated following 48 hours incubation. Growth identified as *Aspergillus terreus*

Microscopic Description:

Aortic mass**:** Generally, approximately 20% of the aorta is expanded up to three-fold with inflammation, necrosis and haemorrhage. The tunica intima, and to a lesser extent, the tunica media, contain multifocal to coalescing areas of dense

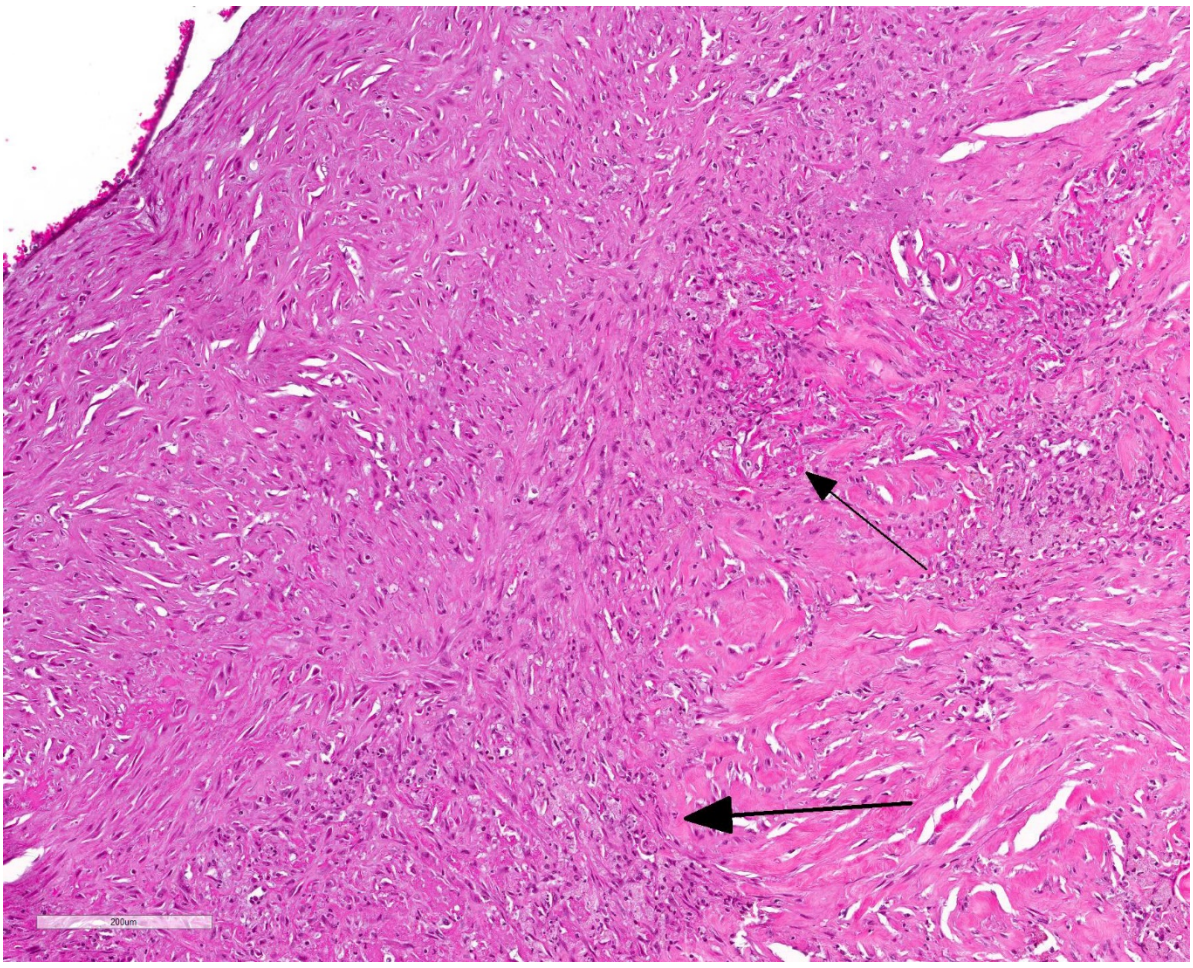

Aorta, dog. The tunica intima is effaced by migration of smooth muscle cells, fibrous connective tissue and elastin, and blends with the underlying tunica media. Within the media there is a dissection which is surrounded by neutrophils, eosinophils, and macrophages (arrows). (HE, 131X)

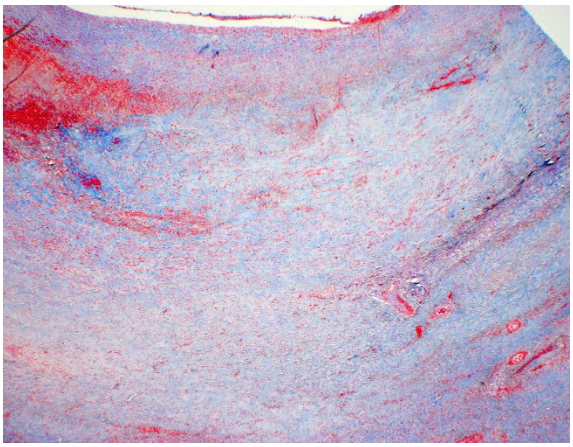

A Masson's trichrome demonstrates the tremendous amount of collagen that expands the wall of the aorta (arrows). The edge of the dissection the red area at upper left. (Masson's trichrome, 40X)

of eosinophilic fibrillary material (fibrin). Macrophages are often epithelioid or forming multinucleated giant cells which engulf or surround hundreds of 3-5 micron-thick, 5-100 micron-long, branching fungal hyphae which are septate with conidial heads and are GMS positive. The tunica media contains large, up to 2000 micron in diameter lakes of extravasated erythrocytes (haemorrhage) admixed with degenerate neutrophils, hyperoesinophilic material, pyknotic and karyorrhectic debris (necrosis). No bacteria are observed on gram stain.

Spleen: In approximately 60% of the tissue section, the white and red pulp are completely effaced by dense infiltrates of lymphocytes and plasma cells which surround hundreds of multifocal with moderate numbers of fungal organisms as described for the aortic mass. The remaining parenchyma contains a reduction in lymphocytes density (depletion) with increased numbers of randomly scattered neutrophils admixed with necrotic debris. aggregates of macrophages, multinucleated giant cells and lesser numbers of neutrophils.

aggregates of degenerate neutrophils and macrophages admixed with large amounts

Macrophages and giant cells often contain or are associated

Contributor's Morphologic Diagnosis:

Aortic mass: Necrotising granulomatous arteritis, severe, generalised, chronic with fungal hyphae (morphology consistent with *Aspergillus terreus*).

Spleen: Granulomatous splenitis, focal, severe, chronic with intralesional fungal hyphae

Contributor's Comment: Aortic aneurysm is a localised dilation of the vessel which may occur secondary to loss of vessel wall integrity. Aneurysms are rare in domestic animals, and may occur secondary to atherosclerosis, medial degeneration, trauma, infection or arterial dissection.[5] In this animal, large amounts of necrosis and inflammation which contain fungal organisms are consistent with a mycotic aneurysm. In this case, the infection has caused a weakening of the vessel wall and

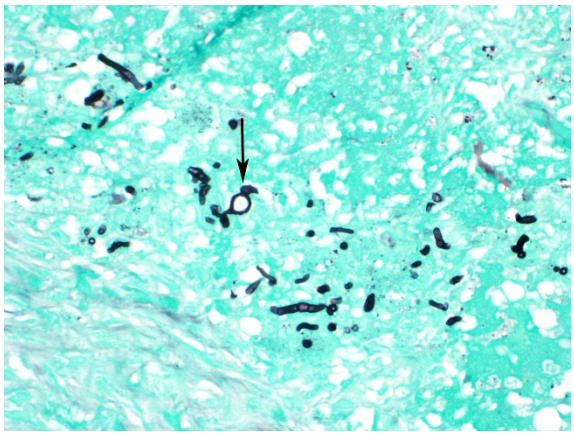

Aorta, dog. A GMS stain demonstrates fungal hyphae in areas of mural necrosis – the hyphae are septate, with parallel walls, and occasionally globose chlamydospore-like swellings (arrow). (HE, 131X)

subsequent rupture, leading to sudden death from acute and massive haemorrhage into the abdomen.

Aspergilli are ubiquitous and can be isolated from soil, air and decomposing organic matter. Infection is acquired from environmental sources, generally by inhalation or ingestion. It is an opportunistic pathogen depending on impaired, overwhelmed or bypassed host defences. Infection may cause local disease, or disseminate to other parts of the body. Evidence of infection and inflammation within the spleen and kidney in this animal is consistent with disseminated disease; however, the original route of infection is undetermined.

Fungal aortic aneurysms have been reported twice previously in dogs.[1,3] In one case, *Graphium* species was isolated from the aneurysm, and *Candida* infection was suspected in the second. In humans, *Aspergillus* species are the most common mycotic infections associated with aneurysms.

A variety of risk factors may be associated with the development of these infections.[1] Reported risk factors in humans include broad-spectrum antibiotic use, mechanical ventilation, parenteral nutrition, renal

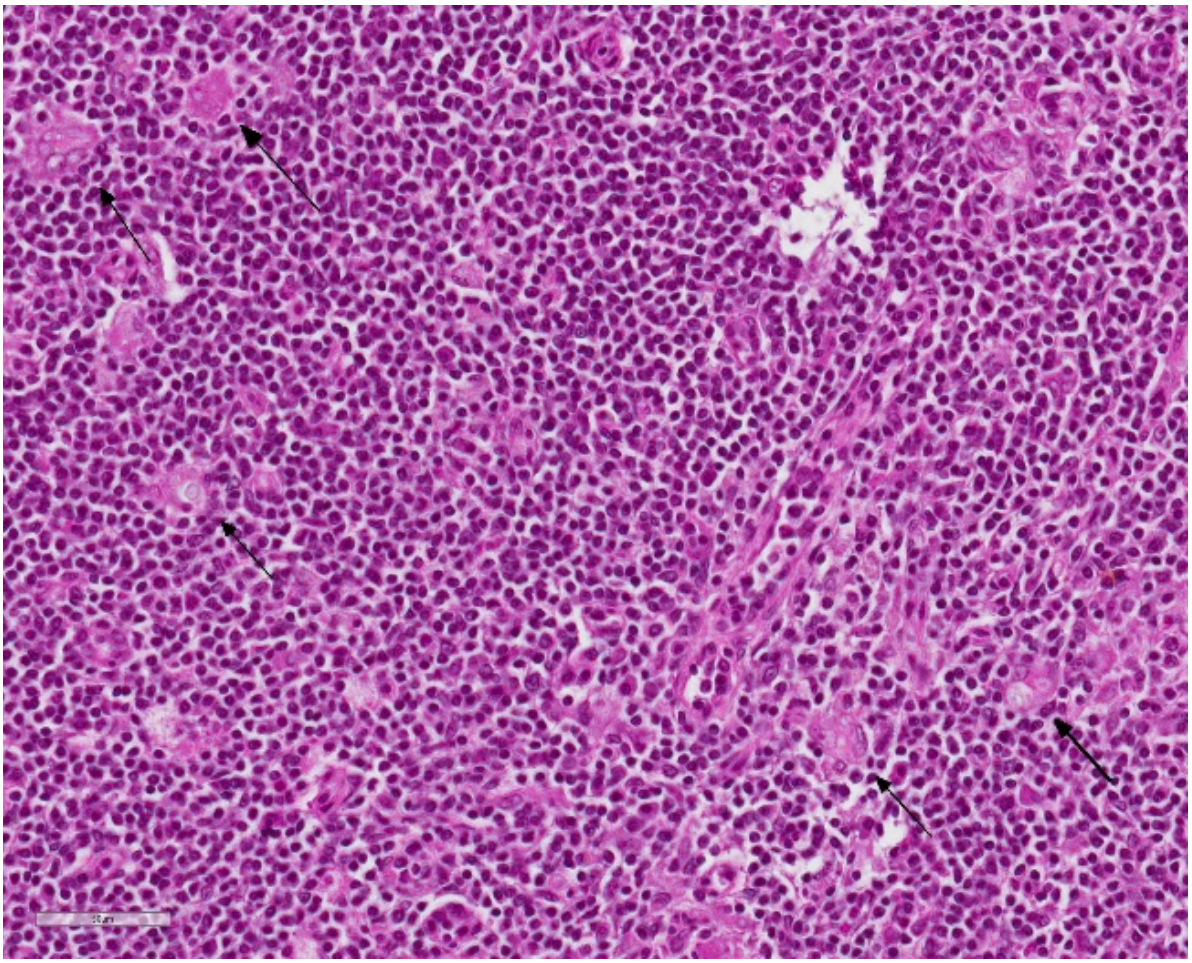

Spleen, dog. there are scattered multinucleated giant cell macrophages which often contain negative outlines of fungal hyphae (arrows) (HE, 400X)

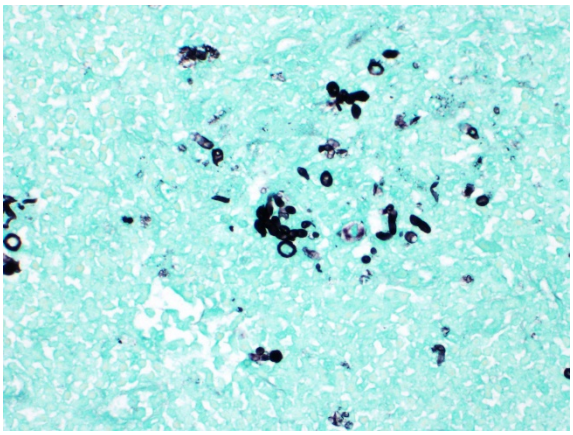

Spleen, dog. A GMS stain demonstrates clusters of fungal hyphae in the spleen. (HE, 400X)

failure, prior surgery, neutropenia, chemotherapy, severe illness, age, and indwelling catheters (especially central venous catheters). Although less commonly reported, veterinary patients appear to have similar risk factors. In one of the case studies cited, however, no predisposing factors were able to be identified.

JPC Diagnosis: 1. Aorta: Elastolysis and fibrosis, transmural, diffuse, severe, with vascularization and dissection.

2. Aorta: Aortitis, pyogranulomatous, focally extensive, severe, with transmural fibrosis and numerous fungal hyphae.

3. Spleen: Splenitis, granulomatous, diffuse, marked with numerous fungal hyphae and lymphoid depletion.

JPC Comment: A caution - the term "mycotic aneurysm" (which may be found repeatedly in Pubmed) is itself a misnomer, as this term, coined by Osler in 1885, refers to a focal aneurysm of an arterial wall due to any infectious cause, not just a fungal one.[6] The term, as applied by Osler, was used to describe the "mushrooming" appearance of the lesion, rather than any particular fungal origin. Most cases of infectious aortitis are the result of opportunistic bacterial infections of pre-existing lesions.

True fungal infections of the aorta are uncommon in all species. They are most commonly dommented in humans, where the may be the result of mycotic infection from other sites (especially in immunocompromised individuals) as well as seen as a devastating complication from a variety of surgical interventions as a result of improper sterilization, including valvular replacement surgery, aortocoronary bypass, and aortic segment replacement.[8]

Documented manifestations of aortic aspergillosis include ascending aortic pseudoaneurysm ansd aspergilloma with supravalvular aortic stenosis.[10] Reports of mycotic aneurysms in animals are even less common. A previous report of *Basidiobolus* infection in a sooty mangabey was published[7] shortly prior to its usage in the Wednesday Slide Conference (WSC Conf. 4, Case 1). The animal was found dead with no premonitory sign following spontaneous rupture of the aneurysm.[7] Aortic aneurysms are well-known in horses and groundhogs[9], both verminous and spontaneous, but only one report of an aortic aneurysm arising from a fungal agent exists.[4]

Few reports of aortic aneurysms due to *Aspergillus terreus* exist for any species (including humans); approximately 90% of reports are the result of infection with *A. fumigatus*. *A terreus* species complex infections are about 4%. [2] Two cases of aortic aneurysm as a result of *A. terreus* infection have been reported, both arising in sites of previous surgery in patients undergoing cancer chemotherapy.[8]

The most common pathogenic species of *Aspergillus* include the members of the *A. fumigatus* species complex, the *A. flaus* species complex, the *A. niger* species

complex, and the *A. terreus* species complex. The *A. terreus* species complex is composed of 16 related species which are found worldwide. They are common soil-borne fungi which can be found in arable soil, compost, and even deserts. They produce light-brown colonies on Sabouraud agar, with characteristic lateral aleurioconidia which attach directly to hyphae. It is used in the pharmaceutical industry to produce lovastatin. [2]

In humans, most *A. terreus* infections are seen in immunocompromised hosts, but chronic pulmonary disease may also be a precipitating factor.[2] In animal species, *A. terreus* has been well documented as a cause of disseminated aspergillosis in the dog,[1,5] with German Shepherd dogs being overrepresented. Breed-associated abnormalities in IgA levels have been postulated as a cause, but not definitively proven. Granulomatous inflamation with fungal hyphae is seen in a number of organs; renal involvement is common (seen in this case, but not submitted) as is myocardial involvement.[1,5] *Aspergillus terreus* is known for a resistance to amphotericin B; 98% of clinical isolates in humans demonstrate a resistance to the drug.[2,8] Luckily, it is the species of *Aspergillus* most susceptible to itraconazone and related antifungals.[2,8]

The moderator noted the presence of vessels within the wall of the aorta – as this is a section of abdominal aorta which should normally be avascular. As a general rule, the walls elastic arteries of small and laboratory animals should not have vasa vasorum; those of ruminants and horses do. The moderator said that he suspected the aneurysm to be the pre-existent lesion and the fungal infection to be secondary.

References:

1. Gershenson RT, et al. Abdominal Aortic Aneurysm Associated with Systemic Fungal Infection in a German Shepherd Dog. *J Am Anim Hosp Assoc.* 2011;47(1):45-49.
2. Lass-Florl, C. Treatment of infections due to *Aspergillus terreus* species complex. *J Fungi* 2018: 4:83-92.
3. Murata Y, et al. Mycotic aneurysm caused by Graphium species in a dog. *J Vet Med Sci.* 2015; 77(10):1285-1288.
4. Okamoto M, Kamitani M, Tunoda N, Tagami M, Nagamine N, Kawata K, Itoh H, Kawasako K, Komine M, Akihara Y, Shimoyama Y, Miyasho T, Hirayama K, Kikuchi N, Taniyama H. Mycotic aneurysm in the aortic arch of a horse associated with invasive aspergillosis. *Vet Rec* 2007; 160:268-270.
5. Robinson WF and Robinson NA. Cardiovascular system. In: Grant Maxie M, ed. *Jubb, Kennedy and Palmer's Pathology of Domestic Animals.* vol 3, 6th ed. Elsevier, Missouri. 2016:68-69.
6. Salzberger LA, Cavuoti D, Barnard J. Fatal *Salmonella* aortitis with mycotic aneurysm rupture. *Am J Forens Med Path* 2002; 23(4):382-385.
7. Sharma P, Cohen JK, Lockhart SR, Hurst SF, Drew CP. Ruptured mycotic aortic aneurysm in a sooty mangabey (*Cercocebus atys*).
8. Silva ME, Malagolowkin MH, Hall TR, Sadeghi AM, Krogstad P.

Mycotic aneurysm of the thoracic aorta due to *Aspergillus terreus*: case report and review. *Clin Inf Dise* 200; 31:1144-1148.
9. Snyder RL Ratcliffe HL. *Marmota monax*: a model for studies of cardiovascular, cerebrovascular and neoplastic disease. *Acta Zool Pathol Antvep* 1969; 48:256-273
10. Watanabe, I, Nakayama T, Yamada E, Tsukino M, Hayashi E. Invasive aspergillosis in the aortic arch with infectious *Aspergillus* lesions in pulmonary bullae. *Med Mycol Case Rep* 2015; 7:15-19.
10.

CASE III: WSC Case 1 (JPC 4049886).

Signalment: 22Y 6M 12D, female, common squirrel monkey (*Saimiri sciureus*).

History: Patient was found dead in its enclosure. Patient had been exhibiting abnormal behavior the day prior. A necropsy was performed and tissue specimens were submitted in formalin for histopathologic evaluation.

Gross Pathology: There were multiple, multifocal, up to 1 mm diameter dark red-black foci throughout the cerebral gray matter. A small amount of bruising and emorrhage was noted in the rostral mandible.

Laboratory Results (clinical pathology, microbiology, PCR, ELISA, etc.)**:** None.

Microscopic Description: Diffusely, cerebral meningeal and parenchymal vessels are transmurally expanded and effaced by variable amounts of amorphous, finely fibrillar to waxy, pale eosinophilic material (amyloid). Multifocally, affected vessels are surrounded by mild to moderate amounts of fibrinoid exudate and acute to chronic hemorrhage as well as mild to moderate numbers of gitter cells that occasionally contain golden-brown globular intracytoplasmic pigment (hemosiderin), lymphocytes and plasma cells and fewer gemistocytic astrocytes and occasional multinucleate giant cells. There are multifocal small (10-25 um) round parenchymal deposits (senile plaques) often adjacent to affected vessels.

Contributor's Morphologic Diagnosis:

Cerebrum, vessels: Amyloidosis, transmural, diffuse, severe, with hemorrhage, fibrinoid exudation, astrogliosis, senile plaques and occasional multinucleate giant cells.

Contributor's Comment:

The histomorphologic findings in the cerebrum are consistent with cerebral amyloid angiopathy (CAA) – a vascular disorder caused by the accumulation of amyloidogenic proteins in the walls of cerebral blood vessels.[4] In severe cases, CAA can result in other vasculopathic changes such as microhemorrhages, fibrinoid extravasation and focal gliosis.[4] In some cases, vascular/perivascular inflammation, fibrinoid necrosis and leukoencephalopathy have been associated with vascular β-amyloid deposition.[4] The

predilection to developing age-related CAA has been confirmed in the squirrel monkey and they are an animal model for CAA in humans, in whom it has been shown to increase the risk of intracerebral bleeding and has been associated with up to 20% of non-traumatic hemorrhagic strokes in the elderly.[4] Additionally, CAA is a risk factor for cognitive decline (even in the absence of stroke) and may worsen the dementia of Alzheimer's disease (AD).[4] Currently, there are no practical antemortem diagnostic tests or treatments for CAA. CAA-related vasculopathies arise in squirrel monkeys but are not common. In severely affected animals (as in this case), microhemorrhages and fibrinoid exudation may occur. Several studies support squirrel monkeys as an optimal biological model for idiopathic CAA and for testing the safety and efficacy of β-amyloid reduction strategies such as β-amyloid-immunization therapy for AD.[4]

The pathogenesis of CAA remains obscure; however, failure of active/passive elimination of β-amyloid from the aging brain may play an important role.[4] Squirrel monkeys naturally develop β-amyloid deposits in the form of CAA and senile plaques starting at approximately 13 years of age.[4] Their life span in captivity is up to 30 years. Additionally, their cerebrovascular and immune systems are similar to humans. The β-amyloid precursor protein in squirrel monkeys is 99.5% homologous to human βAPP751 and the amino acid sequence of β-amyloid is identical in the two species.[2] Severely affected arterioles show loss of smooth muscle cells in the tunica media leading to weakening of the vascular wall and an increased propensity to rupture,

Cerebrum, squirrel monkey. Fragments of cerebrum are presented for examination. A subgross magnification, no lesions are visible, save for a focal area of hemorrhage at lower right. (HE 6X).

leading to intracerebral bleeding.[2] Amyloid accumulation in cerebral vessels is known to induce degeneration of the entire neurovascular unit. Not only does the accumulation of insoluble amyloid species in vascular walls cause alterations of smooth muscle and endothelial cell layers, but amyloid deposition and concomitant microhemorrhages also occur in capillaries lacking the smooth muscle layer.[5] Complement activation products co-localize with cerebral parenchymal and vascular deposits in AD and non-β-amyloid amyloidosis indicating that the chronic inflammatory response, most likely initiated by the deposits, is a general phenomenon.[5] Once complement components are generated, they participate in several key steps of amyloidogenesis (aggregation, microglial activation and phagocytosis).[5] Other markers of inflammation in AD include elevated cytokines and chemokines as well as accumulation of activated cytokine-expressing microglia found in or near pathologic lesions.[5]

Capillaries are especially vulnerable to CAA in squirrel monkeys,[4] while in humans,

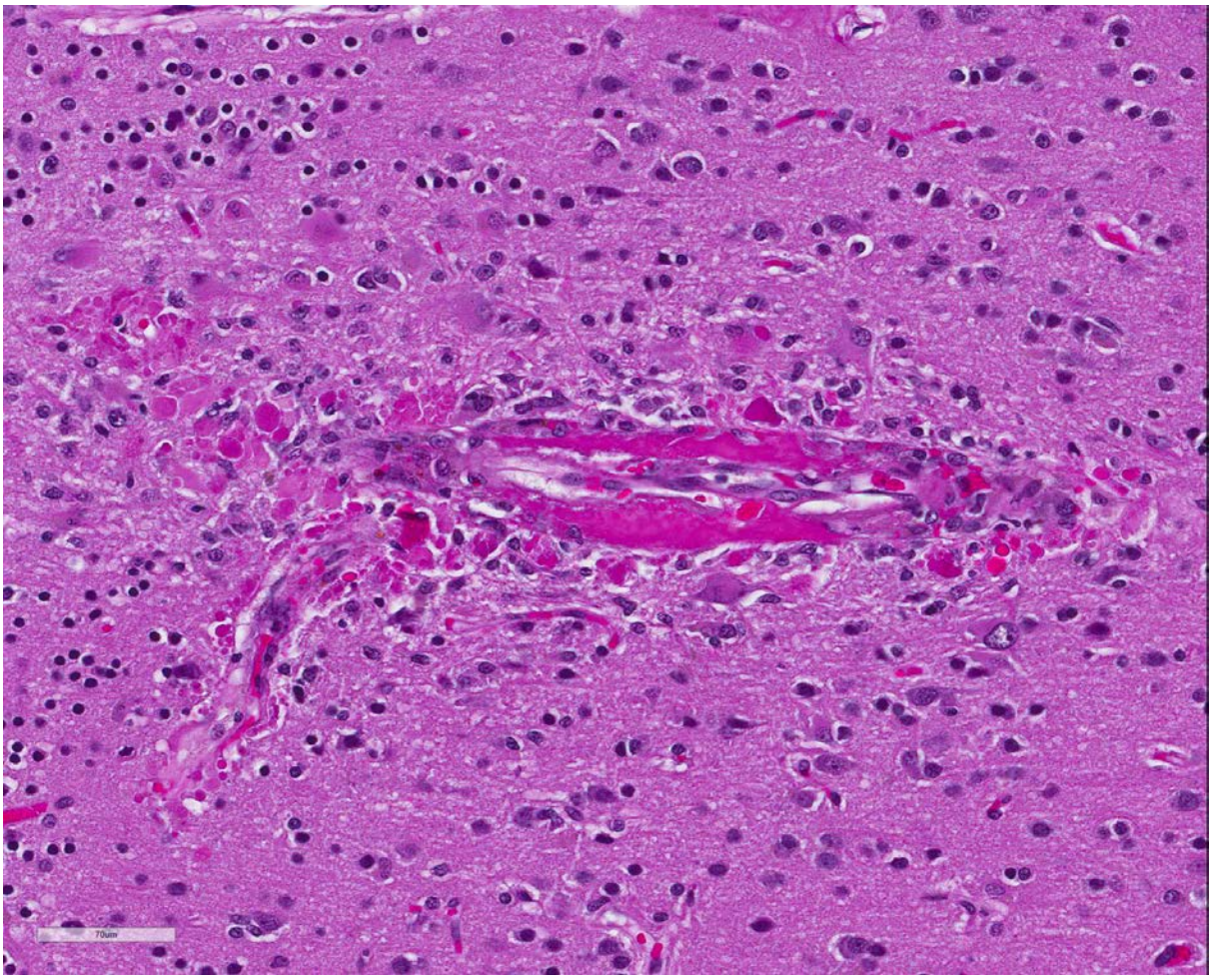

Cerebrum, squirrel monkey. Parenchymal vessel walls are expanded by brightly eosinophilic amyloid and surrounded by macrophages, astrocytes, and globules of extruded protein. (HE 6X).

leptomeningeal and cortical arteries and arterioles are especially vulnerable. Both (vessels and parenchyma) types of β-amyloid deposits occur primarily in the neocortex with the highest density of lesions in the rostral cortex, diminishing caudally.[4] Distribution and quantity of deposits are highly symmetrical in the right and left hemispheres.[2] In the squirrel monkey, aggregated β-amyloid occupies meningeal and parenchymal arteries/arterioles as well as numerous parenchymal capillaries.[4] Few capillaries are congophilic and, as in humans, veins are seldom amyloidotic.[4] In the arteriolar wall, the basal lamina of the tunica media is the primary site of β-amyloid accumulation.[4] The tunica adventitia is also frequently involved.[4] When severe, there is effacement of hypocellularity of the vascular wall – especially within the tunica media.[4] In contrast to humans, large parenchymal senile plaques are relatively infrequent in aged squirrel monkeys and when they occur they are usually small (10-25 um in diameter) and spherical.[4] Amyloidotic vessels occasionally may be surrounded by

reactive microglia; however, they are more often associated with reactive astrocytes.[4]

CAA is ultrastructurally composed of classic amyloid fibrils and is the principal type of cerebral β-amyloidosis in squirrel monkeys.[4] The basal lamina of amyloidotic vessels is enlarged and distended by masses of classic amyloid fibrils. In capillaries, β-amyloid accumulates in the basal lamina and tunica adventitia (due to lack of tunica media proper). In some cases, β-amyloid in parenchymal and vascular lesions is coextensive.[4] Additional diagnostic tests include Congo Red special histochemical stain, β-amyloid immunohistochemistry, Thioflavin T fluorescent stain and the Shtrasburg method. CAA has also been reported in a sooty mangabey.[5] This case was reviewed in consultation with Dr. Derek Mathis, MD neuropathologist.

Contributing Institution:

http://www.wpafb.af.mil/AFRL

JPC Diagnosis: Cerebrum, small and medium-caliber arteries: Amyloidosis , multifocal, moderate, with multifocal fibrinoid necrosis, and minimal perivascular granulomatous inflammation.

JPC Comment: The contibutor has done an excellent job in describing the syndrome of cerebrovascular amyloidosis (cerebral amyloid angiopathy – CAA) in the squirrel

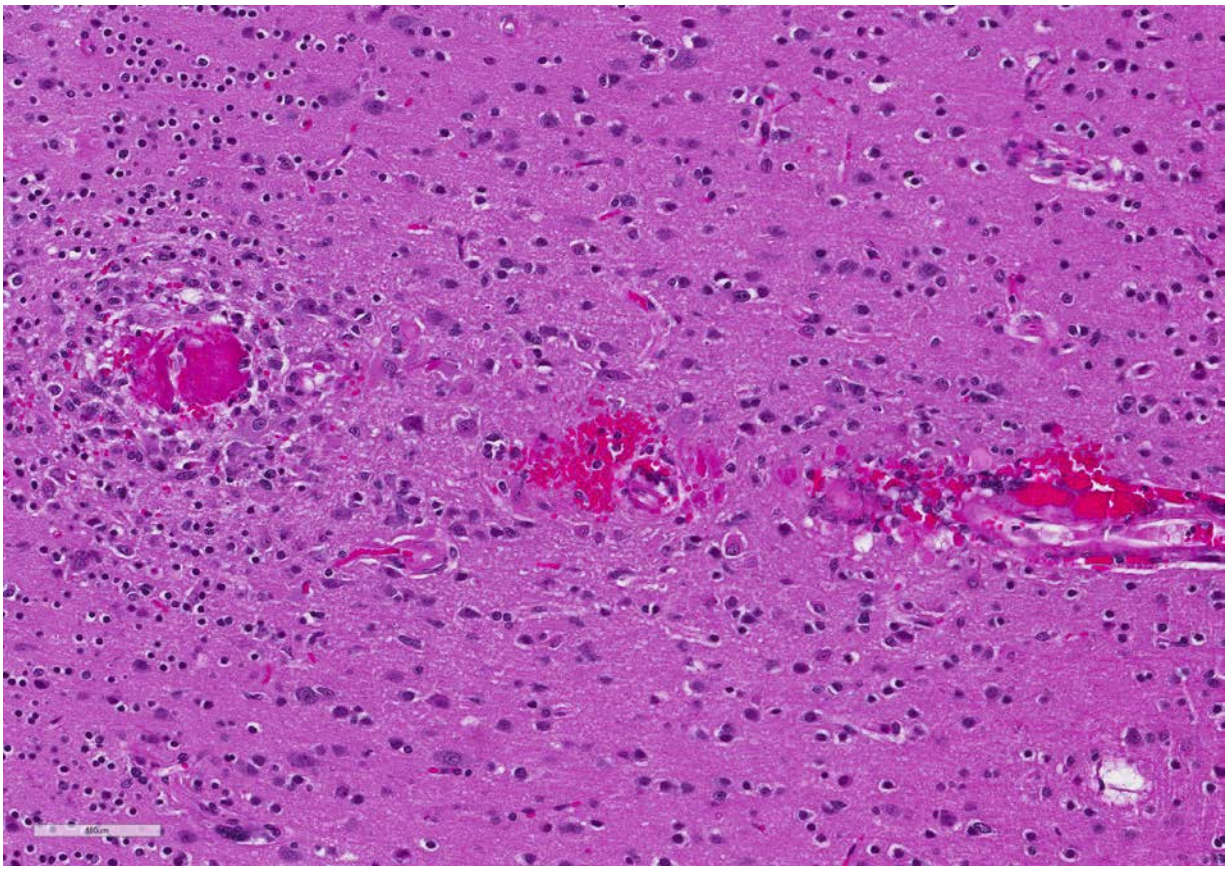

Macrophages, glial cells and rare gemistocytic astrocytes surround remnants of a thrombosed vessel (left). The walls of nearby vessels are expanded with amyloid and there is focal hemorrhage. There is gliosis of the surrounding parenchyma. (HE 254X).

monkey, perhaps the best animal model for a significant health problems in aging humans. Increasingly sophisticated imaging technologies are available today for antemortem detection CAA in squirrel monkeys. Magnetic resonance imaging has detected two distinct patterns associated with cerebrovascular amyloid – amyloid-related imaging abnormalities (ARIA). T-2 weighted MRI has identified an edematous type (ARIA-E), that appears as a hyperintense signal, and a hemosiderotic type (ARIA-H) which demonstrates a hypointense signal. The ARIA-E type demonstrates astrocytic and microglial hypertrophy in the white and grey matter.[6]

In humans, β-amyloid peptide (Aβ) is an integral part (along with tauopathy) in the development of Alzheimer's disease, and the misfolding of Aβ is considered the initiating event in the development of Alzheimer's disease (AD).[6] On its own, it is not associated with dementia or neurodegeneration in humans[6], but is considered a major cause of spontaneous intracerebral hemorrhage.[1]

CAA is commonly seen in elderly humans, and advancing age is the strongest risk factor for its development.[1] (Another risk factor, shared with AD, is the apoliporotein E (ApoE) epsilon IV (e4) allele).[4] Up to 40% of non-demented and 60% of demented individuals between the ages of 80 and 90 years may demonstrate CAA at autopsy.[1] One study suggests that it may be seen in up to 95% of humans with dementia if looked for diligently. A number of manifestations of CAA in humans in the absence of Alzheimer's disease have been described, to include spontaenous cortical hemorrhage (with associated microbleeds and siderosis), post-hemorrhage cognitive impairment, and transient focal neurological episodes ("amyloid spells").[1] A recent study demonstrated significant cortical thinning in individuals with CAA.[3]

As mentioned above in context with the spider monkey, the currently accepted pathogenesis for CAA is not overproduction of Aβ, but deficiencies in clearance. Excess interstitial fluid in the brain is drained along arteries in the brain, bolstered by the pulsation of these vessels. The predominant theory of deposition is that as this perivascular drainage system fails with age, Aβ is progressive trapped in the expanding perivascular compartment, which allows for aggregation and deposition along vascular basement membranes.[1]

Regarding the comparative pathology of CAA, in addition to the squirrel monkey, there are a number of mouse models which overexpress Aβ and develop senile plaues and CAA, but no significant neurodegeneration.[7] A number of researchers have suggested species-specific differences in post-translational characteristics and the the formation of species-specific Aβ isoforms as a potential reason for the lack of associated neurodegenerative disease in some species. Squirrel monkeys also manifest extensive Aβ deposition, but not the additional lesions associated with Alzheimer's disease.[7]

The concurrent presence of amyloidosis and fibrinoid necrosis was interesting in this case. The moderator described histologic differences in the two which are best appreciated without the use of a condenser. In addition, the moderator demonstrated the presence of giant cells adjacent to arteries containing mural amyloid, as well as the discontinuity of arterial walls when stained with smooth muscle actin (most appreciable on arteries cut on longitudinal section.)

References:

1. Charidimou A, Boulouis G, Gurol ME, Ayata C, Bacskai, Frosch MP, Viswanathan A, Greenberg. Emerging concepts in sporadic cerebral amyloid angiopathy. *Brain* 2017; 140:1829-1850.
2. D'Angelo OM, Dooyema J, Courtney C, Walker LC and Heuer E. Cerebral amyloid angiopathy in an aged sooty mangabey (Cercocebus atys). Comp Med (2013) 63(6): 515-520.
3. DeSimone CV, Graff-Radford J, El-Harasis MA, Rabinstein AA, Asirvatham SJ, Homes DR. Cerebral amyloid angiopathy: diagnosis, clinical implications, and management strategies in atrial fibrillation. *J Am College Cardiol* 2017; 70(6):1173-1181.
4. Elfenbein HA, Rosen RF, Stephens SL, Switzer RC, Smith Y, Pare J, Mehta PD, Warzok R and Walker LC. Cerebral β-amyloid angiopathy in aged squirrel monkeys. *Histol Histopathol* (2007) 22:155-167.
5. Ghiso J, Fossati S and Rostagno A. Amyloidosis Associated with Cerebral Amyloid Angiopathy: Cell Signaling Pathways Elicited in Cerebral Endothelial Cells. *J Alzheimers Dis* (2014).
6. Heuer E, , Jacobs J, Du R, Wang S, Kiefer OP, Cintron AF, Dooyemy J, Meng Y, Zhang X, Walker L. Amyloid related imaging abnormalities (ARIA) in an aged squirrel monkey with cerebral amyloid angiopathy. *J Alzheimers Dis* 2017; 57(2): 519-530.
7. Rosen RF, Tomidokoro Y, Farberg AS, Dooyema, Ciliax B, Preuss Tm, Neubert, TA, Ghiso JA, LeVine H, Walker LC. Comparative pathobiology of Aβ and the unique susceptibility of humans to Alzheimer's disease. *Neurobiol Aging* 2016; 44:185-196.

CASE IV: 21465 (JPC 4135536).

Signalment: 18 month old male Bassett hound (*Canis lupus familiaris*)

History: Mild ataxia, with cardiac enlargement of uncertain origin.

Gross Pathology: The dog has body weight of 17.0 kg. Watery joint fluid, with synovial hyperplasia, is present in several larger joints, but is particularly marked in the left coxofemoral joint. The subcutaneous fascia is thicker than expected over the muscles of the rear limbs, with reduced adipose tissue. The corneas are bilaterally cloudy. Thick dense spongy bone was present in cross-sections of the anterior calvarium. The

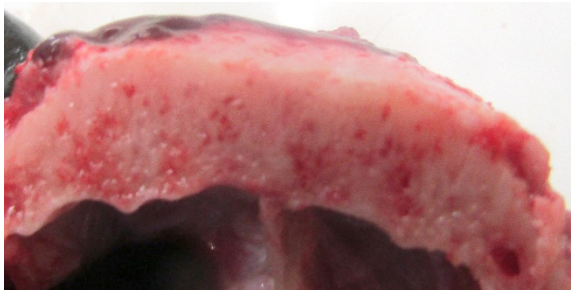

Calvarium, dog. Cross-section of bone of the anterior calvarium, showing increased width are reduced spongy texture. (Photo courtesy of: Veterinary Medical Diagnostic Laboratory, University of Missouri, 610 East Campus Loop, Columbia MO 65211, http://vmdl.missouri.edu/; http://vpbio.missouri.edu/)

Ribs, dog. Pleural aspect of the right costochondral junction, showing spatulate ribs. (Photo courtesy of: Veterinary Medical Diagnostic Laboratory, University of Missouri, 610 East Campus Loop, Columbia MO 65211, http://vmdl.missouri.edu/; http://vpbio.missouri.edu/)

costochondral junctions of the ribs are mildly offset, with a spatulate form. The skeletal muscles are pale, especially masseters and maxillary muscles. Both interventricular heart valves are extensively and irregularly somewhat irregularly, but have, rounded, smooth surfaces, and a gelatinous texture. Associated chordae tendonae are pearly white.

Laboratory Results: A mutation was found in the α-L iduronase gene by PCR.

Microscopic Description: Submitted tissues consist of thoracic aorta and heart with muscular arteries in the epicardial fat.

The elastic aortic wall is has elevated, plaque-like thickenings in the intima that bulge into the lumen, but remain covered by a single layer of flat endothelium. In the media, smooth muscle cells have a regimented appearance, and are separated into stacks by elastic fibers and increased interstitial ground substance with H&E (Fig. 5). Medial myocytes are diffusely contain unstained, well-defined cytoplasmic vacuoles. Despite this generally well-organized microanatomy, there is multifocal disorganization of the wall, a band of vacuolated macrophages located in the intima and inner media (Fig. 6), multifocal medial vacuolation around the vasa vasorum (Fig 7). These areas contain a multitude of foamy macrophages that form disorganized islands in the superficial wall and contribute to the substance of the plaques. Similar vacuoles occur in the muscularis of muscular arteries in the epicardial fat (Fig. 8) with disorganization of the vascular wall. The adventitia of these arteries contains increased ground substance and vacuolated macrophages in both muscularis and adventitia. There is very mild increase in lipofuscin on either side of cardiomyocyte nuclei sectioned longitudinally (not shown).

Movat's pentachrome staining was used to differential stain to determine the stromal components of the plaques (Fig.9). This stain produces black staining of elastin, while mucopolysaccharides stain green, collagen yellow, and muscle stains red. Small elastin fibers of the tunica intima is disorganized, and the plaque is easily demarcated from the internal elastic lamina of the media. Myocytes are outlined by elastin as well. The plaque is less intensely stained green, detecting mucopolysaccharides in its ground

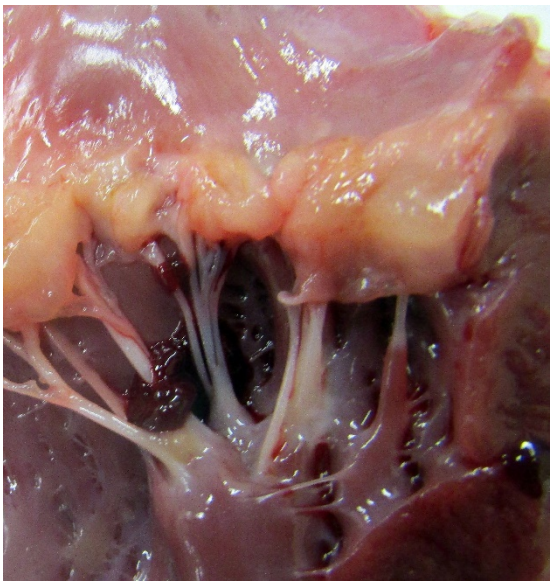

Tricuspid valve. Valve leaflets are enlarged. (Photo courtesy of: Veterinary Medical Diagnostic Laboratory, University of Missouri, 610 East Campus Loop, Columbia MO 65211, http://vmdl.missouri.edu/; http://vpbio.missouri.edu/)

substance. Elastin staining is less organized in the intimal plaque and around the vasa vasorum. With Alcian blue-PAS 1.0 and 2.5, blue staining of sulfomucins predominated between the medial myocytes (Fig 10), but cytoplasmic vacuoles are shaded in pink along the edges (neutral and carboxymucins mucins). Vacuoles are found within muscle cells of the epicardial arteries.

Laboratory Results (clinical pathology, microbiology, PCR, ELISA, etc.)**:**

A mutation was found in the α-L iduronase gene by PCR.

Contributor's Morphologic Diagnosis:

Arteriopathy, with aortic plaques and stromal dysplasia, consistent with mucopolysaccharidosis

Contributor's Comment:

As a group, the mucopolysaccharidoses result from defective glycosaminoglycan catabolism. [9, 10] They are characterized by accumulation of glycoaminoglycans (GAG) in lysosomes. The most severe form, a deficiency of α-L iduronidase, causes Hurler's syndrome (MPSI), and results in increased retention of both dermatan sulfate and heparin sulfate in cells and interstitium.[9] Both metabolites are shed in urine of patients. Failure to hydrolyze these two substrates results in their accumulation in lysosomes, triggering complex of intracellular events leading to clinical signs that are directly linked to mechanical consequences of GAG storage.[5] Common findings in humans include laryngeal and tracheal narrowing, hearing and visual deficits, gargoyle faces, skeletal deformities, and heart valve disease with cardiomyopathy due to cardiac rigidity.[9,10]

Over 100 enzyme defects have been described in people of severe or intermediate phenotype.[10] α-L iduronidase deficiency has

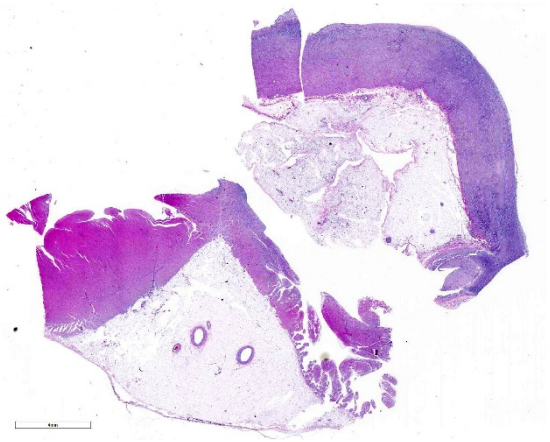

Atrium (left) and aorta (right). Two tissue sections are presented for examination. The wall of the aorta is markedly thickened with abnormal alternating of increased density and pallor at subgross examination. (HE 6X)

been described in dogs,[3, 11, 12] knockout mice,[2] and cats.[4] Even after replacement therapy, there is over a two-fold increase in expression of lysosomal and proteasome function in 19-month-old Plott hounds affected by MPSI.[2] Downregulated were genes associated with cell adhesion, cytoskeleton and calcium regulation. Immunoregulatory genes were also elevated. This could mean that GAGs produce an inflammatory environment that exacerbates disease.[2] Up-regulation of extracellular cathepsin B may also increase pathology due to elastin catabolism.[6]

The known mutation in Plott hounds is G to A point mutation in the donor splice site of intron, [4, 8] resulting in retained transcription of intron, but premature termination at the intron-exon junction due to the presence of a stop codon. Homozygous recessives completely lack the enzyme protein or its activity.[8] Mucopolysaccharidosis I has described in a Rottweiler, Afghan hound, this Bassett and a Boston terrier, but information about the specific genetic mutations in these breeds is not known.

Enzyme replacement abrogates part of the clinical syndrome and increases the survival time in humans and dogs, but patients still have a considerable residual disease burden.[1, 10] Enzyme replacement does not correct heart valvulopathy, cardiac stiffness or vasculopathy, and death from cardiac manifestations of disease is common, even after treatment. Bone abnormalities remain, and may require surgical intervention. Dogs given genetically-corrected hematopoietic stem cells had increased GAG clearance, reduced GAGs in the brain and improved craniofacial appearance. It is noted that people with severe gene mutations like W70X, Q70X and missense A327P, G51D have no functional enzyme activity and the authors indicated that they must be referred for therapy shortly after birth to slow the progression of disease.[10]

Histologically, affected dogs have unstained vacuoles are present in many organs, particularly mesodermal tissues such as fascia, cartilage, blood vessels, heart valves and cerebral leptomeninges.[11]

Lyons examined the branches of the terminal aorta of MPSI-affected dogs that lacked α-L-iduronase enzyme activity. [7] Vascular wall thickness is particularly increased near branch points, locations associated with turbulent flow. Reduced shear stress alters the metabolism of endothelial cells, resulting in increased permeability and leakage. Macrophages may also contribute to degradation of internal elastic lamina, as demonstrated in this case.[7] These asymmetric plaques are characterized by extensive intimal thickening and disruption of the internal elastic lamina, often with significant (60-70%) narrowing of the vascular lumens. Lumenal narrowing was probably more significant in the cases in this study compared to the submitted tissue, because only the terminal branches of the aorta were used in the study. The plaques contained GAG-laden macrophages, fibroblasts and smooth muscle cells, with loss of the endothelial basement membrane and reduced claudin production.[7] CD18+ macrophages were scattered or clustered below the endothelium (Figs. 6, 7). Enzyme treatment makes intimal plaques more

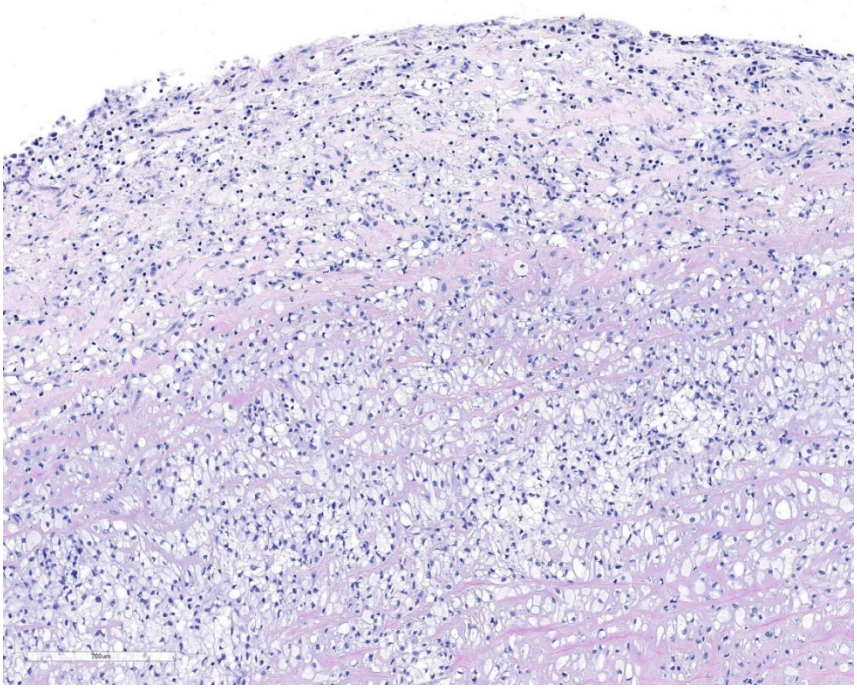

Atrium (left) and aorta (right). Two tissue sections are presented for examination. The wall of the aorta is markedly thickened with abnormal alternating of increased density and pallor at subgross examination. (HE 6X)

JPC Diagnosis: Aorta: Smooth muscle vacuolation, diffuse, severe, with multifocal necrosis **,** intimal histiocytic plaque formation , medial neovascularization, and fibrosis.

JPC Comment: The contributor has done an excellent job in describing the Mucopolysaccharidoses in the dog, and also in man.

The mucopolysaccharidoses are a group of lysosomal storage diseases arising from genetic deficiencies of enzymes needed to catabolize the mucopolysaccharides, a group of glycosamino-glycans constructed by attaching long-chain carbohydrates to proteins. Most of these diseases were first described in humans in the 1970's, and a number of animal models of spontaneous disease have been subsequently identified (Table 1). They are most commonly found in the interstitial ground substance and include dermatan sulfate, chondroitin sufate, keratan sulfate and heparan sulfate. These undegraded or partially degraded glycosaminoglycans accumulate in lysosomes in a number of cells, including macrophages and long-lived post-mitotic cells such as fibroblasts and myocytes.

While the accumulation of partially degraded mucopolysaccharides within lysosomes appears histologically to be a relatively benign process largely resulting in

organized, with reduced macrophages and more laminar organization of fibrous tissue in treated dogs after several months. Similar pathology has been found in human patients and null mice.[1] In affected humans, the disease most commonly affects the coronary arteries. In mice, dilation of the aortic root was more common and coronary artery disease was uncommon; species differences exist in disease manifestations. This progressive vascular changes in MPS-I shares some morphological similarities to atherosclerotic plaques.

Contributing Institution:

Veterinary Medical Diagnostic Laboratory, University of Missouri, 610 East Campus Loop, Columbia MO 65211, http://vmdl.missouri.edu/; http://vpbio.missouri.edu/)

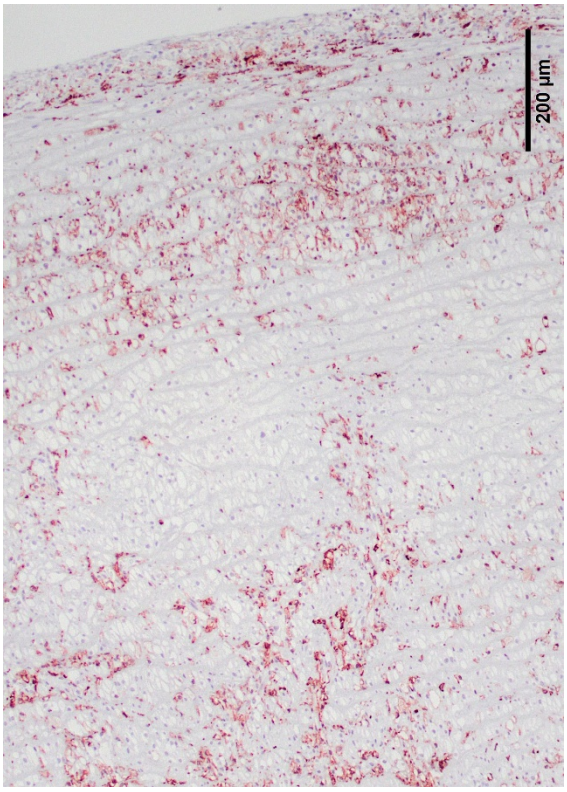

Aorta, dog. Low magnification of a plaque and underlying tunica intima shows the infiltration of the wall by numerous IBA-1- positive histiocytes. (anti IBA-1, 40X). (Photo courtesy of: Veterinary Medical Diagnostic Laboratory, University of Missouri, 610 East Campus Loop, Columbia MO 65211, http://vmdl.missouri.edu/; http://vpbio.missouri.edu/)

cytomegaly, the buildup of these products within lysosomes results in tremendous enlargement and overpopulation of these organelles. This results in hindrance of normal cellular processes, leading to cell death. In addition, the accumulation of autophagic substrate within lysosomes may proceed to a level in which apoptosis may be triggered.

MPS 1, or Hurler's disease, is considered a prototypical, and one of the the most severe forms of mucopolysaccharidoses. It results from a deficiency of α-L-iduronidase, required to hydrolyze the terminal α-L-iduronic acid residues from dermatan and heparan sulfate. In humans, three distinct clinical manifestations of the condition exist: MPS I H or Hurler's syndrome, MPS I S or Scheie syndrome, and the intermediate phenotypes, collectively referred to as MPS I H/S or Hurler-Scheie syndrome.[9] MPS I H is the most severe, with an early onset (most cases are diagnosed between 6 and 24 months of age) and marked cognitive delay as one of the symptoms. It is a progressive disease which untreated results in death before the 10th year, and includes enlarged liver and spleen, skeletal deformites, coarse faces, and joint stiffness. Affected individuals develop significant hearing loss and an enlarged tongue, along with congnitive delay that relegates affected individuals to only rudimentary language skills. Communicating hydrocephalus often develops at 2-3 years of age. MPS I S, or Scheie syndrome, on the other end of the severity spectrum, is a much more limited phenotype, sharing joint stiffness (an early and often presenting sign), aortic valve disease, corneal clouding and other ocular abnormalities, but not the cognitive delay, and diagnosis is often made between 10-20 years of age.[9]

Treatment of Hurler's disease has advanced dramatically in recent years, and includes allogeneic hematopoietic stem cell transplants (HSCT) and enyme replacement therapy with human recombinant laronidase.[10] HSCT is considered the most appropriate treatment for MPS I H, and has been shown to be successful in halting progression of cognitive delay when used in patients before 2.5 years of age. Enzyme replacement therapy has been shown to be effective in cases of MPS I S and may be initiated in more severely affected individuals prior to more definitive HSCT; however, it is not recommended for Hurler's syndrome due to the limited ability of laronidase to cross the blood-brain barrier.[10]

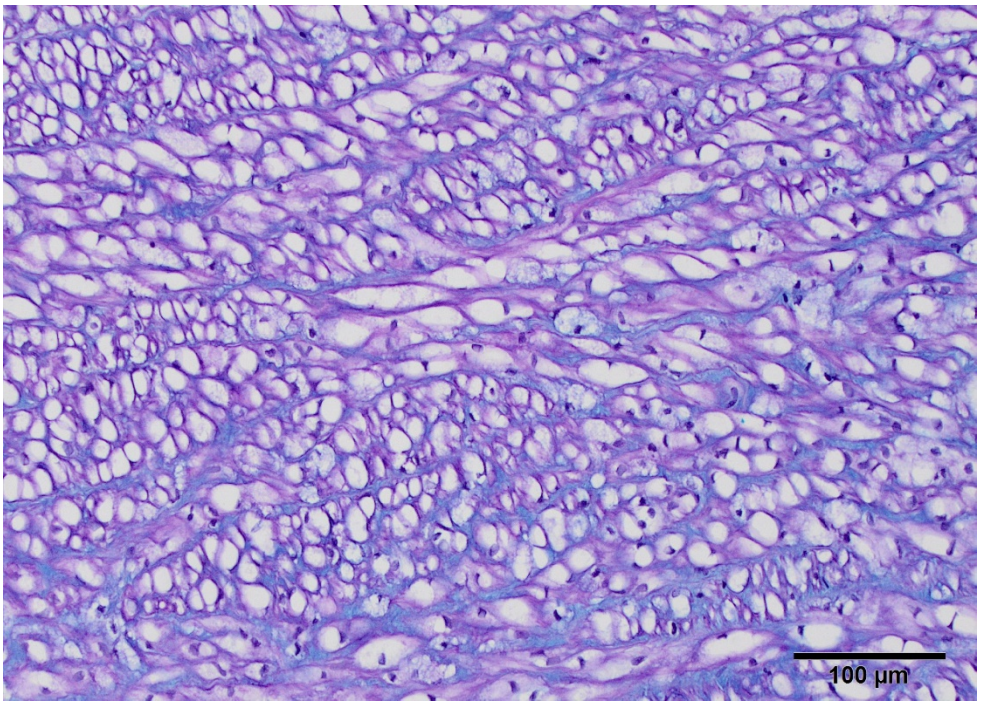

An Alcian blue 2.5 stain demonstrates accumulation of mucinous extracellular matrix in the wall of the aorta (MEMA – mucinous extracellular matrix accumulation.) (Alcian blue 2.5, 400X)

References:

1. Braunlin E, Mackey-Bojack S, Oanoskaltsis A, et al. Cardiac functional and histopathologic findings in humans and mice with mucopolysaccharidosis type I: implications for assessment of therapeutic interventions in Hurler syndrome. Pediatr Res. 2006;59:27-32.

2. Gonzalez EA, Martins GR, Tavares AMV, et al. Cathepsin B inhibition attenuates cardiovascular pathology in mucopolysaccharidosis I mice.Lice Science. 2018;196:102-109.

3. Haskins ME. Animal models of mucopolysaccharidosis and their clinical relevance. *Acta Paediatr*. 2007;96:56-92.

4. Haskins ME, Aguirre GD, Jezyk PF, Desnick RJ, Patterson DF. The pathology of the feline model of mucopolysaccharidosis I. *Am J Pathol.* 1983:112:27-36.

5. Hinderer C, Katz N, Louboutin J-P, et al. Abnormal polyamine metabolism is unique to the neuropathic forms of MPS: potential for biomarker development and insight into pathogenesis. *Human Molec Genet.* 2017; 26:3837-3849.

6. Khalid O, Vera MU, Gordts PL, et al. Immune-mediated inflammation may contribute to the pathogenesis of cardiovascular disease in mucopolysaccharidosis. *Plos One.* 2016;DOI:10.1371/journal.pone.010850.

7. Lyons JA, Dickson PI, Wall JS, et al. Arterial pathology in canine mucopolysaccharidosis-I and response to therapy. Lab Invest. 2010;91:665-674.

8. Menon KP, Tieu PT, Neufeld EF. Architecture of the canine IDUA gene and mutation underlying canine mucopolysaccharidosis I. Genomics 1992;14:763-768.

dosis I. Genomics 1992; 14:763-768.

9. Neufeld E, Muenzer JA. The mucopolysaccharidoses. Ch 61 in

Eds. Scriver CR, Beaudet AL, Sly WS,Valle D. *The Metabolic Basis of Inherited Disease, vol 2,* 6th ed. UDA:McGraw-Hill; 1989:1565-1587.

10. Parini R, Deodoro F, Di Rocco M, et al. Open issues in mucopolysaccharidosis I-Hurler. *Orphanet J Rare Dis*. 2017;12:112. DOI 10.1186/s13023-017-0662-9.

11. Shull RM, Helman RG, Spellacy E, Constantopoulos G. Munger RJ, Neufeld EF. Morphologic and biochemical studies of canine mucopolysaccharidosis I. *Am J Pathol*. 1984;114:487-495.

12. Spellacy E, Shull RM, Constantopoulos G, Neufeld EF. A canine model of human alpha-L-iduronidase deficiency. *Proc Natl Acad Sci USA*. 1983;80:6091-3065.

Self-Assessment - WSC 2019-2020 Conference 18

1. Which of the following histochemical stains will highlight both collagen and elastin?
    a. Verhoeff-van Gieson
    b. Luxol fast blue
    c. Masson's trichrome
    d. Movat's pentachrome

2. Which of the following structures are not visualized in portal areas in cases of intrahepatic arteriovenous fistulae?
    a. Lymphatics
    b. Bile ducts
    c. Portal veins
    d. Arterioles

3. Which of the following species of *Aspergillus* is most often recovered from infections in all species of animals and man?
    a. Aspergillus deflectus
    b. Aspergillus flavus
    c. Aspergillus fumigatus
    d. Aspergillus terreus

4. Which of the following is true concerning cerebral amyloid angiopathy in the squirrel monkey?
    a. It results in neurodegenerative disease similar to Alzheimer's disease in humans.
    b. Veins are primarily affected.
    c. There are no viable tests for antemortem presence.
    d. Both meningeal and parenchymal vessels are affected.

5. Which of the following enzyme deficiencies results in MPS 1 in man and animals?
    a. B-glucuronidase
    b. arylsulfatase B
    c. Iduronate-2-sulfatase
    d. α-L-iduronidase

Please email your completed assessment for grading to Dr. Bruce Williams at bruce.h.williams12.civ@mail.mil. Passing score is 80%. This program (RACE program 33611) is approved by the AAVSB RACE to offer a total of 0.5 CE Credits, with a maximum of 12.5 CE Credits being available to any individual Veterinary Medical Professionals for the 2019-2020 Wednesday Slide Conference. This RACE approval is for the subject matter categories of: SCIENTIFIC using the delivery method of NON-INTERACTIVE DISTANCE. This approval is valid in jurisdictions which recognize AAVSB RACE.

Joint Pathology Center
Veterinary Pathology Services

WEDNESDAY SLIDE CONFERENCE 2019-2020

C o n f e r e n c e 19

19 February 2020

Conference Moderator:

Molly Church, VMD, Ph.D, DACVP
Assistant Professor, Pathobiology
University of Pennsylvania School of Veterinary Medicine
4005 MJR-VHUP
3900 Delancey Street
Philadelphia, PA, 19104

CASE I: 17041318 (JPC 4117490).

Signalment: 3-month-old, female, Aberdeen-Angus calf (*Bos taurus*)

History: Paraparesis and inability to stand with the hindlimbs were noted for 6 days. Clinical signs were not improved with penicillin treatments and progressed to lateral recumbency and hindlimb paralysis. Rigidity of the head and neck was noted. The calf had no deep pain and no patellar reflex in both hindlimbs, whereas deep pain was normal in the forelimbs. Cranial nerve responses were intact and normal. Omphalitis was present, and body temperature, pulse and respiratory rates were normal. The calf was euthanized and submitted for necropsy.

Gross Pathology: Multiple pale white streaks were seen on the epicardium. On cut surfaces of the heart, multiple irregular, pale white foci were observed in the myocardium, especially in the papillary muscle. Similar pale white streaks and irregular pale foci were noted in the skeletal muscles throughout the body, including the shoulders, brisket, quadriceps, and tongue.

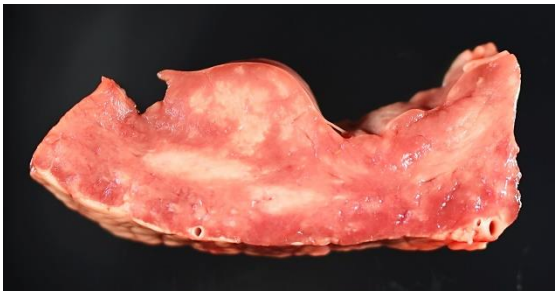

Heart, calf. The cut surface of the myocardium demonstrates numerous irregular pale white foci. (Photo courtesy of: Oklahoma State University, Department of Veterinary Pathobiology, College of Veterinary Medicine, 250 McElroy Hall, Stillwater, OK 74078, https://cvhs.okstate.edu/Veterinary_Pathobiology)

Spinal cord (left) heart (right), calf. In both tissues, there are coalescing areas of necrosis. (HE, 6X).

A large abscess was found at the base of the umbilicus. All lung lobes were wet and heavy and slightly reddened. An increased lobular pattern was noted in the cranioventral lung lobes.

The entire length of the spinal cord was sectioned and examined after fixation. A demarcated, regionally extensive, brown focus of malacia was found in the lumbar spinal cord. Other significant gross abnormalities were not observed in the rest of spinal cord segments or the brain.

Laboratory results: Hepatic vitamin E level and trace mineral analysis (including selenium) were all within normal limits. *Trueperella pyogenes* was recovered from the umbilical abscess.

Microscopic Description: Heart: Multifocal to confluent necrotic foci are randomly distributed in the myocardium. Cardiomyocyte degeneration and necrosis characterized by hypereosinophilia, fragmentation, pyknosis, karyorrhexis, and mineralization is widespread. Loss of cardiomyocytes and collapse of endomysium are accompanied by fibrosis and infiltrates of lymphocytes, macrophages, and few neutrophils. Small clusters (10-50 µm in diameter) of intracytoplasmic protozoal tachyzoites are commonly found in the cardiomyocytes and occasionally in Purkinje fibers at the periphery of necrotic foci or non-inflamed areas. Tachyzoites are basophilic, crescent-shaped, approximately 5 x 2 µm, with a prominent central nucleus. Spherical protozoal tissue cysts, measuring 10-20 µm in diameter are uncommonly seen containing a thin (< 1 µm), eosinophilic cyst wall and numerous tightly packed bradyzoites. Multiple Anichkov cells are observed within areas of necrosis and fibrosis.

Spinal cord: In the lumbar spinal cord, more than 70% of the parenchyma is obscured by regionally extensive necrosis and accompanying inflammatory infiltrates. Lesions center on the ventral sulcus and the gray matter, extending to the white matter, and are characterized by marked spongiosis, disruption and loss of neuropil, neuronal degeneration and loss, replaced by numerous foamy gitter cells, foci of gliosis, and scattered lymphocytes and plasma cells. Clusters of protozoal tachyzoites and tissue cysts are commonly identified within the neuropil (Figs. 3 & 5) and vascular endothelium (Fig. 4), and occasionally also found within glial cells and neurons. Multifocally, Virchow-Robin spaces and the leptomeninges are expanded by moderate numbers (2-5 layers) of lymphocytes and neutrophils. Endothelial cells are hypertrophic, and occasionally contain intracytoplasmic protozoal tachyzoites. Axonal degeneration with spheroids is prominent. The central canal is disrupted by inflammation and filled with proteinaceous fluid, neutrophils, lymphocytes, cellular debris and intralesional tachyzoites. The lining ependymal cells are attenuated or necrotic and lost.

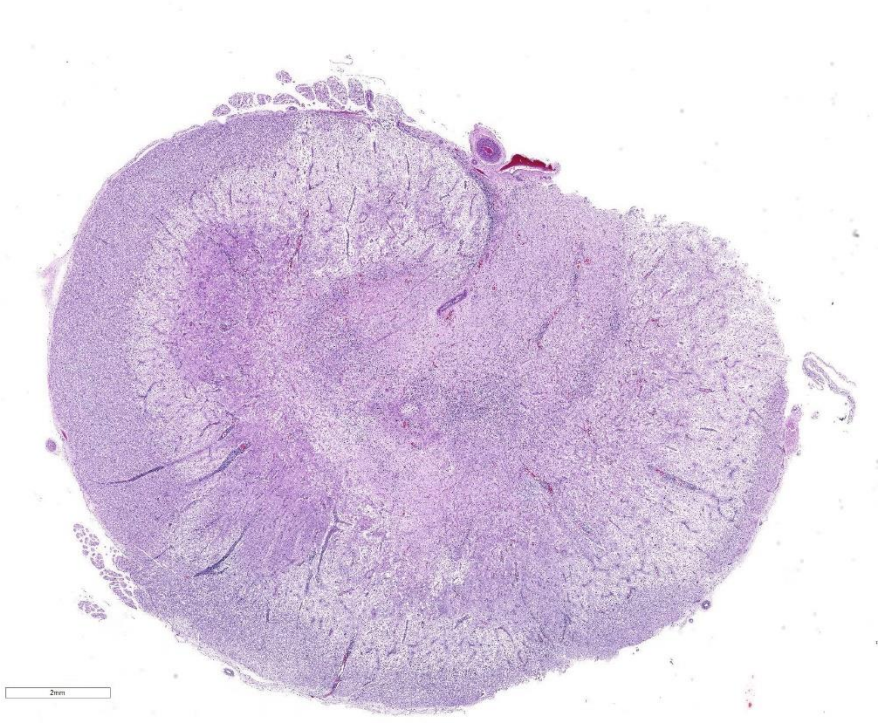

Spinal cord, calf. The degree of malacia within the spinal cord results in a lack of delineation between grey and white matter. (HE 10X)

Contributor's Morphologic Diagnosis:

Heart: Marked, chronic-active, multifocal to coalescing necrotizing myocarditis, lymphohistiocytic, with fibrosis, mineralization, abortive myocardial regeneration and intralesional protozoal tachyzoites and tissue cysts.

Lumbar spinal cord: Severe, subacute, multifocal and regionally extensive, necrotizing meningomyelitis, lymphohistiocytic and neutrophilic, with spongiosis, gliosis, perivascular cuffing, neuroaxonal degeneration and intralesional protozoal tachyzoites and tissue cysts.

Contributor's Comment: The microscopic findings are consistent with apicomplexan protozoal infection-associated myocarditis and meningomyelitis. The causative protozoans are confirmed as *Neospora caninum* by their characteristic ultrastructural features. Similar lesions and microorganisms were also identified in the skeletal muscles throughout the body, and to a lesser extent, in the brainstem and the cerebrum of this calf.

Neosporosis is a significant cause of abortion and stillbirth in both beef and dairy cattle worldwide.[1-5] The causative agent, *Neospora caninum*, is an apicomplexan protozoal parasite known as a major pathogen of cattle and dogs.[1-3] Abortion may occur from 3 months gestation to term with a peak at 5-6 months gestation in the affected cows.[2] Other than reproductive failure, *N. caninum* infection rarely causes clinical disease in adult cattle and calves.[1] However, occasionally, neurologic disease as a result of encephalomyelitis may occur in congenitally infected calves less than 4 months of age[2] and clinical signs such as ataxia, hyperextension of limbs, weakness and paralysis have been reported.[2,3,6,7,8]

Dogs and several wild canids are the definitive hosts of *N. caninum*, whereas cattle and other warm-blooded animals serve as intermediate hosts.[1,5] The pathogenesis of *N. caninum* infection in cattle is not fully understood. Both transplacental and

horizontal transmissions play an important role in bovine neosporosis.[1,6] Transplacental transmission occurs when tissue cysts are reactivated in the persistently infected cow (endogenous) or when the oocysts are ingested by the naïve cow (exogenous).[1,6] *N. caninum* is transmitted efficiently from the pregnant cows to their offspring during pregnancy, and the consequences of infection include abortion, birth of a weak calf occasionally with neurologic signs, or birth of a persistently infected but clinically healthy calf.[1,3] Abortion is believed to be a result of one or more of the following mechanisms: (1) primary parasite-induced placental damage; (2) fetal tissue damage due to parasite multiplication; (3) maternal immune expulsion of the fetus (Th1-type immunoresponse) due to *N. caninum* induced pro-inflammatory cytokines in the placenta.[1,3] Cow-to-cow transmission has not yet been proven.[1] The only demonstrated natural mode of postnatal infection in cattle is ingestion of sporulated *N. caninum* oocysts from the environment (e.g. contaminated canine feces).[9]

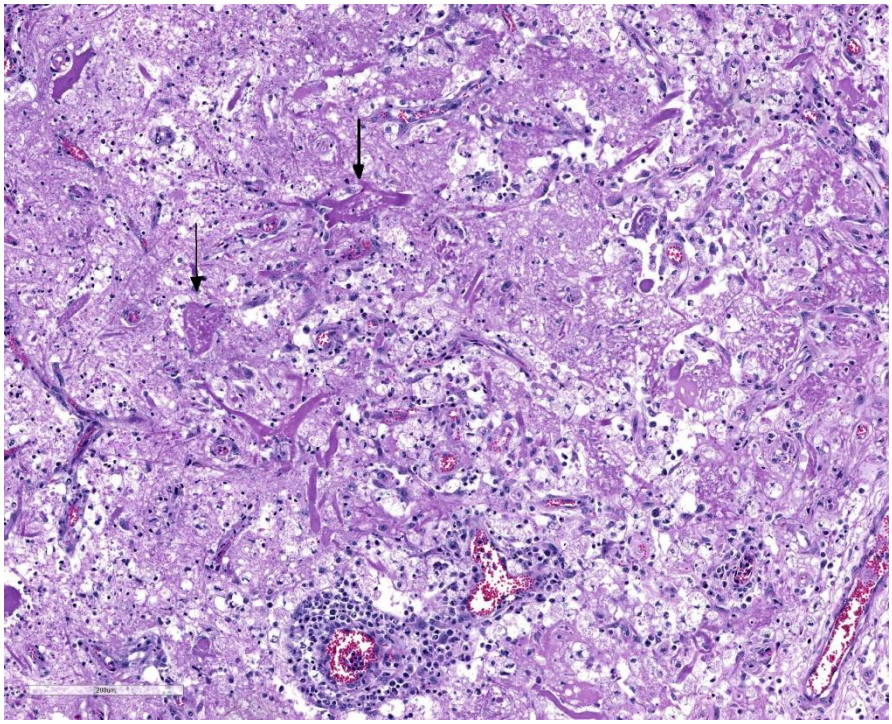

Spinal cord, calf. Within the malacic and edematous grey matter, there is ischemic necrosis of remaining neutrons. Vessels are often cuffed by multiple layers of neutrophils, macrophages, and lymphocytes. (HE 154X)

Neospora caninum is an intracellular protozoa and has three infectious stages, including sporozoites, tachyzoites and bradyzoites.[1] Sporozoites are present in oocysts that are shed in the feces of the definitive host. Tachyzoites and bradyzoites are found in the tissues of both intermediate and definitive hosts.[1-3] Tachyzoites are rapidly dividing forms, crescent-shaped, approximately 6 x 2 µm with a centrally placed nucleus. They may infect a variety of cells including neural cells, vascular endothelial cells, myocytes, hepatocytes, renal cells, alveolar macrophages and placental trophoblasts.[1] Bradyzoites are slowly replicating forms present within the tissue cysts. They are slender, approximately 6.5 x 1.5 µm with a terminally located nucleus and contain several Periodic Acid Schiff positive amylopectin granules.[1] Tissue cysts found in infected calves are usually smaller (<50 µm in diameter) with thinner (<2 µm thick) walls compared to those in dogs (up to 107 µm in diameter).[1]

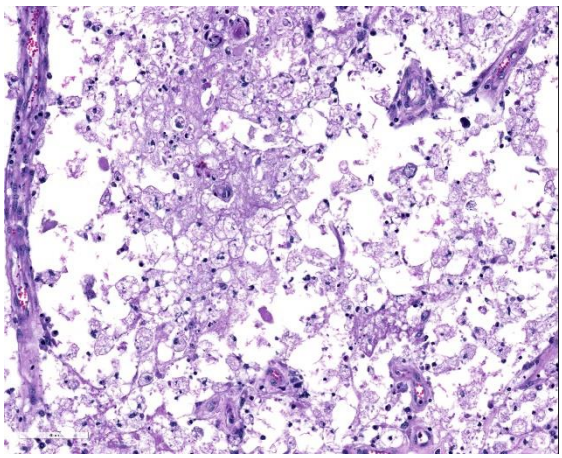

Spinal cord, calf. There are extensive areas of necrosis within deep white matter in all funiculi, with dilation and loss of myelin sheaths, enclosed nerve fibers, and replacement by numerous Gitter cells. (HE 273X)

In the current case, the lesions were most severe in the lumbar spinal cord, heart, and the skeletal muscles. Interestingly, the gross lesions somewhat resembled those of calves with vitamin E/selenium deficiency (white muscle disease), because of the widespread myonecrosis. However, neosporosis was confirmed on histopathology by demonstrating numerous *N. caninum* organisms. Minor lesions were also noted in the brainstem and cerebrum, characterized by foci of necrosis with gliosis, aggregates of mononuclear cells and prominent perivascular cuffing. Furthermore, the vitamin E and selenium levels were within normal limits in this calf.

Microscopically, abortifacient apicomplexan protozoans such as *N. caninum*, *Toxoplasma gondii*, and *Sarcocystis cruzi*, can be indistinguishable in HE stained sections.[2,5] *Toxoplasma gondii* is seen in rodents, dogs, cats, and human with CNS and reproductive diseases but it has not been proven to cause abortion in cattle.[2] A recent study documented that some species of *Sarcocystis*, specifically *S. cruzi*, can cause neurologic disease in calves and adult cattle.[10] However, it was suggested that if apicomplexan-like protozoans are seen in the brain tissue of aborted calves, they can be assumed to be *N. caninum*.[2]

Ultrastructurally, *N. caninum*, *T. gondii*, and *S. cruzi* have different morphologies that can be distinguished from each other.[2,11] *N. caninum* contains 8-12 electron-dense rhoptries and numerous micronemes cranial to the nucleus, whereas *T. gondii* contains few (4-8) spongy or honeycomb-like rhoptries, few micronemes, and many micropores.[11] Individual merozoites of *S. cruzi* are smaller (3-5 x 2-3 µm) compared to the others and they have numerous micronemes but lack rhoptries.[2,10]

Immunohistochemistry staining is a useful tool to identify *N. caninum* organisms on histopathology slides, but false positives due to cross reactions to *T. gondii* have been

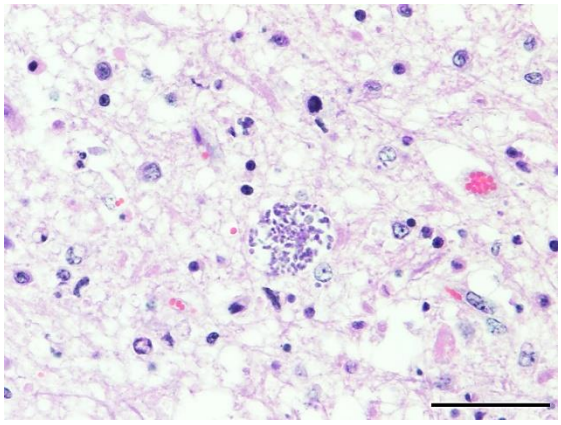

Spinal cord, calf. Tissue cysts containing numerous tachyzoites are present within cells within the neuropil. (HE 400X) (Photo courtesy of: Oklahoma State University, Department of Veterinary Pathobiology, College of Veterinary Medicine, 250 McElroy Hall, Stillwater, OK 74078, https://cvhs.okstate.edu/Veterinary_Pathobiology)

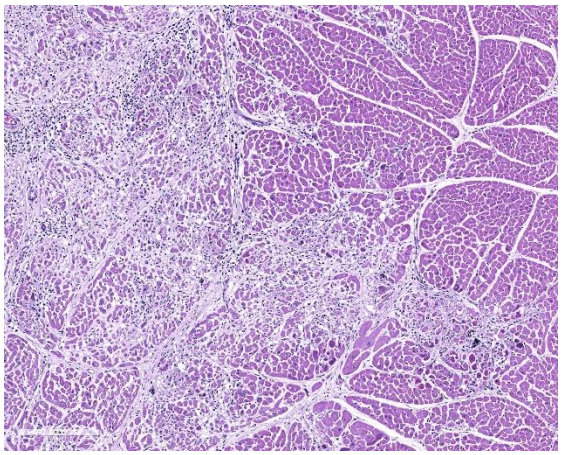

Heart, calf. The myocardium contains large, coalescing areas of necrosis and myofiber loss. (HE 128X)

reported in some studies.[2,12] PCR is another commonly used method for diagnosis and many PCR assays targeting different *N. caninum* genes have been published.[2,12] Serology is a practical tool to diagnose *N. caninum*-related abortions. It has an advantage of antemortem diagnosis of the disease and is commonly used as a screening test in herds.[2]

Contributing Institution:

Oklahoma State University
Department of Veterinary Pathobiology
College of Veterinary Medicine
250 McElroy Hall
Stillwater, OK 74078
https://cvhs.okstate.edu/Veterinary_Pathobiology

JPC Diagnosis: 1. Spinal cord, grey and white matter: Myelitis, necrotizing, multifocal to coalescing, severe with mild multifocal lymphohistiocytic and neutrophilic meningitis, and numerous intra- and extracellular apicomplexan zoites.

2. Heart: Myocarditis, necrotizing, subacute, multifocal to coalescing, marked, with occasional intracellular apicomplexan zoites.

JPC Comment: The contributor has provided an excellent review of *Neospora*, a common finding in bovine abortion in many parts of the US. The comment is so well-constructed, that our comment in turn will focus on some lesser known, but interesting "facts" about *Neospora* that are often overlooked in its review.

While not an author on the original Norwegian paper by Bjerkas et al. describing *Neospora* as an "unidentified cyst-forming sporozoon" causing encephalomyelitis and myositis in three consecutive litters of dogs, a PubMed search for both "Neospora" and "Dubey" brings up an amazing 277 titles.

In the last thirty years, *Neospora caninum* has appeared eleven times in the Wednesday Slide Conference, (and a twelfth submission

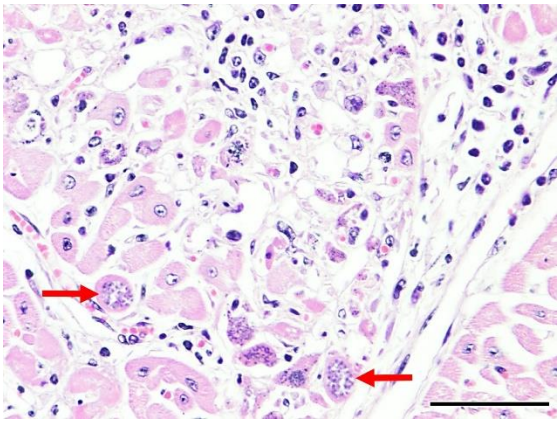

Heart, calf. Tissue cysts are present within cardiomyocytes as well. (HE 400X) (Photo courtesy of: Oklahoma State University, Department of Veterinary Pathobiology, College of Veterinary Medicine, 250 McElroy Hall, Stillwater, OK 74078, https://cvhs.okstate.edu/Veterinary_Pathobiology)

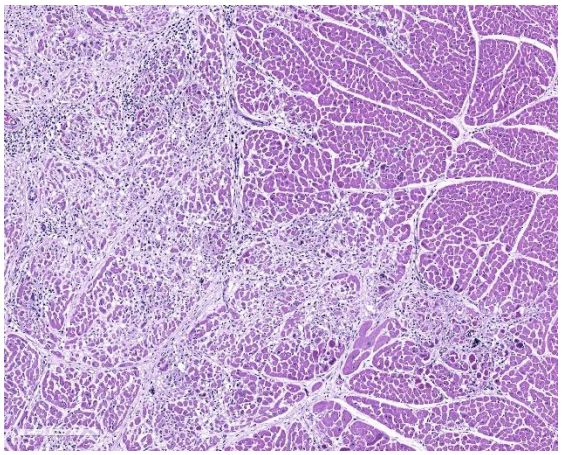

Heart, calf. The myocardium contains large, coalescing areas of necrosis and myofiber loss. (HE 128X)

was diagnosed as *Sarcocystis* by Dr. J.P. Dubey based on ultrastructural analysis and later, immunohistological confirmation). In the WSC, it has actually been submitted more often in the dog, from the brain (4), spinal cord (3), skin (2) and skeletal muscle (1). In the ox, this will be the second case in the spinal cord, and the first submission of the heart lesion; a previously presented case was diagnosed in the brainstem.

In addition to the very characteristic infections in intermediate hosts such as cattle and dogs (dogs also serve as the definitve host), it has also been found in aberrant hosts (usually singular cases) to include sheep, water buffalo, horses, goats, white-tailed deer, a raccoon, and a rhinoceros. Dr. Dubey stresses that simply finding DNA of *N. caninum*, or antibodies to the organism, is not synonymous with identiifying the viable apicomplexan parasite histologically. Serologic positivity to *N. caninum* has been well documented in humans, but disease has not.[13]

Dubey et al considers *N. caninum* to be one of the most "efficiently transplacentally transmitted parasites among all known microbes in cattle," with all calves in some herds being born infected but asymptomatic.[13] In some parts of the US, it is such a common cause of abortion in calves that, even in the absence of finding characteristic tissue cysts, the presence of glial nodules in the brain and areas of necrosis in the heart or liver is considered adequate proof of its etiology. Cow-to-cow (horizontal) transmission has not been established.[14] While previously identified in the CNS of adult horses, a recent publication documents the presents of *Neospora* tachyzoites in the lung, liver and heart of an equine abortus, suggesting that *N. caninum* should now be considered as an uncommon

Heart, calf. Electron micrography of the apicomplexan zoites demonstrates multiple rhoptries (arrow) and numerous micronemes (arrowhead). (Photo courtesy of: Oklahoma State University, Department of Veterinary Pathobiology, College of Veterinary Medicine, 250 McElroy Hall, Stillwater, OK 74078, https://cvhs.okstate.edu/Veterinary_Pathobiology)

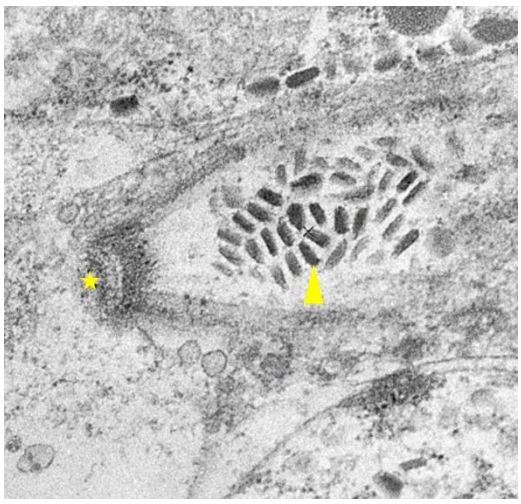

Heart, calf. Electron micrography of the apicomplexan zoites demonstrates a conoid ring (star) and numerous micronemes (arrowhead). (Photo courtesy of: Oklahoma State University, Department of Veterinary Pathobiology, College of Veterinary Medicine, 250 McElroy Hall, Stillwater, OK 74078, https://cvhs.okstate.edu/Veterinary_Pathobiology)

cause of equine abortion as well. [15]

References:

1. Dubey JP, Buxton D, Wouda W. Pathogenesis of bovine neosporosis. *J Comp Pathol*. 2006;134(4):267-289.

2. Dubey JP, Schares G. Diagnosis of bovine neosporosis. *Vet Parasitol*. 2006;140(1-2):1-34.

3. Innes EA, Wright S, Bartley P, et al. The host-parasite relationship in bovine neosporosis. *Vet Immunol Immunopathol*. 2005;108(1-2):29-36.

4. Helman RG, Stair EL, Lehenbauer TW, et al. Neosporal abortion in Oklahoma cattle with emphasis on the distribution of brain lesions in aborted fetuses. *J Vet Diagn Invest*. 1998;10(3):292-295.

5. Dubey JP, Schares G. Neosporosis in animals--the last five years. *Vet Parasitol*. 2011;180(1-2):90-108.

6. Marugan-Hernandez V. *Neospora caninum* and Bovine Neosporosis: Current Vaccine Research. *J Comp Pathol*. 2017;157(2-3):193-200.

7. Uesaka K, Koyama K, Horiuchi N, et al. A clinical case of neosporosis in a 4-week-o ld holstein friesian calf which developed hindlimb paresis postnatally. *J Vet Med Sci*. 2018;80(2):280-283.

8. De Meerschman F, Focant C, Detry J, et al. Clinical, pathological and diagnostic aspects of congenital neosporosis in a series of naturally infected calves. *Vet Rec*. 2005;157(4):115-118.

9. McCann CM, McAllister MM, Gondim LFP, et al. *Neospora caninum* in cattle: Experimental infection with oocysts can result in exogenous transplacental infection, but not endogenous transplacental infection in the subsequent pregnancy. *International Journal for Parasitology*. 2007;37(14):1631-1639.

10. Dubey JP, Calero-Bernal R, Verma SK, et al. Pathology, immunohistochemistry, and neurological sarcocystosis in cattle. *Vet Parasitol*. 2016;223:147-152.

11. Lindsay DS, Speer CA, Toivio-Kinnucan MA, et al. Use of infected cultured cells to compare ultrastructural features of *Neospora caninum* from dogs and *Toxoplasma gondii*. *Am J Vet Res*. 1993;54(1):103-106.

12. van Maanen C, Wouda W, Schares G, et al. An interlaboratory comparison of immunohistochemistry and PCR methods for detection of *Neospora caninum* in bovine

foetal tissues. *Vet Parasitol*. 2004;126(4):351-364.

13. Dubey JP, Schares G, Ortega-Mora LM. Epidemiology and control of neosporosis and Neospora caninum. *Clin Microbiol Rev* 2007; 20(2):323-367.

14. Dubey JP. Review of *Neospora caninum* and neosporosis in animals. *Korean J Parasit* 2003; 41(1):1-16.

15. Anderson JA, Alves DA, Cerquieira-Cezar CK, da Silva AF, Murata FHA, Norris JK, Howe DK, Dubey JP. Histologically, immunohistochemically, ultrastructurally, and molecularly confirmed neosporosis abortion in an aborted equine fetus. *Vet Parasit* 2019; 270:20-24.

CASE II: 18-0311 (JPC 4136399).

Signalment: 4-year-old male castrated mixed breed dog (*Canis familiaris*)

History: One year prior to euthanasia, the patient began exhibiting bruxism in periods of stress. This worsened to more frequent periods of anxiety and loud bruxism persisting for hours. Five months prior to euthanasia (seven months after onset of clinical signs), the patient became hyperreactive to stimuli around the face and head, showed unclassified ataxia and balance problems, and began to walk into objects. On presentation to the Neurology Service at the university, the patient had vestibular/cerebellar ataxia and an inconsistent menace response bilaterally. Fundic examination was normal. The MRI report stated that the cerebrum had widened cerebral sulci, a severely dilated ventricular system, and small basal nuclei, thalamus, and cerebellum with prominent folia. The patient's clinical signs continued to progress, and euthanasia was elected due to quality of life concerns.

Brain, dog. Multiple cross sections demonstrate marked atrophy of the cerebral and cerebellar cortex, with hydrocephalus ex vacuo. (Photo courtesy of: University of Pennsylvania School of Veterinary Medicine, Department of Pathobiology, http://www.vet.upenn.edu/research/academic-departments/)

Gross Pathology: The cerebral cortex was severely atrophied with widening of the sulci and secondary dilation of the lateral ventricles (hydrocephalus). The cerebellum appears slightly small. No additional abnormalities were detected on gross examination.

Laboratory results: None

Microscopic Description:

Sections of cerebellum or cerebellum with brainstem are submitted. The cerebellar cortex is mildly diffusely atrophied, with slight thinning and marked pallor of the cerebellar folia. Within the folia, there is marked loss of neurons within the granule cell layer, with fine vacuolation of the remaining parenchyma. Purkinje cells are irregularly spaced, with scattered necrosis and loss. Neurons and glial cells frequently contain abundant pale eosinophilic cytoplasmic storage material that has a globular or granular appearance. The material often peripheralizes the nucleus and variably distends the perikaryon. Affected neurons are degenerate, with cytoplasmic

Cerebellum, dog. The cerebellar folia (top and left) are markedly thin and hypocellular. The granular layer is indistinct. (HE, 8X)

swelling and central chromatolysis. The neuroparenchyma is mildly hypercellular, with increased numbers of glial cells, predominately microglia. Similar changes are detected in neurons throughout the entire central nervous system (cerebral cortex, cerebellum, brainstem nuclei, and spinal cord grey matter) and retina (slides not submitted).

Histochemical stains are applied to multiple sections of central nervous system tissue (see photomicrographs). The cytoplasmic storage material stains magenta with Periodic acid-Schiff (PAS) and is positive with Luxol fast blue.

Contributor's Morphologic Diagnosis:

Cerebellum: Severe chronic neuronal degeneration and loss with abundant intracytoplasmic storage material and cortical atrophy

Contributor's Comment: Although the recognition of intracellular storage material can be relatively straightforward, definitive identification of the material and subsequent categorization of the storage disease can pose a diagnostic challenge for veterinary pathologists. In this case, an extensive histologic survey of the major organs identified intracytoplasmic pigment only in the central nervous system (CNS) and retina, with the neurons most severely affected. The microscopic appearance, histochemical staining pattern, and cellular distribution of the pigment are most consistent with a type of neuronal ceroid lipofuscinosis (NCL), although definitive diagnosis requires electron microscopy and/or genetic testing.[3,6,13]

NCLs are neurodegenerative diseases characterized by the accumulation of lipopigment material within cells, always and most severely affecting neurons.[3] Like other lysosomal storage diseases, a mutation in a protein (typically an enzyme) critical to the metabolic pathway of digesting a material leads to accumulation of the now indigestible material in residual bodies, gradually leading to cell dysfunction and death.[6,20] More than 360 mutations in over a dozen genes have been identified as causes of these diseases in humans[8,20,21], dogs[1,2,9,10,13], sheep[22], pigs[4], horses[23], goats[7], and cattle[10]. NCL has been described in cats, although a genetic cause has not been identified in this species.[5] The vast majority of mutations are within genes coding for lysosomal enzymes, although endoplasmic reticulum and Golgi apparatus proteins have also been implicated.[13,15,16,20,21]

The accumulated ceroid-lipofuscin lipopigment in NCL is similar to both ceroid and lipofuscin but is not truly a variant of

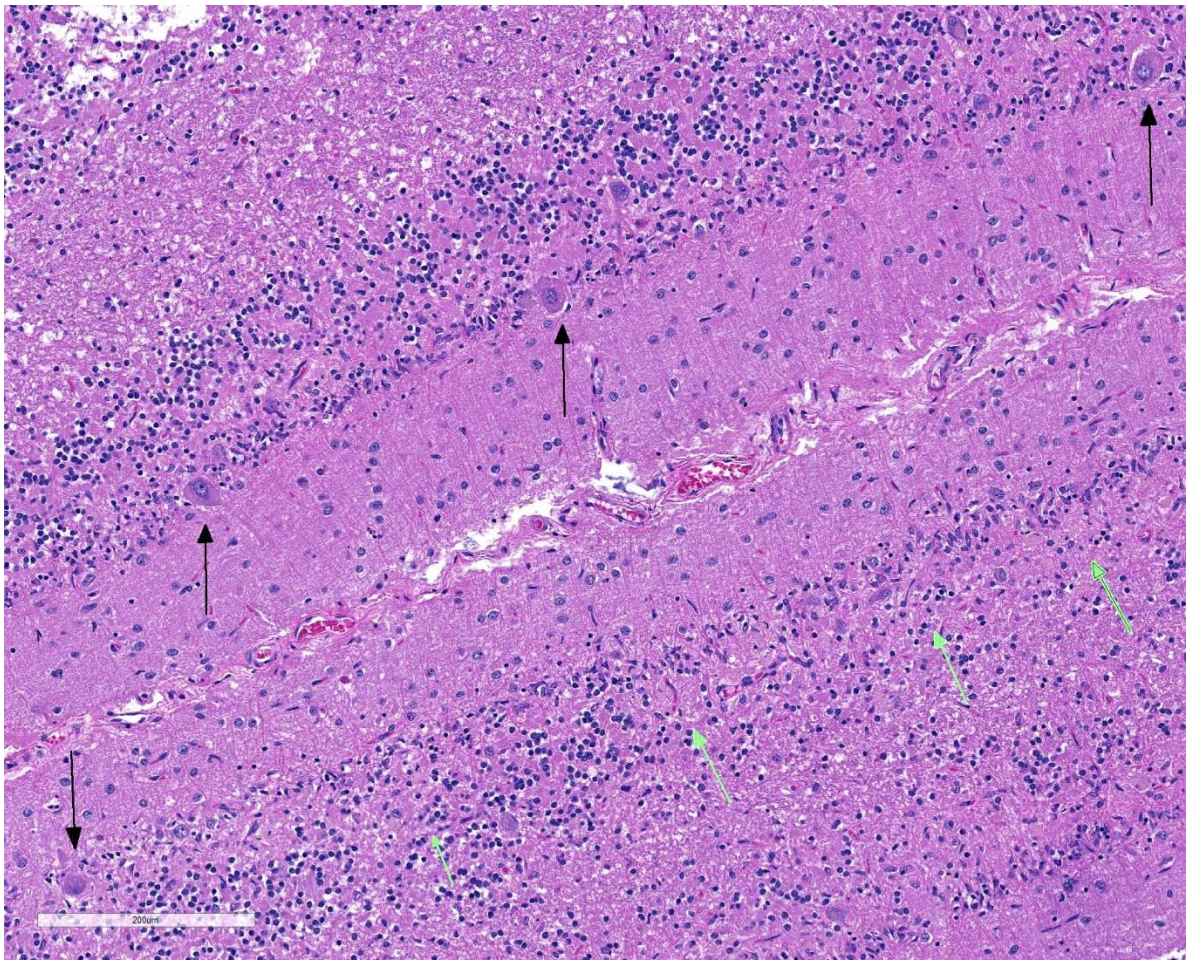

Cerebellum, dog. There is marked loss of Purkinje cells with a very prominent stretch of hypocellular granular layer without any overlying Purkinje cells at bottom right (green arrows) (HE, 163X)

either. Ceroid is a pigment that accumulates within cells due to a pathological process, such as a nutritional deficiency. Lipofuscin is also a pigment that accumulates within post-mitotic cells with age as a "wear-and-tear" material. The NCL lipopigment is composed primarily of protein with lesser lipid components.[13,15] The specific protein component is determined by mutation, but is typically derived from subunit C of mitochondrial ATP synthase[13], or less commonly from a sphingolipid activator protein.[18,20]

Ceroid-lipofuscin is yellow-gold to lightly eosinophilic on H&E staining. In cases of NCL, there are globular or botryoid accumulations within the axon hillock that displace the nucleus and Nissl substance. The material stains positively with PAS and Luxol fast blue stains and is variably acid-fast positive.[3] Ultrastructurally, the lipopigment has characteristic "curvilinear" or "fingerprint bodies" approximately 15 nm in diameter.[3,6,13,20] The material will autofluoresce under ultraviolet light, particularly in unstained paraffin-embedded tissue sections[13,15]

Neurons throughout the CNS are always affected, although the material may also accumulate in neurons of the peripheral nervous system neurons (e.g. in the intestinal plexi) as well as other cells in the CNS, including astrocytes, oligodendrocytes, and microglia. Later in

disease, cells in tissues outside of the nervous system may also accumulate storage material, including hepatic Kupffer cells and epithelial cells in the kidneys, pancreas, lungs, reproductive organs, skin, endocrine organs, salivary glands, etc.[13,16,20]

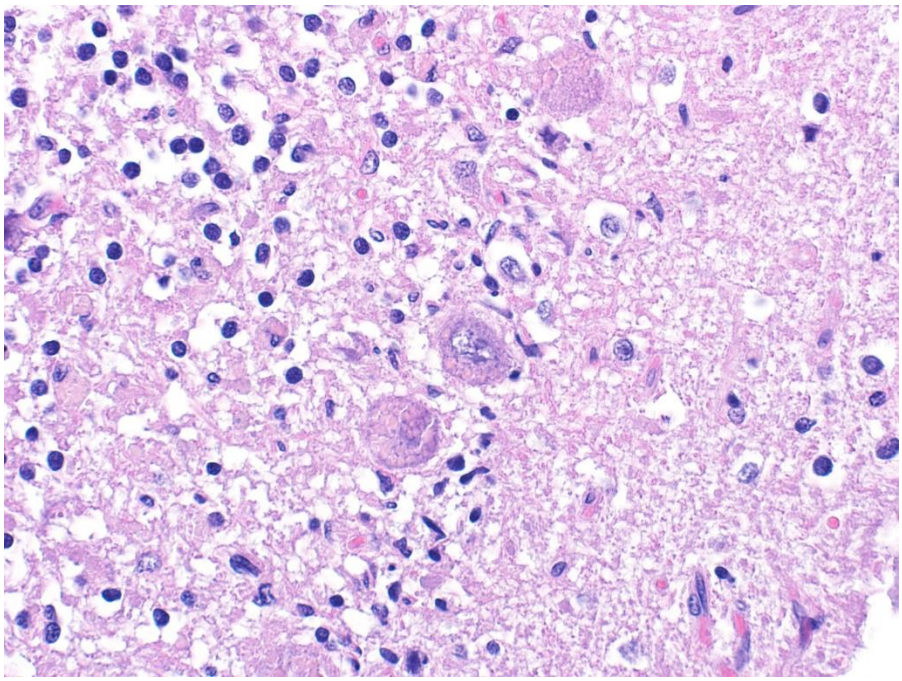

Cerebellum, dog. Remaining Purkinje cells contain numerous intracytoplasmic vacuoles containing a tan-pink granular material (ceroid). Glial cells/macrophages in the adjacent granular layer also contain similar material in their cytoplasm. (HE, 400X) (Photo courtesy of: University of Pennsylvania School of Veterinary Medicine, Department of Pathobiology, http://www.vet.upenn.edu/research/academic-departments/)

Affected individuals show progressive cognitive decline, visual and motor deficits, and seizures.[13,14] Age of onset can vary greatly, with most affected animals showing signs early in life, however there are late forms as well.[6,15] The disease is invariably fatal, with death occurring within months or up to a few years after clinical signs first present.[3,20]

Contributing Institution:

University of Pennsylvania
School of Veterinary Medicine
Department of Pathobiology
http://www.vet.upenn.edu/research/academic-departments/

JPC Diagnosis: Cerebellum: Neuronal degeneration, necrosis, and loss, diffuse, severe, with marked neuronal intracellular granular pigment accumulation, gliosis, and neuronophagia.

JPC Comment: The contributor has provided an excellent review of neuronal-ceroid lipofuscinosis in animals.

The disease was first described in humans by Dr. Otto Christian Stengel in Germany as a juvenile onset disorder resulting in blindness and progressive dementia. In 1902, English neurologist and pediatrician Frederick Eusace Batten described a similar disorder in two members of the same family, but was also the first to describe the neuropathology of cerebral and ocular macular degeneration, and it is from this investigator that the disease was called Batten's disease for many years (with that term now being restricted to certainly particular forms of the disease).[18]

Today, at least 14 affected genes have been implicated in NCL (neuronal ceroid-lipofuscinosis), which result in various manifestations that may appear in infants, toddlers, juveniles, and adult onset form. Eight of these 14 genes have been identified

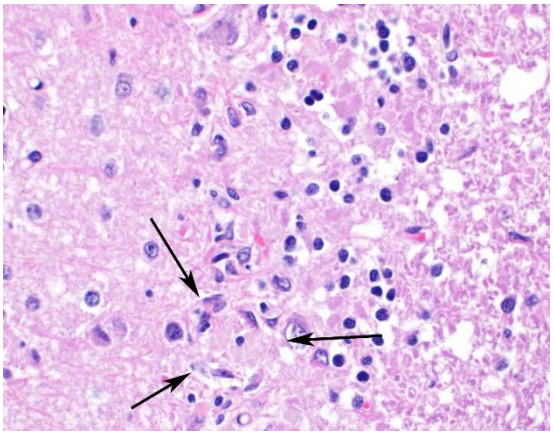

Cerebellum, dog. Within the Purkinje cell layer, there are neuronophagic nodules (arrows) populated by glial cells and macrophages containing abundant phagocytosed ceroid from effete Purkinje cells. (HE, 400X)

in canine CNL, as noted in Table 1, below.[12] A number of schemes are used in the classification of NCLs in humans, to include the historical schema, largely based on onset, a classification scheme based on abnormal genes and accumulated proteins, and one based on typical ultrastructural findings and abnormal enzymatic activities. A review of these classifications and a very good overall review of the disease in general in humans is available by Nita et al. below.[18]

Although there are a wide diversity of mutated genes, affected proteins, and manifestations, the NCLs are traditionally grouped together due to the common presence of autofluorescent pigment accumulation within neurons and other cells. Like many lysosomal storage diseases, many of the identified abnormal gene products in the variants of NCL accumulate in lysosomes, as do ceroid lipoportain pigments. While early attempts at classification assumed that the appearance of inclusions were specific for each variant, more recent investigation has shown that they are not specific for each disease, may vary with tissue examined, and the same NCL may include more than one pattern of inclusion.[18]

References:

1. Awano T, Katz ML, O'Brien DP, Sohar I, et al. A frame shift mutation in canine TPP1 (the ortholog of human CLN2) in a juvenile Dachshund with neuronal ceroid

Table 1
Summary of canine NCL-associated disease sequence variants.[a]

Disease	Gene	Sequence variant	Amino acid change	Affected dog breed
CLN1	*PPT1*	c.736_737insC	p.F246Lfs*29	Dachshund [20]
CLN1	*PPT1*	c.124 + 1G > A	Splice variant	Cane Corso [12]
CLN2	*TPP1*	c.325delC	p.A108Pfs*6	Dachshund [21]
CLN5	*CLN5*	c.619C > T	p.Q207X	Border Collie [19]
				Australian Cattle Dog [14]
				Mixed breed [5,18]
CLN5	*CLN5*	c.934_935delAG	p.E312Vfs*6	Golden Retriever [22]
CLN6	*CLN6*	c.829 T > C	p.W277R	Australian Shepherd [23]
CLN7	*MFSD8*	c.491 T > C	p.F282Lfs*13	Chinese Crested [13]
				Chihuahua [24,25]
CLN8	*CLN8*	c.491 T > C	p.L164P	English Setter [15]
CLN8	*CLN8*	c.585G > A	p.W195X	Australian Shepherd & Australian Cattle Dog [17]
				German Shorthaired Pointer[b]
CLN8	*CLN8*	g.30852988_30902901del	CLN8 absence	Alpenländische Dachsbracke [26]
CLN8	*CLN8*	c.349dupT	p.Glu117*	Saluki [6]
CLN10	*CTSD*	c.597G > A	p.M199I	American Bulldog [27]
CLN12	*ATP13A2*	c.1623delG	p.P541 fs*56	Tibetan Terrier [28]
CLN12	*ATP13A2*	c.1118C > T	p.Thr373Ile	Australian Cattle Dog [29]

[a] Updated from previous published list [5].
[b] This report.

(Reprinted from reference 12).

lipofuscinosis. Molec Genet Metab. 2006; 89: 254-260.
2. Awano T, Katz ML, O'Brien DP, Taylor JF, et al. A mutation in the cathepsin D gene (CTSD) in American bulldogs with neuronal ceroid lipofuscinosis. Molec Genet Metab. 2006; 87: 341-348.
3. Cantile C, Youssef, S. Nervous system. In: Maxie MG, ed. Jubb, Kennedy, and Palmer's Pathology of Domestic Animals. Vol 1. 6th ed. St. Louis, MO: Saunders Elsevier; 2016: 290-292.
4. Cesta MF, Mozzachio K, Little PB, Olby NJ, Sills RC, Brown TT. Neuronal ceroid lipofuscinosis in a Vietnamese pot-bellied pig (Sus scrofa). Vet Pathol. 2006;43(4):556-560.
5. Chalkley MD, Armien AG, Gilliam DH, Johnson GS, Zeng R, Wünschmann A, Kovi RC, Katz ML. Characterization of neuronal ceroid-lipofuscinosis in 3 cats. Vet Pathol. 2014;51(4):796-804.
6. Ferreira CR, Gahl WA. Lysosomal Storage Diseases. Translational Science of Rare Diseases. 2017; 2: 1–71.
7. Fiske RA, Storts RW. Neuronal ceroid-lipofuscinosis in Nubian goats. Vet Pathol. 1988; 25: 171-173.
8. Gao HL, Boustany RMN, Espinola JA, Cotman SL, et al. Mutations in a novel CLN6-encoded transmembrane protein cause variant neuronal ceroid lipofuscinosis in man and mouse. Am J Hum Genet. 2002; 70: 324-335.
9. Goebel HH, Bilzer T, Dahme E, Malkusch F. Morphological studies in canine (Dalmatian) neuronal ceroid-lipofuscinosis. Am J Med Genet Suppl. 1988; 5: 127-139.
10. Guo J, Johnson GS, Brown HA, Provencher ML. A CLN8 nonsense mutation in the whole genome sequence of a mixed breed dog with neuronal ceroid lipofuscinosis and Australian shepherd ancestry. Molec Genet Metab. 2014; 112: 302-309.
11. Guo J, Johnson GS, Cook J, Harris OK, Mhlanga-Mutangadura T, Schabel RD, Jensen CA, Katz ML. Neuronal ceroid lipofuscinosis in a German Shorthaired Pointer associated with a previously reported CLN8 nonsense variant. *Mol Gen Metabol Rep* 2019; 21. Htps://doi.org/10.1016/j.ymgm4.2019.100521.
12. Harper PAW, Walker KH, Healy PJ, Hartley WJ, et al. Neurovisceral ceroid-lipofuscinosis in blind Devon cattle. Acta Neuropathologica. 1988; 75: 632-636.
13. Jolly RD, Palmer DN, Studdert VP, Sutton RH, et al. Canine ceroid-lipofuscinoses: A review and classification. Journal of Small Animal Practice. 1994; 35: 299-306.
14. Katz ML, Narstrom K, Johnson GS, O'Brien DP. Assessment of retinal function and characterization of lysosomal storage body accumulation in the retinas and brains of Tibetan terriers with ceroid-lipofuscinosis. Am Jour Vet Research. 2005; 66:67-76.
15. Katz ML, Rustad E, Robinson GO, Whiting REH, Student JT, Coates JR, Narfstrom K. Canine neuronal ceroid lipofuscinoses: Promising models for preclinical testing of therapeutic interventions. Neurobiology of Disease. 2017; 108: 277-287.
16. Melville SA, Wilson CL, Chiang CS, Studdert VP. A mutation in canine CLN5 causes neuronal ceroid

lipofuscinosis in border collie dogs. Genomics. 2005; 86: 287-294.
17. Nakamoto Y, Yamato O, Uchida K, Nibe K. Neuronal Ceroid-Lipofuscinosis in longhaired chihuahuas: Clinical, pathologic, and MRI findings. J Am Anim Hosp Assoc. 2011; 47: E64-E70.
18. Nita DA, Mole SE, Minassian BA. Neuronal ceroid lipofuscinoses. *Epileptic Disord* 2016; 18(Supple 2):S73-S88.
19. Palmer DN, Tyynela J, vanMil HC, Westlake VJ, Jolly RD. Accumulation of sphingolipid activator proteins (SAPs) A and D in granular osmiophilic deposits in miniature schnauzer dogs with ceroid-lipofuscinosis. J Inherit Metab Dis. 1997; 20: 74-84.
20. Pastores GM, Maegawa GHB. Neuropathic Lysosomal Storage Disorders. Neurol Clin. 2013 November; 31(4): 1051–1071.
21. Sun, A. Lysosomal storage disease overview. Ann Transl Med 2018; 6(24):476.
22. Tammen I, Houweling PJ, Frugier T, Mitchell NL, et al. A missense mutation (c. 184C > T) in ovine CLN6 causes neuronal ceroid lipofuscinosis in Merino sheep whereas affected South Hampshire sheep have reduced levels of CLN6 mRNA. Biochim Biophys Acta. 2006;1762: 898-905.
23. Url A, Bauder B, Thalhammer J, Nowotny N, et al. Equine neuronal ceroid lipofuscinosis. Acta Neuropathologica. 2001; 101: 410-414.

CASE III: KSU VDL (JPC 4032559).

Signalment: 4-month-old female Hereford bovine calf.

History: The calf presented to the referring DVM with opisthotonus, head tilt, and ataxia. The calf was treated with tulathromycin (Draxxin) and dexamethasone for suspected otitis. Amprolium and sucralfate were given for 5 days for suspected nervous coccidiosis. The calf was presented to KSU teaching hospital a month later in sternal recumbency and was unable to stand. The physical examination revealed bilateral dorsolateral strabismus, variable nystagmus, and positive pupillary, menace, and palpebral reflexes with strong tongue tone. The ear exam was normal. There was no response to oxytetracycline, thiamine and dexamethasone. The calf was not eating or drinking and occasionally took few sips of water. The calf was euthanized.

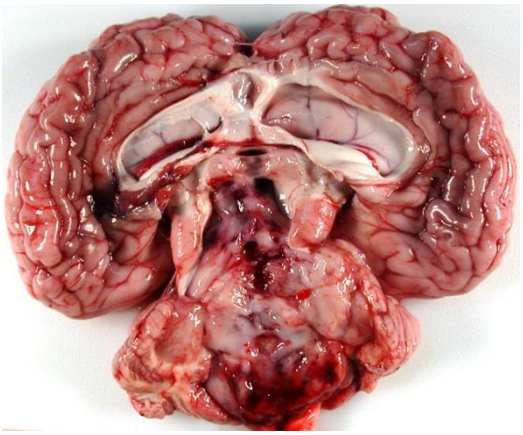

Cerebellum, calf. The fourth ventricle is replaced and expanded by a friable, pale white mass with multifocal hemorrhages. The mass extends into and occludes the mesencephalic aqueduct. Both lateral ventricles are markedly dilated. (Photo courtesy of: Department of Diagnostic Medicine and Pathobiology, Kansas State Veterinary College of Veterinary Medicine, 1800 Denison Avenue, Manhattan, KS 66506 http://www.vet.k-state.edu/depts/dmp/index.htm)

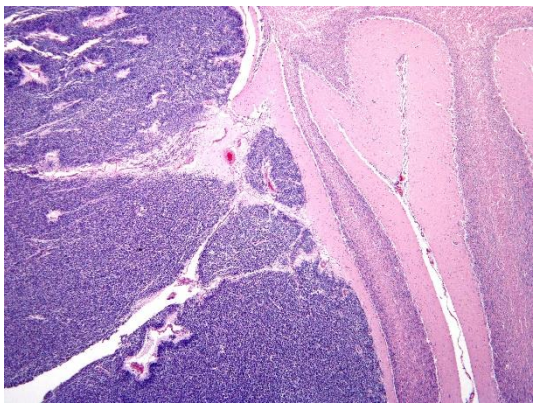

Cerebellum, calf. Subgross view of neoplastic cells compressing and peripherally invading the cerebellum. (Photo courtesy of: Department of Diagnostic Medicine and Pathobiology, Kansas State Veterinary College of Veterinary Medicine, 1800 Denison Avenue, Manhattan, KS 66506 http://www.vet.k-state.edu/depts/dmp/index.htm)

Gross Pathology: The calf was in good body condition. A soft, friable, gelatinous, pale white mass completely filled and expanded the fourth ventricle and compressed the cerebellar vermis and extended cranially and occluded the mesencephalic aqueduct. The lateral ventricles were markedly distended with cerebrospinal fluid that was pale yellow and cloudy. Multifocally, mild to moderate hemorrhages were present within the mass.

Laboratory results: None

Microscopic Description:

Brain: Expanding the fourth ventricle, compressing and superficially invading the brainstem and cerebellum is a moderately well-delineated, unencapsulated, highly cellular neoplasm composed of round to fusiform cells arranged in sheets supported by a scant fibrovascular stroma. Frequently, three to five cell-layer thick neoplastic cells also palisade around the capillaries (pseudorosettes). Occasionally, the cells palisade around a central fibrillar material (rosettes). The cells have scant eosinophilic cytoplasm and oval to elongate nuclei containing coarsely stippled chromatin and 1-4 nucleoli. There are 10 mitotic figures in ten 400X fields. The cells have variably distinct borders and there is mild anisocytosis and anisokaryosis. Within the neoplasm there are multifocal areas of necrosis, hemorrhage and a few lymphocytic infiltrates.

Histochemical stains are applied to multiple sections of central nervous system tissue (see photomicrographs). The cytoplasmic storage material stains magenta with Periodic acid-Schiff (PAS) and is positive with Luxol fast blue.

Contributor's Morphologic Diagnosis:

Brain, cerebellum and brainstem: Medulloblastoma with bilateral marked hydrocephalus of lateral ventricles.

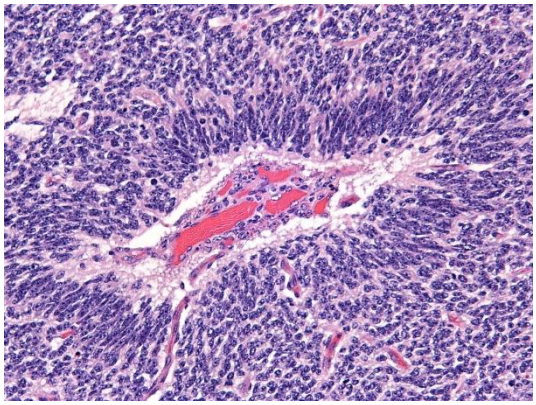

Cerebellum, calf. Neoplastic cells palisade around capillaries (pseudorosettes). (Photo courtesy of: Department of Diagnostic Medicine and Pathobiology, Kansas State Veterinary College of Veterinary Medicine, 1800 Denison Avenue, Manhattan, KS 66506 http://www.vet.k-state.edu/depts/dmp/index.htm)

Contributor's Comment:

Medulloblastoma is a malignant brain tumor that is thought to arise from an undifferentiated germ cells found below the pia mater during fetal and neonatal life.[2,11] The terminology medulloblastoma is exclusively used to indicate embryonal tumors arising in the cerebellum while similar neoplasms in other locations of the brain are called primitive neuroectodermal tumors (PNET).[2] In animals, it is reported in calves[5], young dogs[12], cats[7], baboons[1] and rats[9]. Medulloblastomas occur more frequently in children (80 %) and is the second most common malignant tumor in the central nervous system of children.[5]. In children, the neoplasm arises from the vermis and in adults it is located in cerebellar hemisphere. In humans, these neoplasms are seen more commonly in males but no such sex predisposition has been reported in animals.[2]

Medulloblastomas are malignant tumors that can invade into adjacent neuropil and disseminate via cerebrospinal fluid (CSF). Grossly, medulloblastomas are soft, friable, gray masses that arise from the cerebellum and expand the fourth ventricle. The neoplasm can obstruct the ventricles leading to obstructive hydrocephalus. Microscopically, the cells are round to polygonal, forming sheets or bands with scant cytoplasm and an elongated nucleus sometimes resembling a 'carrot'. Occasionally, the neoplastic cells can form Homer Wright and Flexner-Wintersteiner-like rosettes.[2,8]

There is variability in the immunohisto-chemical staining characteristics of cells

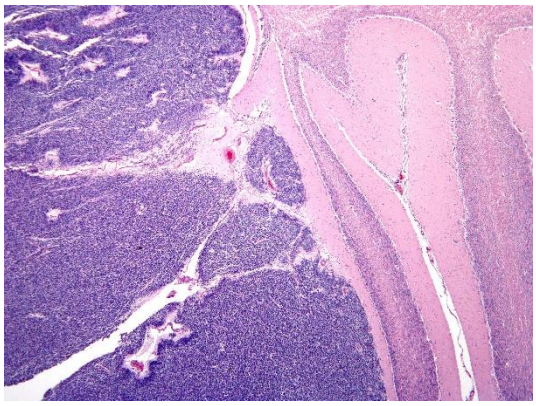

Cerebellum, calf. Neoplastic cells surrounding a central fibrillar material (Homer Wright rosettes). (Photo courtesy of: Department of Diagnostic Medicine and Pathobiology, Kansas State Veterinary College of Veterinary Medicine, 1800 Denison Avenue, Manhattan, KS 66506 http://www.vet.k-state.edu/depts/dmp/index.htm)

owing to the stages of differentiation. In one study of canine medulloblastoma, primitive neuroepithelium stained for vimentin and S-100; differentiated neurons stained for neuron specific enolase (NSE) and synaptophysin; differentiated astrocytes labeled positive for glial fibrillary acidic protein (GFAP), vimentin, NSE, and neurofilament.[12] In addition, the telomerase activity and c-kit expression were recently reported in canine medulloblastomas.[9]

Immunohistochemistry was performed in the current case for NSE, synaptophysin, GFAP, vimentin, cytokeratin, and S-100. The neoplastic cells were immunopositive for vimentin and S-100 and negative for GFAP, NSE, synaptophysin and cytokeratin, suggesting that the neoplastic cells are undifferentiated. Differentiation along neuronal and glial lineage is less common in animals than in humans.[2]

Contributing Institution:

Department of Diagnostic Medicine and Pathobiology
Kansas State Veterinary College of Veterinary Medicine
1800 Denison Avenue
Manhattan, KS 66506
http://www.vet.k-state.edu/depts/dmp/index.htm

JPC Diagnosis: Cerebellum: Primitive neuroectodermal tumor (medulloblastoma).

JPC Comment: Medulloblastoma is a form of primitive neuroepithelial tumor that likely arises from the external germinal cell zone, which lies directly beneath the meninges in the developing cerebellum.[6] Normally, during fetal development, cerebellar granular cells develop in the external germinal zone then migrate past Purkinje cells to form the granule cell layer.

Activation of the hedgehog pathway has been shown not only to regulate normal growth, but is also involved in the tumorigenesis of several neoplasms, including medulloblastomas.[4] More specifically, the Patched gene (*Ptc*) controls growth and pattern formation in early neural development and the adult cerebellum.[3] *Ptc* gene encodes a Sonic hedgehog (*Shh*) receptor and a tumor suppressor protein. While many subtle aspects of signaling have not been completely elucidated, it is clear that a complex interaction between *Shh* and *Ptc* is required for normal development. Shh binds to Ptc, activates smoothened (*Smo*) which leads to over expression of *Gli-1* and some *Wnt* and *TGF-ß* gene families.[3,4] (Hedgehog effectors *Gli-1* and *BclII* have also been shown to be overexpressed in medulloblastomas).[3] *Ptc*-knockout mice (which allow for unregulated expression of *Shh* target genes have a high incidence of PNET formation – eight percent of *Ptc*-heterozyogous mice develop tumors as early as 5 weeks.[6] Tumor incidence increases with age in *Ptc*-heterozygous mice with an incidence of about 30% at six months of age.[6] In humans, *Ptc* mutation has been associated with basal cell carcinoma, fibroma, medulloblastoma and rhabdomyosarcoma.[4]

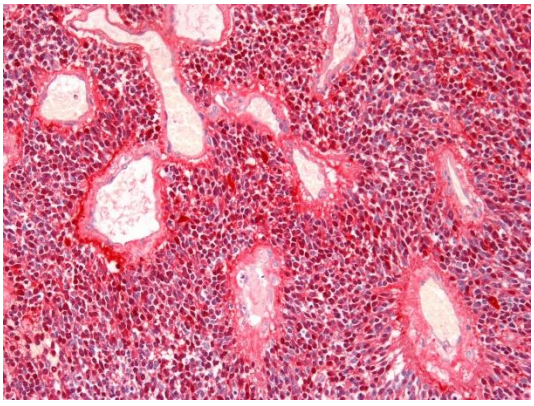

Cerebellum, calf. Neoplastic cells are immunopositive for S-100. (Photo courtesy of: Department of Diagnostic Medicine and Pathobiology, Kansas State Veterinary College of Veterinary Medicine, 1800 Denison Avenue, Manhattan, KS 66506 http://www.vet.k-state.edu/depts/dmp/index.htm)

References:

1. Berthe J, Barneon G, Richer G, Mazue G. Medulloblastoma in a baboon (*Paio paio*). *Lab Anim Sci.* 1980; 30: 703-705.

2. Cummings J, de Lahunta A. *Veterinary Neuropathology,* Mosby, St. Louis, MO, 1995; 378-379.

3. Goodrich LV, Milenković L, Higgins KM, Scott MP: Altered neural cell fates and medulloblastoma in mouse patched mutants. Science 277:1109-1113, 1997

4. Hahn H, Wojnowski L, Specht K, Kappler R, Calzada-Wack J, Potter D, Zimmer A, Müller U, Samson E,

Quintanilla-Martinez L, Zimmer A: Patched target Igf2 is indispensable for the formation of medulloblastoma and rhabdomyosarcoma. J Biol Chem 275:28341-28344, 2000

5. Jolly RD, Alley MR. Medulloblastoma in calves: A report of three cases. *Vet Pathol.* 1969; 6: 463-468.

6. Kim JYH, Nelson AL, Algon SA, Graves O, Sturla LM, Goumnerova LC, Rowitch DH, Segal RA, Pomeroy SL: Medulloblastoma tumorigenesis diverges from cerebellar granule cell differentiation in patched heterozygous mice. Developmental Biology 263:50-66, 2003

7. Kitagawa H, Koie, Kanayama K, Sakail T. Medulloblastoma in a cat: clinical and MRI findings. *J Small Anim Pract.* 2003; 44: 139-142

8. Koestner A, Bilzer T, Schulman F, Summers B, Van Winkle T: Histological classification of tumors of the nervous system of domestic animals. *In: World Health Organization, International Histological Classification of Tumors of Domestic Animals, ed.* Armed Institute of Pathology, Washington, DC, 1999; 25-25

9. Krinke G, Kuafmann W, Mahrous A, Schaetti, P. Morphologic characterization of spontaneous nervous system tumors in mice and rats. *Toxicol Pathol.* 2000; 28: 178-192

10. Madrioli L, Biserni R, Panarese S, Morini M, Gandini G, Bettini G. Immunohistochemical profiling and telomerase activity of a canine medulloblastoma. *Vet Pathol.* 2011; 48: 814-816

11. Maxie M G, Youssef S: The nervous system. In: Jubb, Kennedy, and Palmer's Pathology of domestic animals. Vol. 1. 5th ed., Elsevier, Edinburg, 2007; 450-451

12. Steinberg H, Galbreath EJ. Cerebellar medulloblastoma with multiple differentiations in a dog. *Vet Pathol.* 2005; 35:543-546.

CASE IV. WSC 1920 Conf 19 Case 4 (JPC 4033564).

Signalment: 16-year-old, female spayed Maine coon cat (*Felis catus*)

History: The cat originally presented for an acute episode of collapse, left hemiparesis, and increased respiratory rate and respiratory effort. Neurological examination revealed anisocoria, a left head turn, and ambulatory left hemiparesis with proprioceptive deficits in the left fore and

Spinal cord, cat. Four large red raised nodules are present on the ventral aspect of the spinal cord from C3-C5. (Photo courtesy of: Animal Medical Center, 510 East 62nd St. New York, NY 10065, http://www.amcny.org/)

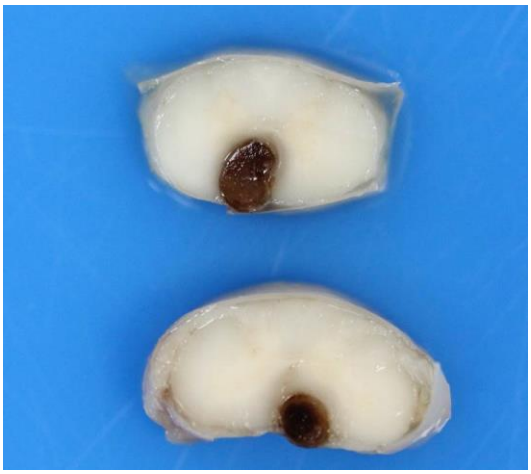

Spinal cord, cat. Cross section of one of the nodules demonstrating its extension and compression of the ventral funiculi. (Photo courtesy of: Animal Medical Center, 510 East 62nd St. New York, NY 10065, http://www.amcny.org/)

hind limbs. The neuroanatomical localization was multifocal with suspicion for C1-C5 myelopathy. Hematology and serum biochemistry profile were unremarkable, with the exception of a moderately elevated creatine kinase (1024 IU/L, RI: 64-440 IU/L). Thoracic radiographs revealed a patchy interstitial lung pattern presumed secondary to parenchymal disease. MR imaging of the brain and cervical spinal cord revealed an ill-defined hyperintensity in the left ventrolateral portion of the spinal cord at the cranial aspect of the C3. No intracranial abnormalities were detected, and an incidental unilateral otitis media was observed. Cisternal CSF analysis revealed moderately increased protein (184 mg/dL) and a moderately increased nucleated cell count with a mixed cell pleocytosis (150 nucleated cells/uL, 52% small mononuclear cells/mature lymphocytes, 27% nondegenerative neutrophils and 21% large monocytoid mononuclear cells with scattered erythrocytes and rare erythrophagia). A vascular event was the most likely differential, but infectious etiologies could not be completely ruled-out. Titers for *Cryptococcus* and *Toxoplasma* were declined by the owner. The following day the cat's neurological examination and ability to ambulate had already improved. The cat was discharged with antibiotics and instructions to recheck with the neurology service and consult with the cardiology department. Serial neurological examinations revealed mild persistent paraparesis.

Eighteen months later the cat represented in congestive heart failure with a history of chronic progressive paraparesis. The owner elected euthanasia.

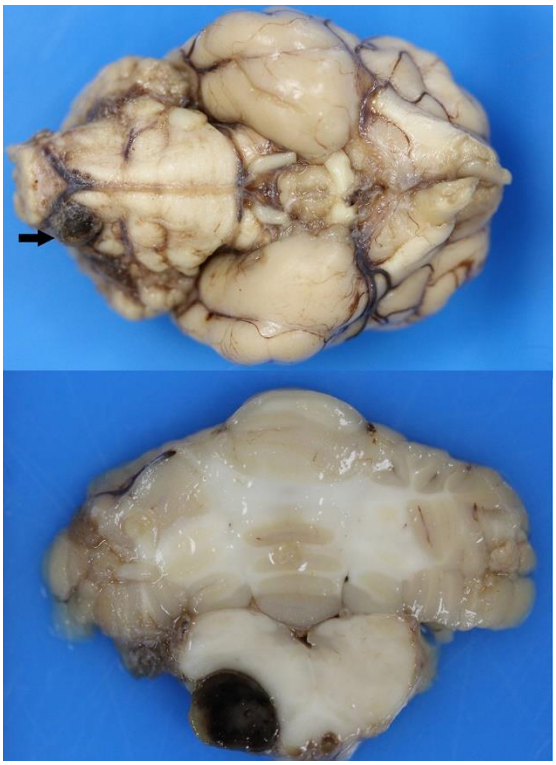

Spinal cord, cat. A similar blood-filled nodule is present arising from the basilar artery at the ventral lateral aspect of the medulla. (Photo courtesy of: Animal Medical Center, 510 East 62nd St. New York, NY 10065, http://www.amcny.org/)

Gross Pathology: Macroscopic examination of the spinal cord revealed four large, multifocal, dark red, raised nodules (presumed telangiectasia) at the ventral aspect of the mid body of C3-C4 and C4-C5, involving the cervical intumescence. These foci ranged from 3 x 2 mm to 1 mm in diameter. An additional, similar, small, dark red focus at ventral midline of the distal thoracic spinal cord measured approximately 1 mm in diameter, and three dark red, slightly raised, nodules were present on the ventral aspect of the lumbar spinal cord at L3 and L4, the largest measuring 5 x 2.5 mm (Figure 1B). When the nodules were sectioned, they were found to be homogenously dark red, and extended into the spinal cord parenchyma, at least 2.5 mm into the cervical segments (Figure 2), and 3 mm into the lumbar segments. In the brain, a large, well-demarcated, dark red, homogeneous, firm, round mass at the ventral lateral aspect of the medulla measured 6 x 5 x 7 mm and was adjacent to a branch of the basilar artery (arrow, Figure 3). When sectioned, the mass was well-demarcated, homogeneously dark red, and compressed the adjacent medullary parenchyma (Figure 3). A nodule in the left thyroid gland was observed, and the heart was moderately enlarged with dilation of the left atrium and auricle. There was no evidence of thromboembolism in the caudal aorta or iliac arteries.

Laboratory results: Serum biochemistry profile revealed a mildly elevated T4 concentration (5.0 ug/dL, (RI: 0.8-4.7 ug/dL) and mild azotemia (BUN 51 mg/dL, RI: 14-36 mg/dL; creatinine 2.0 mg/dL, RI: 0.6-2.4 mg/dL).

Microscopic Description:

Microscopic evaluation of the spinal cord revealed severe aneurysmal dilation of the ventral spinal artery at C3-4, C4-5 (Figure 4), L3 and L4. The tunica intima and media of the dilated vessels were thickened by deposition of hyaline, acellular eosinophilic material (hyalinosis, Figure 5) and occasionally, increased populations of spindle cells. In regions of most severe arterial dilation, the arterial wall was attenuated. Luminal thrombi were present within the affected arteries, with foci of re-canalization. Intramural arterial and periarterial hemorrhage was observed, with periarterial hemosiderin- and hematoidin-containing macrophages (Figure 6), sometimes intermixed with lymphocytes and plasma cells. These severely dilated vessels compressed the adjacent parenchyma. The ventral funiculi of the cervical and lumbar spinal cord exhibited variable amounts of white matter myelin vacuolation, with swollen, eosinophilic axons (spheroids), rare myelomacrophages, increased populations of glial cells, including microglia with rod morphology and reactive astrocytes, few Gitter cells, hemorrhage, and accumulation of eosinophilic material (possible edema). Within the ventral grey matter of the lumbar section, there was mild hemorrhage. Few corpora amylacea and Rosenthal fibers were present, most notably in the section of lumbar spinal cord. Occasional aggregates of eosinophilic material were observed in spinal nerves. A focus of hemorrhage intermixed with few hemosiderin containing macrophages was adhered to the dura in a section of cervical spinal cord. In regions of vascular hyalinosis, Congo Red stains were

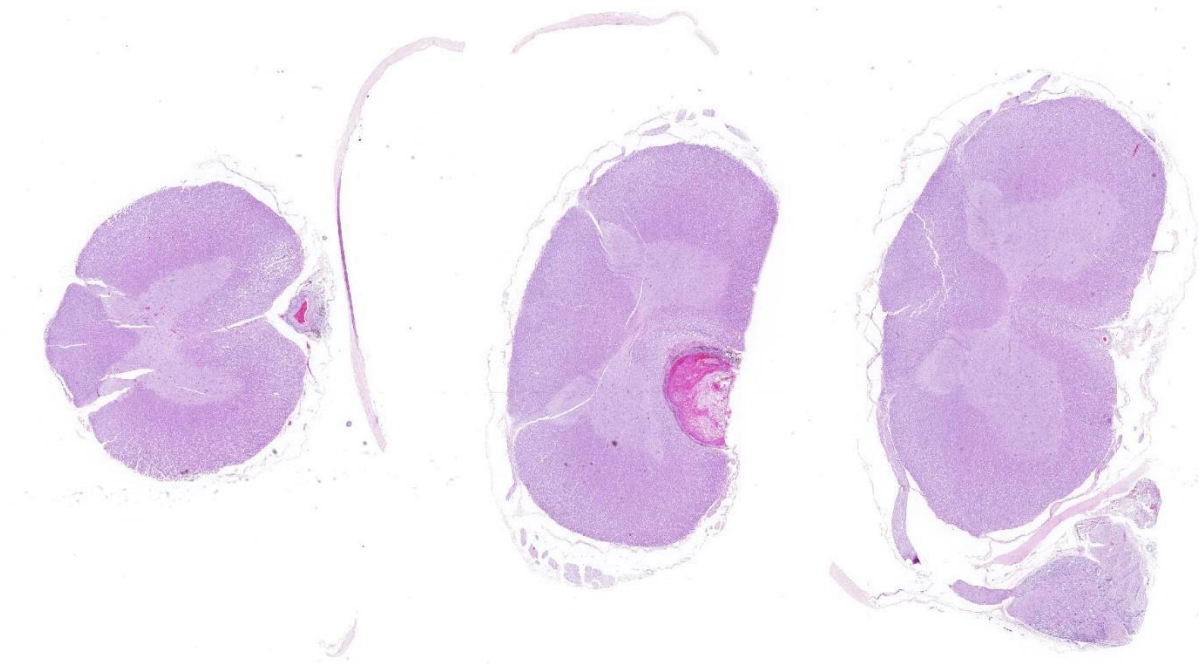

Spinal cord, cat. Three sections of cervical spinal cord are submitted, with thrombosis and marked dilation of the middle spinal artery present in the section in the middle. On the section at the left, the artery is patent, but the wall is markedly thickened. (HE, 8X)

negative for amyloid, and hyaline material stained magenta with Periodic acid Schiff (PAS) stains (Figure 7).

Histologic evaluation of the medullary mass in the brain (not included) revealed a severely dilated, thrombosed artery, adjacent to a lateral branch of the basilar artery (presumed to represent a communicating branch), with compression of the surrounding brain parenchyma and midline shift at the level of the olivary nucleus and deep arcuate fibers. Vessels were attenuated or the tunica intima and media were thickened by deposition of hyaline, acellular eosinophilic material (hyalinosis) and less frequently, spindle cell populations, with thrombosis, mural hemorrhage, periarteriolar hemosiderin-containing macrophages and lymphocytes. Congo red stains were negative for amyloid in regions of arterial hyalinosis. The regional white matter exhibited myelin vacuolation, spheroid formation and necrosis, characterized by white matter rarefaction and Gitter cell infiltration, with rare neuronal chromatolysis and necrosis.

Contributor's Morphologic Diagnosis:

Spinal cord (cervical and lumbar segments): Severe, focal to multifocal ventral spinal hyaline arteriopathy (arteriolosclerosis) with severe dilation, thrombosis, intramural and periarteriolar hemorrhage and hemosiderosis

Spinal cord (cervical and lumbar segments): Severe, ventromedial white matter vacuolation with spheroid formation, gliosis, edema and hemorrhage

Contributor's Comment: The ventral spinal artery was severely dilated,

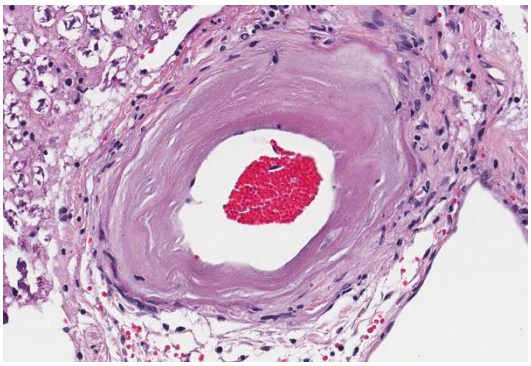

Spinal cord, cat. The tunica media of affected vessels contains a patchy deposition of hyaline eosinophilic protein, collagen and the adventitia contains circumferential lamellar collagen and fibrocytes. (HE, 100X) (Photo courtesy of: Animal Medical Center, 510 East 62nd St. New York, NY 10065, http://www.amcny.org/)

thrombosed, and thickened by deposition of hyaline material, resulting in grossly visible lesions. Damage to the spinal cord was interpreted to be multifactorial, caused by both ischemic and compressive damage. Arteriosclerosis literally translates to "hardening of the arteries" and in veterinary medicine, encompasses arteriolosclerosis and atherosclerosis. In humans, arteriosclerosis includes the two aforementioned categories as well as Monckeberg medial calcific sclerosis.[3] These lesions all result in stiffening and thickening of the arterial wall.[3]

Arteriolosclerosis is defined as a lesion of arterioles, which are small arterial vessels with 1 or 2 layers of smooth muscle cells.[3] Arteriolosclerosis includes hyaline and hyperplastic lesions.[1,,3,8] In humans, arteriolar hyalinosis occurs with benign hypertension and is associated with impaired autoregulation, hypothesized to be caused by hemodynamic injury with leakage of plasma components into the vessel wall.[1,9] This lesion can also be seen with aging, diabetes mellitus, and focal segmental glomerulosclerosis (FSGS).[9] Hyperplastic arteriolosclerosis in people is more commonly linked to malignant hypertension, the histologic changes of which includes thickening of the arteriolar wall by concentric layers of hyperplastic smooth muscle cells. Recommendations have been made to term the hyaline subtype as intimal hyalinosis and hyperplastic arteriolosclerosis as fibromuscular intimal thickening.[3]

Hypertension has been linked to arteriolosclerosis in cats, reported in association with chronic renal disease, hyperthyroidism, primary hyperaldosteronism, and chronic anemia.[4,6,7] Between 65 and 100% of cats with systemic hypertension and concurrent hypertensive ocular lesions have evidence of reduced renal function.[4] However, this relationship is complex, and it cannot always be determined whether systemic hypertension is a cause or consequence of renal damage.[4] Systemic hypertension may be less prevalent in the hyperthyroid feline population than previously thought (reported ranges from 9-23%), and approximately 20% will develop hypertension following treatment, although not all will be azotemic.[4] Feline target organs that can incur damage secondary to hypertension include the eye, kidney, central nervous system and cardiovascular system.[4,6] The effects of hypertension on the eyes and heart have been described in cats.[4,6,7] Hypertensive encephalopathy in the

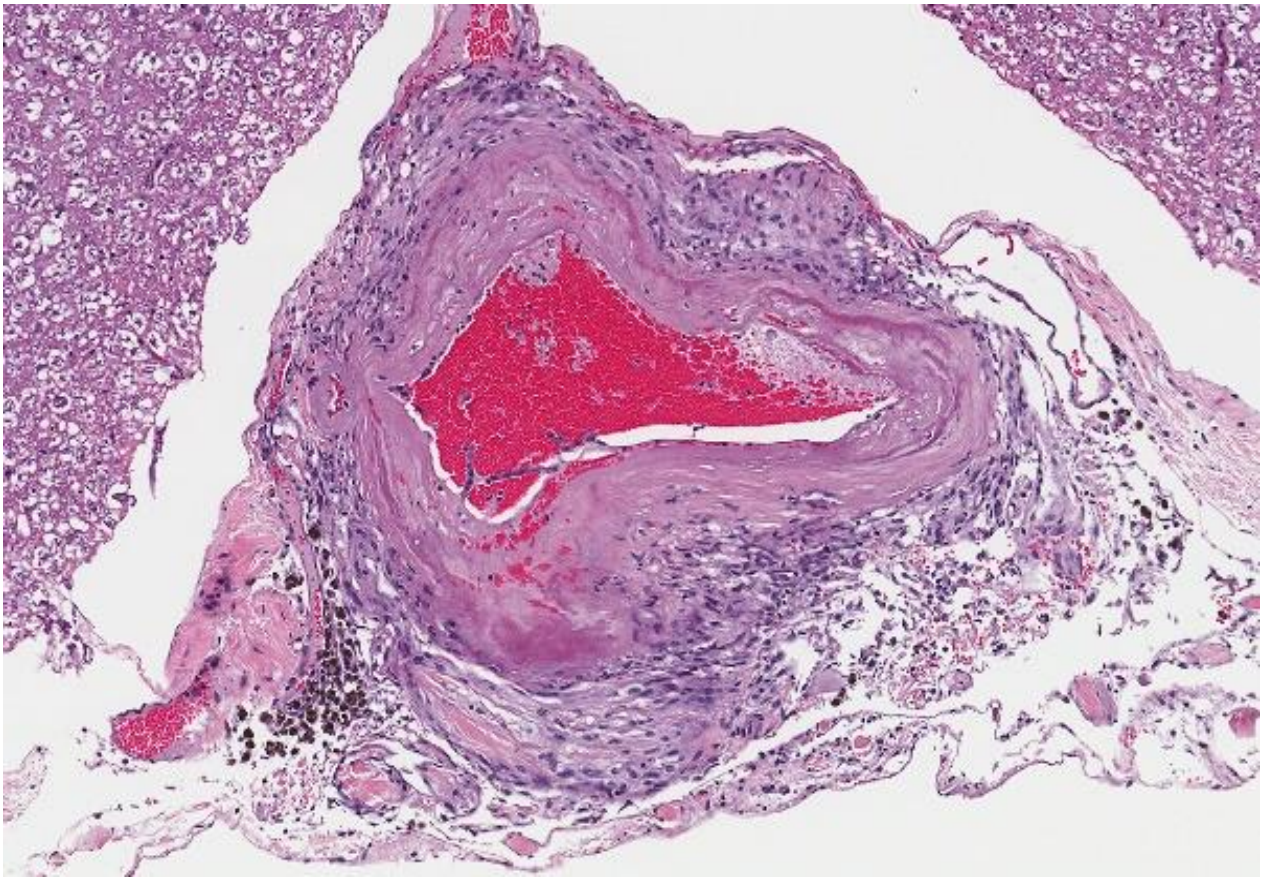

Spinal cord, cat. The tunica media of affected vessels contains a patchy deposition of hyaline eosinophilic protein, collagen and the adventitia contains circumferential lamellar collagen and fibrocytes. (HE, 100X) (Photo courtesy of: Animal Medical Center, 510 East 62nd St. New York, NY 10065, http://www.amcny.org/)

cat typically occurs following a precipitous and sustained rise in blood pressure that exceeds the limits of cerebral arterial autoregulation.[1]

Experimentally induced hypertensive encephalopathy in 2 cats was described.[1] Macroscopic abnormalities included cerebellar herniation, external hemorrhages and widening and flattening of the cerebral gyri (edema). Histologic evaluation revealed severe pallor and rarefaction of the cerebral white matter with regional widening of periarteriolar spaces and accumulation of PAS positive protein droplets. Vascular lesions were described as arteriolar hyalinosis and hyperplastic arteriolosclerosis of pial arterioles. Rare ischemic changes and microhemorrhages were also found within the brain.[1] The pathogenesis is thought to involve autoregulatory failure of cerebral arterial blood flow during elevations of blood pressure. Forced vessel overdistension leads to blood brain barrier breakdown, opening of endothelial tight junctions and leakage of plasma proteins into the extracellular space and formation of vasogenic edema. Vascular dilation often starts segmentally, but can become diffuse, leading to generalized, interstitial cerebral edema. Clinical signs of hypertensive

encephalopathy in cats can include ataxia, lethargy, seizures, stupor, and blindness.[1]

In this case, hypertension was documented (200 mmHg), and the cat had a history of hyperthyroidism, mild azotemia, cardiomyopathy and moderate histologic lesions in the kidneys consistent with chronic renal disease. Based upon the ACVIM consensus guidelines for classification of blood pressure, this cat is in risk category IV, with severe risk of target organ damage.[4] Thus, hypertension may have played a role in the formation of hyaline arteriopathy, however, the reason for the predilection in the CNS for the ventral spinal artery, basilar artery and branches is unknown. It is possible that thrombosis may have played a role in the formation of these changes, although similar vascular lesions were observed in the lungs and heart. The diameter of the ventral spinal artery in cats is the smallest at the level of C2, which is a potential predisposing factor for thrombosis.[10] Evaluation of the brain did not reveal the histologic changes described in the experimentally induced hypertensive cats[1] and histologic retinal arteriolar changes were not identified. Aneurysmal dilation of the ventral spinal artery has not been previously described as a sequel to hypertension in cats, however, ischemic lesions in the spinal cord of cats have been frequently reported.[6,10,11] Predisposing medical conditions were reported to include chronic renal disease, hypertension, cardiomyopathy, and hyperthyroidism.[10,11] In one case series of 19 cats with ischemic myelopathy, the most commonly affected regions of spinal cord included the C1-C5 (30%) and C6-T2 (30%) regions of the spinal cord, based upon MRI findings, with cervical spinal cord lesions in the region supplied by the ventral spinal artery.[11]

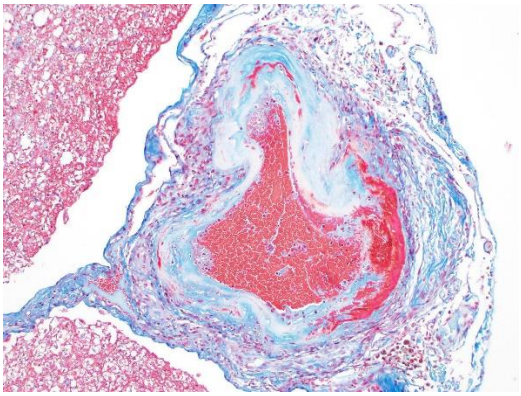

Spinal cord, cat. A Masson's trichrome stain highlights the deposition of collagen within the wall of damaged arteries. (Photo courtesy of: Animal Medical Center, 510 East 62nd St. New York, NY 10065, http://www.amcny.org/)

Although not present in this case, atherosclerosis is a lesion of arteriosclerosis in which fatty degenerative changes occur, and are typified by the presence of atheroma or fibrofatty plaque formation. In dogs, lipid is more frequently observed in the tunica media and adventitia, as opposed to the tunica intima in humans.[7] Atherosclerotic susceptibility amongst animals is variable, with atherosensitive species including humans, rabbits, chickens and pigs, and atheroresistant species including dogs, cats, cattle, goats and rats. In dogs, atherosclerosis is almost always found in conjunction with endocrine diseases, most notably hypothyroidism and diabetes mellitus.[7]

Contributing Institution:

Animal Medical Center, 510 East 62nd St. New York, NY 10065

http://www.amcny.org/

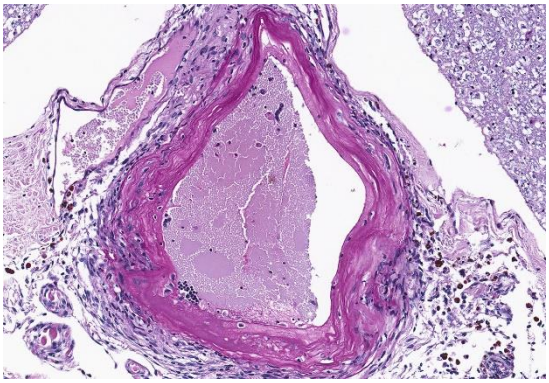

Spinal cord, cat. Hyaline material stains strongly positive with PAS. (Photo courtesy of: Animal Medical Center, 510 East 62nd St. New York, NY 10065, http://www.amcny.org/)

JPC Diagnosis: 1. Ventral spinal artery: Arteriosclerosis, diffuse, severe with aneurysmal dilatation, thrombosis, recanalization, and mural hyaline degeneration, and fibrosis.

2. Spinal cord, ventral funiculi: Axonal degeneration and loss, diffuse, mild to moderate.

JPC Comment: The contributor has provided an excellent review of hypertension and subsequent vascular change in cats. This particular case was subsequently published by Rylander et al.[10] in 2014, as part of a case series involving 5 cats.

Vascular disease resulting from feline hypertension has been previously seen in the Wednesday Slide Conference in 2017 (hypertensive retinopathy), and 2010 (hypertensive encephalopathy). While a common thread of chronic renal disease is associated with most cases[1] (and seen in this case), a number of other conditions may be responsible for hypertension in cats as well: hyperthyroidism (also noted in the clinical history in this case), diabetes mellitus, pheochromocytoma, hyperaldosteronism, and erythropoietin therapy.[5]

The pathogenesis of hypertensive encephalopathy is thought to involve the development of vasogenic edema as a result of sudden increases in blood pressure that exceed the autoregulatory capacity of the vasculature in the brain, resulting in endothelial injury and breakdown of the blood-brain barrier.[5] A recent publication by the moderator[2] has detailed the systemic pathology and resultant vascular and parenchymal lesions of feline hypertensive encephalopathy. In this case review of 12 cats, the median age was 12 years, without apparent breed predilection. All 12 had measured hypertension, from 16—300mm Hg. 11 of 12 animals had chronic tubulointerstitial nephritis and 4/12 had concurrent hyperthyroidism (which is consistent with previous publications). 6/12 had choroidal arteriopathy, and 5/12 had left ventricular hypertrophy.[2]

Neurological signs were most often localized to the prosencephalon and/or posterior fossa (brainstem and cerebellum), with 8/12 casts demonstrating cranial neve deficits, 50% had altered mentation ranging from dull to comatose. 5/12 developed seizure activity.[2]
]

Gross lesions were only seen in 4/12 cases, to include cerebral edema with or without displacement of the cerebellum. In this study, the primarily histologic lesion was bilaterally symmetrical regional to diffuse cerebral edema of the white matter, most severe at the dorsal aspect of white matter tracts.[2] Areas of edema separated myelin sheaths, and were populated by subjectively increased numbers of glial cells, including Alzheimer II astrocytes; gemistocytic astrocytes were seen in 3/12 cases.

Leptomeningeal arteriosclerosis was identified in 9/12 cases, with 8 of 12 demonstrating hyaline change. Lamellar fibrosis of the serosa ("onion-skinning") was relatively uncommon, being seen in 2 cases, one with the highest arterial pressure, and one with the longest history of systemic hypertension.[2]

References:

1. Brown CA, Munday JS, Mathur S, Brown SA. Hypertensive encephalopathy in cats with reduced renal function. *Vet Pathol*. 2005; 42:642-649.

2. Church ME, Turek BJ, Durham AC. Neuropathology of spontaneous hypertensive encephalopathy in cats. *Vet Pathol* 2019; 56(5):778-782.

3. Fishbein GA, Fishbein MC. Arteriosclerosis, rethinking the current classification. *Arch Pathol Lab Med.* 2009; 133:1309-1316.

4. Jepson R. Feline systemic hypertension, classification and pathogenesis. *J Fel Med Surg*. 2011; 13:25-34.

5. Kent M. The cat with neurological manifestations of systemic disease; key conditions impacting on the CNS. *Journal of Feline Med Surg.* 2009;11:395-407.

6. Littman MP. Spontaneous systemic hypertension in 24 cats. *J Vet Intern Med*. 1994; 8:79-86.

7. Maggio F, DeFrancesco TC, Atkins CE, Pizzirani S, Gilger BC, Davidson MG. Ocular lesions associated with systemic hypertension in cats: 69 cases (1985-1998). *J Am Vet Med Assoc.* 2000; 217(5):695-702.

8. Maxie MG, Robinson WF. Cardiovascular system. In: Jubb, Kennedy, and Palmer's Pathology of Domestic Animals, vol 3, 5th ed. New York, NY: Elsevier Limited; 2007:56-61.

9. Olsen JL. Hyaline arteriolosclerosis: new meaning for an old lesion. Editorial. *Kidney Intl.* 2003; 63:1162-1163.

10. Rylander H, Eminaga S, Palus V, Steinberg H, Caine A, Summers BA, Gehrke J, West C, Fox PR, Donovan TA, Cherubini GB. Feline ischemic myelopathy and encephalopathy secondary to hyaline arteriopathy in five cats. *J Feline Med Surg* 2014; 16(10):832-9.

11. Theobald A, Volk H, Dennis R, Berlato D, DeRisio L. Clinical outcome in 19 cats with clinical and magnetic resonance imaging diagnosis of ischaemic myelopathy (2000-2011). J Fel Med Surg. 2012; 15(2): 132-141.

Self-Assessment - WSC 2019-2020 Conference 19

1. True or false. The primary mode of transmission of *Neospora caninum* between cattle is horizontal.
    a. True
    b. False

2. Which of the following is the definitive host of *Neospora caninum*?
    a. Dog
    b. Cat
    c. Cattle
    d. Opossum

3. Aside from the cerebrum, neuronal lysosomes accumulated ceroid and disease-specific proteins is often seen in neurons in which of the following tissues?
    a. Sciatic nerve
    b. Retina
    c. Auerbach's plexi in the intestine
    d. Spinal ganglia

4. Medulloblastomas are thought to arise from cells in which layer of the cerebellum?
    a. Purkinje
    b. External germinal zone
    c. Molecular
    d. Granular

5. Which of the following is most often associate4d with feline hypertensive encephalopathy/myelopathy?
    a. Hyperthyroidism
    b. Pheochromocytoma
    c. Chronic renal disease
    d. Diabetes mellitus

Please email your completed assessment for grading to Dr. Bruce Williams at bruce.h.williams12.civ@mail.mil. Passing score is 80%. This program (RACE program 33611) is approved by the AAVSB RACE to offer a total of 0.5 CE Credits, with a maximum of 12.5 CE Credits being available to any individual Veterinary Medical Professionals for the 2019-2020 Wednesday Slide Conference. This RACE approval is for the subject matter categories of: SCIENTIFIC using the delivery method of NON-INTERACTIVE DISTANCE. This approval is valid in jurisdictions which recognize AAVSB RACE.

Joint Pathology Center
Veterinary Pathology Services

WEDNESDAY SLIDE CONFERENCE 2019-2020

C o n f e r e n c e 20

25 March 2020

CASE I: T-1708131 (JPC 4117493).

Signalment: Seven-month-old, female, domestic short hair cat, *Felis catus*

History: The animal presented to the referring veterinarian for general malaise and chronic weight loss. The cat returned home with the owner and was subsequently found dead a few days later. The carcass was submitted to the Tifton Veterinary Diagnostic and Investigational Laboratory (TVDIL) for necropsy.

Gross Pathology: At necropsy, the musculature was mildly atrophied. The oral mucosa was pale beige to grey. Lung lobes were mottled dark red to beige with frequent pinpoint pale foci. Liver had numerous 1 mm to 25 mm in diameter, slightly firm, pale foci. Multifocal to coalescing, irregular, and yellow beige foci, ranging from 2 to 20 mm in diameter were also observed on renal capsule and in renal cortices. Mesenteric lymph nodes were markedly enlarged. There was no other grossly visible lesion at necropsy.

Laboratory results: Bacterial culture on the lung and liver yielded no bacterial growth. Fluorescent antibody tests on lung, spleen, and kidney were negative for both feline infectious peritonitis and feline leukemia virus. PCR for feline coronavirus on pooled

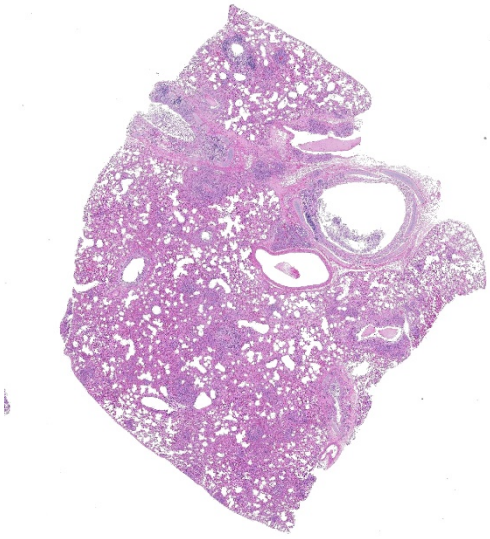

Lung, cat. A single section of lung is presented for examination. At subgross examination, arterioles are surrounded by a cellular infiltrate, and there is exudate within airways. (HE 5X).

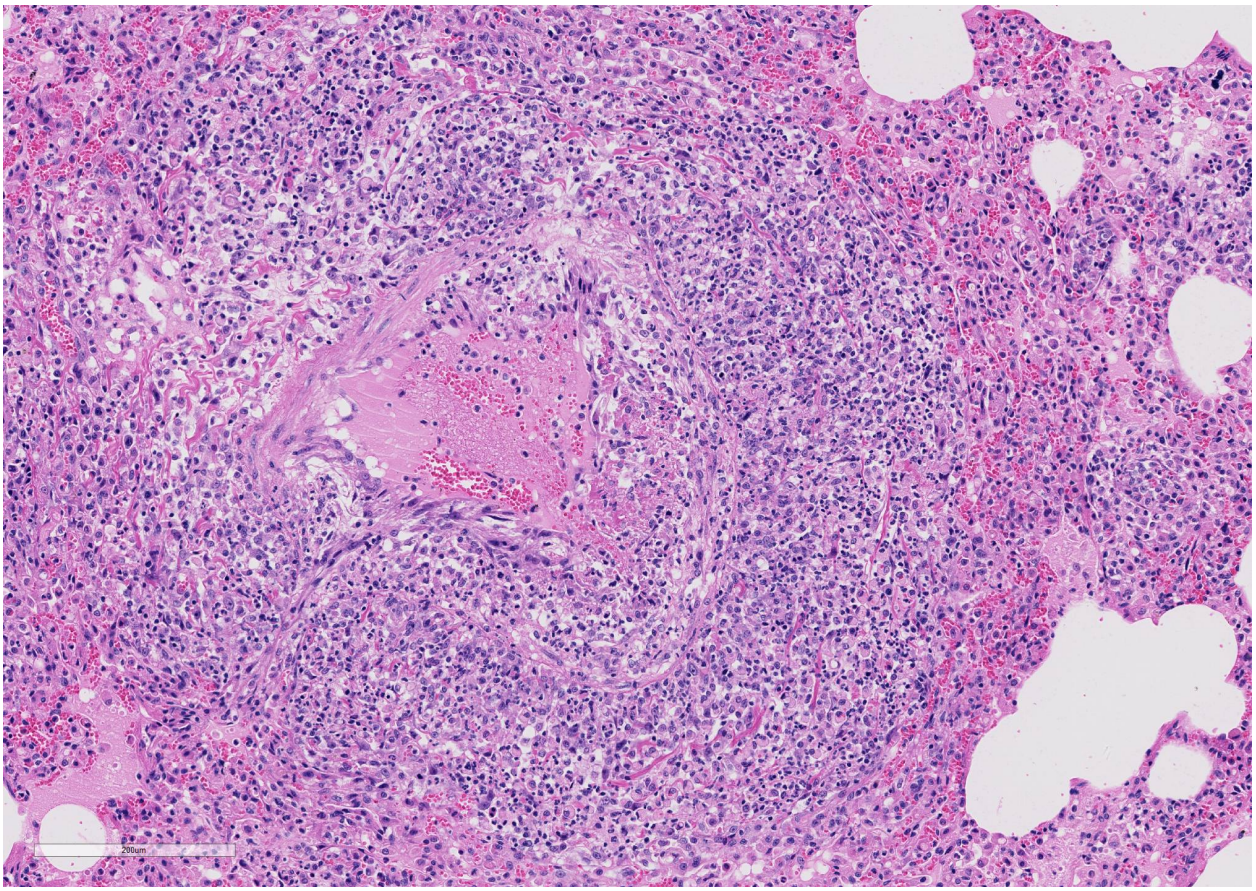

Lung, cat. A single section of lung is presented for examination. At subgross examination, arterioles are surrounded by a cellular infiltrate, and there is exudate within airways. (HE 5X).

samples from lung, kidney, liver, and brain was positive.

Microscopic Description: Lung sections were congested and disrupted by multifocal to coalescing areas of marked inflammation composed of large numbers of macrophages and neutrophils admixed with fewer plasma cells and lymphocytes. Occasional inflammatory foci contained multinucleated giant cells. Multifocally, tunica media and tunica intima of the pulmonary vessels were disrupted and expanded by an eosinophilic fibrillar material, degenerate neutrophils, and karyorrhectic debris. Scattered vessels were partially occluded by thrombi. Alveoli often contained an eosinophilic material admixed with low to moderate numbers of macrophages. A few bronchioles and bronchi contained an eosinophilic wispy material admixed with low numbers of macrophages and neutrophils. The peribronchiolar lymphoid tissue was hyperplastic. The pleural mesothelium exhibited mild hypertrophy. In a few regions, the pleural surface was overlaid with fibrin mats that contained degenerate neutrophils (not present in all sections).

Contributor's Morphologic Diagnosis:

1. Pneumonia, interstitial, pyogranulomatous, subacute to chronic, multifocal to coalescing, marked with vasculitis, lung.
2. Nephritis, interstitial, pyogranulomatous to plasmacytic, subacute to chronic, multifocal to coalescing, marked with vasculitis, kidney (not present in slide).

3. Hepatitis, pyogranulomatous to plasmacytic, subacute to chronic, multifocal to coalescing, marked, liver (not present in slide).
4. Meningoencephalitis, neutrophilic and histiocytic to plasmacytic, subacute to chronic, multifocal, marked with vasculitis, brain (not present in slide).
5. Lymphadenitis, pyogranulomatous to plasmacytic, subacute to chronic, multifocal to coalescing, marked, mesenteric and splenic lymph nodes (not present in slide).
6. Myocarditis, necrotizing to pyogranulomatous, subacute to chronic, multifocal, moderate to marked, heart (not present in slide).
7. Cystitis, interstitial, pyogranulomatous, subacute to chronic, multifocal, moderate to marked, urinary bladder (not present in slide).

Contributor's Comment: Histopathology confirmed a marked pyogranulomatous interstitial pneumonia with vasculitis. Similar foci of pyogranulomatous inflammation and vasculitis were observed in the kidney, liver, brain, lymph nodes, heart, and urinary bladder. The pattern of multisystemic pyogranulomatous inflammation with vasculitis was consistent with the noneffusive form of feline infectious peritonitis (FIP). PCR on fresh samples of lung, liver, kidney, and brain were positive for feline

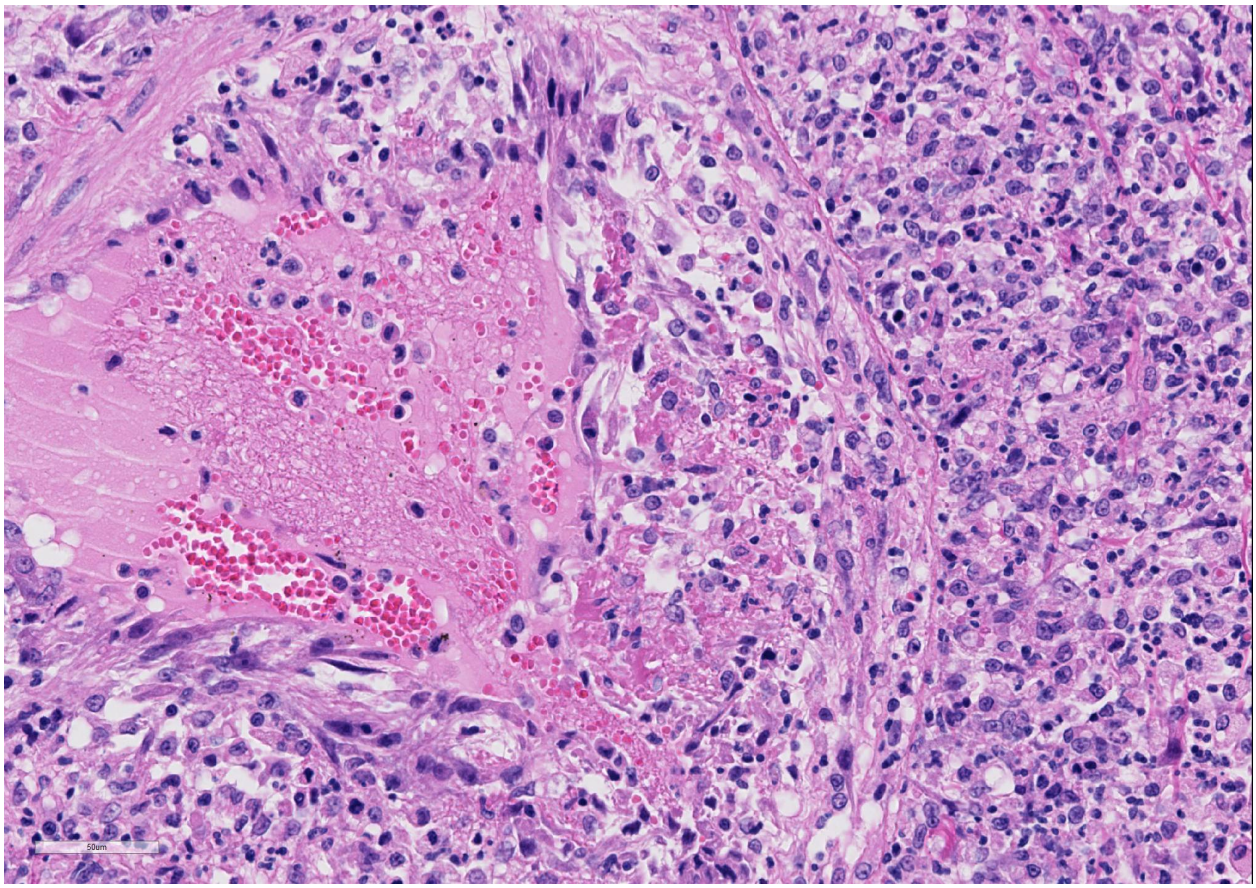

Lung, cat: Higher magnification of the affected vessel demonstrating segmental necrosis, mural fibrin and hemorrhage, and effacement of the wall by infiltrating neutrophils and macrophages, admixed with abundant cellular debris. (HE, 400X).

coronavirus. These results in conjunction with the histopathologic lesions confirmed FIP.

FIP is a fairly common infectious disease of cats with a low morbidity, yet high mortality. FIP is a coronaviral disease that can affect cats of any age, but is most prevalent among cats <3 years of age and especially from 4 to 16 months of age.[4] The disease continues to be a major killer of young cats.[3] In general, FIP tends to affect young cats, but can still occur in middle-aged to older cats. Purebred cats and male cats appear to be more susceptible.[4] It has also been well documented in virtually every species of Felidae, and FIP of domestic cats and cheetahs has been historically intertwined.[2,4]

Coronaviruses have adapted themselves over thousands of years to virtually every species of mammals and birds, and are a common cause of transient enteritis and respiratory disease.[3] The causative agent of FIP is feline coronavirus and more specifically, the feline infectious peritonitis virus (FIPV) biological pathotype. The virus is an Alphacoronavirus in the family Coronaviridae.[5] The other pathotype is feline enteric coronavirus (FECV), which is restricted to the intestinal tract and generally considered to be avirulent.[5] The exact pathogenesis of the viral infection and development of clinical disease is not fully elaborated, but the ability of the virus to replicate within macrophages is important in the development of FIP.[5,6] Mutation of FECV to a virulent FIPV has been considered as a possible contributing factor to the development of feline infectious peritonitis.[4,5,6] Other factors contributing to FIP include viral strain, genetic predisposition, and the host's immune response (e.g. ineffective cell mediated immunity of the host will favor an FIP virus infection).[5,6] The role of genetic factors in resistance or susceptibility to FIP is based on both indirect and direct observations. Pedigreed cats are more likely to develop FIP than random-bred cats and certain breeds are also more severely affected than others.[3]

Resistance to FIP is complicated and involves genetic susceptibility, age at the time of exposure and a number of stressors that occur at the same time as infection and have a negative impact on the ability of the infected cat to eliminate the virus. The time period between initial FECV exposure and clinical signs of disease can be as short as 2–3 weeks, as long as several months or, rarely, years, reflecting the time it takes for mutant FIPVs to evolve, or for the infection to progress from a subclinical to clinical disease. After an onset of overt clinical disease, a return to normal health is extremely uncommon and rarely may a cat will make an apparent recovery, but only to have clinical signs recur months and even years later. The disease course is generally shorter in younger cats and cats with effusive disease than in older cats and cats with non-effusive disease.[3]

FIP manifests itself in two forms the non-effusive ("dry") form as displayed in this case and the effusive ("wet") form. Despite the distinct nomenclature, these forms likely represent the two extremes of a spectrum. The effusive form typically presents with multiple acutely developing effusions in body cavities predominantly the abdominal and pleural cavities. Also, serosal surfaces often have fibrin deposits with necrotic foci in the associated parenchyma.[5] The noneffusive form however is chronic and characterized by multisystemic vasculitis and perivascular inflammation. The inflammatory infiltrate is classically histiocytic to pyogranulomatous with variable numbers of neutrophils, plasma cells and lymphocytes.[5] The lesions are commonly observed in the kidney, eye, brain, lung, liver, lymph nodes, and serosal surfaces. Grossly, the noneffusive form of FIP can present

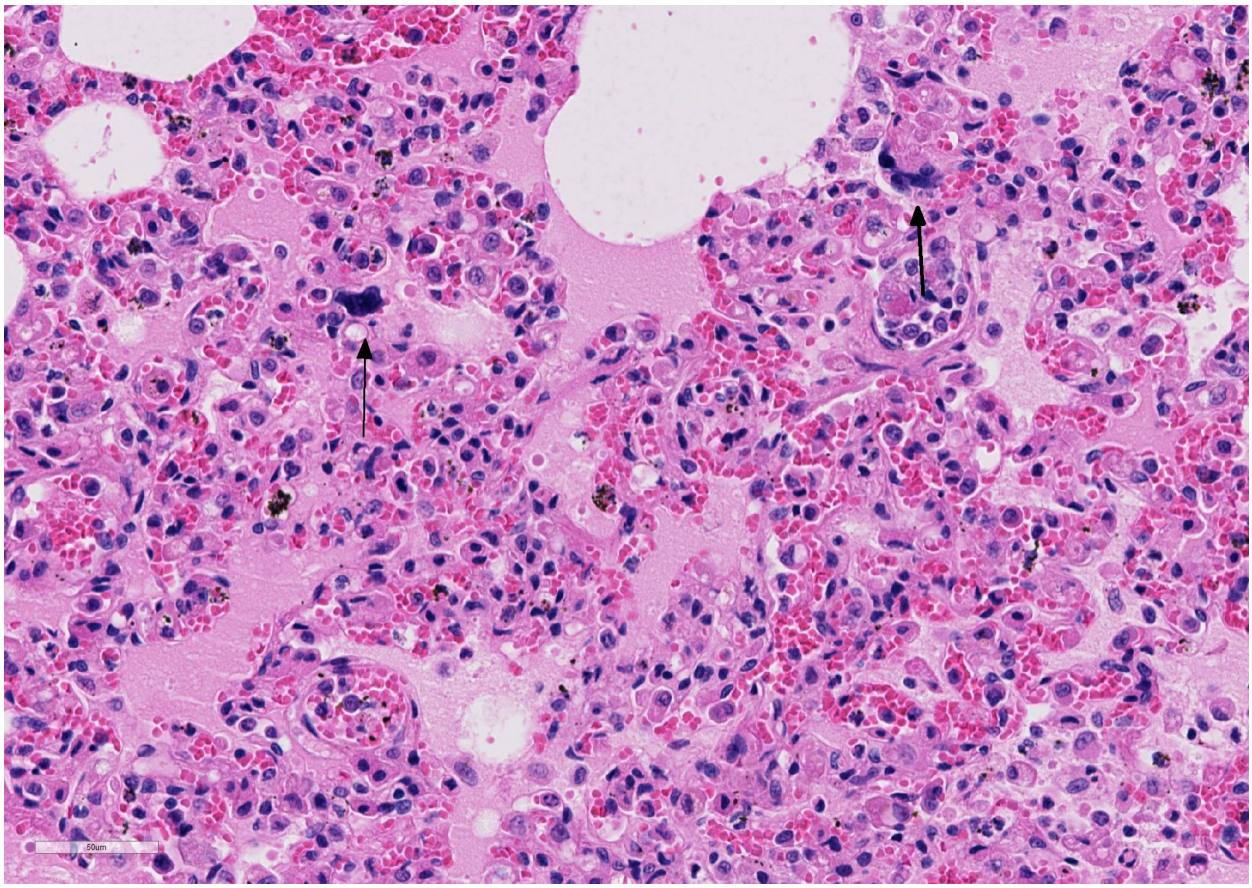

Lung, cat: Throughout the section, alveolar spaces are flooded with edema fluid. Alveolar septa are markedly congested, contain scattered fibrin thrombi, and rare megakaryocytes (arrows). (HE, 125X).

similar to systemic bacterial, fungal or protozoal infections and disseminated neoplasia, especially lymphoma.[5]

Diagnosis of FIP is based first and foremost on consideration of the age of the patient, origin, clinical signs and physical examination. Abdominal distension with ascites, dyspnea with pleural effusion, jaundice, hyperbilirubinuria, discernible masses on the kidneys and/or mesenteric lymph nodes, uveitis and a range of neurological signs associated with brain and/or spinal cord involvement are all common in cats with either the effusive or non-effusive form of FIP. At this point, the diagnosis of FIP can be made with reasonable certainty.[5]

The diagnosis of feline infectious peritonitis is typically based on the gross lesions and histopathology in combination with molecular diagnostics and/or immunohohistochemistry.[5] Other ancillary tests such as serology (e.g. ELISA) or fluorescent antibody testing can help support the diagnosis of FIP,[5] but may be less reliable.

Contributing Institution: The University of Georgia, College of Veterinary Medicine, Department of Pathology, Tifton Veterinary Diagnostic & Investigational Laboratory, Tifton, GA 31793; http://www.vet.uga.edu/dlab/tifton/index.php

JPC Diagnosis: Lung: Phlebitis, lymphohistiocytic, diffuse, severe, with fibrinoid necrosis, diffuse moderate interstitial pneumonia and marked alveolar and interstitial edema.

JPC Comment: The contributor has provided a fine overview of the disease of feline infectious peritonitis. Over the last decade, extensive research has provided insight into the "internal mutation theory" that the mutations transforming FeCV to FIPV occur internally within each individual. Three different genes have been identified have been identified with this conversion.[3]

The ORF 3c gene (whose protein product is unknown) was the first mutated gene to be identified, and approximately 2/3 of FIP viruses have ORF3c truncating mutations resulting in the ability to replicate in macrophages. (Other mutated ORF 3c genes which are not truncated (in this case causing a premature stop codons) do not confer this ability on the virus.[3]

Multiple mutations of the S gene, which encodes the fusion protein, has been identified in mutated forms in FIPVs and in FIP-infected cats, but not in FECVs. Single nucleotide alterations, including at the S1/S2 cleavage have been associated with macrophage tropism. [3]

Macrophage activation is one of the most important drivers of FIP in the cat. The typical vasculitis in FIP is as seen in this case - a vasculitis almost exclusively affecting veins and driven by virus-infected macrophages.[1] This phlebitis has been purported to develop as a result of interaction between the viral-infected monocytes and activated endothelial cells. The preponderance of vascular lesions is limited to veins in a number of organs (kidney, lung, meninges, eyes, liver), suggesting that not all endothelial cells share responsiveness to macrophages-secreted cytokines.[1] The incredible outpouring of fluid from affected vessels in the wet form of FIP (and likely the tremendous amount of fluid in the lungs of FIP cats such as this submission) has been associated with overproduction of vascular endothelial growth factor by virally-infected macrophages. Other cytokines overproduced by macrophages in FIP-infected cats include TNF-alpha, GM-CSF and G-CSF.[1] Macrophages secrete the adhesion molecule CD18 in order to attach to activated endothelium, and matrix malloproteinases to digest the vascular basement membrane at sites of emigration. The relative lack of lymphocytes in these lesions helps distinguish this lesion from a true immune-medicated vasculitis.[1]

References:

1. Kipar A, Meli ML. Feline infectious peritonitis: still an enigma? *Vet Pathol* 2014, 51(2):505-526.
2. Pearks Wilkerson AJ, Teeling EC, Troyer JL, et al. Coronavirus outbreak in cheetahs: Lessons for SARS. Current Biolo. 2004; 14, R227–R228.
3. Pedersen NC. An update on feline infectious peritonitis: Virology and Immunopathogenesis. The Vet J. 201 (2014) 123–132.
4. Pedersen NC. An update on feline infectious peritonitis: Diagnostics and Therapeutics. The Vet J. 201 (2014) 133–141.
5. Uzal FA, Plattner BL, Hostetter JM. Alimentary System. In: Maxie MG ed. *Jubb, Kennedy, and Palmer's Pathology of Domestic Animals.* 6th ed. Elsevier: St. Louis, MO; 2016; 2: 253-255.
6. Zachary JF. Mechanisms of microbial infections. In: Zachary, JF ed. *Pathologic Basis of Veterinary Disease.* 6thed. Elsevier: St. Louis, MO; 2017; 217-218.

CASE II: 19-2535 DVD (JPC 4135747).

Signalment: One-year old female sheep

History: Two yearling sheep in a group of fifteen died within the span of two weeks. A field necropsy with limited tissue collection was performed by the primary veterinarian.

Gross Pathology: Clinician reported adequate internal fat, heavy and wet lungs, and several < 1 cm in diameter abscesses in the liver.

Laboratory results: Quantitative PCR for ovine herpesvirus 2 revealed high copy numbers of viral DNA in liver and lung (73,400 and 195,000 copies/5 ng total tissue DNA).

In situ hybridization: Leukocytes demonstrate positive intranuclear staining for ovine herpesvirus 2.

Microscopic Description: Kidney: Multifocal vessels within the renal cortex and the arcuate arteries are transmurally disrupted by moderate numbers of densely packed macrophages, lymphocytes, plasma cells, and a few neutrophils. The endothelial cells are circumferentially plump, and the internal elastic lamina of the tunica intima is multifocally interrupted or obscured by the mixed inflammation admixed with small amounts of hypereosinophilic fibrillar material, shrunken and hypereosinophilic cellular silhouettes that have pyknotic nuclei (necrosis), and eosinophilic granular debris. The tunica media and adventitia are expanded by increased numbers of plump fusiform cells and collagenous connective tissue (hypertrophy). The mixed inflammation fills the periportal connective tissue and multifocally obscures the venous silhouettes. The renal parenchyma adjacent to the affected arteries is also expanded by small to moderate numbers of lymphocytes and plasma cells.

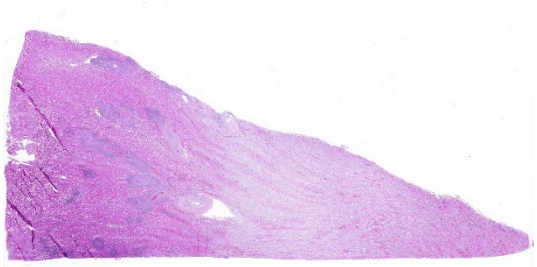

Kidney, sheep. A wedge of kidney is submitted for examination. All arterioles (arcuate, lobar, interlobar) are outlined by hypercellularity. (HE, 8X)

Other tissues:

Liver: Multifocally within the portal triads or around hepatic arteries, the walls of the arteries are similarly disrupted. The mixed inflammation fills the periportal connective tissue and multifocally obscures the venous silhouettes.

Lung: A group of arteries adjacent to the cartilage of a bronchus is similarly disrupted by mixed inflammation that surrounds and extends into the wall.

Heart: A large caliber artery is disrupted by smaller amounts of mixed inflammation. All arteries have moderate to marked medial hypertrophy and thickening.

Contributor's Morphologic Diagnosis:

Vasculitis, histiocytic and lymphoplasmacytic, multifocal, chronic, marked with vascular hypertrophy; liver, kidney, heart, and spleen

Contributor's Comment: The presented case is consistent with systemic necrotizing vasculitis of sheep, a sporadic disease affecting individuals or clusters of sheep ranging from 5 months to 3 years old in the literature.[2,7,9,10] Clinical signs of this disease may vary, and subcutaneous and joint swelling, diarrhea, chronic weight loss, and hemorrhage into body cavities with a case of aneurysmal dilation and rupture of the

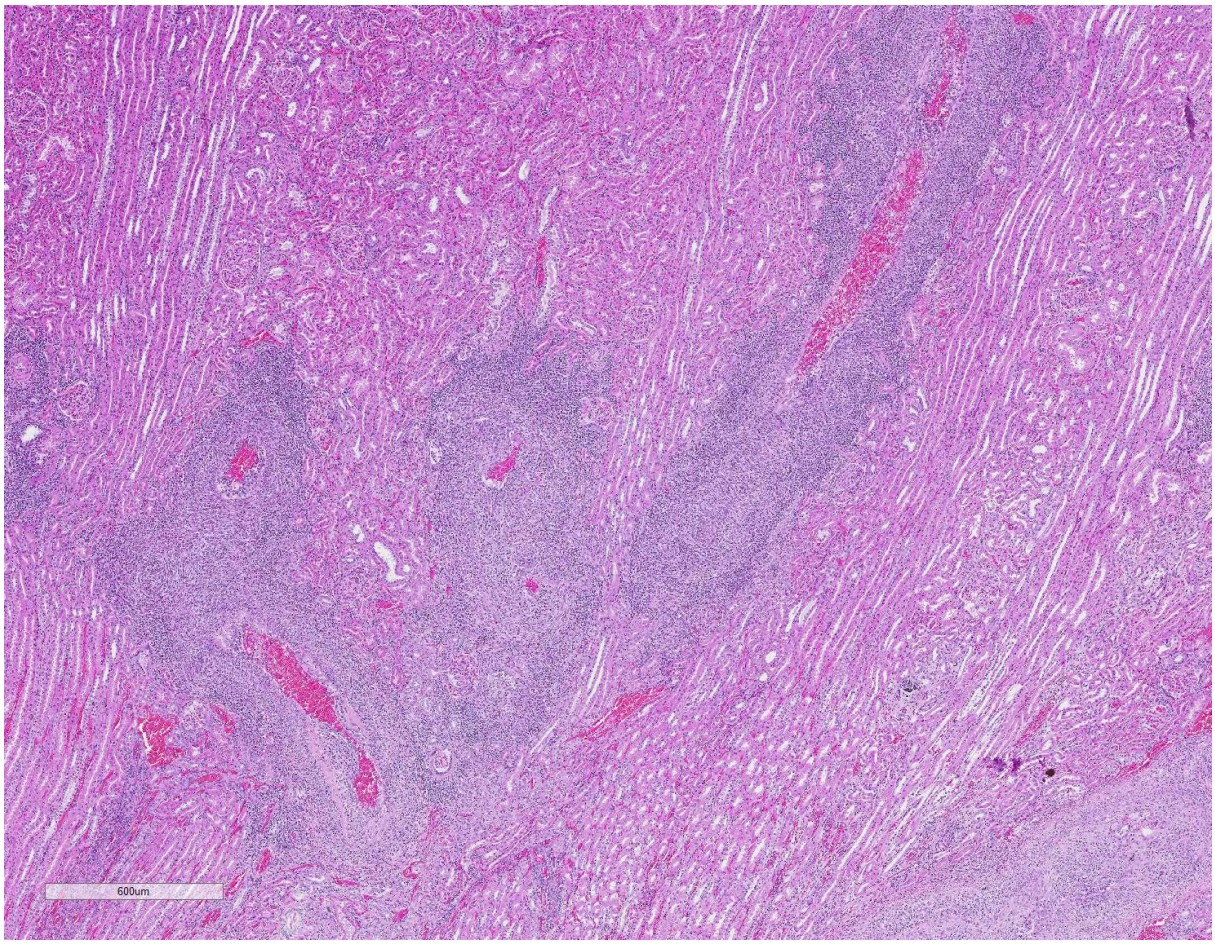

Kidney, sheep. Higher magnification showing effacement of medium-caliber arterioles by a lymphohistiocytic infiltrate which extends into and effaces the surrounding renal parenchyma. (HE, 8X)

gastroduodenal artery have been described. Histologically, the findings are characterized by a primarily circumferential lymphocytic inflammation disrupting small- to medium-sized arteries. The inflammation and local necrosis is often most densely affecting the adventitia and outer muscular wall, but can extend to be transmural in affected vessels. Comparisons between systemic necrotizing vasculitis of sheep and polyarteritis nodosa have been described,[2] and the etiology in individual cases are often speculated to be viral or immune-mediated.[9,10]

Recently, infection with the gammaherpesvirus ovine herpesvirus 2 (OvHV-2) has been demonstrated to be associated with systemic necrotizing vasculitis in sheep.[7] Our presented case recapitulates this association by identifying OvHV-2 nucleic acid within the vascular lesion via *in situ* hybridization. OvHV-2, a causative agent for malignant catarrhal fever (MCF) affecting several ruminant species such as cattle, deer, and confined bison, is generally thought to be a subclinical infection in domestic sheep. Like other herpesviruses, OvHV-2 establishes persistent infection in sheep, which are the natural hosts, and the virus is shed throughout the lifetime of the host. Although complete details of the epidemiology and viral life cycle of OVH-2 infection in domestic sheep remain to be determined, the majority of lambs acquire OvHV-2 at about

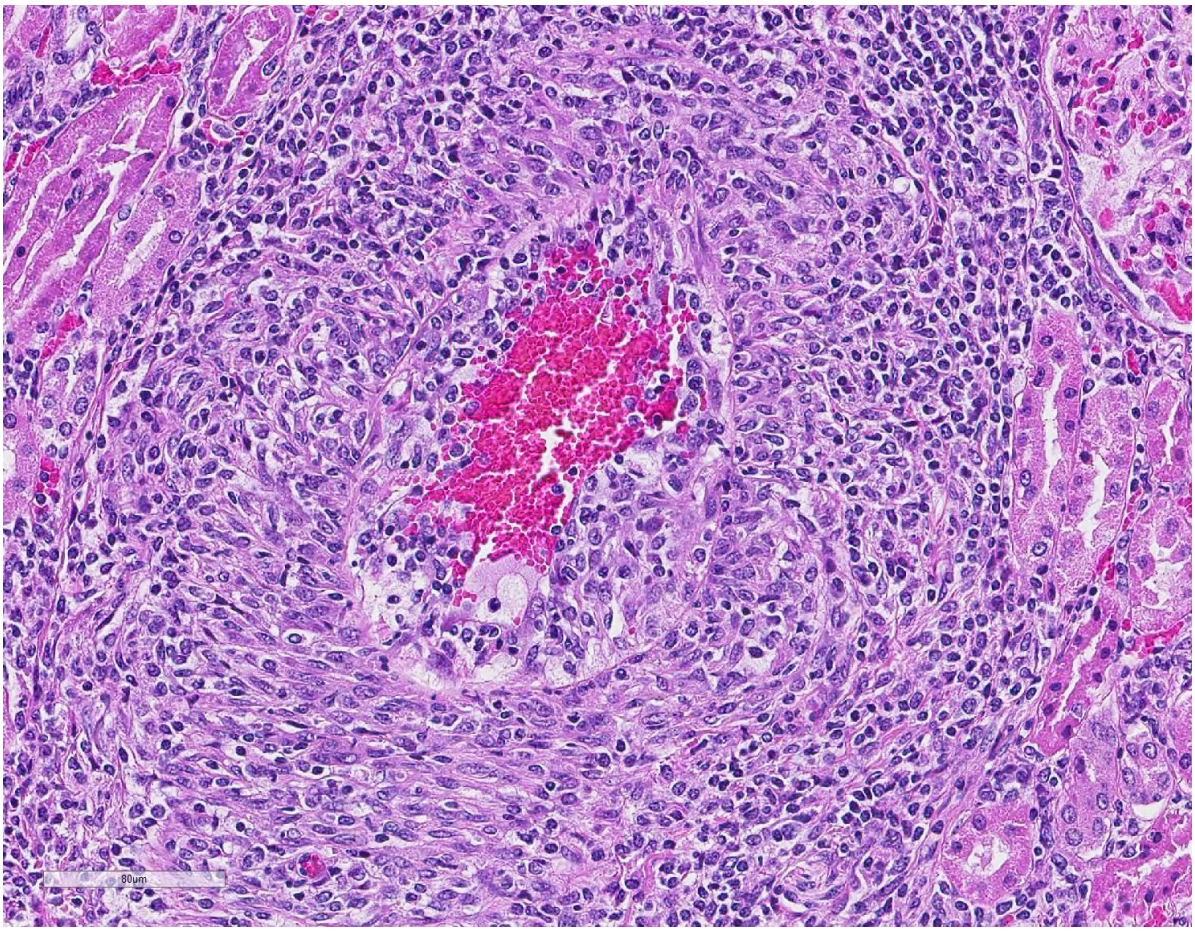

Kidney, sheep. The tunica intima is effaced by inflammatory cells, infiltrating smooth muscle cells and collagen. Similar changes affect the tunica media and inflammatory cells, with a predominance of lymphocytes replace the adventitia and extend into the surrounding parenchyma. (HE, 283X)

10 weeks of age, and the highest levels of viral DNA is detected in nasal secretions when individuals are between 6 and 9 months of age.[5] Viral DNA is detected in peripheral blood leukocytes of lambs earlier than in nasal secretions, which suggest that initial infection may occur in lymphocytes.[4] Diagnosis of OVH-2 associated MCF-like syndrome in sheep is a diagnostic challenge given that the virus is readily detectable in clinically healthy animals. Supportive evidence for diagnosis in this case included characteristic vasculitis in multiple organs, quantitative PCR demonstrating high copy numbers of OVH-2 DNA in tissue, and in situ hybridization revealing OHV-2 genomic material within lesion leukocytes.

Differentials for viral-associated vasculitis in sheep are summarized in Table 1, below.

Name	Virus	Associated Disease	Ancillary testing
Bluetongue	Orbivirus	Vascular thrombosis, tissue infarction, and hemorrhage +/- vascular inflammation	PCR of affected tissues

Maedi-Visna / Ovine Progressive Pneumonia	Small Ruminant Lentivirus	Chronic lymphocytic pneumonitis, encephalitis, arthritis, mastitis and vasculitis	Positive lentivirus ELISA with concurrent and characteristic lesions, IHC
Border Disease	Pestivirus	Disseminated nodular periarteritis with a predilection for CNS tissues	Viral isolation and/or rt-PCR

Table 1. Differential diagnoses for viral vasculitides in sheep.[1,3,6,11]

Contributing Institution: Washington State University Department of Veterinary Microbiology and Pathology (https://vmp.vetmed.wsu.edu/)

Washington State Animal Disease Diagnostic Laboratory (https://waddl.vetmed.wsu.edu/)

JPC Diagnosis: Kidney, arteries: Arteritis, lymphohistiocytic, multifocal, chronic, severe, with moderate perivascular lymphohistiocytic nephritis.

JPC Comment: The contributor has provided a concise but thorough review of malignant catarrhal fever (MCF) in sheep. MCF has been a frequent contribution to the WSC over the years (Table 2), even before ovine herpesvirus-2 (OvH-2) was identified as a potential cause. In addition to ovine herpesvirus-2, five other MCF-inducing viruses have been identified in ungulates, including alcelaphine herpesviruses 1 and 2, caprine herpesviruses 2 and 3, and ibex malignant catarrhal virus.[8]

The contributor has mentioned the difficulty in establishing the diagnosis of MCF in sheep. Clinically healthy sheep are thought to be widely infected with OvH-2, and would normally be PCR-positive for the present of this virus. A recent paper[7] described a diagnostic protocol utilizing a combination of in-situ hybridization and quantitative PCR to compare viral nucleic acid between tissues of vasculitis and those of clinical healthy normal carriers; it suggested that the presence of ISH positivity in vascular lesions and high levels of OvH-2 DNA may be used to confirm cases of ovine MCF.[7]

Other unique features of MCF in the sheep have impacted the elucidation of its pathogenesis. Unlike other MCF viruses, such as alcelaphine herpesvirus-1, the virus cannot be grown in cell culture, relegating researchers to used pooled secretions from multiple lambs. In AHV-1 infection in susceptible ruminants, lymphoid hyperplasia in which the nodes are populated by large lymphocytes heralds early infection, but these changes are not seen in OVH-2 infection, in which viral distribution is limited, and lesion development is proportional to viral infection and distribution.[8] One particular group has recently published a report of their development of a specific OvH-2 ISH probe with high specificity (it does not react with

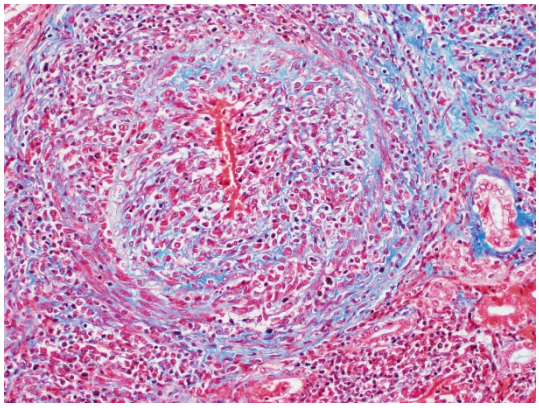

Kidney, sheep. A Masson-Trichrome demonstrates the amount of collagen within the wall of the inflamed arteriole. (Masson's trichrome, 400X)

AHV-1, ibex-McFV, and CpHV-2). The particular probe was shown to be effective in both experimental and natural infections, even in cases with low viral copy number, and that ISH signals correlate positively with lesion severity.[8]

References:

1. Cutlip RC, Lehmkuhl HD, Schmerr MJF, Brogden KA. Ovine progressive pneumonia (maedi-visna) in sheep. *Vet Micro* 1988; 17(3), 237–250.
2. Ferreras MC, Benavides J, Fuertes M., García-Pariente C, Muñoz M. Pathological features of systemic necrotizing vasculitis (polyarteritis nodosa) in sheep. *J Comp Path,* 2013; 149(1), 74–81.
3. García-Pérez A, Minguijón E, Barandika JF, Aduriz G, Povedano. Detection of Border Disease Virus in fetuses, stillbirths, and newborn lambs from natural and experimental infections. *J Vet Diagn Investig*, 2009; 21(3), 331–337.
4. Li H, Hua, Y, Snowder G., Crawford TB. Levels of ovine herpesvirus-2 DNA in nasal secretions and blood of sheep: implications for transmission. *Vet Microbiol* 2001, 79(4): 301–310.
5. Li, H, Taus NS, Lewis GS, Kim O, Traul DL. Shedding of ovine herpesvirus-2 in sheep nasal secretions: the predominant mode for transmission. *J Clin Microbiol* 2004; 42(12): 5558–5564.
6. Maclachlan NJ, Drew CP, Darpel KE, & Worwa G. The pathology and pathogenesis of bluetongue. *J of Comp Path* 2009; 141(1): 1–16.
7. Pesavento PA, Dange RB, Carmen Ferreras M, Dasjerdi A, Pérez V.. Systemic necrotizing vasculitis in sheep is associated with ovine herpesvirus 2. *Vet Pathol* 2019; 56(1): 87–92.
8. Pesavento PA, Cunha CW, Li H, Jackson K, O'Toole, D. In situ hybridization for localization of ovine herpesvirus2, the agent of sheep-associated malignant catarrhal fever in formalin fixed tissues. *Vet Pathol* 2019; 56(1) 78-86.
9. Rae CA. Lymphocytic enteritis and systemic vasculitis in sheep. *Can Vet J* 1994*;* 35(10): 622–625.
10. Wessels M, Strugnell B, Woodger N, Peat M, La Rocca, SA. Systemic necrotizing polyarteritis in three weaned lambs from one flock. *J of Vet Diagn Investig* 2017; 29(5): 733–737.
11. Zakarian B, Barlow RM, Rennie JC, Head, KW. Periarteritis in experimental border disease of sheep. *J of Comp Path* 1976; 86(3), 477–487.

CASE III: Blank label (JPC 4117883).

Signalment: 1-year-old, Aberdeen Angus steer*, Bos taurus*

History: Found dead in pen.

Lung, ox. A ~2L blood clot filled the pericardial sac. There is a full thickenss tear at the base of the pulmonary artery. (Photo courtesy of: Colorado State University Veterinary Diagnostics Laboratories, 200 West Lake Street, Fort Collins, CO 80523-1644, http://csu-cvmbs.colostate.edu/vdl/Pages/default.aspx)

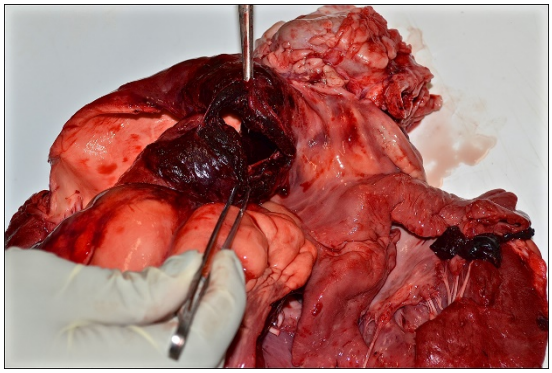

Lung, ox. Close up of the tear at the base of the pulmonary artery with marked hemorrhage within the arterial wall. (Photo courtesy of: Colorado State University Veterinary Diagnostics Laboratories, 200 West Lake Street, Fort Collins, CO 80523-1644, http://csu-cvmbs.colostate.edu/vdl/Pages/default.aspx

Gross Pathology: Presented for postmortem examination was a 1-year-old Black Angus steer in adequate body condition (BCS 2.5 out of 5) with minimal postmortem autolysis. A mild amount of edema expanded the subcutaneous fascia of the ventral thorax and mandible. Markedly distending the pericardial sac and enveloping the heart was a large ~2L coagulum of blood (Figure 1). The wall of the right ventricle was markedly thickened and firm, with a 1:1 ratio of right to left ventricular free walls. The pulmonary artery was severely dilated and there was a 4 x 2 cm acute full thickness tear at the base of the pulmonic outflow track (Figure 2). The intimal surface of the pulmonary artery was irregularly roughened and granular and the tear had hemorrhagic borders. The liver was slightly enlarged with rounded borders and was slightly firm in texture on cut section. The remainder of the post mortem examination was within normal limits.

1. Heart/pulmonary artery: Severe right ventricular concentric hypertrophy with pulmonary artery aneurysm, acute rupture, and hemopericardium with cardiac tamponade.
2. Liver: Moderate chronic passive congestion.

Laboratory results:

Bacteriology - Aerobic culture, lung

No significant growth

Molecular diagnostics - lung

Mycoplasma PCR: Not detected

Bovine respiratory syncytial virus (BRSV) real-time PCR: Not detected

Bovine herpesvirus-1 (IBR) real-time PCR: Not detected

Bovine viral diarrhea virus (BVDV) real-time PCR: Not detected

Microscopic Description: Lung: Diffusely throughout sections examined, the vascular lumina of small to large caliber muscular arteries, and to a lesser extent intraparenchymal pulmonary veins, are diminished due to marked expansion of the tunica intima and media by hypertrophic and hyperplastic smooth muscle and fibroplasia. Severely affected vessels are also segmentally to circumferentially expanded by poorly organized and edematous adventitial fibrosis which supports multiple cross sections of proliferative capillary profiles (complex plexiform arteriopathy/vasa vasorum hypertrophy). Adjacent alveolar spaces are occasionally compressed and collapsed. Vessels are internally lined by endothelial cells which are plump and reactive. Rare vessels are partially to completely occluded by organized thrombi. The tunica intimal and medial hypertrophy of both arteries and (to a lesser extent) veins was confirmed on a Van Gieson stain.

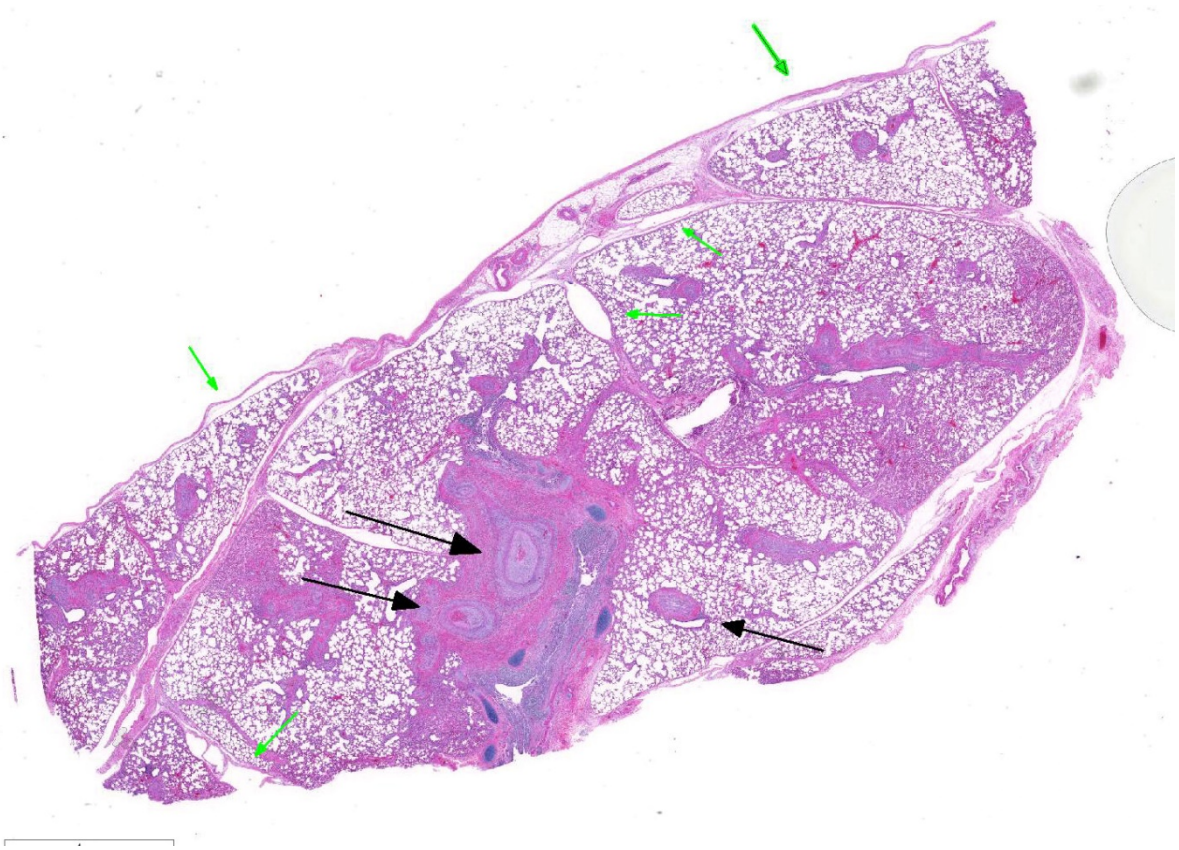

Lung, ox. At subgross magnification, the walls of pulmonary arteries are markedly expanded (black arrows), and there is marked edema and emphysema affecting the interlobular septa and pleura (green arrows). (HE, 6X)

There are multifocal regions of mild alveolar interstitial necrosis. In these areas alveolar septae are lined by hyalinized webs of fibrin. In other locations alveolar septae are lined by plump hyperplastic type II pneumocytes. Alveolar spaces are multifocally expanded by fibrinous and edematous exudates which support scant numbers of neutrophils and plump foamy alveolar macrophages. The pleural surface and interlobular septae are mildly expanded by edema.

Contributor's Morphologic Diagnosis:

1. Lungs, pulmonary arteries: Severe diffuse chronic arterial mural hypertrophy and hyperplasia with adventitial fibrosis and vasa vasorum hypertrophy (plexiform arteriopathy).
2. Lungs, pulmonary veins: Multifocal mild segmental mural hypertrophy.

Contributor's Comment: The most significant gross lesion detected on post mortem examination was severe right ventricular concentric hypertrophy with pulmonary artery aneurysm, rupture, and hemopericardium. Histologic lesions within the lungs are consistent with high mountain disease, also known as brisket disease, due to typical presentation with submandibular, cervical, and cranioventral thoracic subcutaneous edema.

Brisket disease was clinically recognized in Colorado in the early 1900's and was initially reported by Glover and Newsom in the *Colorado Agriculture Experimental Station* bulletin in 1915 and 1917.[2,3] In 1959

Alexander and Jensen reported that this condition is associated with right ventricular hypertrophy in both natural cases as well as in experimental cattle residing at high altitude.[1] Chronic hypoxia and pulmonary hypertension were proposed as an underlying etiology.

In acute hypoxic conditions, such as encountered at high altitude (elevation > 1600m), pulmonary arteriolar vasoconstriction results in both pulmonary hypertension and vascular shunting.[5] Chronicity results in remodeling of pulmonary arteries, including hypertrophy of the tunica intima, media, and adventitia, which further increases pulmonary resistance to flow. Neary et. al speculated that proximal remodeling of large pulmonary arteries (in additional to precapillary arterioles) may play a role in the pathogenesis of bovine pulmonary hypertension.[8] Stenmark et al. introduced an "outside in" hypothesis which postulates that vascular remodeling may be initiated by activated pro-inflammatory adventitial fibroblasts which mediate remodeling in adventitial, medial, and intimal layers and induce proliferation of the vasa vasorum.[6,10] Long-standing pulmonary hypertension may result in cor pulmonale or right ventricular cardiac hypertrophy and eventually right-sided congestive heart failure.[5]

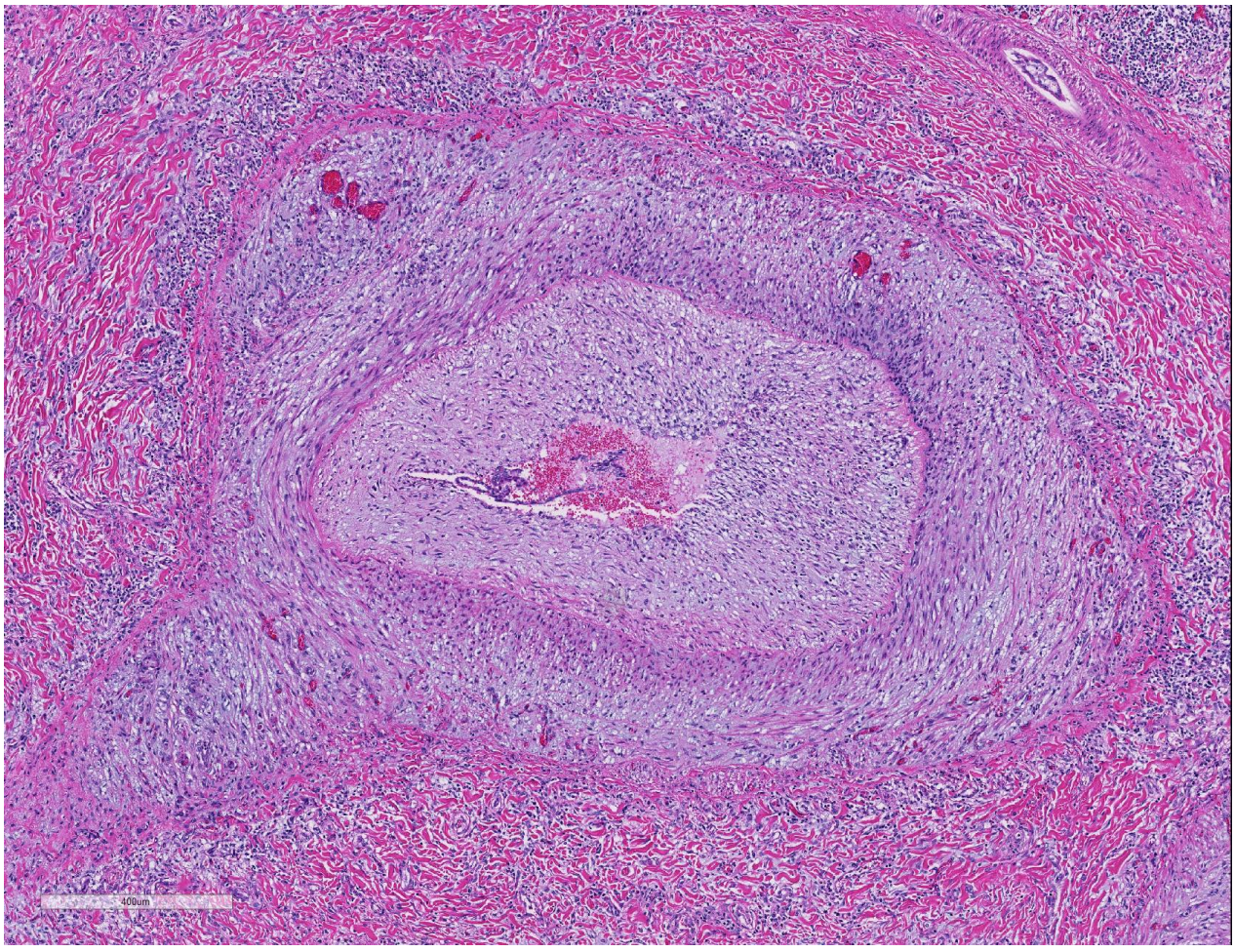

Lung, ox. At subgross magnification, the walls of pulmonary arteries are markedly expanded (black arrows), and there is marked edema and emphysema affecting the interlobular septa and pleura (green arrows). (HE, 40X)

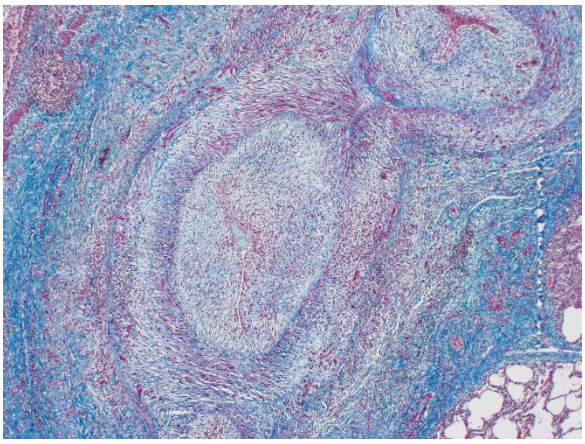

Lung, ox. A Masson's trichrome demonstrates the amount of fibroplasia within the walls of the hypertrophied arterioles. (Masson's trichrome, 40X)

Pulmonary hypertension is detected in live cattle by direct measurement of pulmonary arterial pressure (PAP) via catheterization of the right ventricle. Routine pulmonary arterial pressure testing (PAP) was initiated in the 1960s and early studies concluded that the degree of pulmonary hypertension detected by the PAP measurement was directly related to the degree of histologic pulmonary arterial hypertrophy.[5] Thus a pulmonary arterial pressure above 30 mmHg is considered diagnostic for pulmonary hypertension in cattle and it is recommended bulls with an elevated PAP be removed from breeding stock.

As demonstrated in this case by Verhoff-Van Gieson elastin staining, vascular lesions are not limited solely to pulmonary arteries but also rarely involve pulmonary veins. The degree of this lesion is mild in this case, but may be playing a perpetuating role in the underlying pathogenesis of this disease.

In addition to cattle, cardiac and pulmonary arterial remodeling was described in various zoo mammals housed at high altitudes at African Safari in Puebla, Mexico (elevation 2,100m) (8). Species included in this study were 10 maras (*Dolichotis patagonum*), 2 cotton-top tamarins (*Saguinus oedipus oedipus*), 2 capybaras (*Hydrochaeris hydrochaeris*), a Bennet's wallaby (*Macropus rufogriseus*), a nilgai antelope (*Boselaphus tragocamelus*), and a scimitar-horned oryx (*Oryx dammah*).[9]

It is important to rule out other diseases that may mimic brisket disease such as hardware disease, cardiomyopathy, heart failure secondary to chronic pneumonia, diffuse pulmonary parenchymal disease such as pulmonary fibrosis, or disseminated pulmonary abscesses, parasitic pneumonia, pulmonary intoxications, and/or emphysema.[7] In this case, the histologic changes consistent with a mild interstitial pneumonia retrospectively prompted a comprehensive bovine respiratory disease screen for case completeness; no underlying infectious etiologies were identified.

Given the history of this animal being raised along the Colorado Front Range (elevation ~1700m) combined with the gross and histologic diagnoses we conclude the constellation of these findings are consistent with bovine high altitude pulmonary hypertension with core pulmonale, pulmonary aneurysm and rupture.

Contributing Institution:

Colorado State University Veterinary Diagnostics Laboratories
200 West Lake Street
1644 Campus Delivery
Fort Collins, CO 80523-1644

http://csu-cvmbs.colostate.edu/vdl/Pages/default.aspx

JPC Diagnosis: Lung, pulmonary arterioles: Smooth muscle hypertrophy and hyperplasia, diffuse, severe, with mural fibroplasia, venous fibroplasia, and multifocal alveolar edema.

JPC Comment: The World Health Organization has classified six different types of pulmonary hypertension: pulmonary arterial hypertension, pulmonary veno-occlusive disease, hypertension resulting from left heart disease, hypertension with pulmonary disease or hypoxemia (which includes chronic forms of altitude disease), chronic thromboembolic pulmonary disease, and pulmonary hypertension with unclear multifactorial mechanisms.[11]

In humans, altitude disease ("mountain sickness") takes both an acute and chronic form. Acute exposure to hypoxic conditions at high altitude (2500 ft above sea level) manifests within 6-12 hours, characterized by headache, loss of appetite, vomiting, dizziness, and fatigue. Two theories as to its pathogenesis predominate: a) acute cerebral hyperperfusion resulting from impeded autoregulation of cerebral blood vessels and increased levels of VEG-F and circulating radicals, and b) inhibition of astrocytic Na-K ATPase and resulting edema and irritation of sensory trigeminal nerve fibers. If unattended, especially in additional altitude is attained, life-threatening cerebral or pulmonary edema may result.[4]

Chronic hypoxia resulting from high altitude in humans results in significant remodeling of small- and medium caliber pulmonary arterioles. The remodeling is the result of increased proliferation, decreased apoptosis, and migration of a population of less well-differentiated pulmonary artery smooth muscle cells. In addition, a mural population of fibroblasts may differentiate into a smooth muscle phenotype, while maintaining the ability to secrete matrix proteins. The end result of both proliferations results in effacement of the tunica intima and expansion of all layers of the arterial wall by smooth muscle hyperplasia, disarray, and fibrosis. In

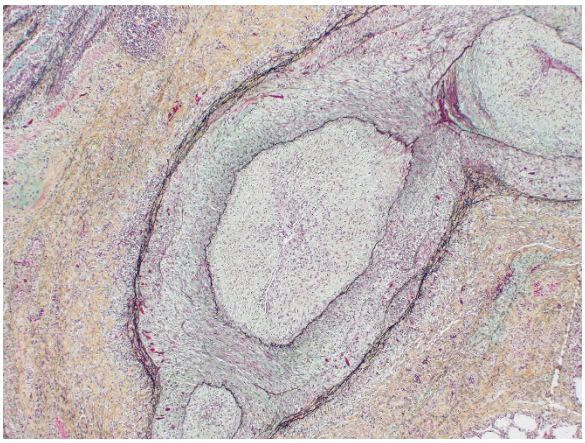

Lung, ox. The internal elastic lamina is largely intact, although the tunica intima is markedly expanded by migrating smooth muscle cells and fibroplasia which markedly compromises the limen. . (Masson's trichrome, 40X).

affected lungs, previously non-muscularized precapillary vessels may develop a muscular wall. However, all of these changes are reversible after prolonged re-exposure to normal oxygen levels.[4]

Plexiform lesions are not seen in remodeling of pulmonary arteries in chronic hypoxia in humans, and are associated with the most severe group of diseases resulting in pulmonary hypertension - those in WHO group 1, pulmonary arterial hypertension. This group includes the idiopathic and congenital forms of pulmonary arterial hypertension, which results in severe, non-reversible remodeling changes of pulmonary arterial remodeling, to include fibrinoid arteritis and plexiform lesion development.[11] An excellent example of these changes may be seen in WSC 25, Case 4 of 2018-2019, in a West Highland White Terrier, a breed in which several cases of idiopathic pulmonary hypertension similar to that seen in humans have been documented.

Several animal models for pulmonary hypertension exist. Chronic exposure of rats and mice to diminished levels of oxygen in normo- and hypobaric settings have been utilized for years and produce predictable

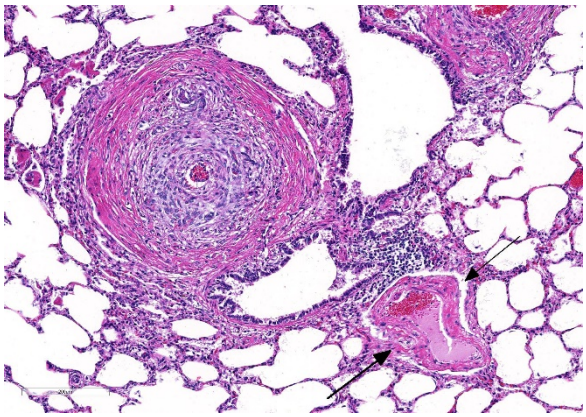

Lung, ox. Multifocally, there is fibrosis of walls of the larger pulmonary veins (arrows). (HE, 100X)

and reproducible results, depending on the strain of rodent. Fawn-hood rats appear to produce the most dramatic tissue changes. Oral administration of monocrotaline, a toxic pyrrolizidine alkaloid derived from *Crotalus spectabilis* also produces arterial changes consistent with pulmonary hypertension in rats dosed orally. While the precise mechanism is unknown, the prevailing hypothesis suggests direct endothelial damage to pulmonary arterioles. In addition, several genetically engineered mouse strains, including a BMPR2 knock out model (a genetic mutation seen in humans with severe forms of pulmonary arterial hypertension) have been developed.[11]

References:

1. Alexander AF, Jensen R. Gross Changes in Cattle with High Mountain (Brisket) Disease and in Experimental Cattle Maintained at High Altitudes. *Am J Vet Res* 20:680–689. 1959.
2. Glover GH, Newsom IE. Brisket Disease (Dropsy of High Altitude). *The Agriculture Experiment Station of the Colorado Agricultural College* Bulletin No. 204. January, 1915.
3. Glover GH, Newsom IE. Brisket Disease. *The Agriculture Experiment Station of the Colorado Agricultural College* Bulletin No. 204. May 1917.
4. Grimminger J, Richer M, Tello K, Sommer N, Hening G, Ghofrani HA. Thin air resulting in high pressure: Mountain sickness and hypoxia-induced pulmonary hypertension. *Can Resp J* 2017;https://doi.org/10.1155/2017/8381653.
5. Holt TN, Callan RJ. Pulmonary Arterial Pressure Testing for High Mountain Disease in Cattle. *Vet Clin North Am - Food Anim Pract*. 2007.
6. Li M, Riddle SR, Frid MG, et al. Emergence of Fibroblasts with a Proinflammatory Epigenetically Altered Phenotype in Severe Hypoxic Pulmonary Hypertension. *J Immunol*. 2011.
7. Malherbe CR, Marquard J, Legg DE, Cammack KM, O'Toole D. Right ventricular hypertrophy with heart failure in Holstein heifers at elevation of 1,600 meters. *J Vet Diagn Invest*. 2012.
8. Neary JM, Gould DH, Garry FB, Knight AP, Dargatz DA, Holt TN. An investigation into beef calf mortality on five high-altitude ranches that selected sires with low pulmonary arterial pressures for over 20 years. *J Vet Diagnostic Investig*. 2013.
9. Para A, Garner MM, Dipl ACVP. Pulmonary Arterial Disease Associated With Right-Sided Cardiac Hypertrophy and Congestive Heart Failure in Zoo Mammals Housed At 2,100 M Above Sea. *J zoo Wildl Med*. 2015.
10. Stenmark KR, Frid MG, Yeager M, et al. Targeting the Adventitial Microenvironment in Pulmonary

Hypertension: A Potential Approach to Therapy that Considers Epigenetic Change. *Pulm Circ*. 2012.
11. Stenmark KR, Mcyrick B, Galie N, Mooi WJ, McMurtyr IF. Animal models of pulmonary arterial hypertension: the hope for etiological discovery and pharmacological cure. *AmJ Phiol Lung Cell Mol Physiol* 2009; 197: L1013-1032.

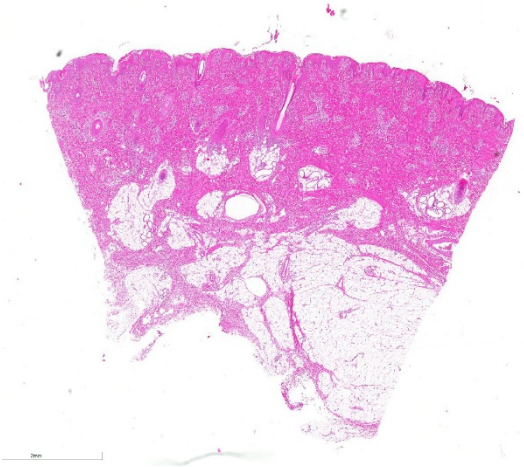

Haired skin, pig: One section of haired skin with subcutis is presented for examination. (HE, 5X)

CASE IV: LE-2 (JPC 4049442).

Signalment: Porcine, breed unspecified (*Sus scrofa domestica*), 14-weeks-old, neutered male, body weight 56.6 kg

History: This pig was submitted from a feeder-to-finish pig farm. Due to alterations of the skin a contagious disease was suspected. Therefore, the pig was euthanized and submitted for a complete post mortem examination. A more detailed clinical history was not available.

Gross Pathology: The carcass showed multiple cutaneous red macules and patches measuring up to 2 cm in diameter that were predominately located on the head, over the scapulae, as well as at the distal extremities and the anus.

Peripheral and visceral lymph nodes were enlarged measuring up to three times of their normal size. Their cut surfaces contained multiple slightly elevated white foci measuring 0.2 cm in diameter (indicative of a marked follicular hyperplasia) and displayed a red marginal coloration (consistent with a moderate blood resorption). Furthermore, both kidneys had multiple red foci measuring 0.1 cm in diameter that were restricted to the cortex; renal alterations were interpreted as a diffuse moderate acute glomerulonephritis. In addition, lungs showed a mild to moderate suppurative bronchopneumonia in both cranial lobes.

Laboratory results: PCR was positive for the detection of porcine Circovirus type 2 in tissue samples of brain, lungs and kidneys.

PCR was negative for the detection of classical swine fever virus in tissue samples of brain, lungs, lymph nodes, tonsils and spleen.

Microscopic Description: Haired skin: Multifocally, vascular walls of dermal capillaries, arterioles and venules showed deposition of homogenous eosinophilic material associated with loss of normal architecture interpreted as fibrinoid degeneration. Endothelial cells were swollen and bulged into vascular lumens (activated endothelial cells) or showed different stages of degeneration or necrosis (karyopyknosis and karyorrhexis). Some affected vessels were surrounded by a few extravasated erythrocytes and/or were cuffed by moderate numbers of inflammatory cells that extended within the adjacent dermis.Some affected vessels contained intraluminal fibrin thrombi and/or moderate numbers of neutrophils. The inflammatory infiltrates consisted of

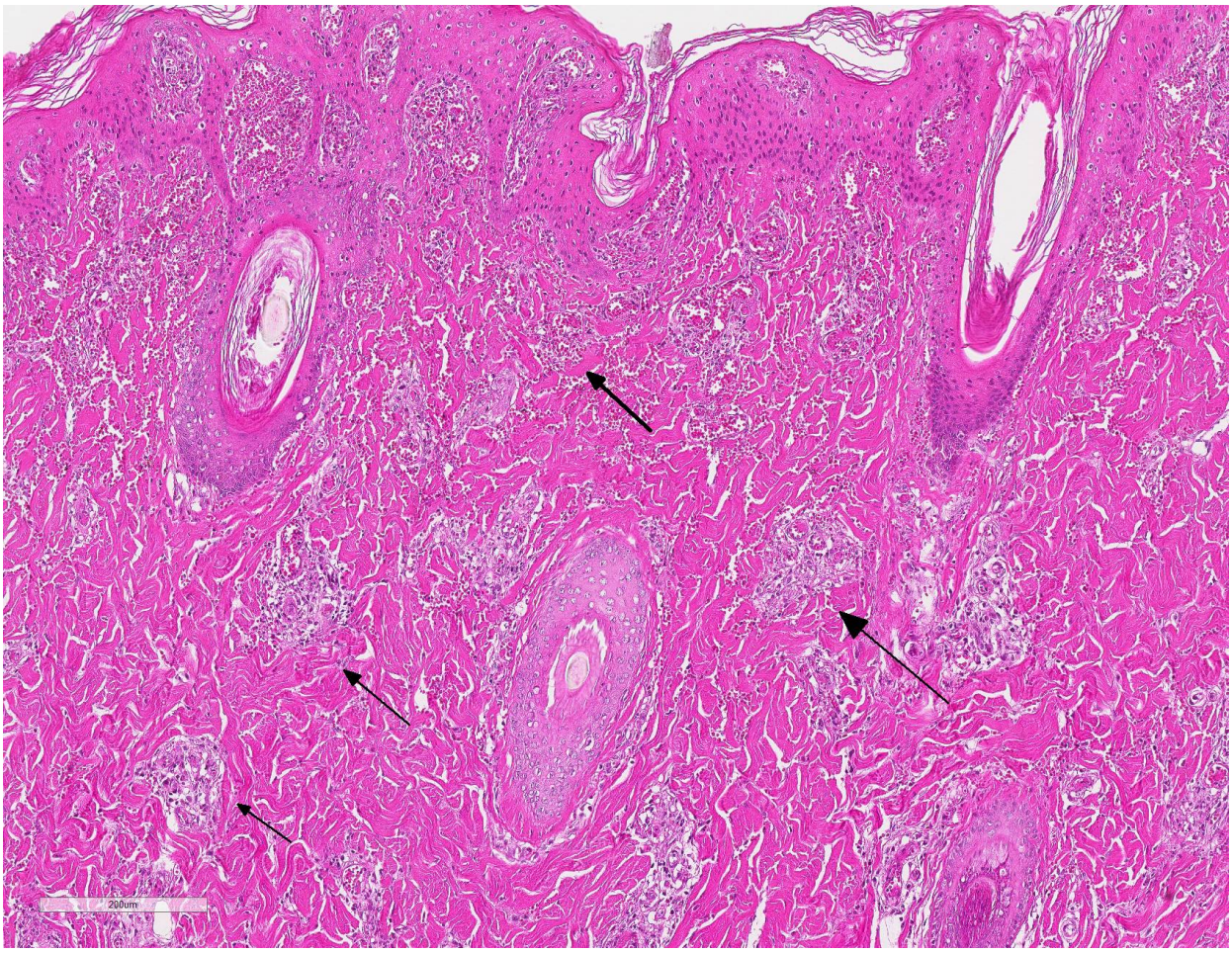

Haired skin, pig: All vessels within the dermis are outlined by edema and a cellular infiltrate (arrows). (HE, 25X)

predominately mononuclear cells (macrophages, lymphocytes, plasma cells) and a few neutrophils. Furthermore, a diffuse mild to moderate perivascular edema existed. The epidermis showed mild irregular epidermal hyperplasia and mild orthokeratotic basket-woven hyperkeratosis. In some slides, the described vascular lesions were also observed within the subcutis.

Contributor's Morphologic Diagnosis:
Haired skin, dermis and subcutis: Perivasculitis and vasculitis, necrotizing and mixed-cellular, acute to subacute, multifocal, moderate, with perivascular hemorrhage and edema

Contributor's Comment: Porcine circovirus type 2 (PCV2) belongs to the family Circoviridae, that encompass the two genera Circovirus and Gyrovirus. Porcine circovirus type 1 (PCV1) and type 2, beak and feather disease virus, canary, goose, pigeon, duck, finch and gull circovirus belong to the genus Circovirus. The genus Gyrovirus contains only the chicken anemia virus (CAV).[13]

The replication of the virions takes place within the nucleus of the host cell during the S phase of the mitosis by using the host cell DNA polymerase. PCV2 is reported as the smallest known pathogenic virus of our domestic animals with a size of approximately 16 to 20 nm in diameter.[13]

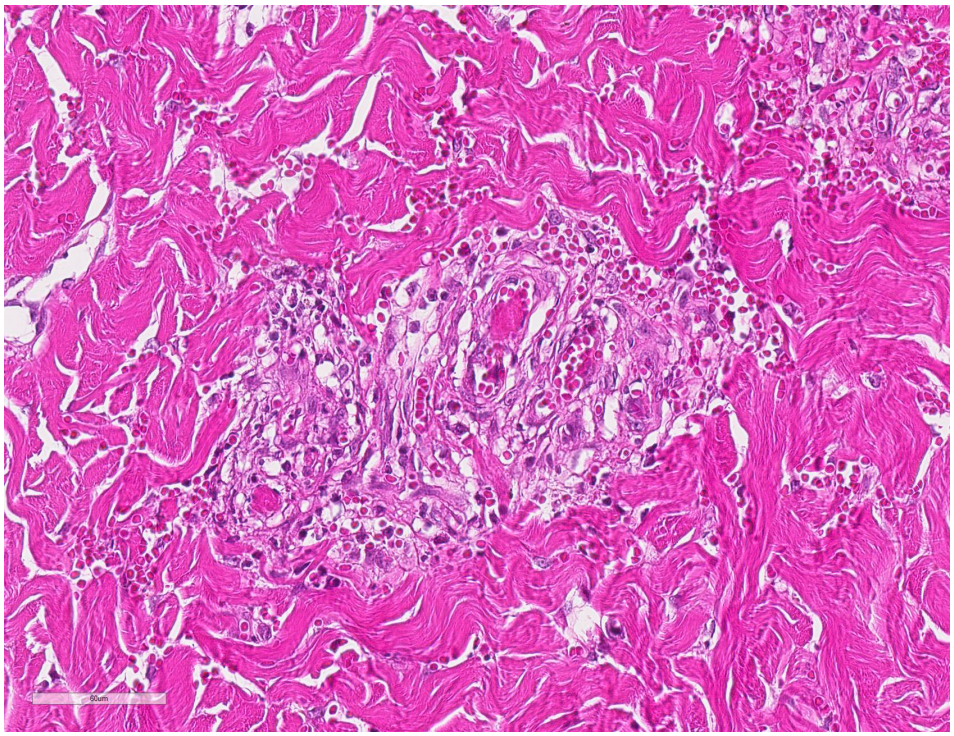

Haired skin, pig: Vessels have smudgy indistinct walls with mural inflammation, debris, luminal thrombi, and perivascular hemorrhage (vasculitis). (HE, 400X)

The porcine circovirus was first mentioned in 1974 from Tischer and colleagues.[11] It had been isolated from a pig kidney cell line PK 15 as a contaminant. At this time it was thought to be a picornavirus.[11] In the 1980s the same investigator group classified the virus as a porcine circovirus.[12] It has an isometric shape. The DNA is a covalently closed circular molecule. Furthermore, DNA is single stranded and has a genome size of 1.76 kb.[12]

In 1997, Clark described a new pig disease that occurred in Canada and called it the Post-Weaning Multisystemic Wasting Syndrome (PMWS).[3] Typical pathomorphologic findings are interstitial pneumonia characterized by mononuclear cellular infiltrates including predominately large macrophages and numerous multinucleated syncytial cells as well as enlarged lymph nodes characterized by a lymphoid depletion, an infiltration with large histiocytic cells and multinucleated syncytial cells.[3] In some cases, intralesional histiocytic cells display intracytoplasmic basophilic inclusions (botryoid inclusion bodies).[3,6] At this time the porcine circovirus has been suggested as the infectious agent.[3]

A comparison of the viruses of the pig kidney cell line PK 15 with those isolated from the animals with PMWS showed that they were antigenically distinct. Allan and colleagues designated the original PCV isolate from the pig kidney cell line PK 15 as PCV1 and the disease associated circovirus as PCV2.[1]

Retrospective studies showed the presence of PCV2 back to the 1970s in the United Kingdom pig population and at least since 1962 in Northern Germany.[4,6] Nowadays, a global distribution within the pig population is known.[7] PCV2 can be found in healthy as well as in diseased pigs.[2] It is speculated that a breakout of a PCV2-associated disease is multifactorial in causality, like host susceptibility, immune modulation, coinfection.[7] Viruses spread via fecal-oral route, but vertical transmission has also been demonstrated.[13]

Opriessnig and Langohr summarized the diversity of PCV2-associated diseases in pigs.[9] Those can be divided into subclinical PCV2 infection, PCV2-associated systemic infection, PCV2-associated respiratory disease, PCV2-associated enteritis, PCV2-associated reproductive failure and PCV2-

associated porcine dermatitis and nephropathy syndrome (PDNS).[8]

In the present case, microscopic examination of enlarged lymph nodes revealed lymphocytic depletion as well as infiltration by numerous multinucleated giant cells (syncytial cells). Furthermore, lungs showed a marked diffuse interstitial non-suppurative pneumonia and a moderate multifocal acute suppurative bronchopneumonia. The kidneys displayed histologically a multifocal moderate non-suppurative interstitial nephritis, a suppurative glomerulonephritis and a multifocal marked necrotizing vasculitis and perivasculitis.

PCV2-associated PDNS is characterized by typical gross lesions of the skin and the kidneys together with the hallmark microscopic lesions (systemic vasculitis and glomerulonephritis) and detection of PCV2 mRNA or antigen. Higgins mentioned PDNS also in association with drugs, other infectious agents and neoplasia.[5]

Therefore in the present case, PCV2-associated PDNS is most likely due to the gross lesions, histopathological findings and the detection of PCV2 mRNA within multiple tissues of this pig.

The proposed pathogenesis of PDNS is a type III hypersensitivity reaction with deposition of immune complexes in vessel walls and glomerular tuffs. In regards to the PCV2-associated PDNS, Rosell and collegues couldn't always detect porcine circovirus nucleic acid in vascular and glomerular lesions.[10] They supposed a transient deposition and a promptly removal of immune complexes or that the immune complexes lack of viral genome and only contain viral protein.

One of the major differential diagnoses of a disseminated acute vasculitis and glomerulonephritis is classical swine fever, in addition other viremic or septicemic diseases have to be ruled out. Further virological examination is required in such cases, i.e. PCR and/or virus culture, to definitively rule out the presence of a highly contagious and notifiable disease. The present case was negative for classical swine fever virus.

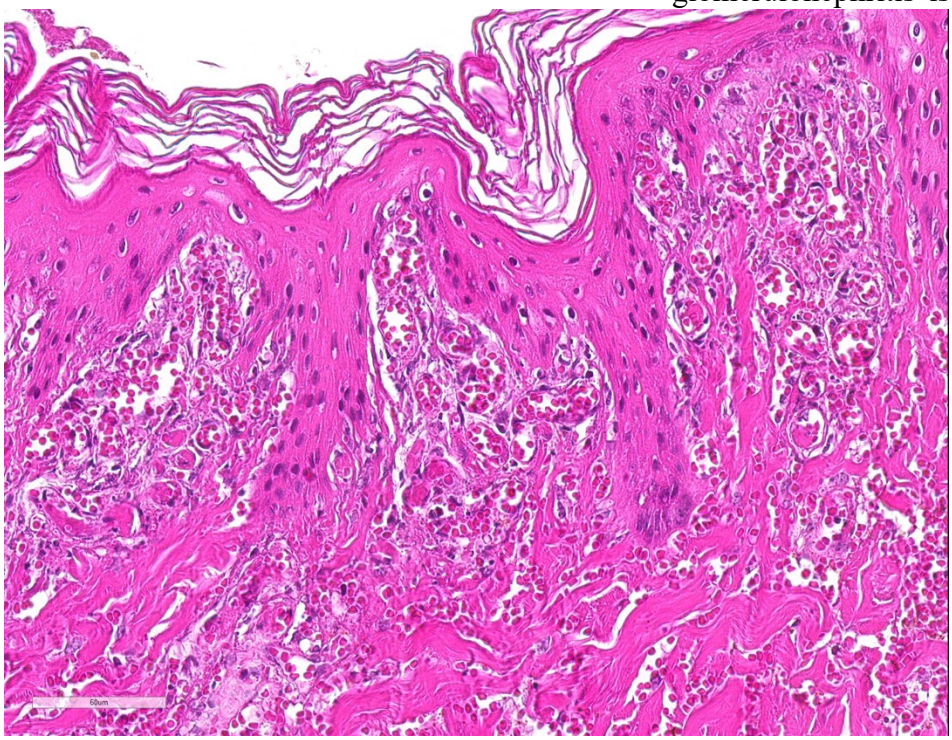

Haired skin, pig: There is marked congestion and hemorrhage within dermal pegs and necrosis of the overlying epidermis. (HE, 400)

In case several animals of this farm may present with similar lesions, management

practices, disinfection, control of coinfections and PCV2 vaccines should be recommended.[8]

Contributing Institution:

Institute of Pathology

Faculty of Veterinary Medicine

University of Leipzig

Director Professor H.-A. Schoon

An den Tierkliniken 33

04103 Leipzig

Germany

http://pathologie.vetmed.uni-leipzig.de/

JPC Diagnosis: Haired skin: Vasculitis, necrotizing, diffuse, severe, with multifocal dermal and epidermal necrosis.

JPC Comment: The contributor has provided an excellent review of the history of porcine circovirus-2 investigation. PCV-2 has made a number of appearances in the WSC demonstrating the wide spectrum of disease associated with this virus. Previous WSC submissions falling into this category include two previous cases of PCV-associated myocarditis (WSC 2019, Conference 17 Case 2 and WSC 2016, Conf 8, Case 2), cerebellar vasculitis and necrosis (WSC 2014, Conf 21, Case 4), granulomatous lymphadenitis and hepatitis (WSC 2013 Conf 25 Case1) and

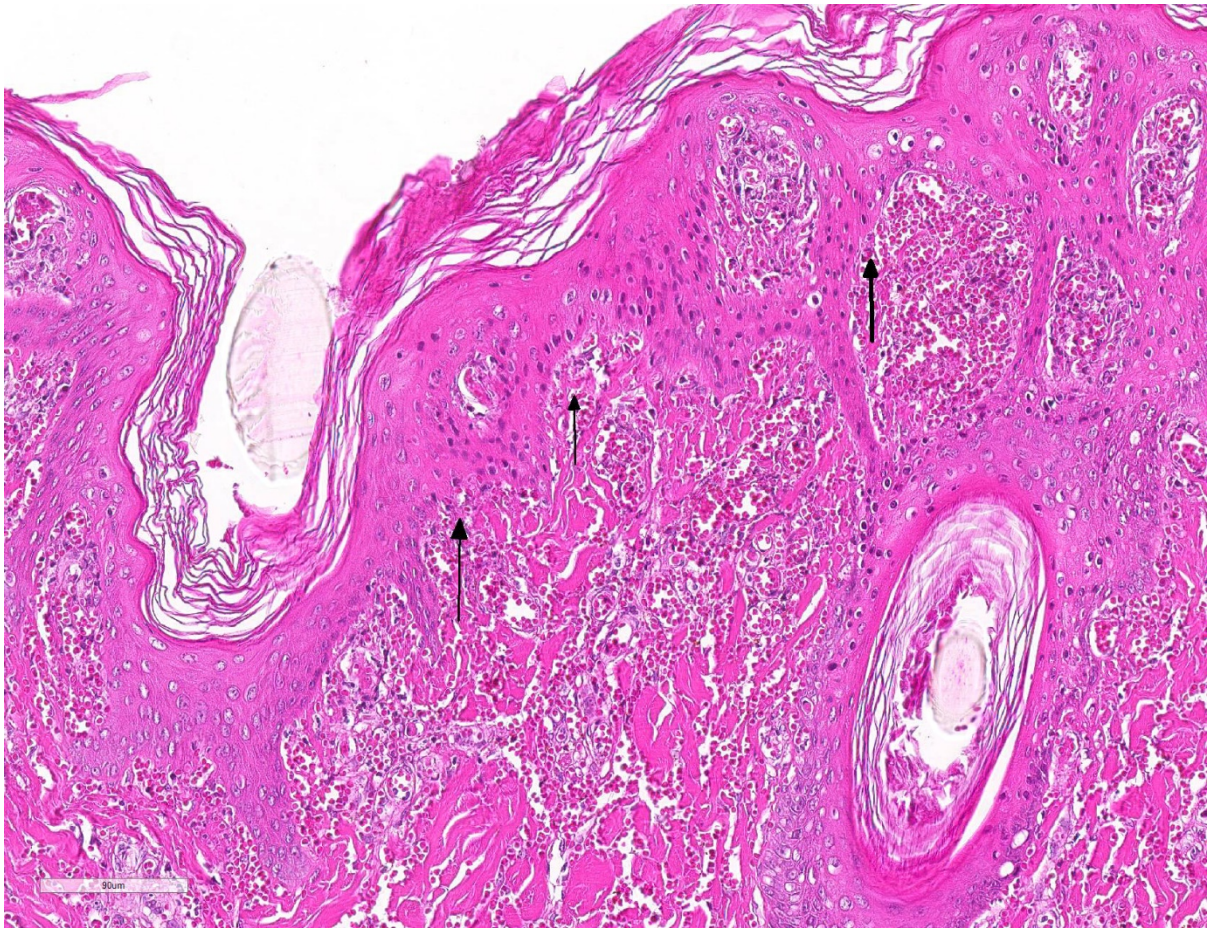

Haired skin, pig: There is profound hemorrhage within the superficial epidermis, and segmental areas full-thickness epidermal necrosis (black arrows) characterized by hypereosinophilic and nuclear pyknosis. Note the viable, more vesicular nuclei in the apidermis at left, and then the lower left portion of the hair follicle. (HE, 231X)

tubulointerstitial nephritis (WSC 2011, Conf 7, Case 3.)

Vasculitis is a common lesion in association with PCV-2 infection. Porcine dermatitis and nephritis syndrome is characterized by a necrotizing and neutrophilic vasculitis of arterioles and capillaries of the skin and kidney (to include glomerular capillaries). Fibrinoid necrosis of septal capillaries within the lung and resultant focal alveolar hemorrhage and edema has been widely reported in the US and Europe.[7] Necrotizing vasculitis within the cerebellum has been documented in porcine multisystemic wasting disease. Finally, cases of myocarditis in piglets are often associated with lymphohistiocytic coronary arteritis and periarteritis.[7,8]

The presumed pathogenesis of vasculitis in various forms of PCVAD is a Type III hypersensitivity reaction. In Type III hypersentivity, systemic disease results from the formation of antibodies to a protein (in this case, viral protein) with deposition of antigen-antibody complexes within the walls of vessels. Vessels in which blood is filtered to form other bodily fluids, such as urine and synovial fluid, are most affected (resulting in glomerulonephritis and polyarthritis respectively). Anitbodies (IgG and IgM) which have the ability to bind complement or bind to Fc receptors on leukocytes are the most likely to result in vascular lesions of fibrinoid necrosis. Analysis of damaged vessels may demonstrate the presence of immune complexes or complement, although levels in vessels outside the kidney may be low. PCV-2 antigen has been demonstrated within the walls of damaged blood vessels.

The effects of PCV-2 on vessels remains to be elucidated, but previous studies have shone light on some of its effects. PCV-2 antigen has been demonstrated in endothelial and inflammatory cells within the walls of vessels in both experimentally- and naturally-infected pigs. PCV-2 has the ability to infect endothelial cells, causing them to increase the expression of surface procoagulant activity. PCV-2 antigen has been identified in endothelial and inflammatory cells within necrotic vessels in infected pigs with granulomatous lymphadinitis as well as a peracute syndrome of acute pulmonary edema syndrome.[8]

References:

1. Allan G, Meehan B, Todd D, Kennedy S, McNeilly F, Ellis J, Clark E G, Harding J, Espuna E, Botner A, Charreyre C. Novel porcine Circoviruses from pigs with wasting disease syndromes. *Vet Rec.* 1998;142(17):467-468.
2. Allan GM, Ellis JA. Porcine circoviruses: a review. *J Vet Diagn Invest.* 2000;12:3–14.
3. Clark EG. Post-weaning wasting syndrome. *Proc Am Ass Swine Prac.* 1997;28:499–501.
4. Grierson SS, King DP, Sandvik T, Hicks D, Spencer Y, Drew TW, Banks M. Detection and genetic typing of type 2 porcine circoviruses in archived pig tissues from the UK. *Arch Virol.* 2004;149(6):1171–1183.
5. Higgins RJ. Glomerulo-nephropathy syndrome. *Pig Vet J.* 1993;31:160–163.
6. Jacobsen B, Krueger L, Seeliger F, Bruegmann M, Segalés J, Baumgaertner W. Retrospective study on the occurrence of porcine circovirus 2 infection and associated entities in Northern Germany. *Vet Microbiol.* 2009;138(1-2):27-33.
7. Kumar V, Abbas AK, Aster JC. Diseases of the immune system. *In:* Robbins and Cotran Pathologic Basis of Disease, 9th ed. Philadelphia, PA, Elsevier Saunders, 2015.
8. Opriessnig T, Meng XJ, Halbur PG. Porcine circovirus type 2 associated disease (PCVAD): Update on current terminology,

clinical manifestations, pathogenesis, diagnosis, and intervention strategies. *J Vet Diagn Invest.* 2007;19:591-615.
9. Opriessnig T, Langohr I. Current state of knowledge on porcine circovirus type 2-associated lesions. *Vet Pathol.* 2013;50(1):23-38.
10. Rosell C, Segalés J, Ramos-Vara JA, Folch JM, Rodriguez-Arrioja GM, Duran CO, Balasch M, Plana-Durán J, Domingo M. Identification of porcine circovirus in tissues of pigs with porcine dermatitis and nephropathy syndrome. *Vet Rec.* 2000;146:40-43.11. Tischer I, Rasch R, Tochtermann G. Characterization of papovavirus- and picornavirus-like particles in permanent pig kidney cell lines. *Zbl Bakt Hyg.* 1974:A 226:153-167.

12. Tischer I, Gelderblom H, Vettermann W, Koch MA. A very small porcine virus with a circular single-stranded DNA. *Nature.* 1982;295:64-66.
13. Truyen U. [Familie Circoviridae. In: Selbitz H-J, Truyen U, Peter V-W, eds. *Tiermedizinische Mikrobiologie, Infektions- und Seuchenlehre.* 9. Auflage. Stuttgart: Enke-Verlag]. 2011;487-492.

Self-Assessment - WSC 2019-2020 Conference 20

1. Which of the following cells is considered the primary driver in the vasculitis associated with feline infectious peritonitis
    a. B cells
    b. Macrophages
    c. T cells
    d. Endothelial cells

2. Which of the following is considered a good test for the diagnosis of malignant catarrhal fever in sheep?
    a. Serology
    b. PCR
    c. Immunophenotyping vascular inflammation
    d. None of the above

3. Which of the following is a consistent lesion in chronic high altitude disease in cattle ?
    a. Left ventricular hypertrophy
    b. Remodeling of pulmonary veins
    c. Right ventricular hypertrophy
    d. Hemopericardium

4. Which of the following, when administered to rats, results in lesions consistent with pulmonary hypertension?
    a. Streptozotocin
    b. Monocrotaline
    c. Salicylic acid
    d. Dimethyl benzene

5. Which of the following is most likely responsible for the vasculitis seen in porcine dermatitis and nephritis syndrome?
    a. Type I hypersensitivity
    b. Type II hypersensitivity
    c. Type III hypersensitivity
    d. Type IV hypersensitivity

Please email your completed assessment for grading to Dr. Bruce Williams at bruce.h.williams12.civ@mail.mil. Passing score is 80%. This program (RACE program 33611) is approved by the AAVSB RACE to offer a total of 0.5 CE Credits, with a maximum of 12.5 CE Credits being available to any individual Veterinary Medical Professionals for the 2019-2020 Wednesday Slide Conference. This RACE approval is for the subject matter categories of: SCIENTIFIC using the delivery method of NON-INTERACTIVE DISTANCE. This approval is valid in jurisdictions which recognize AAVSB RACE.

Joint Pathology Center
Veterinary Pathology Services

WEDNESDAY SLIDE CONFERENCE 2019-2020

C o n f e r e n c e 21

3 April 2020

CASE I: B-14-0576 (JPC 4066399).

Signalment: 9-year-old spayed female Old English sheepdog

History: The dog had a one-month history of rostral mandibular swelling displacing mandibular incisors and canine teeth. A previous incisional (Jamshidi) biopsy diagnosis was osteosarcoma. A computed tomography scan showed a soft tissue attenuating mass with pinpoint mineral attenuating foci and heterogeneous contrast enhancement; the mass was markedly displacing teeth and causing marked bony lysis and mild osseous proliferation of the rostral mandible (Fig. 1). The mass and rostral mandible including the tissues rostral to teeth 309 and 409 were removed via mandibulectomy and submitted as a surgical biopsy.

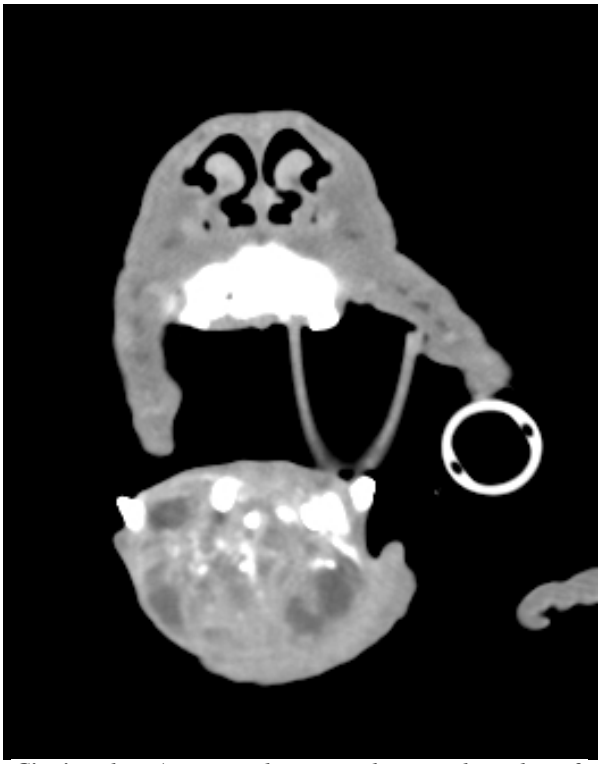

Gingiva, dog. A computed tomography scan showed a soft tissue attenuating mass with pinpoint mineral attenuating foci and heterogeneous contrast enhancement. (Photo courtesy of: University of Wisconsin-Madison, School of Veterinary Medicine, 2015 Linden Drive, Madison, WI 53706 www.vetmed.wisc.edu)

Gross Pathology: The mandible contained a smooth surfaced mass covered in mucosal epithelium, which extended from just caudal

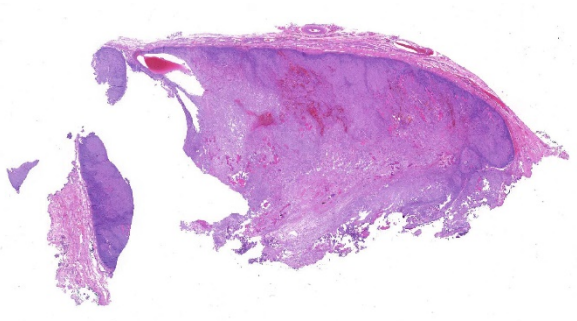

Gingiva, dog. A well demarcated mass expands the gingiva. (HE, 5X)

to the canine teeth to rostral to the incisors, expanding tissue between teeth and widely separating the incisors. The mass measured 4.8 x 4.8 x 3.7 cm, and was firm but not hard and lacked bony texture. On midline section the mass was white to red to dark red, with multifocal cavitated areas filled with watery brown fluid. The interior of the mass was soft with no bony texture.

Laboratory results: NA.

Microscopic Description: The mandible contains and is effaced by an unencapsulated, well-demarcated, multilobulated mass which is composed of polygonal cells arranged in cords,

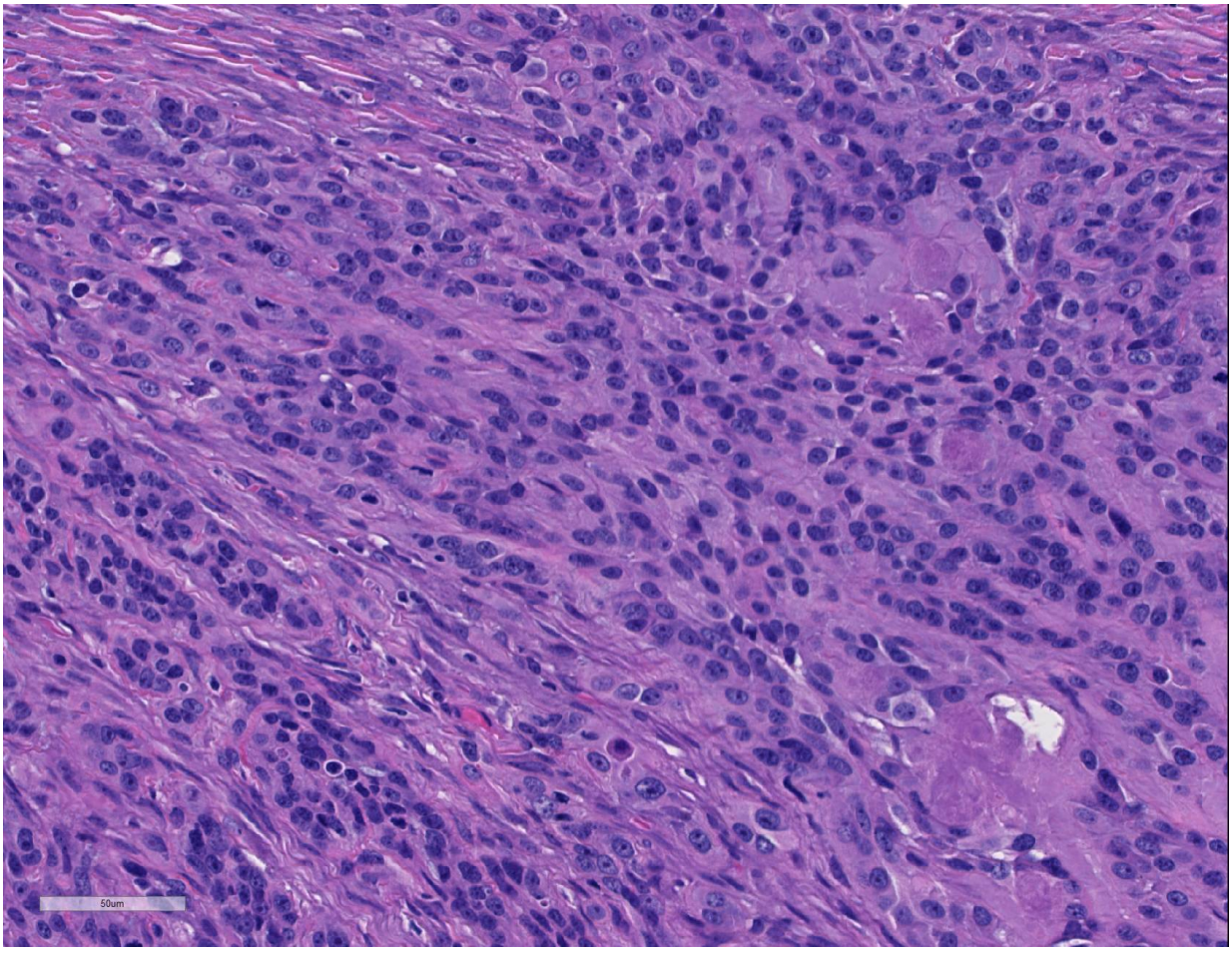

Gingiva, dog. Neoplastic cells (which are most dense along the periphery) are cuboidal and form think cords of palisading cells on a moderate fibrous stroma. In this region, small islands of amyloid separate some cords of cells (arrows). (HE, 400X)

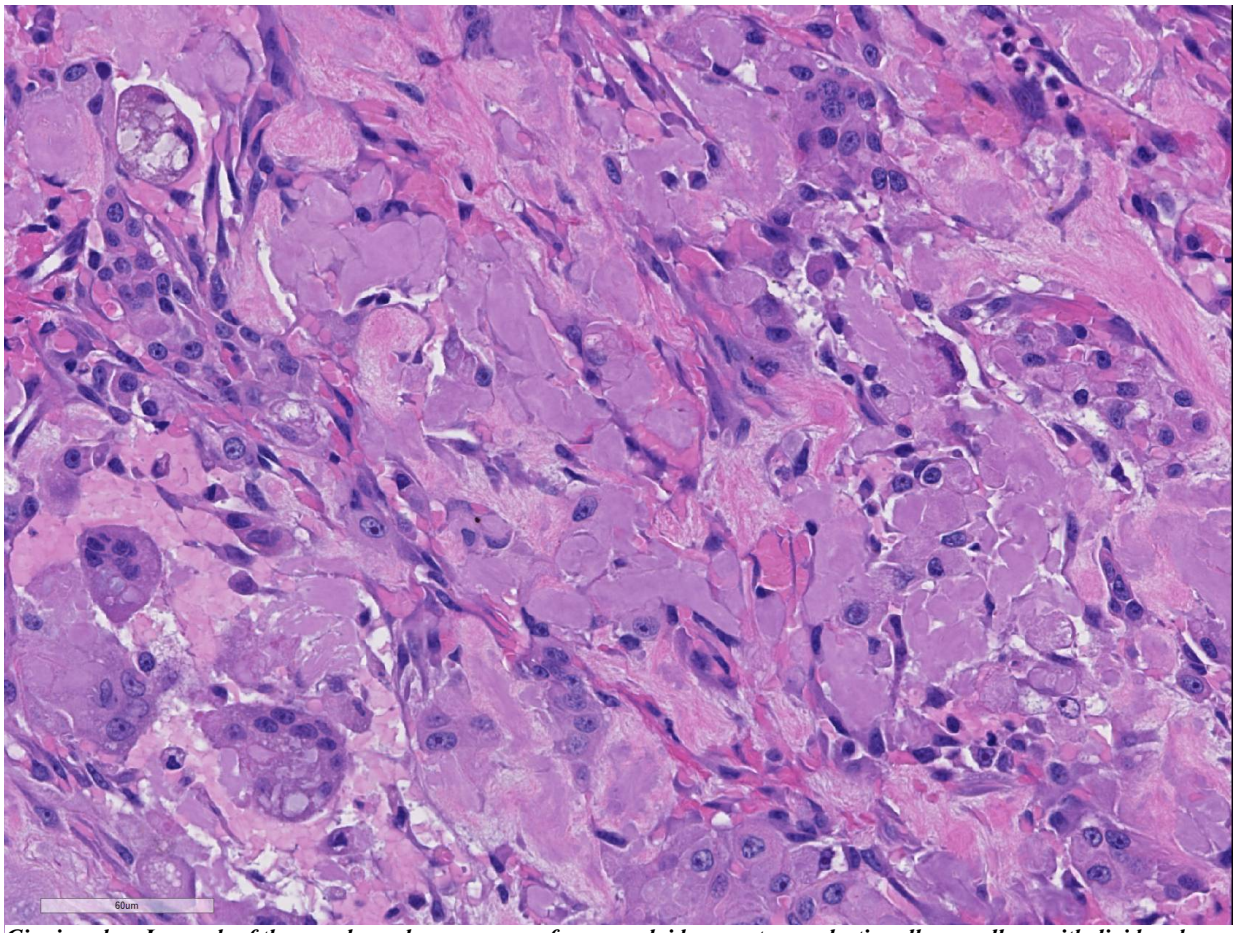

Gingiva, dog. In much of the neoplasm, large masses of way amyloid separate neoplastic cells as well as epithelioid and multinucleated foreign body type macrophages. (HE, 400jX)

trabeculae, and few small islands, supported by moderate amounts of fibrovascular stroma and with large amounts of extracellular amyloid. The cells are most dense near the edge of the mass, with increasing amounts of matrix centrally, with some central areas showing fewer neoplastic cells and increased amounts of fibrous connective tissue, or cavities of hemorrhage. The cells have distinct borders with rare prominent intercellular bridges, moderate amounts of eosinophilic cytoplasm, oval nuclei with finely stippled chromatin and 1-2 prominent magenta nucleoli. Anisocytosis and anisokaryosis are moderate. Few binucleate and rare multinucleate cells are noted. Mitotic figures are 2 per ten 400x fields. Many cells contain small to large amounts of amphophilic smudgy amorphous material (intracellular amyloid). In some areas cells are larger with more abundant eosinophilic cytoplasm, which occasionally forms concentric lamellae around the nucleus (keratin).

In many areas, cells are separated by moderate to large amounts of extracellular eosinophilic to amphophilic, smudgy, amorphous material (amyloid). In few areas, the cells are separated by islands and trabeculae of densely fibrillar eosinophilic matrix which has a less basophilic tincture than the amyloid and is often mineralized. There are multifocal areas of hemorrhage or

necrosis, with few large cavities filled with hemorrhage. Centrally there are regions of loose immature fibrous connective tissue containing few islands of neoplastic cells and matrix. Multifocally the mass is surrounded by a band of moderately cellular collagenous connective tissue with evenly spaced stellate cells reminiscent of periodontal ligament; multifocally these regions have many congested blood vessels and few regular trabeculae of woven bone.

A Congo Red histochemical stain stains the amyloid red, and under polarized light this material has a faint green birefringence.

Pancyokeratin (AE1/AE3) and vimentin immunohistochemistry both show strongly positive cytoplasmic labeling in neoplastic cells. The amyloid is weakly immunopositive for pancytokeratin.

Contributor's Morphologic Diagnosis:

Rostral mandible: amyloid-producing odontogenic tumor

Contributor's Comment: Amyloid-producing odontogenic tumor (APOT) is a rare neoplasm reported in dogs and cats.[1] Histologically they are characterized by odontogenic epithelium with extracellular and intracellular congophilic amyloid matrix. Features of odontogenic epithelium include thin trabeculae and islands of cells with centrally located cells having long intercellular bridges, and peripheral

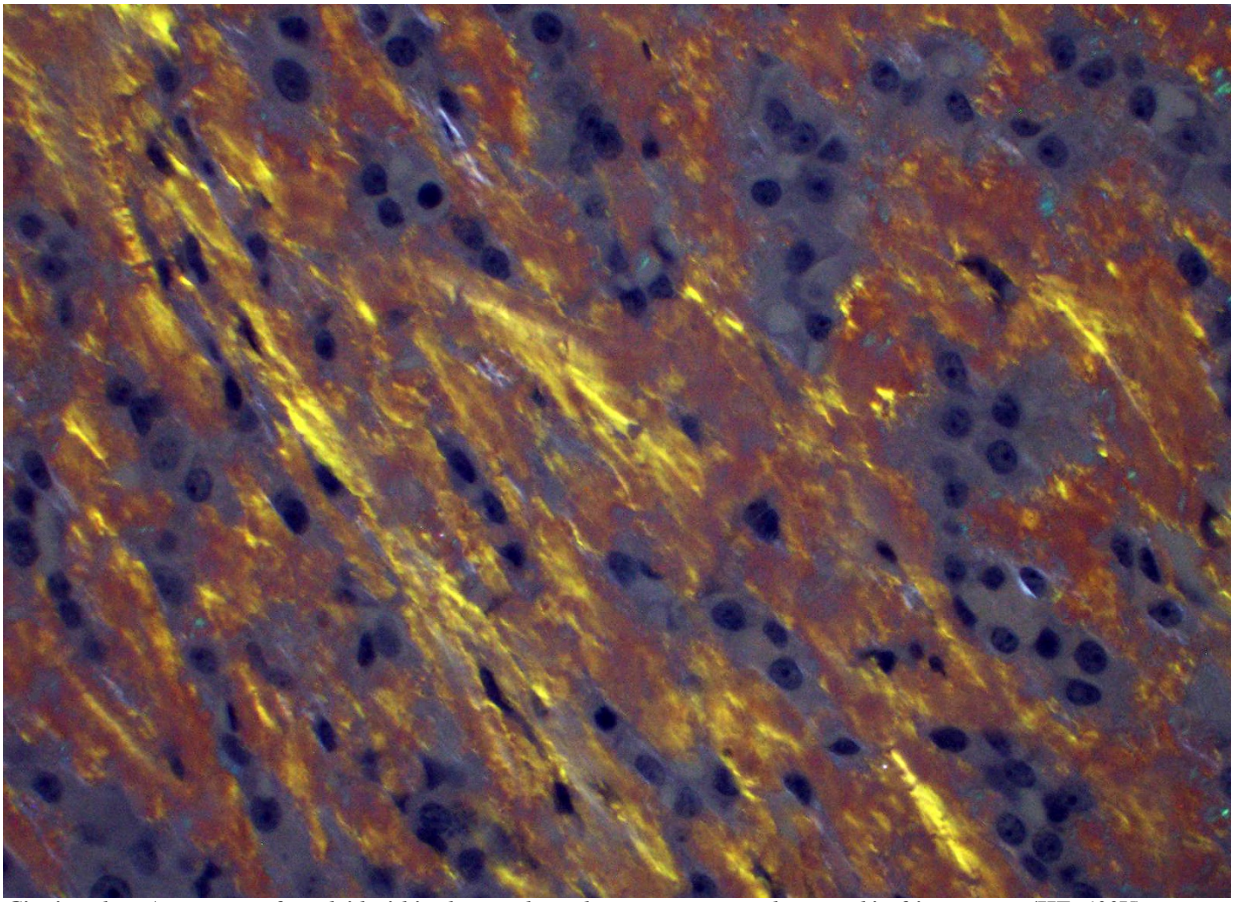

Gingiva, dog. Aggregates of amyloid within the neoplasm demonstrate an apple-green birefringence. (HE, 400X)

palisading cells with apical nuclei and basilar cytoplasmic clearing. These classical features may be difficult to demonstrate in some tumors, as in this case. Odontogenic epithelium may co-express both cytokeratin and vimentin,[3] as demonstrated in the immunohistochemistry results. Biologic behavior is slowly progressive but metastatic APOT has not been reported. Complete surgical removal is the treatment of choice. The nature of the amyloid protein in this tumor is reported to be a combination of enamel proteins.[2] This tumor has also been referred to as 'calcifying epithelial odontogenic tumor', but the term is borrowed from a human condition with several distinctly different features from APOT, including mineralization of matrix and sheets of polygonal cells.[1,4] APOT is not reported in humans.

Contributing Institution:

University of Wisconsin-Madison, School of Veterinary Medicine, 2015 Linden Drive Madison, WI 53706
www.vetmed.wisc.edu

JPC Diagnosis: Gingiva: Amyloid-producing ameloblastoma.

JPC Comment: Amyloid-producing odontogenic tumors (APOT), are rare tumors of the oral cavity and have been reported in dogs, cats, and in a goat, horse, rabbit, moose, Bengal tiger and a prairie dog.[6,9] These rare tumors have been reported to comprise between 1 and 4% of odontogenic neoplasms in the dog.[8] It has also been recently reported in the facial skin of cats within the supraorbital and labial skin.[4]

This history of this neoplasm has not been without controversy, as evidenced by the many names by which it has been referred to over the years. Originally diagnosed in humans in 1958 by J.J. Pindborg, the neoplasm in many early veterinary texts was referred to as a calcifying epithelial odontogenic tumor (CEOT) or "Pindborg tumor", but a 1994 publication by Gardner et al provided evidence that the human and veterinary versions of the neoplasm were distinct entities and proposed the name amyloid-producing odontogenic tumor.[9] Recent publications have suggested that the CEOT and APOT may be two stages along a spectrum of a tumor which produces a variety of substances such as dental hard substances such as cementum and dentin, amyloid, and keratin[9]. In a recently published textbook on veterinary oral and maxillofacial pathology, the tumor is referred to as an amyloid-producing ameloblastoma.[9]

These neoplasms are unencapsulated neoplasm that may arise either centrally or peripherally within the bone, which while widely considered benign, may aggressively invade bone.[8,9] The tissue or origin is not clear, and current thought of origin include some component of odontogenic epithelium of the dental lamina, stratum intermedium of the enamel organ, or Hertwig's epithelial root sheath.[9] The appearance of the epithelial component may vary widely from traditional columnar to spindled or even round in less differentiated regions of the tumor.[9] Some feline tumors may even have melanin granules within the epithelial component.[9] Pancytokeratin and vimentin may be helpful in differentiating between

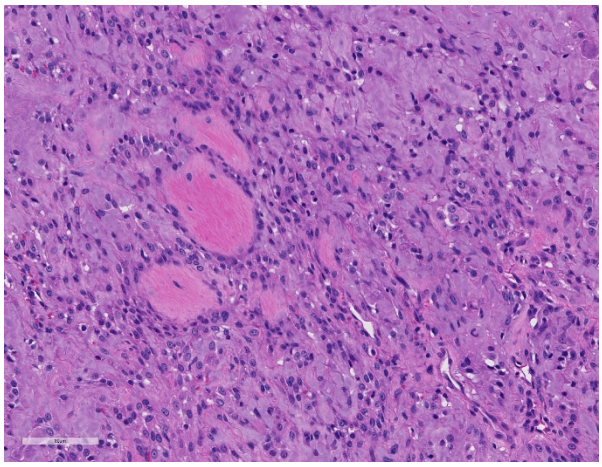

Gingiva, dog. Odontogenic cells occasionally surround islands of dental hard substance within the neoplasm. (HE, 100X)

epithelial, stromal, and inflammatory components.

The deposition of amyloid is the defining characteristic of this particular neoplasm. Amyloid within APAs has been shown to be different from AA, AL, and senile cardiovascular amyloid.[8] Odontogenic amyloid ameloblast-associated protein (ODAM), a feature of human CEOTs has not been identified within these tumors (supporting their distinction from the human CEOT), a number of other amyloid-related proteins have been found in canine and feline APAs, including amyloid protein of canine APOT, ameloblastin (also present in cat APAs), amelogenin, and sheathlin.[4,8] While the amyloid material in this case demonstrates congophilia and green birefringence on polarized light, the material is not always birefringent.[9] Some authors believe that the amyloid-like material represents dysplastic tooth matrix, as immunohistochemical analysis of the amyloid protein in several studies has indicated that it is of ameloblastic origin.[1, 3]

References:

1. Delaney MA, Singh K, Murphy CL, Solomon A, Nel S., Boy SC. Immunohistochemical and biochemical evidence of ameloblastic origin of amyloid-producing odontogenic tumors in cats. *Vet Pathol* 50(2): 238-242.
2. Head KW et al. Histologic classification of the tumors of the alimentary system in domestic animals. Washington DC, Armed Forces Institute of Pathology CL Davis DVM Foundation, 2003.
3. Hirayama K, Miyasho T, Ohmachi T, Watanabe T, Yokota H, Taniyama H. Biochemical and immunohistochemical characterization of the amyloid in canine amyloid-producing odontogenic tumor. *Vet Pathol*. 2010;**47**:915-22.
4. Hirayama,K, Endoh C, Kagawa Y, Ohmachi T, Yamagami T, Nomura K, Matsuida K, Okamotis M. Taniyama H. Amyloid producing odontogenic tumors of the facial skin in three cats. *Vet Pathol* 2017; 54(2): 218-221.
5. Izzati UZ, Hidaka Y, Hirai T, Yamaguchi R. Immunohistochemical profile of ameloblastic carcinoma arising from an amyloid-producing odontogenic tumor in a miniature dachshund. *J Comp Path* 2019; 106:54-58.
6. Kok, MK, Chamgers JK, Ushio N, Miwa Y, Nakayhama H, Uchida K. Amyloid-producing odontoameloblastoma in a black-tailed prairie dog. *J Comp Path* 2018; 159:26-30.
7. Miles CR, Bell CM, Pinkerton ME, Soukup JW. Maxillary ameloblastic fibroma in a dog. *Vet Pathol.* 2011;**48**:823-6.
8. Munday JS. Lohr CV, Kiupel M. Tumors of the alimentary tract. *In:*

Meuten DJ, ed., Tumors in Domestic Animals, 5th Ed, Ames IA: Wiley and Sons, 2017: 536-537.
9. Murphy BG, Bell CM, Soukup JW. Tumors composed of odontogenic epithelium and fibrous stroma. *In:* Veterinary Oral and Maxillofacial Pathology. Hoboken, NJ: Wiley and Sons, 2020, pp. 105-108
10. Regezi JA, Sciubba JJ, Jordan RCK. Odontogenic tumors. *In* Oral Pathology: Clinical pathologic correlations. St Louis MO Saunders Elsevier, 2008.

CASE II: H17-0922-03 (JPC 4122528).

Signalment: 4 year-old neutered male rabbit (*Oryctolagus cuni*culus).

History: The owner had noticed dysorexia and weight loss. A mandibular mass associated with malocclusion was diagnosed by the attending veterinarian. CT scan showed left mandibular neoplastic infiltration with osteolysis and periosteal reaction but no infiltration of the mandibular lymph nodes.

The animal was referred to the Centre Hospitalier Universitaire Vétérinaire d'Alfort (ChuvA) for a surgical exeresis with a left hemimandibulectomy. The animal died of cardiac arrest 30 minutes after the surgery during the recovery phase.

Gross Pathology: A non-ulcerated, firm, infiltrating, left mandibular mass measuring 1.5 x 2 cm in diameter with a central depressible zone caused an incisor malocclusion.

Laboratory results: NA.

Microscopic Description: Gingiva with mandibular bone:

A relatively well-delineated, unencapsulated neoplasm focally infiltrates the mandibular bone. It is admixed with preexisting dental and osseous structures, and is composed of several tissue types. The first is a dense proliferative fibrous mesenchymal tissue composed of fusiform to stellate cells (reminiscent of periodontal ligament) with multifocal osseous metaplasia. The second consists in squamous epithelial nests, sometimes with cystic degeneration (accumulating desquamated cells and red blood cells in the lumen). The third component is an inconstant association of epithelial and mesenchymal structures variably mimicking normal teeth. The best differentiated areas are organized around a loose mesenchyme reminiscent of the dental pulp (ectomesenchyme), covered by a single layer of cubic to columnar cells (odontoblasts) producing an orange tubular matrix (dentin). A hypereosinophilic amorphous material (enamel) lies against the dentin; it is synthetized by a well-differentiated columnar single-layered epithelium with an inverted polarity (apical nuclei and clear basal pole) and forming palisades (ameloblasts). Their apical pole is inconstantly in contact with stellate vacuolated epithelial cells (less differentiated: stellate reticulum). The infiltrated mandibular bone in contact with the tumor is multifocally osteolytic with Howship's lacunae containing osteoclasts and woven bone lined by osteoblasts.

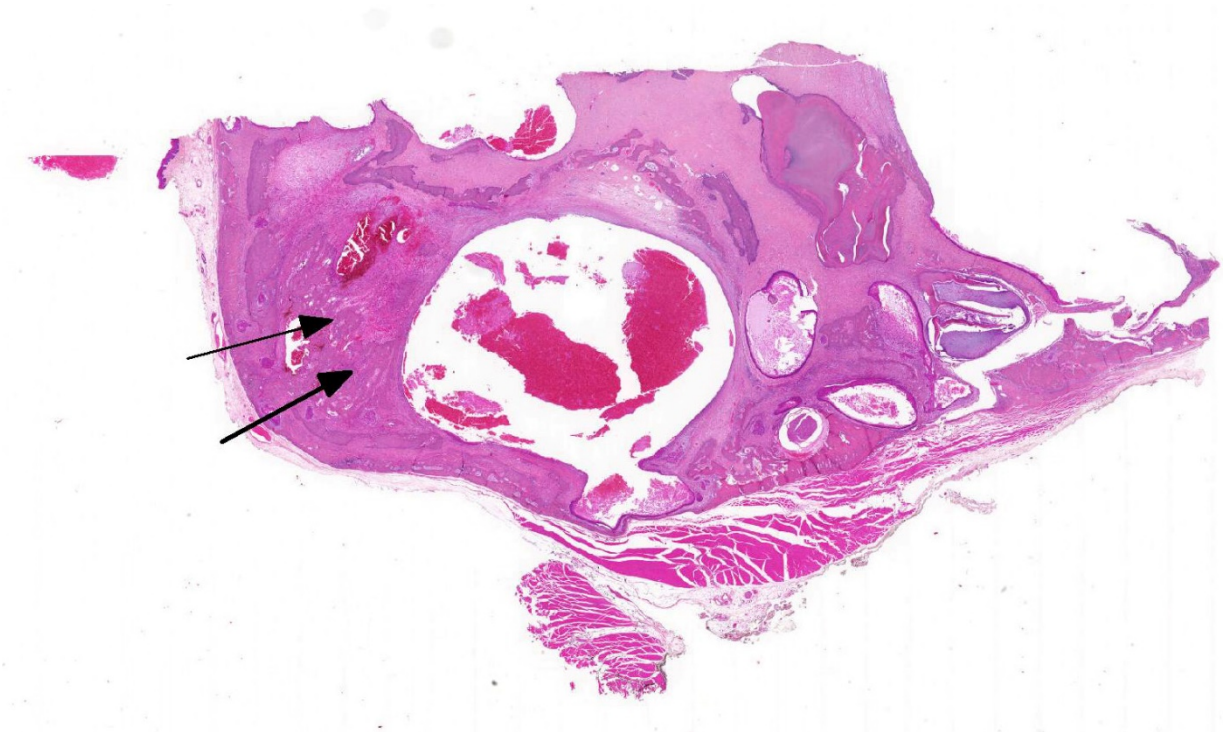

Alveolar bone, rabbit. The jaw bone (skeletal muscle at bottom) is effaced by a variably cystic neoplasm. Areas of bone lysis and resorption are evident and there is a large area of reactive woven bone formation adjacent to the neoplasm (arrows). (HE, 6X)

Contributor's Morphologic Diagnosis:

Gingiva with mandibular bone: Odontogenic tumor – Complex odontoma

Contributor's Comment: Odontogenic tumors are predominantly described in dogs and cats, and are rare in other species.[3,7] Due to their similarities and the complex organization of the teeth, they present a diagnostic challenge. Identification and classification of odontogenic tumors are based on recognizing developing or fully developed teeth tissues or odontogenic epithelium.

Knowledge of odontogenesis and components of teeth is therefore essential.

Teeth develop from two embryonic tissues[8]: oral cavity Malpighian epithelium and embryonic mesenchyme (ectomesenchyme).

At first, a fragment of oral Malpighian epithelium invaginates in embryonic mesenchyme to form the dental lamina. The latter progressively differentiates in enamel organ, an epithelial structure composed by central stellate reticulum, lined by external and internal ameloblastic epithelium (bell stage). The embryonic mesenchyme condenses under the internal ameloblastic epithelium to form the "dermal papilla", the future dental pulp. These epithelial and mesenchymal dental structures have an inductive effect on each other. It is called *reciprocal odontogenic induction*:

1) Internal ameloblastic epithelium promotes the differentiation of the superior part of the dental papilla in an odontoblast layer.

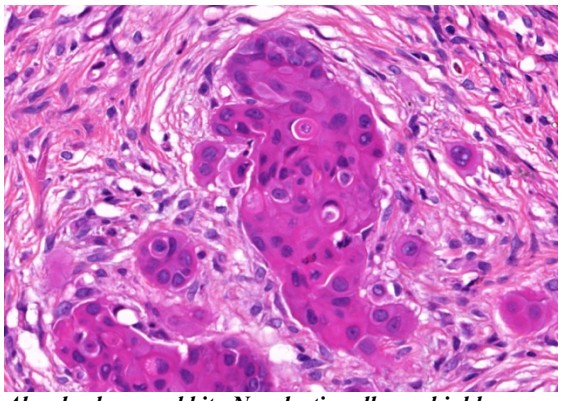

Alveolar bone, rabbit. Neoplastic cells are highly invasive, forming small nests or islands or simply individual cells surrounded by a schirrous response. Neoplastic cells exhibit occasional keratinization. (HE, 400X)

2) Odontoblasts secrete dentin which accumulates at the odontoblasts-ameloblasts interface.
3) Presence of dentin is necessary to enamel synthesis by ameloblasts. Enamel accumulates between the dentin layer and ameloblasts.

After odontogenesis, amelobasts degenerate during dental eruption, except in hypsodont species with continuously erupting teeth (such as rodents and rabbits).

The classification and diagnosis of odontogenic tumors is based on the quantity and localization of odontogenic epithelium, production of enamel, and presence or absence of ectomesenchyme (dentin, cementum, mesenchyme resembling the periodontal ligament or the dental pulp). Visualization of dental hard tissue such as enamel, dentin or cementum is helpful in recognizing an odontogenic tumor but is an inconstant finding.[3]

These tumors are separated in three groups:

1) **Tumors with only odontogenic epithelium** (without odontogenic ectomesenchyme):

Ameloblastoma, Canine acanthomatous ameloblastoma, Ameloblastic carcinoma, Amyloid producing odontogenic tumor

2) **Tumors with mesenchyme and/or odontogenic ectomesenchyme:** *Cementoma/cementoblastoma, Odontogenic myxoma/myxosarcoma, Peripheral odontogenic fibroma (previously called epulis)*

3) **Tumors with odontogenic epithelium and odontogenic ectomesenchyme** (with or without hard tissue):

Ameloblastic fibroma, Infiltrative inductive ameloblastic fibroma, Ameloblastic fibro-odontoma, ameloblastic Fibro-dentinoma, Ameloblastic fibro-odontosarcoma, Complex odontoma, Compound odontoma.

In our case, the concurrent identification of dentin, odontoblasts, mesenchyme tissue resembling periodontal or dental pulp (= ectomesenchyme), as well as ameloblasts producing enamel and stellate reticulum (= odontogenic epithelium), confirms this

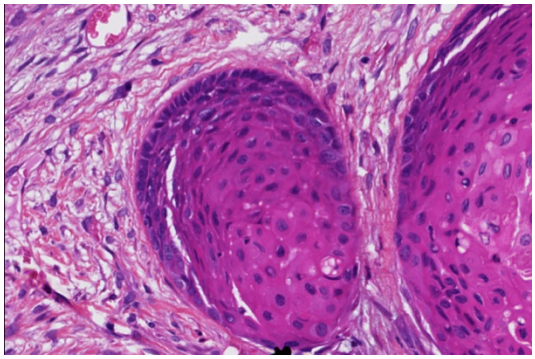

Alveolar bone, rabbit. Neoplastic cells rarely exhibit odontogenic features, including peripheral palisading and antibasilar nuclei.. (HE, 400XX)

neoplasm as an odontogenic tumor and directs the diagnosis towards a mixed odontogenic tumor. An odontoma is a dental tumor in which cell differentiation has resulted in formation of dentin and enamel. They are two types: *Complex* (poorly differentiated) and *Compound* (well differentiated, with denticle formation) [4] . The apparent disorganization of the odontogenic elements (absence of well-differentiated denticles) leads us to conclude that this particular neoplasm is a complex odontoma.

Complex odontoma are described in horses, dogs, cattle, rats and are located on the mandibular or maxillary arch. The etiology of odontomas is yet not known. Several hypotheses have been formulated: local trauma (and that continuously erupting teeth might be more sensitive to trauma), malocclusion (which may disrupt normal dental eruption), and infection.[1,9]

Furthermore, carcinogens such as methylnitrosourea may induce development of odontomas and other odontogenic tumors in rats.[1,9] In the literature, odontomas are rarely described in rabbits but are well characterized in prairie dogs: this tumor is the third tumor in frequency (9.4%) in that species, after hepatocellular carcinoma (35.8%) and lymphoid tumors (14%); affected animals are between 2 and 6 years

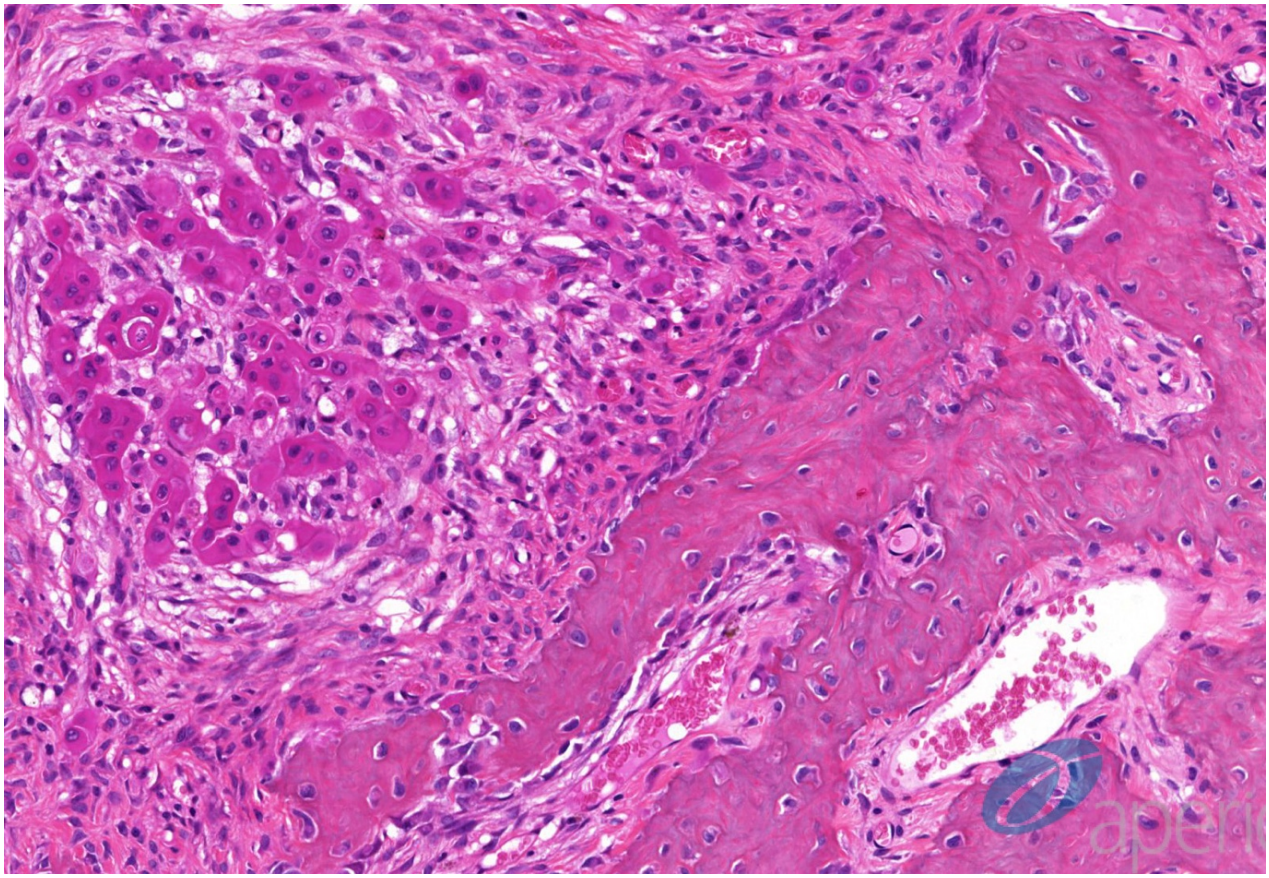

Alveolar bone, rabbit. Islands of neoplastic cells are surrounded by a schirrous response and abundant proliferative woven bone. (HE, 28X)

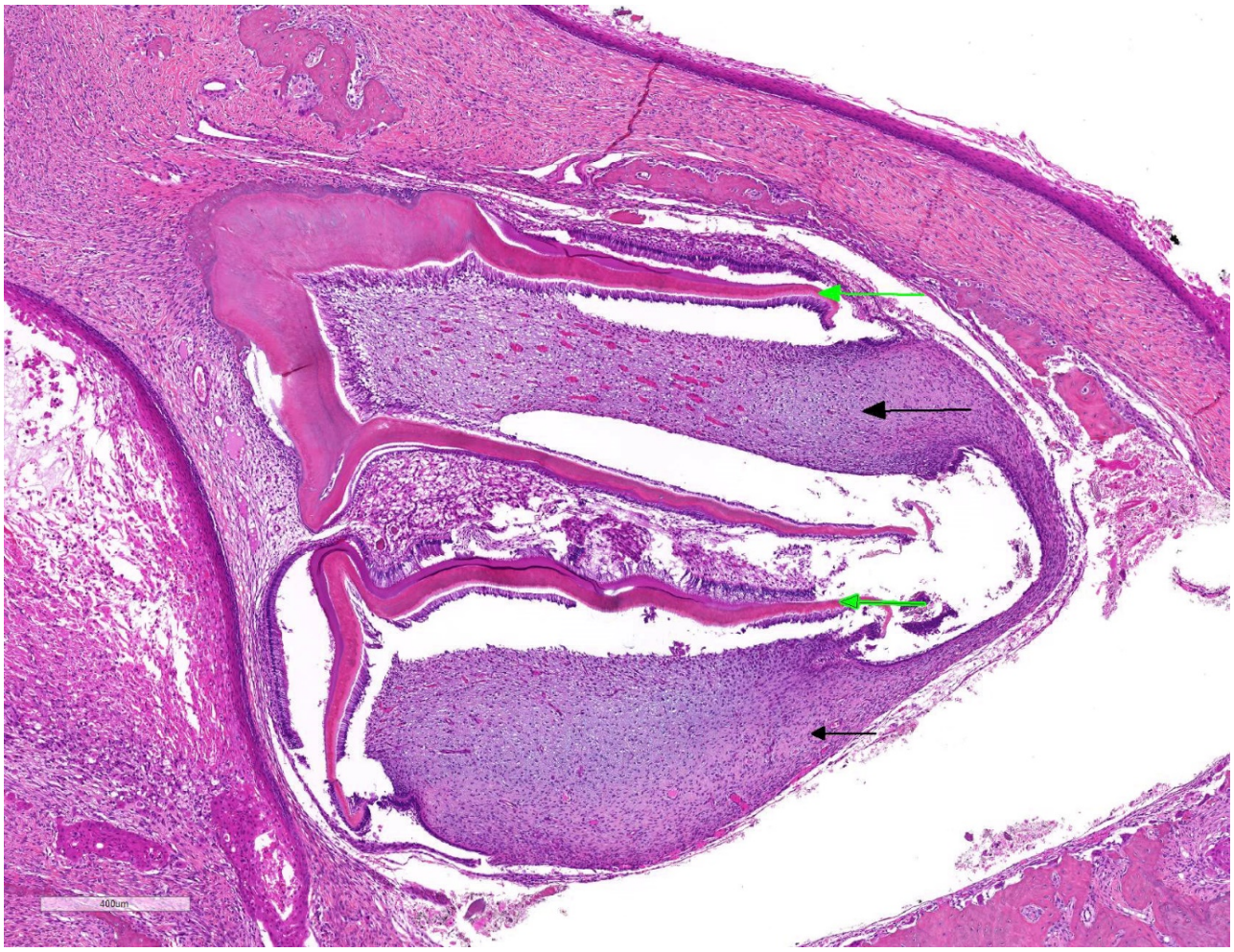

Alveolar bone, rabbit. The developing tooth is dysplastic with undulant enamel and dentin (green arrows) and widened dental papilla (black arrow), consistent with odontodysplasia. (HE, 51X)

of age, both maxillary and mandibular arches are affected but animals only display symptoms in maxillary tumors (anatomic proximity with the hard palate, posterior choanae and the posterior nasal meatus).[5]

Distinguishing complex odontoma from ameloblastic fibro-odontoma can be quite challenging. In both cases, diagnosis is based on identifying odontogenic epithelium reminiscent of the enamel organ, a loose odontogenic ectomesenchyme resembling dental pulp, and several types of hard dental tissue (dentin, cementum, enamel). In some case, the diagnostis is not possible by histopathology alone.[3] The age of animal and the type of tooth growth (continuously erupting or not) may be required to refine the diagnosis.

All odontogenic tumors are benign but locally aggressive. Only one case of malignant fibro-odontoma has been described, in a dog.[6] Surgical excision is curative in most cases, but may be quite complex to perform.

Contributing Institution:

Unité d'Histologie, d'Embryologie et d'Anatomie pathologique, Biopôle

Département des Sciences Biologiques et Pharmaceutiques
Ecole Nationale Vétérinaire d'Alfort
7 avenue du Général De Gaulle
94704 Maisons Alfort Cedex
FRANCE

JPC Diagnosis: Gingiva and alveolar bone: Carcinoma with odontodysplasia.

JPC Comment: In the sections we examined, the primary lesion was composed of a malignant, invasive epithelial neoplasm surrounded by a scirrhous response and woven bone proliferation. These features are consistent with a carcinoma. Potential sources for carcinoma include odontogenic epithelium (i.e. ameloblastic carcinoma; AC) or gingival epithelium (i.e. squamous cell carcinoma; SCC). There is substantial overlap between these diagnoses as both form islands of pleomorphic epithelial cells that can have some keratinization.

Generally, SCC has a greater degree of keratinization, is more inflammatory, and is associated with (potentially ulcerated) gingival mucosa. AC should have some features of odontogenic epithelium and can arise from either the gingival mucosa or deeper in submucosal connective tissue or jaw, without any evident connection to the gingival mucosa.[4] In this case, although both odontogenic epithelial features (there was rare palisading of cells with antibasilar nuclei) and keratinization were present, neither were prominent. Additionally, gingival mucosa was not present in the examined sections and we could not determine if this neoplasm arose from the overlying mucosa. Taken together, we favored a more general diagnosis of "carcinoma with odontodysplasia."

Odontodysplasia (OD) was evident in the developing teeth at the edge of the sections examined. Histologically, OD is a malformation of a tooth (or multiple teeth) or the components of a tooth. It occurs due to trauma to the dental germ during odontogenesis. Dysplastic teeth often fail to erupt.[4] There is substantial histologic overlap between OD and odontoma and distinguishing between these two can be difficult to impossible. The presence of concurrent inflammation/trauma (trauma in this case was from carcinoma with abundant scirrhous response and bony proliferation) should assist the pathologist in diagnosing OD over odontoma.

(A note of thanks to Dr. Brian Murphy of UCDavis for assistance with this very challenging case. His recent volume in oral and maxillofacial pathology was used in the determination of the JPC morphologic diagnosis in all of the cases this week.)

References:

1. Jang DD, Kim CK, Ahn B, Kang JS, Nam KT, Kim DJ, Han DU, Jung K, Chung HK, Ha SK, Choi C, Cho WS, Kim J, Chae C. Spontaneous complex odontoma in a Sprague-Dawley rat. *J Vet Med* 2002, 64 (3): 289-291.
2. Miwa Y, Nakata M, Takimoto H, Chambers JK, Uchia K. Spontaneous oral tumors in 18 rabbits (2005-2015). *J Small Anim Pract* 2019, https://doi.org/10.1111/jsap.13082

3. Munday JS. Lohr CV, Kiupel M. Tumors of the alimentary tract. *In:* Meuten DJ, ed., Tumors in Domestic Animals, 5th Ed, Ames IA: Wiley and Sons, 2017: 536-537.
4. Murphy BG, Bell CM, Soukup JW. Tumors composed of odontogenic epithelium and fibrous stroma. *In:* Veterinary Oral and Maxillofacial Pathology. Hoboken, NJ: Wiley and Sons, 2020: pp. 113-118
5. Pellizzone I, Vitolo GD, D'Acierno M, Stefanello D, Forlani A, Broich G. *l.* Lateral approach for excision of maxillary incisor pseudo-odontoma in prairie dogs *(Cynomys ludovicianus). In Vivo* 2016; 30: 60-68.
6. Ueki H, Sumi A, Takaishi H, Ito H, Oyamada T, Yoshikawa H. Malignant ameloblastic fibro-odontoma in a dog. *Vet. Pathol* 2004; 41: 183-185.
7. Uzal FA, Plattner BL, Hostetter JM. Alimentary System. *In*: Maxie MG ed., *Jubb, Kennedy, and Palmer's Pathology of Domestinc Animals, Vol 2.:* St. Louis, MO; Elsevier, 2017.pp. 22-28.
8. https://www.askjpc.org/wsco/wsc/wsc05/05wsc04
9. https://www.askjpc.org/wsco/wsc_showcase2.php?id=YlNvSG1QSENqZ09rK0Z6d09BUmdzUT09

CASE III: S2018-0004 (DVD) (JPC 4117676)

Signalment: 13 year old, female, Red-tailed boa (*Boa constrictor ortonii*)

History: This boa developed a mass along the inner (palatine) left maxillary dental arcade, and despite antimicrobial therapy, it continued to grow. Radiographs demonstrated widening of the bone with lysis. The mass was resected and submitted for histopathological examination.

Gross Pathology: The sample received was a 3.5 cm x 1.8 cm x 1.4 cm fleshy to firm, oblong, pink to dark red and purple mass with three teeth embedded on one lateral side. On cut section, the mass appeared to extend to the deep margin and was composed of multifocal, tan, soft regions and firm, white, bony regions.

Laboratory results: NA.

Microscopic Description: Gingiva with mandibular bone:

Oral mass: Expanding the submucosa and raising the overlying mucosal epithelium is a poorly demarcated, unencapsulated, neoplasm composed of epithelial and mesenchymal elements that frequently form haphazardly arranged, variably sized and shaped, tooth-like structures on a moderate fibrovascular stroma. Islands and wavy aggregates of brightly eosinophilic extracellular material with fine tubular

Head, boa. Pre-operative image of an expansile mass arising from the left maxillary, dental arcade. (Photo courtesy of: Wildlife Conservation Society, 2300 Southern Blvd., Bronx, NY 10460, https://www.wcs.org/)

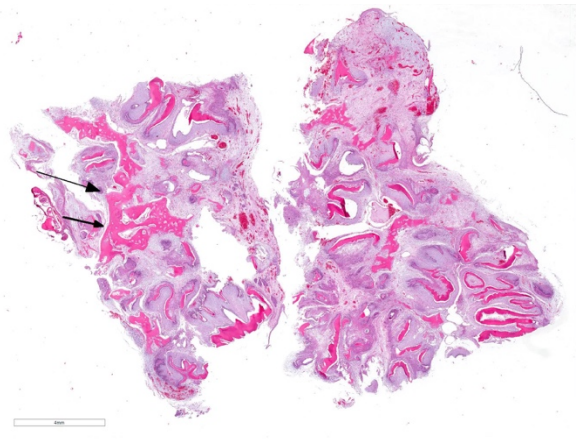

Maxilla, boa. Two sections of the mass are submitted for examination. Numerous attempts at recapitulating teeth with brightly eosinophilic dentin efface the maxillary bone (arrows). (HE, 7X)

cavities (dentin) and an occasional adjacent clear gap are surrounded on one aspect by a layer of well-differentiated, palisading odontoblasts and on the other aspect by variably thick rows and sheets of tightly packed columnar to polygonal shaped cells with apically oriented nuclei (ameloblasts). The ameloblasts are often arranged in palisading rows overlying loosely arranged stellate to fusiform cells with prominent intracellular bridging (stellate reticulum). In other regions, odontogenic epithelium is more haphazardly arranged in sheets, small follicles, or branching, anastamosing trabeculae and islands that have a peripheral palisade of cells and infiltrate into the surrounding mesenchyme. Occasionally, islands and trabeculae bud off from rows of ameloblasts bordering dentin material. Within the mass, neoplastic odontogenic epithelium occasionally form cords and nests that are not associated with dentin, with multifocal areas of prominent cellular vacuolation (degeneration) or loss of cells and accumulation of pale, basophilic wispy material admixed with sloughed cells and pyknotic nuclear debris. The neoplastic cells have distinct cell borders with small to moderate amounts of eosinophilic cytoplasm, round to oval nuclei with finely stippled chromatin and one to two, small central nucleoli. There is mild to multifocally moderate anisocytosis and anisokaryosis in this population with 6 mitotic figures in ten 400x figures. Multifocally, neoplastic cells undergo abrupt keratinization. Spindle to stellate mesenchymal cells with an accompanying vascular component (dental pulp) are often present centrally within the tooth-like structures. Infrequently, the eosinophilic dentin material is surrounded by small numbers of multinucleated odontoclasts. Multifocally, there are trabeculae of moderately cellular, woven new bone and small amounts of existing lamellar bone that are occasionally surrounded by small numbers of osteoblasts or small numbers of multinucleated osteoclasts in Howship's lacunae. The overlying mucosa is largely ulcerated and the subjacent submucosa is expanded by increased clear space and pale eosinophilic proteinaceous material (edema). In one section (slide 2), the ulcerated mucosa is covered by a dense band of eosinophilic degenerate material, with small to moderate numbers of granulocytes infiltrating into the subjacent submucosa. Scattered throughout the mass and submucosa are small to moderate numbers of histiocytes, lymphocytes and plasma cells.

Contributor's Morphologic Diagnosis:

Oral mass, inner (palatine) left dental arcade: Ameloblastoma arising in an odontoma (previously odontoameloblastoma) with mucosal ulceration and proliferative new bone

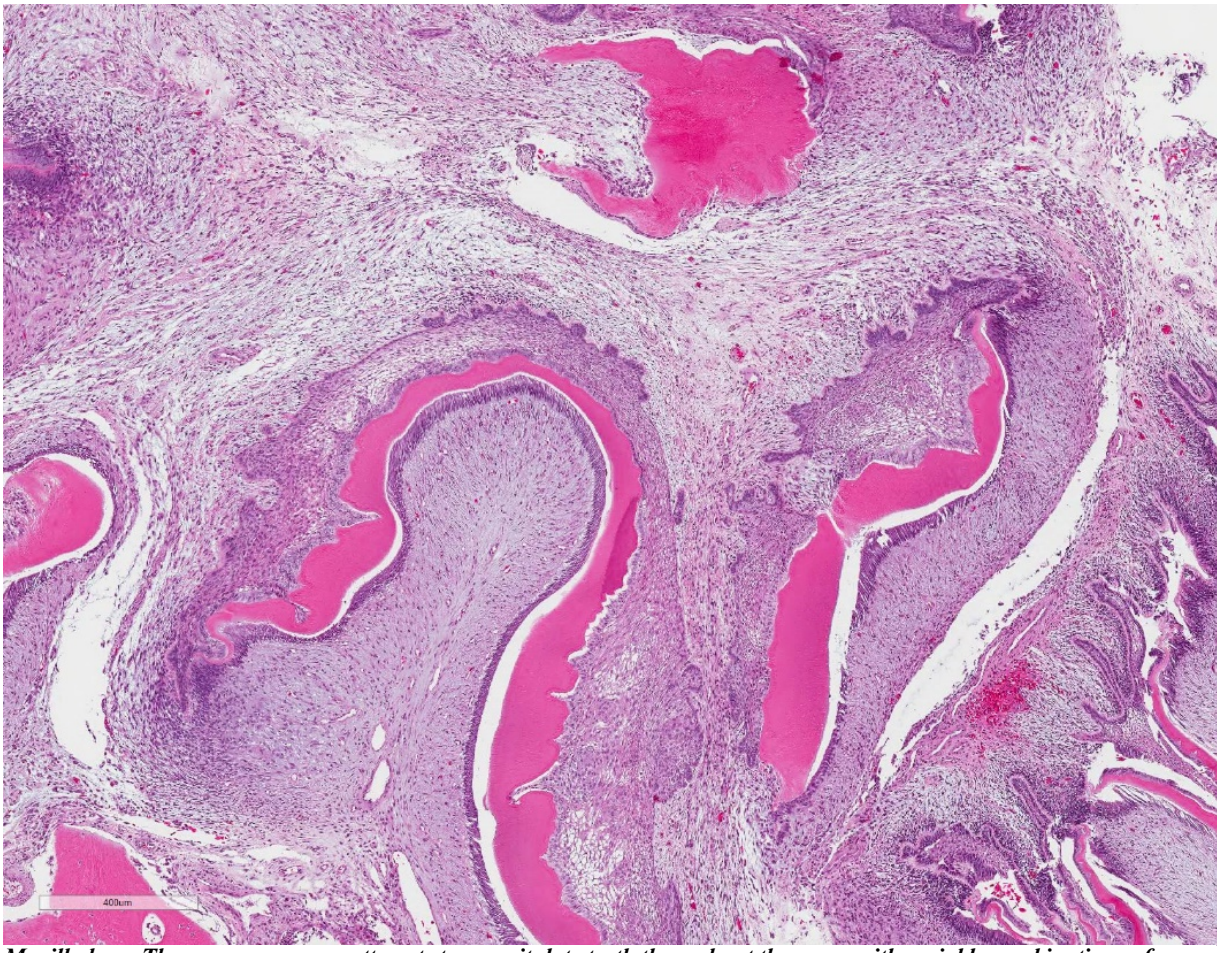

Maxilla boa. There are numerous attempts to recapitulate teeth throughout the mass, with variable combinations of ameloblasts, stellate reticulum, tubular dentin, odontoblasts, and mesenchyme resembling dental pulp. (HE 54X)

Contributor's Comment: Histologic evaluation of the oral mass revealed a mixed odontogenic tumor containing a neoplastic population of odontogenic epithelium (ameloblastoma) as well as a differentiated mesenchymal component and tooth-like structures (odontoma). The combination of these two findings was most consistent with an ameloblastoma arising in an odontoma (AAO) or odontoameloblastoma (OA), an uncommon odontogenic neoplasm in veterinary and human medicine. In the most recent (2017) WHO classification of head and neck tumors, the term odontoameloblastoma (or ameloblastic odontoma) was discussed.[7] The current consensus concluded that, due to the lack of evidence that these tumors begin or recur as odontoameloblastomas, and that they often recur as ameloblastomas, the term ameloblastoma arising in an odontoma (AAO) was more appropriate.

Odontoameloblastomas have been reported in domestic and non-domestic mammalian species, but to our knowledge have not been recognized in reptiles.[1,4,5,8,13] An ameloblastoma has been reported in a wild black rat snake, with a single mass on the mandible.[2] In humans, OA or AAO are often locally aggressive with behavior and prognosis similar to ameloblastomas. In the

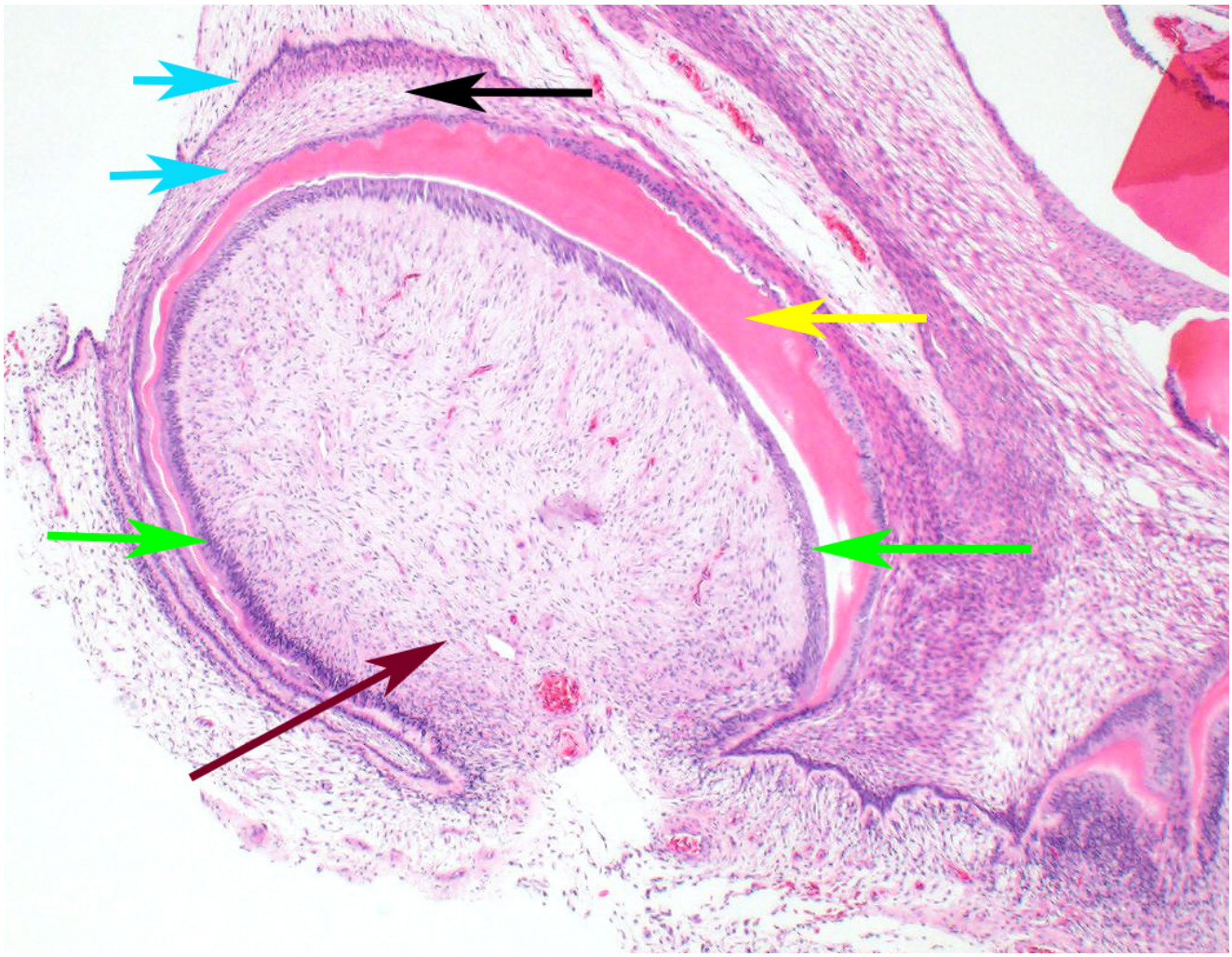

Maxilla, boa. In a particularly well-formed prototooth at the edge of one section, a rudimentary enamel organ containing two layers of ameloblasts (blue arrows) separated by stellate reticulum-like tissue (black arrow), abuts a layer of dentin (yellow arrow), a layer of odontoblasts (green arrows), and surrounds vascular mesenchyme resembling dental pulp. (HE 40X)

veterinary literature, odontoameloblastomas are similarly locally aggressive and expansile with destruction of the adjacent bone of the jaw. The mandible is a common site of the primary tumor, [1,4,5,8,13] though the lesion was maxillary in this case.

Diagnosis of an odontoameloblastoma relies on the presence of three components: neoplastic odontogenic epithelium, a mesenchymal component reminiscent of dental pulp, and dental matrix (dentin and enamel). Differentiation of an odontoameloblastoma or AAO from other mixed odontogenic tumors relies not only on the presence of these components but also the relative amount. Differentials such as an ameloblastic fibro-odontoma and ameloblastic fibroma should have a predominant ectomesenchyme (pulp stroma) component, and odontomas (both complex and compound), should have less odontogenic epithelium.

In this case, the mass did extend to the margins of the examined sections, and bony lysis was suspected on radiographs. However, no gross evidence of recurrence was noted at 4 months follow up.

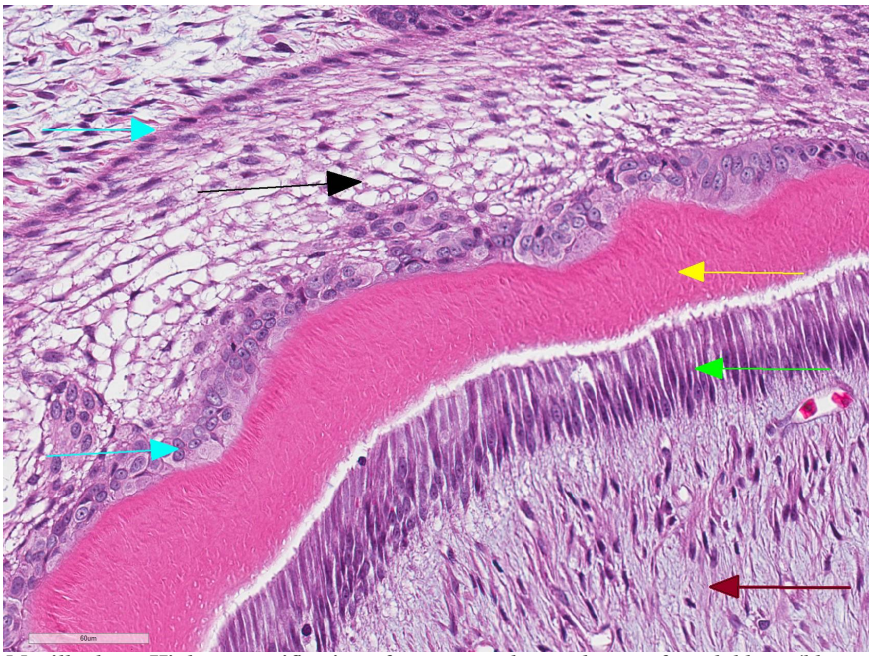

Maxilla, boa. Higher magnification of a prototooth., two layers of ameloblasts (blue arrows) are separated by stellate reticulum-like tissue (black arrow), abut a layer of dentin (yellow arrow), a layer of odontoblasts (green arrows), and surrounds vascular mesenchyme resembling dental pulp. (HE, 380X)

Contributing Institution:

Wildlife Conservation Society
2300 Southern Blvd.
Bronx, NY 10460
https://www.wcs.org/

JPC Diagnosis: Gingiva and alveolar bone: Compound odontoma.

JPC Comment: This case is an excellent example of the difficulties of subclassifying odontogenic neoplasms, especially those in exotic species. While attendees had no problem identifying odontogenic epithelium and mineralized dental matrix, the issue of differentiating ectomesenchyme of the dental papilla from the surround loose fibrous stroma of the neoplasm, especially in a reptile, proved to be a challenge.

While careful consideration was given to the contributor's diagnosis of odontoameloblastoma, we prefer a very slightly altered diagnosis of odontoma. While we agree that this is a neoplasm composed of odontogenic epithelium, dental hard substance, and ectomesenchyme, in the sections we examined, we could not identify an overwhelming odontogenic epithelial proliferation to make the diagnosis of OA. The diagnosis of OA requires a greater proportion of odontogenic epithelium than in odontoma. In this case, the odontogenic epithelium was generally associated with prototeeth (i.e. well-formed denticles), as is seen in odontomas. While there are some areas of the tumor in which sheets of odontogenic epithelium are present without the formation of dental matrix or any apparent inductive effect on the surrounding mesenchyme, the majority of the neoplasm is composed of areas in which these three components are clearly represented.

Odontogenic neoplasms have been rarely reported in snakes, with a single previous report of ameloblastoma in a wild black rat snake (*Pantherophis alleghanensis)*[2] and a peripheral odontogenic fibromyxoma in a red tail boa (*Boa constrictor constrictor)* co-infected with arenavirus (inclusions were

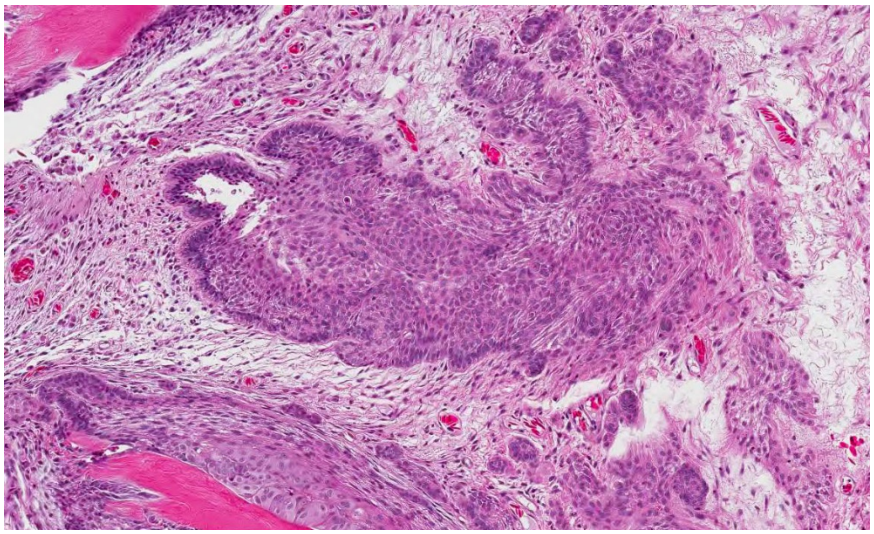

Maxilla, boa. In some areas, sheets of odontogenic epithelium, lacking any mineralized matrix or inductive effect, infiltrate the stroma. (Photo courtesy of: Wildlife Conservation Society, 2300 Southern Blvd., Bronx, NY 10460, https://www.wcs.org/)

not seen in the neoplastic cells, unfortunately.)[7]

Snakes, like most reptiles (with the exception of some lacertids to include bearded dragons), fish, and amphibians are polyphydont, with continuous tooth renewal as opposed to humans, which are diphyodont, or monophyodont animals with continuously growing teeth (i.e, mice.) In polyphyodon models, teeth are not regenerated following tooth loss, but are continually developed under a highly complex and coordinated process including a number of important genes and gene products to include sonic hedgehog and Wnt/b-catenin. Those readers interested in this process are referred to references 6 and 9.

References:

1. Burrough ER et al. Spontaneous odontoameloblastoma in a female Sprague Dawley rat. *JVDI*. 2010.22:998-1001.
2. Comolli JR et al. Ameloblastoma in a wild black rat snake (Pantherophis alleghaniensis). *JVDI*. 2015. 27(4): 536-539.
3. Dubielzig RR. Odontogenic tumors and cysts. In: Meuten DJ, ed. *Tumors in Domestic Animals*. 4th ed. Ames, IA: Iowa State University Press; 2002:402-409.
4. Dubielzig RR, Griffith JW. An odontoameloblastoma in an adult sheep. Vet Pathol. 1982. 19:318-320.
5. Elvio L, et al. Odontoameloblastoma in a calf. J Vet Dent. 2013. 30:248-250.
6. Gaete M, Tucker AS. Organized emergence of multiple-generations of teeth in snakes is dysregulated by activation of Wnt/beta-catenin signaling. *PLOS One* 2013; 8(9):e77784.
7. Hellebuyck T, Pasmans F, Ducatelle R, Saey V, Martel A. Detection of arenavirus in a peripheral odontogenic fibromyxoma in a red tail boa with inclusion body disease. *J Vet Diagn Invest* 2014; 27(2):245-248.
8. Murphy B et al. Mandibular odontoameloblastoma in a rat and a horse. *JVDI*. 2017. 29(4):536.
9. Murphy BG, Bell CM, Soukup JW. Tumors composed of odontogenic epithelium and fibrous stroma. *In:* Veterinary Oral and Maxillofacial Pathology. Hoboken, NJ: Wiley and Sons, 2020: pp. 113-118.
10. Richman JM, Handrigan GR. Reptilian tooth development. *Genesis* 2011; 49:247-260.

11. Uzal FA et al. Alimentary system. In: Maxie MG, ed. *Jubb, Kennedy and Palmer's Pathology of Domestic Animals*. 6th ed. St. Louis, MO: Elsevier; 2016:22-24.
12. Wright JM et al. Update from the 4th Edition of the World Health Organization Classification of Head and Neck Tumours: Odontogenic and Maxillofacial Bone Tumors. *Head Neck Pathol.* 2017.11(1):68-77.
13. Yanai T et al. Odontoameloblastoma in a Japanese monkey (macaca fuscata). Vet Pathol. 1995. 32:57-59

CASE IV: AR17-0027-7 DVD (JPC 4117660).

Signalment: 4-month-old male prairie vole (*Microtus ochrogaster*)

History: On the day of necropsy, this animal was found hunched, and had dried blood around the anus and on the feces. Euthanasia via C02 and cervical dislocation was performed due to poor prognosis.

Gross Pathology: The roots of both first mandibular molars extended ventrally (2x2x1 mm) beyond the body of the mandible, and had blackened tips. The roots of both of the second mandibular molars extended from the body of the mandible, curling laterally and dorsally (3x2x1 mm). The tooth roots of maxillary molars 2 and 3 extended through the skull and into the ventral cranial vault, in the area of the pituitary gland, with the cranial pair extending in 1x1x1 mm and the caudal pair, 3x2x2 mm. An intussusception was present involving the ansa spiralis coli and proximal colon.

Laboratory results: NA.

Microscopic Description:

Sagittal section of the skull: The molar roots extend cranially, the first molar (M1) compresses the nasal sinuses, and the second and third molars (M2 and M3) extend into the cranial vault. The pulp cavities and dentin have irregularly scalloped edges, and the stellate reticulum is retained. The cortical bone overlying the molars is thin, irregularly scalloped, and has many smooth (resting) and haphazard (reversal) basophilic lines throughout. The bone is lined by closely spaced osteoblasts and fewer osteoclasts in Howship's lacunae, and some osteocytes are pale without cellular detail, or are not present in lacunae (necrosis).

Contributor's Morphologic Diagnosis:

Dental dysplasia with invasion of the cranium, maxillary molars

Degeneration and regeneration, multifocal, chronic, moderate, maxilla

Contributor's Comment: This animal was one of sixteen cases of laboratory prairie voles (*Microtus ochrogaster*) at our facility which presented with varying degrees of molar apical elongation in the mandible and/or maxilla. The animals ranged from 4 to 13 months old, and both genders were represented. All cases had bilateral mandibular molar roots that extended apically beyond the body of the mandible, and fourteen voles had maxillary molars which extended apically through the skull into the cranial vault and compressed the nasal sinuses. The histologic findings for all of these animals revealed dental dysplasia

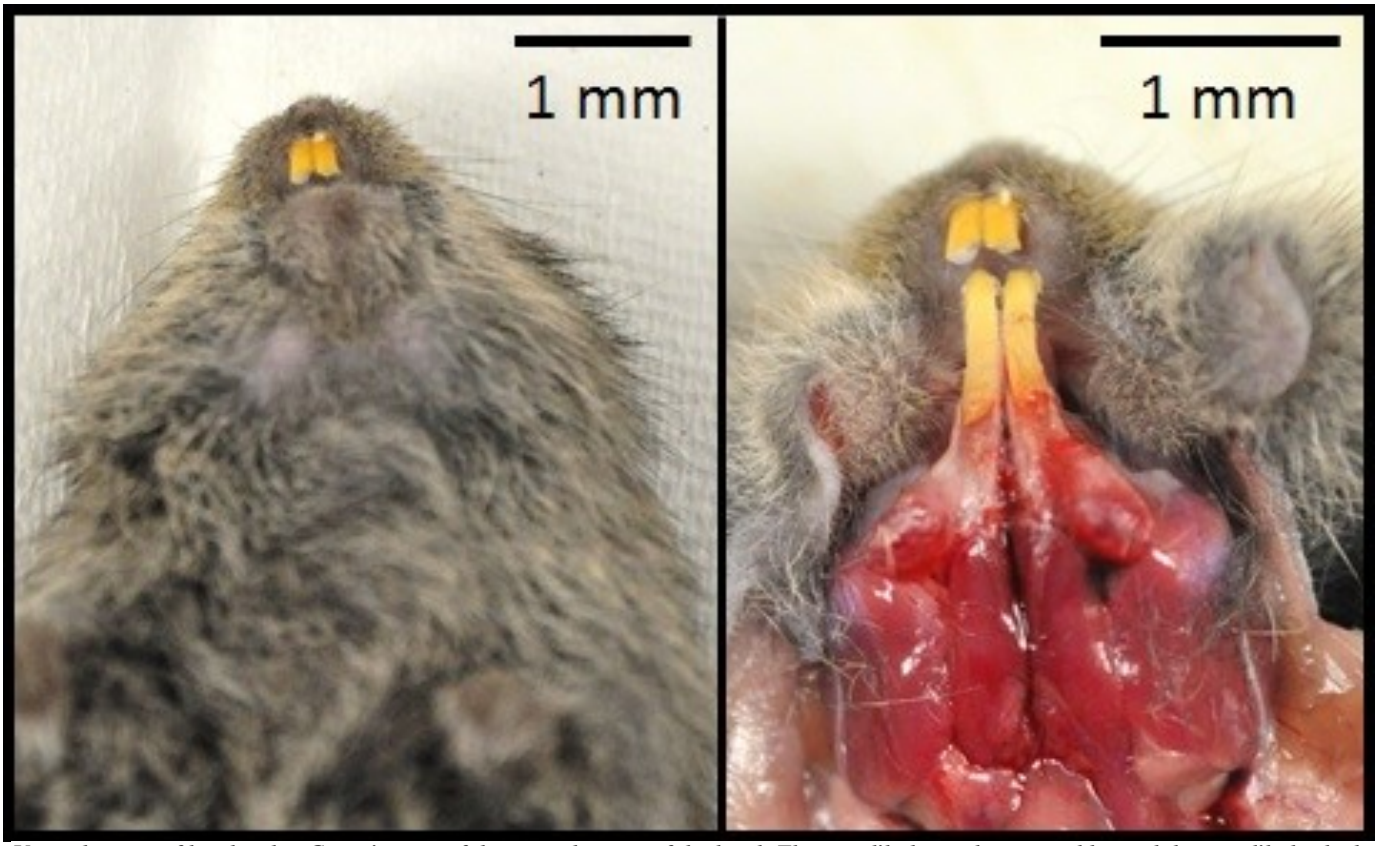

Ventral aspect of head, vole: Gross images of the ventral aspect of the head: The mandibular molars extend beyond the mandibular body. (Photo courtesy of: Department of Comparative Medicine, Wake Forest School of Medicine, 1 Medical Center Boulevard, Winston-Salem, NC 27157)

with abnormal dentin, irregular pulp cavities, and marked remodeling of the surrounding bone.

There was neither apparent correlation between age and the size of the mandibular root protuberances, nor between the size and any clinical sign. Six prairie voles had oral lesions (abscessation, food impaction, ulceration, osteomyelitis) which were attributed to the dental deformity, three had concurrent coronal incisor overgrowth, and two died of sepsis secondary to oral infection. The brain was unaffected in all but three cases where cerebral compression was noted.

Prairie voles have aradicular hypsodont dentition[10], which displays continual growth of teeth throughout life, offsetting the wear incurred from a fibrous diet. Other terms for this pattern of growth are hypselodont or elodont dentition.[8] Unlike other rodents including mice (*Mus musculus*) which have only continual growth of the incisors, all vole teeth, including the one incisor and three molars in each quadrant, continually grow. Other animals with complete aradicular hypsodont dentition include rabbits, guinea pigs, and chinchillas.[12] It has been proposed that the persistence of the stellate reticulum plays a role in the perpetual tooth growth in the incisors of mice and vole teeth.[8] The stellate reticulum is a stem cell niche within the cervical loop of the proximal tooth which sits between the inner and outer enamel epithelia.[9] Epithelial

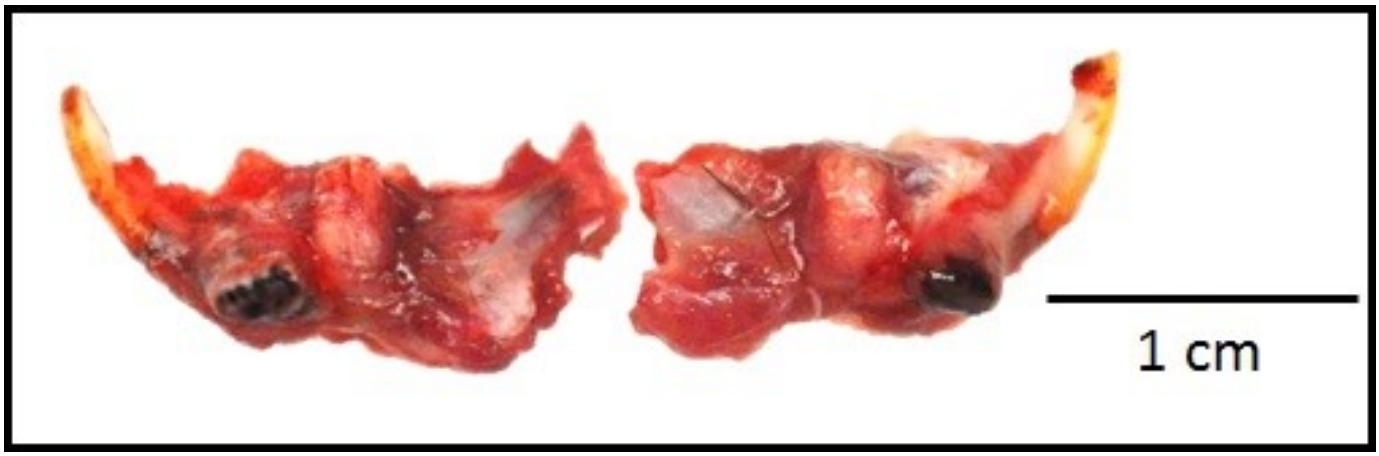

***Mandibles, vole:** The roots of the first and second mandibular molars extend beyond the body of the mandible. The first mandibular molars have blackened tips, and the second mandibular molars curl laterally and dorsally. (Photo courtesy of: Department of Comparative Medicine, Wake Forest School of Medicine, 1 Medical Center Boulevard, Winston-Salem, NC 27157)*

stem cells are thought to be located within the stellate reticulum and enamel epithelium (also known as Hertwig's epithelial root sheath) at the edge of the cervical loop. Stellate reticulum stem cells migrate to the inner enamel epithelium and support proliferating cells which then relocate distally to differentiate into ameloblasts.[14] In mice, the stellate reticulum of the molars regresses during maturation, explaining the cessation of growth. The regulation of growth in mouse incisors and the molars of sibling voles (*Microtus rossaiemeridionalis*) have been shown to be under the influence of FGF10, *Sox*2+ and Notch signaling, in addition to potential influence of BMP4.[2,14] The histology presented from this case showed retention of the stellate reticulum in the maxillary molars of an adult vole with dental dysplasia. Normal teeth from unaffected adult animals in this cohort also had retained stellate reticulum.

Similar findings in a colony of prairie voles at another facility have been studied, and it was speculated that a spontaneous mutation in dental stem cell regulatory genes was responsible for the condition. The inheritance was considered to be complex, as experimental inbreeding of affected animals produced no gross molar changes in the F2 offspring by 8-12 months of age.[8] In both this study and observations from our cases some animals were lethargic, moribund, or found dead, which was thought to have been attributable to the invasion of the skull and compression of the brain, although a definitive link could not be established.

A number of *Microtus* species (including *M. californicus californicus, M californicus vallicola, M. montanus, M. pennsylvanicus,* and *M. socialis*) have been reported with this abnormality[4]. Molar apical elongation in a colony of captive Amargosa voles (*Microtus californicus scirpensis*) was attributed to clinical signs including abnormal mentation, ocular discharge and abnormal mastication. Histology of these lesions showed variable hyperplasia, dysplasia, and atrophy of the inner and outer enamel epithelial layers.[4] A Japanese field vole (*Microtus montebelli*) from one study presented with maxillary molar macrodontia that protruded apically and invaded the brain as deep as the

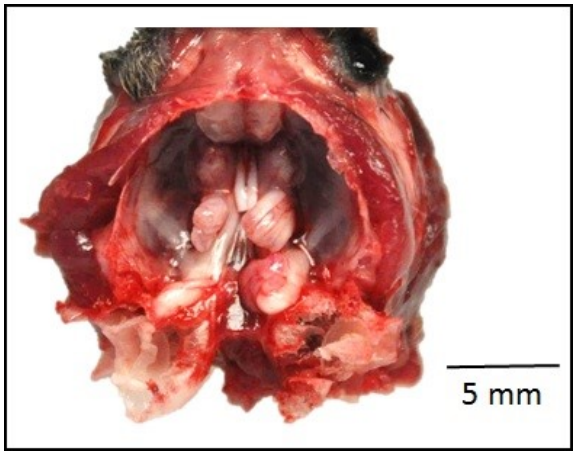

Ventral cranium: The tooth roots of maxillary molars 2 and 3 extend into the cranial vault. (Photo courtesy of: Department of Comparative Medicine, Wake Forest School of Medicine, 1 Medical Center Boulevard, Winston-Salem, NC 27157)

thalamic nuclei.[13] Coronal molar overgrowth without incisor abnormalities has been reported in a colony of laboratory pine voles (*Microtus pinetorum*). Changes in the husbandry of the pine vole colony, which included increasing dietary roughage and adding hard wood as enrichment, appeared to prevent further occurrence of this lesion.[3]

Although the stellate reticulum was also retained in the incisors of the adult voles in our cases, none of the incisors displayed apical elongation. This suggests that the cause of the dysplasia is more complex than simply a mutation in the stellate reticulum, or perhaps the incisor and molar stem cell niches are dissimilar. Another supposition is the possibility that a causative mutation may only affect the molar-specific mechanic and transduction pathway, or there may be differences in the periodontal ligament anchorage between incisors and molars.[8] Some studies have suggested that the cause of molar apical elongation is multifactorial, including genetic predisposition, deficient occlusal attrition and environmental factors such as inadequate roughage in the diet.[4]

A colony of Steppe lemmings (*Lagurus lagurus*), which are aradicular hypsodonts in the same subfamily as voles, had apical odontogenic dysplasia of the mandibular and maxillary molars with cranial vault invasion. In contrast, on histology, the apical overgrowths were composed of highly disorganized mature odontogenic structures, and more closely resembled hamartomas, which in aradicular hypsodonts have been termed elodontomas[5].Changes comparable to molar apical elongation and elodontoma formation occur in many aradicular hypsodont animals, including rabbits, squirrels, and degus.[1,6,7] These findings indicate that some degree of apical molar overgrowth is intrinsic in species with this dentition.[4]

Contributing Institution:

Wake Forest School of Medicine
Department of Pathology, Section on Comparative Medicine

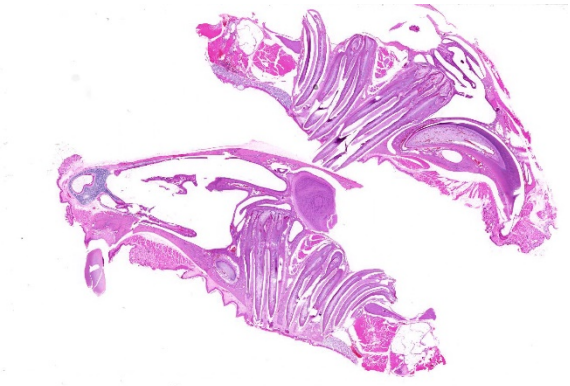

Sagittal section of head, vole. Two sagittal section of the head are presented for evaluation. There is marked elongation of the cheek teeth in both sections and they protrude into the overlying maxillary sinus. (HE, 5X)

Medical Center Boulevard, Winston-Salem, NC 27157
www.wakehealth.edu

JPC Diagnosis: Head, sagittal section, cheek teeth: Odontogenic dysplasia with alveolar bone remodeling, and penetration of the maxillary sinus and calvarium.

JPC Comment: The contributor has given us an excellent review of dental growth in rodents as well as the available literature on dysplastic teeth lesions in the rodent. Hyperplasia and dysplasia with apical elongation appears to be a considerable problem in voles of the genus *Microtus*. The changes noted in this particular case are similar to those which were well-described in a captive colony of Amargosa voles (*Microtus californicus scirpensis*) by Imai et al.[4]

In these particular voles the lesion of molar apical elongation (MAE) was characterized by a combination of hyperplasia and to a lesser extent dysplasia which was seen in 63% of the colony. The single predisposing factor in this particular report was age. The authors believe the entity to be multifactorial as a result of a) the nature of continuous growth of hypsodont teeth, inadequate occlusal attrition, and c) a possible genetic inheritance.

That particular paper also describes, with excellent photomicrographs, many of the changes seen in this condition. While it has often been referred to as dentinal dysplasia in rodents, the disorganization of elements seen in true odontogenic dysplasia is not evident in this particular sample other than mild compression of the intercuspal loops and scalloping of the dentin, so we prefer the overall diagnosis of hyperplasia as described by Imai et al. than dysplasia in this particular 4-month-old individual. It might be true that this lesion might become more dysplastic over time as the animal matured.

Sagittal section of head, vole. The molar apices (black arrows) have grown dorsally through the maxilla into the maxillary sinus, compressing the turbinate bones. The olfactory lobe (within the cranium) is highlighted by the green arrow. (HE, 16X)

The term odontogenic dysplasia has been applied to a number of proliferative masses in rodents and lagomorphs over the years, and used interchangeably with odontoma, pseudo-odontoma, and elontoma (all of which incorrectly imply a neoplastic origin.) The etiology of these masses is likely to be disruption of the embryonic enamel organ by a variety of means, including irritation, microtrauma, or infection. It is characterized by a disorganized mass of odontogenic epithelium with significant mineralized dental matrix (dentin, enamel, and in the case of hypsodont teeth, cementum.)[11]

References:

1. Boy SC, Steenkamp G. Odontoma-like tumours of squirrel elodont incisors–elodontomas. J Comp Pathol. 2006;135(1):56–61.
2. Harada H, Kettunen P, Jung HS, Mustonen T, Wang YA, Thesleff I. Localization of putative stem cells in dental epithelium and their association with Notch and FGF signaling. J Cell Biol. 1999; 147(1): 105–120.
3. Harvey SB, Alworth LC, Blas-Machado U. Molar malocclusions in pine voles (*Microtus pinetorum*). J Am Assoc Lab Anim Sci. 2009; 48(4): 412–415.
4. Imai DM, Pesapane R, Conroy CJ, Alarcón CN, Allan N, Okino RA, Fung J, Murphy BG, Verstraete FJM, Foley JE. Apical Elongation of Molar Teeth in Captive Microtus Voles. Vet Pathol. 2018 Jul;55(4):572-583. doi: 10.1177/0300985818758469. Epub 2018 Apr 17.
5. Imbschweiler I, Schauerte N, Henjes C, Fehr M, Baumgärtner W. Odontogenic dysplasia in the molar teeth of Steppe lemmings (*Lagurus lagurus*). Vet J. 2011 Jun;188(3):365-8.
6. Jekl V, Hauptman K, Skoric M, et al. Elodontoma in a degu (Octodon degus). JExot Pet Med. 2008;17(3):216–220.
7. Jekl V, Redrobe S. Rabbit dental disease and calcium metabolism--the science behind divided opinions. J Small Anim Pract. 2013 Sep;54(9):481-90. doi: 10.1111/jsap.12124.
8. Jheon A, Prochazkova M, Sherman M, Manoli DS, Shah NM, Carbone L, Klein O. Spontaneous emergence of overgrown molar teeth in a colony of prairie voles (*Microtus ochrogaster*). Int J Oral Sci. 2015 Mar; 7(1): 23–26.
9. Juuri E, Saito K, Ahtiainen L, Seidel K, Tummers M, Hochedlinger K, Klein OD, Thesleff I, Michon F. Sox2+ stem cells contribute to all epithelial lineages of the tooth via Sfrp51 progenitors. Dev Cell. 2012; 23(2): 317–328.
10. Mushegyan V, Eronen JT, Lawing AM, Sharir A, Janis C, Jernvall J, Klein OD. Continuously growing rodent molars result from a predictable quantitative evolutionary change over 50 million years. Cell Rep. 2015 May 5;11(5):673-80.
11. Murphy BG, Bell CM, Soukup JW. Odontogenic dysplasia. *In:* Veterinary Oral and Maxillofacial Pathology. Hoboken, NJ: Wiley and Sons, 2020: pp. 39-41.
12. Renvoisé E, Michon F. An Evo-Devo perspective on ever-growing teeth in mammals and dental stem cell maintenance. Front Physiol. 2014 Aug 28;5:324
13. Sugita S, Uchiumi O, Fujiwara K, Niida S, Fukuta K. Brain deformation caused by hyperplasia molar teeth (macrodonts) in the Japanese field vole (*Microtus montebelli*). Exp Anim. 1995 Oct;43(5):769-72.
14. Tummers M, Thesleff I. Root or crown: a developmental choice orchestrated by the differential regulation of the epithelial stem cell niche in the tooth of two rodent species. Development. 2003 Mar;130(6):1049-57.

Self-Assessment - WSC 2019-2020 Conference 21

1. Which of the following is true concerning amyloid-producing odontogenic tumors?
    a. The amyloid has been shown to be of ameloblastic origin.
    b. The amyloid is of the AA type as a result of chronic periodontal disease.
    c. APOTs are confined to the gingiva.
    d. APOTs are the most common odontogenic tumor in the dog.

2. Which of the following odontogenic tumors would likely have relatively well-formed denticles contained within?
    a. Complex odontoma
    b. Compound odontoma
    c. Odontoameloblastoma
    d. Amyloid-producing ameloblastoma

3. True or false. The maturation process often seen in odontomas results in less mineralized dental matrix over time?
    a. True
    b. False

4. Most reptiles, amphibians and fish fall into which of the following classifications?
    a. Edentulous
    b. Diphyodont
    c. Polyphyodont
    d. Monophyodont

5. Which of the following is a common finding in captive moles of the genus *Microtus*?
    a. Ameloblastomas
    b. Compound odontoma
    c. Apical elongation of the cheek teeth
    d. Dentinal dysplasia of the incisors

Please email your completed assessment for grading to Dr. Bruce Williams at bruce.h.williams12.civ@mail.mil. Passing score is 80%. This program (RACE program 33611) is approved by the AAVSB RACE to offer a total of 0.5 CE Credits, with a maximum of 12.5 CE Credits being available to any individual Veterinary Medical Professionals for the 2019-2020 Wednesday Slide Conference. This RACE approval is for the subject matter categories of: SCIENTIFIC using the delivery method of NON-INTERACTIVE DISTANCE. This approval is valid in jurisdictions which recognize AAVSB RACE.

Joint Pathology Center
Veterinary Pathology Services

WEDNESDAY SLIDE CONFERENCE 2019-2020

C o n f e r e n c e 22

15 April 2020

CASE I: NO-16-1279 (JPC 4099471).

Signalment: Adult male white-headed capuchin (*Cebus capucinus*).

History: Several New World and Old World monkeys (white-headed capuchin (*Cebus capucinus*), booted macaque (*Macaca ochreata*), and sooty mangabey (*Cercocebus atys*)) in this primate facility had a sudden onset of severe depression, fatigue, lethargy, and sleepiness, then died within a few hours after first clinical signs.

Gross Pathology: A 3.45 Kg adult male white-headed capuchin (*Cebus capucinus*) was in fair nutritional condition (body condition score of 4/9). Scleral and oral mucosa was diffusely pale pink. The heart was moderately enlarged and veins were dilated with clotted blood. There were multiple foci of slightly pale discoloration scattered throughout the left ventricular wall and near the heart apex. The discolored pale tan areas extended approximately 5-7 mm into the underlying myocardium. The apical region of pallor was approximately 3 mm in diameter at the epicardial surface. Lung lobes were diffusely pink; however, the right middle lobe had multifocal distinctly dull red demarcated, depressed areas.

The liver was slightly enlarged; the tip of the right lateral liver lobe extended 5-10 mm caudal to the costal margin.

Throughout the cerebrum and meninges, vessels were dilated and prominent. All other organs were grossly unremarkable.

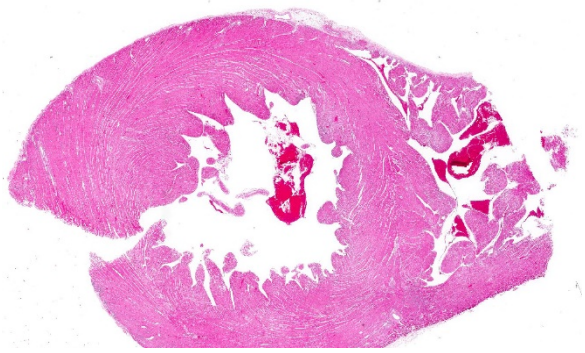

Heart, capuchin monkey. A cross section of the left tentacle and tip of left atrium is submitted for examination. There are no lesions at subgross examination. (HE, 5X)

Laboratory results:

- Bacteriology: Rare colonies of *Staphylococcus aureus* were isolated from submitted pulmonary tissue, and no bacterial colonies were isolated from submitted hepatic tissue.

- Virology: Virus isolation demonstrated prominent cytopathic effects from submitted fresh frozen pooled specimens including heart and brain. Encephalomyocarditis virus was detected from cell culture supernatant by PCR and confirmed by genetic sequencing. PCR to detect Herpesvirus, West Nile virus, and *Francisella tularensis* were negative.

Microscopic Description: All representative sections of the heart contain similar inflammatory processes and will be described collectively; however, the degree of severity varies between sections. Multifocally, within examined sections of left and right cardiac ventricles, there are variably dense interstitial infiltrates of

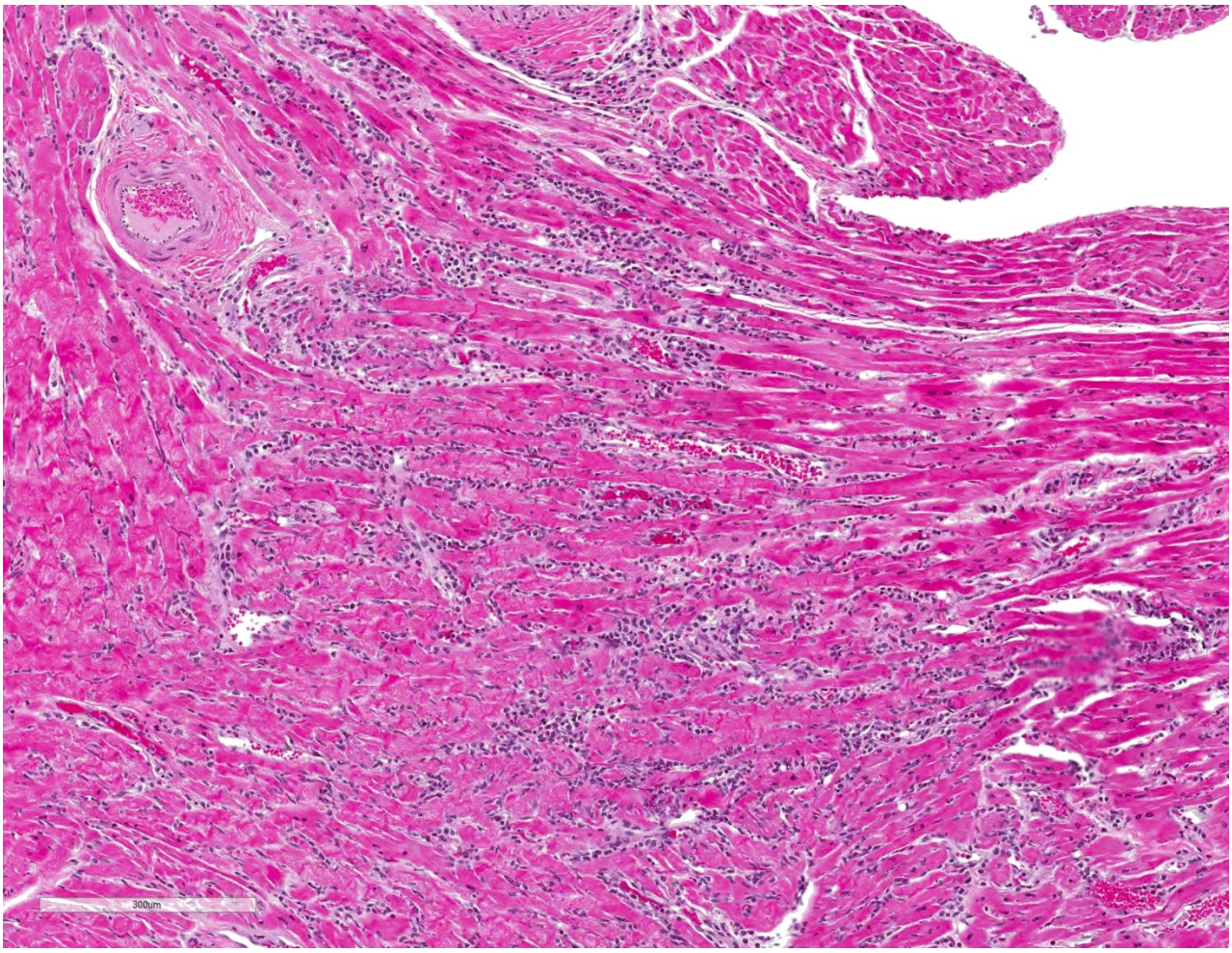

Heart, capuchin monkey. Multifocally and randomly, the interstitium is markedly expanded by a cellular infiltrate. (HE, 100X)

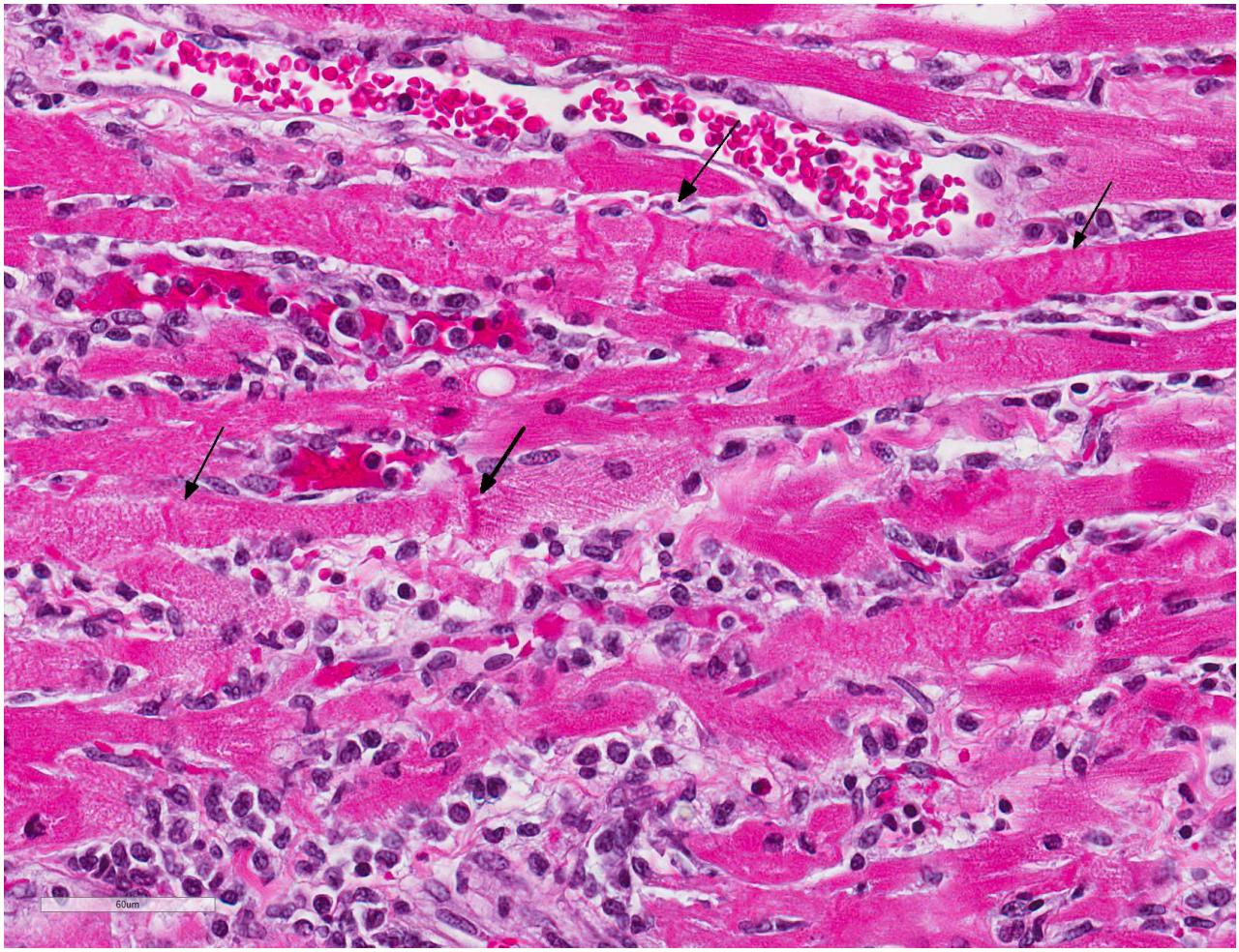

Heart, capuchin monkey. In areas of inflammation, moderate numbers of lymphocytes and macrophages expand the interstitium. Cardiac myocytes demonstrate necrotic chantes including shrinkage, fragmentation contraction band formation (black arrows), pyknosis andkaryorrhexis. (HE, 400X)

mixed inflammatory cells dissecting around the myocardial fibers and surrounding occasional vessels in some areas. These leukocytes include lymphocytes, plasma cells, and histiocytes mixed with fewer neutrophils. The affected cardiomyocytes are variably degenerating or necrotic characterized by hypereosinophilia, loss of cellular detail, formation of contraction bands, and nuclear pyknosis and karyorrhexis. In some areas, there is intracytoplasmic and extracellular basophilic granular mineralization.

Contributor's Morphologic Diagnosis:

Heart: Myocarditis, necrotizing, moderate to severe, multifocal to coalescing

Contributor's Comment:

Encephalomyocarditis virus (EMCV) is a small non-enveloped single-stranded RNA virus, classified as a member of family *Picornaviridae*, genus *Cardiovirus*. The virus is known to cause myocarditis and encephalitis in a variety of domestic mammals including pigs and several zoo and wildlife species including non-human primates.[1,3,5,6,12] EMCV infection is also

sporadically reported in humans, although the vast majority of cases are mild and asymptomatic.[10]

Rodents are considered to be reservoir hosts for EMCV in some studies,[1,5] though studies have associated EMCV inoculation with severe to fatal myocarditis and necrotizing pancreatitis in Mongolian gerbils (*Meriones unguiculatus*) as well as acute orchitis in Syrian hamsters (*Mesocricetus auratus*).[7,8]

Infected non-human primates have a rapid disease course including severe depression and lethargy progressing to acute heart failure and death within 24 hours of clinical presentation. In some cases, the affected animal may suffer from progressive respiratory distress prior to death.[2, 5] As in this case, gross findings are typically limited to the heart as evidenced by pale white discoloration or variable petechial and ecchymotic hemorrhage.[1,2,5]

Hydropericardium, hydrothorax, pulmonary congestion, and ascites may be observed in some cases. [2,3] The principal histologic findings of EMCV-infected non-human primates include multifocal regions of myocardial degeneration and necrosis with associated variable degrees of lymphocytic to mixed interstitial inflammatory infiltrates.

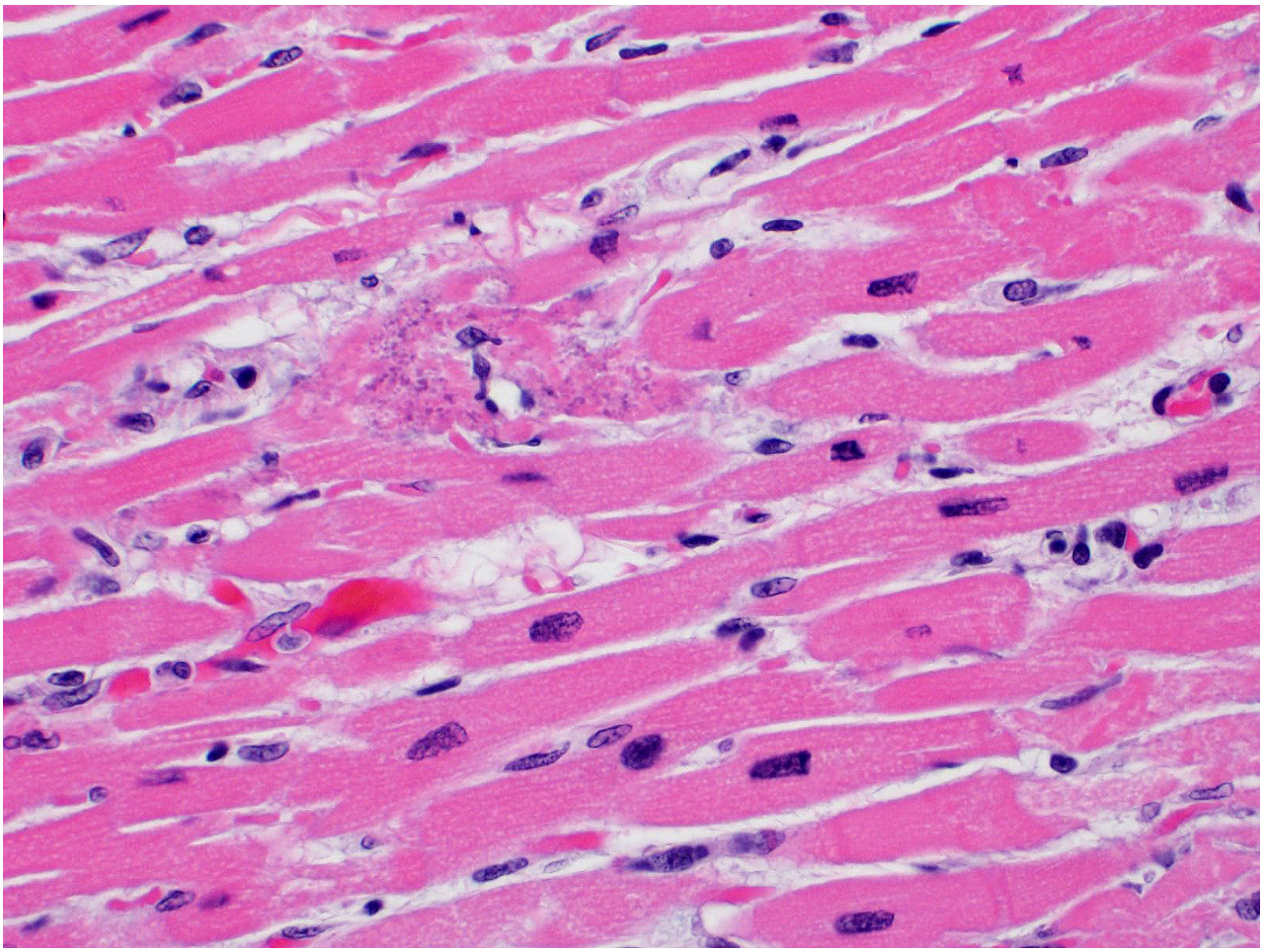

Heart, capuchin monkey. Necrotic myofibers are occasionally stippled with granular mineral. (HE, 400X)

Neural lesions are uncommon in non-human primates, which suggests a cardiotropic nature of the virus in these hosts;[4] however, some studies showed neurotropism of this virus in naturally and experimentally infected animals.[1,6] Other infectious diseases that can be associated with myocarditis in non-human primates include West Nile virus, *Trypanosoma cruzi*, and *Borrelia burgdorferi*.

Contributing Institution:

Diagnostic Center for Population and Animal Health and the Department of Pathobiology and Diagnostic Investigation, College of Veterinary Medicine, Michigan State University. 4125 Beaumont Rd. Lansing, MI 48910
www.animalhealth.msu.edu;
www.pathobiology.msu.edu

JPC Diagnosis: Heart: Myocarditis, necrotizing and lymphocytic, multifocal, random, mild to moderate, with mild lymphocytic epicarditis and endocarditis.

JPC Comment: EMCV was first identified in a captive gibbon in 1945 that died suddenly from pulmonary edema and myocarditis. Mice inoculated with edema fluid from the affected monkey developed myocarditis and hindlimb paralysis. A similar virus was isolated 4 years later in the Mengo district of Entebbe, Uganda from a paralyzed rhesus macaque which was shown to be antigenically indistinct via sero-neutralization, but both viruses were considered distinct from the Theiler's murine encephalomyelitis virus (another cardiovirus).[2] The first outbreak in swine was noted in Panama in 1958.[2]

Although mice are considered to be the natural reservoir, rats are often implicated in transmission to other species, including non-human primates and swine. Transmission is most likely the result of fecal contamination of feeds, although horizontal transmission has been identified in swine and suspected in non-human primates.[11]

This virus has been shown to infect a wide range of non-human primates, including rhesus macaques, mandrills, chimpanzees, marmosets, owl monkeys and squirrel monkeys. [11] There have been a number of significant outbreaks in captive baboons, suggesting that this species may be uniquely susceptible.[11] Many infected primates are found dead with minimal premonitory signs, or suffer from rapidly progressing biventricular heart failure with prominent edema and froth or fluid from the nose and mouth. As mentioned by the contributor, the clinical picture in non-human primates is primarily that of cardiac infection, however, neurotropic strains may also cause lymphocytic infiltrates in the cerebrum.[11]

Encephalomyocarditis virus will also cause cardiovascular disease in a number of other species including pygmy hippopotamuses and exotic hoofstock, lemurs, tapirs, rhinoceroses, and elephants[9] (perhaps explaining the elephant's mythic fear of the mouse.) Transmission within zoo collections is considered the result of fecal and infected carcass contamination of feed. Myocarditis and heart failure is always present; neurologic lesions are uncommon.[9]

While considered a zoonosis, disease in humans is mild and somewhat controversial. Human cell lines are readily infected. EMCV has been incriminated in a number of cases of febrile human illness with clinical signs of headache, nausea and malaise, when EMCV virus was detected using molecular techniques in the absence of other viruses. Seropositivity to EMCV has ranged from 3-15% in the general population with higher rates in humans with occupational exposure and hunters. [2]

References:

1. Canelli E, Luppi A, Lavazza A, et al. Encephalomyocarditis virus infection in an Italian zoo. *Virol J*. 2010;7(64). Published online 2010 Mar 18.
2. Carocci M, Bakkali-Kassimi L. The encephalomyocarditis virus. *Virulence*. 2012;3(4):351-367.
3. Citino SB, Homer BL, Gaskin JM, et al. Fatal encephalomyocarditis virus infection in a Sumatran orangutan (*Pongo pygmaeus abelii*). *J Zoo Animal Med*. 1988;19(4):214-218.
4. Craighead JE. Pathogenicity of the M and E variants of the encephalomyocarditis (EMC) virus. *Am J Pathol.* 1966;48(2):333-345.
5. Jones P, Cordonnier N, Mahamba C, et al. Encephalomyocarditis virus mortality in semi-wild bonobos (*Pan panicus*). *J Med Primatol*. 2011;40(3):157-163.
6. LaRue R, Myers S, Brewer L, et al. A wild-type porcine encephalomyocarditis virus containing a short poly(C) tract is pathologic to mice, pigs, and cynomolgus macaques. *J Virol*. 2003;77(17):9136-9146.
7. Matsuzaki H, Doi K, Mitsuoka T, et al. Experimental encephalomyocarditis virus infection in Mongolian gerbils (*Meriones unguiculatus*). *Vet Pathol*. 1989;26:11-17.
8. Shigesato M, Takeda M, Hirasawa K, et al. Early development of encephalomyocarditis (EMC) virus-induced orchitis in Syrian hamsters. *Vet Pathol.* 1995;32:186-186.
9. Terio KA, McAloose D, St Leger J eds., *In:* Pathology of Wildlife and Zoo Animals; London: Associated Press, 2019
10. Tesh R. The prevalence of encephalomyocarditis virus neutralizing antibodies among various human populations. *Am J Trop Med Hyg*. 1978;27(1):144-148.
11. Wachtman L, Mansfield C. Viral diseases of non-human primates. *In:* Abee CR, Mansfield K, Tardiff S, Morris T, eds. Nonhuman Primates in Biomedical Research: Diseases. London, Academic Press 2012, pp 73-74.
12. Wells SK, Gutter AE, Soike KF, et al. Encephalomyocarditis virus: epizootic in a zoological collection. *J Zoo Wildl Med*. 1989;20(3):291-296.

CASE II: Case 2 (DVD) (JPC 4136179).

Signalment: 2.9 year old male rhesus macaque (*Macaca mulatta*)

History: The animal was assigned to a study investigating the effects of co-stimulatory blockade on delaying rejection of renal porcine xenotransplants. The animal presented with acute severe dyspnea one-month post-transplantation.

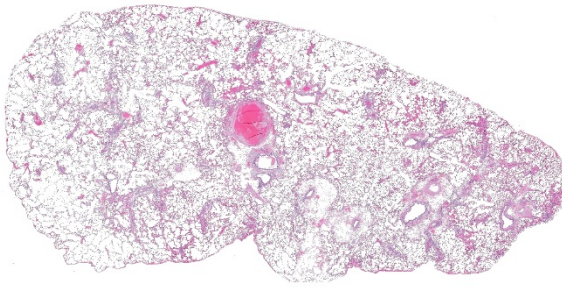

Lung, rhesus macaque. At subgross examination, pulmonary arterioles are highlight by marked edema, vessels throughout the section are outlined by a cellular infiltrate, and there is a large focal central pulmonary thrombus. (HE, 6X)

Gross Pathology: Red-tinged foam and liquid was present surrounding the nares and muzzle. Similar foam was present within the larynx and trachea. There was approximately 5mL of straw-colored fluid within the pleural cavity with few floating fibrin aggregates. The lungs were wet, heavy, failed to collapse, and were mottled red-pink.

Laboratory results:

Hematologic and serum biochemical analyses demonstrated a leukocytosis ($11x10^3$) with mild neutrophilia, lymphopenia, monocytosis, mild anemia, mild hypoproteinemia with low-normal albumin, mild azotemia, hyperphosphatemia, hyperglycemia, and hyperkalemia.

Microscopic Description: Lungs: There are numerous small and medium caliber blood vessels that are lined by endothelial cells with markedly enlarged nuclei and cytoplasm (cytomegaly) and occasional Cowdry type-A eosinophilic intranuclear inclusion bodies. Affected vessels are frequently infiltrated by neutrophils, lymphocytes, and histiocytes within the tunica media and intima (vasculitis). Multiple vessels are surround by abundant clear space (perivascular edema) and lesser amount of free erythrocytes (hemorrhage). Few larger vessels have abundant proliferation of the tunica intima with infiltration by neutrophils There are scattered coalescing regions where alveolar spaces contain free erythrocytes, fibrin, neutrophils, necrotic debris, and increased numbers of alveolar macrophages that frequently contain abundant eosinophilic

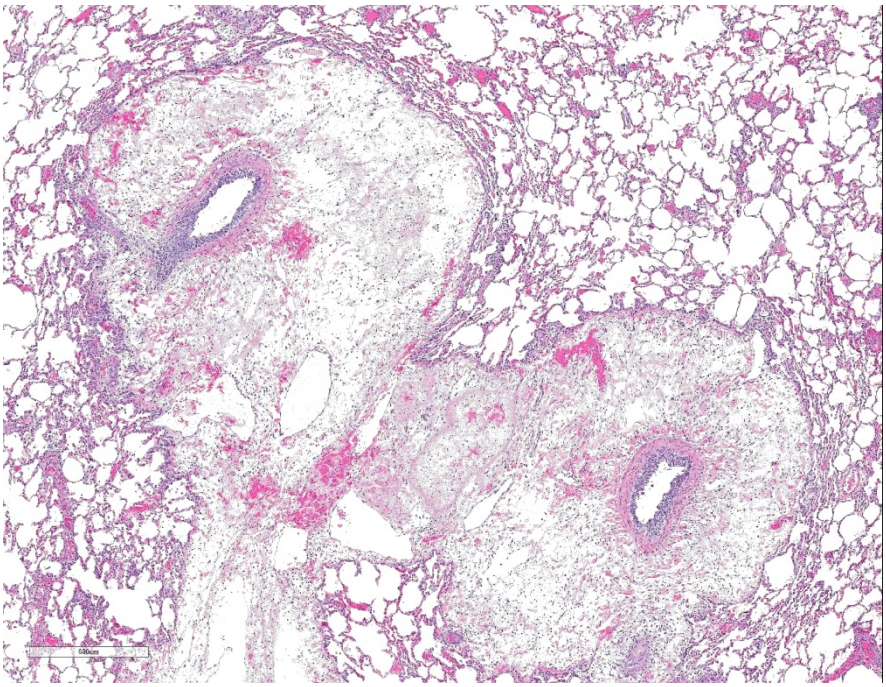

Lung, rhesus macaque. Higher magnification of the marked edema which expands arteriolar adventitia and compresses adjacent alveoli. Lymphatics are markedly expanded and there is multifocal hemorrhage. (HE, 38X)

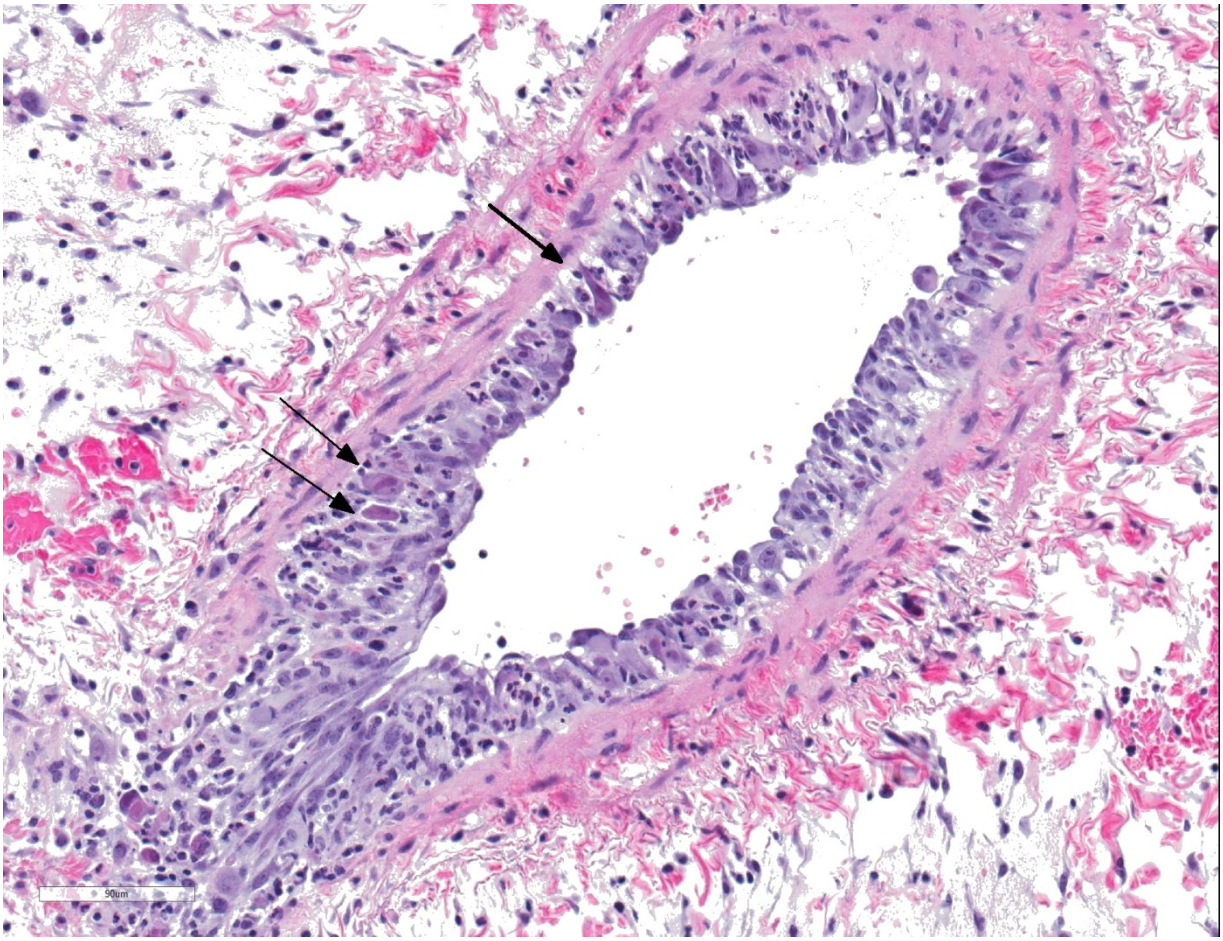

Lung, pulmonary arteriole, rhesus macaque. There is marked hyperplasia and hypertrophy of arteriolar endothelium and several hypertrophic endothelial cells contain large oblong intranuclear viral inclusions (arrows). The intima and inner media is expanded by edema, infiltrating neutrophils, and cellular debris. (HE, 240X)

cytoplasm (alveolar edema). There are multiple patchy regions where alveolar septae are expanded by similar mixed inflammatory cells. There are rare intranuclear inclusion bodies present within histiocytes and type-1 pneumocytes.

Contributor's Morphologic Diagnosis:

Lungs: Severe, multifocal widespread, neutrophilic and lymphocytic small and medium artery vasculitis with endothelial cytomegaly, Cowdry type-A intranclear inclusions (cytomegalovirus) and perivascular edema; Mild to moderate, multifocal to coalescing, neutrophilic and lymphocytic interstitial pneumonia with alveolar edema and hemorrhage.

Contributor's Comment: Rhesus cytomegalovirus (*macacine herpesvirus 3*), is a double-stranded DNA virus in the family betaherpesvirus that is commonly identified in non-specific pathogen free colonies of rhesus macaques, with 50% of infants seropositive by 6 months of age and almost 100% by 1 year old.[22] Transmission is believed to be horizontal, as vertical transmission is exceedingly rare, which mimics the human virus[4]. Infections are usually asymptomatic with the virus

remaining latent until an immunosuppressive event occurs, allowing for recrudescence.

Specifically, T-cells play an important role in controlling CMV replication,[16] which are also the target of many immunosuppressive therapies in organ transplantation and in SIV and type-D retroviral infections.[1] Cytomegaloviral infection/recrudescence has been reported as a complication leading to death or euthanasia in multiple nonhuman primate species undergoing solid organ or stem cell transplantation, including rhesus[13,15] and cynomolgus[12] macaques and baboons.[2]

Although it is difficult to assess the complication rates in nonhuman primate transplant studies due to the relatively small numbers of animals reported in the literature, the rate of post-transplantation infections is thought to be 14%.[10] These infections can be classified as early (<1 month), intermediate (1-6 months), or late (>6 months) infections. Generally, early infection etiologies most frequently include bacteria or Candida[17], while intermediate infections are typified by the viral infections such as cytomegalovirus, Epstein-Barr virus, varicella zoster virus, herpes B virus, human herpesvirus-6, and simian immunodeficiency virus.[10] It is probably more accurate to consider these as re-emergent latent pre-transplantation viral infections rather than de novo post-operative infections.

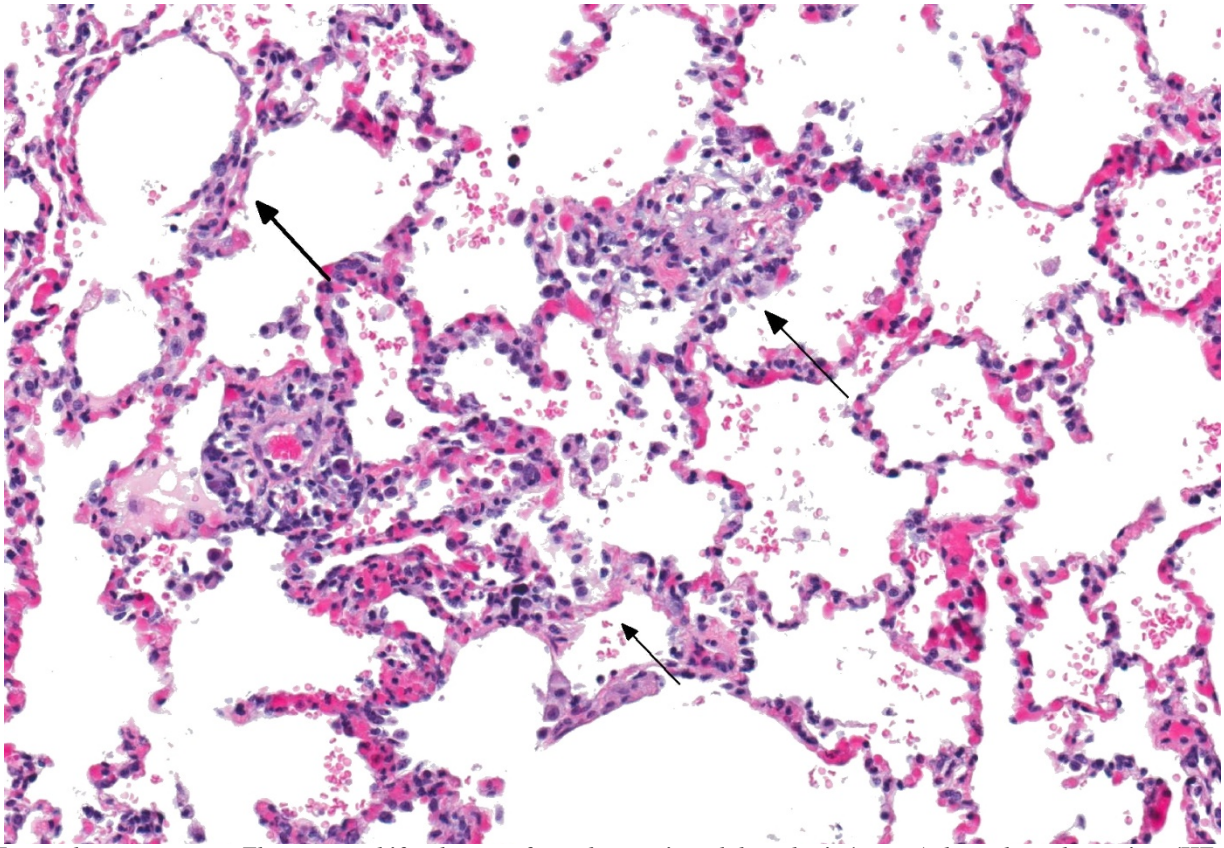

Lung, rhesus macaque. There are multifocal areas of septal necrosis and thrombosis (arrows) throughout the section. (HE, 220X).

In humans, CMV is most commonly associated with HIV and transplant-associated immunosuppression.[8,19,20] CMV-related diseases in these cases include chorioretinitis, gastrointestinal diseases (colitis, esophagitis, gastritis, hepatitis), pneumonia, encephalitis and myelitis, and adrenal adenitis. Lesions associated with cytomegaloviral infection in nonhuman primates result from disseminated infections, which are almost always linked to immunosuppression. Diseases resulting from disseminated infection include: necrotizing enteritis, encephalitis, lymphadenitis, and/or pneumonitis/interstitial pneumonia.[1] Typically, alveolar septa are lined by hypertrophied type 2 pneumocytes and contain cytomegaly with large intranuclear Cowdry type-A inclusion bodies within the septa and lining. Alveolar spaces contain fibrin, alveolar macrophages, and neutrophils. Similar lesions can also be found in spleen, liver, kidney, and testis. The similarities between humans and nonhuman primates regarding pathogenesis and gross and histologic lesions makes nonhuman primates an ideal model for studying CMV in immunosuppressed patients.

Within the present case, only pulmonary lesions (and resultant hydrothorax) were observed, with classical cytomegaloviral inclusions observed predominately within vascular endothelial cells, and alveolar septa and macrophages much less frequently observed. Endotheliitis in the lungs and other organs from cytomegalovirus has also been described in immunosuppressed humans.[9,21] Vasculitis is a less common pathologic finding than alveolitis, but can cause perivascular and alveolar edema and hemorrhage, as well as pleural effusion.[11,18] In rhesus macaques, CMV has also been reported to cause hypophysitis[5] and facial neuritis[3] with co-infection with SIV, and mesenchymoproliferative enteropathy with co-infection with SIV and simian polyomavirus.[14]

Contributing Institution:

Division of Pathology, Yerkes National Primate Research Center, Emory University

http://www.yerkes.emory.edu/research/divisions/pathology/index.html

JPC Diagnosis: Lung: Pneumonia, interstitial, necrotizing and neutrophilic, multifocal to coalescing, moderate, with necrotizing vasculitis and numerous endothelial and pneumocyte karyomegalic viral inclusions.

JPC Comment: The contributor has provided an excellent and concise review of cytomegalovirus, and their importance in both primate and transplant research.

Present in most if not all mammalian species, cytomegaloviruses (CMV) are slow-growing viruses that result in a life-long latent infection, with recrudescence and clinical disease only in times of severe immunosuppression. In order to do this, cytomegaloviruses have developed unique methods of preventing the host from clearing the infection, which are only now beginning to come to light.

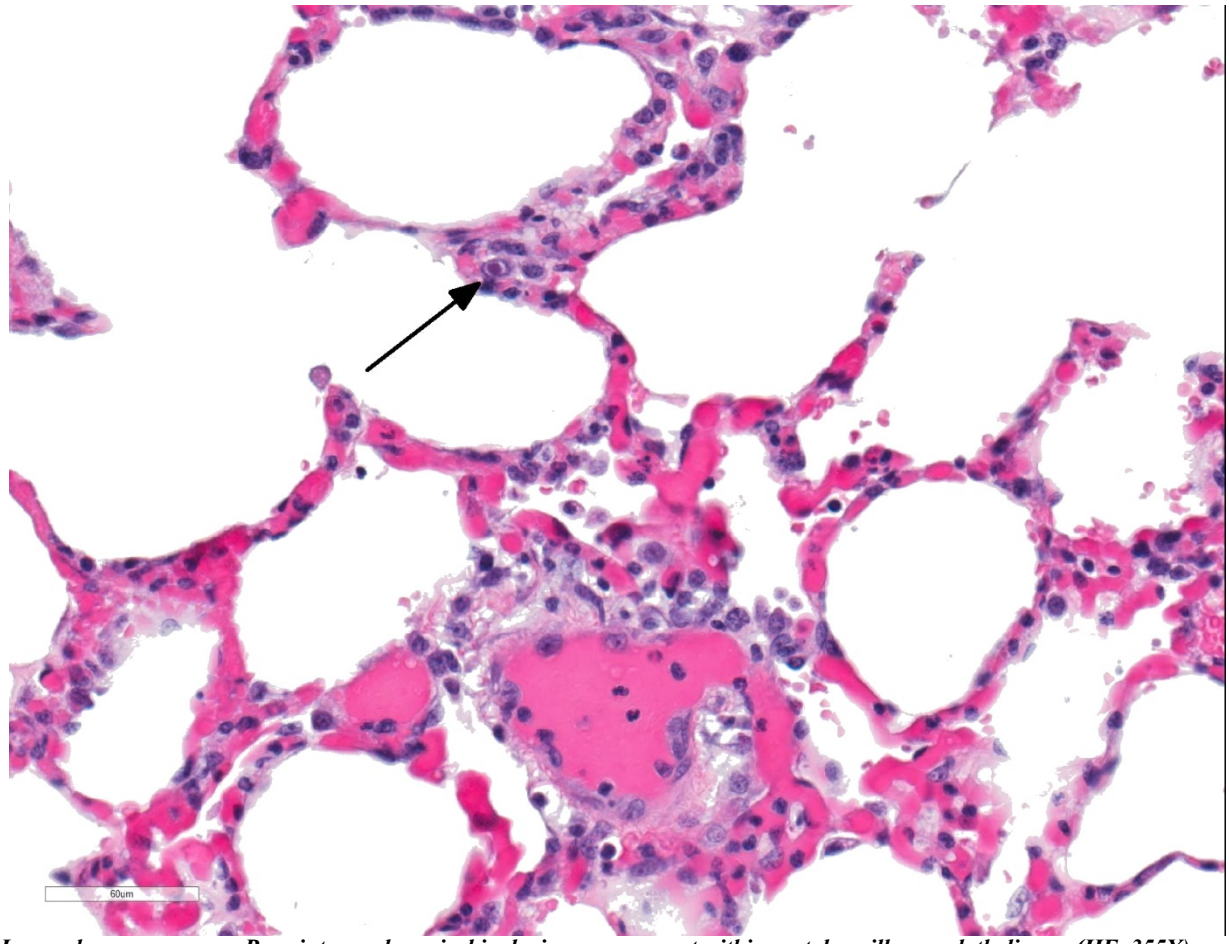

Lung, rhesus macaque. Rare intranuclear viral inclusions are present within septal capillary endothelium. (HE, 355X).

As shown in the mouse model (murine cytomegalovirus is a well-researched agent due to its similarity to human CMV), toll-like receptors and cellular stress responses will activate intrinsic methods of cell death following CMV infection. In order to combat this, CMV has developed ways to counteract a number of key factors which inhibit cellular death, i.e., "death inhibitors".[6]

One method is a viral protein which inhibits mitochondrial outer membrane permeabilization, a key step in apoptosis, by producing vMIA (viral mitochondria-localized inhibitor of apoptosis), which inhibits the activator Bak and sequesters Bax at the mitochondrial membrane.[6]

CMV also produces a viral protein, UL38, which results in accumulation of the activating transcription factor 4 (ATF4) and suppression of JNK activity. ATF4 helps to resolve cell stress by inducing the production of proteins that facilitate protein folding within the ER, and the inactivation of JNK inhibits activation of Bim and Bcl-2, further stabilizing the mitochondrial membrane.[6]

CMP infection also modifies so-called "death receptors" at the cell surface, such as the TNF-related apoptosis-inducing ligand (TRAIL). An open reading frame on M166, a CMV viral-encoded protein inhibits the expression of this receptor at the cell surface. Other viral proteins inhibit Fas-induced cell death by binding to pro-caspase

8 and inhibiting its activation.[6] Several proteins also inhibit activators of null killer cells at the level of the NKG2D cell receptor (CD226).[7]

References:

1. Abee CR, Mansfield K, Tardiff S, Morris T: Nonhuman Primates in Biomedical Research, Second ed., pp. 19-20. Elsevier, Oxford, 2012

2. Asano M, Gundry SR, Izutani H, Cannarella SN, Fagoaga O, Bailey LL. Baboons undergoing orthotopic concordant cardiac xenotransplantation surviving more than 300 days: effect of immunosuppressive regimen. *J Thorac Cardiovasc Surg*. 2003;125**:** 60-69; discussion 69-70.

3. Assaf BT, Knight HL, Miller AD. Rhesus Cytomegalovirus (Macacine Herpesvirus 3)–Associated Facial Neuritis in Simian Immunodeficiency Virus–Infected Rhesus Macaques (Macaca mulatta). *Veterinary Pathology*. 2014;52**:** 217-223.

4. Barry PA, Lockridge KM, Salamat S, et al. Nonhuman primate models of intrauterine cytomegalovirus infection. *ILAR J*. 2006;47**:** 49-64.

5. Berg MR, Owston MA, Gauduin M-C, Assaf BT, Lewis AD, Dick EJ. Cytomegaloviral hypophysitis in a simian immunodeficiency virus-infected rhesus macaque (Macacca mulatta). *Journal of Medical Primatology*. 2017;46**:** 364-367.

6. Brune W, Andoniou CE. Die another day: inhibition of cell death pathways by cytomegalovirus. *Viruses* 2017; 9(9):doi 10.3390/v9090249.

7. De Pelsmaeker S, Romero N, Vitale M, Favoreel HW. Herpes virus evasion of natural killer cells. *J Virol* 2018; 92(11): doi 10.1128/JVI.02105-17.

8. . Drew WL. Cytomegalovirus infection in patients with AIDS. *Clin Infect Dis*. 1992;14**:** 608-615.

9. . Golden MP HS, Wanke CA, Albrecht MA. Cytomegalovirus Vasculitis- Case Reports and Review of the Literature. *Medicine*. 1994;73**:** 246-255.

10.. Haustein S, Kolterman A, Sundblad J, Fechner J, Knechtle S. Nonhuman primate infections after organ transplantation. *ILAR J*. 2008;49**:** 209-219.

11. . Herry I CJ, Antoine M, Meharzi J, Michelson S, Parrot A, Rozenbaum W, Mayaud C. Cytomegalovirus-induced alveolar hemorrhage in patients with AIDS: a new clinical entity? *Clin Infect Dis*. 1996;22**:** 616-620.

12. Jonker M, Ringers J, Kuhn EM, t Hart B, Foulkes R. Treatment with anti-MHC-class-II antibody postpones kidney allograft rejection in primates but increases the risk of CMV activation. *Am J Transplant*. 2004;4**:** 1756-1761.

13. Kean LS, Adams AB, Strobert E, et al. Induction of Chimerism in Rhesus Macaques through Stem Cell Transplant and Costimulation Blockade-Based Immunosuppression. *American Journal of Transplantation*. 2007;7**:** 320-335.

14. Macri SC, Knight HL, Miller AD. Mesenchymoproliferative Enteropathy Associated With Dual Simian Polyomavirus

and Rhesus Cytomegalovirus Infection in a Simian Immunodeficiency Virus–Infected Rhesus Macaque (Macaca mulatta). *Veterinary Pathology*. 2012;50**:** 715-721.

15. Pearson TC, Trambley J, Odom K, et al. Anti-CD40 therapy extends renal allograft survival in rhesus macaques. *Transplantation*. 2002;74**:** 933-940.

16. Rowshani AT, Bemelman FJ, van Leeuwen EM, van Lier RA, ten Berge IJ. Clinical and immunologic aspects of cytomegalovirus infection in solid organ transplant recipients. *Transplantation*. 2005;79**:** 381-386.

17. Rubin R, Schaffner A, Speich R. Introduction to the Immunocompromised Host Society Consensus Conference on Epidemiology, Prevention, Diagnosis, and Management of Infections in Solid-Organ Transplant Patients. *Clinical Infectious Diseases*. 2001;33**:** S1-4.

18. Salomon N GT, Perlman DC, Laya L, Eber C, Mildvan D. Clinical features and outcome of HIV-related cytomegalovirus pneumonia. *AIDS*. 1997;11**:** 319-324.

17. Schulman LL RD, Austin JH, Rose EA. Cytomegalovirus pneumonitis after cardiac transplantation. *Arch Intern Med*. 1991;151**:** 1118-1124.

19. Sia IG, Patel R. New strategies for prevention and therapy of cytomegalovirus infection and disease in solid-organ transplant recipients. *Clin Microbiol Rev*. 2000;13**:** 83-121, table of contents.

20. Smith FB, Arias JH, Elmquist TH, Mazzara JT. Microvascular Cytomegalovirus Endothelialitis of the Lung. *Chest*. 1998;114**:** 337-340.

21. Vogel P, Weigler BJ, Kerr H, Hendrickx AG, Barry PA. Seroepidemiologic studies of cytomegalovirus infection in a breeding population of rhesus macaques. *Lab Anim Sci*. 1994;44**:** 25-30.

CASE III: 61726-1 (DVD) (JPC 4117676)**.**

Signalment: 2-year-old, female Angolan Colobus monkey (Colobus angolensis palliatus)

History: This monkey was found down and unresponsive at morning check and transported to the hospital immediately. She

Cerebrum, colobus monkey. A large area of necrosis involving the grey matter is present at lower left. There are multifocal areas of hypercellularity outlining vessels within the white matter of the corona radiata and adjacent grey matter. (HE, 5X)

had no significant history prior to this event, and keepers reported no recent cause for concern. On physical examination she was obtunded and ataxic, with decreased lung sounds on the left and mild crackles on the right. A small abrasion was present on the left ischial pad. On a CT scan, there was a severe, diffuse, nodular/bronchiolar pattern throughout the lungs with a left-sided alveolar pattern. No apparent soft tissue asymmetry was noted. The animal failed to respond to supportive care and was humanely euthanized later the same day due to poor prognosis.

Gross Pathology: Postmortem examination revealed evidence of interstitial pneumonia, nephritis characterized by coalescing tan, red-rimmed nodules, and a prominent focus of hemorrhage in the rostral left cerebrum.

Laboratory results:

Clinical pathology:

- A CBC showed a mild non-regenerative anemia (HCT 30), thrombocytopenia (158,000/ul), and increased fibrinogen (400 mg/dl). A serum chemistry was unremarkable.

Microscopic Description: Cerebrum: Approximately 15-20% of the parenchyma, of which the majority is gray matter, is affected by multifocal to coalescing

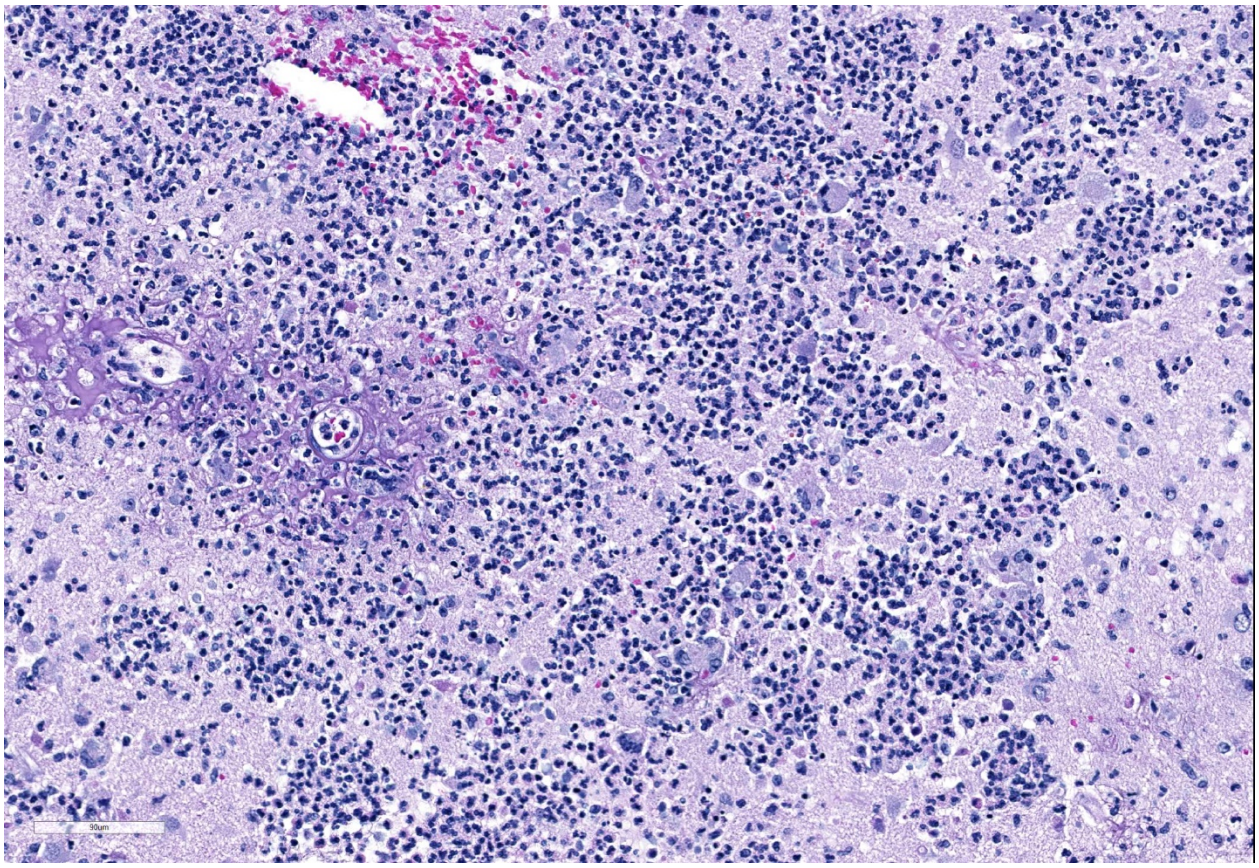

Cerebrum, colobus monkey. The affected area is infiltrated by innumerable viable and degenerate neutrophils and few macrophages/Gitter cells and foreign body-type macrophages. Vessels are necrotic with exudation of fibrin into the surrounding parenchyma. (HE, 242X)

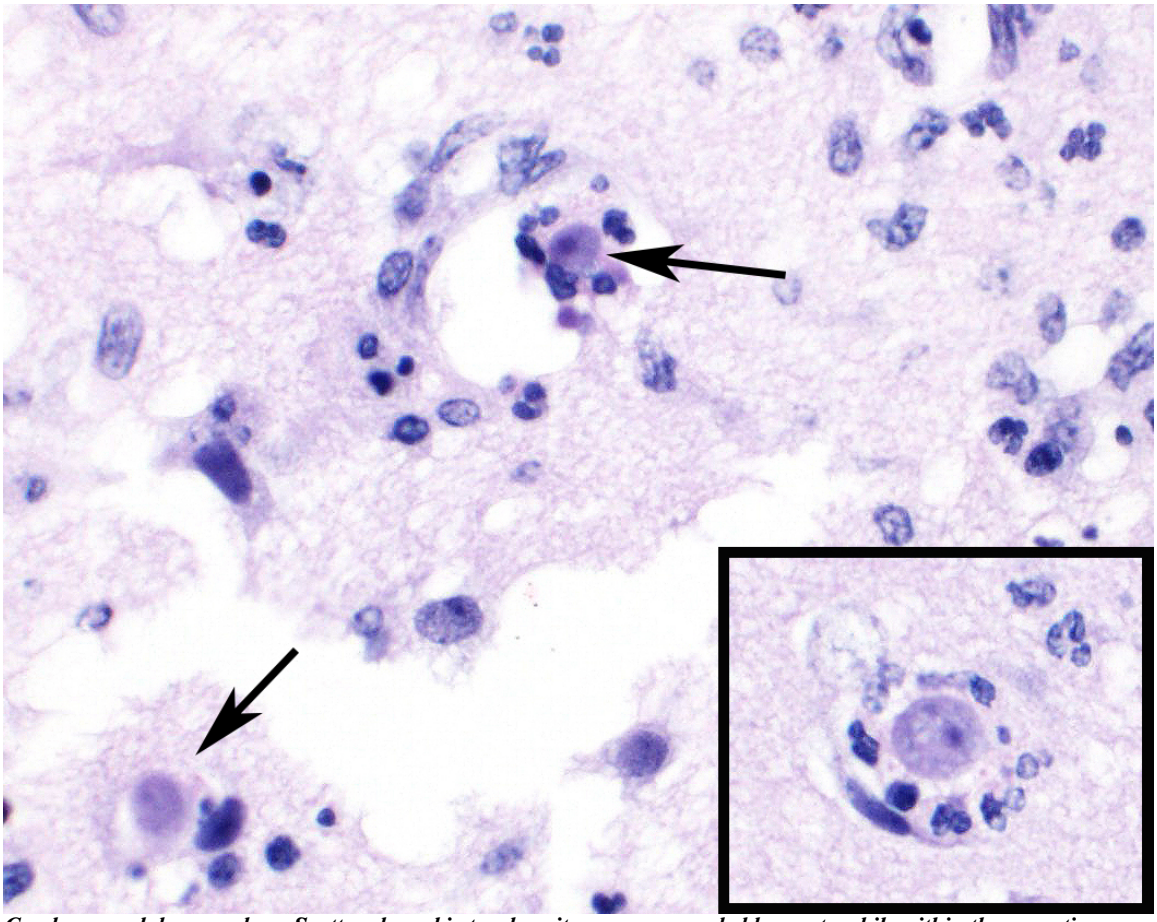

Cerebrum, colobus monkey. Scattered amebic trophozoites are surrounded by neutrophils within the necrotic area. (HE, 242X)

rarefaction, necrosis, and hemorrhage, and is infiltrated by large numbers of neutrophils with fewer histocytes and lymphocytes. Vessel walls in this region are frequently diffusely hyalinized, disrupted and expanded by eosinophilic fibrillar material and karyorrhectic debris (fibrinoid necrosis), and infiltrated by neutrophils (vasculitis). Moderate numbers of amoebic trophozoites measuring from 15-30 micrometers in diameter with a 4-6 micrometer karyosome (nucleus), up to three endosomes (nucleoli), and amphophilic, lacy to vacuolated cytoplasm are scattered throughout the inflamed region. There are increased numbers of glial cells (gliosis), and astrocytes have large nuclei with open chromatin (reactive astrocytosis). The meninges are expanded by large numbers of lymphocytes, plasma cells, and histiocytes with fewer neutrophils. Vessels in surrounding parenchyma are surrounded by large numbers of lymphocytes and plasma cells, which multifocally infiltrate vessel walls.

Immunohistochemistry:

Balamuthia immunohistochemistry: positive

Acanthamoeba immunohistochemistry: negative

Naegleria immunohistochemistry: negative

Contributor's Morphologic Diagnosis:

Brain, cerebrum: Severe, marked, regionally extensive, necrotizing, pyogranulomatous, meningoencephalitis with cavitation, fibrinoid vascular necrosis, vasculitis, and amoebae.

Contributor's Comment: Infections with free-living amoeba are an emerging disease in both human and animal populations. The major differentials for free-living amoeba infecting animal and human tissues include *Balamuthia* sp, *Acanthamoeba* sp, and *Naegleria fowleri*. These three organisms can be difficult to distinguish from each other based on light microscopy alone except for a few distinguishing features. The distinguishing feature of *Naegleria fowleri*, is that it does not form cysts in the brain, whereas *Balamuthia* sp. and *Acanthamoeba* sp. do.[8]

Acanthamoeba and *Balamuthia* are very similar morphologically and can be difficult to diagnose without additional diagnostics such as immunohistochemistry or PCR. One feature that may assist in distinguishing between the two is that *Balamuthia* can have multiple nucleoli within its trophozoite stage, whereas *Acanthamoeba* only has one nucleolus. Also, *Balamuthi*a trophozoites are slightly larger and tend to be more pleomorphic than *Acanthamoeba* trophozoites.[5] The size of the amoeba (trophozoites 15-30 micrometers in greatest dimension) along with the occasional presence of multiple endosomes or nucleoli in this case is consistent with *Balamuthia mandrillaris*, which was subsequently confirmed by immunohistochemistry.

Balamuthia mandrillaris was first discovered in a 3-year old female mandrill baboon

(*Mandrillus sphinx*) from the San Diego Zoo Safari Park that died of amoebic encephalitis in 1986. The species name *mandrillaris* comes from this index case.[7] Since the first case, additional sporadic cases have been identified at the San Diego Zoo and San Diego Zoo Safari Park over the years.[5] In addition, the agent was subsequently found to be an important human pathogen, explaining a number of historical human cases of amoebic encephalitis that failed to stain with antibodies against *Acanthamoeba* and *Naegleria.*[1]

Balamuthia mandrillaris is a soil-dwelling organism. The pathogenesis of the infection remains uncertain, but open skin lesions are thought to be a risk factor in human cases.[6] The animal in this case did have an abrasion on an ischial pad, which could have been a portal of entry. Exposure to blowing dust, mud puddles, or other soil contaminated water are thought to be additional potential risk factors.[4] These infections are not transmissible and are not zoonotic. Individuals infected with free-living amoeba tend to be immunocompromised in some way, with a number of human patients being infected with AIDS[6]; however, immunocompromise is not required for infection. Morbidity is overall low, but mortality is relatively high with human and animal infections.[4]

Common organ systems infected in humans include skin and the central nervous system. Lesions are typically granulomatous and necrotizing. Unlike other free-living

amoeba, *Balamuthia mandrillaris* can cause disseminated chronic infections that are indistinguishable from metastatic neoplasia.[1] Overall, free-living amoeba infections are important to have as a differential for various presentations in both animal and human patients.

Contributing Institution:

San Diego Zoo Global Disease Investigations
P.O. Box 120551

San Diego, CA 92112-0551
https://institute.sandiegozoo.org/disease-investigations

JPC Diagnosis: Cerebrum: Meningoencephalitis, necrotizing and pyopgranulomatous, focally extensive, severe with vasculitis, thrombosis, gliosis, and numerous amebae.

JPC Comment: Free-living amebae are ubiquitous protozoans in the environment, of which four generally are considered pathogenic for humans and animals: *Acanthamoeba*, *Balamuthia mandrillaris*, *Naegleria fowleri*, and *Sappinia pedata.*[1,3] As a group, they may act as vectors for a wide range of pathogenic bacilli, as well as hosts for a range of viruses, including coxsackieviruses and adenoviridae pathogenic for humans. Other viruses, the so-called giant viruses, may act as

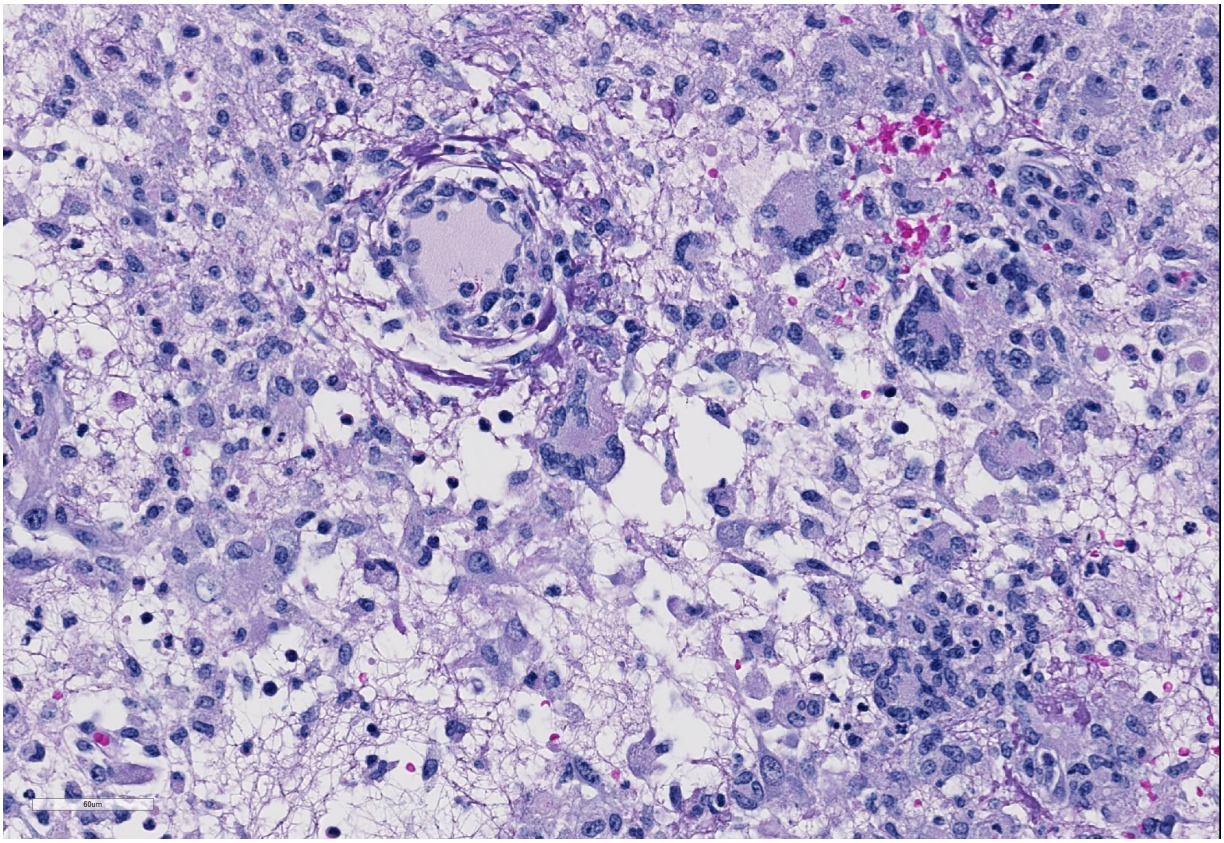

Cerebrum, colobus monkey. In more longstanding areas of infection, liquefaction predominates with large numbers of uni- and multinucleated Gitter cells. (HE, 348X)

endocytobionts, including representatives of the *Mimi*-, *Moumo*- and *Megaviridae*, as well as *Pandoviridae*. Human infections with free-living amebae, while uncommon, are especially problematic due to their high mortality, non-specific symptoms, and lack of effective treatment.

Balamuthia mandrillaris is also a cause of granulomatous amebic encephalitis which usually results from hematogenous spread from soil-contaminated wounds and which ranges in duration between *Acanthamoeba* and *Naegleria* (discussed below). A recent review of human cases from the CDC's free-living ameba registry identified 109 cases in the US within the last forty years[3] with 99% resulting in encephalitis; 6% had skin lesions as well. 68% of cases were male, with people of Hispanic ethnicity most frequently affected, and California, Texas, and Arizona had the most cases. Immunosuppressed patients accounted for less than 40% of this study. Due to the non-specific clinical signs and laboratory diagnostics, only 25% of patients received an antemortem diagnosis of *Balamuthia* infection.[3]

In humans, *Balamuthia* is thought to enter by inhalation or cutaneous wounds; hematogenous spread is supported by the tendency for trophozoites to cluster around vessels, as well as its propensity to infect multiple organs. In 2009, organ transplantation was identified as another method of transmission with kidney recipients of a donor that died of *Balamuthia* encephalitis.[3]

Acanthamoeba appear to be most often associated with disease in humans and animals, with 18 distinct genotypes based on nuclear small-subunit ribosomal DNA rather than morphology. The most common condition associated with infection in humans is a chronic keratitis, seen in immunocompetent patients associated with improper handling of contact lenses, exposure to contaminated water, or trauma. Risk factors of contact lens users include the use of all-in-one solutions, showering while wearing contact lenses, and poor contact lens hygiene.[4] Other species of free-living amoeba which may have been identified in cases of keratitis include *Hartmanella, Vahlkamphiae*, and *Allovahlkampfiae spelae.*[4]

Granulomatous amebic encephalitis is a well-documented syndrome in humans resulting from hematogenous spread, often from the lower respiratory tract or skin lesions. It shows a chronic fatal progression with luckily only 150 documented cases worldwide.[4] Due to its hematogenous origins, areas of granulomatous inflammation are seen throughout all parts of the brain. Cutaneous acanthamoebiasis is also an uncommon opportunistic condition primarily seen in immunosuppressed patients, resulting in erythematous sores and skin ulcers.[4]

Primary amebic meningoencephalitis (PAM) is another rare fatal disease in humans caused by *Naegleria fowleri.* This condition generally occurs in healthy children and adults swimming or bathing in in warm freshwater ponds. Infective amebae migrate along olfactory nerves from the nose to the

brain; fatal infection proceeds rapidly and is almost always fatal. Due to this unique entry portal, areas of lytic necrosis are clustered at the base of the brain, hypothalamus, pons, and occasionally seen in posterior areas such as the medulla oblongata.[4]

References:

1.Balczun C, Scheid PL. Free-living amoebae as hosts for and vectors of intracellular microorganisms with public health significance. *Viruses* 2017; 9:^%, doi 10-3390/v9040065.

2. Bravo FG, Alvarez PJ, Gotuzzo E. Balamuthia mandrillaris infection of the

skin and central nervous system: an emerging disease of concern to many specialties in medicine. Curr Opin Infect Dis. 2011 Apr;24(2):112-7.

3. Cope JR, Landa J, Nether cut H, Collier SA, Glaser C, Moser M, Puttagunta R, Yoder JS, Ali IK, Roy S. Th epidemiology and clinical features of *Balamuthia mandrillaris* disease in the United States, 1974-2016. *Clin Inf Dis* 2019, 68(11):1815-1822.

4. Krol-Turminska K, Olender A. Human infections caused by free-living amoebae. Ann Agric Environ Med. 2017 May 11 ;24(2):254-260.

5. Rideout BA, Gardiner CH, Stalis IH, et al. Fatal infections with Balamuthia mandril/aris (a free-living amoeba) in gorillas and other Old World primates. Vet Pa tho I. 1997 Jan;34(1): 15-22.

6. Trabelsi H, Dendana F, Sellami A, et al. Pathogenic free-living amoebae: epidemiology and clinical review. Pathol Biol (Paris). 2012 Dec;60(6):399-405.

7. Visvesvara GS, Martinez AJ, Schuster FL, et al. Leptomyxid ameba, a new agent of amebic meningoencephalitis in humans and animals. J Clin Microbial. 1990 Dec;28(12):2750-6.

8. Visvesvara GS, Moura H, Schuster FL. Pathogenic and opportunistic free-living amoeba: Acanthamoeba spp., Balamuthia mandrillaris, Naegleria fowleri, and Sappinia diploidea. FEMS lmmunol Med Microbial 2007; 50:1-26.

CASE IV: WSC 1920 Conf 22 Case 4 DVD (JPC 4100234).

Signalment: 26-year-old, male intact Geoffroy's spider monkey (*Ateles geoffroyi)*

History: The previous year, this animal had episodes of depression and diarrhea and was diagnosed with *Campylobacter hyointestinalis*. At that time, treatment led to complete resolution of signs. The following year, the monkey presented with lethargy and loose stool. Weight loss of 2 kg had occurred over the previous two months and symptomatic treatment including fluids and antibiotics was provided. The animal died the following day.

Gross Pathology: On necropsy, the markedly dilated large intestine contained a large amount of homogenous, brownish, turbid, thick fluid. The most aborad ileal mucosa, the cecal mucosa, and large

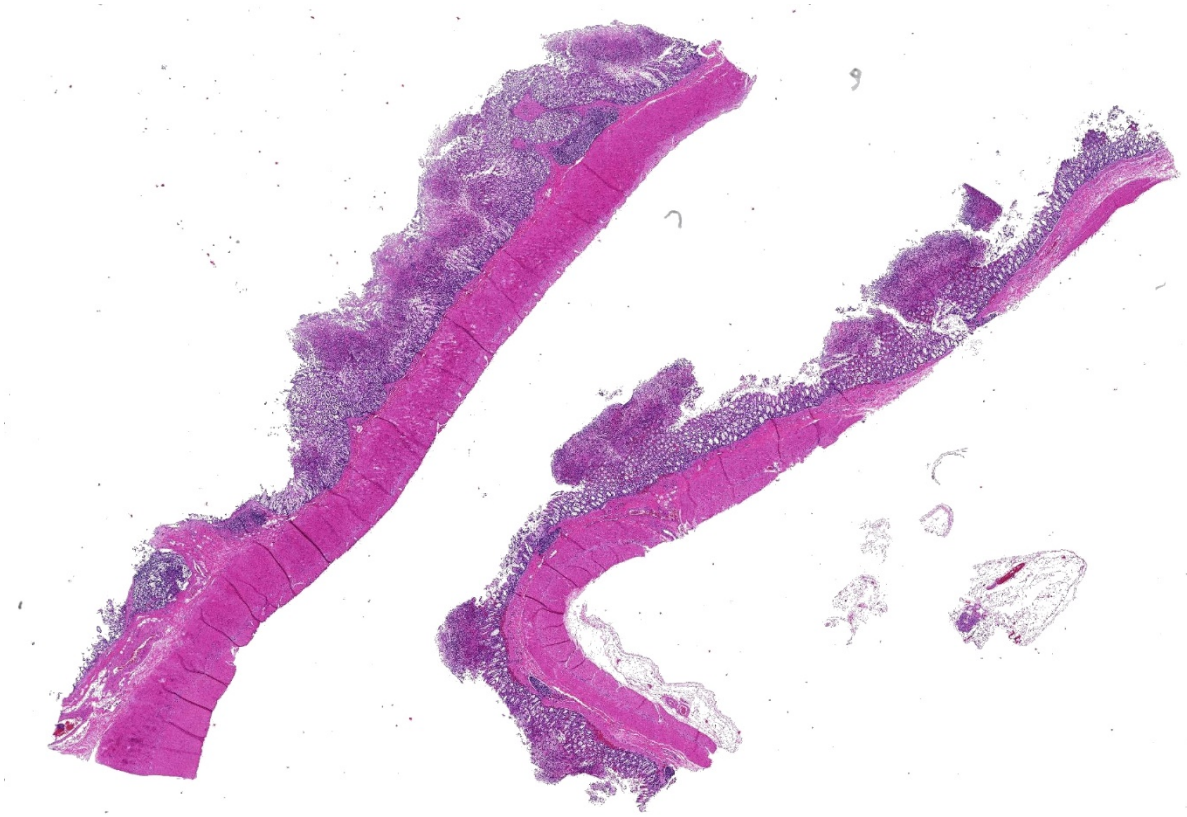

Intestine, spider monkey. Multifocally, the mucosa is effaced by foci of eosinophilic cellular debris that occasionally extends superficially and laterally from the mucosa surface. (HE, 5X)

portions of the colonic mucosa were covered by pale brown membranous material that was easily removable. Underneath this material, the mucosa was reddened but appeared otherwise intact. While the cecal mucosa was almost entirely coated by the pseudomembranous material, particularly in the colon, the pseudomembraneous material was distributed multifocally in numerous geographical to round, up to 3 to 4mm in diameter convex deposits that were roughly evenly spaced.

Laboratory results:

Bacteriology – aerobic and anaerobic cultures were negative. A culture for *Clostridium difficile* specifically was positive. There was no evidence of a parasitic infection based on the negative result of fecal flotation. Viral particles were not detected in the colonic content at electron microscopy.

Microscopic Description: Two to three full-thickness sections of similarly affected cecum and colon are evaluated. Multifocally, there are 'volcano lesions' composed of aggregations of sloughed epithelial cells, numerous degenerate and non-degenerate neutrophils, few erythrocytes, and fibrin within and extending from the underlying eroded epithelium and lamina propria into the lumen. Along the luminal aspect of these aggregates, frequent individual and clustered rod-shaped, straight pale basophilic bacteria up to 10 um long, occasionally with a visible

clearing (oval spores), are admixed with cocci-shaped and shorter rod-shaped bacteria. The underlying epithelium is intact within some of these areas and partially to completely necrotic in others, with variable extension of inflammatory infiltrates into the mucosa. The superficial mucosa subjacent to some of these lesions is necrotic, with sparing of the remainder of the crypts. The lamina propria is moderately expanded by plasma cells, lymphocytes, and degenerate leukocytes. Necrosis extends full thickness overlying some of the underlying lymphoid follicles (Peyer's patches/gastrointestinal-associated lymphoid tissue) within the sections of ileum and cecum. Small aggregates of fibrin are present within the lumina of a small to moderate number of the capillaries of the lamina propria and submucosa. The submucosa is multifocally expanded by small numbers of lymphocytes, plasma cells, and lower numbers of eosinophils, with mild to moderate increased submucosal clear space within some sections (edema). There is mild to moderate submucosal congestion.

Contributor's Morphologic Diagnosis:

Cecum and colon, typhlocolitis, erosive and fibrinonecrotizing (pseudomembranous), multifocal, marked, acute

Contributor's Comment: *Clostridium difficile* is a toxin-producing, gram-positive, spore-forming anaerobe best known for its role in causing pseudomembranous colitis in

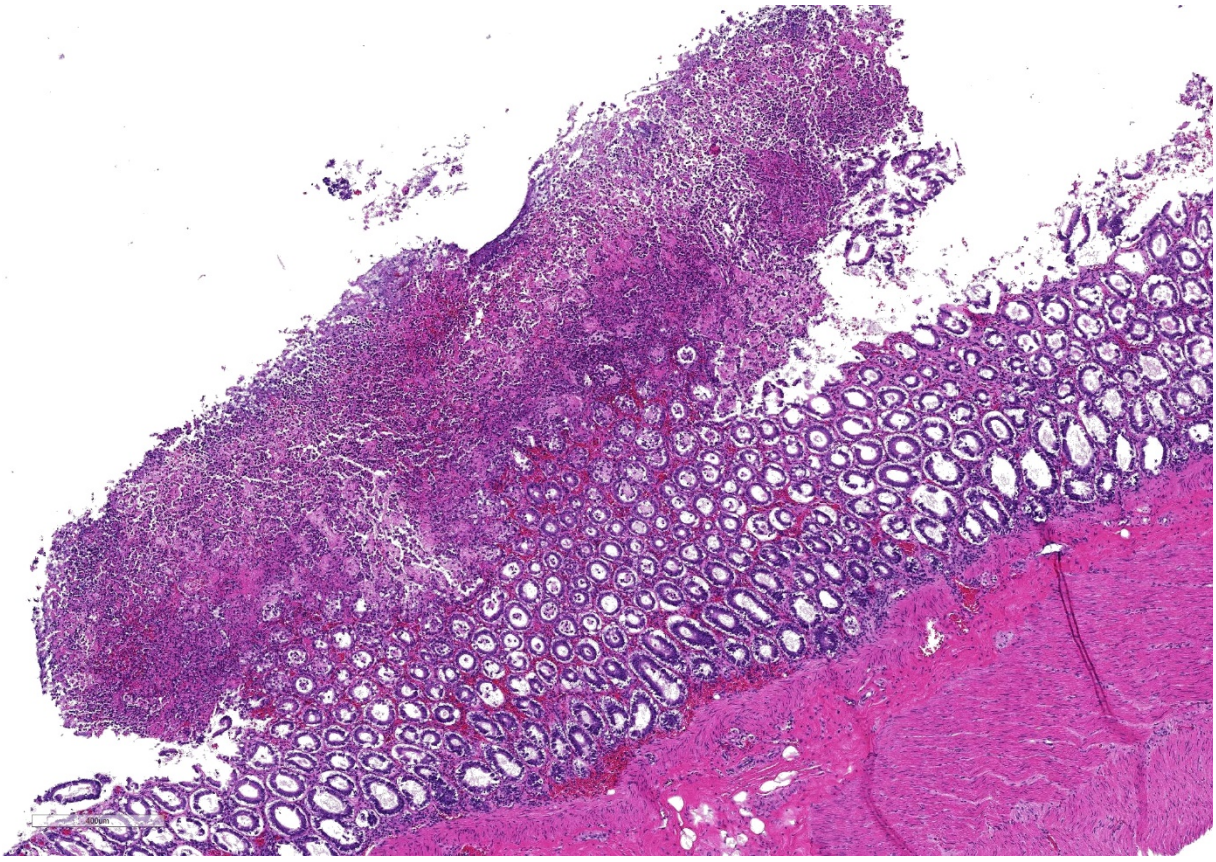

Intestine, spider monkey. Higher magnification of a characteristic "volcano" lesion, with abundant necrotic cellular debri arising over the mucosa. (HE, 20X)

humans (often referred to as *Clostridium difficile*-associated disease or CDAD), often associated with antibiotic administration.[5] As use of antibiotics has increased, so has reported cases of pseudomembranous colitis, with *C. difficile* acting as a source of a potent enterotoxin. To the author's knowledge, *Clostridium difficile*-related pseudomembranous colitis with characteristic 'volcano' lesions has not been described in New World monkeys, with a single reported case in a marmoset within the 2016 Wednesday Slide Conference that displayed more severe and diffuse histologic changes and a case report of several cotton-top tamarins that died suddenly following antibiotic therapy for *Campylobacter spp.* associated diarrhea, with identification of *Clostridium difficile* toxin within the feces in all and pseudomembranous colitis in two of the five described cases.[8]

In humans, several papers have described various morphologic stages of lesion in cases of pseudomembranous colitis, beginning with a focal epithelial necrosis with exudation of fibrin and neutrophils, followed by presence of a marked exudate extending through the area of mucosal ulceration and forming the classic "volcano" lesion, ultimately leading to a more diffuse and severe mucosal ulceration and necrosis with presence of a pseudomembrane.[5,7,10] In this case, the volcano-like lesions were a prominent feature. Similar 'volcano lesions' have been described within piglets diagnosed with *Clostridium difficile*-associated typhlocolitis and within mice and hamsters and are reported rarely in horses.[2,3,6]

While CDAD is considered well-described in humans and has been characterized in several animal species, the challenges of definitive diagnosis are ongoing. Cultures of *Clostridium difficile* are capable of isolating the bacteria, but interpretation of results is not clear-cut, given the isolation of *C. difficile* in low numbers from asymptomatic animals that have not been treated with antibiotics and in higher numbers from asymptomatic animals following antibiotic treatment.[2,13] For this reason, toxinotyping of cultured isolates is necessary to rule out presence of a non-toxigenic strain of *C. difficile*, though this is more readily available in human medicine than in veterinary medicine. Toxinotyping is a PCR-restriction fragment length polymorphism-based method that classifies strains of *C. difficile* based on variations in the pathogenicity locus (PaLoc), which is the region that codes for toxin A and toxin B, and groups strains by those with identical changes within the PaLoc region. Many isolates of *C. difficile* have been identified with varying toxigenic properties, with 34 toxinotypes reported based on sequence variations in the A and B toxin genes. PCR ribotyping allows further characterization of strains of *C. difficile* and their relatedness, which has been of particular interest due to geographical variation in the prevalence of various ribotypes.[14]

The primary virulence factors of *C. difficile* are two major exotoxins, toxin A and toxin B. Toxin A and Toxin B are both enterotoxins, while Toxin B is also a cytotoxin. Alone or together, these toxins have the ability to glycosylate and inactivate Ras GTPases, disabling key cell signaling

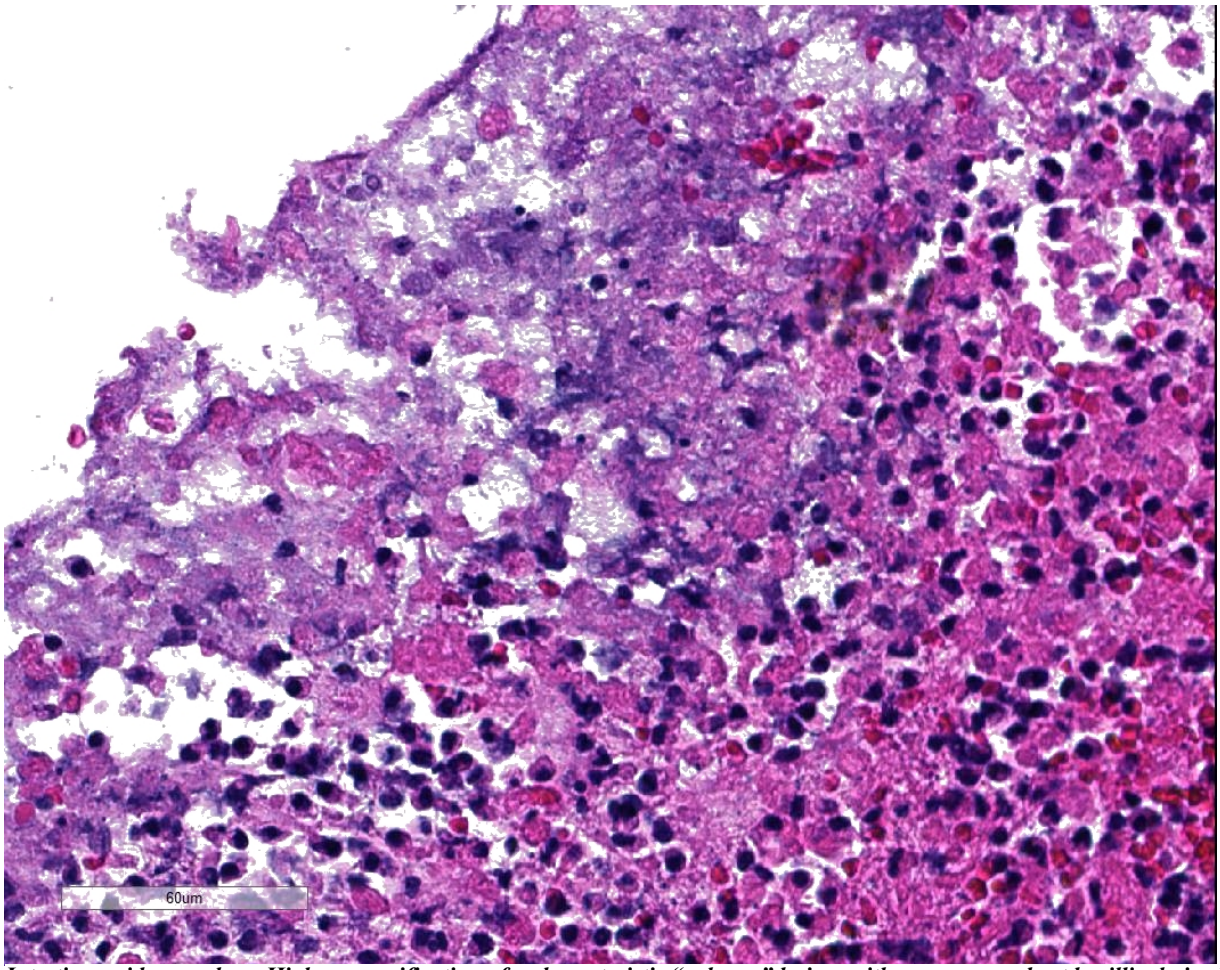

Intestine, spider monkey. Higher magnification of a characteristic "volcano" lesion, with numerous robust bacilli admixed with degenerating neutrophils, hemorrhage, and cellular debris. (HE, 400X)

pathways, and glycosylate Rho and interfere with its regulation of cytoskeletal actin.[14] Fecal ELISA is commonly used to identify one or both of these toxins, and was utilized in this case to confirm the presence of *Clostridium difficile* A and B toxins in three of four other similarly affected monkeys within the same colony, though samples were not available for submission from this particular individual at the time of diagnosis.

Almost any antibiotic can cause disruption of the intestinal microbiota and subsequent *Clostridium difficile* infection, with clindamycin frequently implicated in human cases, along with other antibiotics such as cephalosporins and broad-spectrum penicillins that are widely prescribed.[5] Resolution of clinical signs is often successful with vancomycin or metronidazole treatment.[13] *C. difficile* infection has been more widely reported in the equine and implicated in gastrointestinal disease in the dog and cat, though there is controversy as to the importance of antibiotic exposure as a risk factor in development of CDAD in these species.[2,12] Diet change and environmental stressors have also been implicated in disruption of the gastrointestinal flora and subsequent

colonization and development of CDAD in several species.[2,6]

Contributing Institution:

University of Minnesota Department of Veterinary Population Medicine/Minnesota Veterinary Diagnostic Laboratory - https://www.vetmed.umn.edu/departments/veterinary-population-medicine ; https://www.vdl.umn.edu/

JPC Diagnosis: Cecum, colon (per contributor): Typhlocolitis, necrotizing, multifocal to coalescing, marked, with numerous extracellular bacilli.

JPC Comment: *C. difficile* has been the cause of disease in a wide variety of mammalian species. First identified from feces of clinically healthy human babies in the 1930s, the organism was originally named *Bacillus difficilis* because of the difficulties encountered in cultivating it. In humans, most infected people will remain asymptomatic, with the remainder developing variable GI signs ranging from watery diarrhea to pseudomembranous colitis[1], particularly if they have been recently hospitalized or the recipient of antibiotics.

In humans, *C. difficile* associated disease (CDAD) was always assumed to affect individuals of any age except during the neonatal period, as it was thought that this specific group may lack specific *C. difficile* toxin receptors. Although between 25 and 70% of human neonates are colonized with *C. difficile*, these microorganisms have been largely considered part of the commensal microbiota. Recently, however, two 9- and 18- month-old children were diagnosed with CDAD, providing evidence that *C. difficile* is a potential cause of bloody diarrhea in neonates and young infants. In most animal species, CDAD is not age-dependent. The exception to this are pigs, which are almost exclusively affected during the neonatal period, up to approximately one week of age.[11]

The gut microbiota is the primary protection against *C. difficile* overgrowth and overt disease. In addition to antibiotic administration, alteration in bile acids (which promote the germination of *C. difficile)* has been noted in affected human patients, adding another potential factor in CDAD.[1] An emerging treatment for recurrent *C. difficile* infection is fecal microbiota transplants, which showed significantly higher rates of resolution of recurrent CDAD than those with conventional antibiotic treatment. In the Netherlands, one large medical center has set up the "Netherlands Donor Feces Bank" and a panel of internal medicine and infectious disease specialists review each case to ensure it fits a rigid set of inclusion criteria, accepting 80% of referrals and posting a 90% rate of success.[1]

In clinical disease, the bacillus is not infective. Mucosal necrosis and loss of barrier integrity is the result of liberation of a number of enzymes, including collagenase, hyaluronidase, and chondroitin-sulfatase, as well as the previously mentioned toxins, which act on the epithelial cell cytoskeleton, leading to enterocyte disassociation, fluid loss, and local inflammation.[1]

C. difficile-associated disease (CDAD) affects a wide range of other mammals – while always resulting in enterocolitis, its manifestation varies widely with the affected species. Table 1 summarizes the severity of disease in various species by enteron segment.

Table 1. Summary of lesion distribution by species.[3]

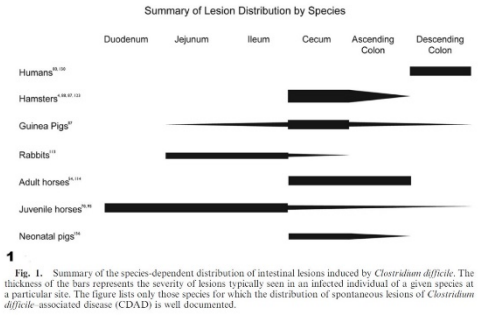

Fig. 1. Summary of the species-dependent distribution of intestinal lesions induced by *Clostridium difficile*. The thickness of the bars represents the severity of lesions typically seen in an infected individual of a given species at a particular site. The figure lists only those species for which the distribution of spontaneous lesions of *Clostridium difficile*–associated disease (CDAD) is well documented.

In rodents, CDAD is primarily cecal, resulting in ulcerative and rarely proliferative typhlitis and death. In pigs, the disease results in ulcerative typhitis or colitis with development of "volcano ulcers". An additional gross finding of mesocolonic edema[4] (as well as diarrhea) makes CDAD a differential diagnosis for edema disease in swine.[2] The difference is that *C. difficile* infections occurs in young piglets (1-7 days of age), while edema disease is a disease of weanling age pigs. It has been suggested as a pathogen for enteritis in young calves[4] as well as an agent that can cause necrotic enteritis in poultry.[10] In some Latin American countries, a linkage between high incidence in poultry and high prevalence of CDAD in humans has been identified.[4] In rabbits, the lesion is primarily seen in the small intestine and concentrated in the ileum, often following antibiotic administration. It has also been reported sporadically in dogs, cats, ostriches, prairie dogs, and experimentally in non-human primates.[11]

References:

1. Czaepiel J, Drozdz M, Pituch H, Kuijper EJ, Perucki W, Mielimonka A, Goldman S, Wultariska D, Garlicki A, Biesiade. *Clostridium difficile* infection: a review. *Europ J Clin Microbiol Inf Dis* 2019; 38:1211-1221.
2. Diab, SS, Songer G, and Uzal, FA. *Clostridium difficile* infection in horses: A review. *Veterinary Microbiology* 2013;167:42-49.
3. Hutton ML, Mackin KE, Chakravorty A, and Lyres D. Small animal models for the study of *Clostridium difficile* disease pathogenesis. *FEMS Microbiology Letters* 2014;352(2):140-149.
4. Kachrimanidou, M, Tzika E, Filioussis. Clostidioides (Clostridium) difficile in food-producing animals, horses and hosuehod pets: a comprehensive review. *Microorgainisms* 2019; 7(12):667:doi 10.3390/microorganisms7120667.
5. Kelly CP, Pothoulakis C, LaMont JT. Clostridium difficile colitis. *New England Journal of Medicine.* 1994; 330:257-262.
6. McElroy MC, Hill M, Moloney G, Aogain MM, McGettrick S, O'Doherty A, Rogers TR. Typhlocolitis associated with Clostridium difficile ribotypes 078 and 110 in neonatal piglets from a commercial Irish pig herd. *Ir Vet J* 2015; 69:10.
7. Price AB, Davies DR. Pseudomembranous colitis. *J Clin Path* 1977;30:1-12.
8. Rolland RM, Chalifoux LV, Snook SS, Ausman LM, Johnson LD. Five spontaneous deaths associated with Clostridium difficile in a colony of cotton-top tamarins (*Saguinus*

Oedipus). *Lab Anim Sci.* 1997;47(5):472-476.

9. Uzal FA, Plattner BL, Hostetter JM. Alimentary system. In: Maxie MG, ed. *Jubb, Kennedy, and Palmers Pathology of Domestic Animals*. 6th ed. Vol 2. St. Louis, MO: Elsevier; 2016:183-183, 191-194.
10. Uzal FA, Navarro MA, Li J, Freedman JC, Shrestha A, McCline BA. Comparative pathogenesis of enteric clostridial infections in humans and animals. *Anaerobe* 2018; 53:11-20.
11. Weese, JS and Armstrong, J. Outbreak of Clostridium difficile-associated disease in a small animal veterinary teaching hospital. *J Vet Intern Med* 2003;17(6):813-816.
12. Zar FA, Bakkanagari SR, Moorthi KMLST, Davis MB. A comparison of vancomycin and metronidazole for the treatment of *Clostridium difficile*-associated diarrhea, stratified by disease severity. *Clinical Infectious Diseases*. 2007;45(3):302-307.
13. Zhu S, Zhang L, Zhang C, Chen X, Chen Q, Li Z. Comparison of polymerase chain reaction ribotyping, toxinotyping and nutritional aspects of toxin production of *Clostridium difficile* strains. *Biomed Rep* 2014;2(4):477-480.

Self-Assessment - WSC 2019-2020 Conference 22

1. Which of the following is NOT susceptible to encephalomyocarditis virus?
    a. Rodents
    b. Hoofstock
    c. Reptiles
    d. Elephants

2. Cytomegaloviruses belong to which family of viruses?
    a. Polyomavirus
    b. Retrovirus
    c. Coronavirus
    d. Herpesvirus

3. Which of the following is most often associated with cytomegalovirus infection in primates?
    a. Long-term antibiotic administration
    b. Recent hospitalization
    c. Transplantation
    d. Immunosuppression

4. Which of the following is NOT considered a free-living ameoba?
    a. Entamoeba histolytica
    b. Acanthamoeba sp.
    c. Balamuthia mandrillaris
    d. Naegleria fowleri

5. Which of the following is the most definitive way to diagnose clinical *C. difficile* infection?
    a. Culture
    b. Immunohistochemistry
    c. PCR
    d. Toxinotyping

Please email your completed assessment for grading to Dr. Bruce Williams at bruce.h.williams12.civ@mail.mil. Passing score is 80%. This program (RACE program 33611) is approved by the AAVSB RACE to offer a total of 0.5 CE Credits, with a maximum of 12.5 CE Credits being available to any individual Veterinary Medical Professionals for the 2019-2020 Wednesday Slide Conference. This RACE approval is for the subject matter categories of: SCIENTIFIC using the delivery method of NON-INTERACTIVE DISTANCE. This approval is valid in jurisdictions which recognize AAVSB RACE.

Joint Pathology Center
Veterinary Pathology Services

WEDNESDAY SLIDE CONFERENCE 2019-2020

C o n f e r e n c e 23

22 April 2020

CASE I: 69887 (JPC 4117530).

Signalment: Neutered male Domestic Short Hair cat of unknown age, *Felis catus*

History: The animal was a rescue shelter cat current on all vaccinations. The animal was presented with dyspnea, hemoptysis and subsequent cardiac arrest.

Gross Pathology: The most notable postmortem findings were restricted to the lungs, which were uncollapsed, moist, firm, meaty and diffusely mottled dark red to pink with multifocal to coalescing 2-4mm white/tan raised round nodules. Impression smear of these nodules showed numerous degenerate neutrophils and macrophages. There were also multifocal, dome shaped, raised, 1-2 cm nodules with central cavitations containing few ovoid, reddish-brown ~5 x 10 mm adult trematodes.

Laboratory results: NA.

Microscopic Description: Lung: Pyogranulomatous inflammation effaces and replaces up to 40% of the lung parenchyma and occludes bronchi and bronchioles. This inflammation is composed of numerous degenerate and viable neutrophils and macrophages with fewer multinucleated giant cells, lymphocytes and plasma cells. Associated with inflammation, there are

Lungs, cat. The lung lobes are uncollapsed, moist, firm, meaty, and diffusely mottled dark red to pink with multifocal to coalescing, 2-4 mm white to tan/grey, raised, round nodules. (Photo courtesy of: Johns Hopkins University School of Medicine, Department of Molecular and Comparative Pathobiology, http://www.hopkinsmedicine.org/mcp)

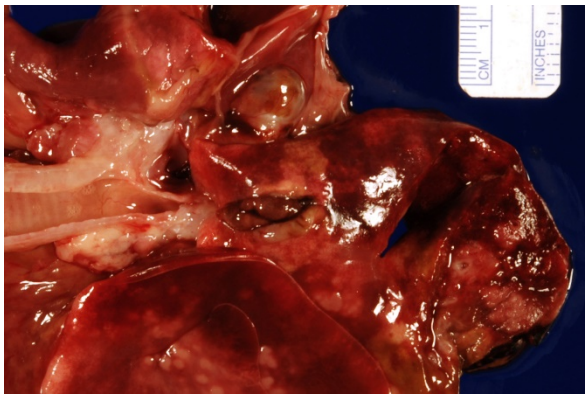

Lung, cat. There are multifocal, dome-shaped, raised 1-2 cm nodules with central cavitations containing few ovoid, reddish-brown, approximately 5x10 mm adult trematodes. (Photo courtesy of: Johns Hopkins University School of Medicine, Department of Molecular and Comparative Pathobiology, http://www.hopkinsmedicine.org/mcp)

multiple adult trematodes, parasitic eggs and multifocal bacterial colonies in the alveolar, bronchiolar and bronchial lumena. Adult trematodes are ~ 6mm X 4mm with a 40um thick spiny tegument and a spongy parenchyma that contains numerous subtegumental vitellaria with eosinophilic globular yolk material, centrally located uterus with numerous egg, few testis containing sperms, and intestinal caeca. The parasite eggs in the adult trematode and airways are 50um X 120um and embryonated with curved 110um X 30um larva, and have 1-3um thick, gold-brown, operculate, ansiotropic shell. Bacterial colonies are composed of numerous 1-2um cocci enmeshed in a brightly eosinophilic protein matrix (Splendore-Hoeppli material). Bronchi and bronchioles are partially filled with sloughed epithelial cells and low numbers of macrophages, neutrophils, lymphocytes and plasma cells and surround by moderate numbers of the same inflammatory cells, hyperplastic peribronchial mucous glands and mild fibrosis. Many bronchi containing adult trematodes are lined by lined by squamous epithelium (squamous metaplasia). Less affected areas have pigment-laden macrophages, eosinophilic proteinaceous material (edema) and hemorrhage. Multifocally, small and medium caliber blood vessels have tunica media and intima thickened by hypertrophic and vacuolated smooth muscle cells and endothelial cells, respectively, and multifocally surrounded by paler connective tissue separated by clear space (edema). There is multifocal bronchiolar and alveolar smooth muscle hypertrophy. The pleura is thickened up to 50um by inflammatory infiltrate and increased fibrosis and lined by plump and cuboidal mesothelial cells (reactive).

Contributor's Morphologic Diagnosis:

Lung, pneumonia pyogranulomatous and lymphoplasmacytic, multifocal to

Paragonimus kellicotti eggs. (Photo courtesy of: Johns Hopkins University School of Medicine, Department of Molecular and Comparative Pathobiology, http://www.hopkinsmedicine.org/mcp)

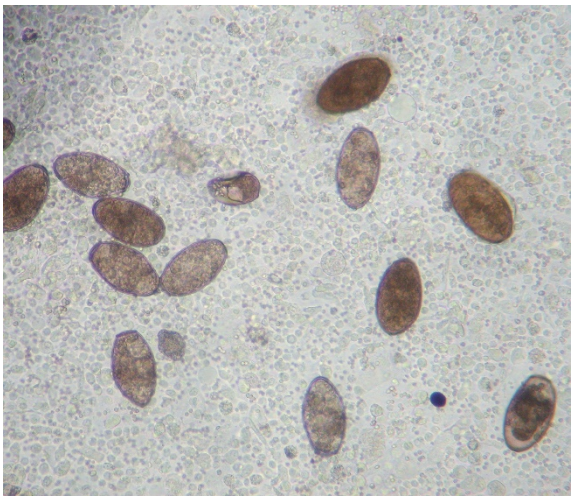

Paragonimus kellicotti eggs. (Photo courtesy of: Johns Hopkins University School of Medicine, Department of Molecular and Comparative Pathobiology, http://www.hopkinsmedicine.org/mcp)

coalescing, chronic active, severe with pleuritis and trematode adults and eggs and bacterial cocci

Etiologic diagnosis: Pulmonary paragonimiasis

Cause: *Paragonimus kellicotti*

Contributor's Comment: Pulmonary paragonimiasis is a parasitic disease caused by trematodes of the genus *Paragonimus* and the family *Troglotrematidae*. It is an important food-borne zoonotic disease affecting crayfish eating mammals and human worldwide, but it is most common in China, southeast Asia, and North America.[1] At least 28 species of *Paragonimus* have been discovered.[1] *P. westermani* (China and southeast Asia) and *P. kellicotti* (North America) are the two most common species.[2]

Adult trematodes are usually found in the lung of definitive hosts (human and wild and domestic animals, including dogs and cats).[1] Trematodes are also rarely found in other viscera and brain (extrapulmonary paragonimosis).[1] The first and second intermediate hosts are small aquatic snails (cercariae stage) and crayfish or crabs (metacercariae stage), respectively.[2,4] Once the second intermediate hosts are ingested by definitive hosts such as dogs and cats, the metacercariae are liberated into the intestine and subsequently migrate across the peritoneal and pleural cavities into the lung where they mature, form cysts and cause pyogranulomatous inflammation and fibrosis.[2,4]. The mature adults lay eggs into the bronchioles or bronchi and the eggs are coughed up the tracheobronchial tree, swallowed and passed in feces or excreted in the sputum.[2,4] In the external environment, the eggs hatch and release ciliated miracidia, which infect the first intermediate hosts such as aquatic snails.[2]

Clinical signs include intermittent cough, weakness and lethargy (4). Pathologic lesions are principally due to the presence

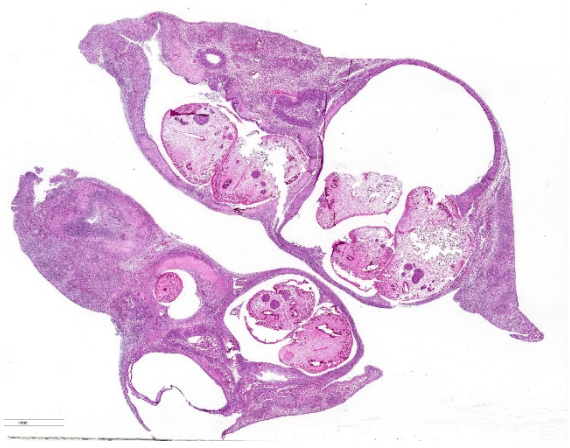

Lung, cat. Two sections of lung are presented, with cross sections of cysts containing paired adult trematodes. The remainder of each section is atelectatic with patch areas of inflammation. (HE, 7X)

Lung, cat. Higher magnification of the adult trematode, demonstrating a spiked tegument, spongy body cavity, numerous vitellarian glands (black arrows), cross section of cecum (green arrow) and testes (yellow arrows). (HE, 67X)

and migration of adult trematodes and eggs and metabolites produced by trematodes (1). Common pulmonary lesions include pyogranulomatous pneumonia, catarrhal and eosinophilic bronchitis and pleuritis (4). In addition, pneumothorax also can happen rarely due to rupture of parasitic cysts (4). Ectopic extrapulmonary paragonimosis occur more often than in other mammalian species (1). Common sites extrapulmonary Paragonimosis are the brain, spinal cord, abdominal cavity and subcutis (1).

Contributing Institution:

Johns Hopkins University School of Medicine
Department of Molecular and Comparative Pathobiology
http://www.hopkinsmedicine.org/mcp

JPC Diagnosis: Pneumonia, pyogranulomatous, multifocal, mild with encysted adult trematode and eggs.

.

JPC Comment: Paragonimiasis is an uncommon acquired infection of crustacean-eating animals. Of the approximately 30 named species of *Paragonimus*, ten are considered pathogenic, but the overwhelming number of cases occur, as mentioned above, as a result of *P. westermani* infection in Asia, and *P. kellicotti* in the United States.

P. rudis was the first lung fluke to be described by Natere in 1828, *P. westermani* was first described by Conrad Kerbert in 1878 in a Bengal tiger at the Amsterdam Zoo and named for the zoo's curator, C.F Westerman. The next year, B.S. Ringer identified the first case of human paragonimiasis in the lung, and the following year, Patrick Manson and Erwin von Baetz independently diagnosed cases by viewing fluke eggs in human sputum for the first time. The first case of *P. kellicotti* in the U.S. was identified in a dog in Ohio by Kellicott in 1894, and in a cat by Ward, and the first human case of *P. kellicotti* was identified by Abend in 1910.

Human paragonimiasis is far more common in Asia, where it is considered endeminc in some areas of China and Southeast Asia in humans who eat raw, undercooked, or alcohol-pickled freshwater crayfish. In the U.S., cases of non-native paragonimiasis (*P. westermani* infection from eating imported Asian crabs) still outweigh cases of native paragonimiasis (*P. kellicotti* infection from consuming raw or undercooked crayfish).

Published risk factors for cases of native paragonimiasis include young males (males outweigh females 15:1), alcohol consumption, and paddling, boating, or camping along the upper Mississippi river valley, with a particular concentration in the state of Missouri. Many cases of nonnative paragonimiasis arise as a result of eating poorly cooked imported crabs, often in sushi restaurants. In parts of Asia where "drunken crabs" (ethanol-picked crabs) are a delicacy, up to 30% of the local population have antibodies to *P. westermani*. A resurgence in consumption of wild boar meat in Japan has resulted in a number of cases of infection with *P. miyazakii.*

The contributor has described the complex life cycle of lung flukes with multiple intermediate hosts. Young pathologists are often intrigued by the very characteristic presence of two hermaphroditic flukes in each cyst (as illustrated in this case). *Paragonimus* flukes are indeed hermaphroditic, with presence of both testicular and ovarian tissue within an individual. While under certain circumstances they can self-fertilized, cross-fertilization is generally the rule (hence the presence of two flukes) and the cysts are known as "mating cysts".)

In humans, the prepatent period for both nonnative and native paragonimasis is 2 to 16 weeks with an average of 10 weeks. The initial clinical signs occur days following ingestion with abdominal cramps, diarrhea and fever (likely the period of migration of metacercaria out of the intestine.). After 2-16 weeks, a constellation of clinical signs occur, including fever, "rusty" hemoptysis

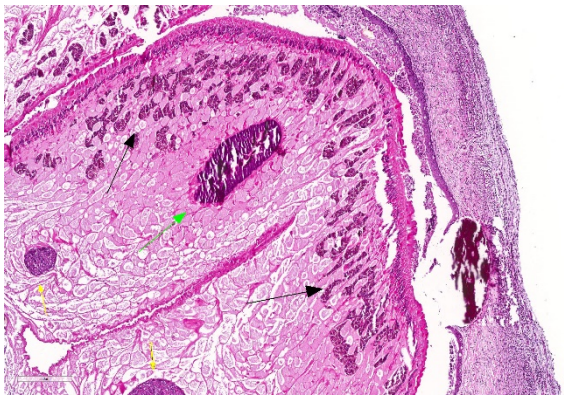

Lung cat. Cross section of encysted adult trematode demonstrating spiny tegument and spongy parenchyma, and cross sections of ceca (black arrows), vitellarian glands (green arrows), testes (blue arrows) and uterus with eggs (red arrows). (HE, 40X).

(due to the presence of red blood cells from rusty mating cysts.), and peripheral eosinophilia. Respiratory infections are the rule, although aberrant migration may result in cutaneous infections (*trematoda larval migrans)* or cerebral infections. Complications of respiratory infections in humans include pneumothorax, constrictive pleuritis and pleural effusions. Following diagnosis, treatment with praziquantel generally effects a cure.

References:

1. Madarame H, Suzuki H, Saitoh Y, Tachibana M, Habe S, Uchida A and Sugiyama H. Ectopic (subcutaneous) *Paragonimus miyazakii* infection in a dog. Vet Pathol. 2009 Sep;46(5):945-8.
2. Blair D. (2014) Paragonimiasis. In: Toledo R., Fried B. (eds) Digenetic Trematodes. Advances in Experimental Medicine and Biology, vol 766. Springer, New York, NY.
3. Gardiner CH, Poyton SL. An Atlas of Metazoan Parasites in Animal Tissue. Washington, DC: Armed Forces Institute of Pathology; 1990:46-48.

4. Caswell JL, Williams KJ. Respiratory System. In: Maxie ME, ed. Jubb, Kennedy, and Palmer's Pathology of Domestic Animals. 6th ed. Vol 2, Philadelphia, PA: Elsevier; 2016:591.

CASE II: PV300 (JPC 4119013).

Signalment: A 6.9 years old, female spayed, mixed breed (*canis familiaris*).

History: Ascites. Ultrasound examination revealed many cysts in the abdominal cavity. The cysts were sampled on exploratory laparotomy.

Gross Pathology: Open and friable cyst approximately 7 cm in diameter. On section many spaces, approximately 2 cm in diameter that contain clear fluid.

Laboratory results: NA.

Microscopic Description: The tissue sections consist of mesenteric/peritoneal fat with peritoneal connective tissue with minimal fibrosis and mononuclear cell infiltration. There is formation of many cystic spaces composed of a wall of mature fibrous tissue with an inner layer of palisading macrophages surrounding degenerate cestode larvae with a thick, smooth capsule, a subjacent layer of somatic cells and a loose body cavity with numerous calcareous corpuscles. No scolices are observed.

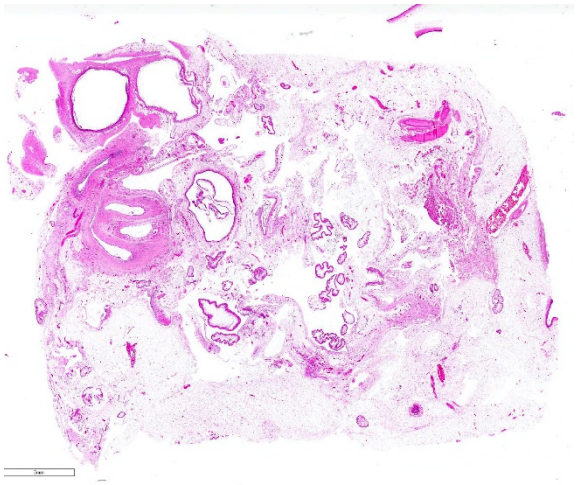

Mesentery, dog. Subgross examination of a section of mesenteric fibroadipose tissue contains cross sections of numerous metacestodes which are both encysted and free in the tissues. (HE, 7X)

Contributor's Morphologic Diagnosis:

Mild chronic peritonitis with cestode larvae - most compatible with canine peritoneal larval cestodiasis

Contributor's Comment: Most parasites found in the peritoneal cavity occur during their normal migration to another site. Only a few larval and adult helminths use the abdominal cavity as their normal habitat. Cysticerci may be found on the peritoneum in rabbits and ruminants during their normal development; they are nonpathogenic and incite no tissue response beyond a thin bland fibrous capsule. Rarely, cysticerci are reported in the abdomen of carnivores, which are abnormal hosts.[10]

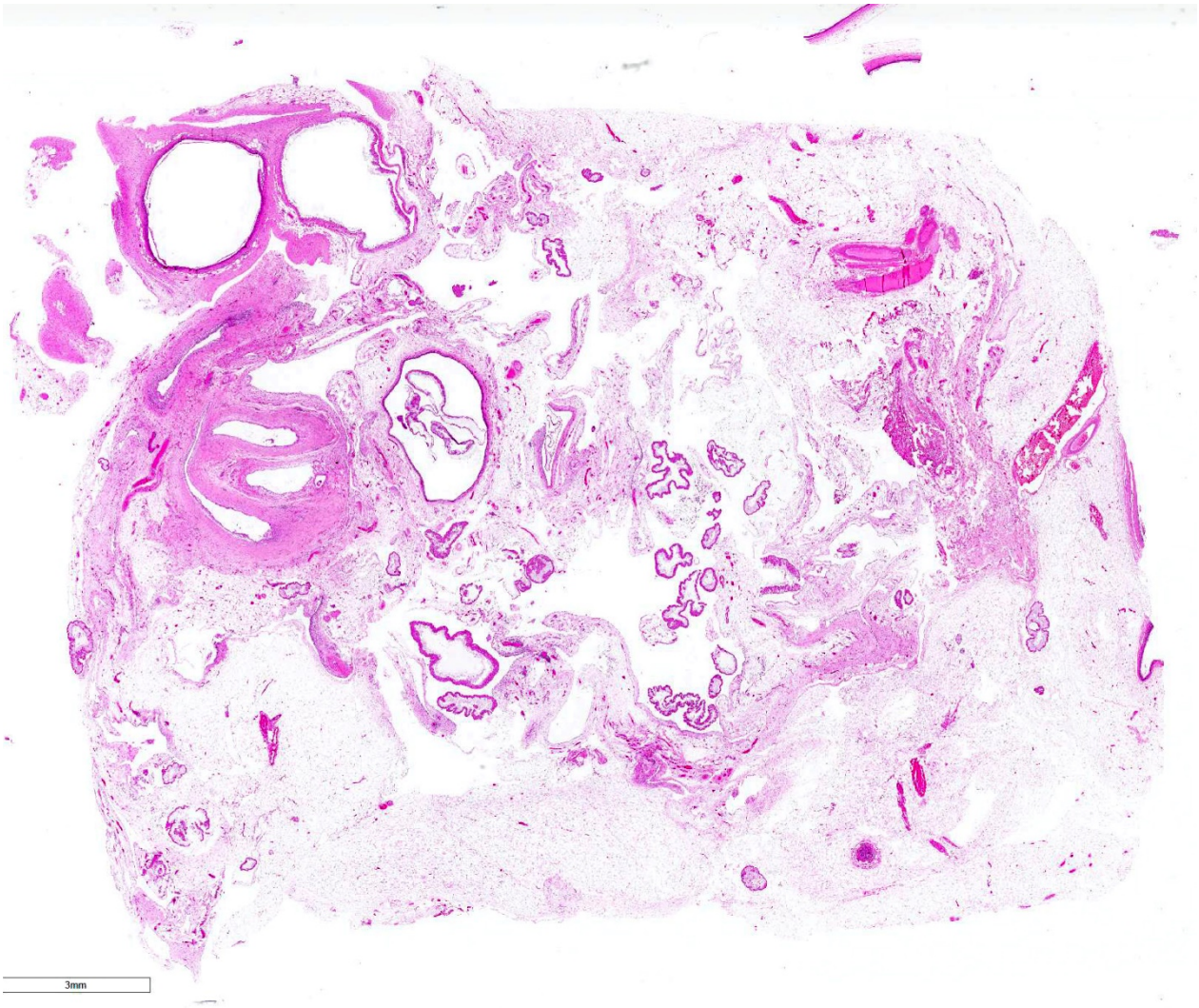

Mesentery, dog. Higher magnification of degenerating metacestodes within fibrous cysts (black arrows) and viable asexually replicating metacestodes free in the tissue. (HE 38X)

The etiology in this case is most compatible with infection with the tapeworm *Mesocestoides* spp. The larvae of *Mesocestoides* can proliferate extensively in the abdominal cavity of carnivores and cause a pyogranulomatous and proliferative peritonitis known as parasitic ascites or canine peritoneal larval cestodiasis (CPLC).[1,9,10]The diagnosis in this case was confirmed by PCR. The differential diagnosis is infection with *Spirometra* spp. which may also encyst in the peritoneal cavity of carnivores.

Canine peritoneal larval cestodiasis (CPLC) is an unusual parasitic disease in dogs that is caused by asexual proliferation of larval *Mesocestoides*. *Mesocestoides* spp. are tapeworm parasites. Adult worms reside in the intestinal tracts of their final hosts, which include carnivores, birds and occasionally humans. Infection with adult worms is usually asymptomatic. In contrast, the third stage larvae, called tetrathyridium, live in the serosal cavities of second intermediate hosts, which include amphibians, reptiles, birds, and rodents.

Dogs and cats can also harbor tetrathyridia in their peritoneal cavities.[6,9] Proglottids from adult parasites are not directly infectious to definitive or secondary intermediate host species.[6,9]

Diagnosis of infection by *Mesocestoides* spp. can be confirmed by morphologic identification of tetrathyridia or by PCR.

Recommended treatment involves long term therapy with praziquantel.[8] Praziquantel has been reported effective to eliminate peritoneal tetrathyridia definitely. Early recognition of CPLC improves the prognosis, as it may be an incidental, but severe finding.[8]

Contributing Institution:

Department of Veterinary Resources
Weizmann Institute
Rehovot 76100, Israel
http://www.weizmann.ac.il/vet/

JPC Diagnosis: Fibroadipose tissue: Encysted and free tetrathyridia multiple with mild granulomatous steatitis.

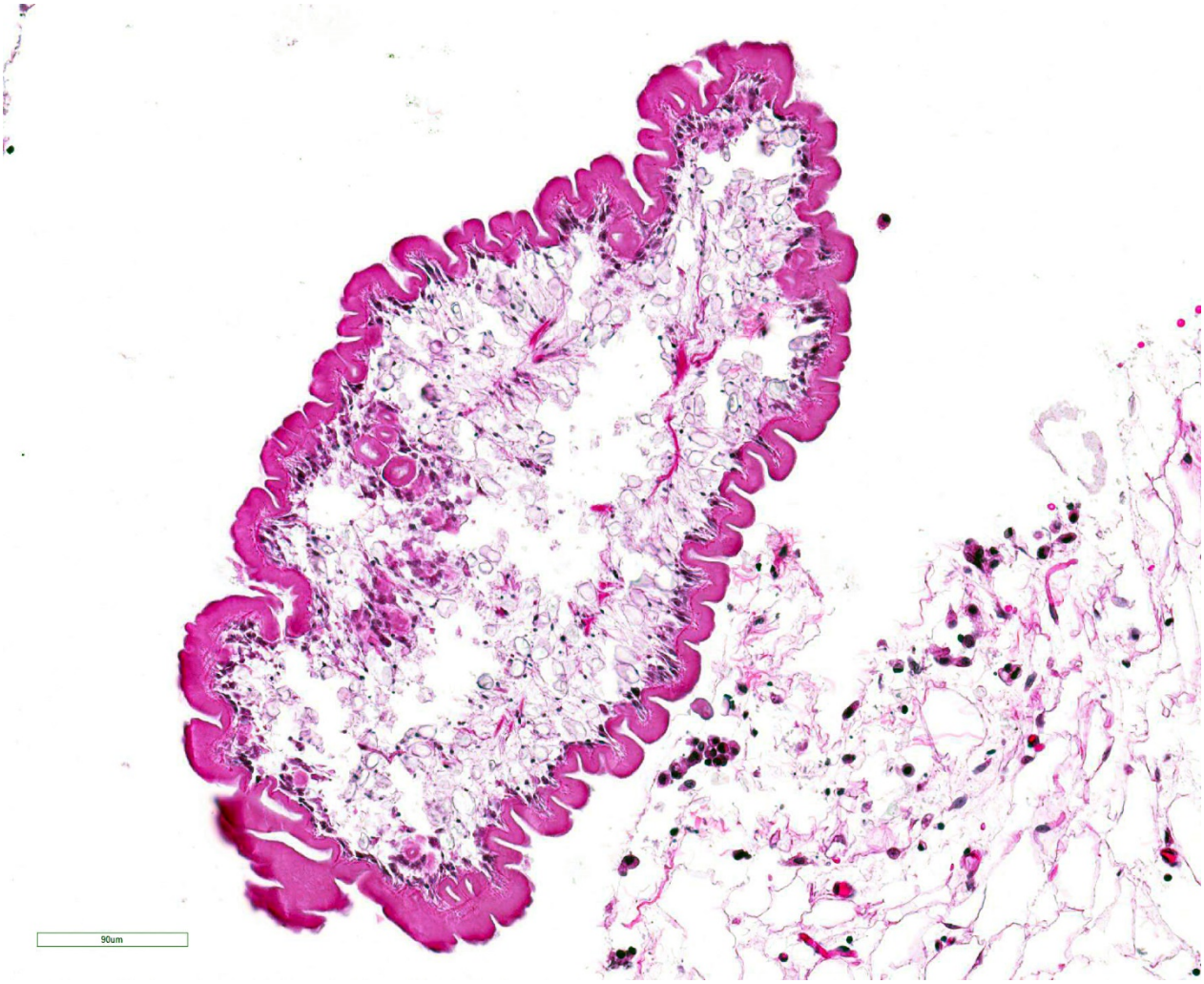

Mesentery, dog. Cross-section of a mesocestode (tetrathyridium) demonstrating a thick eosinophilic tegument, subtegumental somatic cell nuclei, a spongy parenchymatous body and numerous oval clear calcareous corpuscles. (HE 246X)

JPC Comment: The uniqueness of the cyclophyllidean cestodes belonging to the Family Mesocestoidae is matched only by the continued mystery of its life cycle. First identified in 1863, published life cycles remain presumptive 150 years later. Gravid proglottids are shed in the feces of a carnivore definitive host (which is rarely man).[2,7] Eggs are contained within the parauterine organ, a structure unique to *Meoscestoides* and a diagnostic feature when examining proglottids.[7] Eggs lack a shell, and possess an emybryophore enveloping the naked oncosphere.[7] The eggs are ingested by the first intermediate host (presumptively an arthropod) where it develops into a second, as yet undescribed larval (or metacestode) stage. The metacestode possesses all of the somatic structures of the eventual adult cestode with the exception of reproductive organs. [7] The arthropod host is then consumed by a vertebrate secondary host, usually an amphibian or reptile (but rodents and birds may also serve as intermediate hosts), where upon the larva passes through a series of post-larval forms, ultimately becoming a tetrathyridia, the infective stage for the final carnivore host.[2] Terrestrial carnivores including dogs, cats, procyonids, mustelids, and opossums, are most commonly identified as definitive hosts.[2] While in the secondary intermediate host or the definitive host, tetrathyridia possess the ability to divide asexually, sometimes achieving large numbers and infections similar to that illustrated in this case. Only in the definitive carnivore host does the tetrathyridium evaginate, attach to the intestinal mucosa, and mature into an adult cestode.[2]

Human infections with metacestodes are quite rare, and only two genera *(M. lineatum* in Asia, Europe and Africa and *M. variablilis* in North America) have been reported in these cases.[4] Most cases involve the consumption of uncooked viscera or blood containing metacestodes (tetrathyridia).[4]

In the dog, the disease is referred to as canine peritoneal larval cestodiasis, and this type of infection is less commonly seen in cats.[1,3] Asexual proliferation of tetrathyridia results in variable degrees of granulomatous peritonitis with occasional extension into abdominal organs and the thoracic cavity. Clinical signs are generally vague, and include lethargy, weight loss, vomiting, and ascites. Some cases are identified during routine OHE and castration (including WSC 2014, Conference 3 Case 3.)[1,3]

In 2014, a similar asexually proliferative metacestode infection was first identified in a captive juvenile Borneo orangutan which we had been American-born and currently resided in a zoo in Michigan. Cestode parasites of the genus *Versteria* are most commonly seen in small mammals including mustelids and weasels. Atypical infection of this non-human primate manifested as cysts within the liver, lung, and spleen containing numerous metacestodes which were identified as unique members of the genus *Versteria* with 12% difference from the DNA of the closest species (*V. mustelae).*[5]

References:

1. Boyce W et al. Survival analysis of dogs diagnosed with canine peritoneal larval cestodiasis (Mesocestoides spp.). *Vet Parasitol* 2011. 180:256– 261
2. Centers for Diseases Control: DPDX – Identifcation of Parasites of Public Health Concern. https://www.cdc.gov/dpdx/mesocestoidiasis/index.html
3. Crosbie PR, Boyce WM, Platzer EG. Diagnostic procedures and treatment of eleven dogs with peritoneal infections caused by Mesocestoides spp. *J Am Vet Med Assoc* 1998; 213:1578-1583.
4. Fuenza MV, Galan-puchdes MT, Maline JB. A new case report of human *Mesocestoides* infection in the United States. *Am J Trop Med Hyg* 2003; 68(5)566-567.
5. Goldberg TL, Gendron-Fitzpatrick A, Deering KM, Wallace RS, Clyde VL, Lauck M, Rosen GE, Bennett AJ, Greiner EC, O'Connor DH. Fatal metacestode infction in Bornean orangutan caused by unknown Versteria species. *Emerg Inf Dis* 2014; 20(1):109-113.
6. Kashiide T et al. Case report: First confirmed case of canine peritoneal larval cestodiasis caused by Mesocestoides vogae (syn. M. corti) in Japan. *Vet Parasitol* 2014. 20:154–157.
7. McAlister CT, Tkach VV, Conn DB. Morphological ad molecular characterization of post-larval pretetrathrydia of Mesocestoides sp. (Cestoda Cyclophyllida) from Ground Skink from Southeastern Oklahoma. *J Parasitol* 2018; 104(1):246-253.
8. Papini R et al. Effectiveness of praziquantel for treatment of peritoneal larval cestodiasis in dogs: A case report. *Vet Parasitol* 2010. 170:158–16,
9. Uzal FA et al. Alimentary system. In: Jubb, Kennedy and Palmer's *Pathology of Domestic Animals*. Ed: M Grant Maxie. 6th ed. vol. 2, Elsevier, 2016:223.
10. Uzal FA et al. Alimentary system. In: Jubb, Kennedy and Palmer's *Pathology of Domestic Animals*. Ed: M Grant Maxie. 6th ed. vol. 2, Elsevier, 2016:255.
11. Wirtherle N et al. First case of canine peritoneal larval cestodosis causedby Mesocestoides lineatus in Germany. *Parasitology International*. 2007. 56:317–320

CASE III: 61290 (JPC 4117380).

Signalment: 7.5 year old, female Malayan Snail-eating turtle, *Malayemys subtrijuga*

History: This captive-hatched animal was found dead with no history of clinical signs.

Gross Pathology: An approximately 2.0 cm long by 0.3 cm diameter off-white to yellow,

Lung, turtle. Numerous adult pentastomes are present within the lungs and one is contained within on of the mainstem bronchi. (Photo courtesy of: Disease Investigations, Institute for Conservation Research, San Diego Zoo Global, PO Box 120551, San Diego, CA 92112, http://institute.sandiegozoo.org/disease-investigations)

Pentastome. Adult pentastomes are pseudosegmented and had a flattened anterior end with four hooklets. (Photo courtesy of: Disease Investigations, Institute for Conservation Research, San Diego Zoo Global, PO Box 120551, San Diego, CA 92112, http://institute.sandiegozoo.org/disease-investigations)

round parasite (identified as a pentastome) was within the caudal oral cavity near the base of the tongue. Approximately 5-10 similar parasites were throughout the parenchyma of each lung, and a single parasite was folded within the lumen of the right bronchus. Under a dissecting scope, the parasites had a slightly expanded and flattened anterior end with four hooks on the flattened surface.There was very subtle banding or pseudosegmentation of the parasite body, and most of the body cavity was filled with a thick, highly convoluted white to off-white tubular structure (presumed uterus). The turtle's lungs were diffusely pink-red and wet, yet floated when placed in 10% neutral buffered formalin.

Two smaller grey-tan, coiled, round pentastome nymphs measuring approximately 1.0 cm long by 0.1 cm diameter were in the adventitia of the mid esophagus, adjacent to the medial aspect of the left lung. No adipose stores were present, and there was some watery coelomic fluid.

Laboratory results: Parasite Identification: Whole parasites were submitted to the Zoological Medicine and Wildlife Disease Laboratory at the University of Florida for speciation using a pentastome PCR assay, which resulted in a sequence that identified the parasites as *Sebekia mississippiensis*.

Microscopic Description: Lung (sections from 3 blocks): There is some variability between slides. The interstitium of faveolar septa is diffusely expanded by edema and variable numbers of inflammatory cells with occasional foci of hemorrhage. The inflammatory infiltrate consists of predominately granulocytes, lymphocytes and plasma cells with fewer histiocytes and

Pentastome. Much of the body of the female contains a convoluted egg-filled uterus. (Photo courtesy of: Disease Investigations, Institute for Conservation Research, San Diego Zoo Global, PO Box 120551, San Diego, CA 92112, http://institute.sandiegozoo.org/disease-investigations)

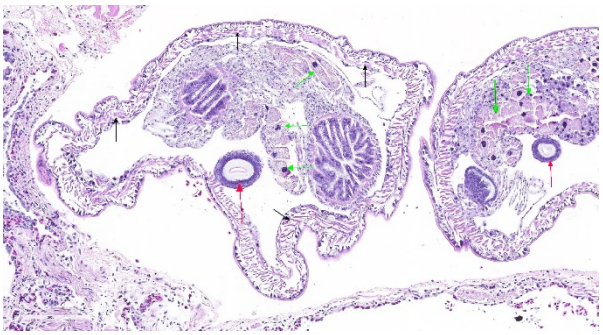

Lung, turtle. Cross sections of the anterior end of the pentastomes demonstrates a thin cuticle, coelom, skeletal muscle (black arrows), chitinous hooklets (red arrows) and cross sections of an intestinal tract bordered by large eosinophilic glandular cells (green arrows). (HE ,140X)

melanomacrophages. A few 1-2 mm diameter metazoan parasites expand and compress faveoli, fill a bronchial lumen, or are embedded in pleural connective tissue, depending on the section. These parasites have features consistent with pentastomes, including a thin, undulating to pseudosegmented eosinophilic cuticle which contains occasional openings lined by refractile, eosinophilic material (sclerotized pores). Underlying the cuticle, striated skeletal muscle fascicles with subcuticular glands make up the body wall, which encloses a body cavity containing a multicellular digestive tract lined by eosinophilic glands and a reproductive tract. In sections of mature parasites, the uterus is filled with developing eggs. Chitinous hooks are present in some sections. Also present in faveolar lumina are variable amounts of sloughed respiratory epithelium mixed with granulocytes, macrophages, red blood cells, debris and bacteria. The faveolar epithelium is frequently absent, hypertrophied or hyperplastic. There are 1-2 discrete heterophilic granulomas within the interstitium in some sections. These occasionally contain folded, hyalinized, eosinophilic membranous material (presumed pentastome cuticle).

Contributor's Morphologic Diagnosis:

Lungs: Moderate, diffuse, granulocytic and lymphoplasmacytic interstitial pneumonia with epithelial erosion and hyperplasia and adult and nymph pentastomes

Contributor's Comment: Pentastomiasis is a disease caused by a group of blood-sucking endoparasites with a world-wide distribution.[5] Variably considered a separate phylum or a subclass of phylum Arthropoda, Pentastomida is an interesting group of obligate parasites most closely related to branchiurans, or fish lice, a type of crustacean arthropod.[5,7] The distribution of definitive hosts and fossil records show pentastomids first appeared when reptiles flourished during the Mesozoic era.[7,9] Approximately 90% of pentastomes use reptiles as definitive hosts, and the life cycle is indirect.[7,9]

Adult pentastomes typically reside in the lower respiratory tract and produce larvated

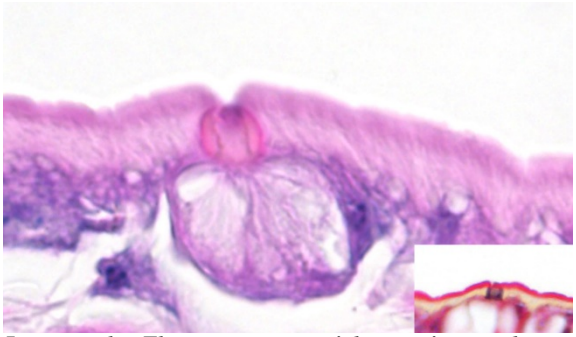

Lung, turtle. The pentastome cuticle contains regular spaced sclerotzedc openings, which stain black with a Movat's pentachrome (inset) (HE and Movat's pentachrome, 400X) (Photo courtesy of: Disease Investigations, Institute for Conservation Research, San Diego Zoo Global, PO Box 120551, San Diego, CA 92112, http://institute.sandiegozoo.org/disease-investigations)

ova that are swallowed and expelled from the definitive host in feces.[5] Intermediate hosts of various pentastomids are mostly fish and mammals, which can include humans, with additional animals able to serve as paratenic hosts.[7] Some definitive hosts can harbor nymph and adult stages.[7,9] The intermediate host ingests ova from contaminated water, vegetation, or fecal matter. Once ingested, the first stage nymph emerges from the egg, penetrates the gastrointestinal tract, and migrates through viscera. Here the nymph encysts and molts multiple times to become an infective nymph. Once the intermediate host is ingested by the definitive host, nymphs excyst and migrate to the lungs where they mature, completing the lifecycle.[5,7]

Infections in reptile hosts vary in severity from incidental to fatal. Adult pentastomes in their natural host often incite only mild inflammation; however, clinical signs in captive reptiles can include lethargy, anorexia, dyspnea, pneumonia, and sudden death.[1,4,5] The eggs can be detected in feces or lung wash samples.[2,4] Clinical signs are due to tissue destruction or inflammation associated with parasite migration, from parasite molting which can elicit a hypersensitivity reaction, from respiratory tract obstruction, or from secondary bacterial infections.[4,7,9] The turtle in this report had significant inflammation throughout the lungs, including a few heterophilic granulomas that appeared to be associated with molted cuticle, as well as obstruction of a primary bronchus by an adult worm.

The most defining characteristic of pentastomids in histologic tissue sections is the presence of sclerotic pores that open into the cuticle within the body wall. These pores produce cuticle during molts.[2] Better visualization of the pores can be achieved by using a Movat pentachrome stain that stains the typically eosinophilic sclerotic pore black. Additional identifying features include two paired hooks surrounding the mouth, striated musculature, acidophilic glands encircling the intestinal tract, and pseudosegmentation.[2]

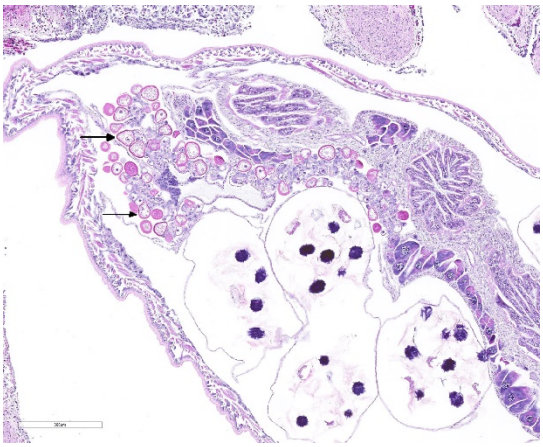

Lung, turtle. Cross-section of a female pentastome demonstrates a uterus with developing ova and multiple cross-sections of a uterus with fully developed eggs (HE, 100X)

Malayan snail-eating turtles are carnivorous turtles with diverse diets including items such as fish, earthworms, aquatic insects, and, of course, snails. Its diet in captivity consisted of earthworms, processed turtle brittle and gel, and occasional snails. Fish were not reported to be component of its diet, although mosquito fish were sometimes present in the water system in which it was housed. The pentastomid species recovered from this turtle was *Sebekia mississippiensis*, for which fish (including mosquito fish) are intermediate hosts.[1,6]

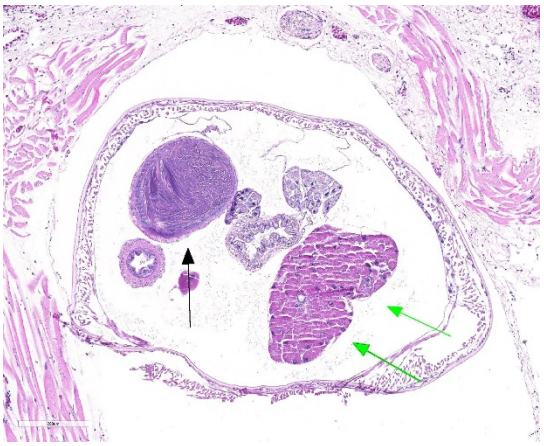

Lung, turtle. Cross-section of a male pentastome demonstrates sperm- filled testis (black arrow) and eosinophilic glandular cells (green arrows). (HE, 115X)

Sebekia sp. are pentastomids of crocodilians, and *Sebekia mississippiensis* is specifically of the American alligator.[1, 6] High mortality rates among hatchling crocodilians infected with *Sebekia* sp. has been previously reported, along with a single report of a dermal infection in a woman.[1,6,7] Pentastomes are less frequently reported in turtles than other reptiles, but infections with *Diesingia* (family Sebekidae) have been seen.[4,7,9] Both adults and nymphs were present in this turtle, which could indicate autoinfection or a continued source of reinfection. It could also act as both a definitive and intermediate host. A second snail-eating turtle in the collection was subsequently screened for pentastome infection and was negative. Screening of fish and proper freezing protocols prior to feeding can help reduce incidence of this parasite in susceptible captive animals.[1,7]

Contributing Institution:

Disease Investigations
Institute for Conservation Research
San Diego Zoo Global
PO Box 120551
San Diego, CA 92112

http://institute.sandiegozoo.org/disease-investigations

JPC Diagnosis: Lung: Pneumonia, bronchointerstitial, granulocytic, mild to moderate, chronic, with intra- and extrapulmonary pentastomes.
2. Lung: Granuloma, heterophilic, focal.

JPC Comment: The contributor has presented an excellent review of pentastome infections in reptiles. To expand on their histology, pentastome have two pairs of hooks surrounding the mouth which led early researchers to believe that they had five heads (leading to the name "pentastomes").[2] The presence and staining of sclerotized openings (unique to pentastomes) with Movat's pentachrome is important as these structures are present in all life stages, and is maintained even in degenerate or calcified specimens.[2]

Pentastomes utilize a wide range of intermediate hosts, and occasionally end up in human intermediate hosts. Most human infections involve the species *Armillifer armillatus* (whose definitive host is the python) or *A. grandis.* Intermediate hosts are infected by eating water and vegetation contaminated with eggs passed in the feces of respiratory secretions of snakes. Human infections are most common in regions of African where snake meat is eaten, although some infections are likely acquired by ingesting water or vegetation contaminated with the feces or respiratory

secretions of snakes. Autopsy studies have demonstrated a 22% infection rate in certain African countries, and a 45% incidence in autopsy is some parts of Malaysia.[8]

Poorly cooked snake meat may be purchased at markets and eaten by inhabitants of certain parts of Africa, and adult pentastomes (referred to locally as "snake springs") are spit out.[10] Chewing the pentastomes may result in liberation of eggs. After ingestion, 4-legged primary larvae migrate through the viscera, and following several molts, transformed in the legless nymphs which are characteristically found on serosal membranes and rarely within viscera.[10] While most infections in these regions are the result of *A. armillifer*, a significant number of cases of pentastomiasis may be seen with *A. grandis*.[8] While cases of *A. armillifer* result in more traditional peritoneal encysted nymphs, *A. grandis* has a predilection for ocular infections, with blindness as a common result.

References:

1. Adams L, Isaza R, Greiner E. Fatal Pentasomiasis in Captive African Dwarf crocodile Hatchlings (Osteolaemus tetraspis). Journal of Zoo and Wildlife Medicine. 2001;32(4): 500-502.
2. Gardiner, CH, Poynton, SL. *An Atlas of Metazoan Parasites in Animal Tissues*. Washington DC: Armed Forces Institute of Pathology; 1999 59-60.
3. Ioannou P, Vamvoukaki R. Armillifer infections in humans: a systematic review. *Trop Me and Inf Disease* 2019; 16;4(2). pii: E80. doi: 10.3390/tropicalmed4020080.
4. Jacobson ER. *Infectious Disease and Pathology of Reptiles.* Boca Raton, FL: CRC Press, Taylor & Francis Group; 2007 590-592.
5. Meyers WM, Neafie RC. Pentastomiasis. In Meyers, WM, ed: Topics on the Pathology of Protozoan and Invasive Arthropod Disease. Ebook; 2011: 1-10.
6. Moreland, AF, Forrester, DJ,Delany MF. Sebekia mississippiensis (Pentastomida) from Juvenile American Alligators in North Central Florida. The Helminthological Society of Washington. 1989;56(1): 42-43.
7. Paré JA. An Overview of Pantastomiasis in Reptiles and Other Vertebrates. Journal of Exotic Pet Medicine. 2008;17(4): 285-294.
8. Potters I, Desaive C, Van Den Broucke S, Esbroeck MJ, Lynen L. Unexpected infection with *Armillifer* parasites. *Emerg Inf Dis* 2017; 23(12): 2116-2118.
9. Riley J. The Biology of Pentastomids. Advances in Parasitology. 1986;25: 45-128.
10. Tappe D, Sulyok M, Riu T, Rozsa L, Bodo I, Schoen C, Muntau B, Babocsay G, Hardi R. Co-infections in visceral pentastomiasis, Democratic Republic of the Congo. *Emerg Inf Dis* 2016; 22(8):1333-1339.

CASE IV: S1601842 (JPC 4101199).

Signalment: Two week old, male Arabian foal (*Equus caballus*)

History: The foal was found in right lateral recumbency. It had appeared in good health

the day before, although it was observed to fall once while nursing when the mare moved; however it immediately stood back up and resumed nursing. On physical examination the foal was afebrile, and had a heart rate of 100, and respiratory rate of 28. The foal was unable to rise, remain standing when assisted to rise, or maintain sternal recumbency. Front limb movement appeared hypermetric, the foal intermittently flailed with a rigid head and neck, and exhibited intermittent horizontal nystagmus. No external evidence of trauma was detected. The umbilical stump and limb joints appeared within normal limits, the abdomen appeared taut, and the sclerae were slightly yellow-tinged. Abdominal ultrasound revealed an intact urinary bladder, and possible thickening of the small intestinal wall.

The foal was euthanized the same day due to a poor prognosis.

Gross Pathology: The carcass was in good postmortem condition and well-fleshed. Conjunctival mucosa, sclera and gingival mucosa were slightly yellow tinged, and there was multifocal, moderate subcutaneous hemorrhage of the subcutis of right upper eyelid, and caudodorsal cranium (overlying interparietal and occipital bones). Cranial meninges were congested with two small, focal hemorrhages on the dorsolateral aspect of the right cerebral hemisphere.

The trachea contained scant stable foam, and the lungs were spongy and pink with mild, multifocal red mottling. There was a small dark red nodule of approximately 0.3cm in diameter on the cardiac right atrioventricular valve. The stomach contained a small amount of fragmented roughage (hay) and no milk curds. The cecum and large colon contained plentiful sand and the large intestinal mucosa was diffusely red. The small colon contained loose, malodorous feces.

Laboratory results: Rare mixed bacterial flora was isolated from liver on aerobic culture, and large numbers of *Escherichia coli* and mixed bacterial flora were isolated from small intestine and large colon. Salmonella PCR was negative on liver, small intestine and colon, and ELISA testing for both *Clostridium perfringens* toxins and *Clostridium difficile* toxins, was negative on small intestinal and cecal contents.

No parasite eggs were detected in feces. Heavy metal analysis of the liver detected a marginally deficient selenium concentration, while other tested minerals were within acceptable ranges for the species.

No aerobic bacterial pathogens were isolated from a submitted sample of dam's milk, and

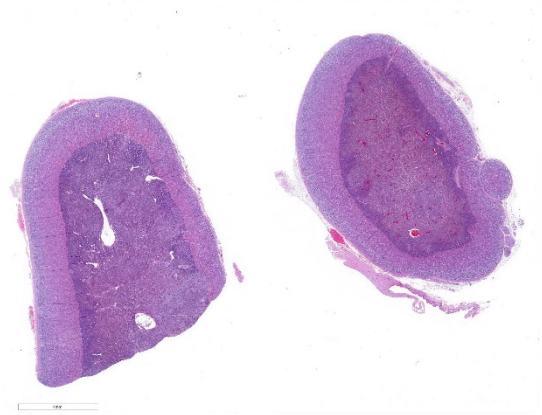

Adrenal gland, foal. Approximately 50% of the adrenal medulla is replaced by coalescing areas of necrosis and inflammation which extend into the adrenal cortex. (HE, 7X)

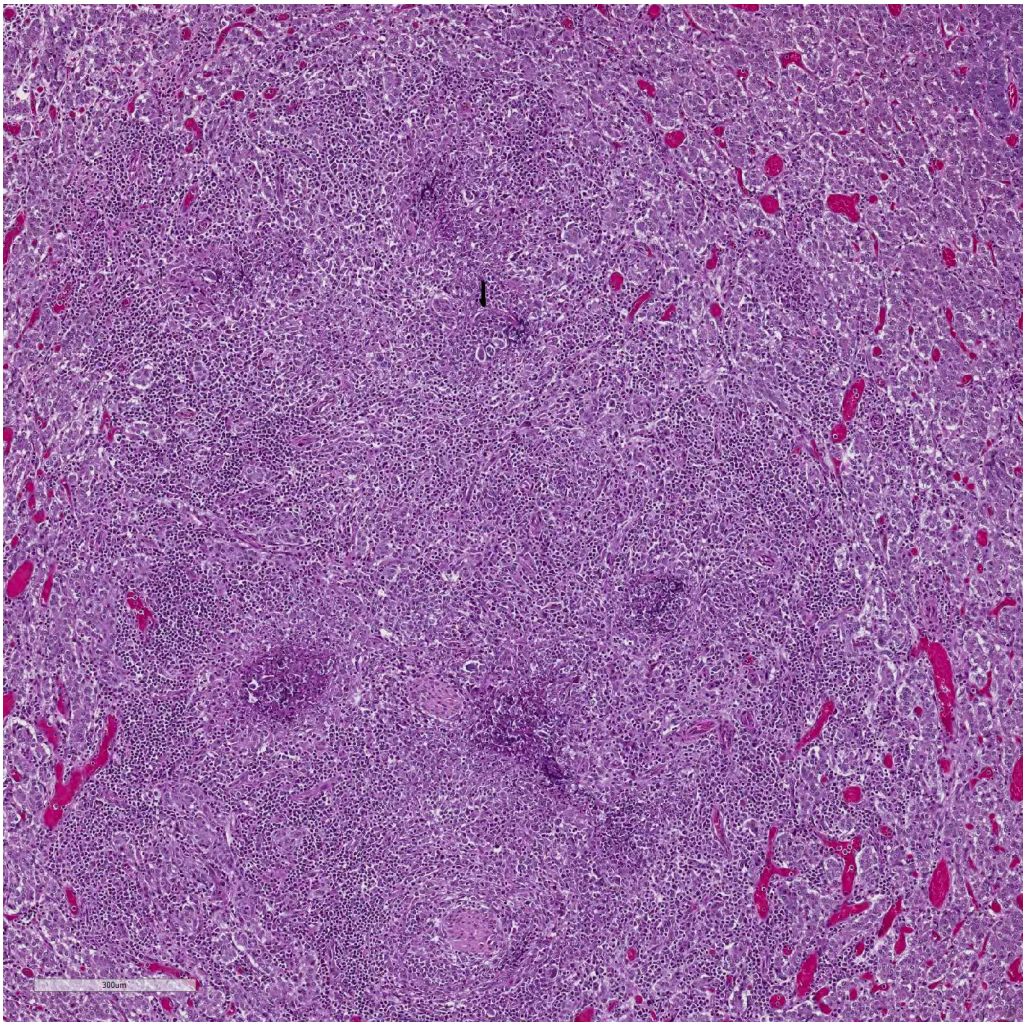

Adrenal gland, foal. Approximately 50% of the adrenal medulla is replaced by coalescing areas of necrosis and inflammation which extend into the adrenal cortex. (HE, 7X)

Clostridium botulinum toxin testing was negative on a submitted feed sample (mare and foal pellet).

Microscopic Description: Adrenal gland: The medulla is extensively disrupted by multifocal to coalescent, variably sized foci of granulomatous inflammation characterized by densely cellular aggregates of Langhans-type multinucleated giant cells and epithelioid cells, and large numbers of admixed and/or peripheral lymphocytes and plasma cells. Some of the granulomas are centrally necrotic and there are scattered tangentially and cross-sectioned larval and adult rhabditid nematodes with a diameter of 10-25um, and fewer thin-walled, multicellular to larvated, ovoid eggs. In a small number of tangentially sectioned nematodes it is possible to identify anatomical features such as a rhabditiform esophagus with isthmus and terminal bulb, dark basophilic granular structures of 2-3 um within the pseudocoelom, and a smooth cuticle.

Contributor's Morphologic Diagnosis:

Adrenalitis, granulomatous, lymphoplasmacytic, multifocal to coalescent, moderate to severe, with multifocal necrosis and rhabditiod nematodes, etiology presumptive *Halicephalobus gingivalis*.

Contributor's Comment: In addition to the adrenalitis, histologic examination of the brain sections from this foal identified the presence of granulomatous to

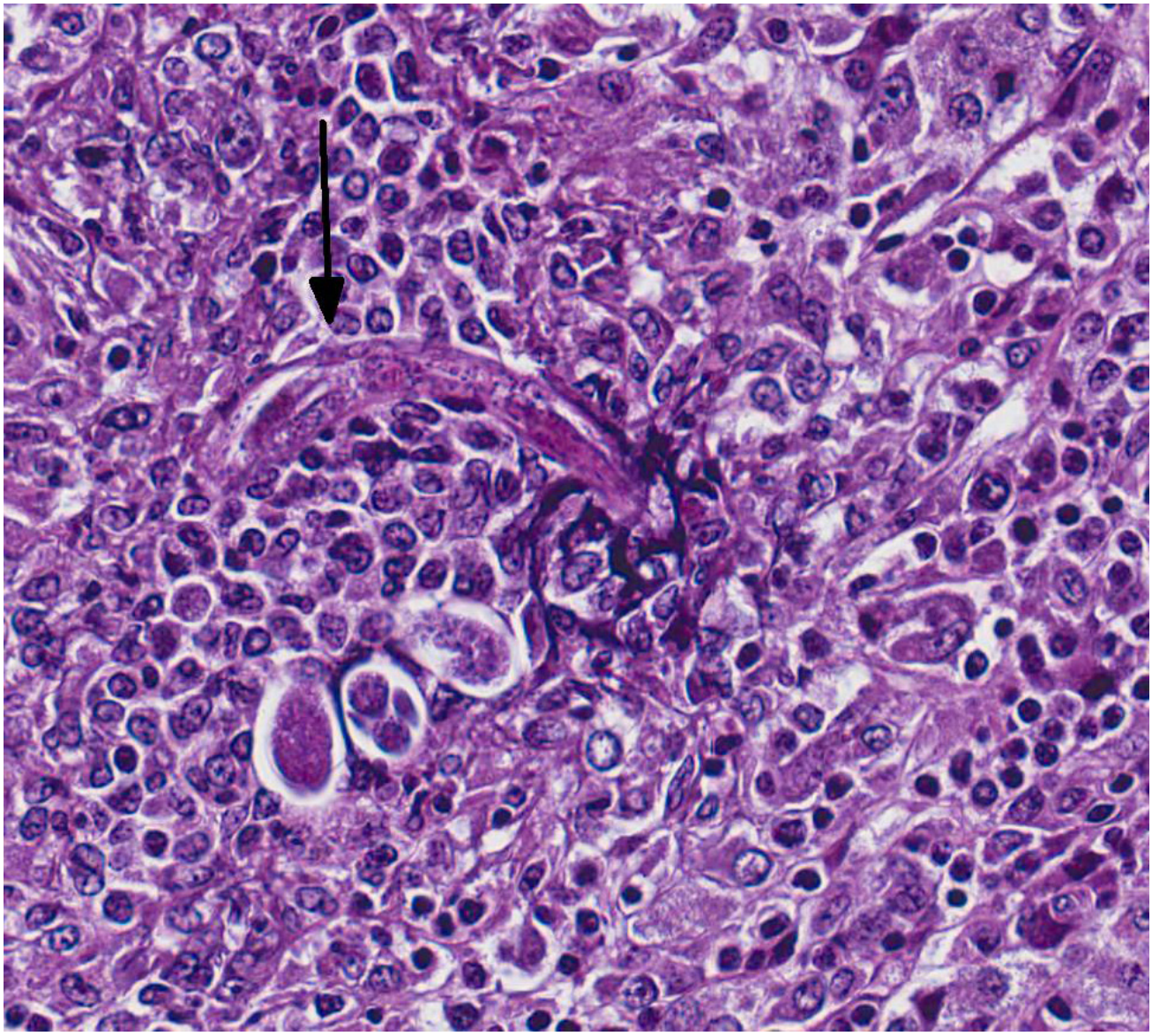

Adrenal gland, foal. Approximately 50% of the adrenal medulla is replaced by coalescing areas of necrosis and inflammation which extend into the adrenal cortex. (HE, 7X)

lymphohistiocytic meningoencephalitis, with multifocal malacia and rhaditid nematodes that were morphologically consistent with *Halicephalobus gingivalis.*

Halicephalobus gingivalis is a free-living nematode of soil, decaying organic matter and horse manure, and a facultative parasite primarily of horses and rarely of humans.[5,7,9] although there is one published report of an outbreak of halicephalobiasis producing meningoencephalitis in a group of dairy calves in Denmark.[3] Little is known about the life cycle and method of transmission; however it has been speculated that the portal of entry is mostly penetration of mucous membranes (particularly oropharyngeal following ingestion) and skin wounds, with subsequent, predominantly hematogenous spread to other organs.[3,5,6,7,9]

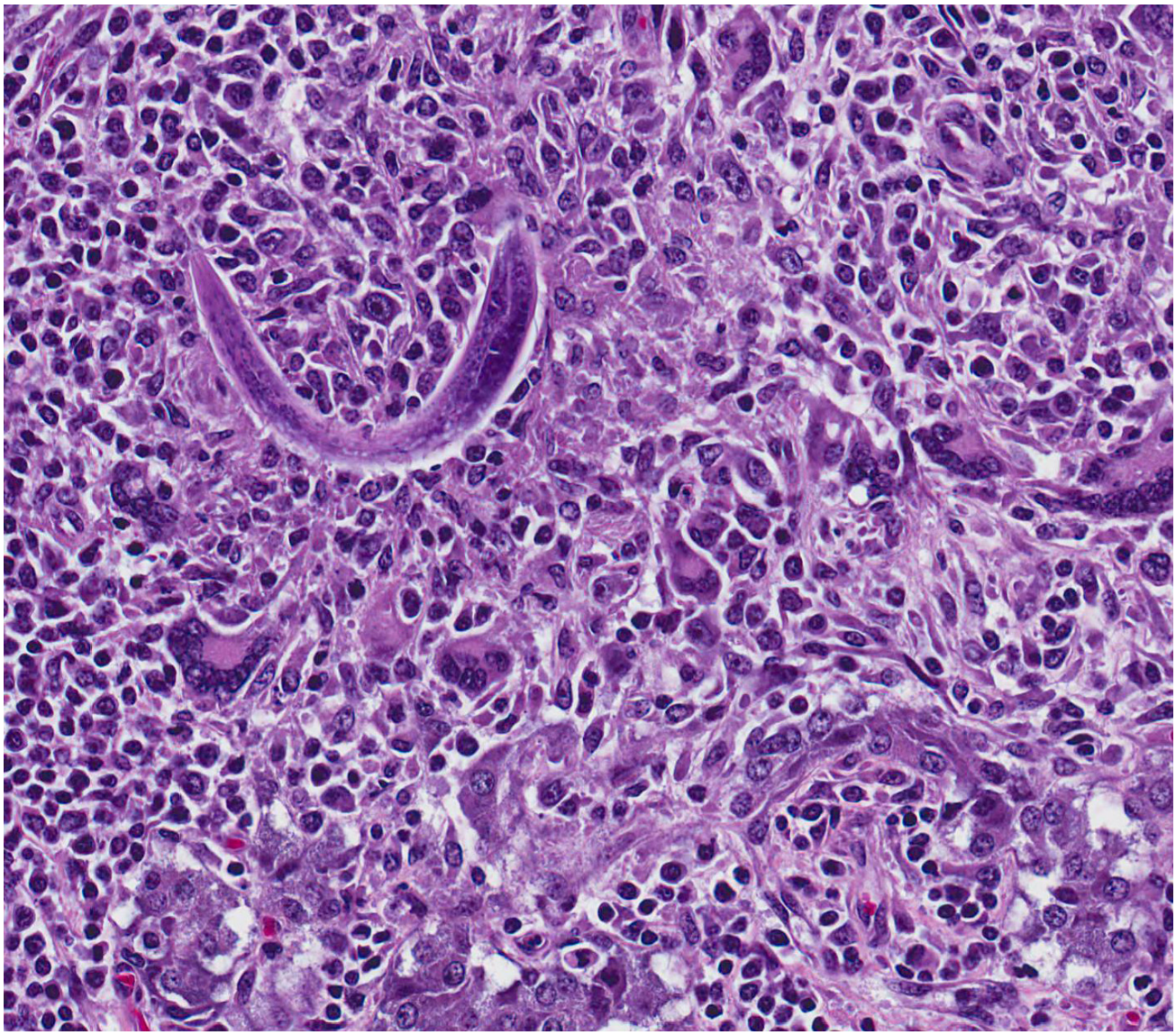

Adrenal gland, foal. Some areas of inflammation surrounding nematodes contain numerous foreign body type giant cells. The posterior end of the female rhabditoid nematode contains a deeply basophilic genital tract. (HE, 400X)

In one documented case of a fatal *H.gingivalis* infection in a 5 year old boy, he developed meningoencephalitis 8 days after falling into a horse manure spreader, acquiring manure-contaminated facial lacerations.[7,9] Only female nematodes, larvae and eggs have been detected in tissues, and as such nematode reproduction in the host is thought to be asexual with parthenogenetic females. [3,5,6,7,9] Sexual reproduction is believed to occur during the free-living part of the life cycle, and both males and females have been found in the environment.[3]

In horses, the organs/tissues most commonly affected are the meninges/brain, with or without involvement of the spinal cord and central/spinal nerves, kidney, mandibular bone and maxillary bone/sinuses, gingiva, eye, and prepuce, with less frequent reports

of involvement of adrenal gland, lung, mammary gland and testicle.[5,7,9]

Halicephalobus gingivalis infection of young foals is very rare.[3,9] Strong evidence of a transmammary route of infection was documented in one case[8] in which a 3-week-old foal presented with neurologic signs and was diagnosed postmortem with leptomeningoencephalitis caused by rhabditiod nematodes morphologically compatible with *H.gingivalis. A* biopsy of the dam's mammary gland taken the previous year was diagnosed at the time as a nematode infection, and retrospectively as mastitis caused by infection with *H.gingivalis.*

Diagnosis of halicephalobiasis is mostly performed postmortem by histologic identification of consistent lesions and morphologically compatible rhabditoid nematodes; however the nematodes can also be extracted from macerated and sieved fresh tissue, washed, centrifuged and examined by light microscopy.[3] If there is renal involvement, the nematode may also be shed in the urine, and can be collected by centrifugation of a urine sample. These methods enhance the ability to identify the characteristic features of adult female *H.gingivalis* including the rhabditiform esophagus with a corpus, isthmus and 2 esophageal bulbs, and the didelphic reproductive tract with reflexed ovary at the posterior end.[7] Identification of the nematode can be confirmed by sequencing of extracted ribosomal DNA.[3,6,7]

Contributing Institution:

Disease Investigations
Institute for Conservation Research
San Diego Zoo Global
PO Box 120551
San Diego, CA 92112

http://institute.sandiegozoo.org/disease-investigations

JPC Diagnosis: Adrenal gland: Adrenalitis, granulomatous, multifocal to coalescing, severe, with adult and larval rhabditoid nematodes.

JPC Comment: The contributor has provided an excellent and comprehensive review of disease associated with *Halicephalobus* gingivalis. The genus *Halicephalobu*s comprises eight species of small nematodes belonging to the Family Rhabditoida, which also includes *Rhabdias, Strongyloides,* and *Pelodera*.

The morphology of *Halicephalobus* is unique and characteristic. Rhabditoids are one of three families which have platymyarian-coeloyarian musculature, with the others being the strongyles and oxyurids.[4] All stages of the parasite possess the characteristic "rhabditiform esophagus" – a unique structure with a corpus, isthmus and bulb. *Halicephalobus* adult females possess a single genital tract as opposed to the paired tracts of *Strongyloides.* For this reason, only one egg is seen per cross-section of an adult female.[4] A fortuitous section can also demonstrate the dorsoflexed ovary mentioned by the contributor, which is also unique to the genus.[4]

Only females of *Strongyloides* and *Halicephalobus* are parasitic. *Halicephalobus* females (which are the only gender recovered from lesions) are not hermaphroditic and likely not parthenogenetic,– males live in decaying plant material, soil, and fresh and salt water, as do both genders of the other seven species.[2,5] Vectors have not been identified for this particular parasite; infections are presumed to be the result of ingestion, inhalation, or direct contact with infected plant matter or water with wounds or mucous membranes. Parasitic females migrate along vessels to numerous organs – in domestic equids, the brain, lymph nodes and kidneys are commonly infected.[2]

Less than ten cases of human halicephalobiasis have been reported, making this a very uncommon disease in humans. Halicephalobiasis in humans manifests as encephalitis and myelitis, and cases have been invariably fatal, due to not only the non-specific signs of disease but also the unfamiliarity of human physicians with this parasite.[8]

In humans, neurological disease associated with helminth infection may occur with a number of nematodes, including *Toxocara canis*, *Angiostrongylus cantonensis, Baylisascaris procyonis, Strongyloides stercoralis,* and nematodes lesser known to veterinarians, such as *Gnathostoma spinigerum* and *Lagochilascaris minor.*[8] Humans are atypical hosts for *Gnathostoma* sp., which utilizes a copepod of the genus *Cyclops* as a primary intermediate hosts and a wide range of vertebrates as second intermediate hosts. Humans may contract gnathostomiasis from eating undercooked seafood containing the larval nematodes (Asian swamp eels are a common source in areas of SE Asia. .As humans are aberrant hosts for this parasite, larva will migrate through a number of tissues, never completing their life cycle. *Lagochiascaris minor* is an ascarids which uses the mouse as an intermediate host and a cat for a definitive host. Accidental ingestion of undercooked rodent meat may result in visceral larval migrans in the human.[1]

References:

1. Campos DMB, Barbosa AP, De Oliveira JA, Tavares GG, Cravo PVL, Ostermayer AL. Human lagochilascariasis – a rare helmintic diseas. *PLoS Neglect Trop Dis*; s11(6): e0005510.
2. Cantile C, Youssef S. Nervous system. *In:* Maxie MG, ed. Jubb, Kennedy, and Palmer's Pathology of Domestic Animals. Vol 1. 6th ed. Philadelphia, PA: Elsevier; 2016:390.
3. Enemark HL et al. An outbreak of bovine menigoencephalomyelitis with identification of *Halicephalobus gingivalis*. Vet Parasitol 2016; 218: 82-86.
4. Gardiner CH, Poynton SL. Morphologic characteristics of rhabditoids in tissue section. *In*: An Atlas of Metazoan Parasites in Animal Tissues. Washington DC, AFIP Press, pp. 14-16.
5. Henneke C et al. The distribution pattern of *Halicephalobus gingivalis* in a horse is suggestive of a

haematogenous spread of the nematode. *Acta Vet Scand* 2014; 56: 1-4.
6. Jung JY et al. Meningoencephalitis caused by *Halicephalobus gingivalis* in a Thoroughbred gelding. *J Vet Med Sci* 2014; 76(2): 281-284.
7. Lim CK et al. First human case of fatal *Halicephalobus gingivalis* meningoencephalitis in Australia. *J Clin Microb* 2015; 53(5): 1768-1774.
8. Papadi B, Boudreaux C. Tucker JA, Mathison B, Bishop H, Eberhard ME. Case report Halicepahlobus gingivalis: a rare cause of fata meningoencehalomyelitis in humans. *Am J Trop Med Hyg* 2013; 88(6):1062-1064.
9. Wilkins PA et al. Evidence of *Halicephalobus delatrix* (*H. gingivalis*) from dam to foal. *J Vet Intern Med* 2001; 15: 412-417.

Self-Assessment - WSC 2019-2020 Conference 23

1. Which of the following is the primary mode of transmission of *Paragonimus kellicotti*?
    a. Eating feces of an infected mammal
    b. Aerosolized sputum
    c. Eating crustaceans
    d. Eating snails

2. Tetrathyridia of *Mesocestoides* species are found in which of the following?
    a. First intermediate host
    b. Second intermediate host
    c. Definitive carnivore host
    d. B and C

3. Metacestodes possess all but which of the structures seen in the adult cestode?
    a. Calcareous corpuscles
    b. Parauterine organs
    c. Reproductive tract
    d. Gastrointestinal tract

4. Pentastomes are most closely related to which of the following?
    a. Tapeworms
    b. Insects
    c. Crustaceans
    d. Acanthacephalans

5. Which of the following is not a morphologic characteristic of *Halicephalobus* in tissue section?
    a. Esophagus with corpus, isthmus, and bulb
    b. Paired genital tract
    c. Platymyarian-coelomyarian musculature
    d. Presence of only females and larva in lesions

Please email your completed assessment for grading to Dr. Bruce Williams at bruce.h.williams12.civ@mail.mil. Passing score is 80%. This program (RACE program 33611) is approved by the AAVSB RACE to offer a total of 0.5 CE Credits, with a maximum of 12.5 CE Credits being available to any individual Veterinary Medical Professionals for the 2019-2020 Wednesday Slide Conference. This RACE approval is for the subject matter categories of: SCIENTIFIC using the delivery method of NON-INTERACTIVE DISTANCE. This approval is valid in jurisdictions which recognize AAVSB RACE.

Joint Pathology Center
Veterinary Pathology Services

WEDNESDAY SLIDE CONFERENCE 2019-2020

C o n f e r e n c e 24

29 April 2020

CASE I: S62/16 (JPC 4084944). Tissue from a horse (*Equus caballus*).

Signalment: Horse, pony, adult.

History: Incidental finding during scheduled euthanasia of several ponies in the course of a parasitological study.

Gross Pathology: Mesenteric arteries of several ponies were thickened and stiffened. After opening of the vessels luminal larval nematodes were present in some animals. On cross sections the vessel lumina were narrowed and filled by thrombi with numerous entrapped grayish to white or transparent nematode larvae of approximately 1 to 2 cm in length and 1 mm in thickness.

Laboratory results: None.

Microscopic Description: Mesenteric artery: The endothelium, tunicae interna and media are widely replaced and expanded by abundant granulation tissue and massive inflammatory infiltrate. The infiltrate is composed of mainly macrophages, viable and degenerate neutrophils, eosinophils and few lymphocytes. Numerous thin-walled small caliber blood vessels, lined by plump endothelial cells and oriented perpendicular to the vascular lumen as well as increased numbers of mostly circular arranged fibroblasts and fibrocytes delineate the

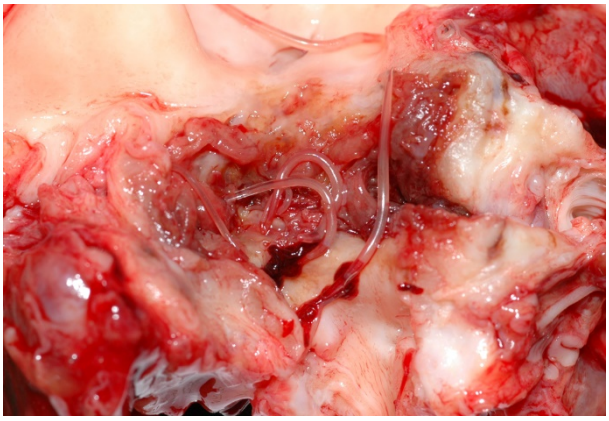

Mesenteric artery, horse. A dilated aspect of one of the mesenteric arteries contains numerous large strongyle nematodes. (Photo courtesy of: Department of Veterinary Pathology, Freie Universitaet Berlin http://www.vetmed.fu-berlin.de/en/einrichtungen/institute/we12/index.html)

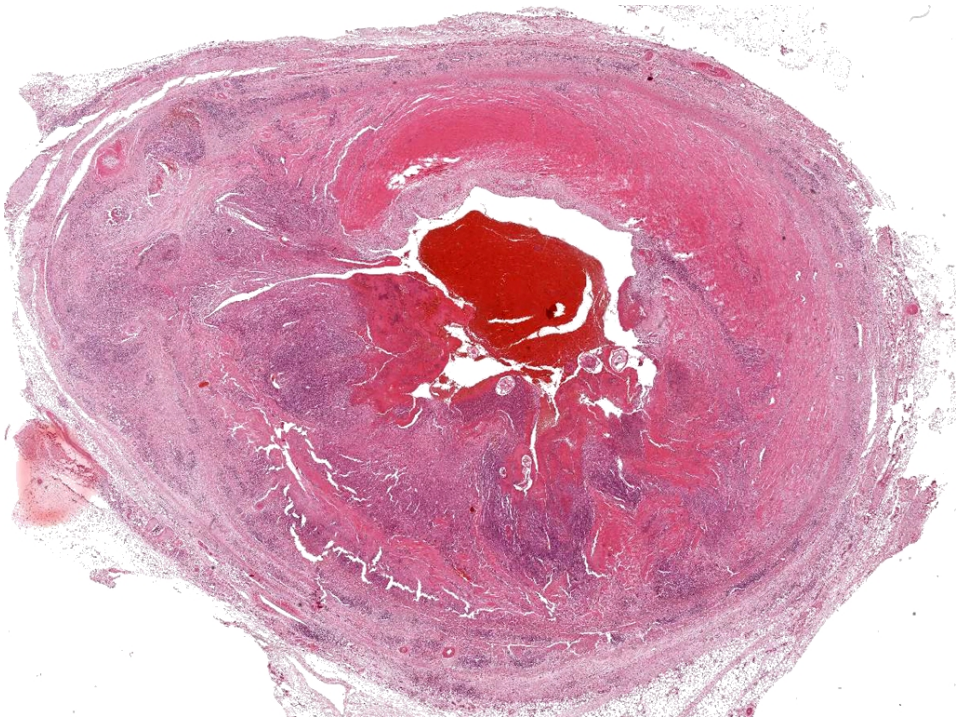

Mesenteric artery, horse. A dilated aspect of one of the mesenteric arteries contains numerous large strongyle nematodes. (Photo courtesy of: Department of Veterinary Pathology, Freie Universitaet Berlin http://www.vetmed.fu-berlin.de/en/einrichtungen/institute/we12/index.html)

inflammation in the periphery. The arterial lumen is partially occluded by an eosinophilic, amorphous material (fibrin thrombus) containing alternating layers of erythrocytes, viable and degenerate neutrophils, and fibrin (lines of Zahn) with multiple cross sections of nematode larvae. Larvae are up to 250 µm in diameter with a smooth cuticle, a pseudocoelom, platymyarian-meromyarian muscles, prominent lateral cords, and a large central intestine, lined by few multinucleated cells with a prominent brush border.

Contributor's Morphologic Diagnosis:

Mesenteric artery: Arteritis, severe, chronic-active, segmental, granulomatous and eosinophilic with (white) thrombus-formation and intralesional larval nematodes consistent with *Strongylus vulgaris*

Contributor's Comment: Virtually all horses are affected by strongylid infections, of which the most damaging to the host is the infection with the large strongyle *Strongylus vulgaris*[4]. Infectious 3rd larvae of *S. vulgaris* are ingested and exsheath in the small intestine. After penetrating the intestinal mucosa, they molt to the 4th stage of 1 mm length and migrate in or along the intima to the cranial mesenteric artery. These larvae can cause large subserosal hemorrhages called *hemomelasma ilei*. After a maturation period of 3 to 4 months the 10 to 18 mm long 5th larvae (immature adult) returns to the wall of the cecum or colon via arterial lumen and encapsulate in the subserosa forming 5 to 8 mm large nodules. After rupture of the nodules with release into the intestinal lumen and another 1 to 2 months of maturation the adult nematodes produce eggs that are shed with the feces and develop outside the horse to the 3rd larvae.[6,7]

The two other common large strongyles affecting horses are *S. edentatus* and *S. equinus*. *S. edentatus* travels via the portal

system to the liver, molts to the 4th stage and re-enters the cecum via the hepatic ligaments. *S. equinus* molts in the walls of the ileum, caecum and colon, travels via the peritoneal cavity to the liver and later also the pancreas, molts to the 5th stage and return into the cecal lumen probably by direct penetration.[7]

Gross lesions can range from small visible tracts to thrombotic lesions as in this case. Thrombembolic intestinal infarction, especially of the large bowel and the colon can be the consequence.[7] Chronic infections may lead to thickening or even scarring of the affected vessels. Another possible consequence is weakening of the vessel walls with subsequent aneurysm-formation and rupture.[6] Debilitating disease with pyrexia, anorexia, depression, diarrhea and colic are more common in foals with high larval burden and consequence to toxic products from decaying larvae. A degree of host resistance can be slowly acquired under natural conditions, but all ages remain susceptible.[6] In addition to the aortic-iliac thrombosis *S. vulgaris* may also cause cerebrospinal nematodiasis.[7]

The number of infections decreased with improvement of anthelmintics but increase again due to upcoming resistances, especially in cases of infestation with small strongyles (cyathostominosis).[5] That's why the European Union made anthelmintics available on prescription-only basis[1]. This in turn led to an increased need of *intra vitam* diagnosis of nematosis. Especially the "traditional" egg count methods may be misleading as studies indicated that horses with counts below 100 eggs per gram can harbor cyathostomes burdens in the order of 100,000 luminal worms.[4] However. until now no reliable alternative method has been found.[1,5,6] That's why the number of strongylid infections seen in necropsy will possibly increase in near future.

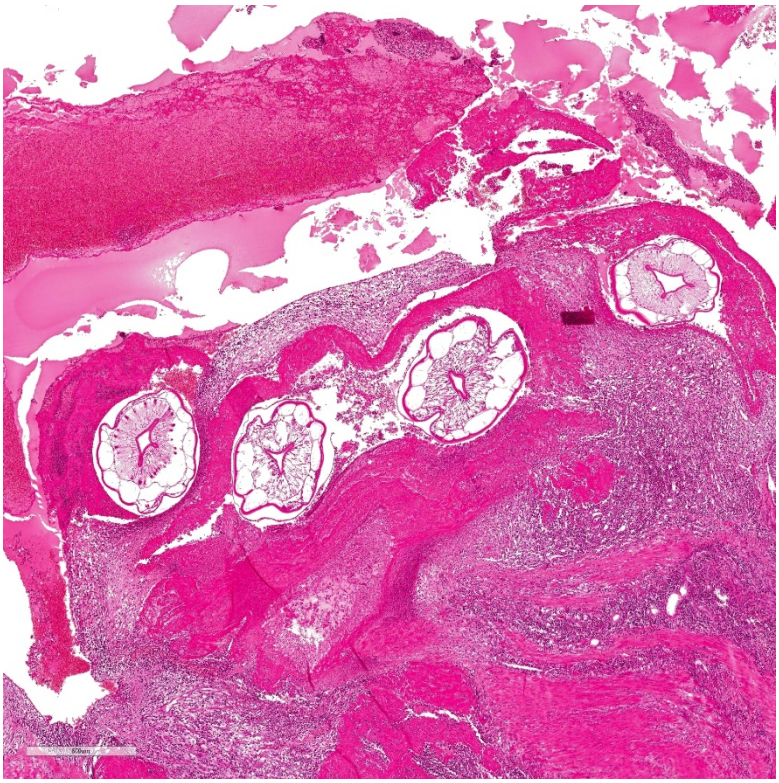

Mesenteric artery, horse. Larvae are up to 250 µm in diameter with a smooth cuticle, a pseudocoelom, platymyarian-meromyarian muscles (M), prominent lateral cords (LC), and a large central intestine, lined by few multinucleated cells with a prominent brush border (B). (Photo courtesy of: Department of Veterinary Pathology, Freie Universitaet Berlin http://www.vetmed.fu-

Contributing Institution:

Department of Veterinary Pathology, Freie Universitaet Berlin

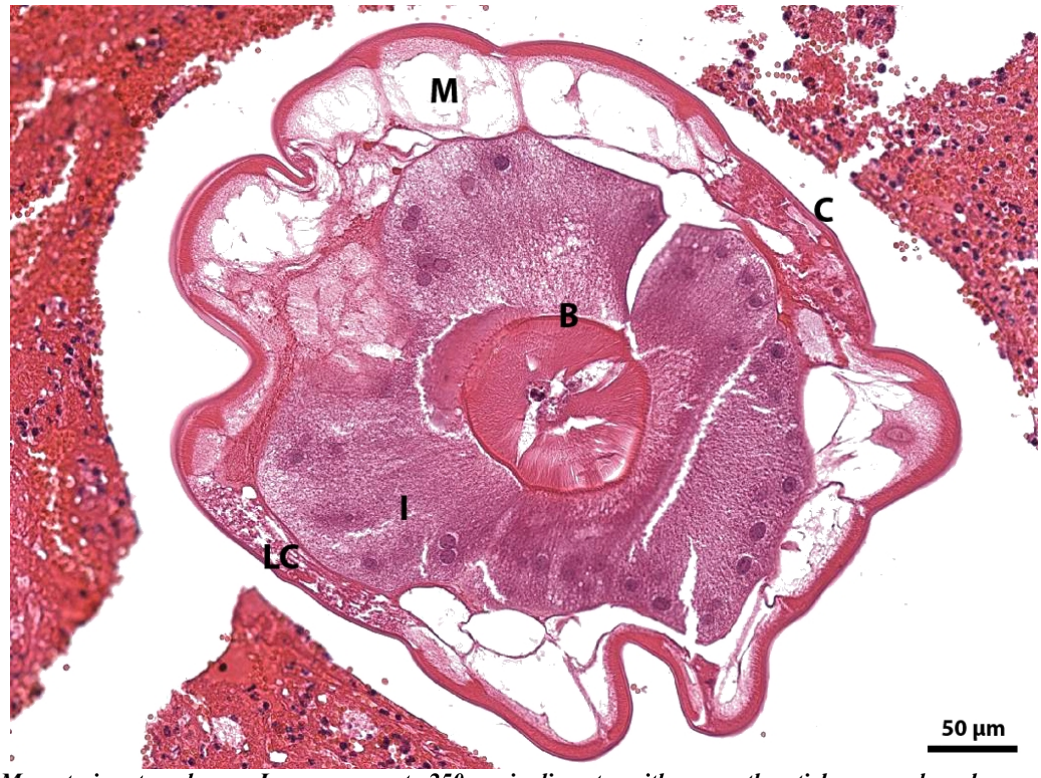

Mesenteric artery, horse. Larvae are up to 250 µm in diameter with a smooth cuticle, a pseudocoelom, platymyarian-meromyarian muscles (M), prominent lateral cords (LC), and a large central intestine, lined by few multinucleated cells with a prominent brush border (B). (Photo courtesy of: Department of Veterinary Pathology, Freie Universitaet Berlin http://www.vetmed.fu-berlin.de/en/einrichtungen/institute/we12/index.html)

http://www.vetmed.fu-erlin.de/en/einrichtungen/institute/we12/index.html

JPC Diagnosis: Mesenteric artery: Arteritis, proliferative, granulomatous and eosinophilic, transmural, chronic**,** diffuse, severe, with thrombosis and luminal larval strongyles.

JPC Comment: Even with the widespread use of ivermectin among horse owners, the classic lesion of *Strongylus vulgaris* have turned up in the WSC twice in the last 6 years (WSC 2013-2014 Conference 24 Case 4, and WSC 2017-2018 Conference 21 Case 4, 2017-2018.)

Before the widespread use of ivermectin, up to 90% of equine colic was attributed to strongyle infection (as 90% of horses with colic without obvious signs of obstruction had lesions associated with infection).

Arterial infarctions of the colon in animals with *S. vulgaris* infections have been well-documented in association with *S. vulgaris* infection and a source of puzzlement for veterinarians for many years. The lesion occurs in a small number of animals with remodeled mesenteric arteries, while the vast majority of infected do not show evidence of infarction. Several theories have been put forth about their cause, but none proven. It is compelling to think that pieces of the large thrombus in mesenteric arteries might break off and embolize to the affected regions, but its occurrence has never been documented. Another theory is vasospasm of the colonic arteries due to vasoactive substances liberated by the larvae or components of the thrombus (similar to the enhancement of ischemia induced in human myocardial infarcts by the thromboxane liberated by

platelets). Yet another theory is that the thickened arterial walls place pressure on the autonomic plexi, interfering with gut innervation.[7]

As mentioned by the contributor, reliable antemortem diagnosis of *S. vulgaris* infection is a continuing problem. Within the last few years, several potential antemortem diagnostic techniques have been proposed. Real-time identification of *S. vulgaris* antigens in fecal samples have been shown to be more effective in identifying infected animals than larval isolation techniques.[3] Recently an ELISA test measuring antibodies to recombinant *S. vulgaris* SXP protein was shown to be 73.3% sensitive and 81.1% specific for *S. vulgaris* infection.[2]

References:

1. Andersen UV, Howe DK, Olsen SN, Nielsen MK: Recent advances in diagnosing pathogenic equine gastrointestinal helminths: the challenge of prepatent detection. *Vet Parasitol* 2013; 192: 1-9.
2. Anderson UV, Howe DK, Dangoudoubiyam S, Toft N, Reinemeyer CR, Lyons ET, Olsen SN, Monrad J, Nejsum P, Nielsen MK. SvSXP: a Strongylus vulgaris antigen with potential for prepatent diagnosis. *Parasit Vect* 2013; 6:84.
3. Kaspra A, Pfister K, Nielsen MK, Silaghi C, Fink H, Scheuerle MC. Detection of Strongylus vulgaris in quine faecal samples by real-time PCR and larval culture - method comparison and occurrence assessment. *BMC Vet Res* 2017; 13:19, doi: 10.1186/s12917-016-0918-y.
4. Nielsen MK, Baptiste KE, Tolliver SC, Collins SS, Lyons ET: Analysis of multiyear studies in horses in Kentucky to ascertain whether counts of eggs and larvae per gram of feces are reliable indicators of numbers of strongyles and ascarids present. *Vet Parasitol* 2010; 174: 77-84.
5. Nielsen MK, Pfister K, von Samson-Himmelstjerna G: Selective therapy in equine parasite control--application and limitations. *Vet Parasito* 2014; *l* 202: 95-103.
6. Robinson WF, Robinson NA: Cardiovascular System. In: Jubb, Kennedy and Palmer's Pathology of Domestic Animals: Sixth Edition, pp. 1-101.e101. 2015
7. Uzal FA, Plattner BL, Hostetter JM: Alimentary System. In: Jubb, Kennedy and Palmer's Pathology of Domestic Animals: Sixth Edition, pp. 1-257.e252. 2015.
8. White NA: Thromboembolic colic in horses. *Comp Contin Educ* 1985; 7: S156-S163.

CASE II: Case 2 (JPC 4048931). Tissue from a horse (*Equus caballus*).

Signalment: 7 month-old, male, thoroughbred, horse (*Equus caballus*)

History: Foal tissue samples were submitted from a farm with a herd of about 300 horses of different ages and sexes. Foals were weaned between four to seven months of age. After weaning, all foals were grouped in batches of about 35 animals based on age. The facilities where the foals were daily handled were the same used for the management of other animals of different ages.

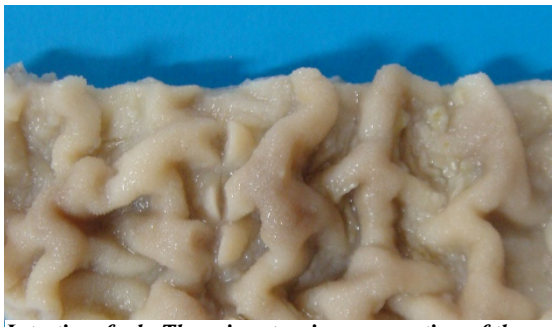

Intestine, foal. There is extensive corrugation of the intestinal mucosa. (Photo courtesy of the Veterinary School. Universidade Federal de Minas Gerais. (www.vet.ufmg.br)

Every year cases of diarrhea were reported with variable severity and characteristics in foals of different ages. Thirty-nine foals, nine from generation 2011 and 30 from generation 2012, showed clinical signs of pasty diarrhea evolving to liquid diarrhea. The body temperature varied between 39.5 to 41.0°C within 48 hours, in addition to lack of appetite and dehydration. In foals with three to six months of age, hypoproteinemia associated with submandibular edema were frequently observed. The duration of the clinical signs was from a few days to a few weeks.

Seven of 39 foals had clinical signs of diarrhea and three of these animals died. A seven-month-old foal died four days after the onset of clinical signs and intestinal samples were submitted to the Laboratory.

Gross Pathology: Grossly, large amounts of blood-tinged fluid was observed in the peritoneal cavity. The serosa of the small intestine was hyperemic. Thickening of the intestinal wall was associated with a clear corrugation and thickening of the mucosa folds with consequent reduction of intestinal lumen.

Laboratory results: Eleven fecal and serum samples from this group of foals were also submitted to the laboratory. All samples were negative for the detection of *Cryptosporidium*, *Salmonella* spp. and, *Clostridium perfringens*. Three foals were seropositive for *Lawsonia intracellularis* (1:60 – Immunoperoxidase monolayer assay). All foals were negative for *L. intracellularis* by PCR in fecal samples.

Immunohistochemistry staining using *L. intracellularis* specific antibodies demonstrated antigen labeling at the cytoplasmic apex of enterocytes and inside macrophages in the lamina propria of the duodenum, ileum and large intestine.

Microscopic Description: Histological analysis of the duodenum, jejunum, ileum and large intestine demonstrated enterocyte hyperplasia of the crypts associated with an

Intestine, foal. A section of small intestine is presented for examination. At subgross magnification, there is marked villar blunting, and expansion of the submucosal by marked edema. (HE, 6X)

intense diffuse marked decrease in the number of goblet cells. Rare crypts were dilated and the lumen filled with cell debris and neutrophils (crypt abscess). In addition, crypts were present in some areas of the submucosa.

Contributor's Morphologic Diagnosis:

Small intestine, horse: Moderate diffuse proliferative enteropathy with mild multifocal adenomatosis.

Contributor's Comment: Reported clinical signs, gross and microscopic findings, all consistent with the literature[11,13] and associated with IHC positive signal for *L. intracellularis,* allowed us to reach the diagnosis of equine proliferative enteropathy (EPE). Unlike pigs, in which lesions and immunostaining are more concentrated in the final third of the small intestine, in horses they can also be found in the duodenum,[9] as reported in this case. The lesions of the large intestine are less frequent, but in our case, histologic lesions compatible with EPE were also found in colon.

Affected animals had ages ranging from a few days to 21 months of age; however, diarrhea associated with submandibular edema (consequent of the hypoproteinemia) was observed more frequently in foals from three to six months old, the age group in which these animals are more susceptible and affected by *L. intracellularis*.[8,9] This predisposition is probably associated with the decline of maternal antibodies,[7] as well as stressors such as weaning, the move to new paddocks and barns, worming and/or vaccination programs and/or early

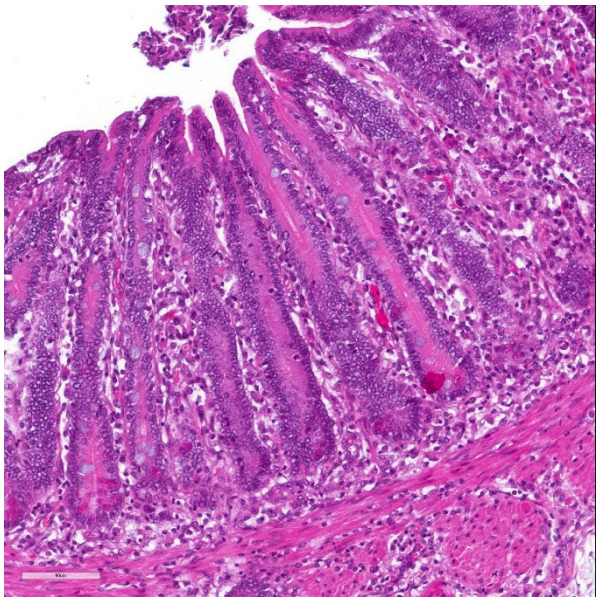

Intestine, foal. There is marked blunting of villi, resulting in a crypt:villus ratio of 1:5 or higher. Crypts are elongated with numerous mitotic figures. An infiltrate of macrophages and fewer lymphcoytes, eosinophils, and neutrophils separates crypts and lifts them off of the underlying muscularis mucosa. (HE,150X)

conditioning programs,[4] which were reported in this farm.

Animals with hypoproteinemia were treated with erythromycin, with clinical improvement in some of these animals. Treatment with erythromycin was effective for EPE in other reports[2,8] and is considered one of the treatments of choice for suspected cases of the disease. Disease progression varies from days to weeks, and the prognosis is good, if timely diagnosis and appropriate treatment are performed. Late diagnosed or untreated cases lead to death.[10]

Seropositivity for *L. intracellularis* in animals negative by PCR in fecal samples can be explained by the sensitivity of the last technique and/or by the course of the infection. There are many PCR inhibitors in fecal material that reduces the sensitivity of

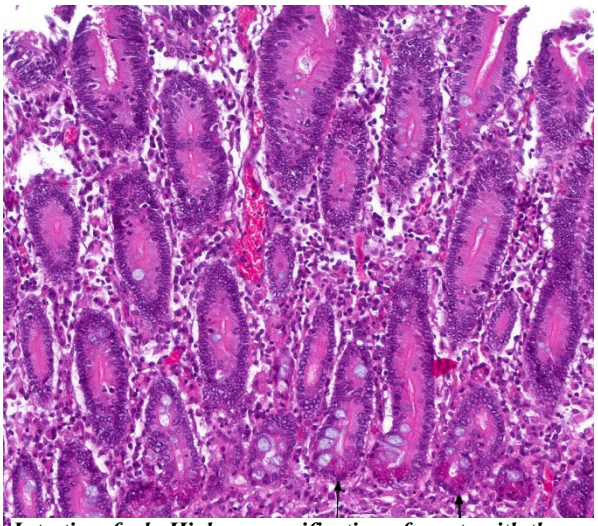

Intestine, foal. Higher magnification of crypts with the expansion of the lamina propria by inflammatory cells. In areas of ulceration, higher numbers of neutrophils are present. Paneth cells (only seen in the equine small intestine) are present at the bottom of crypts and contain numerous brightly eosinophilic granules (black arrows). (HE, 242X)

the technique; as a result, the amount of shed bacteria in the feces could be below the detection threshold. In addition, serum antibodies against *L. intracellularis* last much longer then the bacteria fecal shedding.[10]

Contamination of colts in this report may have occurred through the feces of other positive horses due to daily use of the same facilities for all ages. *L. intracellularis* subclinical infection seems to be common in horses and fecal shedding of viable bacteria can be a source of infection for susceptible foals.[5,11] Wild and domestic animals, like dogs, cats, opossums (*Didelphis* spp.), and bush dogs (*Canis thous*) sighted on the property, can also be sources of contamination. Bacterial DNA has been detected in the feces of domestic and wild animals trapped in farms with the occurrence of EPE.[11]

The EPE is present in horse farms in Brazil and despite the report of a clinical case of the disease[6] and the detection of *L. intracellularis* in feces and serology in foals in other Brazilian states,[5] EPE remains neglected in the differential diagnosis with other enteric disease in foals.

Contributing Institution:

Veterinary School. Universidade Federal de Minas Gerais. (www.vet.ufmg.br)

JPC Diagnosis: 1. Small intestine: Enteritis, proliferative, diffuse, marked with villar blunting, crypt herniation, histiocytic and eosinophilic enteritis and submucosal edema.

2. Mesentery: Fat atrophy, diffuse, moderate with lymphohistiocytic steatitis.

JPC Comment: *Lawsonia intracellularis* is a gram-negative, non-spore-forming, obligate intracellular bacterium named after Dr. Gordon Lawson, a long-term researcher at the University of Edinburgh on porcine proliferative enteropathy and the first to grow the bacterium in pure culture in 1993. This curve-shaped bacterium lives within the apical cytoplasm of a number of mammalian species, as well as chickens and ostriches, but has not been identified as an infectious agent in humans. A list of species which it has been identified in includes ferrets, swine, horses, dogs, rats, sheep, deer, ratites, nonhuman primates, and guinea pigs.[14] There are a number of subtleties of infection between species, with ferrets affected in the colon rather than small intestine, and with species like the rabbit and horse having a more profound inflammatory component. Marked

glandular proliferation of epithelium (historically referred to as "adenomatosis") characterizes the infection in hamsters and some ages of swine. Cross-species infections are often unpredictable – for example, hamsters may be infected with swine isolates (but not horse isolates) while rabbits may be infected with horse-derived strains (but not those of swine).[12,14]

The bacterium possesses a single flagellum which provides an important boost to pathogenicity by allowing it to penetrate the mucus layer in the early stages of infection. Internalization of the bacilli within apical enterocytes occurs within 3 hours, but as of yet, the events associated with this important step have not been characterized.[14] The bacilli induces cellular proliferation of crypt epithelium, and lives free within the cytoplasm, undergoing binary fission and replication itself within 2-6 days. Infected cells may release bacilli into the crypt lumen via balloon-like cytoplasmic protrusions, and these bacilli can then infect adjacent enterocytes.[14]

In horses, the disease is referred to as equine proliferative enteropathy (EPE). Primarily affecting foals around weaning (2-8 months), it may also be seen in adult animals. Weight loss, hypoalbuminemia, peripheral edema, colic, diarrhea and leukocytosis are seen (but may also be seen in other gastrointestinal diseases of young horses such as infection with *Parascaris equorum* and cyathostomiasis), and ultrasound reveals prominently thickened loops of small intestine (resulting from the mucosal thickening and submucosal edema[3] evident on this slide).

Real time PCR is used to identify the bacterium in feces and is a very useful antemortem diagnostic test. Affected horses shed bacteria for 14-21 days following active infection, as compared to pigs, which shed bacilli up to 12 weeks. (This is why subclinical infections in the pig are much more readily identified than in horses.)[14] Identification of bacilli within crypt enterocytes may be done at autopsy, but some cases may yield negative results in PCR-positive animals.[3]

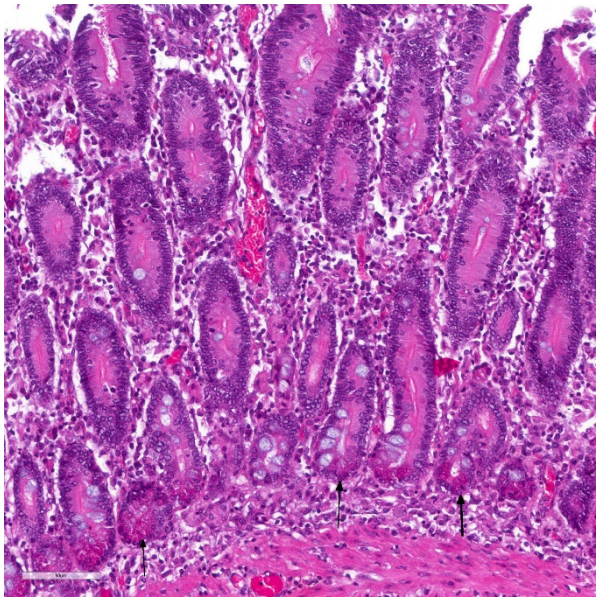

Intestine, foal. Multifocally, hyperplastic crypts herniate into the underlying mucosa. (HE, 50X)

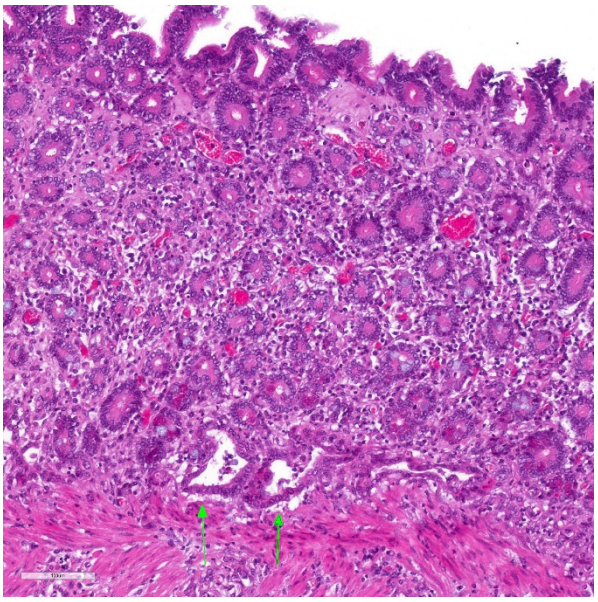

Intestine, foal. Markedly inflamed segment of intestine with crypt abscesses (green arrows). (HE, 144X)

While PPE is considered a proliferative and inflammatory intestinal disease resulting in ill thrift and hypoproteinemia, a 2013 report by Arroyo et al.[1] described an outbreak of ulcerative and necrohemorrhagic disease in weanling foals more reminiscent of the hemorrhagic enteropathy seen as a variant of *L. intracellularis* infection seen in swine (known as porcine hemorrhagic enteropathy.) These foals, in addition to ulceration, hemorrhage, and the presence of the organism in 3 of 5 cases) failed to demonstrate the marked crypt hyperplasia which is common in horses and most other species. The two other foals in this group were negative for organisms on WS and immunohistochemistry, but were PCR-positive on antemortem fecal samples.[1]

Another mystery is how foals are infected. Exposure to swine is uncommon in horse farms today. One recent study examined rodents and stray cats in the vicinity of horse farms and found a 28% per cent detection rate for cats (via serology and PCR) and variable but lesser rates for a range of rodents. The range of infected animals varied greatly between farms, but suggests wild rodents or other mammals as potential sources on infection.[7]

References:

1. Arroyo LG, ter Woort F, Baird JD, Tatiersky L, DeLay J, van Drewuel T. *Lawsonia intracellularis*-associated ulcerative and necrohemorrhagic enteritis in 5 weanline foals. *Can Vet J* 2013; 54:853-858.
2. Bihr TP. Protein-losing enteropathy caused by *Lawsonia intracellularis* in a weanling foal. *Can Vet J.* 2003;44:65-66.
3. Bohin AM, Olsen SN, Laursen SH, OHman A, van Galen G. *Lawsonia intracellularis*-associated equine proliferative enteropathy in Danish weanlig foals. *Acta Vet Scand* 2019; 61:12 doi 10.1186/s13028-019-0447-3.
4. Frazer ML. *Lawsonia intracellularis* infection in horses: 2005–2007. *J Vet Intern Med.* 2008;22:1243–1248.
5. Guimarães-Ladeira CV, Palhares MS, Oliveira JS, et al. Shedding and serological cross-sectional study of *Lawsonia intracellularis* in horses in the state of Minas Gerais, Brazil. *Equine Vet. J.* 2009;41(6):593-596.
6. Guttmann PM, Viscardi V, Lessa DAB, et al. Equine Proliferative Enteropathy Caused by *Lawsonia intracellularis* in a Foal in Brazil. *J. Equine Vet. Science.* 2014;34:701-703
7. Hwang JM, Seo MJ, Yeh JY. *Lawsonia intracellularis* in the feces of wild rodents and stray cats captured around equine farms. *BMC*

Vet Res, 2017; 13:233 doi 10.1186/s/s12917-017-1155-8
8. Lavoie JP, Drolet R, Parsons D, et al. Equine proliferative enteropathy: a cause of weight loss, colic, diarrhea and hypoproteinaemia in foals on the breeding farms in Canada. *Equine Vet J.* 2000;32(5):418-25.
9. Pusterla N, Gebhart C. *Lawsonia intracellularis* infection and proliferative enteropathy in foals. *Vet Microbiol.* 2013;167(1-2):34-41.
10. Pusterla N, Higgins JC, Smith P, et al. Epidemiological survey on farms with documented occurrence of equine proliferative enteropathy due to *Lawsonia intracellularis*. *Vet Rec.* 2008;163(5):156-158.
11. Pusterla N, Wattanaphansak S, Mapes S, et al. Oral Infection of Weanling Foals with an Equine Isolate of *Lawsonia intracellularis*, Agent of Equine Proliferative Enteropathy. *J Vet Intern Med* 2010;24:622–627.
12. Sampieri F, Vannucci FA, Allen AL, Pusterla N, Antonopoulos AJ, Ball KR, Thompson J, Dowling PM, Hamilton DL, Gebhart CJ. Species specificity of equine and porcine *Lawsonia intracellularis* isolates in laboratory animals. *Can J Vet Res* 2013: 77:261-272.
13. Vannucci FA, Pusterla N, Mapes SM, et al. Evidence of host adaptation in *Lawsonia intracellularis* infections. *Vet Res*. 2012;20:43-53.
14. Vannucci FA and Gebhart CJ. Recent advances in understanding the pathogenesis of Liawonia intracelullaris infections. *Vet Pathol* 2014; 51(2) 465-477.

CASE III: S1706449 (JPC 4117527)**.** Tissue from a horse (*Equus caballus*).

Signalment: Two-year-old Quarter horse gelding

History: Colic of unknown duration which could not be controlled with non-steroidal anti-inflammatory drugs (banamine and others) and was euthanized.

Gross Pathology: The carcass was in good nutritional condition, well-muscled and with adequate subcutaneous, perirenal and pericardial adipose tissue. The abdomen contained approximately 1 liter of red, thin, opaque fluid. Affecting three quarters of the right dorsal colon, extending distally from the diaphragmatic flexure, were the following changes: the serosa was diffusely red to dark red; the wall was transmurally thickened up to 2 cm and dark red and wet; the mucosa was mottled red to dark red to brown with a diffusely corrugated appearance; and the ingesta was semi-liquid green plant material that was red-tinged. There was a sharp line of demarcation between this region and the distal one quarter of the right dorsal colon, which had a slightly less thickened wall and diffusely tan serosa and mucosa). There was extensive petechiation of the epicardial surfaces of the atria and ventricles of the heart. No other significant gross abnormalities were observed in the rest of the carcass.

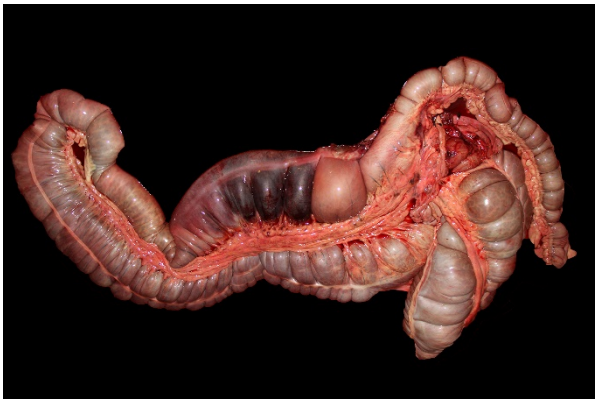

Right dorsal colon, horse. Segmentally, three-quarters of the right dorsal colon is distended and edematous with marked reddening of the serosa and a sharp line of demarcation between the affected area and the unaffected quarter. (Photo courtesy of: California Animal Health and Food safety Laboratory system, San Bernardino branch, University of California, Davis.)

Laboratory results: Aerobic and anaerobic culture of colon tissue and content grew large mixed flora; culture of colon content for *Clostridium difficile* was negative. ELISAs for toxins A and B of *C. difficile* and for alpha, beta and epsilon toxins of *Clostridium perfringens*, respectively were negative. Salmonella culture and PCR were negative on colon tissue. Aerobic culture of liver and lung grew small numbers *of Streptococcus equi* ssp. *zooepidemicus* and mixed flora.

Microscopic Description: Colon: Diffusely, there is transmural congestion, edema and hemorrhage. The whole thickness of the mucosa is necrotic and presents lymphoplasmacytic and neutrophilic infiltration. The mucosal and submucosal vasculature presents fibrin thrombi and thrombotic vessels show fibrinoid necrosis and infiltration with viable and degenerate neutrophils. These vessels are frequently surrounded by hemorrhage and viable and degenerate leukocytes. The sub-mucosa is greatly expanded by homogeneous eosinophilic edema and diffuse infiltration of lymphocytes, plasma cells, macrophages and neutrophils. The lymphatic vessels are dilated and contain large amounts of fibrin, red blood cells and neutrophils, both viable and degenerate. Large numbers of mix bacteria admixed with fibrin and cell debris cover the denudated superficial mucosa. The serosal blood vessels are also thrombotic and present fibrinoid necrosis.

Contributor's Morphologic Diagnosis:

Colon, right dorsal: Colitis, severe, diffuse, acute, necrotizing with severe fibrinonecrotizing vasculitis, fibrin thrombosis and massive submucosal edema and congestion

Contributor's Comment: Microscopic examination confirmed severe necrotizing right dorsal colitis with extensive vasculitis and many fibrin thrombi. Given the morphologic diagnosis, location, exclusion of *C. difficile*, *C. perfringens* and *Salmonella spp*., and history of banamine administration, this is likely consequence of

Right dorsal colon, horse. The mucosa of the affected segment is corrugated and mottled dark red to brown. (Photo courtesy of: California Animal Health and Food safety Laboratory system, San Bernardino branch, University of California, Davis.)

nonsteroidal anti-inflammatory drugs (NSAIDs) toxicity.[3,8]

NSAIDs cause ulceration of the small intestine and colon in horses and other animals. In horses, even low doses of phenylbutazone can cause ischemic damage to the intestinal mucosa.[8] Stress and/or dehydration are considered contributory factors to the pathogenesis of this condition.[8] Because the right dorsal colon is preferentially involved, the condition is usually named *"right dorsal colitis";* however, lesions in other parts of the colon and in the small intestine may also occur.[4,6,7] The pathogenesis of this condition is associated with decreased production of prostaglandin E_2 and nitric oxide. Decreased prostaglandin is due to NSAID inhibition of cyclooxygenase 2 (COX-2).[8]

Morphologically, right dorsal colitis cannot be differentiated from some of the most common infectious colitis of horses (e.g. *C. difficile, C. perfringens* and *Salmonella spp.* infections). There are no specific tests to confirm the diagnosis of NSAID's toxicity, and the diagnosis should therefore be based on a history of NSAIDs administration and ruling out infectious causes of colitis. While location of the lesion in the right dorsal colon helps to establish a diagnosis of NSAIDs toxicity, it should be kept in mind that these drugs can also affect other parts of the alimentary canal in horses.[8]

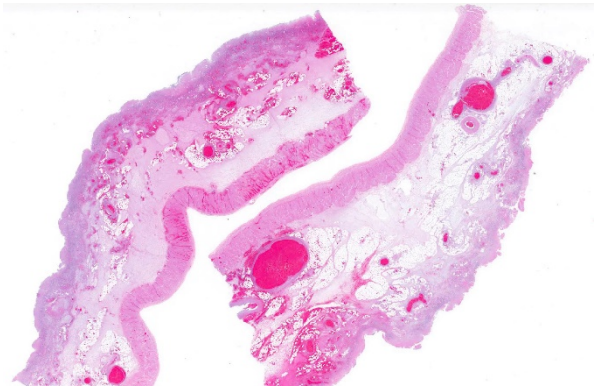

Right dorsal colon, horse. At subgross magnification, there is diffuse necrosis of the mucosal, profound submucosal edema, and marked congestion with hemorrhage and edema in all layers of the gut wall. (HE, 5X)

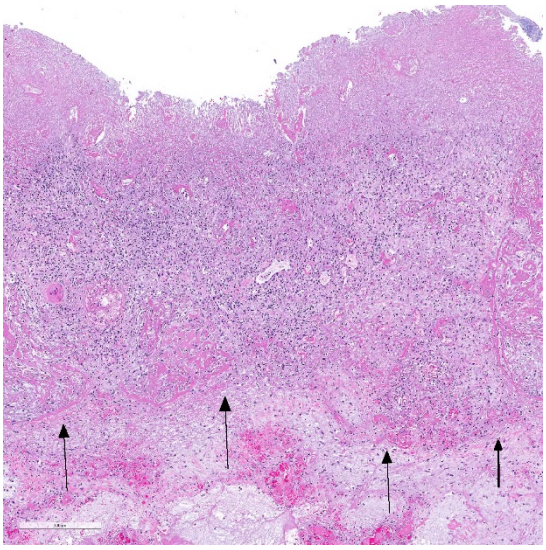

Right dorsal colon, horse. At subgross magnification, there is diffuse necrosis of the mucosal, profound submucosal edema, and marked congestion with hemorrhage and edema in all layers of the gut wall. (HE, 5X)

Contributing Institution:

California Animal Health and Food safety Laboratory system, San Bernardino branch, University of California, Davis.

JPC Diagnosis: Colon: Mucosal necrosis, diffuse, with transmural vascular fibrinoid necrosis and thrombosis, and severe submucosal edema.

JPC Comment: Since the mid-1980's, overuse of non-steroidal anti-inflammatory drugs has been associated with a variety of lesions in horses, to include ulceration of various segments of the gastrointestinal tract, as well as papillary necrosis in the kidney and

vascular damage in multiple organs.[2] Hypovolemia has been shown to potentiate their anti-prostaglandin effects, making their usage particularly hazardous in horses with endotoxemia or colic. The published toxic dose for phenylbutazone in the horse is 8.8 mg/kg BW[5] while in hypovolemic animals it is lowered to 6.0 mg/kg BW[1].

Gastrointestinal ulceration may be seen in a number of sites in the GI tract with aggressive NSAID use, to include the mouth, esophagus, and glandular stomach. While the reason for the particular susceptibility of the right dorsal colon is largely unknown, a number of theories have been advanced but not proven. The slow transit time and proximal narrowing as it enters the small colon may allow increased mucosal contact time for orally dosed NSAIDs bound to feed particles. Concentration gradients within the dorsal colon may also play a role, as the dorsal colon differs from the ventral colon in that fluid may be secreted as well as absorbed.[1]

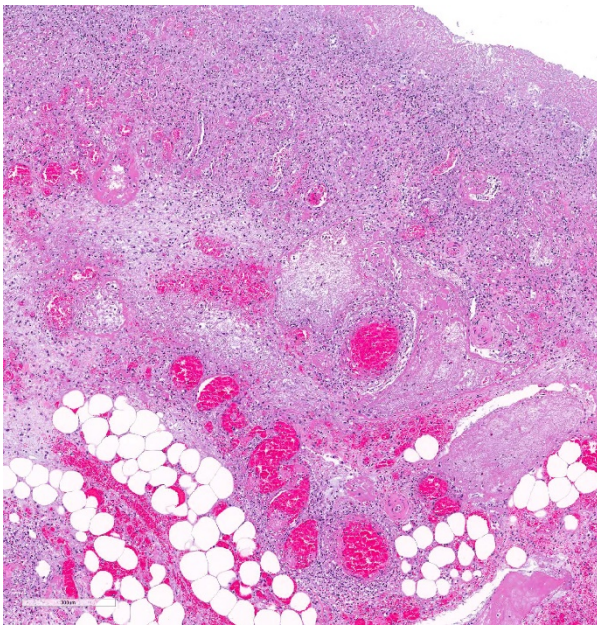

Right dorsal colon, horse. There is fibrinoid necrosis of vessels of all sizes in the mucosa and submucosa (black arrows). The submucosal adipose tissue is a good marker for colon in the horse in sections in which mucosa is totally necrotic. (HE, 83X)

Both acute and chronic syndromes of right dorsal colitis have been described, with horses with acute disease manifesting with colic, diarrhea, fever, depression, and shock. More chronic disease results in intermittent colic with weight loss, soft but not diarrheic feces and ventral edema. Hypoproteinemia and hypoalbuminemia are commonly seen in both acute and chronic presentations, with more severe levels and panhypoproteinemia seen in cases with more chronic courses.[2]

At necropsy, areas of ulceration may be interrupted by islands of regenerating mucosa, and in chronic cases, colonic submucosal fibrosis, stenosis and impaction may be evident.[2]

References:

1. Galvin N, Dillon H, McGovern F. Right dorsal colitis in the horse: minimreview and reports on three cases in Ireland. *Irish Vet J* 2004; 57(8): 467-473.
2. Karcher LF, Gill SG, Anderson WI, King JM. Right dorsal colitis. *J Vet Int Med* 1990; 4:247-253.
3. Jones SL, Davis J, Rowlingson K. 2003. Ultrasonographic findings in horses with right dorsal colitis: five cases (2000–2001*). J Am Vet Med Assoc* 222:1248–1251.
4. Marshall JF, Blikslager AT. 2011. The effect of nonsteroidal anti-inflammatory drugs on the equine intestine. *Equine Vet J* Suppl 39:140-144.
5. Meschter CL, Gilbert M, Krook L, Maylin G, Corradino R. The effects of phenylbutaxone of the morphology

of prostaganding concentras of the pyloric mucosa f the equine stomach. *Vet Pathol* 1990; 27:244-253.
6. Parfitt JR, Driman DK. 2007. Pathological effects of drugs on the gastrointestinal tract: a review. *Hum Pathol* 38:527-536.
7. Rotting AK, Freeman DE, Constable PD, Eurell JA, Wallig MA. 2004. Effects of phenylbutazone, indomethacin, prostaglandin E_2, butyrate, and glutamine on restitution of oxidant-injured right dorsal colon of horses in vitro. *Am J Vet Res* 65:1589–1595.
8. Uzal FA, Plattner BL, Hostetter JM. Alimentary system. 2016. In: Maxie G ed., Jubb, Kennedy and Palmer's Pathology of domestic animals. Vol. 2, pp. 1-257. Elsevier, St. Louis, MO.

CASE IV: WSC Case 2 (DVD) (JPC 4083951). Tissue from a horse (*Equus caballus*).

Signalment: 26-year-old male horse (*Equus ferus caballus*), breed not documented

History: This horse was part of a protocol for which blood samples were collected periodically to provide blood and/or blood products for use in other research projects. The horse was ataxic, lethargic, and exhibited reported neurologic signs for approximately 2 days prior to being euthanized.

This horse was part of a research project conducted under an IACUC approved protocol in compliance with the Animal Welfare Act, PHS Policy, and other federal statutes and regulations relating to animals and experiments involving animals. The facility where this research was conducted is accredited by the Association for Assessment and Accreditation of Laboratory Animal Care, International and adheres to principles stated in the 8th edition of the Guide for the Care and Use of Laboratory Animals, National Research Council, 2011.

Gross Pathology: Due to extenuating circumstances and adverse weather conditions, the only portion of this animal harvested for necropsy was the head. Because the horse exhibited neurologic signs prior to euthanasia, both rabies and herpes tests were performed on postmortem brain samples at the local diagnostic laboratory, and were negative. Upon gross examination of the brain, it was noted that the pituitary gland was dark red, soft, and enlarged, measuring 2.5 x 2.5 x 3 cm.

Laboratory results: Rabies and herpes tests: Negative.

Microscopic Description: Pituitary gland: Expanding the pars intermedia, compressing adjacent tissue, is a well-circumscribed,

Pituitary gland in situ, horse. The pituitary gland extends upward out of the sella turcica. (Photo courtesy of : USAMRIID, Pathology Division, 1425 Porter Street, Frederick, MD 21702-5011, http://www.usamriid.army.mil/)

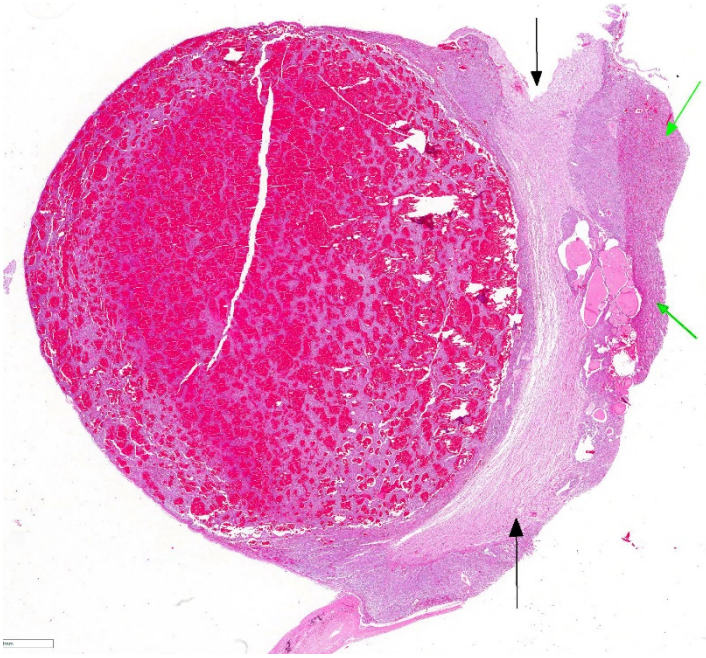

Pituitary gland, horse. A 1.75cm nodule arising from the pars intermedia, compressing the adjacent pars nervosa (black arrow) and pars glandularis (green arrow). (HE, 8X)
)

partially encapsulated, moderately cellular neoplasm composed of polygonal cells arranged in nests and packets supported by a fine fibrovascular stroma. Neoplastic cells have indistinct cell borders, moderate amounts of granular, often microvacuolated eosinophilic cytoplasm, a round, antibasilar nucleus with finely stippled chromatin, and up to 3 variably distinct nucleoli. Mitosis average less than one per 10 HPFs. Anisocytosis and anisokaryosis are mild to moderate. Diffusely throughout the neoplasm, neoplastic cells often surround variably sized and shaped blood-filled cystic spaces and occasionally palisade around blood vessels, forming pseudorosettes. Neoplastic cells occasionally form follicles lined by low cuboidal cells and filled with homogenous eosinophilic material (colloid) and cellular debris. Occasionally, scattered throughout the neoplasm and adjacent pars nervosa, there are globules of gold-brown pigment (hemosiderin) and bright yellow pigment (hematoidin) accompanied by hemosiderin-laden macrophages. There is multifocal, minimal hemorrhage.

Contributor's Morphologic Diagnosis:

Pituitary gland, pars intermedia: Adenoma, breed unspecified, equine.

Contributor's Comment: Adenoma of the pars intermedia is the most common pituitary tumor in the horse.[1] Grossly, the tumors are well circumscribed, partially encapsulated, multinodular, space occupying lesions that tend to expand, and subsequently compress, the overlying hypothalamus.[1] Microscopically, neoplastic cells are polygonal to spindle shaped with eosinophilic, granular cytoplasm, and an oval, hyperchromatic nucleus. Neoplastic cells are arranged in nodules, rosettes, bundles, or follicular structures separated by fine, fibrovascular septa, often containing numerous capillaries.[1,4]

Secondary compression of the hypothalamus can greatly diminish its normal function, resulting in the clinical syndrome associated with the tumor, termed Pituitary Pars Intermedia Dysfunction (PPID). PPID is one of the most commonly diagnosed equine endocrinopathies.[7] PPID was originally imprecisely termed "equine Cushing's disease," due to its similarities to human Cushing's disease. However, in human Cushing's disease, the pars distalis, rather than the pars intermedia, is affected. Additionally, in humans, the condition is

usually not neoplastic, and exhibits more adrenal gland involvement.[5] Since the hypothalamus is responsible for regulating body temperature, appetite, and cyclic shedding of hair, clinical signs in the horse include hyperhidrosis, polyphagia, hirsutism, polyuria, polydipsia, laminitis, muscle atrophy, fat accumulation, lethargy, and some metabolic abnormalities, among others.[1,5,6,7] Hypothalamus compression and resultant PPID is not limited in causation to neoplasia, and can also result from pituitary hypertrophy and hyperplasia, with the pituitary gland enlarging 2 to 5 times its normal weight.[5]

There are conflicting reports whether there is a gender predisposition in horses with PPID. Historically, literature has reported that female horses are more frequently affected than males, while others have noted a weak association with gelding sex.[4] Still other studies report no sex differences in the risk for developing PPID, including a review with meta-analysis of 6 studies.[3] However, there is overall consensus that PPID is a chronic progressive disease that overwhelmingly affects older horses, and is considered one of the most common diseases of horses 15 years of age and older.[5,6] The population of aged horses has considerably increased within the past two decades, and clients are becoming more informed and aware of equine age-associated diseases.[5] A recent report that investigated disease prevalence in older horses found that pituitary pars intermedia adenoma was the most common neoplasm in horses 15 years of age and older, and that PPID was the most common specific diagnosis.[6] Additionally, when accounting for the reason for euthanasia, PPID was found to be the second-most common cause of death in aged horses, with disease of the digestive system as the first.[6]

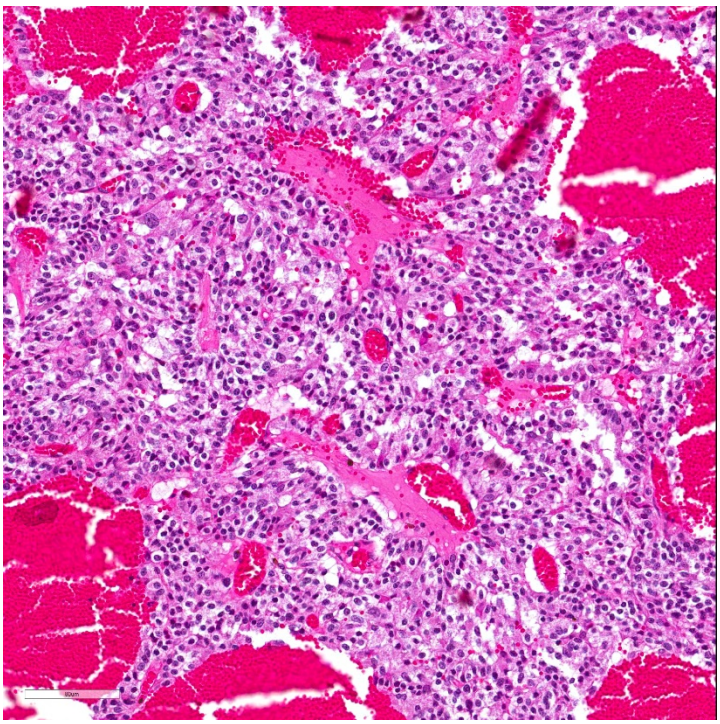

Pituitary gland, horse. Neoplastic cells form vague nests and packets and palisade along blood vessels. Numerous areas of hemorrhage and drop are present throughout the mass. (HE, 274X)

Note: Opinions, interpretations, conclusions, and recommendations are those of the authors and are not necessarily endorsed by the U.S. Army.

Contributing Institution:

USAMRIID
Pathology Division
1425 Porter Street
Frederick, MD 21702-5011
http://www.usamriid.army.mil/

JPC Diagnosis: Pituitary gland, pars intermedia: Adenoma.

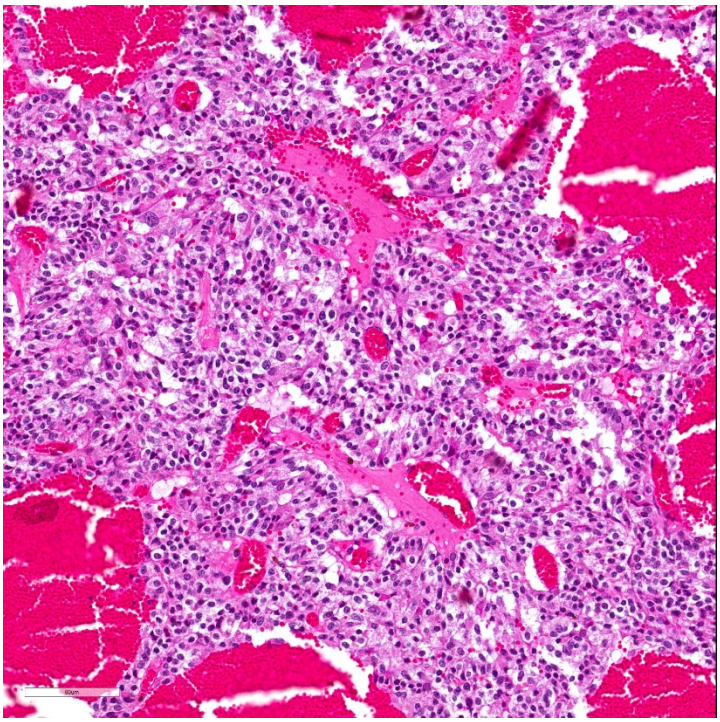

Pituitary gland, horse. Neoplastic cells palisade along vessels, forming pseudorosettes. (HE, 275X)

JPC Comment: The contributor has provided a very concise but thorough review of this particular neoplasm (largely restricted to the dog and horse), as well as the very important and common condition of pars pituitary intermedia disease (PPID). It bears repeating that the two entities are different, in that the pituitary pars intermedia adenoma (PI adenoma) is a common neoplasm in older horses, while PPID is the clinical syndrome arising from the compression of the hypothalamus from neoplasms or hyperplastic lesions of the pituitary. Characteristic clinical signs of PPID in the horse include hirsutism, delayed shedding, polydipsia and polyuria, weight loss, laminitis, and reproductive disorders in mares.[2]

A histologic and stereologic study was performed on 124 horses, and a number of histologic findings were significantly correlated with age, to include follicles and cysts within the pars intermedia, lipofuscin in the pars nervosa, and focal chromophobe hyperplasia in the pars glandularis. Highlighting the difference between adenoma and PPID, in this study, 22/124 horses had adenomas of the pars intermedia, but only 4/124 demonstrated clinical signs associated with PPID. In this study, most PI adenomas were considered incidental findings and non-functional. (Interestingly, in another review of old age lesions in the horse, in a total of 40 horses with PI adenoma, 23 were euthanized because of the pituitary adenoma. Interestingly, stereological review of PI adenomas showed that the neoplastic cells of PI adenomas causing PPID were larger by volume than those in horses without PPID.

Pituitary adenomas may also be part of a constellation of endocrine tumors in horses.

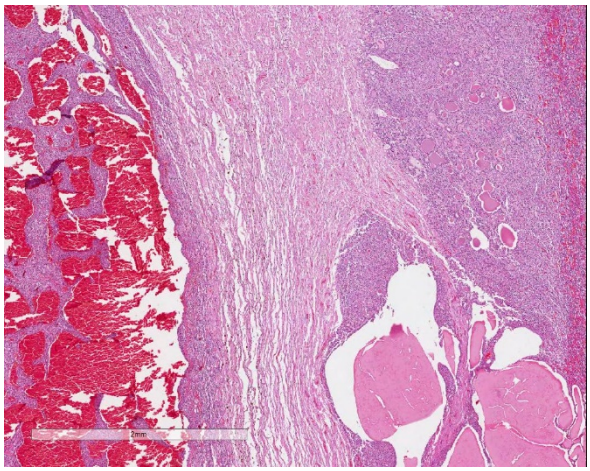

Pituitary gland, horse. Non-neoplastic areas of the pars intermedia (right) contain clusters of colloid-filled follicles. (HE, 275X)

In a recent multicenter study on equine pheochromocytoma, 18/37 (49%) animals had a concurrent PI adenoma, and 8/37 had a third neoplasm (thyroid adenoma, C-cell carcinoma), ultimately resulting in a diagnosis of multiple endocrine neoplasia. In humans, type I multiple endocrine neoplasia (MEN) includes pheochromocytoma and pituitary gland tumors.

References:

1. Capen CC. Endocrine glands. In: Maxie MG, ed. *Jubb, Kennedy, and Palmer's Pathology of Domestic Animals*. Vol 3. 5th ed. Philadelphia, PA: Elsevier Saunders; 2007:326-376.
2. Hatazoe T, Kawaguchi H, Hobo S, Misumi K. Pituitary pars intermedia dysfunction (equine Cushing's disease) in a thoroughbred stallion: a single report. *J Equine Sci* 2015*; 26(4):125-128.*
3. Leitenbacher J, Herbach N. Age-related qualitative histological and quantitative stereological changes in the equine pituitary. *J Comp Path* 2016; 154:215-224.
4. Luethy D, Habecker P, Murphy B, Nolen-Walston R. Clinical and pathological featurs of pheochromocytoma in the horse a multi-center retrospective study of 37 cases (2007-2014). *J Vt Inten Med* 2016; 30:309-313.
5. McFarlane D. Endocrine and metabolic disorders. In: Smith BP, ed. *Large Animal Internal Medicine,* 4th ed. St. Louis, MO: Elsevier; 2009:1340-1344.
6. Miller MA, Moore GE, Bertin FR, Kritchevsky JE. What's new in old horses? Postmortem dignoses in mature and aged equids. *Vet Pathol.* 2016;53(2):390-398.
7. Rohrbach BW, Stafford JR, Clermont RS, et al. Diagnostic frequency, response to therapy, and long-term prognosis among horses and ponies with pituitary par intermedia dysfunction, 1993–2004. J Vet Intern Med. 2012; 26(4):1027–1034.

Self-Assessment - WSC 2019-2020 Conference 24

1. Arterial infarcts of which of the following are seen with *S. vulgaris* infection ?
    a. Right kidney
    b. Ileum
    c. Colon
    d. Spleen

2. In which of the following species has *Lawsonia intracellularis* NOT been documented?
    a. First intermediate host
    b. Second intermediate host
    c. Definitive carnivore host
    d. B and C

3. In which of the following species is *Lawsonia intracellularis* infection located in the colon rather than the small intestine ?
    a. Swine
    b. Poultry
    c. Horses
    d. Ferrets

4. Which of the following segments of colon is often affected with aggressive use of non-steroidal antinflammatory drugs?
    a. Small colon
    b. Right ventral colon
    c. Right dorsal colon
    d. Left dorsal colon

5. Which of the following is not associated with pituitary pars intermedia dysfunction in the horse?
    a. Laminitis
    b. Colic
    c. Polyuria
    d. Hirsutism

Please email your completed assessment for grading to Dr. Bruce Williams at bruce.h.williams12.civ@mail.mil. Passing score is 80%. This program (RACE program 33611) is approved by the AAVSB RACE to offer a total of 0.5 CE Credits, with a maximum of 12.5 CE Credits being available to any individual Veterinary Medical Professionals for the 2019-2020 Wednesday Slide Conference. This RACE approval is for the subject matter categories of: SCIENTIFIC using the delivery method of NON-INTERACTIVE DISTANCE. This approval is valid in jurisdictions which recognize AAVSB RACE.

Joint Pathology Center
Veterinary Pathology Services

WEDNESDAY SLIDE CONFERENCE 2019-2020

C o n f e r e n c e 25

13 May 2020

CASE I: 15/692 (JPC 4137583).Tissue from a horse (*Equus caballus*).

Signalment: 11 years, mare, American Quarter Horse, *Equus caballus*, horse.

History: The horse had a firm, well-defined tumor on the left side of the neck. The tumor was excised for pathological examination.

Gross Pathology: A skin biopsy measuring 4x2x2 cm was received. There was a tumor in the dermis, not adherent to the epidermis, that consisted of a brown, homogeneous but somewhat lobulated, medium firm tissue. The tumor was surrounded by a thin sheath of connective tissue in the deeper areas and on the sides.

Laboratory results: None.

Microscopic Description: In the deep dermis of the skin there is a non-encapsulated, infiltrative, medium cell rich, moderately demarcated tumor that consists of spindle shaped cells and numerous multinucleated giant cells (MGCs), in sparse amounts of stroma. There are two growth patterns in the tumor, one with tightly packed spindle shaped cells growing in bundles with few MGCs and another with numerous MGCs and fewer loosely arranged spindle cells.

The spindle shaped tumor cells are medium sized, with small to moderate amounts of eosinophilic cytoplasm and an oval to cigar

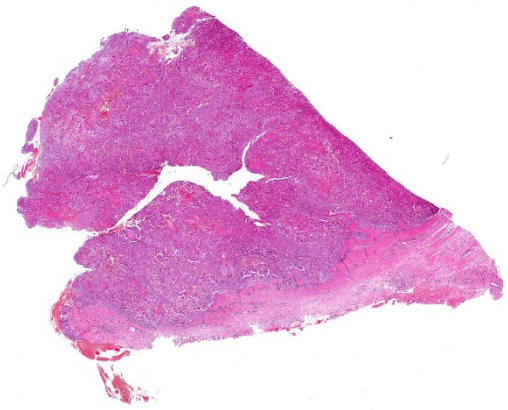

Subcutis, horse: Dermal elements are effaced by a multilobular neoplasm which extends to three cut borders. (HE, 5X)

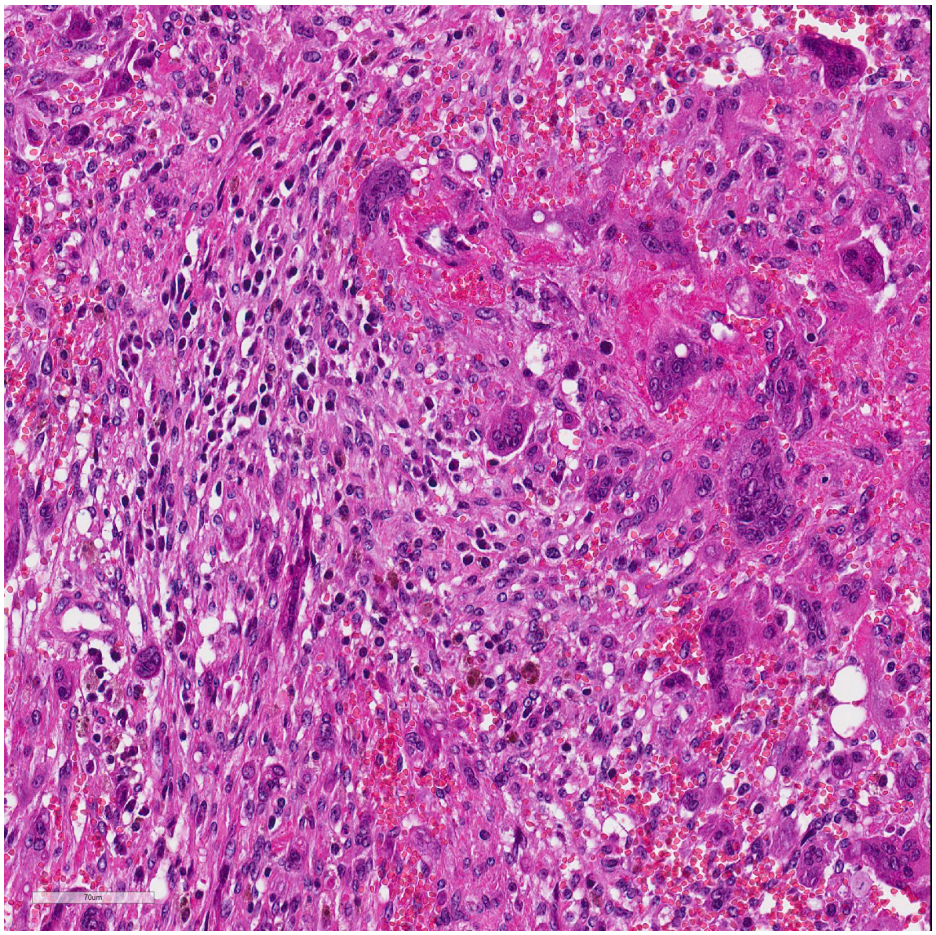

Subcutis, horse: The neoplasm is composed of two distinct cell types with a spindle cell component (left), and multinucleated giant cells (right). The stroma contains low to moderate numbers of lymphocytes and plasma cells, hemorrhage, and hemosiderin-laden macrophages. (HE, 300X)

shaped nucleus with finely stippled chromatin and 1-3 small nucleoli. The spindle shaped cells have mild to moderate anisocytosis and anisokaryosis. The MGCs are elongated, oval or round, they have abundant eosinophilic cytoplasm and oval or round nuclei with finely stippled chromatin and 1-3 small nucleoli. The MGCs are highly variable in shape, size, and nucleus number (up to 37). Mitotic figures are 2 per 10 HPF.

There are some multifocal necrotic areas in the tumor tissue. The areas with numerous MGCs often have hemorrhage, and there are multifocal inflammatory cell infiltrates with lymphocytes, plasma cells and macrophages with yellow to brown pigment (hemosiderin). Small amounts of pigment is also present in the cytoplasm of some MGCs. No acid-fast mycobacteria was detected in a Ziehl-Neelsen stained section.

Immunohistochemistry staining with the muscle marker desmin showed positive staining in the spindle shaped cells. Immunohistochemistry staining with antibody for α smooth muscle actin was variable. Areas with compact growth of spindle shaped cells had a combination of strongly positive cells and negative cells. In areas with numerous MGCs, the spindle cells were weakly positive. All MGCs were negative, in both desmin and α smooth muscle actin stained slides.

Contributor's Morphologic Diagnosis:

Skin: Undifferentiated pleomorphic sarcoma with numerous MGCs

Contributor's Comment: Undifferentiated pleomorphic sarcoma is a rare tumor that also has been termed malignant fibrous histiocytoma, giant cell tumor of soft parts, extraskeletal giant cell tumor and anaplastic

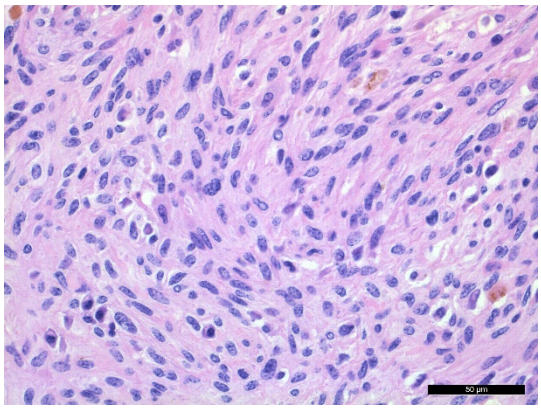

Subcutis, horse: Higher magnification of the spindle cell component of the neoplasm. (Photo courtesy of: Norwegian University of Life Sciences, Faculty of Veterinary Medicine www.nmbu.no)

sarcoma with giant cells. The cellular origin of the tumor cells are controversial. Sarcomas with combined spindle shaped cells, vacuolated histiocyte-like cells, and variable amounts of pleomorphic MGCs and a collagenous stroma have in the past often been diagnosed as malignant fibrous histiocytoma. But the term undifferentiated pleomorphic sarcoma is now preferred as these tumors most likely represent a diverse group neoplasms.[5,6]

A meta-analysis of 43 case reports and case series, totaling 82 human patients, showed that giant cell rich malignancies may be of highly variable origin, and may arise from both skeletal and many extraskeletal tissue types.[4]

The tumor in the present case is dominated by spindle shaped cells and numerous MGCs, with few mononuclear histiocyte-like cells. Also in areas with numerous MGCs, most other cells were spindle shaped. The spindle shaped cells were immunohistochemically positive for desmin and variably positive for α smooth muscle actin.

In a study of 21 cases of equine giant cell tumor of soft parts,[2] tumors with a morphology comparable to the present case were described. The tumor cells were immunohistochemically positive for vimentin and negative for cytokeratin, smooth-muscle actin, CD3, CD79a, CD31 and desmin. CD18 expression was detected only in the MGCs in the tumors, and it was suggested that the MGCs represent a secondary non-neoplastic cellular population.

It is suggested that within the undifferentiated pleomorphic sarcoma group there is a tumor of primitive myofibroblasts origin in dogs and cats that is analogous to the entity malignant fibrous histiocytoma (MFH) in humans.[5] The fibroblastic/myofibroblastic cells in MFH stain positive for vimentin and variably for actin and desmin, and the MGCs should show the same positivity as the fibroblastic cells.[5] This was however not the case in the present tumor, where desmin and actin negative MGCs were present between desmin and smooth muscle actin positive spindle shaped cells.

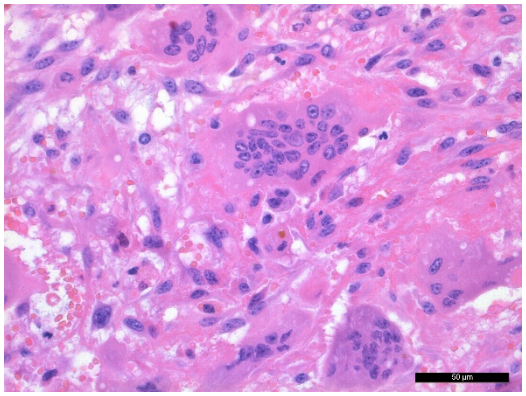

Subcutis, horse: Higher magnification of the multinucleated component of the neoplasm. (Photo courtesy of: Norwegian University of Life Sciences, Faculty of Veterinary Medicine www.nmbu.no)

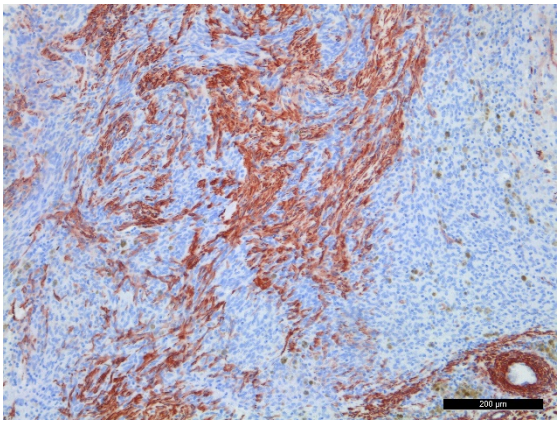

Subcutis, horse: Spindle cells demonstrate multifocal smooth muscle actin positivity. (Photo courtesy of: Norwegian University of Life Sciences, Faculty of Veterinary Medicine www.nmbu.no) (anti-SMA, 200X)

Specific antibodies for further differentiation between myofibroblasts and smooth muscle cell differentiation or origin were not available. Thus a distinction between a myofibroblastic fibrosarcoma with MGCs or a leiomyosarcoma with MGCs could not be made. In human leiomyosarcomas, a giant cell variant is recognized, and in these tumors the MGCs are proposed to be osteoclast-like cells.[3]

Contributing Institution:

Norwegian University of Life Sciences, Faculty of Veterinary Medicine
www.nmbu.no

JPC Diagnosis: Subcutis (presumptive): Pleomorphic (anaplastic) sarcoma with giant cells.

JPC Comment: The contributor has provided a concise review of this tumor, which has been shrouded in controversy for many years. It has appeared twice in the WSC in the subcutis of the horse (WSC 1994-1995, Conf 20 Case 3 and WSC 1991-1992 Conf 3, Case 4). Two submissions of malignant fibrous histiocytoma in the skin of the rat have also been submitted (WSC 1976-1977, Conf 29 Case 1 and WSC 1987-1988, Conf 21, Case 4.)

Giant cell tumors of soft parts have been described in a number of species, including baboons, Syrian hamsters, cats, and in a mule, as well as humans.[2] A recent publication describes them in rabbits.[1] In the rabbit, they most often arise in the subcutaneous tissues as well. In humans, they may be classified as superficial (affecting the skin and subcutis) or deep (affecting tendons, fascia, and skeletal muscles of the thighs). Deep tumors often recapitulate giant cell tumors of bone, and are positive for CD68 and tartrate-resistant acid phosphatase (TRAP) and occasionally positive for smooth muscle actin (as seen in this case).[2]

One of the major differentials for this neoplasm, both from a morphologic and a immunohistochemical standpoint, is

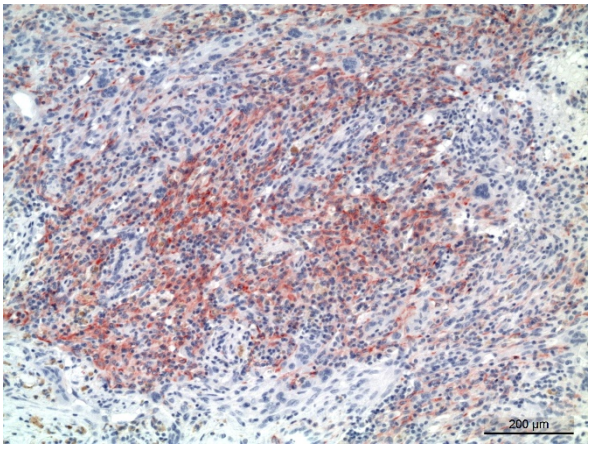

Subcutis, horse: Spindle cells demonstrate multifocal desmin positivity. (Photo courtesy of: Norwegian University of Life Sciences, Faculty of Veterinary Medicine www.nmbu.no) (anti-desmin, 100X)

histiocytic sarcoma. In the study of 21 horses with this neoplasm, 19/21 horses demonstrated CD18 positivity within the multinucleated giant cell population, but not in the spindle cell population.[2] For this reason, several authors have posited that the multinucleated cell population may be a reactive population of histiocytic cells in a spindle cell neoplasm[2,5], but exactly why they arise in a neoplasm with a fibroblastic/myofibroblastic phenotype is yet unclear.

A recent report of a tumor of this type in a Warmblood horse discusses another variant of this tumor, which has years ago been included under the umbrella term "giant cell tumor of soft parts" but more recently termed "benign giant cell tumor of tendon sheath."[7] This particular variant has been reported in dog, cats and horses. Other authors believe this neoplasm actually represents a form of pigmented villonodular synovitis, as it often arises in or near joints and shares a common feature of numerous hemosiderin-laden macrophages.[7] A case of pigmented villonodular synovitis in a reticulated giraffe appeared in the WSC 2015-2016 as Conference 9, Case 1, and the case discussion reflects a similar controversy of nature and origin.

The immunohistochemistry reported by the contributor in this case is also somewhat problematic, as the 21 cases in the retrospective by Bush *et al.*[2] were negative for smooth muscle actin and desmin, but this particular neoplasm demonstrated patchy immunopositivity. This is in agreement with the current thinking that this neoplasm, which has gone under many names over the years, is not a single neoplasm with different variants, but a collection of several neoplasms which are histologically and immunohistochemically diverse.[2,5] Consultation with a veterinary pathologist with extensive experience in similar tumors suggested an alternative theory on the origin of these lesions, in that they may be reparative in nature rather than neoplastic (personal communication, L. Craig, University of Tenn.) A similar morphology is seen in peripheral giant cell granulomas in the oral cavity of the dog and cat – a biphasic population of spindle and multinucleate cells within a background of granulation tissue. (See WSC 2017-2018 Conf 11, Case 4). While the origin of these tumors is not yet elucidated in veterinary species, human pathologists have considered peripheral giant cell granulomas to represent a reparative rather than neoplastic response.

References:

1. Bertram, CA, Garner MM, Reavill D, Klopfleisch R, Kiupel M. Giant cell sarcomas in domestic rabbits (*Oryctolagus cuniculus). Vet Pathol* 2020; DOI: 10.1177/0300985820921814
2. Bush JM, Powers BE. Equine giant cell tumor of soft parts: a series of 21 cases (2000-2007). *J Vet Diagn Invest*. 2008;20:513-516.
3. Gibbons CLMH, Sun SG, Vlychou M. et al. Osteoclast-like cells in soft tissue leiomyosardomas. *Virchows Arch*. 2010;456:317-323.
4. Gore MR. Giant cell rich malignancies: A metaanalysis. *Ann Med Health Sci Res*. 2018;8:225-232
5. Hendrick MJ. Mesenchymal tumors of the skin and soft tissues. In:

Meuten DJ, ed. *Tumors in domestic animals*. 5th ed. Ames, Iowa, USA: Wiley Blackwell; 2017:142-175.
6. Mauldin E, Peters-Kennedy J. Integumentary system. In: Maxie MG, ed. *Jubb, Kennedy, and Palmer's pathology of domestic animals*. Vol 1. 6th ed. St. Louis, Missouri, USA: Elsevier; 2016:509-736.
7. Zimmerman K, Almy F, Saunders G, Crisman M, Leonardi, L. An unusual case of giant cell tumor of soft parts in an American Warmblood horse. *Open Vet J* 2019, 9(1):44-48.

CASE II: MU11478 (JPC 4115990).
Tissue from a horse (*Equus caballus*).

Signalment: A 20-day-old female brown and white goat (*Capra aegagrus hircus)*.

History: This goat had a weeklong history of lameness in the left front leg. It improved slightly after a dose of banamine and florfenicol and then lameness progressed. At the time of euthanasia, there was swelling and clinical lameness in both carpal joints.

Heart, goat. The pericardial sac contains abundant fibrin. (Photo courtesy of: Veterinary Medical Diagnostic Lab, University of Missouri, www.vmdl.missouri.edu)

The goat was nursing poorly, and the owner requested euthanasia on humane grounds.

Gross Pathology: The goat kid weighed 5.7 kg at necropsy. Lesions were limited to the joints. In addition, there was marked, tan to white, caseous to fibrinous exudate, with increased synovial fluid volume, expanding multiple joints and multifocally infiltrating into the surrounding extracapsular tissue. The left and right shoulders, carpi, coxofemoral, right stifle, and right tarsal joints were affected.

The thoracic cavity contained marked, multifocal, yellow-tan fibrinous exudate that was multifocally adhered to the pleura, body wall, and pericardium, with numerous easily broken adhesions. The lungs are multifocally tan and red, mildly firm, and float in formalin.

Laboratory results: Small colonies of bacteria were isolated on sheep blood agar from swabs of the right carpus, right shoulder and left fetlock. Polymerase chain reaction identified them as *Mycoplasma mycoides* subsp. *capri.*

Microscopic Description: In all joints examined, there was marked edema and inflammation of the synovial membrane. The least affected specimen still contains recognizable synovial villi (Fig 2). Neutrophilic inflammation occurred in the joint lumen and infiltrating villi (Fig 3), admixed with other leukocytes. The synovial lining was ulcerated in other joints, with more fibrin in the joint lumen. The synovium and joint capsules were expanded by edema, moderate fibrosis and granulation tissue. Multifocally within the synovium,

capsule, joint space, ligament, and adjacent fat and muscle, there were aggregates of

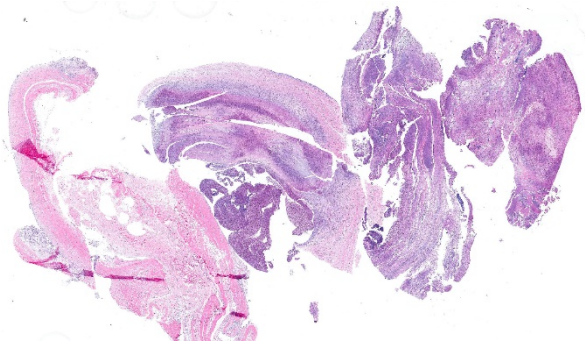

Joint, goat. The joint capsule and synovium is at left, several large lamellated clots of suppurative inflammation are present to the right. (HE, 7X)

necrotic neutrophils with fewer macrophages, similar to those comprising the separated inflammation in the specimens submitted. Unfortunately, in these particular specimens, it is only possible to identify the sheets of necrotic neutrophils, not their location. The extent of inflammation is illustrated in Fig 4, taken from another affected joint.

Contributor's Morphologic Diagnosis:

Subacute fibrinosuppurative and necrotizing polyarthritis

Contributor's Comment: The synovial lesions found in this goat are characteristic of *Mycoplasma mycoides* subsp. *capri* infection, with regard to the extent and severity of inflammation. Clumps of degenerate neutrophils and extension of inflammatory cells across the joint capsule and occasionally into muscle are dissimilar to arthritis of neonatal bacteremia, or early lentiviral infection. Several species of mycoplasma, including *M. capricolum* subsp. *capricolum* (the etiology of contagious caprine pleuropneumonia), *M. putrifaciens* and *M agalactia* can produce similar arthritis.[9,11] This particular goat had fibrinous pleuritis as well, and pleuropneumonia is often described as the most common pathologic finding in herd outbreaks, which can produce explosive disease and high morbidity and mortality. In contrast, arthritis associated with neonatal bacteremia yields a more localized suppurative intra-articular exudate with less extensive synovitis. Lentiviral infection leads to synovial proliferation and a lymphohistiocytic exudate.

Mycoplasma mycoides subsp. *capri* has been described in herd outbreaks involving hundreds of goats,[3,5,12] and, although this outbreak involved only kids less than a month of age, adults can also be affected. Adults can carry the organism in the ear canal, and isolation or PCR are the main methods of detecting carriers to eliminate them from the herd.[1] Kids acquire the infection by ingesting the agent through milk or colostrum containing mycoplasma.[5] Experimental infection after systemic

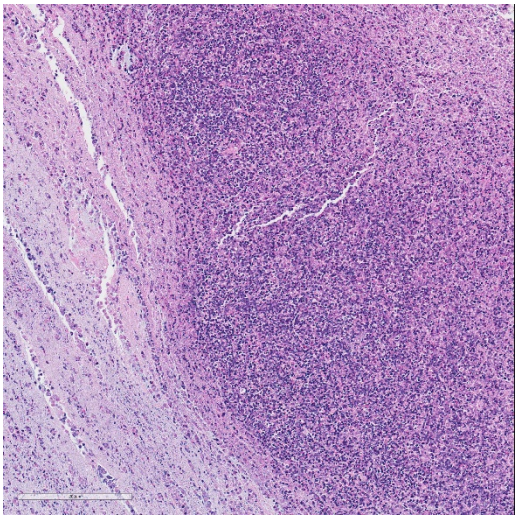

Joint, goat. Higher magnification of the lamellated suppurative exudate within the joint. (HE, 182X)

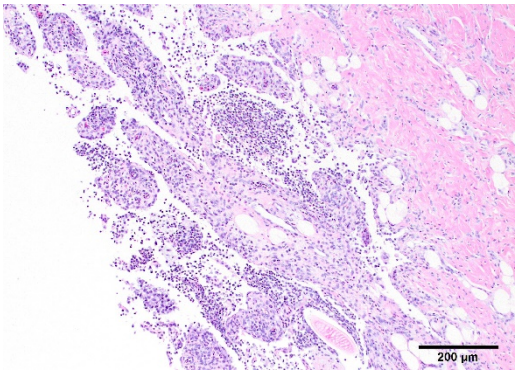

Joint, goat. Remnant synovial villi are surrounded and infiltrated by large numbers of neutrophils. (Photo courtesy of: Veterinary Medical Diagnostic Lab, University of Missouri, www.vmdl.missouri.edu) (HE, 200X)

innoculation[8] recapitulates the disease in multiple organ systems.

It is important to recognize that organisms of the mycoides group of mycoplasmas is somewhat distantly related from most other species[6,4] and that PCR tests that can speciate this group of organisms must be used or the organism may escape detection.[2,7,10]

Contributing Institution:

Norwegian University of Life Sciences, Faculty of Veterinary Medicine
www.nmbu.no

JPC Diagnosis: Synovium and periarticular soft tissue: Synovitis, fibrinosuppurative, chronic, diffuse, severe, with synovial ulceration and granulation tissue formation.

JPC Comment: Outbreaks of disease in young goats due to *Mycoplasma mycoides* subsp. *capri* have been reported to cause serious disease around the world for many years. In addition to polyarthritis, the agent may also result in septicemia as well as respiratory disease in kids. The disease is introduced into a herd by healthy carriers, and as mentioned by the contributor, transmitted to young kids via infected milk (up to 50% of does shedding mycoplasma in the milk do not show clinical signs).[1] The feeding of pooled milk by bottle appears to be the most common route of infection. Disease outbreaks often occur following stress, such as the onset of cold weather or overcrowding. Infected animals may be successfully treated with tylosin, and closer attention to husbandry practices; a long period allowed for kids to nurse from their dams appears to be useful in preventing recurrence of the disease in out years.

Mycoplasma agalactiae, the causative agent of contagious agalactiae in goat, may also cause arthritis in neonatal goats.[5] An outbreak in Greece demonstrated polyarthritis in 1-3 day old kids the season after the doe herd had contracted contagious agalactia, and the dams of the affected kids had been treated during that time for mastitis. (Affected dairy goats usually shed mycoplasma in the milk for a year, although prolonged shedding for periods up to 8 years

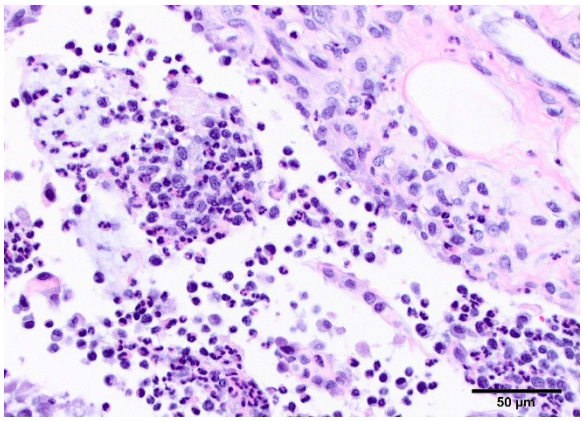

Joint, goat. Higher magnification of the remnant synovium. (Photo courtesy of: Veterinary Medical Diagnostic Lab, University of Missouri, www.vmdl.missouri.edu)

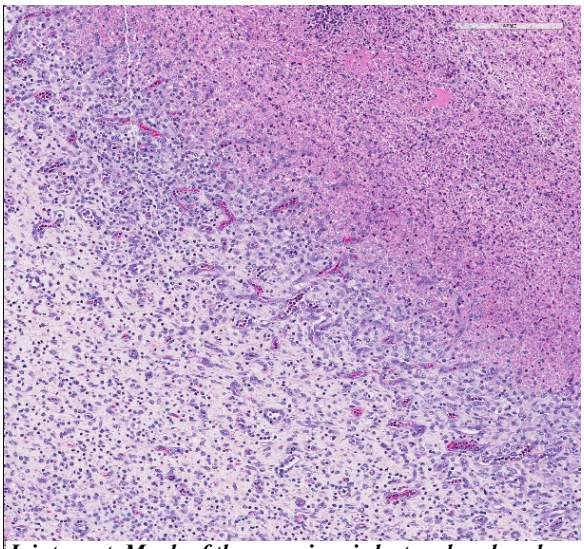

Joint, goat. Much of the synovium is lost and replaced with densely cellular granulation tissue. (HE, 100X)

have been reported.)[5] *Mycoplasma mycoides* subsp. *mycoides* has also been reported to cause polyarthritis in goats as well.[5]

Since the submission of this case, the contributors have published a case study in the Journal of Veterinary Diagnostic Information. Over a three-year period, 8 goat kids, averaging 2 weeks of age, were submitted for autopsy. 5 of the 8 goats had concurrent respiratory disease (pleuropneumonia, interstitial pneumonia, or pleuritis), 2 had meningitis, and 1 (presumptive the individual in this case) had pericarditis as well. PCR testing of colonies grown on sheep blood trypticase soy agar from affected animals using universal 16S rRNA forward and reverse primers identified the isolates as *M. mycoides* subsp. *capri.*

References:

1. Agnello S, Chetta M, Vicari D, Mancuso R, Manno C, Puleio R, Console A, Nicholas RAJ, Loria GR. Severe outbreaks of polyarthritis in kids caused by Mycoplasma mycoides subspecies capiri in Sicily. *Vet Rec* 2012; 170,416b doi: 10.1136/vr.100481
2. Amores J, et al. Comparison of culture and PCR to detect *Mycoplasma agalactia* and *Mycoplasma mycoides* subsp. *Capri* in ear swabs taken from goats. *Vet Microbiol.* 2010;**140**:105-108.
3. Becker CAM, Ramos F, Sillal E, et al. Development of a multiplex real-time PCR for contagious agalactia diagnosis in small ruminants. *J Microbiol Meth.* 2012;**90**:73-79.
4. DaMassa AJ, Eakenell PS, Brooks DL. Mycoplasmas of goats and sheep. *J Vet Diagn Invest*. 1992;**4**:101-113.
5. Filioussis G, Giadinis ND, Petridou EJ, Karavanis , Papageorgios K, Karatzias H. Congenital polyarthritis in goat kids attributed to Mycoplasma agalactiae. *Vet Rec 2011; 169,364b doi: 10.1136/vrd627*
6. Fischer A, Shapiro B, Muriuki C, et al. The origin of the '*Mycoplasma mycoides'* cluster coincides with domestication of ruminants. *PLOS ONE* 2012;**7**:e36150.
7. Johnson GC, Fales WH, Shoemake BM, Adkins PR, Middleton JR, Williams III F, Zinn M, Michell WJ, Calcutt MJ. An outbreak of Mycoplasma mycoides subspecies capri arthritis in young goats: a case study. *J Vet Diagn Invest* 2019; 31(3):453-457.
8. Kinde H, DaMasse AJ, Wakenell PS, et al. Mycoplasma infection in a commercial goat dairy caused by *Mycoplasma agalactia* and *Mycoplasma mycoides* subsp. *mycoides* (caprine biotype). *J Vet Diagn Invest* 1994;**6**:423-427.

9. Liu W, Fang L, Li M, et al. Comparative genomics of Mycoplasma: analysis of conserved essential genes and diversity of pan-genome. *PLOS ONE* 2012;**7**:e35698.
10. McAuliffe L, Ellis RJ, Lawes JR, ,et al. 16S rDNA PCR and denaturing gradient gel electrophoresis; a single generic test detecting and differentiating *Mycoplasma* species. *J Med Microbiol.* 2005;**54**:731-739.
11. Nakagawa M, Taylor WD, Yedloutschnig RJ. Pathology of goats and sheep experimentally infected with *Mycoplasma mycoides* var. *capri*. *Nat Inst Hlth Quart.*1976:**16:**65-77.
12. Nicholas RAJ. Improvements in the diagnosis and control of diseases of small ruminants caused by mycoplasmas. *Small Rum Res*. 2002;**45**:145-149.
13. Richter DJ, Rurangirwa FJ, Call DR, et al; Development of a bead-based multiplex PCR assay for the simultaneous detection of multiple *Mycoplasma* species *Vet Microbiol.* 2011;**153**

CASE III: 17-137-W4 (JPC 4117671)**.**

Signalment: ~6 month old, female, Yorkshire cross, *Sus scrofa*

History: Animal arrived at the university on 10/3/17. Observed limping on right front limb on 10/6/17, three days after arrival. The lameness progressed despite NSAID and antibiotic administration. The animal was also observed coughing occasionally with mucous production. Radiographs indicated soft tissue swelling and evidence of pneumonia. The decision was made to euthanize by the investigator on 10/12/17 due to lack of response to treatments and

Right front foot, pig. There is marked swelling of the right front foot with several abrasions on the cranial surface. (Photo courtesy of: University of Pittsburgh, Division of Laboratory Animal Resources, http://www.dlar.pitt.edu/)

inability to use in the following week's study. A complete necropsy was performed by the veterinary pathologist on 10/13/17.

Gross Pathology: The right front foot swelling was associated with a large joint abscess between P2 and P3. Approximately 20mL of tan foul smelling fluid was expressed when the joint capsule was cut.

Right front foot, pig. The lateral joint space of P2 and P3 contains suppurative exudate and the synovium is proliferative and grey-red. (Photo courtesy of: University of Pittsburgh, Division of Laboratory Animal Resources,

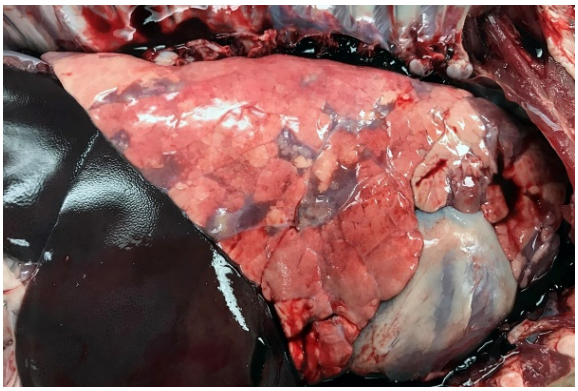

Lung, pig. Multiple lobules are depressed and dark red with extensive greyish foci. (Photo courtesy of: University of Pittsburgh, Division of Laboratory Animal Resources, http://www.dlar.pitt.edu/)

The synovium was proliferative and tan-grey to dark red between the lateral P2 - P3 joint. There was also circumferential severe swelling of the surrounding soft tissues. The lungs contained multifocal lobular dark red firm areas. On cut section, lobules were dark red to grey with white-grey foci that seemed to be associated with the airways. Cultures of the lung were submitted.

Laboratory results: Cultures from both the lungs and joint were positive for the bacterial organism *Trueperella pyogenes.*

Microscopic Description: Lungs: Affecting 75% of the section, there are multifocal to coalescing areas of necrosis composed of numerous viable and degenerate neutrophils with fewer macrophages admixed with abundant karyorrhectic and eosinophilic cellular debris and cloud-like bacterial colonies. Necrotic foci are surrounded by many epithelioid macrophages, reactive fibroblasts, and fewer lymphocytes with an outside rim of organizing granulation tissue and collagen. In less affected areas, the perivascular interstitium and alveolar septa are infiltrated and expanded by variable numbers of macrophages, neutrophils, and lymphocytes. Alveoli are often filled with proteinaceous fluid (edema), fibrin, foamy macrophages, and neutrophils. Most airways contain various amounts of neutrophils, fibrin, edema fluid, and sometimes bacterial organisms. Numerous blood vessels in the lung sections contain fibrin thrombi.

Joint, P2-P3: The synovial lining is diffusely ulcerated and covered in a layer of hyalinized fibrin and necrosuppurative debris. The joint capsule contains microabscesses composed of a central necrotic core surrounded by a rim of epithelioid macrophages, more peripheral reactive fibroblasts and lymphocytes, with an outside layer of organizing granulation tissue and collagen. The synovial membrane is thickened up to 5 times normal and forms villous projections in areas. Villi are expanded by edema, fibrin, congested blood vessels, fibroblasts, organizing granulation tissue and fibrous connective tissue.

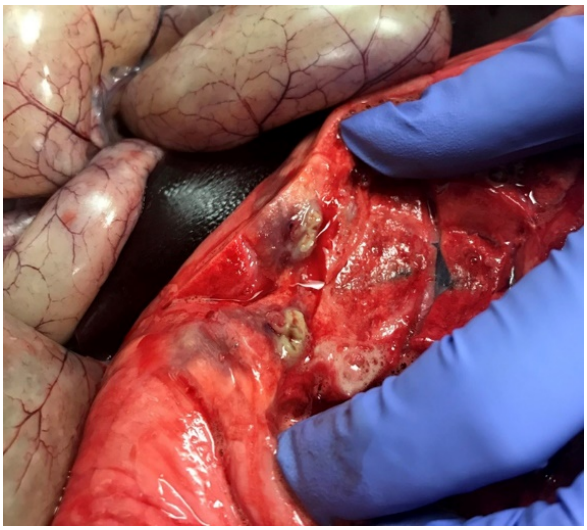

Lung, pig. On cut section, the greyish foci that appear to be associate with the airways.(Photo courtesy of: University of Pittsburgh, Division of Laboratory Animal Resources, http://www.dlar.pitt.edu/)

Contributor's Morphologic Diagnosis:

Pneumonia, necrosuppurative, multifocal to coalescing, severe, chronic, with bacteria, etiology consistent with *Trueperella pyogenes.*

P2-P3 synovitis, necroulcerative, diffuse, chronic, with microabscesses and bacteria, etiology consistent with *Trueperella pyogenes.*

Contributor's Comment: The lesions in this animal indicated chronic infection in both the joint space (P2-P3) and the lung was due to *Trueperella* which was cultured from both locations. Due to the severity and chronicity of the lesions, it is not possible to determine whether they occurred as a result of direct infection (i.e.: inhalation, focal wound) or embolic spread. The large amount of airway inflammation in the lungs suggests possible infection by inhalation, but embolic spread was likely also a factor.

T. pyogenes is a commensal and an opportunistic pathogen that causes abscessation and pneumonia in several large animal species including pigs and ruminants. In addition to pneumonia and abscesses, other potential lesions include metritis, udder lesions, pneumonia, arthritis, endocarditis, lymphadenitis and osteomyelitis. It is a gram-positive, non-motile, non-spore-forming, short, rod-shaped, coryneform bacterium that is ubiquitous in the environment and can be found on the mucous membranes of domestic animals leading to subsequent spread to any other organ system in the body.[2,3,4,7]

Haired skin, lung: Sections of lung and haired skin are submitted for examination. Both have one or more abscesses and the deep margin of the skin section appears to be a draining tract. (HE, 5X)

Although *T. pyogenes* is can infect companion animals and humans, it is an uncommon clinical pathogen.[1] In ruminants and pigs, however, it can cause significant disease and lead to condemnation at slaughter. Although treatment with antibiotics can clear the infections, this pathogen can also develop resistance to commonly used antibiotics such as tetracycline and doxycycline.[2,4,7]

Contributing Institution:

University of Pittsburgh, Division of Laboratory Animal Resources

http://www.dlar.pitt.edu/

JPC Diagnosis: 1. Haired skin, deep dermis: Abscess, with draining tract.

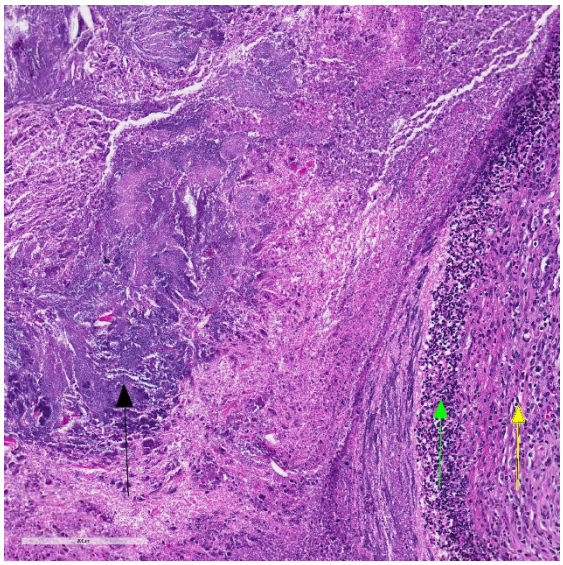

Haired skin: High magnification of the dermal abscess with numerous bacterial colonies (black arrow), peripheral layer of degenerating neutrophils and eosinophils (green arrow), abscess wall (yellow arrow). HE, 186X)

2. Lung: Pneumonia, embolic, chronic-active, focally extensive, severe.

JPC Comment: Well-known for its opportunistic infections in ruminants, *Trueperella pyogenes* is a common cause of suppurative lesions in swine as well. *T. pyogenes* is a common inhabitant of the mucosal flora in healthy animals, and can be cultured from feces of healthy swine. Infected swine can shed it in urine, feces and discharges from the upper respiratory tract, teats, and vulva.[6]

As an opportunist, it colonizes areas of inflammation or infection caused by other agents, and is a common isolate in longstanding lesions such as abscesses when the inciting agent has long disappeared. The bacterium possess a number of virulence factors which help in colonization of a number of surfaces, including neuraminidases, fimbria and collagen-, fibrin-, and fibrinogen binding proteins. Other virulence factors assist in tissue damage, including pyolysin, a cholesterol-binding exotoxin which results in cytotoxicity in a variety of cells, including neutrophils, macrophages, epithelial cells, erythrocytes, and fibroblasts.[5] The cytolytic activity of pyolysin is similar to other exotoxins secreted by gram-positive bacteria, by binding to the cell membrane and forming transmembrane pores.[5]

T. pyogenes is one of, if not the most common, bacterium isolated with suppurative processes in swine, and it may be responsible not only for focal lesions, but (as a result of hematogenous dissemination (as demonstrated in this case)) multisystemic infections as well. It is a common agent of pneumonia, pleuritic, osteoarthritis, polyarthritis, mastitis, endocarditis, valvulitis, and reproductive infections.[5,6] It may result in pyelonephritis or mastitis in non-pregnant sows, and pyometra with fetal maceration in pregnant sows. It may also be part of a mixed infection, and infections are often associated with immunosuppression from common swine viruses, such as porcine arterivirus (PRRSV).[5]

Abscesses in a variety of organs are characterized by a thick wall and yellow-green pus. Intramuscular or subcutaneous abscesses may show few clinical signs except a loss of body condition in pigs, but will often result in carcass condemnation at slaughter, especially in cases with multiple abscesses or visceral involvement.[5]

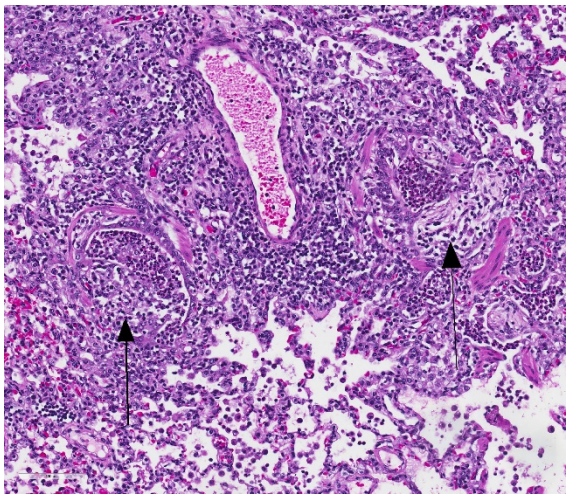

Lung, pig. Plugs of fibrous connective tissue are growing into bronchioles following effacement of the wall y suppurative and eosinophilic inflammation (bronchiolitis obliterans). (HE, 218X)

References:

1. Billington SJ, Post KW, Jost BH. Isolation of Arcanobacterium (Actinomyces) pyogenes from cases of feline otitis externa and canine cystitis. J Vet Diagn Invest. 2002; 14:159-162.
2. Buddle JR, O'Hara AJ. Enzootic pneumonia of pigs a diagnostic dilemma. Aust Vet J. 2005;83:134_139.
3. Craig LE, Dittmer KE, Thompson KG. Bones and Joints. In: Maxie MG, ed. Jubb, Kennedy, and Palmer's Pathology of Domestic Animals. Vol. 2. 6th ed. London, UK: Saunders Elsevier; 2016. Volume 1:148
4. Ribeiro MG, Risseti RM, Bolaños CAD, Caffaro KA, de Morais ACB, Lara GHB, Zamprogna TO, Paes C, Listoni FJP, Franco MMJ. rueperella pyogenes multispecies infections in domestic animals: a retrospective study of 144 cases (2002 to 2012). Veterinary Quarterly. 2015; 35(2): 82-87.
5. Rzewuska M, Kwiecien E, Chrobak-Chmiel D, Kizerwetter-Swida M, StefanskaI, Gierynska M. Pathogenicity and virulence of Truperella pyogenes: a review. *Int J Molec Sci* 2019; 20(11). pii: E2737. doi: 10.3390/ijms20112737.
6. Taylor DJ. Misclennaeous bacterial infections. *In:* Zimmerman JJ, Karriker LA, Ramirez A, Schwartz KJ, Stevenson GW eds., Diseases of Swine 10th ed. Ames IA, John J. Wiley & Sons, pp. 867-868.
7. Zhang D, Zhao J, Wang Q, Liu Y, Tian C, Zhao Y, Yu L, Liu, M. Trueperella pyogenes isolated from dairy cows with endometritis in Inner Mongolia, China: Tetracycline susceptibility and tetracycline-resistance gene distribution. Microbial Pathogenesis. 2017:51-56

CASE IV: 25681 (JPC 4115969).

Signalment: 2 year old neutered male American Quarter Horse (*Equus ferus caballus)*

History: The horse had a history of muscle wasting and pyrexia that did not respond to corticosteroids or NSAIDS. There was ultrasonographic evidence of mineralization of multiple internal organs that led to euthanasia.

Gross Pathology: The horse weighed 406 kg and was fair body condition. Skeletal muscle of the gluteal and biceps groups of both rear limbs contained patchy pale areas. Tongue and cardiac muscle are similarly

affected. The lungs failed to collapse, even after incision, and were firm and somewhat gritty. Patches of endocardium had a wrinkled appearance, were hard and had a pale gray color. Both kidneys had multiple wedge-shaped, pale, gritty cortical foci. Petechial hemorrhages and erosions were found in the glandular stomach.

Laboratory results:

Test	**December 7**	**December 16**	**Reference**
WBC	15.44 X 10^3 /ul ↑	21.76 X 10^3 /ul ↑	5.40-14.3 X 10^3 /ul
Segs	13.74 X 10^3 /ul ↑	17.41 X 10^3 /ul ↑	2.26-8.85 X 10^3 /ul
Fibrinogen	0.4 gm/dL	0.6 gm/dL ↑	0.1-0.4 gm/dL
Urea Nitrogen	21 mg/dL	39 mg/dL ↑	11-24 mg/dL
Creatinine	0.9 mg/dL	2.1 mg/dL ↑	0.9-1.7 mg/dL
Cl-	96 meq/L	94 meq/L	95-105 meq/L
Calcium	11.5 mg/dL	11.1 mg/dL	11.0-12.9 mg/dL
Phosphorus	4.1 mg/dL ↑	8.7 mg/dL ↑	1.8-2.1 mg/dL
Triglyceride	58 mg/dL ↑	84 mg/dL ↑	14-62 mg/dL
AST	>10,000 U/L ↑	5324 U/L ↑	203-415 U/L
CK	>80,000 U/L ↑	6136 U/L ↑	112-496 U/L
Urine 2/07/18	Brown, opaque, pH 9.0		
Heme	3+		
Urine specific gravity	1.063		
Urine Sediment Cytology	Marked amorphous material		
Strep equi SEM ELISA	Moderately positive		

Microscopic Description: Two sections of muscle are submitted, one minimally and one extensively affected (gluteal). There is multifocal, degeneration, necrosis and mineralization involving single or clustered myofibers. Associated with degenerating fibers are infiltrating macrophages, multi-nucleate giant cells, lymphocytes and neutrophils. Foci of degenerate fibers are associated with mild to moderate interstitial fibrosis. Multinucleate regenerating muscle fibers have lightly basophilic nuclei, and central nuclei are present. Small to medium-

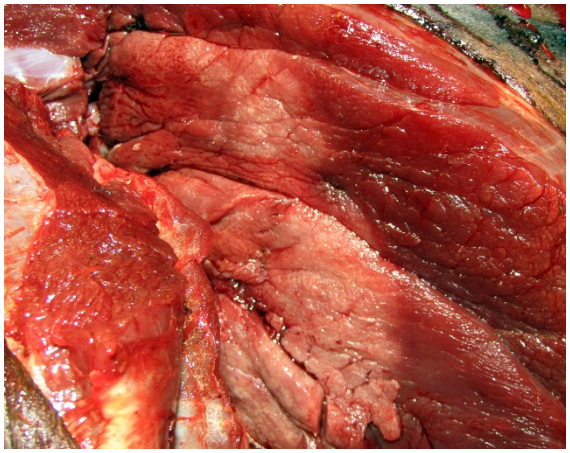

Skeletal muscle, horse. There are patches of pallor within the gluteal muscles. (Photo courtesy of : Veterinary Medical Diagnostic Lab, University of Missouri, www.vmdl.missouri.edu)

sized arterioles in affected areas are characterized by coagulative necrosis and mineralization affecting the tunica intima and tunica media.

Other microscopic diagnoses (not found on the tissues submitted) include mineralization of alveolar walls and arteries of the lung, mineralization of the epicardium, endocardium and muscle of the heart and aorta, and multifocal mineralization of the renal cortex, gastric mucosa and tongue muscle.

Contributor's Morphologic Diagnosis:

Chronic-active necrotizing myodegeneration with myofiber mineralization and attempted muscle regeneration

Contributor's Comment: This animal has characteristic lesions in muscle and other organs consistent with systemic calcinosis.[3,5,8] Skeletal muscles affected by this condition undergo gross atrophy. Large muscles, especially the gluteal, have more severe and extensive lesions, and the more severely affected specimen submitted is gluteal muscle. Other muscles can be much less affected. Histologic lesions are severe muscle necrosis. Necrosis in this case is associated with acute contraction bands, sarcoplasmic vacuolation, loss of striations and dystrophic calcification. Foci involving multiple fibers within a single muscle appear to be random, and segmental. Involvement of multiple fibers in one spot, in association with vascular mineralization suggests that vascular damage may influence lesion distribution. Macrophage infiltrate and regenerative changes are often concurrently present in foci where multiple fibers are involved. Acute and chronic damage exists

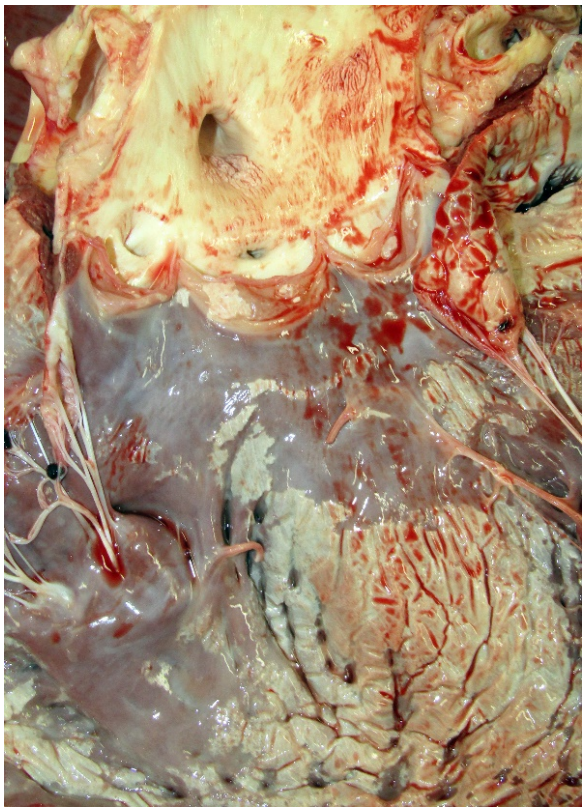

Heart, horse. There is significant mineralization of the left ventricular endocardium, aorta, and aortic valves. (Photo courtesy of : Veterinary Medical Diagnostic Lab, University of Missouri, www.vmdl.missouri.edu)

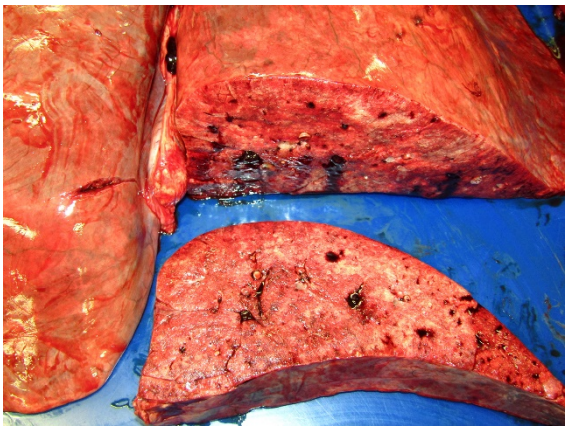

Lung, horse. The lung lobes fail to collapse and contain multiple calcified foci. (Photo courtesy of : Veterinary Medical Diagnostic Lab, University of Missouri, www.vmdl.missouri.edu)

side-by-side, although the regeneration does not appear to be conspicuously successful.

Systemic calcinosis is an invariably fatal multisystemic disease of horses that is thought to be a manifestation of calciphylaxis. Caliciphylaxis, or Systemic Uremic Arteriopathy in humans most often occurs in advanced uremia, prolonged dialysis, and renal transplantation. Muscle manifestations can be present, may be the presenting complaint,[4,6] and are manifest as a subacute proximal myopathy. Cutaneous calcification is the most common site of calcium deposition in people, along with calcification of multiple internal organs. Patients also have elevated serum phosphate and normal serum calcium.

The equine disease affects younger horses, primarily Quarter horses and Paint horses. Tissue mineralization is multisystemic, and clinical signs relate to the severity of mineral deposition in various organs. This animal presented with muscle weakness and ataxia, and the muscular system is usually involved. In this horse, mineralization of the lung and heart was also severe, even though the horse presented with signs of lameness. Numerous organs can be affected, including the liver and intestine in the analogous human disease. Only a handful of equine cases have been reported.

The equine disease may be immune-mediated, with some similarities to dermatomyositis, but there is not yet immunologic support for this hypothesis. In some humans, the presence of suspected lupus was found in one patient,[6] and vascular complement deposition has been found in another patient, providing potential support for this idea.[1]

Mineralization of soft tissue may be dystrophic (deposition of mineral on dead tissue) or metastatic (deposition of mineral on otherwise normal tissue).

Muscle calcification can occur without vascular damage. Direct sarcolemmal damage causes contraction bands in muscle fibers. Calcium entry into muscle fibers eventually results in mitochondrial overload.

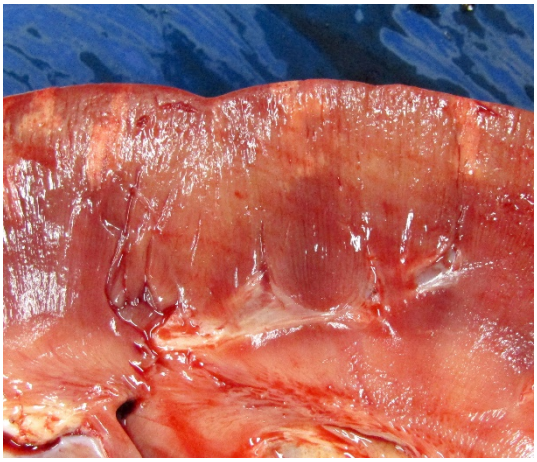

Kidney, horse. Gritty pale foci in the renal cortex have an infarct-like distribution (HE, 275X). (Photo courtesy of : Veterinary Medical Diagnostic Lab, University of Missouri, www.vmdl.missouri.edu)

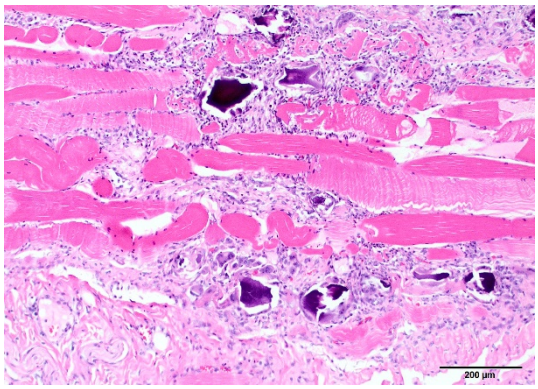

Skeletal muscle, horse: A central, degenerating blood vessel (arrow) co-exists with degenerating and mineralized fibers. (HE, 400X)

Mineralization is a hyperacute event that is virtually concurrent muscle degradation by calpains.[2]

However, dystrophic mechanisms are more likely in calciphylaxis due to the occurrence of vascular mineralization and thrombosis that is associated with calcification of myofibers. This multifocal distribution of muscle lesions that contain more to less acute damage also suggests that arteriolar damage is primary. Calcification can develop on otherwise normal tissue (metastatic) when the Ca X P product exceeds 65. In this patient, the Ca X P product was 47 on a first chemistry and 97 on a second. Calcification may be a result of RANK-l and TNF activation of osteoclasts, and hyperphosphatemia. The mechanism is thought to be through parathyroid hormone release. Vitamin D can also produce hyperphosphatemia, which usually results in hypercalcemia; serum calcium was within normal limits in this horse and the amplified Ca X P product was primarily due to hyperphosphatemia. Attempts to measure parathyroid hormone in the patient were unsuccessful due to prolonged sample storage.

In people, administration of parathyroid hormone and corticosteroid exacerbates the calciphylaxis and leads to death. It is argued that arteriolar smooth muscle is not normal in uremic patients[7] and uremic patients without calciphylaxis have vascular mineralization anyway. In any event, since corticosteroids are a mainstay of therapy for myositis in veterinary medicine, misdiagnosis is unlikely to improve clinical outcome.

Contributing Institution:

Veterinary Medical Diagnostic Lab
University of Missouri
www.vmdl.missouri.edu

JPC Diagnosis: Skeletal muscle: Myositis, necrotizing and granulomatous, polyphasic, diffuse, severe, with mineralization.

JPC Comment The contributor has provided an excellent review of systemic calcinosis in the horse, as well as cellular mechanisms of tissue calcification. In this particular specimen, the wide range of changes in affected myofibers (ranging from acute swelling and hyalinization, to fragmentation and mineralization) indicates a polyphasic lesion, one that occurs over time. In monophasic lesions, such as may be seen with acute myopathic toxic injury, such as ionophore toxicosis, skeletal muscle lesions are approximately at the identical stage or degeneration or necrosis.[3]

A wide range of conditions can result in

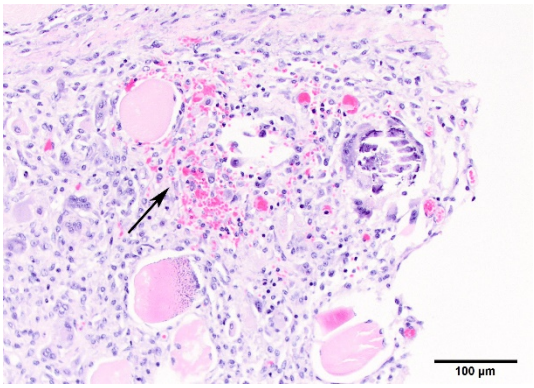

Skeletal muscle, horse. Acute degeneration coexists with mineralization, interstitial fibrosis, and regenerative multinucleate cells in one focus of damage. (HE, 200X)

local or systemic muscular calcification in horses, both dystrophic and metastatic. Traumatic damage to myofibers, such as may be seen with injections, will result in monophasic dystrophic calcification. A range of plant toxicoses may result in either monophasic lesions (in acute overwhelming intoxications) or polyphasic lesions (which are more common, in prolonged grazing). Toxicosis with sublethal doses of ionophores may result in monophasic lesions with mineralization of effected myofibers. Some species of *Cassia* result in monophasic skeletal muscle lesions in horses and ruminants; recumbent animals often do not recover. A number of plants including *Cestrum diurnum*, *Trisetum flavescens*, and plants of the genus *Solanum* accumulate analogs of activated Vitamin D, which result in excessive absorption of calcium from the intestine and subsequent metastatic calcification of skeletal muscle and many other organs. These lesions are polyphasic and progressive, and skeletal muscle mineralization is considered to be one of the earliest affected sites. Vitamin E-selenium imbalance may result in significant polyphasic damage to myocardial and skeletal muscle (particularly the muscles of deglutition and the neck and shoulder muscles) in foals, and less severe lesions within the skeletal muscles in adult horses. Recurrent non-lethal cases of exertional myopathies may present as polyphasic lesions.[3]

References:

1. Aouizerate J, Valleyrie-Allanore L, Limal N, et al. Ischemic myopathy revealing systemic calciphylaxis. *Muscle & Nerve*. 2017;**56**:529-533.
2. Cooper BJ, Valentine B. Muscle and Tendon. In: Maxie MG, ed. In: *Pathology of Domestic Animals, vol.1.* 6th ed. St. Louis:Elsevier; 2017:161-162.
3. Durwood-Akhurst SA, Valberg SJ. Immune-mediated muscle diseases of the horse. *Vet Pathol.* **2018**;55:68-75.
4. Eldelstein CL, Wickham MK, Kirby PA. Systemic calciphylaxis presenting as painful, proximal myopathy. *Postgrad Med J.* 1992;**68**:201-211.
5. Fales-William A, Sponseller B, Flaherty H. Idiopathic arterial medial calcification of the thoracic arteries in an adult horse. *J Vet Diagn Invest.* 2008;**20**:692-697.
6. Randall DP, Fisher MA, Thomas C. Rhabdomyolysis as the presenting manifestation of calciphylaxis. *Muscle & Nerve.* 2000;**23**:289-293.
7. Rogers NM, Teubner DJO, Coates TH. Calcific uremic arteriopathy: advances in pathogenesis and treatment. *Semin Dialysis.* 2007;**20**:150-167.
8. Tan, J-Y, Valbberg SJ, Sebastian MM, et al. Suspected systemic

calcinosis and calciphylaxis in 5 horses. *Can Vet J.* 2010;**51**:993-999.

Self-Assessment - WSC 2019-2020 Conference 25

1. True or False. Undifferentiated sarcoma with giant cells (giant cell tumors of soft parts) are tumors of histiocytic origin.
    a. True
    b. False

2. Which of the following is NOT commonly seen with *Mycoplasma mycoides* subsp. *Capri* infection in young goats?
    a. Rhinitis
    b. Pneumonia
    c. Septicemia
    d. Polyarthritis

3. The causative agent of contagious agalactia in goats is ?
    a. Mycoplasma agalactiae
    b. *Mycoplasma mycoides* subsp *capricolum*
    c. *Mycoplasma mycoides* subsp *capri*
    d. *Mycoplasma uberis*

4. Which of the following is considered the primary virulence factor resulting in tissue damage of *Trueperella pyogenes*?
    a. Perforin
    b. Pyolysin
    c. YOPS
    d. Type III secretion system

5. Which of the following is a common gross lesion in systemic calcinosis in horses?
    a. Corneal stromal mineralization
    b. Gross atrophy of skeletal muscles
    c. Cutaneous calcification
    d. Extensive metacarpal and metatarsal periosteal new bone growth.

Please email your completed assessment for grading to Dr. Bruce Williams at bruce.h.williams12.civ@mail.mil. Passing score is 80%. This program (RACE program 33611) is approved by the AAVSB RACE to offer a total of 0.5 CE Credits, with a maximum of 12.5 CE Credits being available to any individual Veterinary Medical Professionals for the 2019-2020 Wednesday Slide Conference. This RACE approval is for the subject matter categories of: SCIENTIFIC using the delivery method of NON-INTERACTIVE DISTANCE. This approval is valid in jurisdictions which recognize AAVSB RACE.